



PATHOGENOMICS OF THE GENUS BRUCELLA AND BEYOND

EDITED BY: Axel Cloeckert, Michel Stanislas Zygmunt, Nieves Vizcaino,
Adrian Whatmore and Holger C. Scholz

PUBLISHED IN: Frontiers in Microbiology and Frontiers in Veterinary Science



frontiers

Frontiers eBook Copyright Statement

The copyright in the text of individual articles in this eBook is the property of their respective authors or their respective institutions or funders. The copyright in graphics and images within each article may be subject to copyright of other parties. In both cases this is subject to a license granted to Frontiers.

The compilation of articles constituting this eBook is the property of Frontiers.

Each article within this eBook, and the eBook itself, are published under the most recent version of the Creative Commons CC-BY licence.

The version current at the date of publication of this eBook is CC-BY 4.0. If the CC-BY licence is updated, the licence granted by Frontiers is automatically updated to the new version.

When exercising any right under the CC-BY licence, Frontiers must be attributed as the original publisher of the article or eBook, as applicable.

Authors have the responsibility of ensuring that any graphics or other materials which are the property of others may be included in the CC-BY licence, but this should be checked before relying on the CC-BY licence to reproduce those materials. Any copyright notices relating to those materials must be complied with.

Copyright and source acknowledgement notices may not be removed and must be displayed in any copy, derivative work or partial copy which includes the elements in question.

All copyright, and all rights therein, are protected by national and international copyright laws. The above represents a summary only. For further information please read Frontiers' Conditions for Website Use and Copyright Statement, and the applicable CC-BY licence.

ISSN 1664-8714

ISBN 978-2-88971-285-4

DOI 10.3389/978-2-88971-285-4

About Frontiers

Frontiers is more than just an open-access publisher of scholarly articles: it is a pioneering approach to the world of academia, radically improving the way scholarly research is managed. The grand vision of Frontiers is a world where all people have an equal opportunity to seek, share and generate knowledge. Frontiers provides immediate and permanent online open access to all its publications, but this alone is not enough to realize our grand goals.

Frontiers Journal Series

The Frontiers Journal Series is a multi-tier and interdisciplinary set of open-access, online journals, promising a paradigm shift from the current review, selection and dissemination processes in academic publishing. All Frontiers journals are driven by researchers for researchers; therefore, they constitute a service to the scholarly community. At the same time, the Frontiers Journal Series operates on a revolutionary invention, the tiered publishing system, initially addressing specific communities of scholars, and gradually climbing up to broader public understanding, thus serving the interests of the lay society, too.

Dedication to Quality

Each Frontiers article is a landmark of the highest quality, thanks to genuinely collaborative interactions between authors and review editors, who include some of the world's best academicians. Research must be certified by peers before entering a stream of knowledge that may eventually reach the public - and shape society; therefore, Frontiers only applies the most rigorous and unbiased reviews. Frontiers revolutionizes research publishing by freely delivering the most outstanding research, evaluated with no bias from both the academic and social point of view. By applying the most advanced information technologies, Frontiers is catapulting scholarly publishing into a new generation.

What are Frontiers Research Topics?

Frontiers Research Topics are very popular trademarks of the Frontiers Journals Series: they are collections of at least ten articles, all centered on a particular subject. With their unique mix of varied contributions from Original Research to Review Articles, Frontiers Research Topics unify the most influential researchers, the latest key findings and historical advances in a hot research area! Find out more on how to host your own Frontiers Research Topic or contribute to one as an author by contacting the Frontiers Editorial Office: frontiersin.org/about/contact

PATHOGENOMICS OF THE GENUS BRUCELLA AND BEYOND

Topic Editors:

Axel Cloeckaert, Institut National de recherche pour l'agriculture, l'alimentation et l'environnement (INRAE), France

Michel Stanislas Zygmunt, Institut National de recherche pour l'agriculture, l'alimentation et l'environnement (INRAE), France

Nieves Vizcaino, University of Salamanca, Spain

Adrian Whatmore, Animal and Plant Health Agency, United Kingdom

Holger C. Scholz, Institut für Mikrobiologie der Bundeswehr, Germany

Citation: Cloeckaert, A., Zygmunt, M. S., Vizcaino, N., Whatmore, A., Scholz, H. C., eds. (2021). Pathogenomics of the Genus *Brucella* and Beyond. Lausanne: Frontiers Media SA. doi: 10.3389/978-2-88971-285-4

Table of Contents

- 06 Editorial: Pathogenomics of the Genus *Brucella* and Beyond**
Axel Cloeckaert, Michel S. Zygmunt, Holger C. Scholz, Nieves Vizcaino and Adrian M. Whatmore
- 11 *Brucella abortus* Strain 2308 Wisconsin Genome: Importance of the Definition of Reference Strains**
Marcela Suárez-Esquivel, Nazareth Ruiz-Villalobos, Amanda Castillo-Zeledón, César Jiménez-Rojas, R. Martin Roop II, Diego J. Comerci, Elías Barquero-Calvo, Carlos Chacón-Díaz, Clayton C. Caswell, Kate S. Baker, Esteban Chaves-Olarte, Nicholas R. Thomson, Edgardo Moreno, Jean J. Letesson, Xavier De Bolle and Caterina Guzmán-Verri
- 17 *COX-2* Inhibition Reduces *Brucella* Bacterial Burden in Draining Lymph Nodes**
Aurélie Gagnaire, Laurent Gorvel, Alexia Papadopoulos, Kristine Von Bargen, Jean-Louis Mège and Jean-Pierre Gorvel
- 30 Extended Multilocus Sequence Analysis to Describe the Global Population Structure of the Genus *Brucella*: Phylogeography and Relationship to Biovars**
Adrian M. Whatmore, Mark S. Koylass, Jakub Muchowski, James Edwards-Smallbone, Krishna K. Gopaul and Lorraine L. Perrett
- 44 MLVA Genotyping Characteristics of Human *Brucella melitensis* Isolated from Ulanqab of Inner Mongolia, China**
Zhi-Guo Liu, Dong-Dong Di, Miao Wang, Ri-Hong Liu, Hong-Yan Zhao, Dong-Ri Piao, Guo-Zhong Tian, Wei-Xing Fan, Hai Jiang, Bu-Yun Cui and Xian-Zhu Xia
- 54 *Brucella* and Osteoarticular Cell Activation: Partners in Crime**
Guillermo H. Giambartolomei, Paula C. Arriola Benitez and M. Victoria Delpino
- 63 Genetic Diversity of *Brucella* Reference and Non-reference Phages and Its Impact on *Brucella*-Typing**
Jens A. Hammerl, Cornelia Göllner, Claudia Jäckel, Holger C. Scholz, Karsten Nöckler, Jochen Reetz, Sascha Al Dahouk and Stefan Hertwig
- 75 *Brucella* Genital Tropism: What's on the Menu**
Jean-Jacques Letesson, Thibault Barbier, Amaia Zúñiga-Ripa, Jacques Godfroid, Xavier De Bolle and Ignacio Moriyón
- 80 Erythritol Availability in Bovine, Murine and Human Models Highlights a Potential Role for the Host Aldose Reductase During *Brucella* Infection**
Thibault Barbier, Arnaud Machelart, Amaia Zúñiga-Ripa, Hubert Plovier, Charlotte Hougardy, Elodie Lobet, Kevin Willemart, Eric Muraille, Xavier De Bolle, Emile Van Schaftingen, Ignacio Moriyón and Jean-Jacques Letesson
- 93 Exploring the Diversity of Field Strains of *Brucella abortus* Biovar 3 Isolated in West Africa**
Moussa Sanogo, David Fretin, Eric Thys and Claude Saegerman
- 101 Prevalence, Host Range, and Comparative Genomic Analysis of Temperate *Ochrobactrum* Phages**
Claudia Jäckel, Stefan Hertwig, Holger C. Scholz, Karsten Nöckler, Jochen Reetz and Jens A. Hammerl

- 117 ***Systems Biology Analysis of Temporal In vivo Brucella melitensis and Bovine Transcriptomes Predicts host:Pathogen Protein–Protein Interactions***
Carlos A. Rossetti, Kenneth L. Drake, Sara D. Lawhon, Jairo S. Nunes, Tamara Gull, Sangeeta Khare and Leslie G. Adams
- 135 ***Modulation of Microtubule Dynamics Affects Brucella abortus Intracellular Survival, Pathogen-Containing Vacuole Maturation, and Pro-inflammatory Cytokine Production in Infected Macrophages***
Juliana Alves-Silva, Isabela P. Tavares, Erika S. Guimarães, Miriam M. Costa Franco, Barbara C. Figueiredo, João T. Marques, Gary Splitter and Sergio C. Oliveira
- 145 ***Identification of lptA, lpxE, and lpxO, Three Genes Involved in the Remodeling of Brucella Cell Envelope***
Raquel Conde-Álvarez, Leyre Palacios-Chaves, Yolanda Gil-Ramírez, Miriam Salvador-Bescós, Marina Bárcena-Varela, Beatriz Aragón-Aranda, Estrella Martínez-Gómez, Amaia Zúñiga-Ripa, María J. de Miguel, Toby Leigh Bartholomew, Sean Hanniffy, María-Jesús Grilló, Miguel Ángel Vences-Guzmán, José A. Bengoechea, Vilma Arce-Gorvel, Jean-Pierre Gorvel, Ignacio Moriyón and Maite Iriarte
- 159 ***African Lineage Brucella melitensis Isolates from Omani Livestock***
Jeffrey T. Foster, Faith M. Walker, Brandy D. Rannals, M. Hammad Hussain, Kevin P. Drees, Rebekah V. Tiller, Alex R. Hoffmaster, Abdulmajeed Al-Rawahi, Paul Keim and Muhammad Saqib
- 173 ***The Fast-Growing Brucella suis Biovar 5 Depends on Phosphoenolpyruvate Carboxykinase and Pyruvate Phosphate Dikinase but Not on Fbp and GlpX Fructose-1,6-Bisphosphatases or Isocitrate Lyase for Full Virulence in Laboratory Models***
Amaia Zúñiga-Ripa, Thibault Barbier, Leticia Lázaro-Antón, María J. de Miguel, Raquel Conde-Álvarez, Pilar M. Muñoz, Jean J. Letesson, Maite Iriarte and Ignacio Moriyón
- 186 ***Genomic Insertion of a Heterologous Acetyltransferase Generates a New Lipopolysaccharide Antigenic Structure in Brucella abortus and Brucella melitensis***
Estrella Martínez-Gómez, Jonas Stähle, Yolanda Gil-Ramírez, Amaia Zúñiga-Ripa, Mona Zaccheus, Ignacio Moriyón, Maite Iriarte, Göran Widmalm and Raquel Conde-Álvarez
- 200 ***Genotypic Expansion Within the Population Structure of Classical Brucella Species Revealed by MLVA16 Typing of 1404 Brucella Isolates From Different Animal and Geographic Origins, 1974–2006***
Gilles Vergnaud, Yolande Hauck, David Christiany, Brendan Daoud, Christine Pourcel, Isabelle Jacques, Axel Cloeckaert and Michel S. Zygmunt
- 211 ***BASI74, a Virulence-Related sRNA in Brucella abortus***
Hao Dong, Xiaowei Peng, Yufu Liu, Tonglei Wu, Xiaolei Wang, Yanyan De, Tao Han, Lin Yuan, Jiabo Ding, Chuanbin Wang and Qingmin Wu
- 220 ***Characterization of Cell Envelope Multiple Mutants of Brucella ovis and Assessment in Mice of Their Vaccine Potential***
Rebeca Singh Sidhu-Muñoz, Pilar Sancho, Axel Cloeckaert, Michel Stanislas Zygmunt, María Jesús de Miguel, Carmen Tejedor and Nieves Vizcaino

- 241** *WadD, a New Brucella Lipopolysaccharide Core Glycosyltransferase Identified by Genomic Search and Phenotypic Characterization*
Miriam Salvador-Bescós, Yolanda Gil-Ramírez, Amaia Zúñiga-Ripa, Estrella Martínez-Gómez, María J. de Miguel, Pilar M. Muñoz, Axel Cloeckeaert, Michel S. Zygmunt, Ignacio Moriyón, Maite Iriarte and Raquel Conde-Álvarez
- 255** *Comparative Genomics and in vitro Infection of Field Clonal Isolates of Brucella melitensis Biovar 3 Did Not Identify Signature of Host Adaptation*
Marion Holzapfel, Guillaume Girault, Anne Keriell, Claire Ponsart, David O'Callaghan and Virginie Mick
- 261** *Phenotypic and Molecular Characterization of Brucella microti-Like Bacteria From a Domestic Marsh Frog (Pelophylax ridibundus)*
Maryne Jaÿ, Guillaume Girault, Ludivine Perrot, Benoit Taunay, Thomas Vuilmet, Frédérique Rossignol, Pierre-Hugues Pitel, Elodie Picard, Claire Ponsart and Virginie Mick
- 268** *Transcriptomic Analysis of the Brucella melitensis Rev.1 Vaccine Strain in an Acidic Environment: Insights Into Virulence Attenuation*
Mali Salmon-Divon, Tamar Zahavi and David Kornspan
- 280** *Genomic Characterization Provides New Insights for Detailed Phage- Resistant Mechanism for Brucella abortus*
Xu-ming Li, Yao-xia Kang, Liang Lin, En-Hou Jia, Dong-Ri Piao, Hai Jiang, Cui-Cai Zhang, Jin He, Yung-Fu Chang, Xiao-Kui Guo and YongZhang Zhu
- 290** *Genetic and Phenotypic Characterization of the Etiological Agent of Canine Orchiepididymitis Smooth Brucella sp. BCCN84.3*
Caterina Guzmán-Verri, Marcela Suárez-Esquivel, Nazareth Ruíz-Villalobos, Michel S. Zygmunt, Mathieu Gonnet, Elena Campos, Eunice Viquez-Ruiz, Carlos Chacón-Díaz, Beatriz Aragón-Aranda, Raquel Conde-Álvarez, Ignacio Moriyón, José María Blasco, Pilar M. Muñoz, Kate S. Baker, Nicholas R. Thomson, Axel Cloeckeaert and Edgardo Moreno
- 303** *Genetic Diversity of Brucella melitensis in Kazakhstan in Relation to World-Wide Diversity*
Elena Shevtsova, Gilles Vergnaud, Alexandr Shevtsov, Alexandr Shustov, Kalysh Berdimuratova, Kasim Mukanov, Marat Syzdykov, Andrey Kuznetsov, Larissa Lukhnova, Uinkul Izbanova, Maxim Filipenko and Yerlan Ramankulov
- 314** *Polymorphisms in Brucella Carbonic Anhydrase II Mediate CO₂ Dependence and Fitness in vivo*
Juan M. García Lobo, Yelina Ortiz, Candela Gonzalez-Riancho, Asunción Seoane, Beatriz Arellano-Reynoso and Félix J. Sangari
- 327** *Taxonomic Organization of the Family Brucellaceae Based on a Phylogenomic Approach*
Sébastien O. Leclercq, Axel Cloeckeaert and Michel S. Zygmunt
- 339** *Omp2b Porin Alteration in the Course of Evolution of Brucella spp.*
Axel Cloeckeaert, Gilles Vergnaud and Michel S. Zygmunt
- 348** *Application of Whole Genome Sequencing and Pan-Family Multi-Locus Sequence Analysis to Characterize Relationships Within the Family Brucellaceae*
Roland T. Ashford, Jakub Muchowski, Mark Koylass, Holger C. Scholz and Adrian M. Whatmore



Editorial: Pathogenomics of the Genus *Brucella* and Beyond

Axel Cloeckaert^{1*}, Michel S. Zygmunt¹, Holger C. Scholz², Nieves Vizcaino³ and Adrian M. Whatmore⁴

¹ INRAE, Université de Tours, UMR, ISP, Nouzilly, France, ² Centre for Biological Threats and Special Pathogens, Highly Pathogenic Microorganisms (ZBS 2), Robert Koch Institute, Berlin, Germany, ³ Departamento de Microbiología y Genética, Universidad de Salamanca, Salamanca, Spain, ⁴ Department of Bacteriology, Animal and Plant Health Agency, Weybridge, United Kingdom

Keywords: *Brucellaceae*, *Brucella*, *Ochrobactrum*, genetics/genomics, diversity, evolution, cell envelope, virulence

Editorial on the Research Topic

Pathogenomics of the Genus *Brucella* and Beyond

INTRODUCTION

Brucellosis, caused by members of the genus *Brucella*, is an economically important disease in production animals causing abortion and infertility. Human brucellosis is associated with animal reservoirs and transmitted via the food chain or direct contact with diseased animals. This collection of 30 review, opinion and original research articles add to understanding of this group in fundamental areas from emerging genomic approaches and their application, through to knowledge of diverse aspects of lifestyle and pathogenicity.

BRUCELLA WITHIN THE FAMILY BRUCELLACEAE

One ongoing debate is how *Brucella* should be classified taxonomically, both internally within the genus, and in terms of wider relationships with other members of family *Brucellaceae*. This debate has continued for years, promoted by the emergence of genetically atypical *Brucella* strains distinct from classical *Brucella* species, and the discovery of many new non-*Brucella* members of the family *Brucellaceae*. Two papers in the Research Topic explore genetic relationships within *Brucellaceae* using whole genome sequencing (WGS). Leclercq et al. compared 145 *Brucellaceae* genomes with over 40 others from the wider order *Rhizobiales* to resolve phylogenetic ambiguities. They positioned the entire genus *Brucella* as a single genomic clade within current *Ochrobactrum* species diversity, while also separating *Ochrobactrum* species themselves into two distinct clades. The authors speculate that one species, *Ochrobactrum intermedium*, is undergoing genome reduction that may lead to an animal-associated pathogenic lifestyle rather than a saprophytic lifestyle. This mirrors genome reduction thought to have occurred in the evolution of the highly pathogenic *Brucella* species (Wattam et al., 2014). Ashford et al. focused in depth on the *Brucellaceae* family again showing that *Ochrobactrum*, as defined at the time of writing, is a polyphyletic group splitting into two clades. The study also recognized substantial currently unindexed diversity in *Ochrobactrum* spp. and *Pseudochrobactrum* spp. when non-type strains were included in the analysis.

OPEN ACCESS

Edited by:

Martin G. Klotz,
Washington State University,
United States

Reviewed by:

Jerod Skyberg,
University of Missouri, United States

*Correspondence:

Axel Cloeckaert
Axel.Cloeckaert@inrae.fr

Specialty section:

This article was submitted to
Infectious Diseases,
a section of the journal
Frontiers in Microbiology

Received: 26 April 2021

Accepted: 02 June 2021

Published: 08 July 2021

Citation:

Cloeckaert A, Zygmunt MS,
Scholz HC, Vizcaino N and
Whatmore AM (2021) Editorial:
Pathogenomics of the Genus *Brucella*
and Beyond.
Front. Microbiol. 12:700734.
doi: 10.3389/fmicb.2021.700734

NOVEL *BRUCELLA* SPECIES AND STRAINS

An emerging theme of recent years has been the recognition of new groups of strains expanding known ecological niches and genetic diversity of the genus *Brucella* (Moreno, 2020; Whatmore and Foster, 2021). Guzmán-Verri et al. characterized a novel *Brucella* sp. from a dog presenting with orchiepididymitis in Costa Rica. The isolate, BCCN84.3, displays smooth colonial morphology and clusters within the classical *Brucella* clade containing all the major pathogenic species. The genome contains all the genes required for virulence but is distinct from the classical rough species *Brucella canis*, associated with brucellosis in dogs. The authors fall short of assigning a taxonomic name, citing current difficulties around the ongoing debate of the *Brucella* species concept, but raising awareness of this group will allow its significance, dispersal and zoonotic potential to be explored. With similar regard to the theme of extending ecological niches Jay et al. identified an isolate similar to *Brucella microti*—a species originally described in voles but since found in wild boar, foxes and persisting in soil—in a domestic marsh frog in France. While many *Brucella inopinata*-like strains of the genetically atypical *Brucella* group have been associated with various species of tropical frogs recently (Scholz et al., 2016) this is the first finding of other species, closer to classical *Brucella* species, in amphibians.

MOLECULAR TYPING, EVOLUTION, PHYLOGEOGRAPHY

Several papers used molecular tools to explore *Brucella* diversity at the sub-species level particularly focusing on the major pathogenic species *Brucella melitensis* (ovine/caprine), *Brucella abortus* (bovine), and *Brucella suis* (porcine). The Topic included papers that used two of these approaches, multi-locus variable number of tandem repeat analysis (MLVA) and multi-locus sequence analysis (MLSA), to examine the global population structure of the genus. Whatmore et al. reported application of an extended MLSA tool to a globally and temporally diverse collection of >500 isolates, as well as the launch of an online database allowing the community to interrogate existing data and compare new profiles. Despite relatively low resolution, over 100 sequence types were identified by MLSA and new insights into the global evolutionary history of the genus were provided with evidence of the existence of lineages with restricted host or geographical ranges. Notably extensive previously undescribed genetic diversity was noted in African isolates with two early branching *B. abortus* clades appearing confined to Africa while other, later emerging, lineages have spread globally. A further important observation was the lack of congruence between biovar, long used as a crude epidemiological marker in these species, and genotype, particularly in *B. melitensis* but also to some extent in *B. abortus*. In a similar study Vergnaud et al. used MLVA to examine the population structure of a collection of >1,400 *Brucella* isolates from different animal and geographic origins isolated over three decades. In contrast to the situation

in more rapidly evolving bacteria MLVA in *Brucella* provides useful resolution even at global/taxonomic levels as well as for local epidemiology, a point confirmed as authors highlighted the congruence of MLVA groupings with those reported in the above MLSA study. Once again work highlighted a lack of congruence between biovar and genotype and suggested that, particularly for *B. melitensis*, the biovar concept is of limited value and genome-based methods may be better placed to answer questions regarding epidemiology and tracking epidemic strains in the future.

In the topic MLVA was also applied in local situations to explore transmission pathways. Brucellosis is a serious public health problem in China (Jiang et al., 2020). Liu et al. characterized isolates of *B. melitensis* from Ulanqab using MLVA to suggest lack of control of animal movements or movement of contaminated food products between regions. In a larger study in Kazakhstan Shevtsova et al. examined >1,300 human derived isolates of *B. melitensis* showing that, as in the Liu et al. study above, isolates cluster within the previously identified “Eastern Mediterranean” group of *B. melitensis*. Both studies highlight once again the lack of any clear relationship between biovar and genotype in *B. melitensis*. Much less is known about *Brucella* diversity in Africa—Sanogo et al. reviewed MLVA types of *B. abortus* biovar 3 isolates in West Africa and highlighted the need for more studies to understand the epidemiology of brucellosis in this region. Foster et al. used MLVA, along with SNP assays, to identify a lineage of *B. melitensis* circulating in multiple animal species in Oman distinct from most other Middle Eastern isolates associated with endemic disease. The lineage appears most closely related to isolates from North Africa suggesting an African origin for some *B. melitensis* isolates in Oman likely through livestock trade. This study once again hinted at substantial under-sampled *Brucella* genetic diversity in Africa.

Cloekaert et al. examined genes encoding Omp2 porins. These represent some of the most genetically diverse *Brucella* genes and were historically used as typing tools. Utilizing WGS data the authors propose an evolutionary pathway from two ancestral genes in genetically atypical *Brucella* through progressive genetic loss in *omp2b* on the path to the classic pathogenic species. Changes appear to reflect extensive recombination events with *omp2a* and were correlated to increasing sugar permeability of the porin that the authors speculate might be related to environmental adaptation to survive conditions on the pathway to the current status as intracellular pathogens.

Comparative genomics was applied by Holzapfel et al. to examine *B. melitensis* isolates from an outbreak infecting different hosts (human, bovine, and ovine) in order to identify evidence of host adaptation. Only a single SNP, and no genome rearrangements at all, were seen although the possibility of differences in expression in different hosts was not explored. Another important comparative genomic study provided a contrasting picture of genomic stability and highlights a common concern in microbiology—variability between reference strains assumed to represent a single common entity. *B. abortus* 2308 is a reference strain often used in virulence studies or as a

challenge strain in vaccine trials. Suárez-Esquivel et al. compared the genomes of *B. abortus* 2308 stocks from three laboratories and revealed significant differences, particularly in indels related to insertional elements, suggesting that variability accumulated due to transposition events. The study challenges the idea that reference strains are non-changing entities in time and space and may question the validity of comparison between studies using the “same” reference strain.

PHAGE BIOLOGY AND TYPING

Three papers focus on phage or phage resistance. Lytic phages have been used historically to type *Brucella* strains and Hammerl et al. sequenced known reference phage and, analogous to the situation described above, the same reference phage from different laboratories were not always genetically identical and may display differences in host range. The same study also analyzed 22 non-reference brucellaphages suggesting some new candidates that may be useful in diagnostics. Jäckel et al. also explored phage in the related *Ochrobactrum* group, showing for the first time that active prophages are common in this group. Li et al. examined a smooth phage resistant *B. abortus* strain isolated in China and compared it with phage sensitive strains. Although they failed to categorically identify a mechanism of phage resistance a number of indels and point mutations differentiating the strains were identified.

BRUCELLA CELL ENVELOPE AND SURFACE STRUCTURES

Three papers focus on the role and properties of lipopolysaccharide (LPS) and lipids of the *Brucella* cell envelope. *Brucella* LPS plays a major role in virulence impairing recognition by the innate immune system and delaying immune responses (Roop et al., 2021). The LPS core is a branched structure involved in resistance to complement and polycationic peptides. Mutants in glycosyltransferases required for the synthesis of the lateral branch not linked to the O-polysaccharide (O-PS) are attenuated, and have been proposed as vaccine candidates. The chemical structure of the *Brucella* LPS core suggests that, in addition to the already identified WadB and WadC glycosyltransferases, others could be implicated in the synthesis of this lateral branch. By screening *B. abortus* LPS mutants Salvador-Bescós et al. identified a new glycosyltransferase gene named *wadD*. A *wadD* mutant lost reactivity against antibodies that recognize the core section while keeping an intact O-PS. WadD glycosyltransferase may thus be involved in the addition of one or more sugars to the core lateral branch. Further experiments indicated its role in resistance to components of the innate immune system and in chronic stages of infection. These results corroborate and extend studies indicating that the *Brucella* LPS core is a branched structure that constitutes a steric impairment preventing elements of the innate immune system protecting against *Brucella*.

Conde-Álvarez et al. investigated *Brucella* homologs of *lptA*, *lpxE*, and *lpxO*, three genes that in some pathogens encode

enzymes involved in masking the LPS pathogen-associated molecular pattern (PAMP), to avoid rapid recognition by innate immunity. They encode putative enzymes involved in lipid A or other lipids modification. In this study, despite their participation in cationic peptide resistance of *B. melitensis*, none of the *B. melitensis* mutants for the respective genes were attenuated in dendritic cells or mice, which suggest they are not significantly involved in alteration of the PAMP properties of *Brucella* LPS and free-lipids, and were not positively selected during the adaptation to intracellular life.

Smooth (S) LPS (S-LPS) is a major virulence factor in smooth *Brucella* species carrying an O-PS on the LPS core. The O-PS consists of an *N*-formyl-perosamine homopolymer and constitutes the major antigen in serodiagnostic tests. Martínez-Gómez et al. report that the *Brucella* O-PS can be structurally and antigenically modified using *wbdR*, the acetyltransferase gene involved in *N*-acetyl-perosamine synthesis in *Escherichia coli* O157:H7. Introducing *wbdR* into the *Brucella* genome resulted in loss of the main *Brucella* O-PS immunodominant epitopes. *wbdR* constructs produced chronic infections in mice and triggered antibodies to new immunogenic epitope(s) that can be differentiated from those evoked by the wild-type strain in S-LPS ELISAs. These results raise the possibility of developing vaccines that are both antigenically tagged, and lack diagnostic epitopes of virulent field strains, thereby solving the diagnostic interference created by current *Brucella* vaccines.

A fourth paper focuses on the cell envelope of *Brucella ovis*, a non-zoonotic species lacking a specific vaccine. *B. ovis* presents a narrow host range (rams), a unique biology relative to other *Brucella* species, and important distinct surface properties. To develop a specific vaccine, Sidhu-Muñoz et al. investigated multiple mutants for nine cell-envelope-related genes. Among several combinations of mutations investigated in a mouse virulence model, a *B. ovis* mutant deleted for three genes (*omp10*, *ugpB*, and *omp31*) appeared an interesting vaccine candidate. It showed similar infectious behavior to the wild-type strain up until week 3 post-infection, but was then totally cleared from the spleen. In mice protection assays, in comparison to the live attenuated *B. melitensis* Rev1 reference vaccine, the triple mutant induced limited splenomegaly, a significantly higher antibody response against whole *B. ovis* cells, and better protection against challenge with a virulent *B. ovis* strain. As this vaccine candidate lacks *Omp31*, a highly immunogenic *B. ovis* protein, differentiation between infected and vaccinated animals may also be possible.

INTRACELLULAR LIFESTYLE

Six papers in the topic focus on factors important in the intracellular lifestyle of *Brucella*. Rossetti et al. analyzed the *in vivo* temporal transcriptional profile of *B. melitensis* during the initial 4 h interaction with cattle. It revealed that *in vivo* *Brucella* sense and actively regulate their metabolism through transition to an intracellular lifestyle. Other *Brucella* pathways involved in virulence, such as ABC transporters and T4SS, were

repressed suggesting a silencing strategy to avoid stimulation of the innate immune response very early in the infection process. It supports the idea that *Brucella* employ a stealthy strategy at the onset of infection. Further, using other approaches, unanticipated interactions were identified suggestive of new virulence factors and mechanisms responsible for evasion of the immune response.

Live attenuated *B. melitensis* Rev.1 vaccine is widely used to control small ruminant brucellosis. Following uptake by the host cell, *Brucella* replicate inside a membrane-bound compartment whose acidification is essential for pathogen survival. By comparative transcriptome analysis of Rev.1 and virulent strain 16M, Salmon-Divon et al. identified 403 genes responding differently to acidic conditions in the two strains, consisting of genes involved in crucial cellular processes, including metabolic, biosynthetic, and transport processes. A number of genes downregulated in Rev.1 under acidic conditions were identified, possibly explaining the attenuated virulence of Rev.1.

The microtubule (MT) cytoskeleton regulates several cellular processes related to the host immune system. Alves Silva et al. used nocodazole to induce MTs depolymerization and paclitaxel or recombinant (r) TIR (Toll/interleukin-1 receptor) domain containing protein (TcPB) to induce MT stabilization in bone marrow-derived macrophages infected with *B. abortus*. In this infection model, intracellular trafficking and maturation of *Brucella*-containing vesicles (BCVs) appeared affected by partial destabilization or stabilization of the MTs network. Complementary macrophage infection experiments indicated that modulation of MTs affects crucial steps of *B. abortus* pathogenesis, including BCV maturation, intracellular survival and IL-12 secretion in infected macrophages.

Some *Brucella* isolates require increased CO₂ for growth, especially on initial isolation. By comparing differences in gene content among different CO₂-dependent and CO₂-independent *Brucella* strains, Garcia Lobo et al. confirmed that carbonic anhydrase (CA) II is the enzyme responsible for this phenotype. *Brucella* species contain two CAs of the β family, CA I and CA II. Genetic polymorphisms were identified for both of them in different isolates, but only those putatively affecting the activity of CA II correlated with the CO₂ requirement of the corresponding isolate. CO₂-independent mutants arise easily *in vitro*, and carry compensatory mutations that produce a functional full-length CA II. Unlike *in vitro* growth, growth *in vivo* in a mouse model of infection provided a significant advantage to the CO₂-dependent strain. This could explain why some *Brucella* isolates are CO₂-dependent in primary isolation.

Several genes associated with intracellular trafficking and multiplication have been identified in *Brucella* spp. However, the sophisticated post-transcriptional regulation and coordination of gene expression that enable adaptation to changes in environment and evasion of host cell defenses are not fully understood. Bacteria small RNAs (sRNAs) play a significant role in post-transcriptional regulation in a number of bacteria. Dong et al. identified several sRNAs in *Brucella* spp., and found that over-expression of a sRNA, termed BASI74, led to alteration in virulence of *Brucella* in a macrophage infection model. The expression of BASI74 increased when *B. abortus* was grown in acidic media. Four genes were identified as targets of BASI74.

Among them, BABI1154, was predicted to encode a cytosine-N4-specific DNA methyltransferase, which protects cellular DNA from the restriction endonuclease in *Brucella*. BASI74 thus plays an important role in *Brucella* survival in a macrophage infection model, speculatively by its connection with stress responses or impact on restriction-modification systems.

The best-characterized brucellae infect livestock, behaving as stealthy facultative intracellular parasites. This stealthiness depends on envelope molecules with reduced PAMPs, as revealed by low lethality and the ability to persist in mice of these bacteria. Infected cells are often engorged with brucellae without signs of distress, suggesting that stealthiness could also reflect an adaptation of the parasite metabolism to use local nutrients without harming the cell. Zúñiga-Ripa et al. compared key metabolic abilities of virulent *B. abortus* 2308 and *B. suis* strain 513, representative of the ancestral biovar 5 found in wild rodents. Strain 513 used a larger number of C substrates and showed faster growth *in vitro*, two features similar to those of *B. microti*, a species phylogenomically close to strain 513 infecting voles. However, whereas *B. microti* shows enhanced lethality and reduced persistence in mice, strain 513 was similar to *B. abortus* 2308 in this regard. Further analyses showed similarities and discrepancies in metabolic pathways of the strains studied that may reflect a progressive adaptation of brucellae to intracellular growth.

IMMUNE AND CELLULAR RESPONSES

Establishment of a Th1-mediated immune response characterized by the production of IL-12 and IFN γ is essential to control brucellosis. Leukotrienes derived from arachidonic acid (AA) metabolism negatively regulate a protective Th1 immune response against bacterial infections. Gagnaire et al. demonstrated that *B. abortus* strongly stimulates the prostaglandin (PG) pathway in dendritic cells (DC). They also showed induction of AA production by infected cells correlated with expression of *Ptgs2*, encoding the downstream cyclooxygenase-2 (COX-2) enzyme in infected DC. By comparing infection routes (oral, intradermal, intranasal, and conjunctival), the intradermal inoculation route was identified as the more potent in inducing *Ptgs2* expression but also in inducing a local inflammatory response in the draining cervical lymph nodes (CLN). NS-398, a specific inhibitor of COX-2 enzymatic activity decreased *B. melitensis* burden in the CLN after intradermal infection. This effect was accompanied by a decrease of IL-10 and a concomitant increase of *Ifng* expression. Altogether, these results suggest *Brucella* has evolved to take advantage of the PG pathway in the harsh environment of the CLN to persist and to subvert immune responses. This work also proposed that novel strategies to control brucellosis may include the use of COX-2 inhibitors.

Giambartolomei et al. reviewed mechanisms of osteoarticular brucellosis, a common presentation of human disease. The three commonest forms of osteoarticular involvement are sacroiliitis, spondylitis, and peripheral arthritis. *B. abortus* induces bone damage through diverse mechanisms where TNF- α and the

receptor activator of nuclear factor kappa-B ligand, the natural modulator of bone homeostasis, are involved. These processes are driven by inflammatory cells. In addition, *B. abortus* has a direct effect on osteoarticular cells and tilts homeostatic bone remodeling. These bacteria inhibit bone matrix deposition by osteoblasts, and modify the phenotype of these cells to produce matrix metalloproteinases and cytokine secretion, contributing to bone matrix degradation. *B. abortus* also affects osteoclasts by inducing osteoclastogenesis and osteoclast activation; thus, increasing mineral and organic bone matrix resorption, contributing to bone damage. Pathology induced by *Brucella* also involves joint tissue and analysis of *B. abortus*-infected synoviocytes indicated bacteria also replicate in their reticulum indicating use of this cell type for intracellular replication during the osteoarticular localization of the disease.

GENITAL TROPISM

Erythritol is the preferential carbon source for most brucellae. Since this polyol is abundant in genital organs of ruminants and swine, it is accepted that erythritol accounts, at least partially, for the characteristic genital tropism of brucellae. Nevertheless, proof of erythritol availability and essentiality during *Brucella* intracellular multiplication has remained elusive. A study by Barbier et al., using wild-type *B. abortus* and erythritol utilization mutants, showed that erythritol was available, but not required, for *B. abortus* multiplication in bovine trophoblasts. Mice and

humans have been considered to lack erythritol but this study showed it is available, but not required, for multiplication in human and murine trophoblastic and macrophage-like cells, and in mouse spleen and conceptus. These results led to the hypothesis that there may be erythritol in tissues of mammals other than ungulates, with evidence for the involvement of the host aldose reductase, an enzyme that can catalyze the synthesis of polyols including erythritol.

In a linked opinion article Letesson et al. noted the coincidence between the possible presence of lactate, glutamate, and glycerol in the placenta and male genital organs and fluids, favored habitats of brucellae, and nutritional requirements of *Brucella* identified in classical studies performed many decades ago (Gerhardt et al., 1950).

CONCLUSION

In conclusion, this Research Topic provides a comprehensive and up-to-date summary of multiple aspects of *Brucella* pathogens, from their taxonomic position within the family *Brucellaceae* to their main pathogenic mechanisms and induced immune responses.

AUTHOR CONTRIBUTIONS

All authors listed have made a substantial, direct and intellectual contribution to the work, and approved it for publication.

REFERENCES

- Gerhardt, P., Tucker, L. A., and Wilson, J. B. (1950). The nutrition of *Brucellae*: utilization of single amino acids for growth. *J. Bacteriol.* 59, 777–782.
- Jiang, H., O'Callaghan, D., and Ding, J. B. (2020). Brucellosis in China: history, progress and challenge. *Infect. Dis. Poverty* 9, 55. doi: 10.1186/s40249-020-00673-8
- Moreno, E. (2020). The one hundred year journey of the genus *Brucella* (Mayer and Shaw 1920). *FEMS Microbiol. Rev.* 45:fuaa045. doi: 10.1093/femsre/fuaa045
- Roop, R. M., Barton, I. S., Hoppersberger, D., and Martin, D. W. (2021). Uncovering the hidden credentials of *Brucella* virulence. *Microbiol. Mol. Biol. Rev.* 85, e00021–e00019. doi: 10.1128/MMBR.00021-19
- Scholz, H. C., Mühldorfer, K., Shilton, C., Benedict, S., Whatmore, A. M., Blom, J., et al. (2016). The change of a medically important genus: worldwide occurrence of genetically diverse novel *Brucella* species in exotic frogs. *PLoS ONE* 11:e0168872. doi: 10.1371/journal.pone.0168872
- Wattam, A. R., Foster, J. T., Mane, S. P., Beckstrom-Sternberg, S. M., Beckstrom-Sternberg, J. M., Dickerman, A. W., et al. (2014). Comparative phylogenomics and evolution of the *Brucellae* reveal a path to virulence. *J. Bacteriol.* 196, 920–930. doi: 10.1128/JB.01091-13
- Whatmore, A. M., and Foster, J. T. (2021). Emerging diversity and ongoing expansion of the genus *Brucella*. *Infect. Genet. Evol.* 92:104865. doi: 10.1016/j.meegid.2021.104865

Conflict of Interest: The authors declare that the research was conducted in the absence of any commercial or financial relationships that could be construed as a potential conflict of interest.

Copyright © 2021 Cloekaert, Zygmunt, Scholz, Vizcaino and Whatmore. This is an open-access article distributed under the terms of the Creative Commons Attribution License (CC BY). The use, distribution or reproduction in other forums is permitted, provided the original author(s) and the copyright owner(s) are credited and that the original publication in this journal is cited, in accordance with accepted academic practice. No use, distribution or reproduction is permitted which does not comply with these terms.



Brucella abortus Strain 2308 Wisconsin Genome: Importance of the Definition of Reference Strains

Marcela Suárez-Esquivel¹, Nazareth Ruiz-Villalobos¹, Amanda Castillo-Zeledón¹, César Jiménez-Rojas¹, R. Martin Roop II², Diego J. Comerci³, Elías Barquero-Calvo⁴, Carlos Chacón-Díaz^{1,4}, Clayton C. Caswell⁵, Kate S. Baker^{6,7}, Esteban Chaves-Olarte⁴, Nicholas R. Thomson^{6,8}, Edgardo Moreno^{1,9}, Jean J. Letesson¹⁰, Xavier De Bolle¹⁰ and Caterina Guzmán-Verri^{1,4*}

OPEN ACCESS

Edited by:

Axel Cloeckaert,
French National Institute
for Agricultural Research (INRA),
France

Reviewed by:

Suzana P. Salcedo,
Molecular Microbiology and Structural
Biochemistry, France
Renee M. Tsois,
University of California, Davis, USA
Thomas A. Ficht,
Texas A&M University, USA

*Correspondence:

Caterina Guzmán-Verri
catguz@una.cr

Specialty section:

This article was submitted to
Infectious Diseases,
a section of the journal
Frontiers in Microbiology

Received: 24 July 2016

Accepted: 16 September 2016

Published: 29 September 2016

Citation:

Suárez-Esquivel M, Ruiz-Villalobos N,
Castillo-Zeledón A, Jiménez-Rojas C,
Roop II RM, Comerci DJ,
Barquero-Calvo E, Chacón-Díaz C,
Caswell CC, Baker KS,
Chaves-Olarte E, Thomson NR,
Moreno E, Letesson JJ, De Bolle X
and Guzmán-Verri C (2016) *Brucella*
abortus Strain 2308 Wisconsin
Genome: Importance of the Definition
of Reference Strains
Front. Microbiol. 7:1557.
doi: 10.3389/fmicb.2016.01557

¹ Programa de Investigación en Enfermedades Tropicales, Escuela de Medicina Veterinaria, Universidad Nacional de Costa Rica, Heredia, Costa Rica, ² Department of Microbiology and Immunology, Brody School of Medicine, East Carolina University, Greenville, NC, USA, ³ Instituto de Investigaciones Biotecnológicas "Dr. Rodolfo A. Ugalde", Instituto Tecnológico de Chascomús, Universidad Nacional de San Martín, Consejo Nacional de Investigaciones Científicas y Técnicas, Comisión Nacional de Energía Atómica, Grupo Pecuario, Centro Atómico Ezeiza, Buenos Aires, Argentina, ⁴ Centro de Investigación en Enfermedades Tropicales, Facultad de Microbiología, Universidad de Costa Rica, San José, Costa Rica, ⁵ Center for Molecular Medicine and Infectious Diseases, Department of Biomedical Sciences and Pathobiology, Virginia–Maryland College of Veterinary Medicine, Virginia Tech, Blacksburg, VA, USA, ⁶ Wellcome Trust Sanger Institute, Hinxton, UK, ⁷ Department of Functional and Comparative Genomics, Institute of Integrative Biology, University of Liverpool, Liverpool, UK, ⁸ The London School of Hygiene and Tropical Medicine, London, UK, ⁹ Instituto Clodomiro Picado, Universidad de Costa Rica, San José, Costa Rica, ¹⁰ Unité de Recherche en Biologie des Microorganismes, Université de Namur, Namur, Belgium

Brucellosis is a bacterial infectious disease affecting a wide range of mammals and a neglected zoonosis caused by species of the genetically homogenous genus *Brucella*. As in most studies on bacterial diseases, research in brucellosis is carried out by using reference strains as canonical models to understand the mechanisms underlying host pathogen interactions. We performed whole genome sequencing analysis of the reference strain *B. abortus* 2308 routinely used in our laboratory, including manual curated annotation accessible as an editable version through a link at <https://en.wikipedia.org/wiki/Brucella#Genomics>. Comparison of this genome with two publically available 2308 genomes showed significant differences, particularly indels related to insertional elements, suggesting variability related to the transposition of these elements within the same strain. Considering the outcome of high resolution genomic techniques in the bacteriology field, the conventional concept of strain definition needs to be revised.

Keywords: *Brucella*, *Brucella abortus*, reference genome, reference strain, WGS

INTRODUCTION

Brucella is a bacterial genus responsible for brucellosis, a disease in animals causing infertility, pre-term birth, or abortion (Moreno and Moriyón, 2006). It is also one of the most worldwide spread bacterial zoonosis, not only causing human suffering but also representing a significant economic burden on animal industries. Because this severe and debilitating disease has not been adequately addressed at some national and international level, it is considered by WHO (2014) as one of the “forgotten neglected zoonosis,” constituting a major burden for poor rural communities.

The main etiological agent of cattle brucellosis is *B. abortus* associated with abortion, infertility, reproductive failure, and decreased milk production (Harmon et al., 1989; Xavier et al., 2009; Neta et al., 2010). Humans usually become infected when in contact with infected animals or their derived products, particularly non-pasteurized dairy products (Spink, 1956). Several *B. abortus* reference strains have been described and used as models to understand *Brucella* pathogenesis or as challenge strains for vaccine testing (Meyer and Morgan, 1973; Chain et al., 2005; Halling et al., 2005; Singh et al., 2015).

Genetic drift causing loss of virulence or antigenic properties has been reported in several *Brucella* vaccines strains (Bosserey, 1991; Mukherjee et al., 2005; Jacob et al., 2006; Miranda et al., 2013), but very little is known on the genetic stability of reference strains.

Brucella abortus strain 2308 was originally described as a highly virulent strain recovered in 1940 from an aborted fetus of a cow which had been in contact with cattle experimentally infected with a mixture of *B. abortus* cultures (Jones et al., 1965). Since then it has been widely used as a reference and challenge strain within the brucellosis research community (Trant et al., 2010; Dabral et al., 2014; Miranda et al., 2015; Olsen et al., 2015; Truong et al., 2016; Zhu et al., 2016). Whole Genome Sequencing (WGS) of this strain was first carried out by Chain et al. (2005), who found conservation in chromosome synteny with other sequenced *B. abortus* genomes and also some differences that were suggested to be strain specific. In 2009, the results of a WGS analysis from a strain named *B. abortus* 2308A were publically available under accession number GCA_000182625.1. No additional information regarding the isolates used in these two WGS projects was provided.

We performed WGS, functional annotation and manual curation of reference strain *B. abortus* 2308 kept at the Tropical Disease Research Program, Veterinary School, National University in Costa Rica and compared it with these two published *B. abortus* 2308 genomes. Significant differences were found among the genomes, challenging the idea of reference strains as a non-changing entities in time and among laboratories. The use and communication of standardized quality control and experimental design protocols could help interpretation and follow up of reported results.

MATERIALS AND METHODS

Strain Description

All procedures involving live *B. abortus* were carried out according to the “Reglamento de Bioseguridad de la CCSS 39975-0,” year 2012, after the “Decreto Ejecutivo #30965-S,” year 2002 and research protocol approved by SIA 0434-14 from the National University, Costa Rica. A vial of *B. abortus* strain 2308 was obtained at the Tropical Disease Research Program, Veterinary School, National University, Costa Rica, from Dr. Ignacio Moriyón at University of Navarra, Pamplona, Spain. He received it in 1983 from Dr. Lois M. Jones from the laboratory of Prof. David T. Berman at University of Wisconsin Madison as a lyophilized vial coming originally from the National

Animal Disease Center at Ames, IA, USA. From this, bacteria were expanded in trypticase soy agar, assayed biochemically to assure properties (Alton et al., 1988) and stored at -70°C in 20% glycerol. For master seed preparation, recommendations for identification, maintenance and to rule out attenuation were followed as suggested (Alton et al., 1988). Therefore, before master seed storage, a passage in mice was performed using 10^5CFU from an overnight culture in 100 μL PBS for intraperitoneal inoculation. Bacteria were recovered from the spleen after 3 weeks after plating in trypticase soy agar and a single colony expanded in trypticase soy broth overnight (Bosserey, 1991; Grilló et al., 2012). Trypticase soy broth aliquots were prepared with 20% glycerol and stored at -70°C as a master seed. Protocols for experimentation with mice were revised and approved by the Comité Institucional para el Cuido y Uso de los Animales of the Universidad de Costa Rica (CICUA-47-12) and were in agreement with the corresponding law, Ley de Bienestar de los Animales, of Costa Rica (law 7451 on animal welfare). Mice were housed in the animal building of the Veterinary School, Universidad Nacional, Costa Rica. Animals were kept in cages with water and food *ad libitum* under biosafety containment conditions previous to and during the experiment.

Finally, a master seed aliquot was grown in tryptic soy agar for phenotypical and biochemical characterization (Alton et al., 1988), MLVA-16 (Le Flèche et al., 2006), Bruce-ladder PCR (López-Goñi et al., 2011) and infection of Raw macrophages as described (Palacios-Chaves et al., 2011). Aliquots were used only once and discharged.

Due to its origin, this strain is from herein referred as *B. abortus* strain 2308 Wisconsin (*B. abortus* 2308W).

WGS, Assembly and Annotation

A bacteriological loop sample from a frozen master seed aliquot of *B. abortus* 2308W was inoculated in trypticase soy broth and grown overnight. DNA was extracted using the Promega Wizard Genomic DNA Purification kit, and stored at -70°C until used.

WGS was performed at the Wellcome Trust Sanger Institute on Illumina platforms according to *in house* protocols (Quail et al., 2009, 2012), resulting in 4 396 650 reads, depth of coverage: 128.76 ± 34.84 , an error rate of 0.005 and a duplication rate of 0.0017.

The SNPs discovery performed in this study used raw reads with a base quality score of Q33. Sequence variation was called by BCFtools¹ if the depth of coverage is greater than 5, the variant is present in at least 75% of reads at that position, the variant is present on both strands, and the mapping quality is greater than 30. Each SNP was manually investigated using BamView (Carver et al., 2010).

For WGS assembly and alignment, sequencing reads were *de novo* assembled using Velvet Optimiser (Zerbino and Birney, 2008; Page et al., 2016) and 18 contigs (N50 = 294779) were ordered using Abacas (Assefa et al., 2009) against *B. abortus* 9–941 (accession numbers NC_006932 and NC_006933). To detect mis-assemblies, raw data were mapped back against the

¹<https://samtools.github.io/bcftools/bcftools.html>

2308W genome assembly using SMALT 0.5.8² which resulted in 99.89% mapping. Two more assembly controls were performed by mapping the 2308W raw reads against 2308 reference genome (NC_007618 and NC_007624) or 9–941 reference genome. This resulted in 98.88 and 98.77% mapping, respectively.

Annotation was automatically transferred from a previously WGS obtained from *B. abortus* 2308 (NC_007618 and NC_007624). In order to facilitate the 2308W annotation review, a BLAST comparison (Altschul et al., 1997) between 2308W chromosomes, *B. abortus* 9–941, *B. melitensis* 16M (accession NC_003317.1 and NC_003318.1) and *B. suis* (NC_004310.3 and NC_004311.2) was performed. Visualizations were done with Artemis and BLAST comparisons with the Artemis Comparison Tool (Rutherford et al., 2000). Each coding region (CDS) was checked manually and curation was performed according to available experimental information and literature search on *B. abortus* 2308. Major findings were summarized in **Supplementary Table S1** and a link to an editable version is available at <https://en.wikipedia.org/wiki/Brucella#Genomics>.

Sequencing info has been deposited at the European Nucleotide Archive (ENA)³ under the accession code ERS568782.

Genome Comparison among *B. abortus* 2308 Strains

A BLAST comparison using the genome here described, *B. abortus* 2308W (assembly accession ERS568782) and two previously published genomes: *B. abortus* 2308 (Chain et al., 2005; accession number NC_007618 and NC_007624); and

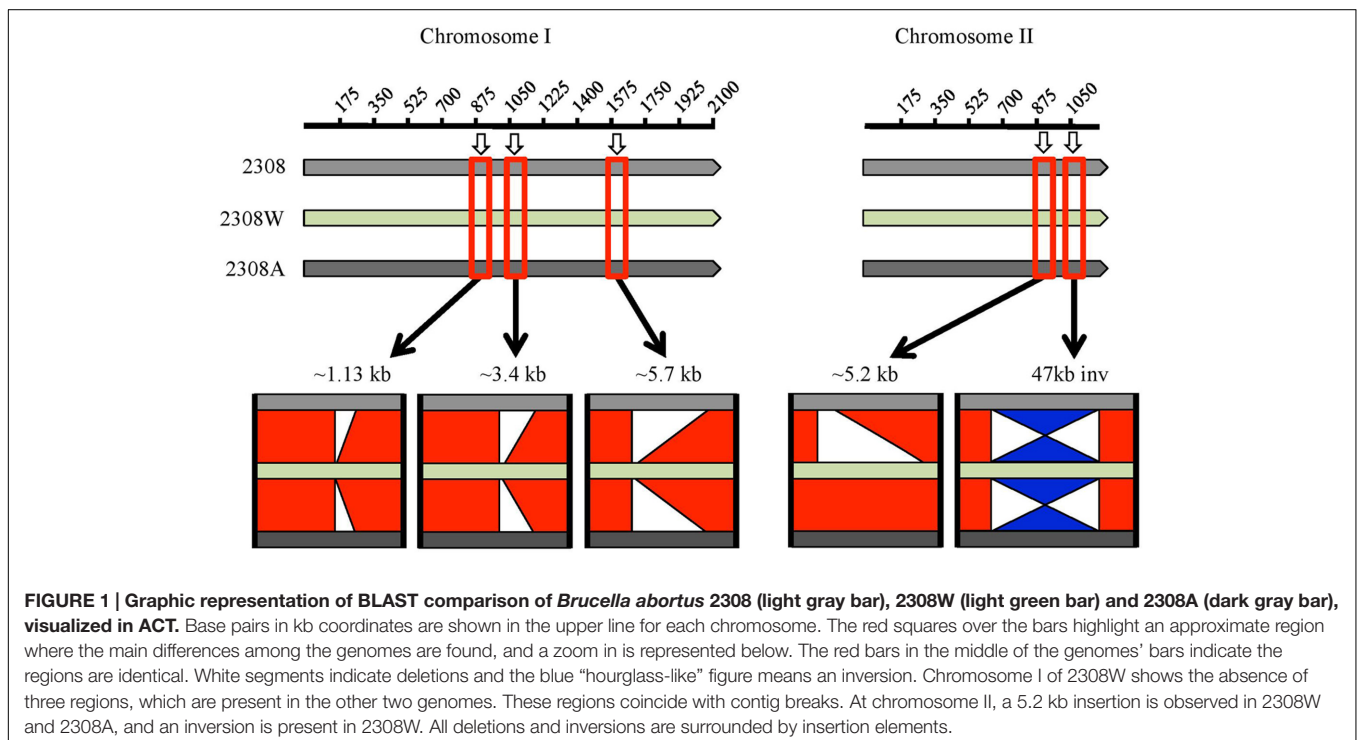
B. abortus str. 2308A (assembly accession GCA_000182625.1; contigs accession numbers ACOR01000001-ACOR01000009) was performed. Visualizations were done with Artemis and ACT (Rutherford et al., 2000).

As the 2308A genome is reported as contigs, raw sequencing data were downloaded and *de novo* assembly using Velvet Optimizer (Zerbino and Birney, 2008) was performed followed by ordering with Abacas (Assefa et al., 2009), using *B. abortus* 9–941 genome as reference as per the analysis of our strain.

RESULTS AND DISCUSSION

For comparative analysis, we performed WGS analysis of the 2308 strain that has been used in our laboratory and referred here as *B. abortus* 2308W, to distinguish its genome from previously reported ones (2308 and 2308A). The genome consists of two chromosomes, chromosome I is 2.10 kb in size and chromosome II is 1.16 kb. Automated annotation and manual curation were performed and summarized in **Supplementary Table S1**. An editable spreadsheet was also created in order to facilitate updates in the annotation or additional relevant comments (e.g., virulence, function, mutants availability) and is available through a link at <https://en.wikipedia.org/wiki/Brucella#Genomics>.

A BLAST comparison of this genome with those two previously reported showed major differences summarized in **Figure 1** and detailed in **Supplementary Table S2**. Three major deletions in chromosome I in *B. abortus* 2308W were detected relative to *B. abortus* 2308 and 2308A of 1.13, 3.4, and 5.7 kb. It is important to point out that these three deletions are located at the end of contigs and surrounded by repetitive sequences so may



represent incompletely assembled contiguous sequences, rather than genuine deletions. Regions containing repetitive sequences are proven difficult to assemble and sequence, regardless the sequencing technology used (Bidmos and Bayliss, 2014). The 1.13 kb deletion contains the 2308 loci BAB1_0934 to BAB1_0937 associated to IS711 elements and transposases. The 3.4 kb deletion includes loci BAB1_1102–BAB1_1104; the first two CDSs are predicted proteins of unknown function and the third one is predicted to be a site-specific recombinase, DNA invertase. These loci fall within a larger 8.1 kb genomic island named GI-1, encoding mainly predicted proteins and phage-related proteins (Rajashekara et al., 2004). Five CDSs are part of the 5.7 kb region absent in chromosome I of 2308W (BAB1_2221–BAB1_2225). They encode tRNAs and rRNAs genes with copies elsewhere in the genome (Supplementary Table S2). These copies are represented by a higher number of reads as compared with average for the rest of the CDS (9700 versus 3200 reads), suggesting that contig breaks are caused by mis-assembly of the repeated copies of the tRNA and rRNA genes during the assembly.

An insertion of a 5.2 kb segment in chromosome II was observed in 2308W and 2308A, relative to 2308 (Chain et al., 2005). This region displayed even read coverage as compared to the rest of the 2308W genome. It includes four genes encoding sugar binding proteins, proteins involved in nitrogen metabolism as well as the transcriptional activator FtrB involved in regulation of carbon and amino acid metabolism (BAW_20862–BAW_20865). The adjacent loci (BAW_20861 and BAW_20866) contain sequence partial deletions in 2308 (corresponding to BAB2_0903) or 2308W (corresponding to BAB2_0904). Also evident is an inversion of the 47 kb GI-5 (Rajashekara et al., 2004) in 2308W as compared to 2308 and 2308A that results in deletion of BAB2_1075, encoding an IS3 transposase. Notably, insertion elements were detected alongside all of the indel regions. These observations show not only how unstable the *B. abortus* 2308 genome is but also that chromosomal rearrangements are a source of genetic variability, probably as consequence of IS mediated transposition events (Tsoktouridis et al., 2003; Ocampo-Sosa and García-Lobo, 2008; Mancilla et al., 2012).

According to the National Collection of Cultures (NCTC) in England, reference strains are “stipulated in internationally recognized standard methods as definitive control strains for various microbiological testing procedures⁴.” The fact that *Brucella* is regarded as a genetically homogeneous genus, but significant differences are present in *B. abortus* 2308 stored in different laboratories raises a broader question and challenges the concept of “reference strain.” In the case of *B. abortus* 2308 this is even more relevant, since this strain has been regarded as the canonical challenge organism in vaccine trials where different results about its survival in mice models are reported (Montaraz and Winter, 1986; Ko et al., 2002; Yang et al., 2006).

⁴ <https://www.phe-culturecollections.org.uk/collections/nctc.aspx>

There are probably several reasons for these contrasting results. Some, such as differences due to strain handling can be accounted by using standardized quality control and experimental design protocols. Probably more difficult to control are genome changes. Reference strains are usually isolates obtained from clinical cases used in research labs as infection models, and as such, are subject of genetic modification according to the environment (Hopkins et al., 1981; Turse et al., 2011). A detailed description of the strain used, including a publically available WGS, as well as growth, propagation and maintenance conditions included with reported results could help readers to better assess the reported observations.

AUTHOR CONTRIBUTIONS

MS-E performed bioinformatics analysis, manual curation, and prepared tables and figures. NR-V performed molecular typing and manual curation. AC-Z, CJ-R, RR, and DC performed manual curation. CC provided data for manual curation. EB-C and CC-D performed biochemical typing and provided data for manual curation. KB performed bioinformatics analysis and edited the manuscript. EC-O and EM analyzed data. NT performed bioinformatics analysis and manual curation. XD and JL performed manual curation, organized, and analyzed data. CG-V designed the study, analyzed data, performed manual curation, and wrote the manuscript. All authors edited the final version of the manuscript.

FUNDING

This study was funded by Fondos del Sistema del Consejo Nacional de Rectores (FEES-CONARE) Costa Rica, and Wellcome Trust. NR-V, AC-Z, and CJ-R were partially sponsored by University of Costa Rica scholarships. KB is in receipt of a WT clinical research fellowship (106690/A/14/Z). KB and NT were funded by the Wellcome Trust, grant number 098051

ACKNOWLEDGMENTS

We are grateful to Daphne Garita for technical assistance. We thank Dr. Andrew Page and Dr. Gordon Dougan for helpful discussions.

SUPPLEMENTARY MATERIAL

The Supplementary Material for this article can be found online at: <http://journal.frontiersin.org/article/10.3389/fmicb.2016.01557>

TABLE S1 | 2308W annotation.

TABLE S2 | Genomic differences among 2308W, 2308 and 2308A.

REFERENCES

- Alton, G. G., Jones, L. M., Angus, R. D., and Verger, J. M. (1988). *Techniques for the Brucellosis Laboratory*. Paris: Institut National de la Recherche Agronomique.
- Altschul, S. F., Madden, S. L., Schäffer, A. A., Zhang, J., Zhang, Z., Miller, W., et al. (1997). Gapped BLAST and PSI-BLAST: a new generation of protein database search programs. *Nucleic Acids Res.* 25, 3389–3402. doi: 10.1093/nar/25.17.3389
- Assefa, S., Keane, T. M., Otto, T. D., Newbold, C., and Berriman, M. (2009). ABACAS: algorithm-based automatic contiguation of assembled sequences. *Bioinformatics* 25, 1968–1969. doi: 10.1093/bioinformatics/btp347
- Bidmos, F. A., and Bayliss, C. D. (2014). Genomic and global approaches to unravelling how hypermutable sequences influence bacterial pathogenesis. *Pathogens* 3, 164–184. doi: 10.3390/pathogens3010164
- Bosseray, N. (1991). *Brucella melitensis* Rev. 1 living attenuated vaccine: stability of markers, residual virulence and immunogenicity in mice. *Biologicals* 19, 355–363. doi: 10.1016/S1045-1056(05)80025-9
- Carver, T., Bohme, U., Otto, T. D., Parkhill, J., and Berriman, M. (2010). BamView: viewing mapped read alignment data in the context of the reference sequence. *Bioinformatics* 26, 676–677. doi: 10.1093/bioinformatics/btq010
- Chain, P., Comerci, D. J., Tolmasky, M. E., Larimer, F. W., Malfatti, S. A., Vergez, L. M., et al. (2005). Whole-genome analyses of speciation events in pathogenic *Brucellae*. *Infect. Immun.* 73, 8353–8361. doi: 10.1128/IAI.73.12.8353-8361.2005
- Dabral, N., Martha-Moreno-Lafont, Sriranganathan, N., and Vemulapalli, R. (2014). Oral immunization of mice with gamma-irradiated *Brucella neotomae* induces protection against intraperitoneal and intranasal challenge with virulent *B. abortus* 2308. *PLoS ONE* 9:e107180. doi: 10.1371/journal.pone.0107180
- Grilló, M.-J., Blasco, J. M., Gorvel, J. P., Moriyón, I., and Moreno, E. (2012). What have we learned from brucellosis in the mouse model? *Vet. Res.* 43:29. doi: 10.1186/1297-9716-43-29
- Halling, S. M., Peterson-Burch, B. D., Bricker, B. J., Zuerner, R. L., Qing, Z., Li, L.-L., et al. (2005). Completion of the genome sequence of *Brucella abortus* and comparison to the highly similar genomes of *Brucella melitensis* and *Brucella suis*. *J. Bacteriol.* 187, 2715–2726. doi: 10.1128/JB.187.8.2715-2726.2005
- Harmon, B. G., Adams, L. G., Templeton, J. W., and Smith, R. (1989). Macrophage function in mammary glands of *Brucella abortus*-infected cows and cows that resisted infection after inoculation of *Brucella abortus*. *Am. J. Vet. Res.* 50, 459–465.
- Hopkins, I. G., Thornton, D. H., and Hebert, C. N. (1981). Comparison of *Brucella abortus* (strain 544) variants. *J. Biol. Stand.* 9, 421–429. doi: 10.1016/S0092-1157(81)80033-9
- Jacob, J., Hort, G. M., Overhoff, P., and Mielke, M. E. A. (2006). In vitro and in vivo characterization of smooth small colony variants of *Brucella abortus* S19. *Microbes Infect.* 8, 363–371. doi: 10.1016/j.micinf.2005.07.003
- Jones, L. M., Montgomery, V., and Wilson, J. (1965). Characteristics of carbon dioxide-independent cultures of *Brucella abortus* isolated from cattle vaccinated with strain 19. *J. Infect. Dis.* 115, 312–320. doi: 10.1093/infdis/115.3.312
- Ko, J., Gendron-Fitzpatrick, A., Ficht, T. A., and Splitter, G. A. (2002). Virulence criteria for *Brucella abortus* strains as determined by interferon regulatory factor 1-deficient mice. *Infect. Immun.* 70, 7004–7012. doi: 10.1128/IAI.70.12.7004-7012.2002
- Le Flèche, P., Jacques, I., Grayon, M., Al Dahouk, S., Bouchon, P., Denoeud, F., et al. (2006). Evaluation and selection of tandem repeat loci for a *Brucella* MLVA typing assay. *BMC Microbiol.* 6:9. doi: 10.1186/1471-2180-6-9
- López-Goñi, I., García-Yoldi, D., Marín, C. M., de Miguel, M. J., Barquero-Calvo, E., Guzmán-Verri, C., et al. (2011). New Bruce-ladder multiplex PCR assay for the biovar typing of *Brucella suis* and the discrimination of *Brucella suis* and *Brucella canis*. *Vet. Microbiol.* 154, 152–155. doi: 10.1016/j.vetmic.2011.06.035
- Mancilla, M., Marín, C. M., Blasco, J. M., Zárraga, A. M., López-Goñi, I., and Moriyón, I. (2012). Spontaneous excision of the O-polysaccharide wkbA glycosyltransferase gene is a cause of dissociation of smooth to rough *Brucella* colonies. *J. Bacteriol.* 194, 1860–1867. doi: 10.1128/JB.06561-11
- Meyer, M. E., and Morgan, W. J. B. (1973). Designation of neotype strains and of biotype reference strains for species of the genus *Brucella* meyer and shaw. *Int. J. Syst. Bacteriol.* 23, 135–141. doi: 10.1099/00207713-23-2-135
- Miranda, K. L., Dorneles, E. M. S., Pauletti, R. B., Poester, F. P., and Lage, A. P. (2015). *Brucella abortus* S19 and RB51 vaccine immunogenicity test: evaluation of three mice (BALB/c, Swiss and CD-1) and two challenge strains (544 and 2308). *Vaccine* 33, 507–511. doi: 10.1016/j.vaccine.2014.11.056
- Miranda, K. L., Poester, F. P., Minharro, S., Dorneles, E. M. S., Stynen, A. P. R., and Lage, A. P. (2013). Evaluation of *Brucella abortus* S19 vaccines commercialized in Brazil: immunogenicity, residual virulence and MLVA15 genotyping. *Vaccine* 31, 3014–3018. doi: 10.1016/j.vaccine.2013.04.054
- Montaraz, J. A., and Winter, A. J. (1986). Comparison of living and nonliving vaccines for *Brucella abortus* in BALB/c mice. *Infect. Immun.* 53, 245–251.
- Moreno, E., and Moriyón, I. (2006). “The genus *Brucella*,” in *The Prokaryotes*, eds M. Dworkin, S. Falkow, E. Rosenberg, K.-H. Schleifer, and E. Stackebrandt (New York, NY: Springer), 315–456. doi: 10.1007/0-387-30745-1
- Mukherjee, F., Jain, J., Grilló, M. J., Blasco, J. M., and Nair, M. (2005). Evaluation of *Brucella abortus* S19 vaccine strains by bacteriological tests, molecular analysis of ery loci and virulence in BALB/c mice. *Biologicals* 33, 153–160. doi: 10.1016/j.biologicals.2005.04.003
- Neta, A. V. C., Mol, J. P. S., Xavier, M. N., Paixão, T. A., Lage, A. P., and Santos, R. L. (2010). Pathogenesis of bovine brucellosis. *Vet. J.* 184, 146–155. doi: 10.1016/j.tvjl.2009.04.010
- Ocampo-Sosa, A. A., and García-Lobo, J. M. (2008). Demonstration of IS711 transposition in *Brucella ovis* and *Brucella pinnipedialis*. *BMC Microbiol.* 8:17. doi: 10.1186/1471-2180-8-17
- Olsen, S. C., McGill, J. L., Sacco, R. E., and Hennager, S. G. (2015). Immune responses of bison and efficacy after booster vaccination with *Brucella abortus* strain RB51. *Clin. Vaccine Immunol.* 22, 440–447. doi: 10.1128/CDVI.00746-14
- Page, A. J., De Silva, N., Hunt, M., Quail, M. A., Parkhill, J., Harris, S. R., et al. (2016). Robust high throughput prokaryote *de novo* assembly and improvement pipeline for Illumina data. *Microbiol. Soc. 2*, 1–7. doi: 10.1101/052688
- Palacios-Chaves, L., Conde-Álvarez, R., Gil-Ramírez, Y., Zúñiga-Ripa, A., Barquero-Calvo, E., Chacón-Díaz, C., et al. (2011). *Brucella abortus* ornithine lipids are dispensable outer membrane components devoid of a marked pathogen-associated molecular pattern. *PLoS ONE* 6:e16030. doi: 10.1371/journal.pone.0016030
- Quail, M. A., Kozarewa, I., Smith, F., Scally, A., Stephens, P. J., Durbin, R., et al. (2009). A large genome centre's improvements to the Illumina sequencing system. *Nat. Methods* 5, 1005–1010. doi: 10.1038/nmeth.1270.A
- Quail, M. A., Otto, T. D., Gu, Y., Harris, S. R., Skelly, T. F., McQuillan, J. A., et al. (2012). Optimal enzymes for amplifying sequencing libraries. *Nat. Methods* 9, 10–11. doi: 10.1038/nmeth.1814
- Rajashekara, G., Glasner, J. D., Glover, D. A., and Splitter, G. A. (2004). Comparative whole-genome hybridization reveals genomic islands in *Brucella* species. *J. Bacteriol.* 186, 5040–5051. doi: 10.1128/JB.186.15.5040-5051.2004
- Rutherford, K., Parkhill, J., Crook, J., Horsnell, T., Rice, P., Rajandream, M.-A., et al. (2000). Artemis: sequence visualization and annotation. *Bioinformatics* 16, 944–945. doi: 10.1093/bioinformatics/16.10.944
- Singh, D. K., Kumar, A., Tiwari, A. K., Sankarasubramanian, J., Vishnu, U. S., Sridhar, J., et al. (2015). Draft genome sequence of *Brucella abortus* virulent strain 544. *Genome Announc.* 3:e00419-15. doi: 10.1128/genomeA.00419-15
- Spink, W. (1956). “The evolution of the concept that brucellosis is a disease of animals and man,” in *The Nature of Brucellosis* (Minneapolis, MN: University of Minnesota Press), 464.
- Trant, C. G. M. C., Lacerda, T. L. S., Carvalho, N. B., Azevedo, V., Rosinha, G. M. S., Salcedo, S. P., et al. (2010). The *Brucella abortus* phosphoglycerate kinase mutant is highly attenuated and induces protection superior to that of vaccine strain 19 in immunocompromised and immunocompetent mice. *Infect. Immun.* 78, 2283–2291. doi: 10.1128/IAI.01433-09
- Truong, Q. L., Cho, Y., Park, S., Park, B.-K., and Hahn, T.-W. (2016). *Brucella abortus* mutants lacking ATP-binding cassette transporter proteins are highly attenuated in virulence and confer protective immunity against virulent *B. abortus* challenge in BALB/c mice. *Microb. Pathog.* 95, 175–185. doi: 10.1016/j.micpath.2016.04.009
- Tsoktouridis, G., Merz, C. A., Manning, S. P., Giovagnoli-Kurtz, R., Williams, L. E., Mujer, C. V., et al. (2003). Molecular characterization of *Brucella abortus* chromosome II recombination. *J. Bacteriol.* 185, 6130–6136. doi: 10.1128/JB.185.20.6130-6136.2003

- Turse, J. E., Pei, J., and Ficht, T. A. (2011). Lipopolysaccharide-deficient *Brucella* variants arise spontaneously during infection. *Front. Microbiol.* 2:54. doi: 10.3389/fmicb.2011.00054
- WHO (2014). "The control of neglected zoonotic diseases," in *WHO Conference Report*, ed. NZD4 organising committee, (Geneva: WHO Press), 48.
- Xavier, M. N., Paixão, T. A., Poester, F. P., Lage, A. P., and Santos, R. L. (2009). Pathological, immunohistochemical and bacteriological study of tissues and milk of cows and fetuses experimentally infected with *Brucella abortus*. *J. Comp. Pathol.* 140, 149–157. doi: 10.1016/j.jcpa.2008.10.004
- Yang, X., Becker, T., Walters, N., and Pascual, D. W. (2006). Deletion of *znuA* virulence factor attenuates *Brucella abortus* and confers protection against wild-type challenge. *Infect. Immun.* 74, 3874–3879. doi: 10.1128/IAI.01957-05
- Zerbino, D. R., and Birney, E. (2008). Velvet: algorithms for de novo short read assembly using de Bruijn graphs. *Genome Res.* 18, 821–829. doi: 10.1101/gr.074492.107
- Zhu, L., Feng, Y., Zhang, G., Jiang, H., Zhang, Z., Wang, N., et al. (2016). *Brucella suis* strain 2 vaccine is safe and protective against heterologous *Brucella* spp. infections. *Vaccine* 34, 395–400. doi: 10.1016/j.vaccine.2015.09.116
- Conflict of Interest Statement:** The authors declare that the research was conducted in the absence of any commercial or financial relationships that could be construed as a potential conflict of interest.
- Copyright © 2016 Suárez-Esquivel, Ruiz-Villalobos, Castillo-Zeledón, Jiménez-Rojas, Roop II, Comerci, Barquero-Calvo, Chacón-Díaz, Caswell, Baker, Chaves-Olarte, Thomson, Moreno, Letesson, De Bolle and Guzmán-Verri. This is an open-access article distributed under the terms of the Creative Commons Attribution License (CC BY). The use, distribution or reproduction in other forums is permitted, provided the original author(s) or licensor are credited and that the original publication in this journal is cited, in accordance with accepted academic practice. No use, distribution or reproduction is permitted which does not comply with these terms.



COX-2 Inhibition Reduces *Brucella* Bacterial Burden in Draining Lymph Nodes

Aurélien Gagnaire¹, Laurent Gorvel², Alexia Papadopoulos¹, Kristine Von Bargen¹, Jean-Louis Mège³ and Jean-Pierre Gorvel^{1*}

¹ Aix Marseille Univ, CNRS, INSERM, CIML, Centre d'Immunologie de Marseille-Luminy, Marseille, France, ² Department of Pathology and Immunology, Washington University School of Medicine, St. Louis, MO, USA, ³ Aix Marseille Univ, INSERM, CNRS, IRD, URMITE, Marseille, France

OPEN ACCESS

Edited by:

Axel Cloeckert,
French National Institute for
Agricultural Research (INRA), France

Reviewed by:

Gregory T. Robertson,
Colorado State University, USA
Diego J. Comerchi,
Universidad Nacional de San Martín
(CONICET), Argentina
Jean Celli,
Washington State University, USA

*Correspondence:

Jean-Pierre Gorvel
gorvel@ciml.univ-mrs.fr

Specialty section:

This article was submitted to
Infectious Diseases,
a section of the journal
Frontiers in Microbiology

Received: 13 October 2016

Accepted: 28 November 2016

Published: 12 December 2016

Citation:

Gagnaire A, Gorvel L,
Papadopoulos A, Von Bargen K,
Mège J-L and Gorvel J-P (2016)
COX-2 Inhibition Reduces *Brucella*
Bacterial Burden in Draining Lymph
Nodes. *Front. Microbiol.* 7:1987.
doi: 10.3389/fmicb.2016.01987

Brucella is a Gram-negative facultative intracellular bacterium responsible for a chronic disease known as brucellosis, the most widespread re-emerging zoonosis worldwide. Establishment of a Th1-mediated immune response characterized by the production of IL-12 and IFN γ is essential to control the disease. Leukotrienes derived from arachidonic acid (AA) metabolism are known to negatively regulate a protective Th1 immune response against bacterial infections. Here, using genomics approaches we demonstrate that *Brucella abortus* strongly stimulates the prostaglandin (PG) pathway in dendritic cells (DC). We also show an induction of AA production by infected cells. This correlates with the expression of *Ptgs2*, a gene encoding the downstream cyclooxygenase-2 (COX-2) enzyme in infected DC. By comparing different infection routes (oral, intradermal, intranasal and conjunctival), we identified the intradermal inoculation route as the more potent in inducing *Ptgs2* expression but also in inducing a local inflammatory response in the draining cervical lymph nodes (CLN). NS-398, a specific inhibitor of COX-2 enzymatic activity decreased *B. melitensis* burden in the CLN after intradermal infection. This effect was accompanied by a decrease of *Ii10* and a concomitant increase of *Iifng* expression. Altogether, these results suggest that *Brucella* has evolved to take advantage of the PG pathway in the harsh environment of the CLN in order to persist and subvert immune responses. This work also proposes that novel strategies to control brucellosis may include the use of COX-2 inhibitors.

Keywords: *Brucella*, COX-2, dendritic cells, intradermal infection, prostaglandins

Abbreviations: 5-LO, 5-Lipoxygenase; AA, Arachidonic Acid; BMDC, Bone marrow-derived dendritic cell; Ccl2, C-C-chemokine ligand 2; Ccr7, C-C-chemokine receptor 7; CFU, Colony forming units; CLN, Cervical lymph nodes; COX-2, Cyclooxygenase-2; DC, Dendritic cells; DMSO, Dimethyl sulfoxide; EP, Prostaglandin E receptor; Foxp3, Forkhead box 3; GM-CSF, Granulocyte macrophage colony-stimulating factor; Gzmb, Granzyme B; IFN, Interferon; IL, Interleukin; LPS, Lipopolysaccharide; moDC, Monocyte derived dendritic cell; MOI, Multiplicity of infection; NOS₂, Nitric oxide synthase 2; NS-398, *N*-[2-(cyclohexyloxy)-4-nitrophenyl]-methanesulfonamide; PBMC, Peripheral blood mononuclear cells; PG, Prostaglandins; PTGDS, Prostaglandin D synthase; PTGER, Prostaglandin E receptor; *Ptgs2*, Prostaglandin-endoperoxide synthase 2; Th1, T helper 1; TLR, Toll-like receptor; TNF- α , Tumor Necrosis Factor α ; TSA, Tryptic Soy Agar; TSB, Tryptic Soy Broth.

INTRODUCTION

Brucellosis is a disease caused by a Gram-negative facultative intracellular bacterium belonging to the genus *Brucella*. It is the most widespread re-emerging zoonosis worldwide affecting more than half a million people each year (Seleem et al., 2010). *Brucella* affects a wide range of land and aquatic mammals including humans and livestock. Animals are *Brucella* primary hosts in which the bacterium has a particular tropism for the reproductive system, often leading to spontaneous abortion and sterility responsible for severe economic losses (Pappas, 2010). *Brucella* can be transmitted to humans in close contact with infected animals mostly by ingestion of contaminated food or inhalation of aerosolized contaminated particles (Moreno, 2014). The *Brucella* species presenting the most important zoonotic potential for humans are *B. melitensis*, *B. abortus*, *B. suis*, and *B. canis* (Moreno, 2014). In human, the disease is characterized by an acute phase, which mainly manifests itself by asthenia, recurrent undulant fever and influenza-like symptoms. If the disease is not cured, it can evolve into chronic brucellosis, which may result in serious complications such as endocarditis or neurobrucellosis (Franco et al., 2007; Dean et al., 2012). Currently, there is no effective vaccine to prevent the disease in human highlighting the importance to understand the physiopathology of the disease.

To establish a persistent infection, *Brucella* behaves as a stealthy pathogen (Barquero-Calvo et al., 2007), using various strategies to modulate the host immune response. For instance, its unusual LPS plays a central role showing a low endotoxicity and being poorly recognized by Toll-like-receptor 4 (TLR4) (Lapaque et al., 2005; Lapaque et al., 2009; Conde-Álvarez et al., 2012). *Brucella* can also modulate the protective Th1 immune response characterized by the secretion of pro-inflammatory cytokines such as IL-1 β , IFN γ , TNF- α , or IL-12 (Zhan and Cheers, 1995; Zhan et al., 1996; Martirosyan et al., 2011) by inducing an early IL-10 secretion orchestrated by CD4⁺CD25⁺ T cells (Xavier et al., 2013).

It has also been shown that *B. abortus* can activate the 5-LO responsible for the synthesis of leukotrienes derived from AA (Fahel et al., 2015). The 5-LO activity impacts on pro-inflammatory cytokine secretion including IL-12 and IFN γ *in vivo* (Fahel et al., 2015). Thus, 5-LO seems to function as a negative regulator of the protective Th1 response during mice infection with *B. abortus*. However, AA can be metabolized by different enzymes including the COX also known as PtgS (Harizi et al., 2008). COX enzymes are responsible for the rate-limiting step in the biosynthesis of PG and other prostanoids among them thromboxanes and prostacyclins (Figure 1). Three known isoforms of COX have been identified so far: COX-1, COX-2 and COX-3 whose physiological function is not yet fully elucidated (Chandrasekharan et al., 2002; Chandrasekharan and Simmons, 2004). The constitutively and ubiquitously expressed COX-1 isoform is involved in basal and constitutive PG production. On the contrary, COX-2 is expressed at very low levels and is highly inducible following pro-inflammatory stimuli such as cytokines or endotoxins. COX-2 converts AA into prostaglandin H₂ (PGH₂), which is then converted into prostaglandin D₂, prostaglandin E₂ (PGE₂), prostacyclins, or thromboxane A₂

depending on cell specific enzymes expression (Figure 1). The context as well as the panel of PG receptors will define the pro- or anti-inflammatory action of these lipid mediators. Thus, PG have immunomodulatory traits that can worsen or improve bacterial clearance. This dual activity is observed during *Salmonella* Typhimurium infection in mice. Indeed, COX-2 inhibition during the acute stage of the disease increases bacterial load whereas at later stage it enhances mouse survival (Bowman and Bost, 2004). A similar pattern is observed in mice infected with *Mycobacterium tuberculosis* (Rangel Moreno et al., 2002).

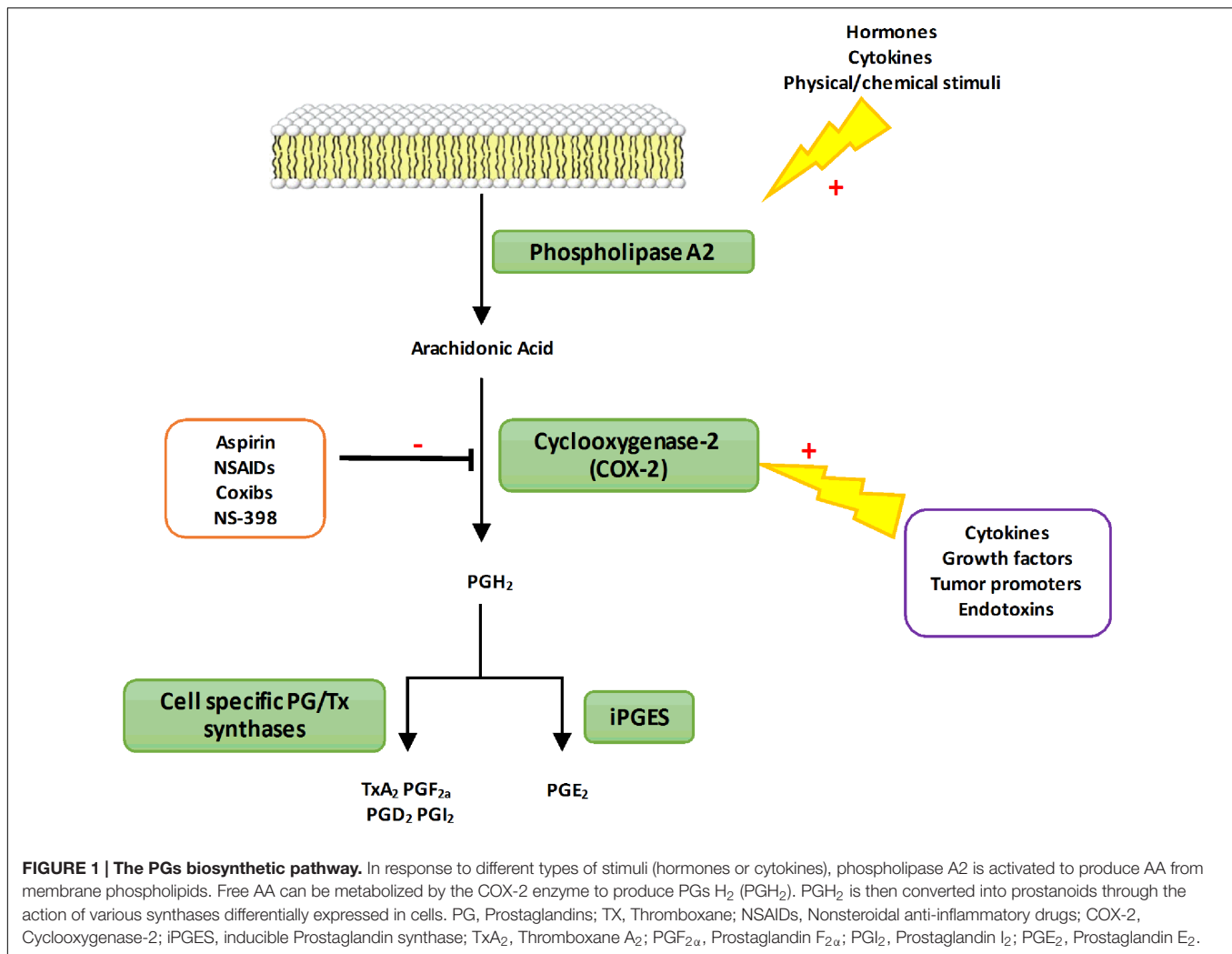
Cyclooxygenase-2 has been shown to have different outcomes during several bacterial and viral infections (Steer and Corbett, 2003; Agard et al., 2013) but little is known about its role during *Brucella* infection. Some studies have reported the impact of *B. abortus* and *B. melitensis* LPS on COX-2 expression in monocytes (López-Urrutia et al., 2001). Both smooth-LPS (S-LPS) were found to induce COX-2 expression in THP-1 cell line and rat-peritoneal macrophages in a dose-dependent manner. PGE₂ synthesis and its impact in bovine PBMC infected with live and γ -irradiated *B. abortus* have also been assessed showing that IL-2 and IFN γ suppression was independent on COX-1 and COX-2 (Stevens and Olsen, 1994) but these *in vitro* studies were not confirmed *in vivo*.

The aim of our study is to determine whether COX-2 is involved in protection against *Brucella* infection or exacerbation of the *Brucella* burden. We have investigated the ability of *B. abortus* to stimulate the AA-COX-2 pathway in infected human moDC and in mouse GM-CSF BMDC and studied the impact of COX-2 inhibition *in vivo* after intradermal infection with *B. melitensis*. Here, we demonstrate that *B. abortus* enhances AA production in human moDC and *Ptgs2* expression both in human moDC and murine GM-CSF BMDC. The comparison of different inoculation routes allowed us to identify the intradermal route as the more potent to induce *Ptgs2* expression and local inflammatory response in CLN. COX-2 inhibition decreases the bacterial burden in CLN characterized by a decrease of *Il10* and an increase of *Ifng* expression. Thus, further development of COX-2 inhibitors may represent a novel therapeutic strategy against *Brucella*.

MATERIALS AND METHODS

Ethics Statement

This study was carried out in strict accordance with the guidelines of the Council of the European Union (Directive 86/609/EEC) regarding the protection of animals used for experimental and other scientific purposes. The experimental protocol was approved by the institutional animal care and use committee of the Aix-Marseille University (N° 87-848, October 19, 1987, Paris, modified by Decree 2001-464 and Decree 2001-131 relative to European Convention, EEC directive 86/609). All experiments were done in accordance with French and European guidelines for animal care. Blood was obtained from the Etablissement Français du Sang. As it is a commercial product, the Ethics Committee agreement is not required.



Mice and Bacteria

Six to eight weeks old females C57BL/6 (Charles River Laboratories) were maintained under pathogen-free conditions and fed sterile food and water *ad libitum*. All infections were performed under Animal Biosafety Level 3 facility.

Bacterial Strains

Orentia tsutsugamushi strain Kato (CSUR R163) (gift from Dr. Jean-Louis Mège, URMITE, Marseille, France) was propagated in L929 cells (ATCC), as previously described (Barry et al., 2012). Briefly, highly infected cells were sonicated, or lysed using glass beads for *O. tsutsugamushi*, and centrifuged at $500 \times g$ for 10 min to remove cell debris. Supernatants were collected and centrifuged at $10,000 \times g$ for 10 min to pellet the bacteria. Live bacteria were quantified using infected cell-counting units. *Coxiella burnetii* organisms (RSA493 Nile Mile strain) (gift from Dr. Jean-Louis Mège, URMITE, Marseille, France) were obtained by passage in BALB/c mice (Charles River Laboratories) and culture in L929 cells. The concentration of organisms was determined by immunofluorescence using

specific antibodies and/or PCR using known concentrations of bacterial DNA. The quantification of organisms was performed as previously described (Barry et al., 2012). Bacterial viability was assessed using the LIVE/DEAD Bac Light bacterial viability kit (Invitrogen). *Brucella abortus* strain 2308 and *Brucella melitensis* strain 16M (gift from Dr. Ignacio Moriyon, University of Pamplona, Spain) were grown on TSA (Sigma-Aldrich) at 37°C for 7 days, as previously described (Pizarro-Cerdá et al., 1998). The Twist-Marseille (CNCM I-2202) strain of *Tropheryma whippelii* (gift from Dr. Jean-Louis Mège, URMITE, Marseille, France), a bacterium known to live in macrophages, was cultured in HEL cells and purified. Quantification of inocula was performed by measuring the percentage of infected cells by immunofluorescence, as previously described (Gorvel et al., 2010).

Isolation of Human moDC

Peripheral blood mononuclear cells from buffy coats were recovered from the Ficoll-Hypaque (GE healthcare) interface after centrifugation at $700 \times g$ for 20 min. Monocytes and T lymphocytes were isolated from PBMCs using

magnetic beads coupled to antibodies specific for CD14 and CD3, respectively, as described by the manufacturer (Miltenyi Biotec). The purity of the monocyte and T-cell preparations was assessed by flow cytometry and was greater than 98%. Monocytes were then incubated in RPMI 1640 (Gibco) containing 20 mM HEPES, 2 mM glutamine, 10% fetal calf serum (FCS) (Invitrogen), 0.1 ng/mL IL-4 and 1 ng/mL granulocyte-macrophage colony-stimulating factor (GM-CSF) (R&D Systems) for 7 days to obtain moDC.

In vitro Generation of BMDC

Bone marrow-derived dendritic cells were prepared from 6 to 8 week-old females C57BL/6 mice as previously described (Salcedo et al., 2008). Briefly, tibias and femurs were flushed with RPMI-5%FCS (Eurobio)-50 μ M β -mercaptoethanol (Sigma—Aldrich) to extract bone marrow.

In order to generate GM-CSF-BMDC, 3.10^6 cells per well were seeded onto 6-well plates in medium supplemented with supernatant of J558L GM-CSF producing cell line (gift from Dr. Philippe Pierre, Centre d'Immunologie de Marseille-Luminy, Marseille, France). The medium was changed at day 2.5.

In vitro Infection Assays

GM-CSF-DC were infected with *B. abortus* smooth virulent strain 2308 using a MOI of 30:1. Bacteria were centrifuged onto cells at $400 \times g$ for 10 min at 4°C. Then, cells were incubated for 30 min at 37°C with 5% CO₂. After two washes with medium, cells were incubated for one hour with medium containing antibiotic [gentamicin (Sigma—Aldrich) at 50 μ g/ml] in order to kill the extracellular bacteria. Thereafter, the antibiotic concentration was decreased at 10 μ g/ml until the end of the infection time.

In Vivo Bacterial Challenge

Brucella melitensis 16M with a chromosomal integration of DsRed was used in this study. *B. melitensis* were grown under shaking in TSB (Sigma—Aldrich) containing 25 μ g/ml kanamycin (Sigma—Aldrich) at 200 rpm for 16 h at 37°C. Inocula were prepared by pelleting bacteria and by adjusting bacterial concentration in endotoxin free PBS (Gibco) to obtain the right concentration depending on the inoculation route. Oral infection was performed as previously described (von Bargen et al., 2014). Briefly, pelleted bacteria were re-suspended to previously heat-sterilized 5% milk and adjusted at respective MOI in 5% milk (Scharlau). For all the other inoculation routes, mice were anesthetized with Ketamine/Xylazine (Virbac). For intranasal infection, the bacterial inoculum containing 10^5 CFU suspended in 35 μ L of endotoxin free PBS (Gibco) was applied onto mice nostril via pipet. For intradermal infection, the bacterial inoculum containing 10^4 CFU suspended in 10 μ L of endotoxin free PBS was injected into the ear pinna. For conjunctival infection, the bacterial inoculum containing 10^9 CFU suspended in 10 μ L was applied onto conjunctival surfaces (5 μ L per eye). In some experiments, the selective COX-2 inhibitor NS-398 (Cayman Chemicals) were administered by intraperitoneal injection (15 mg/kg) right after intradermal infection. A stock

solution of NS-398 was prepared in DMSO (Sigma—Aldrich) and was diluted in PBS just prior to treatment to the right concentration in a 1:3 (DMSO:PBS) ratio for a total volume of 100 μ L per mouse or vehicle control (DMSO:PBS alone).

Treatments were repeated daily for 7 days. At 8 and 29 days post-infection mice were sacrificed by cervical dislocation. Immediately after sacrifice, CLN (including mandibular, accessory mandibular, and superficial parotid lymph nodes referred here as CLN; Van den Broeck et al., 2006) and spleens were collected, weighted, and proceeded for bacterial count and RNA extraction.

Analysis of Organ Bacterial Burden

Spleens and CLN were removed and homogenized in Triton X-100 (Sigma—Aldrich) 0.1%. Serial dilutions were performed in PBS, and plated in triplicate onto TSA agar. CFU were enumerated after 3–4 days of culturing at 37°C.

Microarrays

Monocyte derived dendritic cells (5.10^6 cells per well) were plated in 6-well plates and stimulated or not with *B. abortus* (MOI of 300:1) for 6 hours, and total RNA was then extracted using the RNeasy minikit (Qiagen) and DNase treatment. This study utilized the 4X44k Human Whole Genome microarrays (Agilent Technologies), representing 44,000 probes. Reverse transcription, samples labeling, and hybridization were performed according to the protocols specified by the manufacturer (One-Color Microarray-Based Gene Expression Analysis). Three samples per experimental condition were included in the analysis. The slides were scanned at a 2-mm resolution with a G2505C DNA microarray scanner (Agilent Technologies).

RNA Extraction, RT, and q-PCR

Total RNAs from infected GM-CSF-BMDC were extracted using RNeasy Micro Kit (Qiagen) following manufacturer's instructions. CLN were stabilized in RNAlater (Qiagen) immediately after sampling. Organs were homogenized in RLT buffer (Qiagen) and then extracted using RNeasy Micro Kit (Qiagen) following manufacturer's instructions. cDNAs were obtained by using Quantitech Reverse Transcription Kit (Qiagen) following manufacturer's instructions using 300 ng of RNA as a matrix. qPCR were conducted using a 7500 Fast-Real-time PCR (Applied Biosystem) with SYBER Green (Takara) following manufacturer's instructions. HPRT was used as housekeeping gene to determine Δ Ct. Fold change compared to base line expression in uninfected cells, or control mice was determined using $2^{-\Delta\Delta C_t}$ method where $\Delta\Delta C_t = (C_{t\text{target}} - C_{t\text{HPRT}})_{\text{infected}} - (C_{t\text{target}} - C_{t\text{HPRT}})_{\text{non-infected}}$ as previously described (Papadopoulos et al., 2016). mRNAs whose expression level was twice as high compared to control were considered as significantly up-regulated. Primers used in this study are listed in Table 1.

Arachidonic Acid Quantification

Monocyte derived dendritic cells were stimulated by bacterial pathogens (MOI 50:1 for *T. whipplei* or 20:1 for others) or

TABLE 1 | Primers used for analysis of gene expression upon infection.

Genes	Forward Primers	Reverse Primers
<i>HPRT</i>	AGCCCTCTGTGTGCTCAAGG	CTGATAAAATCTACAGTCATAGGAATGGA
<i>lfn</i>	TCAAGTGGCATAGATGTGGAAGAA	TGGCTCTGCAGGATTTCATG
<i>Il6</i>	GAGGATACCACTCCCAACAGACC	AAGTGCATCATCGTTGTTTCATACA
<i>Gzmb</i>	ATCAAGGATCAGCAGCCTGA	CATGATGTCATTGGAGAATGTCT
<i>Nos2</i>	CAGCTGGGCTGTACAAACCTT	CATTGGAAGTGAAGCGTTTCG
<i>Ptgs2 (Cox2)</i>	ACCTCTGCGATGCTCTTCC	TCATACATTCCCAACGGTTT
<i>Ccl2</i>	GCCTGCTGTTCCACAGTTGC	ATTGGGATCATCTTGCTGGT
<i>Ccr7</i>	GTGGTGGCTCTCCTTGTCT	GAAGCACACCGACTCGTACA
<i>Il10</i>	GGTTGCCAAGCCTTATCGGA	ACCTGCTCCACTGCCTTGCT
<i>Foxp3</i>	AGGAGCCGCAAGCTAAAAGC	TGCTTCGTGCCCACTGT
<i>Tnf</i>	CATCTTCTCAAAATTGAGTGACAA	TGGGAGTAGACAAGGTACAACCC
<i>Il4</i>	ACTCTTTCGGGCTTTTCGAT	TTGCATGATGCTCTTTAGGC

Escherichia coli LPS (Sigma—Aldrich) (1 µg/ml) for 16 h, suspended in 0.3 mL of cold methanol (MeOH). Fatty acid methyl esters (FAME) extraction was performed as previously described (Schutter and Dick, 2000; Ecker et al., 2012), 15 µL of MeOH/Deuterium-labeled eicosanoids (LTB4-d4 and 5-HETE-d8, 400 ng/ml) standard solution were added to 0.2 ml of homogenate. After centrifugation, supernatants were diluted in 10 mL of hydrochloric acid (HCl) 0.02 M and submitted to solid-phase extraction on C18 cartridge (Macherey Nagel). After complete loading, columns were washed, dried and lipid mediators were eluted in methyl formate (MeFor). Solvent was evaporated under N₂ and samples were dissolved within 30 µL MeOH and stored at −80°C.

For AA quantification, 0.1 ml of homogenates were extracted in dichloromethane/methanol/water, in the presence of 2 µg glyceryl triheptadecanoate (Sigma—Aldrich) and hydrolyzed in potassium hydroxide (KOH) (0.5 M in MeOH) at 50°C for 30 min. Lipids were transmethylated in 14% boron trifluoride MeOH solution (Sigma—Aldrich) and hexane at 80°C for 1 h. FAME were extracted with hexane, dried and dissolved in ethyl acetate.

Fatty acid methyl esters were analyzed by gas—liquid chromatography as previously described (Lepage and Roy, 1986) on a Clarus 600 Perkin Elmer system using Fawewax RESTEK fused silica capillary columns (30 m × 0.32 mm i.d., 0.25 µm film thickness). Oven temperature was programmed from 110°C to 220°C at a rate of 2°C per min and the carrier gas was hydrogen (0.5 bar). The injector and the detector were at 225°C and 245°C, respectively. LC-MS/MS analysis was performed on UHPLC system (Agilent LC1290 Infinity) coupled to Agilent 6460 triple quadrupole MS (Agilent Technologies) equipped with electrospray ionization source. Separation was done at 40°C on a Zorbax SB-C18 column (2.1 mm, 50 mm, 1.8 µm) (Agilent Technologies). The mobile phases were, respectively water, ACN and FA (75/25/0.1) (A) and ACN, FA (100/0.1) (B). The linear gradient was as follows: 0% B at 0 min, 85% B at 8.5 min, 100% B at 9.5 min, 100% B at 10.5 min, and 0% B at 12 min. The flow rate was 0.35 mL/min. The autosampler was set at 5°C and the injection volume was 5 µL. Electrospray ionization was performed in negative ion mode with a spray voltage fixed at −3500 V. After optimization, source conditions were as follows:

source temperature was 325°C, nebulizer gas (nitrogen) flow rate was 10 L/min, sheath gas temperature was 400°C and sheath gas (nitrogen) flow rate was 12 L/min. Analyses were acquired in multiple reaction mode (MRM) using nitrogen as collision gas. For each compound the conditions of separation: retention time in minute (RT), and of quantification were defined: specific Q1/Q3 transition (T) fragmentor (F), and collision energy (CE). Thus, optimized parameters were as follows: LTB4 (RT: 4.32 min, T: 335/195, F: 115 V; CE: 4 V), LTB4-d4 (RT: 4.31 min, T: 339/197, F: 120 V, CE: 6 V). Peak detection, integration and quantitative analysis were performed using Mass Hunter Quantitative analysis software (Agilent Technologies).

Statistical Analysis

The results are expressed as mean ± SD and statistical significance was assessed using the unpaired, two-tailed Student's *t*-test or by analysis of variance (ANOVA) followed by Tukey's multiple comparison test provided by GraphPad Prism software when more than two conditions were analyzed simultaneously. *p* values over 0.05 were not considered as significant.

RESULTS

B. abortus Infection of moDC and GM-CSF-BMDC Stimulates AA-Cyclooxygenase Pathway

We first measured the AA concentration in *B. abortus* infected moDC culture supernatants at 16 h post-infection. In parallel, other intracellular bacteria (*T. whipplei*, *C. burnetii*, *O. tsutsugamushi*) were tested. Only *B. abortus* and *O. tsutsugamushi* induced a significant AA production compared to non-stimulated moDC (Figure 2A).

AA can be metabolized by the COX pathway (Harizi et al., 2008). Thus, to determine the impact of *B. abortus* on this pathway, we analyzed the transcriptional profile of several key genes involved in the PG and leukotriene pathways in infected cells (Figure 2B). Compared to unstimulated cells, infected human moDC strongly expressed *PTGS2*

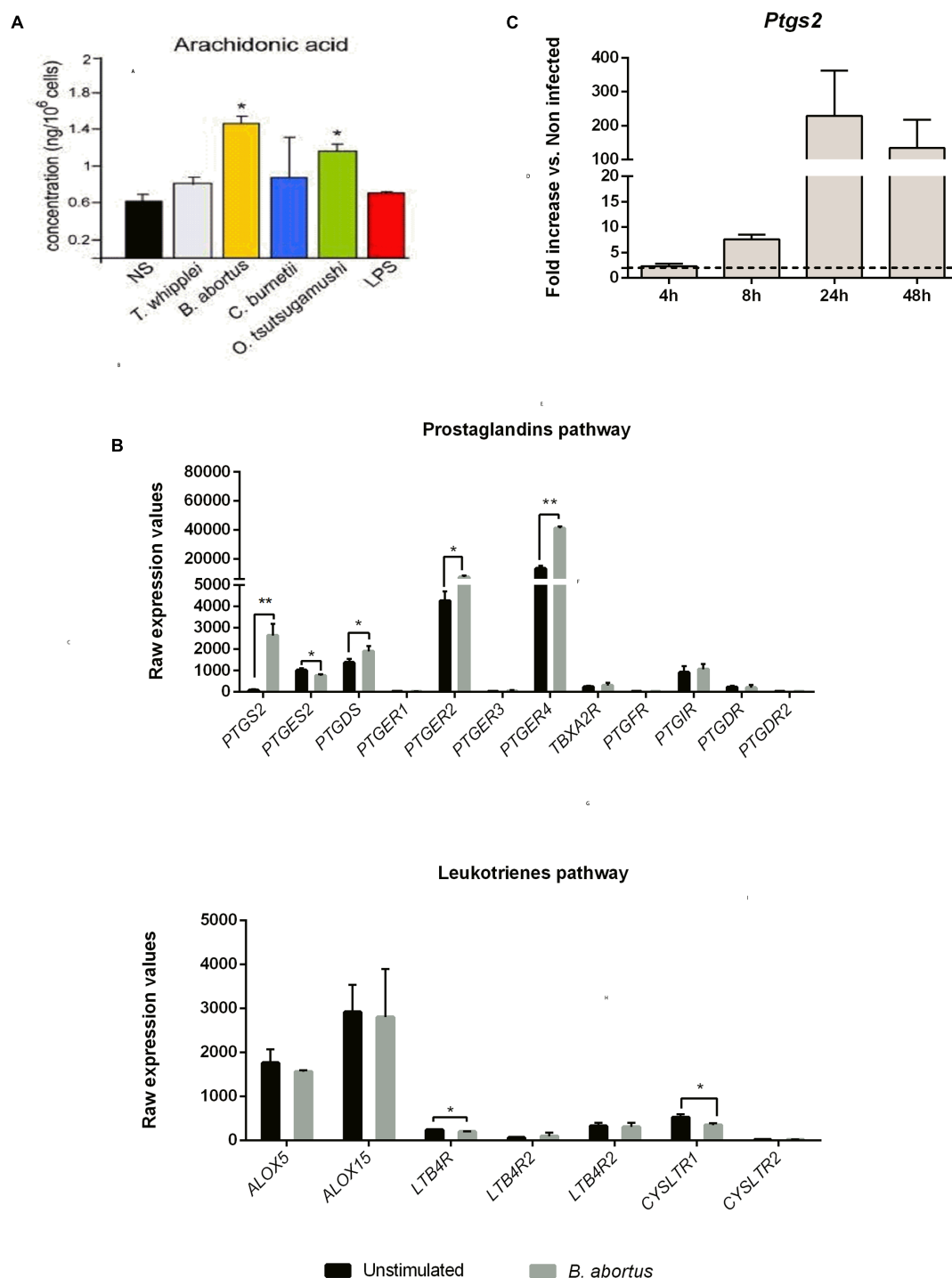


FIGURE 2 | Prostaglandins pathway highlights induced AA metabolism in human moDC and mice GM-CSF BMDC upon *Brucella abortus* infection. (A) moDC were stimulated or not (NS) during 16 h with *Tropheryma whipplei* (30:1), *B. abortus* (20:1), *Coxiella burnetii* (20:1), *Orentia tsutsugamushi* (20:1), or *Escherichia coli* LPS (1 μ g/mL) and then treated for AA dosage. The AA concentration after infection was compared to unstimulated condition using unpaired, two-tail Student's *t*-test (* p < 0.05) (Results of three independent experiments). Results are given as mean \pm SD. (B) Transcriptomic analysis. moDC were stimulated or not with *B. abortus*, for 6 h. RNA was extracted, and a microarray was performed. Statistical analysis was performed using unpaired, two-tail Student's *t*-test (* p < 0.05; ** p < 0.005; *** p < 0.001) and results are given as mean \pm SD (Results of three independent experiments). (C) GMCSF BMDC from C57BL/6 mice were infected with *B. abortus* 2308 (30:1). At 4, 8, 24, and 48 h post-infection, cells were recovered and RNA was extracted. Gene expression is represented as a fold increases between non-infected and infected cells. Statistical analyses were performed by using the comparative CT Method ($\Delta\Delta$ CT method) given by $2^{-\Delta\Delta$ CT}. The dotted line represents a fold increase of 2, the statistical significant threshold in this method. Results are given as mean \pm SD (Results of three independent experiments).

(33 times higher) and in a lesser extent *PTGER2*, *PTGER4* and *PTGDS* (1.7, 3.1, and 1.3 times higher, respectively) (**Figure 2B**, upper panel). On the contrary, none of the genes involved in the leukotriene pathway were up-regulated following *Brucella* infection (**Figure 2B**, lower panel).

We next investigated the expression of *Ptgs2* in murine GM-CSF-derived DC at 4, 8, 24, and 48 h post-infection. We observed that as in human DC, murine *Ptgs2* mRNA level was strongly up regulated. *Ptgs2* expression was time-dependent, reaching a peak at 24 h post-infection (229.4-fold up regulated compared to non-infected cells) (**Figure 2C**).

These results show that *B. abortus* infection is capable of stimulating the AA metabolic pathway and downstream PG pathway both in human and mice DC.

Intradermal Infection Is Characterized by a Strong *Ifng* and *Ptgs2* Signature

We next investigated the involvement of the PTGS-2 pathway *in vivo* upon infection in mice. We have first compared three different *Brucella* strains (*B. abortus* 2308, *B. melitensis* 16M, and *B. suis* 1330) and their ability to colonize CLN at 8 and 15 days post-infection using the oral infection model we previously shown to induce a specific colonization of CLN (von Bargen et al., 2014). We avoided to use intraperitoneal inoculation since it is associated to systemic infection and recedes from *Brucella* physiological routes of infection or vaccination (Grilló et al., 2012). Although bacterial loads in CLN were very similar at any time point for all *Brucella* species (Supplementary Figure 1A), *B. melitensis* and *B. suis* induced a higher lymphadenopathy compared to *B. abortus* at 15 days post-infection suggesting an enhanced inflammatory response in the CLN (Supplementary Figure 1B). We then decided to continue this study with *B. melitensis* 16M.

WT C57BL/6 mice were inoculated with *B. melitensis* by oral administration (with 10^9 bacteria per mouse) as previously described (von Bargen et al., 2014) or by intranasal (with 10^5 bacteria per mice), conjunctival (10^9 bacteria per mice) or intradermal (10^4 bacteria per mice) routes. Mice were sacrificed at 8 and 29 days post-infection and the weight and bacterial load of CLN and spleens were measured (**Figures 3A,B**).

At 8 days post-infection, the intradermal route was the only route capable of inducing lymphadenopathy compared to mock-treated mice and to other inoculation methods (**Figure 3A**, Left panel). No splenomegaly was observed at 8 days post-infection compared to mock-treated mice (**Figure 3A**, Right Panel). These results correlated with bacterial loads. CFU numbers in CLN were higher in mice infected intradermally compared to the other infection routes (**Figure 3B**, Left panel). However, spleens were poorly colonized as observed in all infection conditions (**Figure 3B**, Right panel). At 29 days post-infection, all inoculation routes resulted in lymphadenopathy and induced splenomegaly (**Figure 3A**). The increase in CLN and spleen weight was not associated with an increase in bacterial load (**Figure 3B**). This suggests the establishment of an inflammatory response in these organs.

We next investigated the local immune response induced by *Brucella* infection in the spleens and CLN by extracting mRNA at 8 and 29 days post-infection. Results were analyzed as a fold increase compared to their mock counterparts. No significant response was observed in the spleen for any infection routes (Supplementary Figure 2). On the contrary, a clear inflammatory response was observed in the CLN of mice infected intradermally from 8 days post-infection onwards (**Figure 3C**). This response led to a strong up-regulation of *Ifng*, *Gzmb* and *Ptgs2* mRNAs (64, 18.6, and 30.8-fold, respectively) (**Figure 3C**). At 29 days post-infection, *Ifng*, *Gzmb*, and *Il6* mRNA levels strongly decreased whereas a strong up-regulation of *Ptgs2* and in a lesser extent *Nos2* and *Ccl2* mRNA levels remained (**Figure 3C**). The inflammatory response was less pronounced using the other inoculation routes. Indeed, no significant changes between day 8 and 29 were observed in terms of mRNA expression levels except for conjunctival inoculation displaying an increase of *Nos2* and *Ccl2* mRNA levels (Fold change: 10.3 and 2.9, respectively) (**Figure 3C**).

In conclusion, the intradermal infection route is the most potent at inducing inflammatory genes expression and *Ptgs2* seems to be a robust marker of *Brucella* intradermal infection compared to intranasal, conjunctival or oral infection routes. At 29 days post-infection following *B. melitensis* intradermal inoculation, the expression of *Il6* was significantly higher compared to intranasal infection. *Nos2* (compared to the oral and intranasal routes), *Ptgs2* and *Ccl2* genes (compared to all the other routes) were also increased (**Figure 3C**). Interestingly, no systemic response was observed in mice sera at any time independently from the inoculation route except for IFN- γ after intradermal infection. However, low but significant amounts of TNF- α were detected in the sera of mice infected intradermally at 8 days post-infection (Supplementary Figure 3).

Overall, these results strongly suggest that in the CLN after intradermal infection a robust inflammatory response characterized by an *Ifng* and a *Ptgs2* signature takes place.

COX-2 Inhibition Reduces Bacterial Burden *In vivo*

After having identified that the intradermal route was the more potent to induce *Ptgs2* expression during *B. melitensis* infection, we evaluated *in vivo* the involvement of COX-2 during infection. WT C57BL/6 mice were challenged intradermally with *B. melitensis* (10^4 bacteria per mice) and were given NS-398, a specific COX-2 inhibitor, or DMSO vehicle (mock control) by intraperitoneal administration daily for 7 days.

We first looked at CLN and spleen weights at 8 days post-infection. Independently of the treatment, infected mice presented a lymphadenopathy compared to uninfected mice. However, NS-398 treatment induced a decrease in CLN weight compared to non-treated infected mice (**Figure 4A**, Left panel). This effect was consistent with the anti-inflammatory properties of NS-398. No significant effect could be observed in the spleen (**Figure 4A**, Right panel). This response was accompanied by a decrease of CFU numbers in CLN in treated mice (**Figure 4A**,

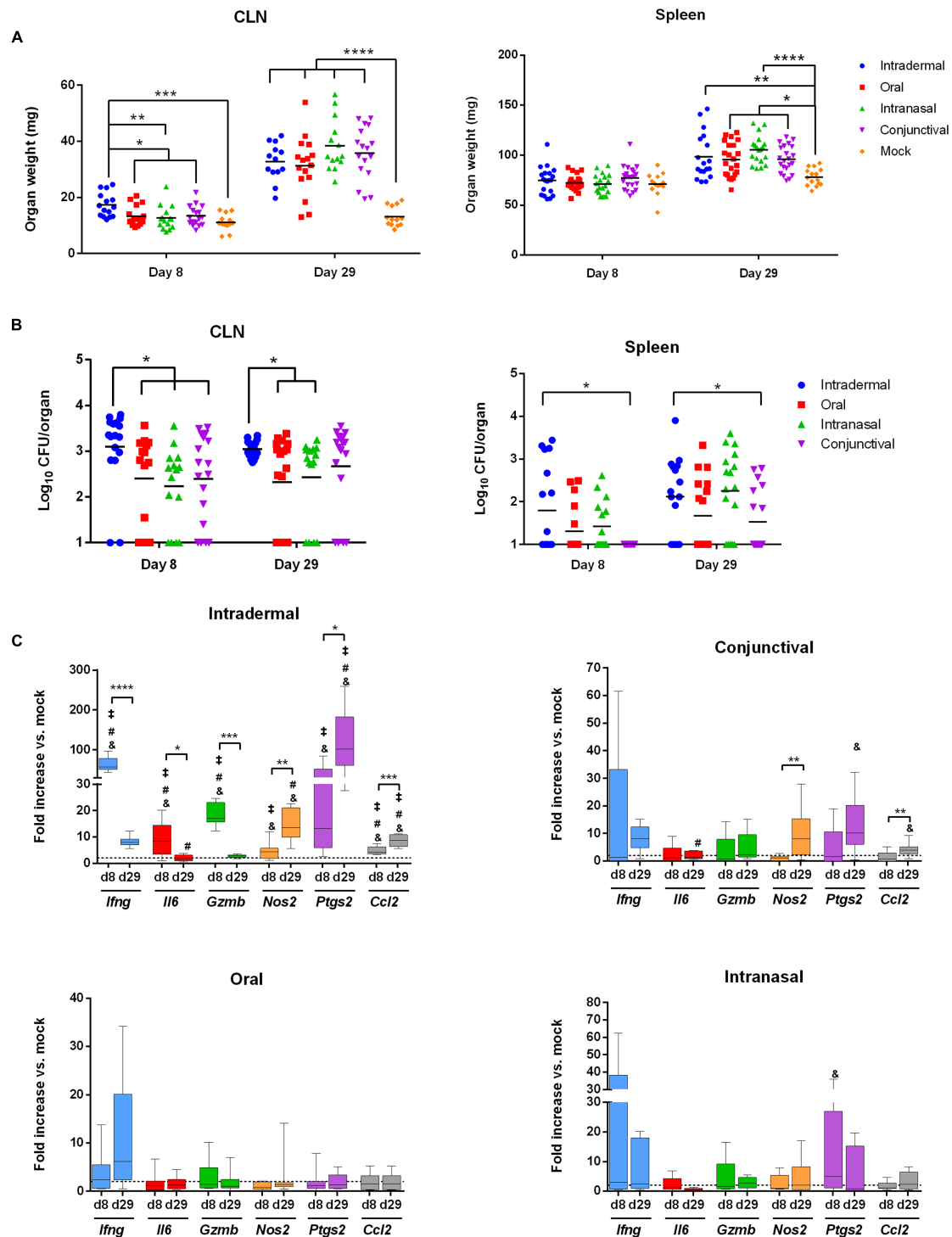


FIGURE 3 | The intradermal inoculation pathway induces a strong local inflammatory response in CLN. C57BL/6 mice ($n = 5$ per group) were infected using the routes of infection described in the methods section. At 8 and 29 days post-infection, mice were sacrificed and organs were weighed and analyzed for their bacterial loads by plating homogenates on nutrient agar. Data represent mean of CLN (Left panel) and spleen (Right panel) weight (A) or CFU per organ (B) from three independent experiments. Analysis significance was determined using ANOVA ($*p < 0.05$; $**p < 0.005$; $***p < 0.001$; $****p < 0.0001$). (C) C57BL/6 mice ($n = 5$ per group) were infected using different routes of infection as described in methods section. At 8 and 29 days post-infection, total RNA of the CLN was extracted and analyzed for inflammatory response gene expression by reverse transcription real-time PCR. Results are given as fold increase compared to the signal obtained for mock-infected mice. Statistical significance was determined using unpaired, two-tailed Student's t -test (Results of three independent experiments) ($*p < 0.05$; $**p < 0.005$; $***p < 0.001$; $****p < 0.0001$) and $\&$ significant compared to the oral route; $\#$ significant compared to the intranasal route and $\$$ significant compared to the conjunctival route using ANOVA.

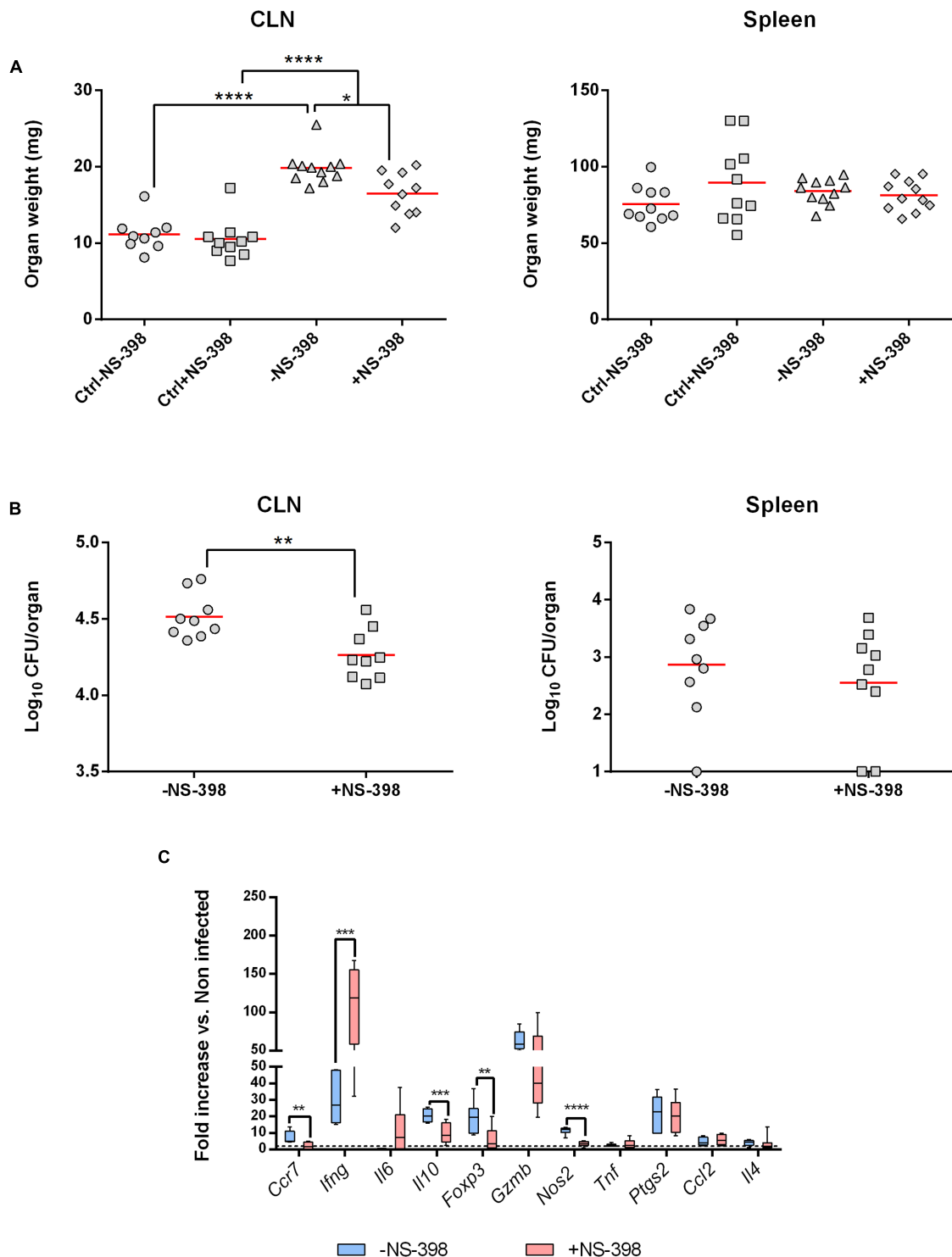


FIGURE 4 | Cyclooxygenase-2 inhibition induces a decrease of bacterial burden in draining lymph nodes. C57BL/6 mice ($n = 5$) were infected with *B. melitensis* (10^4 bacteria per mice) intradermally into ear pinnae. After infection mice received 15 mg/kg of COX-2 inhibitor (NS-398) or DMSO (mock-treated mice) intraperitoneally daily for 7 days. Data represent two independent experiments. **(A)** At 8 days post-infection mice were sacrificed and organs were harvested and CLN (Left panel) and spleen (Right panel) were weighted. Statistical significance was determined using ANOVA ($*p < 0.05$; $****p < 0.0001$). **(B)** At 8 days post-infection mice were sacrificed and organs were harvested and analyzed for their CLN (Left panel) or spleen (Right panel) bacterial loads by plating homogenates on nutrient agar. Statistical significance was determined using unpaired, two-tailed Student's *t*-test ($**p < 0.005$). **(C)** At 8 days post-infection, total RNA of the CLN was extracted and analyzed for expression of genes involved in inflammatory response by reverse transcription real-time PCR. Results are given as fold increase compared to the signal obtained for mock-infected mice. Statistical significance was determined using unpaired, two-tailed Student's *t*-test ($**p < 0.005$; $***p < 0.001$; $****p < 0.0001$).

Left panel) and no significant response was observed in the spleen (Figure 4B, Right Panel).

The local inflammatory response in NS-398-treated mice was characterized by a strong decrease of *Il10* and *Nos2* expression and in a lesser extent of *Ccr7* and *Foxp3* compared to untreated mice. However, *Ifng* mRNA level strongly increased following NS-398 treatment. All the other genes tested did not exhibit any significant changes in their expression (Figure 4C).

Altogether, these results indicate that inhibition of COX-2 decreases bacterial load in CLN by acting on *Il10* and *Ifng* expression levels.

DISCUSSION

In this study, we investigated the impact of *Brucella* spp. infection on the COX-2 metabolic pathway. We first assessed the ability of *B. abortus* to stimulate AA production in DC. We also confirmed using a genomic approach that PG pathway downstream partners were overexpressed. We observed that *B. abortus* triggers a higher level of AA in human moDC infected with *B. abortus* compared to cells infected with other intracellular bacteria (*C. burnetii*, *T. whipplei*, *O. tsutsugamushi*). This response was accompanied by an increase of *Ptgs2* mRNA levels in both human and murine DC. Interestingly, we did not detect any major change in the expression profile of the leukotriene pathway and specifically for *ALOX5*, the gene encoding for the 5-LO in humans. This result is contradictory with previously published data showing that 5-LO was strongly up-regulated in *Brucella* infected spleens as early as one-week post-infection in mice and was accompanied by leukotriene B₄ and lipoxin A₄ production (Fahel et al., 2015). This discrepancy may be explained by the *in vitro* DC model used in our study compared to total splenocytes used in the study published in 2015 and also possible differences between the mouse and human models. Moreover, cells expressing 5-LO have not yet been identified *in vivo*, thus, it could be possible that DC are not the source of leukotrienes during *B. abortus* infection.

Transcriptional profiling showed an increase of *PTGER2*, *PTGER4*, and *PTGSD* expression in infected human moDC compared to unstimulated cells. Interestingly, it has been reported that PGE₂ can stimulate IL-10 secretion by mature BMDC leading to a decrease of IL-12 secretion. This effect is dependent on the expression of EP2/EP4 receptors encoded by *Ptger2* and *Ptger4*, respectively (Harizi et al., 2003). Similarly, macrophage treatments with PG analogs stimulating the EP2/EP4 receptors lead to an increase of IL-10 secretion and concomitantly a decrease of TNF- α secretion (Shinomiya et al., 2001). Moreover, in a *Pseudomonas aeruginosa* intranasal infection model, this immunomodulatory effect towards IL-10 secretion seems to be mediated by EP2 since EP2^{-/-} mice presented a lower bacterial burden in the lung (Sadikot et al., 2007). Considering the negative impact of IL-10 on the establishment of a protective immune response during brucellosis, PG pathway could contribute to bacterial persistence.

Then, we determined the levels of expression of *Ptgs2* *in vivo* using different infection routes. For this purpose, we chose to study physiologically relevant inoculation routes such as

nasal, oral, and conjunctival infection routes that mimic natural exposure to bacteria. We also included the intradermal infection route often used for vaccination (Kim et al., 2012). We focused on CLN since CLN also drains the eye (Hamrah and Dana, 2007) and the nasal mucosa (Wolters et al., 1999) and we previously shown that this organ was preferentially targeted by *Brucella* after oral inoculation (von Bargen et al., 2014). COX-2 being important during inflammatory process, contrary to the *in vitro* experiments, we decided to use *B. melitensis* as it seems that this species induced an enhanced inflammation in CLN compared to *B. abortus*.

As anticipated, we observed a tropism of bacteria for the CLN and a marked lymphadenopathy compared to mock-treated mice as soon as 8 days post-infection in mice infected intradermally and in all conditions at 29 days post-infection. This effect was particularly marked when using the intradermal route. When looking at the local immune response in CLN, we observed that the intradermal route induced a particular gene signature characterized by a strong up-regulation of *Ifng* and *Ptgs2* mRNA levels compared to the other tested routes. However, we cannot exclude a difference in terms of kinetics due to the fact that intradermal infection delivers directly the bacteria into the tissue. On the contrary, oral, intranasal, and conjunctival inoculations expose bacteria to physiological barriers such as mucosal surfaces that can delay the bacterial trafficking to the draining lymph nodes. Indeed, we observed that at 8 days post-infection bacterial load was significantly higher after intradermal infection but this difference tends to be reduced at later time points. Moreover, using a *Yersinia pestis* intradermal infection model it has been shown that bacterial dissemination does not involve bacteria active transport through phagocytes to the draining lymph nodes (Gonzalez et al., 2015). At the beginning of the chronic phase (29 days post-infection), we observed a strong decrease of *Ifng*, *Il6*, *Gzmb* concomitant with and an increase of *Nos2*, *Ptgs2* mRNA levels. Interestingly, it has recently been shown that synergic induction of COX-2 by IFN- γ and TNF- α limits type-1 immune response in tumor microenvironment by concomitant action of IL-10, NOS2, and Indoleamine 2,3-dioxygenase (Wong et al., 2016). Thus, we can hypothesize that the induction of *Ptgs2* is beneficial for the bacteria.

We then used a specific COX-2 inhibitor (NS-398) and demonstrated the beneficial potential of such an inhibition in favor of the host. Indeed, COX-2 inhibition correlated with a decrease in bacterial load in CLN concomitant with a decrease of *Ccr7*, *Il10*, *Foxp3*, *Nos2* mRNA levels and an increase of *Ifng* expression. At early time points, the induction of *Ptgs2* gene expression could be used by the bacteria to stimulate not only their replication but also the migration of the infected cells to other secondary organs as suggested by the effect on *Ccr7* expression. It is also known that Th1 immune response characterized by IFN- γ and IL-12 secretion is important to control infection and that production of IL-10 has a negative impact in the course of brucellosis control by the host (Zhan and Cheers, 1995; Brandao et al., 2012). Then, we can hypothesize that the beneficial effect observed in the presence of COX-2 inhibitor treatment can be associated with a strong Th1 response. Moreover, it has been demonstrated that in absence of IL-10,

mice are more resistant to *Brucella* infection and this effect is correlated with an increase of pro-inflammatory cytokine secretion (Corsetti et al., 2013). The decrease of *Il10* mRNA levels is also accompanied by a decrease of *Foxp3* expression, a marker of regulatory T lymphocytes (T-reg). After intraperitoneal infection, it has been shown that CD4⁺CD25⁺ T cells produce IL-10 during acute brucellosis that favor bacterial persistence in mice (Xavier et al., 2013). CD4⁺CD25⁺ T cell population in parotid and retropharyngeal lymph nodes has been shown to increase following conjunctival infection in sheep (Suraud et al., 2007). CD4⁺CD25⁺ T cells with regulatory activity express the transcription factor *Foxp3* (Hori et al., 2003). Interestingly, following NS-398 treatment, we observed a significant decrease of *Foxp3* expression. This finding is in accordance with the decrease of *Il10* expression. Thus, we hypothesize that infection stimulates regulatory/suppressor T-cells that can favor bacterial persistence through the secretion of IL-10. A similar effect has been described during *Mycobacterium tuberculosis* infection where COX-2/PGE₂ axis stimulates T-reg expansion (Garg et al., 2008; Holla et al., 2016). Thereby, T-reg accumulation contributes to the decrease of bacterial clearance in infected mice (Kursar et al., 2007). During *Francisella tularensis* live vaccine strain intranasal infection, the inhibition of the COX-1 and COX-2 increased the number of IFN- γ producing T lymphocytes in the lung leading to a decrease of the bacterial load (Woolard et al., 2008). This is correlated with our observations showing that COX-2 inhibition leads to an increase of *Ifng* mRNA levels in CLN.

Our results corroborate other studies which have investigated the involvement of the COX-2 pathway during bacterial infection by *Pseudomonas aeruginosa* (Sadikot et al., 2007), *Burkholderia pseudomallei* (Asakrah et al., 2013), and *Streptococcus pyogenes* (Goldmann et al., 2010). COX-2 inhibition translates into a decrease of bacterial burden in CLN. It would be interesting to look at later time points to know whether or not COX-2 inhibition can cause a bacterial clearance. Taken together, our results suggest that *Brucella* has taken advantage of the PG pathway to survive and replicate in host cells and that COX-2 inhibition is not only crucial to control brucellosis but also other bacterial infectious diseases.

REFERENCES

- Agard, M., Asakrah, S., and Morici, L. A. (2013). PGE(2) suppression of innate immunity during mucosal bacterial infection. *Front. Cell. Infect. Microbiol.* 3:45. doi: 10.3389/fcimb.2013.00045
- Asakrah, S., Nieves, W., Mahdi, Z., Agard, M., Zea, A. H., Roy, C. J., et al. (2013). Post-exposure therapeutic efficacy of COX-2 inhibition against *Burkholderia pseudomallei*. *PLoS Negl. Trop. Dis.* 7:e2212. doi: 10.1371/journal.pntd.0002212
- Barquero-Calvo, E., Chaves-Olarte, E., Weiss, D. S., Guzmán-Verri, C., Chacón-Díaz, C., Rucavado, A., et al. (2007). *Brucella abortus* uses a stealthy strategy to avoid activation of the innate immune system during the onset of infection. *PLoS ONE* 2:e631. doi: 10.1371/journal.pone.0000631
- Barry, A. O., Boucherit, N., Mottola, G., Vadovic, P., Trouplin, V., Soubeyran, P., et al. (2012). Impaired stimulation of p38 α -MAPK/Vps41-HOPS by LPS from pathogenic *Coxiella burnetii* prevents trafficking to microbicidal phagolysosomes. *Cell Host Microbe* 12, 751–763. doi: 10.1016/j.chom.2012.10.015

AUTHOR CONTRIBUTIONS

AG, J-PG, and J-LM conceived and designed the experiments. AG, LG, AP, and KVB performed the experiments. AG, LG, and J-PG analyzed the data. AG and J-PG wrote the paper.

FUNDING

J-PG was financed by an institutional grant from the Centre National de la Recherche Scientifique for equipment, consommables, and salary, by an institutional grant from the Institut National de la Santé et de la Recherche Médicale for equipment and consommables and by the grant n°CS2012-2016 from the Fondation pour la Recherche Médicale, for equipment and consommables. AG and AP were financed by a fellowship from the Aix Marseille Université. J-LM was financed by the Assistance Publique des hôpitaux de Marseille for ressources and salary. J-PG and KVB were financed by the Agence National de la Recherche, grant n° ANR10-BLAN-000 for ressources and salary, respectively.

ACKNOWLEDGMENTS

The authors would like to thank Hugues Lelouard, Johnny Bonnardel, and Clara Degos for providing and supporting in establishment of protocols and for valuable discussions. We deeply thank Dr. Ignacio Moriyon for providing the *Brucella* strains as well as Dr. Philippe Pierre for the J558L GM-CSF producing cell line. Also, we are very grateful to the BSL-3 core facilities staff at the Immunophenomique Center (CIPHE).

SUPPLEMENTARY MATERIAL

The Supplementary Material for this article can be found online at: <http://journal.frontiersin.org/article/10.3389/fmicb.2016.01987/full#supplementary-material>

- Bowman, C. C., and Bost, K. L. (2004). Cyclooxygenase-2-mediated prostaglandin E2 production in mesenteric lymph nodes and in cultured macrophages and dendritic cells after infection with *Salmonella*. *J. Immunol.* 172, 2469–2475. doi: 10.4049/jimmunol.172.4.2469
- Brandao, A. P., Oliveira, F. S., Carvalho, N. B., Vieira, L. Q., Azevedo, V., Macedo, G. C., et al. (2012). Host susceptibility to *Brucella abortus* infection is more pronounced in IFN-gamma knockout than IL-12/beta2-microglobulin double-deficient mice. *Clin. Dev. Immunol.* 2012:589494. doi: 10.1155/2012/589494
- Chandrasekharan, N. V., Dai, H., Roos, K. L., Evanson, N. K., Tomsik, J., Elton, T. S., et al. (2002). COX-3, a cyclooxygenase-1 variant inhibited by acetaminophen and other analgesic/antipyretic drugs: cloning, structure, and expression. *Proc. Natl. Acad. Sci. U.S.A.* 99, 13926–13931. doi: 10.1073/pnas.162468699
- Chandrasekharan, N. V., and Simmons, D. L. (2004). The cyclooxygenases. *Genome Biol.* 5:241. doi: 10.1186/gb-2004-5-9-241
- Conde-Álvarez, R., Arce-Gorvel, V., Iriarte, M., Manček-Keber, M., Barquero-Calvo, E., Palacios-Chaves, L., et al. (2012). The lipopolysaccharide core of

- Brucella abortus* acts as a shield against innate immunity recognition. *PLoS Pathog.* 8:e1002675. doi: 10.1371/journal.ppat.1002675
- Corsetti, P. P., de Almeida, L. A., Carvalho, N. B., Azevedo, V., Silva, T. M., Teixeira, H. C., et al. (2013). Lack of endogenous IL-10 enhances production of proinflammatory cytokines and leads to *Brucella abortus* clearance in mice. *PLoS ONE* 8:e74729. doi: 10.1371/journal.pone.0074729
- Dean, A. S., Crump, L., Greter, H., Hattendorf, J., Schelling, E., and Zinsstag, J. (2012). Clinical manifestations of human brucellosis: a systematic review and meta-analysis. *PLoS Negl. Trop. Dis.* 6:e1929. doi: 10.1371/journal.pntd.0001929
- Ecker, J., Scherer, M., Schmitz, G., and Liebisch, G. (2012). A rapid GC-MS method for quantification of positional and geometric isomers of fatty acid methyl esters. *J. Chromatogr. B Anal. Technol. Biomed. Life Sci.* 897, 98–104. doi: 10.1016/j.jchromb.2012.04.015
- Fahel, J. S., de Souza, M. B., Gomes, M. T., Corsetti, P. P., Carvalho, N. B., Marinho, F. A., et al. (2015). 5-Lipoxygenase negatively regulates Th1 response during *Brucella abortus* infection in mice. *Infect. Immun.* 83, 1210–1216. doi: 10.1128/IAI.02592-14
- Franco, M. P., Mulder, M., Gilman, R. H., and Smits, H. L. (2007). Human brucellosis. *Lancet Infect. Dis.* 7, 775–786. doi: 10.1016/S1473-3099(07)70286-4
- Garg, A., Barnes, P. F., Roy, S., Quiroga, M. F., Wu, S., García, V. E., et al. (2008). Mannose-capped lipaarabinomannan- and prostaglandin E2-dependent expansion of regulatory T cells in human *Mycobacterium tuberculosis* infection. *Eur. J. Immunol.* 38, 459–469. doi: 10.1002/eji.200737268
- Goldmann, O., Hertzén, E., Hecht, A., Schmidt, H., Lehne, S., Norrby-Teglund, A., et al. (2010). Inducible cyclooxygenase released prostaglandin E2 modulates the severity of infection caused by *Streptococcus pyogenes*. *J. Immunol.* 185, 2372–2381. doi: 10.4049/jimmunol.1000838
- Gonzalez, R. J., Lane, M. C., Wagner, N. J., Weening, E. H., and Miller, V. L. (2015). Dissemination of a highly virulent pathogen: tracking the early events that define infection. *PLoS Pathog.* 11:e1004587. doi: 10.1371/journal.ppat.1004587
- Gorvel, L., Al Moussawi, K., Ghigo, E., Capo, C., Mege, J. L., and Desnues, B. (2010). *Tropheryma whipplei*, the Whipple's disease bacillus, induces macrophage apoptosis through the extrinsic pathway. *Cell Death Dis.* 1:e34. doi: 10.1038/cddis.2010.11
- Grilló, M. J., Blasco, J. M., Gorvel, J. P., Moriyón, I., and Moreno, E. (2012). What have we learned from brucellosis in the mouse model? *Vet. Res.* 43, 29. doi: 10.1186/1297-9716-43-29
- Hamrah, P., and Dana, M. R. (2007). Corneal antigen-presenting cells. *Chem. Immunol. Allergy* 92, 58–70. doi: 10.1159/000099254
- Harizi, H., Corcuff, J. B., and Gualde, N. (2008). Arachidonic-acid-derived eicosanoids: roles in biology and immunopathology. *Trends Mol. Med.* 14, 461–469. doi: 10.1016/j.molmed.2008.08.005
- Harizi, H., Grosset, C., and Gualde, N. (2003). Prostaglandin E2 modulates dendritic cell function via EP2 and EP4 receptor subtypes. *J. Leukoc. Biol.* 73, 756–763. doi: 10.1189/jlb.1002483
- Holla, S., Stephen-Victor, E., Prakhar, P., Sharma, M., Saha, C., Udupa, V., et al. (2016). Mycobacteria-responsive sonic hedgehog signaling mediates programmed death-ligand 1- and prostaglandin E2-induced regulatory T cell expansion. *Sci. Rep.* 6:24193. doi: 10.1038/srep24193
- Hori, S., Nomura, T., and Sakaguchi, S. (2003). Control of regulatory T cell development by the transcription factor Foxp3. *Science* 14, 1057–1061.
- Kim, Y. C., Jarrahan, C., Zehrung, D., Mitragotri, S., and Prausnitz, M. R. (2012). Delivery systems for intradermal vaccination. *Curr. Top. Microbiol. Immunol.* 351, 77–112. doi: 10.1007/82_2011_123
- Kursar, M., Koch, M., Mittrücker, H. W., Nouailles, G., Bonhagen, K., Kamradt, T., et al. (2007). Cutting edge: regulatory T cells prevent efficient clearance of *Mycobacterium tuberculosis*. *J. Immunol.* 178, 2661–2665. doi: 10.4049/jimmunol.178.5.2661
- Lapaque, N., Moriyon, I., Moreno, E., and Gorvel, J. P. (2005). *Brucella* lipopolysaccharide acts as a virulence factor. *Curr. Opin. Microbiol.* 8, 60–66. doi: 10.1016/j.mib.2004.12.003
- Lapaque, N., Muller, A., Alexopoulou, L., Howard, J. C., and Gorvel, J. P. (2009). *Brucella abortus* induces Irgm3 and Irga6 expression via type-I IFN by a MyD88-dependent pathway, without the requirement of TLR2. TLR4, TLR5 and TLR9. *Microb. Pathog.* 47, 299–304. doi: 10.1016/j.micpath.2009.09.005
- Lepage, G., and Roy, C. C. (1986). Direct transesterification of all classes of lipids in a one-step reaction. *J. Lipid Res.* 27, 114–120.
- López-Urrutia, L., Alonso, A., Bayón, Y., Nieto, M. L., Orduña, A., and Sánchez Crespo, M. (2001). *Brucella* lipopolysaccharides induce cyclooxygenase-2 expression in monocytic cells. *Biochem. Biophys. Res. Commun.* 289, 372–375. doi: 10.1006/bbrc.2001.5995
- Martirosyan, A., Moreno, E., and Gorvel, J. P. (2011). An evolutionary strategy for a stealthy intracellular *Brucella* pathogen. *Immunol. Rev.* 240, 211–234. doi: 10.1111/j.1600-065X.2010.00982.x
- Moreno, E. (2014). Retrospective and prospective perspectives on zoonotic brucellosis. *Front. Microbiol.* 5:213. doi: 10.3389/fmicb.2014.00213
- Papadopoulos, A., Gagnaire, A., Degos, C., de Chastellier, C., and Gorvel, J. P. (2016). *Brucella* discriminates between mouse dendritic cell subsets upon in vitro infection. *Virulence* 7, 33–44. doi: 10.1080/21505594.2015.1108516
- Pappas, G. (2010). The changing *Brucella* ecology: novel reservoirs, new threats. *Int. J. Antimicrob. Agents* 36(Suppl. 1), S8–S11. doi: 10.1016/j.ijantimicag.2010.06.013
- Pizarro-Cerdá, J., Méresse, S., Parton, R. G., van der Goot, G., Sola-Landa, A., Lopez-Goni, I., et al. (1998). *Brucella abortus* transits through the autophagic pathway and replicates in the endoplasmic reticulum of nonprofessional phagocytes. *Infect. Immun.* 66, 5711–5724.
- Rangel Moreno, J., Estrada García, I., De La Luz García Hernández, M., Aguilar Leon, D., Marquez, R., and Hernández Pando, R. (2002). The role of prostaglandin E2 in the immunopathogenesis of experimental pulmonary tuberculosis. *Immunology* 106, 257–266. doi: 10.1046/j.1365-2567.2002.01403.x
- Sadikot, R. T., Zeng, H., Azim, A. C., Joo, M., Dey, S. K., Breyer, R. M., et al. (2007). Bacterial clearance of *Pseudomonas aeruginosa* is enhanced by the inhibition of COX-2. *Eur. J. Immunol.* 37, 1001–1009. doi: 10.1002/eji.200636636
- Salcedo, S. P., Marchesini, M. I., Lelouard, H., Fugier, E., Jolly, G., Balor, S., et al. (2008). *Brucella* control of dendritic cell maturation is dependent on the TIR-containing protein Btp1. *PLoS Pathog.* 4:e21. doi: 10.1371/journal.ppat.0040021
- Schutter, M. E., and Dick, R. P. (2000). Comparison of fatty acid methyl ester (FAME) methods for characterizing microbial communities. *Soil Sci. Soc. Am. J.* 64, 1659–1668. doi: 10.2136/sssaj2000.6451659x
- Seleem, M. N., Boyle, S. M., and Sriranganathan, N. (2010). Brucellosis: a re-emerging zoonosis. *Vet. Microbiol.* 140, 392–398. doi: 10.1016/j.vetmic.2009.06.021
- Shinomiya, S., Naraba, H., Ueno, A., Utsunomiya, I., Maruyama, T., Ohuchida, S., et al. (2001). Regulation of TNF α and interleukin-10 production by prostaglandins I(2) and E(2): studies with prostaglandin receptor-deficient mice and prostaglandin E-receptor subtype-selective synthetic agonists. *Biochem. Pharmacol.* 61, 1153–1160. doi: 10.1016/S0006-2952(01)00586-X
- Steer, S. A., and Corbett, J. A. (2003). The role and regulation of COX-2 during viral infection. *Viral Immunol.* 16, 447–460. doi: 10.1089/088282403771926283
- Stevens, M. G., and Olsen, S. C. (1994). In vitro effects of live and killed *Brucella abortus* on bovine cytokine and prostaglandin E2 production. *Vet. Immunol. Immunopathol.* 40, 149–161. doi: 10.1016/0165-2427(94)90030-2
- Suraud, V., Olivier, M., Bodier, C. C., and Guilloteau, L. A. (2007). Differential expression of homing receptors and vascular addressins in tonsils and draining lymph nodes: effect of *Brucella* infection in sheep. *Vet. Immunol. Immunopathol.* 15, 239–250. doi: 10.1016/j.vetimm.2006.11.008
- Van den Broeck, W., Derore, A., and Simoens, P. (2006). Anatomy and nomenclature of murine lymph nodes: descriptive study and nomenclature standardization in BALB/cAnNCrl mice. *J. Immunol. Methods* 30, 12–19. doi: 10.1016/j.jim.2006.01.022
- von Bargen, K., Gagnaire, A., Arce-Gorvel, V., de Bovis, B., Baudimont, F., Chasson, L., et al. (2014). Cervical lymph nodes as a selective niche for *Brucella* during oral infections. *PLoS ONE* 10:e0121790. doi: 10.1371/journal.pone.0121790
- Wolters, D. A., Coenen-de Roo, C. J., Mebius, R. E., van der Cammen, M. J., Tirion, F., Miltenburg, A. M., et al. (1999). Intranasally induced immunological tolerance is determined by characteristics of the draining lymph nodes: studies with OVA and human cartilage gp-39. *J. Immunol.* 15, 1994–1998.

- Wong, J. L., Obermajer, N., Odunsi, K., Edwards, R. P., and Kalinski, P. (2016). Synergistic COX2 Induction by IFN γ and TNF α Self-Limits Type-1 immunity in the human tumor microenvironment. *Cancer Immunol. Res.* 4, 303–311. doi: 10.1158/2326-6066.CIR-15-0157
- Woolard, M. D., Hensley, L. L., Kawula, T. H., and Frelinger, J. A. (2008). Respiratory *Francisella tularensis* live vaccine strain infection induces Th17 cells and prostaglandin E2, which inhibits generation of gamma interferon-positive T cells. *Infect. Immun.* 76, 2651–2659. doi: 10.1128/IAI.01412-07
- Xavier, M. N., Winter, M. G., Spees, A. M., Nguyen, K., Atluri, V. L., Silva, T. M., et al. (2013). CD4+ T cell-derived IL-10 promotes *Brucella abortus* persistence via modulation of macrophage function. *PLoS Pathog.* 9:e1003454. doi: 10.1371/journal.ppat.1003454
- Zhan, Y., and Cheers, C. (1995). Endogenous interleukin-12 is involved in resistance to *Brucella abortus* infection. *Infect. Immun.* 63, 1387–1390.
- Zhan, Y., Liu, Z., and Cheers, C. (1996). Tumor necrosis factor alpha and interleukin-12 contribute to resistance to the intracellular bacterium *Brucella abortus* by different mechanisms. *Infect. Immun.* 64, 2782–2786.
- Conflict of Interest Statement:** The authors declare that the research was conducted in the absence of any commercial or financial relationships that could be construed as a potential conflict of interest.

Copyright © 2016 Gagnaire, Gorvel, Papadopoulos, Von Bargen, Mège and Gorvel. This is an open-access article distributed under the terms of the Creative Commons Attribution License (CC BY). The use, distribution or reproduction in other forums is permitted, provided the original author(s) or licensor are credited and that the original publication in this journal is cited, in accordance with accepted academic practice. No use, distribution or reproduction is permitted which does not comply with these terms.



Extended Multilocus Sequence Analysis to Describe the Global Population Structure of the Genus *Brucella*: Phylogeography and Relationship to Biovars

Adrian M. Whatmore*, Mark S. Koylass, Jakub Muchowski, James Edwards-Smallbone, Krishna K. Gopaul and Lorraine L. Perrett

FAO/WHO Collaborating Centre for Reference and Research in Brucellosis and OIE Brucellosis Reference Laboratory, Department of Bacteriology, Animal and Plant Health Agency, Addlestone, UK

OPEN ACCESS

Edited by:

Jorge Blanco,
University of Santiago de Compostela,
Spain

Reviewed by:

Vanesa García,
University of Santiago de Compostela,
Spain

Ana Cristina Ferreira,
Instituto Nacional de Investigação
Agrária e Veterinária, Portugal

*Correspondence:

Adrian M. Whatmore
adrian.whatmore@apha.gsi.gov.uk

Specialty section:

This article was submitted to
Infectious Diseases,
a section of the journal
Frontiers in Microbiology

Received: 10 November 2016

Accepted: 06 December 2016

Published: 21 December 2016

Citation:

Whatmore AM, Koylass MS,
Muchowski J, Edwards-Smallbone J,
Gopaul KK and Perrett LL (2016)
Extended Multilocus Sequence
Analysis to Describe the Global
Population Structure of the Genus
Brucella: Phylogeography and
Relationship to Biovars.
Front. Microbiol. 7:2049.
doi: 10.3389/fmicb.2016.02049

An extended multilocus sequence analysis (MLSA) scheme applicable to the *Brucella*, an expanding genus that includes zoonotic pathogens that severely impact animal and human health across large parts of the globe, was developed. The scheme, which extends a previously described nine locus scheme by examining sequences at 21 independent genetic loci in order to increase discriminatory power, was applied to a globally and temporally diverse collection of over 500 isolates representing all 12 known *Brucella* species providing an expanded and detailed understanding of the population genetic structure of the group. Over 100 sequence types (STs) were identified and analysis of data provided insights into both the global evolutionary history of the genus, suggesting that early emerging *Brucella abortus* lineages might be confined to Africa while some later lineages have spread worldwide, and further evidence of the existence of lineages with restricted host or geographical ranges. The relationship between biovar, long used as a crude epidemiological marker, and genotype was also examined and showed decreasing congruence in the order *Brucella suis* > *B. abortus* > *Brucella melitensis*. Both the previously described nine locus scheme and the extended 21 locus scheme have been made available at <http://pubmlst.org/brucella/> to allow the community to interrogate existing data and compare with newly generated data.

Keywords: *Brucella*, brucellosis, multilocus sequence, molecular typing, zoonosis

INTRODUCTION

Brucellosis remains one of the world's most important zoonotic diseases and continues to have a significant impact on animal and human health in much of the world particularly in South America, Southern Europe, Africa, the Middle East, and much of Asia (Pappas et al., 2006). Recent years have seen the beginning of an expansion of the genus *Brucella* (Whatmore, 2009) from the six classically identified species [*Brucella abortus* (cattle), *Brucella melitensis* (sheep and goats), *Brucella suis* (pigs, hares, reindeer), *Brucella canis* (dogs), *B. ovis* (sheep), and *B. neotomae* (rodents)] with the description of six additional species (*Brucella microti* (voles), *Brucella pinnipedialis* (pinnipeds), *Brucella ceti* (cetaceans), *Brucella papionis* (baboons), *Brucella vulpis* (foxes), and *Brucella inopinata*

(isolated from a human case—natural host unknown). Although *Brucella* have long been known to represent a highly homogeneous genus, even for a time being classified as a monospecific genus (Verger et al., 1985), the known diversity of the group was extended greatly by the description of this latter species (De et al., 2008; Wattam et al., 2012) and *B. vulpis* (Hofer et al., 2012; Scholz et al., 2016). These groups are often described as “atypical” in the literature reflecting their genetic separation from classical species. A number of other isolates that await formal taxonomic description originating from sources as diverse as humans, frogs, fish, and additional rodents will likely extend diversity within both the classical group and newly emerging “atypical” *Brucella* in the near future (Tiller et al., 2010a,b; Godfroid et al., 2011; Eisenberg et al., 2012; Scholz and Vergnaud, 2013; Whatmore et al., 2015; Eisenberg et al., 2016).

Of the species described above *B. melitensis*, *B. abortus*, and *B. suis* are the most significant in terms of both animal and human disease impact. Where achieved, control has reflected a combination of measures including animal vaccination and/or control strategies (“test and slaughter”) along with improved food hygiene standards. International trade standards are applied as part of efforts to help control spread of these pathogens (World Organisation for Animal Health, 2011). *B. canis* and *B. ovis* are less economically significant pathogens of animals and, of these species, only *B. canis* is known to cause rare infections of humans (Marzetti et al., 2013). The significance of *Brucella* infection in the marine ecosystem remains uncertain (Nymo et al., 2011) and there is only evidence of one genotype causing serious, but rarely reported, naturally acquired infections of humans (Whatmore et al., 2008). *B. inopinata* has been confined to a single human case with no reservoir of infection identified and, while *B. microti* appears highly virulent in its natural host and other rodents (Jiménez de Bagüés et al., 2010), any pathogenic potential for man remains to be elucidated.

The three major species, *B. melitensis*, *B. abortus*, and *B. suis* are divided into biovars by a biotyping scheme that for many years has been the gold standard for *Brucella* characterisation at both the species and subspecies level. The scheme, based on a combination of growth characteristics, biochemical reactions, serotyping and bacteriophage typing, distinguishes the six classical species and further subdivides the major species into seven (*B. abortus*), five (*B. suis*) or three (*B. melitensis*) biovars, respectively. The homogeneity of the classical species meant that slow progress was made in identifying molecular markers to consistently define species and particularly to type at the subspecies level. Thus, in spite of the obviously limited resolution offered, biovars became commonly used epidemiological markers with particular biovars associated with certain geographical areas or certain hosts. However biotyping in its traditional form is expensive, time-consuming, involves hazardous culture and its rather subjective nature means it needs to be carried out by highly experienced scientists and is likely prone to inconsistency between laboratories. Further this traditional method is likely to become increasingly less relevant as the genus expands and new species emerge that diverge from classical criteria. As more molecular diversity has become apparent with technological advances biotyping is increasingly being replaced by the use of

frontline molecular tools notably various diagnostic PCRs based on genomic deletions or SNPs (Foster et al., 2008; Gopaul et al., 2008, 2010; López-Góñi et al., 2008). However the performance of such tools is critically dependent on their design being based on an accurate and comprehensive understanding of the population genetic structure of the groups they are designed to separate (Keim et al., 2004).

This paper updates current understanding of the population structure of *Brucella* based on an extended (from an existing nine locus scheme—Whatmore et al., 2007) and extensive multilocus sequence analysis (MLSA) examining 21 independent genetic loci applied to a geographically and temporally diverse collection of over 500 *Brucella* isolates. The data significantly add to understanding of the genetic diversity of the group providing insights into evolutionary history, phylogeography, the relationship between genotype and biovar and provides a comprehensive framework to further understanding of these issues, for the future placement of newly emerging or atypical isolates and for the rational design of robust and accurate rapid diagnostic assays.

METHODS

Bacteriology

Isolates were minimally cultured on serum dextrose agar and DNA preparations or crude lysates were prepared by standard procedures described previously (Whatmore et al., 2006) to serve as PCR template. Biotyping was undertaken by standard approaches as described elsewhere (Alton et al., 1988; Whatmore, 2009).

MLSA

A 21 locus MLSA scheme (BruMLSA21) was developed by identifying an additional 12 informative housekeeping gene loci and adding these to the BruMLSA9 scheme described earlier (Whatmore et al., 2007). Loci and corresponding primers used in the scheme are described in **Table S1**. These were designed such as that identical PCR procedures could be applied to all 21 loci and thus PCR parameters and downstream purification and sequencing procedures were all as described previously (Whatmore et al., 2007). BruMLSA21 profiles of 508 isolates representing all 12 *Brucella* species (172 *B. abortus*, 84 *B. melitensis*, 100 *B. suis*, 24 *B. canis*, 11 *B. ovis*, 73 *B. ceti*, 20 *B. pinnipedialis*, 7 *B. microti*, 3 *B. neotomae*, 2 *B. papionis*, 2 *B. vulpis*, 1 *B. inopinata* and 9 unclassified *Brucella* isolates) were obtained and used in the analysis described here. Sequences of two strains *B. abortus* 9–941 and *B. abortus* 2308 were extracted from previously published whole genome sequences (Chain et al., 2005; Halling et al., 2005).

Data Analysis

A representative strain of each genotype (sequence type or ST) was used for phylogenetic analysis. Sequences of the 21 loci were concatenated to produce a 10,257 bp sequence (including indels) for each genotype. Phylogenetic analysis was performed with the MEGA software, Version 5.2 (Tamura et al., 2011). Neighbour joining trees were constructed using the Jukes-Cantor model and

the percentage bootstrap confidence levels of internal branches were calculated from 1000 resamplings of the original data.

Minimum spanning trees were constructed in Bionumerics using the predefined template and the categorical coefficient. STs are represented by circles and the size of the circle is indicative of the number of isolates of that particular type. The coloring inside the circles indicates the *Brucella* species (**Figure 2**) or geographical origin (**Figures 4, 6, 8**). The different line types connecting genotypes reflect different numbers of shared loci as described in figure legends. The maximum neighbor difference used to create complexes indicated by the gray shading is given in individual figure legends.

PubMLST

In common with MLST/MLSA schemes for most other bacteria, an open and expandable database has been established at the PubMLST website using the Bacterial Isolate Genome Sequence Database (BIGSdb) platform (Jolley and Maiden, 2010). Databases containing allele descriptions and allelic profiles for both BruMLSA9 (Whatmore et al., 2007) and the extended BruMLSA21 described here, and a corresponding isolate database, are available at <http://pubmlst.org/brucella/> where data can be interrogated and submissions of new data are encouraged. All BruMLSA21 data that forms the basis of the analyses described in this communication, as well as a significant volume of previously undescribed BruMLSA9 data, have been deposited in these databases.

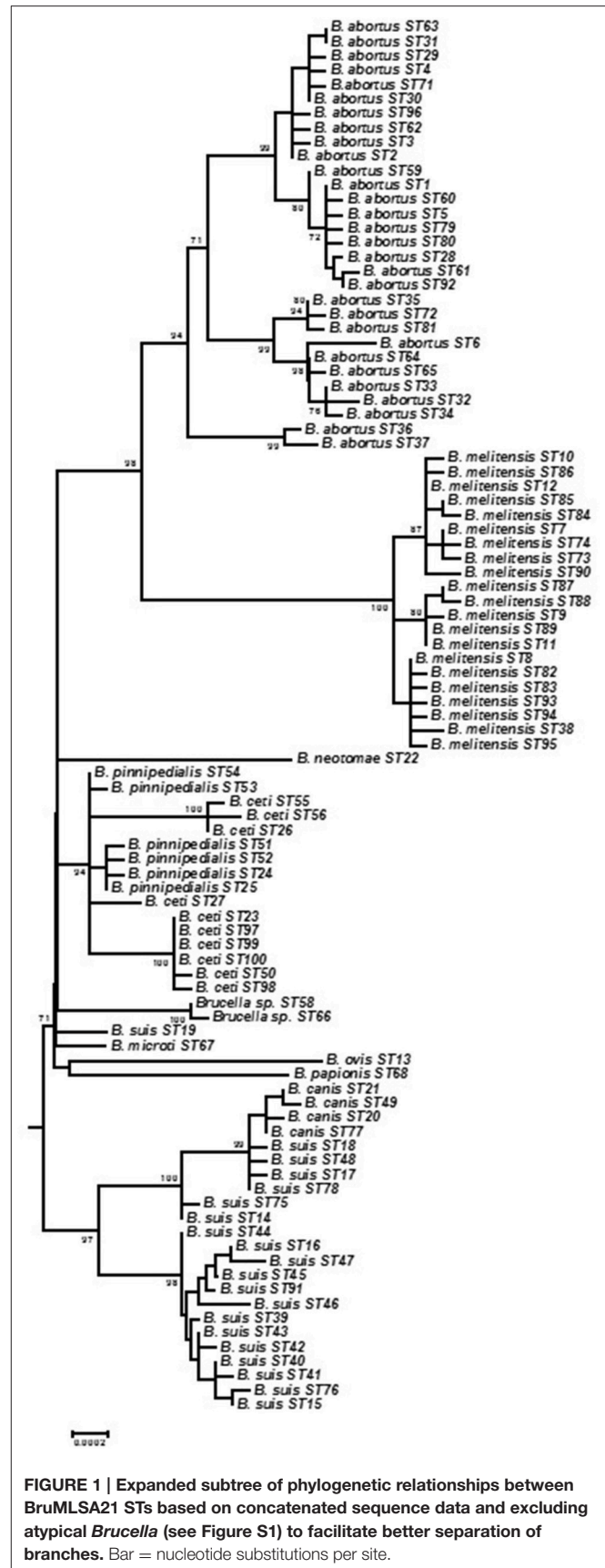
Other Molecular Testing

Confirmation of isolates as *B. abortus* vaccine strains S19 and RB51 was performed using previously described PCR assays (Sangari and Agüero, 1994; Vemulapalli et al., 1999) and confirmatory SNP based typing (Gopaul et al., 2010).

RESULTS AND DISCUSSION

Extension of Existing MLSA Scheme

A previously described MLSA scheme based on nine loci (BruMLSA9) provided limited resolution dividing 161 *Brucella* isolates into only 27 STs reflecting the relative genetic homogeneity of the classical *Brucella* species (Whatmore et al., 2007). In order to provide a supplementary scheme with increased resolution this scheme was extended by the addition of fragments representing 12 additional informative housekeeping genes to characterize 21 distinct loci in total. Here we describe its application to a temporally and geographically diverse collection of over 500 *Brucella* isolates representing all known species and biovars, and including all type strains, to describe the global population structure of the genus. The collection divided into 101 BruMLSA21 STs (**Table S2**) with the number of alleles varying from 10 in the case of *caiA* and *fbaA* to 27 in the case of *glk*, a gene included in BruMLSA9, and previously shown to be the most variable in this scheme. Strains of *B. vulpis* and the *B. inopinata*-like isolate BO2 failed to amplify a product at one locus (*mviM*) and were not assigned a BruMLSA21 ST although they have a full BruMLSA9 profile and ST. In addition the application of BruMLSA9 to a larger isolate collection than previously increased



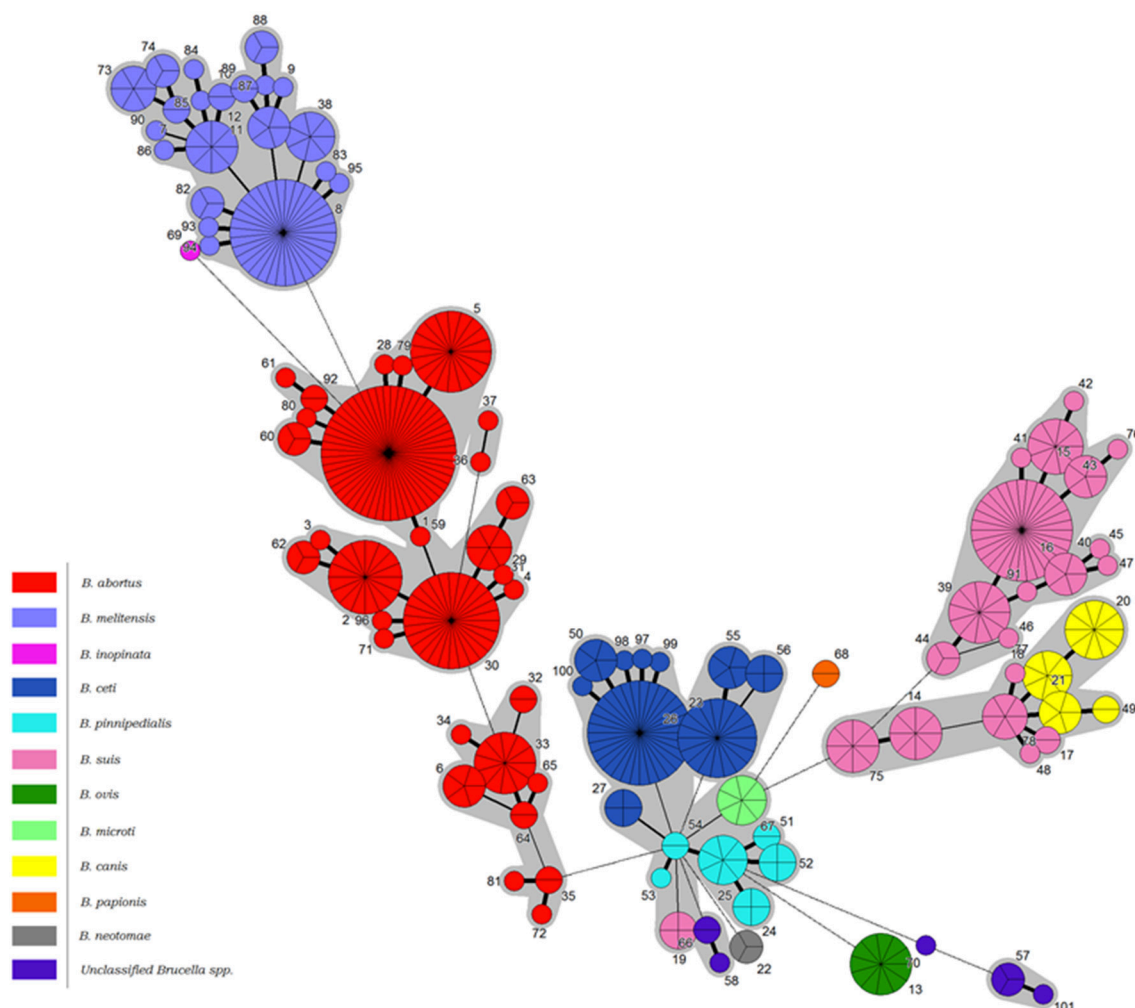


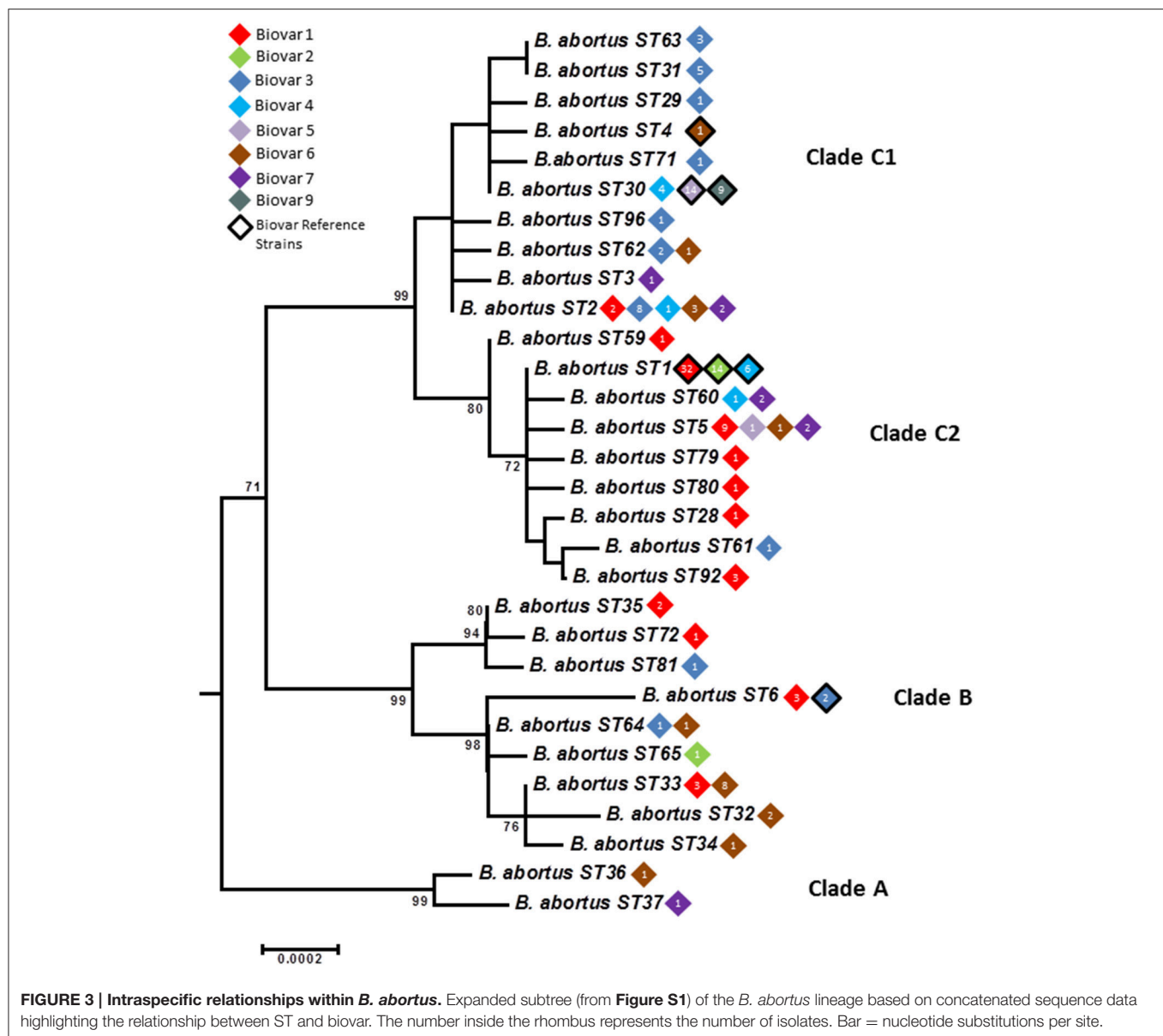
FIGURE 2 | Minimum spanning tree of BruMLSA21 profiles described in this study. Each circle denotes a particular ST type with the size of the circle illustrating the number of isolates of that particular type. The coloring inside the circles indicates the *Brucella* species. Thick solid lines joining two types denote types differing at a single locus, thinner solid lines types differing at two or three loci, and the thinnest solid lines types differing at four or five loci. Dashed lines indicate types differing at >5 loci. The gray halos surrounding groupings represent clusters defined in Bionumerics created if neighbors differed in no more than 5 of 21 loci.

the number of BruMLSA9 STs from 27 to 60 when applied to the strain collection described here (Table S2).

Overarching Population Structure

Individual allele sequences for each individual ST were concatenated to form a 10,257 bp length sequence for analysis with 493 (4.81%) sites being polymorphic excluding indels. With 219 polymorphic sites (2.14%) diversity is much reduced if only the core *Brucella* group are considered (i.e., without BruMLSA21 STs 57, 69, 70, and 101 representing *B. inopinata* and unclassified isolates from Australian rodents). Phylogenetic analysis based on all 101 STs is shown in Figure S1 and illustrates the overall structure of the genus with *B. inopinata* and isolates from Australian rodents comprising early branching groups in the genus as currently described. Studies of a number of other groups including isolates from frogs (Eisenberg et al., 2012; Whatmore et al., 2015; Scholz et al., accepted) and foxes (*B.*

vulpis) (Scholz et al., 2016) for which BruMLSA9, or partial BruMLSA21, data are available confirm that these isolates also belong to the genetically atypical *Brucella* but that they are clearly much more closely affiliated to the genus *Brucella* than to the nearest phylogenetic neighbor *Ochrobactrum*. Figure 1 shows the core *Brucella* only as an expanded subtree to facilitate resolution. BruMLSA21 confirms the separation into clear clades comprising *B. abortus*/*B. melitensis*, *B. suis*/*B. canis*, *B. ceti*/*B. pinnipedialis*, *B. ovis*/*B. papionis*, and *B. neotomae*. These clades appear to have radiated virtually simultaneously from a common ancestor into host specific lineages. This was previously also seen with BruMLSA9 analysis and it was initially hoped that the additional discrimination offered by BruMLSA21 would help resolve this. However, it is now apparent that even whole genome sequencing phylogenies suggest the same explosive radiation has occurred although the reasons for this remain unclear (Audic et al., 2011; Wattam et al., 2014). Two additional short branches



represent *B. suis* biovar 5 (BruMLSA21 ST19) and *B. microti*—the greater resolution offered by whole genome sequencing has suggested that the former is a very early branching group of the *B. suis*/*B. canis* lineage while the latter is just basal to the classical *Brucella* lineage (Audic et al., 2011; Wattam et al., 2014).

One additional lineage corresponds to BruMLSA21 STs 58 and 66—these represent historical isolates obtained by APHA in the 1960s reportedly associated with human infections in Thailand and originally characterized as atypical *B. suis*. These isolates might, with additional analysis, merit description as a novel species and illustrate the value of MLSA in placing novel isolates in the context of the complete extant understanding of the population structure of the genus. Such data adds to the evidence base facilitating description of novel species as has been

the case for *B. papionis*, *B. inopinata*, *B. microti*, and *B. vulpis* (Scholz et al., 2008, 2010, 2016; Whatmore et al., 2014) and for other emerging atypical *Brucella* awaiting formal taxonomic description (Tiller et al., 2010a; Eisenberg et al., 2012; Whatmore et al., 2015).

Construction of a minimum spanning tree treating data categorically and defining clusters on the basis of neighbors differing in no more than five of the 21 loci revealed a similar relationship (Figure 2). Under these analysis conditions *B. melitensis* constituted a single complex, the more diverse *B. abortus* three complexes corresponding to Clades A, B, and C described below by intraspecies phylogenetic analysis, and *B. suis* biovars 1–4/*B. canis* two complexes, one corresponding to biovar 2 and the other biovars 1, 3, and 4 and *B. canis*. *B. papionis*, *B. ovis*, and *B. neotomae* all constitute separate groups

while the remaining major central complex contains *B. ceti*, *B. pinnipedialis*, *B. microti*, and *B. suis* biovar 5 isolates.

Intraspecies Relationships within *B. Abortus*: Phylogeography and Biovar

Only six *B. abortus* STs were described initially by BruMLSA9—application of BruMLSA21 to a wider strain collection significantly increased known diversity of *B. abortus* with 30 STs identified. Isolates comprise three major clades A, B, and C (Figures 3, 4)—the two early branching clades A and B comprise isolates entirely originating from widely across Africa (Senegal, Nigeria, Zimbabwe, Sudan, Mozambique, Kenya, Chad, and Uganda) with clade A representing a previously undescribed clade that substantially increases known diversity of *B. abortus*. These clades consist predominantly isolates of biovars 1, 3, and 6 including the biovar 3 reference strain Tulya.

In contrast to the geographical restriction of clades A and B, isolates of clade C have a global distribution with in particular ST1 and ST2 appearing to be widely distributed across many

continents. As shown in Figure 3 this clade splits into two subclades—in clade C1 the most common genotype to biovar association is with biovar 3. However one ST, ST30 is associated exclusively with isolates of biovars 4, 5, and 9 and includes virtually all isolates of the latter two biovars and their reference strains. The vast majority of these isolates originate from the UK (prior to brucellosis eradication) with most of the few remaining isolates from other parts of Western Europe. Consistent with this biovar 5 was colloquially known as “*British melitensis*” (Corbel and Banai, 2005) and is differentiated from biovar 9, colloquially known as “*H₂S producing melitensis*” (Corbel and Banai, 2005), only by H₂S production. The remaining isolates of ST30 represent biovar 4 which is also seen in genetically distinct lineages and differs from biovar 5 and 9 only in its inability to grow in the presence of thionin. While the overall picture within Clade C is of global dispersal there is evidence that individual genotypes may reflect types with restricted geographical range that may be endemic in certain regions—notably STs 63 and 31 were exclusively associated with East Asia (India, Sri Lanka, and

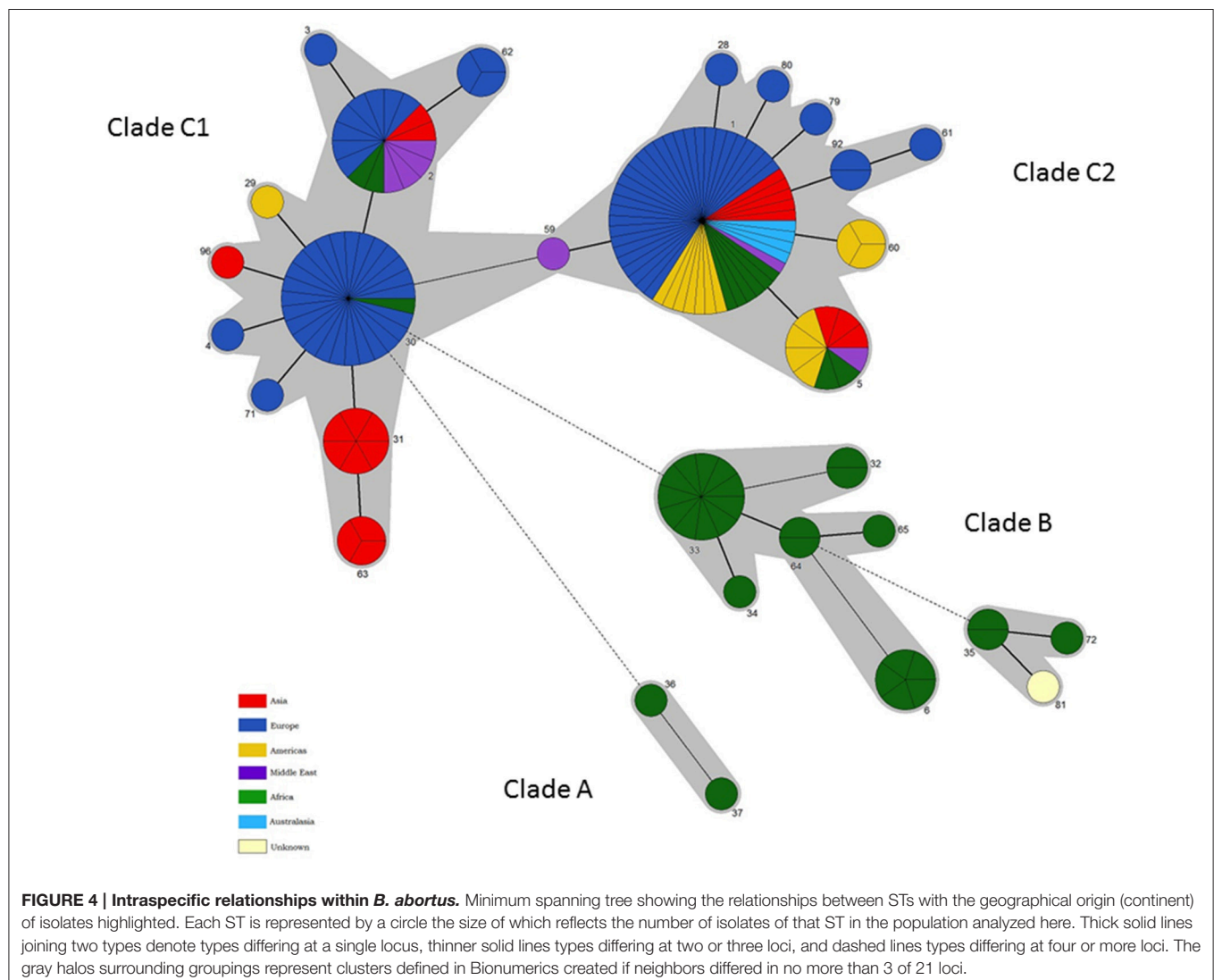
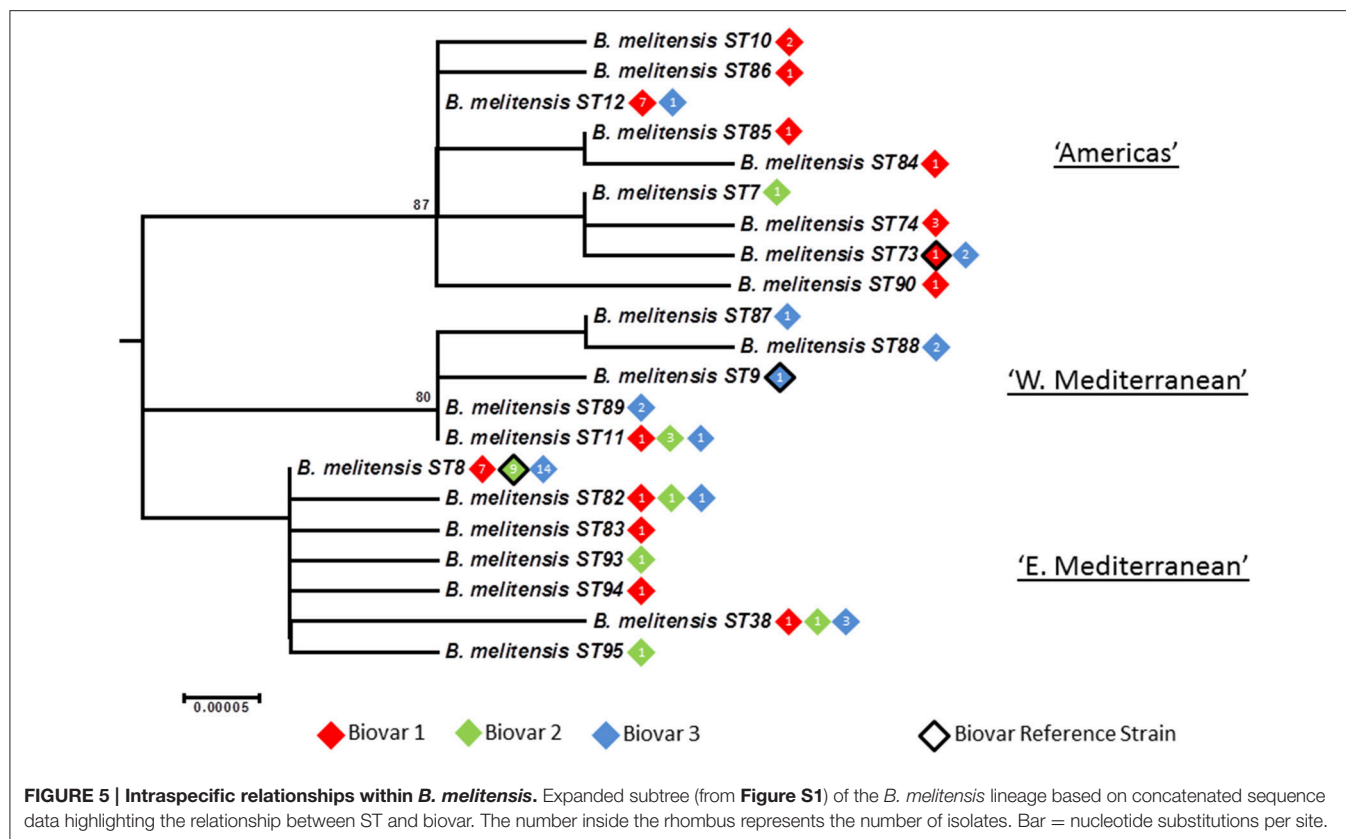


FIGURE 4 | Intraspecific relationships within *B. abortus*. Minimum spanning tree showing the relationships between STs with the geographical origin (continent) of isolates highlighted. Each ST is represented by a circle the size of which reflects the number of isolates of that ST in the population analyzed here. Thick solid lines joining two types denote types differing at a single locus, thinner solid lines types differing at two or three loci, and dashed lines types differing at four or more loci. The gray halos surrounding groupings represent clusters defined in Bionumerics created if neighbors differed in no more than 3 of 21 loci.



Thailand). Much more detailed local analysis, enabled by the work described here, will help better understand the genotypes prevalent at local levels.

Clade C2 appears more strongly associated with biovar 1 isolates. The particularly widely dispersed genotype, ST1, consists of isolates of biovar 1, 2, and 4 including the reference strains for all these biovars. Biovars 1 and 2 differ only in fuchsin susceptibility while biovar 4 isolates show a different pattern of agglutination with monospecific sera. *B. abortus* biovars 1, 2, and 4 have been shown historically to be closely genetically related (e.g., Gargani and López-Merino, 2006) and, based on these findings it is still not possible to identify distinct genetic lineages corresponding to these biovars.

In summary these data, which reflect the first extensive genetic characterisation of *Brucella* from diverse African origins, suggest that *B. abortus* originated in Africa and, the fact that isolates of the two earliest emerging branches (clades A and B) are still confined there to date, may suggest no or limited global spread of these lineages. In contrast the later emerging clade C appears to have been spread globally to all six populated continents. Indeed it is interesting to note that sporadic members of this clade have been isolated from Africa which may suggest these newer lineages were introduced to Africa by cattle importation from Europe such that both the original endemic lineages (Clades A and B) and, probably to a much lesser extent, introduced lineages (Clades C1 and C2) may now circulate in Africa.

While some relationship between genotype and biovar is apparent in *B. abortus* the picture is far from one of complete

congruence. For example isolates of biovar 1 are widely distributed in clades B and C2 and, to a lesser extent in C1. Most isolates in the major early diverging African clade correspond to biovars 1, 3, and 6 (with the latter two biovars separable only by the requirement of biovar 3 for additional CO₂ and use of thionin at 1/25,000 dilution) although, of the reference strains, only that of biovar 3 is found in this clade. Notably clade C1 is also strongly associated with biovar 3—these data appear consistent with reports in the literature of two biovar 3 clades, 3a from Africa (our Clade B) and 3b (our Clade C1) from Europe (Ocampo-Sosa et al., 2005; Ica et al., 2008; Bertu et al., 2015). Biovar 3b isolates have been reported from Spain and Turkey consistent with the sources of isolates falling within clade C1 (Table S2). In contrast, biovars 5 and 9 were almost entirely confined to a single ST within clade C1 suggesting these biovars are congruent with a distinct genetic lineage although clearly genetic separation between these two biovars was not possible using this MLSA scheme. The biovar 6 reference strain is also located in clade C1 albeit with a unique genotype, ST4, consistent with the description of a PCR assay specific for *B. abortus* biovars 3b, 5, 6, and 9 although this notably was only applied to reference strains of the latter three biovars (Ocampo-Sosa et al., 2005). Readers should note that the original biovar 7 reference strain (63/75) has been shown to represent a mixed culture and biovar 7 was thus deleted from *Brucella* taxonomy (Corbel, 1988; Garin-Bastuji et al., 2014). However genetically diverse isolates that possess the phenotypic profile reported for biovar 7 have been included here and reported in other studies (Garin-Bastuji et al.,

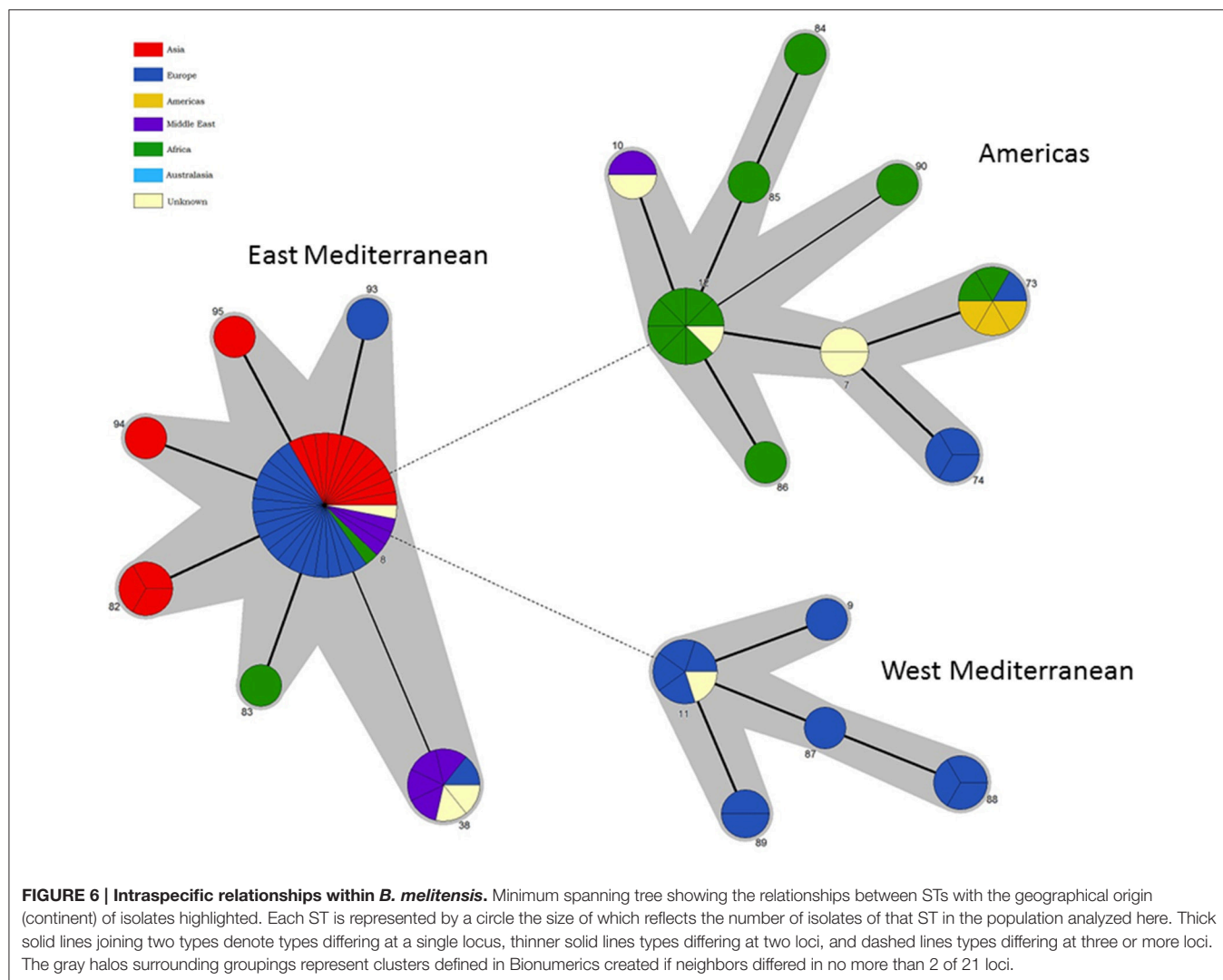
2014; Kim et al., 2016). The genetic diversity of strains with the biovar 7 phenotype questions any move to reintroduce biovar 7 as previously defined. Of the remaining biovars, biovar 2 is almost exclusively associated with ST1 within clade C2 that also includes the majority of biovar 4 strains and a large number of biovar 1 strains. The reference strains for all three biovars 1, 2, and 4 are members of ST1 highlighting the fact that it not possible to identify defined and unique genetic lineages that correspond to these biovars.

Finally both *B. abortus* vaccine strains S19 and RB51 were found to be members of ST5 consistent with the identification of North American field isolates in this ST (the parental strains of the vaccines were North American isolates). Given the sharing of this ST between field and vaccine strains ST5 strains were examined by molecular assays to determine status as vaccine or field strains (Sangari and Agüero, 1994; Vemulapalli et al., 1999; Gopaul et al., 2010). These analyses identified that a substantial proportion of isolates in this ST appear to represent S19 vaccine re-isolated from the field (Table S2).

Intraspecies Relationships within *B. melitensis*: Phylogeography and Biovar

Application of BruMLSA21 to a wider *B. melitensis* strain collection identified 21 STs in contrast to the 6 STs previously described by BruMLSA9. Isolates cluster into three distinct lineages (Figures 5, 6) that correspond to the “Americas,” “West Mediterranean,” and “East Mediterranean” lineages described previously on the basis of MLVA data (Al Dahouk et al., 2007). Only a small number of isolates from the Americas were examined here and while isolates from USA and Argentina are included in the Americas clade more than 60% of the isolates of this clade are of African origin. African isolates included in this clade originate widely across the continent (Ethiopia, Somalia, Nigeria, Tanzania, Sudan, Zimbabwe) and, as few African isolates are seen in the “West Mediterranean” and “East Mediterranean” lineages, it appears that this lineage may be endemic in Africa.

In agreement with the previous designation isolates falling in the “West Mediterranean” lineage were exclusively reported from Italy, France, the former Yugoslavia and Germany. In contrast



the “East Mediterranean” lineage, while including isolates from Greece, Turkey, Cyprus, and the Balkan States, also extends much more widely into the Middle East and Asia (Thailand, India, Pakistan, Mongolia, and Afghanistan). Although numbers are small some BruMLSA21 STs appear geographically restricted—for example ST82 associated with Thailand (and in agreement with the identification by a recent whole genome sequence analysis of a separate lineage within the “East Mediterranean” cluster including the ST82 defining strain and strains from Malaysia and the Philippines—Tan et al., 2015) and ST38 to the Middle East. However ST8, by far the most frequently seen *B. melitensis* ST, appears widely distributed across Europe and Asia from Portugal to Afghanistan and Mongolia.

While each of the three lineages contains one of the *B. melitensis* biovar reference strains (“West Mediterranean” Ether biovar 3; “East Mediterranean” 63/9 biovar 2; “Americas” 16M biovar 1) there is no clear relationship between genotype and biovar. While the majority of isolates in the “Americas” lineage belong to biovar 1 (81%) and in the “West Mediterranean” lineage belong to biovar 3 (64%), isolates of both other biovars were apparent in both of these lineages. In addition virtually equivalent numbers of all three biovars are seen in both the “East Mediterranean” lineage overall and the most common

and widely dispersed BruMLSA21 ST8 specifically. Early MLVA studies highlighted a lack of congruence between genotype and biovar (Whatmore et al., 2006) and a growing body later MLVA studies (e.g., Al Dahouk et al., 2007; Jiang et al., 2011, 2013), taken together with data presented here using markers more appropriate for determining phylogeny, suggest that the biovar concept, which is the case of *B. melitensis* is reliant solely on serological reaction, is of extremely limited epidemiological value for *B. melitensis*.

Intraspecific Relationships of *B. suis*/*B. canis* Lineage: Phylogeography and Biovar

As with other species application of BruMLSA21 to a wider *B. suis* strain collection significantly increased the number of STs identified in BruMLSA9 from 6 to 20. In contrast to *B. abortus* and *B. melitensis* there is a strong congruency between genotype and biovar. Excluding *B. suis* biovar 5 there are two genetically divergent major clades (Figure 7), one comprising to biovar 2 isolates and the second comprising an early branching group corresponding to biovar 1 isolates, biovar 3 and 4 isolates and *B. canis* isolates forming a terminal group on this branch. Thus only

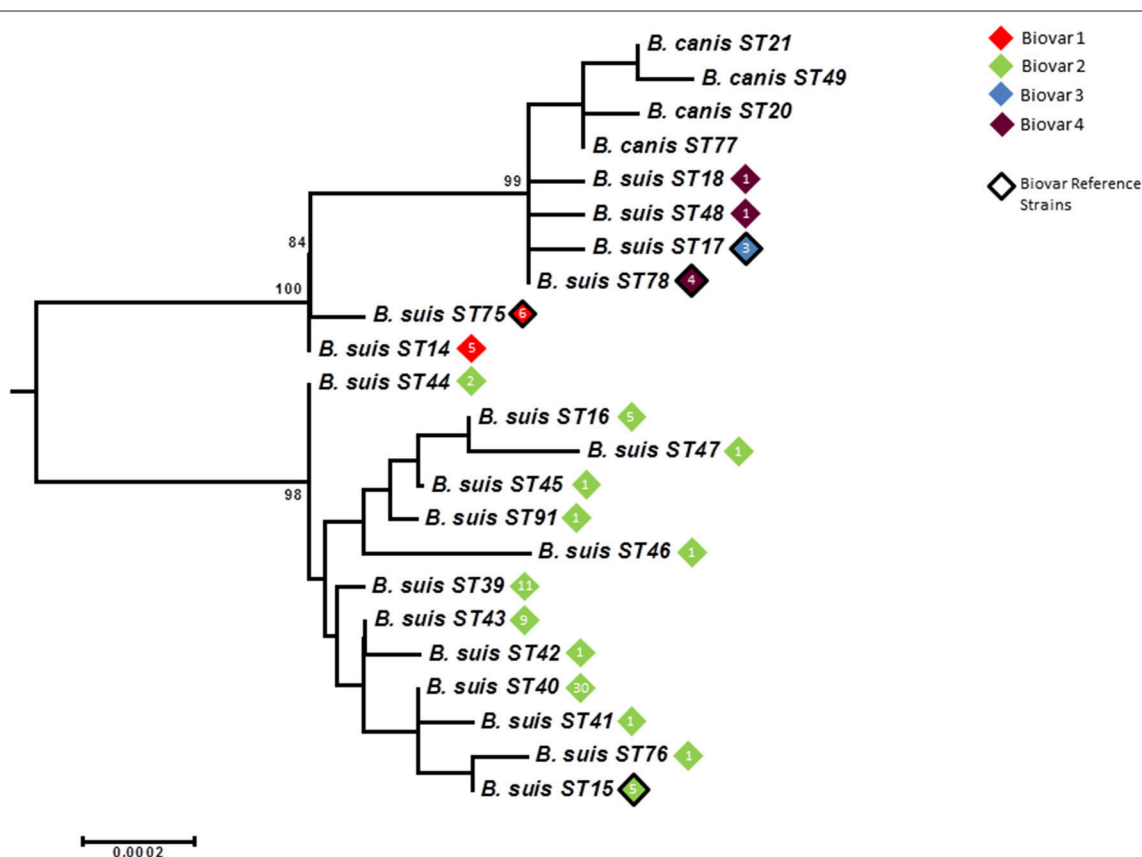


FIGURE 7 | Intraspecific relationships within the *B. suis*/*B. canis* lineage. Expanded subtree (from Figure S1) of the *B. suis*/*B. canis* lineage based on concatenated sequence data highlighting the relationship between ST and biovar. The number inside the rhombus represents the number of isolates. Bar = nucleotide substitutions per site.

biovar 3 and 4 isolates do not represent clearly separated clusters although, in contrast to BruMLSA9 where they share a genotype, the small number of biovar 3 isolates included do correspond to a single unique BruMLSA21 ST (ST17).

Only biovar 2 has sufficient isolates to ascertain possible phylogeographic associations (**Figure 8**). Here the vast majority of STs are associated with Central and Northern European isolates where it is likely that movement of strains in wildlife reservoirs (hares and wild boar) has dispersed genotypes widely. However two genotypes ST39 and ST44 are confined to the Iberian peninsula suggesting they correspond to the Iberian clone of *B. suis* biovar 2 described previously on the basis of PCR-RFLP, MLVA and subsequent whole genome mapping (Ferreira et al., 2016).

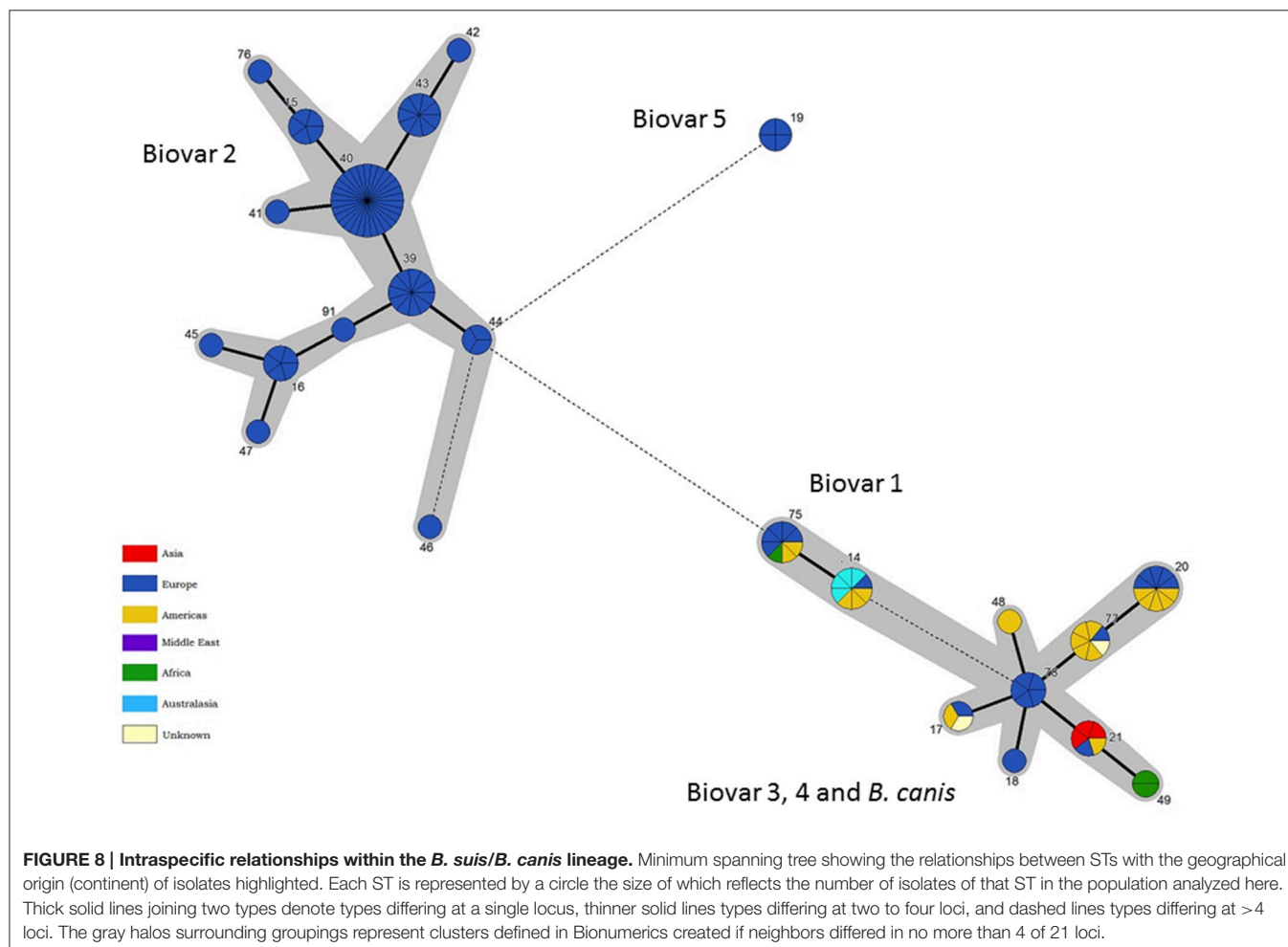
Intraspecies Relationships of *B. pinnipedialis* and *B. ceti*

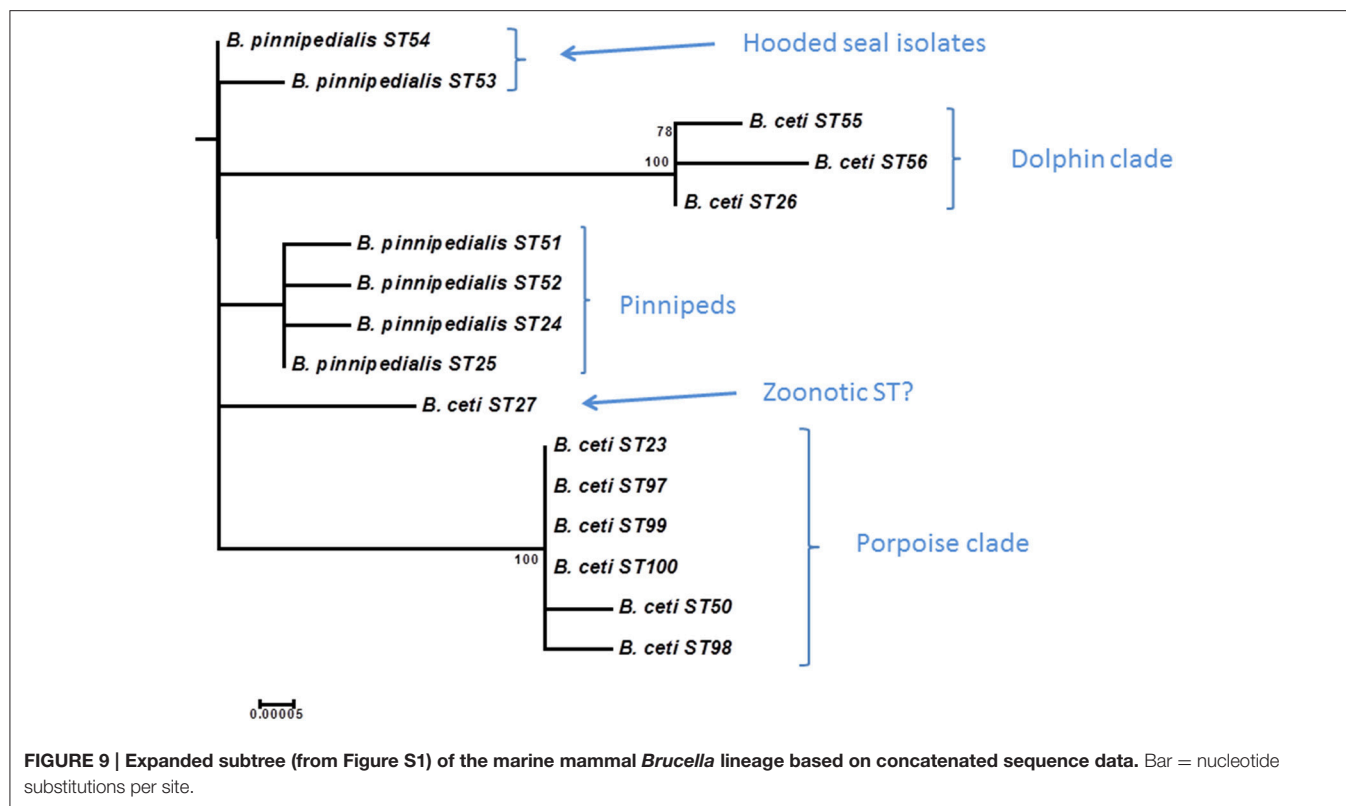
Grouping of marine mammal *Brucella* remains largely consistent with that described by BruMLSA9 with an increase in STs from 5 to 16 (**Figure 9** and **Table S2**). As suggested previously phylogeny appears inconsistent with taxonomy in this group and *B. ceti* appears paraphyletic with two distinct clusters (ST26

complex and ST23 complex) that appear to have preferred hosts of dolphins or porpoises, respectively (Groussaud et al., 2007; Dawson et al., 2008). The increased resolution of BruMLSA21 allows further subdivision of isolates of BruMLSA9 ST24 and ST25 associated with various species of seals for example identifying two BruMLSA21 STs (ST53 and ST54) that appear to be specific for hooded seals in this dataset, a finding consistent with the previous description of a hooded seal specific clade on the basis of MLVA (Groussaud et al., 2007; Maquart et al., 2009). The remaining ST, ST27 has previously been associated with human zoonotic infection (Whatmore et al., 2008) and remains distinct from the main marine mammal *Brucella* clusters. These data again highlight that phylogenetic relationships suggest that a taxonomic rearrangement of *Brucella* from marine mammals might be appropriate (Whatmore, 2009).

Remaining Species

No diversity was identified in *B. microti*, *B. neotomae*, *B. papionis*, and *B. ovis*. In large part this may reflect the very limited sampling of these rarely or recently isolated species although *B. ovis* has been more extensively sampled with isolates from across the globe included here. These data, and complementary MLVA





data, which also reveals relatively limited diversity within *B. ovis* (Whatmore et al., 2006), suggest that *B. ovis*, while relatively well-separated from other classical species, may represent an extremely genetically restricted group.

Only a single isolate of *B. inopinata* has been formally described although the increasing isolation of diverse genetically atypical *Brucella* from various hosts might point toward consideration of whether the description of *B. inopinata* should be expanded to include all these early-branching *Brucella* isolates.

CONCLUSIONS

Although we have previously described the application of BruMLSA21 to address specific issues, for example in the context of addressing the status of *B. abortus* biovar 7 (Garin-Bastuji et al., 2014), full technical details of the scheme, allele calls, ST allelic profiles, and associated metadata have not previously been available to facilitate comparative analysis by others.

To bring *Brucella* into alignment with most other bacterial pathogens the existing BruMLSA9 data (Whatmore et al., 2007) and BruMLSA21 data described here, as well as a large volume of additional unpublished BruMLSA9 data has now been made available via the principle MLST/MLSA database as a resource for the scientific community. The full data set, sampling c. over 740 isolates for BruMLSA9 and more than 500 isolates for BruMLSA21, provide the most comprehensive assessment of the population structure

of the entire genus to date. They provide a framework for understanding the relationship between extant strains, for the placement of newly emerging or discovered strains in the context of extant knowledge and a platform for designing and or assessing the performance of molecular diagnostic assays designed to characterize strains at various taxonomic levels.

The study described here adds to understanding of the phylogeographical relationships within the major *Brucella* species for the first time clearly describing the apparent origin of *B. abortus* in Africa and the global spread of later emerging lineages. Completely novel lineages, such as the early emerging African *B. abortus* lineage, have been revealed which may be significant in understanding the emergence of *B. abortus* as a host specific pathogen. Equally there appear to be clones endemic only locally, such as the *B. abortus* ST63/ST31 Asian clone or the Middle Eastern *B. melitensis* ST38, although much of the world, particularly where brucellosis is most problematic, remains grossly under sampled with insufficient data to draw robust conclusions. It is hoped the publication of these data encourage the application of MLSA (either *per se* or using data extracted from whole genome sequences) more widely to expand the depth of the database described here and further understanding of the global *Brucella* situation.

The data also add significantly to understanding the relationship between biovar and genotype—it is clear that there is there is diminishing congruence in this relationship

from *B. suis* > *B. abortus* > *B. melitensis*. This is not entirely unexpected given a system based on phenotypic or serological markers that may be impacted by factors such as variable expression and the acknowledged subjectivity of the approach combined with the very subtle differences in phenotype of some of the biovars described. Given advances in molecular approaches it would seem timely to consider whether such approaches offer a more meaningful replacement for biotyping. Such assays could be based on genomic rearrangements such as the multiplex Bruceladder (López-Góñi et al., 2008) or SNPs as per existing speciation assays (Scott et al., 2007; Foster et al., 2008; Gopaul et al., 2008) which have the advantage that they can be applied at a number of taxonomic levels (Keim et al., 2004). The crucial point is that they must be designed on the back of a robust population genetic understanding provided by data such as that presented here and iteratively re-examined as knowledge of extant diversity increases. For example it would be very easy to design an assay for *B. abortus* that did not detect the early emerging African lineage if a marker was selected that represented an evolutionary change that occurred beyond this branch.

We welcome submission of new data to the *Brucella* PubMLST website at <http://pubmlst.org/brucella/>.

AUTHORS CONTRIBUTIONS

AW conceived of and designed the study, analyzed the data, and drafted the manuscript. MK, JM, KG, and JE undertook

portions of the experimental work and analysis. LP oversaw strain provision and biotyping.

ACKNOWLEDGMENTS

Brucellosis research at the APHA is supported by the UK Department of the Environment, Food and Rural Affairs (Defra). Development and implementation of MLSA typing was specifically funded as part of projects SE0311 and SE0313 with ongoing support from Defra for database maintenance and expansion. We acknowledge the many colleagues worldwide who have submitted strains to the APHA reference laboratory over the years facilitating the development of an extensive strain collection to support these studies.

SUPPLEMENTARY MATERIAL

The Supplementary Material for this article can be found online at: <http://journal.frontiersin.org/article/10.3389/fmicb.2016.02049/full#supplementary-material>

Figure S1 | Phylogenetic reconstruction of relationships between all 101 BruMLSA21 STs including atypical strains. The tree was constructed with the concatenated sequence data of the 21 loci (>10.2 kb) using the neighbor-joining algorithm with the Jukes-Cantor model in MEGA5.2. Bar = nucleotide substitutions per site.

Table S1 | Technical details of MLSA scheme including details of loci characterized and PCR primer sequences.

Table S2 | Details of BruMLSA21 data described in this study. All data have been deposited at <http://pubmlst.org/brucella/>.

REFERENCES

- Al Dahouk, S., Flèche, P. L., Nöckler, K., Jacques, I., Grayon, M., Scholz, H. C., et al. (2007). Evaluation of *Brucella* MLVA typing for human brucellosis. *J. Microbiol. Methods* 69, 137–145. doi: 10.1016/j.mimet.2006.12.015
- Alton, G. G., Jones, L. M., Angus, R. D., and Verger, J. M. (1988). *Techniques for the Brucellosis Laboratory*. Paris: Institut National de la Recherche Agronomique.
- Audic, S., Lescot, M., Claverie, J. M., Cloeckaert, A., and Zygmunt, M. S. (2011). The genome sequence of *Brucella pinnipedialis* B2/94 sheds light on the evolutionary history of the genus *Brucella*. *BMC Evol. Biol.* 11:200. doi: 10.1186/1471-2148-11-200
- Bertu, W. J., Ducrot, M. J., Muñoz, P. M., Mick, V., Zúñiga-Ripa, A., Bryssinckx, W., et al. (2015). Phenotypic and genotypic characterization of *Brucella* strains isolated from autochthonous livestock reveals the dominance of *B. abortus* biovar 3a in Nigeria. *Vet. Microbiol.* 180, 103–108. doi: 10.1016/j.vetmic.2015.08.014
- Chain, P. S., Commerci, D. J., Tolmasky, M. E., Larimer, F. W., Malfatti, S. A., Vergez, L. M., et al. (2005). Whole-genome analyses of speciation events in pathogenic *Brucellae*. *Infect. Immun.* 73, 8353–8361. doi: 10.1128/IAI.73.12.8353-8361.2005
- Corbel, M. J., and Banai, M. (2005). "Genus I. *Brucella* Meyer and Shaw 1920, 173AL," in *Bergey's Manual of Systematic Bacteriology*, Vol. 2, eds D. J. Brenner, N. R. Krieg, and J. T. Staley (New York, NY: Springer), 370–386.
- Corbel, M. J. (1988). International committee on systematic bacteriology, subcommittee on the taxonomy of *Brucella*. *Int. J. Syst. Bacteriol.* 38, 450–452. doi: 10.1099/00207173-38-4-450
- Dawson, C. E., Stubberfield, E. J., Perrett, L. L., King, A. C., Whatmore, A. M., Bashiruddin, J. B., et al. (2008). Phenotypic and molecular characterisation of *Brucella* isolates from marine mammals. *BMC Microbiol.* 8:224. doi: 10.1186/1471-2180-8-224
- De, B. K., Stauffer, L., Koylass, M. S., Sharp, S. E., Gee, J. E., Helsel, L. O., et al. (2008). Novel *Brucella* strain (BO1) associated with a prosthetic breast implant infection. *J. Clin. Microbiol.* 46, 43–49. doi: 10.1128/JCM.01494-07
- Eisenberg, T., Hamann, H. P., Kaim, U., Schlez, K., Seeger, H., Schauerte, N., et al. (2012). Isolation of potentially novel *Brucella* spp. from frogs. *Appl. Environ. Microbiol.* 78, 3753–3755. doi: 10.1128/AEM.07509-11
- Eisenberg, T., Riße, K., Schauerte, N., Geiger, C., Blom, J., and Scholz, H. C. (2016). Isolation of a novel "atypical" *Brucella* strain from a bluespotted ribbontail ray (*Taeniura lymma*). *Antonie Van Leeuwenhoek*. doi: 10.1007/s10482-016-0792-4. [Epub ahead of print].
- Ferreira, A. C., Dias, R., de Sá, M. I., and Tenreiro, R. (2016). Whole-genome mapping reveals a large chromosomal inversion on Iberian *Brucella suis* biovar 2 strains. *Vet. Microbiol.* 192, 220–225. doi: 10.1016/j.vetmic.2016.07.024
- Foster, J. T., Okinaka, R. T., Svensson, R., Shaw, K., De, B. K., Robison, R. A., et al. (2008). Real-time PCR assays of single-nucleotide polymorphisms defining the major *Brucella* clades. *J. Clin. Microbiol.* 46, 296–301. doi: 10.1128/JCM.01496-07
- Gargani, G., and López-Merino, A. (2006). International Committee on Systematic Bacteriology; Subcommittee on the taxonomy of *Brucella*. *Int. J. Syst. Evol. Microbiol.* 56, 1167–1168. doi: 10.1099/ijs.0.64042-0
- Garin-Bastuji, B., Mick, V., Le Carrou, G., Allix, S., Perrett, L. L., Dawson, C. E., et al. (2014). Examination of taxonomic uncertainties surrounding *Brucella abortus* bv. 7 by phenotypic and molecular approaches. *Appl. Environ. Microbiol.* 80, 1570–1579. doi: 10.1128/AEM.03755-13
- Godfroid, J., Scholz, H. C., Barbier, T., Nicolas, C., Wattiau, P., Fretin, D., et al. (2011). Brucellosis at the animal/ecosystem/human interface at the beginning of the 21st century. *Prev. Vet. Med.* 102, 118–131. doi: 10.1016/j.prevetmed.2011.04.007

- Gopaul, K. K., Koylass, M. S., Smith, C. J., and Whatmore, A. M. (2008). Rapid identification of *Brucella* isolates to the species level by real time PCR based single nucleotide polymorphism (SNP) analysis. *BMC Microbiol.* 8:86. doi: 10.1186/1471-2180-8-86
- Gopaul, K. K., Sells, J., Bricker, B. J., Crasta, O. R., and Whatmore, A. M. (2010). Rapid and reliable single nucleotide polymorphism-based differentiation of *Brucella* live vaccine strains from field strains. *J. Clin. Microbiol.* 48, 1461–1464. doi: 10.1128/JCM.02193-09
- Groussaud, P., Shankster, S. J., Koylass, M. S., and Whatmore, A. M. (2007). Molecular typing divides marine mammal strains of *Brucella* into at least three groups with distinct host preferences. *J. Med. Microbiol.* 56, 1512–1518. doi: 10.1099/jmm.0.47330-0
- Halling, S. M., Peterson-Burch, B. D., Bricker, B. J., Zuerner, R. L., Qing, Z., Li, L. L., et al. (2005). Completion of the genome sequence of *Brucella abortus* and comparison to the highly similar genomes of *Brucella melitensis* and *Brucella suis*. *J. Bacteriol.* 187, 2715–2726. doi: 10.1128/JB.187.8.2715-2726.2005
- Hofer, E., Revilla-Fernández, S., Al Dahouk, S., Riehm, J. M., Nöckler, K., Zygmunt, M. S., et al. (2012). A potential novel *Brucella* species isolated from mandibular lymph nodes of red foxes in Austria. *Vet. Microbiol.* 155, 93–99. doi: 10.1016/j.vetmic.2011.08.009
- Ica, T., Aydin, F., Erdenlig, S., Guler, L., and Büyükcangaz, E. (2008). Characterisation of *Brucella abortus* biovar 3 isolates from Turkey as biovar 3b. *Vet. Rec.* 163, 659–661. doi: 10.1136/vr.163.22.659
- Jiang, H., Fan, M., Chen, J., Mi, J., Yu, R., Zhao, H., et al. (2011). MLVA genotyping of Chinese human *Brucella melitensis* biovar 1, 2 and 3 isolates. *BMC Microbiol.* 11:256. doi: 10.1186/1471-2180-11-256
- Jiang, H., Wang, H., Xu, L., Hu, G., Ma, J., Xiao, P., et al. (2013). MLVA genotyping of *Brucella melitensis* and *Brucella abortus* isolates from different animal species and humans and identification of *Brucella suis* vaccine strain S2 from cattle in China. *PLoS ONE* 8:e76332. doi: 10.1371/journal.pone.0076332
- Jiménez de Bagüés, M. P., Ouahrani-Bettache, S., Quintana, J. F., Mitjana, O., Hanna, N., Bessoles, S., et al. (2010). The new species *Brucella microti* replicates in macrophages and causes death in murine models of infection. *J. Infect. Dis.* 202, 3–10. doi: 10.1086/653084
- Jolley, K. A., and Maiden, M. C. (2010). BIGSdb: scalable analysis of bacterial genome variation at the population level. *BMC Bioinformatics* 11:595. doi: 10.1186/1471-2105-11-595
- Keim, P., Van Ert, M. N., Pearson, T., Vogler, A. J., Huynh, L. Y., and Wagner, D. M. (2004). Anthrax molecular epidemiology and forensics: using the appropriate marker for different evolutionary scales. *Infect. Genet. Evol.* 4, 205–213. doi: 10.1016/j.meegid.2004.02.005
- Kim, J.-Y., Kang, S.-I., Erdenebaatar, J., Vanaabaatar, B., Ulziisaikhan, G., Khursbaatar, O., et al. (2016). Distinctive phenotypic and molecular characteristics of *Brucella abortus* strains isolated from Mongolia. *Turk. J. Vet. Anim. Sci.* 40, 562–568. doi: 10.3906/vet-1511-75
- López-Goní, I., García-Yoldi, D., Marín, C. M., de Miguel, M. J., Muñoz, P. M., Blasco, J. M., et al. (2008). Evaluation of a multiplex PCR assay (Bruce-ladder) for molecular typing of all *Brucella* species, including the vaccine strains. *J. Clin. Microbiol.* 46, 3484–3487. doi: 10.1128/JCM.00837-08
- Maquart, M., Le Flèche, P., Foster, G., Tryland, M., Ramisse, F., Djonje, B., et al. (2009). MLVA-16 typing of 295 marine mammal *Brucella* isolates from different animal and geographic origins identifies 7 major groups within *Brucella ceti* and *Brucella pinnipedialis*. *BMC Microbiol.* 9:145. doi: 10.1186/1471-2180-9-145
- Marzetti, S., Carranza, C., Roncallo, M., Escobar, G. I., and Lucero, N. E. (2013). Recent trends in human *Brucella canis* infection. *Comp. Immunol. Microbiol. Infect. Dis.* 36, 55–61. doi: 10.1016/j.cimid.2012.09.002
- Nymo, I. H., Tryland, M., and Godfroid, J. (2011). A review of *Brucella* infection in marine mammals with special emphasis on *Brucella pinnipedialis* in the hooded seal (*Cystophora cristata*). *Vet. Res.* 42:93. doi: 10.1186/1297-9716-42-93
- Ocampo-Sosa, A. A., Agüero-Balbín, J., and García-Lobo, J. M. (2005). Development of a new PCR assay to identify *Brucella abortus* biovars 5, 6 and 9 and the new subgroup 3b of biovar 3. *Vet. Microbiol.* 110, 41–51. doi: 10.1016/j.vetmic.2005.06.007
- Pappas, G., Papadimitriou, P., Akritidis, N., Christou, L., and Tsianos, E. V. (2006). The new global map of human brucellosis. *Lancet Infect. Dis.* 6, 91–99. doi: 10.1016/S1473-3099(06)70382-6
- Sangari, F. J., and Agüero, J. (1994). Identification of *Brucella abortus* B19 vaccine strain by the detection of DNA polymorphism at the ery locus. *Vaccine* 12, 435–438. doi: 10.1016/0264-410X(94)90121-X
- Scholz, H. C., and Vergnaud, G. (2013). Molecular characterisation of *Brucella* species. *Rev. Sci. Tech.* 32, 149–162. doi: 10.20506/rst.32.1.2189
- Scholz, H. C., Hubalek, Z., Sedláček, I., Vergnaud, G., Tomaso, H., Al Dahouk, S., et al. (2008). *Brucella microti* sp. nov., isolated from the common vole *Microtus arvalis*. *Int. J. Syst. Evol. Microbiol.* 58, 375–382. doi: 10.1099/ijms.0.65356-0
- Scholz, H. C., Nöckler, K., Göllner, C., Bahn, P., Vergnaud, G., Tomaso, H., et al. (2010). *Brucella inopinata* sp. nov., isolated from a breast implant infection. *Int. J. Syst. Evol. Microbiol.* 60, 801–808. doi: 10.1099/ijms.0.011148-0
- Scholz, H. C., Revilla-Fernández, S., Al Dahouk, S., Hammerl, J. A., Zygmunt, M. S., Cloeckert, A., et al. (2016). *Brucella vulpis* sp. nov., isolated from mandibular lymph nodes of red foxes (*Vulpes vulpes*). *Int. J. Syst. Evol. Microbiol.* 66, 2090–2098. doi: 10.1099/ijsem.0.000998
- Scholz, H. C., Muhldorfer, K., Shilton, C., Bendict, S., Whatmore, A. M., and Eisenberg, T. (accepted). Change of a medically important genus: Worldwide emergence of genetically diverse novel *Brucella* species in exotic frogs. *PLoS ONE*.
- Scott, J. C., Koylass, M. S., Stubberfield, M. R., and Whatmore, A. M. (2007). Multiplex assay based on single-nucleotide polymorphisms for rapid identification of *Brucella* isolates at the species level. *Appl. Environ. Microbiol.* 73, 7331–7337. doi: 10.1128/AEM.00976-07
- Tamura, K., Peterson, D., Peterson, N., Stecher, G., Nei, M., and Kumar, S. (2011). MEGA5: molecular evolutionary genetics analysis using maximum likelihood, evolutionary distance, and maximum parsimony methods. *Mol. Biol. Evol.* 28, 2731–2739. doi: 10.1093/molbev/msr121
- Tan, K. K., Tan, Y. C., Chang, L. Y., Lee, K. W., Nore, S. S., Yee, W. Y., et al. (2015). Full genome SNP-based phylogenetic analysis reveals the origin and global spread of *Brucella melitensis*. *BMC Genomics* 16:93. doi: 10.1186/s12864-015-1294-x
- Tiller, R. V., Gee, J. E., Frace, M. A., Taylor, T. K., Setubal, J. C., Hoffmaster, A. R., et al. (2010a). Characterization of novel *Brucella* strains originating from wild native rodent species in North Queensland, Australia. *Appl. Environ. Microbiol.* 76, 5837–5845. doi: 10.1128/AEM.00620-10
- Tiller, R. V., Gee, J. E., Lonsway, D. R., Gribble, S., Bell, S. C., Jennison, A. V., et al. (2010b). Identification of an unusual *Brucella* strain (BO2) from a lung biopsy in a 52 year-old patient with chronic destructive pneumonia. *BMC Microbiol.* 10:23. doi: 10.1186/1471-2180-10-23
- Vemulapalli, R., McQuiston, J. R., Schurig, G. G., Sriranganathan, N., Halling, S. M., and Boyle, S. M. (1999). Identification of an IS711 element interrupting the *wboA* gene of *Brucella abortus* vaccine strain RB51 and a PCR assay to distinguish strain RB51 from other *Brucella* species and strains. *Clin. Diagn. Lab. Immunol.* 6, 760–764.
- Verger, J. M., Grimont, F., Grimont, P. A. D., and Grayon, M. (1985). *Brucella*, a monospecific genus as shown by deoxyribonucleic acid hybridization. *Int. J. Syst. Bacteriol.* 35, 292–295. doi: 10.1099/00207713-35-3-292
- Wattam, A. R., Inzana, T. J., Williams, K. P., Mane, S. P., Shukla, M., Almeida, N. F., et al. (2012). Comparative genomics of early-diverging *Brucella* strains reveals a novel lipopolysaccharide biosynthesis pathway. *Mbio* 3:e00246–212. doi: 10.1128/mBio.00388-12
- Wattam, A. R., Foster, J. T., Mane, S. P., Beckstrom-Sternberg, S. M., Beckstrom-Sternberg, J. M., Dickerman, A. W., et al. (2014). Comparative phylogenomics and evolution of the *Brucellae* reveal a path to virulence. *J. Bacteriol.* 196, 920–930. doi: 10.1128/JB.01091-13
- Whatmore, A. M., Shankster, S. J., Perrett, L. L., Murphy, T. J., Brew, S. D., Thirlwall, R. E., et al. (2006). Identification and characterization of variable number of tandem repeat markers for typing of *Brucella* spp. *J. Clin. Microbiol.* 44, 1982–1993. doi: 10.1128/JCM.02039-05
- Whatmore, A. M., Perrett, L. L., and MacMillan, A. P. (2007). Characterisation of the genetic diversity of *Brucella* by multilocus sequencing. *BMC Microbiol.* 7:34. doi: 10.1186/1471-2180-7-34
- Whatmore, A. M., Dawson, C. E., Groussaud, P., Koylass, M. S., King, A. C., Shankster, S. J., et al. (2008). Marine mammal *Brucella* genotype

- associated with zoonotic infection. *Emerg. Infect. Dis.* 14, 517–518. doi: 10.3201/eid1403.070829
- Whatmore, A. M., Davison, N., Cloeckaert, A., Al Dahouk, S., Zygmunt, M. S., Brew, S. D., et al. (2014). *Brucella papionis* sp. nov., isolated from baboons (*Papio* spp.). *Int. J. Syst. Evol. Microbiol.* 64, 4120–4128. doi: 10.1099/ijs.0.065482-0
- Whatmore, A. M., Dale, E.-J., Stubberfield, E., Muchowski, J., Koylass, M., Dawson, C., et al. (2015). Isolation of *Brucella* from a White's tree frog (*Litoria caerulea*). *JMM Case Rep.* 2015:2. doi: 10.1099/jmmcr.0.000017
- Whatmore, A. M. (2009). Current understanding of the genetic diversity of *Brucella*, an expanding genus of zoonotic pathogens. *Infect. Genet. Evol.* 9, 1168–1184. doi: 10.1016/j.meegid.2009.07.001
- World Organisation for Animal Health (2011). *Manual of Diagnostic Tests and Vaccines for Terrestrial Animals*. Available online from: <http://www.oie.int/international-standard-setting/terrestrial-manual/access-online/>

Conflict of Interest Statement: The authors declare that the research was conducted in the absence of any commercial or financial relationships that could be construed as a potential conflict of interest.

The reviewer VG and handling Editor declared their shared affiliation and the handling Editor states that the process nevertheless met the standards of a fair and objective review.

Copyright © 2016 Whatmore, Koylass, Muchowski, Edwards-Smallbone, Gopaul and Perrett. This is an open-access article distributed under the terms of the Creative Commons Attribution License (CC BY). The use, distribution or reproduction in other forums is permitted, provided the original author(s) or licensor are credited and that the original publication in this journal is cited, in accordance with accepted academic practice. No use, distribution or reproduction is permitted which does not comply with these terms.



MLVA Genotyping Characteristics of Human *Brucella melitensis* Isolated from Ulanqab of Inner Mongolia, China

Zhi-Guo Liu^{1,2†}, Dong-Dong Di^{3†}, Miao Wang², Ri-Hong Liu², Hong-Yan Zhao⁴, Dong-Ri Piao⁴, Guo-Zhong Tian⁴, Wei-Xing Fan³, Hai Jiang^{4*}, Bu-Yun Cui^{4*} and Xian-Zhu Xia^{1,5*}

¹ College of Veterinary Medical Inner Mongolia Agriculture University, Hohhot, China, ² Ulanqab Centre for Endemic Disease Prevention and Control, Health and Family Planning Commission of Ulanqab, Jining, China, ³ Laboratory of Zoonoses, China Animal Health and Epidemiology Center, MOA, Qingdao, China, ⁴ State Key Laboratory for Infectious Disease Prevention and Control, Collaborative Innovation Center for Diagnosis and Treatment of Infectious Disease, National Institute for Communicable Disease Control and Prevention, Chinese Center for Disease Control and Prevention, Beijing, China, ⁵ Institute of Military Veterinary AMMS, Changchun, China

OPEN ACCESS

Edited by:

Adrian Whatmore,
Animal and Plant Health Agency, UK

Reviewed by:

Giuliano Garofolo,
Istituto Zooprofilattico Sperimentale
dell'Abruzzo e del Molise G. Caporale,
Italy
Jeffrey T. Foster,
University of New Hampshire, USA

*Correspondence:

Hai Jiang
jianghai@icdc.cn
Bu-Yun Cui
cui buyun@icdc.cn
Xian-Zhu Xia
xia xzh@cae.cn

[†]These authors have contributed
equally to this work.

Specialty section:

This article was submitted to
Infectious Diseases,
a section of the journal
Frontiers in Microbiology

Received: 17 August 2016

Accepted: 03 January 2017

Published: 18 January 2017

Citation:

Liu Z-G, Di D-D, Wang M, Liu R-H,
Zhao H-Y, Piao D-R, Tian G-Z,
Fan W-X, Jiang H, Cui B-Y and
Xia X-Z (2017) MLVA Genotyping
Characteristics of Human *Brucella*
melitensis Isolated from Ulanqab of
Inner Mongolia, China.
Front. Microbiol. 8:6.
doi: 10.3389/fmicb.2017.00006

Brucellosis is a serious public health problem in Ulanqab, which is a region located in the middle of the Inner Mongolia Autonomous Region adjacent to Shanxi and Hebei provinces. The disease is prevalent in both the latter provinces and Ulanqab with the highest prevalence of brucellosis occurring in Inner Mongolia. The MLVA-16 scheme is a genotyping tool for assessing genetic diversity and relationships among isolates. Moreover, this genotyping tool can also be applied to epidemiological trace-back investigations. This study reports the occurrence of at least two *B. melitensis* biovars (1 and 3) in Ulanqab, encompassing 22 and 94 isolates, respectively. *B. melitensis* biovar 3 was the predominant biovar in the area examined. Panel 1 (MLVA-8) identified three genotypes (42, 63, and 114), with genotype 42 ($n = 101$) representing 87% of the tested strains. MLVA-11 identified eight genotypes (116, 111, 297, 291, and 342–345) from 116 of the analyzed isolates. All of these isolates were identified as belonging to the East Mediterranean group. Genotype 116 ($n = 94$) was the predominant genotype and represented 81% of the isolates. The isolates pertaining to this genotype were distributed throughout most of Ulanqab and neighboring regions. The MLVA-16 scheme showed the presence of 69 genotypes, with 46 genotypes being represented by single isolates. This analysis revealed that Ulanqab brucellosis cases had epidemiologically unrelated and sporadic characteristics. The remaining 23 genotypes were shared (between a total of 70 isolates) with each genotype being represented by two to eight isolates. These data indicate that these cases were epidemiologically related. MLVA genotyping confirmed the occurrence of a multipoint outbreak epidemic and intrafamilial brucellosis. Extensive genotype-sharing events were observed among isolates from different regions of Ulanqab and from other provinces of China. These findings suggest either a lack of control of animal movement between different regions or the circulation of contaminated animal products in the market. Our study is the first comprehensive genotyping and genetic analysis of *B. melitensis* in Ulanqab. We believe that this study will help to improve the effectiveness of brucellosis control programs.

Keywords: *Brucella melitensis*, MLVA, molecular epidemiology, trace-back analysis, Ulanqab, Inner Mongolia

INTRODUCTION

Brucella is a genus of Gram-negative facultative intracellular pathogens that infect humans and a variety of animal species (Shevtsov et al., 2015). Brucellosis is transmitted to humans following direct contact with infected animals or indirectly through the consumption of unpasteurized animal products (Deshmukh et al., 2015). The disease causes severe morbidity in humans and results in many medical challenges globally, especially in poor regions (Corbel, 1997; Pappas et al., 2006; Ducrotoy et al., 2015). Furthermore, animal brucellosis causes abortion and infertility in livestock, resulting in serious economic losses (Araj, 1999).

Since 2000, the incidence of brucellosis has increased rapidly in many regions in China (Deqiu et al., 2002; Jiang et al., 2011). The incidence of brucellosis in Inner Mongolia ranks in the top three incidence rates in Chinese provinces. The incidence of brucellosis in Ulanqab was 177.1/100,000 cases in 2011, 42.2/100,000 cases in 2012, 17.2/100,000 cases in 2013, 24.1/100,000 cases in 2014, and 26.5/100,000 cases in 2015. Ulanqab is a relatively small region in Inner Mongolia, covering a geographical area of 545,000 km², and comprises 11 regions that are extensively pastoral and semi-pastoral. The people that inhabit these regions are economically dependent on small ruminant (sheep) livestock (Jiang et al., 2013). Livestock exchange occurs frequently in this region, and includes import from other areas, internal exchange, livestock foster care, and shifting field grazing. Due to excessive poverty and limitations in relation to control measures, brucellosis is endemic among sheep and humans in these regions. Technical difficulties have meant that previous studies only concentrated on *Brucella* infection surveillance in this region, and adequate attention was not paid to the molecular typing of *Brucella* species. However, rapid and accurate identification and typing procedures are important for epidemiologic surveillance, investigation of outbreaks, and control program follow-up (Whatmore et al., 2006; Al Dahouk et al., 2007; García-Yoldi et al., 2007). Previous studies have confirmed that MLVA (Multiple-locus variable-number tandem repeat analysis) is a useful tool for identifying and genotyping *Brucella* isolates and the resultant data can be used for genetic diversity analysis and epidemiology trace-back investigations (Whatmore et al., 2006; Kattar et al., 2008; Ferreira et al., 2012; Garofolo et al., 2013). In this study, the MLVA-16 scheme was used to type samples and determine the genotyping characteristics and epidemiological links of associated strains. The results of this study contribute to our understanding of the main transmission routes associated with this pathogen as well as effectively informing brucellosis control policies in Ulanqab.

MATERIALS AND METHODS

Ethics Statement

This research was carried out according to the principles of the Declaration of Helsinki. The study is a retrospective investigation of historical strain collections using modern typing methods and the study protocol was approved by the Ethics Committees of the National Institute for Communicable Disease Control

and Prevention and the Chinese Center for Disease Control and Prevention. Informed consent was obtained from all of the patients prior to diagnosis. *Brucella* spp. were isolated from patients' blood samples following confirmation of their consent.

Bacterial Strains

A total of 116 strains were examined. These strains were obtained from 11 Ulanqab counties and three neighboring regions [Suniteyouqi (Xilin Hot City of Inner Mongolia), Datong (Shanxi province), and Shangyi (Hebei province)] from 2011 to 2015. A total of 115 strains were recovered from 114 patients, and one strain was recovered from sheep. Two strains (ws091 and ws101) were obtained from the same patient. The *Brucella* strains were isolated and biotypes were identified using standard procedures (Alton et al., 1975; Al Dahouk et al., 2003). *B. melitensis* 16M, *B. abortus* 544, and *B. suis* 1330 reference strains were used as control strains. Species-level identification was undertaken using *B. abortus*, *B. melitensis*, *B. ovis*, *B. suis* PCR (AMOS-PCR; Bricker and Halling, 1994).

DNA Preparation

DNA was extracted with a Nucleic Acid Automatic Extraction System (LLXBIO China Ltd., China) using a single loop of fresh bacterial cells that were grown for 48 h on *Brucella* agar. DNA concentrations were measured by UV spectrophotometry (NanoDrop 2000, Thermo, US).

Brucella MLVA-16 Genotyping Scheme

MLVA was performed as described previously (Le Flèche et al., 2006; Al Dahouk et al., 2007). The 16 primer pairs were divided into three groups: Panel 1 (MLVA-8: eight loci including bruce06, bruce08, bruce11, bruce12, bruce42, bruce43, bruce45, and bruce55), panel 2A (three loci including bruce18, bruce19, and bruce21), and panel 2B (five loci including bruce04, bruce07, bruce09, bruce16, and bruce30); MLVA-11 (panels 1 and 2A), and MLVA-16 (panels 1, 2A, and 2B). PCR amplifications were performed in 20 µL reaction volumes. The PCR conditions were as follows: initial denaturation at 94°C for 3 min, and then 30 cycles of 94°C for 30 s, 60°C for 30 s, and 72°C for 50 s, with a final extension of 72°C for 3 min. PCR products for the 16 loci were denatured and resolved by capillary electrophoresis on an ABI Prism 3130 automated fluorescent capillary DNA sequencer (Applied Biosystems). Fragments were sized following comparison with a ROX (carboxy-X-rhodamine)-labeled molecular ladder (MapMaker 1000; Bioventures Inc., Murfreesboro, TN, USA) and Gene Mapper software version 4.0 (Applied Biosystems). The fragment sizes were subsequently converted to repeat unit numbers using a published allele numbering system (Le Flèche et al., 2006; Jiang et al., 2013; Scholz and Vergnaud, 2013).

Analysis of MLVA Data

BioNumerics version 5.1 software (Applied Maths, Belgium) was used to analyze the MLVA-16 assay data. Both categorical coefficient and unweighted pair group methods were applied to clustering analysis. Polymorphisms at each locus were quantified using the Hunter-Gaston Diversity index, available

on the HPA website (<http://www.hpa-bioinformatics.org.uk/cgi-bin/DICI/DICI.pl>; Hunter and Gaston, 1988). Resultant genotypes were compared using the web-based Brucella 2012 MLVA database. MLVA-11 was also used to determine phylogeographic relationships between our isolates and 528 isolates from MLVAbank including not available group (2), Africa group (4), America group (75), West Mediterranean group (77), China group (97), and East Mediterranean group (273). Minimum-spanning trees were constructed using the goeBURST algorithm with PHYOVIZ 2.0 (Francisco et al., 2012; Nascimento et al., 2017). MLVA-16 cluster analysis was extended to 194 *B. melitensis* strains including the Ulanqab isolates reported here. Seventy-eight strains from neighboring provinces of Inner Mongolia were utilized for the molecular epidemiology investigation. All MLVA profiles have been submitted to the MLVAbank (<http://microbesgenotyping.i2bc.paris-saclay.fr/>).

RESULTS

Patient Characteristics

Of the 114 *B. melitensis* isolates obtained from unique patients (two isolates were obtained from the same patient), 95% of the strains were isolated from individuals who were engaged in livestock farming and related work [including livestock traffickers ($n = 3$) and slaughterhouse workers ($n = 1$)]. The mean age of the 114 patients was 45.1 years (range 5–73 years), and the ratio of males ($n = 79$) to females ($n = 35$) was 2.26. The relative number of cases that exhibited pain, fever, fatigue, and sweating was 75.8, 46.6, 29.3, and 12.1%, respectively.

Identification and Distribution of *Brucella melitensis*

All of the 116 *Brucella* strains were identified as *B. melitensis* bv. 3 ($n = 94$) and *B. melitensis* bv. 1 ($n = 22$) using the classical biotyping method. These strains were further examined by AMOS-PCR and 731 bp PCR products were obtained. Consistent with the classical biotyping approach, 116 *B. melitensis* strains were observed in the counties and surrounding areas of Ulanqab, including Suniteyouqi (1) (Xilin Hot City of Inner Mongolia), Datong (1) (Shanxi province), and Shangyi (3) (Hebei province) (Figure 1 and Table S1). Strains were predominantly distributed in the Qianshan (76 isolates) area of Ulanqab, especially, Liangcheng (22 isolates), Qianqi (20 isolates), and Fengzhen (18 isolates). An additional 30 strains (from the total of 116 isolates) were isolated from the Houshan area, with five strains being isolated from the areas surrounding Ulanqab. The original locations associated with the other five strains were unknown (Table S1).

MLVA-16 Genotyping Results

In this study, results of a *B. melitensis* isolate diversity analysis confirmed the high discriminatory power of the MLVA-16 panel, with polymorphism levels of 0.985 based on the HGDI, compared to 0.235 and 0.337 for the MLVA-8 and MLVA-11 panels, respectively (Table 1). The HGDI in panel 1 was the highest (0.235) for bruce43. The bruce06, bruce08, bruce11, bruce12, bruce42, and bruce45 loci of panel 1, and bruce18 of panel 2A

showed only one allele (HGDI = 0). In contrast, the greatest variability was detected in panel 2B (diversity index ≥ 0.690) within loci bruce04, bruce16, and bruce30. The bruce04 locus displayed the highest diversity (HGDI = 0.841; Table 1).

Using the complete MLVA-16 scheme including panels 1, 2A, and 2B loci, 116 *B. melitensis* isolates clustered into 69 genotypes, 46 of which were represented by singular independent strains. The other 23 genotypes were shared by two or more isolates. Following analysis of data pertaining to panel 1, the *B. melitensis* population clustered into three known MLVA-8 genotypes: 42 (1-5-3-13-2-2-3-2; $n = 101$), 63 (1-5-3-13-2-3-3-2; $n = 9$), and 114 (1-5-3-13-2-1-3-2; $n = 6$). A dendrogram of the 116 *B. melitensis* strains shows strain identification features, the panel 1 genotype, panel 1+ panel 2A genotype, their geographical origins and the year of isolation (Figure 2). The clustering analysis showed that the 116 isolates formed ten main clusters. Clusters III and IX had two genotypes (114 and 63) and (42 and 63) each, respectively; Clusters VI and VII contained the same two genotypes (42 and 114); Clusters I, II, IV, V, VIII, and X all contained genotype 42.

The phylogeographic relationships of 116 Ulanqab *B. melitensis* isolates were assessed with MLVA-11 and eight different genotypes were identified. Four of these genotypes were previously described (116, 111, 297, and 291) and the remaining four novel genotypes represent single strains with single locus variants of these genotypes, and have been assigned numbers 342–345 in MLVAbank (<http://microbesgenotyping.i2bc.paris-saclay.fr/>). MLVA-11 genotypes 342 (1-5-3-13-2-2-3-2-4-36-8) and 345 (1-5-3-13-2-2-3-2-4-41-9) were single-locus variant (SLV) of MLVA-11 genotype 116 (1-5-3-13-2-2-3-2-4-41-8); MLVA-11 genotypes 343 (1-5-3-13-2-3-3-2-4-41-9) and 344 (1-5-3-13-2-1-3-2-4-46-8) were single-locus variants (SLV) of MLVA-11 genotypes 111 (1-5-3-13-2-3-3-2-4-41-8) and 297 (1-5-3-13-2-2-3-2-4-46-8), respectively. Genotype 116 was the predominant genotype, representing 81% (94/116) of the isolates. This genotype was broadly distributed throughout most of Ulanqab and neighboring regions. Minimum Spanning Tree analysis revealed that all of MLVA-11 genotypes are members of the “East Mediterranean” group (Figure 3 and Table S2).

Cluster Analysis for Ulanqab *B. melitensis* Genotypes

The MLVA-16 scheme indicated that there were 69 MLVA-16 genotypes (Figure 2), 46 of which were represented by unique strains. The other 23 were shared genotypes, with associated genotypes shared between two and eight isolates. The 23 shared genotypes were comprised of 70 clustered strains, with a clustering rate of 60.3% (70/116; Figure 2). The most frequently observed genotype, genotype 18, was present in eight isolates obtained from three regions over a 6-month period in 2015. The six strains that contained the second most frequently observed genotype, genotype 43, were isolated from three regions. Genotypes 6 and 45 were each present in five isolates and each genotype was present in two strains that were isolated from the Zhongqi.

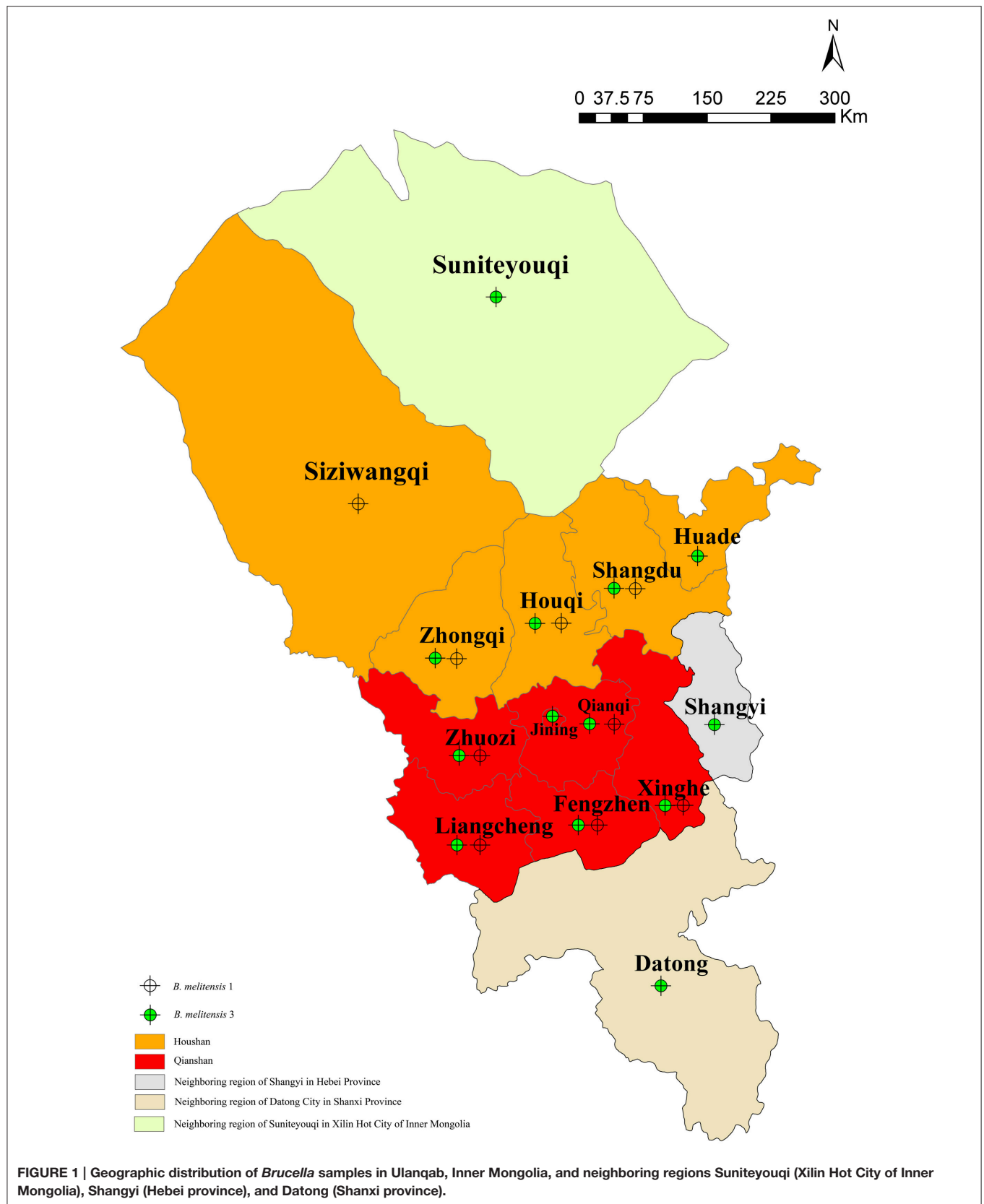


TABLE 1 | Allelic types and Hunter-Gaston diversity index (HGDI) of *B. melitensis* for 16 loci in this study.

Panel and Locus	Diversity	Index Confidence Interval	K	Max (pi)
bruce06	0.000	0.000–0.061	1	1.000
bruce08	0.000	0.000–0.061	1	1.000
bruce11	0.000	0.000–0.061	1	1.000
bruce12	0.000	0.000–0.061	1	1.000
bruce42	0.000	0.000–0.061	1	1.000
bruce43	0.235	0.137–0.333	3	0.871
bruce45	0.000	0.000–0.061	1	1.000
bruce55	0.017	0.000–0.050	2	0.991
Bruce18	0.000	0.000–0.061	1	1.000
bruce19	0.115	0.038–0.193	3	0.940
bruce21	0.034	0.000–0.080	2	0.983
Panel 2A	0.147	0.061–0.233	4	0.922
bruce04	0.841	0.816–0.866	8	0.250
bruce07	0.084	0.015–0.153	3	0.957
bruce09	0.034	0.000–0.080	3	0.983
bruce16	0.791	0.748–0.834	11	0.328
bruce30	0.690	0.643–0.737	6	0.440
Panel 2B	0.983	0.976–0.989	62	0.069
MLVA-16	0.985	0.979–0.992	69	0.069
MLVA-8	0.235	0.137–0.333	3	0.871
MLVA-11	0.337	0.228–0.447	8	0.810

Diversity Index (for VNTR data), A measure of the variation of the number of repeats at each locus. Ranges from 0.0 (no diversity) to 1.0 (complete diversity).

Confidence Interval, Precision of the Diversity Index, expressed as 95% upper and lower boundaries.

K, Number of different repeats present at this locus in this sample set.

Max (pi), Fraction of samples that have the most frequent repeat number in this locus (range 0.0–1.0).

Relevance of MLVA-16 Genotyping for Clinical Case and Trace-Back Analysis of *B. melitensis*

Eleven shared genotypes (Figure 2, genotypes with black shadow) were concurrently recovered from patients who came from the same area, two genotypes (22 and 26) of which were each recovered from patients of the same family. All associated patients contracted brucellosis from direct/indirect contact with infected sheep. Two isolates (genotype 7, ws049; and genotype 16, ws050) were obtained from members of the same family (mother and son) who engaged in sheep farming did not share the same MLVA-16 genotype. Two strains (ws091 and ws101) of genotype 18 were obtained from the same patient (13 days apart). Eighteen genotypes were shared between two or more isolates from two or more regions. The regions that exhibited shared genotypes are shown in Figure 4 and Table S3. All other isolates had distinct genotypes reflecting sporadic cases.

Molecular Epidemiological Investigation of 194 Chinese *B. melitensis* Strains

Five *B. melitensis* strains were obtained from Xilin Hot City of Inner Mongolia (one strain), Hebei province (three strains), and Shanxi province (one strain). MLVA was used to determine

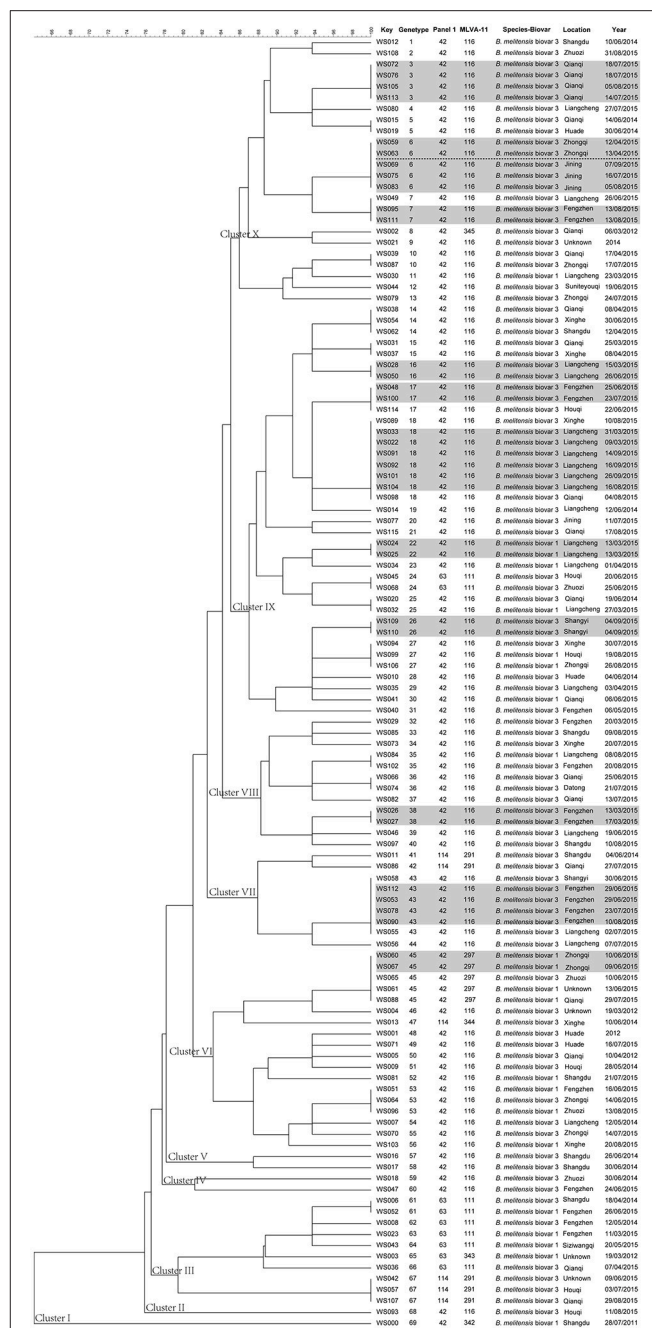


FIGURE 2 | Dendrogram based on the MLVA-16 genotyping assay (UPGMA method), showing relationships between the 116 *B. melitensis* isolates. The columns show the identification numbers, MLVA-16 genotypes, panel 1 genotypes and MLVA-11 (panels 1 and 2A) genotypes, species-biovar, their geographic location, and the year of isolation of the strains.

the epidemiological links between 116 *Brucella* strains from Ulanqab (Table S1) and 78 *Brucella* strains from other provinces of China (Table S4). Ten genotypes were shared by strains from Ulanqab and 10 different provinces of China, including Inner Mongolia, Hebei, Shanxi, Shandong, Guangdong, Zhejiang, Liaoning, Xinjiang, Qinghai, and Beijing. Isolate BJ06-10 was

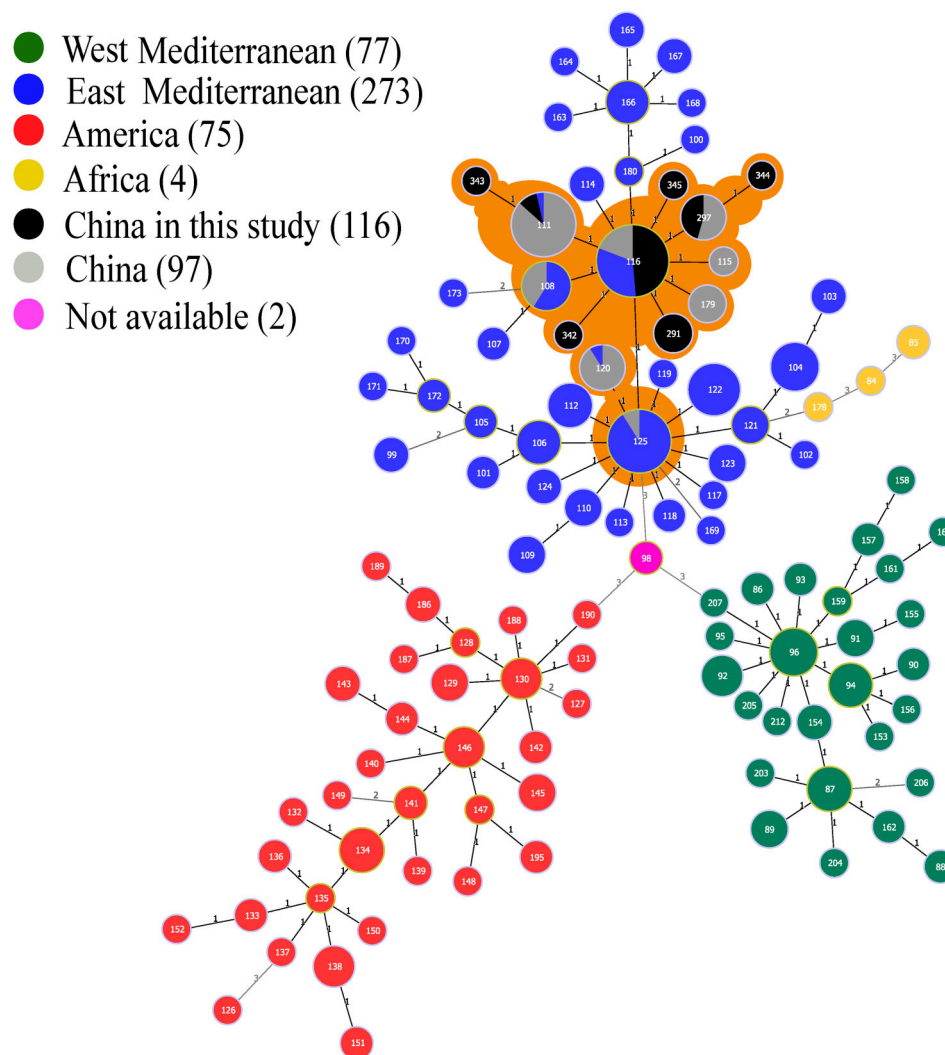


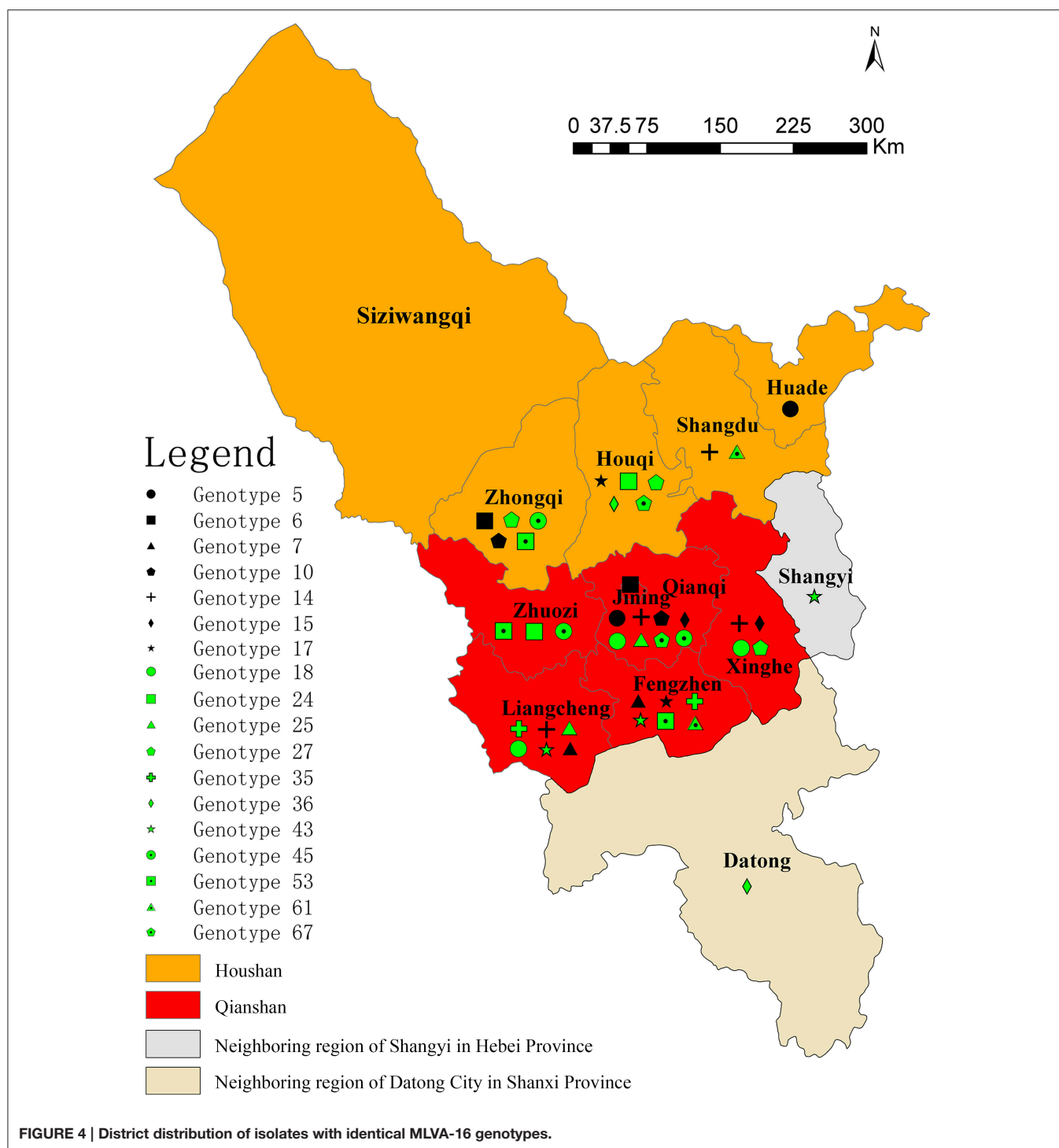
FIGURE 3 | Minimum spanning tree for *B. melitensis* using MLVA-11 data with the East Mediterranean group (blue), the America group (red), the Africa group (yellow), and the West Mediterranean group (blackish green), compared to the China genotypes (gray), and China isolates from our study (black). n.a. not available (pink). Samples with orange shadows indicate the China cluster within the East Mediterranean lineage.

isolated from a microbiology laboratory technician from Beijing hospital and was first reported in China by Jiang et al. (2011). This isolate contained an identical MLVA-16 pattern to isolates ws031 and ws037 from Ulanqab. Isolate ws097 exhibited an identical genotype to strains from four different provinces of China, Inner Mongolia, Shanxi, Hebei, and Guangdong, respectively. Furthermore, only the highest diversity locus (bru04) harbored alleles that were different from strains (TS-bruce051) isolated from Heilongjiang, China. As shown in Table S5, other strains from Ulanqab exhibited identical MLVA-16 profiles to strains isolated from different provinces of China.

DISCUSSION

In the present study, we used MLVA methods to genotype *Brucella* isolates from Ulanqab. A total of 116 *Brucella* isolates

were examined by classical biotyping methods and MLVA typing. All isolates were *B. melitensis* (bv. 1 and bv. 3), and *B. melitensis* bv. 3 was the predominant biovar in this region. These data were in accordance with previous studies where human brucellosis was almost exclusively caused by *B. melitensis* bv. 3 in China (Dequ et al., 2002). Furthermore, nearly all of the associated patients had a history of exposure to sheep. The results reveal that human brucellosis in Ulanqab is more related to infections in sheep than other livestock. Contact with infected domestic animals (sheep) has been identified in another study as the most likely source of infection (Hasanjani Roushan and Ebrahimpour, 2015). Since 2011, S2 vaccine immunization programs have been implemented for sheep for 5 consecutive years in Inner Mongolia. However, human brucellosis continues to occur with a considerable amount of *B. melitensis* infections diagnosed. Consequently, stringent animal quarantine measures could be



a promising control strategy for human brucellosis in this region.

A total of 76 (65.5%) *B. melitensis* strains were isolated from the Qianshan area of Ulanqab. However, the incidence of brucellosis in Houshan, the region directly to the north of Ulanqab, is significantly higher than that in Qianshan districts. This may be related to the underreporting of cases in

low-incidence areas. However, the most important reason relates to the fact that the Qianshan region is close to our hospital, and it is convenient for these individuals to attain a diagnosis and related treatment regimens.

Based on the MLVA-16 marker, our results clearly show that *B. melitensis*, despite the high genetic homogeneity within the genus, is highly polymorphic at the microsatellite level. The

complete MLVA-16 profile offers excellent discriminatory power; the Hunter-Gaston index was 0.985. Panel 2B markers displayed very high discriminatory powers. This result is consistent with previous reports (Jiang et al., 2011; Xiao et al., 2015). With regard to MLVA-8 genotypes, the most frequently observed genotype in this study, genotype 42, was also observed in other regions of China (Jiang et al., 2011; Ma et al., 2016; Sun et al., 2016). MLVA-8 and MLVA-11 yielded three and eight genotypes, respectively; whereas the addition of panel 2B increased the number of genotypes to 69. These findings show that the genotypic variation of Ulanqab isolates was predominantly associated with the highly variable panel 2B loci and to a much lesser extent panel 2A (locus Bruce19 and 21) and panel 1 (loci Bruce 43) loci. In agreement with a previous report (Kilic et al., 2011), this may reflect microevolution through a stepwise mutational event of the most variable loci from a very limited number of ancestors. In addition, there was no clear relationship between biovar and genotype within this *B. melitensis* population. This finding is in agreement with previous studies that used multiple VNTR typing approaches to show that there was no discernible correlation between genotype and biovars (Whatmore et al., 2006). This suggests either that *B. melitensis* biovars do not adhere to specific genetic groups, or that biotyping is so subjective that field strains are often incorrectly assigned masking any potential genetic relationship (Whatmore et al., 2007).

The phylogeographic relationships of the 116 *B. melitensis* isolates from Ulanqab were compared to 528 MLVA profiles from the international database using MLVA-11. A minimum spanning tree analysis revealed the presence of eight different genotypes; all of the strains belonged to the East Mediterranean lineage. Distribution of the MLVA-11 genotypes was consistent in most of the provinces in China. Genotype 116 is the predominant genotype and is likely to have been historically present in this region. Moreover, this genotype was also responsible for the vast majority of *Brucella* infections in China. The four novel genotypes (342–345) represent single strains. Upon comparison with the MLVA international database we observed that the four novel MLVA-11 genotypes (342–345) had been observed for the first time in Ulanqab. No isolates from America and West Mediterranean lineages were observed in this study.

The MLVA-16 genotyping clustering rate was 60.3%, with most isolates differing in one to three loci in panel 2B. The proportion of strains being in clusters suggest that a significant proportion of brucellosis in Ulanqab is due to multiple contaminations from a single source. Four large clusters (genotypes 6, 18, 43, and 45) including strains from different regions. These data show that ongoing transmission of human brucellosis not only in a specific region but also among the regions in Ulanqab. Additionally, the determination that 46 isolates showed distinct genotypes reflected that more than 39.7% (46/116) of the brucellosis cases in Ulanqab had epidemiologically unrelated sporadic characteristics.

Previous studies have confirmed that MLVA-16 genotyping results show good correlation with epidemiological data with epidemiologically related isolates displaying identical or very closely related genotypes (Al Dahouk et al., 2007; Nöckler

et al., 2009; Kilic et al., 2011; Allen et al., 2015). The current study also confirms the occurrence of multipoint outbreak epidemics and intrafamilial brucellosis. The 11 shared genotypes observed during this analysis pertained to 33 *Brucella* strains obtained from the same area. This suggested the occurrence of a multipoint outbreak epidemic from multiple common sources. Meantime, MLVA genotyping also confirmed intrafamilial brucellosis outbreaks in two cases (genotypes 22 and 26), where brucellosis most probably resulted from contact with infected sheep. Other nine shared genotypes confirms the occurrence of multipoint outbreak epidemics. This source of infection also resulted in a higher incidence of brucellosis in other regions of China (Xiao et al., 2015; Ma et al., 2016). In accordance with the previous studies (Kilic et al., 2011), two isolates (genotype 7, ws049; genotype 16, ws050) with different MLVA-16 genotypes were obtained from members of the same family are likely to have resulted from either persistent circulating strains causing sporadic infections or mutation events during the course of the outbreak.

Two isolates from human blood exhibiting identical genotypes were obtained 13 days apart from the same patient, suggesting the occurrence of a singular *B. melitensis* infection. This occurrence is consistent with previous research findings (Kasymbekov et al., 2013). These data confirmed that brucellosis bacteremia persist for at least 13 days (Memish et al., 2000; Pappas et al., 2006; Vrioni et al., 2008). The previous investigations confirmed that strains of low virulence (e.g., *Brucella abortus* S19) are almost always cleared from the bloodstream within a week, whereas virulent strains produce a bacteremia that regularly persists for 4 weeks and may last much longer (Cruickshank, 1957).

Eighteen shared genotypes (5, 6, 7, 10, 14, 15, 17, 18, 24, 25, 27, 35, 36, 43, 45, 53, 61, and 67) including the 58 clustered strains were obtained from two or more regions and displayed identical MLVA-16 profiles. MLVA-16 genotyping confirmed that more than half of the human brucellosis cases in this region resulted from either very close cross-transmission in a singular location or ongoing transmission among different regions. This is likely to have occurred as a result of the frequent trade and exchange of sheep in the associated regions (Garofolo et al., 2013; Shevtsov et al., 2015). In future, a more precise investigation of the strains circulating in animal reservoirs in these regions will be required to confirm this result.

When the strains observed during this analysis were compared with those from neighboring provinces of Inner Mongolia, 10 identical MLVA-16 genotypes were recorded, suggesting possible epidemiological links. Additionally, one strain was isolated from a microbiology laboratory technician in Beijing hospital in 2011 (Jiang et al., 2011). This isolate harbored an identical MLVA-16 profile with two isolates (ws031 and ws037) from Ulanqab. This result suggests that Ulanqab might be the source of infection. It should be noted that isolate ws097 from Ulanqab displayed an identical MLVA-16 profile with strains from four different provinces in China, Inner Mongolia, Shanxi, Hebei, and Guangdong, respectively. This result may be explained by the fact that Inner Mongolia is adjacent to northern Shanxi and Hebei province, and frequent livestock exchange occurs between these areas. These findings reflect either a lack of control in the

movement of infected animals between regions or the circulation of infected animal products in the market. This suggests that inspection mechanisms and measures to ensure the quarantine of livestock exported from endemic regions should be more stringent.

In the present study, 116 *B. melitensis* isolates were genotyped and a comprehensive global genetic analysis was performed. All of the strains belong to the East Mediterranean lineage. We also observed that there was a broad genetic relationship among the analyzed population. Thus, we conclude that the MLVA-16 assay appears to be a very practical and important molecular genotyping tool that is capable of confirming epidemiological linkages in outbreak and trace-back investigations. This study will help to improve the effectiveness of brucellosis control programs.

AUTHOR CONTRIBUTIONS

ZL performed most of the strain isolations and MLVA typing. ZL also drafted the manuscript; DD performed the MLVA cluster analysis and manuscript revision; MW and RL were in charge of epidemiological investigations and data analysis; HZ, GT, and DP prepared the DNA samples; HJ participated in the design of the study and critically reviewed the manuscript; BC, WF, and XX participated in the design of the study and also

managed the project. All authors read and approved the final manuscript.

FUNDING

This study was supported by the Medical and Hygiene Research Projects pertaining to the Inner Mongolia Health and Family Planning Commission (201301094), the National Nature Science Foundation (81271900), the Science and Technology Basic Work Program (2012FY111000), and the public welfare research special projects of Health and Family Planning Commission of China (201302006). The funders contributed to the study design and data collection.

ACKNOWLEDGMENTS

We are grateful to all of the staff in the Brucellosis Clinic, Ulanqab Centre, for endemic disease prevention and assistance in patient screening.

SUPPLEMENTARY MATERIAL

The Supplementary Material for this article can be found online at: <http://journal.frontiersin.org/article/10.3389/fmicb.2017.00006/full#supplementary-material>

REFERENCES

- Al Dahouk, S., Flèche, P. L., Nöckler, K., Jacques, I., Grayon, M., Scholz, H. C., et al. (2007). Evaluation of Brucella MLVA typing for human brucellosis. *J. Microbiol. Methods* 69, 137–145. doi: 10.1016/j.mimet.2006.12.015
- Al Dahouk, S., Tomaso, H., Nöckler, K., Neubauer, H., and Frangoulidis, D. (2003). Laboratory-based diagnosis of brucellosis—a review of the literature. Part II: serological tests for brucellosis. *Clin. Lab.* 49, 577–589.
- Allen, A., Bredon, E., Byrne, A., Mallon, T., Skuce, R., Groussaud, P., et al. (2015). Molecular epidemiology of Brucella abortus in Northern Ireland-1991 to 2012. *PLoS ONE* 10:e0136721. doi: 10.1371/journal.pone.0136721
- Alton, G. G., Jones, L. M., and Pietz, D. E. (1975). Laboratory techniques in brucellosis. *Monogr. Ser. World Health Organ.* 55, 1–163.
- Araj, G. F. (1999). Human brucellosis: a classical infectious disease with persistent diagnostic challenges. *Clin. Lab. Sci.* 12, 207–212.
- Bricker, B. J., and Halling, S. M. (1994). Differentiation of Brucella abortus bv. 1, 2, and 4, Brucella melitensis, Brucella ovis, and Brucella suis bv. 1 by PCR. *J. Clin. Microbiol.* 32, 2660–2666.
- Corbel, M. J. (1997). Recent advances in brucellosis. *J. Med. Microbiol.* 46, 101–103. doi: 10.1099/00222615-46-2-101
- Cruickshank, J. C. (1957). The duration of bacteraemia in relation to the virulence of Brucella strains. *J. Hyg. (Lond.)* 55, 140–147. doi: 10.1017/S0022272400061313
- Deqiu, S., Donglou, X., and Jiming, Y. (2002). Epidemiology and control of brucellosis in China. *Vet. Microbiol.* 90, 165–182. doi: 10.1016/S0378-1135(02)00252-3
- Deshmukh, A., Hagen, F., Sharabasi, O. A., Abraham, M., Wilson, G., Doiphode, S., et al. (2015). In vitro antimicrobial susceptibility testing of human Brucella melitensis isolates from Qatar between 2014 - 2015. *BMC Microbiol.* 15:121. doi: 10.1186/s12866-015-0458-9
- Ducrot, M. J., Ammary, K., Ait Lbacha, H., Zouagui, Z., Mick, V., Prevost, L., et al. (2015). Narrative overview of animal and human brucellosis in Morocco: intensification of livestock production as a driver for emergence? *Infect. Dis. Poverty* 4, 57. doi: 10.1186/s40249-015-0086-5
- Ferreira, A. C., Chambel, L., Tenreiro, T., Cardoso, R., Flor, L., Dias, I. T., et al. (2012). MLVA16 typing of Portuguese human and animal Brucella melitensis and Brucella abortus isolates. *PLoS ONE* 7:e42514. doi: 10.1371/journal.pone.0042514
- Francisco, A. P., Vaz, C., Monteiro, P. T., Melo-Cristino, J., Ramirez, M., and Carriço, J. A. (2012). PHYLOViZ: phylogenetic inference and data visualization for sequence based typing methods. *BMC Bioinformatics* 13:87. doi: 10.1186/1471-2105-13-87
- García-Yoldi, D., Le Fleche, P., Marín, C. M., De Miguel, M. J., Muñoz, P. M., Vergnaud, G., et al. (2007). Assessment of genetic stability of Brucella melitensis Rev 1 vaccine strain by multiple-locus variable-number tandem repeat analysis. *Vaccine* 25, 2858–2862. doi: 10.1016/j.vaccine.2006.09.063
- Garofolo, G., Di Giannatale, E., De Massis, F., Zilli, K., Ancora, M., Cammà, C., et al. (2013). Investigating genetic diversity of Brucella abortus and Brucella melitensis in Italy with MLVA-16. *Infect. Genet. Evol.* 19, 59–70. doi: 10.1016/j.meegid.2013.06.021
- Hasanjani Roushan, M. R., and Ebrahimpour, S. (2015). Human brucellosis: an overview. *Caspian J. Intern. Med.* 6, 46–47.
- Hunter, P. R., and Gaston, M. A. (1988). Numerical index of the discriminatory ability of typing systems: an application of Simpson's index of diversity. *J. Clin. Microbiol.* 26, 2465–2466.
- Jiang, H., Fan, M., Chen, J., Mi, J., Yu, R., Zhao, H., et al. (2011). MLVA genotyping of Chinese human Brucella melitensis biovar 1, 2 and 3 isolates. *BMC Microbiol.* 11:256. doi: 10.1186/1471-2180-11-256
- Jiang, H., Wang, H., Xu, L., Hu, G., Ma, J., Xiao, P., et al. (2013). MLVA genotyping of Brucella melitensis and Brucella abortus isolates from different animal species and humans and identification of Brucella suis vaccine strain S2 from cattle in China. *PLoS ONE* 8:e76332. doi: 10.1371/journal.pone.0076332
- Kasymbekov, J., Imanseitov, J., Ballif, M., Schürch, N., Paniga, S., Pilo, P., et al. (2013). Molecular epidemiology and antibiotic susceptibility of livestock Brucella melitensis isolates from Naryn Oblast, Kyrgyzstan. *PLoS Negl. Trop. Dis.* 7:e2047. doi: 10.1371/journal.pntd.0002047
- Kattar, M. M., Jaafar, R. F., Araj, G. F., Le Flèche, P., Matar, G. M., Abi Rached, R., et al. (2008). Evaluation of a multilocus variable-number tandem-repeat analysis scheme for typing human Brucella isolates in a region

- of brucellosis endemicity. *J. Clin. Microbiol.* 46, 3935–3940. doi: 10.1128/JCM.00464-08
- Kiliç, S., Ivanov, I. N., Durmaz, R., Bayraktar, M. R., Ayaslioglu, E., Uyanik, M. H., et al. (2011). Multiple-locus variable-number tandem-repeat analysis genotyping of human *Brucella* isolates from Turkey. *J. Clin. Microbiol.* 49, 3276–3283. doi: 10.1128/JCM.02538-10
- Le Flèche, P., Jacques, I., Grayon, M., Al Dahouk, S., Bouchon, P., Denoel, F., et al. (2006). Evaluation and selection of tandem repeat loci for a *Brucella* MLVA typing assay. *BMC Microbiol.* 6:9. doi: 10.1186/1471-2180-6-9
- Ma, J. Y., Wang, H., Zhang, X. F., Xu, L. Q., Hu, G. Y., Jiang, H., et al. (2016). MLVA and MLST typing of *Brucella* from Qinghai, China. *Infect. Dis. Poverty* 5, 26. doi: 10.1186/s40249-016-0123-z
- Memish, Z., Mah, M. W., Al Mahmoud, S., Al Shaalan, M., and Khan, M. Y. (2000). *Brucella* bacteraemia: clinical and laboratory observations in 160 patients. *J. Infect.* 40, 59–63. doi: 10.1053/jinf.1999.0586
- Nascimento, M., Sousa, A., Ramirez, M., Francisco, A. P., Carriço, J. A., and Vaz, C. (2017). PHYLOViZ 2.0: providing scalable data integration and visualization for multiple phylogenetic inference methods. *Bioinformatics* 33, 128–129. doi: 10.1093/bioinformatics/btw582
- Nöckler, K., Maves, R., Cepeda, D., Draeger, A., Mayer-Scholl, A., Chacaltana, J., et al. (2009). Molecular epidemiology of *Brucella* genotypes in patients at a major hospital in central Peru. *J. Clin. Microbiol.* 47, 3147–3155. doi: 10.1128/JCM.00900-09
- Pappas, G., Papadimitriou, P., Akritidis, N., Christou, L., and Tsianos, E. V. (2006). The new global map of human brucellosis. *Lancet Infect. Dis.* 6, 91–99. doi: 10.1016/S1473-3099(06)70382-6
- Scholz, H. C., and Vergnaud, G. (2013). Molecular characterisation of *Brucella* species. *Rev. Sci. Tech.* 32, 149–162. doi: 10.20506/rst.32.1.2189
- Shevtsov, A., Ramanculov, E., Shevtsova, E., Kairzhanova, A., Tarlykov, P., Filipenko, M., et al. (2015). Genetic diversity of *Brucella abortus* and *Brucella melitensis* in Kazakhstan using MLVA-16. *Infect. Genet. Evol.* 34, 173–180. doi: 10.1016/j.meegid.2015.07.008
- Sun, M. J., Di, D. D., Li, Y., Zhang, Z. C., Yan, H., Tian, L. L., et al. (2016). Genotyping of *Brucella melitensis* and *Brucella abortus* strains currently circulating in Xinjiang, China. *Infect. Genet. Evol.* 44, 522–529. doi: 10.1016/j.meegid.2016.07.025
- Vrioni, G., Pappas, G., Priavali, E., Gartzonika, C., and Levidiotou, S. (2008). An eternal microbe: *Brucella* DNA load persists for years after clinical cure. *Clin. Infect. Dis.* 46, e131–e136. doi: 10.1086/588482
- Whatmore, A. M., Perrett, L. L., and MacMillan, A. P. (2007). Characterisation of the genetic diversity of *Brucella* by multilocus sequencing. *BMC Microbiol.* 7:34. doi: 10.1186/1471-2180-7-34
- Whatmore, A. M., Shankster, S. J., Perrett, L. L., Murphy, T. J., Brew, S. D., Thirlwall, R. E., et al. (2006). Identification and characterization of variable-number tandem-repeat markers for typing of *Brucella* spp. *J. Clin. Microbiol.* 44, 1982–1993. doi: 10.1128/JCM.02039-05
- Xiao, P., Yang, H., Di, D., Piao, D., Zhang, Q., Hao, R., et al. (2015). Genotyping of human *Brucella melitensis* biovar 3 isolated from Shanxi Province in China by MLVA16 and HOOF. *PLoS ONE* 10:e0115932. doi: 10.1371/journal.pone.0115932

Conflict of Interest Statement: The authors declare that the research was conducted in the absence of any commercial or financial relationships that could be construed as a potential conflict of interest.

Copyright © 2017 Liu, Di, Wang, Liu, Zhao, Piao, Tian, Fan, Jiang, Cui and Xia. This is an open-access article distributed under the terms of the Creative Commons Attribution License (CC BY). The use, distribution or reproduction in other forums is permitted, provided the original author(s) or licensor are credited and that the original publication in this journal is cited, in accordance with accepted academic practice. No use, distribution or reproduction is permitted which does not comply with these terms.



Brucella and Osteoarticular Cell Activation: Partners in Crime

Guillermo H. Giambartolomei, Paula C. Arriola Benitez and M. Victoria Delpino*

Instituto de Inmunología, Genética y Metabolismo – Consejo Nacional de Investigaciones Científicas y Técnicas –
Universidad de Buenos Aires, Buenos Aires, Argentina

OPEN ACCESS

Edited by:

Axel Cloeckaert,
Institut National de la Recherche
Agronomique (INRA), France

Reviewed by:

Gary Splitter,
University of Wisconsin–Madison,
USA

Jean-Pierre Gorvel,
Centre National de la Recherche
Scientifique (CNRS), France

*Correspondence:

M. Victoria Delpino
mdelpino@ffyb.uba.ar

Specialty section:

This article was submitted to
Infectious Diseases,
a section of the journal
Frontiers in Microbiology

Received: 16 December 2016

Accepted: 07 February 2017

Published: 20 February 2017

Citation:

Giambartolomei GH,
Arriola Benitez PC and Delpino MV
(2017) Brucella and Osteoarticular
Cell Activation: Partners in Crime.
Front. Microbiol. 8:256.
doi: 10.3389/fmicb.2017.00256

Osteoarticular brucellosis is the most common presentation of human active disease although its prevalence varies widely. The three most common forms of osteoarticular involvement are sacroiliitis, spondylitis, and peripheral arthritis. The molecular mechanisms implicated in bone damage have been recently elucidated. *B. abortus* induces bone damage through diverse mechanisms in which TNF- α and the receptor activator of nuclear factor kappa-B ligand (RANKL)-the natural modulator of bone homeostasis are involved. These processes are driven by inflammatory cells, like monocytes/macrophages, neutrophils, Th17 CD4⁺ T, and B cells. In addition, *Brucella abortus* has a direct effect on osteoarticular cells and tilts homeostatic bone remodeling. These bacteria inhibit bone matrix deposition by osteoblasts (the only bone cells involved in bone deposition), and modify the phenotype of these cells to produce matrix metalloproteinases (MMPs) and cytokine secretion, contributing to bone matrix degradation. *B. abortus* also affects osteoclasts (cells naturally involved in bone resorption) by inducing an increase in osteoclastogenesis and osteoclast activation; thus, increasing mineral and organic bone matrix resorption, contributing to bone damage. Given that the pathology induced by *Brucella* species involved joint tissue, experiments conducted on synoviocytes revealed that besides inducing the activation of these cells to secrete chemokines, proinflammatory cytokines and MMPS, the infection also inhibits synoviocyte apoptosis. *Brucella* is an intracellular bacterium that replicates preferentially in the endoplasmic reticulum of macrophages. The analysis of *B. abortus*-infected synoviocytes indicated that bacteria also replicate in their reticulum suggesting that they could use this cell type for intracellular replication during the osteoarticular localization of the disease. Finally, the molecular mechanisms of osteoarticular brucellosis discovered recently shed light on how the interaction between *B. abortus* and immune and osteoarticular cells may play an important role in producing damage in joint and bone.

Keywords: osteoarticular brucellosis, B and T cells and *Brucella*, synoviocyte, osteoblast, osteoclastogenesis

OSTEOARTICULAR BRUCELLOSIS- CLINICAL FEATURES

Osteoarticular brucellosis is well documented as a major public health problem in several countries, particularly in the Middle East, the Mediterranean region and Central and South America (Pappas et al., 2006). Although osteoarticular involvement is the most common focal complication of brucellosis; clinical manifestations also include neurological, heart and liver complications

(Buzgan et al., 2010). Its prevalence varies from one report to another, but a recent study has revealed that as many as 47% of brucellosis patients experienced osteoarticular complications (Turan et al., 2011). It can take place at early stages of disease, at any time during the course of illness or some features can be present at the onset of the disease. There are three clinical forms: peripheral arthritis, sacroiliitis, and spondylitis. Peripheral arthritis is the most common one and it affects knees, hips, ankles, and wrists in the context of acute infection (Pappas et al., 2005). The clinical features include joint pain, which may be severe, joint swelling, tenderness; increased local warmth and limitation of movement (Gotuzzo et al., 1982; Rajapakse, 1995; Al-Eissa, 1999; Shaalan et al., 2002). Sacroiliitis also occurs in the context of acute brucellosis. The third form of the osteoarticular disease, spondylitis, remains extremely difficult to treat and often seems to result in residual bone damage (Pappas et al., 2005). The lumbar spine is the usual site of involvement.

The mechanisms involved in bone damage due to *Brucella* infection are not fully understood. Bone damage can be attributed to the direct action of the bacteria or to an immunopathological process due to inflammation triggered by innate immunity. No secreted proteases, toxins or lytic enzymes have been described so far in the bacteria; therefore, it is unlikely that this fact causes a direct deleterious effect, pointing out to innate immune responses as the major cause of osteoarticular pathology.

INTERPLAY BETWEEN BONE AND IMMUNE SYSTEM

The skeleton allows locomotion, calcium storage, and harboring hematopoietic stem cells from which blood and immune cells are derived. Although bone appears to be metabolically inert, it is actually a dynamic organ. Bone is composed of cells and an extracellular matrix which becomes mineralized by the deposition of calcium hydroxyapatite, which gives bone rigidity and strength. Bone has three different cell types: osteoblasts -or bone-forming cells-, osteoclasts -or bone-resorbing cells, whose functions are intimately linked (Ikeda and Takeshita, 2016) and osteocytes, which are terminally differentiated osteoblasts embedded within the mineralized bone matrix. Bone remodeling, a process coordinated between formation and degradation of bone managed by osteoblasts and osteoclasts, respectively, ensures bone homeostasis in healthy individuals. In order to balance bone formation and resorption, osteoblasts secrete RANKL that regulate the differentiation of osteoclasts, and osteocytes are the source of the Wnt antagonist sclerostin, and the Wnt signaling regulated by sclerostin regulate the activity of osteoblast (Karner et al., 2016), and osteocytes also secrete RANKL that regulate osteoclasts activity (Chen et al., 2015).

Several years of investigation have highlighted the interactions between bone and immune cells as well as their overlapping regulatory mechanisms (El-Jawhary et al., 2016). For instance, osteoclasts originate from the same myeloid precursor cells that give rise to macrophages and myeloid dendritic cells. On the other hand, osteoblasts regulate hematopoietic stem cell niches from which blood and immune cells are derived. Moreover, many

of the soluble mediators of immune cells, including cytokines and growth factors, regulate the activities of osteoblasts and osteoclasts.

In physiological conditions, “canonical” osteoclast formation requires macrophage colony-stimulating factor (M-CSF) and receptor activator factor of nuclear factor κ B ligand (RANKL) (Lampiasi et al., 2016). These cytokines act on cells of the monocyte-macrophage lineage, inducing their fusion to form multinucleated active resorbing cells. In the bone milieu, M-CSF is produced by osteoblasts and bone marrow stromal cells. It induces proliferation of osteoclast precursors, and differentiation and survival of mature osteoclasts (Fuller et al., 1993; Tanaka et al., 1993). M-CSF induces RANKL receptor expression, RANK, on mononuclear osteoclast precursors which then interacts with membrane-bound RANKL on surrounding osteoblasts and stromal cells to initiate osteoclasts differentiation (Yasuda et al., 1998). RANKL is present as both a transmembrane molecule and a secreted form. Its interaction with RANK is opposed by osteoprotegerin (OPG), a neutralizing soluble decoy receptor produced by marrow stromal cells and osteoblasts (Grundt et al., 2009). In addition to M-CSF and RANKL, a number of other cytokines and growth factors are known to substitute these two molecules and induce a “non-canonical” osteoclast formation (Lampiasi et al., 2016). Bone-marrow-derived and circulating osteoclast precursors are capable of differentiating into osteoclasts in the presence of M-CSF and substitutes for RANKL such as TNF- α , LIGHT (a receptor expressed in T lymphocytes), APRIL (a proliferation inducing ligand), BAFF (a B cell activating factor), the nerve growth factor, insulin-like growth factor (IGF)-I and II, TGF- β , IL-6, IL-11, IL-8; or in the presence of RANKL and substitutes for M-CSF such as a vascular endothelial growth factor, placental growth factor, FLT-3 ligand and hepatocyte growth factor (Lampiasi et al., 2016). Interestingly, IL-1, IL-7, IL-17, and IL-23 have also been involved in non-canonical osteoclastogenesis (Mori et al., 2013), mostly by inducing indirectly osteoclastogenesis and promoting RANKL release from other cells (Ikeda and Takeshita, 2016) and RANK on osteoclast precursors (Adamopoulos et al., 2010). However, it has been demonstrated that Th17 cells produce RANKL by themselves (Adamopoulos et al., 2010). IL-17 also enhances local inflammation and increases the production of inflammatory cytokines which further promote RANKL expression and activity (El-Jawhary et al., 2016). Most of these molecules are also involved in the immune system regulation and this may explain some of the cross-talk between immune and bone cells (D’Amelio et al., 2006). On the other hand, RANKL has also been involved in immune regulation (D’Amelio et al., 2006, 2009). The significance of non-canonical pathways in physiological bone resorption is uncertain. Yet, they may be important in the context of pathological bone resorption associated with inflammatory lesions of bone where high levels of these cytokines and growth factors are present.

Osteoblasts are specialized mesenchymal cells, responsible for the deposition of bone matrix and osteoclast regulation. Osteoblasts play a very important role in creating and maintaining skeletal architecture. They are the most important cells regulating bone remodeling balance. Osteoblasts express the

parathyroid hormone receptor whose binding to the hormone can activate osteoclast activity by increasing serum calcium levels (Rodan et al., 1981). Together with pre-osteoblasts and stromal cells, osteoblasts produce two key factors acting on osteoclasts: RANKL and OPG (Yasuda et al., 1998). Osteoblasts were proposed to play a major role in haematopoiesis (Visnjic et al., 2001). In the bone marrow, hematopoietic stem cells intermingle with specialized microenvironments -known as stem-cell niches aimed at maintaining their pluripotency and self-renewal ability. Osteoblasts, on the trabecular bone surface, have emerged as a crucial component of this niche, where long-lived antibody-producing B cells are known to reside. CXCL12 and its receptor CXCR4 are involved in the colonization of bone marrow by these B cells and in their retention in the bone marrow, but the localization of CXCL12-expressing cells is not consistent with that of osteoblasts on the trabecular bone surface (Tokoyoda et al., 2004). As it is unclear whether the bone-forming capacity is related to the function required for the niche, it is necessary to carefully reconsider this function for osteoblasts. Recently, osteoclasts have also been involved in the mobilization of stem cells (Kollet et al., 2006), further supporting the intimate relationship between the immune and bone systems.

Although bone is normally resistant to infection, *Brucella* spp. have a tropism for the osteoarticular localization. In this review, we report the current understanding of the interaction between *Brucella*, resident bone cells and immune system cells.

Brucella AND OSTEOBLAST

Infection of murine and human osteoblasts with *B. abortus* is a determining factor in the development of osteomyelitis in bone tissue. *B. abortus* interacts directly with osteoblasts, and replicates inside these cells. As a result of this interaction, modifications occur in the osteoblast metabolism. *B. abortus* inhibits osteoblast differentiation and function, leading to bone loss. Infection induces apoptosis of osteoblasts and also inhibits mineral and organic matrix deposition by these cells. Infection also induces RANKL expression, the main mediator of osteoclast differentiation. All these processes are activated through the p38 and ERK1/2 MAPK pathway (Scian et al., 2012). TNF- α secreted by *B. abortus*-infected macrophages also induces apoptosis and inhibits matrix deposition by osteoblasts (Scian et al., 2012). In addition, infection elicits secretion of chemokines and metalloproteinases (MMPs) (Scian et al., 2011b, 2012). Bone and joint damage can be the result of the inflammatory reaction elicited by MMP activity. Locally increased levels of MMPs have been found in arthritis associated with Lyme disease (Behera et al., 2005) and in periodontitis due to multiple bacteria (Soder et al., 2006). In these pathological processes the main sources of MMPs are inflammatory infiltrating cells (Song et al., 2013). Accordingly, *in vitro* studies have indicated that monocytes and neutrophils infected with *Brucella* secrete MMP-9 and proinflammatory cytokines (Zwerdling et al., 2009; Delpino et al., 2010; Scian et al., 2011b). Osteoblasts have also been shown to produce several MMPs, among which MMP-2 is particularly important because it degrades type I collagen present in bones

and type II collagen present in cartilage (Burrage et al., 2006). *B. abortus* infection of osteoblasts elicits GM-CSF secretion which acts as the major mediator of the increase in MMP-2 production detected in culture supernatants from infected osteoblasts (Scian et al., 2011b). We have also observed an increase in the levels of MMP activity in the synovial fluid from a patient with prepatellar bursitis (Wallach et al., 2010). A common feature of patients with osteoarticular brucellosis is the presence of leukocyte infiltrates (including monocytes and neutrophils) in the synovial fluid of the joints (Gotuzzo et al., 1982; Ibero et al., 1997; Press et al., 2002; Kasim et al., 2004). Accordingly, *B. abortus* infection induces the secretion of IL-8 and MCP-1 by osteoblasts. In conclusion, *B. abortus* may modulate, directly and indirectly, osteoblast function to increase bone resorption.

Brucella AND OSTEOCYTES

Osteocytes are the terminally differentiated forms of osteoblasts embedded in the mineralized bone matrix (Bonewald, 2011). For many years, the bone-bound osteocyte has been considered to be a relatively inactive cell with an unknown role in the bone tissue. Osteocytes are not only the most abundant cell populations of the bone lineage, which comprise up to 95% of bone cells in the adult skeleton, but also the central regulators of the differentiation and activity of both osteoblasts and osteoclasts during bone remodeling (Zhao et al., 2002). Osteocytes form an extensive and multi-functional syncytium throughout the bone. Their location within the matrix confers these cells the ability to sense stress throughout the bone, and to respond accordingly. Osteocytes respond to mechanical load by sending signals to osteoblasts and osteoclasts in the bone and modulating their activity. RANKL, NO and IGF-1 have been identified as such signal factors (Prideaux et al., 2016).

In vitro studies revealed that *B. abortus* may invade murine osteocytes inducing the secretion of MMP-2, RANKL, and proinflammatory cytokines. This inflammatory response induces bone marrow-derived monocytes to undergo osteoclastogenesis via RANKL and TNF- α (Pesce Viglietti et al., 2016).

Osteocytes are trapped within a mineralized matrix. In these conditions, cell-to-cell and cell-to-matrix communication in bone cells mediated by gap junctions and hemichannels, respectively, maintains bone homeostasis. Connexin 43 (Cx-43) is the predominant gap junction protein in bone and it facilitates the communication of cellular signals between cells that are required to maintain viability of osteocytes (Civitelli, 2008; Bivi et al., 2012). *B. abortus* infection inhibits Cx43 expression (Pesce Viglietti et al., 2016). Cx43 deletion in osteocyte cell culture results in increased apoptosis (Bivi et al., 2012). Integrins also control the fate and function of cells by influencing not only their proliferation and differentiation but also apoptosis (Streuli, 2009). *B. abortus* infection reduces the expression of Cx43 expression but does not modify integrin expression on murine osteocytes, which results in the absence of apoptosis (Pesce Viglietti et al., 2016). However, when osteocytes interact with supernatants from *B. abortus*-infected macrophages, the expression of Cx43 is inhibited; also, the

expression of several integrins is affected, inducing osteocyte apoptosis (Pesce Viglietti et al., 2016). This is not surprising given that integrins can link the cellular cytoskeletal network to the extracellular matrix (Geiger et al., 2001), and the detaching of osteocytes from the surrounding extracellular matrix was reported to induce anchorage-dependent cell death, anoikis (Gillmore, 2005).

Taking into account that osteocytes directly control bone remodeling, the modification of the activity of these cells by *B. abortus* infection could have an important contribution to bone damage observed during osteoarticular brucellosis.

Brucella AND FIBROBLAST-LIKE SYNOVIOCYTES

Fibroblast-like synoviocytes are mesenchymal cells that display many characteristics of fibroblasts (Bartok and Firestein, 2010). These cells have been recognized as central mediators of joint damage in inflammatory arthritis of either infectious or noninfectious origins (Inman and Payne, 2003; Bartok and Firestein, 2010).

Human synoviocytes infected with *B. abortus* secrete MMP-2, proinflammatory cytokines, RANKL, and chemokines that can promote the transmigration of monocytes and neutrophils and may mediate an increase in the synovium activation (Scian et al., 2011a). Several investigations have revealed the involvement of RANKL in bone destruction that occurs in rheumatoid arthritis and osteoarticular infectious diseases (Teitelbaum, 2006; Takayanagi, 2007). *Brucella* infection is not the exception as it has been demonstrated that synoviocytes infected with *B. abortus* induces osteoclastogenesis via RANKL, as proved using the natural inhibitor of osteoclastogenesis, OPG (Scian et al., 2013).

Besides their direct pathogenic role due to the production of proinflammatory mediators, *B. abortus* infection inhibits human synoviocyte apoptosis. Smooth *Brucella* species have developed several mechanisms to survive intracellularly, especially inside macrophages. It has been demonstrated that *B. abortus* infects and replicates in primary human synoviocytes (Scian et al., 2011a); this is in line with its capacity to replicate in other nonphagocytic cells such as osteoblasts, astrocytes, hepatocytes and hepatic stellate cells (Delpino et al., 2009, 2012; Garcia Samartino et al., 2010; Scian et al., 2011b). However, at variance with these cells, infection does not induce synoviocyte apoptosis. Moreover, it inhibits apoptosis induced by staurosporine and by culture supernatants from *B. abortus*-infected macrophages and monocytes. This inhibition occurs due to the up-regulation of anti-apoptotic factors such as cIAP-2, clusterin, livin, and P21/CIP/CDNK1A, and the reduction in the expression of pro-apoptotic proteins such as P-p53(S15) and the tumor necrosis factor (TNF) RI/TNFRSF1A (Scian et al., 2013). Thus, *B. abortus* could use these cells as an alternative replicative niche in joints. Accordingly, confocal imaging confirmed that as in macrophages, *B. abortus* replicates within calnexin-positive vacuoles in human primary synoviocytes (Scian et al., 2013). Therefore, interactions of *B. abortus* and synovial fibroblast may

play an important role in the pathogenesis of osteoarticular diseases.

INMUNE CELLS AND OSTEOARTICULAR BRUCELLOSIS

Interactions between Macrophages and *Brucella* in Osteoarticular Brucellosis

Upon infection with *B. abortus*, macrophages release inflammatory mediators that are able to induce the formation of osteoclasts from undifferentiated murine bone marrow cells (Delpino et al., 2012). In chronic inflammatory bone diseases such as rheumatoid arthritis, proinflammatory cytokines TNF- α , IL-1 β , and IL-6, as well as RANKL, have been shown to be important in disease progression and bone loss (Nair et al., 1996; Merkel et al., 1999; Kotake et al., 2001; Haynes, 2004; Wei et al., 2005). TNF- α has been reported to stimulate osteoclastogenesis by a RANKL-independent mechanism (Azuma et al., 2000; Kobayashi et al., 2000). Macrophages infection with *Brucella* elicits the secretion of TNF- α , IL-1 β , and IL-6 but not RANKL. Cytokine production by macrophages and concomitant osteoclastogenesis is not dependent on bacterial viability as both phenomena are induced by heat-killed *Brucella abortus*, suggesting that a structural component of *B. abortus* is responsible for such a response. *B. abortus* lipoproteins seem to be determinant as L-Omp19, a prototypical *B. abortus* lipoprotein (Giambartolomei et al., 2004), mimick the phenotypic and functional changes induced by *B. abortus* which lead to osteoclast activation. This phenomenon is caused by the lipid moiety of the protein as unlipidated Omp19 (U-Omp19) was unable to induce proinflammatory cytokine secretion and concomitant osteoclastogenesis. In addition, when using knockout mice, it was determined that MyD88 and TLR2 are both necessary to induce osteoclastogenesis by *B. abortus* and its lipoproteins as revealed by L-Omp19 stimulation (Delpino et al., 2012).

TNF- α is a potent inducer of bone resorption and it is the main proinflammatory cytokine involved in pathological conditions by activating mature osteoclasts (Thomson et al., 1987; Lerner and Ohlin, 1993; Kitazawa et al., 1994). With the use of TNFR1p55 knockout mice, it was determined that TNF- α signaling through TNFR1 appeared to be the main determinant of macrophage-elicited osteoclastogenesis induced by *B. abortus* and its lipoproteins. The major role of TNF- α in *B. abortus*-induced osteoclastogenesis was also determined in human cells using cytokine-neutralizing antibodies (Delpino et al., 2012). As osteoblasts and synoviocytes secrete MCP-1 in response to *B. abortus* infection (Scian et al., 2011a,b), monocytes can be attracted to the site of infection. In the *in vivo* situation attracted and resident-infected monocytes/macrophage can respond to *Brucella* lipoproteins with the production of TNF- α , thus inducing osteoclastogenesis. In these conditions, proinflammatory cytokines from bone environment induce MCP-1 secretion by human and murine osteoblasts and

human synoviocytes. Therefore, this interaction would create a pathological, vicious circle that exacerbates bone damage.

Role of T Cells in *Brucella*-Induced Bone Loss

The interaction between T cells and osteoclasts is a critical issue in the field of bone infectious and non-infectious diseases (Takayanagi, 2007). Activated T cells tilt bone homeostasis and induce bone destruction under pathological conditions such as estrogen deficiency (Kong et al., 1999; Cenci et al., 2000; Roggia et al., 2001; Kawai et al., 2006) and inflammation (Kong et al., 1999; Kawai et al., 2006) as they become significant sources of RANKL (Kong et al., 1999), TNF- α (Cenci et al., 2000), and IL-17 (Sato et al., 2006). Although these cytokines could induce osteoclast differentiation (Takayanagi, 2010), most T-cell cytokines, as well as IFN- γ , IL-4 and IL-10 inhibit osteoclastogenesis (Takayanagi, 2010). Because infiltration of T cells into the bones and joints is a hallmark pathological finding of osteoarticular brucellosis (Madkour, 2001b; Giambartolomei et al., 2004), it is essential to address whether and how T cells are linked to enhanced osteoclastic bone resorption in this form of brucellosis.

In an *in vitro* model in which murine purified T cells are influenced by the inflammatory milieu elicited by *B. abortus*-infected macrophages, it was demonstrated that T cells may promote the generation of osteoclasts. The pre-activation of these T cells with anti-CD3 induces the secretion of IFN- γ . However, proinflammatory mediators from *B. abortus*-infected macrophages tilt this phenotype to T CD4⁺ cells to secrete RANKL and IL-17 (Giambartolomei et al., 2012). Although RANKL is the major cytokine that regulates osteoclast differentiation (Takayanagi, 2009), in this model based on the use of blocking anti-IL-17 antibodies or osteoclast precursors from IL17R knockout mice it was revealed that IL-17 drives osteoclastogenesis induced by *Brucella*-activated T cells. In addition, IL-6 in the inflammatory milieu from *B. abortus*-infected macrophages is the cytokine that induces IL-17 secretion by T cells (Giambartolomei et al., 2012). IL-17 stimulates osteoclastogenesis indirectly through the induction of proinflammatory cytokines (TNF- α , IL-1 β , and IL-6) by osteoclast precursors. Moreover, it was determined that, with the use of TNFRp55 knockout mice, TNF- α is the main proinflammatory cytokine involved in osteoclastogenesis in the context of T cells influenced by the inflammatory milieu elicited by *B. abortus*-infected macrophages.

It is well known that *Brucella* infection activates the immune system leading to a response that favors the differentiation of T cells toward a Th1 profile (Golding et al., 2001). This response, which involves mainly IFN- γ -producing T cells, is considered to be important in restraining infection (Zhan et al., 1993; Zhan and Cheers, 1995a,b). However, taking into account that there is increased recognition of plasticity within the T helper lineage (Nakayamada et al., 2012), IFN- γ -producing Th1 cells could turn into pathogenic Th17 cells under the influence of the local inflammatory milieu generated by *Brucella*-infected macrophages in the bone, leading to a pro-osteoclastogenic T cell lineage.

Influence of *Brucella*-Activated B Cells on Osteoclastogenesis

The primary function of B cells is the production of antimicrobial immunoglobulins against infecting pathogens. However, B cells may also contribute to the proinflammatory innate host response (Milner et al., 2005; Viau and Zouali, 2005). Activated B cells have long lifespan, and *B. abortus* infection activates B cells (Goenka et al., 2011). Also, B cells provide an infection niche for *B. abortus* (Goenka et al., 2012).

B cells have a close and multifaceted relationship with bone cells (Horowitz et al., 2010) in normal and in pathological conditions. Infiltrating B cells into bones and joints have been found (Young, 2008) in osteoarticular brucellosis. Taken together, these findings suggest that B cells could contribute to infection chronicity (Goenka et al., 2011). In this way, research on human subjects revealed that chronic brucellar lesions on bones and joints characteristically show, at the histological level, an inflammatory response with varying degrees of bone destruction and the presence of infiltrating lymphocytes (Madkour, 2001b). Studies performed *in vitro* with B cells purified from murine spleens have demonstrated that *B. abortus* infection induces the expression of MMP-9, RANKL, and proinflammatory cytokines. Besides the ability of proinflammatory cytokines and RANKL to induce osteoclastogenesis, OPG inhibits osteoclastogenesis induced by B cells indicating that RANKL is the main molecule involved in the induction of bone resorption through the increase in osteoclast differentiation (Pesce Viglietti et al., 2016).

IN VIVO MODELS OF OSTEOARTICULAR BRUCELOSIS

The slow progress made in defining the pathobiology of osteoarticular brucellosis has been hampered by the absence of a suitable animal model in which the variety of disease manifestations observed in humans can be reproduced after experimental infection. Despite not being natural hosts for *Brucella* species that cause diseases in humans, laboratory rodents do not either mimic the spectrum of clinical signs observed in humans. Therefore, although the challenges of clinical brucellosis are associated with its focal involvement, the pathophysiological manifestations in animal models of brucellosis remain poorly characterized.

However, until now, a few studies based on the use of murine models have reported the dynamics of *Brucella* infection in bone. In particular, knockout mice in the IFN- γ signaling pathway have been useful as *in vivo* models of osteoarticular brucellosis. In one of these models, the use of bioluminescent *B. melitensis* to infect intraperitoneally interferon regulatory factor-1 (IRF-1^{-/-}) knockout mice enabled to identify acute infection in many tissues, even in the tail joint (Rajashekara et al., 2005). Similar results were obtained using *B. abortus*-infected IFN- γ knockout mice (Skyberg et al., 2012). Identification of joint localization may provide a model to understand bone pathogenesis of chronic brucellosis in humans (Rajashekara et al., 2005). Wild type Balb/c mice rarely develop spontaneous inflammation in synovial joints

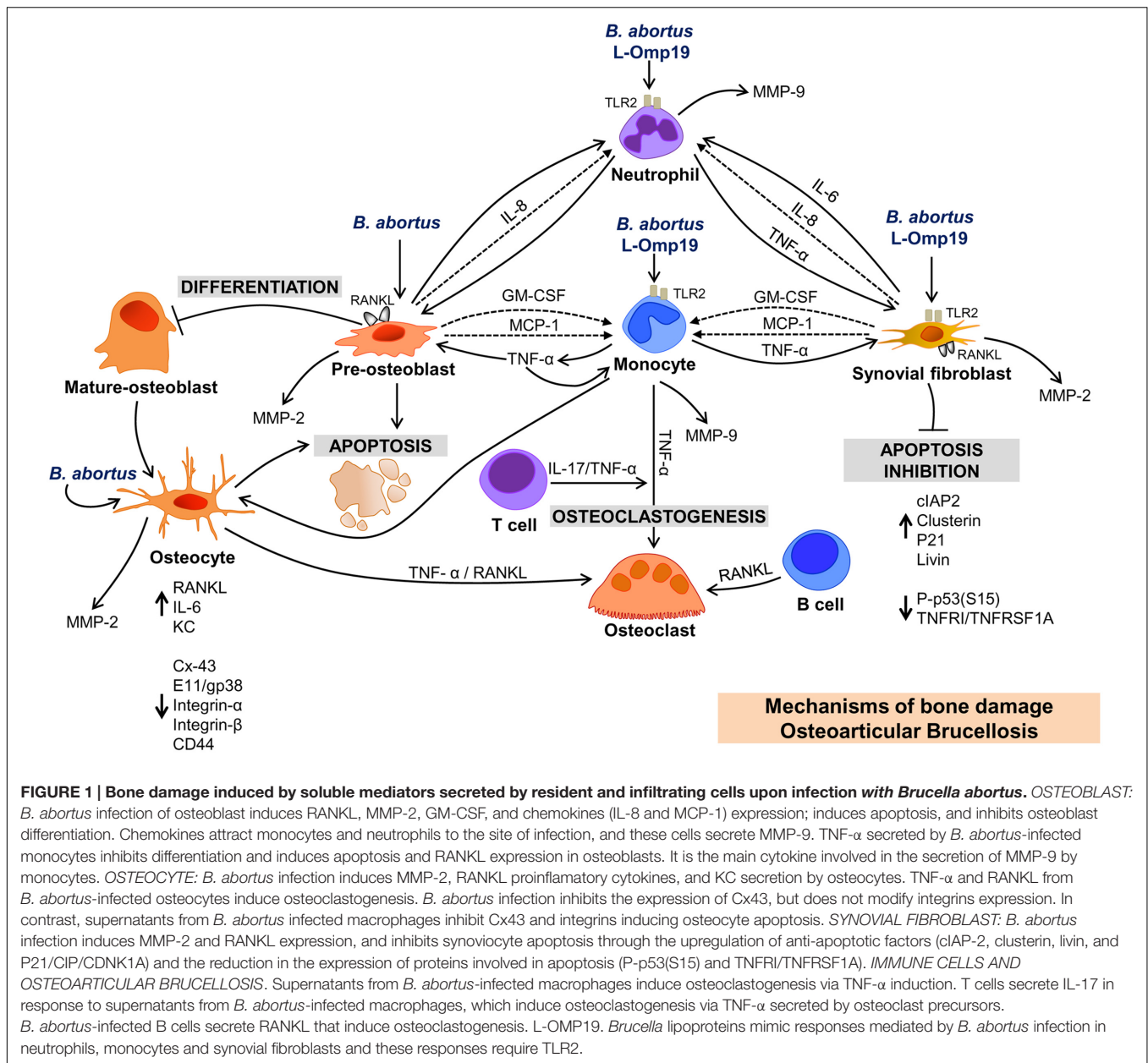


FIGURE 1 | Bone damage induced by soluble mediators secreted by resident and infiltrating cells upon infection with *Brucella abortus*. OSTEObLAST:

B. abortus infection of osteoblast induces RANKL, MMP-2, GM-CSF, and chemokines (IL-8 and MCP-1) expression; induces apoptosis, and inhibits osteoblast differentiation. Chemokines attract monocytes and neutrophils to the site of infection, and these cells secrete MMP-9. TNF- α secreted by *B. abortus*-infected monocytes inhibits differentiation and induces apoptosis and RANKL expression in osteoblasts. It is the main cytokine involved in the secretion of MMP-9 by monocytes. OSTEOCYTE: *B. abortus* infection induces MMP-2, RANKL proinflammatory cytokines, and KC secretion by osteocytes. TNF- α and RANKL from *B. abortus*-infected osteocytes induce osteoclastogenesis. *B. abortus* infection induces MMP-2 and RANKL expression, and inhibits synovial fibroblast apoptosis through the upregulation of anti-apoptotic factors (cIAP-2, clusterin, livin, and P21/CIP/CDNK1A) and the reduction in the expression of proteins involved in apoptosis (P-p53(S15) and TNFR1/TNFRSF1A). IMMUNE CELLS AND OSTEOARTICULAR BRUCELOSIS. Supernatants from *B. abortus*-infected macrophages induce osteoclastogenesis via TNF- α induction. T cells secrete IL-17 in response to supernatants from *B. abortus*-infected macrophages, which induce osteoclastogenesis via TNF- α secreted by osteoclast precursors. *B. abortus*-infected B cells secrete RANKL that induce osteoclastogenesis. L-OMP19. *Brucella* lipoproteins mimic responses mediated by *B. abortus* infection in neutrophils, monocytes and synovial fibroblasts and these responses require TLR2.

(Adarichev et al., 2008; Farkas et al., 2009). However, Balb/c mice infected for 26 weeks with bioluminescent *B. melitensis* exhibited multiple sites of the axial skeletal involvement with inflammatory and non-inflammatory features (Magnani et al., 2013). In these mice, brucellosis-induced arthritis is a progressive disease with postponed onset. In contrast, IRF-1 or IFN- γ knockout mice (Rajashekara et al., 2005; Skyberg et al., 2012; Lacey et al., 2016) develop arthritis much earlier, when *Brucella* is found in high concentrations in the body during the acute stage of the disease. In these conditions, inflammation and presence of bacteria was limited to paw joints and tails (Rajashekara et al., 2005; Skyberg et al., 2012; Lacey et al., 2016).

Despite the limitations of using animal models to study *Brucella* infection, the extensive bacterial dissemination in

the murine host in the conditions indicated above raises novel possibilities for the use of these models. Osteoarticular complications are particularly common in *Brucella*-infected humans, and the mouse model of brucellosis is particularly useful for the use of guided imaging techniques to identify infectious osteoarticular foci. Interestingly, inflammation and *Brucella* foci were independent of the infection route, suggesting that the osteoarticular site is a preferred location for bacterial persistence in the host and the most inflammation-susceptible structure (Skyberg et al., 2012).

The intra-articular knee injection of heat-killed *Brucella* further suggests that joint infection can induce a pro-inflammatory environment, with the induction of osteoclastogenesis (Scian et al., 2011a; Delpino et al., 2012). In

addition, this approach allows corroborating *in vitro* findings such as the role of TNF- α , MyD88 and TLR-2 in *Brucella*-induced osteoclastogenesis (Delpino et al., 2012), and the role of T cells in *Brucella*-induced osteoclastogenesis (Giambartolomei et al., 2012). Further exploration of this model should allow us to determine the relevant parallels to human clinical outcomes.

CONCLUDING REMARKS

Osteoarticular brucellosis is the most common localization of active brucellosis, and bone loss has been reported consistently in its three most frequent forms of osteoarticular involvement (Young, 1989; Madkour, 2001a,b; Aydin et al., 2005; Colmenero et al., 2008). Although the clinical and imaging aspects of osteoarticular brucellosis have been widely described (Madkour, 2001a,b), the pathogenic mechanisms of bone loss caused by *Brucella* have only been partially elucidated at the molecular and cellular levels over the past ten years (Figure 1). The findings presented in this review try to answer key questions about the inflammatory mediators involved in osteoarticular damage caused by *Brucella* and provides an initial background for studying in more detail the role of local and infiltrating

cells in this localization of the disease. As the infection inhibits apoptosis -or cell death- in some osteoarticular cells, it could be possible that these cells act as reservoir of the bacteria allowing the evolution of the disease to chronicity. This could also indicate which cell type may be chosen for therapeutic targeting.

This knowledge could lead to the discovery of new therapeutic treatments that could be co-administered with antibiotics to improve the patient's response to infection and reduce bone damage.

AUTHOR CONTRIBUTIONS

GG helped to draft and to correct the manuscript. PA performed the figure and critical reading of the manuscript. MD drafted the manuscript.

ACKNOWLEDGMENT

This work was supported by grant PICT 2014-1111 from Agencia Nacional de Promoción Científica y Tecnológica (ANPCYT, Argentina).

REFERENCES

- Adamopoulos, I. E., Chao, C. C., Geissler, R., Laface, D., Blumenschein, W., Iwakura, Y., et al. (2010). Interleukin-17A upregulates receptor activator of NF- κ B on osteoclast precursors. *Arthritis Res. Ther.* 12:R29. doi: 10.1186/ar2936
- Adarichev, V. A., Vegvari, A., Szabo, Z., Kis-Toth, K., Mikecz, K., and Glant, T. T. (2008). Congenic strains displaying similar clinical phenotype of arthritis represent different immunologic models of inflammation. *Genes Immun.* 9, 591–601. doi: 10.1038/gene.2008.54
- Al-Eissa, Y. A. (1999). Brucellosis in Saudi Arabia: past, present and future. *Ann. Saudi Med.* 19, 403–405.
- Aydin, M., Fuat Yapar, A., Savas, L., Reyhan, M., Pourbagher, A., Turunc, T. Y., et al. (2005). Scintigraphic findings in osteoarticular brucellosis. *Nucl. Med. Commun.* 26, 639–647.
- Azuma, Y., Kaji, K., Katogi, R., Takeshita, S., and Kudo, A. (2000). Tumor necrosis factor- α induces differentiation of and bone resorption by osteoclasts. *J. Biol. Chem.* 275, 4858–4864. doi: 10.1074/jbc.275.7.4858
- Bartok, B., and Firestein, G. S. (2010). Fibroblast-like synoviocytes: key effector cells in rheumatoid arthritis. *Immunol. Rev.* 233, 233–255. doi: 10.1111/j.0105-2896.2009.00859.x
- Behera, A. K., Hildebrand, E., Scagliotti, J., Steere, A. C., and Hu, L. T. (2005). Induction of host matrix metalloproteinases by *Borrelia burgdorferi* differs in human and murine lyme arthritis. *Infect. Immun.* 73, 126–134. doi: 10.1128/IAI.73.1.126-134.2005
- Bivi, N., Nelson, M. T., Faillace, M. E., Li, J., Miller, L. M., and Plotkin, L. I. (2012). Deletion of Cx43 from osteocytes results in defective bone material properties but does not decrease extrinsic strength in cortical bone. *Calcif. Tissue Int.* 91, 215–224. doi: 10.1007/s00223-012-9628-z
- Bonewald, L. F. (2011). The amazing osteocyte. *J. Bone Miner. Res.* 26, 229–238. doi: 10.1002/jbmr.320
- Burrage, P. S., Mix, K. S., and Brinckerhoff, C. E. (2006). Matrix metalloproteinases: role in arthritis. *Front. Biosci.* 11:529–543.
- Buzgan, T., Karahocagil, M. K., Irmak, H., Baran, A. I., Karsen, H., Evirgen, O., et al. (2010). Clinical manifestations and complications in 1028 cases of brucellosis: a retrospective evaluation and review of the literature. *Int. J. Infect. Dis.* 14, e469–78. doi: 10.1016/j.ijid.2009.06.031
- Cenci, S., Weitzmann, M. N., Roggia, C., Namba, N., Novack, D., Woodring, J., et al. (2000). Estrogen deficiency induces bone loss by enhancing T-cell production of TNF- α . *J. Clin. Invest.* 106, 1229–1237. doi: 10.1172/JCI11066
- Chen, H., Senda, T., and Kubo, K. Y. (2015). The osteocyte plays multiple roles in bone remodeling and mineral homeostasis. *Med. Mol. Morphol.* 48, 61–68. doi: 10.1007/s00795-015-0099-y
- Civitelli, R. (2008). Cell-cell communication in the osteoblast/osteocyte lineage. *Arch. Biochem. Biophys.* 473, 188–192. doi: 10.1016/j.abb.2008.04.005
- Colmenero, J. D., Ruiz-Mesa, J. D., Plata, A., Bermudez, P., Martin-Rico, P., Queipo-Ortuno, M. I., et al. (2008). Clinical findings, therapeutic approach, and outcome of brucellar vertebral osteomyelitis. *Clin. Infect. Dis.* 46, 426–433. doi: 10.1086/525266
- D'Amelio, P., Grimaldi, A., Bernabei, P., Pescarmona, G. P., and Isaia, G. (2006). Immune system and bone metabolism: does thymectomy influence postmenopausal bone loss in humans? *Bone* 39, 658–665. doi: 10.1016/j.bone.2006.03.009
- D'Amelio, P., Isaia, G., and Isaia, G. C. (2009). The osteoprotegerin/RANK/RANKL system: a bone key to vascular disease. *J. Endocrinol. Invest.* 32 (4 Suppl.), 6–9.
- Delpino, M. V., Barrionuevo, P., Macedo, G. C., Oliveira, S. C., Genaro, S. D., Scian, R., et al. (2012). Macrophage-elicited osteoclastogenesis in response to *Brucella abortus* infection requires TLR2/MyD88-dependent TNF- α production. *J. Leukoc. Biol.* 91, 285–298. doi: 10.1189/jlb.04111185
- Delpino, M. V., Barrionuevo, P., Scian, R., Fossati, C. A., and Baldi, P. C. (2010). *Brucella*-infected hepatocytes mediate potentially tissue-damaging immune responses. *J. Hepatol.* 53, 145–154. doi: 10.1016/j.jhep.2010.02.028
- Delpino, M. V., Fossati, C. A., and Baldi, P. C. (2009). Proinflammatory response of human osteoblastic cell lines and osteoblast-monocyte interaction upon infection with *Brucella* spp. *Infect. Immun.* 77, 984–995. doi: 10.1128/IAI.01259-08
- El-Jawhari, J. J., Jones, E., and Giannoudis, P. V. (2016). The roles of immune cells in bone healing; what we know, do not know and future perspectives. *Injury* 47, 2399–2406. doi: 10.1016/j.injury.2016.10.008
- Farkas, B., Boldizsar, F., Tarjanyi, O., Laszlo, A., Lin, S. M., Hutás, G., et al. (2009). BALB/c mice genetically susceptible to proteoglycan-induced arthritis and spondylitis show colony-dependent differences in disease penetrance. *Arthritis Res. Ther.* 11:R21. doi: 10.1186/ar2613

- Fuller, K., Owens, J. M., Jagger, C. J., Wilson, A., Moss, R., and Chambers, T. J. (1993). Macrophage colony-stimulating factor stimulates survival and chemotactic behavior in isolated osteoclasts. *J. Exp. Med.* 178, 1733–1744.
- Garcia Samartino, C., Delpino, M. V., Pott Godoy, C., Di Genaro, M. S., Pasquevich, K. A., Zwerdling, A., et al. (2010). *Brucella abortus* induces the secretion of proinflammatory mediators from glial cells leading to astrocyte apoptosis. *Am. J. Pathol.* 176, 1323–1338. doi: 10.2353/ajpath.2010.090503
- Geiger, B., Bershadsky, A., Pankov, R., and Yamada, K. M. (2001). Transmembrane crosstalk between the extracellular matrix–cytoskeleton crosstalk. *Nat. Rev. Mol. Cell Biol.* 2, 793–805. doi: 10.1038/35099066
- Giambartolomei, G. H., Scian, R., Acosta-Rodriguez, E., Fossati, C. A., and Delpino, M. V. (2012). *Brucella abortus*-infected macrophages modulate T lymphocytes to promote osteoclastogenesis via IL-17. *Am. J. Pathol.* 181, 887–896. doi: 10.1016/j.ajpath.2012.05.029
- Giambartolomei, G. H., Zwerdling, A., Cassataro, J., Bruno, L., Fossati, C. A., and Philipp, M. T. (2004). Lipoproteins, not lipopolysaccharide, are the key mediators of the proinflammatory response elicited by heat-killed *Brucella abortus*. *J. Immunol.* 173, 4635–4642. doi: 10.4049/jimmunol.173.7.4635
- Gilmore, A. P. (2005). Anoikis. *Cell Death Differ.* 12(Suppl. 2), 1473–1477.
- Goenka, R., Guirnalda, P. D., Black, S. J., and Baldwin, C. L. (2012). B Lymphocytes provide an infection niche for intracellular bacterium *Brucella abortus*. *J. Infect. Dis.* 206, 91–98. doi: 10.1093/infdis/jis310
- Goenka, R., Parent, M. A., Elzer, P. H., and Baldwin, C. L. (2011). B cell-deficient mice display markedly enhanced resistance to the intracellular bacterium *Brucella abortus*. *J. Infect. Dis.* 203, 1136–1146. doi: 10.1093/infdis/jiq171
- Golding, B., Scott, D. E., Scharf, O., Huang, L. Y., Zaitseva, M., Lapham, C., et al. (2001). Immunity and protection against *Brucella abortus*. *Microbes Infect.* 3, 43–48.
- Gotuzzo, E., Alarcon, G. S., Bocanegra, T. S., Carrillo, C., Guerra, J. C., Rolando, I., et al. (1982). Articular involvement in human brucellosis: a retrospective analysis of 304 cases. *Semin. Arthritis Rheum.* 12, 245–255.
- Grundt, A., Grafe, I. A., Liegibel, U., Sommer, U., Nawroth, P., and Kasperk, C. (2009). Direct effects of osteoprotegerin on human bone cell metabolism. *Biochem. Biophys. Res. Commun.* 389, 550–555. doi: 10.1016/j.bbrc.2009.09.026
- Haynes, D. R. (2004). Bone lysis and inflammation. *Inflamm. Res.* 53, 596–600.
- Horowitz, M. C., Fretz, J. A., and Lorenzo, J. A. (2010). How B cells influence bone biology in health and disease. *Bone* 47, 472–479. doi: 10.1016/j.bone.2010.06.011
- Ibero, I., Vela, P., and Pascual, E. (1997). Arthritis of shoulder and spinal cord compression due to *Brucella* disc infection. *Br. J. Rheumatol.* 36, 377–381.
- Ikeda, K., and Takeshita, S. (2016). The role of osteoclast differentiation and function in skeletal homeostasis. *J. Biochem.* 159, 1–8. doi: 10.1093/jb/mvv112
- Inman, R. D., and Payne, U. (2003). Determinants of synovial clearance of arthritogenic bacteria. *J. Rheumatol.* 30, 1291–1297.
- Karner, C. M., Esen, E., Chen, J., Hsu, F. F., Turk, J., and Long, F. (2016). Wnt protein signaling reduces nuclear acetyl-CoA levels to suppress gene expression during osteoblast differentiation. *J. Biol. Chem.* 291, 13028–13039. doi: 10.1074/jbc.M115.708578
- Kasim, R. A., Araj, G. F., Afeiche, N. E., and Tabbarah, Z. A. (2004). *Brucella* infection in total hip replacement: case report and review of the literature. *Scand. J. Infect. Dis.* 36, 65–67.
- Kawai, T., Matsuyama, T., Hosokawa, Y., Makihiro, S., Seki, M., Karimbux, N. Y., et al. (2006). B and T lymphocytes are the primary sources of RANKL in the bone resorptive lesion of periodontal disease. *Am. J. Pathol.* 169, 987–998. doi: 10.2353/ajpath.2006.060180
- Kitazawa, R., Kimble, R. B., Vannice, J. L., Kung, V. T., and Pacifici, R. (1994). Interleukin-1 receptor antagonist and tumor necrosis factor binding protein decrease osteoclast formation and bone resorption in ovariectomized mice. *J. Clin. Invest.* 94, 2397–2406. doi: 10.1172/JCI117606
- Kobayashi, K., Takahashi, N., Jimi, E., Udagawa, N., Takami, M., Kotake, S., et al. (2000). Tumor necrosis factor alpha stimulates osteoclast differentiation by a mechanism independent of the ODF/RANKL-RANK interaction. *J. Exp. Med.* 191, 275–286.
- Kollet, O., Dar, A., Shviti, S., Kalinkovich, A., Lapid, K., Sztainberg, Y., et al. (2006). Osteoclasts degrade endosteal components and promote mobilization of hematopoietic progenitor cells. *Nat. Med.* 12, 657–664. doi: 10.1038/nm1417
- Kong, Y. Y., Feige, U., Sarosi, I., Bolon, B., Tafuri, A., Morony, S., et al. (1999). Activated T cells regulate bone loss and joint destruction in adjuvant arthritis through osteoprotegerin ligand. *Nature* 402, 304–309. doi: 10.1038/46303
- Kotake, S., Udagawa, N., Hakoda, M., Mogi, M., Yano, K., Tsuda, E., et al. (2001). Activated human T cells directly induce osteoclastogenesis from human monocytes: possible role of T cells in bone destruction in rheumatoid arthritis patients. *Arthritis Rheum.* 44, 1003–1012. doi: 10.1002/1529-0131(200105)44:5<1003::AID-ANR179>3.0.CO;2-#
- Lacey, C. A., Keleher, L. L., Mitchell, W. J., Brown, C. R., and Skyberg, J. A. (2016). CXCR2 mediates *Brucella*-induced arthritis in interferon gamma-deficient mice. *J. Infect. Dis.* 214, 151–160. doi: 10.1093/infdis/jiw087
- Lampiasi, N., Russo, R., and Zito, F. (2016). The alternative faces of macrophage generate osteoclasts. *Biomed Res. Int.* 2016:9089610. doi: 10.1155/2016/9089610
- Lerner, U. H., and Ohlin, A. (1993). Tumor necrosis factors alpha and beta can stimulate bone resorption in cultured mouse calvariae by a prostaglandin-independent mechanism. *J. Bone Miner. Res.* 8, 147–155. doi: 10.1002/jbmr.5650080205
- Madkour, M. M. (ed.). (2001a). “Bone and joint imaging,” in *Madkour's Brucellosis*, 2nd Edn. Berlin: Springer-Verlag.
- Madkour, M. M. (ed.). (2001b). “Osteoarticular brucellosis,” in *Madkour's Brucellosis*, 2nd Edn. Berlin: Springer-Verlag.
- Magnani, D. M., Lyons, E. T., Forde, T. S., Shekhani, M. T., Adarichev, V. A., and Splitter, G. A. (2013). Osteoarticular tissue infection and development of skeletal pathology in murine brucellosis. *Dis. Model Mech.* 6, 811–818. doi: 10.1242/dmm.011056
- Merkel, K. D., Erdmann, J. M., McHugh, K. P., Abu-Amer, Y., Ross, F. P., and Teitelbaum, S. L. (1999). Tumor necrosis factor-alpha mediates orthopedic implant osteolysis. *Am. J. Pathol.* 154, 203–210.
- Milner, E. C., Anolik, J., Cappione, A., and Sanz, I. (2005). Human innate B cells: a link between host defense and autoimmunity? *Springer Semin. Immunopathol.* 26, 433–452. doi: 10.1007/s00281-004-0188-9
- Mori, G., D'Amelio, P., Faccio, R., and Brunetti, G. (2013). The interplay between the bone and the immune system. *Clin. Dev. Immunol.* 2013:720504. doi: 10.1155/2013/720504
- Nair, S. P., Meghji, S., Wilson, M., Reddi, K., White, P., and Henderson, B. (1996). Bacterially induced bone destruction: mechanisms and misconceptions. *Infect. Immun.* 64, 2371–2380.
- Nakayamada, S., Takahashi, H., Kanno, Y., and O'Shea, J. J. (2012). Helper T cell diversity and plasticity. *Curr. Opin. Immunol.* 24, 297–302. doi: 10.1016/j.coi.2012.01.014
- Pappas, G., Akritidis, N., Bosilkovski, M., and Tsianos, E. (2005). Brucellosis. *N. Engl. J. Med.* 352, 2325–2336.
- Pappas, G., Papadimitriou, P., Akritidis, N., Christou, L., and Tsianos, E. V. (2006). The new global map of human brucellosis. *Lancet Infect. Dis.* 6, 91–99. doi: 10.1016/S1473-3099(06)70382-6
- Pesce Viglietti, A. I., Arriola Benitez, P. C., Giambartolomei, G. H., and Delpino, M. V. (2016). *Brucella abortus*-infected B cells induce osteoclastogenesis. *Microbes Infect.* 18, 529–535. doi: 10.1016/j.micinf.2016.04.001
- Press, J., Peled, N., Buskila, D., and Yagupsky, P. (2002). Leukocyte count in the synovial fluid of children with culture-proven brucellar arthritis. *Clin. Rheumatol.* 21, 191–193.
- Prideaux, M., Findlay, D. M., and Atkins, G. J. (2016). Osteocytes: the master cells in bone remodelling. *Curr. Opin. Pharmacol.* 28, 24–30. doi: 10.1016/j.coph.2016.02.003
- Rajapakse, C. N. (1995). Bacterial infections: osteoarticular brucellosis. *Baillieres Clin. Rheumatol.* 9, 161–177.
- Rajasekara, G., Glover, D. A., Krepps, M., and Splitter, G. A. (2005). Temporal analysis of pathogenic events in virulent and avirulent *Brucella melitensis* infections. *Cell Microbiol.* 7, 1459–1473.
- Rodan, S. B., Rodan, G. A., Simmons, H. A., Walenga, R. W., Feinstein, M. B., and Raisz, L. G. (1981). Bone resorptive factor produced by osteosarcoma cells with osteoblastic features is PGE₂. *Biochem. Biophys. Res. Commun.* 102, 1358–1365.
- Roggia, C., Gao, Y., Cenci, S., Weitzmann, M. N., Toraldo, G., Isaia, G., et al. (2001). Up-regulation of TNF-producing T cells in the bone marrow: a key mechanism by which estrogen deficiency induces bone loss in vivo. *Proc. Natl. Acad. Sci. U.S.A.* 98, 13960–13965.
- Sato, K., Suematsu, A., Okamoto, K., Yamaguchi, A., Morishita, Y., Kadono, Y., et al. (2006). Th17 functions as an osteoclastogenic helper T cell subset that

- links T cell activation and bone destruction. *J. Exp. Med.* 203, 2673–2682. doi: 10.1084/jem.20061775
- Scian, R., Barrionuevo, P., Fossati, C. A., Giambartolomei, G. H., and Delpino, M. V. (2012). *Brucella abortus* invasion of osteoblasts inhibits bone formation. *Infect. Immun.* 80, 2333–2345. doi: 10.1128/IAI.00208-12
- Scian, R., Barrionuevo, P., Giambartolomei, G. H., De Simone, E. A., Vanzulli, S. I., Fossati, C. A., et al. (2011a). Potential role of fibroblast-like synoviocytes in joint damage induced by *Brucella abortus* infection through production and induction of matrix metalloproteinases. *Infect. Immun.* 79, 3619–3632. doi: 10.1128/IAI.05408-11
- Scian, R., Barrionuevo, P., Giambartolomei, G. H., Fossati, C. A., Baldi, P. C., and Delpino, M. V. (2011b). Granulocyte-macrophage colony-stimulating factor- and tumor necrosis factor alpha-mediated matrix metalloproteinase production by human osteoblasts and monocytes after infection with *Brucella abortus*. *Infect. Immun.* 79, 192–202. doi: 10.1128/IAI.00934-10
- Scian, R., Barrionuevo, P., Rodriguez, A. M., Arriola Benitez, P. C., Garcia Samartino, C., Fossati, C. A., et al. (2013). *Brucella abortus* invasion of synoviocytes inhibits apoptosis and induces bone resorption through RANKL expression. *Infect. Immun.* 81, 1940–1951. doi: 10.1128/IAI.01366-12
- Shaalan, M. A., Memish, Z. A., Mahmoud, S. A., Alomari, A., Khan, M. Y., Almuneeff, M., et al. (2002). Brucellosis in children: clinical observations in 115 cases. *Int. J. Infect. Dis.* 6, 182–186. doi: 10.1016/S1201-9712(02)90108-6
- Skyberg, J. A., Thornburg, T., Kochetkova, I., Layton, W., Callis, G., Rollins, M. F., et al. (2012). IFN-gamma-deficient mice develop IL-1-dependent cutaneous and musculoskeletal inflammation during experimental brucellosis. *J. Leukoc. Biol.* 92, 375–387. doi: 10.1189/jlb.1211626
- Soder, B., Airila Mansson, S., Soder, P. O., Kari, K., and Meurman, J. (2006). Levels of matrix metalloproteinases-8 and -9 with simultaneous presence of periodontal pathogens in gingival crevicular fluid as well as matrix metalloproteinase-9 and cholesterol in blood. *J. Periodontol. Res.* 41, 411–417.
- Song, J., Wu, C., Zhang, X., and Sorokin, L. M. (2013). In vivo processing of CXCL5 (LIX) by matrix metalloproteinase (MMP)-2 and MMP-9 promotes early neutrophil recruitment in IL-1beta-induced peritonitis. *J. Immunol.* 190, 401–410. doi: 10.4049/jimmunol.1202286
- Streuli, C. H. (2009). Integrins and cell-fate determination. *J. Cell Sci.* 122(Pt 2), 171–177. doi: 10.1242/jcs.018945
- Takayanagi, H. (2007). Osteoimmunology: shared mechanisms and crosstalk between the immune and bone systems. *Nat. Rev. Immunol.* 7, 292–304. doi: 10.1038/nri2062
- Takayanagi, H. (2009). Osteoimmunology and the effects of the immune system on bone. *Nat. Rev. Rheumatol.* 5, 667–676. doi: 10.1038/nrrheum.2009.217
- Takayanagi, H. (2010). The unexpected link between osteoclasts and the immune system. *Adv. Exp. Med. Biol.* 658, 61–68. doi: 10.1007/978-1-4419-1050-9_7
- Tanaka, S., Takahashi, N., Udagawa, N., Tamura, T., Akatsu, T., Stanley, E. R., et al. (1993). Macrophage colony-stimulating factor is indispensable for both proliferation and differentiation of osteoclast progenitors. *J. Clin. Invest.* 91, 257–263. doi: 10.1172/JCI116179
- Teitelbaum, S. L. (2006). Osteoclasts; culprits in inflammatory osteolysis. *Arthritis Res. Ther.* 8:201.
- Thomson, B. M., Mundy, G. R., and Chambers, T. J. (1987). Tumor necrosis factors alpha and beta induce osteoblastic cells to stimulate osteoclastic bone resorption. *J. Immunol.* 138, 775–779.
- Tokoyoda, K., Egawa, T., Sugiyama, T., Choi, B. I., and Nagasawa, T. (2004). Cellular niches controlling B lymphocyte behavior within bone marrow during development. *Immunity* 20, 707–718. doi: 10.1016/j.immuni.2004.05.001
- Turan, H., Serefhanoglu, K., Karadeli, E., Togan, T., and Arslan, H. (2011). Osteoarticular involvement among 202 brucellosis cases identified in Central Anatolia region of Turkey. *Intern. Med.* 50, 421–428.
- Viau, M., and Zouali, M. (2005). B-lymphocytes, innate immunity, and autoimmunity. *Clin. Immunol.* 114, 17–26.
- Visnjic, D., Kalajic, I., Gronowicz, G., Aguila, H. L., Clark, S. H., Lichtler, A. C., et al. (2001). Conditional ablation of the osteoblast lineage in Col2.3deltat transgenic mice. *J. Bone Miner. Res.* 16, 2222–2231. doi: 10.1359/jbmr.2001.16.12.2222
- Wallach, J. C., Delpino, M. V., Scian, R., Deodato, B., Fossati, C. A., and Baldi, P. C. (2010). Prepatellar bursitis due to *Brucella abortus*: case report and analysis of the local immune response. *J. Med. Microbiol.* 59(Pt 12), 1514–1518. doi: 10.1099/jmm.0.016360-0
- Wei, S., Kitaura, H., Zhou, P., Ross, F. P., and Teitelbaum, S. L. (2005). IL-1 mediates TNF-induced osteoclastogenesis. *J. Clin. Invest.* 115, 282–290. doi: 10.1172/JCI23394
- Yasuda, H., Shima, N., Nakagawa, N., Yamaguchi, K., Kinosaki, M., Mochizuki, S., et al. (1998). Osteoclast differentiation factor is a ligand for osteoprotegerin/osteoclastogenesis-inhibitory factor and is identical to TRANCE/RANKL. *Proc. Natl. Acad. Sci. U.S.A.* 95, 3597–3602.
- Young, E. J. (1989). “Clinical manifestations of human brucellosis,” in *Brucellosis: Clinical and Laboratory Aspects*, eds E. J. Young and M. J. Corbel (Boca Raton, FL: CRC Press).
- Young, E. J. (2008). Family studies in brucellosis. *Infection* 36, 578–579.
- Zhan, Y., and Cheers, C. (1995a). Differential induction of macrophage-derived cytokines by live and dead intracellular bacteria in vitro. *Infect. Immun.* 63, 720–723.
- Zhan, Y., and Cheers, C. (1995b). Endogenous interleukin-12 is involved in resistance to *Brucella abortus* infection. *Infect. Immun.* 63, 1387–1390.
- Zhan, Y., Kelso, A., and Cheers, C. (1993). Cytokine production in the murine response to brucella infection or immunization with antigenic extracts. *Immunology* 80, 458–464.
- Zhao, S., Zhang, Y. K., Harris, S., Ahuja, S. S., and Bonewald, L. F. (2002). MLO-Y4 osteocyte-like cells support osteoclast formation and activation. *J. Bone Miner. Res.* 17, 2068–2079. doi: 10.1359/jbmr.2002.17.11.2068
- Zwerdling, A., Delpino, M. V., Pasquevich, K. A., Barrionuevo, P., Cassataro, J., Garcia Samartino, C., et al. (2009). *Brucella abortus* activates human neutrophils. *Microbes Infect.* 11, 689–697. doi: 10.1016/j.micinf.2009.04.010

Conflict of Interest Statement: The authors declare that the research was conducted in the absence of any commercial or financial relationships that could be construed as a potential conflict of interest.

Copyright © 2017 Giambartolomei, Arriola Benitez and Delpino. This is an open-access article distributed under the terms of the Creative Commons Attribution License (CC BY). The use, distribution or reproduction in other forums is permitted, provided the original author(s) or licensor are credited and that the original publication in this journal is cited, in accordance with accepted academic practice. No use, distribution or reproduction is permitted which does not comply with these terms.



Genetic Diversity of *Brucella* Reference and Non-reference Phages and Its Impact on *Brucella*-Typing

Jens A. Hammerl^{1*}, Cornelia Göllner¹, Claudia Jäckel¹, Holger C. Scholz², Karsten Nöckler¹, Jochen Reetz¹, Sascha Al Dahouk¹ and Stefan Hertwig¹

¹ Department of Biological Safety, German Federal Institute for Risk Assessment, Berlin, Germany, ² German Center for Infection Research, Bundeswehr Institute of Microbiology, Munich, Germany

OPEN ACCESS

Edited by:

Leonard Peruski,
Centers for Disease Control and
Prevention, USA

Reviewed by:

Clayton Caswell,
Virginia Tech, USA
Miklos Fuzi,
Semmelweis University, Hungary

*Correspondence:

Jens A. Hammerl
jens-andre.hammerl@bfr.bund.de

Specialty section:

This article was submitted to
Infectious Diseases,
a section of the journal
Frontiers in Microbiology

Received: 28 December 2016

Accepted: 27 February 2017

Published: 15 March 2017

Citation:

Hammerl JA, Göllner C, Jäckel C,
Scholz HC, Nöckler K, Reetz J,
Al Dahouk S and Hertwig S (2017)
Genetic Diversity of *Brucella*
Reference and Non-reference Phages
and Its Impact on *Brucella*-Typing.
Front. Microbiol. 8:408.
doi: 10.3389/fmicb.2017.00408

Virulent phages have been used for many years to type *Brucella* isolates, but until recently knowledge about the genetic makeup of these phages remains limited. In this work the host specificity and genomic sequences of the original set (deposited in 1960) of VLA *Brucella* reference phages Tb, Fi, Wb, Bk2, R/C, and Iz were analyzed and compared with hitherto described brucellaphages. VLA phages turned out to be different from homonymous phages in other laboratories. The host range of the phages was defined by performing plaque assays with a wide selection of *Brucella* strains. Propagation of the phages on different strains did not alter host specificity. Sequencing of the phages Tb_V, Fi_V, Wb_V, and R/C_V revealed nucleotide variations when compared to same-named phages previously described by other laboratories. The phages Bk2_V and Iz_V were sequenced for the first time. While Bk2_V exhibited the same deletions as Wb_V, Iz_V possesses the largest genome of all *Brucella* reference phages. The duplication of a 301 bp sequence in this phage and the large deletion in Bk2_V, Wb_V, and R/C_V may be a result of recombination caused by repetitive sequences located in this DNA region. To identify new phages as potential candidates for lysotyping, the host range and Single Nucleotide Polymorphisms (SNPs) of 22 non-reference *Brucella* phages were determined. The phages showed lysis patterns different from those of the reference phages and thus represent novel valuable candidates in the typing set.

Keywords: *Brucella*, phage, genome, virulent, lysotyping

INTRODUCTION

Brucellae are highly infectious and facultative intracellular bacterial pathogens causing brucellosis, a frequent zoonosis with more than 500,000 human cases reported worldwide every year (de Figueiredo et al., 2015). Infections may lead to reproductive failure and abortion in animals and a feverish multiorgan disease in humans. Up to now, 12 species were allocated to the genus *Brucella* (Godfroid et al., 2013). Six of them, *B. melitensis*, *B. abortus*, *B. suis*, *B. canis*, *B. ovis*, and *B. neotomae*, recovered from goats, cattle, pigs, dogs, sheep, and desert rats, respectively, belong to the “classical” or “historical” *Brucella* species (<http://www.bacterio.net/brucella.html>). Later on, “novel” *Brucella* species were isolated from cetaceans (*B. ceti*) and pinnipeds (*B. pinnipedialis*; Foster et al., 2007), voles (*B. microti*; Scholz et al., 2008b), baboons (*B. papionis*;

Whatmore et al., 2014), red foxes (*B. vulpis*; Scholz et al., 2016) and from a human breast implant infection (*B. inopinata*; Scholz et al., 2010). Recently, a novel *Brucella* spp. reservoir in amphibians (e.g., Big-eyed tree frog: *Leptopelis verniculatus*; African bullfrogs: *Pyxicephalus edulis*; White's tree frog: *Litoria caerulea*) was discovered (Eisenberg et al., 2012; Fischer et al., 2012; Whatmore et al., 2015; Soler-Lloréns et al., 2016). Genetically, all *Brucella* species are closely related exhibiting genome similarities of >90% at the nucleotide level (Al Dahouk et al., 2010). Furthermore, because of the close genetic relationship of several genetic loci (e.g., 16S rRNA, 98.7% and *recA*, 85.5%) and a biochemical profile similar to *Ochrobactrum* spp., particularly atypical *Brucella* species like *B. microti* and *B. inopinata* are often misidentified using commercially available biochemical test systems (Scholz et al., 2008a,c).

Identification and subtyping of brucellae is time-consuming and laborious. Suspicious colonies on agar plates are primarily identified by a slide agglutination test using polyvalent *Brucella* antiserum (anti-S serum; Alton et al., 1975). Alternatively, PCR detection systems targeting the *bcs31* gene and the intergenic sequence IS711 exist that are suited for the molecular detection of *Brucella* spp. (Baily et al., 1992; Hinic et al., 2008). Moreover, some multiplex PCR assays (e.g., AMOS, Bruceladder) were established for further species differentiation (López-Goñi et al., 2008; Mayer-Scholl et al., 2010). However, none of the available molecular typing systems cover all currently known species and biovars of the genus *Brucella*. In microbiological routine testing, the identification of species and biovars is based on specific properties of the bacteria (e.g., CO₂ requirement, H₂S production, urease activity, agglutination with monospecific A, R, and M sera, growth on media with thionin or basic fuchsin, metabolization of different substrates) and in particular susceptibility to lytic *Brucella* reference phages (Al Dahouk et al., 2010).

Phages which infect and lyse *Brucella* strains are known for over half a century (Parnas et al., 1958; Brinley-Morgan et al., 1960; Jablonski, 1962). After some basic characterization, a typing set comprising five reference phages [Tb (Tbilisi), Fi (Firenze), Wb (Weybridge), Bk (Berkeley), R/C] was developed (Corbel, 1984). Some years later the typing set was complemented by phage Iz (Izatnagar; Joint FAO/WHO Expert Committee on Brucellosis, 1986) and since then has been used in many diagnostic laboratories worldwide. The same holds true for a set of *Brucella* reference strains serving as controls for lysotyping. The original typing set has also been modified by adding other phages, e.g., S708, Bk2, F1, F25, and Np, some of which are mutants of the reference phages (Moreira-Jacob, 1968; Corbel et al., 1988; Rigby et al., 1989; Hammerl et al., 2014). All brucellaphages described so far have a podoviral morphology and are closely related, demonstrated by restriction analysis and southern hybridization (Segondy et al., 1988; Rigby et al., 1989). They are considered as a single taxonomic species (Corbel and Thomas, 1976; Ackermann et al., 1981). As a consequence, some phages possess an almost identical host specificity (Morgan, 1963; Calderone and Pickett, 1965). For a better identification and discrimination of isolates, *Brucella* lysotyping is mostly carried out by spot assays using both a routine test dilution (RTD),

which is the highest dilution of a phage suspension producing confluent lysis of a propagator strain, and a 10,000 × RTD phage suspension. The main drawback of this procedure is that it cannot clearly distinguish between strains, in which the phages propagate, and those which are merely killed by the so-called *lysis from without* effect caused by a collapse of the cell wall in response to an overwhelming number of adsorbed phage particles (Corbel, 1984). Similar to growth inhibition, lysis from without is rather unspecific and more difficult to interpret than single plaques that unequivocally illustrate a phage infection (Jones et al., 1968). Furthermore, host range variants of *Brucella* reference phages have been isolated, particularly after changing the propagator strain (Corbel et al., 1988). Hence, it is not surprising that even studies, in which the same reference phages were tested, may show inconsistent results (Morris et al., 1973). For that reason it is important to know the biological and genetic properties of the typing phages exactly. First DNA sequences of phage Tb were reported by Zhu et al. (2009). The analysis of whole genome sequences of diagnostic brucellaphages confirmed their close relationship, even though phage Tb deposited in two different institutes revealed some sequence deviations, mainly point mutations (Flores et al., 2012; Farlow et al., 2014; Tevdoradze et al., 2015). Indeed, besides two InDels ~2.4 and 0.4 kb in size, the genomes of the investigated phages notably differ by single nucleotide polymorphisms (SNPs). Many of them were found in a gene probably encoding a tail collar protein, which has been suggested to be a determinant of host specificity. The importance of individual amino acids of the tail collar protein for the host range of the phages, however, has not yet been investigated.

In this work, the host specificity and genomes of six VLA *Brucella* reference phages (designated Tb_V, Fi_V, Wb_V, Bk2_V, R/C_V, and Iz_V herein) were analyzed in detail. The genome sequences of Bk2_V and Iz_V will be presented for the first time. The phages were compared with homonymous phages originating from other laboratories. Bioinformatic analyses revealed DNA repeats within the phage genomes, which may be important for the acquisition, loss or duplication of DNA sequences. The host range determination of 22 non-reference phages disclosed some potential candidates useful for lysotyping.

MATERIALS AND METHODS

Bacterial Strains, Media, and Growth Conditions

Detailed information on all strains used in this study is given in **Table S1**. Cultivation of the bacteria was performed as previously described (Alton et al., 1975). Solid and overlay agar contained 1.8 and 0.7% (w/v) bacto-agar No. 1 (Oxoid, Wesel, Germany), respectively.

Propagation of Bacteriophages

Relevant data on brucellaphages used in this study are given in **Table S2**. The reference phages Tb_V, Bk2_V, Wb_V, Fi_V, R/C_V, and Iz_V were obtained from the Weybridge bacteriophage collection in form of unopened lyophilized phage stocks produced by the OIE Brucellosis Reference Centre of the Veterinary Laboratories

Agency (VLA, Addlestone, UK) in 1973. Lyophilized phages were suspended in 5 ml of SM-buffer (100 mM NaCl, 8 mM MgSO₄ 7H₂O, 50 mM Tris-HCl, pH 7.5). The suspensions were used for plaque assays by the softagar overlay method as previously described (Sambrook and Russell, 2001). In contrast to phage R/C_V, which was propagated on *B. ovis* strain 63/290, Tb_V, Fi_V, Bk2_V, Wb_V, and Iz_V were propagated on *B. abortus* vaccine strain S19. Besides the standard reference phages which are globally used for *Brucella*-typing, other brucellaphages were included in the study. While lyophilized A422 and M51 stocks from 1960 were also provided by VLA, the origin of the phages F1, F1m, F1u, F25, F25u, F44, F45, F48, FO1, P, P2, 3, 6, 7, 10I, 12m, 24II, 45II, 212XV, and 371XXIX is unknown. Lyophilized stocks of these phages prepared at the BfR in 1973 were used for further investigation. However, there is no information available on how these phages were propagated before lyophilization. To ensure the purity of all brucellaphages, a three-fold successive single plaque separation was performed. After the third plaque separation purified phages were used for the preparation of high titer lysates (>10⁹ PFU/ml). To accomplish this, 10⁶ PFU were applied to 20 ml of an early logarithmic growing (McFarland 1.0–1.5) *Brucella* culture followed by incubation for 24–48 h on a rotational shaker (100 rpm) under microaerobic conditions. Thereafter, lysates were centrifuged for 10 min at 7,500 × g to remove cellular debris. Supernatants were subjected to sterile filtration (0.45 and 0.2 μm; Merck Millipore, Schwalbach, Germany) and DNaseI-/RNaseA-treatment (10 μg/ml wt/vol each; Roche, Mannheim, Germany). Phage particles were concentrated and purified by discontinuous CsCl-step gradients (CsCl, 1.3 to 1.7 g ml⁻¹) as described previously (Sambrook and Russell, 2001). Phage bands recovered from CsCl-gradients were desalted using 100K Amicon Ultra centrifugal filter columns (Merck Millipore).

Host Range Determination

Host range analyses were carried out by spot assays on *Brucella* spp. reference and type strains ($n = 26$; **Table S1**) and field isolates as well as reference strains of *Ochrobactrum* spp. ($n = 119$), *Yersinia enterocolitica* O:9 ($n = 7$), *Mesorhizobium* sp. ($n = 6$), *Sinorhizobium meliloti* ($n = 5$), and *Pseudomonas* ($n = 5$; data not shown). Two hundred microliters of each strain were mixed with 5 ml of pre-warmed *Brucella*-broth soft agar (0.7%) and poured onto a lysogeny-broth (LB) agar plate. Ten microliter aliquots of 1:10 serial dilutions of each lysate were spotted onto the overlay agar. Agar plates were visually inspected after incubation for 24 and 48 h at 37°C. Phages that did not affect bacterial growth were classified as non-infectious (negative: –). Phages were classified as infectious (positive: +) when single plaques were identified in spotting zones of the tested lysates. In case of growth inhibition (GI) visible by an even but decreased bacterial growth within the spotting areas, the respective phage/strain combinations were further investigated by preparing phage lysates. For this purpose, 10⁷ phages were applied to 20 ml of an early exponential growing *Brucella* culture (McFarland: 1.0–1.5). After incubation at 37°C for 48 h, lysates were purified as described above. Propagation of phages was determined by plaque assays (Sambrook and Russell, 2001). Four

hundred microliters of a *Brucella* culture (McFarland: 5.0–7.0) were mixed with 100 μl aliquots of 1:10 serial dilutions of each lysate, incubated for 20 min at room temperature, added to 5 ml of pre-warmed *Brucella*-broth soft agar (0.7%) and poured onto LB agar plates. After incubation for 24 and 48 h at 37°C, agar plates were visually inspected for plaque activity. If phage replication occurred, the lysates contained more than 10⁷ infectious particles. Strains which increased the phage titer were finally classified as susceptible (positive: +).

Isolation of Phage DNA, Whole Genome Sequencing, and Bioinformatic Analysis

Phage DNA extraction from CsCl-purified particles was performed as previously described (Hammerl et al., 2016). Determination of phage genomic sequences was conducted using a Roche 454 genome sequencer FLX titanium system by GATC Biotech AG (Konstanz, Germany). Library generation and 454 FLX sequencing were carried out according to the procedure of the manufacturer (Roche/454 Life Sciences, Branford, Connecticut, USA). Sequence reads were assembled using the Roche/454 Newbler software at default settings (454 Life Sciences Corporation, Software release 2.3) resulting in one contig with an average sequence coverage of >100 per consensus base. Sequence analysis and alignments were carried out using Accelrys Gene v2.5 (Accelrys Inc., San Diego, CA, USA). Bioinformatic analysis and genome annotation were performed as described previously (Hammerl et al., 2014, 2016).

PCR Analysis

PCR was performed in an Eppendorf Mastercycler ep Gradient (Eppendorf, Hamburg, Germany) according to standard protocols. Single reactions were carried out with ~10 ng/μl phage DNA and 2.5 μl of each primer in a final volume of 50 μl using Qiagen DNA polymerase amplification components (Qiagen, Hilden, Germany). For PCR amplification the following parameters were used: initial template denaturation at 96°C for 120 s followed by 35 cycles including denaturation at 96°C for 15 s, annealing at 55°C for 5 min and elongation for 210 s at 72°C. A final elongation step at 72°C for 1 min was added. Purification of PCR products was performed by using the MSB spin PCRapace kit (Strattec, Birkenfeld, Germany). The nucleotide sequence of the PCR products was determined by Sanger sequencing (Eurofins Genomics, Ebersberg, Germany).

Nucleotide Sequence Accession Number

The complete nucleotide sequences of the brucellaphages were submitted to GenBank under the accession numbers HF569092 (Wb_V), HF569091 (Tb_V), HF569089 (Fi_V), HF569091 (Bk2_V), HF569090 (R/C_V), and KY056619 (Iz_V).

RESULTS AND DISCUSSION

Host Range Determination of the VLA *Brucella* Reference Phages

A comprehensive study with 10 *Brucella* species represented by 26 reference and type strains was performed to elucidate in which strains the group I to group VI *Brucella* reference

phages Tb_V, Fi_V, Wb_V, Bk2_V, R/C_V, and Iz_V (Corbel, 1987) replicate and which strains are merely lysed by lysis from without at high MOIs. Lytic activity of the phages was quantified by plaque assays (titration) allowing an accurate determination of the hosts' susceptibility. If no plaque formation occurred and only growth inhibition was observed, we examined propagation of the phages using liquid cultures of the respective strains (see section Materials and Methods). The phages Tb_V (group I) and Fi_V (group II) showed almost identical lysis patterns (Table 1). They infected reference strains of the eight *B. abortus* biovars (bv1–7, 9), *B. neotomae* 5K33, *B. microti* CCM4915 and two strains of the recently identified species *B. vulpis* (Scholz et al., 2016). On the other hand, *B. suis* 1,330 (bv1) was only lysed by phage Tb_V, but not by Fi_V. Data that have been published on the susceptibility of *B. suis* 1,330 to phage Tbilisi are rather contradictory. While several articles reported that this strain was not lysed by the phage at RTD (Jones et al., 1968; Flores et al., 2012), other authors obtained plaques with both Tbilisi and Firenze (Rigby et al., 1989). Another deviation from published data concerns *B. melitensis* 16M (bv1), for which we and also others could not confirm infection by Tbilisi and Firenze, whereas Rigby et al. (1989) reported on plaque formation caused by these phages (Rigby et al., 1989). This raises the question about the reasons for these discrepancies? One possible explanation is that in our study and in the study of Rigby et al. (1989), phages were propagated on the *B. abortus* vaccine strain S19 (bv1), which makes host adaptation as a reason for different lysis patterns improbable. Furthermore, the slightly different methodologies applied to determine lysis patterns might not account for diverging results. It is more likely that the phages and/or indicator strains used in the two studies were actually not identical, perhaps due to mutations in genes important for phage infection. Of course, this presumption can only be confirmed by whole genome sequencing of the used strains and phages. For phage Tbilisi different variants (Tb_M and Tb_V) have already been described (Foster et al., 2007; Flores et al., 2012). In addition, it has been demonstrated that the propagation of brucellaphages on different indicator strains caused changes in the phage genome, which might alter host specificity (Tevdoradze et al., 2015). However, lysis patterns of the phages have not yet been determined and compared. We therefore address this issue in detail.

Unlike Tb_V and Fi_V, the phages Wb_V (group III), Bk2_V (group IV), R/C_V (group V), and Iz_V (group VI) revealed lysis patterns that correlated well with published data. The species *B. ceti* and *B. inopinata* were not infected by any phage. Five phages inhibited the growth of the *B. ceti* reference strain but replication of the phages did not occur. Though, a number of *B. ceti* strains isolated from cetaceans were lysed by Weybridge and Izatnagar in another study (Foster et al., 2007). In contrast, for *B. inopinata* which is currently represented only by its type strain BO1, no lytic phage has been found so far. Since this strain harbors an active prophage (Hammerl et al., 2016) that might affect the susceptibility to other phages, the importance of the prophage was analyzed in more detail (see next chapter). To avoid misinterpretation of phage typing results, plaque assays allowing a quantitative determination of the lytic activity are certainly better suited than spot assays using high

titer lysates, since lysis from without effects are too variable to identify species unequivocally. We also studied infection of other species (*Ochrobactrum* spp., *Mesorhizobium* sp., *Sinorhizobium meliloti*, *Yersinia enterocolitica* O:9, *Pseudomonas* sp.) by the brucellaphages and detected growth inhibition of some strains (data not shown). As the zones of growth inhibition looked similar to halos obtained with *Brucella*, such results could be misleading.

Propagation of the Phages on Alternative Strains Did Not Alter Lysis Patterns

In this set of experiments the question should be answered whether lytic specificity of the phages may be affected by a change of propagator strains. For that reason Tb_V, Wb_V, R/C_V, and Iz_V were co-cultivated with *B. abortus* S19, *B. melitensis* 16M, *B. suis* 1,330 and *B. ovis* 63/290. After overnight incubation, phages were isolated and used for the next co-cultivation with the respective strain. This procedure was repeated 20 times corresponding to ~500 generations. Thereafter, host ranges of the phages were examined by plaque assays testing all reference and type strains (Table S1). Following this procedure, no change of lysis patterns was detected. Furthermore, no adaptation of the phages to new hosts was observed. Phage R/C_V e.g., remained its specificity and infected exclusively rough strains. The data suggest that even though propagation of brucellaphages on different strains may cause genomic changes (Tevdoradze et al., 2015) this is not necessarily associated with an alteration of the host range. However, the number of phage particles released from individual strains can differ significantly (data not shown). Thus, lysates of the same phage exhibited different titers which may bias a result. To avoid diverging lysis patterns, we recommend to propagate diagnostic brucellaphages on the same indicator strain and to examine the phage genomes by sequencing if results are inconsistent.

Since many phages have been isolated from *Brucella* cultures, a lysogenic state termed pseudolysogeny has been suggested for these phages (Renoux and Suire, 1963). Lysogeny may influence the susceptibility of the bacteria to phages. We investigated *B. abortus* S19 colonies that had survived infection by phage Tb_V. The isolated colonies were passaged several times. While a release of phage particles after mitomycin C treatment (Hammerl et al., 2016) was not observed, Tb_V was identified in initial cultures by PCR. In addition, electron microscopy revealed Tb_V particles adsorbed to the cell wall (data not shown). Even after repeated cultivation, the phage was no longer detectable. The data indicate that strain *B. abortus* S19 may serve as carrier for Tb_V but that there is obviously no integration of the phage genome into the bacterial chromosomes. We also did not observe any immunity of the Tb_V-carrying bacteria against superinfection by the same or other *Brucella* reference phages. Similar results were published by other authors (Morris et al., 1973; Corbel and Morris, 1975). To elucidate whether Tb_V-induced cell lysis may be affected by endogenous prophages providing immunity to superinfection, a S19 derivative (S19lys) containing the temperate phage BiPBO1 (Hammerl et al., 2016) was studied. Tb_V lysed the lysogenic strain like the original strain without

TABLE 1 | Host range determination of *Brucella* reference phages.

<i>Brucella</i> spp. (Strain)	<i>Brucella</i> phage group					
	I Wb _V	II Fi _V	III Bk2 _V	IV Tb _V	V R/C _V	VI Iz _V
<i>B. abortus</i>	+	+	+	+	–	+
<i>B. abortus</i> (S19)	2 × 10 ⁹	2 × 10 ⁹	2 × 10 ⁹	2 × 10 ⁹	NL	2 × 10 ⁹
<i>B. abortus</i> bv1 (544)	7 × 10 ⁷	4 × 10 ⁷	2 × 10 ⁸	2 × 10 ⁸	NL	6 × 10 ⁷
<i>B. abortus</i> bv2 (86/8/59)	1 × 10 ⁸	1 × 10 ⁸	1 × 10 ⁹	1 × 10 ⁸	NL	3 × 10 ⁸
<i>B. abortus</i> bv3 (Tulya)	1 × 10 ⁸	6 × 10 ⁶	1 × 10 ⁷	2 × 10 ⁸	NL	3 × 10 ⁷
<i>B. abortus</i> bv4 (292)	2 × 10 ⁸	6 × 10 ⁶	1 × 10 ⁷	3 × 10 ⁷	NL	3 × 10 ⁷
<i>B. abortus</i> bv5 (B3196)	1 × 10 ⁸	1 × 10 ⁷	1 × 10 ⁸	1 × 10 ⁷	NL	1 × 10 ⁷
<i>B. abortus</i> bv6 (870)	6 × 10 ⁷	6 × 10 ⁷	1 × 10 ⁷	2 × 10 ⁷	NL	3 × 10 ⁷
<i>B. abortus</i> bv7 (63/75)	4 × 10 ⁷	1 × 10 ⁶	3 × 10 ⁸	7 × 10 ⁷	NL	7 × 10 ⁶
<i>B. abortus</i> bv9 (C68)	8 × 10 ⁷	2 × 10 ⁷	3 × 10 ⁷	3 × 10 ⁷	NL	2 × 10 ⁷
<i>B. melitensis</i>	±	–	+	–	–	+
<i>B. melitensis</i> bv1 (16M)	1 × 10 ⁷	NL	1 × 10 ⁸	NL	NL	1 × 10 ⁸
<i>B. melitensis</i> bv2 (63/9)	NL	NL	1 × 10 ⁷	NL	NL	5 × 10 ⁶
<i>B. melitensis</i> bv3 (Ether)	3 × 10 ⁷	NL	6 × 10 ⁷	NL	NL	5 × 10 ⁷
<i>B. suis</i>	±	–	±	±	–	±
<i>B. suis</i> bv1 (1330)	1 × 10 ⁹	NL	2 × 10 ⁸	5 × 10 ⁷	NL	2 × 10 ⁸
<i>B. suis</i> bv2 (Thomsen)	GI	NL	GI	GI	NL	GI
<i>B. suis</i> bv3 (686)	1 × 10 ⁷	NL	3 × 10 ⁷	NL	NL	3 × 10 ⁷
<i>B. suis</i> bv4 (40)	5 × 10 ⁸	NL	4 × 10 ⁸	NL	NL	3 × 10 ⁸
<i>B. suis</i> bv5 (513)	5 × 10 ⁸	NL	5 × 10 ⁸	NL	NL	2 × 10 ⁸
<i>B. ovis</i>	–	–	–	–	+	–
<i>B. ovis</i> (63/290)	NL	NL	NL	NL	2 × 10 ⁸	NL
<i>B. neotomae</i>	+	+	+	+	–	+
<i>B. neotomae</i> (5K33)	1 × 10 ⁹	2 × 10 ⁷	2 × 10 ⁸	1 × 10 ⁸	NL	1 × 10 ⁸
<i>B. canis</i>	–	–	–	–	–	–
<i>B. canis</i> (RM6/66)	NL	NL	NL	NL	1 × 10 ⁷	NL
<i>B. ceti</i>	–	–	–	–	–	–
<i>B. ceti</i> (B1/94)	GI	GI	GI	GI	NL	GI
<i>B. pinnipedialis</i>	+	–	+	–	–	–
<i>B. pinnipedialis</i> (B2/94)	4 × 10 ⁶	NL	2 × 10 ⁶	NL	NL	NL
<i>B. microti</i>	+	+	+	+	–	+
<i>B. microti</i> (CCM 4915)	1 × 10 ⁹	2 × 10 ⁵	5 × 10 ⁸	2 × 10 ⁷	NL	2 × 10 ⁸
<i>B. inopinata</i>	–	–	–	–	–	–
<i>B. inopinata</i> (BO1)	NL	NL	NL	NL	NL	NL
<i>B. vulpis</i>	+	+	+	+	–	+
<i>B. vulpis</i> (FH60HL)	2 × 10 ⁹	3 × 10 ⁷	1 × 10 ⁹	2 × 10 ⁸	NL	5 × 10 ⁸
<i>B. vulpis</i> (FH965HL)	1 × 10 ⁹	2 × 10 ⁸	1 × 10 ⁹	4 × 10 ⁸	NL	2 × 10 ⁸

+, Plaque formation, –, no plaque formation. bv, biovar; NL, no lysis; GI, growth inhibition.

the prophage. Thus, BiPBO1 did not affect Tb_V propagation. However, lysates prepared with strain S19lys contained both Tb_V and BiPBO1 which could be easily identified by their

different plaque morphologies. As the BiPBO1 prophage was induced by infection with Tb_V, lysogeny has to be taken into account when lysates of brucellaphages are prepared. Otherwise,

incorrect results might be obtained when the phages are used for typing.

HindIII Restriction Analysis Is Suited to Allocate Bk2_V and Iz_V to Existing Phage Groups

Previous studies on the *Brucella* reference phages Tbilisi, Weybridge, Bk2, and R/O (an instable variant of phage R/C) showed that their genomes cannot be distinguished by restriction analysis using the endonucleases BamHI, EcoRI, and PvuII, because identical fragment patterns were obtained (Segondy et al., 1988). In contrast, phage Nepean (Np) revealed some differences, e.g., an additional 1.0 kb fragment in the HindIII digest (Rigby et al., 1989). The hitherto sequenced brucellaphage genomes mainly differed by two major InDels and can thus be assigned to two groups (Flores et al., 2012; Farlow et al., 2014; Tevdoradze et al., 2015). The presence or absence of these sequences should be traceable by use of suitable restriction enzymes. We analyzed HindIII restriction patterns of the VLA reference phages in detail to ascertain whether the yet not sequenced phages Bk2_V and Iz_V belong to one of the existing groups. As documented in **Figure 1**, phage Tb_V and Fi_V showed two additional restriction fragments, 5.0 kb and 2.8 kb in size, which were absent in Wb_V and R/C_V. These fragments comprise DNA sequences that are missing in the latter phages. The fragments were also absent in the Bk2_V restriction digest. This suggests that Bk2_V may exhibit identical deletions as Weybridge and R/C. The two above mentioned restriction fragments of Tb_V and Fi_V were detected in Iz_V indicating that this phage resembles Tb_V and Fi_V in this respect. In summary, restriction analysis using HindIII is a fast and easy method to determine whether a new phage contains deletions similar to already known brucellaphages.

The VLA *Brucella* Reference Phages Are Not Identical to Same-Named Phages in Other Laboratories

Host range analyses showed that the six VLA reference phages infected a distinct range of strains, even though some phages revealed almost identical lysis patterns. The only difference that was observed between Tb_V and Fi_V was *B. suis* strain 1,330 that was infected by Tb_V but not by Fi_V. Similarly, the host range of Wb_V, Bk2_V and Iz_V only differed by one or two strains (**Table 1**). To allow a comparison between host specificity and genome variations, the phages were sequenced, two of them (Bk2_V and Iz_V) for the first time. The remaining four phages (Tbilisi, Firenze, Weybridge, and R/C) have already been characterized in previous studies but none of the genomic sequences determined in this work was identical to those described by other authors. Tb_V showed eight SNPs compared to phage Tb_W deposited at the Félix d'Hérelle Reference Center for Bacterial Viruses, Université Laval, Canada (Farlow et al., 2014). Five SNPs are silent mutations, two others lying within ORF21 (neck protein) and ORF44 (hypothetical protein) caused an amino acid exchange and one (within ORF14) is an insertion

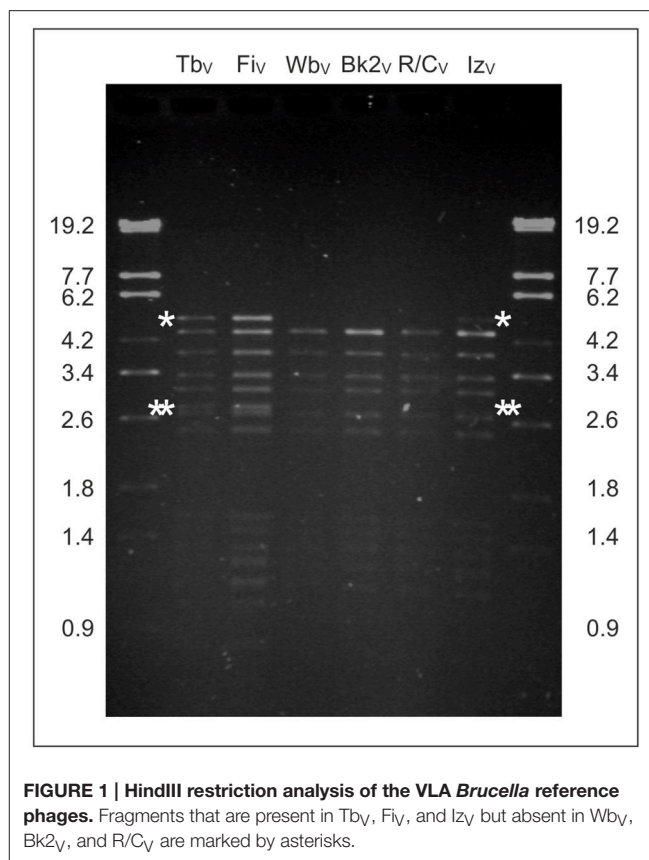


FIGURE 1 | HindIII restriction analysis of the VLA *Brucella* reference phages. Fragments that are present in Tb_V, Fi_V, and Iz_V but absent in Wb_V, Bk2_V, and R/C_V are marked by asterisks.

resulting in a truncated protein of unknown function. All these SNPs plus 14 additional SNPs exist when Tb_V is compared with Tb_E isolated at Eliava, Tbilisi, Ukraine (Tevdoradze et al., 2015). Differences to Tb_M (Gamaleya Scientific Research Institute of Epidemiology and Microbiology, Moscow, Russia) are even more pronounced and have already been addressed by Farlow et al. (2014). Contrary to Tb_V, Fi_V exhibited only two SNPs compared to Firenze in Laval. One SNP is located in an intergenic region, the other SNP caused an amino acid exchange at the C-terminus of a hypothetical protein. Wb_V showed five single nucleotide deviations to its counterpart in Laval. Three of them are located in genes (ORF16 and ORF23) for structural proteins, one in ORF27 probably encoding a tail collar protein and one in ORF57 for a primase/DNA polymerase. All of them caused amino acid exchanges. The most pronounced discrepancies between two phages with identical designations were found in R/C. The genomic sequence of the VLA R/C phage strain is 45 bp shorter than that of R/C in Laval. Furthermore, nine SNPs and two InDels were identified. Most deviations (four amino acid exchanges and one deletion of two amino acids) were found in the tail collar protein. Two frame shift mutations leading to radically changed gene products are present in ORF11 and ORF14 encoding a hypothetical protein and a primase/DNA polymerase, respectively. Quite the opposite was observed for Bk2_V. The host range of this phage differs significantly from that of Bk (Corbel, 1987; Farlow et al., 2014) but on the genome only one SNP located in the tail

collar protein gene leading to an amino acid exchange was detected.

Phage Iz_V exhibits the largest genome (41,446 bp) of all hitherto described brucellaphages. It contains a 301 bp duplicated nucleotide sequence located between the ORFs 23 and 24, which code for tail fiber proteins. Apart from this deviation, the Iz_V genome composition is similar to those of Tb_V and Fi_V as it does not carry the two deletions present in other *Brucella* reference phages (**Figure 2**). However, based on the SNP data the closest relative of Iz_V is not Tb_V or Fi_V, but phage Bk2_V. Besides the two InDels there are only five SNPs in these two phages. All of the SNPs are similarly present in the phages Tb_V, Fi_V, Wb_V, and R/C_V. The SNPs are located in genes for the large terminase subunit, neck protein, a hypothetical protein and the primase/DNA polymerase (**Table S3**). Tb_V and Fi_V revealed 17 additional SNPs which are spread all over the phage genomes (**Figure 2**). Another interesting feature of Iz_V is that the gene for the primase/DNA polymerase contains an internal stop codon, caused by the deletion of a single nucleotide. Therefore, in Iz_V the largest gene of brucellaphages is splitted into two smaller ORFs. While the primase/DNA polymerase of Tb_V, for instance, comprises 780 amino acids, the ORFs 57 and 58 of Iz_V encode polypeptides of 496 and 284 amino acids. Because of the frame shift mutation, the eight C-terminal amino acids of the large Iz_V polypeptide diverge from the Tb_V protein. The small polypeptide exhibits no differences to the Tb_V sequence. Our analysis of the R/C_V genomic sequence revealed that this phage also contains

a stop codon within the primase/DNA polymerase gene. In this phage polypeptides of 236 and 555 amino acids are encoded. The data demonstrate that several variants of the primase/DNA polymerase exist in brucellaphages. Whether the two proteins of Iz_V and R/C_V possess the same activity as their larger counterpart in Tb_V is unknown and has to be clarified by further experiments.

On the basis of host range and whole genome analyses, Farlow et al. (2014) divided the Laval reference phages into three groups. Group I is composed of Tbilisi and Firenze, group II includes Berkeley, R/C and Pr from Mexico and group III contains Weybridge and S708. Some of these phages were also investigated in this study. However, since the VLA and Laval reference phages are not identical, they cannot be easily compared. From the data obtained in our study, the VLA reference phages can be allocated to four groups. As in the classification mentioned above, Tb_V and Fi_V belong to group I. Group II consists of Wb_V and Bk2_V, which exhibited an almost identical host range and which are genetically closely related. Phage R/C_V represents group III. It possesses an unique host specificity and showed some deletions and frame shift mutations not occurring in the other reference phages. The fourth group is represented by Iz_V which does not fit to the other groups, neither by its host range, nor in terms of its genomic sequence. Due to the close overall DNA homologies of brucellaphages and because nucleotide variations can be observed after changing the host strain (Tevdoradze et al., 2015), the question arises, whether it really makes sense to group these phages. In addition, it should be considered that *Brucella*

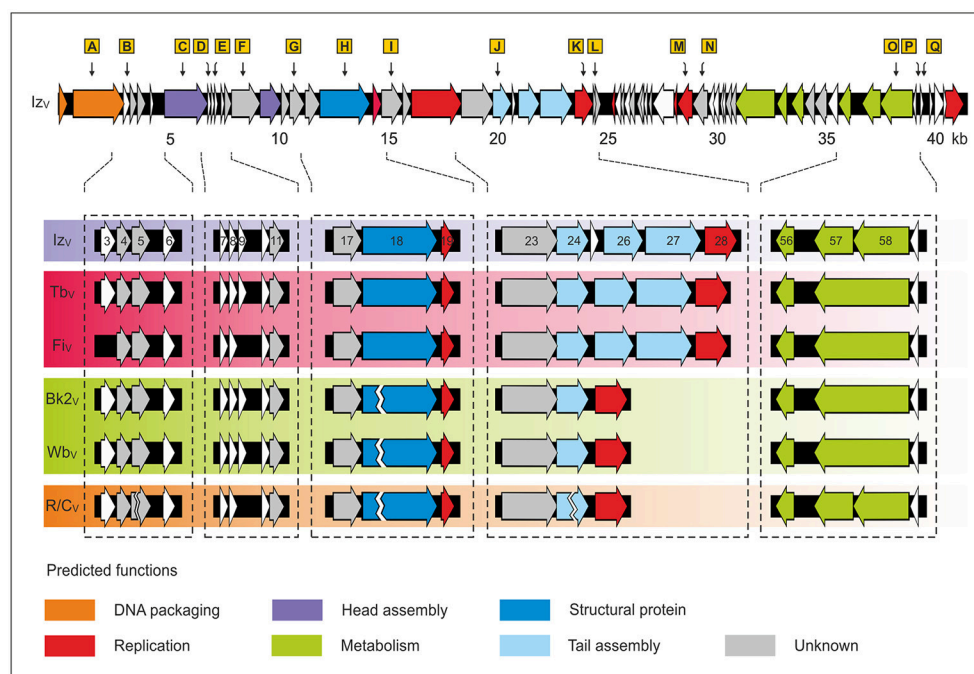


FIGURE 2 | Genome organization of the VLA *Brucella* reference phages. The upper panel shows the gene map of Iz_V. Putative genes are colored according to the predicted functions of their gene products **Table S4**. SNPs identified by comparison with the other reference phages are indicated by orange rectangles (A–Q). For a better overview, only one SNP per gene is shown. A list with all SNPs is presented in **Table S3**. The lower panel illustrates the gene composition of the six VLA reference phages. Relevant genes are numbered. In Wb_V, Bk2_V and R/C_V ORF27 and ORF28 are deleted, while ORF18 exhibits only a partial deletion. In Iz_V and R/C_V ORF57 is splitted into two ORFs Iz_V additionally contains the novel ORF 25 generated by sequence duplication.

strains having the same designation do not need to be identical. This also can distort results, e.g., the determination of the host range of the phages.

Identification of Repetitive DNA Sequences Possibly Involved in Genomic Rearrangements

Sequence determination of *Brucella* reference phages disclosed a 2.4 kb DNA fragment comprising two genes for tail fiber proteins present in Tb_V, Fiv, and Iz_V, but absent in Wb_V, Bk2_V, and R/C_V (Figure 3). Subsequent InDel analysis revealed some remarkable consistencies among various phages. Compared to the other reference phages, Wb_V, Bk2_V, and R/C_V show exactly the same deletion of 2,443 bp. In Tb_V, Fiv, and Iz_V, the fragment is flanked by a 9 bp direct repeat termed RS-A and RS-B (5'-GACCAACCC-3', Figure 3). A third copy of this sequence (RS-C) exists in reverse complement orientation ~700 bp apart from RS-A. By contrast, the Wb_V, Bk2_V, and R/C_V genomes contain only one copy of this sequence, adjacent to the deleted fragment. Notably, the 301 bp sequence that is duplicated in Iz_V also borders with one end on RS-A. At the other end of the duplicated sequence, a similar motif (5'-ACCAAACCC-3') is located in reverse complement orientation (Figure 3). This sequence does not exist in the other VLA *Brucella* reference phages. The duplication resulted in the generation of the new ORF 25 in Iz_V. These data suggest that the identified repeats may be important for the acquisition, loss or duplication of DNA sequences in brucellaphages. The additional 1.0 kb HindIII fragment identified in phage Nepean but not in other reference phages has also been suggested to be a repetition as it hybridized to Tbilisi DNA (Tevdoradze et al., 2015). It would be interesting to learn whether the repetition in this phage is similarly flanked by the repeats described above.

New Phages May Be Helpful to Improve the Typing Set

This study, and also those of other authors revealed several difficulties that may arise, when certain *Brucella* strains are typed using the existing reference phage typing set. The main reasons for this are the very similar host ranges of the phages and the fact that lysis from without effects, which are more difficult to interpret than plaques, have yet been included in the evaluation of lysis patterns. In addition, there are apparently host range variants of the reference phages, which further exacerbate the situation because it makes the comparison of data collected in different laboratories difficult. We therefore determined the host range of 22 non-reference phages deposited in the *Brucella* phage collection of the BfR (Table S2) to identify further candidates for typing. The analysis disclosed a very similar host specificity of the phages (Table 2). Though, the host range was clearly different from those of the reference phages. Like Tb_V and Fiv, none of the phages lysed strains of *B. melitensis* and *B. pinnipedialis*. All phages infected at least two, most of them even three *B. suis* biovars, namely bv1, bv4, and bv5. In this regard, the phages resemble Wb_V, Bk2_V, and Iz_V. Lysis of *Brucella* species was similar to the reference phages. The exact analysis of the

phages' host range also revealed some individual differences. This particularly pertained to the *B. suis* bv5 strain 513 that was not lysed by five phages. *Brucella microti* CCM4915^T was resistant only to one phage. Besides these specificities, all phages infected the same strains. It should, however, be emphasized that the phages produced a reduced number (up to 4 log units) of plaques on *B. suis* and *B. microti* strains. This has to be considered when the phages are used for typing. Two of the non-reference phages (A422 and M51) have been already studied by Morris et al. (1973). While we found plaques on *B. suis* with both phages, the other authors reported on lytic activity at RTD only for M51. It is conceivable that their A422 lysate did not contain enough active phage particles to cause lysis at RTD. Nevertheless, in spite of this discrepancy, the data of this study suggest that the reference phage typing set could be complemented by additional phages, which would make the discrimination of some *Brucella* species and strains more reliable.

The sequence analysis of the *Brucella* reference phages disclosed several SNPs (>50 SNPs, regions A–Q, Figure 2), most of them causing amino acid exchanges or deletions. Because no data were available about the genomes of the 22 non-reference phages, we examined all SNP positions by PCR using 23 different primer pairs. The study showed that all phages differed in at least one SNP and that none of the phages exhibited the two large deletions found in Wb_V, Bk2_V, and R/C_V. Taking into account all SNPs, two clusters of non-reference phages were assigned. One cluster (cluster B) consists of the phages A422 and M51 whose closest relatives are Wb_V, Bk2_V, Iz_V, and R/C_V. The remaining phages form a cluster (cluster C), which is related to cluster B (Figure 4). As the neck and tail collar protein genes of brucellaphages have been suspected to be important for host specificity (Flores et al., 2012; Farlow et al., 2014; Tevdoradze et al., 2015), we focused on the occurrence of SNPs within these genes. In the six VLA reference phages, the neck and tail collar protein genes exhibited five and seven SNPs, respectively. The analysis of the non-reference phages revealed even higher numbers of SNPs, some of which are located at the same position as in the reference phages (Table S3). A comparison of SNPs within the neck and tail collar protein genes with the host ranges of the phages did not provide evidence for amino acids that may decide on the strains that are infected. However, among 18 non-reference phages that exhibited an identical host range, 10 amino acid exchanges were observed in the neck protein and 11 in the tail collar protein, indicating that these positions do not determine specificity. Hence, even though the neck and tail collar protein genes are hotspots for nucleotide variations, it remains open which sequences are the key factor defining the host range of the phages.

CONCLUSIONS

Lytic phages have been applied for decades to identify and discriminate *Brucella* species and biovars. Moreover, the set of reference phages used in different laboratories is basically the same. The phages were isolated many years ago and they were distributed to diagnostic laboratories worldwide. The same holds true for *Brucella* reference and type strains serving as

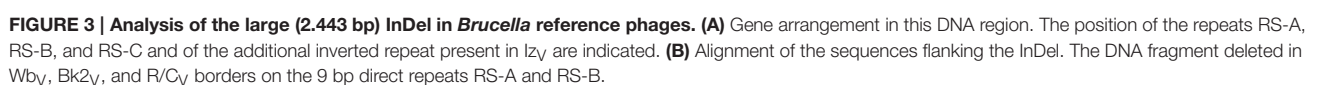
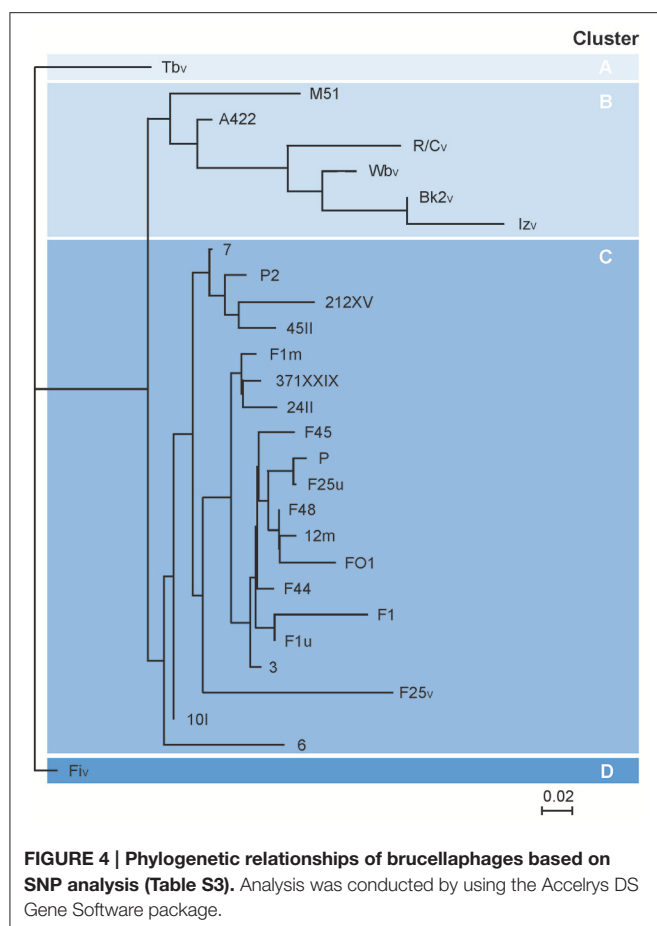


TABLE 2 | Host range of other brucellaphages.

<i>Brucella strain</i>	F44	P	45 III	FO1	F1m	F1u	F25u	F45	F48	3	6	7	10I	12m	24II	212 XV	371 XXIX	P2	M51	A 422	F25	F1
<i>B. abortus</i> 544	+	+	+	+	+	+	+	+	+	+	+	+	+	+	+	+	+	+	+	+	+	+
<i>B. abortus</i> 86/8/59	+	+	+	+	+	+	+	+	+	+	+	+	+	+	+	+	+	+	+	+	+	+
<i>B. abortus</i> Tulya	+	+	+	+	+	+	+	+	+	+	+	+	+	+	+	+	+	+	+	+	+	+
<i>B. abortus</i> 292	+	+	+	+	+	+	+	+	+	+	+	+	+	+	+	+	+	+	+	+	+	+
<i>B. abortus</i> B3196	+	+	+	+	+	+	+	+	+	+	+	+	+	+	+	+	+	+	+	+	+	+
<i>B. abortus</i> 870	+	+	+	+	+	+	+	+	+	+	+	+	+	+	+	+	+	+	+	+	+	+
<i>B. abortus</i> 63/75	+	+	+	+	+	+	+	+	+	+	+	+	+	+	+	+	+	+	+	+	+	+
<i>B. abortus</i> C86	+	+	+	+	+	+	+	+	+	+	+	+	+	+	+	+	+	+	+	+	+	+
<i>B. melitensis</i> 16M	-	-	-	-	-	-	-	-	-	-	-	-	-	-	-	-	-	-	-	-	-	-
<i>B. melitensis</i> 63/9	-	-	-	-	-	-	-	-	-	-	-	-	-	-	-	-	-	-	-	-	-	-
<i>B. melitensis</i> Ether	-	-	-	-	-	-	-	-	-	-	-	-	-	-	-	-	-	-	-	-	-	-
<i>B. suis</i> 1330	(+)	(+)	(+)	(+)	(+)	(+)	(+)	(+)	(+)	(+)	(+)	(+)	(+)	(+)	(+)	(+)	(+)	(+)	(+)	(+)	(+)	(+)
<i>B. suis</i> Thomsen	-	-	-	-	-	-	-	-	-	-	-	-	-	-	-	-	-	-	-	-	-	-
<i>B. suis</i> 686	-	-	-	-	-	-	-	-	-	-	-	-	-	-	-	-	-	-	-	-	-	-
<i>B. suis</i> 40	(+)	(+)	(+)	(+)	(+)	(+)	(+)	(+)	(+)	(+)	(+)	(+)	(+)	(+)	(+)	(+)	(+)	(+)	(+)	(+)	(+)	(+)
<i>B. suis</i> 513	-	(+)	-	(+)	(+)	(+)	(+)	(+)	(+)	(+)	-	(+)	(+)	(+)	(+)	(+)	(+)	(+)	(+)	-	-	(+)
<i>B. canis</i> RM 6/66	-	-	-	-	-	-	-	-	-	-	-	-	-	-	-	-	-	-	-	-	-	-
<i>B. neotomae</i> 5K33	+	+	+	+	+	+	+	+	+	+	+	+	+	+	+	+	+	+	+	+	+	+
<i>B. ovis</i> 63/290	-	-	-	-	-	-	-	-	-	-	-	-	-	-	-	-	-	-	-	-	-	-
<i>B. ceti</i> B1/94	-	-	-	-	-	-	-	-	-	-	-	-	-	-	-	-	-	-	-	-	-	-
<i>B. pinnipedialis</i> B2/94	-	-	-	-	-	-	-	-	-	-	-	-	-	-	-	-	-	-	-	-	-	-
<i>B. microti</i> CCM4915 ^T	(+)	(+)	(+)	(+)	(+)	(+)	(+)	(+)	(+)	(+)	-	(+)	(+)	(+)	(+)	(+)	(+)	(+)	(+)	(+)	(+)	(+)
<i>B. inopinata</i> BO1	-	-	-	-	-	-	-	-	-	-	-	-	-	-	-	-	-	-	-	-	-	-
<i>B. vulpis</i> F60 H	+	+	+	+	+	+	+	+	+	+	+	+	+	+	+	+	+	+	+	+	+	+
<i>B. vulpis</i> F965 H	+	+	+	+	+	+	+	+	+	+	+	+	+	+	+	+	+	+	+	+	+	+

+, Plaque formation; (+), reduced plaque formation in comparison to *B. abortus* strain S19; -, no plaque formation.



controls. After sequencing of the first *Brucella* reference phages, it became obvious that there is not only one Tbilisi, Firenze, or Weybridge phage but some variants of the prototypes revealing distinct sequence alterations. Nucleotide variations particularly occur in genes probably involved in host specificity. Therefore, it is not surprising that the VLA reference phages investigated in this study partially exhibited a host range different from homonymous phages in other laboratories. However, it is important to point out that in our study, lytic activity was defined as the ability of the phages to form plaques, while rather unspecific lysis from without effects caused by extremely

high numbers of phages were not evaluated. We think that this practice delivers more reliable data because single plaques are much easier to interpret than halos of lysis which may look very different. Results can also be biased when typing phages are propagated on different hosts, or when strains containing endogenous phages are infected. The *B. abortus* vaccine strain S19 is a well-suited host because it is susceptible to many *Brucella* phages and a Biosafety Level 2 (BSL2) organism. Thus, there are some issues that should be considered when brucellaphages are applied for typing. One main problem with lysotyping of *Brucella* strains is the similar host specificity of the reference phages. The situation could be improved by adding new phages to the typing set, which exhibit an individual host range. Our analysis of 22 non-reference brucellaphages revealed some new candidates that could be applied for routine diagnostics.

AUTHOR CONTRIBUTIONS

JH, HS, KN, and SH designed the study. JH, CG, CJ, and JR performed the experiments. JH, CG, CJ, HS, JR, SA, and SH analyzed the data. JH, CJ, and SH wrote the manuscript and prepared the tables and figures. All authors edited the manuscript.

ACKNOWLEDGMENTS

The study was financially supported by a grant of the German Federal Institute for Risk Assessment (1332-488). Parts of the study were conducted within the Ess-B.A.R. project (FKZ: 13N13982).

SUPPLEMENTARY MATERIAL

The Supplementary Material for this article can be found online at: <http://journal.frontiersin.org/article/10.3389/fmicb.2017.00408/full#supplementary-material>

Table S1 | Bacterial strains used in this study.

Table S2 | Bacteriophages used in this study.

Table S3 | Single Nucleotide Polymorphisms (SNPs) among brucellaphages.

Table S4 | ORF analysis of brucellaphage Iz.

REFERENCES

- Ackermann, H. W., Simon, F., and Verger, J. M. (1981). A survey of *Brucella* phages and morphology of new isolates. *Intervirology* 16, 1–7. doi: 10.1159/000149240
- Al Dahouk, S., Scholz, H. C., Tomaso, H., Bahn, P., Göllner, C., Karges, W., et al. (2010). Differential phenotyping of *Brucella* species using a newly developed semi-automated metabolic system. *BMC Microbiol.* 10:269. doi: 10.1186/1471-2180-10-269
- Alton, G. G., Jones, L. M., and Pietz, D. E. (1975). *Laboratory Techniques in Brucellosis*. Geneva: WHO
- Baily, G. G., Krahn, J. B., Drasar, B. S., and Stoker, N. G. (1992). Detection of *Brucella melitensis* and *Brucella abortus* by DNA amplification. *J. Trop. Med. Hyg.* 95, 271–275.
- Brinley-Morgan, W. J., Kay, D., and Bradley, D. E. (1960). *Brucella* bacteriophage. *Nature* 188, 74–75. doi: 10.1038/188074a0
- Calderone, J. G., and Pickett, M. J. (1965). Characterization of Brucellaphages. *J. Gen. Microbiol.* 39, 1–10. doi: 10.1099/00221287-39-1-1
- Corbel, M. J. (1984). Properties of *Brucella*-phages lytic for non-smooth *Brucella* strains. *Dev. Biol. Stand.* 56, 55–62.
- Corbel, M. J. (1987). *Brucella* phages: advances in the development of a reliable phage typing system for smooth and non-smooth *Brucella* isolates. *Ann. Inst. Pasteur. Microbiol.* 138, 70–75. doi: 10.1016/0769-2609(87)90056-1
- Corbel, M. J., and Morris, J. A. (1975). Studies on a smooth phage resistant variant of *Brucella abortus* II. Mechanism of phage resistance. *Br. J. Exp. Pathol.* 56, 1–7.

- Corbel, M. J., and Thomas, E. L. (1976). Properties of some new *Brucella* phage isolates; evidence for lysogeny within the genus. *Dev. Biol. Stand.* 31, 38–45.
- Corbel, M. J., Tolari, F., and Yadava, V. K. (1988). Characterisation of a new phage lytic for both smooth and non-smooth *Brucella* species. *Res. Vet. Sci.* 44, 45–49.
- de Figueiredo, P., Ficht, T. A., Rice-Ficht, A., Rossetti, C. A., and Adams, L. G. (2015). Pathogenesis and immunobiology of brucellosis: review of *Brucella*-host interactions. *Am. J. Pathol.* 185, 1505–1517. doi: 10.1016/j.ajpath.2015.03.003
- Eisenberg, T., Hamann, H. P., Kaim, U., Schlez, K., Seeger, H., Schauerte, N., et al. (2012). Isolation of potentially novel *Brucella* spp. from frogs. *Appl. Environ. Microbiol.* 78, 3753–3755. doi: 10.1128/AEM.07509-11
- Farlow, J., Filippov, A. A., Sergueev, K. V., Hang, J., Kotorashvili, A., and Nikolich, M. P. (2014). Comparative whole genome analysis of six diagnostic brucellaphages. *Gene* 541, 115–122. doi: 10.1016/j.gene.2014.01.018
- Fischer, D., Lorenz, N., Heuser, W., Kämpfer, P., Scholz, H. C., and Lierz, M. (2012). Abscesses associated with a *Brucella inopinata*-like bacterium in a big-eyed tree frog (*Leptopelis vermiculatus*). *J. Zoo Wildl. Med.* 43, 625–628. doi: 10.1638/2011-0005R2.1
- Flores, V., López-Merino, A., Mendoza-Hernandez, G., and Guarneros, G. (2012). Comparative genomic analysis of two brucellaphages of distant origins. *Genomics* 99, 233–240. doi: 10.1016/j.ygeno.2012.01.001
- Foster, G., Osterman, B. S., Godfroid, J., Jacques, I., and Cloeckaert, A. (2007). *Brucella ceti* sp. nov. and *Brucella pinnipedialis* sp. nov. for *Brucella* strains with cetaceans and seals as their preferred hosts. *Int. J. Syst. Evol. Microbiol.* 57(Pt 11), 2688–2693. doi: 10.1099/ijs.0.05269-0
- Godfroid, J., Al Dahouk, S., Pappas, G., Roth, F., Matope, G., Muma, J., et al. (2013). A “One Health” surveillance and control of brucellosis in developing countries: moving away from improvisation. *Comp. Immunol. Microbiol. Infect. Dis.* 36, 241–248. doi: 10.1016/j.cimid.2012.09.001
- Hammerl, J. A., Al Dahouk, S., Nöckler, K., Göllner, C., Appel, B., and Hertwig, S. (2014). F1 and tbilisi are closely related brucellaphages exhibiting some distinct nucleotide variations which determine the host specificity. *Genome Announc.* 2:e01250-13. doi: 10.1128/genomeA.01250-13
- Hammerl, J. A., Göllner, C., Al Dahouk, S., Nöckler, K., Reetz, J., and Hertwig, S. (2016). Analysis of the first temperate broad host range brucellaphage (BiPBO1) isolated from *B. inopinata*. *Front. Microbiol.* 7:24. doi: 10.3389/fmicb.2016.00024
- Hinic, V., Brodard, I., Thomann, A., Cvetnic, Z., Makaya, P. V., Frey, J., et al. (2008). Novel identification and differentiation of *Brucella melitensis*, *B. abortus*, *B. suis*, *B. ovis*, *B. canis*, and *B. neotomae* suitable for both conventional and real-time PCR systems. *J. Microbiol. Methods* 75, 375–378. doi: 10.1016/j.mimet.2008.07.002
- Jablonski, L. (1962). Variability of *Brucella* phages. *Nature* 193, 703–704. doi: 10.1038/193703a0
- Jones, L. M., Merz, G. S., and Wilson, J. B. (1968). Phage typing reactions on *Brucella* species. *Appl. Microbiol.* 16, 1179–1190.
- Joint FAO/WHO Expert Committee on Brucellosis (1986). *Technical Report Series joint FAO/WHO Expert Committee on Brucellosis*. World Health Organization.
- López-Goñi, I., García-Yoldi, D., Marín, C. M., de Miguel, M. J., Muñoz, P. M., Blasco, J. M., et al. (2008). Evaluation of a multiplex PCR assay (Bruce-ladder) for molecular typing of all *Brucella* species, including the vaccine strains. *J. Clin. Microbiol.* 46, 3484–3487. doi: 10.1128/JCM.00837-08
- Mayer-Scholl, A., Draeger, A., Göllner, C., Scholz, H. C., and Nöckler, K. (2010). Advancement of a multiplex PCR for the differentiation of all currently described *Brucella* species. *J. Microbiol. Methods* 80, 112–114. doi: 10.1016/j.mimet.2009.10.015
- Moreira-Jacob, M. (1968). New group of virulent bacteriophages showing differential affinity for *Brucella* species. *Nature* 219, 752–753. doi: 10.1038/219752a0
- Morgan, M. J. B. (1963). The examination of *Brucella* cultures for lysis by phage. *J. Gen. Microbiol.* 1963, 437–443. doi: 10.1099/00221287-30-3-437
- Morris, J. A., Corbel, M. J., and Phillip, J. I. (1973). Characterization of three phages lytic for *Brucella* species. *J. Gen. Virol.* 20, 63–73. doi: 10.1099/0022-1317-20-1-63
- Parnas, J., Feltynowski, A., and Bulikowski, W. (1958). Anti-*Brucella* phage. *Nature* 182, 1610–1611. doi: 10.1038/1821610a0
- Renoux, G., and Suire, A. (1963). Spontaneous lysis and phage-carrier state in *Brucella* cultures. *J. Bacteriol.* 86, 642–647.
- Rigby, C. E., Cerqueira-Campos, M. L., Kelly, H. A., and Surujballi, O. P. (1989). Properties and partial genetic characterization of Nepean phage and other lytic phages of *Brucella* species. *Can. J. Vet. Res.* 53, 319–325.
- Sambrook, J. F., and Russell, D. W. (2001). *Molecular Cloning: A Laboratory Manual*, Vol. 3. New York, NY: Cold Spring Harbor Laboratory Press.
- Scholz, H. C., Al Dahouk, S., Tomaso, H., Neubauer, H., Witte, A., Schloter, M., et al. (2008a). Genetic diversity and phylogenetic relationships of bacteria belonging to the *Ochrobactrum-Brucella* group by recA and 16S rRNA gene-based comparative sequence analysis. *Syst. Appl. Microbiol.* 31, 1–16. doi: 10.1016/j.syapm.2007.10.004
- Scholz, H. C., Hubalek, Z., Sedláček, I., Vergnaud, G., Tomaso, H., Al Dahouk, S., et al. (2008b). *Brucella microti* sp. nov., isolated from the common vole *Microtus arvalis*. *Int. J. Syst. Evol. Microbiol.* 58(Pt 2), 375–382. doi: 10.1099/ijs.0.05356-0
- Scholz, H. C., Nöckler, K., Göllner, C., Bahn, P., Vergnaud, G., Tomaso, H., et al. (2010). *Brucella inopinata* sp. nov., isolated from a breast implant infection. *Int. J. Syst. Evol. Microbiol.* 60(Pt 4), 801–808. doi: 10.1099/ijs.0.011148-0
- Scholz, H. C., Pfeffer, M., Witte, A., Neubauer, H., Al Dahouk, S., Wernery, U., et al. (2008c). Specific detection and differentiation of *Ochrobactrum anthropi*, *Ochrobactrum intermedium* and *Brucella* spp. by a multi-primer PCR that targets the recA gene. *J. Med. Microbiol.* 57(Pt 1), 64–71. doi: 10.1099/jmm.0.47507-0
- Scholz, H. C., Revilla-Fernández, S., Al Dahouk, S., Hammerl, J. A., Zygmunt, M. S., Cloeckaert, A., et al. (2016). *Brucella vulpis* sp. nov., isolated from mandibular lymph nodes of red foxes (*Vulpes vulpes*). *Int. J. Syst. Evol. Microbiol.* 66, 2090–2098. doi: 10.1099/ijsem.0.000998
- Segondy, M., Allardet-Servent, A., Caravano, R., and Ramuz, M. (1988). Common physical map of four *Brucella* bacteriophage genomes. *FEMS Microbiol. Lett.* 56, 177–182. doi: 10.1111/j.1574-6968.1988.tb03173.x
- Soler-Lloréns, P. F., Quance, C. R., Lawhon, S. D., Stuber, T. P., Edwards, J. F., Ficht, T. A., et al. (2016). A *Brucella* spp. isolate from a Pac-man frog (*Ceratophrys ornata*) reveals characteristics departing from classical brucellae. *Front. Cell. Infect. Microbiol.* 6:116. doi: 10.3389/fcimb.2016.00116
- Tevdoradze, E., Farlow, J., Kotorashvili, A., Skhirtladze, N., Antadze, I., Gunia, S., et al. (2015). Whole genome sequence comparison of ten diagnostic brucellaphages propagated on two *Brucella abortus* hosts. *Virol. J.* 12:66. doi: 10.1186/s12985-015-0287-3
- Whatmore, A. D., Dale, E. J., Stubberfield, E., Muchowski, J., Koylass, M., Dawson, C., et al. (2015). Isolation of *Brucella* from a White's tree frog (*Litoria caerulea*). *JMM Case Rep.* 2:e000017. doi: 10.1099/jmmcr.0.000017
- Whatmore, A. M., Davison, N., Cloeckaert, A., Al Dahouk, S., Zygmunt, M. S., Brew, S. D., et al. (2014). *Brucella papionis* sp. nov., isolated from baboons (*Papio* spp.). *Int. J. Syst. Evol. Microbiol.* 64(Pt 12), 4120–4128. doi: 10.1099/ijs.0.065482-0
- Zhu, C. Z., Xiong, H. Y., Han, J., Cui, B. Y., Piao, D., Li, Y. F., et al. (2009). Molecular characterization of Tb, a new approach for an ancient brucellaphage. *Int. J. Mol. Sci.* 10, 2999–3011. doi: 10.3390/ijms10072999

Conflict of Interest Statement: The authors declare that the research was conducted in the absence of any commercial or financial relationships that could be construed as a potential conflict of interest.

Copyright © 2017 Hammerl, Göllner, Jäckel, Scholz, Nöckler, Reetz, Al Dahouk and Hertwig. This is an open-access article distributed under the terms of the Creative Commons Attribution License (CC BY). The use, distribution or reproduction in other forums is permitted, provided the original author(s) or licensor are credited and that the original publication in this journal is cited, in accordance with accepted academic practice. No use, distribution or reproduction is permitted which does not comply with these terms.



Brucella Genital Tropism: What's on the Menu

Jean-Jacques Letesson^{1*}, Thibault Barbier¹, Amaia Zúñiga-Ripa², Jacques Godfroid³, Xavier De Bolle¹ and Ignacio Moriyón²

¹ Research Unit in Microorganisms Biology, University of Namur, Bruxelles, Belgium, ² Facultad de Medicina, Departamento de Microbiología y Parasitología, Edificio de Investigación, Instituto de Salud Tropical e Instituto de Investigación Sanitaria de Navarra, Universidad de Navarra, Pamplona, Spain, ³ Arctic Infection Biology, UiT - The Arctic University of Norway, Tromsø, Norway

Keywords: brucellosis, tropism, placenta, epididymis, metabolism, erythritol, lactate, glutamate

OPEN ACCESS

Edited by:

Axel Cloeckaert,
Institut National de la Recherche
Agronomique, France

Reviewed by:

Roy Martin Roop II,
East Carolina University, USA
Gregory T. Robertson,
Colorado State University, USA
Luis Ernesto Samartino,
INTA Instituto Patobiología, Argentina

*Correspondence:

Jean-Jacques Letesson
jean-jacques.letesson@fundp.ac.be

Specialty section:

This article was submitted to
Infectious Diseases,
a section of the journal
Frontiers in Microbiology

Received: 18 January 2017

Accepted: 10 March 2017

Published: 28 March 2017

Citation:

Letesson J-J, Barbier T,
Zúñiga-Ripa A, Godfroid J, De Bolle X
and Moriyón I (2017) Brucella Genital
Tropism: What's on the Menu.
Front. Microbiol. 8:506.
doi: 10.3389/fmicb.2017.00506

If things such as Tripadvisor web-site or Foursquare apps existed for bacteria, for sure, to the question “What is the best place to eat near me?” or “Where can I find my favorite food?” *Brucella* would be advised “male and female genital organs” as a first choice with millions of positive comments from previous and highly satisfied congeneric visitors. The friendly ambiance and the relish for the specialties of the chef are illustrated by the fact that the infected bovine concepts can host up to 10¹⁴ brucellae (Alexander et al., 1981; Corner, 1983).

As expected, these bacteria are not welcome visitors: they cause brucellosis, a highly contagious zoonosis that affects many species of wild and domestic animals (Zheludkov and Tsirelson, 2010; Atluri et al., 2011) and represents a serious burden for livestock and humans worldwide (McDermott et al., 2013). In their hosts, these gram-negative coccobacilli replicate in an endoplasmic reticulum-derived vacuole of professional (macrophages, dendritic cells) and non-professional (e.g., trophoblastic cells) phagocytes (Atluri et al., 2011), and in sexually mature animals have a pronounced tropism for genital organs causing orchitis, epididymitis and infertility in males, and abortion (most often in the last third of gestation) and sterility in females (Moreno and Moriyón, 2006). This genital tropism also holds true in humans as *Brucella* induces epididymo-orchitis and can infect the placenta even if abortion is rare (Anderson et al., 1986; Queipo-Ortuño et al., 2006). Sexual secretions and aborted tissues of animals contain billions of bacteria and, as the brucellae cannot survive long in the environment, these high numbers grant transmission via aerosols, ingestion or sexual intercourse (Poester et al., 2013). Therefore, the localization and abundant multiplication in the reproductive tract of animals is crucial in the biology of this parasite.

Although identified as a characteristic of the disease in ruminants by the end of the Nineteenth century (reviewed in Huddleson et al., 1943), the reason(s) underlying the genital tropism of *Brucella* and subsequent intense multiplication are still to be deciphered. Clearly, any unifying hypothesis should consider properties shared by both the male and female organs of the target species, which rules out some possibilities. For instance, although *Brucella* is carried by blood cells (Anderson et al., 1986; Vitry et al., 2014), the (erythro-)phagocytic properties of the trophoblasts as an entry gate to the placenta cannot be invoked to explain the localization in seminal vesicles. On the other hand, immune privilege (Filippini et al., 2001) in testis and semen or local immunosuppression at the feto-maternal interface (Warning et al., 2011) could well be part of the explanation. Yet, tolerance cannot be enough: an intense multiplication needs timely and effective sources of carbon, nitrogen and energy. Following this idea, we will argue here that some peculiarities of the metabolism of these organs provide nutrients that match the metabolic abilities of *Brucella* and are thus playing a prominent role.

Although, the link with *Brucella* metabolism may not be immediately evident, female and male genital organs have some common metabolic features, the most obvious one being a rather high production of fructose. This is, for example, the case of epitheliochorial and synepitheliochorial placentas (e.g., those of cows, ewes and sows) where fructose is in fact the major sugar. To a lesser extent, fructose is also present in other types of placentas like those of dogs, cats, guinea pigs, rabbits, rats, and ferrets (Alexander et al., 1955; Håstein and Velle, 1968; Battaglia and Meschia, 1978; Reitzer et al., 1979; Kim et al., 2012). A similar dominance of fructose over glucose occurs in epididymes, seminal fluids and oviducts of several mammals (boars, bulls, rats, guinea pigs, etc.) where it serves as the primary energy source for spermatozooids (Frenette et al., 2004; Frenette, 2006; Pruneda et al., 2006; Larose et al., 2012). In all these organs, fructose originates from glucose through the Polyol Pathway, initially described in the fetal tissues of ungulates (Hers, 1956). In this pathway, glucose is reduced to sorbitol in a reaction catalyzed by the aldose reductase (AR) and this C6 polyol is then oxidized to fructose by sorbitol dehydrogenase, which uses NAD as electron acceptor. Since AR uses as proton/electron donor the NADPH furnished by the Pentose Phosphate (PP) Pathway (or hexose monophosphate shunt), there is a connection between the PP and Polyol pathways. Fructose, however, does not support growth of all *Brucella* strains (McCullough and Beal, 1951), and what are noteworthy here are some intricacies of these two pathways.

The PP pathway is known to occur, among other places, in the testes, ovaries, adrenal cortex, and placenta where the NADPH it produces is crucially needed for the synthesis of steroid hormones (Ferrier, 2013). In 1967, Clark et al. (1967) proposed that this pathway was involved in the production of erythritol, a C4 sugar alcohol they identified among other polyols in bovine semen. This suggests a prominent albeit indirect role for the PP pathway in *Brucella* genital tropism because previous work not only had shown that erythritol is the preferred carbon/energy source of *B. abortus*, *B. melitensis* and *B. suis* (McCullough and Beal, 1951) but also had reported that it displayed “vitamin-like” properties stimulating the growth of these *Brucella* spp. in catalytic amounts (Keppie et al., 1965). Since then, the high concentrations of erythritol in fetal fluids, placental tissue, epididymis and semen of the preferred hosts of those *Brucella* species have been postulated as important in the genital tropism of these pathogens in ruminants (Smith et al., 1962; Clark et al., 1967; Essenberg et al., 2002) and, indeed, recent evidence strongly suggests its presence in various concentrations in cells and tissues of other *Brucella* hosts where it was not detected previously (Lowrie and Kennedy, 2001; Burkhardt et al., 2005; Jauniaux et al., 2005). Moreover, speculating on the origin of erythritol in bovine fetal fluids, where it was first identified in animal tissues, Pearce had the insight that: “it may arise from D-erythrose, a possible product of the pentose phosphate pathway, and act as an intermediate between D-erythrose and D-erythrulose as sorbitol acts as an intermediate between glucose and fructose” (Pearce et al., 1962). In fact, in bovine genital organs erythritol concentration parallels that of fructose and is very likely produced by the action of AR because, in addition to a very broad ability to reduce

aldehydes to their corresponding alcohols, its K_m is far lower for D-erythrose ($4 \cdot 10^{-4}$ M/L) than for glucose ($7 \cdot 10^{-2}$ M/L) (Hayman and Kinoshita, 1965). AR would thus bridge the Polyol and PP pathways by both acting on a PP sugar and using a PP coenzyme.

It is worth noting that AR activity increases during pregnancy (Håstein and Velle, 1968). Thus, erythritol production could rise following a dynamics that overlaps with the increased susceptibility to *Brucella* colonization that occurs during the second half of pregnancy, as shown by field experience, repeated observations with *B. melitensis* vaccine Rev 1 (which displays a comparatively high residual virulence, Blasco, 1997) and controlled experiments in cattle (Crawford et al., 1987). Studying chorioallantoic membrane explants, Samartino and Enright found that the replicative capability of the bacteria was better in late gestational placental tissue than in tissue harvested earlier (Samartino and Enright, 1992). Later on they found that erythritol production was highest at mid pregnancy (Samartino et al., 1994). However, they pointed out also that erythritol was unlikely to be the only or even main factor operating in their *in vitro* system as experiments with *B. abortus* S19, which is inhibited by erythritol, yielded results not different from those obtained with the virulent strain (Samartino and Enright, 1992). Even though an interpretation is obscured by the isolation of erythritol-resistant mutants of S19 (Corner and Alton, 1981), this vaccine is still able to induce abortions in pregnant cattle (albeit only in a low proportion; Nicoletti, 1976), which also suggests the existence of other metabolic factors that would allow its efficient growth in placentas.

In this context, it is important to note that, although erythritol is a *Brucella* preferential carbon source, the placenta and the male genital organs and fluids also have high concentrations of glycerol, lactate, and glutamate (Figure 1).

In late pregnancy, due to the enhanced adipose tissue lipolytic activity, the maternal plasma concentration of glycerol is consistently elevated. Because of the rapid and efficient conversion of maternal glycerol into glucose there is little direct glycerol transfer to the fetus by the placenta (Palacin et al., 1987). The glycerol gradient between maternal plasma and fetal blood is greater in species with epitheliochorial placentation (i.e., ruminants) than in accidental hosts that like humans have a hemochorial placenta (Herrera, 2002). Glycerol has also been described, either free or as glyceryl-phosphoryl-choline, in bull and ram semen where it is taken by spermatozoa and metabolized through an oxidative process into lactate (Britton, 1962; Clark et al., 1967). Concerning the latter substrate, the placenta of different mammals, even under aerobic conditions, produces lactate in relatively large amounts, presumably from maternal glucose, and supplies it to the fetus where it is an important metabolic substrate. Likewise, male germ cells preferentially use lactate and pyruvate over glucose as an energy substrate (Battaglia and Meschia, 1978; Père, 2003; Goldberg et al., 2010). Finally, glutamate is also available in genital tissues of at least sheep. While it appears that neutral and basic amino acids are transported from the ovine placenta into fetal blood, the acidic amino acids glutamate and aspartate are not. In fact, glutamate is delivered by the fetal lamb to the placenta in large amounts and

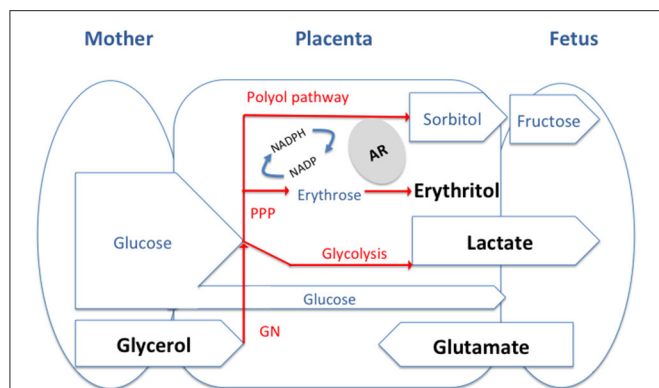


FIGURE 1 | General model of the feto-maternal interface and of the main carbon source available for *Brucella*. The substrates we discuss in the paper are in Bold and are likely to be present at different levels in tissues of different host depending on the type of placentation. PPP, pentose phosphate pathway; GN, gluconeogenesis; AR, aldose reductase.

then converted to glutamine before being released back into the fetal circulation (Battaglia and Meschia, 1978; Wu et al., 2015). Glutamate is also the main free amino acid in the testis and semen of most mammalian species, where it occurs mainly in the seminal plasma (Setchell et al., 1967; Keil et al., 1979).

Amazingly glutamate, lactate and glycerol match the three carbon (and nitrogen for glutamate) sources identified by Gerhardt et al. (1950) as suitable to formulate a defined minimal medium for *Brucella* growth that obviated the need for complex amino acid mixtures. Gerhardt et al. reported that only glutamate among 20 amino acids and related nitrogen compounds was used as sole source of carbon, nitrogen and energy by S19 and two wild-type *B. abortus* strains (Gerhardt et al., 1950). Even though this is not true for all *B. suis* strains and at least some *B. abortus* and *B. melitensis* strains are respectively auxotrophic for specific amino acids or require a CO₂ supply for growing on glutamate (Plommet, 1991), the fact stands that all *Brucella* species have in common a remarkable capacity to oxidize exogenous glutamate (Verger and Grayon, 1977; Jacques et al., 2007). As expected, genomic and mutant analysis show that the brucellae keep a conventional enzymatic machinery for using glutamate both for amino acid synthesis and as a C source feeding the Krebs cycle (Ronneau et al., 2014).

Although, reports on lactate as a source of C for *Brucella in vitro* are few, it has been noted that it is very effectively used and that it can even advantageously replace glucose (Gerhardt and Wilson, 1948). These effects can be explained, at least in part, by the existence of a lactate permease and a primary L-lactate dehydrogenase coupled to the electron transport chain whose efficiency is similar to that of the primary erythritol-1-phosphate dehydrogenase (Rest, 1975). Similarly, there are few studies on glycerol *in vitro*, and it is unclear whether the growth promoting effect observed by Gerhard and Wilson relate only to an ability to act as an excellent complementary C source for lactate (Gerhardt and Wilson, 1948). On one hand, the rather

high concentration of glycerol in Gerhard and Wilson's medium seems metabolically unnecessary and it has been interpreted to mean that non-nutritional properties, such as a proper control of the E_h of the medium, could contribute (Gerhardt, 1958). On the other, even though impurities such as vitamins or amino acids in the reagent used in early studies cannot be ruled out (Gerhardt, 1958; Plommet, 1991), recent observations *in vitro* also support the complementarity role of glycerol (Zúñiga-Ripa et al., 2014).

It seems, therefore, a plausible hypothesis that there is an adequacy between the presence and abundance of privileged nutrients in the male and female genitals organs and the nutritional preferences of *Brucella* in some simple defined media. Strong candidates are erythritol, lactate, glycerol and glutamate, in all likelihood in various combinations and proportions. To test this hypothesis would require assaying defined metabolic mutants for their residual virulence in reproductive tissues (e.g., male or female genital tissue colonization, induction of fetal pathology and abortion) of natural hosts. Regrettably, in most countries, governmental regulations represent a bottleneck for this kind of research that is almost impossible to circumvent and, although imperfect, the mouse model remains as the only feasible surrogate.

It has been suggested that rather than facultative intracellular parasites, the brucellae should be described as intracellular facultative extracellular bacteria (Moreno and Moriyón, 2002) and, indeed, their ability to persist outside the host is very limited at least for the classical species. As emphasized above, they circumvent their precarious condition in the environment by being released in numbers so high that make contagion highly probable. From this perspective, the coincidences discussed here are unlikely to be accidental. If our hypothesis is proven true, the identification of erythritol, lactate, glycerol and glutamate as effective substrates for *Brucella* growth *in vitro* would be more than a mere coincidence as it would reflect metabolic preferences suitable for a pathogen that relies on genital tropism to close its biological cycle. These bacteria have been described as "stealthy" because of their ability not to be detected effectively by innate immunity. Could we also consider them as "gourmet" or "greedy" to describe a key step of their behavior in their hosts?

AUTHOR CONTRIBUTIONS

JJL, TB, IM, AZR, XDB, and JG had discussion about the content and corrected the paper. JJL and IM wrote the paper.

ACKNOWLEDGMENTS

This work was supported by grants from the Communauté Française de Belgique (Action de Recherches Concertées 08/13–015) and by the Interuniversity Attraction Poles Programme initiated by the Belgian Science Policy Office. Research at the Department of Microbiology and Parasitology of the University of Navarra is supported by The Institute for Tropical Health and by MINECO grant AGL2014-58795-CA.

REFERENCES

- Alexander, B., Schnurrenberger, P. R., and Brown, R. R. (1981). Numbers of *Brucella abortus* in the placenta, umbilicus and fetal fluid of two naturally infected cows. *Vet. Rec.* 108:500. doi: 10.1136/vr.108.23.500
- Alexander, D. P., Huggett, A. S., Nixon, D. A., and Widdas, W. F. (1955). The placental transfer of sugars in the sheep: the influence of concentration gradient upon the rates of hexose formation as shown in umbilical perfusion of the placenta. *J. Physiol.* 129, 367–383. doi: 10.1113/jphysiol.1955.sp005360
- Anderson, T. D., Meador, V. P., and Cheville, N. F. (1986). Pathogenesis of placentitis in the goat inoculated with *Brucella abortus*. I. Gross and histologic lesions. *Vet. Pathol.* 23, 219–226. doi: 10.1177/030098588602300301
- Atluri, V. L., Xavier, M. N., de Jong, M. F., den Hartigh, A. B., and Tsois, R. M. (2011). Interactions of the human pathogenic *Brucella* species with their hosts. *Annu. Rev. Microbiol.* 65, 523–541. doi: 10.1146/annurev-micro-090110-102905
- Battaglia, F. C., and Meschia, G. (1978). Principal substrates of fetal metabolism. *Physiol. Rev.* 58, 499–527.
- Blasco, J. M. (1997). A review of the use of *B. melitensis* Rev 1 vaccine in adult sheep and goats. *Prev. Vet. Med.* 31, 275–283. doi: 10.1016/S0167-5877(96)01110-5
- Britton, H. G. (1962). Some non-reducing carbohydrates in animal tissues and fluids. *Biochem. J.* 85, 402–407. doi: 10.1042/bj0850402
- Burkhardt, S., Jiménez de Bagüés, M. P., Liautard, J.-P., and Köhler, S. (2005). Analysis of the behavior of eryC mutants of *Brucella suis* attenuated in macrophages. *Infect. Immun.* 73, 6782–6790. doi: 10.1128/IAI.73.10.6782-6790.2005
- Clark, J. B., Graham, E. F., Lewis, B. A., and Smith, F. (1967). D-mannitol, erythritol and glycerol in bovine semen. *J. Reprod. Fertil.* 13, 189–197. doi: 10.1530/jrf.0.0130189
- Corner, L. A. (1983). Three aspects of bovine brucellosis: epidemiology, the role of bulls and vaccines. *New South Wales Vet. Proc.* 19, 47–48.
- Corner, L. A., and Alton, G. G. (1981). Persistence of *Brucella abortus* strain 19 infection in adult cattle vaccinated with reduced doses. *Res. Vet. Sci.* 31, 342–344.
- Crawford, R. P., Adams, L. G., and Williams, J. D. (1987). Relationship of fetal age at conjunctival exposure of pregnant heifers and *Brucella abortus* isolation. *Am. J. Vet. Res.* 48, 755–757.
- Essenberg, R. C., Seshadri, R., Nelson, K., and Paulsen, I. (2002). Sugar metabolism by *Brucellae*. *Vet. Microbiol.* 90, 249–261. doi: 10.1016/S0378-1135(02)00212-2
- Ferrier, D. R. (2013). *Biochemistry*, 6 Edn., ed H. R. A Lippincott (Boca Raton, FL: CRC Press; Taylor & Francis Group) 33487–2742.
- Filippini, A., Riccioli, A., Padula, F., and Lauretti, P. (2001). Immunology and immunopathology of the male genital tract: control and impairment of immune privilege in the testis and in semen. *Hum. Reprod.* 7, 444–449. doi: 10.1093/humupd/7.5.444
- Frenette, G. (2006). Polyol pathway in human epididymis and semen. *J. Androl.* 27, 233–239. doi: 10.2164/jandrol.05108
- Frenette, G., Lessard, C., and Sullivan, R. (2004). Polyol pathway along the bovine epididymis. *Mol. Reprod. Dev.* 69, 448–456. doi: 10.1002/mrd.20170
- Gerhardt, P. (1958). The nutrition of brucellae. *Bacteriol. Rev.* 22, 81–98.
- Gerhardt, P., and Wilson, J. B. (1948). The nutrition of brucellae: growth in simple chemically defined media. *J. Bacteriol.* 56, 17–24.
- Gerhardt, P., Tucker, L. A., and Wilson, J. B. (1950). The nutrition of *Brucellae*: utilization of single amino acids for growth. *J. Bacteriol.* 59, 777–782.
- Goldberg, E., Eddy, E. M., Duan, C., and Odet, F. (2010). LDHC: the ultimate testis-specific gene. *J. Androl.* 31, 86–94. doi: 10.2164/jandrol.109.008367
- Hästein, T., and Velle, W. (1968). Placental aldose reductase activity and foetal blood fructose during bovine pregnancy. *J. Reprod. Fertil.* 15, 47–52. doi: 10.1530/jrf.0.0150047
- Hayman, S., and Kinoshita, J. H. (1965). Isolation and properties of lens aldose reductase. *J. Biol. Chem.* 240, 877–882.
- Herrera, E. (2002). Lipid metabolism in pregnancy and its consequences in the fetus and newborn. *Endocrine*. doi: 10.1385/ENDO:19:1:43
- Hers, H. G. (1956). The mechanism of the transformation of glucose in fructose in the seminal vesicles. *Biochim. Biophys. Acta* 22, 202–203. doi: 10.1016/0006-3002(56)90247-5
- Huddleson, I., Hardy, A., Debono, J. E., and Giltner, W. (1943). *Brucellosis in Man and Animals*. ed I. F. Huddleson (New York, NY; London: The Commonwealth Fund, Humphrey Milford, Oxford-University Press).
- Jacques, I., Grayon, M., and Verger, J.-M. (2007). Oxidative metabolic profiles of *Brucella* strains isolated from marine mammals: contribution to their species classification. *FEMS Microbiol. Lett.* 270, 245–249. doi: 10.1111/j.1574-6968.2007.00675.x
- Jauniaux, E., Hempstock, J., Teng, C., Battaglia, F. C., and Burton, G. (2005). Polyol concentrations in the fluid compartments of the human conceptus during the first trimester of pregnancy: maintenance of redox potential in a low oxygen environment. *J. Clin. Endocrinol. Metab.* 90, 1171–1115. doi: 10.1210/jc.2004-1513
- Keil, M., Wetterauer, U., and Heite, H. J. (1979). Glutamic acid concentration in human semen—its origin and significance. *Andrologia* 11, 385–391. doi: 10.1111/j.1439-0272.1979.tb02224.x
- Keppie, J., Williams, A., Witt, K., and Smith, H. (1965). The role of erythritol in the tissue localization of the brucellae. *Br. J. Exp. Pathol.* 46, 104–108.
- Kim, J., Song, G., Wu, G., and Bazer, F. W. (2012). Functional roles of fructose. *Proc. Natl. Acad. Sci. U.S.A.* 109, E1619–E1628. doi: 10.1073/pnas.1204298109
- Larose, J., Laflamme, J., Côté, I., Lapointe, J., Frenette, G., Sullivan, R., et al. (2012). The polyol pathway in the bovine oviduct. *Mol. Reprod. Dev.* 79, 603–612. doi: 10.1002/mrd.22067
- Lowrie, D. B., and Kennedy, J. F. (2001). Erythritol and threitol in canine placenta: possible implication in canine brucellosis. *FEBS Lett.* 23, 69–72. doi: 10.1016/0014-5793(72)80287-4
- McCullough, W. G., and Beal, G. A. (1951). Growth and manometric studies on carbohydrate utilization of *Brucella*. *J. Infect. Dis.* 89, 266–271. doi: 10.1093/infdis/89.3.266
- McDermott, J., Grace, D., and Zinsstag, J. (2013). Economics of brucellosis impact and control in low-income countries. *Rev. Off. Int. Epizoot.* 32, 249–261. doi: 10.20506/rst.32.1.2197
- Moreno, E., and Moriyón, I. (2002). *Brucella melitensis*: a nasty bug with hidden credentials for virulence. *Proc. Natl. Acad. Sci. U.S.A.* 99, 1–3. doi: 10.1073/pnas.022622699
- Moreno, E., and Moriyón, I. (2006). *The Prokaryotes*. eds M. Dworkin, S. Falkow, E. Rosenberg, K.-H. Schleifer, and E. Stackebrandt (New York, NY: Springer).
- Nicoletti, P. (1976). A preliminary report on the efficacy of adult cattle vaccination using Strain 19 in selected dairy herds in Florida. *Proc. Annu. Meet. U.S. Anim. Health Assoc.* 80, 91–106.
- Palacin, M., Lasunción, M. A., and Herrera, E. (1987). Lactate production and absence of gluconeogenesis from placental transferred substrates in fetuses from fed and 48-H starved rats. *Pediatr. Res.* 22, 6–10. doi: 10.1203/00006450-198707000-00002
- Pearce, J., Williams, A., Harris-Smith, P. W., Fitzgeorge, R., and Smith, H. (1962). The chemical basis of the virulence of *Brucella abortus*: II. Erythritol, a constituent of bovine foetal fluids which stimulates the growth of br. abortus in bovine phagocytes. *Br. J. Exp. Pathol.* 43, 1–7.
- Père, M.-C. (2003). Materno-foetal exchanges and utilisation of nutrients by the foetus: comparison between species. *Reprod. Nutr. Dev.* 43, 1–15. doi: 10.1051/rnd:2003002
- Plommet, M. (1991). Minimal Requirements for Growth of *Brucella suis* and Other *Brucella* Species. *Zentralblatt für Bakteriologie* 275, 436–450. doi: 10.1016/S0934-8840(11)80165-9
- Poester, F. P., Samartino, L. E., and Santos, R. L. (2013). Pathogenesis and pathobiology of brucellosis in livestock. *Rev. Off. Int. Epizoot.* 32, 105–115. doi: 10.20506/rst.32.1.2193
- Prunedu, A., Pinart, E., Bonet, S., Yeung, C.-H., and Cooper, T. G. (2006). Study of the polyol pathway in the porcine epididymis. *Mol. Reprod. Dev.* 73, 859–865. doi: 10.1002/mrd.20481
- Queipo-Ortuño, M. I., Colmenero, J. D., Muñoz, N., Baeza, G., Clavijo, E., and Morata, P. (2006). Rapid diagnosis of brucella epididymo-orchitis by real-time polymerase chain reaction assay in urine samples. *J. Urol.* 176, 2290–2293. doi: 10.1016/j.juro.2006.07.052
- Reitzer, L. J., Wice, B. M., and Kennel, D. (1979). Evidence that glutamine, not sugar, is the major energy source. *J. Biol. Chem.* 254, 2669–2676.
- Rest, R. F. (1975). Characterization of the electron transport system in *Brucella abortus*. *J. Bacteriol.* 122, 139–144.
- Ronneau, S., Moussa, S., Barbier, T., Conde-Alvarez, R., Zúñiga-Ripa, A., Moriyón, I., et al. (2014). *Brucella*, nitrogen and virulence. *Crit. Rev. Microbiol.* 42, 1–19. doi: 10.3109/1040841X.2014.962480

- Samartino, L. E., and Enright, F. M. (1992). Interaction of bovine chorioallantoic membrane explants with three strains of *Brucella abortus*. *Am. J. Vet. Res.* 53, 359–363.
- Samartino, L. E., Traux, R. E., and Enright, F. M. (1994). Invasion and replication of *Brucella abortus* in three different trophoblastic cell lines. *Zentralblatt Veterinarmedizin Reihe B.* 41, 229–236. doi: 10.1111/j.1439-0450.1994.tb00223.x
- Setchell, B. P., Hinks, N. T., Voglmayr, J. K., and Scott, T. W. (1967). Amino acids in ram testicular fluid and semen and their metabolism by spermatozoa. *Biochem. J.* 105, 1061–1065. doi: 10.1042/bj1051061
- Smith, H., Williams, A. E., Pearce, J. H., Keppie, J., Harris-Smith, P. W., Fitz-George, R. B., et al. (1962). Foetal erythritol: a cause of the localization of *Brucella abortus* in bovine contagious abortion. *Nature* 193, 47–49. doi: 10.1038/193047a0
- Verger, J.-M., and Grayon, M. (1977). Oxidative metabolic profiles of “*Brucella*” species. *Ann. Sclavo.* 19, 46–60.
- Vitry, M. A., Hanot Mambres, D., Deghelt, M., Hack, K., Machelart, A., Lhomme, F., et al. (2014). *Brucella melitensis* invades murine erythrocytes during infection. *Infect. Immun.* 82, 3927–3938. doi: 10.1128/IAI.01779-14
- Warning, J. C., McCracken, S. A., and Morris, J. M. (2011). A balancing act: mechanisms by which the fetus avoids rejection by the maternal immune system. *Reproduction* 141, 715–724. doi: 10.1530/REP-10-0360
- Wu, X., Xie, C., Zhang, Y., Fan, Z., Yin, Y., and Blachier, F. (2015). Glutamate-glutamine cycle and exchange in the placenta-fetus unit during late pregnancy. *Amino Acids* 47, 45–53. doi: 10.1007/s00726-014-1861-5
- Zheludkov, M. M., and Tsirelson, L. E. (2010). Reservoirs of *Brucella* infection in nature. *Biol. Bull. Russ. Acad. Sci.* 37, 709–715. doi: 10.1134/S106235901007006X
- Zúñiga-Ripa, A., Barbier, T., Conde-Alvarez, R., Martínez-Gómez, E., Palacios-Chaves, L., Gil-Ramírez, Y., et al. (2014). *Brucella abortus* depends on pyruvate phosphate dikinase and malic enzyme but not on Fbp and GlpX fructose-1,6-bisphosphatases for full virulence in laboratory models. *J. Bacteriol.* 196, 3045–3057. doi: 10.1128/JB.01663-14

Conflict of Interest Statement: The authors declare that the research was conducted in the absence of any commercial or financial relationships that could be construed as a potential conflict of interest.

Copyright © 2017 Letesson, Barbier, Zúñiga-Ripa, Godfroid, De Bolle and Moriyón. This is an open-access article distributed under the terms of the Creative Commons Attribution License (CC BY). The use, distribution or reproduction in other forums is permitted, provided the original author(s) or licensor are credited and that the original publication in this journal is cited, in accordance with accepted academic practice. No use, distribution or reproduction is permitted which does not comply with these terms.



Erythritol Availability in Bovine, Murine and Human Models Highlights a Potential Role for the Host Aldose Reductase during *Brucella* Infection

Thibault Barbier¹, Arnaud Machelart¹, Amaia Zúñiga-Ripa², Hubert Plovier¹, Charlotte Hougardy¹, Elodie Lobet¹, Kevin Willemart¹, Eric Muraille³, Xavier De Bolle¹, Emile Van Schaftingen⁴, Ignacio Moriyón² and Jean-Jacques Letesson^{1*}

¹ Research Unit in Biology of Microorganisms, Department of Veterinary Medicine, University of Namur, Namur, Belgium,

² Departamento de Microbiología y Parasitología, Instituto de Salud Tropical, Instituto de Investigación Sanitaria de Navarra, Universidad de Navarra, Pamplona, Spain, ³ Laboratoire de Parasitologie, Faculté de Médecine, Université Libre de Bruxelles, Brussels, Belgium, ⁴ WELBIO and de Duve Institute, Université Catholique de Louvain, Brussels, Belgium

OPEN ACCESS

Edited by:

Axel Cloeckaert,
Institut National de la Recherche
Agronomique (INRA), France

Reviewed by:

Alessandra Occhialini,
Université de Montpellier, France
Roy Martin Roop II,
East Carolina University, United States
Renee M. Tsois,
University of California, Davis,
United States

*Correspondence:

Jean-Jacques Letesson
jean-jacques.letesson@fundp.ac.be

Specialty section:

This article was submitted to
Infectious Diseases,
a section of the journal
Frontiers in Microbiology

Received: 20 April 2017

Accepted: 30 May 2017

Published: 13 June 2017

Citation:

Barbier T, Machelart A,
Zúñiga-Ripa A, Plovier H,
Hougardy C, Lobet E, Willemart K,
Muraille E, De Bolle X,
Van Schaftingen E, Moriyón I and
Letesson J-J (2017) Erythritol
Availability in Bovine, Murine
and Human Models Highlights
a Potential Role for the Host Aldose
Reductase during *Brucella* Infection.
Front. Microbiol. 8:1088.
doi: 10.3389/fmicb.2017.01088

Erythritol is the preferential carbon source for most brucellae, a group of facultative intracellular bacteria that cause a worldwide zoonosis. Since this polyol is abundant in genital organs of ruminants and swine, it is widely accepted that erythritol accounts at least in part for the characteristic genital tropism of brucellae. Nevertheless, proof of erythritol availability and essentiality during *Brucella* intracellular multiplication has remained elusive. To investigate this relationship, we compared Δ eryH (erythritol-sensitive and thus predicted to be attenuated if erythritol is present), Δ eryA (erythritol-tolerant but showing reduced growth if erythritol is a crucial nutrient) and wild type *B. abortus* in various infection models. This reporting system indicated that erythritol was available but not required for *B. abortus* multiplication in bovine trophoblasts. However, mice and humans have been considered to lack erythritol, and we found that it was available but not required for *B. abortus* multiplication in human and murine trophoblastic and macrophage-like cells, and in mouse spleen and conceptus (fetus, placenta and envelopes). Using this animal model, we found that *B. abortus* infected cells and tissues contained aldose reductase, an enzyme that can account for the production of erythritol from pentose cycle precursors.

Keywords: *Brucella*, erythritol, aldose reductase, murine model, bovine trophoblast, human trophoblast, pentose phosphate cycle, polyol pathway

INTRODUCTION

To survive and multiply any pathogen must harvest nutrients and consequently adapt to the carbon, energy and nitrogen sources that are available in the host. Pathogenesis is therefore not only a matter of virulence determinants, metabolism also enables virulence (de Lorenzo, 2014; Nataro, 2015). In this context, a paradigm of the correlation between metabolism and pathogenicity has been the preferential use of erythritol by the brucellae (McCullough and Beal, 1951; Smith et al., 1962), a group of facultative intracellular bacteria that cause brucellosis, a worldwide extended

zoonosis (Zinsstag et al., 2011). A relevant part of the symptomatology of this disease is related to the particular tropism of the pathogen for the reproductive tract of ungulates and swine, which results in orchitis, epididymitis, abortion and infertility (Moreno and Moriyón, 2006). Massive intratrophoblastic colonization occurs in brucellosis by *B. abortus* in cows, *B. melitensis* in goats and sheep, *B. ovis* in sheep, *B. suis* in sows and *B. canis* in bitches (reviewed in Anderson et al., 1986b), and the infection of trophoblasts is a key step in the loss of integrity of the placenta that leads to abortion (Samartino and Enright, 1993) and subsequent dissemination. These events are critical in the biology of *Brucella* as these bacteria do not survive long in the environment and are transmitted mostly by contact with aborted tissues and fluids as well as venereally and congenitally (Moreno and Moriyón, 2006). Although not detected in early studies, more recent literature from endemic areas report a correlation between adverse pregnancy outcomes and *Brucella* infection (Khan et al., 2001; Karcaaltincaba et al., 2010; Al-Tawfiq and Memish, 2013; Vilchez et al., 2015), and epididymo-orchitis occurs in up to 20% of infected males (Navarro-Martinez et al., 2001).

The reasons for the preferential colonization of reproductive organs by the brucellae are not fully understood, and they may involve nutritional, immune, and hormonal factors (Samartino and Enright, 1993; Letesson et al., 2017). One of the molecular bases that is proposed to account, at least partially, for this tropism is the existence of erythritol in the target organs of ungulates (Smith et al., 1962). Present in substantial amounts in fetal fluids, placenta, seminal vesicles and semen of several ungulate species (Smith et al., 1962; Keppie et al., 1965; Clark et al., 1967), this four carbon polyol promotes *Brucella* growth at low concentrations and is also a preferred carbon source (McCullough and Beal, 1951; Smith et al., 1962). Bovine fetal tissues that were obtained from 6 to 7 months pregnant cattle (the time after which *Brucella* abortion often occurs) (Williams et al., 1962) and chorioallantoic membrane explants (Enright and Samartino, 1994) have been described to produce high amounts of erythritol. Nevertheless, other observations are not consistent with erythritol being the only factor in *Brucella* localization *in vivo*. First, although *B. ovis* and *B. canis* are unable to catabolize erythritol, they cause genital infections and abortion in sheep and dogs, respectively (Blasco, 1990; Carmichael, 1990). Second, vaccine *B. abortus* S19 is inhibited by erythritol (Jones et al., 1965) (see also below) and can cause genital infections and abortion in cattle. Third, high erythritol concentrations are not found in human or rodents (Keppie et al., 1965), hosts in whose reproductive tracts *Brucella* can localize and even multiply in cognate trophoblastic cell lines (Bosseray, 1980, 1983; Tobias et al., 1993; Kim et al., 2005; Salcedo et al., 2013). This last evidence, however, may need to be reinterpreted because *B. suis* mutants *eryB* and *eryC* (see below), which cannot catabolize erythritol, are attenuated in human macrophage-like THP-1 cells, murine J774 cells and BALB/C mice (Köhler et al., 2002; Burkhardt et al., 2005). As discussed below, the phenotype of these mutants suggests the presence of erythritol in these cells in amounts that are high enough to effect on *Brucella* multiplication.

The attenuation observed for some *ery* mutants has been attributed to the strong growth inhibition caused by erythritol that can be observed *in vitro* (Burkhardt et al., 2005). This bacteriostatic effect was identified very early as one of the markers of vaccine *B. abortus* S19 (Jones et al., 1965) and it was traced to an interrupted assimilation pathway (see below) (Sperry and Robertson, 1975). The mechanism of erythritol catabolism has been recently revised (Barbier et al., 2014) and proceeds through a five step pathway (Figure 1A). The first step, catalyzed by the EryA kinase, is an ATP-dependent phosphorylation that, while highly efficient, becomes futile when the downstream pathway is interrupted (i.e., when either EryB, EryC, EryH or EryI are not functional), as occurs in *B. abortus* S19. The consequence is that the ATP that was invested cannot be recovered and becomes depleted, hence the observed growth inhibition (Sperry and Robertson, 1975). This “toxicity” phenotype has prevented the carrying out of mutant-based analyses to investigate whether erythritol is actually used during infection and to what extent it contributes to *Brucella* multiplication during infection.

To clarify these issues, we exploited the phenotypes caused by mutations in different steps of the erythritol pathway as a reporting system. This system was based on a comparison of *B. abortus* 2308 wild type (WT) and mutants *eryA* (erythritol kinase) and *eryH* (isomerase; blocked in D-3-tetrol-4-P/D-erythrulose-4-P conversion) (Figure 1A). As discussed above, the erythritol kinase mutant is erythritol-tolerant but, since it cannot metabolize erythritol, it should be attenuated if erythritol is a crucially needed nutrient (i.e., a major or even the only C source) in the replicative niche. However, the *eryH* mutant is predicted to be erythritol-sensitive, and therefore, it should be attenuated if erythritol is present. Using this reporting system, we found that erythritol was available but not required for *B. abortus* multiplication in bovine trophoblastic cells and, notably, also in human trophoblastic cells, in murine and human macrophage-like cells and in the spleen and conceptus of mice. These results led us to hypothesize that there should be a source of erythritol in tissues of mammals other than ungulates, and we present evidence for the involvement of the host aldose reductase (AR), an enzyme in the polyol pathway that can catalyze the synthesis of a plethora of polyols including erythritol.

RESULTS

B. abortus 2308 Δ *eryA* and Δ *eryH* Mutants Are Erythritol-Tolerant and Sensitive, Respectively

We first constructed the non-polar mutants Δ *eryA* and Δ *eryH* of *B. abortus* 2308. Using a chemically defined medium, we confirmed for Δ *eryH* (Barbier et al., 2014) and demonstrated for Δ *eryA* their inability to grow with erythritol as the sole carbon source (Supplementary Figure S1). We found no growth defect in a rich medium that lacked erythritol (2YT [10% yeast extract, 1% tryptone, 5% NaCl]) (Dozot et al., 2010), a result that makes broader metabolic defects in these mutants unlikely. We made

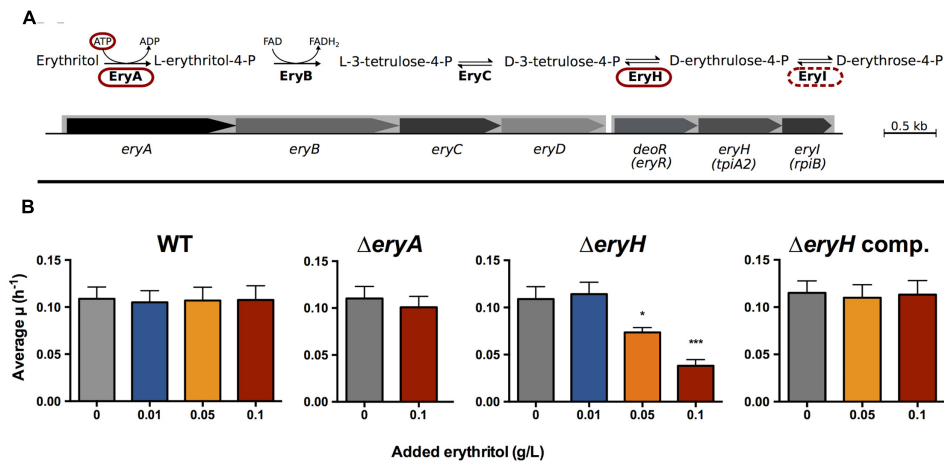


FIGURE 1 | *Brucella abortus* Δ eryA and Δ eryH are erythritol-tolerant and erythritol-sensitive. **(A)** Revised erythritol catabolic pathway (the mutants used in this investigation are circled); **(B)** Growth of *B. abortus* 2308 WT, Δ eryA, Δ eryH and complemented Δ eryH mutants in 2YT medium supplemented with increasing concentrations of erythritol. Values are the average of biological and technical triplicates plus the standard deviation (* $p < 0.05$; *** $p < 0.001$ [Student's *t*-test]).

the same observation using a Δ eryI mutant (not shown), which was as expected.

A critical requirement for using these mutants as reporters of erythritol availability was that Δ eryA and Δ eryH should be erythritol-tolerant and erythritol-sensitive, respectively. To prove these correlation, we grew Δ eryA and Δ eryH in 2YT medium that was supplemented with increasing concentrations of erythritol (**Figure 1B**). Whereas erythritol did not affect the growth of the mutant Δ eryA at the highest concentration tested, it markedly inhibited the growth of the mutant Δ eryH at a concentration as low as 0.05 g/L, which is in the inhibitory range for vaccine S19 (Keppie et al., 1967) and for an *eryC* mutant of *B. suis* 1330 (Burkhardt et al., 2005). Since we could restore the WT phenotype of the Δ eryH mutant by complementation (**Figure 1B**), we concluded that deletion of *eryH* caused both the inability to grow on erythritol and its toxicity. As expected from the activity of EryI (downstream of EryA, **Figure 1A**), the Δ eryI mutant was also inhibited by erythritol (not shown) and, as it phenocopied Δ eryH, below we present only the data obtained with the latter mutant.

Another critical requirement of any reporter system is specificity. To test the specificity, we studied the growth of WT and Δ eryH in 2YT medium supplemented with polyols (0.1 g/L) with structures close to erythritol (**Supplementary Figure S2**) that have been reported in male or pregnant female genital organs (Clark et al., 1967; Brusati et al., 2005; Jauniaux, 2005; Regnault et al., 2010; Larose et al., 2012). Since we did not detect any inhibitory effects for glycerol, ribitol, arabitol, xylitol, sorbitol, mannitol or dulcitol, the toxicity was specific for erythritol.

Erythritol Is Available But Not Essential for *B. abortus* Multiplication in Bovine and Human Trophoblastic Cells

Since brucellae multiply intensively in bovine trophoblasts (Anderson and Cheville, 1986; Anderson et al., 1986a), we tested

our reporting system in a suitable bovine trophoblastic cell line (Samartino et al., 1994). As shown in **Figure 2A**, no differences could be evidenced between the WT and the mutants at 2 h post infection (p.i.), a time when bacteria have not yet reached their replicative niche (Samartino et al., 1994). At later times, Δ eryH (erythritol-sensitive) but not Δ eryA (erythritol-tolerant) failed to multiply at the level of the WT strain. These results are consistent with the availability of erythritol in the replicative niche of *B. abortus* in bovine trophoblasts.

These observations and the recent description that *Brucella* can colonize human trophoblastic cell lines (Salcedo et al., 2013; Fernandez et al., 2016) prompted us to test our reporting system in trophoblastic cells other than those of bovine origin. When we infected human BeWo trophoblastic cells with *B. abortus* 2308 WT, Δ eryA or Δ eryH, we observed that the mutants were indistinguishable from the WT 2 h after infection and that only the multiplication of the erythritol-sensitive mutant Δ eryH was significantly reduced at later times (**Figure 2B**). These observations are in apparent conflict with previous studies that reported only very low erythritol concentrations in human fetal tissues (Keppie et al., 1965; Clark et al., 1967; Amin and Wilshire, 1997). However, results obtained with cell lines do not necessarily reflect the *in vivo* situation and the parallelism with the results in bovine trophoblastic cells indicated that, while not being required for optimal bacterial replication, erythritol should be available in human BeWo cells at a concentration above that which is toxic for the sensitive mutant.

Erythritol Is Available But Not Essential for *B. abortus* Multiplication in RAW 264.7 and THP-1 Macrophage-Like Cells

Macrophages are another cell type in which *Brucella* multiplies extensively. For this reason, RAW 264.7 murine macrophages and THP-1 human macrophage-like cells were infected with the erythritol catabolic mutants (**Figure 3**). Although both were

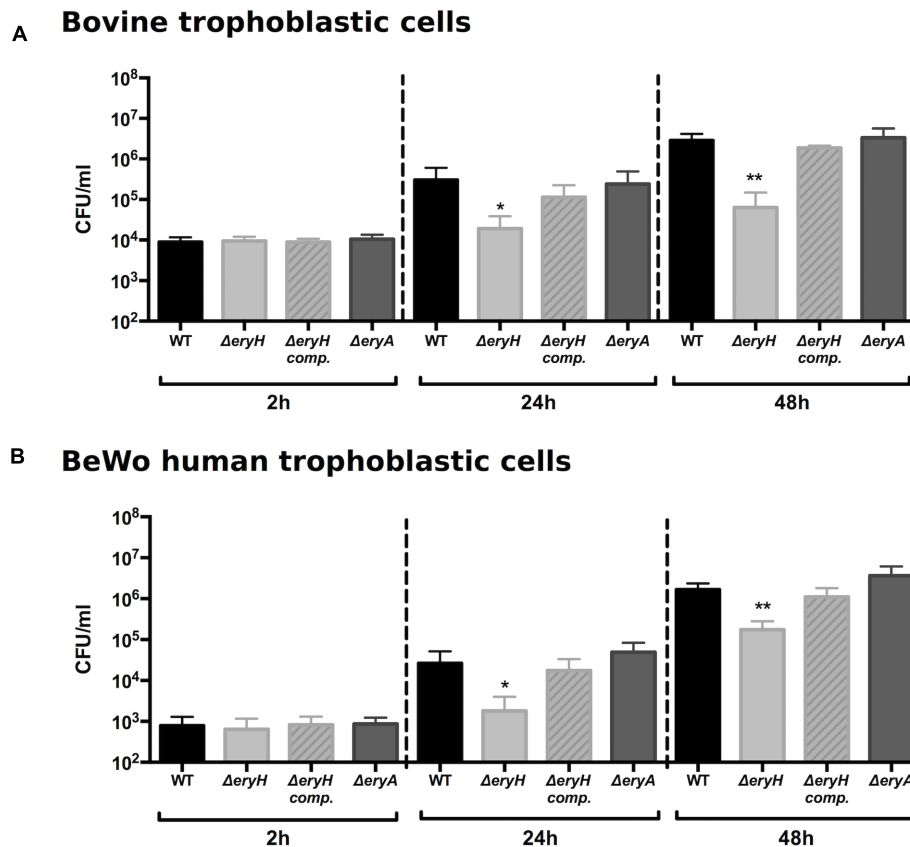


FIGURE 2 | *Brucella abortus* $\Delta eryH$ but not *B. abortus* 2308 $\Delta eryA$ or the complemented *B. abortus* $\Delta eryH$ (*eryH* comp.) are attenuated in bovine (A) and human trophoblastic (B) cells. Values are the average of biological and technical triplicates plus the standard deviation (* $p < 0.05$; ** $p < 0.01$; *** $p < 0.001$ [Student's *t*-test]).

able to invade these cells to the same extent as the WT (i.e., resulted in the same CFU/ml at 2 h p.i.), the erythritol-sensitive mutant was found in lower numbers 24 and 48 h after infection. These results are in agreement with those of Burkhardt et al. (2005) who showed that a *B. suis* 1330 $\Delta eryC$ mutant was erythritol-sensitive and attenuated in macrophages. Indeed, these authors also reported $\Delta eryC$ attenuation in mice and suggested an availability of erythritol *in vivo*.

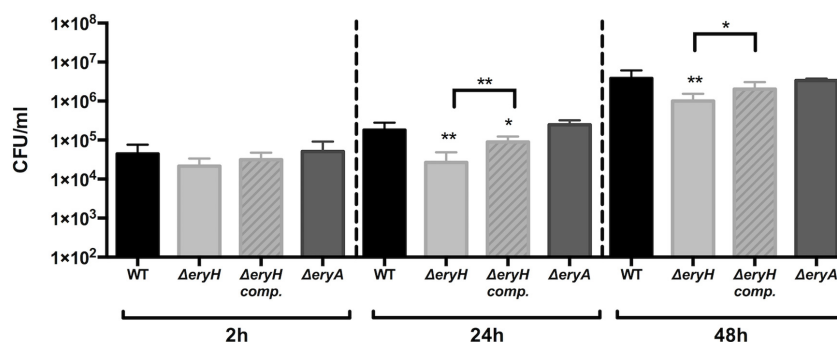
Erythritol Availability and Essentiality Are Time-Dependent in C57BL/6 Mouse Spleens

In C57BL/6 mice that were infected intraperitoneally with either *B. abortus* 2308 WT or the erythritol catabolic mutants, the CFU numbers/spleen of both $\Delta eryA$ and $\Delta eryH$ were significantly lower than those of the WT 3 days after infection (Figure 4). After 9 days, only the erythritol-sensitive mutant showed significantly reduced CFU numbers, and consistent with this, splenomegaly was lower in the corresponding group of mice. Although splenomegaly was reduced in the $\Delta eryH$ -infected group, no differences in the CFU numbers of the mutants were observed 30 days after infection. These results are also in line with those

of Burkhardt et al. (2005) who also found reduced CFU/spleen for the *B. suis* $\Delta eryC$ at early times (7 days or less) but not 28 days after infection. On the other hand, they are only in partial agreement with those of Sangari et al. (1998). These authors found that the CFU/spleen of a *B. abortus* 2308 erythritol sensitive Tn5 mutant and the parental strain were similar 7, 14, and 28 days after infection. The discrepancy is thus limited to the results obtained 7 days after infection but as earlier times were not studied and the CFU/spleen at longer times coincide with the our observations, it seems possible that the differences could relate to the protocols (breed of mice [BalB/c versus C57BL/6], Tn5 polarity effects on regulators downstream and possibly others).

Bearing in mind the properties of the mutants in our reporting system, these results suggest that the availability and importance of erythritol as a carbon source in the spleen of mice changes during the course of infection. During a splenic infection everything including the bacterial load, the type of infected cells, the type of recruited cells, the splenic microarchitecture and the immune environment is evolving in a dynamic way. Therefore, it may be not so surprising that 3 days after infection (that is to say before the peak of splenic infection and before any detectable splenomegaly) *Brucella* is in a compartment where erythritol is available (attenuation of $\Delta eryH$) but also required (attenuation

A THP-1 human monocytic cells



B RAW 264.7 murine macrophages

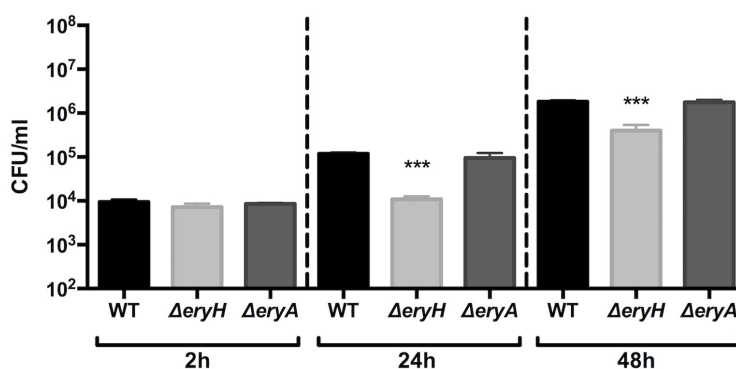


FIGURE 3 | *Brucella abortus* $\Delta eryH$ but not *B. abortus* 2308 $\Delta eryA$ or the complemented *B. abortus* $\Delta eryH$ (*eryH* comp.) are attenuated in human (A) and murine (B) macrophage-like cells. Values are the average plus the standard deviation of three experiments for THP-1 and of one representative replicate for RAW 264.7 (* $p < 0.05$; ** $p < 0.01$; *** $p < 0.001$ [Student's *t*-test]).

of $\Delta eryA$); later on, changes in one or several parameters (i.e., infected cells or immune environment) might lead to a change in the nutrients that are available which makes erythritol, while available (attenuation of $\Delta eryH$) less needed (no attenuation of $\Delta eryA$). Afterward, erythritol availability would progressively dwindle because both mutants reached a WT-like bacterial load at 30 days p.i.

Erythritol Is also Available in the *B. abortus*-Infected Murine Conceptus

The well-known genital tropism of *Brucella* prompted us to investigate erythritol availability in the mouse conceptus. We infected C57BL/6 mice in either early (6 days) or late (14 days) pregnancy with *B. abortus* WT, $\Delta eryA$ and $\Delta eryH$ (Bosseray, 1980). Then, we determined the CFU in fetuses, placenta and fetal envelopes 1 and 9 days p.i., which in both groups corresponds to post-conception day 15. The results (Figure 5) showed a systemic distribution of the three strains in the conceptus with the placenta being the most heavily infected organ, as expected from its barrier function (Bosseray, 1980). For the mice that were infected at day 6 post-conception, only the erythritol-sensitive strain $\Delta eryH$ was present in significantly lower numbers in the

fetus and placenta. When mice were infected late in pregnancy, only $\Delta eryH$ was attenuated, and attenuation was observed in all tissues. These results strongly suggest that erythritol is available but not crucially required for *B. abortus* to multiply in the murine conceptus.

Aldose Reductase Is Expressed in RAW 264.7 Macrophages and Tissues Infected by *B. abortus*

The polyol pathway has been suggested to be involved in the synthesis of erythritol in mammalian tissues (Pearce et al., 1962) and the key enzyme, AR, can catalyze the conversion of erythrose into erythritol (Hayman and Kinoshita, 1965; Kardon et al., 2008). Thus, we examined whether there was a connection between AR and the ability of *Brucella* to multiply in cells and tissues.

First, we studied whether AR is expressed in some of the cells in which our reporting system indicated the presence of erythritol. We found that the enzyme was detectable by immunofluorescence and that AR gene expression was observed in uninfected RAW 264.7 macrophages that were cultured in standard media; no noticeable changes were noted when

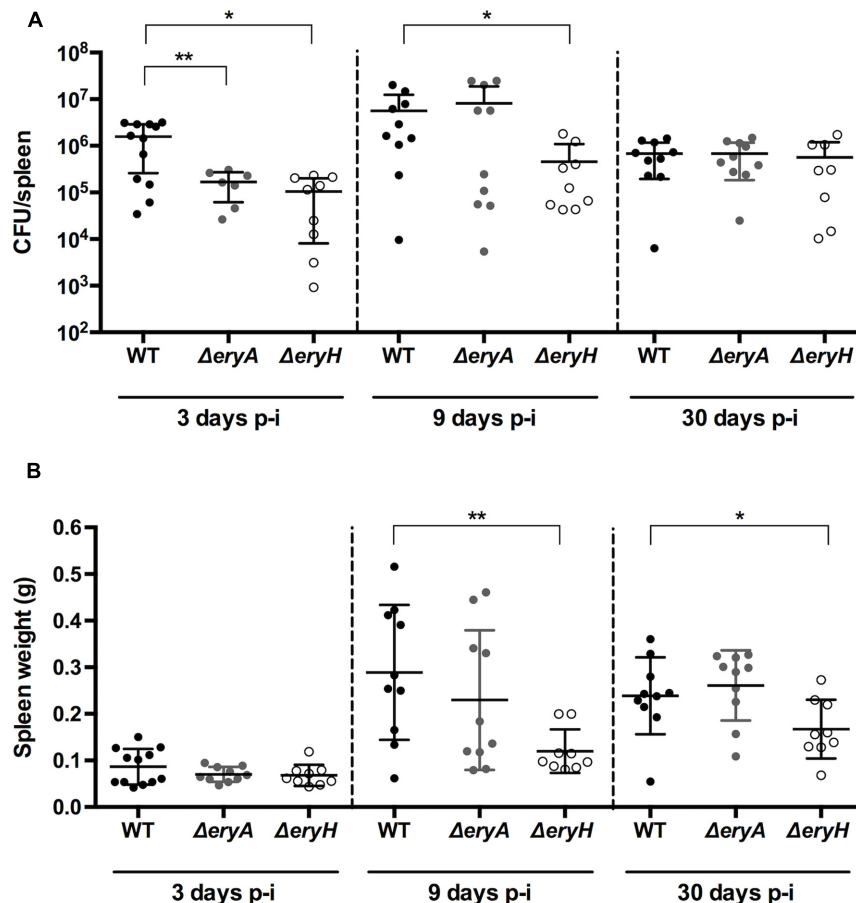


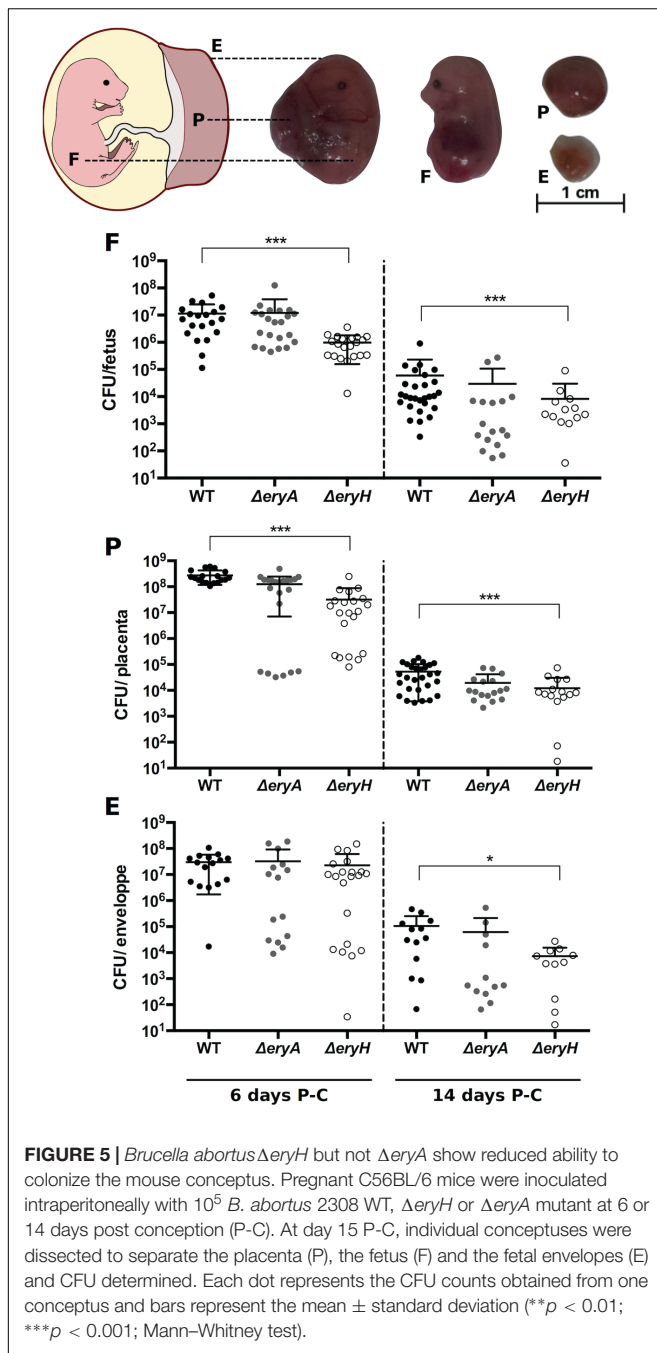
FIGURE 4 | The *B. abortus* erythritol catabolic mutants Δ eryA and Δ eryH are attenuated in C57BL/6 mice. Mice were infected with 5×10^4 CFU, and CFU in the spleen (**A**) and spleen weights (**B**) determined at the indicated intervals. Each dot represents the CFU counts of one individual mouse, and bars the mean \pm standard deviation (* $p < 0.01$; ** $p < 0.001$; Mann-Whitney test).

these cells were infected by *Brucella* (data not shown). Since AR is induced by hyperglycemia (≥ 20 mM glucose; 5 mM being normoglycemic) (González et al., 1984; Tawata et al., 1992) and the DMEM-HG culture medium contains 25 mM glucose, we also measured the dependence of the expression of gene *Akr1b3* (which codes for mouse AR) on glucose as an indirect and complementary test for AR activity. In RAW 264.7 macrophages that were grown in a range (2.8 [0.5 g/L], 5.6 [1.0 g/L] and 25 mM [4.5 g/L]) of glucose concentrations, we found that expression of *Akr1b3* was modulated by glucose (Figure 6A), a result that strongly suggests that AR is active in these cells in culture. Although the glucose concentration did not affect the multiplication of the Δ eryH mutant during the first 2 h after infection, its inhibition was significant at 24 and 48 h (Figure 6B) suggesting that erythritol is available in cells that are grown in the range of physiological glucose concentrations that induce AR gene expression.

Second, we examined the AR and bacterial distributions in the conceptuses of mice that were infected intraperitoneally with

B. abortus 2308-mCherry at 6 days post conception. Bacteria and AR-positive cells were located preferentially in the junctional zone of the placenta just underneath the decidua basalis and in a cellular sheet surrounding the fetus apposed on the internal face of the distended decidua parietalis (Figure 7A). Infected cells were positive for cytokeratin 7 (Figures 7B,C) and thus trophoblastic in nature (Croy et al., 2013), probably being trophoblastic giant cells (Kim et al., 2005). As expected, some infected trophoblasts were also scattered in the decidua after mid-gestation (Hu and Cross, 2010). Bacteria were found almost exclusively in AR-positive cells (Figure 8).

Finally, we investigated mouse spleens 9 days after infection, a time at which the erythritol-sensitive strain Δ eryH showed attenuation. We found intense AR-staining in the red pulp (Supplementary Figure S3), with small clusters of CD11b-positive cells [often iNOS positive and corresponding to granulomas (Copin et al., 2012)], which are frequently associated with AR. In contrast, we hardly detected AR in spleens of non-infected mice; when we did, AR was mostly restricted to scattered CD11b-negative cells in the red pulp.



DISCUSSION

In this work, we set up and validated a reporting system to detect the presence and catabolism of erythritol in the *Brucella* replicative niche, and this system demonstrated the availability of this polyol in infection models of bovine, human and murine origin, extending previous research in macrophages and mice (Burkhardt et al., 2005) to trophoblastic cell lines. Indeed, because erythritol is present in comparatively large amounts in the placenta and genital tissues of ruminants and swine and because *Brucella* is

found inside trophoblastic cells of ruminants and uses erythritol very efficiently, it has been widely assumed that trophoblasts produce erythritol. However, most evidence is limited to extracts of fetal allantoic and amniotic fluids, cotyledons, whole placenta, seminal vesicles and testis (Smith et al., 1962; Williams et al., 1962; Clark et al., 1967), and to the best of our knowledge, only one work has reported the presence of erythritol in trophoblasts of bovine origin (Enright and Samartino, 1994). Our work confirms this pattern and provides the first experimental data that support the presence of erythritol in human and murine trophoblastic cells. In addition, we demonstrate for the first time that the catabolism of erythritol is not essential to the infectious processes in these infection models.

The fact that bovine and human trophoblastic cells and murine models give similar results contrasts with the low erythritol concentrations that were reported in fetal fluids of humans and mice (approximately 60 μ g/ml in cows and less than 2 μ g/ml in humans or mice) (Keppie et al., 1965; Amin and Wilsmore, 1997). Based on our *in vitro* toxicity assays in 2YT, it can be speculated that erythritol concentration should reach 50–100 μ g/ml to result in Δ eryH attenuation during infection. If correct, these differences in erythritol measurements in fetal fluids could reflect the particular composition of the *Brucella* replicative niche during infection. It is apparently puzzling that, although our reporting system shows that erythritol is catabolized “*in vivo*,” it also shows that erythritol is not an essential carbon source, indicating a complex nutritional situation in the replicative niche where erythritol, but also alternative C sources, should be available in various and evolving proportions based on the time of infection, the type of cell infected and other variables. A possible explanation for this situation could be the presence of an active polyol pathway because this pathway (which depends on AR; see below) can supply not only erythritol but also other polyols such as glycerol, arabitol, mannitol and inositol that are in fact found in fetal tissues and reproductive systems of several *Brucella* hosts (Jauniaux, 2005). These polyols, erythritol included, may not be critical individually but could be alternative carbon sources. Of course, a definite answer needs specific investigations carried out in the natural host species, not only with *B. abortus*, *B. melitensis* and *B. suis* but also with *B. ovis* and *B. canis*, the two classical species not stimulated by erythritol.

Since our reporting system showed erythritol in cells in which its presence has not been described, we looked for possible biosynthetic mechanisms in mammal tissues. Over 50 years ago, Pearce et al. (1962) proposed that erythritol “*may arise from D-erythrose [. . .] as an intermediate between D-erythrose and D-erythrulose as sorbitol acts as an intermediate between glucose and fructose.*” The enzyme responsible for the conversion of glucose to sorbitol is the aldose reductase (AR, AKR1B1 in human and bovines, AKR1B3 in mice) of the polyol pathway, which oxidizes sorbitol to fructose. Thus, we investigated the presence of AR in cells and tissues where *B. abortus* multiplied and where the presence of erythritol

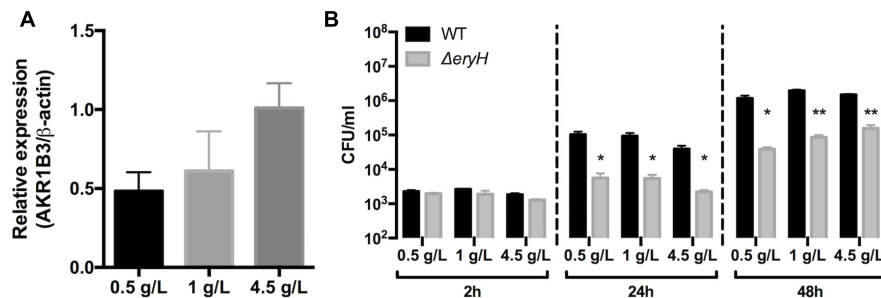


FIGURE 6 | The expression of Aldose reductase gene *Akr1b3* in RAW 264.7 macrophages depends on glucose concentration. **(A)** Expression of gene *Akr1b3* measured by qRT-PCR in macrophages cultured with 0.5, 1, and 4.5 g/L of glucose. **(B)** Multiplication of *B. abortus* 2308 WT and $\Delta eryH$ in macrophages cultured with 0.5, 1, and 4.5 g/L of glucose. All experiments were performed in biological and technical duplicates ($*p < 0.05$; $**p < 0.01$; $***p < 0.001$ [Student's *t*-test]).

was detected. We found that AR was present in RAW 264.7 macrophages independently of an infection, that 9 days after infection there was a sharp increase in AR in the splenic red pulp where clusters of CD11b⁺ (indicative of *Brucella*-induced granulomas) cells co-localized with AR and that AR and *B. abortus* co-localized in the infected murine conceptus. There is abundant indirect evidence that this coexistence of AR and brucellae in the laboratory models parallels the situation in the natural hosts. Actually, tissues characteristically targeted by brucellae such as the placenta of cows, sheep and pigs, and the epididymis, seminal fluids and oviduct of pigs, cattle and some rodents, which are among those tissues whose fructose concentrations are high or are predominant over glucose, contain abundant amount of AR (Clark et al., 1967; Frenette, 2006; Pruneda et al., 2006). Moreover, AR (AKR1B1) has also been recently identified by proteomics as differentially produced in bovine chorioallantoic membranes that were infected by *Brucella* (Mol et al., 2016). Indeed, AR can reduce a broad range of aldehydes to their corresponding alcohols (Håstein and Velle, 1968) and significantly its affinity is far higher for erythrose than for glucose (Hayman and Kinoshita, 1965; Kardon et al., 2008). Furthermore, a role of AR in erythritol generation in these tissues is consistent with the fact that the pentose phosphate pathway, which can supply D-erythrose, is active in testes, ovaries and placenta (Ferrier, 2013). Although further research is necessary, all these indirect evidences together with the data presented here, lend support to the hypothesis that AR accounts for erythritol production in cells that have been invaded by brucellae, as well as for the apparently puzzling observation that erythritol is not essential for *Brucella* multiplication. In preliminary experiments, we have found that treatment of murine macrophages with the potent AR inhibitor Sulindac (Ratcliff et al., 1999) impairs *B. abortus* 2308 intracellular multiplication, an observation that is also consistent with our hypothesis. It is also worth commenting that AR is a moonlighting protein that in addition to its function in the polyol pathway, has been linked to inflammation regulation (Ramana and Srivastava, 2010) and is involved in the hormonal regulation of pregnancy and parturition. Some AR are, as a matter of fact, involved in progesterone degradation and are also the main human, murine and bovine prostaglandin

F2 α (PGF2 α) synthase (Madore et al., 2003; Kabututu et al., 2008; Bresson et al., 2011, 2012). It is thus tempting to hypothesize that AR could represent an actor in the context of *Brucella*-host interaction at the crossroad of metabolism, inflammation and abortion, a possibility that deserves further investigation.

MATERIALS AND METHODS

Bacterial Strains and Culture Conditions

Escherichia coli DH10B were grown in LB medium. *B. abortus* 2308 NaI^R and derived strains were grown at 37°C in rich medium 2YT (16 g/L bacto tryptone 10 g/L yeast extract and 5 g/L NaCl; BD Difco) or in a chemically defined medium (Barbier et al., 2014) composed of 2.3 g/L K₂HPO₄; 3 g/L KH₂PO₄; 0.1 g/L Na₂S₂O₃; 5 g/L NaCl; 0.2 g/L nicotinic acid; 0.2 g/L thiamine; 0.07 g/L pantothenic acid; 0.5 g/L (NH₄)₂SO₄; 0.01 g/L MgSO₄; 0.1 mg/L MnSO₄; 0.1 mg/L FeSO₄; 0.1 mg/L biotin and 2 g/L of erythritol. Growth was monitored using an automated plate reader (Bioscreen C, Lab Systems) following the OD (600 nm) with continuous shaking at 37°C. The growth rate was calculated as follows: $(\ln(OD_{t2}) - \ln(OD_{t1})) / (t2 - t1)$. The Δt was set for 7 h, i.e., approximately two division times, and incremented over the log phase every 0.5 h (0–7 h; 0.5–7.5 h, ...) resulting in a set of values whose mean is the average growth rate, μ . When required, the medium was supplemented with chloramphenicol (20 mg/ml), nalidixic acid (25 mg/ml), sucrose (5%), agar (15 g/L, BD Difco) and polyols (concentrations annotated in the manuscript). Unless otherwise stated, reagents were purchased from Sigma-Aldrich.

Construction of an mCherry-producing *B. abortus* 2308 strain was performed following the same procedure that was validated for *B. melitensis* (Copin et al., 2012). Construction of the in-frame deletion in *eryA* was done following a previously described strategy (Barbier et al., 2014). Briefly, approximately 750 bp upstream and downstream of BAB2_0372 were amplified by PCR from genomic DNA of *B. abortus* 2308. The obtained PCR

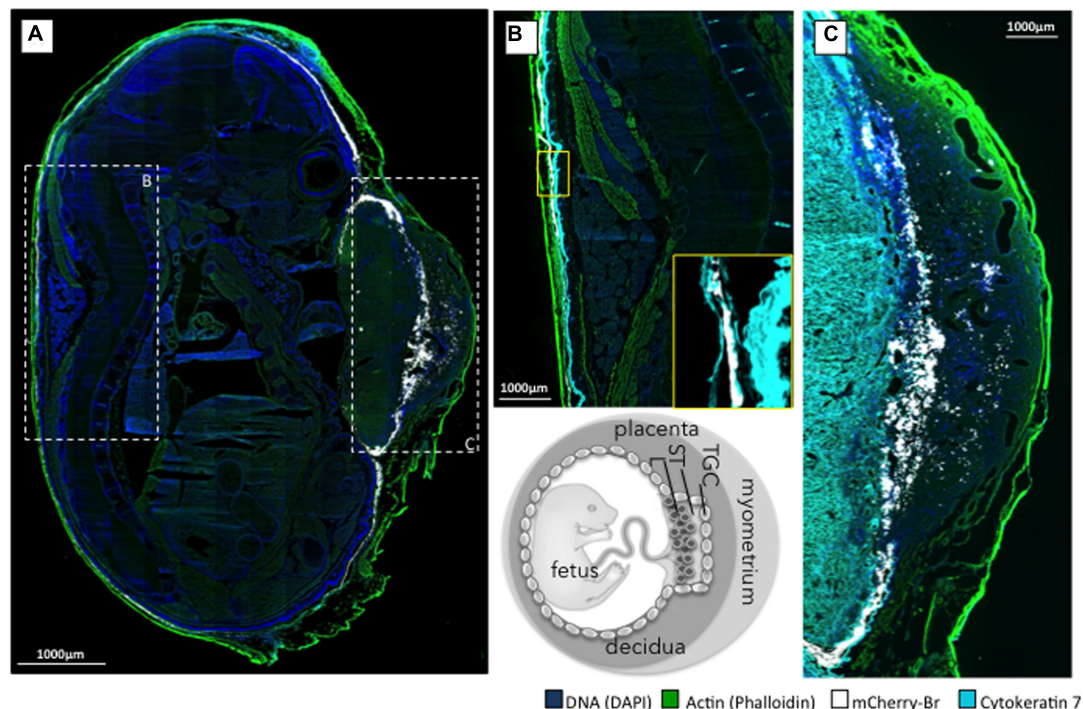


FIGURE 7 | Localization of *B. abortus* 2308 in murine conceptus. Pregnant mice were infected intraperitoneally at 6 days post-conception with 10^5 CFU of *B. abortus* mCherry (white), and the conceptuses were obtained at post-conception day 15. **(A)** Mosaic reconstitution (210 individual images taken at $10\times$ magnification) of a sagittal section of an infected murine conceptus stained for DNA (DAPI/blue) and actin (phalloidin/green); dashed squares B and C circumscribe the prototypal zone corresponding to **(B,C)**. **(B)** Cytokeratine-7 immunostaining (light blue) of trophoblastic cells of the dorsal part of the conceptus with a close up of the infected trophoblastic cells lining the decidua parietalis (yellow square). **(C)** Cytokeratine-7 immunostaining (light blue) of the placenta at the level of the decidua basalis. TGC, trophoblast giant cell; ST, spongiotrophoblast; L, labyrinth.

products were, respectively, flanked by SpeI/BamHI (SpeI_F: 5'-ACTAGTCTTGGCGGAACTTGACTGG-3'; BamHI_R: 5'-ATACGCGGATCCGCGATAACGCATGGCTGACACAGG-3') and BamHI/SphI restriction sites (BamHI_F: 5'-TATCGCGGATCCGCGTATGGCAAATAAGGAAACATTGAATG-3'; SphI_R: 5'-GCATGCGCGCTTGTCGTGGTTCTG-3'). A third PCR joined the two fragments together using primers SpeI_F and SphI_R, which was followed by ligating this product into an EcoRV-digested pGEM plasmid (Promega). After sequence verification (Beckman Coulter Genomics), the ± 1500 bp insert was excised as a SpeI – SphI fragment and cloned into a pNPTS138 suicide vector (Kan^R, Suc^S). The acquisition of this vector by *Brucella* after mating with conjugative S17 *E. coli* was selected by kanamycin and nalidixic acid resistance. The loss of the plasmid concomitant with either a deletion or a return to WT phenotype was then selected on sucrose. Mutants were identified using PCR with primers that were located external to the deletion. The Δ eryH and Δ eryI strains were previously characterized (Barbier et al., 2014). For complementation, *eryH* was amplified by PCR from genomic DNA of *B. abortus* 2308 as a BamHI/XhoI fragment (BamHI_F: 5'-gcgggatccatgaccaaattctggattgg-3'; XhoI_R: 5'-ttaattcgcttgaaccttggtcgagccg-3'). Fragments were cloned into an EcoRV-digested pGEM, sequenced and then transferred into a pBBR1MCS1 (Cm^R). The Δ eryH strain with

the construct was then transformed by conjugation with the construction and selected for with the newly acquired resistance to chloramphenicol.

All *Brucella* were handled under BSL-3 containment according to the Directive 98/81/CE du Conseil du 26 octobre 1998 and to a law of the Gouvernement wallon du 4 juillet 2002.

Cell Culture and Infection

RAW 264.7 murine macrophages were routinely cultured in Dulbecco's modified Eagle's medium with high glucose (DMEM, Gibco) supplemented with 10% heat-inactivated fetal calf serum (FCS, Gibco). THP-1 human macrophage-like cells were cultured in RPMI 1640 medium (Gibco) that was supplemented with 10% FCS and 2 mM L-glutamine. Cells were differentiated into adherent monocytes by overnight treatment with 5 nM phorbol myristate (PMA). Bovine trophoblastic CL2 cells were kindly provided by Pr. Cynthia Baldwin (University of Massachusetts, Amherst, MA, United States) and cultured in RPMI 1640 supplemented with 10% FCS and 0.05 mM 2-mercaptoethanol (Gibco) as previously described (Parent et al., 2012). BeWo human trophoblastic cells (ATCC clone CCL-98) were cultured in DMEM-F12 Ham medium (Gibco) that was supplemented with 10% FCS and 2 mM L-glutamine as already described (Salcedo et al.,

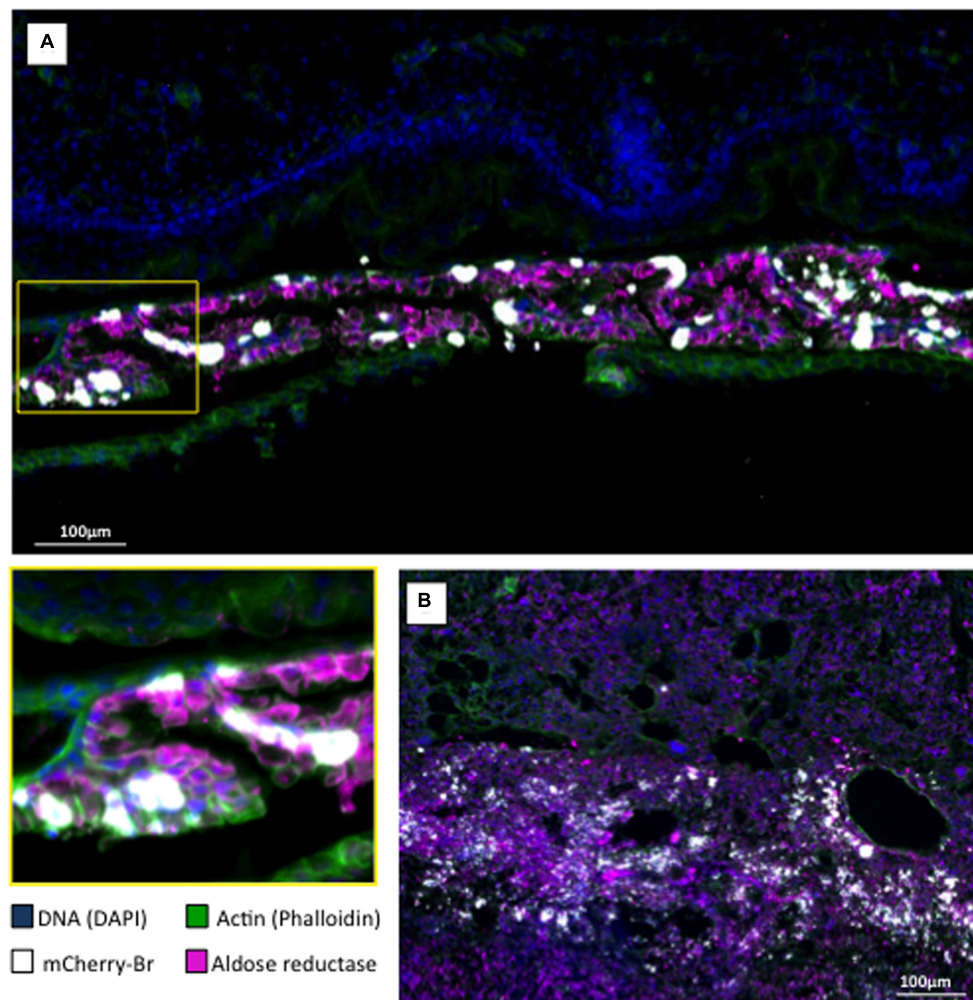


FIGURE 8 | Aldose reductase localization in *B. abortus* infected murine conceptus. Pregnant mice were intraperitoneally infected at post-conception day 6 with 10^5 CFU of a *B. abortus* mCherry (mCherry-Br; white color). Conceptus were obtained at post-conception day 15 and stained for DNA (DAPI/blue) and actin (phalloidin/green). **(A)** Aldose reductase immunostaining (purple) of the trophoblastic layer surrounding the fetus (the area in the yellow square corresponds to the lower left panel of the Figure). **(B)** Aldose reductase immunostaining (purple) of the placenta at the level of the decidua basalis.

2013). All cells were maintained at 37°C with a 5% CO₂ atmosphere.

For experiments in which RAW 264.7 were cultured with various glucose concentrations, DMEM with no glucose (Gibco) was supplemented with the appropriate amount of filter-sterilized glucose. Cells were cultured under these conditions for at least 2 passages prior to infection. Infections were performed as described elsewhere (Salcedo et al., 2013; Zúñiga-Ripa et al., 2014). Briefly, cells were seeded in 24-well plates at an appropriate density (2.105 cells/ml THP-1 cells and 4.104 cells/ml for RAW 264.7 and trophoblastic cells) and infected 24 h later with a multiplicity of infection (MOI) of 100. The cells were centrifuged at 1000 RPM for 10 min at 4°C before being incubated for 1 h at 37°C with 5% CO₂; they were then washed with fresh medium and incubated for 1 h with medium containing 50 μg/ml of gentamicin. The medium was then replaced with a fresh medium that contains 10 μg/ml of this antibiotic. At 2, 24, and 48 h after

infection, cells were washed with PBS and treated for 10 min at room temperature with PBS Triton X100 0.1%; after this treatment, the lysates were collected, diluted, plated on TSB and incubated at 37°C for approximately 3 days to enumerate the CFUs.

For immunofluorescence staining, cells were seeded on coverslip and treated as described previously (Francis et al., 2017). At the end of the process, the cells were fixed in 2% paraformaldehyde, pH 7.4, at 37°C for 15 min.

C57BL/6 Mice Infection

The procedures used and the handling of mice complied with current European legislation (directive 86/609/EEC) and the corresponding Belgian law “Arrêté royal relatif à la protection des animaux d’expérience du 6 avril 2010 publié le 14 mai 2010.” The Animal Welfare Committee of the Université de Namur (Belgium) reviewed and approved the complete protocols

(Permit Number 16/277). All infections were performed at an Animal Biosafety Level 3 facility.

To obtain the inoculum, bacteria from an overnight culture of *Brucella* in rich medium were pelleted, washed with RPMI 1640 and diluted in this medium. Intraperitoneal infection was carried out as previously described (Copin et al., 2012). Briefly, 500 μ l of suspension (10^5 CFU) was injected into groups of 8 to 12 C57BL/6 mice for each tested strain. Mice were euthanized 3, 9, and 30 days post-infection by cervical dislocation, the spleens were isolated, weighted and homogenized in 1 ml of PBS Triton X100 0.1%, and the CFU were counted on tryptic soy agar plates.

The procedure that was used to infect pregnant mice was adapted from previous reports (Bosseray, 1982; Kim et al., 2005; Pennington et al., 2012). Estruses of 6–14 weeks old C57BL/6 females were synchronized 3 days before mating pairs were set up with males that were 3–4 months old. Then, the presence of a vaginal plug was checked daily, and potentially fertilized females were isolated. That day corresponds to day 0 post-fecundation (PF). Four to five pregnant females were infected intraperitoneally with 500 μ l of bacterial suspension that was prepared as previously described (10^5 bacteria) at day 6 or 14 PF. At day 15 PF, mice were anesthetized with isoflurane (Zoetis) and euthanized by cervical dislocation. Conceptuses were removed from maternal uterine horns and transferred to sterile Petri dishes on ice, where they stayed for 15 min. Placenta, fetuses and surrounding fetal membranes were then further isolated and weighed. Tissues were homogenized in 1 ml PBS Triton X100 0.1% with an Ultra-Turrax homogenizer, the homogenates were serially diluted in PBS, and their CFU were counted.

Immunofluorescence Microscopy

Fetuses and spleens were fixed for 2 h at room temperature in 2% paraformaldehyde (pH 7.4), washed in PBS, and incubated overnight at 4°C in a 20% PBS-sucrose solution. The tissues were then embedded in Tissue-Tek OCT compound (Sakura) and frozen in liquid nitrogen, and cryostat sections (thickness, 5 μ m for spleens and 10 μ m for fetus) were prepared. For the staining, tissue sections were rehydrated in PBS and incubated in a PBS solution that contained 1% blocking reagent (PBS-BR 1%, Boehringer) for 20 min before they were incubated overnight in PBS-BR 1% containing mAbs or the following reagents: DAPI nucleic acid stain Alexa Fluor 350 or 488 phalloidin (Molecular Probes) to visualize the structure of the organ, and rat biotin-coupled anti-mouse CD11b (BD Pharmingen), rabbit anti-mouse iNOS (Calbiochem), rabbit anti-mouse Cytokeratin 7 (ab 181598, Abcam), and rabbit anti-mouse AR (CPA3124, Cohesion Biosciences) to stain the cells of interest. The samples were incubated with the appropriate secondary reagents [Alexa Fluor 568 streptavidin (Molecular Probes) or Alexa Fluor 647-coupled donkey anti-rabbit IgG (Molecular Probes)] for 2 h. Slides were mounted in Fluoro-Gel medium (Electron Microscopy Sciences, Hatfield, PA, United States). Labeled tissue sections were visualized with an Axiovert M200 inverted microscope (Zeiss, Jena, Germany) that was equipped with a high-resolution monochrome camera (AxioCam HR, Zeiss).

Images (1384 pixels \times 1036 pixels, 0.16 μ m/pixel) were acquired sequentially for each fluorochrome with A-Plan 10 \times /0.25 N.A. and LD-Plan-NeoFluar 63 \times /0.75 N.A. dry objectives and recorded as eight-bit gray-level *.zvi files. At least three slides per organ were analyzed from three different animals, and the results are representative of two independent experiments.

For immunostaining of AR in RAW 264.7 murine macrophages, the primary antibody that was used was the same that was used for staining in mice with a goat anti-rabbit IgG Alexa 488 (Life Technologies) as the secondary antibody.

Measurement of the Murine Aldose Reductase AKR1B3 Expression in RAW 264.7 by qRT-PCR

RNA from cells cultivated in a T75 flask was extracted with TriPure isolation reagent (Roche) according to the instructions of the manufacturer and DNA contamination was eliminated by incubation with DNase I (Fermentas). Then, RNA was first reverse transcribed (two steps) by SuperScript II (Invitrogen) into cDNA, which was then amplified in a LightCycler 96 Instrument (Roche) with FastStart Universal SYBR Green Master (Roche) as the fluorescent dye. The specificity of the SYBR Green assays was assessed by melting-point analysis and gel electrophoresis. The results were normalized using the housekeeping b-actin gene. Primer sequences are described in Supplementary Table S1.

AUTHOR CONTRIBUTIONS

TB, AZ-R, IM and J-JL conceived the study. AM and EM were responsible for the immunofluorescence microscopy analysis. XDB supervised all the molecular approaches. HP, CH, and EL contributed in the mutant construction, growth curves and tested them in cells and mice. TB and AZ-R were the main researchers involved in mutant and metabolic tests. EVS brought a lot of input in the aldose reductase and polyol pathway. J-JL, TB, and IM wrote the paper. All the authors read and commented on the paper.

FUNDING

J-JL's team is supported by an FNRS grant (Fonds de la Recherche Fondamentale Collective Grant N° 2452110) and by the Interuniversity Attraction Poles Programme initiated by the Belgian Science Policy Office. TB has a Ph.D. grant as "Aspirant FNRS." AM and EL have a Ph.D. grant from the FRIA. Research at the University of Navarra is supported by grants from the Ministerio de Economía y Competitividad of Spain (AGL2011-30453-C04-00) and the Institute for Tropical Health. The E.V.S. laboratory is supported by a Welbio grant of the Walloon Region and by a grant from the Fonds de la Recherche Scientifique Médicale. EM is a Research Associate at the Fonds de la Recherche Scientifique (FRS)–FNRS (Belgium).

SUPPLEMENTARY MATERIAL

The Supplementary Material for this article can be found online at: <http://journal.frontiersin.org/article/10.3389/fmicb.2017.01088/full#supplementary-material>

FIGURE S1 | *Brucella abortus* 2308 Δ eryA and Δ eryH are not able to grow with erythritol as the only carbon source. The growth of the Δ eryA mutant was monitored in rich medium 2YT or in chemically defined medium with erythritol as the only carbon source and compared to Δ eryH (Barbier:2014 cm). As expected, the growth of the deletion strains is abolished when only erythritol is available.

FIGURE S2 | The growth of the erythritol-sensitive *B. abortus* 2308 Δ eryH strain is not affected by other polyols. Growth was monitored in 2YT supplemented with polyols structurally close to erythritol that are also found in fetal fluids and tissues. The growth of the Δ eryH mutant was not affected by any of the polyols tested

REFERENCES

- Al-Tawfiq, J. A., and Memish, M. A. (2013). Pregnancy associated brucellosis. *Recent Pat. Antiinfect. Drug Discov.* 8, 47–50. doi: 10.2174/1574891X11308010009
- Amin, J. D., and Wilshire, A. J. (1997). The effects of crude placental extract and erythritol on growth of *Chlamydia psittaci* (ovis) in McCoy cells. *Vet. Res. Commun.* 21, 431–435. doi: 10.1023/A:1005807402736
- Anderson, T. D., and Cheville, N. F. (1986). Ultrastructural morphometric analysis of *Brucella abortus*-infected trophoblasts in experimental placentitis. Bacterial replication occurs in rough endoplasmic reticulum. *Am. J. Pathol.* 124, 226–237.
- Anderson, T. D., Cheville, N. F., and Meador, V. P. (1986a). Pathogenesis of placentitis in the goat inoculated with *Brucella abortus*. II. Ultrastructural studies. *Vet. Pathol.* 23, 227–239.
- Anderson, T. D., Meador, V. P., and Cheville, N. F. (1986b). Pathogenesis of placentitis in the goat inoculated with *Brucella abortus*. I. Gross and histologic lesions. *Vet. Pathol.* 23, 219–226.
- Barbier, T., Collard, F., Zúñiga-Ripa, A., Moriyón, I., Godard, T., Becker, J., et al. (2014). Erythritol feeds the pentose phosphate pathway via three new isomerases leading to D-erythrose-4-phosphate in *Brucella*. *Proc. Natl. Acad. Sci. U.S.A.* 111, 17815–17820. doi: 10.1073/pnas.1414622111
- Blasco, J. M. (1990). “*Brucella ovis*,” in *Animal Brucellosis*, eds K. H. Nielsen and J. R. Duncan (Boca Raton, FL: CRC Press), 352–378.
- Bosseray, N. (1980). Colonization of mouse placentas by *Brucella abortus* inoculated during pregnancy. *Br. J. Exp. Pathol.* 61, 361–368.
- Bosseray, N. (1982). Mother to young transmission of *Brucella abortus* infection in mouse model. *Ann. Rech. Vét.* 13, 341–349.
- Bosseray, N. (1983). Kinetics of placental colonization of mice inoculated intravenously with *Brucella abortus* at day 15 of pregnancy. *Br. J. Exp. Pathol.* 64, 612–616.
- Bresson, E., Boucher-Kovalik, S., Chapdelaine, P., Madore, E., Harvey, N., Laberge, P. Y., et al. (2011). The human aldose reductase AKR1B1 qualifies as the primary prostaglandin F synthase in the endometrium. *J. Clin. Endocrinol. Metab.* 96, 210–219. doi: 10.1210/jc.2010-1589
- Bresson, E., Lacroix-Pépin, N., Boucher-Kovalik, S., Chapdelaine, P., and Fortier, M. A. (2012). The prostaglandin F synthase activity of the human aldose reductase AKR1B1 brings new lenses to look at pathologic conditions. *Front. Pharmacol.* 3:98. doi: 10.3389/fphar.2012.00098/abstract
- Brusati, V., Jóźwik, M., Jóźwik, M., Teng, C., Paolini, C., Marconi, A. M., et al. (2005). Fetal and maternal Non-glucose carbohydrates and polyols concentrations in normal human pregnancies at term. *Pediatr. Res.* 58, 700–704. doi: 10.1203/01.PDR.0000180549.86614.73
- Burkhardt, S., Jiménez de Bagüés, M. P., Liautard, J.-P., and Köhler, S. (2005). Analysis of the behavior of *eryC* mutants of *Brucella suis* attenuated in macrophages. *Infect. Immun.* 73, 6782–6790. doi: 10.1128/IAI.73.10.6782-6790.2005
- Carmichael, L. E. (1990). “*Brucella canis*,” in *Animal Brucellosis*, eds K. H. Nielsen and J. R. Duncan (Boca Raton, FL: CRC Press), 336–350.
- Clark, J. B., Graham, E. F., Lewis, B. A., and Smith, F. (1967). D-mannitol, erythritol and glycerol in bovine semen. *J. Reprod. Fertil.* 13, 189–197. doi: 10.1530/jrf.0.0130189
- Copin, R., Vitry, M.-A., Hanot Mambres, D., Machelart, A., De Trez, C., Vanderwinden, J.-M., et al. (2012). In situ microscopy analysis reveals local innate immune response developed around *Brucella* infected cells in resistant and susceptible mice. *PLoS Pathog.* 8:e1002575. doi: 10.1371/journal.ppat.1002575.g009
- Croy, B. A., Yamada, A. T., DeMayo, F. J., and Adamson, S. L. (2013). *The Guide to Investigation of Mouse Pregnancy*. Amsterdam: Academic Press.
- de Lorenzo, V. (2014). From the selfish gene to selfish metabolism: revisiting the central dogma. *Bioessays* 36, 226–235. doi: 10.1002/bies.201300153
- Dozot, M., Poncet, S., Nicolas, C., Copin, R., Bouraoui, H., Mazé, A., et al. (2010). Functional characterization of the incomplete phosphotransferase system (PTS) of the intracellular pathogen *Brucella melitensis*. *PLoS ONE* 5:e12679. doi: 10.1371/journal.pone.0012679
- Enright, F. M., and Samartino, L. E. (1994). Mechanisms of abortion in *Brucella abortus* infected cattle. *Proc. Annu. Meet. U.S. Anim. Health Assoc.* 98, 55–63. doi: 10.1186/1471-2164-14-426
- Fernandez, A. G., Ferrero, M. C., Hielpos, M. S., Fossati, C. A., and Baldi, P. C. (2016). Proinflammatory response of human trophoblastic cells to *Brucella abortus* infection and upon interactions with infected phagocytes. *Biol. Reprod.* 94, 48. doi: 10.1095/biolreprod.115.131706
- Ferrier, D. R. (ed.) (2013). *Biochemistry*, 6 Edn. Hagerstown: Lippincott Williams & Wilkins.
- Francis, N., Poncin, K., Fioravanti, A., Vassen, V., Willemart, K., Ong, T. A. P., et al. (2017). CtrA controls cell division and outer membrane composition of the pathogen *Brucella abortus*. *Mol. Microbiol.* 103, 780–797. doi: 10.1111/mmi.13589
- Frenette, G. (2006). Polyol pathway in human epididymis and semen. *J. Androl.* 27, 233–239. doi: 10.2164/jandrol.05108
- González, R. G., Barnett, P., Aguayo, J., Cheng, H. M., and Chylack, L. T. (1984). Direct measurement of polyol pathway activity in the ocular lens. *Diabetes Metab. Res. Rev.* 33, 196–199. doi: 10.2337/diab.33.2.196
- Hästein, T., and Velle, W. (1968). Placental aldose reductase activity and foetal blood fructose during bovine pregnancy. *J. Reprod. Fertil.* 15, 47–52. doi: 10.1530/jrf.0.0150047
- Hayman, S., and Kinoshita, J. H. (1965). Isolation and properties of lens aldose reductase. *J. Biol. Chem.* 240, 877–882.
- Hu, D., and Cross, J. C. (2010). Development and function of trophoblast giant cells in the rodent placenta. *Int. J. Dev. Biol.* 54, 341–354. doi: 10.1387/ijdb.082768dh
- Jauniaux, E. (2005). Polyol concentrations in the fluid compartments of the human conceptus during the first trimester of pregnancy: maintenance of redox potential in a low oxygen environment. *J. Clin. Endocrinol. Metab.* 90, 1171–1175. doi: 10.1210/jc.2004-1513

- Jones, L. M., Montgomery, V., and And Wilson, J. B. (1965). Characteristics of carbon dioxide-independent cultures of *Brucella abortus* isolated from cattle vaccinated with strain 19. *J. Inf. Dis.* 115, 312–320. doi: 10.1093/infdis/115.3.312
- Kabututu, Z., Manin, M., Pointud, J. C., Maruyama, T., Nagata, N., Lambert, S., et al. (2008). Prostaglandin F2 synthase activities of aldo-keto reductase 1B1, 1B3 and 1B7. *J. Biochem.* 145, 161–168. doi: 10.1093/jb/mvn152
- Karcaaltincaba, D., Sencan, I., Kandemir, O., Guvendag Guven, E. S., and Yalvac, S. (2010). Does brucellosis in human pregnancy increase abortion risk? Presentation of two cases and review of literature. *J. Obstet. Gynaecol. Res.* 36, 418–423. doi: 10.1111/j.1447-0756.2009.01156.x
- Kardon, T., Stroobant, V., Veiga-da-Cunha, M., and Van Schaftingen, E. (2008). Characterization of mammalian sedoheptulokinase and mechanism of formation of erythritol in sedoheptulokinase deficiency. *FEBS Lett.* 582, 3330–3334. doi: 10.1016/j.febslet.2008.08.024
- Keppie, J., Williams, A., Witt, K., and Smith, H. (1965). The role of erythritol in the tissue localization of the brucellae. *Br. J. Exp. Pathol.* 46, 104–108.
- Keppie, J., Witt, K., and Smith, H. (1967). The effect of erythritol on the growth of S19 and other attenuated strains of *Brucella abortus*. *Res. Vet. Sci.* 8, 294–296.
- Khan, M. Y., Mah, M. W., and Memish, Z. A. (2001). Brucellosis in pregnant women. *Clin. Infect. Dis.* 32, 1172–1177. doi: 10.1086/319758
- Kim, S., Lee, D., Watanabe, K., Furuoka, H., Suzuki, H., and Watarai, M. (2005). Interferon- γ promotes abortion due to *Brucella* infection in pregnant mice. *BMC Microbiol.* 5:22. doi: 10.1186/1471-2180-5-22
- Köhler, S., Foulongne, V., Ouahrani-Bettache, S., Bourg, G., Teyssier, J., Ramuz, M., et al. (2002). The analysis of the intramacrophagic virulome of *Brucella suis* deciphers the environment encountered by the pathogen inside the macrophage host cell. *Proc. Natl. Acad. Sci. U.S.A.* 99, 15711–15716. doi: 10.1073/pnas.232454299
- Larose, J., Laflamme, J., Côté, I., Lapointe, J., Frenette, G., Sullivan, R., et al. (2012). The polyol pathway in the bovine oviduct. *Mol. Reprod. Dev.* 79, 603–612. doi: 10.1002/mrd.22067
- Letesson, J.-J., Barbier, T., Zúñiga-Ripa, A., Godfroid, J., De Bolle, X., and Moriyón, I. (2017). *Brucella* genital tropism: what's on the menu. *Front. Microbiol.* 8:506. doi: 10.3389/fmicb.2017.00506
- Madore, E., Harvey, N., Parent, J., Chapdelaine, P., Arosh, J. A., and Fortier, M. A. (2003). An aldose reductase with 20-hydroxysteroid dehydrogenase activity is most likely the enzyme responsible for the production of prostaglandin F2 in the bovine endometrium. *J. Biol. Chem.* 278, 11205–11212. doi: 10.1074/jbc.M208318200
- McCullough, W. G., and Beal, G. A. (1951). Growth and manometric studies on carbohydrate utilization of *Brucella*. *J. Infect. Dis.* 89, 266–271. doi: 10.1093/infdis/89.3.266
- Mol, J. P. S., Pires, S. F., Chapeaurouge, A. D., Perales, J., Santos, R. L., Andrade, H. M., et al. (2016). Proteomic profile of *Brucella abortus*-infected bovine chorioallantoic membrane explants. *PLoS ONE* 11:e0154209. doi: 10.1371/journal.pone.0154209
- Moreno, E., and Moriyón, I. (2006). “The genus *Brucella*,” in *The Prokaryotes*, eds M. Dworkin, S. Falkow, E. Rosenberg, K.-H. Schleifer, and E. Stackebrandt (New York, NY: Springer), doi: 10.1007/0-387-30745-1_17
- Nataro, J. P. (2015). “Pathogenesis — Thoughts from the front line,” in *Metabolism and Bacterial Pathogenesis*, eds T. Conway and P. S. Cohen (Washington, DC: American Society of Microbiology), 17–26. doi: 10.1128/microbiolspec.MBP-0012-2014
- Navarro-Martinez, A., Solera, J., Corredoira, J., Beato, J. L., Martinez, A. E., Atienzar, M., et al. (2001). Epididymo-orchitis due to *Brucella melitensis*: a retrospective study of 59 patients. *Clin. Infect. Dis.* 33, 2017–2022. doi: 10.1086/324489
- Parent, M. A., Bellaire, B. H., Murphy, E. A., Roop, R. M., Elzer, P. H., and Baldwin, C. L. (2012). *Brucella abortus* siderophore 2,3-dihydroxybenzoic acid (DHBA) facilitates intracellular survival of the bacteria. *Microb. Pathog.* 32, 239–248. doi: 10.1006/mpat.2002.0500
- Pearce, J., Williams, A., Harris-Smith, P. W., Fitzgeorge, R., and Smith, H. (1962). The chemical basis of the virulence of *Brucella abortus*: II. Erythritol, a constituent of bovine foetal fluids which stimulates the growth of *Br. abortus* in bovine phagocytes. *Br. J. Exp. Pathol.* 43, 31–37.
- Pennington, K. A., Schlitt, J. M., and Schulz, L. C. (2012). Isolation of primary mouse trophoblast cells and trophoblast invasion assay. *J. Vis. Exp.* 59:e3202. doi: 10.3791/3202
- Pruneda, A., Pinart, E., Bonet, S., Yeung, C.-H., and Cooper, T. G. (2006). Study of the polyol pathway in the porcine epididymis. *Mol. Reprod. Dev.* 73, 859–865. doi: 10.1002/mrd.20481
- Ramana, K. V., and Srivastava, S. K. (2010). Aldose reductase: a novel therapeutic target for inflammatory pathologies. *Int. J. Biochem. Cell Biol.* 42, 17–20. doi: 10.1016/j.biocel.2009.09.009
- Ratliff, D. M., Martinez, F. J., Vander Jagt, T. J., Schimandle, C. M., Robinson, B., Hunsaker, L. A., et al. (1999). Inhibition of human aldose and aldehyde reductases by non-steroidal anti-inflammatory drugs. *Adv. Exp. Med. Biol.* 463, 493–499. doi: 10.1007/978-1-4615-4735-8_62
- Regnault, T. R. H., Teng, C., de Vrijer, B., Galan, H. L., Wilkening, R. B., and Battaglia, F. C. (2010). The tissue and plasma concentration of polyols and sugars in sheep intrauterine growth retardation. *Exp. Biol. Med.* 235, 999–1006. doi: 10.1258/ebm.2010.009360
- Salcedo, S. P., Chevrier, N., Lacerda, T. L. S., Ben Amara, A., Gerart, S., Gorvel, V. A., et al. (2013). Pathogenic brucellae replicate in human trophoblasts. *J. Infect. Dis.* 207, 1075–1083. doi: 10.1093/infdis/jit007
- Samartino, L. E., and Enright, F. M. (1993). Pathogenesis of abortion of bovine brucellosis. *Comp. Immunol. Microbiol. Infect. Dis.* 16, 95–101. doi: 10.1016/0147-9571(93)90001-L
- Samartino, L. E., Traux, R. E., and Enright, F. M. (1994). Invasion and replication of *Brucella abortus* in three different trophoblastic cell lines. *Zentralbl. Veterinarmed. B* 41, 229–236. doi: 10.1111/j.1439-0450.1994.tb00223.x
- Sangari, F. J., Grilló, M. J., Jimenez de Bagues, M. P., González-Carreró, M. I., García-Lobo, J. M., Blasco, J. M., et al. (1998). The defect in the metabolism of erythritol of the *Brucella abortus* B19 vaccine strain is unrelated with its attenuated virulence in mice. *Vaccine* 16, 1640–1645. doi: 10.1016/S0264-410X(98)00063-2
- Smith, H., Williams, A., Pearce, E. J., Keppie, J., Harris-Smith, P. W., Fitz-George, R. B., et al. (1962). Foetal erythritol: a cause of the localization of *Brucella abortus* in bovine contagious abortion. *Nature* 193, 47–49. doi: 10.1038/193047a0
- Sperry, J. F., and Robertson, D. C. (1975). Inhibition of growth by erythritol catabolism in *Brucella abortus*. *J. Bacteriol.* 124, 391–397.
- Tawata, M., Ohtaka, M., Hosaka, Y., and Onaya, T. (1992). Aldose reductase mRNA expression and its activity are induced by glucose in fetal rat aortic smooth muscle (A10) cells. *Life Sci.* 51, 719–726. doi: 10.1016/0024-3205(92)90480-D
- Tobias, L., Cordes, D. O., and Schurig, G. G. (1993). Placental pathology of the pregnant mouse inoculated with *Brucella abortus* strain 2308. *Vet. Pathol.* 30, 119–129. doi: 10.1177/030098589303000204
- Vilchez, G., Espinoza, M., D'Onadio, G., Saona, P., and Gotuzzo, E. (2015). Brucellosis in pregnancy: clinical aspects and obstetric outcomes. *Int. J. Infect. Dis.* 38, 95–100. doi: 10.1016/j.ijid.2015.06.027
- Williams, A. E., Keppie, J., and Smith, H. (1962). The chemical basis of the virulence of *Brucella abortus*. III. Foetal erythritol a cause of the localisation of *Brucella abortus* in pregnant cows. *Br. J. Exp. Pathol.* 43, 530–537.
- Zinsstag, J., Schelling, E., Solera, J., Blasco, M. J., and Moriyón, I. (2011). “Brucellosis,” in *Handbook of Zoonoses*, eds R. S. Palmer, L. Soulsby, R. P. Torgeson, and G. D. Brown (Oxford: Oxford University Press), 54–62.
- Zúñiga-Ripa, A., Barbier, T., Conde-Alvarez, R., Martínez-Gómez, E., Palacios-Chaves, L., Gil-Ramírez, Y., et al. (2014). *Brucella abortus* depends on pyruvate phosphate dikinase and malic enzyme but not on Fbp and GlpX fructose-1,6-bisphosphatases for full virulence in laboratory models. *J. Bacteriol.* 196, 3045–3057. doi: 10.1128/JB.01663-14

Conflict of Interest Statement: The authors declare that the research was conducted in the absence of any commercial or financial relationships that could be construed as a potential conflict of interest.

Copyright © 2017 Barbier, Machelart, Zúñiga-Ripa, Plovier, Hougardy, Lobet, Willemart, Muraille, De Bolle, Van Schaftingen, Moriyón and Letesson. This is an open-access article distributed under the terms of the Creative Commons Attribution License (CC BY). The use, distribution or reproduction in other forums is permitted, provided the original author(s) or licensor are credited and that the original publication in this journal is cited, in accordance with accepted academic practice. No use, distribution or reproduction is permitted which does not comply with these terms.



Exploring the Diversity of Field Strains of *Brucella abortus* Biovar 3 Isolated in West Africa

Moussa Sanogo^{1*}, David Fretin², Eric Thys³ and Claude Saegerman⁴

¹ Central Veterinary Laboratory of Bingerville, LANADA, Bingerville, Ivory Coast, ² Department of Bacteriology and Immunology, Veterinary and Agro-chemical Research Centre, Brussels, Belgium, ³ Department of Biomedical Sciences, Institute of Tropical Medicine, Antwerp, Belgium, ⁴ Research Unit of Epidemiology and Risk Analysis Applied to Veterinary Sciences (UREAR-ULg), Faculty of Veterinary Medicine, Fundamental and Applied Research for Animal and Health Center, University of Liège, Liège, Belgium

OPEN ACCESS

Edited by:

Adrian Whatmore,
Animal and Plant Health Agency,
United Kingdom

Reviewed by:

Takehiko Kenzaka,
Osaka Ohtani University, Japan
Heinrich Neubauer,
Friedrich Loeffler Institute Greifswald,
Germany

*Correspondence:

Moussa Sanogo
ssanogomoussas@gmail.com

Specialty section:

This article was submitted to
Infectious Diseases,
a section of the journal
Frontiers in Microbiology

Received: 13 December 2016

Accepted: 19 June 2017

Published: 30 June 2017

Citation:

Sanogo M, Fretin D, Thys E and
Saegerman C (2017) Exploring the
Diversity of Field Strains of *Brucella*
abortus Biovar 3 Isolated in West
Africa. *Front. Microbiol.* 8:1232.
doi: 10.3389/fmicb.2017.01232

Brucellosis is one of the most widespread bacterial zoonotic diseases in the world, affecting both humans and domestic and wild animals. Identification and biotyping of field strains of *Brucella* are of key importance for a better knowledge of the epidemiology of brucellosis, for identifying appropriate antigens, for managing disease outbreaks and for setting up efficient preventive and control programmes. Such data are required both at national and regional level to assess potential threats for public health. Highly discriminative genotyping methods such as the multiple locus variable number of tandem repeats analysis (MLVA) allow the comparison and assessment of genetic relatedness between field strains of *Brucella* within the same geographical area. In this study, MLVA biotyping data retrieved from the literature using a systematic review were compared using a clustering analysis and the Hunter-Gaston diversity index (HGD). Thus, the analysis of the 42 MLVA genotyping results found in the literature on West Africa [i.e., from Ivory Coast (1), Niger (1), Nigeria (34), The Gambia (3), and Togo (3)] did not allow a complete assessment of the actual diversity among field strains of *Brucella*. However, it provided some preliminary indications on the co-existence of 25 distinct genotypes of *Brucella abortus* biovar 3 in this region with 19 genotypes from Nigeria, three from Togo and one from Ivory Coast, The Gambia, and Niger. The strong and urgent need for more sustainable molecular data on prevailing strains of *Brucella* in this sub-region of Africa and also on all susceptible species including humans is therefore highlighted. This remains a necessary stage to allow a comprehensive understanding of the relatedness between field strains of *Brucella* and the epidemiology of brucellosis within West Africa countries.

Keywords: molecular epidemiology, brucellosis, *Brucella*, *Brucella abortus* biovar 3, biotyping, MLVA, West Africa

INTRODUCTION

Brucellosis is one of the most widespread bacterial zoonotic diseases in the world, affecting both humans and domestic and wild animals (Maurin, 2005; Corbel, 2006). The disease is caused by Gram-negative facultative intracellular bacteria of the genus *Brucella*. According to the World Health Organization (WHO), about 500,000 new cases of human brucellosis are reported annually worldwide (Corbel, 1997; Pappas et al., 2006). In animals, brucellosis is responsible

for many economic losses because of abortions, decrease in production (particularly reduced milk production), losses of calves, viable but weak calves, reproductive disorders, and costs of intervention. With its impact on productivity, this disease contributes worsening the deficit of animal protein especially for populations in developing countries, where food needs are continuously increasing (Perry, 2002). In areas where people's livelihood heavily depends on livestock, the impact of brucellosis might therefore exacerbate poverty (Cáceres, 2010).

In spite of its status as a neglected tropical disease, bovine brucellosis remains the most widespread disease in animals and the main concern in Sub-Saharan African countries (Akakpo and Bornarel, 1987; Corbel, 1997; McDermott and Arimi, 2002; Bronsvoort et al., 2009). For a better understanding of the epidemiology of bovine brucellosis, phenotypic, and genotypic knowledge on prevailing *Brucella* spp. are required in both human and animal hosts. Thus, *Brucella* causing brucellosis has been investigated throughout the years in different regions of the world including West Africa. In this part of Africa, the presence and the endemicity of brucellosis were confirmed, with *Brucella abortus* biovar 3 being the most commonly isolated strains in cattle (Sanogo et al., 2013a).

This paper compares and investigates the relatedness between the prevailing field strains of *B. abortus* biovar 3 from West Africa.

MATERIALS AND METHODS

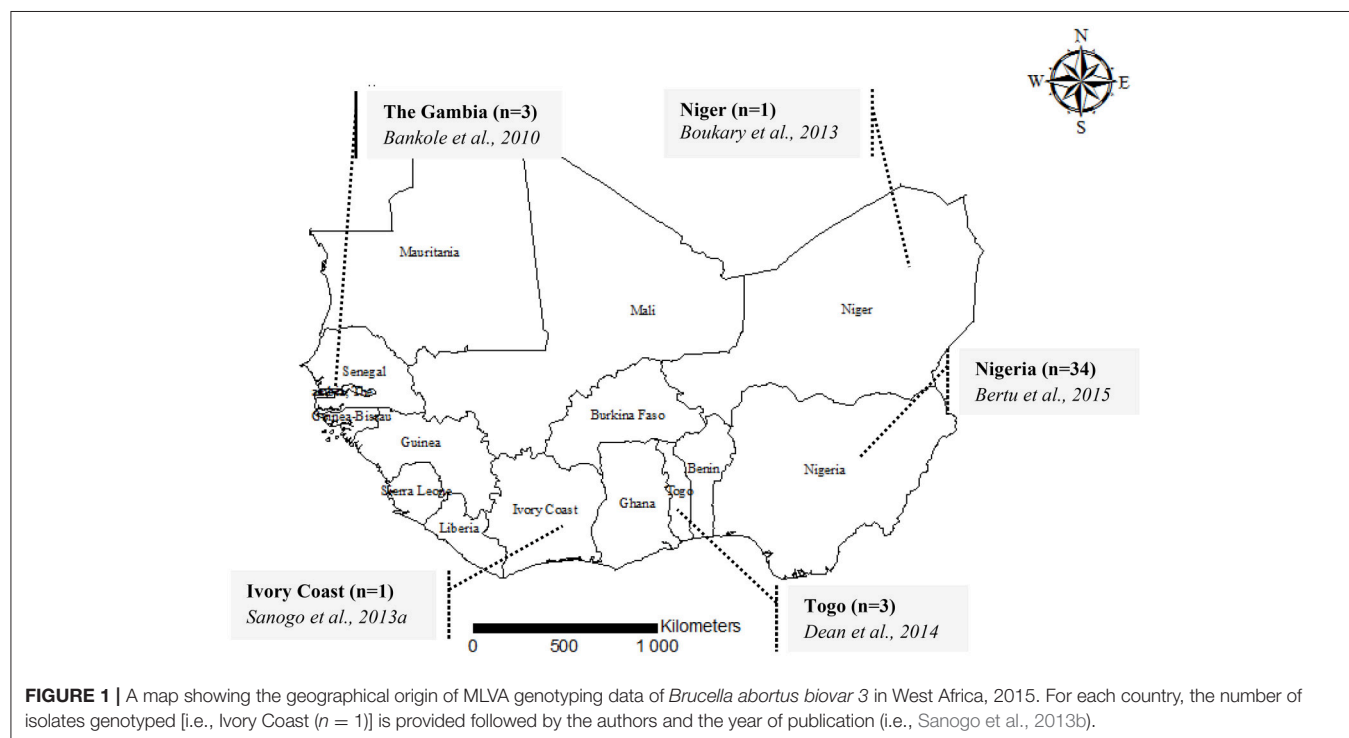
Study Area

With a surface area of 5 112 903 km² representing a fifth of the African continent, West Africa is one of the four major regions of

Sub-Saharan Africa. This region includes 14 countries including Benin, Burkina Faso, Cape Verde, The Gambia, Ghana, Guinea, Ivory Coast, Liberia, Mali, Niger, Nigeria, Senegal, Sierra Leone, and Togo (Figure 1). These countries comprise almost 25% of the cattle population of the continent with about 70 million heads of cattle of different types (*Bos taurus* type, *Bos indicus* type and crossbreds) (FAO, 2017). These cattle are mostly raised extensively in sedentary herds. This region is also characterized by the existence of frequent livestock movements between countries through transhumance or commercial exchanges.

Prevailing Field Strains of *Brucella abortus* Biovar 3 from West Africa

A Preferred Reporting Items of Systematic reviews and Meta-Analyses (PRISMA) approach (Moher et al., 2009) was used to identify available and accessible information in the literature on typing of prevailing field strains of *Brucella* in both human and animals through general internet search engines, including Google Scholar and PubMed, with no language and time period restrictions. The search strategy was adapted according to the database. Search terms were composed by combinations of keywords. In Google Scholar, “Brucellosis+*Brucella*+MLVA+typing+genotyping+Sub-saharan+Africa” was used while in PubMed, the following search algorithm was used: (((Brucellosis) OR *Brucella*)) AND (((genotyping) OR typing) OR MLVA)) AND ((Africa) OR sub-Saharan Africa). Firstly, titles and abstracts were screened and available full texts were screened for relevant information. Thus, studies reporting information on genotyping data of field strains of *B. abortus* biovar 3 from sub-Saharan Africa and especially West Africa were considered and were given a



particular focus for final inclusion. When provided, Multiple Locus Variable number of tandem repeats Analysis (MLVA) data [e.g., the number of repeats in a set of variable number of tandem repeats (VNTR) loci] were extracted from the selected paper, summarized, and subjected to further analysis. A flow diagram summarizing the literature search strategy is presented in **Figure 2**.

Multiple Locus Variable Number of Tandem Repeats Analysis

MLVA profiles of field strains of *B. abortus* biovar 3 isolated from West Africa were used in this study (**Figure 1**). Briefly, MLVA consists of the assessment of the number of repeats in a set of variable number of tandem repeats (VNTR) loci. In MLVA 16, two sets of VNTRs gathered into 8 microsatellite markers (panel 1: Bruce06, Bruce08, Bruce11, Bruce12, Bruce42, Bruce43, Bruce45, Bruce55) and 8 microsatellite markers (panel 2) comprising two groups (panel 2A: Bruce18, Bruce19, Bruce21; and panel 2B: Bruce04, Bruce07, Bruce09, Bruce16, Bruce30) are examined (Le Flèche et al., 2006; Maquart et al., 2009). The number of repetitions of each locus of each panel, constituting the MLVA profile, is derived from the size of the band of the PCR products (Le Flèche et al., 2006).

Comparison of MLVA Profiles

Diversity and relatedness among field strains of *B. abortus* biovar 3 from West Africa were assessed by calculating the Hunter-Gaston diversity index (HGDI), a numerical index measuring the probability that two strains consecutively taken from a given

population would be placed into different typing groups (Hunter and Gaston, 1988) (<http://www.hpa-bioinformatics.org.uk/cgi-bin/DICI/DICI.pl>). The relatedness between the distinct MLVA profiles of West African strains and neighbor profiles originating from Africa in the public MLVA *Brucella* database on MLVAnet (<http://mlva.u-psud.fr/brucella/>) was also assessed with a Ward hierarchical clustering analysis using the *hclust* function and the *cluster* package in R software (<http://www.r-project.org>). Using results of a Ward linkage clustering analysis of the number of variable tandem repeats, a dendrogram of clustered MLVA profiles of West African strains was also generated. In order to assess potential relatedness with others prevailing strains from sub-Saharan Africa, comparison of the 25 distinct MLVA profiles from West Africa includes three lately published *B. abortus* biovar 3 MLVA profiles from Tanzania (Mathew et al., 2015) and five other sub-Saharan Africa *B. abortus* biovar 3 field strains and neighbor profiles from the *Brucella* MLVA database, namely Kenya (Muendo et al., 2012), Sudan, Uganda, and Chad (Le Flèche et al., 2006) (**Table 1**).

RESULTS

In order to explore the genetic diversity of field strains of *B. abortus* biovar 3 from West Africa, available and accessible MLVA genotyping data were retrieved from the literature (**Figures 1, 2**). Among 57 published papers initially retrieved from the literature search, only 10 papers report MLVA genotyping data of West African *B. abortus* biovar 3 strains. These 10 papers include four

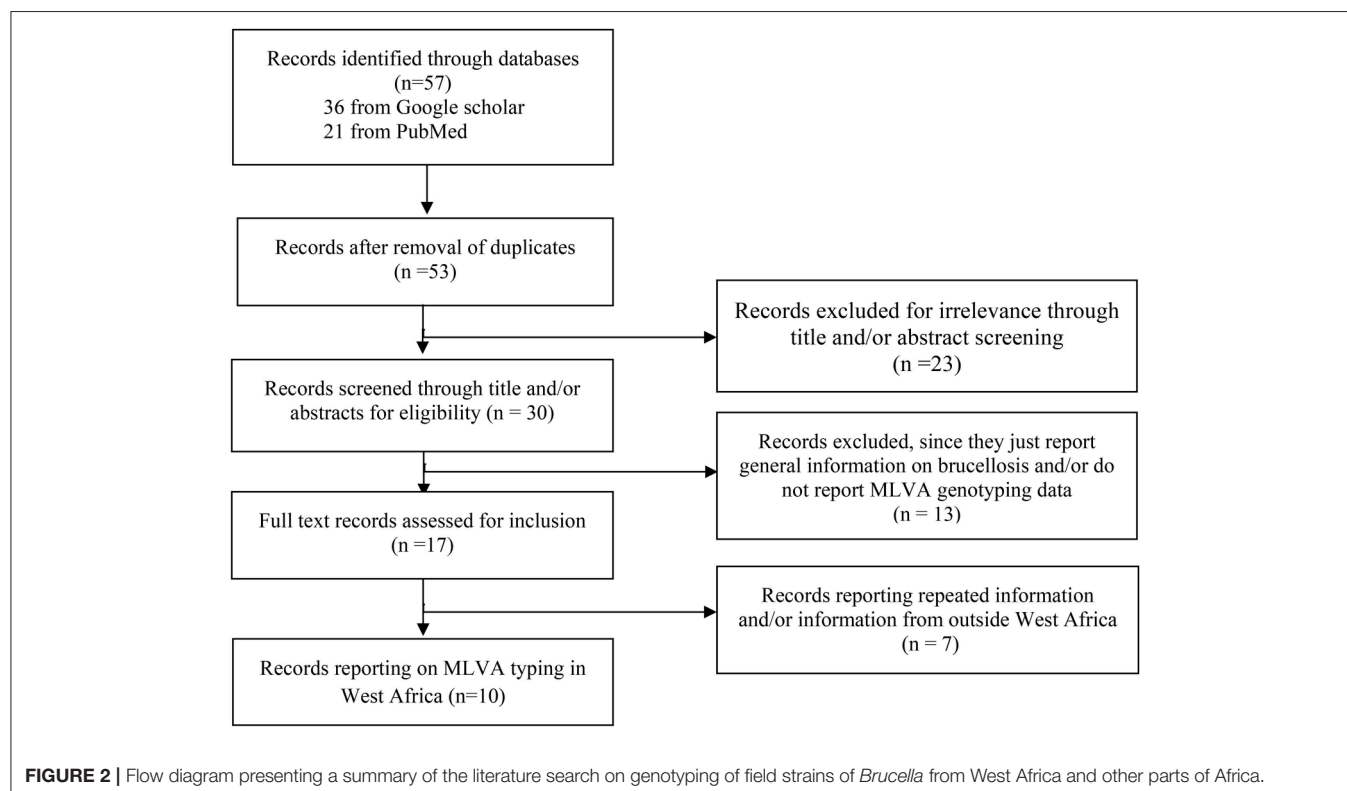


TABLE 1 | Multiple Loci Variable Number Tandem Repeats analysis (MLVA) distinct profiles of West African isolates of *B. abortus* biovar 3 and some close neighbor profiles from Africa retrieved from literature and from the *Brucella* MLVA bank.

Id	VNTR locus																	References		
	aStrains																			
	Bruc06	Bruc08	Bruc11	Bruc12	Bruc42	Bruc43	Bruc45	Bruc55	Bruc18	Bruc19 ^b	Panel 2A				Panel 2B			Period of collection	Location	Host
	Bruc06	Bruc08	Bruc11	Bruc12	Bruc42	Bruc43	Bruc45	Bruc55	Bruc18	Bruc19 ^b	Bruc21	Bruc04	Bruc07	Bruc09	Bruc16	Bruc30				
1	Ref Strain Tulya	3	5	5	11	2	2	3	3	8	40	8	6	5	3	11	5	Uganda	Human	Le Flèche et al., 2006
2	^c Ref Strain BCCN 93_26	3	5	5	11	2	2	3	3	6	40	8	6	8	3	7	7	Sudan	Dromedary	Le Flèche et al., 2006
3	^d Ref Strain BfR7	3	5	5	11	2	2	3	3	6	–	8	6	4	3	8	4	Chad	Cattle	Le Flèche et al., 2006
4	^e IVC_isolate	3	5	4	11	2	2	3	3	7	21	8	4	5	3	7	3	Ivory Coast	Cattle	Sanogo et al., 2013b
5	Niger_isolate	3	5	3	11	2	2	3	3	8	21	8	6	2	3	12	7	Niger	Cattle	Boukary et al., 2013
6	The_gambia_isolate	3	5	4	11	2	2	3	3	7	–	8	5	5	3	3	5	The Gambia	Cattle	Bankole et al., 2010
7	Togo_1	3	5	3	11	2	2	3	3	10	41	8	4	2	3	8	4	Togo	Cattle	Dean et al., 2014
8	Togo_2	3	5	3	11	2	2	3	3	8	41	8	4	2	3	5	4	Togo	Cattle	Dean et al., 2014
9	Togo_3	3	5	3	11	2	2	3	3	8	41	8	4	2	3	6	4	Togo	Cattle	Dean et al., 2014
10	Nigeria_602	3	4	4	12	2	1	3	3	6	40	8	7	4	3	4	5	Nigeria	Cattle	Bertu et al., 2015
11	Nigeria_603	3	4	4	11	2	1	3	3	6	40	8	7	4	3	4	6	Nigeria	Cattle	Bertu et al., 2015
12	Nigeria_604	3	4	4	11	2	2	3	3	6	40	9	8	4	3	3	5	Nigeria	Cattle	Bertu et al., 2015
13	Nigeria_605	3	4	4	11	2	2	3	3	6	42	8	7	6	3	6	5	Nigeria	Cattle	Bertu et al., 2015
14	Nigeria_606	3	4	4	11	2	2	3	3	6	40	8	8	4	3	5	6	Nigeria	Cattle	Bertu et al., 2015
15	Nigeria_607	3	4	4	11	2	2	3	3	6	40	8	8	4	4	7	5	Nigeria	Sheep	Bertu et al., 2015
16	Nigeria_608	3	4	4	10	2	2	3	3	6	40	8	8	4	4	8	5	Nigeria	Cattle	Bertu et al., 2015
17	Nigeria_609	3	4	4	10	2	3	3	3	6	40	8	6	7	4	8	8	Nigeria	Cattle	Bertu et al., 2015
18	Nigeria_610	3	4	4	10	2	2	3	3	6	40	8	5	10	3	14	6	Nigeria	Cattle	Bertu et al., 2015
19	Nigeria_611	3	4	4	10	2	2	3	3	6	40	8	5	10	3	9	6	Nigeria	Cattle	Bertu et al., 2015
20	Nigeria_612	3	4	4	11	2	2	3	3	6	42	9	8	3	3	8	5	Nigeria	Sheep	Bertu et al., 2015
21	Nigeria_613	4	4	4	12	2	2	3	3	6	44	9	5	10	3	8	6	Nigeria	Cattle	Bertu et al., 2015
22	Nigeria_614	3	3	4	12	2	1	3	3	7	46	9	5	9	3	8	7	Nigeria	Cattle	Bertu et al., 2015
23	Nigeria_615	3	3	4	12	2	1	3	3	7	46	9	8	2	3	6	5	Nigeria	Cattle	Bertu et al., 2015
24	Nigeria_616	3	3	4	12	2	1	3	3	7	48	9	7	3	1	6	5	Nigeria	Cattle	Bertu et al., 2015
25	Nigeria_617	3	5	4	11	2	1	3	3	7	40	8	5	10	3	4	6	Nigeria	Cattle	Bertu et al., 2015
26	Nigeria_618	3	5	4	11	2	2	3	3	6	40	8	8	4	3	4	5	Nigeria	Horse	Bertu et al., 2015
27	Nigeria_619	3	5	4	11	2	1	3	3	6	40	8	5	10	3	4	6	Nigeria	Cattle	Bertu et al., 2015
28	Nigeria_620	4	5	4	12	2	2	3	3	7	40	8	8	4	3	4	5	Nigeria	Horse	Bertu et al., 2015
29	Kenya_11-KEBa2	3	5	4	11	2	2	3	3	7	40	8	6	5	3	12	5	Kenya	Cattle	Muendo et al., 2012
30	Kenya_12-KEBa1	3	5	4	11	2	2	3	3	7	40	8	6	6	3	11	6	Kenya	Cattle	Muendo et al., 2012
31	Tanzania_O64	2	4	2	12	3	2	3	3	5	–	8	7–8	2	6	7	4	Tanzania	Cattle	Mathew et al., 2015
32	Tanzania_O65	2	4	2	12	3	2	3	3	5	42–44	8	7–8	2	6	8	4	Tanzania	Cattle	Mathew et al., 2015
33	Tanzania_O66	2	4	2	12	3	2	3	3	5	42–44	8	7–8	2	6	8	4	Tanzania	Cattle	Mathew et al., 2015

^aFor each country, when the same MLVA profile is shared by more than one strain, only one genotype or distinct MLVA profile is presented. Here the 25 distinct genotypes of *Brucella abortus* biovar 3 obtained from 42 MLVA profiles found in the literature on West Africa (19 genotypes out of 34 profiles from Nigeria, 3 out of 3 profiles from Togo, 1 distinct genotype out of 3 profiles from the Gambia, 2 from each single profile reported from Ivory Coast and Niger) are presented with 5 strains from East Africa and 3 references strains from the MLVA bank;

^badditional locus comprised in the MLVA-16 and absent in MLVA-15;

^c*Brucella* Culture Collection;

^dFederal Institute for Risk Assessment;

^eisolate from Ivory Coast.

review papers reporting already published data covering sub-Saharan Africa in general (Boukary et al., 2013; Ducrottoy et al., 2017) and West Africa in particular (Sanogo et al., 2013a; Dean et al., 2014). Except from Nigeria, where strains came from both imported and autochthonous cattle and from sheep ($n = 2$) and horse ($n = 2$), strains originating from other countries were obtained from autochthonous cattle. None of the retrieved MLVA profiles were reported from humans so far. A total of 42 MLVA genotyping results were reported in the literature. Comparison of MLVA profiles of *B. abortus* biovar 3 field strains reported so far within West Africa revealed the presence of 25 distinct genotypes [e.g., a single genotype from the three strains isolated from The Gambia (Bankole et al., 2010), one from the unique strain from Niger (Boukary et al., 2013), one from the unique strain from Ivory Coast (Sanogo et al., 2013b), three genotypes from the three strains from Togo (Dean et al., 2014), and 19 genotypes from the 34 strains from Nigeria (Bertu et al., 2015)] (Figure 1).

While considering only panel 1 (MLVA 8), which is indicative of the species, diversity indexes of 0.620 (95% CI: 0.532–0.708), 0.580 (95% CI: 0.428–0.732), 0.477 (95% CI: 0.316–0.638), 0.280 (95% CI: 0.085–0.475), and 0.153 (95% CI: 0.000–0.332) were observed, respectively, at locus Bruce08, Bruce12, Bruce43, Bruc11, and Bruc06 with different genotypes. The others loci showed identical number of repeating units among the genotypes observed (e.g., Bruce42: 1; Bruce45: 1; Bruce55: 1) (Table 2). Highest diversity indexes were observed with the set of markers

composing panel 2, especially at Bruce16 (HGDI = 0.870, 95% CI: 0.808–0.932), known as one of the most variable locus. Within this panel 2, while considering highly discriminative markers (i.e., Bruce04, Bruce07, Bruce09, Bruce16, and Bruce30), three to nine different alleles were found.

DISCUSSION

For many years, *Brucella* spp. causing bovine brucellosis were characterized using both phenotypic and genotypic methods. While *B. abortus* biovar 1 have been reported as the most encountered in cattle worldwide (Corbel, 1997), in the USA (Bricker et al., 2003), and in Latin America (Acha and Szyfres, 2003; Lucero et al., 2008; Minharro et al., 2013), *B. abortus* biovar 3 was predominant in both native cattle and buffalo from eastern Africa and China (Timm, 1982; Domenech et al., 1983). *B. abortus* biovar 3 was also identified as the most commonly isolated in cattle from West Africa and Sub-Saharan Africa (Sanogo et al., 2013a; Bertu et al., 2015). In West Africa, where only *B. abortus* was reported so far, field strains of *B. abortus* biovar 3 were characterized mostly in cattle using a combination of bacteriological phenotypic typing and MLVA genotyping approaches. These West African isolates were mostly characterized from autochthonous cattle and from hygroma fluid samples. Phenotypic methods consisted of bacteriological isolation and identification and relied on a combination of morphological, cultural, serological and biochemical characteristics in order to characterize suspicious colonies (Alton et al., 1988). However, phenotypic typing methods may fail to correctly classify or differentiate some strains as in Nigeria (Bertu et al., 2015). Therefore, conventional bacteriological identification needs to be supplemented by molecular methods such as the VNTR analysis (MLVA). MLVA is a powerful molecular tool for typing and for assessing the potential relationships between *Brucella* spp. isolates from different sources of infection and from different geographical origins. It is a particularly useful method to study the molecular epidemiology of *Brucella* where a high discriminatory power is required (Bricker et al., 2003; Cutler et al., 2005; Le Flèche et al., 2006). Wherever possible, more accurate and discriminative typing methods such as the enhanced AMOS-ery PCR and MLVA should be used in complementarity with conventional biotyping methods (Ocampo-Sosa et al., 2005; Bankole et al., 2010; Sanogo et al., 2013b; Dean et al., 2014; Bertu et al., 2015).

Using panel 1 (MLVA8), 10 genotypes were obtained while 18 genotypes were obtained using the combination of panel 1 and 2B (MLVA11). The analysis of the complete MLVA16 (panels 1, 2A and 2B) revealed 25 distinct genotypes. Clustering analysis of the different MLVA profiles suggested the co-existence of distinct clonal complexes (Figure 3). While the three strains isolated from The Gambia shared the same profile, distinct profiles co-existed in Nigeria and Togo. The Togolese strains appeared to be related to many Nigerian strains and isolates from The Gambia. On the other hand, isolates from Niger and Ivory Coast appeared to be genetically related. In Nigeria where distinct profiles also co-exist, some isolates were more related to eastern African isolates originating from Tanzania and Kenya. These observations might

TABLE 2 | The Hunter Gaston Diversity Index for different loci of West African field strains of *B. abortus* biovar 3 (i.e., from Ivory Coast, Niger, Nigeria, The Gambia, and Togo) based on MLVA 16 data.

	Panel	Locus	Diversity index	95% Confidence interval	Number of alleles	Max(pi)
Panel 1		Bruce06	0.153	0.000–0.332	2	0.920
		Bruce08	0.620	0.532–0.708	3	0.480
		Bruce11	0.280	0.085–0.475	2	0.840
		Bruce12	0.580	0.428–0.732	3	0.600
		Bruce42	0.000	0.000–0.237	1	1.000
		Bruce43	0.477	0.316–0.638	3	0.680
		Bruce45	0.000	0.000–0.237	1	1.000
		Bruce55	0.000	0.000–0.237	1	1.000
Panel 2	Panel 2a	Bruce18	0.617	0.474–0.759	4	0.560
		Bruce19	0.720	0.547–0.893	8	0.520
		Bruce21	0.380	0.206–0.554	2	0.760
	Panel 2b	Bruce04	0.793	0.730–0.857	5	0.320
		Bruce07	0.833	0.755–0.912	8	0.320
		Bruce09	0.290	0.077–0.503	3	0.840
		Bruce16	0.870	0.808–0.932	9	0.240
		Bruce30	0.733	0.617–0.849	6	0.440

Diversity Index (for VNTR data): a measure of the variation of the number of repeats at each locus. It ranges from 0.0 (no diversity) to 1.0 (complete diversity).
Confidence Interval: precision of the Diversity Index, expressed as 95% upper and lower boundaries.
max (pi): fraction of samples that have the most frequent repeat number in this locus (range 0.0–1.0).

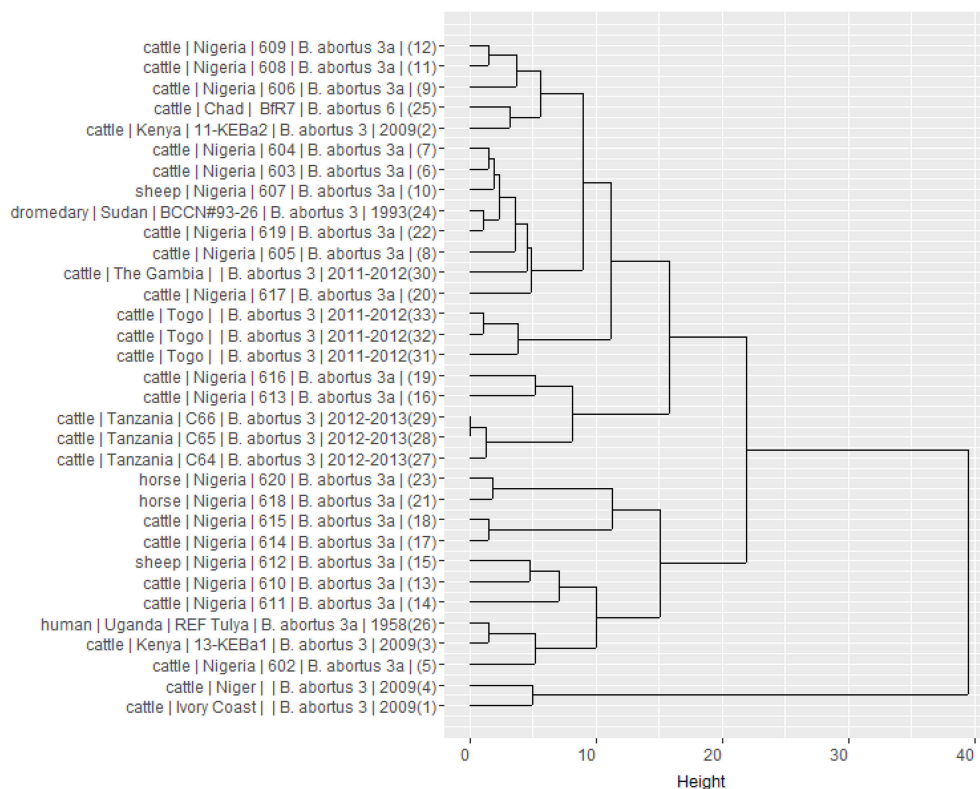


FIGURE 3 | Dendrogram clustered MLVA profiles showing the relation between the 25 West African isolates of *B. abortus* biovar 3 and eight neighbor profiles from Africa retrieved in the literature and from the *Brucella* MLVA bank. It is built from results of a Ward linkage cluster analysis of the number of variable tandem repeats (VNTR) of the MLVA 16 loci. For each strain, information on host, country of origin, strain reference, species and biovar, year of isolation (when available) and number of order in the database are provided.

suggest a possible relation between African *B. abortus* biovar 3 strains. Indeed, despite the relative limited number of strains compared, these results provide some preliminary indications on the co-existence of different genetic profiles among the prevailing field strains of *B. abortus* biovar 3 in this sub-region (Dean et al., 2014; Bertu et al., 2015). This heterogeneity among *B. abortus* biovar 3 strains originating from Africa was already described, with the North African strains more closely related to European *B. abortus* biovar 3b strain lineage and the sub-Saharan African strains more related to *B. abortus* biovar 3a lineage (Ocampo-Sosa et al., 2005; Ica et al., 2008; Bertu et al., 2015; Mathew et al., 2015; Ducrotoy et al., 2017). However, despite the genotypic diversity observed, the closeness of most of sub-Saharan African strains with the human reference Tulya strain from Uganda, put forward the hypothesis of the possible dominance of lineage 3a among West African *B. abortus* biovar 3 (Bertu et al., 2015; Ducrotoy et al., 2017) and a possible common historical origin of brucellosis in this region. Indeed, this lineage commonly isolated in West Africa is known to be confined in the African continent where *B. abortus* is believed to originate (Whatmore et al., 2016). Such a hypothesis associated with the observed polymorphisms is in line with unrestricted livestock movements through transhumance and trade among countries composing this sub-region (OECD, 2008), which might favor

frequent introduction and reintroduction of the pathogen. So far, data on prevailing strains of *Brucella* in both animal and human hosts are still scarce and irregularly reported (Sanogo et al., 2013a). In order to challenge such hypothesis and allow a better understanding of the epidemiology of brucellosis in West Africa, more molecular typing results are needed. In West Africa, brucellosis (or evidence of its presence) was reported in most of the 14 countries so far (Mangen et al., 2002; Boukary et al., 2013). Adequate and efficient control of brucellosis in this region implies a comprehensive understanding of its epidemiology at West African region scale, in order to include prevailing strains causing the disease and adjust diagnostic tools. Indeed, additional data on prevailing field strain of *Brucella* are required to identify the sources of infection and to understand the transmission pathways of this infection between animals and from animal to humans (Adone and Pasquali, 2013).

In conclusion, the number of strains analyzed in this study precludes an actual complete and comprehensive assessment of the relatedness of field strains of *B. abortus* biovar 3 in cattle from West Africa but provides preliminary indications on the co-existence of distinct profiles in this sub-region, in line with other recent findings (Bertu et al., 2015; Ducrotoy et al., 2017). More extended knowledge of prevailing strains in livestock and other hosts remains necessary to actually assess their

diversity and to fully understand the molecular epidemiology of *Brucella* infection, distribution, and transmission patterns within West Africa and across the whole African continent (Godfroid et al., 2013). By allowing comparison among strains, MLVA genotyping methods would also be useful as a surveillance tool of the distribution of brucellosis in West Africa, where frequent movements of livestock between countries are expected to play a role in the spread of *Brucellae*. So far, MLVA data from West Africa are not available from MLVA public database. It might be therefore suggested that studies publishing MLVA typing results explicitly report, share details profiles and be more informative. This is particularly critical for a sub-region where resources and molecular epidemiological investigations are limited.

Formal collaboration between countries and their respective public health actors is required for sharing available information and for implementing harmonized surveillance and control strategies. Such collaboration coupled with adoption of the concept of “One health approach” would be particularly beneficial in a regional framework, especially in West Africa where national resources and capabilities for prevention, control and surveillance of infectious diseases of public importance such as brucellosis are still scarce (Saegerman et al., 2010, 2012;

Marcotty et al., 2013). It is also essential to ensure a sustainable system of data collection on prevailing strains covering the whole West African region with a better coverage of other susceptible domestic and wild animals in order to document sources of human infections and to produce strong molecular evidence informing on the epidemiologic links between strains of *Brucella* within this region.

AUTHOR CONTRIBUTIONS

MS performed the literature review and the clustering analyses. MS and CS wrote the manuscript and all authors including DF and ET reviewed, commented and approved the final manuscript.

ACKNOWLEDGMENTS

The authors are grateful to the Institute of Tropical Medicine of Antwerp, to the bacteriology and immunology department of the Veterinary Agrochemical Research Centre of Brussels and the University of Liège in Belgium for their respective support. We are also grateful to Marie J. Ducrotoy, Virginie Mick, and Wilson Bertu for providing the MLVA profile from Nigeria.

REFERENCES

- Acha, P. N., and Szyfres, B. (eds.). (2003). “Brucellosis,” in *Zoonoses and Communicable Diseases Common to Man and Animals: Vol 1: Bacterioses and Mycoses, 3rd Edn*, (Washington, DC: Pan American Health Organization), 40–67.
- Adone, R., and Pasquali, P. (2013). Epidemiosurveillance of brucellosis. *Rev. Sci. Tech. Off. Int. Epiz.* 32, 199–205. doi: 10.20506/rst.32.1.2202
- Akakpo, A. J., and Bornarel, P. (1987). Epidémiologie des brucelloses animales en Afrique tropicale: enquêtes clinique, sérologique et bactériologique. *Rev. Sci. Tech. Off. Int. Epiz.* 6, 981–1027. doi: 10.20506/rst.6.4.313
- Alton, G. G., Jones, L. M., Angus, R. D., and Verger, J. M. (1988). *Techniques for the Brucellosis Laboratory*. Paris: INRA.
- Bankole, A. A., Saegerman, C., Berkvens, D., Fretin, D., Geerts, S., Ieven, G., et al. (2010). Phenotypic and genotypic characterisation of *Brucella* strains isolated from cattle in The Gambia. *Vet. Rec.* 166, 753–756. doi: 10.1136/vr.b4862
- Bertu, W. J., Ducrotoy, M. J., Mu-oz, P. M., Mick, V., Zú-iga-Ripa, A., Bryssinckx, W., et al. (2015). Phenotypic and genotypic characterization of *Brucella* strains isolated from autochthonous livestock reveals the dominance of *B. abortus* biovar 3a in Nigeria. *Vet. Microbiol.* 180, 103–108. doi: 10.1016/j.vetmic.2015.08.014
- Boukary, A. R., Saegerman, C., Abatih, E., Fretin, D., Alambédji Bada, R., De Deken, R., et al. (2013). Seroprevalence and potential risk factors for *Brucella* spp. infection in traditional cattle, sheep and goats reared in urban, periurban and rural areas of Niger. *PLoS ONE* 8:e83175. doi: 10.1371/journal.pone.0083175
- Bricker, B. J., Ewalt, D. R., and Halling, S. M. (2003). *Brucella* “HOOFprints”: strain typing by multi-locus analysis of variable number tandem repeats (VNTRs). *BMC Microbiol.* 3:15. doi: 10.1186/1471-2180-3-15
- Bronsvort, B. M. D., Koterwas, B., Land, F., Handel, I. G., Tucker, J., Morgan, K. L., et al. (2009). Comparison of a flow assay for brucellosis antibodies with the reference cELISA test in West African *Bos indicus*. *PLoS ONE* 4:e5221. doi: 10.1371/journal.pone.0005221
- Cáceres, S. B. (2010). *Comparative Veterinary Capacity in Western Africa: Implications for Livestock Development*. Livestock Research for Rural Development. Available online at: <http://www.lrrd.org/lrrd22/10/burg22180.htm> (Accessed May 26, 2017).
- Corbel, M. J. (1997). Brucellosis: an overview (1st International conference on emerging zoonosis). *Emerg. Infect. Dis.* 3, 213–221. doi: 10.3201/eid0302.970219
- Corbel, M. J. (2006). *Brucellosis in Humans and Animals*. Geneva: World Health Organization (WHO) Press.
- Cutler, S. J., Whatmore, A. M., and Commander, N. J. (2005). Brucellosis - new aspects of an old disease. *J. Appl. Microbiol.* 98, 1270–1281. doi: 10.1111/j.1365-2672.2005.02622.x
- Dean, A. S., Schelling, E., Bonfoh, B., Kulo, A. E., Boukaya, G. A., and Pilo, P. (2014). Deletion in the gene BruAb2_0168 of *Brucella abortus* strains: diagnostic challenges. *Clin. Microbiol. Infect.* 20, O550–O553. doi: 10.1111/1469-0691.12554
- Domenech, J., Corbel, M. J., Thomas, E. L., and Lucet, Ph. (1983). La brucellose bovine en Afrique centrale: VI. Identification et typage des souches isolées au Tchad et au Cameroun. *Rev. Elev. Med. Vet. Pays Trop.* 36, 19–25.
- Ducrotoy, M., Bertu, W. J., Matope, G., Cadmus, S., Conde-Álvarez, R., Gusi, A. M., et al. (2017). Brucellosis in Sub-Saharan Africa: current challenges for management, diagnosis and control. *Acta Trop.* 165, 179–193. doi: 10.1016/j.actatropica.2015.10.023
- FAO (Food And Agricultural Organization) (2017). FAOSTAT. Food and Agricultural Organization Statistic Division Available online at: <http://www.fao.org/faostat/fr/#data/QA> (Accessed May 26, 2017).
- Godfroid, J., Al Dahouk, S., Pappas, G., Roth, F., Matope, G., Muma, J., et al. (2013). A “One Health” surveillance and control of brucellosis in developing countries: moving away from improvisation. *Comp. Immunol. Microbiol. Infect. Dis.* 36, 241–248. doi: 10.1016/j.cimid.2012.09.001
- Hunter, P. R., and Gaston, M. A. (1988). Numerical index of the discriminatory ability of typing systems: an application of Simpson's index of diversity. *J. Clin. Microbiol.* 26, 2465–2466.
- Ica, T., Aydin, F., Erdenlig, S., Guler, L., and Büyükcangaz, E. (2008). Characterization of *Brucella abortus* biovar 3 isolates from Turkey as biovar 3b. *Vet. Rec.* 63, 659–661. doi: 10.1136/vr.163.22.659
- Le Flèche, P., Jacques, I., Grayon, M., Al Dahouk, S., Bouchon, N. P., Denoeud, F., et al. (2006). Evaluation and selection of tandem repeat loci for a *Brucella* MLVA typing assay. *BMC Microbiol.* 6:9. doi: 10.1186/1471-2180-6-9
- Lucero, N. E., Ayala, S. M., Escobar, G. I., and Jacob, N. R. (2008). *Brucella* isolated in humans and animals in Latin America from 1968 to 2006. *Epidemiol. Infect.* 136, 496–503. doi: 10.1017/S0950268807008795

- Mangen, M. J., Otte, J., Pfeiffer, D., and Chilonda, P. (2002). *Bovine Brucellosis in sub-Saharan Africa: Estimation of Sero-Prevalence and Impact on Meat and Milk Offtake Potential*. Rome: FAO Livestock Information and Policy Branch; AGAL. Livestock Policy Paper n°8.
- Maquart, M., Le Flèche, P., Foster, G., Tryland, M., Ramisse, F., Djønne, B., et al. (2009). MLVA-16 typing of 295 marine mammal *Brucella* isolates from different animal and geographic origins identifies 7 major groups within *Brucella ceti* and *Brucella pinnipedialis*. *BMC Microbiol.* 9:145. doi: 10.1186/1471-2180-9-145
- Marcotty, T., Thys, E., Conrad, P., Godfroid, J., Craig, P., Zinsstag, J., et al. (2013). Intersectoral collaboration between the medical and veterinary professions in low-resource societies: the role of research and training institutions. *Comp. Immunol. Microbiol. Infect. Dis.* 36, 233–239. doi: 10.1016/j.cimid.2012.10.009
- Mathew, C., Stokstad, M., Johansen, T. B., Klevar, S., Mdegela, R. H., Mwamengele, G., et al. (2015). First isolation, identification, phenotypic and genotypic characterization of *Brucella abortus* biovar 3 from dairy cattle in Tanzania. *BMC Vet. Res.* 11:156. doi: 10.1186/s12917-015-0476-8
- Maurin, M. (2005). La brucellose à l'aube du 21ème siècle. *Med. Maladies Infect.* 35, 6–16. doi: 10.1016/j.medmal.2004.08.003
- McDermott, J. J., and Arimi, S. M. (2002). Brucellosis in sub-Saharan Africa: epidemiology, control and impact. *Vet. Microbiol.* 90, 111–134. doi: 10.1016/S0378-1135(02)00249-3
- Minharro, S., Mol, J. P., Dorneles, E. M. S., Barbosa, R. P., Neubauer, H., Melzer, F., et al. (2013). Biotyping and genotyping (MLVA16) of *Brucella abortus* isolated from cattle in Brazil, 1977 to 2008. *PLoS ONE* 8:e81152. doi: 10.1371/journal.pone.0081152
- Moher, D., Liberati, A., Tetzlaff, J., Altman, D. G., and The Prisma Group (2009). Preferred reporting items for systematic reviews and meta-analyses: the PRISMA statement. *PLoS Med.* 6:e1000097. doi: 10.1371/journal.pmed.1000097
- Muendo, E., Mbatha, P., Macharia, J., Abdoel, T., Janszen, P., Pastoor, R., et al. (2012). Infection of cattle in Kenya with *Brucella abortus* biovar 3 and *Brucella melitensis* biovar 1 genotypes. *Trop. Anim. Health Prod.* 44, 17–20. doi: 10.1007/s11250-011-9899-9
- Ocampo-Sosa, A. A., Aguero-Balbin, J., and Garcia-Lobo, J. M. (2005). Development of a new PCR assay to identify *Brucella abortus* biovars 5, 6 and 9 and the new subgroup 3b of biovar 3. *Vet. Microbiol.* 110, 41–51. doi: 10.1016/j.vetmic.2005.06.007
- Organization for Economic Co-operation and Development (OECD) (2008). *Livestock and Regional Market in the Sahel and West Africa: Potentials and Challenges*. Paris. Available online at: <http://www.oecd.org/swac/publications/41848366.pdf>
- Pappas, G., Papadimitriou, P., Akritidis, N., Christou, L., and Tsianos, E. V. (2006). The new global map of human brucellosis. *Lancet Infect. Dis.* 6, 91–99. doi: 10.1016/S1473-3099(06)70382-6
- Perry, B. (2002). “Chapter 7: animal disease impact on the poor: study results,” in *Investing in Animal Research to Alleviate Poverty*. Nairobi: International Livestock Research Institute. Available online at: http://ilri.org/infoserv/Webpub/fulldocs/InvestAnim/Book1/media/PDF_chapters/B1_7.pdf
- Saegerman, C., Berkvens, D., Godfroid, J., and Walravens, K. (2010). “Bovine brucellosis,” in *Infectious and Parasitic Diseases of Livestock*, eds P. Lefèvre, J. Blancou, R. Chermette, and G. Uilenberg (Paris: Lavoisier et Commonwealth Agricultural Bureau – International), 971–1001.
- Saegerman, C., Dal Pozzo, F., and Humblet, M.-F. (2012). Reducing hazards for humans from animals: emerging and re-emerging zoonoses. *Ital. J. Public Health* 9, 13–24. doi: 10.2427/6336
- Sanogo, M., Abatih, E., Thys, E., Fretin, D., Berkvens, D., and Saegerman, C. (2013a). Importance of identification and typing of *Brucellae* from West African cattle: a review. *Vet. Microbiol.* 164, 202–211. doi: 10.1016/j.vetmic.2013.02.009
- Sanogo, M., Thys, E., Achi, Y. L., Fretin, D., Michel, P., Abatih, E., et al. (2013b). Bayesian estimation of true prevalence, sensitivity and specificity of Rose Bengal test and indirect ELISA for the diagnosis of bovine brucellosis. *Vet. J.* 195, 114–120. doi: 10.1016/j.tvjl.2012.06.007
- Timm, B. M. (1982). *Brucellosis. Distribution in Man, Domestic and Wild Animals*. Berlin: Springer.
- Whatmore, A. M., Koylass, M. S., Muchowski, J., Edwards-Smallbone, J., Gopaul, K. K., and Perrett, L. L. (2016). Extended multilocus sequence analysis to describe the global population structure of the genus *brucella*: phylogeography and relationship to biovars. *Front. Microbiol.* 7:2049. doi: 10.3389/fmicb.2016.02049

Conflict of Interest Statement: The authors declare that the research was conducted in the absence of any commercial or financial relationships that could be construed as a potential conflict of interest.

Copyright © 2017 Sanogo, Fretin, Thys and Saegerman. This is an open-access article distributed under the terms of the Creative Commons Attribution License (CC BY). The use, distribution or reproduction in other forums is permitted, provided the original author(s) or licensor are credited and that the original publication in this journal is cited, in accordance with accepted academic practice. No use, distribution or reproduction is permitted which does not comply with these terms.



Prevalence, Host Range, and Comparative Genomic Analysis of Temperate *Ochrobactrum* Phages

Claudia Jäckel^{1†}, Stefan Hertwig^{1†}, Holger C. Scholz², Karsten Nöckler¹, Jochen Reetz¹ and Jens A. Hammerl^{1*}

¹ Department of Biological Safety, German Federal Institute for Risk Assessment, Berlin, Germany, ² German Center for Infection Research, Bundeswehr Institute of Microbiology, Munich, Germany

OPEN ACCESS

Edited by:

Yuji Morita,
Aichi Gakuin University, Japan

Reviewed by:

Juan M. Tomas,
University of Barcelona, Spain
Jason Farlow,
Farlow Scientific Consulting Company,
United States
David O'Callaghan,
Université de Montpellier, France

*Correspondence:

Jens A. Hammerl
jens-andre.hammerl@bfr.bund.de

[†]These authors have contributed
equally to this work.

Specialty section:

This article was submitted to
Infectious Diseases,
a section of the journal
Frontiers in Microbiology

Received: 06 March 2017

Accepted: 14 June 2017

Published: 30 June 2017

Citation:

Jäckel C, Hertwig S, Scholz HC,
Nöckler K, Reetz J and Hammerl JA
(2017) Prevalence, Host Range, and
Comparative Genomic Analysis of
Temperate *Ochrobactrum* Phages.
Front. Microbiol. 8:1207.
doi: 10.3389/fmicb.2017.01207

Ochrobactrum and *Brucella* are closely related bacteria that populate different habitats and differ in their pathogenic properties. Only little is known about mobile genetic elements in these genera which might be important for survival and virulence. Previous studies on *Brucella* lysogeny indicated that active phages are rare in this genus. To gain insight into the presence and nature of prophages in *Ochrobactrum*, temperate phages were isolated from various species and characterized in detail. *In silico* analyses disclosed numerous prophages in published *Ochrobactrum* genomes. Induction experiments showed that *Ochrobactrum* prophages can be induced by various stress factors and that some strains released phage particles even under non-induced conditions. Sixty percent of lysates prepared from 125 strains revealed lytic activity. The host range and DNA similarities of 19 phages belonging to the families *Myoviridae*, *Siphoviridae*, or *Podoviridae* were determined suggesting that they are highly diverse. Some phages showed relationship to the temperate *Brucella inopinata* phage BiPB01. The genomic sequences of the myovirus POA1180 (41,655 bp) and podovirus POI1126 (60,065 bp) were analyzed. Phage POA1180 is very similar to a prophage recently identified in a *Brucella* strain isolated from an exotic frog. The POA1180 genome contains genes which may confer resistance to chromate and the ability to take up sulfate. Phage POI1126 is related to podoviruses of *Sinorhizobium meliloti* (PCB5), *Erwinia pyrifoliae* (Pep14), and *Burkholderia cenocepacia* (BcepIL02) and almost identical to an unnamed plasmid of the *Ochrobactrum intermedium* strain LMG 3301. Further experiments revealed that the POI1126 prophage indeed replicates as an extrachromosomal element. The data demonstrate for the first time that active prophages are common in *Ochrobactrum* and suggest that atypical brucellae also may be a reservoir for temperate phages.

Keywords: *Ochrobactrum*, prophage, genome, temperate, lysogeny, phage, *Brucella*

INTRODUCTION

Ochrobactrum species are non-fermenting, aerobic, gram-negative bacilli that are widespread in the environment and have been isolated from various ecological niches, such as water, soil, plants, and animals (Jelveh and Cunha, 1999; Möller et al., 1999; Lebuhn et al., 2000; Goris et al., 2003; Kämpfer et al., 2003; Bathe et al., 2006). Some *Ochrobactrum* strains belonging to

different species were studied for their potential to degrade chemical pollutants and for heavy metal detoxification under a wide range of environmental conditions (El-Sayed et al., 2003; Zhang et al., 2006; Sultan and Hasnain, 2007). The α -proteobacterial genus *Ochrobactrum* belongs to the family *Brucellaceae* and contains to date 16 species, the type species of which is *Ochrobactrum anthropi* (Kämpfer et al., 2011). The closest relatives of *Ochrobactrum* spp. are brucellae (Scholz et al., 2008). *Ochrobactrum intermedium* e.g., shares 98.8% 16S rRNA gene similarity with *Brucella* spp. and is more closely related to this genus than to other *Ochrobactrum* species (Velasco et al., 1998; Lebuhr et al., 2000, 2006). However, while brucellae are well-recognized as important pathogens that cause brucellosis in man and many animal species, *Ochrobactrum* strains, particularly those belonging to the species *O. anthropi* and *O. intermedium*, have for a long time been regarded as opportunistic human pathogens of low virulence, infecting only immunocompromised patients with underlying diseases (Scholz et al., 2008). Nevertheless, the number of publications on opportunistic/nosocomial infections caused by *O. anthropi* has increased over the last decade (Shrishrimal, 2012; Mudshingkar et al., 2013; Siti Rohani and Tzar, 2013). Moreover, a rising number of reported cases included some potentially life-threatening infections, such as endocarditis (Mahmood et al., 2000; Daxboeck et al., 2002; Romero Gomez et al., 2004). The ability of *O. anthropi* to adhere to silicone may play a role in catheter-associated infections (Wi and Peck, 2010; Qasimyar et al., 2014). Some reports describe severe *O. anthropi* infections even in immunocompetent hosts with a clinical presentation similar to brucellosis (Kettaneh et al., 2003; Romero Gomez et al., 2004; Perez-Blanco et al., 2005; Ozdemir et al., 2006). *O. anthropi* often exhibits an intrinsic multi-resistance to antibiotics (Thoma et al., 2009; Johnning et al., 2013). While the location and transmission of virulence and antibiotic resistance genes is commonly associated with mobile genetic elements (MGE) like plasmids and phages, only little is known about MGE of *Ochrobactrum* and the related genus *Brucella*.

In *O. anthropi* ATCC 49188, four plasmids encoding several transporters have been identified which may contribute to the fitness of the strain (Chain et al., 2011). *Ochrobactrum* strain TD contained three linear plasmids, that allowed the strain to use vinyl chloride and ethene as growth substrates (Danko et al., 2004). By contrast, there are yet no reports on phages of *Ochrobactrum*. In *Brucella* the first temperate phage (BiPB01) has recently been described (Hammerl et al., 2016). BiPB01 revealed a broad host range within the genus *Brucella*. Its attachment site within the bacterial chromosome also exists in *Ochrobactrum*. Even though *Ochrobactrum* strains were not lysed by the phage, it showed significant DNA homologies to prophages of *Ochrobactrum*, particularly to a prophage residing in chromosome 1 of the *O. anthropi* strain ATCC 49188 indicating that temperate phages might occur in *Ochrobactrum* spp. as well.

In this study the presence of prophages in *Ochrobactrum* was determined followed by induction experiments to isolate and characterize temperate phages. *In silico* analyses revealed numerous prophages in the published sequences of 19

Ochrobactrum strains. Prophages could be induced by various stress factors. Phage particles were isolated from 19 lysates and characterized in terms of their morphology, host range and genetic relationship. The genomic sequences of two phages (POI1126 and POA1180) were determined and analyzed in detail.

MATERIALS AND METHODS

Bacterial Strains, Media, and Growth Conditions

All strains used in this study were obtained from the strain collections of the Bundeswehr Institute of Microbiology (Munich) and Federal Institute for Risk Assessment (Berlin). Information on the relevant strains is summarized in **Table 1**. If not otherwise indicated bacteria were cultivated aerobically in lysogeny broth (LB) (Carl Roth, Karlsruhe, Germany) at 28°C for 24 h under shaking conditions (180–200 rpm). Solid and overlay agar contained 1.8% (w/v) and 0.6% (w/v) bacto-agar No. 1 (Oxoid, Wesel, Germany), respectively.

Prophage Induction

To optimize the induction of *Ochrobactrum* prophages, various stress factors (mitomycin C, heat, UV) were investigated. At an adsorption ($A_{588\text{nm}}$) of 0.2–0.3, 10 ml bacterial cultures were treated with different mitomycin C concentrations (0.5–10 $\mu\text{g/ml}$), heat (50, 60, or 70°C for 30 and 60 s) or UV (for 30 and 60 s). Thereafter, cultures were incubated under standard conditions for 16–18 h. UV treatment was performed by applying aliquots of the culture into petri dishes ($d = 90\text{ mm}$), which were placed in a distance of 10 cm to an UV lamp (corresponding 45 J m^{-2}). UV radiation treatment was performed for 30 or 60 s. To obtain cell-free lysates, samples were centrifuged for 15 min at $6,000 \times g$ and filtrated through 0.22 μm sterile filters (GE Healthcare, Munich, Germany). Lytic activity was quantified by spotting 10 μl aliquots of a 1:10 dilution series onto lawns of susceptible *Ochrobactrum* strains. All strains were investigated in triplicate under the respective induction conditions. For further characterization, plaques of POA1180 and POI1126 were purified by a three-fold single plaque purification procedure.

Isolation, Propagation, and Purification of POA1180 and POI1126

Phages POA1180 and POI1126 were recovered by mitomycin C (0.5 $\mu\text{g/ml}$) treatment of strains *O. anthropi* O1180 and *O. intermedium* O1126, respectively. High titer lysates were prepared from 200 ml cultures. Cell-free lysates were obtained by centrifugation at $6,000 \times g$ for 30 min and filtration of the supernatants through 0.22 μm sterile pore-size filters (GE Healthcare, Munich, Germany). To remove bacterial DNA and RNA, phage lysates were supplemented with 10 mM MgCl_2 , 10 $\mu\text{g ml}^{-1}$ DNaseI and RNase A (Roche, Mannheim, Germany) followed by an incubation at 37°C for 2 h. Phage particles were concentrated by ultracentrifugation (Beckman) for 4 h at $200,000 \times g$. Concentrated phages were resuspended in SM-buffer and purified by discontinuous gradient (CsCl , 1.35–1.65 g ml^{-1}) centrifugation at $141,000 \times g$ for 18 h (Sambrook

TABLE 1 | Bacterial strains used in this study.

<i>Ochrobactrum</i> spp. strains	Other designation, country (source)	Designation of the Bundeswehr Institute collection
<i>O. anthropi</i>		
O1129	LMG3331, France (unknown)	B-1129
O1154	CCUG20020, Sweden (human blood)	B-1154
O1157	CCUG24695	B-1157
O1163	CCUG34461	B-1163
O1172	LMG3329	B-1172
O1178	LMG33, Denmark (human spinal fluid)	B-1178
O1180	WS4292	B-1180
O1199	DSM20150	B-1199
O1215	LMG5442	B-1215
<i>O. intermedium</i>		
O1126	LMG3301T, France (human blood)	LMG3301T
O1132	LMG3306, France (soil)	B-1132
O1135	OIC8-6	B-1135
O1147	CCUG1838	B-1147
O1191	TD30	B-1191
O1216	LMG5446, USA (bladder)	B-1216
O1218	CCM7036	B-1218
<i>O. tritici</i>		
O1114	LAIII-106	B-1114
O1184	WS1830	B-1184
O1187	WS1846	B-1187
<i>O. dultii</i>		
O1205	CCUG30717, Sweden (human blood)	B-1205
O1206	CCUG43892, Norway (human, amniotic fluid)	B-1206
<i>O. pseudintermedium</i>		
O1164	CCUG34735, Sweden (water)	B-1164
<i>O. oryzae</i>		
O1196	DSM17471, India (deep water rice roots)	B-1196
<i>O. gallinifaeces</i>		
O1142	ISO1965	B-1142
<i>O. haemophilum</i>		
O1166	CCUG38531, Sweden (human blood)	B-1166

ATCC, American Type Culture Collection; BCCM/LMG, Belgian Co-ordinated Collection of Microorganisms.

Host Range Determination of the Phages

The host range of the phages (e.g., POA1180, POI1126) was determined by spot assays. This was performed by applying 100–200 µl of each *Ochrobactrum* spp. strain to 6 ml LB soft agar (0.6%) and pouring of the overlay agar onto a LB agar plate. Aliquots of 1:10 serial dilutions of phage lysates were dropped onto the lawn of the solidified overlay agar. After 24 h spotting areas were visually inspected for plaque formation. Lytic activity was examined on strains of *Ochrobactrum* spp. ($n = 119$), *Brucella* spp. (26 reference and type strains), *Mesorhizobium* ($n = 6$), *Sinorhizobium* ($n = 5$), *Pseudomonas* ($n = 5$) and *Yersinia enterocolitica* O:9 ($n = 4$).

Transmission Electron Microscopy

CsCl-purified phages were applied to pioloform-carbon-coated, 400-mesh copper grids (Plano GmbH, Germany), for 10 min, fixed with 2.5% aqueous glutaraldehyde solution for 1 min, stained with 2% aqueous uranyl acetate solution for 1 min and examined using a JEM-1010 (JOEL, Tokyo, Japan) transmission electron microscope at 80 kV accelerated voltage.

Extraction of Phage DNA and Sequencing

Phage DNA was extracted from CsCl-purified particles by proteinase K/SDS treatment and ethanol precipitation (Sambrook and Russell, 2001). Thereafter, the phage DNA was resuspended in $0.5 \times$ TE-buffer (pH 8.0) for further analyses. Sequencing libraries were prepared using the Nextera XT DNA Sample Preparation Kit according to the recommendations of the manufacturer. Paired-end sequencing was performed on the Illumina MiSeq benchtop using the MiSeq Reagent v3 600-cycle Kit (2×300 cycles) (Illumina, CA, USA). Raw reads were assembled *de novo* using tools of the Pathosystems Resource Integration Center resulting in a single contig with an average sequence coverage of more than 120 and 100 per consensus base for POA1180 and POI1126, respectively. DNA hybridization was conducted using the Roche digoxigenin hybridization system on positively charged nylon membranes according to the manufacture's procedure (Roche, Heidelberg, Germany).

Bioinformatic Analysis

To identify putative prophage sequences in the available *Ochrobactrum* spp. genomes of GenBank (NCBI), the Phage Search Tool-PHAST was used (Zhou et al., 2011). Sequence analysis and alignments were carried out using Accelrys Gene v2.5 (Accelrys Inc., San Diego, CA, USA). Identification of genetic elements like ORFs, transcription terminators, and tRNAs on the phage genome was conducted as previously described (Hammerl et al., 2011, 2016). Similarity and identity values were determined at the NCBI homepage using different BLAST algorithms (Johnson et al., 2008). Annotation of the phage genomes was performed by using Sequin (<https://www.ncbi.nlm.nih.gov/Sequin/>).

Nucleotide Sequence Accession Numbers

The complete nucleotide sequences of the *O. anthropi* POA1180 and *O. intermedium* POI1126 phage genomes were submitted

and Russell, 2001). After centrifugation phage bands were removed and desalted by 100K Amicon Ultra centrifugal filter columns (Merck Millipore, Schwalbach, Germany).

to GenBank under the accession numbers KX669658 and KY417925, respectively.

RESULTS

Prophage Sequences Are Widely Distributed in *Ochrobactrum*

To get a first overview on the presence of prophage DNA in *Ochrobactrum* spp., 19 strains representing several species whose genome sequences have been published, were analyzed by automated *in silico* analyses using the PHAge Search Tool (PHAST) (Zhou et al., 2011). We identified prophage sequences (6.9–91.8 kb in size) in all analyzed *Ochrobactrum* species. Between two and ten putative phage genomes were detected in each strain (Table 2). Highly prevalent was a 17.3–91.8 kb DNA region that showed significant similarity to the *Sinorhizobium meliloti* phage 16-3, which possesses a genome of 60 kb (Deak et al., 2010). The second most frequent prophage was represented by a DNA region of 25.3–56.8 kb revealing close relationship to phage AmM-1 isolated from the Rhizobiales deep-sea bacterium *Aurantimonas* sp. whose genome has a size of 47.8 kb (Yoshida et al., 2015). Most of the remaining prophages in *Ochrobactrum* spp. are similar to other *Rhizobium* phages but homologies to

phages of *Rhodobacter*, *Pseudomonas*, various *Enterobacteriaceae* and even *Bacillus* were also detected (Table 2). According to the results obtained by *in silico* analyses, some of the prophages may be complete and intact. The GC content of the prophages ranges between 49.7 and 65% whereas the average GC content of *O. anthropi* is 56%, suggesting that some *Ochrobactrum* strains may have acquired temperate phages from different hosts through horizontal gene transfer (Table S2).

Ochrobactrum Prophages Can Be Easily Induced by Stress Factors

In this study, 125 *Ochrobactrum* strains of various species deposited in the strain collection of the BfR were analyzed in terms of inducible prophages. We first compared the efficacy of various stress factors (mitomycin C, UV, high temperature) on the release of phage particles. For this purpose, the strains *O. anthropi* O1180 (Figure 1A) and *O. intermedium* O1126 (data not shown) were treated with different concentrations (0.5, 2.5, and 10.0 µg/ml) of mitomycin C, heat (50, 60, 70°C for 30 and 60 s) and UV (45 J m⁻² for 30 and 60 s). Thereafter, the strains were further incubated at 28 and 37°C. At both temperatures bacterial growth was inhibited in response to the tested stress factors, particularly mitomycin C, even though prophage induction at 37°C occurred earlier in most preparations. As shown in Figure 1B even the untreated control of both strains released 10⁴ to 10⁵ phages per milliliter (Table 3). Under stress conditions titers up to 2 × 10⁸ pfu/ml were determined. In general, all tested stress factors were suitable to induce prophages, albeit phage titers achieved in the individual approaches differed significantly from each other. *O. anthropi* strain O1180 revealed much stronger temperature dependence than *O. intermedium* O1126. Some phage titers obtained at 28°C were two to three orders of magnitude higher than those of the corresponding lysates at 37°C. Moreover, whereas UV treatment was the most efficient method to induce prophages in *O. anthropi*, the highest phage titers in *O. intermedium* were achieved with a mitomycin C concentration of 0.5 µg/ml. Thus, *Ochrobactrum* strains diverge significantly regarding their sensitivity to prophage inducers. Based on the results of this study, subsequent induction experiments with a broad range (*n* = 125) of *Ochrobactrum* spp. strains were performed with 0.5 µg/ml mitomycin C at 28°C.

The 125 prepared lysates were tested for their lytic activity by spotting aliquots on all 125 *Ochrobactrum* spp. strains. As an additional indicator for released particles, DNA was isolated from the lysates. Plaques were observed with ~60% of the lysates. Up to 20 strains were susceptible to each lysate. In most cases several *Ochrobactrum* species were lysed. To get a deeper insight into the released phages, 19 lysates originating from *O. anthropi*, *O. intermedium*, *Ochrobactrum tritici*, *O. dultfi*, and *Ochrobactrum* sp., from which significant amounts of encapsidated phage DNA could be isolated (data not shown) were selected for further analyses. Electron microscopic examination revealed phage particles in all lysates, even though four of them did not show lytic activity. According to their morphology, the identified

TABLE 2 | Prophage content of published *Ochrobactrum* sp. genomes.

Strain	Intact (Size)	Questionable (Size)	Incomplete (Size)
<i>O. anthropi</i>			
ATCC 49188	3 (17.2–22.3 kb)	n.d.	2 (17.5–22.6 kb)
ATCC 49687 (OAB)	n.d.	1 (18.0 kb)	1 (13.0 kb)
ML7	3 (41.0–56.8 kb)	3 (12.5–17.8 kb)	n.d.
W13P3	n.d.	5 (15.3–46.3 kb)	1 (7.1 kb)
60a	n.d.	n.d.	2 (8.2–10.5 kb)
CTS-325	n.d.	2 (11.7–22.7 kb)	n.d.
FRAF13	1 (25.3 kb)	1 (54.0 kb)	2 (8.5–26.1 kb)
<i>O. intermedium</i>			
LMG 3301	2 (40.8–48.8 kb)	1 (33.1 kb)	1 (27.4 kb)
2745-2	1 (51.0 kb)	3 (15.5–40.1 kb)	n.d.
M86	3 (23.5–54.3 kb)	4 (9.2–30.5 kb)	2 (6.9–17.3 kb)
CCUG 57381 (299E)	n.d.	n.d.	2 (8.3–10.6 kb)
2745-2	1 (51.0 kb)	n.d.	n.d.
KCJK1738	1 (25.3 kb)	1 (54.0 kb)	2 (8.5–26.1 kb)
<i>Ochrobactrum</i> spp.			
<i>O. pseudogrignonense</i> K8	2 (13.1–13.7 kb)	1 (36.9 kb)	n.d.
<i>Ochrobactrum</i> sp. CDB2	2 (13.8–61.9 kb)	n.d.	1 (26.4 kb)
<i>O. rhizosphaerae</i> SJY1	6 (13.9–91.8 kb)	n.d.	1 (15.1 kb)
<i>Ochrobactrum</i> sp. EGD-AQ16	n.d.	n.d.	3 (7.5–14.9 kb)
<i>Ochrobactrum</i> sp. UNC390CL2Tsu3S39 BS36	1 (23.1 kb)	n.d.	2 (10.2–26.5 kb)

n.d., Not detected.

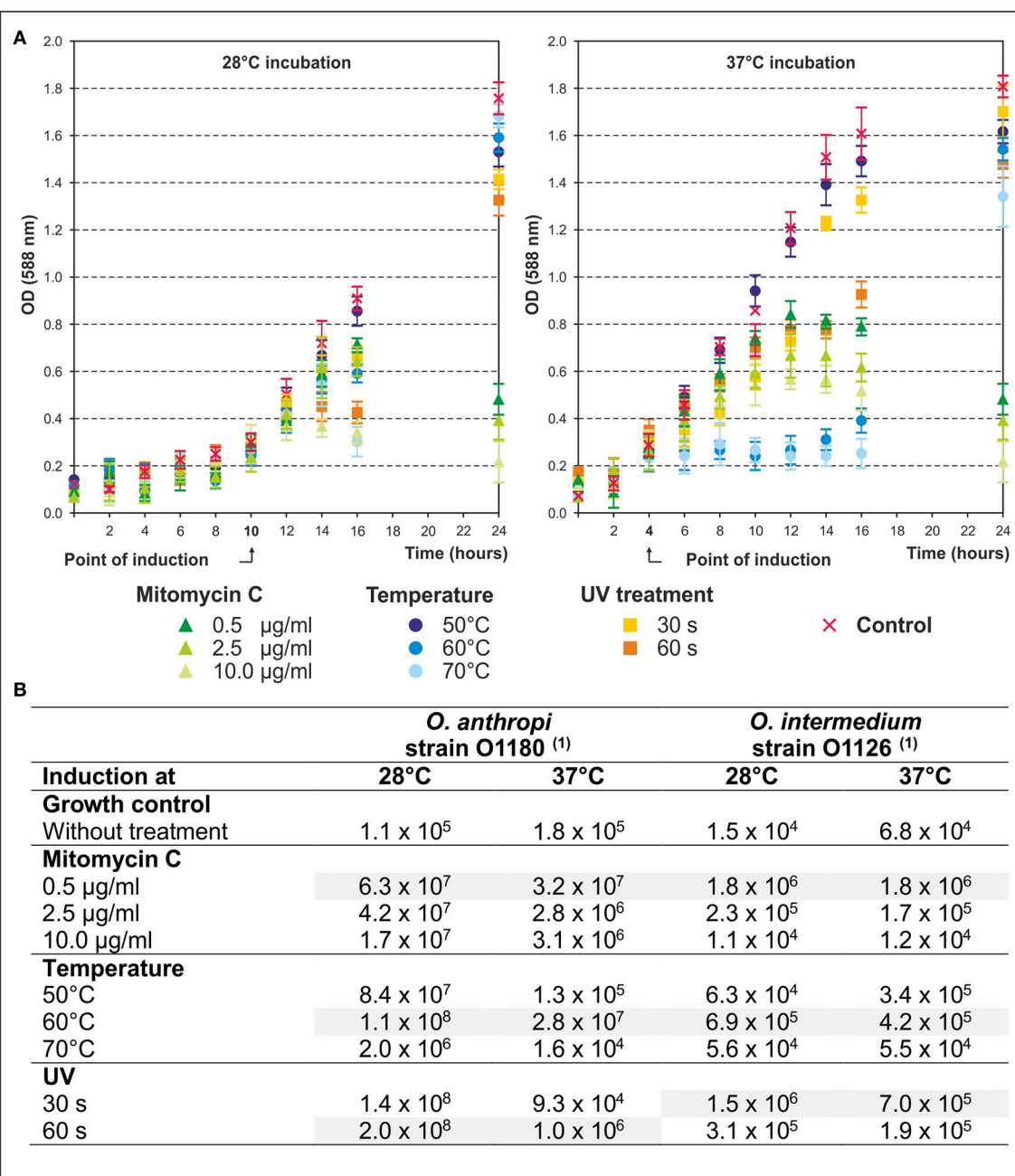


FIGURE 1 | Efficacy of phage release during mitomycin C, temperature, and UV treatment. **(A)** In the diagrams the bacterial growth of *O. anthropi* strain O1180 during stress treatment at 28 and 37°C is shown. Given are mean values of three independent experiments. Error bars indicate the standard deviation from the mean value. The point of induction (OD_{588nm}) is indicated. **(B)** The table summarizes the results of the phage induction by different stress factors. The phage titer is given in pfu/ml. ⁽¹⁾ Plaque formation was investigated on *O. anthropi* strain O1129.

phages belong to different families (Table 4). Most prominent was the family *Myoviridae* represented by phages with an isodiametric or elongated head and a contractile tail. Some lysates contained particles with a long, non-contractile and very short tail, which are members of the *Siphoviridae* and *Podoviridae*, respectively. However, it is important to mention that a number of lysates exhibited various morphotypes

indicating that the respective strains released several phages simultaneously.

Host Range and Genetic Relationships of the Isolated *Ochrobactrum* Phages

Previous experiments demonstrated that most of the investigated *Ochrobactrum* strains harbored one or more prophages inducible

TABLE 3 | Spontaneous lysis of *Ochrobactrum* spp. strains.

<i>Ochrobactrum</i> spp. strain	Number of released phages	Host strain
<i>O. anthropi</i>		
O1178	4 × 10 ⁴ pfu/ml	<i>O. intermedium</i> O1218
O1129	–	<i>O. intermedium</i> O1147
O1157	–	<i>O. intermedium</i> O1147
O1154	–	<i>O. intermedium</i> O1147
O1180	1 × 10 ⁵ pfu/ml	<i>O. anthropi</i> O1129
<i>O. intermedium</i>		
O1216	2 × 10 ⁴ pfu/ml	<i>O. anthropi</i> O1199
O1218	–	<i>O. intermedium</i> O1135
O1132	–	<i>O. anthropi</i> O1163
O1191	–	<i>O. anthropi</i> O1215
O1126	2 × 10 ⁴ pfu/ml	<i>O. anthropi</i> O1129
<i>O. tritici</i>		
O1114	2 × 10 ⁵ pfu/ml	<i>O. anthropi</i> O1172
O1187	2 × 10 ⁵ pfu/ml	<i>O. anthropi</i> O1199
<i>O. dulfi</i>		
O1206	–	<i>O. anthropi</i> O1199
O1205	–	<i>O. anthropi</i> O1215
<i>O. pseudintermedium</i>		
O1164	–	<i>O. intermedium</i> O1135

by mitomycin C, heat and UV. To obtain data on individual phages present in the 19 selected lysates, high titer lysates were prepared by mitomycin C treatment of large culture volumes of the respective *Ochrobactrum* strains (see Section Materials and Methods). Upon purification by CsCl density-gradient centrifugation, 19 phages were isolated and characterized in terms of their host range and genetic relationship. Similar to the data obtained with non-purified lysates, the majority of phages infected several *Ochrobactrum* species, particularly *O. anthropi* and *O. intermedium*, but also strains of *O. tritici*, *O. oryzae*, and *O. pseudintermedium* (Table 5). By contrast, classical and atypical *Brucella* strains were not lysed. Plaques were even and mostly small and rather turbid, as shown for the myovirus POA1180 and the podovirus POI1126 (Figure 2). On the other hand, phage P1218 isolated from *O. intermedium* revealed a very narrow host range and exclusively lysed three strains belonging to this species. Finally, four phages (P1142, P1166, P1184 and P1196) did not infect any *Ochrobactrum* spp. strain. In some cases growth inhibition of indicator strains was observed indicating that phage replication did not occur in those strains.

To determine the genetic relationships of the *Ochrobactrum* phages amongst themselves and to the temperate *Brucella inopinata* phage BiPBO1, restriction patterns of the phage genomes were compared, followed by Southern hybridization (Figure 3). EcoRV restriction analyses revealed numerous fragments and demonstrated that the phages possess double-stranded DNA. Most restriction patterns were unique but

TABLE 4 | Morphology of *Ochrobactrum* spp. phages.

Phage	Family
<i>O. anthropi</i>	
P1178	Myoviridae
P1157	Siphoviridae, icosahedral
P1154	n.d.
P1129	Podoviridae
POA1180	Myoviridae
<i>O. intermedium</i>	
P1216	Myoviridae
P1218	Siphoviridae, icosahedral
P1191	Siphoviridae, icosahedral
P1132	Myoviridae
POI1126	Podoviridae
<i>O. tritici</i>	
P1114	Myoviridae
P1184	Myoviridae
P1187	Podoviridae
<i>O. dulfi</i>	
P1206	Myoviridae
P1205	Siphoviridae, icosahedral
<i>Ochrobactrum</i> spp.	
P1164	Myoviridae
P1142	Siphoviridae, prolate
P1196	Myoviridae
P1166	Siphoviridae

n.d., Not determined

the *O. dulfi* phages P1205 and P1206 exhibited identical profiles. In addition, two *O. intermedium* phages (P1132 and P1135) and the phages P1126 and P1187, isolated from *O. intermedium* and *O. tritici*, respectively, showed very similar patterns. However, the latter two phages differ in their host specificity indicating at least some minor genetic variations. According to the obtained restriction fragments (Figure 3A), genome sizes between 32 and 63 kb were calculated (data not shown). To determine DNA homologies between the phages, Southern hybridizations were performed using three phage DNAs as probes; myovirus POA1180 isolated from *O. anthropi* (Figure 3B), podovirus POI1126 (Figure 3C) isolated from *O. intermedium* and *B. inopinata* phage BiPBO1 (Figure 3D), which already revealed significant homologies to some *Ochrobactrum* prophages (Hammerl et al., 2016). Phage POA1180 did not hybridize to most of the other phages. Weak homologies were detected to POI1126 and to the two *O. dulfi* phages whose restriction patterns were identical. Phage POI1126 hybridized strongly to the *O. anthropi* phage P1129 and to the *O. tritici* phage P1187. Moreover, the homologous restriction fragments were similar in size corroborating the close relationship of these phages. The temperate *B. inopinata* phage BiPBO1 showed relationship to the *O. anthropi* phages

TABLE 5 | Lytic activity of the purified phages.

	<i>O. anthropi</i>					<i>O. intermedium</i>					<i>O. tritici</i>			<i>O. dultii</i>		<i>Ochrobactrum</i> spp.			
	POA1180	P1178	P1129	P1157	P1154	P1216	P1218	POI1126	P1132	P1191	P1114	P1187	P1184	P1206	P1205	P1164	P1196	P1142	P1166
<i>O. anthropi</i> strains (n = 64)																			
O1180	-	-	-	-	-	-	-	-	-	-	-	-	-	-	-	-	-	-	-
O1145	-	-	-	-	-	-	-	-	-	-	-	-	-	-	-	-	-	-	-
O1124	-	-	-	-	-	-	-	-	-	-	-	-	-	-	-	-	-	-	-
O1162	-	-	-	-	-	-	-	-	-	-	-	-	-	-	-	-	-	-	-
O1148	-	-	-	-	-	-	-	-	-	-	-	-	-	-	-	-	-	-	-
O1122	+	-	+	-	-	-	-	+	-	-	-	+	-	-	-	-	-	-	-
O1120	-	-	+	-	-	+	-	+	-	-	-	+	-	-	-	-	-	-	-
O1172	-	-	-	-	-	-	-	+	-	-	+	-	-	-	-	-	-	-	-
O1119	-	-	-	-	-	-	-	+	-	-	-	-	-	-	-	-	-	-	-
O1178	-	-	-	-	-	+	-	+	-	-	-	+	-	-	-	-	-	-	-
O1174	-	-	-	-	-	+	-	+	-	-	-	+	-	-	-	-	-	-	-
O1200	-	-	-	-	-	-	-	-	-	-	-	-	-	-	-	-	-	-	-
O1151	-	-	-	-	-	-	-	+	-	-	-	-	-	-	-	-	-	-	-
O1181	+	-	-	-	-	-	-	-	-	-	-	-	-	-	-	-	-	-	-
O1222	-	-	-	-	-	-	-	-	-	-	-	+	-	-	-	-	-	-	-
O1153	-	-	-	-	-	-	-	-	-	-	-	-	-	-	-	-	-	-	-
O1171	-	-	-	-	-	-	-	-	-	-	-	-	-	-	-	-	-	-	-
O1150	-	-	-	-	-	-	-	-	-	-	-	-	-	-	-	-	-	-	-
O1173	+	-	+	-	-	-	-	+	-	-	-	+	-	-	-	-	-	-	-
O1177	-	-	-	-	-	-	-	-	-	-	-	-	-	-	-	-	-	-	-
O1152	-	-	-	-	-	-	-	+	-	-	-	-	-	-	-	-	-	-	-
O1160	-	-	-	-	-	-	-	-	-	-	-	-	-	-	-	-	-	-	-
O1223	-	-	+	-	-	+	-	+	-	-	(+)	+	-	-	-	-	-	-	-
O1116	+	-	+	-	-	-	-	+	-	-	-	+	-	-	-	-	-	-	-
O1130	-	-	+	-	-	-	-	+	-	-	-	-	-	-	-	-	-	-	-
O1159	-	-	-	-	-	-	-	-	-	-	-	-	-	-	-	-	-	-	-
O1163	-	-	-	-	-	-	-	-	+	-	-	-	-	-	-	-	-	-	-
O1158	-	-	-	-	-	-	-	-	-	-	-	-	-	-	-	-	-	-	-
O1156	+	-	-	-	(+)	-	-	+	-	(+)	-	-	-	-	-	-	-	-	-
O1125	-	-	+	-	-	-	-	+	-	-	-	-	-	-	-	-	-	-	-
O1212	-	-	-	-	-	-	-	-	-	-	-	-	-	-	-	-	-	-	-
O1143	-	-	-	-	-	-	-	+	-	-	-	-	-	-	-	-	-	-	-
O1161	-	-	-	-	-	-	-	-	-	-	-	-	-	-	-	-	-	-	-
O1149	-	+	-	-	-	-	-	+	-	-	-	-	-	-	-	-	-	-	-
O1169	-	-	-	-	-	-	-	-	-	-	-	-	-	-	-	-	-	-	-
O1144	-	-	-	-	-	-	-	-	-	-	-	-	-	-	-	-	-	-	-
O1115	-	-	-	-	-	-	-	-	-	-	-	-	-	-	-	-	-	-	-
O1199	-	-	-	-	-	+	-	-	-	-	-	-	-	-	-	-	-	-	-
O1207	-	-	-	-	-	-	-	+	-	-	-	+	-	-	-	-	-	-	-
O1211	-	-	-	-	-	-	-	-	-	-	-	-	-	-	-	-	-	-	-
O1213	-	-	-	-	-	-	-	-	-	-	-	-	-	-	-	-	-	-	-
O1224	+	-	+	-	-	-	-	+	-	-	-	-	-	-	-	-	-	-	-
O1227	+	-	+	-	-	-	-	+	-	-	-	-	-	-	-	-	-	-	-
O1217	-	-	-	-	-	-	-	-	-	-	-	-	-	-	-	-	-	-	-
O1209	+	-	-	-	-	-	-	-	-	-	-	-	-	-	-	-	-	-	-
O1201	-	-	-	-	-	-	-	+	-	-	-	-	-	-	-	-	-	-	-

(Continued)

TABLE 5 | Continued

	<i>O. anthropi</i>					<i>O. intermedium</i>					<i>O. tritici</i>			<i>O. dulfii</i>		<i>Ochrobactrum</i> spp.			
	POA1180	P1178	P1129	P1157	P1154	P1216	P1218	POI1126	P1132	P1191	P1114	P1187	P1184	P1206	P1205	P1164	P1196	P1142	P1166
O1215	-	-	-	-	-	-	-	-	-	+	-	-	-	-	+	-	-	-	-
O1210	-	-	-	-	-	-	-	-	-	-	-	-	-	-	-	-	-	-	-
O1197	-	-	-	-	-	-	-	-	-	-	-	-	-	-	-	-	-	-	-
O1214	-	-	-	-	-	-	-	+	-	-	-	-	-	-	-	-	-	-	-
O1225	-	-	-	-	-	-	-	-	-	-	-	-	-	-	-	-	-	-	-
O1121	-	-	-	-	-	-	-	-	-	(+)	-	-	-	-	-	-	-	-	-
O1165	-	-	-	-	-	-	-	-	-	-	-	-	-	-	-	-	-	-	-
O1155	+	+	-	+	(+)	-	-	+	-	-	-	-	-	-	(+)	-	-	-	-
O1175	+	-	-	-	-	-	-	-	-	(+)	-	-	-	-	-	-	-	-	-
O1226	-	-	-	-	-	-	-	-	-	-	-	-	-	-	-	-	-	-	-
O1179	-	(+)	-	+	-	-	-	+	-	-	-	-	-	-	-	+	-	-	-
O1123	-	-	-	-	-	-	-	-	-	-	-	-	-	-	-	-	-	-	-
O1176	+	-	-	-	-	-	-	+	-	-	-	-	-	-	-	-	-	-	-
O1202	-	-	-	-	-	-	-	-	-	-	-	-	-	-	-	-	-	-	-
O1129	+	-	-	-	-	+	-	-	-	-	-	+	-	-	-	-	-	-	-
O1157	-	-	-	-	-	-	-	+	-	-	-	-	-	-	-	-	-	-	-
O1154	+	-	-	+	-	-	-	-	-	-	-	-	-	-	-	-	-	-	-
O1128	-	-	-	-	-	-	-	-	-	-	-	-	-	-	-	-	-	-	-
<i>O. intermedium</i> strains (n = 18)																			
O1192	-	-	-	-	-	-	-	-	-	-	-	-	-	-	-	-	-	-	-
O1167	-	-	-	-	-	-	-	-	-	-	-	-	-	-	-	-	-	-	-
O1194	-	-	+	-	-	-	-	+	-	-	-	+	-	-	-	-	-	-	-
O1193	-	+	-	-	-	+	-	-	-	-	-	-	-	-	-	-	-	-	-
O1183	-	-	-	-	-	+	-	+	-	-	-	-	-	-	-	-	-	-	-
O1190	+	-	-	-	-	-	-	-	-	-	-	-	-	-	-	-	-	-	-
O1168	-	-	-	+	-	+	(+)	+	-	-	-	+	-	-	-	-	-	-	-
O1133	-	-	-	-	-	-	-	-	-	-	-	-	-	-	-	-	-	-	-
O1216	-	-	-	-	-	-	-	-	-	-	-	-	-	-	+	-	-	-	-
O1134	-	-	-	-	-	-	-	-	-	-	-	-	-	-	-	-	-	-	-
O1135	-	-	-	-	-	-	+	-	-	-	-	-	-	-	-	-	-	-	-
O1182	-	-	-	-	-	-	-	-	-	(+)	-	+	-	+	-	-	-	-	-
O1132	-	-	-	-	-	-	(+)	-	-	(+)	-	-	-	-	-	-	-	-	-
O1220	-	(+)	+	+	-	-	-	+	-	-	-	+	-	-	-	+	-	-	-
O1147	-	-	+	+	+	+	-	+	+	(+)	-	+	-	+	(+)	+	-	-	-
O1126	-	-	-	-	-	-	-	-	-	-	-	+	-	-	-	+	-	-	-
O1218	-	+	-	-	-	-	-	+	-	-	-	+	-	-	-	-	-	-	-
O1191	-	-	-	-	-	-	-	-	-	(+)	-	-	-	-	-	-	-	-	-
<i>O. tritici</i> strains (n = 9)																			
O1221	-	-	-	-	-	-	-	-	-	-	-	-	-	-	-	-	-	-	-
O1114	-	-	-	-	-	-	-	-	-	-	-	-	-	-	-	-	-	-	-
O1187	-	-	-	-	-	-	-	-	-	-	-	-	-	-	-	-	-	-	-
O1184	-	-	-	-	-	-	-	-	-	-	-	-	-	-	-	-	-	-	-
O1170	-	-	-	-	-	-	-	-	-	-	-	-	-	-	-	-	-	-	-
O1208	-	-	-	-	-	-	-	-	-	-	-	-	-	-	-	-	-	-	-
O1195	-	(+)	-	+	-	-	-	+	-	-	-	-	-	-	-	+	-	-	-

(Continued)

TABLE 5 | Continued

	<i>O. anthropi</i>						<i>O. intermedium</i>				<i>O. tritici</i>			<i>O. dulfi</i>		<i>Ochrobactrum</i> spp.			
	POA1180	P1178	P1129	P1157	P1154	P1216	P1218	POI1126	P1132	P1191	P1114	P1187	P1184	P1206	P1205	P1164	P1196	P1142	P1166
O1140	–	–	–	–	–	–	–	–	–	–	–	–	–	–	–	–	–	–	–
O1146	–	–	–	–	–	–	–	–	–	–	–	–	–	–	–	–	–	–	–
<i>O. dulfi</i> strains (n = 3)																			
O1206	–	–	–	–	–	–	–	–	–	–	–	–	–	–	–	–	–	–	–
O1205	–	–	–	–	–	–	–	–	–	–	–	–	–	–	–	–	–	–	–
O1198	–	–	–	–	–	–	–	(+)	–	–	–	–	–	–	–	+	–	–	–
<i>O. pseudogrignonense</i> strains (n = 3)																			
O1219	–	–	–	–	–	–	–	–	–	–	–	–	–	–	–	–	–	–	–
O1203	–	–	–	–	–	–	–	–	–	–	–	–	–	–	–	–	–	–	–
O1189	+	–	–	–	–	–	–	–	–	–	–	–	–	–	–	–	–	–	–
<i>O. gallinifaecis</i> strains (n = 2)																			
O1141	–	–	–	–	–	–	–	–	–	–	–	–	–	–	–	–	–	–	–
O1142	–	–	–	–	–	–	–	–	–	–	–	–	–	–	–	–	–	–	–
<i>O. grignonense</i> strains (n = 2)																			
O1118	–	–	–	–	–	–	–	–	–	–	–	–	–	–	–	–	–	–	–
O1117	–	–	–	–	–	–	–	–	–	–	–	–	–	–	–	–	–	–	–
<i>O. lupini</i> strains (n = 2)																			
O1136	–	–	–	–	–	–	–	–	–	–	–	–	–	–	–	–	–	–	–
O1137	–	–	–	–	–	–	–	–	–	–	–	–	–	–	–	–	–	–	–
<i>O. pseudintermedium</i> strains (n = 2)																			
O1164	–	–	–	–	–	–	–	–	–	–	–	–	–	–	–	–	–	–	–
O1204	–	+	–	+	–	–	–	–	–	(+)	–	–	–	–	+	–	–	–	–
<i>O. haemophilum</i> strains (n = 1)																			
O1166	–	–	–	–	–	–	–	–	–	–	–	–	–	–	–	–	–	–	–
<i>O. oryzae</i> strains (n = 1)																			
O1196	–	–	+	–	–	+	–	+	–	–	–	+	–	+	–	+	–	–	–
<i>Mesorhizobium</i> sp. strains (n = 2)																			
O1188	–	–	–	–	–	–	–	–	–	–	–	–	–	–	–	–	–	–	–
O1186	–	–	–	–	–	–	–	–	–	–	–	–	–	–	–	–	–	–	–
<i>Pseudomonas kiredjiana</i> strains (n = 1)																			
O1139	–	–	–	–	–	–	–	–	–	–	–	–	–	–	–	–	–	–	–
<i>Pseudomonas saccharolyticum</i> strains (n = 2)																			
O1138	–	–	–	–	–	–	–	–	–	–	–	–	–	–	–	–	–	–	–
O1127	–	–	–	–	–	–	–	–	–	–	–	–	–	–	–	–	–	–	–

+, Strong phage activity; (+), weak phage activity; –, no phage activity.
The gray values indicate a phage activity.

P1129 and P1157 (Figure 3). Based on these results it can be suggested that temperate *Ochrobactrum* phages are genetically highly diverse. To further characterize this diversity, the genomic sequences of myovirus POA1180 and podovirus POI1126 were determined.

The genome of phage POA1180 has a size of 41,655 bp with a GC-content of 56.6%. Fifty-eight putative gene products were assigned of which 55 are located on the same DNA strand. For 32 gene products a functional prediction could be made (Table S1). It is notable that almost no similarities were detected

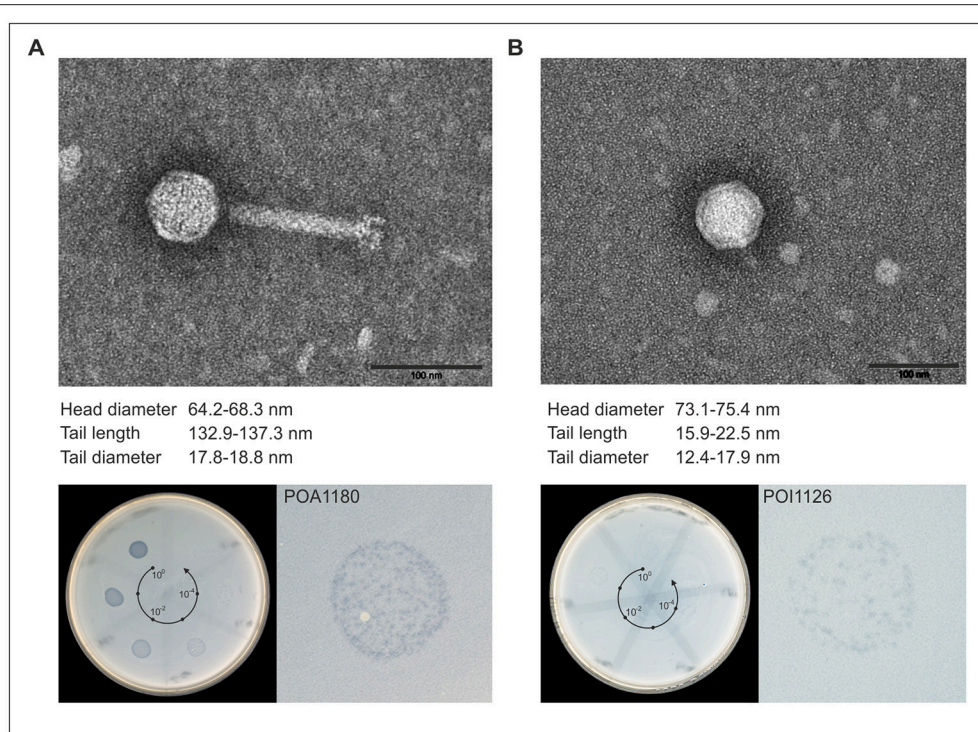


FIGURE 2 | Morphology and lytic activity of POA1180 and POI1126. In the upper part, transmission electron micrographs (TEM) of POA1180 (**A**) and POI1126 (**B**) phage particles isolated from *Ochrobactrum* strains O1180 and O1126, respectively, by mitomycin C induction are shown. The black bar represents a size standard of 100 nm. The lower part demonstrates the lytic activity of the phages POA1180 (**A**) and POI1126 (**B**). The left panels show the lytic activity of the indicated phages during spot testing. On the bacterial lawn of *O. anthropi* strain O1129, 10 μ l of a 1:10 dilution series (spot 1–6) of the P1180 and P1126 phage lysates was applied. The right panels show a six-fold magnification of a representative spotting zone comprising single plaques.

to proteins of other phages. Instead, very similar proteins are encoded by other *Ochrobactrum* strains and strains of the genera *Brucella*, *Agrobacterium*, *Bartonella*, *Burkholderia*, *Rhizobium*, and *Stappia*. The highest similarities exist to a prophage recently identified in *Brucella* strain 10RB9215 isolated from an exotic frog (Scholz et al., 2016). This indicates that closely related prophages are widespread in these bacteria but that reports on the respective phages are scarce. Based on homologies to other proteins, a gene map of phage POA1180 was constructed (**Figure 4**). The left half of the POA1180 genome mainly contains genes for DNA packaging and virion assembly. We identified putative genes for the small (ORF01) and large subunit of the terminase (ORF02), capsid protein, and several tail proteins (e.g., tail tube protein, tape measure protein, and tail fiber protein). The right half of the POA1180 genome contains genes for various proteins. First and foremost, two genes (ORF31 and ORF32) were identified which may confer resistance to chromium. Their products are very similar to proteins of *Rhizobium*, *Mesorhizobium*, and *Sinorhizobium*. While ORF31 encodes a chromate transport protein, the ORF32 product is closely related to chromate resistance proteins. Chromium resistance has already been reported for the *O. tritici* strain 5bv11 but in this strain, the resistance genes are located on a transposon (Morais et al., 2011). Transposase genes (ORF42 and ORF43) are also present on the POA1180 genome, but

whether the chromate resistance genes of this phage can be mobilized, is not known. The POA1180 ORF46 product is similar to sulfate permeases belonging to the CysZ family and may mediate the uptake of sulfate subsequently utilized for the synthesis of sulfur-containing compounds in the cell. Another gene that might be important for *Ochrobactrum* metabolism is ORF53 probably encoding a NAD(P) transhydrogenase. In addition, the right half of the POA1180 phage genome contains genes for an ATPase, transcriptional regulators, a partitioning protein, an exonuclease and the endolysin. However, for most genes located in this region, functional predictions could not be made.

Phage POI1126 possesses a genome of 60,065 bp with a GC-content of 56.2%. Eighty putative genes were assigned, which are equally located on both DNA strands (**Figure 4**). The function of 31 gene products could be predicted on the basis of similarities to known proteins. The closest related phages of POI1126 are the *S. meliloti* phage PCB5, *Erwinia pyrifoliae* phage PEp14 and the *Burkholderia cenocepacia* phages DC1, Bcep22, and BcepIL02. While the lifestyle and morphology of PCB5 have not been documented yet, the other phages are podoviruses like POI1126 (Gill et al., 2011; Lynch et al., 2012). The three *Burkholderia* phages were originally isolated from soil. It has still to be clarified whether these phages are virulent or temperate since they were unable to form stable lysogens.

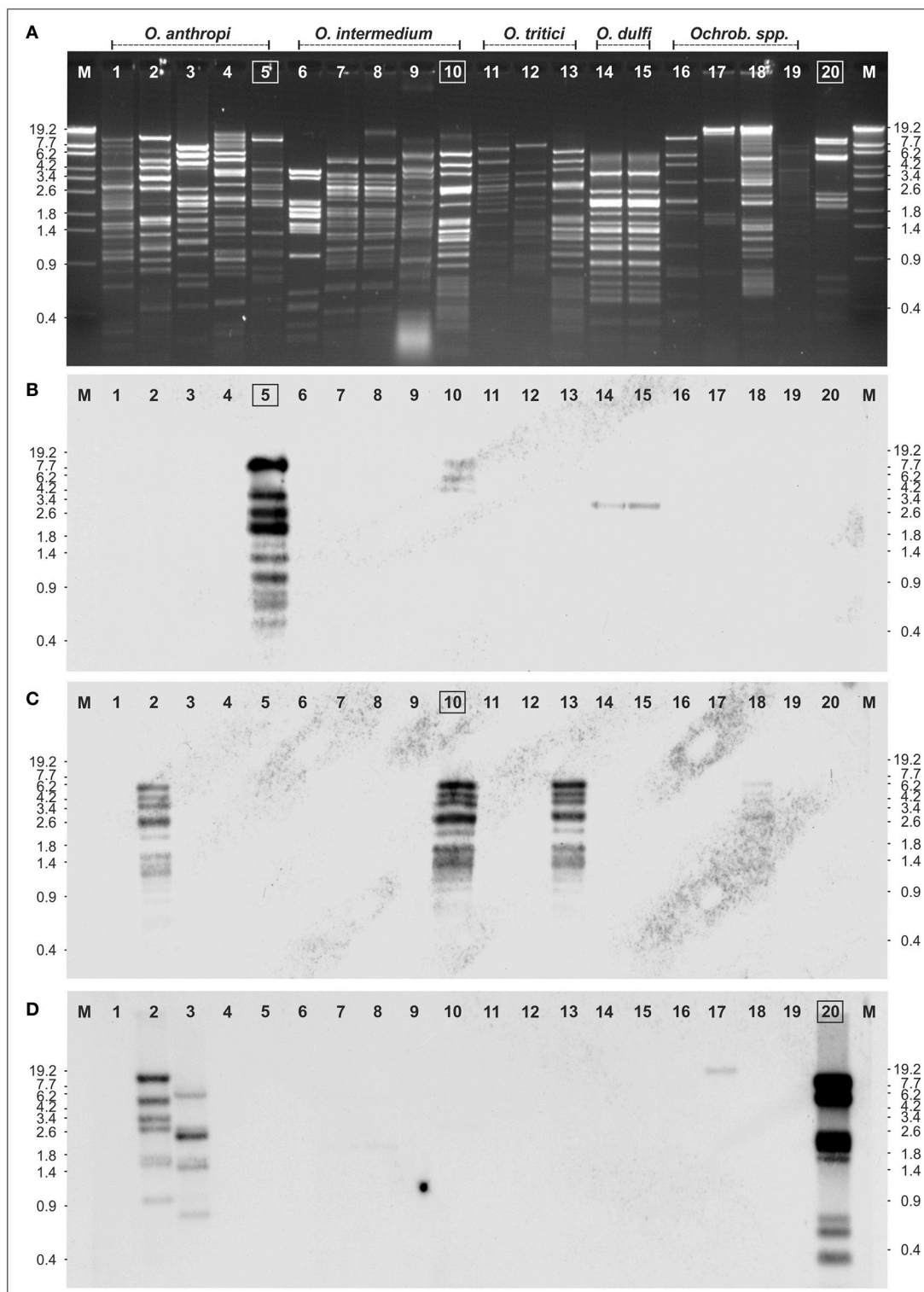


FIGURE 3 | Relationship of 19 *Ochrobacterum* spp. phages. **(A)** EcoRV restriction patterns of the phages. Southern hybridization of POA1180 **(B)**, POI1126 **(C)**, and BiPB01 **(D)** to the isolated *Ochrobacterum* spp. phage DNAs: *Ochrobacterum anthropi* phages P1178 (lane 1), P1129 (lane 2), P1157 (lane 3), P1154 (lane 4), POA1180 (lane 5), *O. intermedium* phages: P1216 (lane 6), P1135 (lane 7), P1132 (lane 8), P1218 (lane 9), POA1126 (lane 10), *O. tritici* phages: P1114 (lane 11), P1184 (lane 12), P1187 (lane 13), *O. dulfii* phages: P1206 (lane 14), P1205 (lane 15), *Ochrobacterum* spp. phages: P1164 (lane 16), P1142 (lane 17), P1166 (lane 18), P1189 (lane 19), and *Brucella inopinata* phage BiPB01 (lane 20). Lanes M, Lambda Eco130I marker DNA.

Although, a recombinase gene and an *attP* site have been detected on the phage genomes the phages may be unable to successfully integrate into the host chromosome. In contrast, phage POI1126 was isolated from an *O. intermedium* strain by induction with mitomycin C suggesting a temperate lifestyle. The analysis of the POI1126 genome disclosed that the phage is almost identical to an unnamed plasmid of the *O. intermedium* strain LMG 3301 (ACQA01000004). We only found one nucleotide variation (deletion) in ORF30. The frame shift mutation led to an exchange of seven C-terminal amino acids in the predicted DNA-methylase protein. The strong homologies to the plasmid of strain LMG 3301 inspired us to analyse the plasmid content of *O. intermedium* strain O1126. This strain indeed contains a plasmid that showed an identical *EcoRV* restriction pattern as phage POI1126 (Figure 5). From these data, it can be assumed that both *O. intermedium* strains, O1126 and LM3301, harbor a temperate phage whose prophage replicates as plasmid. The sequence of the LMG 3301 plasmid deposited at NCBI is framed by a terminal direct repeat of 389 bp. We analyzed the corresponding DNA regions of POI1126 and the plasmid prophage by PCR but did not detect this repetitive sequence. As a consequence the first and last ORF of the LMG 3301 sequence encoding putative DNA methylases are merged in strain O1126. The resulting methylase gene (ORF30) is by far the largest gene of POI1126 (14.526 bp) and preceded by a suitable ribosome

binding site. The genome analysis of the phage revealed two ORFs (38 and 39) probably forming an operon that may be important for plasmid maintenance. Their products are similar to partitioning proteins. Other plasmid-associated genes could not be determined. On the other hand, a putative integrase gene (ORF65) was identified whose function is yet not known. The gene map of phage POI1126 shows that the left half of the genome mainly contains genes for structural proteins and virion assembly, while only few ORFs in the right half could be functionally assigned. It is possible that this part of the genome harbors other genes, which are required for plasmid replication.

The phages POI1126 and POA1180 possess several genes encoding potential methyltransferases (Table S1). To find out whether the genomes of the phages are modified, their DNAs were digested with several restriction endonucleases. None of the obtained restriction patterns of POA1180 coincided with patterns determined by *in silico* analysis. Figure 6A presents *EcoRI* and *EcoRV* profiles of the POA1180 DNA. Using the NEB cutter software, restriction patterns of CpG methylated phage DNA were predicted but also these patterns did not agree with patterns obtained by digestion (Figure 6A). However, a superimposition of the computer-generated *EcoRI* profiles (but not of the *EcoRV* profiles) corresponded well with the restriction pattern observable in agarose gels. This suggests that

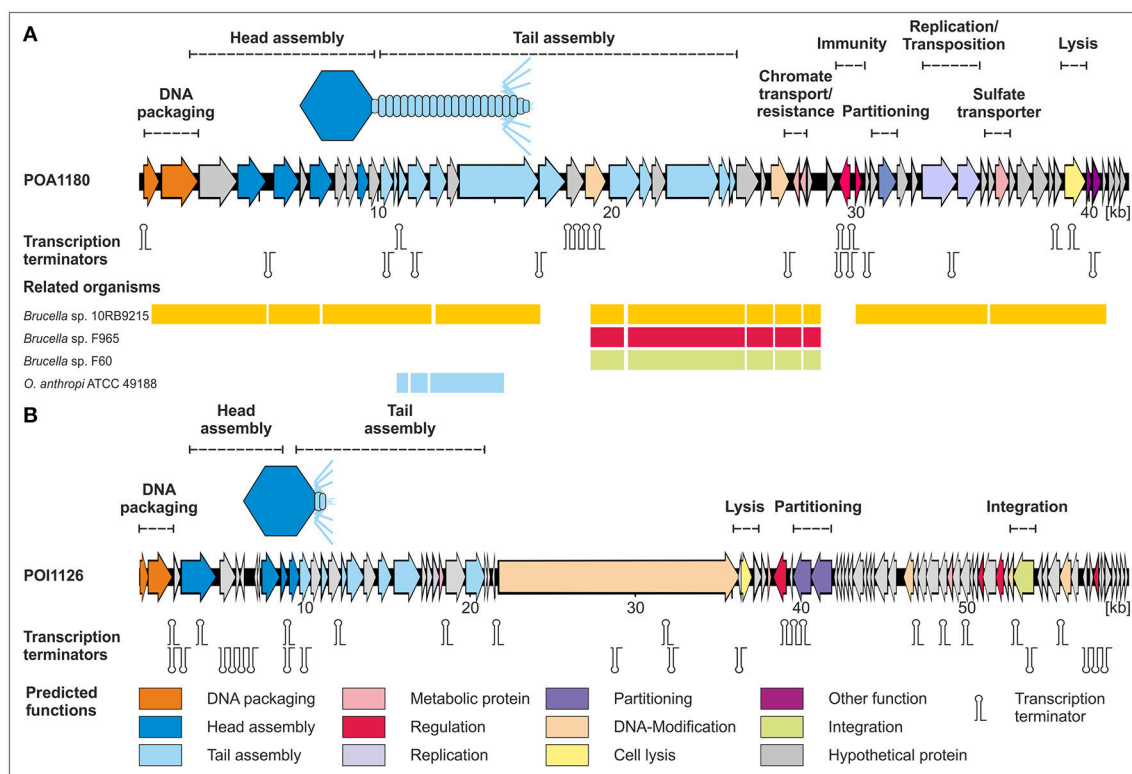
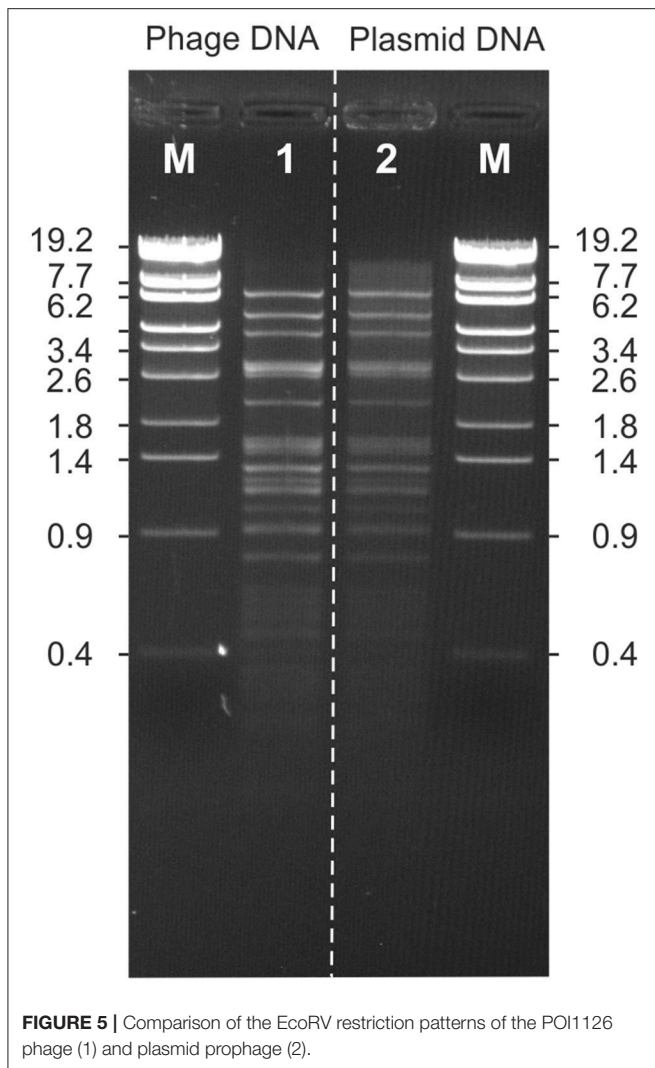


FIGURE 4 | Gene maps of the *Ochrobactrum* phages POA1180 (A) and POI1126 (B). Putative genes are colored according to the predicted functions of their products. The position of putative Rho-independent transcription terminators and tRNAs are indicated. For POA1180 nucleotide similarities (>75%) to closely related *Brucella* and *Ochrobactrum* genomes are shown.



the POA1180 phage DNA contains some modifications, which diverge from modifications known in *E. coli*. On the other hand, the EcoRI and EcoRV restriction patterns of phage POI1126 were in good agreement with patterns predicted for unmethylated DNA (Figure 6B). Thus, the DNA of this phage is either not modified or contains modifications which cannot be traced by the restriction endonucleases used.

DISCUSSION

In this study, temperate *Ochrobactrum* phages were isolated and characterized. Whereas, plasmids of *Ochrobactrum* have already been described (Chain et al., 2011) phages have yet not been investigated. Initial *in silico* analyses of published *Ochrobactrum* spp. genomes revealed that prophages are apparently widespread in this genus, similarly to the related genus *Brucella*, where numerous prophages have been identified (Hammerl et al., 2016). However, while to date only one active temperate phage could be isolated from *Brucella* spp., 72 out of 125 tested

Ochrobactrum strains of different species released phage particles that caused plaques on indicator bacteria. The reason for this incongruity is yet not clear. It is conceivable that in *Brucella* spp. many prophages are defective. Compared to *Ochrobactrum*, the *Brucella* genome is much smaller. The genome reduction is associated with the adaption of brucellae to the intracellular lifestyle (Teyssier et al., 2004) and it is possible that prophage sequences are not conducive for the survival in the intra-host environment. Other reasons could be a high host specificity of *Brucella* phages or an immunity of *Brucella* strains to phage infection due to the presence of inherent prophages. Though, the close relationship between *Brucella* and *Ochrobactrum* does not really support this speculation. Many of the *Ochrobactrum* lysates revealed a rather broad lytic activity against non-lysogenic and lysogenic strains. In addition, as with *B. inopinata* phage BiPBO1, *Ochrobactrum* prophages could be readily induced by mitomycin C, UV, or heat treatment. Moreover, some *Ochrobactrum* strains released significant numbers of phage particles even under non-induced conditions (data not shown). Therefore, it remains obscure, why it is much easier to isolate temperate phages from *Ochrobactrum* than from *Brucella*.

Electron microscopy illustrated that temperate *Ochrobactrum* phages are morphologically diverse. Although, myoviruses are typically lytic while many siphoviruses can integrate into the host genome (Suttle, 2005), most *Ochrobactrum* lysates contained myoviruses. In some lysates two morphotypes (myovirus/podovirus and podovirus/siphovirus) were detected showing that these phages may coexist in the same cell. Phages belonging to different families generally share only little DNA similarity (Jarvis, 1984; Ackermann, 1992; Krylov et al., 1993; Wichels et al., 1998). The majority of the 19 isolated *Ochrobactrum* phages revealed clearly distinguishable restriction patterns. Some patterns were identical but in this case the respective phages varied in their host range indicating that they are related but not identical. Based on the obtained restriction patterns, genome sizes between 32 and 63 kb were calculated, a size range often found in phages (Hatfull, 2008). Southern hybridization experiments confirmed the diversity of the isolated phages. None of the phages revealed significant DNA homology to the myovirus POA1180. Podovirus POI1126 hybridized strongly to two other podoviruses (P1129 and P1187) but not to the remaining phages whereas *B. inopinata* siphovirus BiPBO1 showed similarity to P1129 and P1157. While the relationship of BiPBO1 to the siphovirus P1157 was not surprising, we did not expect signals with P1157, because this phage had been classified as podovirus. A re-examination of the phage isolated from CsCl density-gradient band disclosed that the preparation contained both a podovirus and a siphovirus. The phages could obviously not be separated by CsCl density-gradient centrifugation. Since most *Ochrobactrum* strains are lysogenic or multilytic, prophages may be induced when infected with a phage from outside. As stated above some *Ochrobactrum* strains released high numbers of phage particles spontaneously during growth in culture media. Thus, there is always the possibility, that lysates are contaminated by endogenous phages and because of this fact, it is a challenge to find non-lysogenic, phage sensitive *Ochrobactrum* spp. strains to propagate phages that are of interest.

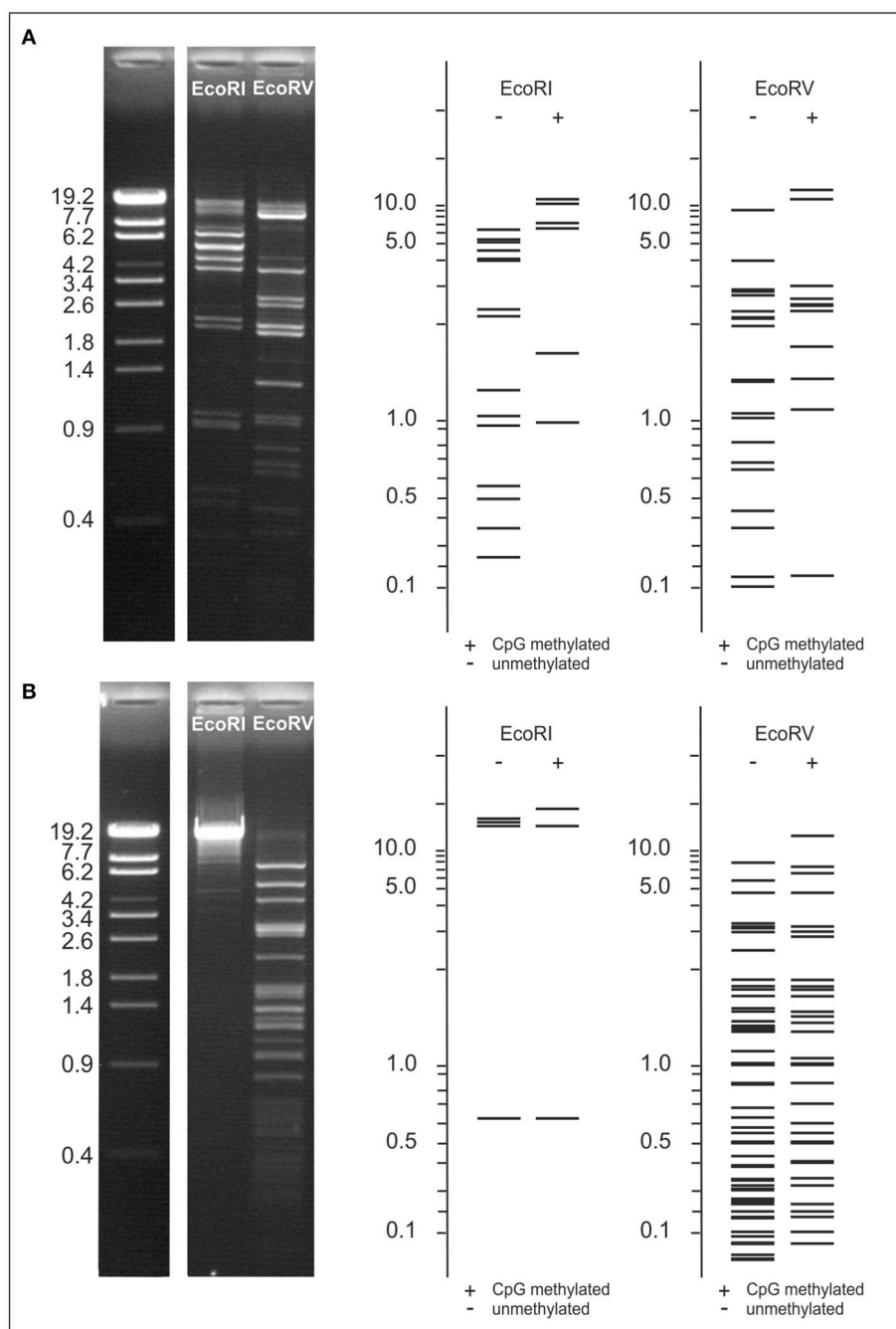


FIGURE 6 | Examination of POA1180 and POI1126 DNA modifications. To compare restriction patterns of the phages, EcoRI and EcoRV digests of POA1180 (**A**) and POI1126 (**B**) were separated on 0.8% agarose gels. Sizes of restriction fragments were determined using the λ Eco130I reference marker. For both phages EcoRI and EcoRV restriction patterns were predicted by computer analysis to compare the *in silico* data with experimental results. Predicted restriction patterns are shown for unmethylated and CpG methylated DNA.

The analysis of the POA1180 phage genomes suggests that it is similarly organized like the genomes of many other temperate phages. The genome contains some functional gene modules, particularly for DNA packaging and virion assembly (Lima-Mendez et al., 2011). Though, for about half of the POA1180 genes, a functional assignment could not be made. One reason

for this ambiguity could be that the closest relatives of POA1180 are prophages identified in other genera of the orders *Rhizobiales*, *Burkholderiales*, and *Rhodobacteriales* and not phage particles that have been characterized in detail. Nevertheless, typical for soil bacteria, some genes were identified on the POA1180 genome, which could be beneficial for its host. Resistance

against chromate has been found in several bacteria including *Ochrobactrum* (Branco and Morais, 2013; Hora and Shetty, 2015), but to the best of our knowledge, the respective genes have yet not been identified on the genome of a temperate phage. The same holds true for the sulfate permease gene which may improve the supply of the host with sulfate (Pilsyk and Paszewski, 2009). These genes may give *Ochrobactrum* a selective advantage in the environment. Since phage POA1180 possesses a rather wide host range within the genus *Ochrobactrum* and because its DNA revealed some modification which may protect it from degradation, it is possible that other *Ochrobactrum* strains may benefit from lysogenic conversion. On the other hand, it becomes clear that those genes would not be beneficial for intracellular bacteria like *Brucella* and this may be one reason why active prophages are so rare in this genus. However, the isolation of phage BiPB01 from *B. inopinata* (Hammerl et al., 2016) and the occurrence of prophages in other non-classical *Brucella* species that are closely related to active *Ochrobactrum* phages (Scholz et al., 2016) suggest that those *Brucella* strains may be carrier of intact phages.

POI1126 is a temperate phage which replicates as plasmid during the lysogenic cycle. Whether POI1126 may integrate into the host chromosome has still to be investigated. The phage contains a putative integrase gene but it is possible that this gene is defective or that the attachment site *attP* is not functional or missing. The relationship of POI1126 to a plasmid

of the *O. intermedium* strain LMG 3301 indicates that plasmid prophages might be common in this genus. Moreover, POI1126 is also related to podoviruses of other genera, e.g., *Burkholderia*. For *B. cenocepacia* phage Bcep22, whose genome showed a close relationship to the LMG 3301 plasmid as well, it has been reported that its prophage is unable to integrate into the host chromosome (Gill et al., 2011). Is it possible that this phage is a plasmid like POI1126? Further experiments are needed to elucidate the lifestyle of this group of podophages.

AUTHOR CONTRIBUTIONS

JH, CJ, HS, KN, and SH designed the study. JH, CJ, and JR performed the experiments. JH, CJ, HS, JR, and SH analyzed the data. All authors prepared the tables and figures, wrote, and edited the manuscript.

ACKNOWLEDGMENTS

The work was supported by the BfR grants 1322-488 and 45-003.

SUPPLEMENTARY MATERIAL

The Supplementary Material for this article can be found online at: <http://journal.frontiersin.org/article/10.3389/fmicb.2017.01207/full#supplementary-material>

REFERENCES

- Ackermann, H. W. (1992). Frequency of morphological phage descriptions. *Arch. Virol.* 124, 201–209. doi: 10.1007/BF01309802
- Bathe, S., Achouak, W., Hartmann, A., Heulin, T., Schloter, M., and Lebuhr, M. (2006). Genetic and phenotypic microdiversity of *Ochrobactrum* spp. *FEMS Microbiol. Ecol.* 56, 272–280. doi: 10.1111/j.1574-6941.2005.00029.x
- Branco, R., and Morais, P. V. (2013). Identification and characterization of the transcriptional regulator ChrB in the chromate resistance determinant of *Ochrobactrum tritici* 5bvl1. *PLoS ONE* 8:e77987. doi: 10.1371/journal.pone.0077987
- Chain, P. S., Lang, D. M., Comerchi, D. J., Malfatti, S. A., Vergez, L. M., Shin, M., et al. (2011). Genome of *Ochrobactrum anthropi* ATCC 49188 T, a versatile opportunistic pathogen and symbiont of several eukaryotic hosts. *J. Bacteriol.* 193, 4274–4275. doi: 10.1128/JB.05335-11
- Danko, A. S., Luo, M., Bagwell, C. E., Brigmon, R. L., and Freedman, D. L. (2004). Involvement of linear plasmids in aerobic biodegradation of vinyl chloride. *Appl. Environ. Microbiol.* 70, 6092–6097. doi: 10.1128/AEM.70.10.6092-6097.2004
- Daxboeck, F., Zitta, S., Assadian, O., Krause, R., Wensch, C., and Kovarik, J. (2002). *Ochrobactrum anthropi* bloodstream infection complicating hemodialysis. *Am. J. Kidney Dis.* 40, E17. doi: 10.1053/ajkd.2002.35759
- Deak, V., Lukacs, R., Buzas, Z., Palvolgyi, A., Papp, P. P., Orosz, L., et al. (2010). Identification of tail genes in the temperate phage 16-3 of *Sinorhizobium meliloti* 41. *J. Bacteriol.* 192, 1617–1623. doi: 10.1128/JB.01335-09
- El-Sayed, W. S., Ibrahim, M. K., Abu-Shady, M., El-Beih, F., Ohmura, N., Saiki, H., et al. (2003). Isolation and identification of a novel strain of the genus *Ochrobactrum* with phenol-degrading activity. *J. Biosci. Bioeng.* 96, 310–312. doi: 10.1016/S1389-1723(03)80200-1
- Gill, J. J., Summer, E. J., Russell, W. K., Cologna, S. M., Carlile, T. M., Fuller, A. C., et al. (2011). Genomes and characterization of phages Bcep22 and BcepIL02, founders of a novel phage type in *Burkholderia cenocepacia*. *J. Bacteriol.* 193, 5300–5313. doi: 10.1128/JB.05287-11
- Goris, J., Boon, N., Lebbe, L., Verstraete, W., and De Vos, P. (2003). Diversity of activated sludge bacteria receiving the 3-chloroaniline degradative plasmid pC1gfp. *FEMS Microbiol. Ecol.* 46, 221–230. doi: 10.1016/S0168-6496(03)00231-9
- Hammerl, J. A., Göllner, C., Al Dahouk, S., Nöckler, K., Reetz, J., and Hertwig, S. (2016). Analysis of the first temperate broad host range brucellaphage (BiPB01) isolated from *B. inopinata*. *Front. Microbiol.* 7:24. doi: 10.3389/fmicb.2016.00024
- Hammerl, J. A., Jäckel, C., Reetz, J., Beck, S., Alter, T., Lurz, R., et al. (2011). *Campylobacter jejuni* group III phage CP81 contains many T4-like genes without belonging to the T4-type phage group: implications for the evolution of T4 phages. *J. Virol.* 85, 8597–8605. doi: 10.1128/JVI.00395-11
- Hatfull, G. F. (2008). Bacteriophage genomics. *Curr. Opin. Microbiol.* 11, 447–453. doi: 10.1016/j.mib.2008.09.004
- Hora, A., and Shetty, V. K. (2015). Partial purification and characterization of chromate reductase of a novel *Ochrobactrum* sp. strain Cr-B4. *Prep. Biochem. Biotechnol.* 45, 769–784. doi: 10.1080/10826068.2014.952385
- Jarvis, A. W. (1984). Differentiation of lactic streptococcal phages into phage species by DNA-DNA homology. *Appl. Environ. Microbiol.* 47, 343–349.
- Jelveh, N., and Cunha, B. A. (1999). *Ochrobactrum anthropi* bacteremia. *Heart Lung* 28, 145–146. doi: 10.1053/hl.1999.v28.a94602
- Johnning, A., Moore, E. R., Svensson-Stadler, L., Shouche, Y. S., Larsson, D. G., and Kristiansson, E. (2013). Acquired genetic mechanisms of a multiresistant bacterium isolated from a treatment plant receiving wastewater from antibiotic production. *Appl. Environ. Microbiol.* 79, 7256–7263. doi: 10.1128/AEM.02141-13
- Johnson, M., Zaretskaya, I., Raytselis, Y., Merezukh, Y., McGinnis, S., and Madden, T. L. (2008). NCBI BLAST: a better web interface. *Nucleic Acids Res.* 36, W5–W9. doi: 10.1093/nar/gkn201
- Kämpfer, P., Buczolits, S., Albrecht, A., Busse, H. J., and Stackebrandt, E. (2003). Towards a standardized format for the description of a novel species (of an established genus): *Ochrobactrum gallinifacis* sp. nov. *Int. J. Syst. Evol. Microbiol.* 53(Pt 3), 893–896. doi: 10.1099/ijs.0.02710-0

- Kämpfer, P., Huber, B., Busse, H.-J., Scholz, H. C., Tomaso, H., Hotzel, H., et al. (2011). *Ochrobactrum pecoris* sp. nov., isolated from farm animals. *Int. J. Syst. Evol. Microbiol.* 61, 2278–2283. doi: 10.1099/ijss.0.027631-0
- Kettaneh, A., Weill, F. X., Poilane, I., Fain, O., Thomas, M., Herrmann, J. L., et al. (2003). Septic shock caused by *Ochrobactrum anthropi* in an otherwise healthy host. *J. Clin. Microbiol.* 41, 1339–1341. doi: 10.1128/JCM.41.3.1339-1341.2003
- Krylov, V. N., Tolmachova, T. O., and Akhverdian, V. Z. (1993). DNA homology in species of bacteriophages active on *Pseudomonas aeruginosa*. *Arch. Virol.* 131, 141–151. doi: 10.1007/BF01379086
- Lebuhn, M., Achouak, W., Schloter, M., Berge, O., Meier, H., Barakat, M., et al. (2000). Taxonomic characterization of *Ochrobactrum* sp. isolates from soil samples and wheat roots, and description of *Ochrobactrum tritici* sp. nov., and *Ochrobactrum grignonense* sp. nov. *Int. J. Syst. Evol. Microbiol.* 50(Pt 6), 2207–2223. doi: 10.1099/00207713-50-6-2207
- Lebuhn, M., Bathe, S., Achouak, W., Hartmann, A., Heulin, T., and Schloter, M. (2006). Comparative sequence analysis of the internal transcribed spacer 1 of *Ochrobactrum* species. *Syst. Appl. Microbiol.* 29, 265–275. doi: 10.1016/j.syapm.2005.11.003
- Lima-Mendez, G., Toussaint, A., and Leplae, R. (2011). A modular view of the bacteriophage genomic space: identification of host and lifestyle marker modules. *Res. Microbiol.* 162, 737–746. doi: 10.1016/j.resmic.2011.06.006
- Lynch, K. H., Stothard, P., and Dennis, J. J. (2012). Characterization of DC1, a broad-host-range Bcep22-like podovirus. *Appl. Environ. Microbiol.* 78, 889–891. doi: 10.1128/AEM.07097-11
- Mahmood, M. S., Sarwari, A. R., Khan, M. A., Sophie, Z., Khan, E., and Sami, S. (2000). Infective endocarditis and septic embolization with *Ochrobactrum anthropi*: case report and review of literature. *J. Infect.* 40, 287–290. doi: 10.1053/jinf.2000.0644
- Möller, L. V., Arends, J. P., Harmsen, H. J., Talens, A., Terpstra, P., and Slooff, M. J. (1999). *Ochrobactrum intermedium* infection after liver transplantation. *J. Clin. Microbiol.* 37, 241–244.
- Moras, P. V., Branco, R., and Francisco, R. (2011). Chromium resistance strategies and toxicity: what makes *Ochrobactrum tritici* 5bvl1 a strain highly resistant. *Biometals* 24, 401–410. doi: 10.1007/s10534-011-9446-1
- Mudshingkar, S. S., Choure, A. C., Palewar, M. S., Dohe, V. B., and Kagal, A. S. (2013). *Ochrobactrum anthropi*: an unusual pathogen: are we missing them? *Indian J. Med. Microbiol.* 31, 306–308. doi: 10.4103/0255-0857.115664
- Ozdemir, D., Soypacaci, Z., Sahin, I., Bicik, Z., and Sencan, I. (2006). *Ochrobactrum anthropi* endocarditis and septic shock in a patient with no prosthetic valve or rheumatic heart disease: case report and review of the literature. *Jpn. J. Infect. Dis.* 59, 264–265.
- Perez-Blanco, V., Garcia-Caballero, J., Dominguez-Melcon, F. J., and Gomez-Limon, I. M. (2005). *Ochrobactrum anthropi* infectious endocarditis in an immunocompetent patient. *Enferm. Infecc. Microbiol. Clin.* 23, 111–112. doi: 10.1157/13071619
- Pilsyk, S., and Paszewski, A. (2009). Sulfate permeases phylogenetic diversity of sulfate transport. *Acta Biochim. Pol.* 56, 375–384.
- Qasimyar, H., Hoffman, M. A., and Simonsen, K. A. (2014). Late-onset *Ochrobactrum anthropi* sepsis in a preterm neonate with congenital urinary tract abnormalities. *J. Perinatol.* 34, 489–491. doi: 10.1038/jp.2014.31
- Romero Gomez, M. P., Peinado Esteban, A. M., Sobrino Daza, J. A., Saez Nieto, J. A., Alvarez, D., and Pena Garcia, P. (2004). Prosthetic mitral valve endocarditis due to *Ochrobactrum anthropi*: case report. *J. Clin. Microbiol.* 42, 3371–3373. doi: 10.1128/JCM.42.7.3371-3373.2004
- Sambrook, J. F., and Russell, D. W. (2001). *Molecular Cloning: A Laboratory Manual (3-Volume Set)*. New York, NY: Cold Spring Harbor Laboratory Press.
- Scholz, H. C., Mühlendorfer, K., Shilton, C., Benedict, S., Whatmore, A. M., Blom, J., et al. (2016). The change of a medically important genus: worldwide occurrence of genetically diverse novel *Brucella* species in exotic frogs. *PLoS ONE* 11:e0168872. doi: 10.1371/journal.pone.0168872
- Scholz, H. C., Pfeffer, M., Witte, A., Neubauer, H., Al Dahouk, S., Wernery, U., et al. (2008). Specific detection and differentiation of *Ochrobactrum anthropi*, *Ochrobactrum intermedium* and *Brucella* spp. by a multi-primer PCR that targets the recA gene. *J. Med. Microbiol.* 57(Pt 1), 64–71. doi: 10.1099/jmm.0.47507-0
- Siti Rohani, A. H., and Tzar, M. N. (2013). *Ochrobactrum anthropi* catheter-related bloodstream infection: the first case report in Malaysia. *Med. J. Malaysia* 68, 267–268.
- Shrishrimal, K. (2012). Recurrent *Ochrobactrum anthropi* and *Shewanella putrefaciens* bloodstream infection complicating hemodialysis. *Hemodial Int.* 16, 113–115. doi: 10.1111/j.1542-4758.2011.00586.x
- Sultan, S., and Hasnain, S. (2007). Reduction of toxic hexavalent chromium by *Ochrobactrum intermedium* strain SDCr-5 stimulated by heavy metals. *Bioresour. Technol.* 98, 340–344. doi: 10.1016/j.biortech.2005.12.025
- Suttle, C. A. (2005). Viruses in the sea. *Nature* 437, 356–361. doi: 10.1038/nature04160
- Teyssier, C., Marchandin, H., and Jumas-Bilak, E. (2004). The genome of alpha-proteobacteria: complexity, reduction, diversity and fluidity. *Can. J. Microbiol.* 50, 383–396. doi: 10.1139/w04-033
- Thoma, B., Straube, E., Scholz, H. C., Al Dahouk, S., Zoller, L., Pfeffer, M., et al. (2009). Identification and antimicrobial susceptibilities of *Ochrobactrum* spp. *Int. J. Med. Microbiol.* 299, 209–220. doi: 10.1016/j.ijmm.2008.06.009
- Velasco, J., Romero, C., Lopez-Goni, I., Leiva, J., Diaz, R., and Moriyon, I. (1998). Evaluation of the relatedness of *Brucella* spp. and *Ochrobactrum anthropi* and description of *Ochrobactrum intermedium* sp. nov., a new species with a closer relationship to *Brucella* spp. *Int. J. Syst. Bacteriol.* 48(Pt 3), 759–768. doi: 10.1099/00207713-48-3-759
- Wi, Y. M., and Peck, K. R. (2010). Biliary sepsis caused by *Ochrobactrum anthropi*. *Jpn. J. Infect. Dis.* 63, 444–446.
- Wichels, A., Biel, S. S., Gelderblom, H. R., Brinkhoff, T., Muyzer, G., and Schutt, C. (1998). Bacteriophage diversity in the North Sea. *Appl. Environ. Microbiol.* 64, 4128–4133.
- Yoshida, M., Yoshida-Takashima, Y., Nunoura, T., and Takai, K. (2015). Genomic characterization of a temperate phage of the psychrotolerant deep-sea bacterium *Aurantimonas* sp. *Extremophiles* 19, 49–58. doi: 10.1007/s00792-014-0702-5
- Zhang, X. H., Zhang, G. S., Zhang, Z. H., Xu, J. H., and Li, S. P. (2006). Isolation and characterization of a dichlorvos-degrading strain DDV-1 of *Ochrobactrum* sp. *Pedosphere* 16, 64–71. doi: 10.1016/S1002-0160(06)60027-1
- Zhou, Y., Liang, Y., Lynch, K. H., Dennis, J. J., and Wishart, D. S. (2011). PHAST: a fast phage search tool. *Nucleic Acids Res.* 39, W347–W352. doi: 10.1093/nar/gkr485

Conflict of Interest Statement: The authors declare that the research was conducted in the absence of any commercial or financial relationships that could be construed as a potential conflict of interest.

Copyright © 2017 Jäckel, Hertwig, Scholz, Nöckler, Reetz and Hammerl. This is an open-access article distributed under the terms of the Creative Commons Attribution License (CC BY). The use, distribution or reproduction in other forums is permitted, provided the original author(s) or licensor are credited and that the original publication in this journal is cited, in accordance with accepted academic practice. No use, distribution or reproduction is permitted which does not comply with these terms.



Systems Biology Analysis of Temporal *In vivo* *Brucella melitensis* and Bovine Transcriptomes Predicts host:Pathogen Protein–Protein Interactions

Carlos A. Rossetti^{1†}, Kenneth L. Drake², Sara D. Lawhon¹, Jairo S. Nunes^{1†}, Tamara Gull^{1†}, Sangeeta Khare^{1†} and Leslie G. Adams^{1*}

¹ Department of Veterinary Pathobiology, College of Veterinary Medicine and Biomedical Science, Texas A&M University, College Station, TX, United States, ² Seralogix, Inc., Austin, TX, United States

OPEN ACCESS

Edited by:

Nieves Vizcaino,
University of Salamanca, Spain

Reviewed by:

Steven Olsen,
Agricultural Research Service (USDA),
United States
Roy Martin Roop II,
East Carolina University, United States
Juan M. Garcia Lobo,
University of Cantabria, Spain

*Correspondence:

Leslie G. Adams
gadams@cvm.tamu.edu

†Present Address:

Carlos A. Rossetti,
Instituto de Patobiología,
CICVyA-CNIA, INTA, CC25
(B1712WAA) Castelar, Buenos Aires,
Argentina;
Jairo S. Nunes,
Takeda Pharmaceuticals International
Co., Cambridge, MA, United States;
Tamara Gull,
Department of Veterinary
Pathobiology, Oklahoma State
University, Stillwater, OK,
United States;
Sangeeta Khare,
National Center for Toxicological
Research, U.S. —Food and Drug
Administration, Jefferson, AR,
United States

To date, fewer than 200 gene-products have been identified as *Brucella* virulence factors, and most were characterized individually without considering how they are temporally and coordinately expressed or secreted during the infection process. Here, we describe and analyze the *in vivo* temporal transcriptional profile of *Brucella melitensis* during the initial 4 h interaction with cattle. Pathway analysis revealed an activation of the “Two component system” providing evidence that the *in vivo* *Brucella* sense and actively regulate their metabolism through the transition to an intracellular lifestyle. Contrarily, other *Brucella* pathways involved in virulence such as “ABC transporters” and “T4SS system” were repressed suggesting a silencing strategy to avoid stimulation of the host innate immune response very early in the infection process. Also, three flagellum-encoded loci (BMEI10150-0168, BMEI1080-1089, and BMEI1105-1114), the “flagellar assembly” pathway and the cell components “bacterial-type flagellum hook” and “bacterial-type flagellum” were repressed in the tissue-associated *B. melitensis*, while *RopE1* sigma factor, a flagellar repressor, was activated throughout the experiment. These results support the idea that *Brucella* employ a stealthy strategy at the onset of the infection of susceptible hosts. Further, through systems-level *in silico* host:pathogen protein–protein interactions simulation and correlation of pathogen gene expression with the host gene perturbations, we identified unanticipated interactions such as VirB11::MAPK8IP1; BtaE::NFKBIA, and 22 kDa OMP precursor::BAD and MAP2K3. These findings are suggestive of new virulence factors and mechanisms responsible for *Brucella* evasion of the host's protective immune response and the capability to maintain a dormant state. The predicted protein–protein interactions and the points of disruption provide novel insights that will stimulate advanced hypothesis-driven approaches toward revealing a clearer understanding of new virulence factors and mechanisms influencing the pathogenesis of brucellosis.

Keywords: interactome model, Bayesian analysis, virulence factors, Peyer's patch

INTRODUCTION

Brucella, an aerobic non-motile Gram-negative coccobacillus, is the etiological agent of brucellosis, a worldwide anthroponozoonotic infectious disease that causes chronic infections with persistent or recurrent bacteremia in susceptible hosts, and mid- to late gestation abortion in pregnant animals. At present, there are 11 recognized species within the genus *Brucella* based on preferential host specificity (O'Callaghan and Whatmore, 2011; Whatmore et al., 2014). Goats and sheep are the preferred hosts for *Brucella melitensis* (Alton, 1990), although this pathogen also infects cattle depending on specific epidemiological conditions (Kalher, 2000; Banai, 2010; Alvarez et al., 2011; Liu et al., 2012; Wareth et al., 2014). *B. melitensis* is also the most pathogenic and the most frequent causative agent of brucellosis in humans (Traxler et al., 2013). Clinically, human brucellosis can be an incapacitating disease that results in intermittent fever, chills, sweats, weakness, myalgia, osteoarticular complications, endocarditis, depression, and anorexia with low mortality (Dean et al., 2012).

The predominant route for *B. melitensis* penetration after natural exposure is the alimentary tract (Adams, 2002). Usually *B. melitensis* enters through the oral mucosa and colonizes the lymph nodes that drain the facial area (Carpenter, 1924; von Bargen et al., 2015); although several studies have isolated *Brucella* from different sections of the alimentary tract and feces revealing the possibility that brucellae invade in multiple sites of the gastrointestinal tract (Carpenter, 1924; Davis et al., 1988). We previously found that under experimental conditions, *B. melitensis* was able to invade the bovine host through the domed epithelium of jejuno-ileal Peyer's patches followed by rapid systemic dissemination (Rossetti et al., 2013). The calf ligated jejuno-ileal loop model has been demonstrated to be a very useful model to study *in vivo* natural host:infectious agent molecular and morphological initial interactions (Santos et al., 2002; Khare et al., 2009, 2012; Winter et al., 2010; Lawhon et al., 2011; Rossetti et al., 2013), a subject that has not been broadly studied in brucellosis.

Brucella lack several classical bacterial virulence factors such as exotoxins, cytotoxins, a capsule, fimbriae, plasmids, resistant strains, lysogenic phages, antigenic variation, or endotoxic lipopolysaccharide among others (Moreno and Moriyón, 2002). *Brucella* has developed a stealthy strategy to avoid being recognized and successfully infect hosts. Succinctly stated, *Brucella* circumvents strong innate immune responses, obstructs the direct action of bactericidal substances, resists destruction by professional phagocytes and maintains the host cells alive to establish long lasting infections (Barquero-Calvo et al., 2007). Although, significant advances have been made lately (de Figueiredo et al., 2015), the molecular pathogenesis of brucellosis is still incompletely understood. To date, fewer than 200 gene products have been identified as *Brucella* virulence factors (He, 2012), and very few related to adhesion and invasion function have been characterized. For instance, the heat shock protein 60 (Hsp60) family proteins on the surface of *Brucella abortus* have been found to bind macrophage and intestinal M cells cellular prion protein (PrP^c) before internalization (Watarai

et al., 2003; Nakato et al., 2012). The SP41 (UgpB) protein that has significant homology with the glycerol-3-phosphate-binding ABC transporter protein interacts with cellular sialic acid residues, facilitating efficient host invasion (Castaneda-Roldán et al., 2006). Other recently characterized proteins in the brucellae genome, such as, BmaC (Posadas et al., 2012), BtaE (Ruiz-Ranwez et al., 2013a), BtaF (Ruiz-Ranwez et al., 2013b) interact with different components of the extracellular matrix, while novel adhesion-encoding regions *inv* (Alva-Perez et al., 2014), or BigA (Czibener et al., 2016) have been demonstrated to promote adhesion and invasion, but their target host molecules have not been identified yet.

A well-recognized *Brucella* virulence factor is the two-component response regulator, BvrR/BvrS, that modulates the host cell cytoskeleton upon *Brucella* invasion (Sola-Landa et al., 1998) and regulates the *Brucella* OMP expression (Guzmán-Verri et al., 2002). Dysfunction of BvrR/S response regulator system induces mutant strains with reduced invasiveness and failure to replicate and survive intracellularly. *Brucella* lipopolysaccharide is also a confirmed virulence factor (Lapaque et al., 2005), that prevents complement-mediated bacterial killing (Allen et al., 1998; Tumurkhuu et al., 2006), provides resistance against antimicrobial peptides such as defensins, lysozyme, and lactoferrin (Martínez de Tejada et al., 1995) and inhibits cell death (Pei and Ficht, 2004; Pei et al., 2006). Additionally, *Brucella* LPS masks recognition of the pathogen-associated molecular patterns (PAMPs) from immune-receptor recognition, and as a consequence, impedes, or attenuates proinflammatory responses and immune system activation (Forestier et al., 2000; Jiménez de Bagués et al., 2004). Simultaneously, the type four secretion system (T4SS) is also a key virulence factor for *Brucella* intracellular survival (O'Callaghan et al., 1999), persistent infection in mice and induction of the host immune response (Rolan and Tsolis, 2007; Roux et al., 2007). This virulence factor, encoded by a *virB* operon, is induced by early phagosome acidification after phagocytosis (Boschiroli et al., 2002; Celli et al., 2003) to translocate effector molecules directly into the host cell cytoplasm. Additional investigations have identified several of these effector proteins, although most of their functions remain undefined (de Jong et al., 2008, 2013; de Barsey et al., 2011; Marchesini et al., 2011, 2016; Salcedo et al., 2013; Ke et al., 2015; Del Giudice et al., 2016). The secretion systems and secretomes of *Brucella* were recently computationally analyzed, resulting in the prediction of 29 host-pathogen specific interactions between cattle and *B. abortus* and 36 host-pathogen interactions between sheep and *B. melitensis* proteins (Sankarasubramanian et al., 2016). The two-component system RegB/A, including the *aceA* encoding isocitrate lyase, has been found to play a critical role in the persistence and *in vivo* pathogenicity of *Brucella suis* (Abdou et al., 2017).

An additional virulence mechanism used by *Brucella* to survive intracellularly is the periplasmic compound cyclic B-1,2 glucan, that interferes with cellular trafficking and maturation of the *Brucella*-containing vacuole by disrupting cholesterol-rich lipid rafts present on phagosomal membranes and preventing the phagosome-lysosome fusion (Arellano-Reynoso et al., 2005; Martirosyan et al., 2012). Other virulence elements reported

to sustain a chronic infection include: phosphatidylcholine, a phospholipid compound abundant in eukaryotic cell membranes that facilitate *Brucella* avoidance of host recognition (Comerci et al., 2006; Conde-Alvarez et al., 2006); PrpA, a proline-racemase family compound that elicits B lymphocyte polyclonal activation (Spera et al., 2006); BtpA and BtpB, *Brucella* TIR-containing effector proteins that suppress innate immunity and modulate host inflammatory responses during infection (Salcedo et al., 2008, 2013); MucR, a transcriptional regulator involved in *Brucella* metabolism, cell wall/envelope biogenesis, replication, type IV secretion system, quorum sensing system, and stress tolerance (Dong et al., 2013) and a flagellar appendage, required for virulence in a mouse infection model (Fretin et al., 2005).

Most of these virulence factors were characterized individually without considering how they are temporally and coordinately expressed or secreted during the infection process. Recently, several experiments have been performed to more fully understand the sequential expression and coordinated regulation of the infection process (Kohler et al., 2002; Al Dahouk et al., 2008; Rambow-Larsen et al., 2008; Lamontagne et al., 2009; Rossetti et al., 2009; Wang et al., 2009; Viadas et al., 2010; Weeks et al., 2010; Hanna et al., 2013; Tian et al., 2013). These experiments using *in vitro* culture media, infected cell cultures, or infected mice were successful for generating initial hypotheses to enhance the understanding of the pathogenesis of brucellosis.

Here, we describe an integrative approach of experimentation and computation to analyze the *in vivo* temporal transcriptional profile of *B. melitensis* during the first 4 h of the interaction with a naturally susceptible host, using the established calf jejuno-ileal loop model of infection. We then performed a system-level analysis by applying both a traditional statistical differential analysis to determine significance of *B. melitensis* gene expression and a pathway and gene ontology (GO) analysis that employed a dynamic Bayesian network (DBN) technique (Khare et al., 2016) to identify perturbations trends over time. The fundamental concept of systems biology is to: (1) perturb a system—(time-course *B. melitensis* infected bovine Peyer's patch), (2) measure systems-wide responses—(*B. melitensis* and bovine transcriptomes), and (3) integrate measured responses into a model—(host:pathogen::Bovine:*B. melitensis* interactome model) to understand the observations and iteratively predict novel interactions and perturbations. The system-level analyses aided understanding of the strategies exploited by *B. melitensis* to invade, survive, and replicate intracellularly; and to identify perturbations of major genes modulating critical cellular pathways in the pathogenesis of brucellosis. Further, through systems-level *in silico* host-pathogen protein-protein interactions (PPIs) simulation (see **File S1**), we were able to make inferred predictions of interactions of close apposition with specific *B. melitensis* expressed genes/proteins to plausible host (bovine) pathway points of disruption or perturbations. The predicted PPIs and the points of disruption provide novel insights that will stimulate advanced iterative hypothesis-driven approaches toward revealing a clearer understanding of new virulence factors and mechanisms contributing to the evasion of the host's protective immune responses.

MATERIALS AND METHODS

Infection Model

The *in vivo* infection model for *Brucella* was described previously (Rossetti et al., 2013). Briefly, five bovine jejuno-ileal segments from four calves were inoculated intraluminally with 3 ml of a suspension containing 1×10^9 CFU of *B. melitensis* 16 M/ml (total of 3×10^9 CFU) at late-log growth phase cultured in F12K medium (ATCC[®]) supplemented with 10% heat-inactivated fetal bovine serum (HI-FBS) (ATCC[®]). One infected segment was removed at every time point (0.25, 0.5, 1, 2, 4 h post-inoculation from each of the four calves.), and six to ten 6 mm biopsy punches were collected from each segment. The mucosal layer of Peyer's patch was immediately dissected, macerated and homogenized in TRI-Reagent[®] (Ambion, Austin, TX). Subsequently, samples were appropriately contained and transported to an inspected and approved BSL-3 laboratory for immediate RNA extraction. Calves were euthanized with an intravenous bolus of sodium pentobarbital at the completion of the procedures. All animal experiments were approved by the Texas A&M University Institutional Animal Care and Research Advisory Committee (AUP#2003-178). Surgeries were performed under biosecurity laboratory III (BSL-3) conditions in CDC-approved isolation buildings at the Texas A&M University experimental farm (College Station, TX).

RNA Isolation, Labeling, and Hybridization

RNA isolation, labeling, and hybridization procedures were performed as described in previous experiments (Rossetti et al., 2010, 2011b). Total RNA from *B. melitensis*-infected bovine Peyer's patches was extracted according to the TRI-Reagent manufacturer's instructions. Tissue-associated *B. melitensis* total RNA was initially enriched (MICROBEnrich[®], Ambion) and then amplified from 30 µg of total RNA from *B. melitensis*-infected bovine Peyer's patches (Rossetti et al., 2010). Briefly, the enriched RNA was precipitated in 100% ethanol at -20°C , washed and re-suspended in 25 µl of DEPC-treated water (Ambion). Immediately, the total amount of RNA was linearly amplified in a 3 step-protocol. First, RNA was reverse transcribed to cDNA using *B. melitensis* genome direct primers (BmGDPs), T7 promoter-template switching primer (T7-TS) (Sigma Genosys, The Woodland, TX) and Moloney Murine Leukemia Virus Reverse Transcriptase (Clontech, Palo Alto, CA). In the next step, the second-strand cDNA was synthesized and purified (Qiagen, Valencia, CA), followed by concentration in a speed-vac with no heat. In the last step, the *in vitro* transcription, was performed using the double-stranded cDNA as the template and T7 polymerase (Ambion). Then, 10 µg of each experimental sample ($n = 44$, i.e., 4 were *in vitro*-grown cultures of *B. melitensis* at late-log phase of growth; 20 were enriched and amplified *B. melitensis* RNA from total RNA from infected bovine Peyer's patches; and an additional 20 were from total RNA of infected bovine Peyer's patches) were reverse transcribed overnight to amino-allyl cDNA using 1.5 µg of *B. melitensis* genomic directed primers (BmGDPs) (Rossetti et al., 2010), labeled with Cy3 (Amersham Pharmacia Biosciences, Piscataway, NJ), mixed with 0.5 µg of Cy5 labeled

B. melitensis gDNA, and applied to a custom 3.2K *B. melitensis* oligoarray (Weeks et al., 2010). Since the enrichment procedure does not eliminate host RNA, total RNA from *B. melitensis*-infected bovine Peyer's patches were also reverse transcribed, labeled and hybridized on *B. melitensis* oligo microarray, due to a potential concern that eukaryotic RNA present in enriched and amplified samples could possibly overlap with sequences of the *B. melitensis* transcripts and cross hybridized with probes on *B. melitensis* oligo microarrays, resulting in falsely detected pathogen genes. The isolation and labeling of *B. melitensis* gDNA has been described in detail elsewhere (Rossetti et al., 2009). Slides were hybridized at 45°C for approximately 20 h in a dark humid chamber (Corning, Corning, NY). Then, washed for 10 min at hybridization temperature with low stringency buffer [1X SSC, 0.2% SDS] followed by two 5-min washes with a higher stringency buffer [0.1X SSC, 0.2% SDS and 0.1X SSC] at room temperature with mild agitation, dried by centrifugation and immediately scanned.

Data Acquisition, Normalization, and Microarray Data Analysis

Immediately after washing, the dried slides were scanned using a commercial laser scanner (GenePix 4100; Axon Instruments Inc., Foster City, CA). Scans were performed using the autoscan feature with the percentage of saturated pixels set at 0.03%. The genes represented on the arrays were adjusted for background and normalized to internal controls using image analysis software (GenePixPro 6.0; Axon Instruments Inc.). Genes with fluorescent signal values below background were disregarded in all analyses. Arrays were initially normalized against *B. melitensis* genomic DNA, and the resulting data were analyzed and modeled using an integrated platform termed the BioSignature Discovery System (BioSignatureDS[®]) (Seralogix, LLC, Austin, TX; <http://www.seralogix.com>) explained in detail elsewhere (Lawhon et al., 2011; Rossetti et al., 2013). The tissue-associated *B. melitensis* gene expression at every time point (0.25–4 h) was compared to the gene expression of the inoculum (i.e., *in vitro*-grown cultures of *B. melitensis* at late-log phase of growth, cultured in F12K medium with 10% HI-FBS; $n = 4$). Significantly expressed genes were determined with the z -test ($p < 0.025$) (enhanced with Bayesian methods of variance estimation) after subtracting those genes also expressed at statistically significant levels when total RNA of *B. melitensis*-infected bovine Peyer's patches was compared to the gene expression of the inoculum. BiosignatureDS tools for statistical z -score gene thresholding, *Brucella* pathway and gene ontology (GO) perturbation scoring (scored using Bayesian Information Criterion and transformed to z -score), and mechanistic gene identification were used for the comprehensive analysis performed in this study. A specialized application was developed to implement algorithms that integrate multiple sources of prior biological knowledge (PBK) into the inference of host-pathogen protein–protein interaction (PPIs) prediction (see **File S1** for complete details). Briefly, we adopted three algorithmic methods for the identification of candidate interaction points for use in network learning between the host and the pathogen from *in vivo* gene

expression data. These algorithmic methods were: (1) a sequence-similarity interaction transference procedure; (2) structural protein domain-based algorithm; and (3) a functional gene-ontology-based algorithm. Gene candidates for inclusion in our interaction prediction process were selected based on interpretation of pathway and GO analyses conducted by our Dynamic Bayesian Network methodology. The *B. melitensis* gene transcriptome was employed and ≈ 600 bovine host genes selected from 12 perturbed and immune response relevant pathways and 10 GO terms to form gene sets representing two “unconnected” system models for starting the “interactome model” network learning process. Those algorithms yielded 348, 68, and 295 potential host-pathogen PPIs, respectively, that comprised the set of potential interactions at the interface of the pathogen and host systems. These potential interactions were then included into the Bayesian host-pathogen network structure learning algorithm. The method employs model structures to initialize learning with biologically relevant structures and utilize actual time-course co-expressed gene and other “omic” data from pathogen and host to search for a set of structures in which the data best fit. Microarray data and metadata are deposited in the Gene Expression Omnibus at the National Center for Biotechnology Information (<http://www.ncbi.nlm.nih.gov/geo/>) Accession #GSE89053.

For microarray results validation, six randomly selected genes with consistently differential expressed from 15 min to 4 h post-infection (p.i.) by microarray results, were analyzed at every time point by quantitative RT-PCR (qRT-PCR) following the protocol described elsewhere (Rossetti et al., 2011b). Primers (Sigma Genosys) of tested genes were designed by Primer Express Software v2.0 (Applied Biosystems) (**Table S1**). For each gene tested, the individual calculated threshold cycles (Ct) were averaged among each condition and normalized to the Ct of the 16S rRNA gene from the same cDNA samples before calculating the fold change using the $\Delta\Delta Ct$ method (Livak and Schmittgen, 2001). For each primer pair, a negative control (water) and an RNA sample without reverse transcriptase (to determine genomic DNA contamination) were included as controls during cDNA quantitation. Statistical significance was determined by Student's t -test and expression differences considered significant when $P < 0.05$. As gene expression by microarray and qRT-PCR were based on z -score and fold-change, respectively, array data were considered valid if the fold change of each gene tested by qRT-PCR was expressed in the same direction as determined by microarray analysis.

RESULTS

B. melitensis Transcriptome Is Perturbed at the Onset of the Infection Process

We previously reported that the number of *B. melitensis* 16M organisms after intraluminal inoculation increased from 15 min to 4 h p.i. (Rossetti et al., 2013) in this model. To study pathogen alterations in gene expression, pathway, and GO perturbations during the initial infection process, *Brucella* RNAs extracted

from infected bovine Peyer's patches at different times p.i. were hybridized on *B. melitensis* microarrays and analyzed. As expected, the traditional z-score analysis ([2.24], 97.5% confidence) identified a total of 2,356 different *B. melitensis* genes (1,221 up-regulated vs. 1,135 down-regulated) differentially expressed (DE) at least once over the 4 h time course p.i., compared to the *in vitro* grown control (Table S2). As opposed to the 1 h-peak of the host gene expression after infection (Rossetti et al., 2013), the total number of perturbed *Brucella* genes is rather constant in the first 4 h p.i. (15 min: 1,899 genes, 30 min: 1,937 genes, 1 h: 1,968 genes, 2 h: 1,909 genes and 4 h: 1,912 genes; Figure 1). The combined analysis of these results, i.e., the host and pathogen transcriptional profiles during bovine Peyer patch infection, clearly indicate that both host and *Brucella* gene expression responses are markedly perturbed at a very early time post-interaction. This is in concordance with other results (He et al., 2006; Rossetti et al., 2011b, 2012), which corroborates an initial transcriptionally perturbed period followed by a more quiescent one.

A group of 1,740 genes (55% of *B. melitensis* genome) was markedly perturbed in the same direction in at least 4 of 5 time points (Table S3). These genes were considered as the core set of genes associated with the adaptive changes of *B. melitensis* during the early *in vivo* bovine Peyer's patch infection, and therefore important in understanding key events in the early modulation of host response. From this set of 1,740 Differentially Expressed (DE) genes, 925 (53%) were activated and 815 (47%) were repressed compared with the *in vitro* grown culture. Interestingly, genes from the core set located on chromosome I were mainly activated (over 1,174 DE genes: 752 were up- and 422 were down-regulated), while genes located on chromosome II were mainly repressed in higher numbers (566 total DE genes: 173 were up- and 393 were down-regulated). Chromosome I encodes the majority of the core metabolic machinery for transcription, translation and protein synthesis, and Chromosome II is overrepresented in genes involved in pathways for utilization of specific substrates (membrane

transport, central intermediary and energy metabolism, and regulation; Paulsen et al., 2002). Altogether, these results suggest that *Brucella* may restrain metabolic functions while inducing transcriptomic modifications to adapt from an extracellular to an intracellular lifestyle. These results are largely in concordance with previous publications (Lamontagne et al., 2009; Rossetti et al., 2011a,b) even though our study analyzes the complexity of *in vivo* invasion process in comparison with pathogen gene expression in other *in vitro* (i.e., one cell line) models of invasion.

Microarray gene expression data were validated by qRT-PCR. Six randomly selected *Brucella* genes, determined to be significantly affected throughout the first 4 h p.i., were chosen for verification at every time point (i.e., 30 data points). As shown by the representative examples in Figure S1, gene expression changes were consistent between microarray and qRT-PCR for genes with increased expression or genes with decreased expression relative to the control.

DISCUSSION

Major *Brucella* Virulence Factors Are Down Regulated at the Onset of the Infection

Within 15–30 min of *in vivo* exposure, *B. melitensis* adhere and immediately penetrate through the intestinal mucosa and Peyer's patch and rapidly disseminate through systemic circulation (Rossetti et al., 2013). Early stage host gene expression of Syndecan 2, Integrin alpha L and Integrin beta 2 genes coincide with initial *Brucella* adhesion which is coupled with simultaneous repression of two intestinal barrier-related pathways (Tight Junction and Trefoil Factors Initiated Mucosal Healing), subverting mucosal epithelial barrier function and facilitating *Brucella* transepithelial migration (Rossetti et al., 2013). To elucidate *Brucella* virulence mechanisms responsible for this host molecular response, we expanded our analysis on pathogen pathways (Table 1) and GO alterations (Tables S4–S8). Note that pathway molecular interactions and annotations are based on those provided by the Kyoto Encyclopedia of Genes and Genomes (KEGG; Kanehisa et al., 2017). Pathways and Gene Ontology groups are comprised of gene sets which may be either activated or repressed in some combination over time. The Bayesian scoring method computes the log-likelihood of the *in vivo* expressed data and measures its goodness-of-fit to a model trained with control data (the *in vitro* inoculum expression data). In this manner, it is possible to determine if a pathway or GO group is activated or repressed. In our computational system biology approach, if the sum of the individual gene scores within a pathway/GO group is positive then the pathway/GO score is considered to be activated. Otherwise, if the sum is negative, the pathway/GO score is considered repressed and assigned a negative score value. Table 1 shows the results of the pathway analysis scoring listed by pathway categories and sorted by activated or repressed state on the 15 min p.i. column. Specific gene expression scores within these pathways are provided in Table S7. Early in the infection process, the pathway category "Environmental Information Processing" has several important pathways involved in *B. melitensis* pathogenicity which are

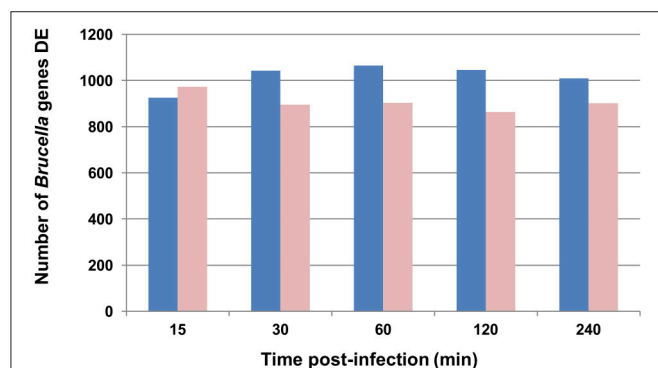


FIGURE 1 | Graphic representation of *B. melitensis* genes differentially expressed (DE) throughout the experiment. Blue bars represent genes activated; light red bars represent genes repressed. For differential analysis, the *in vivo* infected loop gene expression is compared to the *in vitro* log growth phase inoculum as the control.

TABLE 1 | Significantly perturbed pathways (Bayesian z-score >|2.24|) of tissue-associated *B. melitensis* during the first 4 h post-bovine Peyer's patch infection.

KEGG Name	Description	T15	T30	T60	T120	T240
ENVIRONMENTAL INFORMATION PROCESSING						
bme03010	Ribosome	9.63	8.38	11.27	9.53	9.72
bme03020	RNA polymerase	7.64	7.74	10.42	7.9	7.77
bme02060	Phosphotransferase system (PTS)	6.98	6.04	7.9	7.28	6.06
bme00970	Aminoacyl-tRNA biosynthesis	6.82	7.87	9.9	5.6	9.67
bme03060	Protein export	5.29	7.02	8.57	4.61	6.95
bme03410	Base excision repair	-7.33	-5.36	-5.4	-6.28	-5.82
bme03070 bme_M00333*	Type IV secretion system module	-7.67	-9.04	-8.87	-9.52	-6.86
bme03030	DNA replication	-9.41	-6.39	-6.62	-6.69	-6.22
bme02020	Two-component regulatory system	-9.55	8.66	8.65	6.74	9.52
bme02010	ABC transporters	-10.01	-8.34	-9.17	-6.44	-9.83
GLYCAN BIOSYNTHESIS AND METABOLISM						
bme00510 (map00510)*	N-Glycan biosynthesis	-8.34	5.1	7.9	6.02	6.43
bme00512 (map00512)*	O-Glycan biosynthesis	-9.82	-4.26	-4.96	-4.6	-5.59
bme00603	Glycosphingolipid biosynthesis	-9.99	4.81	-6.82	-5.03	-5.18
bme00604 (map00604)*	Glycosphingolipid biosynthesis	-9	-4.92	-6.56	-4.98	-5.46
bme00940 (map00940)*	Phenylpropanoid biosynthesis	-4.74	5.51	6.87	7.05	5.98
CELLULAR PROCESSES						
bme02030	Bacterial chemotaxis	-8.75	-8.68	-7.73	-7.93	-8.25
bme02040	Flagellar assembly	-9.21	-8.29	-9.01	-8.63	-7.17
CARBOHYDRATE METABOLISM						
bme00010	Glycolysis/Gluconeogenesis	8.34	7.05	7.27	6.89	8.52
LIPID METABOLISM						
bme00061	Fatty acid biosynthesis	7.3	7.63	8.34	6.07	7
METABOLISM						
bme00400	Phenylalanine, tyrosine and tryptophan biosynthesis	11.71	9.3	10.01	10.44	9.12
bme00230	Purine metabolism	10.38	9.05	11.96	7.56	8.2
bme00300	Lysine biosynthesis	8.98	6.83	6.77	6.54	5.84
bme00710 (map00710)*	Carbon fixation in photosynthetic organisms	8.89	6.6	6.92	6.42	7.81
bme00620	Pyruvate metabolism	8.66	7.41	8.59	5.99	6.42
bme00950 (map00950)*	Alkaloid biosynthesis I	8.35	7.48	7.04	7.44	6.31
bme00240	Pyrimidine metabolism	8.24	8.72	9.54	7.76	7.26
bme00190	Oxidative phosphorylation	8.09	7.53	10.17	7.87	7.72
bme00271 (map00270)**	Methionine metabolism	8	11.81	9.18	6.73	7.93
bme00740	Riboflavin metabolism	7.49	5.78	10.7	4.36	7.27
bme00720 (map00720)*	Reductive carboxylate cycle (CO ₂ fixation)	7.44	7.79	8.29	6.06	8.31
bme00020	Citrate cycle (TCA cycle)	7.43	8.42	8.95	7.39	8.41
bme00030	Pentose phosphate pathway	7.43	6.62	9.06	6.32	8.85
bme00790	Folate biosynthesis	7.43	6.17	10.52	4.84	7.62
bme00670	One carbon pool by folate	7.29	8.14	10.94	6.59	7.09
bme00251 (map00250)**	Glutamate metabolism	7.19	7.46	8.66	7.82	8.2
bme00760	Nicotinate and nicotinamide metabolism	7.05	6.86	6.85	6.17	8.13
bme00904 (map00904)*	Diterpenoid biosynthesis	6.95	4.35	6.81	3.82	5.08
bme00100 (map00100)*	Biosynthesis of steroids	6.91	6.47	6.88	4.4	6.29
bme00660	C5-Branched dibasic acid metabolism	6.89	7.59	8.19	6.1	6.94
bme00290	Valine, leucine and isoleucine biosynthesis	6.87	7.76	10.18	5.58	5.41
bme00770	Pantothenate and CoA biosynthesis	6.71	10.04	8.42	7.16	7.99
bme00680	Methane metabolism	6.69	7.93	10.68	9.28	7.01
bme00330	Arginine and proline metabolism	6.68	6.67	8.62	5.55	8.6

(Continued)

TABLE 1 | Continued

KEGG Name	Description	T15	T30	T60	T120	T240
bme00621 (map00621)*	Biphenyl degradation	6.62	7.19	8.83	4.13	6.7
bme00730	Thiamine metabolism	6.5	8.39	7.51	5.52	6.54
bme00252 (map00250)**	Alanine and aspartate metabolism	6.36	6.19	8.28	4.05	9.89
bme00072	Synthesis and degradation of ketone bodies	6.26	6.72	9.33	5.34	9
bme00540	Lipopolysaccharide biosynthesis	6.11	5.42	5.98	3	4.94
bme00622	Toluene and xylene degradation	5.95	5.48	5.55	5.36	5
bme00460	Cyanoamino acid metabolism	5.67	6.33	6.96	3.49	5.85
bme00361	Gamma-Hexachlorocyclohexane degradation	5.32	7.54	7.83	5.58	7.45
bme00627	1,4-Dichlorobenzene degradation	5.32	5.1	5.23	5.01	4.73
bme00272 (map00270)**	Cysteine metabolism	5.29	8.32	7.05	5.43	9.11
bme00530 (map00530)*	Aminosugars metabolism	5.15	6	6.99	5.76	7.79
bme00983 (map00983)*	Drug metabolism - other enzymes	4.48	6.72	7.03	7.96	5.98
bme00900	Terpenoid biosynthesis	4.47	5.65	4.86	5.82	7.32
bme00643	Styrene degradation	-2.57	3.65	6.06	3.29	3.13
bme00062 (map00062)	Fatty acid elongation in mitochondria	-3.85	-5.45	-5.31	-4.04	-4.5
bme00472	D-Arginine and D-ornithine metabolism	-4.22	2.97	-3.66	-2.55	-3.76
bme00473	D-Alanine metabolism	-4.56	3.58	-6.23	-5.01	-5.55
bme00785	Lipoic acid metabolism	-4.73	-6.11	-4.56	-3.39	-3.99
bme01053	Biosynthesis of siderophore group nonribosomal peptides	-5.02	-7.26	-6.39	-5.46	8.37
bme00521	Streptomycin biosynthesis	-5.57	-8.27	-6.95	-6.95	-6.03
bme00523	Polyketide sugar unit biosynthesis	-5.68	-4.98	-7.14	-5.33	-6.09
bme00562 (map00562)*	Inositol phosphate metabolism	-6.12	-5.03	-5.59	-5.19	-5.94
bme00960 (map00960)*	Alkaloid biosynthesis II	-6.24	-5.2	-6.06	-4.49	-7.29
bme00561	Glycerolipid metabolism	-6.52	-6.47	-5.85	-6.78	-5.49
bme00780	Biotin metabolism	-6.58	5.58	-8.34	-5.42	-6.92
bme00430	Taurine and hypotaurine metabolism	-6.77	-7.51	-5.9	-4.86	-7.34
bme00471	D-Glutamine and D-glutamate metabolism	-6.78	6.63	-6.03	-5.26	-6.85
bme00520	Nucleotide sugars metabolism	-6.78	-8.13	-9.91	-8.15	-7.92
bme00910	Nitrogen metabolism	-6.93	-7.05	-8.95	-4.62	-8.09
bme00120 (map00120)*	Bile acid biosynthesis	-7	-7.7	-6.81	-4.94	-6.98
bme00791 (map00791)*	Atrazine degradation	-7.07	-8.29	-8.65	-8.67	-5.95
bme00623 (map00623)*	2,4-Dichlorobenzoate degradation	-7.17	8.12	-7.34	-5.59	-8.6
bme00440	Aminophosphonate metabolism	-7.32	-7.74	-7.47	-8.84	-8.42
bme00362	Benzoate degradation via hydroxylation	-7.39	-6.05	-6.55	-7.82	-6.72
bme00930	Caprolactam degradation	-7.59	-8.47	-7.83	-6.26	-7.4
bme00626	Naphthalene and anthracene degradation	-7.67	-8.74	-7.96	-9.4	-9.68
bme00401	Novobiocin biosynthesis	-7.7	-9.01	-6.93	-6.7	-8.07
bme00564	Glycerophospholipid metabolism	-7.8	6.54	7.27	4.05	7.56
bme00750	Vitamin B6 metabolism	-7.87	-7.82	6.75	-6.35	-6.14
bme00363 (map00363)*	Bisphenol A degradation	-7.96	-8.65	-9.7	-4.4	-8.24
bme00903	Limonene and pinene degradation	-8.03	-9	-8.32	-4.84	-7.22
bme00260	Glycine, serine and threonine metabolism	-8.13	8.1	8.28	6.85	8.88
bme00980 (map00980)*	Metabolism of xenobiotics by cytochrome P450	-8.17	-6.12	-5.34	-5.38	-7.51
bme00380	Tryptophan metabolism	-8.21	-8.52	-6.83	-8.29	-7.72
bme00340	Histidine metabolism	-8.22	-7.84	-9.8	-6.14	-7.31
bme00053	Ascorbate and aldarate metabolism	-8.26	-9.15	-7.21	-4.6	-5.25
bme00624	1- and 2-Methylnaphthalene degradation	-8.35	8	9.52	4.59	9.26
bme00982 (map00982)*	Drug metabolism—cytochrome P450	-8.38	-6	-4.92	-4.92	-7.29

(Continued)

TABLE 1 | Continued

KEGG Name	Description	T15	T30	T60	T120	T240
bme00410	Beta-Alanine metabolism	−8.46	−10.2	−6.21	−8.3	−6.83
bme00360	Phenylalanine metabolism	−8.47	6.77	7.76	3.73	8.95
bme00350	Tyrosine metabolism	−8.62	−9.09	−11.2	−5.31	−9.84
bme00310	Lysine degradation	−8.7	−8.34	−7.4	−7.87	−6.92
bme03430 (map03430)*	Mismatch repair	−8.7	−8.39	−7.72	−7.25	−6.91
bme00220	Urea cycle and metabolism of amino groups	−8.78	−8.52	−6.88	−6.64	−8.13
bme01040	Biosynthesis of unsaturated fatty acids	−9.05	−6.42	−6.49	−6.13	−7.2
bme00071	Fatty acid metabolism	−9.35	−9.94	−6.37	−8.2	−6.77
bme00281	Geraniol degradation	−9.41	−8.07	−7.56	−8.65	−9.49
bme00650	Butanoate metabolism	−9.89	−8.32	−7.93	−6.51	−8.96
bme00280	Valine, leucine and isoleucine degradation	−10.19	−7.17	−9.32	−5.61	−8.64
bme00040	Pentose and glucuronate interconversions	−10.28	−8.56	−9.77	8.41	−6.75
bme00640	Propanoate metabolism	−10.89	−7.64	−9.42	−6	−8.92

* Indicates that current KEGG Database only includes the 'map' reference pathway.

** Indicates the "bme" pathway was combined with another pathway in the current KEGG database.

The pathways are organized by category and then sorted by activated or repressed states on the T15 minute p.i. column. Pathway scoring employed the *in vivo* gene expression for the experimental treatment condition and the *in vitro* gene expression from the log growth phase of the inoculum as the control condition. The "bme" pathway molecular interactions were originally based on the 2009 version of Kyoto Encyclopedia of Genes and Genomes (KEGG) database and their KEGG pathway name designators (Kanehisa et al., 2017). Some pathway names indicated with a * or ** required updating to be consistent with the current online KEGG database.

repressed at 15 min p.i. that include "Type IV secretion system," "Type III secretion system," Two-component system," and ABC transporters. It is interesting to note that the Two-component regulatory systems (TCRSs) and Type III secretion system pathways reverse to an activated state at 30 min. p.i. In the cellular processes category, the "Flagellar assembly" and "Bacterial chemotaxis" pathways are also repressed across all time point p.i.

The TCRSs are signal transduction mechanisms that allow microorganisms to sense and respond to changes in environmental conditions. Bioinformatic analysis of *Brucella* genomes has identified 15 predicted *bona fide* TCRS pairs (Lavin et al., 2010). Several of these systems have been characterized in *Brucella* species, such as BvrSR (Sola-Landa et al., 1998), FeuQP (Dorrell et al., 1998), NtrBC (Dorrell et al., 1999), NtrXY (Foulongne et al., 2000; Carrica et al., 2012), PrlSR (Mirabella et al., 2012), the flagellar master regulator FtcR (Leonard et al., 2007), the blue-light-activated LOV HKs (Swartz et al., 2007), RegA (Abdou et al., 2017), and CenR (Zhang et al., 2009). Other TCRSs have been identified by transpositional mutagenesis during global screening for virulence factors (Lestrade et al., 2000; Wu et al., 2006) but remain uncharacterized. Our pathway analysis revealed that the TCRSs were initially repressed at 15 min. p.i. and were then activated for the remaining time points (Table 1) providing evidence that *in vivo* *Brucella* sense and actively regulate their metabolism through the transition to intracellular lifestyle. Changes in expression between 15 min to 30 min p.i. by the TCRSs genes *dctM*, *glnG*, *glnL*, *phoB*, *phoQ*, *citE*, and *divJ* resulted in the TCRSs pathway transitioning from a repressed state to an activated state with the exception of *aceA* which was activated early and then repressed. These genes went from a strongly repressed state to an insignificant expressed state.

Contrarily, other *Brucella* pathways involved in virulence such as "ABC transporters" and "T4SS system" were continuously repressed suggesting a silencing strategy to avoid stimulation of the host's innate immune response very early in the infection process (Table 1). The highly repressed genes associated with the ABC transporters repression included BMEI0196, BMDI0861, PBMII0120, BMEI1138, *proW*, *ybbP*, *pstB*, *potB*, *afuB*, *rbsC* and several others. The T4SS system repression was induced by the repressed genes *virB4*, *virB5*, *virB6*, and *virB9* (Table S2). *In vitro* studies have demonstrated that T4SS is not required for cellular invasion, and its expression begins 15 min after phagocytosis and maximizes at 5 h p.i. (Sieira et al., 2004). It has been shown to be indispensable for intracellular survival of *Brucella* (O'Callaghan et al., 1999; Sieira et al., 2000; Delrue et al., 2005). Under our *in vivo* experimental conditions, expression of genes from the *virB* operon was repressed as was confirmed by qRT-PCR [Figure S1: BMEI0033 (*virB9*)]. In addition, the transcriptional regulator *vjbR* (BMEI1116) that positively regulates the expression of *B. melitensis* *virB* operon (Delrue et al., 2005) was not differentially expressed in our microarray results (Table S2). These data show that the T4SS was repressed during the first 4 h p.i. of *in vivo* infection. Collectively, our results, in addition to those reported earlier (Roux et al., 2007; den Hartigh et al., 2008) that failed to detect differences in the number of *B. abortus* and *B. melitensis* WT and *virB* mutant recovered from mice spleens in the first 3 days p.i., suggest that the *virB* operon may not play a major role in the initial *in vivo* *Brucella* pathogenesis. There are likely *in vivo* environmental signals that modulate the expression of the *virB* operon differently than reported in *in vitro* systems of infection. Identification of the host molecule targets of the T4SS will help characterize its expression based on the host cellular response discussed further in the

next section “Systems biology *in vivo* interactome modeling results.”

Systems Biology *In vivo* Interactome Modeling Results

The simultaneous collection of host and pathogen gene expression data of the bovine host ileal loop infected with *B. melitensis* WT (Rossetti et al., 2013), provided us with a unique opportunity to examine temporal host pathway perturbations concurrent with those of the pathogen. A computational approach based on DBN machine learning was employed to infer protein–protein interactions (PPIs) and to create a novel *in silico* host–pathogen interactome model (File S1). To identify plausible PPIs, a specialized application was developed to implement algorithms that integrate multiple sources of PBK such as from KEGG, BIOCARTA, NCBI, PIBASE, and *Brucella* proteomic analyses (Delvecchio et al., 2002; Wagner et al., 2002; Connolly et al., 2006; Mol et al., 2016), into the inference of host–pathogen protein interactions. Such interactions aid in the identification of mechanisms of host invasion and evasion through manipulation of the host’s immune response system. Our application employed Bayesian networks (BNs) (Friedman et al., 2000; Hartemink et al., 2001) that were expanded by others to include PBK (Imoto et al., 2004; Werhli and Husmeier, 2007). We employed methods similar to Werhli for learning PPIs from expression data and PBK (Werhli and Husmeier, 2007). We adopted three algorithmic methods for the identification of candidate interaction points for use in network learning between the host and pathogen from *in vivo* gene expression data. Through either: (1) protein binding domain, (2) sequence similarity, or (3) Gene Ontology-based functional algorithms of pathogen gene expression with the host gene perturbations, we identified potential *B. melitensis* interactions with host pathways.

The PPI analysis resulted in identifying the *virB* gene that encodes the T4SS proteins to have plausible interaction with a number of genes in the host’s immune response pathways (Table 2 and Table S8). For example, the significantly perturbed *virB11* gene has a high protein domain binding prediction with a negative correlation with the host gene/protein PIK3R2 expression. PIK3R2 is a key regulatory protein in several key pathways including: mTOR signaling, T-cell and B-cell receptor, Integrin-mediated cell adhesion, regulation of actin cytoskeleton, apoptosis, and Toll-like receptor. The host gene PIK3R2 remained activated for all time points p.i. Interestingly, in our host pathway analysis of “Regulation of Actin Cytoskeleton,” the genes ABI2, PPN1, and ARPC5, downstream from PIK3R2, were repressed suggesting a mechanism of host pathway disruption or highjacking. The *VirB11* also had a strong protein domain binding prediction with negative correlation with the host genes MAPK8IP1/2 of the MAPK signaling pathway. The MAPK8IP1/2 host genes were strongly repressed 15 min p.i. and insignificantly expressed thereafter. Downstream of MAPK8IP1/2, the transcription factor JUND and nuclear factor of activated T-cells, cytoplasmic 3, NFATC2 are both strongly repressed.

Brucella flagellum is a virulence factor transiently expressed during vegetative growth and required for persistent infection, but not for internalization *in vivo* (Fretin et al., 2005). In agreement, our results during the first 4 h of infection showed a repression of the three flagellum-encoded loci (BMEI0150-0168, BMEI1080-1089, and BMEI1105-1114) (Table S3), with corresponding repression of the “flagellar assembly” pathway (Table 1), and the cell components “bacterial-type flagellum hook” and “bacterial-type flagellum” (Table S5) in tissue-associated *B. melitensis* compared with *in vitro*-grown cultures. In addition, *RopE1* sigma factor (BMEI0371), a flagellar repressor (Ferooz et al., 2011), was activated throughout the experiment (Table S3). We further examined potential interaction of the flagella-associated genes with the host. Three highly correlated PPIs were identified which included the flagella genes BMEI0324, BMEI1085 (*flgA*), and BMEI1113 (*flgG-2*). The ORF BMEI0324 had strong binding sequence similarity and positive correlation to the host expressed JUN (jun oncogene) which is part of the highly perturbed host pathways: Toll-like Receptor, ErbB Signaling, BRC Signaling, B-cell Signaling, T-cell Signaling, Epithelial Cell Signaling, WNT Signaling, and MAPK Signaling. The flagellum gene *flgA* also had strong binding sequence similarity and positive gene expression correlation to host *CASP2* gene while having a reversed (negative) correlation with the host activated *CASP3* gene. Interestingly, the lowly expressed *CASP2* is only associated with the highly perturbed MAPK signaling pathway, while *CASP3* has several pathway associations that include: Apoptosis, Epithelial Signaling, Natural Killer Cell, and MAPK Signaling. The third flagellum gene *flgG-2* had strong binding sequence similarity to the host *MAP4K1* gene. The highly activated *MAP4K1* is associated with only the host MAPK Signaling pathway. Such interactions may be novel virulence candidates that facilitate circumventing the host immune response. An example of interaction is the pathogen gene *flgA* with the host gene/protein Casp4/6/7/9 which are MAPK pathway genes. Accordingly, down-stream of Casp genes are the repressed *RAC1/2/3* genes of the Rho family of GTPases. *RAC1* has been implicated in various downstream cellular functions, including, but not limited to, cellular plasticity, migration and invasion, cellular adhesions, cell proliferation, and apoptosis.

Host cells identify specific pathogen-associated molecular pattern (PAMP) motifs present in the bacteria by pattern-recognition receptors (PRRs), such as Toll-like Receptors (TLRs). These receptors are key to establishing an important network between the innate and adaptive immune systems. TLR5 is the cellular receptor for extracellular flagellin, a major structural protein of Gram-negative flagella. Binding of flagellin to the extracellular domain of TLR5 rapidly induces a signal cascade that culminates in the production of proinflammatory mediators such as cytokines, chemokines, and costimulatory molecules (Honko and Mizel, 2005). Therefore, the absence of flagellum apparatus during extracellular life while inside the host suggests the *Brucella* strategy is to avoid triggering a host immune response and an initiation of a *Brucella* persistence mechanism (Terwagne et al., 2013). However, our previous analysis showed

TABLE 2 | Interactome model predicted protein–protein interactions (PPIs) between bovine host and *B. melitensis* pathogen.

<i>B. melitensis</i> gene	<i>B. melitensis</i> gene description	Normalized correlation weight	Bovine host gene	Bovine Gene Description	Host gene significantly perturbed	Prediction type	Perturbed Host Pathways
MotB BMEI0324 (BME_RS01570)	Chemotaxis MotB protein	0.268	<i>JUN</i>	jun oncogene	Yes	PD	Toll-like receptor, MAPK, Epithelial cell signaling, GnRH signaling, ErbB signaling, Wnt signaling, BRC signaling, B cell receptor, T cell receptor
MotB BMEI0324 (BME_RS01570)		−0.221	<i>ROCK2</i>	Rho-associated, coiled-coil containing protein kinase 2	Yes	PD	Regulation of actin cytoskeleton, Axon guidance, Integrin-mediated cell adhesion, TGF-beta signaling, CCR@ signaling, Wnt signaling
BMEI0717 (BME_RS03560)	22 kDa OMP precursor	0.208	<i>BAD</i>	BCL2-antagonist of cell death	Yes	BSS	Trefoil Factors Mucosal Healing, VEGF signaling, Apoptosis
BMEI0717 (BME_RS03560)		0.188	<i>MAP2K3</i>	Mitogen-activated protein kinase kinase 3	Yes	BSS	MAPK, GnRH, Toll-like receptor, Fc epsilon RI signaling, Integrin-mediated cell adhesion
BMEI0890 (BME_RS04435, tgt)	tRNA guanosine transglycosylase	0.159	<i>RAP1A</i>	RAP1A, member of RAS oncogene family	No	BSS	MAPK, Integrin-mediated cell adhesion, Leukocyte transendothelial migration
BMEI1077 (BME_RS05395)	Immunogenic membrane protein YajC	−0.206	<i>NRAS</i>	Neuroblastoma RAS viral (v-ras) oncogene homolog	Yes	PD	ErbB signaling, Regulation of actin cytoskeleton, Natural killer cell mediated cytotoxicity, Tight junction, Fc epsilon RI signaling, T cell receptor signaling, GnRH signaling
BMEI1077 (BME_RS05395)		−0.225	<i>CBL</i>	Cas-Bi-M (murine) ecotropic retroviral transforming sequence	No	PD	Jak-Stat signaling, ErbB signaling, Insulin signaling, T cell receptor signaling
BMEI1077 (BME_RS05395)		−0.238	<i>RHOA</i>	ras homolog gene family, member A	Yes	PD	Trefoil factors, Tight junction, TGF-beta signaling, Wnt signaling, Adherens junction, Integrin-mediated cell adhesion, etc.
BMEI1086 (BME_RS05450)	Segregation and condensation protein A	−0.214	<i>CRKL</i>	v-crk sarcoma virus CT10 oncogene homolog	No	BSS	Regulation of actin cytoskeleton, Insulin signaling, ErbB signaling, MAPK
BMEI1582 (BME_RS07890, narL)	Two-component system nitrate/nitrite response regulator	0.145	<i>MKNK1</i>	MAP kinase interacting serine/threonine kinase 1	Yes	BSS	MAPK, Insulin signaling
BMEI1751 (BME_RS08690)	LuxR family transcriptional regulator	−0.102	<i>IRF3</i>	Interferon regulatory factor 3	No	BSS	Toll-like receptor signaling
BMEI1846 (BME_RS09140)	Response regulator receiver protein ExsF	0.202	<i>FLNA</i>	Filamin A, alpha (Actin binding protein 280)	Yes	BSS	MAPK
BMEI1846 (BME_RS09140)		−0.157	<i>CRK</i>	v-crk sarcoma virus CT10 oncogene homolog	Yes	BSS	Regulation of actin cytoskeleton, Insulin signaling, ErbB signaling, MAPK, Integrin-mediated cell adhesion
BtaE (BMEI1873)	trimeric autotransporter adhesin	−0.018	<i>NFKBIA</i>	nuclear factor of kappa light polypeptide gene enhancer in B-cells inhibitor, alpha	No	PD	CD40L Signaling, Apoptosis, Toll-like receptor signaling, Adipocytokine signaling, Epithelial cell signaling in Helicobacter pylori infection, Chronic myeloid leukemia, Prostate cancer, T cell receptor signaling with Antigen Processing, B cell receptor signaling, T cell receptor signaling

(Continued)

TABLE 2 | Continued

<i>B. melitensis</i> gene	<i>B. melitensis</i> gene description	Normalized correlation weight	Bovine host gene	Bovine Gene Description	Host gene significantly perturbed	Prediction type	Perturbed Host Pathways
BtaE (BMEI1873)		0.035	NFATC2	nuclear factor of activated T-cells, cytoplasmic, calcineurin-dependent 2	No	PD	Wnt signaling, VEGF signaling, T cell receptor signaling with Antigen Processing, T cell receptor signaling, MAPK signaling, Calcium signaling, Natural killer cell mediated cytotoxicity, Axon guidance
BtaE		−0.037	MAPK8IP1	mitogen-activated protein kinase 8 interacting protein 1	No		MAPK signaling
BtaE		0.014	RRAS2	related RAS viral (r-ras) oncogene homolog 2	No	BSS	Regulation of actin cytoskeleton, MAPK signaling, Insulin signaling, Axon guidance, Long-term depression, T cell receptor signaling, Natural killer cell mediated cytotoxicity, Gap junction, Tight junction, B cell receptor signaling, Long-term potentiation
BtaE		0.03	RAC3	ras-related C3 botulinum toxin substrate 3 (rho family, small GTP binding protein Rac3)	No	BSS	Integrin-mediated cell adhesion, Colorectal cancer, Pancreatic cancer, VEGF signaling, MAPK signaling, Fc epsilon RI signaling, Toll-like receptor signaling, Regulation of actin cytoskeleton, Adherens junction, Wnt signaling, B cell receptor signaling, Axon guidance
BtaE		−0.028	CCND1	cyclin D1	No	BSS	Colorectal cancer, Wnt signaling, Acute myeloid leukemia, Thyroid cancer, Prostate cancer, Endometrial cancer, Non-small cell lung cancer, Chronic myeloid leukemia, Bladder cancer, Glioma, Pancreatic cancer, Melanoma, Small cell lung cancer, Jak-STAT signaling, Cell cycle
BMEI1872 (BME_RS09280)	Cell surface protein	−0.153	JUND	jun D proto-oncogene	Yes	BSS	MAPK
BMEI0035 (BME_RS10365, virB11)	P-type DNA transfer ATPase VirB11	−0.134	PIK3R2	Phosphoinositide 3 kinase, regulatory subunit 2	Yes	BSS	T cell receptor, mTOR signaling, VEGF signaling, ErbB signaling, Toll-like receptor, Apoptosis, Jak-STAT signaling, Phosphatidylinositol signaling, etc.
BMEI0035 (BME_RS10365, virB11)		−0.168	MAPK8IP1	Mitogen-activated protein kinase 8 interacting protein 1	Yes	PD	MAPK
BMEI0926 (BME_RS14720, minD)	Septum site-determining protein MinD	0.121	RASGRP3	RAS guanyl releasing protein 3	Yes	BSS	MAPK, B cell receptor signaling
BMEI0926 (BME_RS14720, minD)		0.102	CBLB	Cas-Br-M (murine) ecotropic retroviral transforming sequence	Yes	BSS	T cell receptor signaling, Insulin signaling, ErbB signaling, Jak-STAT signaling

(Continued)

TABLE 2 | Continued

<i>B. melitensis</i> gene	<i>B. melitensis</i> gene description	Normalized correlation weight	Bovine host gene	Bovine Gene Description	Host gene significantly perturbed	Prediction type	Perturbed Host Pathways
BMEI0951 (BME_RS14810, narH)	Nitrate reductase beta subunit	0.13	CRK	v-crk sarcoma virus CT10 oncogene homolog	Yes	BSS	Regulation of actin cytoskeleton, Insulin signaling, ErbB signaling, MAPK, Integrin-mediated cell adhesion
BMEI1085 (BME_RS15470, figA)	Flagellar basal body P-ring biosynthesis protein FigA	0.116	CASP4	Caspase 4, apoptosis-related cysteine peptidase	No	BSS	MAPK
BMEI1085 (BME_RS15470, figA)		−0.105	CASP3	Caspase 3, apoptosis-related cysteine peptidase	Yes	BSS	Apoptosis, MAPK, Natural killer cell mediated cytotoxicity
BMEI1113 (BME_RS15605, flig)	Flagellar motor switch protein Flig	−0.112	MAP4K1	Mitogen-activated protein kinase kinase kinase 1	Yes	BSS	MAPK

Higher evidence of possible interaction is inferred if the host gene is also significantly perturbed and correlated with the pathogen gene expression. Prediction type of "Protein Domain" (PD) means that the same binding domains exist between host-pathogen proteins. "Binding sequence similarity" (BSS) is achieved by finding similar sequence in the pathogen as a binding protein domain existing in the host protein. Correlation weights have been normalized so that comparisons between different pathways can be made. The pathways which contain the host PPI genes are listed for each PPI pair. Both the *in vivo* pathogen and host gene expressions were employed in training the models for learning the PPIs.

that TLR5 pathway is activated in *B. melitensis*-infected bovine Peyer's patches during the first hour p.i. (Rossetti et al., 2013), which may have been associated with remnants of flagella in the *in vitro*-growth culture media intraluminally inoculated. More detailed analysis of this pathway showed that down-stream of TLR5 there were several strongly repressed genes including *PIK3C2B*, *PIK3R4*, *STAT1*, *AKT3*, *RAC3*, *IL6*, and *TICAM3*. This may suggest that the pathogen is manipulating important signaling processes by some other mechanism. PPI analysis indicated that virB genes have predicted interactions with *STAT1*, *PIK3C2B*, and *IL6* which may also be circumventing the TLR5 response to flagellin stimulation and preventing the host from mounting an effective immune response.

The complexity of a complete system-level host and *B. melitensis* interaction model ($G_{interactome}$) is illustrated in **Figure 2A**. This Bayesian network model is comprised of approximately 528 nodes (genes) and 987 arcs that connect gene nodes (relationships). Of the 987 arcs, 101 arcs were learned for host-pathogen points of interaction which are highlighted by the orange colored arcs. The number of host genes were limited to a selected set of perturbed host pathways which included MAPK signaling, ErbB signaling, mTOR signaling, WNT signaling, VEGF signaling, Toll-like Receptor signaling, GnRH signaling, Tight junction, Phosphatidylinositol signaling, Notch signaling, Natural killer cell mediated cytotoxicity, and Apoptosis. The intent for using only perturbed pathways was to look for plausible points of pathogen interactions which could influence the hosts immune response. Although this model is visually complex, the model allows for the computational extraction of potentially important mechanisms of interaction. Of the 101 arcs, the prioritization of these interactions can be analyzed according to the most likely to least likely in the following order: "protein domain," "sequence similarity," "GO Functionality," and "Correlated Data". The creation of the interactome model employed only PPI relationships based on protein domain or sequence similarity. For example, **Figure 2B** illustrates the simplification for the interaction between the pathogen's Type IV secretion system and a known cell surface protein, BtaE (Ruiz-Ranwez et al., 2013b), with the host's Toll-like receptor pathway. This demonstrates how predictive information can be employed to interpret host-pathogen responses. The thicker orange arcs are the connections from the pathogen to the host. From this type of analysis, it is possible to understand the state of host's gene expression down-stream from the potential points of interaction/disruption in any of the pathways showing potential manipulation by the pathogen. **Table 2** lists a selected subset of predicted interactions representing the pathogen-host pairs based solely on "protein domain" and "sequence similarity" prediction. A complete listing of predicted PPIs based on protein domain or sequence similarity is provided in **Table S8**. Note that our computational approach did predict interactions of the *B. suis* gene BtaE with several host proteins listed in **Table 2**. BtaE belongs to the type II (trimeric) autotransporter family and is an orthologue of *B. melitensis* BMEI1873. BtaE has been shown to have an active role in host cell adhesion and binding with components of the extracellular matrix such as fibronectin, collagen, and vitronectin (Ruiz-Ranwez et al.,

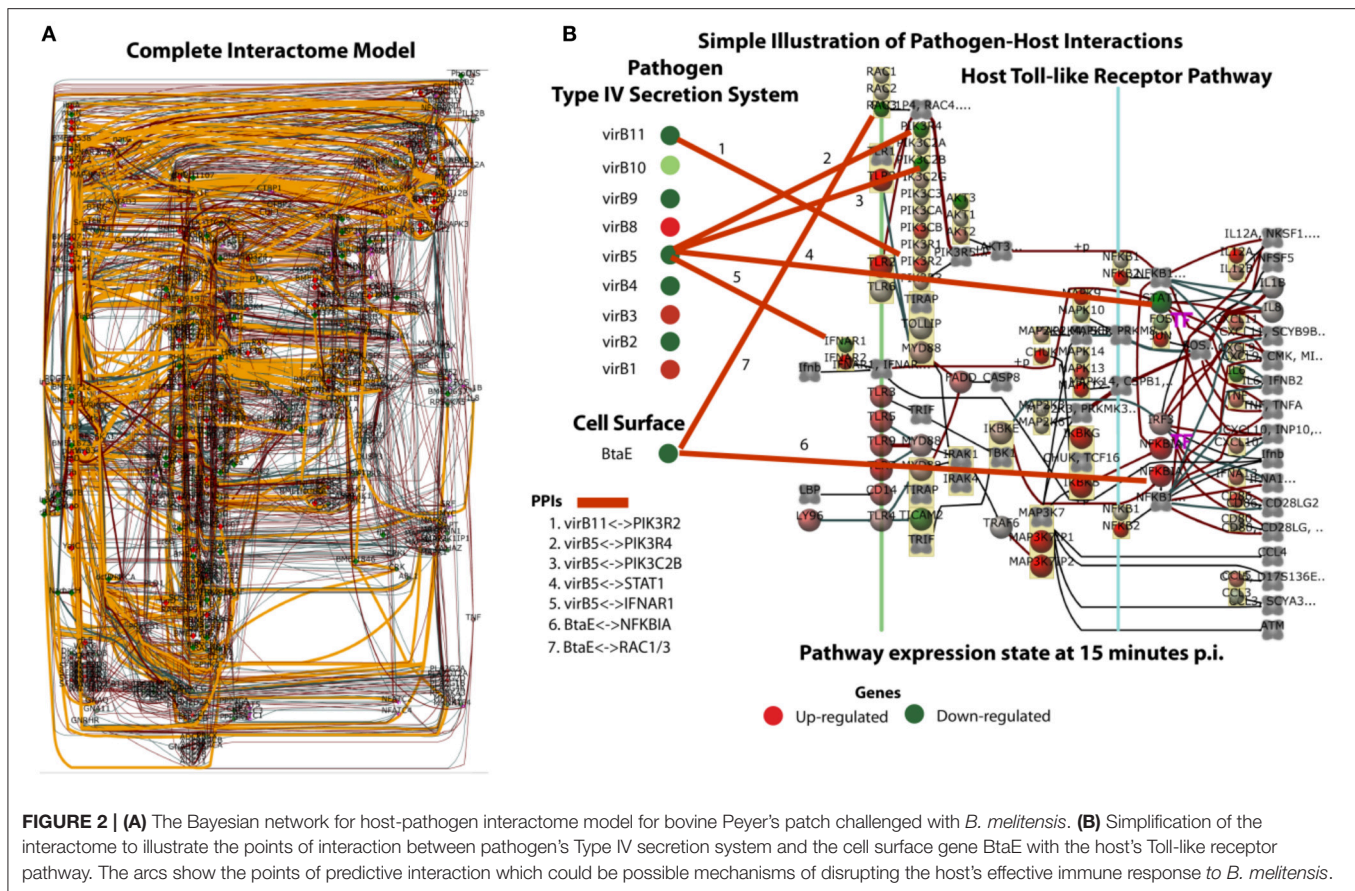


FIGURE 2 | (A) The Bayesian network for host-pathogen interactome model for bovine Peyer's patch challenged with *B. melitensis*. **(B)** Simplification of the interactome to illustrate the points of interaction between pathogen's Type IV secretion system and the cell surface gene BtaE with the host's Toll-like receptor pathway. The arcs show the points of predictive interaction which could be possible mechanisms of disrupting the host's effective immune response to *B. melitensis*.

2013b). The interactome model and its predicted PPI list is the analysis output to be employed for further *in vitro* validation and model refinements. The resulting *B. melitensis* PPI gene set may represent important new virulence factors with the potential to disrupt or hijack the host immune response. **Table 2** also lists the perturbed host pathways in which the host gene PPI is associated, intentionally unfiltered conceptually for subcellular locations so that all PPI are presented. Little is known about the complete secretome of *B. melitensis* during *in vivo* host invasion and proliferation although the secretion systems and secretomes of *Brucella* were recently computationally analyzed which predicted 29 host-pathogen specific interactions between cattle and *B. abortus* and 36 host-pathogen interactions between sheep and *B. melitensis* proteins (Sankarasubramanian et al., 2016). The PPI computational approach employed evidence of host pathway perturbation and gene expression disruption as possible indicators of pathogen interaction. If there was plausible potential for a PPI based on binding domain or sequence similarity to known protein interactions between the pathogen and host protein, then it was included in the PPI in list (**Table 2** and **Table S8**). The list of PPIs can be prioritized based on the normalized correlation weights. The larger the normalized weight indicates stronger likelihood of a relationship between the pathogen and host genes. Note that the normalized correlation weight is an output of structure learning and is employed in the

acceptance or rejection of an arc (edge) in the final Bayesian network. Arc weight is dependent on the number of incoming arcs to a node and other factors and should not be confused as a true correlation measurement between two gene expression values.

It is thought that the unfiltered PPI predictions could, in future experiments, employ such information as normalized correlation weights and cellular localization to help prioritize the selection of which PPI to be experimentally validated. Further, it is proposed that the evidence driven computational approach (*in vivo* host-pathogen responses and machine learning) for predicting bacterial and host cell protein interactions will narrow the focus on likely PPI candidates and will greatly enhance our capacity to design hypothesis-driven experimental approaches to discover which *Brucella* proteins directly participate in host interactions.

In conclusion, the *in silico* interactome modeling offers informative insights leading toward new hypotheses regarding host-pathogen mechanisms of invasion and evasion. This modeling infers that *B. melitensis* has multiple points of host interaction that occur at the early stage post infection. A number of important innate immune response pathways appear to be potential targets of disruption by invading *B. melitensis*, such as Regulation of Actin Cytoskeleton, mTOR Signaling, MAPK, and Toll-like Receptor Signaling appear to be likely targets of

pathogen manipulation that warrant further exploratory research and verification of PPIs. As we have reported and discussed here, identifying interactive host:pathogen PPIs is often the initial step to establish functional significance according to the principle of “guilty by association” (Schauer and Stingl, 2009) that may drive future research to a higher level of understanding of the molecular pathogenesis of brucellosis, thereby facilitating the design of novel immunotherapeutic drugs and vaccines.

ETHICS STATEMENT

This study was carried out in accordance with the recommendations of the Texas A&M University Institutional Animal Care and Research Advisory Committee. The protocol (AUP#2003-178) was approved by the Texas A&M University Institutional Animal Care and Research Advisory Committee.

AUTHOR CONTRIBUTIONS

Conceived and designed the experiments: CR and LA. Performed the experiments: CR, SL, JN, TG, SK, and LA. Analyzed the data: CR, KD, and LA. Writing—original draft: CR, KD, and LA. Writing—review & editing: CR, KD, SL, JN, TG, SK, and LA.

ACKNOWLEDGMENTS

The authors thank Mr. Alan Patranella for the assistance with animal care, and Mrs. Roberta Pugh and Mrs. Doris Hunter for technical support. LA was supported by a grant from the National Institutes of Health (NIH)/National Institute of Allergy and Infectious Diseases 1U54 AI057156-01. LA is also supported by the U.S. Department of Homeland Security National Center of Excellence for Foreign Animal and Zoonotic Disease Defense ONR-N00014-04-1-0 grant. CR was supported by an I.N.T.A.-Fulbright Argentina Fellowship.

SUPPLEMENTARY MATERIAL

The Supplementary Material for this article can be found online at: <http://journal.frontiersin.org/article/10.3389/fmicb.2017.01275/full#supplementary-material>

Figure S1 | Validation of *Brucella melitensis* microarray results by quantitative real time PCR. Six randomly selected *B. melitensis* ORFs that were consistently perturbed in microarray results in the first 4 h p.i. as compared to the inoculum as validated by quantitative RT-PCR. Fold-change was normalized to the expression of *B. melitensis* 16S rRNA and calculated using the $\Delta\Delta C_t$ method. All tested genes at every time point had expression altered in the same direction as microarray. Open bars represent fold-change by microarray analysis and black bars represent fold-change by qRT-PCR.

REFERENCES

Abdou, E., Jiménez De Bagüés, M. P., Martínez-Abadía, I., Ouahrani-Bettache, S., Pantescio, V., Occhialini, A., et al. (2017). RegA plays a key role in oxygen-dependent establishment of persistence and in isocitrate lyase activity, a critical determinant of *in vivo* *Brucella suis* pathogenicity. *Front. Cell. Infect. Microbiol.* 7:186. doi: 10.3389/fcimb.2017.00186

Table S1 | Primers for Real Time PCR analysis of genes in *B. melitensis* samples.

Table S2 | Bayesian z-score of *B. melitensis* genes in tissue-associated *B. melitensis* from 15 min to 4 h post-infection. Genes with z-score $>|2.24|$ were considered differentially expressed. Positive numbers in the body of the table indicate activated genes and negative (–) numbers indicate repressed genes. The tissue-associated *B. melitensis* gene expression at every time point was compared to the gene expression of the inoculum (i.e., *in vitro*-grown cultures of *B. melitensis* at late-log phase of growth). Measured time points were 15 (T15), 30 (T30), 60 (T60), 120 (T120), and 240 (T240) min p.i.

Table S3 | Core set of *B. melitensis* genes differentially expressed ($>|2.24|$) in at least four of five time points in the first 4 h post-infection of bovine Peyer's patch. Genes with z-score $>|2.24|$ were considered differentially expressed. Positive numbers in the body of the table indicate activated genes, negative (–) numbers indicate repressed genes. The tissue-associated *B. melitensis* gene expression at every time point was compared to the gene expression of the inoculum (i.e., *in vitro*-grown cultures of *B. melitensis* at late-log phase of growth). Measured time points were 15 (T15), 30 (T30), 60 (T60), 120 (T120), and 240 (T240) min p.i.

Table S4 | Significantly perturbed Biological Processes (BP) (Bayesian z-score $>|2.24|$) of tissue-associated *B. melitensis* during the first 4 h post-bovine Peyer's patch infection. Measured time points were 15 (T15), 30 (T30), 60 (T60), 120 (T120), and 240 (T240) min p.i. The Bayesian z-scores represent the degree of perturbation of the group of BP genes in tissue-associated *B. melitensis* versus the control. Positive z-scores represent activation of the BP (BP score is dominated by more activated genes), while the negative (–) z-score represents BP repression (BP score is dominated by repressed genes).

Table S5 | Significantly perturbed Cellular Components (CC) (Bayesian z-score $>|2.24|$) of tissue-associated *B. melitensis* during the first 4 h post-bovine Peyer's patch infection. Measured time points were 15 (T15), 30 (T30), 60 (T60), 120 (T120), and 240 (T240) min p.i. The Bayesian z-scores represent the degree of perturbation of the group of CC genes in tissue-associated *B. melitensis* versus the control. Positive z-scores represent activation of the CC (CC score is dominated by activated regulated genes), while the negative (–) z-score represents CC repression (CC score is dominated by repressed genes).

Table S6 | Significantly perturbed Molecular Functions (MF) (Bayesian z-score $>|2.24|$) of tissue-associated *B. melitensis* during the first 4 h post-bovine Peyer's patch infection. Measured time points were 15 (T15), 30 (T30), 60 (T60), 120 (T120), and 240 (T240) min p.i. The Bayesian z-scores represent the degree of perturbation of the group of MF genes in tissue-associated *B. melitensis* versus the control. Positive z-scores represent activation of the MF (MF score is dominated by more activated genes), while the negative (–) z-score represents MF repression (MF score is dominated by repressed genes).

Table S7 | Dynamic Bayesian pathway analysis scores along with the associated individual genes and their Bayesian Scores by time point post-inoculation of tissue-associated *B. melitensis* during the first 4 h post-bovine Peyer's patch infection. Measured time points were 15 (T15), 30 (T30), 60 (T60), 120 (T120), and 240 (T240) min p.i. Positive z-scores represent activation of genes while negative (–) z-scores represent repressed genes.

Table S8 | Comprehensive list of predicted host:pathogen tissue-associated *B. melitensis*:bovine protein–protein interactions (PPI). This list includes only those PPIs which were learned by either known protein domain binding or sequence similarity to known binding domains employing our Bayesian methods for PPI prediction.

File S1 | Host-Pathogen Protein-Protein Interaction (PPIs) Prediction.

Adams, L. G. (2002). The pathology of brucellosis reflects the outcome of the battle between the host genome and the *Brucella* genome. *Vet. Microbiol.* 90, 553–561. doi: 10.1016/S0378-1135(02)00235-3

Al Dahouk, S., Jubier-Maurin, V., Scholz, H. C., Tomaso, H., Karges, W., Neubauer, H., et al. (2008). Quantitative analysis of the intramacrophagic *Brucella suis* proteome reveals metabolic adaptation to late stage of cellular infection. *Proteomics* 8, 3862–3870. doi: 10.1002/pmic.200800026

- Allen, C. A., Adams, L. G., and Ficht, T. A. (1998). Transposon-derived *Brucella abortus* rough mutants are attenuated and exhibit reduced intracellular survival. *Infect. Immun.* 66, 1008–1016.
- Alton, G. G. (1990). “*Brucella melitensis*,” in *Animal Brucellosis*, eds K. Nielsen and J. R. Duncan (Boca Raton, FL: CRC Press, Inc.), 383–409.
- Alva-Perez, J., Arellano-Reynoso, B., Hernandez-Castro, R., and Suarez-Guemes, F. (2014). The *invA* gene of *Brucella melitensis* is involved in intracellular invasion and is required to establish infection in a mouse model. *Virulence* 5, 563–574. doi: 10.4161/viru.28589
- Alvarez, J., Saez, J. L., Garcia, N., Serrat, C., Perez-Sancho, M., Gonzalez, S., et al. (2011). Management of an outbreak of brucellosis due to *B. melitensis* in dairy cattle in Spain. *Res. Vet. Sci.* 90, 208–211. doi: 10.1016/j.rvsc.2010.05.028
- Arellano-Reynoso, B., Lapaque, N., Salcedo, S., Briones, G., Ciocchini, A. E., Ugalde, R. A., et al. (2005). Cyclic B-1,2-glucan is a *Brucella* virulence factor required for intracellular survival. *Nat. Immunol.* 6, 618–625. doi: 10.1038/nri1202
- Banai, M. (2010). Insights into the problem of *B. Melitensis* and rationalizing a vaccination programme in Israel. *Prilozi* 31, 167–180.
- Barquero-Calvo, E., Chaves-Olarte, E., Weiss, D. S., Guzmán-Verri, C., Chacon-Diaz, C., Rucavado, A., et al. (2007). *Brucella abortus* uses a stealthy strategy to avoid activation of the innate immune system during the onset of infection. *PLoS ONE* 2:e631. doi: 10.1371/journal.pone.0000631
- Boschiroli, M. L., Ouahrani-Bettache, S., Foulongne, V., Michaux-Charachon, S., Bourg, G., Allardet-Servent, A., et al. (2002). The *Brucella suis* *virB* operon is induced intracellularly in macrophages. *Proc. Natl. Acad. Sci. U.S.A.* 99, 1544–1549. doi: 10.1073/pnas.032514299
- Carpenter, C. M. (1924). *Bacterium abortum* invasion of the tissues of calves from the ingestion of infected milk. *Cornell Vet.* 14, 16–31.
- Carrica, M. C., Fernandez, I., Marti, M. A., Paris, G., and Goldbaum, F. A. (2012). The NtrY/X two-component system of *Brucella* spp. acts as a redox sensor and regulates the expression of nitrogen respiration enzymes. *Mol. Microbiol.* 85, 39–50. doi: 10.1111/j.1365-2958.2012.08095.x
- Castaneda-Roldán, E. I., Ouahrani-Bettache, S., Saldana, Z., Avelino-Flores, F., Rendón, M. A., Dornand, J., et al. (2006). Characterization of SP41, a surface protein of *Brucella* associated with adherence and invasion of host epithelial cells. *Cell. Microbiol.* 8, 1877–1887. doi: 10.1111/j.1462-5822.2006.00754.x
- Celli, J., De Chastellier, C., Franchini, D. M., Pizarro-Cerdá, J., Moreno, E., and Gorvel, J. P. (2003). *Brucella* evades macrophages killing via VirB-dependent sustained interactions with the endoplasmic reticulum. *J. Exp. Med.* 198, 545–556. doi: 10.1084/jem.20030088
- Comerci, D. J., Altabe, S., De Mendoza, D., and Ugalde, R. A. (2006). *Brucella abortus* synthesizes phosphatidylcholine from coline provided by the host. *J. Bacteriol.* 188, 1929–1934. doi: 10.1128/JB.188.5.1929-1934.2006
- Conde-Alvarez, R., Grillo, M. J., Salcedo, S. P., De Miguel, M. J., Fugier, E., Gorvel, J. P., et al. (2006). Synthesis of phosphatidylcholine, a typical eukaryotic phospholipid, is necessary for full virulence of the intracellular bacterial parasite *Brucella abortus*. *Cell. Microbiol.* 8, 1322–1335. doi: 10.1111/j.1462-5822.2006.00712.x
- Connolly, J. P., Comerci, D., Alefantis, T. G., Walz, A., Quan, M., Chafin, R., et al. (2006). Proteomic analysis of *Brucella abortus* cell envelope and identification of immunogenic candidate proteins for vaccine development. *Proteomics* 6, 3767–3780. doi: 10.1002/pmic.200500730
- Czibener, C., Merwaiss, F., Guaimas, F., Del Giudice, M. G., Serantes, D. A., Spera, J. M., et al. (2016). BigA is a novel adhesin of *Brucella* that mediates adhesion to epithelial cells. *Cell. Microbiol.* 18, 500–513. doi: 10.1111/cmi.12526
- Davis, D. S., Heck, F. C., Williams, J. D., Simpson, T. R., and Adams, L. G. (1988). Interspecific transmission of *Brucella abortus* from experimentally infected coyotes (*Canis latrans*) to parturient cattle. *J. Wildl. Dis.* 24, 533–537. doi: 10.7589/0090-3558-24.3.533
- de Barys, M., Jamet, A., Filopon, D., Nicolas, C., Laloux, G., Rual, J. F., et al. (2011). Identification of a *Brucella* spp. secreted effector specifically interacting with human small GTPase Rab2. *Cell Microbiol.* 13, 1044–1058. doi: 10.1111/j.1462-5822.2011.01601.x
- de Figueiredo, P., Ficht, T. A., Rice-Ficht, A., Rossetti, C. A., and Adams, L. G. (2015). Pathogenesis and immunobiology of brucellosis: review of *Brucella*-host interactions. *Am. J. Pathol.* 185, 1505–1517. doi: 10.1016/j.ajpath.2015.03.003
- de Jong, M. F., Starr, T., Winter, M. G., Den Hartigh, A. B., Child, R., Knodler, L. A., et al. (2013). Sensing of bacterial type IV secretion via the unfolded protein response. *MBio* 4:e00418–12. doi: 10.1128/mbio.00418-12
- de Jong, M. F., Sun, Y. H., Den Hartigh, A. B., Van Dijk, J. M., and Tsois, R. M. (2008). Identification of VceA and VceC, two members of the VjbR regulon that are translocated into macrophages by the *Brucella* type IV secretion system. *Mol. Microbiol.* 70, 1378–1396. doi: 10.1111/j.1365-2958.2008.06487.x
- Dean, A. S., Crump, L., Greter, H., Hattendorf, J., Schelling, E., and Zinsstag, J. (2012). Clinical manifestations of human brucellosis: a systematic review and meta-analysis. *PLoS Negl. Trop. Dis.* 6:e1929. doi: 10.1371/journal.pntd.0001929
- Del Giudice, M. G., Dohmer, P. H., Spera, J. M., Laporte, F. T., Marchesini, M. I., Czibener, C., et al. (2016). VirJ is a *Brucella* virulence factor involved in the secretion of type IV secreted substrates. *J. Biol. Chem.* 291, 12383–12393. doi: 10.1074/jbc.M116.730994
- Delrue, R. M., Deschamps, C., Leonard, S., Nijskens, C., Danese, I., Schaus, J. M., et al. (2005). A quorum-sensing regulator controls expression of both the type IV secretion system and the flagellar apparatus of *Brucella melitensis*. *Cell. Microbiol.* 7, 1151–1161. doi: 10.1111/j.1462-5822.2005.00543.x
- Delvecchio, V. G., Wagner, M. A., Eschenbrenner, M., Horn, T. A., Kraycer, J. A., Estock, F., et al. (2002). *Brucella* proteomes—a review. *Vet. Microbiol.* 90, 593–603. doi: 10.1016/S0378-1135(02)00239-0
- den Hartigh, A. B., Rolan, H. G., De Jong, M. F., and Tsois, R. M. (2008). VirB3 to VirB6 and VirB8 to VirB11, but not VirB7, are essential for mediating persistence of *Brucella* in the reticuloendothelial system. *J. Bacteriol.* 190, 4427–4436. doi: 10.1128/JB.00406-08
- Dong, H., Liu, W., Peng, X., Jing, Z., and Wu, Q. (2013). The effects of MucR on expression of type IV secretion system, quorum sensing system and stress responses in *Brucella melitensis*. *Vet. Microbiol.* 166, 535–542. doi: 10.1016/j.vetmic.2013.06.023
- Dorrell, N., Guigue-Talet, P., Spencer, S., Foulongne, V., O’Callaghan, D., and Wren, B. W. (1999). Investigation into the role of the response regulator NtrC in the metabolism and virulence of *Brucella suis*. *Microb. Pathog.* 27, 1–11. doi: 10.1006/mpat.1999.0278
- Dorrell, N., Spencer, S., Foulongne, V., Guigue-Talet, P., O’Callaghan, D., and Wren, B. W. (1998). Identification, cloning and initial characterisation of FeuPQ in *Brucella suis*: a new sub-family of two component regulatory systems. *FEMS Microbiol. Lett.* 162, 143–150. doi: 10.1111/j.1574-6968.1998.tb12991.x
- Ferooz, J., Lemaire, J., Delory, M., De Bolle, X., and Letesson, J. J. (2011). RpoE1, an extracytoplasmic function sigma factor, is a repressor of the flagellar system in *Brucella melitensis*. *Microbiology* 157, 1263–1268. doi: 10.1099/mic.0.044875-0
- Forestier, C., Deleuil, F., Lapaque, N., Moreno, E., and Gorvel, J. P. (2000). *Brucella abortus* lipopolysaccharide in murine peritoneal macrophages acts as a down-regulator of T cell activation. *J. Immunol.* 165, 5202–5210. doi: 10.4049/jimmunol.165.9.5202
- Foulongne, V., Bourg, G., Cazevielle, C., Michaux-Charachon, S., and O’Callaghan, D. (2000). Identification of *Brucella suis* genes affecting intracellular survival in an *in vitro* human macrophage infection model by signature-tagged transposon mutagenesis. *Infect. Immun.* 68, 1297–1303. doi: 10.1128/IAI.68.3.1297-1303.2000
- Fretin, D., Faucommier, A., Kohler, S., Halling, S. M., Léonard, S., Nijskens, C., et al. (2005). The sheathed flagellum of *Brucella melitensis* is involved in persistence in a murine model of infection. *Cell. Microbiol.* 7, 687–698. doi: 10.1111/j.1462-5822.2005.00502.x
- Friedman, N., Linial, M., Nachman, I., and Pe’er, D. (2000). Using Bayesian networks to analyze expression data. *J. Comput. Biol.* 7, 601–620. doi: 10.1089/106652700750050961
- Guzmán-Verri, C., Manterola, L., Sola-Landa, A., Parra, A., Cloeckaert, A., Garin, J., et al. (2002). The two-component system BvrR/BvrS essential for *Brucella abortus* virulence regulates the expression of outer membrane proteins with counterparts in members of the *Rhizobiaceae*. *Proc. Natl. Acad. Sci. U.S.A.* 99, 12375–12380. doi: 10.1073/pnas.192439399
- Hanna, N., Ouahrani-Bettache, S., Drake, K. L., Adams, L. G., Kohler, S., and Occhialini, A. (2013). Global Rsh-dependent transcription profile of *Brucella suis* during stringent response unravels adaptation to nutrient starvation and cross-talk with other stress responses. *BMC Genomics* 14:459. doi: 10.1186/1471-2164-14-459

- Hartemink, A. J., Gifford, D. K., Jaakkola, T. S., and Young, R. A. (2001). Using graphical models and genomic expression data to statistically validate models of genetic regulatory networks. *Pac. Symp. Biocomput.* 6, 422–433. doi: 10.1142/9789814447362_0042
- He, Y. (2012). Analyses of *Brucella* pathogenesis, host immunity, and vaccine targets using systems biology and bioinformatics. *Front. Cell. Infect. Microbiol.* 2:2. doi: 10.3389/fcimb.2012.00002
- He, Y., Reichow, S., Ramamoorthy, S., Ding, X., Lathigra, R., Craig, J. C., et al. (2006). *Brucella melitensis* triggers time-dependent modulation of apoptosis and down-regulation of mitochondrion-associated gene expression in mouse macrophages. *Infect. Immun.* 74, 5035–5046. doi: 10.1128/IAI.01998-05
- Honko, A. N., and Mizel, S. B. (2005). Effects of flagellin on innate and adaptive immunity. *Immunol. Res.* 33, 83–101. doi: 10.1385/IR.33:1:083
- Imoto, S., Higuchi, T., Goto, T., Tashiro, K., Kuhara, S., and Miyano, S. (2004). Combining microarrays and biological knowledge for estimating gene networks via Bayesian networks. *J. Bioinform. Comput. Biol.* 2, 77–98. doi: 10.1142/S021972000400048X
- Jiménez de Bagues, M. P., Terraza, A., Gross, A., and Dornand, J. (2004). Different responses of macrophages to smooth and rough *Brucella* spp.: relationship to virulence. *Infect. Immun.* 72, 2429–2433. doi: 10.1128/IAI.72.4.2429-2433.2004
- Kalher, S. C. (2000). *Brucella melitensis* infection discovered in cattle for first time, goats also infected. *J. Am. Vet. Med. Assoc.* 216:648. Available online at: <https://www.avma.org/News/JAVMANews/Pages/s030100b.aspx>
- Kanehisa, M., Furumichi, M., Tanabe, M., Sato, Y., and Morishima, K. (2017). KEGG: new perspectives on genomes, pathways, diseases and drugs. *Nucleic Acids Res.* 45, D353–D361. doi: 10.1093/nar/gkw1092
- Ke, Y., Wang, Y., Li, W., and Chen, Z. (2015). Type IV secretion system of *Brucella* spp and its effectors. *Front. Cell Infect. Microbiol.* 5:72. doi: 10.3389/fcimb.2015.00072
- Khare, S., Drake, K. L., Lawhon, S. D., Nunes, J. E., Figueiredo, J. F., Rossetti, C. A., et al. (2016). Systems analysis of early host gene expression provides clues for transient *Mycobacterium avium* ssp *avium* vs. persistent *Mycobacterium avium* ssp *paratuberculosis* intestinal infections. *PLoS ONE* 11:e0161946. doi: 10.1371/journal.pone.0161946
- Khare, S., Lawhon, S. D., Drake, K. L., Nunes, J. E., Figueiredo, J. F., Rossetti, C. A., et al. (2012). Systems biology analysis of gene expression during *in vivo* *Mycobacterium avium* paratuberculosis enteric colonization reveals role for immune tolerance. *PLoS ONE* 7:e42127. doi: 10.1371/journal.pone.0042127
- Khare, S., Nunes, J. S., Figueiredo, J. F., Lawhon, S. D., Rossetti, C. A., Gull, T., et al. (2009). Early phase morphological lesions and transcriptional responses of bovine ileum infected with *Mycobacterium avium* subsp. *paratuberculosis*. *Vet. Pathol.* 46, 717–728. doi: 10.1354/vp.08-VP-0187-G-FL
- Kohler, S., Foulongne, V., Ouahrani-Bettache, S., Bourg, G., Teyssier, J., Ramuz, M., et al. (2002). The analysis of the intramacrophagic virulome of *Brucella suis* deciphers the environment encountered by the pathogen inside the macrophage host cell. *Proc. Natl. Acad. Sci. U.S.A.* 99, 15711–15716. doi: 10.1073/pnas.232454299
- Lamontagne, J., Forest, A., Marazzo, E., Denis, F., Butler, H., Michaud, J. F., et al. (2009). Intracellular adaptation of *Brucella abortus*. *J. Proteome Res.* 8, 1594–1609. doi: 10.1021/pr800978p
- Lapaque, N., Moriyón, I., Moreno, E., and Gorvel, J. P. (2005). *Brucella* lipopolysaccharide acts as a virulence factor. *Curr. Opin. Microbiol.* 8, 60–66. doi: 10.1016/j.mib.2004.12.003
- Lavin, J. L., Binnewies, T. T., Pisabarro, A. G., Ussery, D. W., Garcia-Lobo, J. M., and Oguiza, J. A. (2010). Differences in two-component signal transduction proteins among the genus *Brucella*: implications for host preference and pathogenesis. *Vet. Microbiol.* 144, 478–483. doi: 10.1016/j.vetmic.2010.01.007
- Lawhon, S. D., Khare, S., Rossetti, C. A., Everts, R. E., Galindo, C. L., Luciano, S. A., et al. (2011). Role of SPI-1 secreted effectors in acute bovine response to *Salmonella enterica* serovar Typhimurium: a systems biology analysis approach. *PLoS ONE* 6:e26869. doi: 10.1371/journal.pone.0026869
- Leonard, S., Ferooz, J., Haine, V., Danese, I., Fretil, D., Tibor, A., et al. (2007). FtcR is a new master regulator of the flagellar system of *Brucella melitensis* 16M with homologs in *Rhizobiae*. *J. Bacteriol.* 189, 131–141. doi: 10.1128/JB.00712-06
- Lestrade, P., Delrue, R. M., Danese, I., Didembourg, C., Taminiau, B., Mertens, P., et al. (2000). Identification and characterization of *in vivo* attenuated mutants of *Brucella melitensis*. *Mol. Microbiol.* 38, 543–551. doi: 10.1046/j.1365-2958.2000.02150.x
- Liu, W., Jing, Z., Ou, Q., Cui, B., He, Y., and Wu, Q. (2012). Complete genome sequence of *Brucella melitensis* biovar 3 strain NI, isolated from an aborted bovine fetus. *J. Bacteriol.* 194:6321. doi: 10.1128/jb.01595-12
- Livak, K. J., and Schmittgen, T. D. (2001). Analysis of relative gene expression data using real-time quantitative PCR and the 2- $\Delta\Delta C_T$ method. *Methods* 25, 402–408. doi: 10.1006/meth.2001.1262
- Marchesini, M. I., Herrmann, C. K., Salcedo, S. P., Gorvel, J. P., and Comerchi, D. J. (2011). In search of *Brucella abortus* type IV secretion substrates: screening and identification of four proteins translocated into host cells through VirB system. *Cell. Microbiol.* 13, 1261–1274. doi: 10.1111/j.1462-5822.2011.01618.x
- Marchesini, M. I., Morrone Seijo, S. M., Guaimas, F. F., and Comerchi, D. J. (2016). A T4SS effector targets host cell alpha-enolase contributing to *Brucella abortus* intracellular lifestyle. *Front. Cell. Infect. Microbiol.* 6:153. doi: 10.3389/fcimb.2016.00153
- Martínez de Tejada, G., Pizarro-Cerdá, J., Moreno, E., and Moriyón, I. (1995). The outer membranes of *Brucella* spp. are resistant to bactericidal cationic peptides. *Infect. Immun.* 63, 3054–3061.
- Martirosyan, A., Perez-Gutierrez, C., Banchereau, R., Dutartre, H., Lecine, P., Dullaers, M., et al. (2012). *Brucella* beta 1,2 cyclic glucan is an activator of human and mouse dendritic cells. *PLoS Pathog.* 8:e1002983. doi: 10.1371/journal.ppat.1002983
- Mirabella, A., Yanez Villanueva, R. M., Delrue, R. M., Uzureau, S., Zygmunt, M. S., Cloeckert, A., et al. (2012). The two-component system PrlS/PrIR of *Brucella melitensis* is required for persistence in mice and appears to respond to ionic strength. *Microbiology* 158, 2642–2651. doi: 10.1099/mic.0.060863-0
- Mol, J. P., Pires, S. F., Chapeaurouge, A. D., Perales, J., Santos, R. L., Andrade, H. M., et al. (2016). Proteomic profile of *Brucella abortus*-infected bovine chorioallantoic membrane explants. *PLoS ONE* 11:e0154209. doi: 10.1371/journal.pone.0154209
- Moreno, E., and Moriyón, I. (2002). *Brucella melitensis*: a nasty bug with hidden credentials for virulence. *Proc. Natl. Acad. Sci. U.S.A.* 99, 1–3. doi: 10.1073/pnas.022626999
- Nakato, G., Hase, K., Suzuki, M., Kimura, M., Ato, M., Hanazato, M., et al. (2012). Cutting edge: *Brucella abortus* exploits a cellular prion protein on intestinal M cells as an invasive receptor. *J. Immunol.* 189, 1540–1544. doi: 10.4049/jimmunol.1103332
- O'Callaghan, D., and Whatmore, A. M. (2011). *Brucella* genomics as we enter the multi-genome era. *Brief. Funct. Genomics* 10, 334–341. doi: 10.1093/bfpg/blr026
- O'Callaghan, D., Cazeville, C., Allardet-Servent, A., Boschiroli, M. L., Bourg, G., Foulongne, V., et al. (1999). A homologue of the *Agrobacterium tumefaciens* VirB and *Bordetella pertussis* Ptl type IV secretion systems is essential for intracellular survival of *Brucella suis*. *Mol. Microbiol.* 33, 1210–1220. doi: 10.1046/j.1365-2958.1999.01569.x
- Paulsen, I. T., Seshadri, R., Nelson, K., Eisen, J. A., and Heidelberg, J. F. (2002). The *Brucella suis* genome reveals fundamental similarities between animal and plant pathogens and symbionts. *Proc. Natl. Acad. Sci. U.S.A.* 99, 13148–13153. doi: 10.1073/pnas.192319099
- Pei, J., and Ficht, T. A. (2004). *Brucella abortus* rough mutants are cytopathic for macrophages in culture. *Infect. Immun.* 72, 440–450. doi: 10.1128/IAI.72.1.440-450.2004
- Pei, J., Turse, J. E., Wu, Q., and Ficht, T. A. (2006). *Brucella abortus* rough mutants induce macrophage oncosis that requires bacterial protein synthesis and direct interaction with the macrophage. *Infect. Immun.* 74, 2667–2675. doi: 10.1128/IAI.74.5.2667-2675.2006
- Posadas, D. M., Ruiz-Ranwez, V., Bonomi, H. R., Martin, F. A., and Zorreguieta, A. (2012). BmaC, a novel autotransporter of *Brucella suis*, is involved in bacterial adhesion to host cells. *Cell. Microbiol.* 14, 965–982. doi: 10.1111/j.1462-5822.2012.01771.x
- Rambow-Larsen, A. A., Rajashekara, G., Petersoen, E., and Splitter, G. (2008). Putative quorum-sensing regulator BlxR of *Brucella melitensis* regulates virulence factors including the Type IV Secretion System and flagella. *J. Bacteriol.* 190, 3274–3282. doi: 10.1128/JB.01915-07
- Rolan, H. G., and Tsois, R. M. (2007). Mice lacking components of adaptive immunity show increased *Brucella abortus* virB mutant colonization. *Infect. Immun.* 75, 2965–2973. doi: 10.1128/IAI.01896-06

- Rossetti, C. A., Drake, K. L., and Adams, L. G. (2012). Transcriptome analysis of HeLa cells response to *Brucella melitensis* infection: a molecular approach to understand the role of the mucosal epithelium in the onset of the *Brucella* pathogenesis. *Microbes Infect.* 14, 756–767. doi: 10.1016/j.micinf.2012.03.003
- Rossetti, C. A., Drake, K. L., Siddavatam, P., Lawhon, S. D., Nunes, J. E., Gull, T., et al. (2013). Systems biology analysis of *Brucella* infected Peyer's patch reveals rapid invasion with modest transient perturbations of the host transcriptome. *PLoS ONE* 8:e81719. doi: 10.1371/journal.pone.0081719
- Rossetti, C. A., Galindo, C. L., Everts, R. E., Lewin, H. A., Garner, H. R., and Adams, L. G. (2011a). Comparative analysis of the early transcriptome of *Brucella abortus*-infected monocyte-derived macrophages from cattle naturally resistant or susceptible to brucellosis. *Res. Vet. Sci.* 91, 40–51. doi: 10.1016/j.rvsc.2010.09.002
- Rossetti, C. A., Galindo, C. L., Garner, H. R., and Adams, L. G. (2010). Selective amplification of *Brucella melitensis* mRNA from a mixed host-pathogen total RNA. *BMC Res. Notes* 3:244. doi: 10.1186/1756-0500-3-244
- Rossetti, C. A., Galindo, C. L., Garner, H. R., and Adams, L. G. (2011b). Transcriptional profile of the intracellular pathogen *Brucella melitensis* following HeLa cells infection. *Microb. Pathog.* 51, 338–344. doi: 10.1016/j.micpath.2011.07.006
- Rossetti, C. A., Galindo, C. L., Lawhon, S., Garner, H., and Adams, L. G. (2009). *Brucella melitensis* global gene expression study provides novel information on growth phase-specific gene regulation with potential insights for understanding *Brucella*:host interaction. *BMC Microbiol.* 9:81. doi: 10.1186/1471-2180-9-81
- Roux, C. M., Roldán, H. G., Santos, R. L., Beremand, P. D., Thomas, T. L., Adams, L. G., et al. (2007). *Brucella* requires a functional type IV secretion system to elicit innate immune responses in mice. *Cell. Microbiol.* 9, 1851–1869. doi: 10.1111/j.1462-5822.2007.00922.x
- Ruiz-Ranwez, V., Posadas, D. M., Estein, S. M., Abdian, P. L., Martin, F. A., and Zorreguieta, A. (2013a). The BtaF trimeric autotransporter of *Brucella suis* is involved in attachment to various surfaces, resistance to serum and virulence. *PLoS ONE* 8:e79770. doi: 10.1371/journal.pone.0079770
- Ruiz-Ranwez, V., Posadas, D. M., Van Der Henst, C., Estein, S. M., Arocena, G. M., Abdian, P. L., et al. (2013b). BtaE, an adhesin that belongs to the trimeric autotransporter family, is required for full virulence and defines a specific adhesive pole of *Brucella suis*. *Infect. Immun.* 81, 996–1007. doi: 10.1128/IAI.01241-12
- Salcedo, S. P., Marchesini, M. I., Degos, C., Terwagne, M., Von Bargen, K., Lepidi, H., et al. (2013). BtpB, a novel *Brucella* TIR-containing effector protein with immune modulatory functions. *Front. Cell. Infect. Microbiol.* 3:28. doi: 10.3389/fcimb.2013.00028
- Salcedo, S. P., Marchesini, M. I., Lelouard, H., Fugier, E., Jolly, G., Balor, S., et al. (2008). *Brucella* control of dendritic cell maturation is dependent on the TIR-containing protein Btp1. *PLoS Pathog.* 4:e21. doi: 10.1371/journal.ppat.0040021
- Sankarasubramanian, J., Vishnu, U. S., Dinakaran, V., Sridhar, J., Gunasekaran, P., and Rajendhran, J. (2016). Computational prediction of secretion systems and secretomes of *Brucella*: identification of novel type IV effectors and their interaction with the host. *Mol. Biosyst.* 12, 178–190. doi: 10.1039/C5MB00607D
- Santos, R. L., Zhang, S., Tsois, R. M., Baumler, A. J., and Adams, L. G. (2002). Morphologic and molecular characterization of *Salmonella typhimurium* infection in neonatal calves. *Vet. Pathol.* 39, 200–215. doi: 10.1354/vp.39-2-200
- Schauer, K., and Stingl, K. (2009). 'Guilty by association' - protein-protein interactions (PPIs) in bacterial pathogens. *Genome Dyn.* 6, 48–61. doi: 10.1159/000235762
- Seira, R., Comerci, D. J., Pietrasanta, L. I., and Ugalde, R. A. (2004). Integration host factor is involved in transcriptional regulation of the *Brucella abortus* virB operon. *Mol. Microbiol.* 54, 808–822. doi: 10.1111/j.1365-2958.2004.04316.x
- Seira, R., Comerci, D. J., Sánchez, D. O., and Ugalde, R. A. (2000). A homologue of an operon required for DNA transfer in *Agrobacterium* is required in *Brucella abortus* for virulence and intracellular multiplication. *J. Bacteriol.* 182, 4849–4855. doi: 10.1128/JB.182.17.4849-4855.2000
- Sola-Landa, A., Pizarro-Cerdá, J., Grilló, M. J., Moreno, E., Moriyón, I., Blasco, J. M., et al. (1998). A two-component regulatory system playing a critical role in plant pathogens and endosymbionts is present in *Brucella abortus* and controls cell invasion and virulence. *Mol. Microbiol.* 29, 125–138. doi: 10.1046/j.1365-2958.1998.00913.x
- Spera, J. M., Ugalde, J. E., Mucci, J., Comerci, D. J., and Ugalde, R. A. (2006). A B lymphocyte mitogen is a *Brucella abortus* virulence factor required for persistent infection. *Proc. Natl. Acad. Sci. U.S.A.* 103, 16514–16519. doi: 10.1073/pnas.0603362103
- Swartz, T. E., Tseng, T. S., Frederickson, M. A., Paris, G., Comerci, D. J., Rajashekar, G., et al. (2007). Blue-light-activated histidine kinases: two-component sensors in bacteria. *Science* 317, 1090–1093. doi: 10.1126/science.1144306
- Terwagne, M., Ferooz, J., Rolan, H. G., Sun, Y. H., Atluri, V., Xavier, M. N., et al. (2013). Innate immune recognition of flagellin limits systemic persistence of *Brucella*. *Cell. Microbiol.* 15, 942–960. doi: 10.1111/cmi.12088
- Tian, M., Qu, J., Han, X., Zhang, M., Ding, C., Ding, J., et al. (2013). Microarray-based identification of differentially expressed genes in intracellular *Brucella abortus* within RAW264.7 cells. *PLoS ONE* 8:e67014. doi: 10.1371/journal.pone.0067014
- Traxler, R. M., Lehman, M. W., Bosserman, E. A., Guerra, M. A., and Smith, T. L. (2013). A literature review of laboratory-acquired brucellosis. *J. Clin. Microbiol.* 51, 3055–3062. doi: 10.1128/JCM.00135-13
- Tumurkhuu, G., Koide, N., Takahashi, K., Hassan, F., Islam, S., Ito, H., et al. (2006). Characterization of biological activities of *Brucella melitensis* lipopolysaccharide. *Microbiol. Immunol.* 50, 421–427. doi: 10.1111/j.1348-0421.2006.tb03810.x
- Viadas, C., Rodriguez, M. C., Sangari, F. J., Gorvel, J. P., Garcia-Lobo, J. M., and Lopez-Goni, I. (2010). Transcriptome analysis of the *Brucella abortus* BvrR/BvrS two-component regulatory system. *PLoS ONE* 5:e10216. doi: 10.1371/journal.pone.0010216
- von Bargen, K., Gagnaire, A., Arce-Gorvel, V., De Bovis, B., Baudimont, F., Chasson, L., et al. (2015). Cervical Lymph nodes as a selective Niche for *Brucella* during oral infections. *PLoS ONE* 10:e0121790. doi: 10.1371/journal.pone.0121790
- Wagner, M. A., Eschenbrenner, M., Horn, T. A., Kraycer, J. A., Muej, C. V., Hagius, S., et al. (2002). Global analysis of the *Brucella melitensis* proteome: Identification of proteins expressed in laboratory-grown culture. *Proteomics* 2, 1047–1060. doi: 10.1002/1615-9861(200208)2
- Wang, Y., Chen, Z., Qiao, F., Ying, T., Yuan, J., Zhong, Z., et al. (2009). Comparative proteomics analyses reveal the virB of *B. melitensis* affects expression of intracellular survival related proteins. *PLoS ONE* 4:e5368. doi: 10.1371/journal.pone.0005368
- Wareth, G., Melzer, F., Elschner, M. C., Neubauer, H., and Roesler, U. (2014). Detection of *Brucella melitensis* in bovine milk and milk products from apparently healthy animals in Egypt by real-time PCR. *J. Infect. Dev. Ctries.* 8, 1339–1343. doi: 10.3855/jidc.4847
- Watarai, M., Kim, S., Erdenebaatar, J., Makino, S., Horiuchi, M., Shirahata, T., et al. (2003). Cellular prion protein promotes *Brucella* infection into macrophages. *J. Exp. Med.* 198, 5–17. doi: 10.1084/jem.20021980
- Weeks, J. N., Galindo, C. L., Drake, K. L., Adams, G. L., Garner, H. R., and Ficht, T. A. (2010). *Brucella melitensis* VjbR and C12-HSL regulons: contributions of the N-dodecanoyl homoserine lactone signaling molecule and LuxR homologue VjbR to gene expression. *BMC Microbiol.* 10:167. doi: 10.1186/1471-2180-10-167
- Werhli, A., and Husmeier, D. (2007). Reconstructing gene regulatory networks with bayesian networks by combining expression data with multiple sources of prior knowledge. *Stat. Appl. Genet. Mol. Biol.* 6:15. doi: 10.2202/1544-6115.1282
- Whatmore, A. M., Davison, N., Cloeckaert, A., Al Dahouk, S., Zygmunt, M. S., Brew, S. D., et al. (2014). *Brucella papionis* sp. nov., isolated from baboons (*Papio* spp.). *Int. J. Syst. Evol. Microbiol.* 64, 4120–4128. doi: 10.1099/ijs.0.065482-0
- Winter, S. E., Thiennimitr, P., Winter, M. G., Butler, B. P., Huseby, D. L., Crawford, R. W., et al. (2010). Gut inflammation provides a respiratory electron acceptor for *Salmonella*. *Nature* 467, 426–429. doi: 10.1038/nature09415
- Wu, Q., Pei, J., Turse, C., and Ficht, T. A. (2006). Mariner mutagenesis of *Brucella melitensis* reveals genes with previously uncharacterized roles in virulence and survival. *BMC Microbiol.* 6:102. doi: 10.1186/1471-2180-6-102
- Zhang, X., Ren, J., Li, N., Liu, W., and Wu, Q. (2009). Disruption of the BMEI0066 gene attenuates the virulence of *Brucella melitensis* and

decreases its stress tolerance. *Int. J. Biol. Sci.* 5, 570–577. doi: 10.7150/ijbs.5.570

Conflict of Interest Statement: KD is a Chief Technology Officer in Seralogix, LLC. Seralogix is a bioinformatics research and services company commercializing computational systems biology software tools that are being sponsored by the National Institute of Allergy and Infectious Diseases and the National Human Genome Research Institute. KD participated in conducting certain genomic data processing involving pathway analyses and modeling that helped to provide a more system-level perspective of the host-pathogen interaction to the Texas A&M University researchers. Data were processed by KD utilizing Seralogix's proprietary computational pipeline for biological systems analysis. The relation between Seralogix and Texas A&M University, College of Veterinary Medicine and Biomedical Science is strictly on a collaborative (mutually beneficial) research basis with no financial arrangements, commitments or interests. KD's motivation is to see their computational tools produce results that contribute to the improved understanding of host response to pathogen invasions (an objective of his National Health Institute research grants). KD contributed to the interpretation of the analysis results provided to the Texas A&M University researchers. Seralogix has no ownership of the data, nor results produced by their tools.

The other authors declare that the research was conducted in the absence of any commercial or financial relationships that could be construed as a potential conflict of interest.

Received: 10 March 2017; Accepted: 26 June 2017; Published: 27 July 2017

Citation: Rossetti CA, Drake KL, Lawhon SD, Nunes JS, Gull T, Khare S and Adams LG (2017) Systems Biology Analysis of Temporal In vivo *Brucella melitensis* and Bovine Transcriptomes Predicts host:Pathogen Protein-Protein Interactions. *Front. Microbiol.* 8:1275. doi: 10.3389/fmicb.2017.01275

This article was submitted to Infectious Diseases, a section of the journal *Frontiers in Microbiology*

Copyright © 2017 Rossetti, Drake, Lawhon, Nunes, Gull, Khare and Adams. This is an open-access article distributed under the terms of the Creative Commons Attribution License (CC BY). The use, distribution or reproduction in other forums is permitted, provided the original author(s) or licensor are credited and that the original publication in this journal is cited, in accordance with accepted academic practice. No use, distribution or reproduction is permitted which does not comply with these terms.



Modulation of Microtubule Dynamics Affects *Brucella abortus* Intracellular Survival, Pathogen-Containing Vacuole Maturation, and Pro-inflammatory Cytokine Production in Infected Macrophages

OPEN ACCESS

Edited by:

Axel Cloeckaert,
Institut National de la Recherche
Agronomique (INRA), France

Reviewed by:

Diego J. Comerçi,
Instituto de Investigaciones
Biotecnológicas (IIB-INTECH),
Argentina

Jean-Pierre Gorvel,
Centre National de la Recherche
Scientifique (CNRS), France

*Correspondence:

Sergio C. Oliveira
scozeus1@gmail.com

Specialty section:

This article was submitted to
Infectious Diseases,
a section of the journal
Frontiers in Microbiology

Received: 15 August 2017

Accepted: 27 October 2017

Published: 14 November 2017

Citation:

Alves-Silva J, Tavares IP,
Guimarães ES, Costa Franco MM,
Figueiredo BC, Marques JT,
Splitter G and Oliveira SC (2017)
Modulation of Microtubule Dynamics
Affects *Brucella abortus* Intracellular
Survival, Pathogen-Containing
Vacuole Maturation,
and Pro-inflammatory Cytokine
Production in Infected Macrophages.
Front. Microbiol. 8:2217.
doi: 10.3389/fmicb.2017.02217

**Juliana Alves-Silva¹, Isabela P. Tavares¹, Erika S. Guimarães¹, Miriam M. Costa Franco¹,
Barbara C. Figueiredo¹, João T. Marques¹, Gary Splitter² and Sergio C. Oliveira^{1*}**

¹ Departamento de Bioquímica e Imunologia, Universidade Federal de Minas Gerais, Belo Horizonte, Brazil, ² Department of Pathobiological Sciences, University of Wisconsin-Madison, Madison, WI, United States

The microtubule (MT) cytoskeleton regulates several cellular processes related to the immune system. For instance, an intricate intracellular transport mediated by MTs is responsible for the proper localization of vesicular receptors of innate immunity and its adaptor proteins. In the present study, we used nocodazole to induce MTs depolymerization and paclitaxel or recombinant (r) TIR (Toll/interleukin-1 receptor) domain containing protein (TcPB) to induce MT stabilization in bone marrow-derived macrophages infected with *Brucella abortus*. Following treatment of the cells, we evaluated their effects on pathogen intracellular replication and survival, and in pro-inflammatory cytokine production. First, we observed that intracellular trafficking and maturation of *Brucella*-containing vesicles (BCVs) is affected by partial destabilization or stabilization of the MTs network. A typical marker of early BCVs, LAMP-1, is retained in late BCVs even 24 h after infection in the presence of low doses of nocodazole or paclitaxel and in the presence of different amounts of rTcPB. Second, microscopy and colony forming unit analysis revealed that bacterial load was increased in infected macrophages treated with lower doses of nocodazole or paclitaxel and with rTcPB compared to untreated cells. Third, innate immune responses were also affected by disturbing MT dynamics. MT depolymerization by nocodazole reduced IL-12 production in infected macrophages. Conversely, rTcPB-treated cells augmented IL-12 and IL-1 β secretion in infected cells. In summary, these findings demonstrate that modulation of MTs affects several crucial steps of *B. abortus* pathogenesis, including BCV maturation, intracellular survival and IL-12 secretion in infected macrophages.

Keywords: *Brucella abortus*, microtubules, TcPB, innate immunity, bacterial pathogenesis

INTRODUCTION

The innate immune response is the first line of defense against pathogens. Immune cells sense pathogens through a set of evolutionary conserved pattern recognition receptors (PRRs). Upon recognition of pathogen-associated molecular patterns (PAMPs), some PRRs trigger an inflammatory response, producing cytokines and antimicrobial intermediates leading to the efficient destruction of invading pathogens (Medzhitov and Janeway, 2000; Akira et al., 2006). *Brucella abortus* is a facultative intracellular coccobacillus that causes brucellosis both in humans and cattle and leads to serious economic and public health burden in endemic areas (Pappas et al., 2006). Infection by *B. abortus* causes abortion and sterility in animals; whereas in humans, the disease is characterized by acute inflammation, undulant fever, endocarditis, arthritis, among other pathological manifestations, with approximately half a million new cases occurring each year worldwide (Pizarro-Cerda et al., 1998; Boschirolti et al., 2001; Yang et al., 2013).

Like several bacteria that have undergone a long evolution within mammalian hosts, *Brucella* evolved mechanisms to subvert cell immunosurveillance that ensures bacteria survival, proliferation and persistence within the host (Barquero-Calvo et al., 2007). In this regard, *Brucella* virulence is crucially dependent on its intracellular life cycle. Upon entry into host cells, *Brucella* resides within a membrane-bound compartment, the *Brucella*-containing vesicle (BCV) whose trafficking is controlled by the bacterium (Pizarro-Cerda et al., 1998; Comerci et al., 2001; Delrue et al., 2001; Salcedo et al., 2008; Starr et al., 2008). BCV suffers a maturation process characterized by limited interaction and acquisitions of the endoplasmic reticulum (ER) membrane until it is converted in a organelle competent to sustain bacterial replication. The BCV acidifies and acquires late endosomal marks such as Rab7 and LAMP-1 (Pizarro-Cerda et al., 1998; Celli et al., 2005). This vesicular traffic is largely performed by molecular motors on microtubules (MTs), essential components of the eukaryotic cytoskeleton that are implicated in important functions as cell division, migration, and intracellular signal transduction. Likewise, stabilization and destabilization of MTs directly affects cellular signaling and several signal transduction pathways (Gundersen and Cook, 1999).

Furthermore, bacterial pathogens deliver several effector proteins into host cells for modulating MT cytoskeleton dynamics (Yoshida and Sasakawa, 2003). *B. abortus* encodes a TIR domain-containing protein, TcpB (also termed BtpA) that co-localizes with MTs (Radhakrishnan et al., 2009) and increases the rate of nucleation as well as the polymerization phases of MT formation, acting as a stabilization factor that modulates MTs dynamics (Radhakrishnan et al., 2011). The MT stabilization properties of TcpB are attributed to the BB-loop region of the TIR domain, whereas a BB-loop mutant TcpB exhibits defective MT binding and stabilizing properties (Radhakrishnan et al., 2011).

In this study, we used nocodazole, paclitaxel and recombinant (r) TcpB as MT modulating agents. The complexity of brucellosis pathogenesis emphasizes the importance in understanding the mechanisms governing its intracellular trafficking and life cycle. Therefore, we investigated the effect of MT destabilization and

stabilization on the intracellular trafficking of *B. abortus* as well as host innate immune responses.

MATERIALS AND METHODS

Mice

C57BL/6 mice aged 6–8 weeks were used in this study. Animals were purchased from the animal facility at Federal University of Minas Gerais (UFMG). All the animal experimental procedures were pre-approved by the Institutional Animal Care and Use Committee of UFMG (CETEA #128/2014).

Bacterial Strain

A variation of *B. abortus* virulent strain S2308 which constitutively expresses GFP (*B. abortus*-GFP) from our laboratory collection was used in the present study. Bacteria were grown overnight in Brucella broth medium (BD Biosciences Pharmingen, San Diego, CA, United States) at 37°C under constant agitation, before being used for macrophage infection. All work with *Brucella*, including animal experiments, was conducted in the biosafety cabinet or a primary containment device within a dedicated laboratory. Appropriate laboratory coats, gloves, and protective eyewear were provided to ensure the safety of personnel. All personnel working in the biosafety laboratory were trained and approved for entry by an individual knowledgeable in the biosafety practices.

Pharmacological Reagents

Nocodazole and Paclitaxel were purchased from Sigma–Aldrich, Co. (St. Louis, MO, United States). Stock solutions of 5 mM were prepared for each reagent in dimethyl sulfoxide (DMSO) and kept frozen (–20°C). Further working dilutions were prepared in DMEM medium on the day of the experiments and used fresh.

TcpB Expression and Purification

The expression plasmid containing the coding sequence for the TIR domain-containing protein (TcpB/BtpA) pD444-NH::TcpB was purchased from DNA 2.0 Inc., United States¹, and the expression and purification of TcpB protein performed as previously described (Goncalves de Assis et al., 2015). A poly-lysine column (Thermo Fisher Scientific) was used for endotoxin (LPS) removal according to the manufacturer's instructions.

BMDM Culture

Bone marrow-derived macrophages (BMDMs) were obtained from C57BL/6 mice as previously described (Gomes et al., 2016). Briefly, bone marrow cells from each femur and tibia was flushed with 5 ml of Hanks' balanced salt solution (HBSS). The resulting cell suspension was centrifuged, and the cells were resuspended in Dulbecco's modified Eagle's medium (DMEM; Gibco) containing 10% fetal bovine serum (FBS; Gibco), 1% penicillin-streptomycin, 1% HEPES, and 10% L929 cell-conditioned medium (LCCM) as a source of macrophage colony-stimulating factor (M-CSF). Cells were then plated into 10 cm cell

¹<https://www.dna20.com>

culture dishes and cultured for 10 days in 5% CO₂ atmosphere at 37°C. Four days after seeding, additional 10% LCCM was added to the culture, and on day 7 the medium was replaced by fresh differentiation medium. On the 10th day, differentiation into macrophages was complete, and the cells were released from the dish (using cold PBS) to be re-plated onto 24-well plates for infection. BMDMs were seeded at 5×10^5 cells/well for cytokine secretion and colony forming unit (CFU) analysis, and at 1×10^5 cells/well over sterile 12 mm round glass coverslips for microscopic analysis.

Infection with *B. abortus*

Bone marrow-derived macrophages were infected for 1 h with *B. abortus*-GFP (MOI 200:1) as follows: prior to being infected, cells were washed once with PBS to remove traces of antibiotics from the differentiation media. Three hundred microliters of DMEM (supplemented with 1% FCS) containing bacteria was added to each well, and the cells were centrifuged at 600 g for 10 min before being kept at 37°C for an additional 50 min. At the end of the 1-h period cells were washed once with PBS to remove excess bacteria and media containing nocodazole, paclitaxel or DMSO (controls) were added at different concentrations (see section Results) for a further 4 or 24 h. At the end of the experiments, supernatant was collected for further analysis of cytokine secretion or the cells were fixed in 4% paraformaldehyde for immunofluorescence. For experiments with recombinant (r) TcpB, cells were pre-treated with 1, 5, or 10 µg/mL of rTcpB protein, with no detectable LPS, for 2 h prior to being infected with *B. abortus* (MOI:200) as described above. Cells were then washed once with PBS and cultured in medium containing TcpB (1, 5, or 10 µg/mL) for further 24 h.

Immunofluorescence Microscopy

Infected BMDMs seeded onto glass coverslips and subjected to different treatments, as described above, were fixed in 4% paraformaldehyde, pH 7.4, at room temperature for 30 min. After fixation, cells were washed 3× with PBS and permeabilized with 0.1% saponin for 30 min. Cells were then washed 3× with PBS and incubated overnight with 1:250 rabbit anti-LAMP1 (Cell Signaling) or with 1:500 mouse anti-tubulin. Three washes with PBS were again performed prior to incubation for 1 h with 1:400 anti-rabbit Alexa 546 or 1:400 anti-mouse Alexa 488 secondary antibody. Cover-slips were mounted on slides using ProLong Gold antifade reagent with DAPI (Invitrogen). Images were collected using a Nikon C2 confocal laser microscope. The number of intracellular GFP-expressing bacteria and the percentage of *B. abortus* BCVs containing LAMP-1 were quantified at 24 h using the confocal microscopy images. Images from at least 85 infected cells documented from 3 independent experiments were used for the analysis (see figure legends).

BMDM Viability Assay

The toxicity of nocodazole and paclitaxel treatment was evaluated in live/dead cell viability assays. BMDMs seeded on cover-slips and infected with *B. abortus* (as described above) were treated with 0.5 or 5 µM of nocodazole or paclitaxel (or equivalent amounts of DMSO for control) for 24 h. Then, culture medium

was replaced by PBS containing 1 µg/ml propidium iodide (PI, for dead/injured cells labeling) and 5 µg/ml acridine orange (AO, to label all the cells) for 30 min. Cover slips were then taken for microscopic analyses on an ApoTome 2.0 (Zeiss) microscope adapted with a plan-apochromat 40 × 0.8 objective. HXP 120 C (metal halide) was used for illumination, and images were acquired from AO and PI labeled cells using excitation: BP 470/40; emission BP 525/50 and excitation: BP 550/25; emission BP 605/70, respectively. Zen software was used to collect images as .czi files using an AxioCam HRm camera.

Estimation of *Brucella* CFU in Macrophages

Viable intracellular bacteria were estimated by counting CFUs. Infected macrophages were lysed for 10 min at room temperature in 800 µl of deionized water under manual agitation. Lysates were serially diluted from 10 to 10,000 times in PBS and plated on petri dishes containing *Brucella* Broth Agar. Petri dishes were incubated for 3 days at 37°C to allow proper growth of *Brucella* colonies to be counted as CFUs.

Cytokine Analysis

Supernatant media from BMDMs infected and treated as described above were harvested 24 h after infection and assayed for the secretion of IL-1β, IL-12, IL-6 and TNF-α using ELISA kits (R&D Systems), in accordance with the manufacturer's instructions.

Statistical Analysis

GraphPad Prism computer software, version 6 (GraphPad Software) was used for analysis of the data. As indicated in the text, two-way ANOVA (followed by Bonferroni post-test) or Student's *t*-test were performed. Levels of significance in the analysis were **p* ≤ 0.05, ***p* ≤ 0.01 or ****p* ≤ 0.001 as indicated.

RESULTS

Microtubule Alteration Affects Intracellular *Brucella* Replication

To investigate which aspects of *Brucella* intracellular infection are regulated by MTs, we induced disturbances into the cell cytoskeleton by chemical compounds or added the virulence factor TcpB and evaluated different aspects of host-pathogen interactions, such as: bacterial survival and replication, BCV structure and cytokine secretion. Initially, 0.1, 0.5, 1, 2, 5, and 10 µM of nocodazole (a MT depolymerizing agent) or paclitaxel (a MT stabilizer) were used (data not shown). Then, 0.5 and 5 µM concentrations were selected and cell viability was evaluated (Supplementary Figure 1). Treatment with 5 µM nocodazole for 24 h was the maximum concentration used to induce complete elimination of MT filaments without increase in cell death (Supplementary Figures 1A4,B). Similarly, incubation with 5 µM paclitaxel for 24 h promoted strong MT bundling (Supplementary Figures 1A5,B). Starting concentrations of 0.5 µM nocodazole

and 0.5 μM paclitaxel were used in BMDM cells and also exhibited no effect on cell viability (Supplementary Figure 1A). Immunofluorescence analysis revealed that these lower concentrations of nocodazole and paclitaxel induced only minor alterations on the MT network (Supplementary Figure 1B).

Brucella survival and replication was then evaluated at 24 hours post-infection (hpi) in BMDMs treated with either 0.5 or 5 μM of nocodazole and 0.5 or 5 μM paclitaxel. To ensure that the disruptions on the MT cytoskeleton would not compromise bacteria internalization, macrophages were infected with *Brucella* (MOI 200:1) for 60 min in the absence of drugs. Cells were then washed to remove media containing extracellular *Brucella*, and cultured in medium containing DMSO (vehicle), nocodazole or paclitaxel for the remainder of the experiment. Bacterial load was assessed at 24 hpi by fluorescence microscopy (Figure 1A). Unexpectedly, strong MT disassembly or high MT stabilization in infected macrophages did not affect the intracellular bacterial load at 24 hpi compared to DMSO treated controls (Figure 1B). Conversely, treatment with 0.5 μM nocodazole and 0.5 μM paclitaxel promoted bacterial replication (Figures 1A,B). Despite intense GFP expression observed in imaged intracellular *Brucella*, used as an indication of live bacteria, CFU counts were also performed in infected macrophages to evaluate

viability of the intracellular pathogen. In agreement with the immunofluorescence data, treatment with higher concentrations (5 μM) of nocodazole and paclitaxel had no effect on the viability of intracellular bacteria, whereas treatment with low concentrations of the same drugs promoted bacterial proliferation (Figure 1C). These results indicate that slight alterations in MT dynamics affect *Brucella* replication in BMDMs. Since TcpB also alters MT dynamics (Radhakrishnan et al., 2011), we treated infected cells with rTcpB and evaluated whether this molecule would interfere with *Brucella* survival or replication. *Brucella* growth was evaluated at 24 hpi in BMDMs pre-treated with different concentrations of rTcpB (1, 5, or 10 $\mu\text{g/mL}$) and bacterial load was assessed by microscopy. Interestingly, treatment with rTcpB promoted an increase in intracellular bacterial load in BMDMs infected with *B. abortus* (Figures 2A,B).

Late BCV Composition Is Altered by Modifications of MT Dynamics

The increased number of intracellular *Brucella* in BMDMs treated with 0.5 μM nocodazole or 0.5 μM paclitaxel could be an indication of alterations on BCV trafficking and/or maturation. To evaluate the effect of nocodazole and paclitaxel on BCV composition, we quantified the number of BCVs associated with the late BCV marker, LAMP-1 at 24 hpi, in treated and

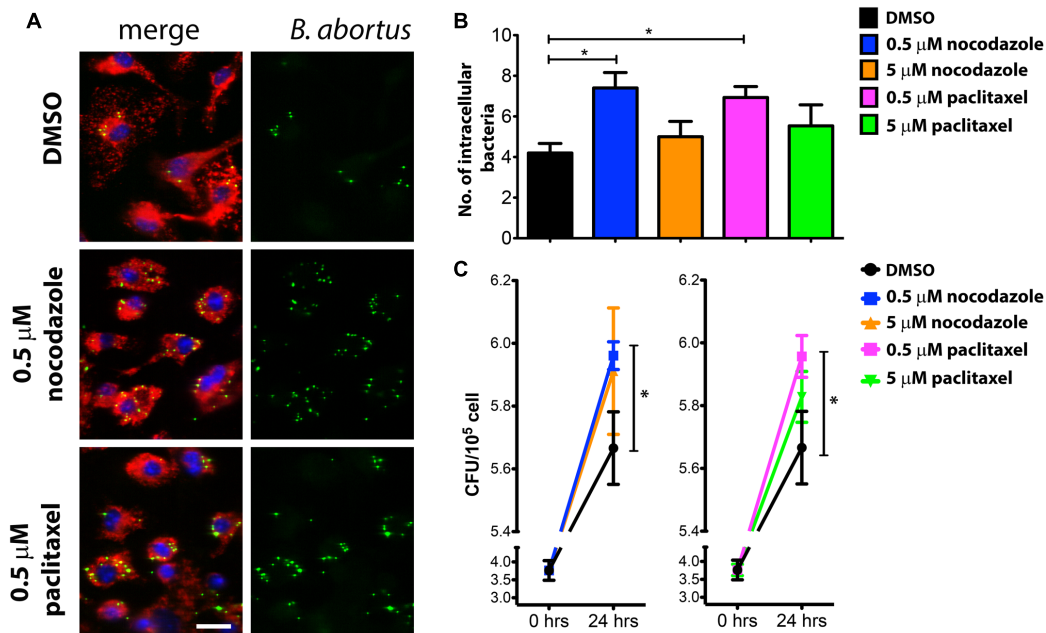


FIGURE 1 | Intracellular bacterial load is increased in BMDMs treated with low doses of nocodazole or paclitaxel. BMDMs were infected with *B. abortus* and treated with nocodazole (0.5 or 5 μM), paclitaxel (0.5 or 5 μM), or vehicle (DMSO) for 24 h. Representative confocal micrographs of infected cells labeled with DAPI in blue and anti-LAMP1 in red are shown on the left (A). GFP-expressing *Brucella* are shown in green. The number of GFP-expressing bacteria/cell was scored and is plotted in (B) as the average number of *Brucella*/macrophage. Data are expressed as mean \pm SE and significant differences in relation to the DMSO control are designated by an asterisk ($p \leq 0.05$, one-way ANOVA). Images are representative of three independent experiments and images from these three experiments were used to compute the graph shown in (B). Number of cells evaluated per condition: DMSO (112), 0.5 μM nocodazole (124), 5 μM nocodazole (93), 0.5 μM paclitaxel (107) and 5 μM paclitaxel (85). Scale bar corresponds to 20 μm . Colony forming unit (CFU) analysis were performed at 0 and 24 hours post-infection (hpi) and the results are plotted in (C). Data are expressed as mean \pm SE of CFU counts obtained in triplicate in two independent experiments. Significant differences in relation to the DMSO control are designated by an asterisk ($p \leq 0.05$, one-way ANOVA).

untreated infected macrophages. Two hours after infection, LAMP-1 association can be found in approximately 83% of BCVs (Figure 3A). Similarly, treatment of infected macrophages with 5 μ M nocodazole or 5 μ M paclitaxel showed no significant differences in percentage of LAMP-1-positive BCVs compared to untreated cells (Figure 3B). However, treatment of infected macrophages with 0.5 μ M of nocodazole or 0.5 μ M of paclitaxel, which cause weaker disturbances of the MT cytoskeleton, induced a dramatic change in LAMP-1 association with late BCVs. Either treatment caused a significant increase (to more than 90%) of LAMP-1 positive BCVs (Figures 3B,C). Similar experiments were performed to evaluate whether treatment with rTcbP would also have any effects on BCV trafficking. At 24 hpi, the number of late BCVs marked with LAMP-1 in untreated and rTcbP-treated infected macrophages was quantified. Treatment of infected macrophages with all studied concentrations of rTcbP induced a dramatic increase in the percentage of BCVs associated with the LAMP-1 marker (Figure 4). Our data support a correlation between TcbP-induced MT stabilization and the regulation of BCV composition during *B. abortus* infection, suggesting a crucial role of TcbP in the maturation of the BCV.

IL-12 and IL-1 β Secretion Induced by *Brucella* Infection in Macrophages Are Regulated by TcbP and Microtubule Network

Staying inside vesicular compartments throughout most of their intracellular life is one of the strategies developed by stealthy pathogens to hide from cytoplasmic innate immune receptors. However, endosomal receptors such as TLR3, TLR7-8 and TLR9, also take part in *Brucella* recognition (Gomes et al., 2016; Campos et al., 2017; Milillo et al., 2017) and likely encounter BCVs during bacterial intracellular trafficking. Since vesicular traffic is largely performed by MTs, we investigated whether treatment of infected macrophages with nocodazole, paclitaxel or rTcbP could also affect innate immune responses against *Brucella* infection. Secretion of IL-1 β , IL-12, IL-6 and TNF- α was measured in untreated as well as drug-treated uninfected macrophages to evaluate any effects of MT disturbance on basal levels of cytokine production. Although MT destabilization with either 0.5 or 5 μ M nocodazole and stabilization with 5 μ M paclitaxel were sufficient to stimulate IL-6 and TNF- α secretion in uninfected BMDM cells (Supplementary Figures 2A,B), their levels were

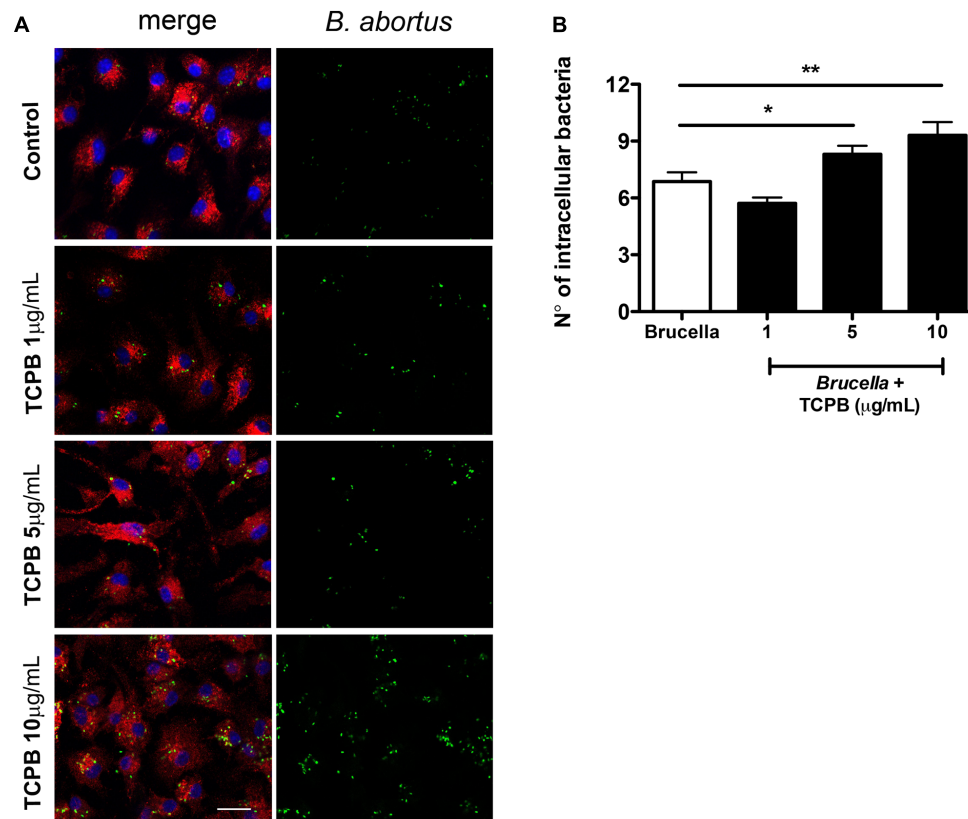


FIGURE 2 | Intracellular bacterial load is increased in BMDMs treated with rTcbP protein. BMDMs were pre-treated with TCPB protein (1, 5, or 10 μ g/mL) for 2 h and infected with *B. abortus* for 24 h. Representative confocal micrographs of infected cells are shown on the left (A) labeled with DAPI in blue and anti-LAMP1 in red. GFP-expressing *Brucella* are shown in green. The number of GFP-expressing bacteria/cell was scored and is plotted in (B) as the average number of *Brucella*/macrophage. Data are expressed as mean \pm SE and significant differences in relation to control are designated by * p < 0.05 and ** p < 0.01, (one-way ANOVA). Images are representative of three independent experiments. At least 85 cells were evaluated per condition. Scale bar corresponds to 20 μ m.

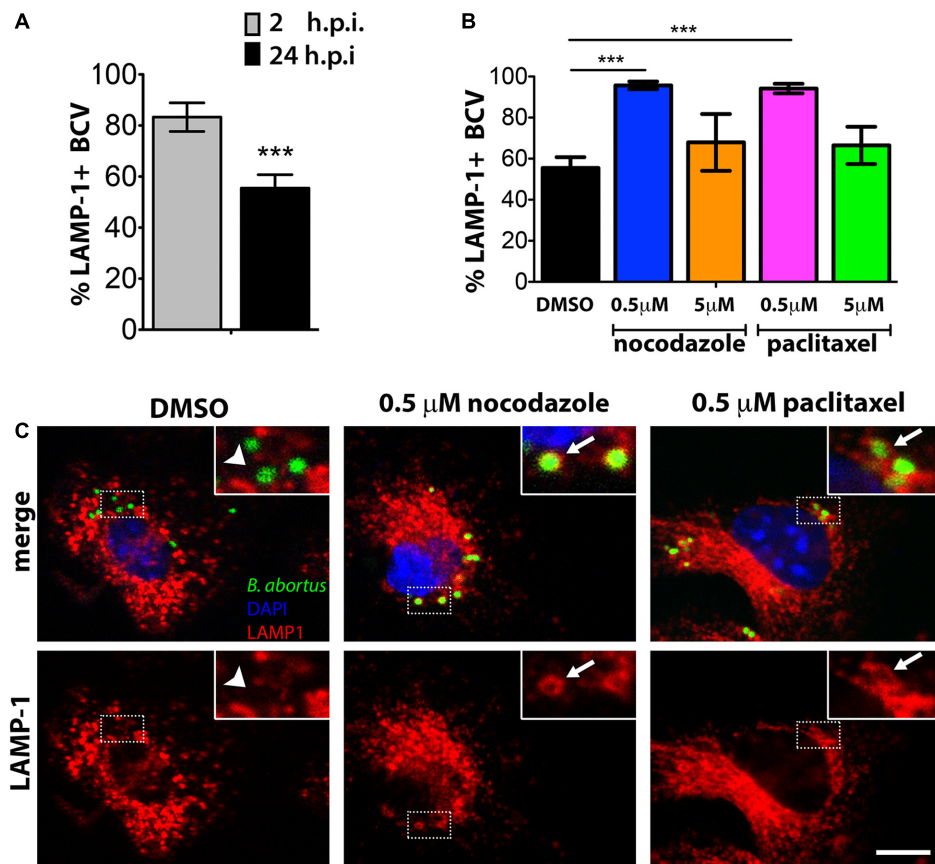


FIGURE 3 | Association of Lamp-1 to late *Brucella*-containing vesicles (BCVs) are increased in BMDMs treated with low doses of nocodazole or paclitaxel. BMDMs were infected with *B. abortus* and treated with nocodazole (0.5 or 5 μM), paclitaxel (0.5 or 5 μM), or vehicle (DMSO) for 24 h. The percentage of LAMP1-positive BCVs was scored per cell, in control cells (DMSO) at 2 and 24 hpi (**A**). For nocodazole and paclitaxel treated cells, LAMP1-positive BCVs were determined at 24 hpi (**B**). Data are mean ± SE of BCVs showing LAMP-1 labeling per cell. Significant differences in relation to the DMSO control are designated by *** $p < 0.001$ (one-way ANOVA). Representative confocal micrographs of BMDMs infected with *Brucella* and treated with DMSO, 0.5 μM nocodazole, or 0.5 μM paclitaxel for 24 h are shown in (**C**). GFP-expressing *Brucella* are shown in green and macrophages were labeled with DAPI in blue and anti-LAMP1 in red on the merge panels. LAMP-1-positive BCVs are exemplified by arrows in inserts of the middle and left panels. BCVs showing weak or no association with LAMP-1 are shown on the right panels (arrow head). Inserts correspond to zoomed images (2.5 times amplification) of boxed areas. Scale bar corresponds to 5 μm.

not significantly different in treated versus untreated *B. abortus* infected macrophages. Also, no difference on secretion of IL-1β was observed in untreated or drug-treated macrophages infected with *B. abortus* (**Figure 5A1**). In contrast, treatment with the lower concentration of rTcPB (1 μg/ml) in infected macrophages promoted a significant increase in IL-1β secretion (**Figure 5A2**). Interestingly, IL-12 production induced by *B. abortus* infection was significantly affected by nocodazole treatment in a dose-dependent manner and a decrease of almost 60% in cytokine secretion was observed in BMDMs treated with 5 μM nocodazole (**Figure 5B1**). In contrast, rTcPB significantly enhanced IL-12 secretion in treated macrophages infected with *B. abortus*, in a dose-dependent fashion (**Figure 5B2**). Additionally, treatment of infected macrophages with either 0.5 or 5 μM paclitaxel had no effect on IL-12 secretion. These results indicate that decrease in IL-12 secretion observed in nocodazole-treated infected macrophages was related to MT destabilization, and the inverse effect promoted by TcPB coincides with the described

feature of this protein as a MT stabilizing agent. In summary, our findings suggest a relevant role for MT dynamics in innate immune responses triggered by *B. abortus* infection.

DISCUSSION

Due to the regulatory roles played by MTs on virtually all cellular processes, it is no surprise that intracellular pathogens, such as *Brucella*, have evolved to take advantage of this cytoskeleton in some of their survival and replication strategies (Radhakrishnan and Splitter, 2012). The intricate network of MT filaments is the main pathway on which vesicles, organelles and different cargos are moved, via molecular motor-mediated transport, inside interphase cells. To survive and replicate inside phagocytic cells, *Brucella* needs to orchestrate structural changes in the vacuoles. One major modification observed during maturation from early to late replicative-BCVs (eBCV to rBCV) is the

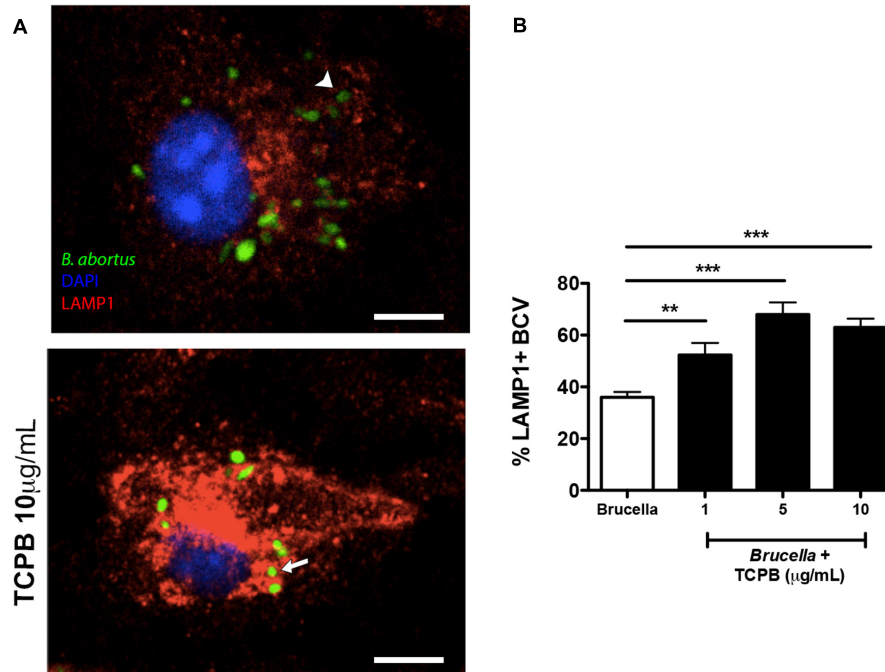


FIGURE 4 | TcpB treatment enhances Lamp-1⁺ marker in late BCVs in infected BMDMs. BMDMs were pre-treated with rTcpB protein (1, 5, or 10 µg/mL) for 2 h and infected with *B. abortus* for 24 h. Representative confocal micrographs of BMDMs infected with *Brucella* and treated with rTcpB 10 µg/mL are shown in (A). GFP-expressing *Brucella* are shown in green and macrophages were labeled with DAPI in blue and anti-LAMP1 in red. LAMP-1-positive BCVs are exemplified by arrows and BCVs showing weak or no association with LAMP-1 are exemplified by arrowheads. Scale bar corresponds to 5 µm. (B) The percentage of LAMP1-positive BCVs was scored per cell 24 hpi. Data are means ± SE of BCVs showing LAMP-1 labeling per cell. Significant differences in relation to the control are designated by ** $p \leq 0.01$ and *** $p \leq 0.001$ (one-way ANOVA).

elimination, over time, of the LAMP-1 marker acquired soon after *Brucella* invades macrophages (Starr et al., 2008; von Bargen et al., 2012; de Souza Filho et al., 2015). However, removal of LAMP-1 from intermediate BCVs is not a requirement for their maturation into rBCVs, since replication of *B. abortus* has been observed in LAMP-1 positive vesicles in THP1 cells and murine macrophages (Bellaire et al., 2005; Starr et al., 2012). Therefore, intermediate steps of BCV trafficking and maturation are still far from being understood. Our results indicate that manipulation of MT dynamics toward the increase of either MT depolymerization or polymerization events at their ends, interfere with BCV maturation and replication of *B. abortus*. However, further analysis with additional markers of different endosomal, Golgi- and ER-derived compartments are necessary to fully characterize the rBCV in nocodazole and paclitaxel treated macrophages. Recently, nocodazole treatment has been shown to interfere with the first steps of *B. abortus* infection in RAW 264.7 cells as pre-treatment of RAW cells with 0.4 µg/ml nocodazole increased adhesion of *Brucella* to the host cell. However, despite the increase in cell attachment, invasion and intracellular growth of bacteria was reduced when compared to control cells (Reyes et al., 2017). Additionally, no alterations were found in the percentage of *Brucella* co-localization with LAMP-1⁺ compartments between control and treated cells. The contrasting results between the Reyes et al. (2017) study and ours may reside in the fact they used a different strain of *B. abortus*

(*B. abortus* 544), as well as performing their experiments using the RAW 264.7 cell line and not BMDMs.

From invasion to dissemination, all stages of the intracellular bacterial life cycle share the same three-dimensional cytosolic space containing the host cytoskeleton. For successful infection and replication, many pathogens hijack the cytoskeleton using effector proteins introduced into the host cytosol by specialized secretion systems (Colonne et al., 2016). Cytoskeletal rearrangement promotes numerous events that are beneficial to the pathogen, including internalization of bacteria, structural support for bacteria-containing vacuoles, altered vesicular trafficking, actin-dependent bacterial movement, and pathogen dissemination. The stealth pathogen *Brucella* is renowned for its silent entry into the host and avoidance of phagolysosomal degradation, and the translocated protein TcpB has been shown to contribute to this strategy by targeting the TLR-dependent arm of the host innate immune defense (Alaidarous et al., 2014). However, the situation seems more complex, as TcpB is also involved in MT dynamics and, recently, in the induction of the unfolded protein response (Radhakrishnan et al., 2011; Smith et al., 2013). In this study, treatment with TcpB causes an increase in intracellular bacterial growth in macrophages that corroborates previous *in vivo* mouse studies that implied TcpB-deficient *Brucella* as defective in systemic spread at early stages of infection (Radhakrishnan et al., 2009). Likewise, *Brucella melitensis* can induce an Unfolded Protein Response via TcpB that

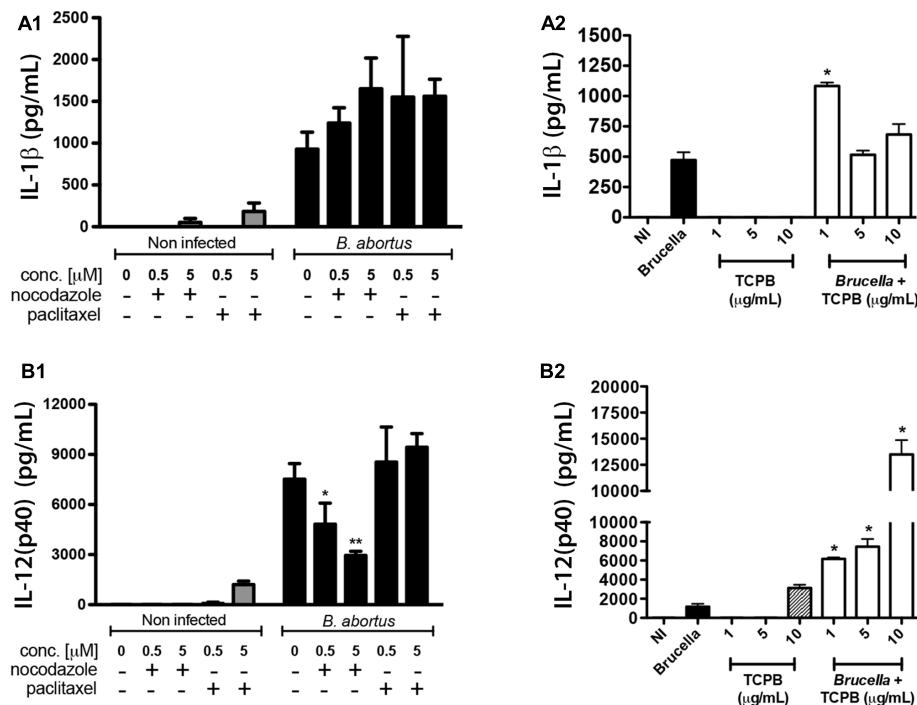


FIGURE 5 | *Brucella*-induced pro-inflammatory cytokines are compromised by alterations on MTs dynamics. Expression of IL-12 (A1,A2) and IL-1β (B1,B2) was evaluated in control (uninfected) and *B. abortus*-infected BMDMs treated with nocodazole (0.5 or 5 μM), paclitaxel (0.5 or 5 μM), rTcPB (1, 5, or 10 μg/mL), or vehicle (DMSO). Supernatants were harvested after 24 h of stimulation and cytokine secretion was determined by ELISA. Significant differences in relation to the infected untreated controls are denoted (* $p \leq 0.05$; ** $p \leq 0.01$, one-way ANOVA).

supports intracellular growth in macrophages (Smith et al., 2013). Increase in LAMP-1⁺ BCVs treated with rTcPB, suggests that the MT bundling generated by TcPB interferes with the vesicular transport along the MT network to the benefit of pathogen survival.

Pro-inflammatory cytokine production by innate immune cells is critical in the process of host control of intracellular pathogens. Herein, we demonstrated that treatment with nocodazole lead to reduced IL-12 production, however, no alteration was observed in IL-1β, IL-6 and TNF-α. Recently, Reyes et al. (2017) reported that *Brucella*-infected nocodazole-treated mice presented higher levels of TNF, IFN-γ, MCP-1, IL-10 and IL-6 as compared to control untreated animals. Interestingly, although not mentioned in their study, their data would suggest that *Brucella*-induced IL-12 expression was robustly reduced by nocodazole treatment as several of these cytokines are dependent on IL-12, a result which corroborates with our findings. Moreover, depolymerization of the MT network disrupted intracellular TLR2 and TLR4 and inhibited IL-12 production in response to *Neisseria meningitidis* infection (Uronen-Hansson et al., 2004). These results suggest that the TLR activation by *N. meningitidis* required for IL-12 production occurs inside DCs and not on the cell surface. We have extensively reported that TLR9 senses *Brucella* CpG to induce IL-12 production (Macedo et al., 2008; Gomes et al., 2016). Therefore, intracellularly expressed TLR9 is likely affected by interference with MT dynamics compromising IL-12 secretion.

TcPB also interferes with innate immune responses following *B. abortus* infection. Subcellular colocalization studies indicate that TcPB colocalizes with the plasma membrane and MTs (Radhakrishnan et al., 2009). Further, the same authors also reported that TcPB affects the dynamics of MT formation stabilizing polymerized tubules (Radhakrishnan et al., 2011). In contrast to nocodazole treatment, rTcPB enhanced IL-12 production in a dose-dependent manner. Additionally, rTcPB-treated macrophages (1 μg/ml) augmented IL-1β secretion after *Brucella* infection. Taking into account that TcPB targets the TIRAP-mediated pathway, leading to subversion of TLR2 and TLR4 signaling and inhibition of NF-κB (Salcedo et al., 2008; Radhakrishnan et al., 2009), IL-12 would be expected to decrease in the presence of rTcPB. However, we and others have demonstrated that TLR9 and not TLR2 and TLR4 is the main receptor involved in IL-12 production by *Brucella* (Giambartolomei et al., 2004; Macedo et al., 2008; Gomes et al., 2016). Furthermore, Salcedo et al. (2013) have reported that TcPB does not inhibit TLR9. Therefore, further studies are necessary to unravel which innate immune pathways are related specifically with TcPB modulation of MTs that affects cytokine production. Detailed investigation on MT-pathogen interactions will provide broad understanding of pathogenicity and host adaptation of several infectious pathogens.

In summary, this study reveals that modulation of MTs affects several crucial steps of *B. abortus* pathogenesis, including BCV maturation, intracellular survival, and IL-12 secretion in

infected macrophages. MTs are potential targets of pathogenic microorganisms to create a replication-permissive niche. Therefore, our results reflect an important relationship between an intracellular bacterial pathogen and MTs that contributes to our understanding of *B. abortus* pathogenicity.

AUTHOR CONTRIBUTIONS

JA-S, JM, GS, and SO designed the project and experiments. JA-S, IT, EG, and BF carried out most of the experiments. JA-S and SO wrote the manuscript. JA-S and EG carried out statistical analysis and prepared figures. SO submitted this paper. All authors reviewed the manuscript.

FUNDING

This work was supported by Conselho Nacional de Desenvolvimento Científico e Tecnológico (CNPQ, Nos:

402527/2013-5, 443662/2014-2, and 302660/2015-1), Coordenação de Aperfeiçoamento de Pessoal de Nível Superior (CAPES, No: 030448/2013-01), Fundação de Amparo à Pesquisa do estado de Minas Gerais (FAPEMIG, Nos: APQ-00837-15, APQ-00704-14 and Rede Mineira de Imunobiológicos No: 00140-16), CAPES/PVE, CAPES/PNPD, CNPq/CT-Biotec, CNPq/CBAB and National Institute of Health R01 AI116453.

ACKNOWLEDGMENT

The authors would like to thank Dr. Gustavo B. Menezes for the use of his Nikon confocal microscope.

SUPPLEMENTARY MATERIAL

The Supplementary Material for this article can be found online at: <https://www.frontiersin.org/articles/10.3389/fmicb.2017.02217/full#supplementary-material>

REFERENCES

- Akira, S., Uematsu, S., and Takeuchi, O. (2006). Pathogen recognition and innate immunity. *Cell* 124, 783–801. doi: 10.1016/j.cell.2006.02.015
- Alaidarous, M., Ve, T., Casey, L. W., Valkov, E., Ericsson, D. J., Ullah, M. O., et al. (2014). Mechanism of bacterial interference with TLR4 signaling by *Brucella* Toll/interleukin-1 receptor domain-containing protein TcpB. *J. Biol. Chem.* 289, 654–668. doi: 10.1074/jbc.M113.523274
- Barquero-Calvo, E., Chaves-Olarte, E., Weiss, D. S., Guzman-Verri, C., Chacon-Diaz, C., Rucavado, A., et al. (2007). *Brucella abortus* uses a stealthy strategy to avoid activation of the innate immune system during the onset of infection. *PLOS ONE* 2:e631. doi: 10.1371/journal.pone.0000631
- Bellaire, B. H., Roop, R. M., and Cardelli, J. A. (2005). Opsonized virulent *Brucella abortus* replicates within nonacidic, endoplasmic reticulum-negative, LAMP-1-positive phagosomes in human monocytes. *Infect. Immun.* 73, 3702–3713. doi: 10.1128/IAI.73.6.3702-3713.2005
- Boschiroli, M. L., Foulongne, V., and O'Callaghan, D. (2001). Brucellosis: a worldwide zoonosis. *Curr. Opin. Microbiol.* 4, 58–64. doi: 10.1016/S1369-5274(00)00165-X
- Campos, P. C., Gomes, M. T., Guimaraes, E. S., Guimaraes, G., and Oliveira, S. C. (2017). TLR7 and TLR3 sense *Brucella abortus* RNA to induce proinflammatory cytokine production but they are dispensable for host control of infection. *Front. Immunol.* 8:28. doi: 10.3389/fimmu.2017.00028
- Celli, J., Salcedo, S. P., and Gorvel, J. P. (2005). *Brucella* coopts the small GTPase Sar1 for intracellular replication. *Proc. Natl. Acad. Sci. U.S.A.* 102, 1673–1678. doi: 10.1073/pnas.0406873102
- Colonne, P. M., Winchell, C. G., and Voth, D. E. (2016). Hijacking host cell highways: manipulation of the host actin cytoskeleton by obligate intracellular bacterial pathogens. *Front. Cell Infect. Microbiol.* 6:107. doi: 10.3389/fcimb.2016.00107
- Comerci, D. J., Martinez-Lorenzo, M. J., Sieira, R., Gorvel, J. P., and Ugalde, R. A. (2001). Essential role of the VirB machinery in the maturation of the *Brucella abortus*-containing vacuole. *Cell Microbiol.* 3, 159–168. doi: 10.1046/j.1462-5822.2001.00102.x
- de Souza Filho, J. A., de Paulo Martins, V., Campos, P. C., Alves-Silva, J., Santos, N. V., de Oliveira, F. S., et al. (2015). Mutant *Brucella abortus* membrane fusogenic protein induces protection against challenge infection in mice. *Infect. Immun.* 83, 1458–1464. doi: 10.1128/IAI.02790-14
- Delrue, R. M., Martinez-Lorenzo, M., Lestrade, P., Danese, I., Bielarz, V., Mertens, P., et al. (2001). Identification of *Brucella* spp. genes involved in intracellular trafficking. *Cell Microbiol.* 3, 487–497. doi: 10.1046/j.1462-5822.2001.00131.x
- Giambartolomei, G. H., Zwerdling, A., Cassataro, J., Bruno, L., Fossati, C. A., and Philipp, M. T. (2004). Lipoproteins, not lipopolysaccharide, are the key mediators of the proinflammatory response elicited by heat-killed *Brucella abortus*. *J. Immunol.* 173, 4635–4642. doi: 10.4049/jimmunol.173.7.4635
- Gomes, M. T., Campos, P. C., Pereira, G. D. S., Bartholomeu, D. C., Splitter, G., and Oliveira, S. C. (2016). TLR9 is required for MAPK/NF- κ B activation but does not cooperate with TLR2 or TLR6 to induce host resistance to *Brucella abortus*. *J. Leukoc. Biol.* 99, 771–780. doi: 10.1189/jlb.4A0815-346R
- Goncalves de Assis, N. R., Batistoni de Moraes, S., Figueiredo, B. C., Ricci, N. D., de Almeida, L. A., da Silva Pinheiro, C., et al. (2015). DNA vaccine encoding the chimeric form of *Schistosoma mansoni* Sm-TSP2 and Sm29 confers partial protection against challenge infection. *PLOS ONE* 10:e0125075. doi: 10.1371/journal.pone.0125075
- Gundersen, G. G., and Cook, T. A. (1999). Microtubules and signal transduction. *Curr. Opin. Cell Biol.* 11, 81–94. doi: 10.1016/S0955-0674(99)80010-6
- Macedo, G. C., Magnani, D. M., Carvalho, N. B., Bruna-Romero, O., Gazzinelli, R. T., and Oliveira, S. C. (2008). Central role of MyD88-dependent dendritic cell maturation and proinflammatory cytokine production to control *Brucella abortus* infection. *J. Immunol.* 180, 1080–1087. doi: 10.4049/jimmunol.180.2.1080
- Medzhitov, R., and Janeway, C. Jr. (2000). Innate immunity. *N. Engl. J. Med.* 343, 338–344. doi: 10.1056/NEJM200008033430506
- Milillo, M. A., Velasquez, L. N., Trotta, A., Delpino, M. V., Marinho, F. V., Balboa, L., et al. (2017). *B. abortus* RNA is the component involved in the down-modulation of MHC-I expression on human monocytes via TLR8 and the EGFR pathway. *PLOS Pathog.* 13:e1006527. doi: 10.1371/journal.ppat.1006527
- Pappas, G., Papadimitriou, P., Akritidis, N., Christou, L., and Tsianos, E. V. (2006). The new global map of human brucellosis. *Lancet Infect. Dis.* 6, 91–99. doi: 10.1016/S1473-3099(06)70382-6
- Pizarro-Cerda, J., Meresse, S., Parton, R. G., van der Goot, G., Sola-Landa, A., Lopez-Goni, I., et al. (1998). *Brucella abortus* transits through the autophagic pathway and replicates in the endoplasmic reticulum of nonprofessional phagocytes. *Infect. Immun.* 66, 5711–5724.
- Radhakrishnan, G. K., Harms, J. S., and Splitter, G. A. (2011). Modulation of microtubule dynamics by a TIR domain protein from the intracellular pathogen *Brucella melitensis*. *Biochem. J.* 439, 79–83. doi: 10.1042/BJ20110577

- Radhakrishnan, G. K., and Splitter, G. A. (2012). Modulation of host microtubule dynamics by pathogenic bacteria. *Biomol. Concepts* 3, 571–580. doi: 10.1515/bmc-2012-0030
- Radhakrishnan, G. K., Yu, Q., Harms, J. S., and Splitter, G. A. (2009). *Brucella* TIR domain-containing protein mimics properties of the toll-like receptor adaptor protein TIRAP. *J. Biol. Chem.* 284, 9892–9898. doi: 10.1074/jbc.M805458200
- Reyes, A. W. B., Hop, H. T., Arayan, L. T., Huy, T. X. N., Min, W., Lee, H. J., et al. (2017). Nocodazole treatment interrupted *Brucella abortus* invasion in RAW 264.7 cells, and successfully attenuated splenic proliferation with enhanced inflammatory response in mice. *Microb. Pathog.* 103, 87–93. doi: 10.1016/j.micpath.2016.11.028
- Salcedo, S. P., Marchesini, M. I., Degos, C., Terwagne, M., Von Bargen, K., Lepidi, H., et al. (2013). BtpB, a novel *Brucella* TIR-containing effector protein with immune modulatory functions. *Front. Cell Infect. Microbiol.* 3:28. doi: 10.3389/fcimb.2013.00028
- Salcedo, S. P., Marchesini, M. I., Lelouard, H., Fugier, E., Jolly, G., Balor, S., et al. (2008). *Brucella* control of dendritic cell maturation is dependent on the TIR-containing protein Btp1. *PLOS Pathog.* 4:e21. doi: 10.1371/journal.ppat.0040021
- Smith, J. A., Khan, M., Magnani, D. D., Harms, J. S., Durward, M., Radhakrishnan, G. K., et al. (2013). *Brucella* induces an unfolded protein response via TcpB that supports intracellular replication in macrophages. *PLOS Pathog.* 9:e1003785. doi: 10.1371/journal.ppat.1003785
- Starr, T., Child, R., Wehrly, T. D., Hansen, B., Hwang, S., López-Otin, C., et al. (2012). Selective subversion of autophagy complexes facilitates completion of the *Brucella* intracellular cycle. *Cell Host Microbe* 11, 33–45. doi: 10.1016/j.chom.2011.12.002
- Starr, T., Ng, T. W., Wehrly, T. D., Knodler, L. A., and Celli, J. (2008). *Brucella* intracellular replication requires trafficking through the late endosomal/lysosomal compartment. *Traffic* 9, 678–694. doi: 10.1111/j.1600-0854.2008.00718.x
- Uronen-Hansson, H., Allen, J., Osman, M., Squires, G., Klein, N., and Callard, R. E. (2004). Toll-like receptor 2 (TLR2) and TLR4 are present inside human dendritic cells, associated with microtubules and the Golgi apparatus but are not detectable on the cell surface: integrity of microtubules is required for interleukin-12 production in response to internalized bacteria. *Immunology* 111, 173–178. doi: 10.1111/j.0019-2805.2003.01803.x
- von Bargen, K., Gorvel, J. P., and Salcedo, S. P. (2012). Internal affairs: investigating the *Brucella* intracellular lifestyle. *FEMS Microbiol. Rev.* 36, 533–562. doi: 10.1111/j.1574-6976.2012.00334.x
- Yang, X., Skyberg, J. A., Cao, L., Clapp, B., Thornburg, T., and Pascual, D. W. (2013). Progress in *Brucella* vaccine development. *Front. Biol.* 8:60–77. doi: 10.1007/s11515-012-1196-0
- Yoshida, S., and Sasakawa, C. (2003). Exploiting host microtubule dynamics: a new aspect of bacterial invasion. *Trends Microbiol.* 11, 139–143. doi: 10.1016/S0966-842X(03)00023-4

Conflict of Interest Statement: The authors declare that the research was conducted in the absence of any commercial or financial relationships that could be construed as a potential conflict of interest.

Copyright © 2017 Alves-Silva, Tavares, Guimarães, Costa Franco, Figueiredo, Marques, Splitter and Oliveira. This is an open-access article distributed under the terms of the Creative Commons Attribution License (CC BY). The use, distribution or reproduction in other forums is permitted, provided the original author(s) or licensor are credited and that the original publication in this journal is cited, in accordance with accepted academic practice. No use, distribution or reproduction is permitted which does not comply with these terms.



Identification of *lptA*, *lpxE*, and *lpxO*, Three Genes Involved in the Remodeling of *Brucella* Cell Envelope

Raquel Conde-Álvarez¹, Leyre Palacios-Chaves², Yolanda Gil-Ramírez¹, Miriam Salvador-Bescós¹, Marina Bárcena-Varela¹, Beatriz Aragón-Aranda¹, Estrella Martínez-Gómez¹, Amaia Zúñiga-Ripa¹, María J. de Miguel³, Toby Leigh Bartholomew⁴, Sean Hanniffy⁵, María-Jesús Grilló², Miguel Ángel Vences-Guzmán⁶, José A. Bengoechea⁴, Vilma Arce-Gorvel⁵, Jean-Pierre Gorvel⁵, Ignacio Moriyón^{1*} and Maite Iriarte^{1*}

OPEN ACCESS

Edited by:

Axel Cloeckaert,
Institut National de la Recherche
Agronomique (INRA), France

Reviewed by:

Diego J. Comerci,
Instituto de Investigaciones
Biotecnológicas (IIB-INTECH),
Argentina
Roy Martin Roop II,
East Carolina University, United States

*Correspondence:

Ignacio Moriyón
imoriyon@unav.es
Maite Iriarte
miriart@unav.es

Specialty section:

This article was submitted to
Infectious Diseases,
a section of the journal
Frontiers in Microbiology

Received: 26 October 2017

Accepted: 20 December 2017

Published: 10 January 2018

Citation:

Conde-Álvarez R, Palacios-Chaves L, Gil-Ramírez Y, Salvador-Bescós M, Bárcena-Varela M, Aragón-Aranda B, Martínez-Gómez E, Zúñiga-Ripa A, de Miguel MJ, Bartholomew TL, Hanniffy S, Grilló M-J, Vences-Guzmán MA, Bengoechea JA, Arce-Gorvel V, Gorvel J-P, Moriyón I and Iriarte M (2018) Identification of *lptA*, *lpxE*, and *lpxO*, Three Genes Involved in the Remodeling of *Brucella* Cell Envelope. *Front. Microbiol.* 8:2657. doi: 10.3389/fmicb.2017.02657

¹ Universidad de Navarra, Facultad de Medicina, Departamento de Microbiología y Parasitología, Instituto de Salud Tropical (ISTUN) e Instituto de Investigación Sanitaria de Navarra (IdISNA), Pamplona, Spain, ² Instituto de Agrobiotecnología, Consejo Superior de Investigaciones Científicas – Universidad Pública de Navarra – Gobierno de Navarra, Pamplona, Spain, ³ Unidad de Producción y Sanidad Animal, Instituto Agroalimentario de Aragón, Centro de Investigación y Tecnología Agroalimentaria de Aragón – Universidad de Zaragoza, Zaragoza, Spain, ⁴ Wellcome-Wolfson Institute for Experimental Medicine, Queen's University Belfast, Belfast, United Kingdom, ⁵ Institut National de la Santé et de la Recherche Médicale, U1104, Centre National de la Recherche Scientifique UMR7280, Centre d'Immunologie de Marseille-Luminy, Aix-Marseille University UM2, Marseille, France, ⁶ Centro de Ciencias Genómicas, Universidad Nacional Autónoma de México, Cuernavaca, Mexico

The brucellae are facultative intracellular bacteria that cause a worldwide extended zoonosis. One of the pathogenicity mechanisms of these bacteria is their ability to avoid rapid recognition by innate immunity because of a reduction of the pathogen-associated molecular pattern (PAMP) of the lipopolysaccharide (LPS), free-lipids, and other envelope molecules. We investigated the *Brucella* homologs of *lptA*, *lpxE*, and *lpxO*, three genes that in some pathogens encode enzymes that mask the LPS PAMP by upsetting the core-lipid A charge/hydrophobic balance. *Brucella lptA*, which encodes a putative ethanolamine transferase, carries a frame-shift in *B. abortus* but not in other *Brucella* spp. and phylogenetic neighbors like the opportunistic pathogen *Ochrobactrum anthropi*. Consistent with the genomic evidence, a *B. melitensis lptA* mutant lacked lipid A-linked ethanolamine and displayed increased sensitivity to polymyxin B (a surrogate of innate immunity bactericidal peptides), while *B. abortus* carrying *B. melitensis lptA* displayed increased resistance. *Brucella lpxE* encodes a putative phosphatase acting on lipid A or on a free-lipid that is highly conserved in all brucellae and *O. anthropi*. Although we found no evidence of lipid A dephosphorylation, a *B. abortus lpxE* mutant showed increased polymyxin B sensitivity, suggesting the existence of a hitherto unidentified free-lipid involved in bactericidal peptide resistance. Gene *lpxO* putatively encoding an acyl hydroxylase carries a frame-shift in all brucellae except *B. microti* and is intact in *O. anthropi*. Free-lipid analysis revealed that *lpxO* corresponded to *olsC*, the gene coding for the ornithine lipid (OL) acyl hydroxylase active in *O. anthropi* and *B. microti*, while *B. abortus* carrying the *olsC* of *O. anthropi* and *B. microti* synthesized hydroxylated OLs. Interestingly, mutants in *lptA*, *lpxE*, or *olsC*

were not attenuated in dendritic cells or mice. This lack of an obvious effect on virulence together with the presence of the intact homolog genes in *O. anthropi* and *B. microti* but not in other brucellae suggests that LptA, LpxE, or OL β -hydroxylase do not significantly alter the PAMP properties of *Brucella* LPS and free-lipids and are therefore not positively selected during the adaptation to intracellular life.

Keywords: lipopolysaccharide, *Brucella*, lipids, cell envelope, PAMP

INTRODUCTION

Brucellosis is the collective name of a group of zoonotic diseases afflicting a wide range of domestic and wild mammals (Whatmore, 2009; Zheludkov and Tsirelson, 2010). In domestic livestock brucellosis is manifested mostly as abortions and infertility, and contact with infected animals and consumption of unpasteurized dairy products are the sources of human brucellosis, an incapacitating condition that requires prolonged antibiotic treatment (Zinsstag et al., 2011). Eradicated in a handful of countries, brucellosis is endemic or even increasing in many areas of the world (Jones et al., 2013; Ducrotoy et al., 2017; Lai et al., 2017).

This disease is caused by facultative intracellular parasites of the genus *Brucella*. Taxonomically placed in the α -2 *Proteobacteria* (Moreno et al., 1990), the brucellae are close to plant pathogens and endosymbionts such as *Agrobacterium*, *Sinorhizobium*, and *Rhizobium* and to soil bacteria such as *Ochrobactrum*, the latter including some opportunistic pathogens, and comparative analyses suggest that soil bacteria of this group are endowed with properties that represent a first scaffold on which an intracellular life style develops (Velasco et al., 2000; Moreno and Moriyón, 2007; Barquero-Calvo et al., 2009). The brucellae owe their pathogenicity mainly to their ability to multiply within dendritic cells, macrophages, and a variety of other cells. Due to their ability to control intracellular trafficking and be barely detected by innate immunity, these bacteria are able to reach a safe intracellular niche before an effective immune response is mounted, and to multiply extensively (Gorvel and Moreno, 2002; Barquero-Calvo et al., 2007). A mechanism used by *Brucella* to scape from the host immune response is the interference with the toll-like receptor (TLR) signaling pathway by the injection of active effectors such as BtpA and BtpB through the Type IV secretion system T4SS. Both effector proteins contain a TIR domain that interferes with TLR signaling by directly interacting with MyD88 (Cirl et al., 2008; Salcedo et al., 2008, 2013; Chaudhary et al., 2012) and contribute to the control of dendritic cell (DC) activation during infection. Moreover, *Brucella* has modified outer membrane (OM) components in order to reduce the pathogen-associated molecular patterns (PAMP) of the cell envelope. In Gram-negative bacteria, these PAMP are created by the conserved composition of the OM lipopolysaccharide (LPS) and the free lipids on which the topology of the OM also depends. However, in addition to free-lipid species present in most Gram-negative bacteria (i.e., cardiolipin, phosphatidylglycerol, and phosphatidylethanolamine), *Brucella* also possesses phosphatidylcholine and amino lipids. Phosphatidylcholine

is a eukaryotic-type phospholipid required for *Brucella* full virulence (Comerci et al., 2006; Conde-Álvarez et al., 2006). Among the amino lipids, only the ornithine lipids (OL) have been investigated which unlike their counterparts in *Bordetella*, do not trigger the release of IL-6 or TNF- α by macrophages, possibly on account of their longer acyl chains that reduce the OL PAMP (Palacios-Chaves et al., 2011). Concerning the LPS, most bacteria carry C1 and C4' glucosamine disaccharides with C12 and C14 acyl and acyl-oxyacyl chains. This highly amphipathic structure, named lipid A, is adjacent to additional negatively charged groups of the core oligosaccharide, namely the heptose phosphates and 2-keto-3-deoxyoctulosonate carboxyl groups (Kastowsky et al., 1992; Moriyón, 2003). This lipid A-core PAMP is so efficiently detected by the innate immunity system that some pathogens partially conceal it by removing phosphate groups or substituting them with arabinosamine and/or ethanolamine, or by hydroxylating the acyl chains (Takahashi et al., 2008; Lewis et al., 2013; Moreira et al., 2013; Needham and Trent, 2013; Llobet et al., 2015; Trombley et al., 2015). In contrast, *Brucella* lipid A is a diaminoglucose disaccharide amide-linked to long (C16, C18) and very long (C28–C30) acyl chains (Velasco et al., 2000; Iriarte et al., 2004; Fontana et al., 2016). Furthermore, negative charges in lipid A phosphates and 2-keto-3-deoxyoctulosonate are counterbalanced by four glucosamine units present in the core (Kubler-Kielb and Vinogradov, 2013; Fontana et al., 2016). As illustrated by the unusually reduced endotoxicity of the *Brucella* LPS this structure is defectively detected by the innate immune response (Lapaque et al., 2005; Martirosyan et al., 2011; Conde-Álvarez et al., 2012). It remains unknown, however, whether *Brucella* LPS undergoes post-synthetic modifications that have been described for other bacteria that could alter its PAMP potential and contribution to virulence. In this work, we investigated in *Brucella* the role of gene homologs to phosphatases, phospho-ethanolamine (pEtN) transferases, and acyl hydroxylases (**Figure 1**) that have been shown in other Gram-negative pathogens to act on LPS and to contribute to overcoming innate immunity defenses.

MATERIALS AND METHODS

Bacterial Strains and Growth Conditions

The bacterial strains and plasmids used in this study are listed in Supplementary Table S1. Bacteria were routinely grown in standard tryptic soy broth or agar either plain or supplemented with kanamycin at 50 μ g/ml, or/and nalidixic at 5 or 25 μ g/ml or/and 5% sucrose. All strains were stored in skim milk at -80°C .

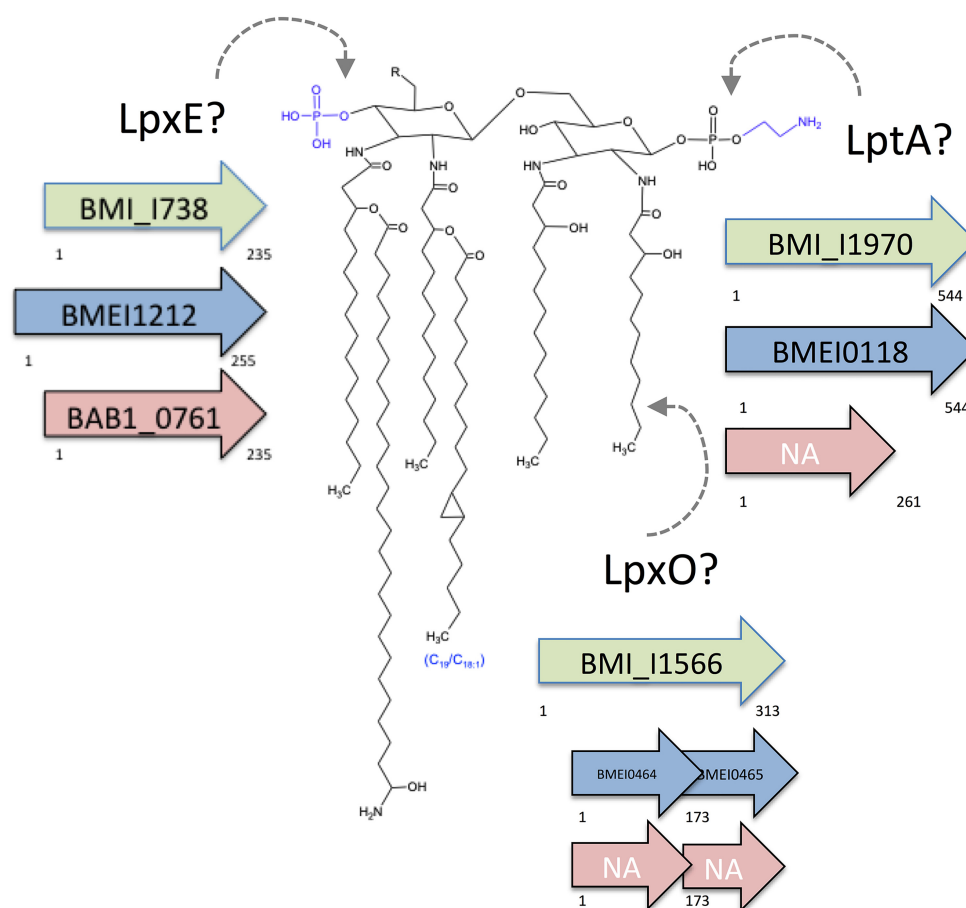


FIGURE 1 | *Brucella* lipid A and hypothetical sites of action of putative LpxE, LptA, and LpxO. The structure proposed is based on acyl-chain and mass spectrophotometry analyses and genomic predictions. The predicted sites of action of LpxE (phosphatase), LptA (pEtN transferase), and LpxO (acyl chain hydroxylase) are indicated, and the corresponding ORF of *B. microti* (green), *B. melitensis* (blue), and *B. abortus* (red) presented (NA, not annotated). The *B. abortus* *lptA* homolog and the *B. melitensis* and *B. abortus* *lpxO* homologs carry a frame-shift mutation.

DNA Manipulations

Genomic sequences were obtained from the Kyoto Encyclopedia of Genes and Genomes (KEGG) database¹. Searches for DNA and protein homologies were carried out using the National Center for Biotechnology Information (NCBI)² and the European Molecular Biology Laboratory (EMBL) – European Bioinformatics Institute server³. Primers were synthesized by Sigma-Genosys (Haverhill, United Kingdom). DNA sequencing was performed by the “Servicio de Secuenciación del Centro de Investigación Médica Aplicada” (Pamplona, Spain). Restriction–modification enzymes were used under the conditions recommended by the manufacturer. Plasmid and chromosomal DNA were extracted with Qiaprep Spin Miniprep (Qiagen) and Ultraclean Microbial DNA Isolation Kits (Mo Bio Laboratories), respectively. When needed, DNA was purified from agarose gels using the Qiack Gel Extraction Kit (Qiagen).

¹<http://www.genome.jp/kegg/>

²<http://www.ncbi.nlm.nih.gov/>

³<http://www.ebi.ac.uk/>

Mutagenesis

To obtain *BmeΔlptA*, *BaΔlpxE*, and *BmiΔolsC* in-frame deletion mutants, directed mutagenesis by overlapping PCR were performed using genomic DNA as template and pJQK (Scupham and Triplett, 1997) as the suicide vector. The corresponding gene was deleted using allelic exchange by double recombination as previously described (Conde-Álvarez et al., 2006).

For the construction of the *BmeΔlptA* mutant, we first generated two PCR fragments: oligonucleotides *lptA*-F1 (5'-GAA CGCGAGACTATGGAAAC-3') and *lptA*-R2 (5'-TGGT GAACGCCAGAAGATAGA-3') were used to amplify a 400-bp fragment including codons 1–26 of *BmelptA* ORF, as well as 324 bp upstream of the *BmelptA* start codon, and oligonucleotides *lptA*-F3 (5'-TCTATCTTCTGGCGTTCACC GCACGACAATCTCTTC-3') and *lptA*-R4 (5'-AATATTCCAT GGCGCATTTTC-3') were used to amplify a 472-bp fragment including codons 506–544 of the *lptA* ORF and 353-bp downstream of the *lptA* stop codon. Both fragments were ligated by overlapping PCR using oligonucleotides *lptA*-F1 and *lptA*-R4 for amplification, and the complementary regions between

lptA-R2 and *lptA*-F3 for overlapping. The resulting fragment, containing the *lptA* deleted allele, was cloned into pCR2.1 (Invitrogen, Barcelona, Spain), sequenced to ensure maintenance of the reading frame, and subcloned into the *Bam*HI and the *Xba*I sites of the suicide plasmid pJQK. The resulting mutator plasmid (pRCI-32) was introduced in *B. melitensis* 16M by conjugation using the *Escherichia coli* S.17 strain (Simon et al., 1983).

For the construction of the *Ba*Δ*lpxE* mutant, we first generated two PCR fragments: oligonucleotides *lpxE*-F1 (5'-CGCGTGTGCCATAGGTATATT-3') and *lpxE*-R2 (5'-TATAGG CAGGGCGCAGAA-3') were used to amplify a 482-bp fragment including codons 1–29 of *lpxE* ORF, as well as 394 bp upstream of the *lpxE*-1 start codon, and oligonucleotides *lpxE*-F3 (5'-TTCTG CGCCCTGCCTATAGATTTCGTTCCGCATGGT-3') and *lpxE*-R4 (5'-CCAATACAC CCGTCATGAGA-3') were used to amplify a 577-bp fragment including codons 226–255 of the *lpxE* ORF and 488-bp downstream of the *lpxE* stop codon. Both fragments were ligated by overlapping PCR using oligonucleotides *lpxE*-F1 and *lpxE*-R4 for amplification, and the complementary regions between *lpxE*-R2 and *lpxE*-F3 for overlapping. The resulting fragment, containing the *lpxE* deleted allele, was cloned into pCR2.1 (Invitrogen, Barcelona, Spain), sequenced to ensure maintenance of the reading frame, and subcloned into the *Bam*HI and the *Xba*I sites of the suicide plasmid pJQK (Scupham and Triplett, 1997). The resulting mutator plasmid (pRCI-36) was introduced in *B. abortus* 2308 by conjugation using the *E. coli* S.17 strain (Simon et al., 1983).

For the construction of the *Bmi*Δ*olsC* mutant, we first generated two PCR fragments: oligonucleotides *olsC*-F1 (5'-TGCTGGATCGTATTCGTCTG-3') and *olsC*-R2 (5'-GCCATAA GCCGATGGAATA-3') were used to amplify a 334-bp fragment including codons 1–15 of *olsC* ORF, as well as 289 bp upstream of the *olsC* start codon, and oligonucleotides *olsC*-F3 (5'-TA GTTCCATCGGCTTATGGCAGGAGGGGCTAGACAACCAC-3') and *olsC*-R4 (5'-AACCAGCGACAGGGTAAGC-3') were used to amplify a 320-bp fragment including codons 286–313 of the *olsC* ORF and 237-bp downstream of the *olsC* stop codon. Both fragments were ligated by overlapping PCR using oligonucleotides *olsC*-F1 and *olsC*-R4 for amplification, and the complementary regions between *olsC*-R2 and *olsC*-F3 for overlapping. The resulting fragment, containing the *lptA* deleted allele, was cloned into pCR2.1 (Invitrogen, Barcelona, Spain), sequenced to ensure maintenance of the reading frame, and subcloned into the *Bam*HI and the *Xba*I sites of the suicide plasmid pJQK (Scupham and Triplett, 1997). The resulting mutator plasmid (pRCI-65) was introduced in *B. microti* CM445 by conjugation using the *E. coli* S.17 strain (Simon et al., 1983).

Deletion of each gene was checked with oligonucleotides *gene*-F1 and *gene*-R4 and internal primers hybridizing in the non-deleted regions.

Complementation of Deleted Genes

For pBME*lpxE* and pBME*lptA* construction we took advantage of the *Brucella* ORFeome constructed with the Gateway cloning Technology (Invitrogen) (Dricot et al., 2004). The clones carrying Bme*lpxE* or Bme*lptA* were extracted and the DNA containing

the corresponding ORF was subcloned in plasmid pRH001 (Hallez et al., 2007) to produce pBME*lpxE* and pBME*lptA*. For pBME*olsC*, *olsC* was amplified using genomic DNA of Bmi-parental as DNA template. The primers used were *olsC*-F6 (5'-GCTTTCCGAACAAGCACTGA-3') and *olsC*-R7 (5'-GCCTCCCTTCACCGTTATT-3'). The resulting PCR product, containing the ORF from 342 bp upstream to 84 bp downstream, was then cloned into pCR2.1 TOPO (Invitrogen) plasmid by "TA cloning" (Life Technologies). The resulting plasmid was sequenced to ensure that the gene was correctly cloned. Then, the gene was subcloned into the *Bam*HI and the *Xba*I sites of the replicative plasmid pBBR1 MCS (Kovach et al., 1994) pBME*lpxE*, pBME*lptA*, and pBME*olsC* were introduced into *Brucella* by conjugation using *E. coli* S.17-1 strain and the conjugants harboring corresponding plasmid were selected by plating onto TSA-Nal-Cm plates.

Sensitivity to Cationic Peptides

Exponentially growing bacteria were adjusted to an optical density equivalent to one of the McFarland scale and the minimal inhibitory concentrations (MICs) of polymyxin B were determined by the *e*-test method on Müller–Hinton agar (Izasa) or by the serial dilution method in a similar broth.

LPS Preparation

Lipopolysaccharide was obtained by methanol precipitation of the phenol phase of a phenol–water extract (Leong et al., 1970). This fraction [10 mg/ml in 175 mM NaCl, 0.05% NaN₃, 0.1 M Tris–HCl (pH 7.0)] was then purified by digestion with nucleases [50 µg/ml each of DNase-II type V and RNase-A (Sigma, St. Louis, MO, United States), 30 min at 37°C] and three times with proteinase K (50 µg/ml, 3 h at 55°C), and ultracentrifuged (6 h, 100,000 × *g*) (Aragón et al., 1996). Free lipids (OLs and phospholipids) were then removed by a fourfold extraction with chloroform–methanol [2:1 (vol/vol)] (Velasco et al., 2000).

Infections in Mice

Seven-week-old female BALB/c mice (Charles River, Elbeuf, France) were kept in cages with water and food ad libitum and accommodated under biosafety containment conditions 2 weeks before the start of the experiments. To prepare inocula, tryptic soy agar (TSA) grown bacteria were harvested and suspended in 10 mM phosphate buffered saline (pH 6.85), and 0.1 ml/mouse containing approximately 5×10^4 colony forming units (CFU) for *B. melitensis* or *B. abortus* and 1×10^4 CFU for *B. microti* was administered intraperitoneally. The exact doses assessed retrospectively by plating dilutions of the inocula. Number of CFU in spleens was determined at different time after inoculation. For this, the spleens were aseptically removed and individually weighed and homogenized in 9 volumes of PBS. Serial 10-fold dilutions of each homogenate were performed and each dilution was plated by triplicate. Plates were incubated at 37°C for 5 days. At several points during the infection process, the identity of the spleen isolates was confirmed by PCR. The individual data were normalized by logarithmic transformation, and the mean log CFU/spleen values and the standard deviations ($n = 5$) were calculated.

Intracellular Multiplication Assays

Bone marrow cells were isolated from femurs of 7–8-week-old C57Bl/6 female and differentiated into dendritic cells [bone-marrow derived dendritic cells (BMDCs)] as described by Inaba et al. (1992). Infections were performed by centrifuging the bacteria onto the differentiated cells (400 × *g* for 10 min at 4°C; bacteria:cells ratio of 30:1 followed by incubation at 37°C for 30 min under a 5% CO₂ atmosphere). BMDCs were gently washed with medium to remove extracellular bacteria before incubating in medium supplemented with 50 µg/ml gentamicin for 1 h to kill extracellular bacteria. Thereafter, the antibiotic concentration was decreased to 10 µg/ml. To monitor *Brucella* intracellular survival at different time-points post-infection, BMDC were lysed with 0.1% (vol/vol) Triton X-100 in H₂O and serial dilutions of lysates were plated onto TSA plates to enumerate the CFU.

Flow Cytometry

To assess activation and maturation, BMDC were analyzed for surface expression of classical maturation markers at 24 h post-treatment with the different *Brucella* strains and derived mutants. Cells were labeled with fluorochrome-conjugated antibodies specific for mouse CD11c:APC-Cy7 (clone N418), IA-IE:PE (MHC class II clone M5/114.15.2) (PE), CD86:FITC (Clone GL-1), CD40:APC (clone 3/23), and CD80:PE-Cy5 (clone 16-10A1), all from BioLegend. Labeled cells were then subjected to multi-color cytometry using a LSR II UV (Becton Dickinson) and the data analyzed using FlowJo Software by first gating on the CD11c⁺ population (100,000 events) prior to quantifying expression of receptors. Cells were stimulated with *E. coli* LPS (055:B5) as a positive control.

Lipid A Extraction

Five milligrams of LPS was hydrolyzed in 5 ml 1% acetic acid by sonication, heating to 100°C for 30 min, and cooling to room temperature. Concentrated HCl was added to the mixture until the pH was 1–2. The solution was converted to a two-phase acidic Bligh–Dyer mixture by adding 5.6 ml of chloroform and 5.6 ml of methanol. Phases were mixed by inverting the tubes and separated by centrifugation at 4000 × *g* for 20 min. The lower phases containing lipid A were collected, washed two times with water, and dried under a stream of nitrogen. Extraction was repeated, and the lower phases (11.2 ml) were combined and neutralized with a drop of pyridine. Samples were evaporated to dryness under a stream of nitrogen.

Mass Spectrometry

Mass spectrometry were acquired on a Bruker Autoflex®Speed TOF/TOF Mass Spectrometer (Bruker Daltonics Inc.) in negative reflective mode with delayed extraction. The ion-accelerating voltage was set at 20 kV. Each spectrum was an average of 300 shots. A peptide calibration standard (Bruker Daltonics Inc.) was used to calibrate the Matrix Assisted Laser Desorption/Ionization Time-of-Flight (MALDI-TOF), and lipid A extracted from *E. coli* strain MG1655 grown in LB medium at 37°C.

Extraction and Analysis of Envelope Lipids

The free-lipid fraction was extracted as described by Bligh and Dyer (1959), and analyzed on a silica gel 60 high-performance thin layer chromatography (HPLC) plates (Merck, Darmstadt, Germany). Chromatography was performed either monodimensionally with chloroform–methanol–water [14:6:1 (volume)] or bidimensionally with chloroform–methanol–water [14:6:1 (volume)] first and chloroform–methanol–acetic acid [13:5:2 (volume)] in the second dimension (Weissenmayer et al., 2002). Plates were developed with 0.2% ninhydrin in acetone at 180°C or 15% sulfuric acid in ethanol at 180°C.

RESULTS

The *Brucella* *lptA* Orthologs Encode a Lipid A Phosphate-Ethanolamine Transferase

A genomic search in the KEGG database revealed that all *Brucella* spp. carry an ORF (BMEI0118 in *B. melitensis*) homologous to *Neisseria meningitidis* *lptA*, a pEtN transferase that modifies lipid A (Cox et al., 2003). Strikingly, in *B. abortus* but not in other *Brucella* spp., all genomic sequences available at KEGG show a deletion of a thymine in position 774 that should result in a truncated protein lacking the amino acids related to the enzymatic activity (Naessan et al., 2008; **Figure 1** and Supplementary Figure S1 and Supplementary Table S2). In addition to *LptA*, two other pEtN transferases have been identified in *N. meningitidis*: *Lpt-3* and *Lpt-6*, which, respectively, modify the LPS core at the third and sixth position of heptose II (Mackinnon et al., 2002; Wright et al., 2004). By multiple sequence alignment, the *B. melitensis* putative pEtN transferase showed highest homology with *Neisseria* *LptA* and also displayed the *LptA* membrane-associated domains not present in *Lpt-3* and *Lpt-6* (ORFs NMB1638, NMB2010, and NMA0408, respectively). Accordingly, it can be predicted that ORF BMEI0118 (henceforth *BmeLptA*) encodes a pEtN transferase that acts on lipid A, a hypothesis fully consistent with the absence of heptose in the *Brucella* LPS core (Iriarte et al., 2004; Fontana et al., 2016).

To test this hypothesis, we constructed a *B. melitensis* non-polar mutant (*BmeΔlptA*) lacking the *LptA* enzymatic domain (amino acids 26–506), which as expected maintained a smooth (S) phenotype (negative crystal violet test and positive coagglutination with anti-S-LPS antibodies). As a consequence of the increased positive charge of the amino group, pEtN has been shown to decrease binding of the polycationic lipopeptide polymyxin B to LPS, and to increase resistance to this antibiotic in a variety of bacteria (Needham and Trent, 2013; Trombley et al., 2015; Herrera et al., 2017). In keeping with this possibility, the *BmeΔlptA* mutant was more sensitive to polymyxin B than the parental strain *B. melitensis* 16M (*Bme*-parental) (**Figure 2A**). In contrast, and consistent with the frame-shift in its *lptA* homolog, *B. abortus* 2308 (*Ba*-parental) displayed polymyxin B sensitivity similar to that of *BmeΔlptA*. Moreover, complementation of *BmeΔlptA* with the multi-copy plasmid

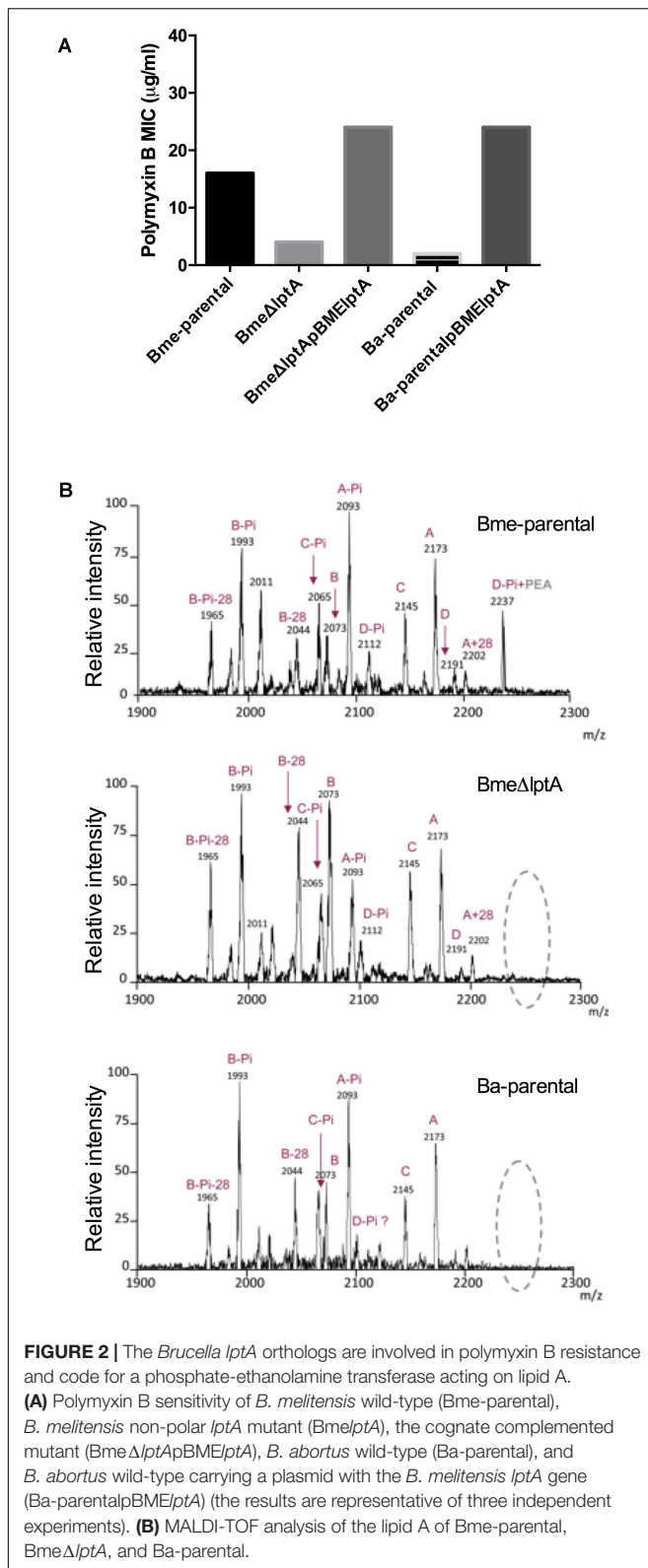


FIGURE 2 | The *Brucella* *lptA* orthologs are involved in polymyxin B resistance and code for a phosphate-ethanolamine transferase acting on lipid A. **(A)** Polymyxin B sensitivity of *B. melitensis* wild-type (Bme-parental), *B. melitensis* non-polar *lptA* mutant (BmeΔ*lptA*), the cognate complemented mutant (BmeΔ*lptA*pBME*lptA*), *B. abortus* wild-type (Ba-parental), and *B. abortus* wild-type carrying a plasmid with the *B. melitensis* *lptA* gene (Ba-parentalpBME*lptA*) (the results are representative of three independent experiments). **(B)** MALDI-TOF analysis of the lipid A of Bme-parental, BmeΔ*lptA*, and Ba-parental.

pBME*lptA* or its introduction into *B. abortus* 2308 leads to restoration of polymyxin B resistance in BmeΔ*lptA* or an increase up to *B. melitensis* level in *B. abortus* (Figure 2A). As expected

both constructs kept the S type features (negative crystal violet test and positive coagglutination with anti-S-LPS antibodies) of the parental strains. *N. gonorrhoeae* shows increased resistance to the action of complement in non-immune serum that is dependent on lipid A-linked pEtN (Lewis et al., 2013). Testing for a similar contribution here, we found that BmeΔ*lptA* was more sensitive than either the parental strain or the complemented mutant (25% vs. no decrease in viability after 3 h of incubation in normal sheep serum) relevant given that *B. melitensis* is characteristically resistant to killing by normal serum.

By MALDI-TOF analysis, the lipid A of Bme-parental was found to contain four main clusters of ions (A, B, C, and D in Figure 2B). BmeΔ*lptA* lipid A was qualitatively identical to Bme-parental with respect to groups A, B, and C but clearly differed in group D (Figure 2B and Supplementary Table S3). In group D, the 2191 m/z species of Ba-parental was consistent with the isotopic mass of a molecule ($C_{120}H_{232}N_4O_{25}P_2$) formed by a hexaacetylated and bisphosphorylated diaminoglucose disaccharide carrying the hydroxylated long and very long chain acyl groups characteristic of *Brucella* (Velasco et al., 2000; Ferguson et al., 2004). According to this interpretation, the signal(s) at 2112 m/z (mass of $-H_2PO_3$ or $-HPO_3^-$, 80.9 - 79.9) could correspond to a monophosphorylated ($C_{120}H_{232}N_4O_{25}P$) 2191 m/z" equivalent. Substitution of this monophosphorylated form with pEtN ($+H_3NCH_2-CH_2-HPO_3^-$ mass 125) should account for signal m/z 2237, in keeping with the fact that m/z 2237 did not appear in the spectrum of the lipids A from either BmeΔ*lptA* or Ba-parental (Figure 2B). Although a clear cut demonstration requires direct analyses of the enzymatic analyses of LptA, these results and the homologies with LptA of other bacteria are consistent with the hypothesis that LptA acts as a pEtN transferase in *B. melitensis* and lacks functionality in *B. abortus*. It is remarkable that pEtN activity was detected for only a fraction (D) of lipid A species. This could be explained by a preferential activity of the enzyme for higher MW lipid A molecules.

The *Brucella* *lpxE* Orthologs Encode a Phosphatase Involved in the Remodeling of the OM

As described above, MALDI-TOF analyses showed the presence of molecular species with a mass compatible with monophosphorylated lipid A. Since lipid A synthesis produces C1 and C4' bisphosphorylated disaccharide backbones (Qureshi et al., 1994), a possible explanation could be its dephosphorylation by a phosphatase such as LpxE, an inner membrane enzyme that in the phylogenetic neighbor *Rhizobium leguminosarum* removes the lipid A phosphate at C1 (Raetz et al., 2009). A search in KEGG showed that all *Brucella* spp. carry an ORF homologous to *R. leguminosarum* *lpxE* (Supplementary Table S2). However, the start codon in the *B. melitensis* 16M homolog (BMEI1212) is annotated to a position different from that determined for other brucellae (Supplementary Table S2), including other *B. melitensis* strains. Thus, whereas the *B. abortus* homolog (BAB1_0671) is predicted to encode a protein of 255 amino acids, the *B. melitensis*

one could encode a protein of either 235 or 255 amino acids (**Figure 1**). Both proteins conserve the consensus sequence of the lipid phosphatase superfamily [KX6RP-(X12–54)-PSGH-(X31–54)-SRX5HX3D] (Stukey and Carman, 2008) which is also present in LpxE from *R. leguminosarum*, *Sinorhizobium meliloti*, and *Agrobacterium tumefaciens* (Karbarz et al., 2003). Although BAB1_0671 and BMEI1212 code for proteins that contain the three motifs conserved in the LpxF phosphatase from *Francisella*, they lack two amino acids of the central motif, NCSFX2G, which seems LpxF specific (Wang et al., 2006, 2007). Thus, the *Brucella* proteins were named BALpxE and BMELpxE.

To study whether BALpxE actually acts as a lipid A phosphatase, we constructed a non-polar mutant (Ba Δ lpxE) and tested it against polymyxin B, since the permanence of a phosphate group in an OM molecule should increase sensitivity to this antibiotic. Mutant Ba Δ lpxE was eight times more sensitive than the parental strain (MIC 0.2 and 1.6 μ g/ml, respectively). Moreover, when we introduced a plasmid containing the BMELpxE ortholog into Ba Δ lpxE, the resistance to polymyxin B was restored (MIC 1.6 μ g/ml). Although final confirmation of this interpretation would require to assay the enzymatic activity of the protein, these results are consistent with the predicted role of lpxE as a phosphatase and its functionality in both *B. abortus* and *B. melitensis* 16M, a strain where the annotation of the start codon was a source of ambiguity.

By MALDI-TOF analysis, the Ba-parental lipid A spectrum showed three of the four predominant clusters of ions (A, B, and C) found in *B. melitensis* (**Figure 2B** and Supplementary Table S3). Cluster A (m/z 2173) was consistent with an hexaacylated bisphosphorylated diaminoglucose disaccharide ($C_{120}H_{232}N_4O_{24}P_2$) and the signal at 2093 m/z , which differed in the mass of one phosphate group (i.e., 80), was consistent with the cognate monophosphorylated lipid A ($C_{120}H_{232}N_4O_{25}P$) (A-Pi, **Figure 2**). Other signals differing in a mass of 14 or 28 units should result from the heterogeneity in acyl chain length that is typical of lipid A. The B and C clusters also contained signals differing in 80 mass units that could correspond to bis- and mono-phosphorylated species. The mass spectrum of Ba Δ lpxE lipid A (not shown) did not differ significantly from that of Ba-parental, and again showed acyl chain heterogeneity in the A, B, C clusters, as well as the -80 m/z signals indicative of mono- and bisphosphorylated lipid A species. As mutation of lpxE is concomitant with an increase in polymyxin B sensitivity, it is tempting to speculate that LpxE directly or indirectly modulates *Brucella* cell envelope by removing an accessible phosphate group from a substrate different from lipid A. Further studies need to be performed to clarify the role of LpxE.

The *Brucella* lpxO Orthologs Encode an Acyl Hydroxylase Acting on Ornithine Lipids

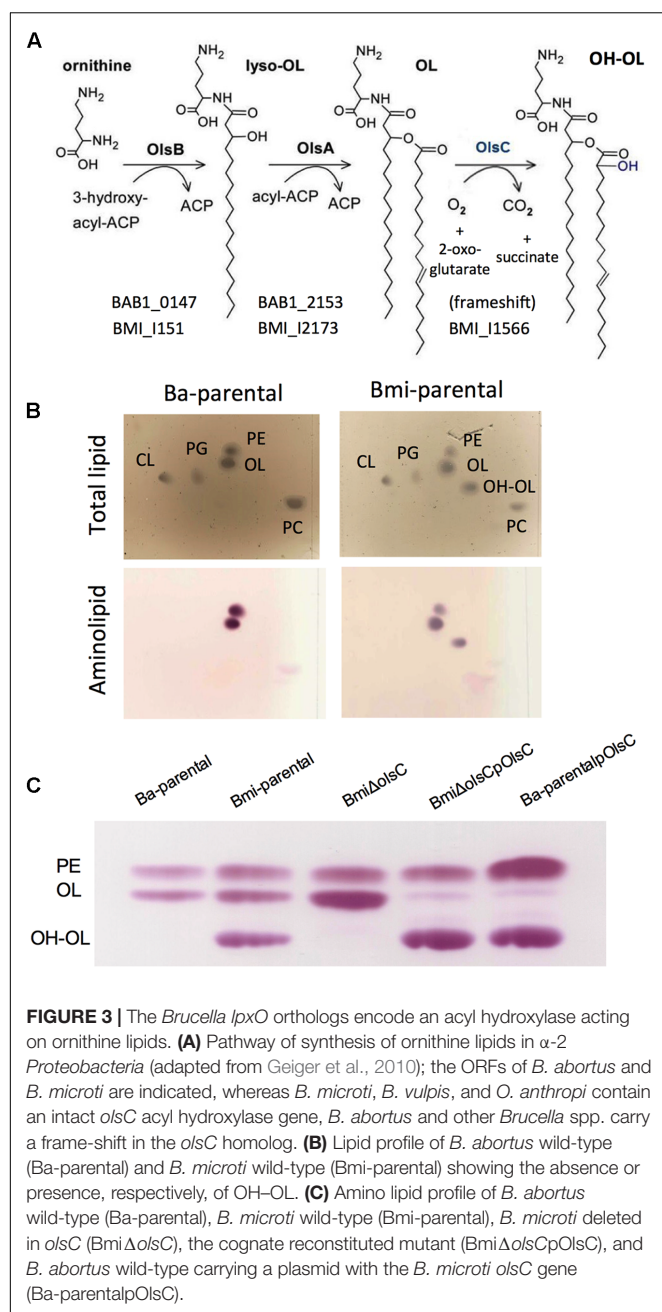
The genomes of all *Brucella* species available at KEGG contain an ORF homologous to *Salmonella* lpxO (Gibbons et al., 2000), which encodes an enzyme hydroxylating the 3'-secondary acyl chain of lipid A. In all *Brucella* spp. except *B. microti* and *B. vulpis*

this ORF presents a frame-shift leading to a truncated protein that lacks the consensus of the aspartyl/asparaginyl β -hydroxylases family to which LpxO belongs (**Figure 1** and Supplementary Table S2). These characteristics are consistent with chemical studies that previously failed to observe S2 hydroxylated fatty acids in *B. abortus* lipid A (Velasco et al., 2000). Moreover, a lpxO homolog is present in *Ochrobactrum anthropi* where S2 hydroxylated fatty acids were also not observed in the lipid A (Velasco et al., 2000), indicating that a role similar to that of *Salmonella* LpxO is unlikely. Thus, the lpxO homologs present in these *B. microti* and *O. anthropi* could be acting on a free lipid and, in fact, it has been reported that the corresponding *R. tropici* homolog is a β -hydroxylase acting on OLs (Vences-Guzmán et al., 2011). If this were the case in *O. anthropi* and the brucellae, the end product [a hydroxylated OL (OH-OL)] of the pathway described previously in members of the *Rhizobiaceae* (**Figure 3A**) should be observed in *O. anthropi* and *B. microti* (and *B. vulpis*) but not in other *Brucella* spp.

To investigate these hypotheses, we compared the free lipids of *B. abortus*, *B. melitensis*, *B. suis*, *B. ovis*, *B. microti*, and *O. anthropi*. As can be seen in **Figure 3B**, *B. microti* but not *B. abortus* produced an amino lipid with the migration pattern predicted for OH-OL (Vences-Guzmán et al., 2011), and results similar to those of *B. microti* were obtained for *O. anthropi* but not for the other *Brucella* spp. tested (not shown). These observations support the interpretation that *O. anthropi* and *B. microti* LpxO are OL hydroxylases and are fully consistent with the aforementioned genomic and chemical evidence. Accordingly, *Brucella* lpxO should be named *olsC*. To confirm this, we examined the amino lipids of a non-polar *olsC* mutant in *B. microti* (Bmi Δ olsC). As predicted, this mutant did not synthesize OH-OL and complementation with a plasmid containing *B. microti* *olsC* restored the wild-type phenotype (**Figure 3C**). Furthermore, introducing this plasmid or a plasmid carrying *O. anthropi* *olsC* into *B. abortus* resulted in the synthesis of OH-OL (**Figure 3C** and Supplementary Figure S2). No difference in polymyxin sensitivity was observed in these constructs or the mutant Bmi Δ olsC when compared to the corresponding parental strains.

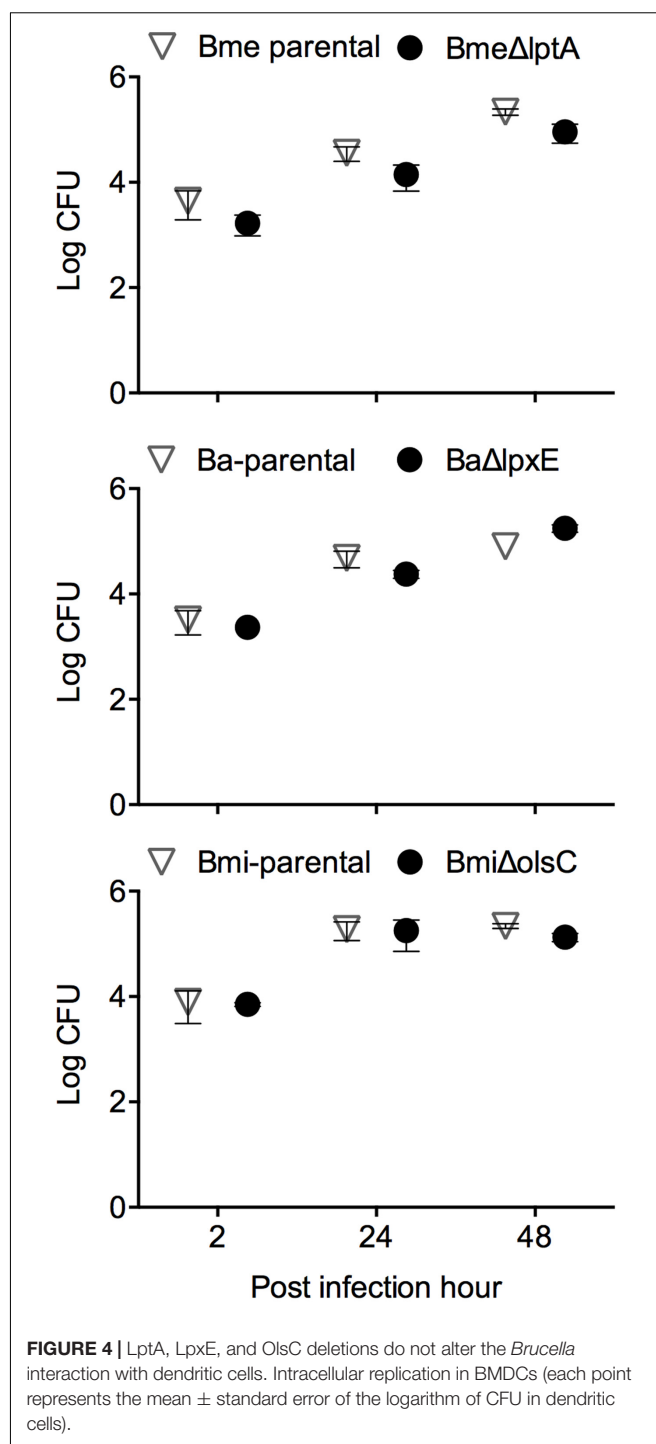
LptA, LpxE, and OlsC Are Not Required for *Brucella* Virulence in Laboratory Models

Brucella abortus, *B. melitensis*, and *B. suis* have been shown to multiply in murine and human monocyte-derived dendritic cells while interfering with their activation and maturation and reducing both antigen presentation and an effective adaptive response (Billard et al., 2007; Martirosyan et al., 2011; Conde-Álvarez et al., 2012; Gorvel et al., 2014; Papadopoulos et al., 2016). To assess whether LptA, LpxE, and OL β -hydroxylase (*OlsC*) were involved, we compared parental and mutant strains of *B. melitensis*, *B. abortus*, and *B. microti* in mouse BMDCs. As shown in **Figure 4**, the kinetics of multiplication of the mutants and wild-type strains were similar. We also performed a phenotypic characterization of MHC II and co-stimulatory



receptors CD86 and CD80 (Figure 5). In agreement with previous studies, these analyses showed that activation and maturation was only partially induced in BMDC infected with *B. melitensis* and *B. abortus* (Martirosyan et al., 2011). In addition, a similar partial-activation profile was evident both for *B. microti*, for which no previous studies exist in infected BMDC, and all of the tested mutants obtained for each of the three *Brucella* spp.

The mouse model has been widely used for testing *Brucella* virulence (Grilló et al., 2012). In this model, the LptA and LpxE mutants and the parental strains behaved identically (Figure 6 upper panels). Deletion of *olsC* in *B. microti* did not



alter the CFU/spleen profile produced by this species which is characterized by a lower lethal dose in mice as well as a faster clearance from mouse spleens (Jiménez de Bagüés et al., 2010; Figure 6, lower left panel). Moreover, when we tested whether the expression of *B. microti olsC* in *B. abortus* could affect virulence, we found no differences between the *B. microti olsC*-carrying and the wild-type *B. abortus* strains (Figure 6, lower right panel).

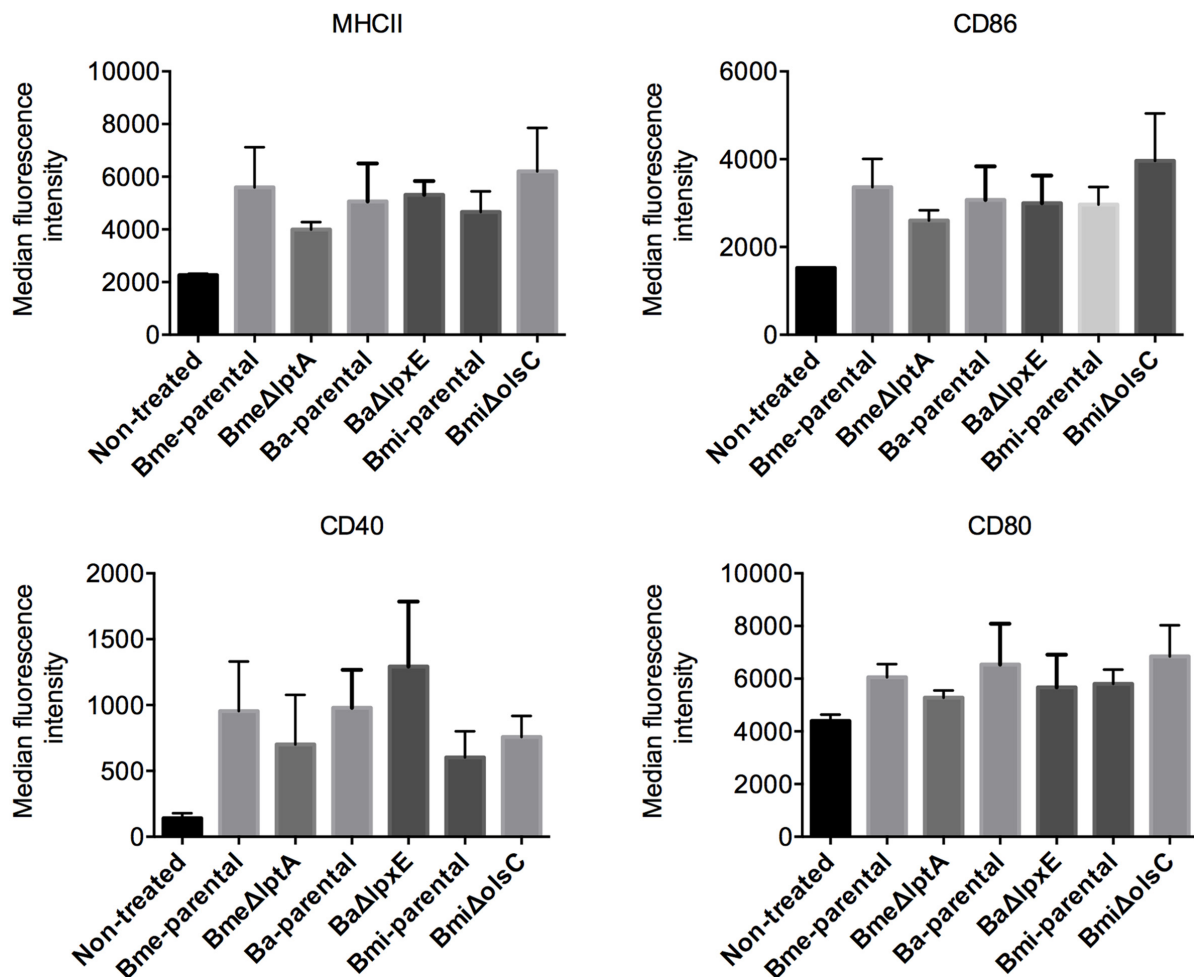


FIGURE 5 | LptA, LpxE, and OlsC deletions do not significantly impact the intrinsic immunogenicity of *Brucella*. Each point represents the mean \pm standard error of the median intensity of surface receptor expression in dendritic cells treated with *Brucella* strains or derived mutants. *E. coli* LPS was used as a positive control for dendritic cell activation.

DISCUSSION

In this work we investigated three *Brucella* ORFs that according to homologies with genes of known function in other pathogens could modify the lipid A and contribute to further altering the LPS PAMP of representative *Brucella* species. The results show that, whereas *Brucella* LptA modifies the lipid A, this is not the case for *lpxE* and *lpxO* (redesignated *olsC*), the former encoding a putative phosphatase acting on an unidentified OM molecule and the latter for an enzyme with OlsC activity.

Our data strongly suggest that *B. melitensis* LptA is involved in the addition of pEtN to lipid A, homologous proteins carrying out this function are not uncommon in Gram-negative pathogens and modulate the properties of lipid A. In *Salmonella* Typhimurium, *Shigella flexneri*, *E. coli*, *Vibrio cholerae*, *Helicobacter pylori*, *Haemophilus ducreyi*, *N. gonorrhoeae*, and *N. meningitidis* pEtN reduces the binding of cationic bactericidal peptides by balancing the negative charge of lipid A (Needham and Trent, 2013; Trombley et al., 2015). Conversely,

pEtN promotes binding to *N. gonorrhoeae* lipid A of factors that downregulate the complement cascade and thwart building of the membrane-attack complex and opsonophagocytosis (Lewis et al., 2013). *N. meningitidis* pEtN also promotes adhesion of non-encapsulated bacteria to endothelial cells (Takahashi et al., 2008). Indeed, properties that parallel some of those observed for the above-listed pathogens can also be attributed to the pEtN transferase counterpart in *Brucella*. An intact *lptA* was related to polymyxin B resistance in *B. melitensis* and the introduction of *B. melitensis* *lptA* into *B. abortus* increases polymyxin B resistance to the level of *B. melitensis*, suggesting that LptA function is severely impaired in *B. abortus*. This is in agreement with the presence of a frame-shift in *B. abortus* *lptA* encompassing the consensus sequence, which makes likely that it codes for a protein with no or residual enzymatic activity. Previous analyses are contradictory with regard to the presence (Casabuono et al., 2017) or absence (Moreno et al., 1990) of ethanolamine in *B. abortus* lipid A but the materials analyzed differ in methods of extraction and presence of *B. abortus* lipid A markers, such as

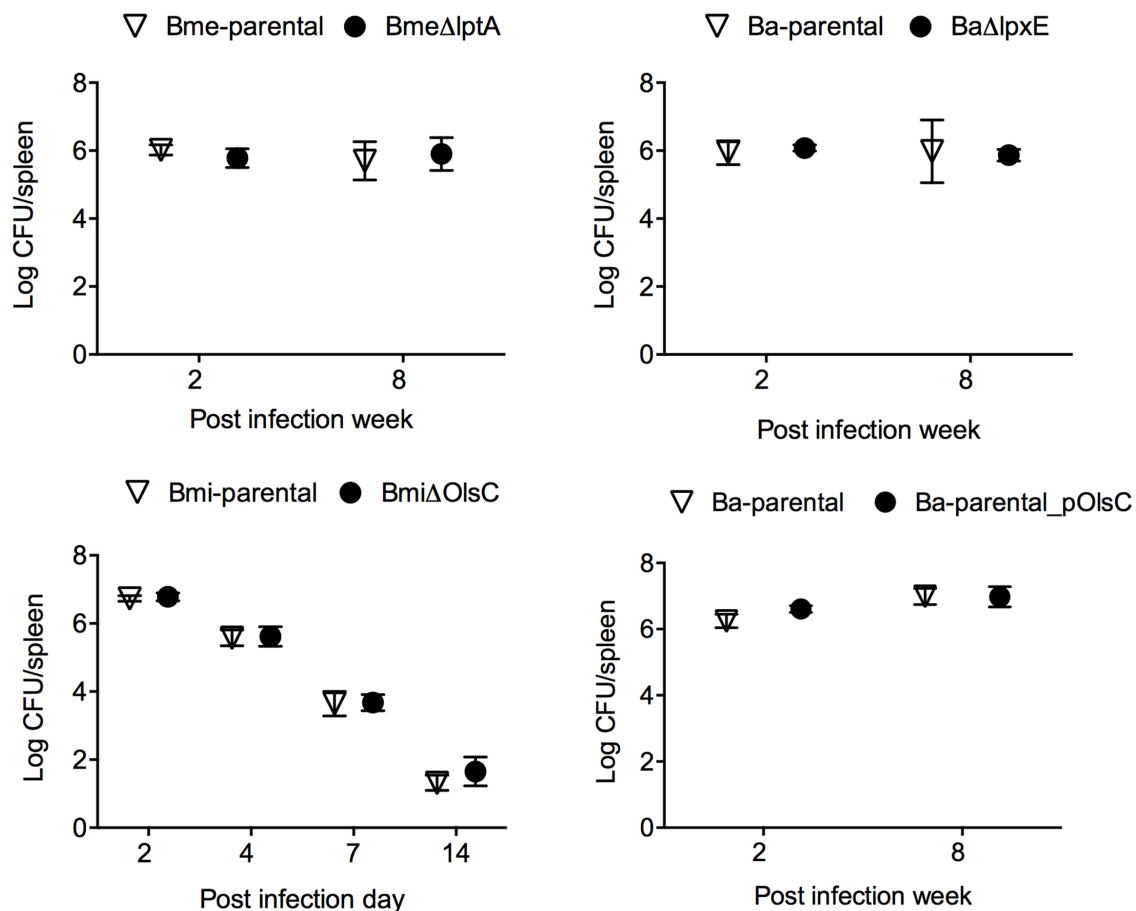


FIGURE 6 | The OM properties that depend on LptA, LpxE, and OlsC are not required for *Brucella* virulence in the mouse model. BALB/c mice were inoculated intraperitoneally with 5×10^4 (Bme-parental, BmeΔlptA, Ba-parental, and BaΔlpxE) or 1×10^4 (Bmi-parental and BmiΔolsC) CFU/mouse and CFU/spleen determined at the indicated times. Each point represents the mean \pm standard error of the logarithm of CFU in the spleens of five animals.

very long chain fatty acids (VCLFA). Although further chemical and enzymatic analyses are necessary for a definite conclusion, our results strongly suggest that, if present, pEtN is in much less amounts in *B. abortus* than in *B. melitensis* lipid A. It is also worth noting that such genetic and phenotypic differences in the lipid A of *B. abortus* and *B. melitensis* could relate to differences in biological properties. The LPS of *B. abortus* and *B. melitensis* is a poor activator of the complement cascade, and this property has been traced to the core and lipid A structure (Moreno et al., 1981; Conde-Álvarez et al., 2012; Fontana et al., 2016). Since *B. abortus* is less resistant than *B. melitensis* to normal serum (González et al., 2008), it is tempting to suggest that, like in *N. gonorrhoeae*, *B. melitensis* pEtN could sequester regulatory elements enhancing complement resistance in this species.

Concerning LpxE, phosphatases acting on lipid A have at least been shown in *Francisella tularensis*, *H. pylori*, *Porphyromonas gingivalis*, and *Capnocytophaga canimorsus*, bacteria where lipid A dephosphorylation is involved both in resistance to bactericidal peptides and the reduction of TLR-4-dependent recognition (Needham and Trent, 2013). Although these properties are

displayed by the LPS of *B. abortus* and *B. melitensis* (Martínez de Tejada et al., 1995; Lapaque et al., 2006; Conde-Álvarez et al., 2012), our results do not support a role for BaLpxE as a lipid A phosphatase. This is consistent with genomic analysis showing that, whereas in bacteria where LpxE acts on lipid A the gene is located together with *lptA* in an operon (Tran et al., 2006; Renzi et al., 2015), *Brucella lpxE* is instead located upstream of three sequences annotated as pseudogenes and downstream, but in the opposite direction, of a cystathionine beta-lyase. On the basis of the data shown here, the origin of monophosphoryl lipid A in *Brucella* remains to be explained. Further, we believe it unlikely to be an artifact resulting from the hydrolytic steps used to obtain lipid A and instead favor the hypothesis of the existence of an as yet unidentified lipid A phosphatase.

LpxE belongs to the type 2 family of phosphatases that can act on lipid A but also on phosphatidylglycerol phosphate, phosphatidic acid, sphingosine phosphate, and lysophosphatidic acid (Brindley and Waggoner, 1998; Sciorra and Morris, 2002). Significantly, LpxE from *Agrobacterium*, although predicted to be a lipid A phosphatase, dephosphorylates

phosphatidyl glycerophosphate (Karbarz et al., 2009) to generate phosphatidylglycerol, a cell envelope phospholipid. Indeed, a hypothetical phosphatidyl glycerophosphate phosphatase activity of *Brucella* LpxE could account for both the polymyxin B sensitivity of the mutated bacteria and the unaltered mass spectra of the lipid A of the mutant. Such a modification of a phospholipid could be meaningful by itself on account of the LpxE-dependent bactericidal peptide resistance but there are other possibilities. In some bacteria (i.e., *Rhizobium*) phosphatidylglycerol is a precursor for the synthesis of amino lipids such as lysyl-phosphatidylglycerol. This synthesis is induced by acid pH and brings about resistance to daptomycin and polymyxin B (Sohlenkamp et al., 2007; Ernst and Peschel, 2011; Arendt et al., 2012). Interestingly, whereas the Δ *lpxE* mutant is impaired for growth at pH 6, the parental *B. abortus* becomes more resistant to cationic peptides (L. Palacios-Chaves and R. Conde-Álvarez, Unpublished observations). These observations suggest the existence in *Brucella* of pH-dependent envelope modifications that require a functional LpxE. Research is in progress to elucidate the mechanisms behind the increased resistance at acid pH and the implication regarding a role for LpxE.

In *S. Typhimurium*, *Pseudomonas aeruginosa*, *Bordetella bronchiseptica*, *Legionella pneumophila*, and *Klebsiella pneumoniae*, LpxO is a Fe²⁺/α-ketoglutarate-dependent dioxygenase that catalyzes the hydroxylation of the 3'-secondary acyl chain of lipid A. LpxO has been implicated indirectly in stress responses at the envelope level (Needham and Trent, 2013) and, in *K. pneumoniae*, it has been shown to be relevant *in vivo* by increasing bactericidal peptide resistance and reducing the inflammatory responses (Llobet et al., 2015). However, as discussed above, previous chemical analysis (Velasco et al., 2000) of lipid A and the evidence presented here indicate that the *Brucella* *lpxO* homolog is not a lipid A hydroxylase but rather an OlsC whose mutation, in contrast with LpxO, does not result in increased sensitivity to polymyxin B. This absence of an effect on polycation resistance is in keeping with both the lack of activity on lipid A and the fact that OL do not play a major role in resistance to polycationic bactericidal peptides in *B. abortus* (Palacios-Chaves et al., 2011). At the same time, it would also appear to rule out, the involvement of this protein in the metabolism of succinate in *B. microti* as has been previously suggested (Audic et al., 2009).

Previous data showing *lptA*, *lpxE*, and *lpxO* to be involved in modulating the properties of the OM in a way that in some cases confers *in vitro* resistance to innate immunity bactericidal peptides, complement, and cytokine responses (Needham and Trent, 2013) have been drawn upon as evidence for a role in virulence. However, to the best of our knowledge, a role *in vivo* has thus far been shown only for *lpxO* from *K. pneumoniae* (Llobet et al., 2015). Moreover, contrasting results have been obtained with mutants both showing bactericidal peptide sensitivity *in vitro* and no phenotype *in vivo* have been reported for at least *H. ducreyi* (Trombley et al., 2015) and may reflect the complexities of the infection processes and/or the inadequacies of the currently available *in vivo* models. Despite their effect on the envelope, our results show that *Brucella* *lptA*,

lpxE, or *olsC* do not play a role in the ability of *Brucella* to replicate in BMDC and do not modulate the activation and maturation profile in these cells. Similarly, the mouse model did not reveal any effect on its ability to colonize and multiply in the spleen. However, further experimental work in the natural hosts and alternative routes of infection might provide evidence on the role in virulence of these genes. The fact that *lptA* and *olsC* are not functional in all *Brucella* spp. must therefore be considered in the context of the models used. While the absence of a functional *lptA* in *B. abortus* suggests that the gene is not essential for the virulence of this species we cannot conclude it to be totally irrelevant. Differences between *B. melitensis* and *B. abortus* related to *lptA* could explain the higher invasiveness of the former species noted by early researchers in studies carried out in guinea pigs, animals that are highly susceptible to brucellosis (Braude, 1951). This possibility together with the presence of intact *lptA* and *olsC* in *Ochrobactrum* and *B. microti* is also compatible with the hypothesis that they represent ancestral characters that are liable to be lost in the absence of a selective pressure during the intracellular life cycle or, in the case of *lptA*, that is no longer present in the ruminant host species (i.e., cattle) to which *B. abortus* is characteristically associated.

ETHICS STATEMENT

Female BALB/c mice (Charles River, France) were kept in cages with water and food *ad libitum* under P3 biosafety conditions in the facilities of “Centro de Investigación Médica Aplicada” (registration code ES31 2010000132) 2 weeks before and during the experiments. The procedures were in accordance with the current European (directive 86/609/EEC) and Spanish (RD 53/2013) legislations, supervised by the Animal Welfare Committee of the University of Navarra, and authorized by the “Gobierno de Navarra” [CEEA045/12 and E36-14 (045-12E1)].

AUTHOR CONTRIBUTIONS

IM, MI, J-PG, JB, and RC-Á conceived the study. RC-Á, LP-C, YG-R, MB-V, MS-B, BA-A, EM-G, AZ-R, MdM, TLB, SH, M-JG, MV-G, and VA-G carried out the experimental work. IM, MI, and RC-Á wrote the paper. All authors participated in the presentation and discussion of results.

FUNDING

This research was supported by the Institute for Tropical Health funders (Obra Social la CAIXA, Fundaciones Caja Navarra and Roviralta, PROFAND, Ubesol, ACUNSA, and Artai) and grants MINECO (AGL2014-58795-C4-1-R, Bru-Epidia 291815-FP7/ERANET/ANIHWA), Aragón Government (Consolidated Group A14), and Marie Curie Career Integration Grant U-KARE (PCIG13-GA-2013-618162). TLB is the recipient of a Ph.D. Fellowship funded by the Department for Employment and Learning (Northern Ireland, United Kingdom).

ACKNOWLEDGMENT

The authors thank A. Delgado-López for excellent technical assistance in the extraction and purification of LPS.

REFERENCES

- Aragón, V., Díaz, R., Moreno, E., and Moriyón, I. (1996). Characterization of *Brucella abortus* and *Brucella melitensis* native haptens as outer membrane O-type polysaccharides independent from the smooth lipopolysaccharide. *J. Bacteriol.* 178, 1070–1079. doi: 10.1128/jb.178.4.1070-1079.1996
- Arendt, W., Hebecker, S., Jäger, S., Nimtz, M., and Moser, J. (2012). Resistance phenotypes mediated by aminoacyl-phosphatidylglycerol synthases. *J. Bacteriol.* 194, 1401–1416. doi: 10.1128/JB.06576-11
- Audic, S., Lescot, M., Claverie, J.-M., and Scholz, H. C. (2009). *Brucella microti*: the genome sequence of an emerging pathogen. *BMC Genomics* 10:352. doi: 10.1186/1471-2164-10-352
- Barquero-Calvo, E., Chaves-Olarte, E., Weiss, D. S., Guzmán-Verri, C., Chacón-Díaz, C., Rucavado, A., et al. (2007). *Brucella abortus* uses a stealthy strategy to avoid activation of the innate immune system during the onset of infection. *PLOS ONE* 2:e631. doi: 10.1371/journal.pone.0000631
- Barquero-Calvo, E., Conde-Álvarez, R., Chacón-Díaz, C., Quesada-Lobo, L., Martirosyan, A., Guzmán-Verri, C., et al. (2009). The differential interaction of *Brucella* and *Ochrobactrum* with innate immunity reveals traits related to the evolution of stealthy pathogens. *PLOS ONE* 4:e5893. doi: 10.1371/journal.pone.0005893
- Billard, E., Dornand, J., and Gross, A. (2007). *Brucella suis* prevents human dendritic cell maturation and antigen presentation through regulation of tumor necrosis factor alpha secretion. *Infect. Immun.* 75, 4980–4989. doi: 10.1128/IAI.00637-07
- Bligh, E. M., and Dyer, W. J. (1959). A rapid method of total lipid extraction and purification. *Can. J. Biochem. Physiol.* 37, 911–917. doi: 10.1139/y59-099
- Braude, A. I. (1951). Studies in the pathology and pathogenesis of experimental brucellosis: I. A comparison of the pathogenicity of *Brucella abortus*, *Brucella melitensis*, and *Brucella suis* for Guinea pigs. *J. Infect. Dis.* 89, 76–86. doi: 10.1093/infdis/89.1.76
- Brindley, D. N., and Waggoner, D. W. (1998). Mammalian lipid phosphate phosphohydrolases. *J. Biol. Chem.* 273, 24281–24284. doi: 10.1074/JBC.273.38.24281
- Casabuono, A. C., Czibener, C., Del Giudice, M. G., Valguarnera, E., Ugalde, J. E., and Couto, A. S. (2017). New features in the lipid A structure of *Brucella suis* and *Brucella abortus* lipopolysaccharide. *J. Am. Soc. Mass Spectrom.* 28, 2716–2723. doi: 10.1007/s13361-017-1805-x
- Chaudhary, A., Ganguly, K., Cabantous, S., Waldo, G. S., Micheva-Viteva, S. N., Nag, K., et al. (2012). The *Brucella* TIR-like protein TcpB interacts with the death domain of MyD88. *Biochem. Biophys. Res. Commun.* 417, 299–304. doi: 10.1016/j.bbrc.2011.11.104
- Cirl, C., Wieser, A., Yadav, M., Duerr, S., Schubert, S., Fischer, H., et al. (2008). Subversion of Toll-like receptor signaling by a unique family of bacterial Toll/interleukin-1 receptor domain-containing proteins. *Nat. Med.* 14, 399–406. doi: 10.1038/nm1734
- Comerci, D. J., Altabe, S., de Mendoza, D., and Ugalde, R. A. (2006). *Brucella abortus* synthesizes phosphatidylcholine from choline provided by the host. *J. Bacteriol.* 188, 1929–1934. doi: 10.1128/JB.188.5.1929-1934.2006
- Conde-Álvarez, R., Arce-Gorvel, V., Iriarte, M., Manček-Keber, M., Barquero-Calvo, E., Palacios-Chaves, L., et al. (2012). The lipopolysaccharide core of *Brucella abortus* acts as a shield against innate immunity recognition. *PLOS Pathog.* 8:e1002675. doi: 10.1371/journal.ppat.1002675
- Conde-Álvarez, R., Grilló, M. J., Salcedo, S. P., de Miguel, M. J., Fugier, E., Gorvel, J. P., et al. (2006). Synthesis of phosphatidylcholine, a typical eukaryotic phospholipid, is necessary for full virulence of the intracellular bacterial parasite *Brucella abortus*. *Cell. Microbiol.* 8, 1322–1335. doi: 10.1111/j.1462-5822.2006.00712.x
- Cox, A. D., Wright, J. C., Li, J., Hood, D. W., Moxon, E. R., and Richards, J. C. (2003). Phosphorylation of the lipid A region of meningococcal lipopolysaccharide: identification of a family of transferases that add phosphoethanolamine to lipopolysaccharide. *J. Bacteriol.* 185, 3270–3277. doi: 10.1128/jb.185.11.3270-3277.2003
- Dricot, A., Rual, J. F., Lamesch, P., Bertin, N., Dupuy, D., Hao, T., et al. (2004). Generation of the *Brucella melitensis* ORFeome version 1.1. *Genome Res.* 14, 2201–2206. doi: 10.1101/gr.2456204
- Ducrotot, M., Bertu, W. J., Matope, G., Cadmus, S., Conde-Álvarez, R., Gusi, A. M., et al. (2017). Brucellosis in sub-saharan Africa: current challenges for management, diagnosis and control. *Acta Trop.* 165, 179–193. doi: 10.1016/j.actatropica.2015.10.023
- Ernst, C. M., and Peschel, A. (2011). Broad-spectrum antimicrobial peptide resistance by MprF-mediated aminoacylation and flipping of phospholipids. *Mol. Microbiol.* 80, 290–299. doi: 10.1111/j.1365-2958.2011.07576.x
- Ferguson, G. P., Datta, A., Baumgartner, J., Roop, R. M., Carlson, R. W., Walker, G. C., et al. (2004). Similarity to peroxisomal-membrane protein family reveals that *Sinorhizobium* and *Brucella* BacA affect lipid-A fatty acids. *Proc. Natl. Acad. Sci. U.S.A.* 101, 5012–5017. doi: 10.1073/pnas.0307137101
- Fontana, C., Conde-Álvarez, R., Stähle, J., Holst, O., Iriarte, M., Zhao, Y., et al. (2016). Structural studies of lipopolysaccharide-defective mutants from *Brucella melitensis* identify a core oligosaccharide critical in virulence. *J. Biol. Chem.* 291, 7727–7741. doi: 10.1074/jbc.M115.701540
- Geiger, O., González-Silva, N., López-Lara, I. M., and Sohlenkamp, C. (2010). Amino acid-containing membrane lipids in bacteria. *Prog. Lipid Res.* 49, 46–60. doi: 10.1016/j.plipres.2009.08.002
- Gibbons, H. S., Lin, S., Cotter, R. J., and Raetz, C. R. H. (2000). Oxygen requirement for the biosynthesis of the S -2-hydroxymyristate moiety in *Salmonella typhimurium* lipid A. *J. Biol. Chem.* 275, 32940–32949. doi: 10.1074/jbc.M005779200
- González, D., Grilló, M.-J., De Miguel, M.-J., Ali, T., Arce-Gorvel, V., Delrue, R.-M., et al. (2008). Brucellosis vaccines: assessment of *Brucella melitensis* lipopolysaccharide rough mutants defective in core and O-polysaccharide synthesis and export. *PLOS ONE* 3:e2760. doi: 10.1371/journal.pone.0002760
- Gorvel, J.-P., and Moreno, E. (2002). *Brucella* intracellular life: from invasion to intracellular replication. *Vet. Microbiol.* 90, 281–297. doi: 10.1016/S0378-1135(02)00214-6
- Gorvel, L., Textoris, J., Banchereau, R., Ben Amara, A., Tantibhedhyangkul, W., von Bargen, K., et al. (2014). Intracellular bacteria interfere with dendritic cell functions: role of the type I interferon pathway. *PLOS ONE* 9:e99420. doi: 10.1371/journal.pone.0099420
- Grilló, M.-J., Blasco, J. M., Gorvel, J. P., Moriyón, I., and Moreno, E. (2012). What have we learned from brucellosis in the mouse model? *Vet. Res.* 43:29. doi: 10.1186/1297-9716-43-29
- Hallez, R., Letesson, J.-J., Vandenhaute, J., and De Bolle, X. (2007). Gateway-based destination vectors for functional analyses of bacterial ORFeomes: application to the min system in *Brucella abortus*. *Appl. Environ. Microbiol.* 73, 1375–1379. doi: 10.1128/AEM.01873-06
- Herrera, C. M., Henderson, J. C., Crofts, A. A., and Trent, M. S. (2017). Novel coordination of lipopolysaccharide modifications in *Vibrio cholerae* promotes CAMP resistance. *Mol. Microbiol.* 106, 582–596. doi: 10.1111/mmi.13835
- Inaba, K., Inaba, M., Romani, N., Aya, H., Deguchi, M., Ikehara, S., et al. (1992). Generation of large numbers of dendritic cells from mouse bone marrow cultures supplemented with granulocyte/macrophage colony-stimulating factor. *J. Exp. Med.* 176, 1693–1702. doi: 10.1084/jem.176.6.1693
- Iriarte, M., González, D., Delrue, R. M., Monreal, D., Conde-Álvarez, R., López-Goñi, I., et al. (2004). “*Brucella* LPS: structure, biosynthesis and genetics,” in

SUPPLEMENTARY MATERIAL

The Supplementary Material for this article can be found online at: <https://www.frontiersin.org/articles/10.3389/fmicb.2017.02657/full#supplementary-material>

- Brucella: Molecular and Cellular Biology*, eds I. López-Goñi and I. Moriyón (Gurgaon: Horizon Bioscience), 159–192.
- Jiménez de Bagüés, M. P., Ouahrani-Bettache, S., Quintana, J. F., Mitjana, O., Hanna, N., Bessoles, S., et al. (2010). The new species *Brucella microti* replicates in macrophages and causes death in murine models of infection. *J. Infect. Dis.* 202, 3–10. doi: 10.1086/653084
- Jones, B. A., Grace, D., Kock, R., Alonso, S., Rushton, J., Said, M. Y., et al. (2013). Zoonosis emergence linked to agricultural intensification and environmental change. *Proc. Natl. Acad. Sci. U.S.A.* 110, 8399–8404. doi: 10.1073/pnas.1208059110
- Karbarz, M. J., Kalb, S. R., Cotter, R. J., and Raetz, C. R. H. (2003). Expression cloning and biochemical characterization of a *Rhizobium leguminosarum* lipid A 1-phosphatase. *J. Biol. Chem.* 278, 39269–39279. doi: 10.1074/jbc.M305830200
- Karbarz, M. J., Six, D. A., and Raetz, C. R. H. (2009). Purification and characterization of the lipid A 1-phosphatase LpxE of *Rhizobium leguminosarum*. *J. Biol. Chem.* 284, 414–425. doi: 10.1074/jbc.M808390200
- Kastowsky, M., Gutberlet, T., and Bradaczek, H. (1992). Molecular modelling of the three-dimensional structure and conformational flexibility of bacterial lipopolysaccharide. *J. Bacteriol.* 174, 4798–4806. doi: 10.1128/jb.174.14.4798-4806.1992
- Kovach, M. E., Phillips, R. W., Elzer, P. H., Roop, R. M., and Peterson, K. M. (1994). pBBR1MCS: a broad-host-range cloning vector. *Biotechniques* 16, 800–802.
- Kubler-Kielb, J., and Vinogradov, E. (2013). The study of the core part and non-repeating elements of the O-antigen of *Brucella* lipopolysaccharide. *Carbohydr. Res.* 366, 33–37. doi: 10.1016/j.carres.2012.11.004
- Lai, S., Zhou, H., Xiong, W., Gilbert, M., Huang, Z., Yu, J., et al. (2017). Changing epidemiology of human brucellosis, China, 1955–2014. *Emerg. Infect. Dis.* 23, 184–194. doi: 10.3201/eid2302.151710
- Lapaque, N., Moriyon, I., Moreno, E., and Gorvel, J.-P. (2005). *Brucella* lipopolysaccharide acts as a virulence factor. *Curr. Opin. Microbiol.* 8, 60–66. doi: 10.1016/j.mib.2004.12.003
- Lapaque, N., Takeuchi, O., Corrales, F., Akira, S., Moriyon, I., Howard, J. C., et al. (2006). Differential inductions of TNF- α and I κ B by structurally diverse classic and non-classic lipopolysaccharides. *Cell. Microbiol.* 8, 401–413. doi: 10.1111/j.1462-5822.2005.00629.x
- Leong, D., Díaz, R., Milner, K., Rudbach, J., and Wilson, J. B. (1970). Some structural and biological properties of *Brucella* endotoxin. *Infect. Immun.* 1, 174–182.
- Lewis, L. A., Shafer, W. M., Dutta Ray, T., Ram, S., and Rice, P. A. (2013). Phosphoethanolamine residues on the lipid A moiety of *Neisseria gonorrhoeae* lipooligosaccharide modulate binding of complement inhibitors and resistance to complement killing. *Infect. Immun.* 81, 33–42. doi: 10.1128/IAI.00751-12
- Llobet, E., Martínez-Moliner, V., Moranta, D., Dahlström, K. M., Regueiro, V., Tomás, A., et al. (2015). Deciphering tissue-induced *Klebsiella pneumoniae* lipid A structure. *Proc. Natl. Acad. Sci. U.S.A.* 112, E6369–E6378. doi: 10.1073/pnas.1508820112
- Mackinnon, F. G., Cox, A. D., Plested, J. S., Tang, C. M., Makepeace, K., Coull, P. A., et al. (2002). Identification of a gene (lpt-3) required for the addition of phosphoethanolamine to the lipopolysaccharide inner core of *Neisseria meningitidis* and its role in mediating susceptibility to bactericidal killing and opsonophagocytosis. *Mol. Microbiol.* 43, 931–943. doi: 10.1046/j.1365-2958.2002.02754.x
- Martínez de Tejada, G., Pizarro-Cerdá, J., Moreno, E., and Moriyón, I. (1995). The outer membranes of *Brucella* spp. are resistant to bactericidal cationic peptides. *Infect. Immun.* 63, 3054–3061.
- Martirosyan, A., Moreno, E., and Gorvel, J.-P. (2011). An evolutionary strategy for a stealthy intracellular *Brucella* pathogen. *Immunol. Rev.* 240, 211–234. doi: 10.1111/j.1600-065X.2010.00982.x
- Moreira, C. G., Herrera, C. M., Needham, B. D., Parker, C. T., Libby, S. J., Fang, F. C., et al. (2013). Virulence and stress-related periplasmic protein (VisP) in bacterial/host associations. *Proc. Natl. Acad. Sci. U.S.A.* 110, 1470–1475. doi: 10.1073/pnas.1215416110
- Moreno, E., Berman, D. T., and Boettcher, L. A. (1981). Biological activities of *Brucella abortus* lipopolysaccharides. *Infect. Immun.* 31, 362–370.
- Moreno, E., and Moriyón, I. (2007). “The genus *Brucella*,” in *The Prokaryotes: Proteobacteria*, Vol. 5, eds S. Falkow, E. Rosenberg, K. H. Schleifer, E. Stackebrandt, and M. Dworkin (Berlin: Springer-Verlag), 315–455.
- Moreno, E., Stackebrandt, E., Dorsch, M., Wolters, J., Busch, M., and Mayer, H. (1990). *Brucella abortus* 16S rRNA and lipid A reveal a phylogenetic relationship with members of the alpha-2 subdivision of the class *Proteobacteria*. *J. Bacteriol.* 172, 3569–3576. doi: 10.1128/jb.172.7.3569-3576.1990
- Moriyón, I. (2003). “Against gram-negative bacteria: the lipopolysaccharide case,” in *Intracellular Pathogens in Membrane Interactions and Vacuole Biogenesis*, ed. J. P. Gorvel (Dordrecht: Kluwer Academic Publishers), 204–230.
- Naessan, C., Egge-Jacobsen, W., Heiniger, R., Wolfgang, M., Aas, F., Røhr, A., et al. (2008). Genetic and functional analyses of PptA, a phospho-form transferase targeting type IV pili in *Neisseria gonorrhoeae*. *J. Bacteriol.* 190, 387–400. doi: 10.1128/JB.00765-07
- Needham, B. D., and Trent, M. S. (2013). Fortifying the barrier: the impact of lipid A remodelling on bacterial pathogenesis. *Nat. Rev. Microbiol.* 11, 467–481. doi: 10.1038/nrmicro3047
- Palacios-Chaves, L., Conde-Álvarez, R., Gil-Ramírez, Y., Zuñiga-Ripa, A., Barquero-Calvo, E., Chacón-Díaz, C., et al. (2011). *Brucella abortus* ornithine lipids are dispensable outer membrane components devoid of a marked pathogen-associated molecular pattern. *PLOS ONE* 6:e16030. doi: 10.1371/journal.pone.0016030
- Papadopoulos, A., Gagnaire, A., Degos, C., de Chastellier, C., and Gorvel, J.-P. (2016). *Brucella* discriminates between mouse dendritic cell subsets upon in vitro infection. *Virulence* 7, 33–44. doi: 10.1080/21505594.2015.1108516
- Qureshi, N., Takayama, K., Seydel, U., Wang, R., Cotter, R. J., Agrawal, P. K., et al. (1994). Structural analysis of the lipid A derived from the lipopolysaccharide of *Brucella abortus*. *J. Endotoxin Res.* 1, 137–148. doi: 10.1177/096805199400100303
- Raetz, C. R. H., Guan, Z., Ingram, B. O., Six, D. A., Song, F., Wang, X., et al. (2009). Discovery of new biosynthetic pathways: the lipid A story. *J. Lipid Res.* 50(Suppl.), S103–S108. doi: 10.1194/jlr.R800060-JLR200
- Renzi, F., Zähringer, U., Chandler, C. E., Ernst, R. K., Cornelis, G. R., and Ittig, S. J. (2015). Modification of the 1-phosphate group during biosynthesis of *Capnocytophaga canimorsus* lipid A. *Infect. Immun.* 84, 550–561. doi: 10.1128/IAI.01006-15
- Salcedo, S. P., Marchesini, M. I., Degos, C., Terwagne, M., Von Bargen, K., Lepidi, H., et al. (2013). BtpB, a novel *Brucella* TIR-containing effector protein with immune modulatory functions. *Front. Cell. Infect. Microbiol.* 3:28. doi: 10.3389/fcimb.2013.00028
- Salcedo, S. P., Marchesini, M. I., Lelouard, H., Fugier, E., Jolly, G., Balor, S., et al. (2008). *Brucella* control of dendritic cell maturation is dependent on the TIR-containing protein Btp1. *PLOS Pathog.* 4:e21. doi: 10.1371/journal.ppat.0040021
- Sciorra, V. A., and Morris, A. J. (2002). Roles for lipid phosphate phosphatases in regulation of cellular signaling. *Biochim. Biophys. Acta* 1582, 45–51. doi: 10.1016/S1388-1981(02)00136-1
- Scupham, A. J., and Triplett, E. W. (1997). Isolation and characterization of the UDP-glucose 4'-epimerase-encoding gene, *galE*, from *Brucella abortus* 2308. *Gene* 202, 53–59. doi: 10.1016/S0378-1119(97)00453-8
- Simon, L. D., Randolph, B., Irwin, N., and Binkowski, G. (1983). Stabilization of proteins by a bacteriophage T4 gene cloned in *Escherichia coli*. *Proc. Natl. Acad. Sci. U.S.A.* 80, 2059–2062. doi: 10.1073/pnas.80.7.2059
- Sohlenkamp, C., Galindo-Lagunas, K. A., Guan, Z., Vinuesa, P., Robinson, S., Thomas-Oates, J., et al. (2007). The lipid Lysyl-phosphatidylglycerol is present in membranes of *Rhizobium tropici* CIAT899 and confers increased resistance to polymyxin B under acidic growth conditions. *Mol. Plant Microbe Interact.* 20, 1421–1430. doi: 10.1094/MPMI-20-11-1421
- Stukey, J., and Carman, G. M. (2008). Identification of a novel phosphatase sequence motif. *Protein Sci.* 6, 469–472. doi: 10.1002/pro.5560060226
- Takahashi, H., Carlson, R. W., Muszynski, A., Choudhury, B., Kim, K. S., Stephens, D. S., et al. (2008). Modification of lipooligosaccharide with phosphoethanolamine by LptA in *Neisseria meningitidis* enhances meningococcal adhesion to human endothelial and epithelial cells. *Infect. Immun.* 76, 5777–5789. doi: 10.1128/IAI.00676-08

- Tran, A. X., Whittimore, J. D., Wyrick, P. B., Mcgrath, S. C., Cotter, R. J., and Trent, M. S. (2006). The lipid A 1-phosphatase of *Helicobacter pylori* is required for resistance to the antimicrobial peptide polymyxin. *J. Bacteriol.* 188, 4531–4541. doi: 10.1128/JB.00146-06
- Trombley, M. P., Post, D. M. B., Rinker, S. D., Reinders, L. M., Fortney, K. R., Zwickl, B. W., et al. (2015). Phosphoethanolamine transferase LptA in *Haemophilus ducreyi* modifies lipid A and contributes to human defensin resistance in vitro. *PLOS ONE* 10:e0124373. doi: 10.1371/journal.pone.0124373
- Velasco, J., Bengoechea, J. A., Brandenburg, K., Lindner, B., Seydel, U., González, D., et al. (2000). *Brucella abortus* and its closest phylogenetic relative, *Ochrobactrum* spp., differ in outer membrane permeability and cationic peptide resistance. *Infect. Immun.* 68, 3210–3218. doi: 10.1128/IAI.68.6.3210-3218.2000
- Vences-Guzmán, M. Á., Guan, Z., Ormeño-Orrillo, E., González-Silva, N., López-Lara, I. M., Martínez-Romero, E., et al. (2011). Hydroxylated ornithine lipids increase stress tolerance in *Rhizobium tropici* CIAT899. *Mol. Microbiol.* 79, 1496–1514. doi: 10.1111/j.1365-2958.2011.07535.x
- Wang, X., McGrath, S. C., Cotter, R. J., and Raetz, C. R. H. (2006). Expression cloning and periplasmic orientation of the *Francisella novicida* lipid A 4'-phosphatase LpxF. *J. Biol. Chem.* 281, 9321–9330. doi: 10.1074/jbc.M600435200
- Wang, X., Ribeiro, A. A., Guan, Z., Abraham, S. N., and Raetz, C. R. H. (2007). Attenuated virulence of a *Francisella* mutant lacking the lipid A 4'-phosphatase. *Proc. Natl. Acad. Sci. U.S.A.* 104, 4136–4141. doi: 10.1073/pnas.0611606104
- Weissenmayer, B., Gao, J. L., Lopez-Lara, I. M., and Geiger, O. (2002). Identification of a gene required for the biosynthesis of ornithine-derived lipids. *Mol. Microbiol.* 45, 721–733. doi: 10.1046/j.1365-2958.2002.03043.x
- Whatmore, A. M. (2009). Current understanding of the genetic diversity of *Brucella*, an expanding genus of zoonotic pathogens. *Infect. Genet. Evol.* 9, 1168–1184. doi: 10.1016/j.meegid.2009.07.001
- Wright, J. C., Hood, D. W., Randle, G. A., Makepeace, K., Cox, A. D., Li, J., et al. (2004). *lpt6*, a gene required for addition of phosphoethanolamine to inner-core lipopolysaccharide of *Neisseria meningitidis* and *Haemophilus influenzae*. *J. Bacteriol.* 186, 6970–6982. doi: 10.1128/JB.186.20.6970-6982.2004
- Zheludkov, M. M., and Tsirelson, L. E. (2010). Reservoirs of *Brucella* infection in nature. *Biol. Bull.* 37, 709–715. doi: 10.1134/S106235901007006X
- Zinsstag, J., Schelling, E., Solera, J., Blasco, J. M., and Moriyón, I. (2011). “Brucellosis,” in *Handbook of Zoonoses*, eds S. R. Palmer, L. Soulsby, P. R. Torgeson, and D. G. Brown (Oxford: Oxford University Press), 54–62.

Conflict of Interest Statement: The authors declare that the research was conducted in the absence of any commercial or financial relationships that could be construed as a potential conflict of interest.

Copyright © 2018 Conde-Álvarez, Palacios-Chaves, Gil-Ramírez, Salvador-Bescós, Bárcena-Varela, Aragón-Aranda, Martínez-Gómez, Zúñiga-Ripa, de Miguel, Bartholomew, Hanniffy, Grilló, Vences-Guzmán, Bengoechea, Arce-Gorvel, Gorvel, Moriyón and Iriarte. This is an open-access article distributed under the terms of the Creative Commons Attribution License (CC BY). The use, distribution or reproduction in other forums is permitted, provided the original author(s) or licensor are credited and that the original publication in this journal is cited, in accordance with accepted academic practice. No use, distribution or reproduction is permitted which does not comply with these terms.



African Lineage *Brucella melitensis* Isolates from Omani Livestock

Jeffrey T. Foster^{1,2*}, Faith M. Walker², Brandy D. Rannals², M. Hammad Hussain^{3,4}, Kevin P. Drees^{1,2}, Rebekah V. Tiller⁵, Alex R. Hoffmaster⁵, Abdulmajeed Al-Rawahi⁴, Paul Keim² and Muhammad Saqib^{3*}

¹ Department of Molecular, Cellular, and Biomedical Sciences, University of New Hampshire, Durham, NH, United States,

² Pathogen and Microbiome Institute, Northern Arizona University, Flagstaff, AZ, United States, ³ Department of Clinical Medicine and Surgery, University of Agriculture, Faisalabad, Pakistan, ⁴ Animal Health Research Center, Ministry of Agriculture and Fisheries, Muscat, Oman, ⁵ National Center for Emerging and Zoonotic Infectious Diseases, Centers for Disease Control, Atlanta, GA, United States

OPEN ACCESS

Edited by:

Axel Cloeckaert,
Institut National de la Recherche
Agronomique (INRA), France

Reviewed by:

Thomas A. Ficht,
Texas A&M University College Station,
United States
Menachem Banai,
Kimron Veterinary Institute, Israel

*Correspondence:

Jeffrey T. Foster
jeff.foster@nau.edu
Muhammad Saqib
drsaqib_vet@hotmail.com

Specialty section:

This article was submitted to
Infectious Diseases,
a section of the journal
Frontiers in Microbiology

Received: 22 June 2017

Accepted: 29 December 2017

Published: 15 January 2018

Citation:

Foster JT, Walker FM, Rannals BD,
Hussain MH, Drees KP, Tiller RV,
Hoffmaster AR, Al-Rawahi A, Keim P
and Saqib M (2018) African Lineage
Brucella melitensis Isolates from
Omani Livestock.
Front. Microbiol. 8:2702.
doi: 10.3389/fmicb.2017.02702

Brucellosis is a common livestock disease in the Middle East and North Africa, but remains poorly described in the region both genetically and epidemiologically. Traditionally found in goats and sheep, *Brucella melitensis* is increasingly recognized as infecting camels. Most studies of brucellosis in camels to date have focused on serological surveys, providing only limited understanding of the molecular epidemiology of circulating strains. We genotyped *B. melitensis* isolates from Omani camels using whole genome SNP assays and VNTRs to provide context for regional brucellosis cases. We identified a lineage of *B. melitensis* circulating in camels as well as in goats, sheep, and cattle in Oman. This lineage is genetically distinct from most genotypes from the Arabian Peninsula and from isolates from much of the rest of the Middle East. We then developed diagnostic assays that rapidly identify strains from this lineage. In analyses of genotypes from throughout the region, Omani isolates were genetically most closely related to strains from brucellosis cases in humans and livestock in North Africa. Our findings suggest an African origin for *B. melitensis* in Oman that has likely occurred through the trade of infected livestock. Moreover, African lineages of *B. melitensis* appear to be undersampled and consequently are underrepresented in genetic databases for *Brucella*. As we begin to more fully understand global genomic diversity of *B. melitensis*, finding and characterizing these unique but widespread lineages is essential. We predict that increased sampling of humans and livestock in Africa will reveal little known diversity in this important zoonotic pathogen.

Keywords: brucellosis, *Brucella melitensis*, camels, Oman, MLVA, SNP genotyping

INTRODUCTION

Brucella melitensis is a ubiquitous and common pathogen of goats and sheep worldwide (Seleem et al., 2010; Moreno, 2014). This pathogen was first identified in Malta by David Bruce in 1887, with subsequent discovery of the role of contaminated goat's milk for brucellosis infections in humans by Themistocles Zammit in 1905 (Vassallo, 1996; Wyatt, 2005). Despite apparent host specificity of *B. melitensis* to caprines, this bacterium also infects camels (Abbas and Agab, 2002; Gwida et al., 2012; Sprague et al., 2012; Wernery, 2014). Arabian camels (*Camelus dromedarius*) occur throughout the deserts of North Africa and across the Middle East to North India, a region where they are critical for meat, milk, leather, wool and transport (Wilson, 1984). Camel brucellosis

was first reported in 1931 and has since been found in all camel-keeping countries in this region but are particularly well documented for infected herds from Africa and the Arabian Peninsula (Gwida et al., 2012).

Camels are not a primary host for *Brucella* spp. but infections with *B. melitensis* occur due to the co-mingling of camels and ruminant livestock (Sprague et al., 2012). In fact, among the highest prevalence rates in camels have been documented when camel herds are intermixed with ruminants (Musa et al., 2008). Despite this cross-species transmission, epidemiological links between brucellosis in camels and other livestock are poorly understood. Prevalence rates of brucellosis in camels vary widely based on several factors, especially animal husbandry practices (Gwida et al., 2012). Camels can also be infected with *B. abortus*, likely due to the commingling of camel herds with infected cattle (Sprague et al., 2012). Thus, brucellosis prevalence in camels is complex and the role of infections in the primary caprine and bovine hosts must be considered. The pathology of brucellosis infection in camels is poorly known as well. Consistent with findings from other livestock, the bacteria appear to localize in reproductive tissues, lymph nodes, and spleen, causing inflammation, edema, and necrosis (Wernery, 2014). Infection of pregnant camels can result in placental and fetal pathologies resulting in abortion (Narnaware et al., 2017). As with brucellosis in other animals, these abortion events likely disseminate the bacteria broadly and allow for transmission to other livestock and to animal handlers. Not surprisingly, the disease is prevalent in Bedouin in Oman (Scrimgeour et al., 1999).

Several serological tests, such as Rose Bengal, tube and serum agglutination tests and ELISAs that have been optimized for testing cattle are used to determine *Brucella* seroprevalence in camels (Gwida et al., 2012), but epidemiological investigations often stop at this point. Furthermore, the lack of validated serological tests that detect *Brucella* infection in camels pose a challenge to definitive diagnosis. A combination of real-time PCR and serological tests provides a solution to many of the diagnostic challenges (Gwida et al., 2011). To determine the causative species, bacterial culturing from milk, blood or tissues of infected animals is performed to recover bacterial isolates. For *B. melitensis*, subsequent testing is required to distinguish the three biovars that are traditionally assessed in characterizing this species.

Brucellosis is a public health concern throughout the Greater Middle East (Pappas and Memish, 2007) and has been considered “hyperendemic” in Saudi Arabia with ~8,000 reported cases per annum (Memish and Mah, 2001). Comprehensive reporting of the disease throughout the region has been elusive due to limited public health infrastructure in many countries. Refai (2002) documented that brucellosis was ubiquitous throughout the Near East, with highest human incidence in Saudi Arabia, Iran, Syria, Jordan, and Oman. In fact, Western Asia contains among the highest incidence of brucellosis globally (Pappas et al., 2006). Human exposure to brucellosis from camels occurs primarily from contaminated milk (Shimol et al., 2012; Garcell et al., 2016). More broadly across other animal hosts, brucellosis infections most often occur in people working in close contact with animal tissues

such as slaughterhouse workers, veterinarians, and farmers (Kaufmann et al., 1980; Whatmore, 2009). Determining the genetic diversity of *B. melitensis* in camels would provide valuable information about disease dispersal and transmission among camels, goats, and sheep in endemic areas, and particularly help better understand the role of camels in human infections.

As part of a brucellosis control program, we collected animal samples from routine surveillance activities. Tissues or bodily fluids were collected and isolates of *B. melitensis* were recovered from camels, goats, sheep, and cattle in the Dhofar governorate of Oman, an area with the highest brucellosis prevalence in the country (El Tahir and Nair, 2011). In 1996, a brucellosis control program that implemented both vaccination and culling of infected animals was initiated in the Dhofar region. As a part of an animal disease surveillance system, the regional Brucellosis Diagnostic Lab in Salalah, Dhofar identified all *Brucella* species that were involved in animal brucellosis cases. Because *B. melitensis* isolates from this region are not well characterized, we took two approaches to assess genetic relationships. First, we placed these isolates into a global phylogeny using single nucleotide polymorphism (SNP)-based genotyping assays specific to major evolutionary lineages of *B. melitensis*. We then genotyped a subset of these samples using multilocus variable number tandem repeats analysis (MLVA), following Huynh et al. (2008), to confirm their placement into well characterized clades. Our results suggest the genetic lineage of *B. melitensis* isolates in camels in Oman extends from North Africa into the Arabian Peninsula.

MATERIALS AND METHODS

Aborted fetuses, placental membranes and vaginal swabs/discharge from aborted animals, and milk secretions and blood from suspected animal brucellosis cases were collected in the Dhofar governorate of southwestern Oman. Samples were handled under BSL-3 containment at the Animal Health Research Center, Ministry of Agriculture and Fisheries, Sultanate of Oman. Putative *Brucella* samples were inoculated on sheep blood agar plates together with *Brucella* selective supplement (SR 0083; Oxoid, Hampshire, UK) and 2.5% glucose. The plates were incubated at 37°C with (10%) or without CO₂ for 7 days. Colonies were presumptively identified as *Brucella* by morphology and Gram staining and further biotyped using standard microbiological lab procedures (Alton et al., 1988; OIE, 2012). *Brucella* genus and species identification was confirmed by PCR (Hinic et al., 2008). Thirty-four isolates of *B. melitensis* were recovered from four animal species: camels ($n = 15$), goats ($n = 8$), cattle ($n = 7$), and sheep ($n = 4$) from 1997 to 2010 (Table 1). These samples are stored in the *Brucella* repository of the Animal Health Research Center. Twenty-hour individual broth cultures ($\sim 2 \times 10^9$ /ml) were pelleted by centrifugation (7,500 rpm) for 10 min and genomic DNA was extracted and purified using Qiagen DNeasy Blood and Tissue Kits (Hilden, Germany) following the manufacturer’s protocol for Gram-negative bacteria.

TABLE 1 | Characteristics of 27 *Brucella melitensis* isolates collected from livestock in Dhofar governorate, Oman.

Year	Collection source	Animal	Location	Catalase	Oxidase	Urease	H ₂ S prod.	CO ₂ req.	Growth on dyes		Phage lysis		Agglutination with monospecific antisera	
									Basic fuchsin	Thionin	Iz ₁	Wb	A	M
1997	placental membrane	camel	Salalah	+	+	+	-	-	+	-	+	-	-	+
1999	aborted fetus	camel	Salalah	+	+	+	-	-	+	-	+	-	-	+
1999	milk	camel	Taqah	+	+	+	-	-	+	-	+	-	-	+
1999	milk	camel	Taqah	+	+	+	-	-	+	-	+	-	-	+
2003	fetus	camel	Mirbat	+	+	+	-	-	+	-	+	-	-	+
2004	vaginal swab/fetus	camel	Salalah	+	+	+	-	-	+	-	+	+	+	+
2004	milk/vaginal swab	camel	Salalah	+	+	+	-	-	+	-	+	+	-	+
2004	aborted material	camel	Salalah	+	+	+	-	-	+	-	+	+	-	+
2004	aborted membranes	camel	Mirbat	+	+	+	-	-	+	-	+	-	-	+
2004	fetal stomach	camel	Rakhyut	+	+	+	-	-	+	-	+	+	-	+
2004	fetal stomach	camel	Dalkut	+	+	+	-	-	+	-	+	-	-	+
2004	fetus	camel	Rakhyut	+	+	+	-	-	+	-	+	+	-	+
2005	milk	camel	Thumrayt	+	+	+	-	-	+	-	+	-	-	+
2005	milk	camel	Thumrayt	+	+	+	-	-	+	-	+	-	-	+
2007	stomach content fetus	camel	Muqshin	+	+	+	-	-	+	-	+	-	-	+
1997	fetus (stomach/lungs)	sheep	Mirbat	+	+	+	-	-	+	-	+	-	-	+
1997	fetus	cow	Taqah	+	+	+	-	-	+	-	+	-	-	+
1997	fetus	sheep	Taqah	+	+	+	-	-	+	-	+	-	-	+
1997	fetus	sheep	Taqah	+	+	+	-	-	+	-	+	-	-	+
1997	vaginal discharge	cow	Salalah	+	+	+	-	-	+	-	+	-	-	+
1997	fetus	sheep	Mirbat	+	+	+	-	-	+	-	+	-	-	+
1998	milk /vaginal discharge	cow	Unknown	+	+	+	-	-	+	-	+	-	-	+
1998	milk	cow	Unknown	+	+	+	-	-	+	-	+	-	-	+
1999	fetus	goat	Shalim	+	+	+	-	-	+	-	+	-	-	+
2000	fetus	cow	Unknown	+	+	+	-	-	+	-	+	-	-	+
2000	vaginal discharge	cow	Unknown	+	+	+	-	-	+	-	+	-	-	+
2000	vaginal discharge	cow	Unknown	+	+	+	-	-	+	-	+	-	-	+

Biotyping indicated that all 27 samples were biovar 1. Seven additional *B. melitensis* isolates from blood samples from goats were also collected from Saham in the Al Batinah North Governorate in 2010, but were not biotyped.

A sub-set of MLVA profiles derived from geographically diverse *B. melitensis* isolates causing human infection was generated at the U.S. Centers for Disease Control and Prevention (CDC) and used in the analysis to understand the distribution of *B. melitensis* genotypes in the region. Samples originating from Egypt with the naming designation starting with “E” were collected from an acute febrile illness surveillance study in Egypt as described by Afifi et al. (2005) and a MLVA study of this sub-set of isolates is described by Tiller et al. (2009). The remainder of the patient samples came from reference diagnostic specimens or were recovered from outbreak or support testing by the CDC. Samples were de-identified prior to analyses. Isolation and DNA extraction methods followed those detailed in Tiller et al. (2009). Three reference strains (16M, 63/9, Rev-1) came from the CDC strain collection but their complete culture history is not known. These strains were MLVA genotyped using the actual isolates rather than using the genome sequence. All strains were minimally passaged after collection from human or animal sources. All culture and manipulation of *Brucella* isolates were conducted in BSL-3 conditions.

To develop a *B. melitensis* SNP genotyping assay, we conducted an *in silico* analysis of 29 *B. melitensis* genomes that were then available in GenBank and generated a phylogenetic tree using Northern Arizona SNP Pipeline (NASP) (Sahl et al., 2016; **Figure 1**). We used default parameters for SNP calling for each genome, which included a minimum of 10X coverage at a locus, at least 90% consensus for a SNP allele, and the requirement that the SNP locus was present in all genomes (i.e., no missing data).

Using these genome sequences, flanking regions were aligned using Sequencher 5.0, and Melt-MAMA (Mismatch Amplification Mutation Assays) were designed (Birdsell et al., 2012) targeting at least two randomly selected SNPs on each major branch (**Table 2**). Changes to primer base composition are detectable in melt-curve analysis, allowing differential fluorescence to determine the allele. Using DNA from the 34 isolates from Omani livestock, we performed Real-Time PCR with SYBR Green incorporation on an Applied Biosystems 7900HT Fast Real-Time PCR system. We ran 5 μ L reactions with 1 μ L DNA standardized to 2 ng/ μ L, when possible, and 4 μ L of PCR reagents. Final concentration per reaction was 1X ABI SYBR Green Universal PCR Master Mix, and 0.15 μ M each of the derived MAMA primer, ancestral MAMA primer, and reverse consensus primer. In practice this converts to 1.28 μ L molecular grade water, 2.5 μ L of 2X Universal PCR Master mix, and 0.08 μ L each of the three primers at 10 μ M each. In melt-MAMA reactions, the derived or ancestral primer containing the SNP allele more effectively amplifies in a competing reaction. Thermocycling conditions were as follows: initial UNG activation of 2 min at 50°C, a hot start of 10 min at 95°C, followed by 40 PCR cycles of 15 s at 95°C for denaturation and 1 min at 60°C for annealing, and a final stage of 15 s at 95°C, 15 s at 60°C, and 15 s at 95°C. Alleles were readily distinguished by the melting step and were confirmed with positive controls for each allele state (Birdsell et al., 2012). The SNP genotyping assays were run on all 34 Omani livestock *B. melitensis* samples.

We also performed MLVA on the 15 camel isolates following the methods of Huynh et al. (2008). Briefly, this is a 15 locus

VNTR panel that uses four multiplex PCRs with fluorescently labeled forward primers (6-FAM, NED, PET, or VIC) and unlabeled reverse primers. Fragment sizes for each locus were visualized by capillary electrophoresis on an ABI 3130 Genetic Analyzer and converted to a repeat number corresponding to each fragment size using the LIZ 1200 size standard in GeneMapper version 4.0. As detailed by Tiller et al. (2009), the MLVA approach we used compares favorably to the more widely used MLVA approach (Le Fleche et al., 2006), although the latter has an expansive database of MLVA genotypes (<http://mlva.u-psud.fr/brucella/>).

RESULTS

In this work, we used SNPs discovered in whole genome comparisons to develop multiple SNP assays that distinguish six major branches in *B. melitensis*. We present details on the assays that provided the greatest peak separation for SNPs found on each branch (**Table 2**). Of particular interest to this study was the phylogenetic placement of isolates from Omani livestock; all 34 of these Omani isolates are part of the clade on the assay branch 2 (**Figure 1**). The finding that Omani livestock samples all came from a distinct branch in the *B. melitensis* phylogeny indicates that these animals all contain relatively closely related isolates from a single lineage.

SNP analyses indicate that all of our *B. melitensis* isolates from Omani camels belong to a distinct clade that also contains isolates originating in Africa (Nigeria, Chad, Tanzania). This key finding was unexpected, as one would predict that isolates from the Arabian Peninsula would be part of the E. Mediterranean lineage that predominates the region (Gyuranecz et al., 2016). Thus, SNP analysis indicates that Omani livestock isolates are part of a group of *B. melitensis* that is related to isolates from Africa and distantly related to most other isolates from the Middle East. Moreover, it suggests that the lineages of *B. melitensis* in Egypt and probably throughout much of N. Africa are distinct from most strains from the rest of the Middle East. Our SNP assays also identify two major groups within the E. Mediterranean clade, branches 4 and 5, suggesting substructure within this group. Interestingly, the African clade isolates are more closely related to isolates from the Americas clade than the E. Mediterranean clade in this rooted tree, a pattern not seen in MLVA (Gyuranecz et al., 2016), likely due to the higher resolution of whole genome sequencing.

MLVA results were compared to our database of MLVA genotypes from the Middle East (Huynh et al., 2008; Tiller et al., 2009). We utilized all MLVA genotypes from the African clade and a representative sample of genotypes from the E. Mediterranean and Americas clades (**Table 3**). A fourth lineage, W. Mediterranean, is not part of our collection, nor was it detected in our sampling so was not included in our phylogeny. The W. Mediterranean clade is largely limited to Italy (Garofolo et al., 2013) but does occur in other countries, including along the Mediterranean (Lounes et al., 2014). Low DNA quality prevented us from running MLVA on the 12 other animal isolates from Oman but this DNA was still of sufficient quality to SNP-based analysis on Real-Time PCR due to the

TABLE 2 | Assay design parameters for primer sets targeting 6 major branches of *Brucella melitensis*.

Branch	Reference genome position	SNP state	Primer	5'→3'	State	% GC content	Primer Tm°C	Primer length (bp)	Amplicon length (bp)	Amplicon Tm°C
1	6028	A/G	F1	ggggcggggcggggcCCGGCGAAATGCTGGCGaTa	D	60	56	20	42	74
			F2	CCGGCGAAATGCTGGCGtTg	A	65	58	20		
			C	GATGCGTATAGCCTTCCTCGC	C	57	56	21		
2	1169400	A/G	F1	ggggcggggcggggcGCAGAAGCGCACTGGAATATgTa	D	48	55	23	58	72
			F2	GCAGAAGCGCACTGGAATATaTg	A	48	55	23		
			C	GGTAAATATGCTGTGCTGTACAGGG	C	44	58	27		
3	1127740	C/T	F1	ggggcggggcggggcCGTAACAGGCAGCAATCTGCAGTc	D	54	59	24	50	73
			F2	CGTAACAGGCAGCAATCTGCACtT	A	50	57	24		
			C	TCAAATATTAAGGGTCGTCCGG	C	55	54	25		
4	870030	T/C	F1	ggggcggggcggggcCGCGGGTTTCTTCATCCAGAAgt	D	63	55	24	51	75
			F2	CGCGGGTTTCTTCATCCAGAAgGc	A	58	61	24		
			C	GCCGGGCGACATCATAGATCG	C	64	60	22		
5	842276	T/C	F1	ggggcggggcggggcGCGCCTCTGCTGCCTcCt	D	74	60	19	49	72
			F2	GCGCCTCTGCTGCCTaCc	A	74	59	29		
			C	GAATCATTATCGTTTCTAGATACATAAAGCC	C	34	56	29		
10	747768	A/C	F1	ggggcggggcggggcGGCGCGGAGCCATATTGgAa	D	60	56	20	55	73
			F2	GGCGCGGAGCCATATTGcAc	A	65	58	20		
			C	CCTTAACCTAGCAATTGGAGGAAC	C	46	58	26		

Reference genome is 16 M (NCBI RefSeq accession numbers NC_003317.1 and NC_003318.1). Branch numbers correspond to branch labels in **Figure 1**. State column refers to Derived (D), Ancestral (A), and Consensus (C), state of the SNP targeted by that specific primer. Tm is the melting temperature for the primers or the amplicon.

smaller amplicons sizes and higher sensitivity of these Real-Time assays (Birdsell et al., 2012). The 10 most stable of the 15 Variable Number Tandem Repeat (VNTR) loci were used in our analyses (VNTRs: 1, 3, 7, 14, 16, 20, 21, 25, 27, 28). Limiting VNTR loci to the most stable markers, or placing greater weighting on these markers, is a common practice in *Brucella* MLVA (e.g., Al Dahouk et al., 2007a). Such a practice reduces homoplasy and allows for understanding deeper phylogenetic relationships but potentially sacrifices more recent epidemiological connections (Keim et al., 2004); this potential loss of resolution was not a concern for our study because we were focused on these deeper connections.

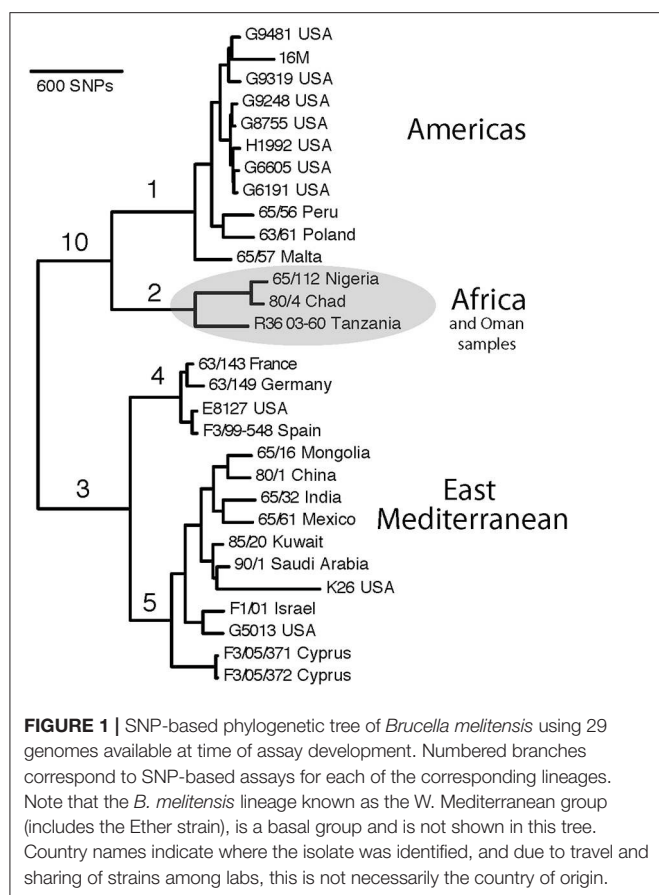
Three distinct lineages of *B. melitensis* were found in our sampling, consistent with geographic groupings of Americas, E. Mediterranean, and Africa clades. Al Dahouk et al. (2007a) first identified the Americas and E. Mediterranean clades but used a different MLVA genotyping scheme (Le Fleche et al., 2006). Subsequent work by Gyuranecz et al. (2016), identified another lineage, the Africa clade. This consistency between the two MLVA schemes, as well as support from whole genome analyses, suggests that either scheme is capable of identifying these major lineages although differentiation of the Africa clade is more pronounced with the Huynh et al. (2008) MLVA scheme. VNTR genotypes were compared using minimum spanning trees in Phylovis 2.0 (Nascimento et al., 2017).

Using MLVA genotyping, the VNTR diversity we observed in these 15 camel isolates divide into 3–6 distinct lineages, depending on clustering criteria (**Figure 2**). Use of all 15 MLVA loci gave similar overall patterns (data not shown).

All camel isolates from Oman, except for one highly similar to a human isolate from Qatar (Q7), are closely related to samples from human patients from Egypt, typically differing from each other by only 1–3 VNTR mutations; indicating that highly related strains circulating across the region in both livestock and humans. Our MLVA results also support the SNP analyses that the Omani camel isolates have greatest similarity to *B. melitensis* isolates from North Africa. Omani camel isolates are related to isolates originating from humans in Egypt, sometimes separated by only one VNTR repeat. Epidemiological trace back may allow for identification of these potential animal to human transmission events. We also note the presence of African lineage isolates in other countries in the region, including Libya, Israel, Syria, Turkey, and Qatar.

DISCUSSION

Our study highlights the presence of a unique lineage of *B. melitensis* in the Middle East, provides assays to quickly identify the strain types circulating and causing animal and human brucellosis in the region, and suggests that substantial diversity remains to be uncovered in Africa. The SNP assays we designed, particularly those for branch 2, allow for rapid identification of African lineage strains and thus can be used to focus on finding new genetic variation among this poorly sampled group. When samples are identified as part of the African lineage, MLVA can then be utilized for higher resolution



analyses, such as understanding the relationships among African isolates and for epidemiological investigations.

SNP Genotyping

The SNP-based results from the whole genome analyses and SNP genotyping support the finding that an African lineage of *B. melitensis* exists in the Arabian Peninsula (e.g., Oman and Qatar), and other nearby countries such as Israel, Turkey, and Syria. Although the African lineage appears to be uncommon elsewhere, it nonetheless has been introduced into many Middle Eastern countries. The two SNP assays specific for branch 2 can quickly identify isolates that are part of this unique African lineage, allowing for a determination of the spread of this clade.

We emphasize that the African clade is a phylogenetic assignment and not a geographic one, and that not all isolates from Africa will be a part of this clade. Accordingly, isolates from Algeria in western North Africa were predominantly from the W. Mediterranean clade (Lounes et al., 2014), suggesting a connection to Europe (especially Italy) rather than the rest of North Africa or other parts of the Middle East. Our SNP findings, and those of Georgi et al. (2017), highlight the power of whole genome analyses and this genomic approach is able to clearly distinguish isolates from the African and E. Mediterranean clades as evolutionarily distinct lineages.

MLVA Genotyping

The MLVA groupings show broad and consistent geographic representations of MLVA types from the Americas, E. Mediterranean clade (consisting primarily of West/Central Asia and Middle Eastern isolates), and Africa. Although this method uses different loci than SNP approaches, these groupings match those from the SNP-based genotyping. Using the MLVA method of Le Fleche et al. (2006), *B. melitensis* isolates from the United Arab Emirates from camels, cattle, and a goat had genotypes from the E. Mediterranean clade but also contained isolates from four camels and a gazelle from the African clade (Gyuranecz et al., 2016). Indeed, the expectation for *B. melitensis* isolates collected from humans or livestock from the Arabian Peninsula and most of the Middle East is membership in the E. Mediterranean clade (Al Dahouk et al., 2007a; Kattar et al., 2008; Kilic et al., 2011). MLVA and whole genome analyses indicate that the E. Mediterranean clade is the principal lineage in the region, continuing from the Middle East along the Mediterranean and into and throughout Asia (Jiang et al., 2011; Tan et al., 2015; Tay et al., 2015). Whole genome comparisons from brucellosis patients infected in the Middle East support this predominance of the E. Mediterranean clade but also identify three isolates of Somali origin from an Africa clade (Georgi et al., 2017). Despite its broad sampling and thousands of genotypes for *B. melitensis*, the MLVA database (<http://mlva.u-psud.fr/brucella/>) contains few representatives from North Africa so it appears to be currently missing much of this genetic diversity. We encourage researchers using the Le Fleche MLVA scheme to genotype samples from this region for a better global understanding of this lineage, after first using our SNP-based assays to identify this clade.

Resolving Apparent Inconsistencies

Our findings challenge common approaches used in *Brucella* epidemiology. While we detail our results from traditional phenotyping approaches, these data are typically not informative for understanding the genetic relationships of isolates within *B. melitensis*. For example, distinguishing the three biovars of *B. melitensis* provides limited resolution when attempting to establish epidemiological links between outbreaks; likely due to the limited association between genotype and phenotype (biovar) in this species (Whatmore et al., 2016). In fact, isolates from biovars 1, 2, and 3 can be closely related genetically (e.g., Jiang et al., 2011) and isolates from the same biovar can be distantly related and from evolutionarily distinct clades (e.g., De Massis et al., 2015). Apparent discrepancies also occur for the country of origin for some isolates; a handful of SNP-based and MLVA genotypes appear to not match the expected clade corresponding to the region. For example, in the SNP phylogeny an isolate from Poland is in the Americas clade, and samples from the USA are in the E. Mediterranean clade. Such discordance is expected. First, as mentioned previously these groupings are phylogenetic assignments and should not be misconstrued as geographic origins. In addition, epidemiological histories of various strains are not always precisely known and the country names may indicate where the isolate was identified and not necessarily the country of origin. Finally, international travel of patients infected

TABLE 3 | MLVA-10 genotypes for 221 isolates of *Brucella melitensis* from the Middle East. Isolates from additional regions added for context.

Sample ID	Country	Host	Lineage	VNTR locus									
				21	14	28	1	16	7	3	27	20	25
1652	Afghanistan	goat	E. Med.	100	123	191	267	225	320	322	389	453	496
1657	Afghanistan	sheep	E. Med.	100	123	215	219	225	308	322	413	453	496
1761	Afghanistan	sheep	E. Med.	100	123	191	267	225	320	322	389	453	496
2011756220	Afghanistan	human	E. Med.	100	123	191	202	225	320	322	381	453	496
2011756221	Afghanistan	goat	E. Med.	100	123	191	219	225	320	322	381	453	496
2013004349	Afghanistan	human	E. Med.	100	123	191	235	225	320	322	381	453	496
25	Afghanistan	human	Americas	100	123	174	227	258	327	370	373	453	496
27	Afghanistan	human	Americas	100	123	174	227	258	327	370	373	453	496
29	Afghanistan	human	Americas	100	123	174	227	258	327	370	373	453	496
31	Afghanistan	human	Americas	100	123	174	227	258	327	370	373	453	496
2008010924	Bosnia	human	E. Med.	100	123	208	227	225	320	386	438	453	496
2011756294	Bosnia	human	E. Med.	100	123	232	251	225	320	354	413	453	496
2008018505	Egypt	human	Africa	100	123	215	219	250	320	403	413	441	496
E1-ABS-9258	Egypt	human	Africa	100	123	215	300	250	316	370	397	441	496
E10-ALX-0769	Egypt	human	Africa	100	123	184	194	250	316	386	446	441	496
E11-ASW-0309	Egypt	human	Africa	100	123	215	227	250	316	419	389	441	496
E12-ABS-9517	Egypt	human	Africa	100	123	191	219	250	316	394	430	441	496
E13-FAY-9671	Egypt	human	Africa	100	123	223	235	250	316	394	397	441	496
E14-BEN-0044	Egypt	human	Africa	100	123	208	314	250	316	394	397	441	496
E15-SHB-10112	Egypt	human	Africa	100	123	174	235	250	316	419	430	441	496
E16-ZAG-0133	Egypt	human	Africa	100	123	215	243	250	316	419	405	441	496
E17-PRS-0241	Egypt	human	Africa	100	123	199	235	250	316	460	413	441	496
E18-SHB-1482	Egypt	human	Africa	100	123	215	243	250	316	403	430	441	496
E19-ALX-0996	Egypt	human	Africa	100	123	199	219	250	316	444	413	441	496
E2-MAL-9273	Egypt	human	Africa	100	123	208	219	250	316	411	430	441	496
E20-MAL-0941	Egypt	human	Africa	100	123	215	227	250	316	435	405	441	496
E21-ABS-10208	Egypt	human	Africa	100	123	208	211	250	316	330	381	441	496
E22-QEN-0166	Egypt	human	Africa	100	123	223	267	250	316	386	397	441	496
E23-ABS-10654	Egypt	human	Africa	100	123	199	243	250	316	338	381	441	496
E24-ALX-1734	Egypt	human	Africa	100	123	199	243	250	316	354	405	441	496
E25-MAL-1462	Egypt	human	Africa	100	123	191	235	250	316	419	413	441	496
E26-SHB-2267	Egypt	human	Africa	100	123	208	243	250	316	378	430	441	496
E27-ALX-2000	Egypt	human	E. Med.	95	123	215	219	217	316	322	413	393	496
E28-SHB-2340	Egypt	human	Africa	95	123	191	227	250	316	322	405	393	496
E29-ASW-1381	Egypt	human	Africa	100	123	199	211	250	316	403	381	441	496
E3-SHB-0395	Egypt	human	Africa	100	123	199	219	250	316	346	405	441	496
E30-AST-0977	Egypt	human	Africa	100	123	199	267	258	316	394	397	441	496
E31-AST-1030	Egypt	human	E. Med.	95	123	215	243	217	316	322	381	425	496
E32-QEN-0364	Egypt	human	Africa	100	123	215	227	250	316	403	373	441	496
E33-ALX-2307	Egypt	human	Africa	100	123	199	267	250	316	419	389	441	496
E34-MAL-1821	Egypt	human	Africa	100	123	191	251	250	316	370	413	441	496
E35-SHB-2580	Egypt	human	Africa	100	123	208	235	250	316	452	430	441	496
E36-ALX-2198	Egypt	human	Africa	100	123	191	243	250	316	435	397	441	496
E37-QEN-0388	Egypt	human	Africa	100	123	223	243	250	316	411	373	441	496
E38-ASW-1553	Egypt	human	Africa	100	123	199	251	250	316	394	389	441	496
E39-ALX-0077	Egypt	human	Africa	100	123	208	283	250	316	428	389	441	496
E4-QEN-0062	Egypt	human	Africa	100	123	223	219	250	316	386	373	441	496
E40-ABS-9024	Egypt	human	Africa	100	123	208	211	250	316	419	389	441	496
E41-SOH-9085	Egypt	human	Africa	100	123	248	243	250	316	346	381	441	496

(Continued)

TABLE 3 | Continued

Sample ID	Country	Host	Lineage	VNTR locus									
				21	14	28	1	16	7	3	27	20	25
E42-SOH-0002	Egypt	human	Africa	100	123	248	243	250	316	346	381	441	496
E43-SHB-9203	Egypt	human	Africa	100	123	199	227	250	316	419	397	441	496
E44-SHB-9204	Egypt	human	Africa	100	123	208	211	258	316	419	397	441	496
E45-SHB-0492	Egypt	human	Africa	100	123	191	227	250	316	468	405	441	496
E46-SHB-0496	Egypt	human	Africa	100	123	191	267	250	316	403	430	441	496
E47-ZAG-0127	Egypt	human	Africa	100	123	199	235	258	316	444	397	441	496
E48-MAL-0966	Egypt	human	Africa	100	123	208	219	250	316	403	397	441	496
E49-MAL-0958	Egypt	human	Africa	100	123	215	243	250	316	419	397	441	496
E5-ABS-9281	Egypt	human	Africa	100	123	191	283	250	316	419	446	441	496
E50-SHB-1580	Egypt	human	Africa	100	123	199	227	250	316	346	430	441	496
E51-SHB-1572	Egypt	human	Africa	100	123	191	243	250	316	354	430	356	496
E52-FAY-10244	Egypt	human	Africa	100	123	191	291	258	316	370	389	441	496
E53-FAY-10257	Egypt	human	Africa	100	123	191	219	258	316	394	389	441	496
E54-BEN-0182	Egypt	human	Africa	100	123	191	227	250	316	452	381	441	496
E55-MAL-1111	Egypt	human	Africa	100	123	215	227	250	316	444	381	441	496
E56-SHB-2081	Egypt	human	Africa	100	123	191	194	250	316	394	389	441	496
E57-ASW-10776	Egypt	human	Africa	100	123	208	202	250	316	411	389	441	496
E58-SHB-2177	Egypt	human	Africa	100	123	199	259	250	316	394	397	441	496
E59-ASW-1220	Egypt	human	Africa	100	123	208	259	250	316	386	405	441	496
E6-SHB-0407	Egypt	human	Africa	100	123	199	267	250	316	403	405	441	496
E60-ASW-1237	Egypt	human	Africa	100	123	199	211	250	316	403	381	441	496
E61-AST-1053	Egypt	human	Africa	100	123	208	235	258	316	394	397	441	496
E62-AST-1008	Egypt	human	Africa	100	123	208	194	258	316	394	397	441	496
E63-AST-1085	Egypt	human	Africa	100	123	199	243	258	316	403	397	441	496
E64-ALX-4	Egypt	human	Africa	100	123	191	202	250	316	403	397	441	496
E65-ALX-107	Egypt	human	Africa	100	123	215	235	250	316	435	389	441	496
E66-MAL-104	Egypt	human	Africa	100	123	199	259	250	316	468	397	441	496
E67-MAL-135	Egypt	human	Africa	100	123	208	243	250	316	460	381	441	496
E68-ABS-52	Egypt	human	Africa	100	123	208	235	258	316	362	389	441	496
E69-ABS-157	Egypt	human	Africa	100	123	199	235	250	316	428	413	441	496
E7-ALX-0404	Egypt	human	Africa	100	123	208	283	250	316	378	397	441	496
E70-ABS-49	Egypt	human	Africa	100	123	199	251	250	316	394	446	441	496
E71-AFI-ABS-134	Egypt	human	Africa	100	123	215	211	217	316	452	413	441	496
E72-MAL-305	Egypt	human	Africa	100	123	208	219	250	316	378	430	441	496
E73-ALX-458	Egypt	human	Africa	100	123	199	259	250	316	386	389	441	496
E74-MAL-293	Egypt	human	Africa	100	123	208	276	250	316	370	413	441	496
E75-ABS-93	Egypt	human	Africa	100	123	199	235	250	316	444	413	441	496
E76-ABS-211	Egypt	human	Africa	100	123	199	235	258	316	403	389	405	496
E77-ALX-467	Egypt	human	Africa	100	123	199	235	250	316	370	389	441	496
E78-ALX-468	Egypt	human	Africa	100	123	208	211	258	316	386	397	441	496
E79-MAL-335	Egypt	human	Africa	100	123	215	211	250	316	386	413	441	496
E8-SHB-0676	Egypt	human	Africa	100	123	191	259	250	316	419	389	441	496
E80-MAL-353	Egypt	human	Africa	100	123	199	219	250	316	394	389	441	496
E81-ALX-535	Egypt	human	Africa	100	123	199	259	250	316	394	389	441	496
E82-ALX-532	Egypt	human	Africa	100	123	191	211	258	316	411	381	441	496
E83-ASW-84	Egypt	human	Africa	100	123	199	251	250	316	378	381	441	496
E9-FAY-9445	Egypt	human	Africa	100	123	199	267	250	316	419	389	441	496
3000409149	Ethiopia	human	Americas	100	123	215	194	258	327	362	381	453	496
2010022407	Greece	human	E. Med.	100	123	215	235	225	320	370	405	453	498

(Continued)

TABLE 3 | Continued

Sample ID	Country	Host	Lineage	VNTR locus									
				21	14	28	1	16	7	3	27	20	25
2006012884	Iran	human	E. Med.	100	123	208	243	225	320	322	397	453	496
2006012885	Iran	human	E. Med.	100	123	208	243	225	320	322	397	453	496
2010022413	Iran	human	Americas	100	123	174	219	258	320	362	405	453	496
3000027166	Iran	human	E. Med.	100	123	199	227	225	320	322	413	453	496
2004017806	Iraq	human	E. Med.	100	123	191	219	225	320	322	413	453	496
2008724248	Iraq	human	E. Med.	100	123	215	211	225	320	338	430	453	496
2012005317	Iraq	human	E. Med.	100	123	191	251	225	320	362	381	453	496
2012017239	Iraq	human	Intermediate	100	123	184	211	225	320	386	389	453	496
2013746956	Iraq	human	E. Med.	100	123	208	219	225	320	354	389	453	496
2013833054	Iraq	human	Intermediate	100	123	199	211	225	320	346	389	453	496
2014001382	Iraq	human	Intermediate	100	123	199	194	225	320	386	397	453	496
2014001698-2	Iraq	human	Intermediate	100	123	199	194	225	320	386	397	453	496
2014001698-3	Iraq	human	Intermediate	100	123	199	194	225	320	386	397	453	496
1988035349	Israel	human	Africa	100	123	208	211	225	320	378	389	441	496
1988035350	Israel	human	E. Med.	100	123	191	235	225	320	362	405	453	496
1988035351	Israel	human	E. Med.	100	123	199	219	225	320	386	389	453	496
1988035352	Israel	human	E. Med.	100	123	199	219	225	320	386	381	453	496
1988035353	Israel	human	E. Med.	100	123	199	219	225	320	386	389	453	496
1988035354	Israel	human	Africa	100	123	208	202	225	320	378	389	441	496
1988035355	Israel	human	E. Med.	100	123	191	235	225	320	362	405	453	496
1988035356	Israel	human	E. Med.	100	123	191	235	225	320	362	405	453	496
1988035357	Israel	human	E. Med.	100	123	191	235	225	320	362	405	453	496
1988035358	Israel	human	E. Med.	100	123	199	219	225	320	386	389	453	496
1988035359	Israel	human	E. Med.	100	123	191	235	225	320	362	405	453	496
1988035360	Israel	human	Intermediate	100	123	199	211	225	320	386	389	453	496
1988035361	Israel	human	Africa	100	123	199	211	225	320	378	389	453	496
1988035362	Israel	human	Intermediate	100	123	199	211	225	320	386	389	453	496
2014002005	Israel	human	E. Med.	100	123	208	227	225	320	322	389	453	496
2002018756	Italy	human	Africa	100	123	199	243	250	320	394	405	441	496
2003018302	Italy	human	Africa	100	123	199	243	250	320	394	405	441	496
3000015492	Jordan	human	E. Med.	100	123	223	202	225	320	362	373	453	496
3000015245	Kazakhstan	human	E. Med.	100	123	199	251	225	320	322	405	453	496
2012016719	Lebanon	human	E. Med.	100	123	191	276	225	320	378	389	453	496
L1	Libya	human	Africa	100	123	199	267	258	316	394	397	441	496
2011756293	Mexico	human	Americas	100	123	174	202	250	320	362	381	453	496
2012005445	Mexico	human	Americas	100	123	174	235	250	327	362	389	453	496
2013005190	Mexico	human	Africa	100	115	184	243	241	320	403	373	441	478
2013005440	Mexico	human	Americas	100	123	174	227	250	327	354	389	453	496
2013007561	Mexico	human	Americas	100	123	174	227	241	327	354	389	453	496
2013746874	Mexico	human	Americas	100	123	174	235	241	327	346	389	453	496
2014001235	Mexico	human	Americas	100	123	174	227	250	320	354	413	453	496
2014001327	Mexico	human	Americas	100	123	174	202	241	327	362	389	453	496
3000015243	Mexico	human	Americas	100	123	174	227	250	327	354	381	453	496
3000015269	Mexico	human	Americas	100	123	174	227	241	327	346	389	453	496
3000023891	Mexico	human	Americas	100	123	174	219	250	327	362	381	453	496
3000023892	Mexico	human	Americas	100	123	174	235	241	327	346	389	453	496
3000023893	Mexico	human	Americas	100	123	174	219	250	327	362	381	453	496
3000023969	Mexico	human	Americas	100	123	174	235	250	327	394	413	453	496
3000026676	Mexico	human	Americas	100	123	174	202	250	327	338	389	453	496

(Continued)

TABLE 3 | Continued

Sample ID	Country	Host	Lineage	VNTR locus									
				21	14	28	1	16	7	3	27	20	25
3000050553	Mexico	human	Americas	100	123	174	211	258	327	362	373	453	496
3000050738	Mexico	human	Americas	100	123	174	211	258	327	362	373	453	496
3000404015	Mexico	human	Americas	100	123	174	267	250	327	370	373	453	496
3000404142	Mexico	human	Americas	100	123	174	227	250	327	354	405	453	496
3000407000	Mexico	human	Americas	100	123	174	219	250	327	354	397	453	496
3000496880	Mexico	human	Americas	100	123	174	211	250	327	362	381	453	496
3000496881	Mexico	human	Americas	100	123	174	211	250	327	362	381	453	496
BTRU #1501	Mexico	human	Americas	100	123	174	227	241	327	394	381	453	496
MEX349	Mexico	human	Americas	100	124	175	219	265	325	362	397	453	493
MEX350	Mexico	human	Americas	100	124	175	219	249	325	387	373	453	493
MEX351	Mexico	human	Americas	100	124	175	219	249	325	386	373	453	493
MEX352	Mexico	human	Americas	100	124	175	178	241	325	362	405	453	493
Bruc-VRC-1	Oman	camel	Africa	101	124	191	202	258	318	380	389	440	491
Bruc-VRC-10	Oman	camel	Africa	101	124	199	186	250	318	348	374	440	491
Bruc-VRC-11	Oman	camel	Africa	101	124	199	186	250	316	348	374	440	492
Bruc-VRC-12	Oman	camel	Africa	101	124	199	259	250	316	348	374	440	491
Bruc-VRC-13	Oman	camel	Africa	101	124	207	235	250	318	348	413	440	491
Bruc-VRC-14	Oman	camel	Africa	101	243	199	124	250	317	348	413	440	491
Bruc-VRC-15	Oman	camel	Africa	101	124	191	226	258	316	356	397	440	491
Bruc-VRC-2	Oman	camel	Africa	101	123	191	235	250	318	340	405	440	491
Bruc-VRC-3	Oman	camel	Africa	101	124	191	227	258	318	356	398	440	492
Bruc-VRC-4	Oman	camel	Africa	101	124	191	210	258	318	404	382	440	491
Bruc-VRC-5	Oman	camel	Africa	101	124	199	210	250	301	397	389	440	491
Bruc-VRC-6	Oman	camel	Africa	101	124	207	227	258	318	356	390	440	491
Bruc-VRC-7	Oman	camel	Africa	101	124	199	226	258	318	356	389	439	491
Bruc-VRC-8	Oman	camel	Africa	101	124	207	227	258	317	356	389	439	491
Bruc-VRC-9	Oman	camel	Africa	101	124	207	227	258	318	356	390	439	492
2010023909	Qatar	human	E. Med.	100	123	191	194	225	320	370	405	453	496
2010023910	Qatar	human	E. Med.	100	123	199	227	225	320	322	405	464	496
2013002770	Qatar	human	Africa	100	123	215	211	250	320	354	397	441	496
Q1-AT-BR-001	Qatar	human	Africa	100	123	215	202	250	316	378	405	441	496
Q10-AT-BR-010	Qatar	human	Africa	100	123	208	211	233	316	322	397	464	496
Q11-AT-BR-011	Qatar	human	E. Med.	100	123	191	227	233	316	346	413	453	496
Q12-AT-BR-012	Qatar	human	E. Med.	100	123	208	219	233	316	322	389	453	496
Q13-AT-BR-013	Qatar	human	Africa	100	123	215	251	250	316	419	389	441	496
Q14-AT-BR-014	Qatar	human	E. Med.	100	123	191	227	233	316	378	389	453	496
Q15-AT-BR-015	Qatar	human	Africa	100	123	199	235	233	316	370	397	453	496
Q16-AT-BR-016	Qatar	human	E. Med.	100	123	191	227	233	316	322	389	464	496
Q17-AT-BR-017	Qatar	human	Africa	100	123	184	267	233	316	378	381	441	496
Q2-AT-BR-002	Qatar	human	Africa	100	123	199	235	233	316	338	397	453	496
Q3-AT-BR-003	Qatar	human	Africa	100	123	215	202	217	316	370	405	441	496
Q4-AT-BR-004	Qatar	human	E. Med.	100	123	191	194	233	316	346	413	453	496
Q5-AT-BR-005	Qatar	human	Africa	100	123	215	202	217	316	370	405	441	496
Q6-AT-BR-006	Qatar	human	Africa	100	123	199	235	258	316	378	397	441	496
Q7-AT-BR-007	Qatar	human	Africa	100	123	232	186	258	316	444	457	441	496
Q8-AT-BR-008	Qatar	human	E. Med.	100	123	199	227	233	316	322	405	453	496
Q9-AT-BR-009	Qatar	human	E. Med.	100	123	191	235	233	316	322	389	464	496
2011756247	reference	type strain 16M	Americas	100	123	174	227	233	327	346	373	453	496

(Continued)

TABLE 3 | Continued

Sample ID	Country	Host	Lineage	VNTR locus									
				21	14	28	1	16	7	3	27	20	25
2011756235	reference	type strain 63/9	E. Med.	100	123	215	267	225	308	322	389	453	496
2010022409	reference	Rev-1 strain	Americas	100	123	174	227	258	327	370	381	453	496
2011019381	Saudi Arabia	human	E. Med.	100	123	232	276	225	320	322	413	464	496
2011756376	Saudi Arabia	human	E. Med.	100	123	208	235	225	320	322	405	464	496
2013008314	Saudi Arabia	human	E. Med.	100	123	199	243	225	320	322	397	453	496
2013008432	Saudi Arabia	human	E. Med.	100	123	199	227	225	320	322	381	453	496
2013012794	Saudi Arabia	human	E. Med.	100	123	215	235	225	320	322	422	464	496
2013016252	Saudi Arabia	human	E. Med.	100	123	199	227	225	320	322	381	453	496
2014003496	Saudi Arabia	human	E. Med.	100	123	223	227	225	320	322	413	464	496
3000015437	Saudi Arabia	human	E. Med.	100	123	191	219	225	320	322	389	453	496
3000015487	Saudi Arabia	human	Americas	100	123	199	227	225	327	386	389	453	496
3000015489	Saudi Arabia	human	E. Med.	100	123	208	235	225	320	322	389	453	496
F4018	Saudi Arabia	human	E. Med.	100	124	207	219	225	317	322	389	452	492
3000358781	Senegal	human	Americas	100	123	174	202	241	320	330	381	453	496
2011756228	Somalia	human	E. Med.	95	123	191	243	225	327	338	389	453	496
2013746792	Somalia	human	E. Med.	95	123	191	243	225	327	338	389	453	496
2013746793	Somalia	human	E. Med.	95	123	191	243	217	327	362	381	453	496
2004017844	Syria	human	Africa	100	123	184	211	225	324	338	397	441	498
2004017845	Syria	human	E. Med.	100	123	199	227	225	320	370	405	441	496
2008724251	Syria	human	Americas	100	123	174	227	250	327	370	381	453	496
2010724533	Syria	human	E. Med.	100	123	208	235	225	320	362	397	453	496
2013746965	Syria	human	Americas	100	123	174	227	258	327	370	373	453	496
2006006287	Turkey	human	Africa	100	123	184	211	233	316	386	430	441	496
2009027624	Turkey	human	E. Med.	100	123	191	202	225	320	346	397	453	496
2013008341	UAE	human	E. Med.	100	123	199	243	225	320	354	413	356	496
3000015259	Uzbekistan	human	E. Med.	100	123	199	243	225	320	322	381	453	496

Country refers to the suspected origin of brucellosis infection although human travel and trade in contaminated animal products may obscure the true origin. Lineage refers to the MLVA branch from **Figure 2**; seven isolates were classified as Intermediate due to genotypes not assigned to one of the three main lineages we investigated (Africa, Americas, E. Mediterranean). VNTR loci follow the numbering of Huynh et al. (2008). Strains not definitively assigned to a lineage were considered Intermediate.

with brucellosis or movement of infected animals may potentially obscure the country of origin unless detailed epidemiological data are available (Al Dahouk et al., 2007b; Garofolo et al., 2013; De Massis et al., 2015; Georgi et al., 2017).

Brucellosis Management

Disease management approaches involving vaccination, treatment with antibiotics, and test-and-slaughter programs for camels can lower disease incidence and even eliminate brucellosis from some farms (Radwan et al., 1995; Abbas and Agab, 2002; Wernery, 2014). Nonetheless, comprehensive elimination of *B. melitensis* in camels from larger regions will require brucellosis management in goats and sheep. Despite calls for the elimination of brucellosis from the Arabian Peninsula for over two decades (Tabbara, 1993), the disease persists throughout the region and indeed continues to be a successful pathogen throughout much of world. High prevalence rates in sheep, goats and cattle, and the hundreds of millions of these animals in the region make brucellosis elimination difficult (Refai, 2002). Although the economic cost of brucellosis to livestock production in Oman is

not well-known, globally the economic burden on both animal and human health is significant and far reaching (Seleem et al., 2010). Understanding historic and contemporary movement of animals infected with brucellosis is an important step in improving disease management strategies.

Brucellosis Movement

The presence of an African lineage from North Africa in the Arabian Peninsula indicates the interconnectedness of livestock in the Greater Middle East, likely due to historical trade and movement between the two regions, although the E. Mediterranean lineage still predominates. Contemporary introductions of *B. melitensis* also appear to occur—the four camels with the African clade genotypes in the United Arab Emirates came from Sudan (Gyuranecz et al., 2016)—connectedness previously suggested by Wernery (2014). Our results also indicate that not all *B. melitensis* isolates from Africa are part of this “Africa” lineage. For example, some samples from Somalia, Kenya, and Egypt appear to be part of the E. Mediterranean clade and Ethiopian and some Egyptian

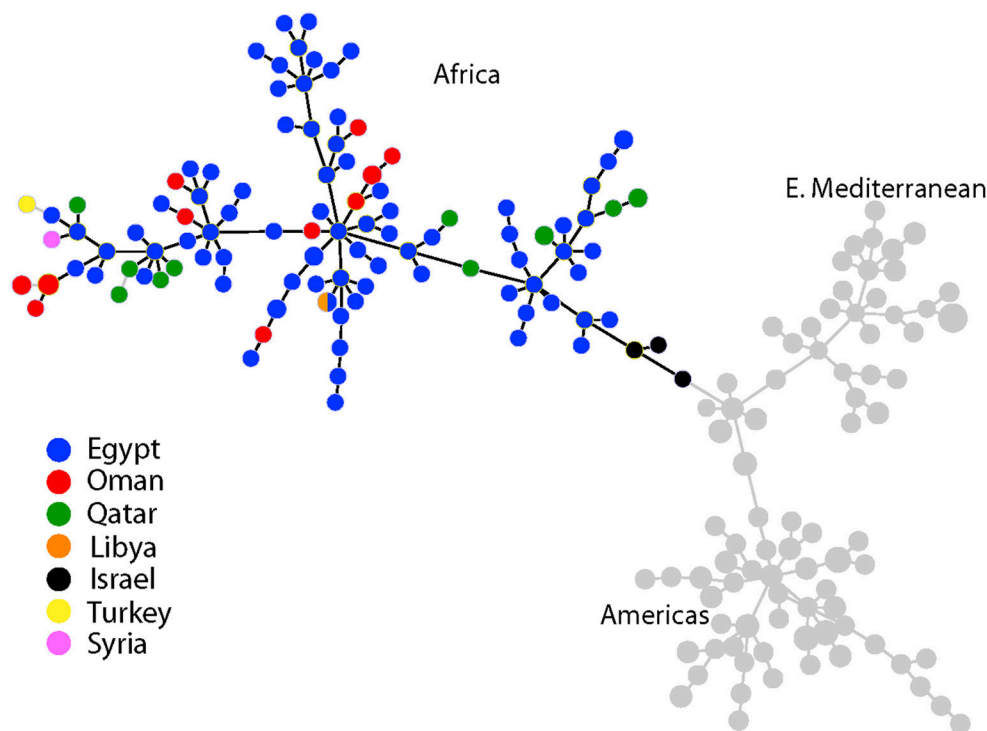


FIGURE 2 | Minimum spanning tree of 221 *Brucella melitensis* isolates based on MLVA-10 genotyping. Country of origin for isolates from the Middle East is represented by the colored circles. Additional isolate details are found in **Table 3**.

samples are part of the Americas clade. Moreover, Lounes et al. (2014) identified isolates from the W. Mediterranean clade in the Maghreb region of Algeria. Even less is known from sub-Saharan Africa, where brucellosis is widespread among livestock (Mcdermott and Arimi, 2002). Clearly, there is tremendous diversity of *B. melitensis* in Africa, potentially due to many introductions of infected livestock from many regions as well as widespread trade. Additional sampling throughout the African continent is needed to better understand the evolutionary history regarding the origins and spread of *B. melitensis* in the region. Although the African lineage may be more localized than the three widely distributed *B. melitensis* clades, substantial undiscovered diversity likely exists, and as we have discovered in Oman, extends beyond the African continent into new lands that have been connected by trade in camels, goats, and sheep.

REFERENCES

- Abbas, B., and Agab, H. (2002). A review of camel brucellosis. *Prev. Vet. Med.* 55, 47–56. doi: 10.1016/S0167-5877(02)00055-7
- Afifi, S., Earhart, K., Azab, M. A., Youssef, F. G., El Sakka, H., Wasfy, M., et al. (2005). Hospital-based surveillance for acute febrile illness in Egypt: a focus on community-acquired bloodstream infections. *Am. J. Trop. Med. Hygiene* 73, 392–399. doi: 10.4269/ajtmh.2005.73.392
- Al Dahouk, S., Le Fleche, P., Nockler, K., Jacques, I., Grayon, M., Scholz, H. C., et al. (2007a). Evaluation of *Brucella* MLVA typing for human brucellosis. *J. Microbiol. Methods* 69, 137–145. doi: 10.1016/j.mimet.2006.12.015

AUTHOR CONTRIBUTIONS

JF, RT, AH, PK, and MS designed the study. MH, AA-R, RT, and MS collected and cultured the samples. JF, FW, BR, KD, and RT analyzed the data. All authors contributed to writing and editing the manuscript.

ACKNOWLEDGMENTS

Funding was provided by the U.S. Department of Homeland Security to PK and JF (HSHQDC-10-C-00139) and by the Agriculture and Fisheries Development Fund (AFDF) of Ministry of Agriculture and Fisheries, Oman. The findings and conclusions in this report are those of the authors and do not necessarily represent the official position of the Centers for Disease Control and Prevention.

- Al Dahouk, S., Neubauer, H., Hensel, A., Schoneberg, I., Nockler, K., Alpers, K., et al. (2007b). Changing epidemiology of human brucellosis, Germany, 1962–2005. *Emerg. Infect. Dis.* 13, 1895–1900. doi: 10.3201/eid1312.070527
- Alton, G. G., Jones, L. M., Angus, R. D., and Verger, J. M. (1988). “Bacteriological methods,” in *Techniques for the Brucellosis Laboratory* (Paris: Institut National de la Recherche Agronomique), 13–61.
- Birdsell, D. N., Pearson, T., Price, E. P., Hornstra, H. M., Nera, R. D., Stone, N., et al. (2012). Melt analysis of mismatch amplification mutation assays (Melt-MAMA): a functional study of a cost-effective SNP genotyping assay in bacterial models. *PLoS ONE* 7:e32866. doi: 10.1371/journal.pone.0032866

- De Massis, F., Ancora, M., Atzeni, M., Rolesu, S., Bandino, E., Danzetta, M. L., et al. (2015). MLVA as an epidemiological tool to trace back *Brucella melitensis* biovar 1 re-emergence in Italy. *Transbound. Emerg. Dis.* 62, 463–469. doi: 10.1111/tbed.12397
- El Tahir, Y. E. H., and Nair, R. R. (2011). Prevalence of brucellosis in the sultanate of Oman with reference to some Middle-East countries. *Vet. Res.* 4, 71–76. doi: 10.3923/vr.2011.71.76
- Garcell, H. G., Garcia, E. G., Pueyo, P. V., Martín, I. R., Arias, A. V., and Alfonso Serrano, R. N. (2016). Outbreaks of brucellosis related to the consumption of unpasteurized camel milk. *J. Infect. Public Health* 9, 523–527. doi: 10.1016/j.jiph.2015.12.006
- Garofolo, G., Di Giannatale, E., De Massis, F., Zilli, K., Ancora, M., Camma, C., et al. (2013). Investigating genetic diversity of *Brucella abortus* and *Brucella melitensis* in Italy with MLVA-16. *Infect. Genetics. Evol.* 19, 59–70. doi: 10.1016/j.meegid.2013.06.021
- Georgi, E., Walter, M. C., Pfalzgraf, M.-T., Northoff, B. H., Holdt, L. M., Scholz, H. C., et al. (2017). Whole genome sequencing of *Brucella melitensis* isolated from 57 patients in Germany reveals high diversity in strains from Middle East. *PLoS ONE* 12:e0175425. doi: 10.1371/journal.pone.0175425
- Gwida, M., El-Gohary, A., Melzer, F., Khan, I., Rosler, U., and Neubauer, H. (2012). Brucellosis in camels. *Res. Vet. Sci.* 92, 351–355. doi: 10.1016/j.rvsc.2011.05.002
- Gwida, M. M., El-Gohary, A. H., Melzer, F., Tomaso, H., Rosler, U., Wernery, U., et al. (2011). Comparison of diagnostic tests for the detection of *Brucella* spp. in camel sera. *BMC Res. Notes* 4:525. doi: 10.1186/1756-0500-4-525
- Gyuranecz, M., Wernery, U., Kreizinger, Z., Juhász, J., Felde, O., and Nagy, P. (2016). Genotyping of *Brucella melitensis* strains from dromedary camels (*Camelus dromedarius*) from the United Arab Emirates with multiple-locus variable-number tandem repeat analysis. *Vet. Microbiol.* 186, 8–12. doi: 10.1016/j.vetmic.2016.02.009
- Hinic, V., Brodard, I., Thomann, A., Cvetnic, Z., Makaya, P. V., Frey, J., et al. (2008). Novel identification and differentiation of *Brucella melitensis*, *B. abortus*, *B. suis*, *B. ovis*, *B. canis*, and *B. neotomae* suitable for both conventional and real-time PCR systems. *J. Microbiol. Methods* 75, 375–378. doi: 10.1016/j.mimet.2008.07.002
- Huynh, L. Y., Van Ert, M. N., Hadfield, T., Probert, W. S., Bellaire, B. H., Dobson, M., et al. (2008). “Multiple locus variable number tandem repeat (VNTR) analysis (MLVA) of *Brucella* spp. identifies species-specific markers and provides insights into phylogenetic relationships,” in *NIH: Frontiers in Research*, ed V. St. Georgiev (Totowa, NJ: Humana Press), 47–54.
- Jiang, H., Fan, M., Chen, J., Mi, J., Yu, R., Zhao, H., et al. (2011). MLVA genotyping of Chinese human *Brucella melitensis* biovar 1, 2 and 3 isolates. *BMC Microbiol.* 11:256. doi: 10.1186/1471-2180-11-256
- Kattar, M. M., Jaafar, R. F., Araj, G. F., Le Fleche, P., Matar, M. G., Rached, R. A., et al. (2008). Evaluation of a multilocus variable-number tandem-repeat analysis scheme for typing human *Brucella* isolates in a region of brucellosis endemicity. *J. Clin. Microbiol.* 45, 3935–3940. doi: 10.1128/JCM.00464-08
- Kaufmann, A. F., Fox, M. D., Boyce, J. M., Anderson, D. C., Potter, M. E., Martone, W. J., et al. (1980). Airborne spread of brucellosis. *Am. N.Y. Acad. Sci.* 353, 105–114. doi: 10.1111/j.1749-6632.1980.tb18912.x
- Keim, P., Van Ert, M. N., Pearson, T., Vogler, A. J., Huynh, L. Y., and Wagner, D. M. (2004). Anthrax molecular epidemiology and forensics: using the appropriate marker for different evolutionary scales. *Infect. Genetics Evol.* 4, 205–213. doi: 10.1016/j.meegid.2004.02.005
- Kilic, S., Ivanov, I. N., Durmaz, R., Bayraktar, M. R., Ayaslioglu, E., Uyanik, M. H., et al. (2011). Multiple-locus variable-number tandem-repeat analysis genotyping of human *Brucella* isolates from Turkey. *J. Clin. Microbiol.* 49, 3276–3283. doi: 10.1128/JCM.02538-10
- Le Fleche, P., Jacques, I., Grayon, M., Al Dahouk, S., Bouchon, P., Denoeud, F., et al. (2006). Evaluation and selection of tandem repeat loci for a *Brucella* MLVA typing assay. *BMC Microbiol.* 6:9. doi: 10.1186/1471-2180-6-9
- Lounes, N., Cherfa, M.-A., Le Carrou, G., Bouyoucef, A., Jay, M., Garin-Bastuji, B., et al. (2014). Human brucellosis in Maghreb: existence of a lineage related to socio-historical connections with Europe. *PLoS ONE* 9:e115319. doi: 10.1371/journal.pone.0115319
- Mcdermott, J. J., and Arimi, S. M. (2002). Brucellosis in sub-Saharan Africa: epidemiology, control and impact. *Vet. Microbiol.* 90, 111–134. doi: 10.1016/S0378-1135(02)00249-3
- Memish, Z. A., and Mah, M. W. (2001). Brucellosis in laboratory workers at a Saudi Arabian hospital. *Am. J. Infect. Control* 29, 48–52. doi: 10.1067/mic.2001.111374
- Moreno, E. (2014). Retrospective and prospective perspectives on zoonotic brucellosis. *Front. Microbiol.* 5:213. doi: 10.3389/fmicb.2014.00213
- Musa, M. T., Eisa, M. Z., El Sanousi, E. M., Abdel Wahab, M. B., and Perrett, L. (2008). Brucellosis in camels (*Camelus dromedarius*) in Darfur, Western Sudan. *J. Comp. Pathol.* 138, 151–155. doi: 10.1016/j.jcpa.2007.10.005
- Narnaware, S. D., Dahiya, S. S., Kumar, S., Tuteja, F. C., Nath, K., and Patil, N. V. (2017). Pathological and diagnostic investigations of abortions and neonatal mortality associated with natural infection of *Brucella abortus* in dromedary camels. *Comp. Clin. Path.* 26, 79–85. doi: 10.1007/s00580-016-2348-4
- Nascimento, M., Sousa, A., Ramirez, M., Francisco, A. P., Carriço, J. A., and Vaz, C. (2017). PHYLOViZ 2.0: Providing scalable data integration and visualization for multiple phylogenetic inference methods. *Bioinformatics* 33, 128–129. doi: 10.1093/bioinformatics/btw582
- OIE, A. H. S. (2012). *Manual of Diagnostic Tests and Vaccines for Terrestrial Animals, Chapter 2.4.3 Bovine brucellosis*. Paris: Office International des Epizooties.
- Pappas, G., and Memish, Z. A. (2007). Brucellosis in the Middle East: a persistent medical, socioeconomic and political issue. *J. Chemother.* 19, 243–248. doi: 10.1179/joc.2007.19.3.243
- Pappas, G., Papadimitriou, P., Akritidis, N., Christou, L., and Tsianos, E. V. (2006). The new global map of human brucellosis. *Lancet Infect. Dis.* 6, 91–99. doi: 10.1016/S1473-3099(06)70382-6
- Radwan, A. I., Bekairi, S. I., Mukayel, A. A., Albokmy, A. M., Prasad, P. V. S., Azar, F. N., et al. (1995). Control of *Brucella melitensis* infection in a large camel herd in Saudi Arabia using antibiotherapy and vaccination with Rev. 1 vaccine. *Rev. Sci. Tech.* 14, 719–732. doi: 10.20506/rst.14.3.860
- Refai, M. (2002). Incidence and control of brucellosis in the Near East region. *Vet. Microbiol.* 90, 81–110. doi: 10.1016/S0378-1135(02)00248-1
- Sahl, J. W., Lemmer, D., Travis, J., Schupp, J., Gilce, J., Aziz, M., et al. (2016). The Northern Arizona SNP Pipeline (NASP): accurate, flexible, and rapid identification of SNPs in WGS datasets. *bioRxiv*. doi: 10.1101/037267
- Scrimgeour, E. M., Mehta, F. R., and Suleiman, A. J. (1999). Infectious and tropical diseases in Oman: a review. *Am. J. Trop. Med. Hyg.* 61, 920–925. doi: 10.4269/ajtmh.1999.61.920
- Seleem, M. N., Boyle, S. M., and Sriranganathan, N. (2010). Brucellosis: a re-emerging zoonosis. *Vet. Microbiol.* 140, 392–398. doi: 10.1016/j.vetmic.2009.06.021
- Shimol, S. B., Dukhan, L., Belmaker, I., Bardenstein, S., Sibirsky, D., Barrett, C., et al. (2012). Human brucellosis outbreak acquired through camel milk ingestion in southern Israel. *Isr. Med. Assoc. J.* 14, 475–478.
- Sprague, L. D., Al-Dahouk, S., and Neubauer, H. (2012). A review on camel brucellosis: a zoonosis sustained by ignorance and indifference. *Pathog. Glob. Health* 106, 144–149. doi: 10.1179/204773212Y.0000000020
- Tabbara, K. F. (1993). Brucellosis: a model for eradication of endemic diseases from the Arabian peninsula. *Ann. Saudi Med.* 13, 1–2. doi: 10.5144/0256-4947.1993.1
- Tan, K.-K., Tan, Y.-C., Chang, L.-Y., Lee, K. W., Nore, S. S., Yee, W. -Y., et al. (2015). Full genome SNP-based phylogenetic analysis reveals the origin and global spread of *Brucella melitensis*. *BMC Genomics* 16:93. doi: 10.1186/s12864-015-1294-x
- Tay, B. Y., Ahmad, N., Hashim, R., Mohamed Zahidi, J. A., Thong, K. L., Koh, X. P., et al. (2015). Multiple-locus variable-number tandem-repeat analysis (MLVA) genotyping of human *Brucella* isolates in Malaysia. *BMC Infect. Dis.* 15:220. doi: 10.1186/s12879-015-0958-0
- Tiller, R. V., De, B. K., Boshra, M., Huynh, L. Y., Van Ert, M. N., Wagner, D. M., et al. (2009). Comparison of two multiple-locus variable-number tandem-repeat analysis methods for molecular strain typing of human *Brucella melitensis* isolates from the Middle East. *J. Clin. Microbiol.* 47, 2226–2231. doi: 10.1128/JCM.02362-08
- Vassallo, D. J. (1996). The saga of brucellosis: controversy over credit for linking Malta fever with goats' milk. *Lancet* 348, 804–808. doi: 10.1016/S0140-6736(96)05470-0
- Wernery, U. (2014). Camelid brucellosis: a review. *Rev. Sci. Tech.* 33, 839–857. doi: 10.20506/rst.33.3.2322

- Whatmore, A. M. (2009). Current understanding of the genetic diversity of *Brucella*, an expanding genus of zoonotic pathogens. *Infect. Genet. Evol.* 9, 1168–1184. doi: 10.1016/j.meegid.2009.07.001
- Whatmore, A. M., Koylass, M. S., Muchowski, J., Edwards-Smallbone, J., Gopaul, K. K., and Perrett, L. L. (2016). Extended multilocus sequence analysis to describe the global population structure of the genus *Brucella*: phylogeography and relationship to biovars. *Front. Microbiol.* 7:2049. doi: 10.3389/fmicb.2016.02049
- Wilson, R. T. (1984). *The Camel*. New York, NY: Longman.
- Wyatt, H. V. (2005). How Themistocles Zammit found Malta Fever (brucellosis) to be transmitted by the milk of goats. *J. R. Soc. Med.* 98, 451–454. doi: 10.1177/014107680509801009

Conflict of Interest Statement: The authors declare that the research was conducted in the absence of any commercial or financial relationships that could be construed as a potential conflict of interest.

Copyright © 2018 Foster, Walker, Rannals, Hussain, Drees, Tiller, Hoffmaster, Al-Rawahi, Keim and Saqib. This is an open-access article distributed under the terms of the Creative Commons Attribution License (CC BY). The use, distribution or reproduction in other forums is permitted, provided the original author(s) or licensor are credited and that the original publication in this journal is cited, in accordance with accepted academic practice. No use, distribution or reproduction is permitted which does not comply with these terms.



The Fast-Growing *Brucella suis* Biovar 5 Depends on Phosphoenolpyruvate Carboxykinase and Pyruvate Phosphate Dikinase but Not on Fbp and GlpX Fructose-1,6-Bisphosphatases or Isocitrate Lyase for Full Virulence in Laboratory Models

OPEN ACCESS

Edited by:

Axel Cloeckaert,
Institut National de la Recherche
Agronomique (INRA), France

Reviewed by:

Roy Martin Roop II,
East Carolina University, United States
Gregory T. Robertson,
Colorado State University,
United States

*Correspondence:

Maite Iriarte
miriart@unav.es
Ignacio Moriyón
imoriyon@unav.es

Specialty section:

This article was submitted to
Infectious Diseases,
a section of the journal
Frontiers in Microbiology

Received: 05 March 2018

Accepted: 19 March 2018

Published: 05 April 2018

Citation:

Zúñiga-Ripa A, Barbier T,
Lázaro-Antón L, de Miguel MJ,
Conde-Álvarez R, Muñoz PM,
Letesson JJ, Iriarte M and Moriyón I
(2018) The Fast-Growing *Brucella*
suis Biovar 5 Depends on
Phosphoenolpyruvate Carboxykinase
and Pyruvate Phosphate Dikinase but
Not on Fbp and GlpX
Fructose-1,6-Bisphosphatases or
Isocitrate Lyase for Full Virulence
in Laboratory Models.
Front. Microbiol. 9:641.
doi: 10.3389/fmicb.2018.00641

Amaia Zúñiga-Ripa¹, Thibault Barbier², Leticia Lázaro-Antón¹, María J. de Miguel³, Raquel Conde-Álvarez¹, Pilar M. Muñoz³, Jean J. Letesson², Maite Iriarte^{1*} and Ignacio Moriyón^{1*}

¹ Departamento de Microbiología y Parasitología e Instituto de Salud Tropical – Instituto de Investigación Sanitaria de Navarra, Universidad de Navarra, Pamplona, Spain, ² Research Unit in Biology of Microorganisms, Namur Research Institute for Life Sciences, University of Namur, Namur, Belgium, ³ Unidad de Producción y Sanidad Animal, Instituto Agroalimentario de Aragón, Centro de Investigación y Tecnología Agroalimentaria de Aragón, Universidad de Zaragoza, Zaragoza, Spain

Bacteria of the genus *Brucella* infect a range of vertebrates causing a worldwide extended zoonosis. The best-characterized brucellae infect domestic livestock, behaving as stealthy facultative intracellular parasites. This stealthiness depends on envelope molecules with reduced pathogen-associated molecular patterns, as revealed by the low lethality and ability to persist in mice of these bacteria. Infected cells are often engorged with brucellae without signs of distress, suggesting that stealthiness could also reflect an adaptation of the parasite metabolism to use local nutrients without harming the cell. To investigate this, we compared key metabolic abilities of *Brucella abortus* 2308 Wisconsin (2308W), a cattle biovar 1 virulent strain, and *B. suis* 513, the reference strain of the ancestral biovar 5 found in wild rodents. *B. suis* 513 used a larger number of C substrates and showed faster growth rates *in vitro*, two features similar to those of *B. microti*, a species phylogenomically close to *B. suis* biovar 5 that infects voles. However, whereas *B. microti* shows enhanced lethality and reduced persistence in mice, *B. suis* 513 was similar to *B. abortus* 2308W in this regard. Mutant analyses showed that *B. suis* 513 and *B. abortus* 2308W were similar in that both depend on phosphoenolpyruvate synthesis for virulence but not on the classical gluconeogenic fructose-1,6-bisphosphatases Fbp-GlpX or on isocitrate lyase (AceA). However, *B. suis* 513 used pyruvate phosphate dikinase (PpdK) and phosphoenolpyruvate carboxykinase (PckA) for phosphoenolpyruvate synthesis *in vitro* while *B. abortus* 2308W used only PpdK. Moreover, whereas PpdK dysfunction causes attenuation of *B. abortus* 2308W in mice, in *B. suis*, 513 attenuation occurred only in the

double PckA-PpdK mutant. Also contrary to what occurs in *B. abortus* 2308, a *B. suis* 513 malic enzyme (Mae) mutant was not attenuated, and this independence of Mae and the role of PpdK was confirmed by the lack of attenuation of a double Mae-PckA mutant. Altogether, these results decouple fast growth rates from enhanced mouse lethality in the brucellae and suggest that an Fbp-GlpX-independent gluconeogenic mechanism is ancestral in this group and show differences in central C metabolic steps that may reflect a progressive adaptation to intracellular growth.

Keywords: *Brucella*, metabolism, gluconeogenesis, pyruvate phosphate dikinase, phosphoenolpyruvate carboxykinase, malic enzyme, isocitrate lyase

INTRODUCTION

In order to survive and efficiently replicate, pathogens need to adjust their metabolism to the nutrients available in their hosts. This is the case of the brucellae, a group of Gram-negative bacteria that infect a wide range of vertebrates (Whatmore, 2009; Zheludkov and Tsirelson, 2010; Soler-Lloréns et al., 2016; Al Dahouk et al., 2017) and include facultative intracellular pathogens causing brucellosis, a worldwide distributed zoonosis. Taxonomically, these bacteria are grouped currently in a single genus with up to 12 closely related species¹, some of which were divided long ago into biovars according to phenotypic criteria (Alton et al., 1988). Recent studies show that most brucellae form a core group, which includes the “classical” species as well as more recent isolates from a variety of mammals, separated from several early diverging brucellae, which in turn are close to environmental bacteria and opportunistic pathogens of the α -2 Proteobacteria (Soler-Lloréns et al., 2016; Al Dahouk et al., 2017). Thus far, the core brucellae that infect domestic ruminants (*Brucella abortus* and *B. melitensis*) and swine (*B. suis* biovars 1, 2, and 3) have deserved greater attention undoubtedly because of their early identification and great impact on public health and animal production. Even though these three species are often described as fastidious because of their slow growth and complex requirements for primary isolation (peptone-yeast extract media, often supplemented with serum), under laboratory conditions the strains investigated are auxotrophic for a few vitamins and, but for some strains that seem to require some amino acids (Plommet, 1991; see also section “Discussion”), they grow on mineral salts with glutamate-lactate-glycerol or glucose (Gerhardt and Wilson, 1948; Plommet, 1991; Barbier et al., 2018). However, there is only limited information on the substrates and pathways in their replicative niche, a vacuole connected to ER cisternae and the outer nuclear membrane (Pizarro-Cerdá et al., 1998; Starr et al., 2008; Ronneau et al., 2014; Zúñiga-Ripa et al., 2014; Barbier et al., 2018; Sedzicki et al., 2018).

The central C metabolism pathways of *Brucella* have been reviewed recently (Barbier et al., 2018). Radiorespirometric and biochemical analyses show that *B. suis* 1330 (reference strain of biovar 1), *B. melitensis* 16M (reference strain of biovar 1) and *B. abortus* 2308 [biovar 1, National Animal Disease Laboratory (Ames, IA, United States)] and S19 (attenuated vaccine strain)

can split hexoses into trioses (Robertson and McCullough, 1968). However, there is no phosphofructokinase (Pfk; **Figure 1**) and glycolysis [i.e., the Embden–Meyerhof–Parnas (EMP)] pathway is thus interrupted. Similarly, although all genes of the Entner–Doudoroff (ED) pathway are present, the dehydratase (Edd) activity could not be detected in the strain tested (S19). Accordingly, the pentose shunt would be the only route that can provide phosphorylated trioses for subsequent oxidation in the tricarboxylic acid (TCA) cycle (Barbier et al., 2018; **Figure 1**). Surprisingly, a *B. abortus* 2308 Wisconsin (2308W; see Supplementary Table S1 and Suárez-Esquivel et al., 2016) double *fbp* and *glpX* mutant (the canonical gluconeogenic fructose-1,6-bisphosphatase genes; **Figure 1**) grows in gluconeogenic media, albeit at a markedly reduced rate (Zúñiga-Ripa et al., 2014). Moreover, attenuation in BALB/c mice was observed for pyruvate phosphate dikinase (PpdK) and malic enzyme (Mae) mutants but not for mutants in Fbp, GlpX, phosphoenolpyruvate carboxykinase (PckA) or isocitrate lyase (AceA; glyoxylate shunt) (**Figure 1**). These observations suggest that *B. abortus* 2308W is endowed with unconventional gluconeogenic enzymes and that, during infection, has access to a limited supply of 6 and 5 C substrates that is compensated through anaplerotic routes by TCA intermediates without a critical role of the glyoxylate shunt.

Phylogenomic analyses show that the core brucellae are less uniform than previously assumed on the basis of DNA:DNA hybridization (Verger et al., 1985). While all *B. abortus* and *B. melitensis* biovars group into two clades, the five recognized biovars of *B. suis* show phylogenomic diversity inconsistent with their grouping into a single species (Moreno et al., 2002; Scholz et al., 2008; Whatmore, 2009; Al Dahouk et al., 2012) and a very wide host range. Biovars 1 and 3 of this nominal species infect swine in the countries of America, Asia, and Europe; biovar 2, swine and hares in Europe; biovar 4, Arctic and Northern Eurasia reindeers; and biovar 5 were isolated from species of wild rodents in Transcaucasia some 30 years ago (Zheludkov and Tsirelson, 2010). Since *B. suis* biovar 5 (reference strain 513) is closer to the ancestral brucellae (Whatmore, 2009; Al Dahouk et al., 2017), in this work, we examined whether it shares with *B. abortus* some relevant nutritional characteristics and steps of the central C metabolism, an information that may help to identify pathways that are conserved and may thus be important in the intracellular life of core brucellae. Here, we report similarities and differences and discuss their potential significance in the lifestyle of these bacteria. The differences and similarities between *B. suis* 513

¹<http://www.bacterio.net/-allnamesac.html>

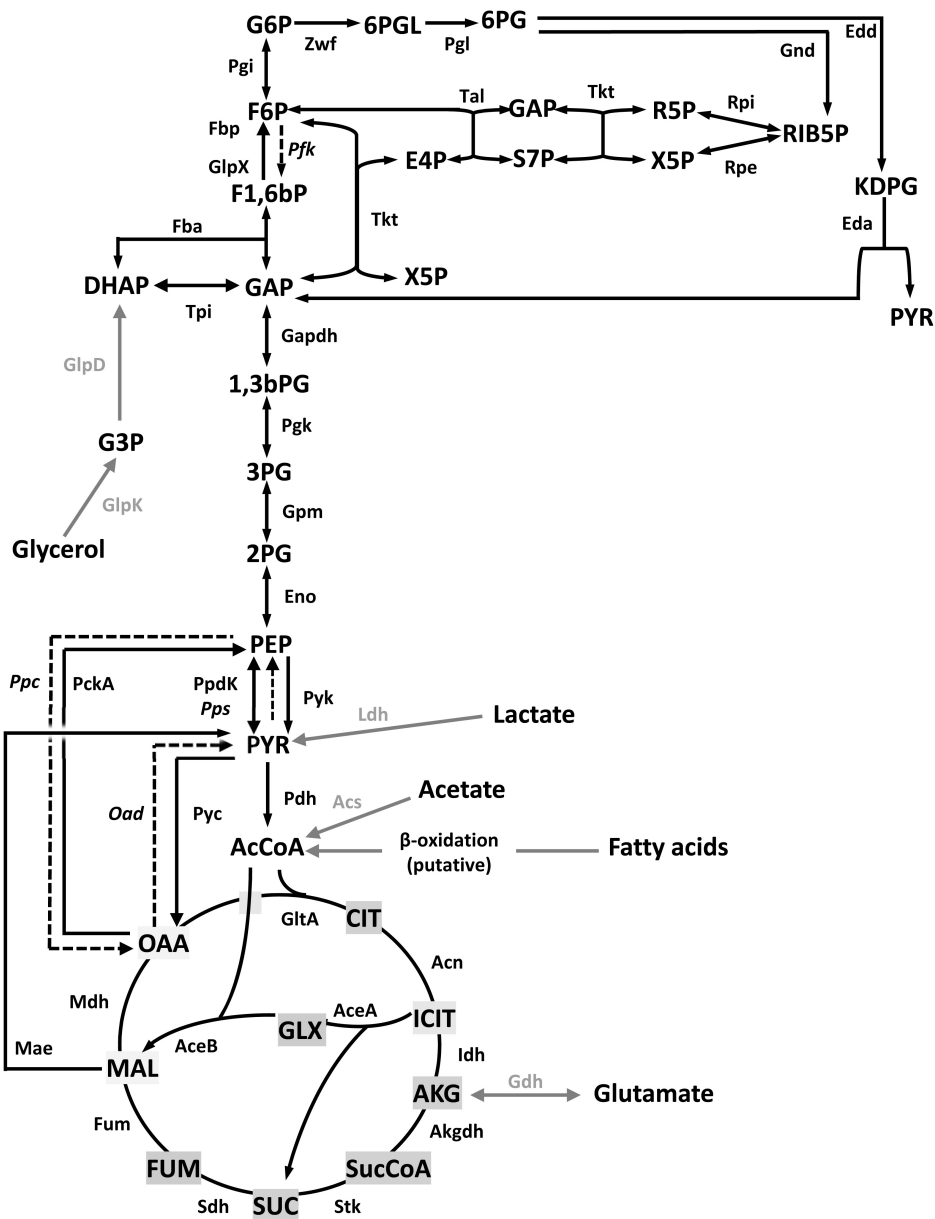


FIGURE 1 | Central C metabolic network of *Brucella* (adapted from Zúñiga-Ripa et al., 2014). The metabolic network includes complete pentoses phosphate, Entner–Doudoroff and gluconeogenesis pathways, as well as a complete tricarboxylic acid cycle including a glyoxylate shunt. The Embden–Meyerhof–Parnas pathway is interrupted due to the lack of phosphofructokinase (Pfk). Black dashed arrows and italics indicate steps for which no putative genes can be identified in *Brucella*. Gray arrows and gray font indicate peripheral pathways. Metabolites: 1,3,bPG, 1,3-bisphosphoglycerate; KDPG, 2-keto-3-deoxy-phosphogluconate; 2PG, 2-phosphoglycerate; 3PG, 3-phosphoglycerate; 6PGL, 6-P-gluconolactone; 6PG, 6-phosphogluconate; AcCoA, acetyl-coenzyme A; AKG, alpha-ketoglutarate; CIT, citrate; ICIT, isocitrate; DHAP, dihydroxyacetone-phosphate; E4P, erythrose-4-phosphate; F1,6bP, fructose-1,6-bisphosphate; F6P, fructose-6-phosphate; FUM, fumarate; G6P, glucose-6-P; GAP, glyceraldehyde-3-phosphate; G3P, glycerol-3-phosphate; GLX, glyoxylate; MAL, malate; OAA, oxaloacetate; PEP, phosphoenolpyruvate; PYR, pyruvate; R5P, ribose-5-P; RIB5P, ribulose-5-P; S7P, sedoheptulose-7-P; SUC, succinate; SucCoA, succinyl-coenzyme A; X5P, xylulose-5-P. Enzymes: Edd, 6-phospho-D-gluconate dehydratase; Gnd, 6-phosphogluconate dehydrogenase; Pgl, 6-phosphogluconolactonase; Acs, acetyl-coenzyme A synthetase; Acn, aconitate hydratase; Akgdh, alpha-ketoglutarate dehydrogenase; GltA, citrate synthase; eno, enolase; Fbp, GlpX, fructose-1,6-bisphosphatase; Fba, fructose bisphosphate aldolase; Fum, fumarase; Zwf, glucose-6-phosphate dehydrogenase; Pgi, glucose-6-phosphate isomerase; Gdh, glutamate dehydrogenase; Gapdh, glyceraldehyde-3-phosphate dehydrogenase; GlpD, glycerol-3-phosphate dehydrogenase; GlpK, glycerol kinase; Idh, isocitrate dehydrogenase; AceA, isocitrate lyase; Eda, 2-dehydro-3-deoxy-phosphogluconate aldolase; Ldh, lactate dehydrogenase; Mdh, malate dehydrogenase; AceB, malate synthase; Mae, malic enzyme; PckA, phosphoenolpyruvate carboxykinase; Ppc, phosphoenolpyruvate carboxylase; Pps, phosphoenolpyruvate synthase; Pfk, phosphofructokinase; Pkg, phosphoglycerate kinase; Gpm, phosphoglycerate mutase; Oad, pyruvate carboxykinase; Pyc, pyruvate carboxylase; Pdh, pyruvate dehydrogenase; Pyk, pyruvate kinase; PpdK, pyruvate phosphate dikinase; Rpi, ribose-5-phosphate isomerase; Rpe, ribulose-5-phosphate-3-epimerase; Sdh, succinate dehydrogenase; Stk, succinyl-coenzyme A synthetase; Tal, transaldolase; Tkt, transketolase; Tpi, triose phosphate isomerase.

and *B. microti* (a species isolated more recently from *Microtus arvalis*), noticed in the course of this study are also discussed.

MATERIALS AND METHODS

Bacterial Strains and Growth Conditions

The bacterial strains and plasmids used in this study are listed in Supplementary Table S1. All *Brucella* were handled under BSL-3 containment. The strains resulting from the genetic manipulations described below were characterized according to standard *Brucella* typing procedures (Alton et al., 1988): colonial morphology after 3 days of incubation at 37°C, crystal violet exclusion, urease, acriflavine agglutination, sensitivity to Tb, Wb, Iz, and R/C phages, agglutination with anti-A and anti-M monospecific sera, CO₂ and serum dependence, and susceptibility to thionine blue, fuchsin, and safranin. Bacteria were routinely grown in standard Peptone-Glucose [Biomérieux; bio-Tryptase (17 g/L), bio-Soyase (3 g/L), Glucose (2.5 g/L), NaCl (5 g/L), K₂HPO₄ (2.5 g/L)] or this media supplemented with agar. The Peptone-Yeast Extract medium used was composed of bacto tryptone (16 g/L), yeast extract (10 g/L), and NaCl (5 g/L) (all from BD Difco). The following antibiotics were used at the indicated concentrations: kanamycin (Km; 50 µg/mL), polymyxin (Pmx; 1.5 µg/mL), and/or chloramphenicol (Cm; 20 µg/mL) (all from Sigma). When needed, media was supplemented with 5% sucrose. All strains were stored in skimmed milk at -80°C (Scharlau).

To study the phenotype of the metabolic mutants constructed, the defined medium of Gerhardt (glutamate-lactate-glycerol) was used (Gerhardt and Wilson, 1948). The components for 1 L medium are: glycerol (30 g), lactic acid (5 g), glutamic acid (1.5 g), thiamine (0.2 mg), nicotinic acid (0.2 mg), pantothenic acid (0.04 mg), biotin (0.0001 mg), K₂HPO₄ (10 g), Na₂S₂O₃·5H₂O (0.1 g), MgSO₄ (10 mg), MnSO₄ (0.1 mg), FeSO₄ (0.1 mg), and NaCl (7.5 g). The pH was adjusted to 6.8–7. In addition, a modification of Plommet's medium was also used (Plommet, 1991; Barbier et al., 2014) and 1 L of this medium is composed of thiamine (0.2 g), nicotinic acid (0.2 g), pantothenic acid (0.07 g), biotin (0.1 mg), K₂HPO₄ (2.3 g), KH₂PO₄ (3 g), Na₂S₂O₃ (0.1 g), MgSO₄ (0.01 g), MnSO₄ (0.1 mg), FeSO₄ (0.1 mg), NaCl (5 g), (NH₄)₂SO₄ (0.5 g), and 1 g/L of substrate. When glutamic acid was used as nitrogen and C source (NH₄)₂SO₄ was not added.

DNA Manipulations

Genomic sequences of the different *Brucella* species were obtained from the database National Center for Biotechnology Information (NCBI) and Kyoto Encyclopedia of Genes and Genomes (KEGG). Searches for DNA and protein homologies were carried out using NCBI BLAST (Altschul et al., 1990). Sequence alignments were performed with Clustal Omega (Goujon et al., 2010; Sievers et al., 2011). Primers were synthesized by Sigma (Haverhill, United Kingdom). DNA sequencing analysis was performed by the Servicio de Secuenciación de CIMA (Centro de Investigación Médica Aplicada, Universidad de Navarra, Pamplona, Spain). Restriction modification enzymes were used under the conditions

recommended by the manufacturer. Plasmid and chromosomal DNA were extracted with QIAprep Spin Miniprep (Qiagen) and Ultraclean Microbial DNA Isolation kit (Mo Bio Laboratories), respectively. When needed, DNA was purified from agarose gels using QIAquick Gel Extraction Kit (Qiagen).

Mutagenesis

Construction of the in-frame deletion mutants *Bs5Δfbp*, *Bs5ΔglpX*, *Bs5ΔfbpΔglpX*, *Bs5ΔpckA*, *Bs5ΔppdK*, *Bs5ΔpckAΔppdK*, *Bs5Δmae*, *Bs5ΔmaeΔpckA*, and *Bs5ΔaceA* was done using previously described plasmids and strategy (Zúñiga-Ripa et al., 2014).

Bs5ΔBMI_I149 (and *Bs5ΔmaeBs5ΔBMI_I149*) was obtained using the plasmid pAZI-25 constructed in this work. First, two PCR fragments were generated: oligonucleotides BMI_I149-F1 (5'-GGTTCGCGCTCTTCTCTTC-3') and BMI_I149-R2 (5'-AAAGTCGAGCGCTTCC TTCT-3') amplified a 266 bp fragment including codons 1–31 of BMI_I149, as well as 161 bp upstream of the BMI_I149 start codon; oligonucleotides BMI_I149-F3 (5'-AGAAGGAAGCGCTCGACTTTAACCCGAACTGATGGAACA-3') and BMI_I149-R4 (5'-TGGACTTGCGATGACAGAAC-3') were used to amplify a 356 bp fragment including the last 240 bp of BMI_I149. A third PCR joined the two fragments together using oligonucleotides BMI_I149-F1 and BMI_I149-R4 for amplification and the complementary regions between BMI_I149-R2 and BMI_I149-F3 for overlapping. The resulting fragment, containing the BMI_I149 deletion allele, was cloned into pCR2.1 (Invitrogen). After sequence verification, the insert was excised as a *Bam*HI-*Xba*I fragment and cloned in a pJQKm suicide vector (Scupham and Triplett, 1997). The acquisition of this vector by *Brucella* after mating with conjugative *Escherichia coli* S17 λpir was selected by Km and Pmx resistance. The loss of the plasmid concomitant with either a deletion or a return to wild type phenotype was then selected on sucrose. The resulting colonies were screened by PCR with primers BMI_I149-F1 and BMI_I149-R4 which amplified a fragment of 622 bp in the mutant and a fragment of 2599 bp in the revertant strain. To check the mutation, an internal primer (BMI_I149-R5) which hybridized in the non-deleted region was used.

For complementation, the plasmid pAZI-19 previously described (Zúñiga-Ripa et al., 2014) was used.

Growth Curves

Growth curves were obtained using a Bioscreen C (Lab Systems) apparatus. To avoid carry over of media by the inoculum and lengthy lag phases, inocula were obtained from bacteria grown in test media as follows. First, the strains were inoculated into 10 mL of peptone-glucose in a 50 mL flask and incubated at 37°C with orbital shaking for 18 h. Then, these bacteria were harvested by centrifugation, resuspended in 10 mL of the test medium (peptone-glucose, peptone-yeast extract, glutamate-lactate-glycerol, glutamate, or lactate) at an OD_{600 nm} of 0.1, and incubated at 37°C with orbital agitation for 18 h. These exponentially growing bacteria were harvested by centrifugation, resuspended at an OD_{600 nm} of 0.1 in the test medium, dispensed as technical replicates in Bioscreen multiwell plates (200 µL/well;

starting OD of 0.05 in the Bioscreen apparatus) and cultivated for 5 days with continuous shaking at 37°C. Absorbance values at 420–580 nm were automatically recorded at 30-min intervals. All experiments were repeated at least three times. Controls with medium and no bacteria were included in all experiments.

Cell Culture and Infection

RAW 264.7 murine macrophages (ATCC TIB-71) were routinely cultured in Dulbecco's Modified Eagle Medium (DMEM; Gibco) with 10% (vol/vol) heat-inactivated fetal bovine serum (Gibco), 1% (vol/vol) L-glutamine (200 mM; Sigma-Aldrich), and 1% (vol/vol) non-essential amino acids (Gibco). Cells were maintained at 37°C with a 5% CO₂ atmosphere.

Infections were performed as previously described (Zúñiga-Ripa et al., 2014). Briefly, cells were seeded in 24-well plates at an appropriate density (1×10^5 cells/well) and infected 24 h later with a multiplicity of infection (MOI) of 50:1. Cells were centrifuged at $400 \times g$, for 10 min at 4°C before being incubated for 15 min at 37°C with 5% CO₂, washed with fresh medium and incubated for 90 min with medium containing 100 µg/mL of gentamycin. The medium was then replaced by a fresh one containing 25 µg/mL of this antibiotic. At each time point, cells were washed three times with 100 mM PBS (pH 7) before processing, lysed with 0.1% (v/v) Triton X-100 in PBS, and plated on peptone-glucose-agar to determine the number of intracellular bacteria. All experiments were performed in triplicate and results are expressed as means and standard errors ($n = 3$) of individual log₁₀ CFU/well. The attenuated *B. abortus virB* mutant was used as a control (Sieira et al., 2000).

Virulence Assays in Mice

Seven-week-old female BALB/c mice (Harlan Laboratories, Bicester, United Kingdom) were accommodated in the facilities of Centro de Investigación y Tecnología Agroalimentaria de Aragón (CITA; Registration code ES502970012025) for 2 weeks before and during the experiments, with water and food *ad libitum* under P3 biosafety containment conditions. The animal handling and other procedures were in accordance with the current European (directive 86/609/EEC) and Spanish (RD 53/2013) legislations, supervised by the Animal Welfare Committee of the CITA (2014-20).

For each strain, inoculum was prepared from cultures on peptone-glucose-agar at 37°C. Bacteria were harvested in 10 mM PBS (pH 7), suspended in this diluent to the appropriate concentration and approximately 5×10^4 CFU in 0.1 mL administered to each mouse intraperitoneally (exact doses were retrospectively assessed). For each strain, mice ($n = 5$ per group) were inoculated and the CFU in spleens was determined at different weeks post-inoculation. Mice were anesthetized by intraperitoneal injection and sacrificed by cervical dislocation; spleens were isolated, weighted, homogenized in 9 vol of PBS and CFU counted on peptone-glucose-agar. The identity of the spleen isolates was confirmed by PCR at several points during the infection process. The individual data were normalized by logarithmic transformation, and the mean log₁₀ CFU/spleen values and

the standard deviation ($n = 5$) were calculated. Statistical significance was evaluated using one-way ANOVA followed by Dunnett's test (* $p < 0.05$, ** $p < 0.01$, *** $p < 0.001$, **** $p < 0.0001$).

RESULTS

Brucella suis 513 (Reference Strain of Biovar 5) Uses a Broad Range of Substrates as the Only C Source but It Is Not Prototrophic for Vitamins

Since the growth characteristics and requirements of *B. suis* 513 are practically unknown, we first examined the ability of this reference strain to grow on common C6, C5, C4, and C3 substrates as the only C source using the vitamins–mineral salts (with ammonium sulfate as N source when necessary) basal medium of Plommet (Plommet, 1991; **Table 1** and **Figures 2–5**). We found that the range of substrates used by *B. suis* 513 as the only C source was broader than that of *B. abortus* 2308W (Suárez-Esquivel et al., 2016). Remarkably, whereas *B. suis* 513 was able to grow efficiently on lactate or glutamate, *B. abortus* 2308W was not (**Table 1** and **Figures 3–5**) and required at least one additional C source (i.e., glutamate-lactate or glutamate-glycerol; not shown and Zúñiga-Ripa et al., 2014). These differences suggested that *B. suis* 513 is more prototrophic than *B. abortus* 2308W (see section “Discussion”), and thus we examined the vitamin requirements of *B. suis* 513. We found that *B. suis* 513

TABLE 1 | Growth of *B. abortus* 2308W and *B. suis* 513 on single C6, C4, and C3 compounds as the only C source¹.

C source	Yield (OD _{600 nm}) ²	
	<i>B. abortus</i> 2308W	<i>B. suis</i> 513
C6		
Glucose	0.00	0.75
Fructose	0.00	0.25
Gluconate	0.00	0.00
Mannose	0.00	0.85
Fucose	0.00	0.60
Inositol	0.00	0.00
C5		
Ribose	0.11	0.90
Xilose	0.19	0.85
Glutamate	0.00	0.60
C4		
Succinate	0.00	0.00
Erythritol	0.70	0.90
C3		
Glycerol	0.00	0.00
Lactate	0.00	0.60
Pyruvate	0.00	0.70

¹C sources (1 g/L) were added to the vitamin-salt broth of Plommet's medium (see section “Materials and Methods”). ²Yields correspond to the stationary phase (obtained at different times depending on the C source).

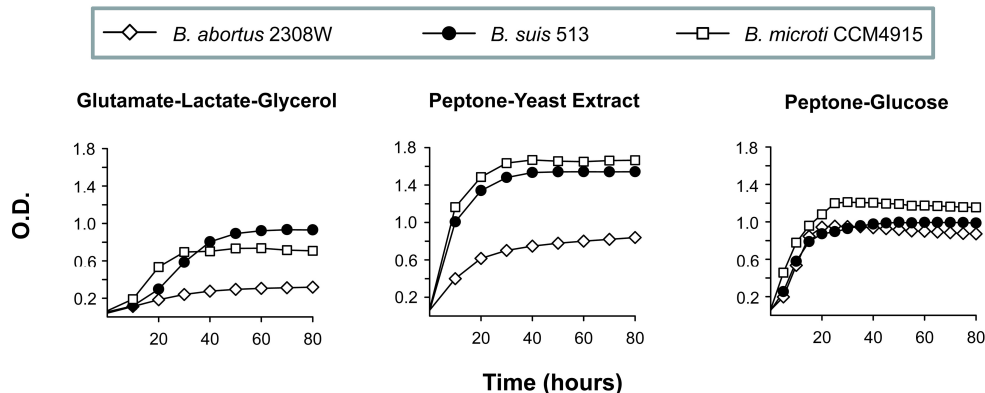


FIGURE 2 | Growth curves in glutamate-lactate-glycerol, peptone-yeast extract, and peptone-glucose of *B. abortus* 2308W, *B. suis* 513, and *B. microti* CCM4915. Each point represents the mean \pm standard error (error bars are within the size of the symbols) of optical density (OD) values of triplicate samples. The experiment was repeated three times with similar results.

required nicotinic acid and thiamine (Supplementary Figure S1), being in this regard not different from *B. abortus*, *B. melitensis*, or the *B. suis* biovars previously studied, all of which require at least these two vitamins (Koser et al., 1941; Koser and Wright, 1942; McCullough and Dick, 1942a,b; McCullough et al., 1946).

***Brucella suis* 513 Shows Faster Growth Rates Than *B. abortus* 2308W in Gluconeogenic Media That Do Not Depend on Fbp and GlpX**

Since the above observations show that we could probe some aspects of the central C pathways of *B. suis* 513 using simple defined media, we compared first the growth of *B. suis* 513 with *B. abortus* 2308W (slow growing) and *B. microti* CCM4915 (usually described as fast growing) under gluconeogenic conditions (Gerhardt's medium, containing glutamate, lactate, glycerol, mineral salts, and vitamins; henceforth glutamate-lactate-glycerol). As can be seen in **Figure 2**, the growth curves suggested higher growth rates for *B. suis* 513 and *B. microti* CCM4915 depending upon the medium. In peptone-yeast extract, a rich but still gluconeogenic medium where growth factors are abundant, *B. suis* 513 and *B. microti* CCM4915 displayed shorter generation times and much higher yields than *B. abortus* 2308W. These differences almost disappeared when peptone was combined with glucose (**Figure 2**). Taken together, these results suggest that *B. suis* 513 and *B. microti* CCM4915, on one hand, and *B. abortus* 2308W, on the other, differ in gluconeogenic abilities, a hypothesis that was examined in the experiments described below.

The brucellae carry homologs of the two canonic fructose-1,6-bisphosphatases (Fbp and GlpX) on which the gluconeogenic pathway depends. Consistent with our previous report (Zúñiga-Ripa et al., 2014), the simultaneous dysfunction of Fbp and GlpX did not affect the growth of *B. abortus* 2308W in peptone-glucose and impaired but did not abrogate its growth in glutamate-lactate-glycerol (**Figure 3**). In contrast, growth of single (*Bs5Δfbp* or *Bs5ΔglpX*) or double (*Bs5ΔfbpΔglpX*)

bisphosphatase mutants of *B. suis* 513 was not compromised to any extent in glutamate-lactate-glycerol (**Figure 3**). Since *B. suis* 513 grew on lactate or glutamate as the sole C source, we also tested the mutants on these gluconeogenic substrates. We found that the ability to grow was not affected on lactate, and only slightly for *Bs5Δfbp* and *Bs5ΔfbpΔglpX* but not for *Bs5ΔglpX* on glutamate (**Figure 3**).

***Brucella suis* 513 and *B. abortus* 2308W Differ in Key Steps Connecting Phosphoenolpyruvate and TCA**

We then investigated whether growth of *B. suis* 513 in complex and gluconeogenic media depends on the steps catalyzed by PpdK (phosphoenolpyruvate \leftrightarrow pyruvate) and PckA (oxaloacetate \rightarrow phosphoenolpyruvate) (**Figure 1**). As observed for *B. abortus* 2308W (**Figure 4** and Zúñiga-Ripa et al., 2014), deletion of *ppdK* (*Bs5ΔppdK*) impaired the growth of *B. suis* 513 on glutamate-lactate-glycerol but not on peptone-glucose (**Figure 4**). On the other hand, deletion of *pckA* had no effect in *B. suis* 513 (mutant *Bs5ΔpckA*; **Figure 4**) or in *B. abortus* 2308W (Zúñiga-Ripa et al., 2014). Although these observations could be interpreted to mean that, like in *B. abortus* 2308W (Zúñiga-Ripa et al., 2014), PckA is not functional and gluconeogenesis depends only on PpdK in *B. suis* 513, we found this hypothesis not to be true because growth on glutamate-lactate-glycerol was abrogated in a double *Bs5ΔpckAΔppdK* mutant (**Figure 4**), indicating that PckA is active in this strain. These results are in keeping with the fact that while *B. abortus* 2308W *pckA* carries a frameshift that generates a premature stop codon (TGA) at position 1474–1476, the orthologous codon in *B. suis* 513 is TGG (tryptophan) (a BLAST search did not reveal any other copy of *pckA* in the *B. abortus* 2308W genome).

We further explored the role of PpdK and PckA by growing *Bs5ΔppdK*, *Bs5ΔpckA*, and *Bs5ΔpckAΔppdK* on lactate or glutamate. But for the expected reduction in growth yields, the results obtained in glutamate paralleled those in glutamate-lactate-glycerol (**Figure 4**), confirming that the

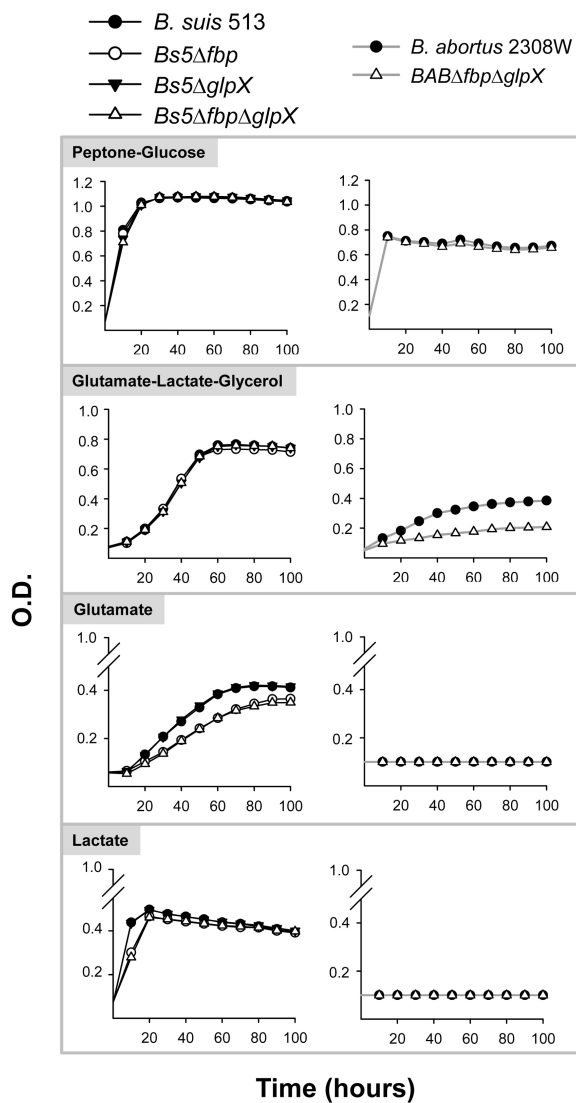


FIGURE 3 | Growth curves in peptone-glucose, glutamate-lactate-glycerol, glutamate, and lactate of *B. suis* 513 and mutants *Bs5Δfbp*, *Bs5ΔglpX*, and *Bs5ΔfbpΔglpX*, and *B. abortus* 2308W and mutant *BABΔfbpΔglpX*. Each point represents the mean \pm standard error (error bars are within the size of the symbols) of an experiment performed in technical triplicates. The experiment was repeated three times with similar results.

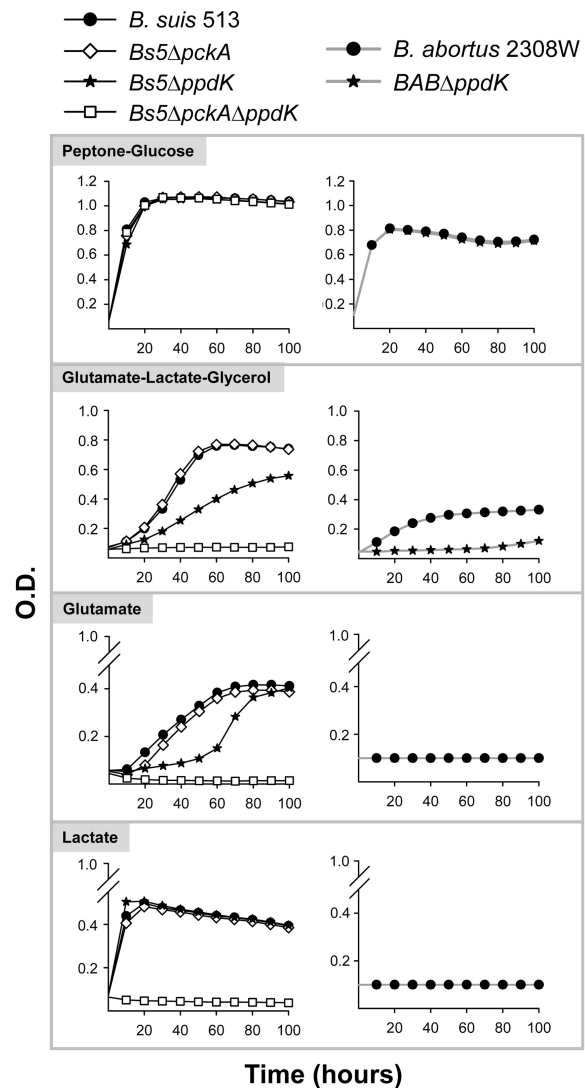


FIGURE 4 | Growth curves in peptone-glucose, glutamate-lactate-glycerol, glutamate, and lactate of *B. suis* 513 and mutants *Bs5ΔpckA*, *Bs5ΔppdK*, and *Bs5ΔpckAΔppdK*, and *B. abortus* 2308W and mutant *BABΔppdK*. Each point represents the mean \pm standard error (error bars are within the size of the symbols) of an experiment performed in technical triplicates. The experiment was repeated three times with similar results.

steps catalyzed by PckA and PpdK set a clear difference in the metabolism of *B. abortus* 2308W and *B. suis* 513 in gluconeogenic substrates. Interestingly, growth of *Bs5ΔppdK* in lactate was unaffected. As the brucellae lack gluconeogenic phosphoenolpyruvate synthase (Pps; **Figure 1**; Barbier et al., 2018), this result means that TCA cycle intermediates derived from the pyruvate obtained from lactate (**Figure 1**) can sustain gluconeogenesis. Since this could implicate a malic enzyme (Mae in **Figure 1**), we investigated the *mae* homologs of *B. suis* 513.

First, we identified a clear homolog of *B. abortus* 2308W *mae* in *B. suis* 513, which is also a homolog of *B. microti*

(strain CCM4915) BMI_I1020. Although in *B. microti* there is a second ORF annotated as *mae* (BMI_I149), its *B. suis* 513 counterpart lacks a thymine at position 1153 that originates a frameshift that could compromise the functionality of the protein. Thus, we started studying the role of the first *mae* identified. Consistent with the presence of an active enzyme furnishing pyruvate from oxaloacetate (**Figure 1**), this *Bs5Δmae* mutant displayed a reduction in growth on glutamate but not on lactate, a phenotype similar to that of its *B. abortus* 2308W counterpart but for the expected differences in growth rates/yields (**Figure 5**). Moreover, growth on glutamate was abrogated in a double *Bs5ΔmaeΔpckA* mutant (**Figure 5**), the

expected result if both Mae and PckA are active and the former acts in tandem with PpdK in gluconeogenesis (Figure 1). On the other hand, these mutants grew normally on lactate (Figure 5), as expected if lactate provides pyruvate for both gluconeogenesis and TCA reactions (Figure 1). Indirectly, the lack of growth of the double mutant on glutamate was coherent with the possibility that the frameshift in the BMI_I149 ortholog results in a non-functional protein, and we confirmed this using a double mutant in the *B. suis* 513 orthologs of BMI_I1020 (*mae*) and BMI_I149. This double mutant displayed the same growth characteristics as the single *Bs5Δmae* (Supplementary Figure S2), strongly suggesting that the protein encoded by the BMI_I149 homolog lacks Mae activity in *B. suis* 513.

The results presented above show that *B. suis* 513 converts malate to pyruvate via Mae, and oxaloacetate to

phosphoenolpyruvate via PckA. Because these TCA cycle intermediates could be replenished by condensation of acetyl-CoA with glyoxylate into malate, we constructed an isocitrate lyase (*AceA*; Figure 1) mutant for *in vivo* studies (see below) on the role of the glyoxylate bypass. As expected, growth of this *B. suis* 513 mutant was identical to that of the parental strain in peptone-yeast extract, and this mutation had no effect on the growth in glutamate-lactate-glycerol, glutamate-glycerol, or lactate-glycerol (results not shown). Similarly, growth was not affected in media containing peptones (not shown), even though acetogenic amino acids (leucine, isoleucine, lysine, phenylalanine, tryptophan, and tyrosine) represent approximately 20% of the peptone amino acid content.

Brucella suis 513 Requires *pckA* or *ppdK* but Not *mae* or *aceA* for Virulence in Mice

Since analysis of the *B. suis* 513 mutants in mice requires a definition of the parameters of virulence of the parental strain in this laboratory model and these have not been studied previously, we first inoculated BALB/c mice with 10^4 and 10^5 CFU of *B. suis* 513. These doses neither caused death nor triggered any signs of septic shock in the next days, a result similar to those that are characteristic of the *Brucella* species infecting domestic ruminants (Grilló et al., 2012). Therefore, we inoculated BALB/c mice intraperitoneally with 5×10^4 CFU of *B. suis* 513 or *B. abortus* 2308W and determined the CFU numbers in spleen in the following weeks (Figure 6A). At week 2 (acute phase of infection; Grilló et al., 2012), *B. suis* 513 reached CFU numbers similar to those obtained with *B. abortus*. Thereafter, although CFU numbers were approximately 1.5 logs lower than those of *B. abortus* 2308W, *B. suis* 513 showed persistence typical of the chronic phase of classical *Brucella* species (Grilló et al., 2012). Virulence of *B. suis* 513 was confirmed in RAW 264.7 macrophages (Figure 6B).

Once we knew these characteristics of *B. suis* 513, we infected BALB/c mice with the above-described *B. suis* 513 mutants and determined the spleen CFU numbers in the acute and chronic phase of infection (i.e., 2 and 8 weeks after infection, respectively). We found that dysfunction of the genes of the gluconeogenic phosphatases Fbp and GlpX did not result in a decrease in the CFU numbers in the spleen of mice at either infection phase (Figure 7). Likewise, neither the *pckA* nor the *ppdK* mutant displayed CFU numbers different from the wild type control in either infection phase (Figure 7). On the other hand, the double *pckA-ppdK* mutant was markedly attenuated in the chronic phase ($p \leq 0.0001$) to the extent that we did not detect any bacteria in the spleens of two of the five mice in this group (limit of detection of this method = 3.3 CFU/mL of the homogenized spleen; Grilló et al., 2012). Altogether, these results strongly suggest that PckA and PpdK are active during the infectious process, either alternatively or simultaneously. In keeping with this interpretation, partial complementation of the double mutant with plasmid pRH001-*ppdK* (pAZI-19; Supplementary Table S1) restored the ability to persist in the spleens of BALB/c mice (Supplementary Figure S3).

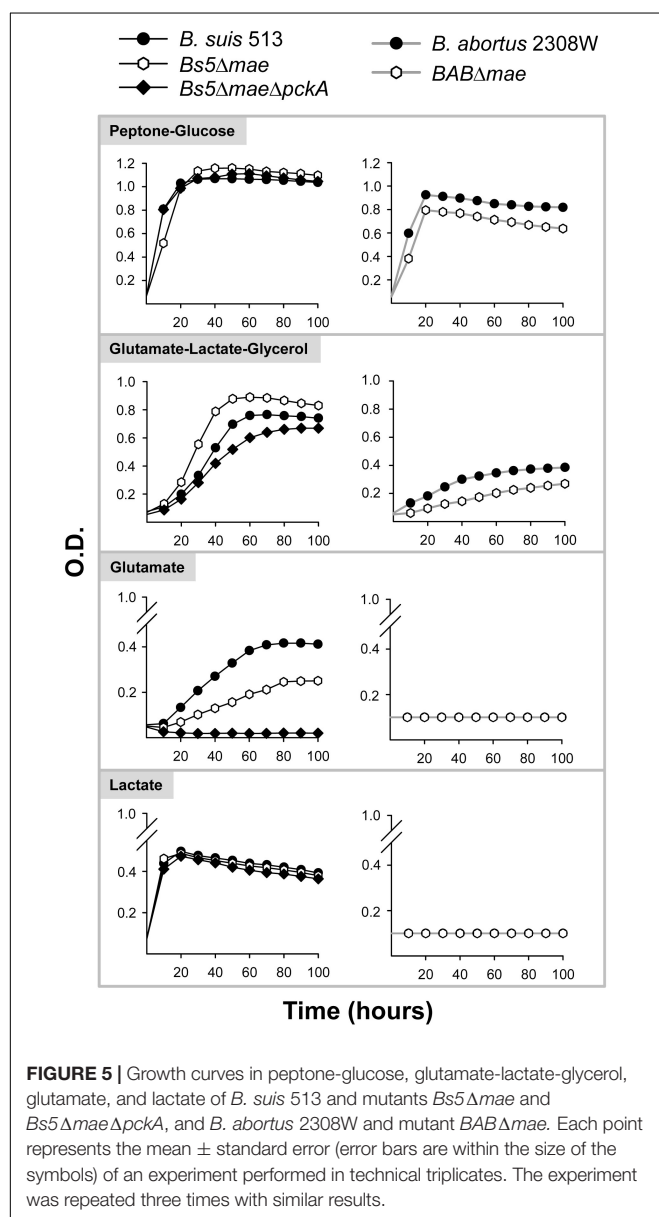


FIGURE 5 | Growth curves in peptone-glucose, glutamate-lactate-glycerol, glutamate, and lactate of *B. suis* 513 and mutants *Bs5Δmae* and *Bs5ΔmaeΔpckA*, and *B. abortus* 2308W and mutant *BABΔmae*. Each point represents the mean \pm standard error (error bars are within the size of the symbols) of an experiment performed in technical triplicates. The experiment was repeated three times with similar results.

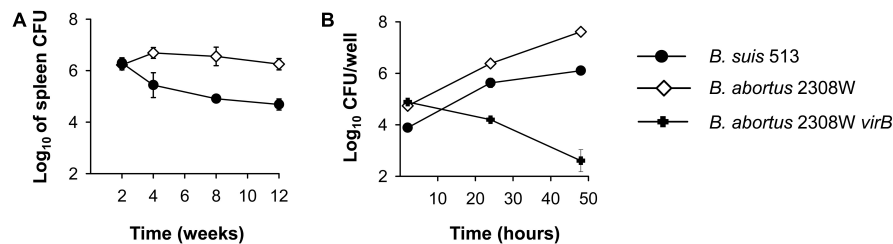


FIGURE 6 | Multiplication of *B. abortus* 2308W and *B. suis* 513 in virulence models. **(A)** Bacterial multiplication in BALB/c mice. Each point is the mean \pm standard deviation ($n = 5$) of the log CFU per spleen. **(B)** Intracellular multiplication in RAW 264.7 macrophages (the *B. abortus* 2308W *virB* mutant is used as a control of attenuation). Values are mean \pm standard errors for triplicate infections and the results shown are representative of three independent experiments.

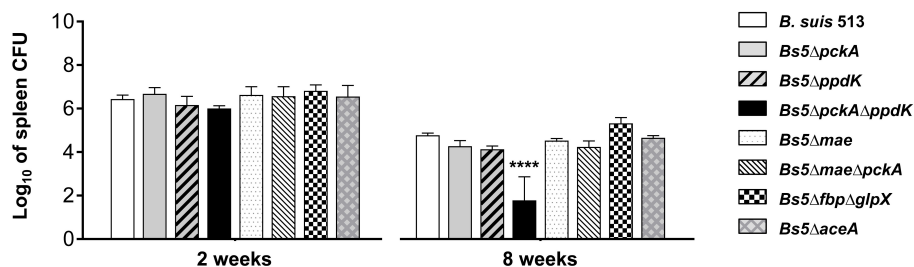


FIGURE 7 | Bacterial loads in the spleens of BALB/c mice at 2 and 8 weeks post-infection of *B. suis* 513 and mutants *Bs5ΔpckA*, *Bs5ΔppdK*, *Bs5ΔpckAΔppdK*, *Bs5Δmae*, *Bs5ΔmaeΔpckA*, *Bs5ΔfbpΔglpX*, and *Bs5ΔaceA*. Statistical differences with *B. suis* 513 were significant at week 8 for *Bs5ΔpckAΔppdK* (**** $p \leq 0.0001$).

We did not find attenuation for *Bs5Δmae* and *Bs5ΔmaeΔpckA* (Figure 7), which indicates that conversion of malate into pyruvate or oxaloacetate into phosphoenolpyruvate (Figure 1) is not essential for multiplication of *B. suis* 513 in BALB/c mouse spleen cells. Also, we did not observe attenuation for *Bs5ΔaceA* (Figure 7), meaning that the glyoxylate shunt is not essential either for *B. suis* 513 multiplication in the spleen of BALB/c mice.

DISCUSSION

Despite repeated isolation from wild rodents in the Caucasus provinces of the former USSR (Meyer, 1976; Vershilova et al., 1983; Corbel, 1984), there is little accessible information on the *in vitro* nutritional requirements and virulence of *B. suis* biovar 5 in standard brucellosis laboratory models. Remarkably, Russian workers described these isolates as displaying “luxurious” growth (Lyamkin et al., 1981) and amino acid oxidative abilities broader than those of *B. suis* biovar 1 (Lyamkin et al., 1982; Vershilova et al., 1983), and on these bases they proposed a new “serobiotype” (*B. murium*; Banai and Corbel, 2010), which was not accepted later at a time when the taxonomic status of *B. suis* seemed clear to the *Brucella* Taxonomy Subcommittee (Meyer, 1976; Vershilova et al., 1983; Corbel, 1984). Consistent with these reports and the proposal, the reference strain *B. suis* 513 displayed growth characteristics departing from those of the classical *Brucella* species, represented in the present work by *B. abortus* 2308W, and were in this regard more similar

to the fast-growing species *B. microti*. Noteworthy, the natural hosts of *B. suis* biovar 5 and *B. microti* are wild rodents, rather than domestic livestock (Vershilova et al., 1983; Corbel, 1984; Scholz et al., 2008) and both are closer to the early diverging brucellae than *B. melitensis*, *B. abortus*, or the other *B. suis* biovars (Whatmore, 2009; Soler-Lloréns et al., 2016; Al Dahouk et al., 2017). Nevertheless, whereas the *B. microti* strain investigated so far (CCM 4915) is lethal at doses higher than 10^4 CFU/mouse and is rapidly eliminated from the spleen at non-lethal doses (Jiménez de Bagüés et al., 2010, 2011), 10^5 CFU of *B. suis* 513 neither caused the death of mice nor triggered any signs of septic shock, and the CFU/spleen profile showed the acute and chronic phases characteristic of *B. abortus*, *B. melitensis*, and among *B. suis* at least that of biovar 1. Although in a different animal model, this observation is in line with those of the Russian workers who found that the *B. suis* biovar 5 isolates were similar to *B. suis* biovar 1 in pathogenicity and subsequent pathomorphological changes in guinea pigs (Lyamkin et al., 1983). It has been pointed out previously that fast growth and lethality correlate in *B. microti* CCM 4915 (Jiménez de Bagüés et al., 2010). It could be that these are two non-causally connected features or that fast growth results in a rapid increase in *Brucella* pathogen-associated molecular pattern (PAMP)-bearing molecules that could reach lethal levels not attained at the same infectious dose by the slow-growing strains. Although we cannot rule out that the fast growth of *B. suis* 513 does not contribute to any extent to lower the CFU/spleen counts by bolstering innate immunity recognition, it is clear that, despite its proximity to *B. microti* in growth rates, host, and phylogenomic position,

B. suis 513 ranks with the classical smooth *Brucella* species in lethality and ability to persist in mice (Jiménez de Bagüés et al., 2011; Grilló et al., 2012). These observations, which should be confirmed in additional strains, suggest differences in key PAMP-bearing molecules and, coherent with this hypothesis is the lack of reactivity of *B. microti* LPS in Western blot with monoclonal antibodies recognizing the core-lipid A of *B. melitensis*, *B. abortus*, and *B. suis* biovars 1, 2, and 5 (Zygmunt et al., 2012; R. Conde-Álvarez, A. Zúñiga-Ripa, S. Köhler, M. Iriarte, and I. Moriyón, unpublished observations). Indeed, the core-lipid A of the classical species bears the PAMP modifications implicated in reduced innate immunity recognition and lower septic shock lethality (Lapaque et al., 2005).

Brucella suis 513 being closer to *B. abortus* 2308W in virulence in mice and macrophages, but more distant in growth rates in gluconeogenic media and in phylogenomic position, these two bacteria represent models suitable for comparing aspects of the central C metabolism of the core brucellae. The inability of *B. abortus* 2308W to grow on simple substrates as the only C source, most notably glucose, has to be interpreted with care, as this does not necessarily mean differences in central C pathways. The same inability has also been noted for the *B. melitensis* 16M strain kept in the laboratory of the authors, which requires methionine to grow on glucose and yet is fully virulent (Barbier et al., 2018). A similar explanation is likely to apply to *B. abortus* 2308W, as the differences with *B. suis* 513 *in vitro* disappear when glucose is combined with peptone (Figure 2). Indeed, these are aspects not related to the central C pathways in which there could be differences among strains with the same reference number kept in different laboratories, as it is the likely case of *B. abortus* 2308 variants (Suárez-Esquivel et al., 2016; see also below). The main differences and similarities that concern the C pathways specifically investigated here are summarized in Figure 8, and their potential significance is discussed below.

In vitro, *B. suis* 513 uses PpdK and PckA for phosphoenolpyruvate synthesis while *B. abortus* 2308W depends only on PpdK. This is likely to reflect the situation *in vivo*, because PpdK dysfunction causes attenuation of *B. abortus* 2308W in mice (Zúñiga-Ripa et al., 2014) but not in *B. suis* 513, in which attenuation occurred only in the double *pckA*-*ppdK* mutant. Although these observations strongly suggest that PckA is not essential for multiplication in the host and that, accordingly, it was not positively selected during evolution, we cannot presently extend this hypothesis to all core brucellae. On one hand, the genomes of all *B. abortus* and *B. melitensis* sequenced strains show the same *pckA* frameshift and subsequent stop codon that results in a truncated protein of 491 amino acids, and this is also true of the only *B. ovis* strain (BOV_2009 strain) sequenced. On the other, the *pckA* homologs of *B. suis* biovar 3 (strain 686), 4 (strain 40), or 5 (strain 513), *B. neotomae* (strain 5K33), *B. ceti* (strain B1/94), and *B. pinnipedialis* (strains M292/94/1 and M163/99/10) encode a protein of the same size (536 amino acids) as the *Agrobacterium tumefaciens* ortholog (for which there is evidence of PckA activity; Liu et al., 2005), *Ochrobactrum anthropi* and *Mesorhizobium loti*. Therefore, whereas the genomic, experimental, and epidemiological data coincide in indicating a

role for PpdK but not for PckA in the virulence of *B. abortus* and *B. melitensis* in ruminants and accidental hosts like humans and canids, the interpretation of the conservation of *pckA* in other brucellae would require studies in the corresponding natural hosts.

The reasons for the conservation of PpdK over PckA in *B. abortus*, *B. melitensis*, and *B. ovis* are not obvious. It may be that, as opposed to the exclusively gluconeogenic role of PckA, the bidirectional nature of the PpdK catalyzed pyruvate \leftrightarrow phosphoenolpyruvate step makes the latter a more versatile enzyme (Figure 8). Although the direction of the C flow remains to be determined, it could indeed change during the life cycle of the bacteria depending on the substrates available at different stages, and in such a scenario *pckA* could become less useful and eventually superfluous. If TCA were the main source of precursors in the animal model, *B. suis* 513 could obtain phosphoenolpyruvate using Mae and PpdK and/or PckA (a possibility suggested by the *in vitro* growth with glutamate; Figure 5), and loss of PckA in *B. abortus* would not affect the Mae and PpdK route (able to supply phosphoenolpyruvate; Figure 8). This simple picture is in keeping with the attenuation of *B. abortus* 2308W *mae* mutants (Zúñiga-Ripa et al., 2014) but not with the virulence of the *B. suis* 513 double *mae*-*pckA* mutant (Figure 7) and the inability of *B. abortus* 2308W to grow with glutamate alone *in vitro* (Table 1 and Figure 3). A hypothesis that could conciliate all the evidence available is that *B. abortus* is complementing the use of malate with a non-TCA substrate able to provide phosphoenolpyruvate, and that *B. suis* 513 uses such a substrate more efficiently, being in this way independent of malate and oxaloacetate. In this regard lactate is an attractive candidate because it can provide pyruvate (and phosphoenolpyruvate using PpdK; Figure 8). Moreover, whereas *B. abortus* 2308W (see below) cannot grow on lactate (Figure 3) and requires glutamate or glycerol as a complement *in vitro* (Zúñiga-Ripa et al., 2014), *B. suis* 513 can use lactate as the only source of C (Figure 3). Recently, on the basis of the availability of glutamate, lactate, and glycerol (and erythritol) in genital tissues, we have speculated that this set of simple C substrates could mimic the nutritional environment in the host (Letesson et al., 2017). It is thus conceivable that the dependence of *B. abortus* on at least two C sources and the loss of PckA reflect a progressive adaptation to such a nutritional environment. In this context, the recent work of Czyż et al. (2017) is also relevant, which described that *B. abortus* 2308 requires lactate dehydrogenase for intracellular survival in THP-1 monocytes. Interestingly, they also found that infected THP-1 monocytes increase glucose consumption and lactate production (a Warburg-like effect). However, the results reported by these authors on the ability of these bacteria to grow on substrates as the only C source do not clearly match those described here. Whereas they reported that a *B. abortus* 2308 strain was able to metabolize glucose, lactate, glutamate, and erythritol by measuring the reduction of a tetrazolium dye in a basal medium containing micromolar concentrations of arginine, glutamate, cystine, and 0.005% yeast extract, we did not find evidence for *B. abortus* 2308W use of lactate, glutamate, or glucose by a direct measurement of growth in mineral salts and vitamins. Although the discrepancies are

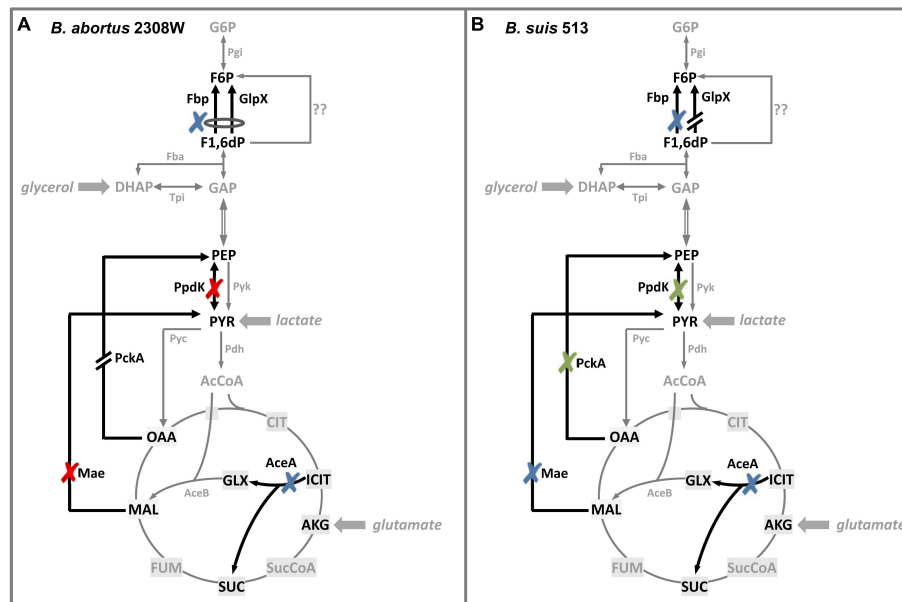


FIGURE 8 | Summary of the results of the central C metabolism enzymes in *B. abortus* 2308W (A) and *B. suis* 513 (B). Glycolysis, gluconeogenesis, TCA cycle, and glyoxylate shunt are shown. Black arrows indicate the steps studied in Zúñiga-Ripa et al. (2014) and in this work. Red crosses indicate attenuated mutants, green crosses specify attenuation when those deletions are combined, blue crosses show steps whose deletion does not affect virulence, broken arrows indicate inactive genes and question marks indicate undescribed enzymes/pathways (for abbreviations, see Figure 1).

difficult to interpret, and they could be due to the use of different basal media or strains (see above), it is important to note that the different ability of 2308W and the 2308 strain used by Czyż et al. (2017) to use lactate *in vitro* as the only C source do not contradict the hypothetical importance of lactate *in vivo*. The L-lactate permease and L-lactate dehydrogenase required for the metabolism of lactate (Barbier et al., 2018 and A. Zúñiga-Ripa, unpublished results) are conserved in all 2308 genomes sequenced and 2308W can use lactate when other substrates are added (Zúñiga-Ripa et al., 2014).

Whereas the experimental and genomic data on the role of PckA and PpdK in the core brucellae agree on the importance of the latter, this is not the case of AceA, the first enzyme of the glyoxylate shunt (Figure 1). Substrates such as fatty acids, some alcohols and esters, waxes, alkenes, and some methylated compounds enter central C metabolism at the level of acetyl-CoA, and this pathway enables some bacteria to use them as the sole C source (Caspi et al., 2018). The pathway may be active in some brucellae. Using a reporter system, we described that *B. abortus* 2308W expresses *aceA* at the beginning of the exponential phase in peptone-yeast extract-glucose but hardly in glutamate-lactate glycerol (Zúñiga-Ripa et al., 2014) and, in a proteomic study in J774 murine macrophages, Al Dahouk et al. (2008) found that *aceA* is expressed in *B. suis* 1330 (biovar 1) 48 h after infection. Also, Abdou et al. (2017) reported that a *B. suis* 1330 (biovar 1) mutant in the *regA* regulator overexpresses *aceA* after 3 days in glutamate-lactate-glycerol in an hypoxic persistence model. Using the *regA* mutant, its complemented strain and an *aceA* mutant grown in glutamate-lactate-glycerol supplemented with 0.05 mM sodium palmitate and 5 mM ammonium sulfate, these

authors found evidence compatible with an active AceA by testing the respective cytosolic fractions with phenylhydrazine in the presence of isocitrate (Abdou et al., 2017). However, the evidence obtained in the analysis of *aceA* mutants in virulence models is not uniform. On one hand, infection of BALB/c mice with a *B. suis* 1330 *aceA* mutant results in lower CFU/spleen in the first 4 weeks but not at later times with respect to a complemented strain that did not fully restore virulence, and the differences are not reproduced in the liver (Abdou et al., 2017). On the other, we observed no attenuation for *B. suis* 513 or, in a previous work (Zúñiga-Ripa et al., 2014), for *B. abortus* 2308W in the spleens of BALB/c mice in the first 8 weeks. For *B. abortus* 2308W and *B. suis* 1330, the discrepancy has been attributed to strain differences (Abdou et al., 2017) and the results with *B. suis* 513 add to the hypothesis of a possible diversity of the brucellae at this level. There are small differences in the amino acid sequence of the respective AceA homologs (Supplementary Figure S4) but these are difficult to interpret without testing the activity of the purified proteins. It would be striking that AceA plays a role on virulence in some core brucellae but not in others, and further research is required to clarify these aspects of the central C metabolism of these bacteria. Thus far, the ability of *Brucella* to grow on fatty acids as the sole C source has not been explored (Gerhardt, 1958), possibly because of the early demonstration of their toxicity for *B. abortus* at very low (10–0.1 mg/L) concentrations (Boyd and Casman, 1951), which could hamper studies *in vitro*.

Both *B. abortus* 2308W and *B. suis* 513 double *fbp-glpX* mutants were able to grow in gluconeogenic media and, as discussed before (Zúñiga-Ripa et al., 2014), this suggests a

hitherto undescribed gluconeogenic pathway (Caspi et al., 2018) possibly implicating a new type of phosphatase. Search for such an enzyme has been elusive (M. C. Durand-Steinhauser, T. Barbier, A. Zúñiga-Ripa, I. Moriyón, and J. J. Letesson, unpublished results) mainly because of the low activity of the hypothetical alternative gluconeogenic pathway in *B. abortus*, as the poor growth in gluconeogenic media reflects (Figure 3 and Table 1). However, the double *fbp-glpX* mutant of *B. suis* 513 displays unscathed gluconeogenic ability in very simple media, a phenotype that is facilitating this investigation. Research in progress confirms the hypothesis that a new gluconeogenic enzyme compatible with a new pathway is in fact active in *B. suis* 513. Also worth commenting upon is the similar phenotype of wild type bacteria of *B. suis* 513 and *B. microti* CCM 4915 but not of *B. abortus* 2308W in gluconeogenic media (Figure 1). This simple observation suggests that gluconeogenesis is similar in the former two species, that the pathway is ancestral in the core brucellae and that there is a reduction of its efficiency in, at least, *B. abortus*. Such a reduction would be coherent with a reduced role or even non-essentiality of the pathway in the natural hosts of at least *B. abortus*, a hypothesis to be tested once the new pathway is fully elucidated.

AUTHOR CONTRIBUTIONS

AZ-R, JL, MI, and IM conceived the study. AZ-R and TB were the main researchers involved in the mutant and metabolic tests. LL-A, RC-Á, MdM, and PM contributed to mutant construction, growth measurements, and experiments in cells and mice. AZ-R and IM wrote the paper. All authors read and approved the manuscript content.

REFERENCES

- Abdou, E., Jiménez de Bagüés, M. P., Martínez-Abadía, I., Ouahrani-Bettache, S., Pantescio, V., Occhialini, A., et al. (2017). RegA plays a key role in oxygen-dependent establishment of persistence and in isocitrate lyase activity, a critical determinant of *in vivo* *Brucella suis* pathogenicity. *Front. Cell. Infect. Microbiol.* 7:186. doi: 10.3389/fcimb.2017.00186
- Al Dahouk, S., Hofer, E., Tomaso, H., Vergnaud, G., Le Flèche, P., Cloeckaert, A., et al. (2012). Intraspecies biodiversity of the genetically homologous species *Brucella microti*. *Appl. Environ. Microbiol.* 78, 1534–1543. doi: 10.1128/AEM.06351-11
- Al Dahouk, S., Jubier-Maurin, V., Scholz, H. C., Tomaso, H., Karges, W., Neubauer, H., et al. (2008). Quantitative analysis of the intramacrophagic *Brucella suis* proteome reveals metabolic adaptation to late stage of cellular infection. *Proteomics* 8, 3862–3870. doi: 10.1002/pmic.200800026
- Al Dahouk, S., Köhler, S., Occhialini, A., Jiménez de Bagüés, M. P., Hammerl, J. A., Eisenberg, T., et al. (2017). *Brucella* spp. of amphibians comprise genomically diverse motile strains competent for replication in macrophages and survival in mammalian hosts. *Sci. Rep.* 7:44420. doi: 10.1038/srep44420
- Alton, G. G., Jones, L. M., Angus, R. D., and Verger, J.-M. (1988). *Techniques for the Brucellosis Laboratory*. Paris: INRA.
- Altschul, S. F., Gish, W., Miller, W., Myers, E. W., and Lipman, D. J. (1990). Basic local alignment search tool. *J. Mol. Biol.* 215, 403–410. doi: 10.1016/S0022-2836(05)80360-2
- Banai, M., and Corbel, M. (2010). Taxonomy of *Brucella*. *Open Vet. Sci. J.* 85–101. doi: 10.2174/1874318801004010085

FUNDING

The work at Departamento de Microbiología y Parasitología, Universidad de Navarra, was supported by MINECO grant AGL2014-58795-C4-1-R and Instituto de Salud Tropical funders (Obra Social la Caixa, Fundacion Caja Navarra, Roviralt, PROFAND, Ubesol, ACUNSA, and Artai). The research at URBM was supported by grants from the Fonds National de la Recherche Scientifique (FNRS; Convention No. 2.4521.10 from Fonds de la Recherche Scientifique Médicale, Belgium) and by the Interuniversity Attraction Poles Programme initiated by the Belgian Science Policy Office. The work at CITA was supported by MINECO grant AGL2014-58795-C4-3-R and Gobierno de Aragón (Consolidated Group A14).

ACKNOWLEDGMENTS

We are grateful to Maria Inácia Corrêa de Sá (Instituto Nacional de Investigação Agrária e Veterinária, Lisbon, Portugal) and Stephan Köhler (Centre d'études d'agents Pathogènes et Biotechnologies pour la Santé, Montpellier, France) for respectively providing the *B. suis* 513 and *B. microti* CCM4915 strains used in this work.

SUPPLEMENTARY MATERIAL

The Supplementary Material for this article can be found online at: <https://www.frontiersin.org/articles/10.3389/fmicb.2018.00641/full#supplementary-material>

- Barbier, T., Collard, F., Zúñiga-Ripa, A., Moriyón, I., Becker, J., Wittmann, C., et al. (2014). Erythritol feeds the pentose phosphate pathway via three new isomerases leading to D-erythrose-4-phosphate in *Brucella*. *Proc. Natl. Acad. Sci. U.S.A.* 111, 17815–17820. doi: 10.1073/pnas.1414622111
- Barbier, T., Zúñiga-Ripa, A., Moussa, S., Plovier, H., Sternon, J. F., Lázaro-Antón, L., et al. (2018). *Brucella* central carbon metabolism: an update. *Crit. Rev. Microbiol.* 44, 182–211. doi: 10.1080/1040841X.2017.1332002
- Boyd, D. M., and Casman, E. P. (1951). Inhibition of a strain of *Brucella abortus* by medium filtered through cotton. *Public Health Rep.* 66, 44–49. doi: 10.2307/4587604
- Caspi, R., Billington, R., Fulcher, C. A., Keseler, I. M., Kothari, A., Krummenacker, M., et al. (2018). The MetaCyc database of metabolic pathways and enzymes. *Nucleic Acids Res.* 46, D633–D639. doi: 10.1093/nar/gkx935
- Corbel, M. J. (1984). International committee on systematic bacteriology. Subcommittee on taxonomy of *Brucella* (Minutes of the Meeting, 10 August 1982, Boston, Massachusetts). *Int. J. Syst. Bacteriol.* 34, 366–367. doi: 10.1099/00207713-34-3-366
- Czyż, D. M., Willett, J. W., and Crosson, S. (2017). *Brucella abortus* induces a Warburg shift in host metabolism that is linked to enhanced intracellular survival of the pathogen. *J. Bacteriol.* 199, e227–e217. doi: 10.1128/JB.00227-17
- Gerhardt, P. (1958). The nutrition of brucellae. *Bacteriol. Rev.* 22, 81–98.
- Gerhardt, P., and Wilson, J. B. (1948). The nutrition of *Brucellae*: growth in simple chemically defined media. *J. Bacteriol.* 56, 17–24.
- Goujon, M., McWilliam, H., Li, W., Valentin, F., Squizzato, S., Paern, J., et al. (2010). A new bioinformatics analysis tools framework at EMBL-EBI. *Nucleic Acids Res.* 38, W695–W699. doi: 10.1093/nar/gkq313

- Grilló, M.-J. J., Blasco, J. M., Gorvel, J.-P. P., Moriyón, I., and Moreno, E. (2012). What have we learned from brucellosis in the mouse model? *Vet. Res.* 43, 1–35. doi: 10.1186/1297-9716-43-29
- Jiménez de Bagüés, M. P., de Martino, A., Quintana, J. F., Alcaraz, A., and Pardo, J. (2011). Course of infection with the emergent pathogen *Brucella microti* in immunocompromised mice. *Infect. Immun.* 79, 3934–3939. doi: 10.1128/IAI.05542-11
- Jiménez de Bagüés, M. P., Ouahrani-Bettache, S., Quintana, J. F., Mitjana, O., Hanna, N., Bessoles, S., et al. (2010). The new species *Brucella microti* replicates in macrophages and causes death in murine models of infection. *J. Infect. Dis.* 202, 3–10. doi: 10.1086/653084
- Koser, S. A., Breslove, B. B., and Dorfman, A. (1941). Accessory growth factor requirements of some representatives of the *Brucella* group. *J. Infect. Dis.* 69, 114–124. doi: 10.1093/infdis/69.2.114
- Koser, S. A., and Wright, M. H. (1942). Further experiments on accessory growth factor requirements of the *Brucella* group. *J. Infect. Dis.* 71, 86–88. doi: 10.1093/infdis/71.1.86
- Lapaque, N., Moriyón, I., Moreno, E., and Gorvel, J. P. (2005). *Brucella* lipopolysaccharide acts as a virulence factor. *Curr. Opin. Microbiol.* 8, 60–66. doi: 10.1016/j.mib.2004.12.003
- Letesson, J.-J., Barbier, T., Zúñiga-Ripa, A., Godfroid, J., De Bolle, X., and Moriyón, I. (2017). *Brucella* genital tropism: What's on the menu. *Front. Microbiol.* 8:506. doi: 10.3389/fmicb.2017.00506
- Liu, P., Wood, D., and Nester, E. W. (2005). Phosphoenolpyruvate carboxykinase is an acid-induced, chromosomally encoded virulence factor in *Agrobacterium tumefaciens*. *J. Bacteriol.* 187, 6039–6045. doi: 10.1128/JB.187.17.6039-6045.2005
- Lyamkin, G. I., Taran, I. F., Safronova, V. M., Tikhenko, N. I., and Shiranovich, M. P. (1983). Taxonomic position and ecology of the causative agent of brucellosis isolated from murine rodents in regions of the northern foothills of the Greater Caucasus. II. The ecological and pathogenetic characteristics of *Brucella* strains isolated from murine rodents. *Zh. Mikrobiol. Epidemiol. Immunobiol.* 6, 31–35. (In Russian).
- Lyamkin, G. I., Taran, I. F., and Tikhenko, N. I. (1982). "Study of *Brucella* strains isolated from rodents in the northern foothills of Greater Caucasus," in *Proceedings of the Conference on Diseases with Natural Focus on the Caucasus*, Stavropol, 96–97.
- Lyamkin, G. I., Tikhenko, N. I., and Resurrection, E. (1981). "Characteristics of *Brucella* isolated in the center of the Caucasus," in *Proceedings of the Conference on Contemporary Problems of Zoonotic Infections*, Stavropol, 99–100.
- McCullough, N. B., and Dick, L. A. (1942a). Physiological studies of *Brucella*: I. Quantitative accessory growth factor requirement of certain strains of *Brucella*. *J. Infect. Dis.* 71, 193–197. doi: 10.1093/infdis/71.3.193
- McCullough, N. B., and Dick, L. A. (1942b). Physiological studies of *Brucella*: II. Accessory growth factor requirement of recently isolated strains of *Brucella abortus*. *J. Infect. Dis.* 71, 198–200. doi: 10.1093/infdis/71.3.198
- McCullough, W. G., Mills, R. C., Herbst, E. J., Roessler, W. G., and Brewer, C. R. (1946). Studies on the nutritional requirements of *Brucella suis* 1. *J. Bacteriol.* 53, 5–15.
- Meyer, M. E. (1976). Evolution and taxonomy in the genus *Brucella*: progesterone induction of filterable forms of *Brucella abortus* type 2 with revertant characteristics essentially indistinguishable *in vitro* from those of *Brucella ovis*. *Am. J. Vet. Res.* 37, 211–214.
- Moreno, E., Cloeckert, A., and Moriyón, I. (2002). *Brucella* evolution and taxonomy. *Vet. Microbiol.* 90, 209–227. doi: 10.1016/S0378-1135(02)00210-9
- Pizarro-Cerdá, J., Méresse, S., Parton, R. G., Van der Goot, G., Sola-Landa, A., López-Goñi, I., et al. (1998). *Brucella abortus* transits through the autophagic pathway and replicates in the endoplasmic reticulum of nonprofessional phagocytes. *Infect. Immun.* 66, 5711–5724.
- Plommet, M. (1991). Minimal requirements for growth of *Brucella suis* and other *Brucella* species. *Zentralbl. Bakteri.* 275, 436–450. doi: 10.1016/S0934-8840(11)80165-9
- Robertson, D. C., and McCullough, W. G. (1968). The glucose catabolism of the genus *Brucella*. I. Evaluation of pathways. *Arch. Biochem. Biophys.* 127, 263–273. doi: 10.1016/0003-9861(68)90225-7
- Ronneau, S., Moussa, S., Barbier, T., Conde-Álvarez, R., Zúñiga-Ripa, A., Moriyón, I., et al. (2014). *Brucella*, nitrogen and virulence. *Crit. Rev. Microbiol.* 42, 507–525. doi: 10.3109/1040841X.2014.962480
- Scholz, H. C., Hubalek, Z., Sedlacek, I., Vergnaud, G., Tomaso, H., Al Dahouk, S., et al. (2008). *Brucella microti* sp. nov., isolated from the common vole *Microtus arvalis*. *Int. J. Syst. Evol. Microbiol.* 58, 375–382. doi: 10.1099/ijls.0.65356-0
- Scupham, A. J., and Triplett, E. W. (1997). Isolation and characterization of the UDP-glucose 4'-epimerase-encoding gene, *galE*, from *Brucella abortus* 2308. *Gene* 202, 53–59. doi: 10.1016/S0378-1119(97)00453-8
- Sedzicki, J., Tschon, T., Low, S. H., Willemart, K., Goldie, K. N., Letesson, J.-J., et al. (2018). 3D correlative electron microscopy reveals continuity of *Brucella*-containing vacuoles with the endoplasmic reticulum. *J. Cell Sci.* 131:jcs210799. doi: 10.1242/jcs.210799
- Sieira, R., Comerci, D. J., Sanchez, D. O., and Ugalde, R. A. (2000). A homologue of an operon required for DNA transfer in *Agrobacterium* is required in *Brucella abortus* for virulence and intracellular multiplication. *J. Bacteriol.* 182, 4849–4855. doi: 10.1128/JB.182.17.4849-4855.2000
- Sievers, F., Wilm, A., Dineen, D., Gibson, T. J., Karplus, K., Li, W., et al. (2011). Fast, scalable generation of high-quality protein multiple sequence alignments using Clustal Omega. *Mol. Syst. Biol.* 7:539. doi: 10.1038/msb.2011.75
- Soler-Lloréns, P. F., Quance, C. R., Lawhon, S. D., Stuber, T. P., Edwards, J. F., Ficht, T. A., et al. (2016). A *Brucella* spp. isolate from a Pac-Man frog (*Ceratophrys ornata*) reveals characteristics departing from classical Brucellae. *Front. Cell. Infect. Microbiol.* 6:116. doi: 10.3389/fcimb.2016.00116
- Starr, T., Ng, T. W., Wehrly, T. D., Knodler, L. A., and Celli, J. (2008). *Brucella* intracellular replication requires trafficking through the late endosomal/lysosomal compartment. *Traffic* 9, 678–694. doi: 10.1111/j.1600-0854.2008.00718.x
- Suárez-Esquivel, M., Ruiz-Villalobos, N., Castillo-Zeledón, A., Jiménez-Rojas, C., Roop, R. M. II, Comerci, D. J., et al. (2016). *Brucella abortus* strain 2308 wisconsin genome: importance of the definition of reference strains. *Front. Microbiol.* 7:1557. doi: 10.3389/fmicb.2016.01557
- Verger, J.-M., Grimont, F., Grimont, P. A. D., and Grayon, M. (1985). *Brucella*, a monospecific genus as shown by deoxyribonucleic acid hybridization. *Int. J. Syst. Bacteriol.* 35, 292–295. doi: 10.1099/00207713-35-3-292
- Vershilova, P. A., Lyamkin, G. I., Malikov, V. E., and Dranovskaia, E. A. (1983). *Brucella* strains from mouse like rodents isolated in the USSR. *Int. J. Syst. Bacteriol.* 33, 399–400. doi: 10.1099/00207713-33-2-399
- Whatmore, A. M. (2009). Current understanding of the genetic diversity of *Brucella*, an expanding genus of zoonotic pathogens. *Infect. Genet. Evol.* 9, 1168–1184. doi: 10.1016/j.meegid.2009.07.001
- Zheludkov, M. M., and Tsirelson, L. E. (2010). Reservoirs of *Brucella* infection in nature. *Biol. Bull.* 37, 709–715. doi: 10.1134/S106235901007006X
- Zúñiga-Ripa, A., Barbier, T., Conde-Álvarez, R., Martínez-Gómez, E., Palacios-Chaves, L., Gil-Ramírez, Y., et al. (2014). *Brucella abortus* depends on pyruvate phosphate dikinase and malic enzyme but not on Fbp and GlpX fructose-1,6-bisphosphatases for full virulence in laboratory models. *J. Bacteriol.* 196, 3045–3057. doi: 10.1128/JB.01663-14
- Zygmunt, M. S., Jacques, I., Bernardet, N., and Cloeckert, A. (2012). Lipopolysaccharide heterogeneity in the atypical group of novel emerging *Brucella* species. *Clin. Vaccine Immunol.* 19, 1370–1373. doi: 10.1128/CVI.00300-12

Conflict of Interest Statement: The authors declare that the research was conducted in the absence of any commercial or financial relationships that could be construed as a potential conflict of interest.

Copyright © 2018 Zúñiga-Ripa, Barbier, Lázaro-Antón, de Miguel, Conde-Álvarez, Muñoz, Letesson, Iriarte and Moriyón. This is an open-access article distributed under the terms of the Creative Commons Attribution License (CC BY). The use, distribution or reproduction in other forums is permitted, provided the original author(s) and the copyright owner are credited and that the original publication in this journal is cited, in accordance with accepted academic practice. No use, distribution or reproduction is permitted which does not comply with these terms.



Genomic Insertion of a Heterologous Acetyltransferase Generates a New Lipopolysaccharide Antigenic Structure in *Brucella abortus* and *Brucella melitensis*

Estrella Martínez-Gómez¹, Jonas Ståhle², Yolanda Gil-Ramírez¹, Amaia Zúñiga-Ripa¹, Mona Zaccheus², Ignacio Moriyón¹, Maite Iriarte¹, Göran Widmalm² and Raquel Conde-Álvarez^{1*}

¹ Instituto de Salud Tropical, Instituto de Investigación Sanitaria de Navarra, Departamento de Microbiología y Parasitología, Universidad de Navarra, Pamplona, Spain, ² Department of Organic Chemistry, Arrhenius Laboratory, Stockholm University, Stockholm, Sweden

OPEN ACCESS

Edited by:

Axel Cloeckaert,
Institut National de la Recherche
Agronomique (INRA), France

Reviewed by:

David Bundle,
University of Alberta, Canada
Diego J. Comerci,
Instituto de Investigaciones
Biotecnológicas (IIB-INTECH),
Argentina

*Correspondence:

Raquel Conde-Álvarez
rconde@unav.es

Specialty section:

This article was submitted to
Infectious Diseases,
a section of the journal
Frontiers in Microbiology

Received: 21 March 2018

Accepted: 07 May 2018

Published: 25 May 2018

Citation:

Martínez-Gómez E, Ståhle J, Gil-Ramírez Y, Zúñiga-Ripa A, Zaccheus M, Moriyón I, Iriarte M, Widmalm G and Conde-Álvarez R (2018) Genomic Insertion of a Heterologous Acetyltransferase Generates a New Lipopolysaccharide Antigenic Structure in *Brucella abortus* and *Brucella melitensis*. *Front. Microbiol.* 9:1092. doi: 10.3389/fmicb.2018.01092

Brucellosis is a bacterial zoonosis of worldwide distribution caused by bacteria of the genus *Brucella*. In *Brucella abortus* and *Brucella melitensis*, the major species infecting domestic ruminants, the smooth lipopolysaccharide (S-LPS) is a virulence factor. This S-LPS carries a *N*-formyl-perosamine homopolymer O-polysaccharide that is the major antigen in serodiagnostic tests and is required for virulence. We report that the *Brucella* O-PS can be structurally and antigenically modified using *wbdR*, the acetyl-transferase gene involved in *N*-acetyl-perosamine synthesis in *Escherichia coli* O157:H7. *Brucella* constructs carrying plasmidic *wbdR* expressed a modified O-polysaccharide but were unstable, a problem circumvented by inserting *wbdR* into a neutral site of chromosome II. As compared to wild-type bacteria, both kinds of *wbdR* constructs expressed shorter O-polysaccharides and NMR analyses showed that they contained both *N*-formyl and *N*-acetyl-perosamine. Moreover, deletion of the *Brucella* formyltransferase gene *wbkC* in *wbdR* constructs generated bacteria producing only *N*-acetyl-perosamine homopolymers, proving that *wbdR* can replace for *wbkC*. Absorption experiments with immune sera revealed that the *wbdR* constructs triggered antibodies to new immunogenic epitope(s) and the use of monoclonal antibodies proved that *B. abortus* and *B. melitensis* *wbdR* constructs respectively lacked the A or M epitopes, and the absence of the C epitope in both backgrounds. The *wbdR* constructs showed resistance to polycations similar to that of the wild-type strains but displayed increased sensitivity to normal serum similar to that of a *per* R mutant. In mice, the *wbdR* constructs produced chronic infections and triggered antibody responses that can be differentiated from those evoked by the wild-type strain in S-LPS ELISAs. These results open the possibilities of developing brucellosis vaccines that are both antigenically tagged and lack the diagnostic epitopes of virulent field strains, thereby solving the diagnostic interference created by current vaccines against *Brucella*.

Keywords: lipopolysaccharide (LPS), bacterial pathogenesis, bacteria, vaccine development, virulence factor, antigen, brucellosis, *Brucella*

INTRODUCTION

The Gram-negative bacteria of the genus *Brucella* are the etiological agents of brucellosis, a zoonosis that causes abortions and infertility in domestic livestock and wildlife and a grave and debilitating disease in humans. Eradicated in a handful of countries, this disease is endemic or increasing in many areas of Asia, Africa, and America due to changing breeding conditions and agricultural intensification, thus representing a serious problem in developing economies throughout the world (Jones et al., 2013; McDermott et al., 2013; Ducrotoy et al., 2015; Lai et al., 2017).

The brucellae are facultative intracellular parasites that, in addition to the ability to control the intracellular trafficking and to adapt their metabolism to the nutrients available in the replicative niche (Martirosyan et al., 2011), owe their pathogenicity to structural peculiarities of the outer membrane (OM) that reduce detection by innate immunity (Lapaque et al., 2005; Barquero-Calvo et al., 2007). The OM of *B. abortus*, *B. suis*, and *B. melitensis* (*Brucella* smooth [S] species found in ruminants and swine), carry a S-LPS poorly recognized by cell receptors, complement and bactericidal peptides. The *Brucella* lipid A is a diaminoglucose disaccharide substituted with very long acyl chains that is linked to a core oligosaccharide carrying a characteristic glucosamine lateral branch (Conde-Álvarez et al., 2012; Kubler-Kielb and Vinogradov, 2013b; Fontana et al., 2016). These lipid A and core structures differ from those of typical LPS, reduce and mask the PAMP of LPS and are thus critical for virulence (Lapaque et al., 2005, 2006; Conde-Álvarez et al., 2012). In *Brucella* S-LPS, mannose and *N*-acetyl-quinovosamine link the core to the O-PS, a homopolymer of *N*-formyl-perosamine (4-formamido-4,6-dideoxy D-mannose) in various proportions of α -(1 \rightarrow 2)- and α -(1 \rightarrow 3)-linkages usually but not always with a terminal cap of at least a tetra-saccharide unit containing α -(1 \rightarrow 3)-linked *N*-formyl-perosamine (Perry and Bundle, 1990; Kubler-Kielb and Vinogradov, 2013a; Zaccheus et al., 2013; Fontana et al., 2016). In at least *B. abortus*, *B. suis*, and *B. melitensis*, the O-PS is involved in the resistance to killing by non-immune serum, reduces the access of complement and bactericidal peptides to OM targets and its loss causes attenuation (Lapaque et al., 2005; González et al., 2008). Although these O-PS properties could be accounted for by topological effects of O-PS length such as a steric hindrance of soluble elements of innate immunity and of non-specific adhesion to host cells (Lapaque et al., 2005; González et al., 2008), it is also possible that *N*-formyl-perosamine is specifically needed for virulence. Testing this hypothesis would require a specific manipulation of the chemical structure of the O-PS in live bacteria. Moreover, such a manipulation could also modify the epitopic structure of the O-PS. Taking into account the prominent role of this section of the S-LPS in serological diagnosis (Ducrotoy et al.,

2016), the development of an antigenic tag for *S. brucellosis* vaccines affecting the diagnostic epitopes of virulent field strains could open the possibility of solving the diagnostic interference created by current brucellosis vaccines, a major problem in the eradication of brucellosis in ruminants (Ducrotoy et al., 2018).

Although to the best of our knowledge genetic modification of *Brucella* O-PS has never been attempted, the genetics of *Brucella* O-PS has been largely elucidated (González et al., 2008; Fontana et al., 2016), and this opens the possibility of manipulating its structure. Since the genes required for perosamine synthesis (*manA*, *manB*, *gmd* and *per*) and its formylation (*wbkC*) are indispensable for O-PS expression, gene replacement seems the simplest strategy, and potential tools are genes carried by the few Gram-negative bacteria endowed of heteropolymeric O-PS with *N*-acylated perosamine (Perry and Bundle, 1990). Here we report that *wbdR*, an O-PS acetyltransferase gene of *Escherichia coli* O157:H7, can replace *wbkC* and generates *Brucella* constructs carrying *N*-acetyl-perosamine. We also describe the effect that this O-PS modification has on the epitopic structure of *B. abortus* and *B. melitensis* and discuss the practical implications in the development of new brucellosis vaccines.

MATERIALS AND METHODS

Bacterial Strains and Growth Conditions

The bacterial strains and plasmids used are listed in Supplementary Table S1. Bacteria were routinely grown in standard tryptic soy broth (TSB; Biomérieux, Solna, Sweden) or agar (TSA; Pronadisa, Laboratorios Conda, Spain) either plain or supplemented with Km at 50 μ g/ml, or Cm at 20 μ g/ml, or nalidixic acid (Nal) at 25 μ g/ml. When needed, media were supplemented with 5% sucrose. All strains were stored in skimmed milk (Scharlau, Barcelona, Spain) at -80°C .

DNA Manipulations

Plasmid and chromosomal DNA were extracted with Qiaprep spin Miniprep (Qiagen GmbH, Hilden, Germany) and Ultraclean Microbial DNA Isolation Kit (Mo Bio Laboratories), respectively. When needed, DNA was purified from agarose gels using a Qiaex Gel extraction kit (Qiagen). DNA sequencing was performed by “Servicio de Secuenciación del Centro de Investigación Médica Aplicada” (Pamplona, Spain) and “Unidad de Genómica del Instituto de Parasitología y Biomedicina López-Neyra” (Granada, Spain). Primers (Supplementary Table S2) were synthesized by Sigma-Genosys Ltd. (Haverhill, United Kingdom).

wbdR-Constructs

Primers *wbdR* attB Fw (5'ggggacaagttgtacaaaaagcaggcttcATGAATTTGTATGGTATTTTGGT3') and *wbdR* attB Rv (5'ggggaccactttgtacagaaagctgggtcTTAAATAGATGTTGGCGATCTT3') were designed based on the sequence of *E. coli* O157:H7¹ and according to Gateway Cloning Technology® (Invitrogen, Barcelona, Spain) instructions. Both primers were used to amplify *wbdR* from the start to the stop codon

¹<http://www.ncbi.nlm.nih.gov/>

Abbreviations: CFU, colony forming units; Cm, chloramphenicol; HMBC, heteronuclear multiple-bond correlation; HSQC, heteronuclear single quantum coherence; Km, kanamycin; LPS, lipopolysaccharide; NMR, nuclear magnetic resonance; O-PS, O-specific polysaccharide; PAMP, pathogen associated molecular pattern; PS, O-PS-core oligosaccharide; R, rough; S, smooth; TOCSY, total correlation spectroscopy; TSA, tryptic soy agar.

using *E. coli* O157:H7 DNA as template, and the resulting product was cloned into pDONR221 (Invitrogen) by site-specific recombination, generating pYRI-5. Then, *wbdR* from pYRI-5 was transferred by site-specific recombination to pRH001 (Hallez et al., 2007). The new plasmid (pYRI-6) was introduced in Ba-parental (*B. abortus* 2308W) by conjugation (Conde-Álvarez et al., 2006) to obtain Ba-pwbdR (Supplementary Table S1).

To obtain a stable *B. abortus*-*wbdR* construct, gene *wbdR* with the 300 bp upstream region containing its promoter was amplified from *E. coli* O157:H7 using primers *wbdR* Fw: 5'-TTCCCCGGGGGAgagttcgccacagtaaatcgaa3' and *wbdR* Rv: 5'-TTCCCCGGGGGAttaaatagatgttgccgatctt3', and cloned in pGEM-T Easy® (Promega, Madison, WI, United States) to obtain pYRI-21. The construction was verified by sequencing. Then, the *EcoRI* fragment of pYRI-21 containing *wbdR* and its promoter was subcloned into the corresponding site of pUC18R6KT-miniTn7TKm (Llobet et al., 2009) to obtain pYRI-27 (pUC18R6KT-miniTn7T-Km-PwbdR). The miniTn7 vector carrying *wbdR* with its own promoter was inserted into Ba-parental chromosome II by the method of Choi et al. (2005) and Choi and Schweizer (2006) modified as follows. First pYRI-27 was introduced in *E. coli* S17.1 λpir and then transferred to *Brucella* using an *E. coli* S17.1 λpir (pYRI-27)-*E. coli* HB101 (pRK2013)-*E. coli* SM10 λpir (pTNS2)-Ba-parental four-parental mating. The resulting Ba::Tn7wbdRKm^R construct was examined by PCR for the correct insertion and orientation of miniTn7 between genes *glmS* and *recG* using the following primers: (i) *GlmS*_B (5'-GTCCTTATGGGAACGGACGT-3') and *Ptn7*-R (5'-CACAGCATAACTGGACTGATT-3') for insertion downstream *glmS*; (ii) *Ptn7*-L (5'-ATTAGCTTACGACGCTACACCC-3') and *RecG* (5'-TATATTCTGGCGAGCGATCC-3') for insertion downstream *recG*; and (iii) *GlmS*_B and *RecG* that only amplify the intergenic region in the absence of the mini-Tn7. The presence of only one copy of the miniTn7 was determined by Southern-blot and sequencing.

To obtain a *wbdR* construct with no Km resistance (Ba::Tn7wbdR), a non-polar *kmR* mutant of Ba::Tn7wbdRKm^R was constructed by overlapping PCR using the Km cassette of pUC18R6KT-miniTn7TKm as template. Primers *kmR*-F1 (5'-AGGAAGCGGAACACGTAGAA-3') and *kmR*-R2 (5'-AATCATGCGAAACGATCCTC-3') amplified a 318-bp fragment including 312-bp upstream of the *kmR* start codon and codons 1 to 2 of the *kmR* ORF, and primers *kmR*-F3 (5'-gagatcggttgcgatgattTTCTTCTGAGCGGGACTCTG-3') and *kmR*-R4 (5'-TGGTCCATATGAATATCCTCCTTA-3') amplified a 268-bp fragment including codons 262–264 of the *kmR* ORF and 256 bp downstream of the *kmR* stop codon. Both fragments were ligated by overlapping PCR using oligonucleotides *kmR*-F1 and *kmR*-R4 for amplification, and the complementary regions between *kmR*-R2 and *kmR*-F3 for overlapping. The resulting fragment, containing the *kmR* deletion allele, was cloned into pCR2.1 (Invitrogen) and subcloned into the *EcoRI* site of the suicide plasmid pNPTS138-Cm (Addgene, LGC Standards, Teddington, United Kingdom) to generate plasmid pRCI-65. This suicide plasmid was used to delete the *kmR* gene of Ba::Tn7wbdRKm^R using the allelic exchange by double

recombination (Conde-Álvarez et al., 2006). Deletion of *kmR* was checked with oligonucleotides *kmR*-F1 and *kmR*-R4.

A Ba::Tn7wbdRΔ*wbkC* mutant potentially expressing only the *wbdR* encoded acetyltransferase was constructed by PCR overlap using genomic DNA of Ba-parental as template. Primers *wbkC*-F1 (5'-AGGTGGCGACAAACGAATAA-3') and *wbkC*-R2 (5'-GCCCATGCCAATCAAGGT-3') amplified a 393-bp fragment including codons 1–29 of the *wbkC* ORF (BAB1_0540), as well as 306 bp upstream of the *wbkC* start codon, and primers *wbkC*-F3 (5'-accttgattggcatgggcAGATGGTTCGGAAGTCCAGATT-3') and *wbkC*-R4 (5'-TCTGAACTCGGCTGGATGAC-3') amplified a 434-bp fragment including codons 212–259 of the *wbkC* ORF and 287-bp downstream of the *wbkC* stop codon. Both fragments were ligated by overlapping PCR using oligonucleotides *wbkC*-F1 and *wbkC*-R4 for amplification, and the complementary regions between *wbkC*-R2 and *wbkC*-F3 for overlapping. The fragment containing the *wbkC* deletion allele was cloned into pCR2.1 and subcloned into the *Bam*HI and the *Xba*I sites of the suicide plasmid pJQK (Scupham and Triplett, 1997). The resulting mutator plasmid pYRI-31 was used to delete the *wbkC* gene of Ba::Tn7wbdR by allelic exchange (Conde-Álvarez et al., 2006). The resulting colonies were screened by PCR with primers *wbkC*-F1 and *wbkC*-R4, which amplify a fragment of 827 bp in the mutant and a fragment of 1373 bp in the parental strain.

Bme::Tn7wbdRKm^R was obtained using the modified miniTn7 site-specific integration vector technology (see above). To obtain Bme::Tn7wbdR and Bme::Tn7wbdRΔ*wbkC* the suicide plasmids pRCI-65 and pYRI-31 (see above and Supplementary Table S1) were used.

Stability of *wbdR* in Ba-pwbdR and Ba::Tn7wbdR

The constructs Ba-pwbdR and Ba::Tn7wbdR were grown in the presence of Km and Cm (plasmid antibiotic markers) or Km (transposon antibiotic marker), adjusted to an O.D.₆₀₀ = 0.109 and CFU counted on TSA and TSA Km/Cm or TSA and TSA Km (transfer 0). A 100 μl aliquot of the culture was inoculated into 10 ml of TSB without antibiotics, the broth incubated for 48 h and CFU counted on TSA and TSA Km/Cm or on TSA and TSA Km. The process was serially repeated five times.

Bacteriological Characterization, Antibiotic Sensitivity and Growth Curves

Colonial morphology, urease, and sensitivity to R/C phage were determined following established *Brucella* typing procedures (Alton et al., 1988). S/R colony morphology was studied by the crystal violet dye exclusion test and acriflavine agglutination (Alton et al., 1988). Autoagglutination was evaluated by measuring the O.D.₆₀₀ of bacterial suspensions in TSB after 6 and 14 days of static incubation at 37°C. To obtain inocula for growth curves, bacteria were first grown in 10 ml of TSB supplemented with antibiotics in a 50 ml flask, incubated with orbital stirring at 37°C for 18 h, harvested by centrifugation and resuspended at a O.D.₆₀₀ of 0.1 in TSB. Then, aliquots were dispensed into Bioscreen plates (200 μl/well) which were incubated in a Bioscreen C (Lab Systems Quesada, Capital Federal, Argentina)

with continuous shaking at 37°C. Growth was monitored at 420–580 nm every 30 min over a 65 h-period (control wells contained sterile TSB). All experiments were performed in triplicate.

LPS and PS Preparations

Crude S-LPS from Ba-parental or *B. abortus wbdR* constructs was obtained by the method of Leong et al. (1970) with modifications. For the wild-type strain, the phenol phase of a phenol-water extract was precipitated with 2 volumes of methanol to obtain the total crude S-LPS. For *wbdR* constructs, this classical precipitation step failed to yield the total of the S-LPS and precipitation was achieved with 6 volumes of methanol. Alternatively, the S-LPS remaining in the supernatant of the methanol precipitation was dialyzed and freeze-dried. These crude S-LPS were resuspended (10 mg/ml) in 175 mM NaCl, 0.05% NaN₃, 0.1M Tris-HCl (pH 7.0), digested once with nucleases (50 µg/ml each of DNase-II type V, and RNase [Sigma, St. Louis, MO, United States] 30 min at 37°C) and then three times with proteinase K (50 µg/ml, 3 h at 55°C). Finally, the S-LPS was recovered by ultracentrifugation (6 h at 100,000 × g in a Beckman Ti70 rotor) (Aragón et al., 1996).

Purified LPS were used to obtain the PS by mild acid hydrolysis in 1% SDS acetate buffer 10 mM (pH 4.5) at 100°C for 2 h, a method that splits the lipid A-core linkage. After cooling at room temperature and brought to pH 7 with 0.2 M NaOH, lipid A and debris were pelleted (10 min at 5000 × g) and the supernatant was dialyzed against distilled water, lyophilized and chromatographed in acetate-pyridine buffer on Sephadex G50. Fractions were analyzed for PS by gel immunoprecipitation in 10% NaCl, 100 mM borate (pH 8.3) (Díaz-Aparicio et al., 1993).

SDS-PAGE and NMR Spectroscopy

LPS were analyzed in 15% polyacrylamide gels (37.5:1 acrylamide/methylenebisacrylamide ratio) in Tris-HCl-glycine and stained by the periodate-alkaline silver method (Tsai and Frasch, 1982).

The ¹H NMR spectrum of the Ba-parental PS (5 mg in 0.55 mL D₂O) was recorded at 25°C and the 1D and 2D NMR spectra of the Ba-*pwbdR* (10 mg in 0.5 mL D₂O), Ba::Tn7*wbdR* (5 mg in 0.55 mL D₂O) and Ba::Tn7*wbdRΔwbkC* PS (10 mg in 0.55 mL D₂O) were recorded at 47°C, 25°C and 25°C, respectively. All experiments were performed on Bruker AVANCE 500 MHz or Bruker AVANCE III 700 MHz spectrometers; both equipped with 5 mm TCI Z-Gradient CryoProbes. ¹H chemical shifts were referenced to internal sodium 3-trimethylsilyl-(2,2,3,3-²H₄)-propanoate (TSP, δ_H 0.00) and ¹³C chemical shifts were referenced to external dioxane in D₂O (δ_C 67.40). Data processing was performed using vendor-supplied software. The assignments of the ¹H and ¹³C resonances of the Ba-parental, Ba-*pwbdR*, Ba::Tn7*wbdR* and Ba::Tn7*wbdRΔwbkC* PS were obtained by analysis of ¹H and ¹³C NMR spectra together with a multiplicity-edited ¹H, ¹³C-HSQC experiment (Parella et al., 1997), ¹H, ¹H-TOCSY using mixing times ranging from 10 to 120 ms (Bax and Davis, 1985), as well as a band-selective constant time ¹H, ¹³C-HMBC experiment of Ba-*pwbdR* PS, which was used

to correlate the N-acyl groups (Claridge and Pérez-Victoria, 2003).

Antibodies and Immunological Tests

To obtain a serum reacting with O-PS carrying both N-formyl- and N-acetyl-perosamine (i.e., the Formyl-Acetyl serum), rabbits were inoculated intravenously with 1 mg/ml of phenol-inactivated Ba-*pwbdR* cells. Then, similar doses were administered intraperitoneally 2 and 4 days later and the animals bled 3 weeks later. The animals (2.5 Kg New-Zealand female rabbits; San Bernardo, Spain) were kept in cages with water and food *ad libitum* in the animal facilities of “Centro de Investigación en Farmacobiología aplicada” (University of Navarra). Rabbits were handled, bled and euthanized according to the Spanish and European recommendations (RD 1201/2005; directive 86/609/ECC), and the protocols approved by the Animal Health Care Department of University of Navarra.

To obtain a serum reacting only with N-acetyl-carrying O-PS (i.e., the Acetyl serum) or N-formyl-carrying O-PS (i.e., the Formyl serum), the Formyl-Acetyl serum was absorbed with Ba-parental or Ba::Tn7*wbdRΔwbkC* cells, respectively. Absorption was performed at 4°C with continuous stirring overnight. Cells were removed (13,200 rpm, 10 min, Eppendorf 5415R centrifuge), and the absorption repeated with incubation for 4 h at room temperature. As a control of absorption, Formyl-Acetyl serum was absorbed with Ba-*pwbdR* cells following the same procedure. Finally aliquots of Formyl-Acetyl or Acetyl serum were subsequently absorbed with cells from rough mutant BaΔ*per* to obtain Formyl-Acetyl-OPS or Acetyl-OPS, respectively.

Monoclonal antibodies 42D2 (C/Y-A>M; preferentially reacting with *B. abortus* and *Yersinia enterocolitica* O:9 O-PS), and 33H8 (C/Y-A = M; equally reacting with *B. abortus*, *B. melitensis* and *Y. enterocolitica* O:9 O-PS) were provided by INGENASA (Madrid, Spain) and the reactivities verified by ELISA using LPS of *B. abortus* 2308, *B. melitensis* 16M and *Yersinia enterocolitica* O:9. Monoclonal antibody A15-6B3 (or 6B3) M; reacting with *B. melitensis* but not *B. abortus* O-PS (Laurent et al., 2004) was a generous gift of J. J. Letesson (University of Namur).

For coagglutination, staphylococci were prepared and sensitized with the appropriate serum (Kronvall, 1973), and the bacteria in 4–6 colonies resuspended in 25 µl of saline on a glass slide and mixed with an equal amount of the sensitized staphylococci.

For Western Blots, SDS-PAGE gels (see above) were electrotransferred onto nitrocellulose sheets (Whatmann, Dassel, Germany), blocked with 3% PBS with 0.05% Tween 20 (PBS-T) overnight, and washed with PBS-T. Immune sera or monoclonal antibodies (see below) were diluted in this same buffer and, after incubation overnight at room temperature and washing the membranes with PBS-T, bound immunoglobulins were detected with peroxidase-conjugated goat anti-rabbit immunoglobulin (Nordic Immunological Laboratories, Tilburg, Netherlands) or peroxidase labeled protein G for mouse sera and 4-chlorine-1-naphthol-H₂O₂.

For ELISA, 96-well ELISA plates (Thermo Scientific, Waltham, MA, United States) were coated with 2.5 µg/ml LPS resuspended in PBS overnight at 4°C. Plates were then washed extensively with PBS-T, and incubated with serial dilutions of the appropriate sera or with monoclonal antibodies at 37°C for 5 h. Then, the plates were washed extensively with PBS-T and bound antibodies were detected with peroxidase-labeled protein G (Alonso-Urmeneta et al., 1988, 1998). The peroxidase activity was detected with 2,2'-azino-bis(3-ethylbenzthiazoline-6-sulphonic acid) (ABTS)/H₂O₂. After 15 min, the color was measured in a microtiter plate reader (Multiscanex, Thermo Scientific, Waltham, MA, United States) at 405 nm.

Infections in Mice

Female BALB/c mice (Harlan Laboratories; Bicester, United Kingdom) were kept in cages with water and food *ad libitum* under P3 biosafety conditions in the facilities of “Centro de Investigación Médica Aplicada” (registration code ES31 2010000132) 2 weeks before and during the experiments. The procedures were in accordance with the current European (directive 86/609/EEC) and Spanish (RD 53/2013) legislations, supervised by the Animal Welfare Committee of the University of Navarra, and authorized by the “Gobierno de Navarra” (CEEA 045/12). To prepare inocula, TSA or TSA-Km grown bacteria were harvested, adjusted spectrophotometrically (O.D.₆₀₀ = 0.170) in 10 mM in PBS and diluted in the same buffer to approximately 5×10^5 CFU/ml (exact doses were assessed retrospectively). For each bacterial strain, five mice were intraperitoneally inoculated with 0.1 mL/mouse. Eight weeks later, mice were bled and CFU numbers in spleen were determined. Statistical significance was evaluated using one-way ANOVA followed by Dunnett's test.

Sensitivity to the Bactericidal Action of Normal Serum

Exponentially growing bacteria were adjusted to 10⁴ CFU/mL in saline and dispensed in triplicate in microtiter plates (45 µL per well) containing fresh normal bovine or ovine serum (90 µL/well). After 15 and 90 min for the bovine serum or 15 and 45 min for the ovine serum at 37°C, brain heart infusion broth was dispensed (200 µL/well), mixed with the bacterial suspension and 100 µL plated on TSA.

Sensitivity to Polycationic Bactericidal Peptides

Bacterial sensitivity was measured as the effect of increasing concentrations of polymyxin B and poly-L-ornithine on cell viability as described elsewhere (Martínez de Tejada et al., 1995).

Surface Charge

The surface charge density was measured as the electrophoretically effective potential (Zeta potential) as previously described (González et al., 2008). Bacteria were grown in TSB, inactivated with 0.5% phenol, washed and resuspended in 1 mM CsCl, 10 mM HEPES 10 mM (pH 7.2) at an O.D.₆₀₀ of 0.2. Measurements were performed at 25°C in a Zetamaster

instrument using the PCS 1.27 software (Malvern Instruments Ltd., Malvern, United Kingdom).

RESULTS

Identification of *wbdR*: A Perosamine Acetyltransferase for Cloning in *Brucella*

The literature describes at least twelve Gram-negative bacteria with O-PS that contain substituted perosamine (Supplementary Table S3). Among them, *E. coli* O157:H7 was selected because its O-PS contains *N*-acetyl-perosamine (D-Rhap4NAc) [O-PS repeating unit: →2)-α-D-Rhap4NAc-(1→3)-α-L-Fucp-(1→4)-β-D-Glcp-(1→3)-α-D-GalpNAc-(1→] and, moreover, the complete genomic sequence is available. Indeed, synthesis of *N*-acetyl-perosamine requires an acetyl-transferase and a putative one, encoded by gene *wbdR*, was found in the O-PS gene cluster of *E. coli* O157:H7. Apparently, no equivalent gene is found in the O-PS cluster of other bacteria carrying *N*-acetyl-perosamine (Albermann and Beuttler, 2008).

Insertion of *wbdR* Into *B. abortus* Chromosome Is Required to Generate a Stable *wbdR* Construct (Ba::Tn7*wbdR*)

wbdR was amplified and cloned into pRH001 to obtain plasmid pYRI-6, which was then introduced into wild-type *B. abortus* 2308W (Ba-parental) to obtain strain Ba-p*wbdR* (Supplementary Table S1). Since plasmids can be lost in the absence of selective pressure and pYRI-6 carries Km/Cm resistance, the stability of Ba-p*wbdR* was studied by serial passage in broth without antibiotics, and aliquots plated on TSA and TSA Km/Cm. One log reduction in CFU/ml was observed on the TSA Km/Cm plates with respect to the TSA plates (Supplementary Figure S1), showing that the construct was not fully stable. To circumvent this problem, a technology that uses the miniTn7 site-specific integration vector was adapted to *Brucella* to integrate *wbdR* into chromosome II (See Experimental Procedures). The new construct (Ba::Tn7*wbdR*Km^R; Supplementary Table S1) was stable in the absence of antibiotic selective pressure (Supplementary Figure S1).

Ba::Tn7*wbdR*Km^R contained *wbkC*, the parental formyltransferase gene, so that it could retain at least part of *N*-formyl-perosamine in its O-PS or no acetyl-perosamine if WbkC activity displaced that of WbdR. To obtain a strain lacking WbkC, the *kmR* cassette was first removed to obtain Ba::Tn7*wbdR* and then *wbkC* deleted to generate Ba::Tn7*wbdR*Δ*wbkC*.

B. abortus wbdR Constructs Produce S-LPS Carrying *N*-acetyl-perosamine

Ba-p*wbdR*, Ba::Tn7*wbdR* and Ba::Tn7*wbdR*Δ*wbkC* were identical to the parental strain in colony morphology and growth (Supplementary Figure S2), oxidase and urease tests and dye sensitivity. Moreover, they did not agglutinate with acriflavine or autoagglutinated (Supplementary Figure S3), and they excluded crystal violet and were resistant to phage R/C

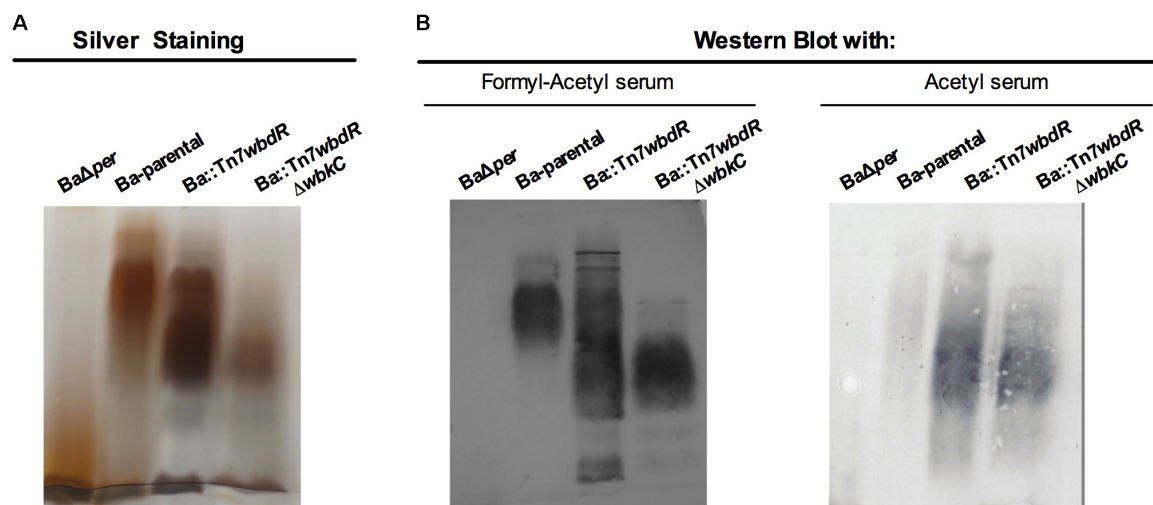


FIGURE 1 | *Brucella abortus wbdR* constructs express an S-LPS that displays a new antigenic structure. SDS-PAGE followed by silver staining (**A**) and Western blots of SDS-proteinase K extracts of the indicated bacteria (**B**). BaΔper is a mutant defective in perosamine synthesis that expresses only R-LPS.

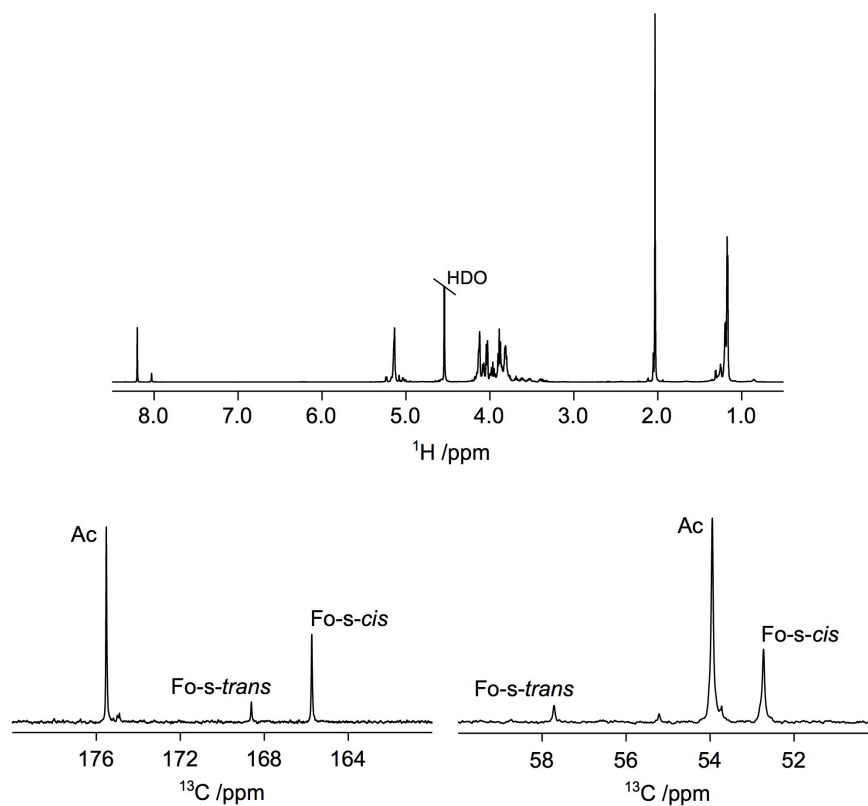


FIGURE 2 | Introduction of *wbdR* into *B. abortus* leads to the expression of *N*-acetyl-perosamine in the O-PS. ^1H NMR spectrum (**Top**) and selected ^{13}C NMR spectral regions corresponding to carbonyl region (**Lower Left**) and region for C4 resonances (**Lower Right**) of *N*-formylated and *N*-acylated perosamine in strain Ba-pwbdR.

(specific for the O-PS-lacking rough [R] brucellae), a set of properties characteristic of strains expressing S-LPS (Alton et al., 1988). Since *wbkC* (i.e., formyl-transferase gene) mutants lack

O-PS (Godfroid et al., 2000), these results strongly suggest that Ba::Tn7wbdRΔwbkC carries a surface O-PS and, therefore, that *wbdR* can replace for *wbkC*, a hypothesis studied by SDS-PAGE

analysis of LPS obtained by the SDS-proteinase K protocol. The LPS of Ba::Tn7*wbdR* and Ba::Tn7*wbdR*Δ*wbkC* (Figure 1A) and Ba::Tn7*wbdR*Km^R and Ba-*pwbdr* (not shown) contained the typical R-LPS and S-LPS fractions present in the parental strain. However, SDS-PAGE also showed that the average molecular weight of the S-LPS fraction of the *wbdR* constructs was lower than that of Ba-parental (Figure 1A).

The ¹H NMR spectrum of the Ba-parental PS (i.e., the core-O-PS obtained by hydrolysis of LPS) (Supplementary Figure S4) was fully consistent with that reported before for *B. abortus* 2.13 (Supplementary Figure S2 in González et al., 2008) showing, among others, resonances from *N*-formyl groups but absence of resonances for *N*-acetyl groups, except for a very small one at δ_H 2.07 consistent with the presence of *N*-acetyl-quinovosamine (the primer for O-PS polymerization) previously investigated in detail using *B. abortus* 2.13. Also, the ¹³C NMR spectrum of Ba-parental PS (Supplementary Figure S4) and ¹³C chemical shifts (Supplementary Table S4) were consistent with those of a *B. abortus* 1119-3 PS (Perry and Bundle, 1990). In contrast, in addition to the expected resonances from *N*-formyl groups at δ_H 8.03 and 8.20 (~0.3 equivalents), the ¹H NMR spectrum of the Ba-*pwbdr* PS revealed a conspicuous resonance from an *N*-acetyl group at δ_H 2.03 (~0.6 equivalents) (Figure 2). Moreover, the ¹³C NMR spectrum showed resonances in the carbonyl region at δ_C 175.5 from the *N*-acetyl group and at δ_C 168.6 and 165.7 from the two conformations of the *N*-formyl group, (Engström et al., 2017) in the region for nitrogen-carrying carbon atoms at δ_C 53.9 from C4 of perosamine carrying the *N*-acetyl group and at δ_C 57.7 and 52.7 from C4 of perosamine substituted by the *N*-formyl group (Figure 2) as well as a resonance from the methyl group of the *N*-acetyl group at δ_C 23.0 supporting the proposed substitution pattern. This was confirmed by a ¹H,¹³C-BS-CT-HMBC NMR experiment in which heteronuclear correlations

over two and/or three bonds could be observed; in particular, correlations were observed at δ_C/δ_H 165.7/3.96 and 168.6/3.40 between the carbonyl atom of the *N*-formyl group and H4 of perosamine as well as at δ_C/δ_H 175.5/3.89 and 175.5/2.03 between the carbonyl atom of the *N*-acetyl group and H4 of perosamine and the methyl protons of the *N*-acetyl group, respectively, fully consistent with NMR chemical shifts of perosamine with these substituents (Kenne et al., 1988).

Subsequent NMR analysis showed that an *N*-acetyl group was also present in the Ba::Tn7*wbdR* PS since a singlet in the ¹H NMR spectrum was observed at 2.05 ppm. Formyl group substitution was still evident from resonances at 8.05 and 8.22 ppm (Figure 3A). These findings were supported by ¹³C NMR resonances at, *inter alia*, 165.7, 168.5, and 175.6 ppm (cf. the above Ba-*pwbdr* PS). In strain Ba::Tn7*wbdR*Δ*wbkC*, in which the formyl-transferase gene has been deleted, a prominent ¹H NMR resonance at δ_H 2.05 confirmed the presence of an *N*-acetyl group in the PS. Notably, and most importantly, any resonances from *N*-formyl groups in the ¹H spectral region at ~8 ppm were completely absent (Figure 3B) confirming the successful transformation into an *N*-acetyl-only substituted PS, additionally supported by ¹³C NMR data, *inter alia*, a resonance at 175.6 ppm.

Taken together, the above results show that cloning of *E. coli wbdR* in *B. abortus* resulted in expression of S-LPS molecules whose O-PS contain *N*-formyl plus *N*-acetyl-perosamine residues or only *N*-acetyl-perosamine depending on the simultaneous presence of *wbkC* and *wbdR* or of only *wbdR*, respectively. The degree of polymerization of the *N*-acetyl-perosamine containing O-PS was, however, reduced when compared to the parental O-PS.

The O-PS of *B. abortus wbdR* Constructs Displays a New Antigenic Structure Lacking the *Brucella C* Epitopes

To probe for epitopic changes, polyclonal immune sera specifically recognizing O-PS carrying only *N*-formyl-perosamine, both *N*-formyl-perosamine and *N*-acetyl-perosamine or only *N*-acetyl-perosamine (henceforth anti-Formyl, anti-Formyl-Acetyl, and anti-Acetyl sera, respectively) were obtained by immunization and cross-absorption (see Material and Methods). By coagglutination, only the bacteria containing an intact *wbkC* reacted with the anti-Formyl or anti-Formyl-Acetyl sera. On the other hand, only the *wbdR* constructs agglutinated with the anti-Acetyl serum, and titration of serial dilutions of cell suspensions showed that the reactivity of Ba::Tn7*wbdR*Δ*wbkC* with this serum was slightly higher (1/32 titer) than that of Ba::Tn7*wbdR* or Ba-*pwbdr* (1/16 titer). These analysis proved the surface exposure of the O-PS antigens and, taking into account that polyclonal sera represent a wide spectrum of specificities, avidities and titers, they prove the existence of surface immunogenic epitope(s) associated with the expression of *N*-acetyl-perosamine and the loss of those associated with *N*-formyl-perosamine in Ba::Tn7*wbdR*Δ*wbkC*. To prove that the new epitopes were in fact carried by the S-LPS, we used the purified molecule. iELISA (Figure 4) showed epitopic changes, and Western-blots (Figure 1B) also

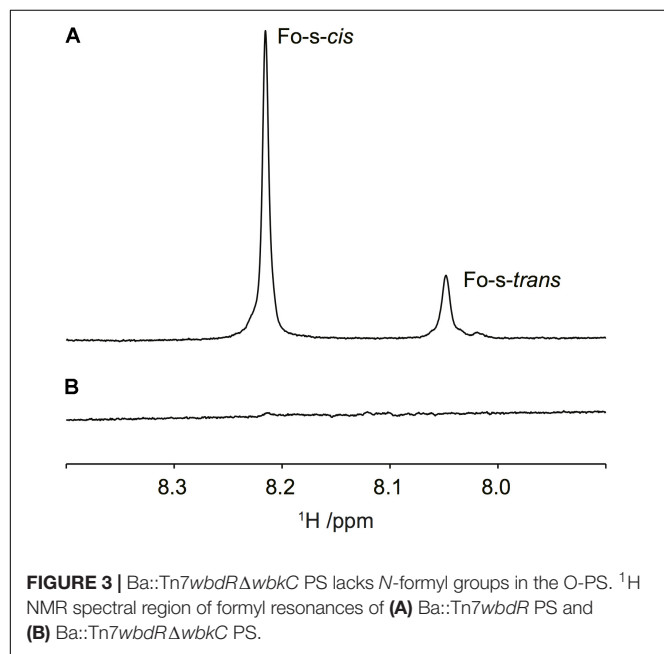


FIGURE 3 | Ba::Tn7*wbdR*Δ*wbkC* PS lacks *N*-formyl groups in the O-PS. ¹H NMR spectral region of formyl resonances of (A) Ba::Tn7*wbdR* PS and (B) Ba::Tn7*wbdR*Δ*wbkC* PS.

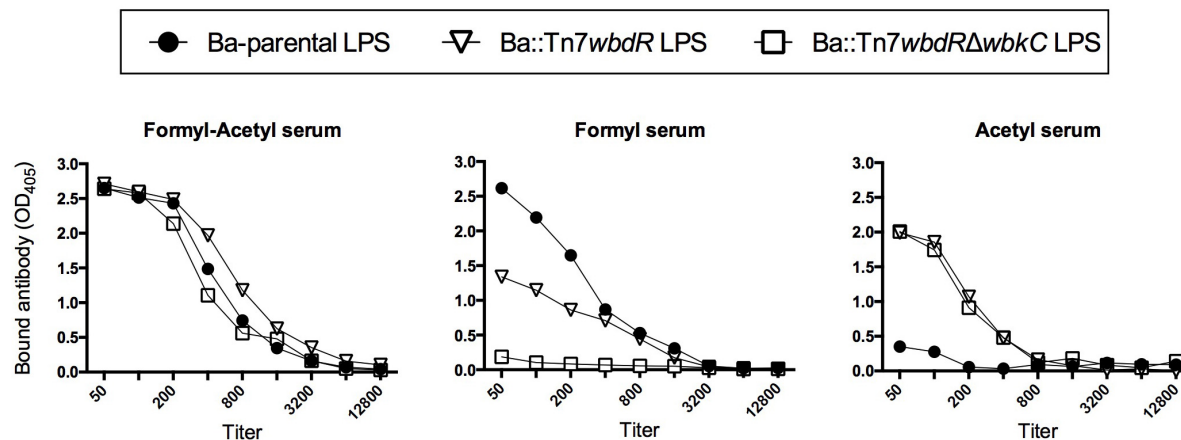


FIGURE 4 | *N*-acetyl-perosamine generates new epitopes in the S-LPS. The ELISAs were performed with the S-LPS of Ba-parental or *B. abortus wbdR*-constructs and anti Ba-*pwbdR* rabbit sera either plain (Formyl-acetyl serum) or adsorbed with Ba::Tn7wbdRΔwbkC (Formyl serum) or with Ba-parental (Acetyl serum).

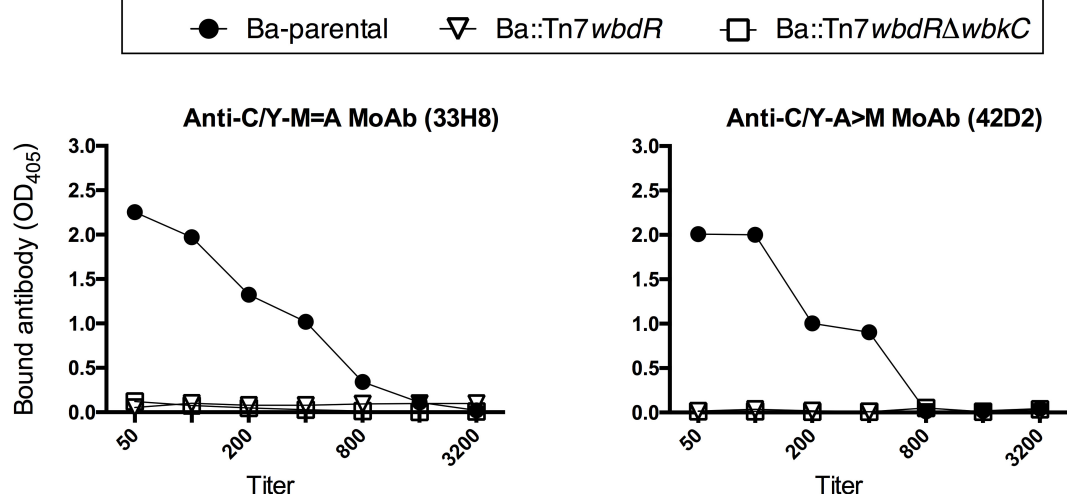


FIGURE 5 | *N*-acetyl-perosamine alters the epitopic structure of S-LPS. Upper panels: Reactivity with monoclonal antibodies of C/Y-A = M and C/Y-A>M specificities in an ELISA performed with the S-LPS of Ba-parental or *B. abortus wbdR*-constructs.

demonstrated that the differences in average molecular weight observed by SDS-PAGE (Figure 1A) corresponded in fact to O-PS heterogeneity. None of the above results changed when the same sera were adsorbed with cells of the R mutant BaΔ*per* (Supplementary Figure S5). Altogether, these results support the conclusion that the epitopes generated by *N*-acetyl-perosamine were absent from wild-type *B. abortus* and that the *N*-acetyl-perosamine O-PS homopolymer of Ba::Tn7wbdRΔwbkC lacked the *N*-formyl-perosamine related epitopes present in the parental strain and the Ba::Tn7wbdR construct. Although the O-PS of brucellae carries overlapping epitopes that are all detected with polyclonal sera, monoclonal antibodies allow for analyses with more refined structural implications. Thus, we probed the O-PS with monoclonal antibodies of A, M and C epitopes specificities. In contrast to the Ba-parental S-LPS, the S-LPS from *wbdR*-constructs did not react with the C/Y-A = M (Cby33H8)

and C/Y-A>M (42D2) monoclonal antibodies (Figure 5 and Supplementary Figure S6). Ba-parental is a biovar 1 strain that lacks the M epitope (Alton et al., 1988; Douglas and Palmer, 1988) and, as expected, the reactivity of the antibody to the M epitope A156B3 was negative for all these S-LPS (data not shown).

***B. abortus wbdR* Constructs Display Increased Sensitivity to Normal Serum but Not to Bactericidal Polycations**

S brucellae but not R mutants are resistance to the bactericidal action to polycations and complement in non-immune serum (Lapaque et al., 2005). The minimal inhibitory concentration of polymyxin B was the same for Ba-parental, Ba::Tn7wbdR and Ba::Tn7wbdRΔwbkC (Figure 6A), and the lack of differences was

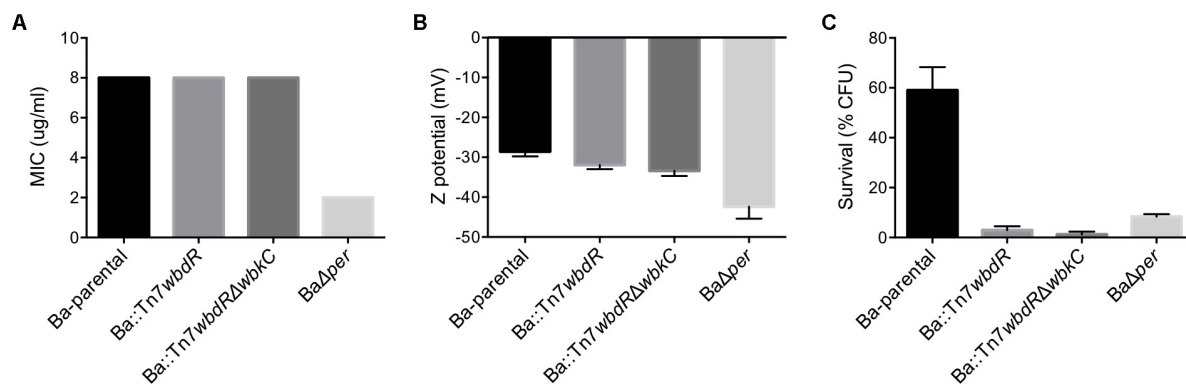


FIGURE 6 | *Brucella abortus wbdR* constructs display increased sensitivity to normal serum but not to bactericidal polycations. Polymyxin B sensitivity (representative results of three independent experiments) **(A)**, surface charge (Z potential) (mean of \pm SD of three independent experiments) **(B)** and survival after 90 min of incubation in normal bovine serum (media \pm standard error of three technical replicates representative of three independent experiments) **(C)** of Ba-parental, Ba::Tn7wbdR, Ba::Tn7wbdRΔwbkC and the R mutant BaΔper.

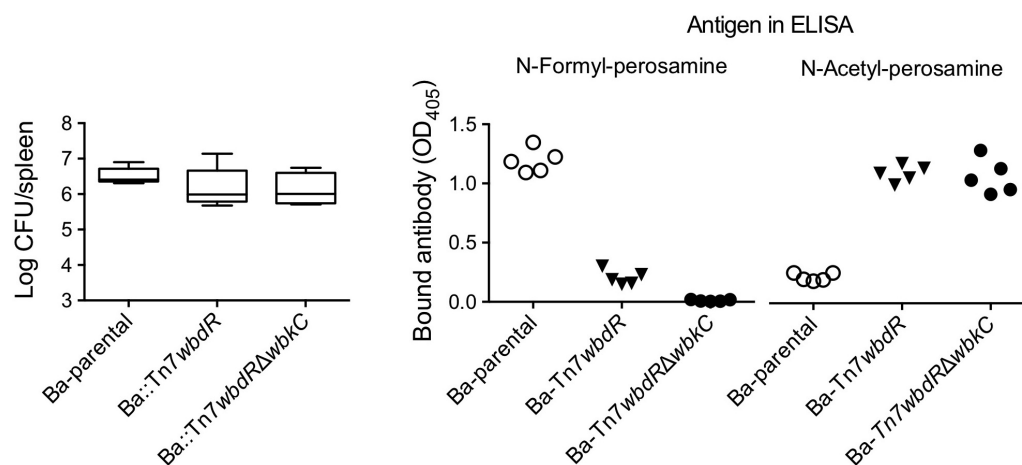


FIGURE 7 | *Brucella abortus wbdR* constructs produce chronic infections in mice that trigger antibodies to the new epitopes. **(Left)** Bacterial loads in the spleens of BALB/c mice at 8 weeks post-infection. **(Center and Right)** Reactivity of sera from mice infected with Ba-parental, Ba::Tn7wbdR or Ba::Tn7wbdRΔwbkC in ELISA performed with the S-LPS of Ba-parental (N-Formyl-perosamine iELISA) or Ba::Tn7wbdRΔwbkC (N-Acetyl-perosamine iELISA). The ODs correspond to the serum dilution (1:50) showing the maximal discrimination between the wild-type and the *wbdR* constructs.

confirmed with poly-L-ornithine (not shown). Consistent with this phenotype, Ba::Tn7wbdR and Ba::Tn7wbdRΔwbkC showed only a small increase in negative surface charge as compared to Ba-parental (**Figure 6B**). On the other hand, Ba::Tn7wbdR and Ba::Tn7wbdRΔwbkC were more sensitive than Ba-parental to the killing action of bovine normal serum and strikingly this susceptibility was similar to that of the R mutant BaΔper (**Figure 6C**). This increased sensitivity was confirmed with sheep normal serum (not shown).

***B. abortus wbdR* Constructs Produce Chronic Infections in Mice That Trigger Antibodies to the New Epitopes**

The above-described experiments were complemented with analyses in the mouse model. As shown in **Figure 7**, the strains carrying N-acetyl O-PS kept the ability to multiply in the spleens

and persisted in the chronic phase, a characteristic of virulent *S. brucellae*. To test whether the infection triggers antibodies corresponding to the above-described epitopic changes, we tested the sera of these animals. Whereas those infected with Ba-parental developed antibodies strongly reacting in an iELISA with the wild-type N-formyl-perosamine LPS, the sera of mice infected with *wbdR* constructs displayed almost no reaction (**Figure 7**), and the reverse picture was obtained in an iELISA with the N-Acetyl-perosamine LPS from Ba::Tn7wbdRΔwbkC (**Figure 7**).

The *wbdR*-Encoded Acetyl-transferase Is Also Active in *B. melitensis*

When the Tn7 technology was used to insert *wbdR* in the chromosome II of *B. melitensis* 16M (Bme-parental), the resulting Bme::Tn7wbdR construct was also S according to the standard

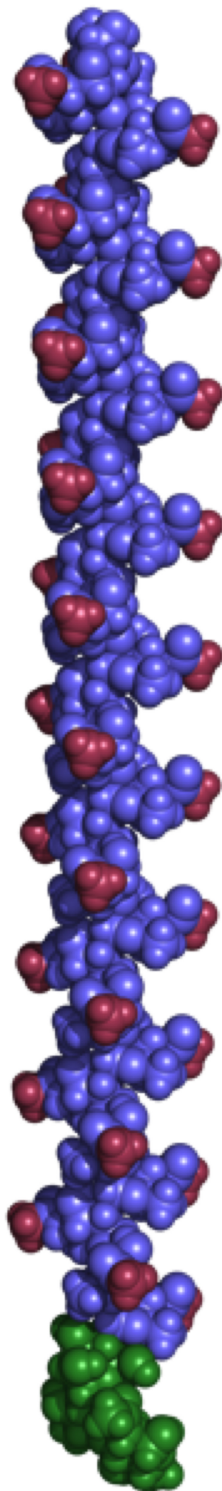


FIGURE 8 | Novel epitopes are accessible for antibodies in the O-PS of Ba::Tn7wbdRΔwbkC. The polysaccharide structure containing 30 residues of →2)-α-D-Rhap4NAc-(1→ connected to two adaptor sugars and a primer →4)-α-D-Manp-(1→3)-α-D-Manp-(1→3)-β-D-QuipNAc which links to the core, was generated by CarbBuilder v2.1.17 and visualized with PyMol 1.3. Methyl groups of *N*-acetyl groups in perosamine residues are highlighted in red color.

tests for S and R brucellae (Alton et al., 1988). Like its *B. abortus* counterpart, this construct coagglutinated with the anti-Formyl-Acetyl, anti-Acetyl and anti-Formyl sera showing that its O-PS contained *N*-acetyl and *N*-formyl-perosamine. Moreover, when *wbkC* was deleted, the resulting Bme::Tn7wbdRΔwbkC strain coagglutinated with the anti-Formyl-Acetyl and anti-Acetyl sera but not with the anti-Formyl serum.

Bme::Tn7wbdR and Bme::Tn7wbdRΔwbkC synthesized a S-LPS with a S fraction of average molecular weight lower than that of the parental strain (Supplementary Figure S7A), being in this regard also similar to the *B. abortus* equivalents. Also, whereas the S-LPS of Bme-parental, Bme::Tn7wbdR and Bme::Tn7wbdRΔwbkC reacted with the anti-Formyl-Acetyl serum, only the S-LPS of the *wbdR*-constructs reacted with the anti-Acetyl serum (Supplementary Figure S7B). In addition, Bme::Tn7wbdRΔwbkC was the only strain that produced a LPS that did not react with the anti-Formyl serum (Supplementary Figure S7B). With respect to the M and C epitopes carried by *B. melitensis* 16M (a biovar 1 strain) (Alton et al., 1988; Douglas and Palmer, 1988), the monoclonal antibodies Cby33H8 (C/Y epitope) and A156B3 (M epitope) did not react with the LPS of Bme::Tn7wbdRΔwbkC (Supplementary Figure S7B). As expected, the reactivity of the monoclonal antibody 42D2 to the A>M epitope was negative with all S-LPS obtained in the *B. melitensis* background (Supplementary Figure S7B). These results show that expression of *wbdR* in a *B. melitensis* background results in the synthesis of O-PS carrying *N*-acetyl-perosamine with epitopic modifications that parallel those observed in the *B. abortus* background.

DISCUSSION

The results presented in this work demonstrate that *wbdR*, the acetyl-transferase gene involved in the synthesis of the *N*-acetyl-perosamine of the heteropolymeric O-PS repeating unit of *E. coli* O157:H7, can replace for the autochthonous *N*-formyl-transferase gene *wbkC* in representative strains of *B. abortus* and *B. melitensis* biovars 1. In all *Brucella* examined thus far that carry *N*-formyl-perosamine in the O-PS, the sugar linkages vary from almost exclusively α-(1→2) to various proportions of α-(1→2) and α-(1→3), and the arrangement and proportion of these linkages relate to the overlapping A, M, C and C/Y epitopes whose distribution varies among the different *Brucella* serovars (Alton et al., 1988; Meikle et al., 1989; Weynants et al., 1997; Kubler-Kielb and Vinogradov, 2013a; Zaccheus et al., 2013; Zygmunt et al., 2015; Ducrotoy et al., 2016). The O-PS of *B. abortus* 1119-3, a typical biovar 1 strain, contains over 95% α-(1→2)-linkages and is A, C, C/Y, and that of *B. melitensis* 16M, which is M, C, C/Y, displays a 4:1 proportion of α-(1→2) and α-(1→3)-linkages (Bundle et al., 1987; Meikle et al., 1989). Since *wbdR* was functional in both backgrounds it can be proposed that the polymerization of *N*-acetyl-perosamine by the *Brucella* O-PS glycosyltransferases takes place no matter the kind of linkage [α-(1→2) or α-(1→3)] in the native O-PS. Therefore, even though the experiments were carried out in two strains,

it seems likely that *wbdR* can replace for *wbkC* in other *S-Brucella* species that carry *N*-formyl-perosamine homopolymers in the S-LPS (i.e., *B. suis*, *B. ceti*, *B. pinnipedialis*, *B. neotomae*, and *B. microti*). However, such an independence of the kind of linkage does not mean that the autochthonous O-PS biosynthetic machinery is as efficient in synthesizing the wild-type and the *N*-acetyl-perosamine O-PS. We observed that the degree of O-PS polymerization is reduced in the latter, and the present state of knowledge on gram-negative O-PS biosynthesis makes only possible to speculate on the causes. First, it is conceivable that the activities of the heterologous acyl-transferase, which belongs to a taxonomically distant bacterium, and the native enzymes (the glycosyltransferases for formylperosamine polymerization) are not optimal in the heterologous environment and substrates, respectively. Moreover, although to the best of our knowledge systems regulating the length of homopolymeric OPS (*wzm/wzt* dependent) are not known for any bacteria, it could be that such systems work differently on heterologous sugars and/or are affected by a reduced flow of precursors. The lack of stability of the Ba-*pwbdR* may also be explained by these hypothetical biosynthetic and export defects.

The substitution of the formamide by the acetamide group in perosamine resulted in a profound modification of the epitopic structure of the O-PS. For the *wbdRΔwbkC* constructs, reactivity with monoclonal antibodies of C/Y and A>M (in *B. abortus*), or C/Y-A = M and M (in *B. melitensis*) specificity was severely hampered. This is consistent with the critical role of the formamide group in the interaction with the binding site of monoclonal antibody Yst9.1 (an anti-*Y. enterocolitica* O:9 antibody of C/Y reactivity) and with the observation that chemical removal of the formyl group followed by full *N*-acetylation reduces functional antibody affinities one thousand fold below those of the natural antigen (Caroff et al., 1984; Bundle, 1989; Oomen et al., 1991). For the *wbdR* constructs that conserved the formyl-transferase gene *wbkC*, the *N*-formyl plus *N*-acetyl-perosamine O-PS also lost the reactivity with the monoclonal antibodies tested. Since the binding sites of monoclonal antibodies of A, C/Y and M specificities have been estimated to accommodate five or less *N*-formyl-perosamine residues (Bundle, 1989; Oomen et al., 1991), the results strongly suggest that the acetamide groups in these O-PS are interspersed among the formamide ones thereby disrupting the interaction with the antibodies. Further NMR studies or the validation of the binding site of monoclonal antibodies by crystal structure analysis of complexes with oligosaccharides would be necessary to confirm this interpretation. The observations with monoclonal antibodies were complemented with the polyclonal sera because the anti-Ba-*pwbdR* serum and the absorptions conducted to obtain the Anti-Acetyl reagent demonstrated that the acetamide group was associated with the appearance of new epitope(s) absent from the wild-type strains. Taking into account that the acetamido group is larger than the formamido one, it remains to be analyzed in detail whether *N*-acetyl-perosamine O-PS induces antibodies that can still bind *N*-formyl-perosamine O-PS and their affinity. Topologically, previous molecular modeling and analysis of the antibody

binding sites shows that the *N*-formyl-perosamine formamido group is exposed on *Brucella* wild-type O-PS (Bundle, 1989; Peters et al., 1990). Modeling using CarbBuilder (Kuttel et al., 2016) shows that in the *wbdRΔwbkC* constructs the acetamide methyl group is exposed (Figure 8) thus replacing the formyl hydrogen atom of the 4-amido substituent of the wild-type O-PS, which accounts for the change in antibody reactivity to these O-PS.

One relevant question is to what extent if any the O-PS modifications described here alter properties that are associated with virulence, and this has been partially studied here. The O-PS is known to be critical in the marked resistance of *S. brucellae* to the bactericidal action of complement in non-immune serum (Eisenschenk et al., 1995). This resistance results from a hindrance by *Brucella* O-PS of C1 access to the outer membrane proteins combined with the reduced activation of the complement cascade that depends on the structural peculiarities of its core and lipid A (Eisenschenk et al., 1999; Lapaque et al., 2005; Conde-Álvarez et al., 2012). The experiments presented in this work show that bacteria carrying *N*-acetyl-perosamine O-PS are more sensitive to normal serum than the wild-type strains. Studies with *E. coli* O111B4 and *Salmonella montevideo* have demonstrated that the resistance of these bacteria to normal serum correlates with the degree of O-PS polymerization and coverage of the cell surface by LPS (Goldman et al., 1984; Joiner et al., 1984; Grossman et al., 1987). Since the SDS-PAGE and Western-blot analyses show shorter O-PS for the *B. abortus wbdR* constructs than for the wild-type bacteria, this difference could account for the increased serum sensitivity of the former, in parallel to the observations in *E. coli* and *S. montevideo*. This hypothesis is compatible with the lack of an effect of *N*-acetyl-perosamine on the resistance to polymyxin B as the core and lipid A sections should not be affected by *wbdR*. Indeed, these are the sections involved in the resistance to bactericidal peptides in *B. abortus* and *B. melitensis* (Moreno et al., 1981; Conde-Álvarez et al., 2012; Fontana et al., 2016) and, in fact, a change in surface charge that could reveal an exposure of anionic groups was not detected. It is worth noting that serum sensitivity did not result in a significant decrease of the bacteria in their ability to multiply in the spleens of mice (and hence intracellularly in a variety of cells [Copin et al., 2012]) and to reach the chronic phase. Although this could be interpreted to mean that serum resistance is not relevant in *S. Brucella* virulence, the result could also reflect the limitations of the mouse model and/or the route of infection in this model. Studies in sheep using *wbdR* and *wbdRΔwbkC* modified *B. melitensis* Rev 1 vaccine are in progress to analyze these aspects and to study whether the structural modifications and epitopes detected under laboratory conditions are meaningful in these natural hosts. In this connection, it is also worth commenting on the potential practical application of the *wbdR* constructs, the main motivation of the present work.

The best available brucellosis vaccines (i.e., strains *B. melitensis* Rev 1 and *B. abortus* S19) carry O-PS and induce antibodies that interfere in the best diagnostic tests and thus in serological diagnosis (Ducrotoy et al., 2018). Although this problem can be significantly reduced by a judicious choice of the route and age of vaccination, the interference is troublesome. This problem is

particularly important in Rev 1 because this vaccine is used not only against *B. melitensis* but also against *B. ovis*, an R species devoid of O-PS that infects sheep. Because of the serological interference, countries that have eradicated *B. melitensis* ban the use of Rev 1 and are thus without immunoprophylactic tools to combat *B. ovis*. Accordingly, it is generally acknowledged that a brucellosis vaccine that would not interfere with serodiagnosis, or a test that would discriminate antibodies to wild-type O-PS elicited by S vaccines and virulent S brucellae would represent a definite asset. Concerning the second possibility, suggestive work with synthetic oligosaccharides has been presented recently and, moreover, immunizations with the corresponding glyconjugates proposed for vaccination (Ganesh et al., 2014; Bundle and McGiven, 2017; Mandal et al., 2017). The results presented here suggest that *wbdR* could be used for differentiating the antibody response occurring during an infection by wild-type strains from that induced upon vaccination with *wbdR* modified strains. Since the method described here works in both *B. melitensis* and *B. abortus*, the background strain could be one of the existing S vaccines (i.e., *B. melitensis* Rev1 and *B. abortus* S19) but also a totally new vaccine. Concerning the ancillary serological test, there is also a variety of possibilities. Classical buffered *Brucella* antigen agglutination and complement fixation tests use whole bacteria and, as the O-PS is surface exposed, they could be implemented with cells from a *wbdR*-modified strain, more likely of the *wbdRΔwbkC* type. Logistic difficulties posed by these tests can be circumvented using immunoenzymatic assays, and the LPS of the *wbdR* modified strains, or the hydrolytic polysaccharide if cross-reactivity at LPS core level poses a problem, are a clear alternative (Ducrotoy et al., 2016). Studies in natural hosts are in progress to investigate whether these tests combined with formamido-tagged vaccines are useful tools in the control of animal brucellosis.

REFERENCES

- Albermann, C., and Beutler, H. (2008). Identification of the GDP-N-acetyl-d-perosamine producing enzymes from *Escherichia coli* O157:H7. *FEBS Lett.* 582, 479–484. doi: 10.1016/j.febslet.2008.01.005
- Alonso-Urmeneta, B., Marín, C., Aragón, V., Blasco, J. M., Díaz, R., and Moriyón, I. (1998). Evaluation of lipopolysaccharides and polysaccharides of different epitopic structures in the indirect enzyme-linked immunosorbent assay for diagnosis of brucellosis in small ruminants and cattle. *Clin. Diagn. Lab. Immunol.* 5, 749–754.
- Alonso-Urmeneta, B., Moriyón, I., and Blasco, J. E. M. (1988). Enzyme-linked immunosorbent assay with *Brucella* native hapten polysaccharide and smooth lipopolysaccharide. *J. Clin. Microbiol.* 26, 2642–2646.
- Alton, G. G., Jones, L. M., Angus, R. D., and Verger, J.-M. (1988). *Techniques for the Brucellosis Laboratory*. Paris: INRA.
- Aragón, V., Díaz, R., Moreno, E., and Moriyón, I. (1996). Characterization of *Brucella abortus* and *Brucella melitensis* native haptens as outer membrane O-type polysaccharides independent from the smooth lipopolysaccharide. *J. Bacteriol.* 178, 1070–1079. doi: 10.1128/jb.178.4.1070-1079.1996
- Barquero-Calvo, E., Chaves-Olarte, E., Weiss, D. S., Guzmán-Verri, C., Chacón-Díaz, C., Rucavado, A., et al. (2007). *Brucella abortus* uses a stealthy strategy to avoid activation of the innate immune system during the onset of infection. *PLoS One* 2:e631. doi: 10.1371/journal.pone.0000631
- Bax, A., and Davis, D. G. (1985). MLEV-17-based two-dimensional homonuclear magnetization transfer spectroscopy. *J. Magn. Reson.* 65, 355–360. doi: 10.1016/0022-2364(85)90018-6

AUTHOR CONTRIBUTIONS

RC-Á, MI, and IM conceived and coordinated the study. GW supervised the NMR studies. EM-G, YG-R, AZ-R, JS, MZ, MI, and RC-Á performed the experiments and genomic analyses. RC-Á, GW, and IM wrote the manuscript. All authors analyzed the results and approved the final version of the manuscript.

FUNDING

This work was supported by grants from the Swedish Research Council, the Knut and Alice Wallenberg Foundation, by MINECO (grant AGL2014-58795-CA-R1), and Institute for Tropical Health funders (Obra Social la CAIXA, Fundaciones Caja Navarra and Roviralta, PROFAND, Ubesol, ACUNSA, and Artai).

ACKNOWLEDGMENTS

We thank A. Delgado-López for excellent technical assistance in the extraction and purification of LPS. Monoclonal antibody A15-6B3 was a generous gift of Prof. J. J. Letesson (University of Namur).

SUPPLEMENTARY MATERIAL

The Supplementary Material for this article can be found online at: <https://www.frontiersin.org/articles/10.3389/fmicb.2018.01092/full#supplementary-material>

- Bundle, D. R. (1989). Antibody combining sites and oligosaccharide determinants studied by competitive binding, sequencing and X-ray crystallography. *Pure Appl. Chem.* 61, 1171–1180. doi: 10.1351/pac198961071171
- Bundle, D. R., Cherwonogrodzky, J. W., and Perry, M. B. (1987). Structural elucidation of the *Brucella melitensis* M antigen by high-resolution NMR at 500 MHz. *Biochemistry* 26, 8717–8726. doi: 10.1021/bi00400a034
- Bundle, D. R., and McGiven, J. (2017). Brucellosis: improved diagnostics and vaccine insights from synthetic glycans. *Acc. Chem. Res.* 50, 2958–2967. doi: 10.1021/acs.accounts.7b00445
- Caroff, M., Bundle, D. R., Perry, M. B., Cherwonogrodzky, J. W., and Duncan, J. R. (1984). Antigenic S-type lipopolysaccharide of *Brucella abortus* 1119-3. *Infect. Immun.* 46, 384–388.
- Choi, K.-H., Gaynor, J. B., White, K. G., Lopez, C., Bosio, C. M., Karkhoff-Schweizer, R. R., et al. (2005). A Tn7-based broad-range bacterial cloning and expression system. *Nat. Methods* 2, 443–448. doi: 10.1038/nmeth765
- Choi, K.-H., and Schweizer, H. P. (2006). mini-Tn7 insertion in bacteria with single attTn7 sites: example *Pseudomonas aeruginosa*. *Nat. Protoc.* 1, 153–161. doi: 10.1038/nprot.2006.24
- Claridge, T. D. W., and Pérez-Victoria, I. (2003). Enhanced ¹³C resolution in semi-selective HMBc: a band-selective, constant-time HMBC for complex organic structure elucidation by NMR. *Organ. Biomol. Chem.* 1, 3632–3634. doi: 10.1039/B307122G
- Conde-Álvarez, R., Arce-Gorvel, V., Iriarte, M., Manèk-Keber, M., Barquero-Calvo, E., Palacios-Chaves, L., et al. (2012). The lipopolysaccharide core of *Brucella abortus* acts as a shield against innate immunity recognition. *PLoS Pathog.* 8:e1002675. doi: 10.1371/journal.ppat.1002675

- Conde-Álvarez, R., Grilló, M. J., Salcedo, S. P., de Miguel, M. J., Fugier, E., Gorvel, J.-P., et al. (2006). Synthesis of phosphatidylcholine, a typical eukaryotic phospholipid, is necessary for full virulence of the intracellular bacterial parasite *Brucella abortus*. *Cell. Microbiol.* 8, 1322–1335. doi: 10.1111/j.1462-5822.2006.00712.x
- Copin, R., Vitry, M. A., Hanot Mambres, D., Machelart, A., De Trez, C., Vanderwinden, J. M., et al. (2012). In Situ microscopy analysis reveals local innate immune response developed around *Brucella* Infected cells in resistant and susceptible mice. *PLoS Pathog.* 8:e1002575. doi: 10.1371/journal.ppat.1002575
- Díaz-Aparicio, E., Aragón, V., Marín, C., Alonso-Urmeneta, B., Font, M., Moreno, E., et al. (1993). Comparative analysis of *Brucella* serotype A and M and *Yersinia enterocolitica* O:9 polysaccharides for serological diagnosis of brucellosis in cattle, sheep, and goats. *J. Clin. Microbiol.* 31, 3136–3141.
- Douglas, J. T., and Palmer, D. A. (1988). Use of monoclonal antibodies to identify the distribution of A and M epitopes on smooth *Brucella* species. *J. Clin. Microbiol.* 26, 1353–1356.
- Ducrottoy, M. J., Bertu, W. J., Matope, G., Cadmus, S., Conde-Álvarez, R., Gusi, A. M., et al. (2015). Brucellosis in Sub-Saharan Africa: current challenges for management, diagnosis and control. *Acta Trop.* 165, 179–193. doi: 10.1016/j.actatropica.2015.10.023
- Ducrottoy, M. J., Conde-Álvarez, R., Blasco, J. M., and Moriyón, I. (2016). A review of the basis of the immunological diagnosis of ruminant brucellosis. *Vet. Immunol. Immunopathol.* 171, 81–102. doi: 10.1016/j.vetimm.2016.02.002
- Ducrottoy, M. J., Muñoz, P. M., Conde-Álvarez, R., Blasco, J. M., and Moriyón, I. (2018). A systematic review of current immunological tests for the diagnosis of cattle brucellosis. *Prev. Vet. Med.* 151, 57–72. doi: 10.1016/j.prevetmed.2018.01.005
- Eisenschien, F. C., Houle, J. J., and Hoffmann, E. M. (1995). Serum sensitivity of field isolates and laboratory strains of *Brucella abortus*. *Am. J. Vet. Res.* 56, 1592–1598.
- Eisenschien, F. C., Houle, J. J., and Hoffmann, E. M. (1999). Mechanism of serum resistance among *Brucella abortus* isolates. *Vet. Microbiol.* 68, 235–244. doi: 10.1016/S0378-1135(99)00075-9
- Engström, O., Mobarak, H., Stähle, J., and Widmalm, G. (2017). Conformational dynamics and exchange kinetics of N-Formyl and N-Acetyl groups substituting 3-Amino-3,6-dideoxy- α -D-galactopyranose, a Sugar found in Bacterial O-Antigen polysaccharides. *J. Phys. Chem. B* 121, 9487–9497. doi: 10.1021/acs.jpcc.7b05611
- Fontana, C., Conde-Álvarez, R., Stähle, J., Holst, O., Iriarte, M., Zhao, Y., et al. (2016). Structural studies of lipopolysaccharide defective mutants from *Brucella melitensis* identify a core oligosaccharide critical in virulence. *J. Biol. Chem.* 291, 7727–7741. doi: 10.1074/jbc.M115.701540
- Ganesh, N. V., Sadowska, J. M., Sarkar, S., Howells, L., McGiven, J., and Bundle, D. R. (2014). Molecular recognition of *Brucella* A and M Antigens dissected by synthetic oligosaccharide glycoconjugates leads to a disaccharide diagnostic for brucellosis. *J. Am. Chem. Soc.* 136, 16260–16269. doi: 10.1021/ja5081184
- Godfroid, F., Cloeckart, A., Taminiau, B., Danese, I., Tibor, A., De Bolle, X., et al. (2000). Genetic organisation of the lipopolysaccharide O-antigen biosynthesis region of *Brucella melitensis* 16M (wbk). *Res. Microbiol.* 151, 655–668. doi: 10.1016/S0923-2508(00)90130-X
- Goldman, R. C., Joiner, K., and Leive, L. (1984). Serum-resistant mutants of *Escherichia coli* O111 contain increased lipopolysaccharide, lack an O antigen-containing capsule, and cover more of their lipid A core with O antigen. *J. Bacteriol.* 159, 877–882.
- González, D., Grilló, M.-J., de Miguel, M.-J., Ali, T., Arce-Gorvel, V., Delrue, R.-M., et al. (2008). Brucellosis vaccines: assessment of *Brucella melitensis* lipopolysaccharide rough mutants defective in core and O-polysaccharide synthesis and export. *PLoS One* 3:e2760. doi: 10.1371/journal.pone.0002760
- Grossman, N., Schmetz, M. A., Foulds, J., Klima, E. N., Jimenez, L. V. E., Leive, L. L., et al. (1987). Lipopolysaccharide size and distribution determine serum resistance in *Salmonella montevideo*. *J. Bacteriol.* 169, 856–863. doi: 10.1128/jb.169.2.856-863.1987
- Hallez, R., Letesson, J. J., Vandenhaute, J., and De Bolle, X. (2007). Gateway-based destination vectors for functional analyses of bacterial ORFomes: application to the Min system in *Brucella abortus*. *Appl. Environ. Microbiol.* 73, 1375–1379. doi: 10.1128/AEM.01873-06
- Joiner, K. A., Schmetz, M. A., Goldman, R. C., Leive, L., and Frank, M. M. (1984). Mechanism of bacterial resistance to complement-mediated killing: inserted C5b-9 correlates with killing for *Escherichia coli* O111B4 varying in O-antigen capsule and O-polysaccharide coverage of lipid A core oligosaccharide. *Infect. Immun.* 45, 113–117.
- Jones, B. A., Grace, D., Kock, R., Alonso, S., Rushton, J., Said, M. Y., et al. (2013). Zoonosis emergence linked to agricultural intensification and environmental change. *Proc. Natl. Acad. Sci. U.S.A.* 110, 8399–8404. doi: 10.1073/pnas.1208059110/-/DCSupplemental
- Kenne, L., Unger, P., and Wehler, T. (1988). Synthesis and nuclear magnetic resonance studies of some N-acylated methyl 4-amino-4,6-dideoxy- α -D-mannopyranosides. *J. Chem. Soc. Perkin Trans. 1*, 1183–1186. doi: 10.1039/P19880001183
- Kronvall, G. (1973). A rapid slide-agglutination method for typing Pneumococci by means of specific antibody adsorbed to protein A-containing Staphylococci. *J. Med. Microbiol.* 6, 187–190. doi: 10.1099/00222615-6-2-187
- Kubler-Kielb, J., and Vinogradov, E. (2013a). Reinvestigation of the structure of *Brucella* O-antigens. *Carbohydr. Res.* 378, 144–147. doi: 10.1016/j.carres.2013.03.021
- Kubler-Kielb, J., and Vinogradov, E. (2013b). The study of the core part and non-repeating elements of the O-antigen of *Brucella* lipopolysaccharide. *Carbohydr. Res.* 366, 33–37. doi: 10.1016/j.carres.2012.11.004
- Kuttel, M. M., Stähle, J., and Widmalm, G. (2016). CarbBuilder: software for building molecular models of complex oligo- and polysaccharide structures. *J. Comput. Chem.* 37, 2098–2105. doi: 10.1016/j.carres.2011.02.013
- Lai, S., Zhou, H., Xiong, W., Gilbert, M., Huang, Z., Yu, J., et al. (2017). Changing epidemiology of human Brucellosis, China, 1955–2014. *Emerg. Infect. Dis.* 23, 184–194. doi: 10.3201/eid2302.151710
- Lapaque, N., Moriyón, I., Moreno, E., and Gorvel, J.-P. (2005). *Brucella* lipopolysaccharide acts as a virulence factor. *Curr. Opin. Microbiol.* 8, 60–66. doi: 10.1016/j.mib.2004.12.003
- Lapaque, N., Takeuchi, O., Corrales, F., Akira, S., Moriyón, I., Howard, J. C., et al. (2006). Differential inductions of TNF- α and IGTP, IIGP by structurally diverse classic and non-classic lipopolysaccharides. *Cell. Microbiol.* 8, 401–413. doi: 10.1111/j.1462-5822.2005.00629.x
- Laurent, T. C., Mertens, P., Dierick, J. F., Letesson, J.-J., Lambert, C., and De Bolle, X. (2004). Functional, molecular and structural characterisation of five anti-*Brucella* LPS mAb. *Mol. Immunol.* 40, 1237–1247. doi: 10.1016/j.molimm.2003.11.037
- Leong, D., Díaz, R., Milner, K., Rudbach, J., and Wilson, J. B. (1970). Some structural and biological properties of *Brucella* endotoxin. *Infect. Immun.* 1, 174–182.
- Llobet, E., March, C., Giménez, P., and Bengoechea, J. A. (2009). *Klebsiella pneumoniae* OmpA confers resistance to antimicrobial peptides. *Antimicrob. Agents Chemother.* 53, 298–302. doi: 10.1128/AAC.00657-08
- Mandal, S. S., Duncombe, L., Ganesh, N. V., Sarkar, S., Howells, L., Hogarth, P. J., et al. (2017). Novel solutions for vaccines and diagnostics to combat Brucellosis. *ACS Central Sci.* 3, 224–231. doi: 10.1021/acscentsci.7b00019
- Martínez de Tejada, G., Pizarro-Cerdá, J., Moreno, E., and Moriyón, I. (1995). The outer membranes of *Brucella* spp. are resistant to bactericidal cationic peptides. *Infect. Immun.* 63, 3054–3061.
- Martirosyan, A., Moreno, E., and Gorvel, J.-P. (2011). An evolutionary strategy for a stealthy intracellular *Brucella* pathogen. *Immunol. Rev.* 240, 211–234. doi: 10.1111/j.1600-065X.2010.00982.x
- McDermott, J. J., Grace, D., and Zinsstag, J. (2013). Economics of brucellosis impact and control in low-income countries. *Rev. Sci. Tech.* 32, 249–261. doi: 10.20506/rst.32.1.2197
- Meikle, P. J., Perry, M. B., Cherwonogrodzky, J. W., and Bundle, D. R. (1989). Fine structure of A and M antigens from *Brucella* biovars. *Infect. Immun.* 57, 2820–2828.
- Moreno, E., Berman, D. T., and Boettcher, L. A. (1981). Biological activities of *Brucella abortus* lipopolysaccharides. *Infect. Immun.* 31, 362–370.
- Oomen, R. P., Young, N. M., and Bundle, D. R. (1991). Molecular modeling of antibody-antigen complexes between the *Brucella abortus* O-chain polysaccharide and a specific monoclonal antibody. *Prot. Eng.* 4, 427–433. doi: 10.1093/protein/4.4.427

- Parella, T., Sanchez-Ferrando, F., and Virgili, A. (1997). Quick recording of pure absorption 2D TOCSY, ROESY, and NOESY spectra using pulsed field gradients. *J. Magn. Reson.* 125, 145–148. doi: 10.1006/jmre.1996.1069
- Perry, M. B., and Bundle, D. R. (1990). “Lipopolysaccharide antigens and carbohydrates of *Brucella* BT - advances in brucellosis research,” in *Advances in Brucellosis Research*, ed. G. L. Adams (College Station, TX: A&M University Press), 76–88.
- Peters, T., Brisson, J. R., and Bundle, D. R. (1990). Conformational analysis of key disaccharide components of *Brucella* A and M antigens. *Can. J. Chem.* 68, 979–988. doi: 10.1139/v90-154
- Scupham, A. J., and Triplett, E. W. (1997). Isolation and characterization of the UDP-glucose 4'-epimerase-encoding gene, *galE*, from *Brucella abortus* 2308. *Gene* 202, 53–59. doi: 10.1016/S0378-1119(97)00453-8
- Tsai, C. M., and Frasch, C. E. (1982). A sensitive silver stain for detecting lipopolysaccharides in polyacrylamide gels. *Anal. Biochem.* 119, 115–119. doi: 10.1016/0003-2697(82)90673-X
- Weynants, V. E., Gilson, D., Cloeckaert, A., Tibor, A., Denoel, P. A., Godfroid, F., et al. (1997). Characterization of smooth lipopolysaccharides and O polysaccharides of *Brucella* species by competition binding assays with monoclonal antibodies. *Infect. Immun.* 65, 1939–1943.
- Zaccheus, M. V., Ali, T., Cloeckaert, A., Zygmunt, M. S., Weintraub, A., Iriarte, M., et al. (2013). The Epitopic and structural characterization of *Brucella suis* Biovar 2 O-Polysaccharide demonstrates the existence of a new M-Negative C-Negative Smooth *Brucella* Seroovar. *PLoS One* 8:e53941. doi: 10.1371/journal.pone.0053941
- Zygmunt, M. S., Bundle, D. R., Ganesh, N. V., Guiard, J., and Cloeckaert, A. (2015). Monoclonal antibody-defined specific C Epitope of *Brucella* O-polysaccharide revisited. *Clin. Vacc. Immunol.* 22, 979–982. doi: 10.1128/CVI.00225-15

Conflict of Interest Statement: RC-Á, AZ-R, MI, and IM are inventors of patent EP15201717.4 covering potential uses of *wbdR* constructs.

The other authors declare that the research was conducted in the absence of any commercial or financial relationships that could be construed as a potential conflict of interest.

Copyright © 2018 Martínez-Gómez, Stähle, Gil-Ramírez, Zúñiga-Ripa, Zaccheus, Moriyón, Iriarte, Widmalm and Conde-Álvarez. This is an open-access article distributed under the terms of the Creative Commons Attribution License (CC BY). The use, distribution or reproduction in other forums is permitted, provided the original author(s) and the copyright owner are credited and that the original publication in this journal is cited, in accordance with accepted academic practice. No use, distribution or reproduction is permitted which does not comply with these terms.



Genotypic Expansion Within the Population Structure of Classical *Brucella* Species Revealed by MLVA16 Typing of 1404 *Brucella* Isolates From Different Animal and Geographic Origins, 1974–2006

Gilles Vergnaud¹, Yolande Hauck¹, David Christiany¹, Brendan Daoud¹, Christine Pourcel¹, Isabelle Jacques^{2,3}, Axel Cloeckaert^{2*} and Michel S. Zygmunt²

OPEN ACCESS

Edited by:

Leonard Peruski,
Centers for Disease Control
and Prevention (CDC), United States

Reviewed by:

Francisco Ruiz-Fons,
Consejo Superior de Investigaciones
Científicas (CSIC), Spain
Menachem Banai,
Kimron Veterinary Institute, Israel

*Correspondence:

Axel Cloeckaert
axel.cloeckaert@inra.fr

Specialty section:

This article was submitted to
Infectious Diseases,
a section of the journal
Frontiers in Microbiology

Received: 26 March 2018

Accepted: 21 June 2018

Published: 12 July 2018

Citation:

Vergnaud G, Hauck Y, Christiany D,
Daoud B, Pourcel C, Jacques I,
Cloeckaert A and Zygmunt MS (2018)
Genotypic Expansion Within
the Population Structure of Classical
Brucella Species Revealed by
MLVA16 Typing of 1404 *Brucella*
Isolates From Different Animal
and Geographic Origins, 1974–2006.
Front. Microbiol. 9:1545.
doi: 10.3389/fmicb.2018.01545

¹ Institute for Integrative Biology of the Cell, CEA, CNRS, Univ. Paris-Sud, Université Paris-Saclay, Gif-sur-Yvette, France,
² ISF, INRA, Université François Rabelais de Tours, UMR 1282, Nouzilly, France, ³ IUT de Tours, Tours, France

Previous studies have shown the usefulness of MLVA16 as a rapid molecular identification and classification method for *Brucella* species and biovars including recently described novel *Brucella* species from wildlife. Most studies were conducted on a limited number of strains from limited geographic/host origins. The objective of this study was to assess genetic diversity of *Brucella* spp. by MLVA16 on a larger scale. Thus, 1404 animal or human isolates collected from all parts of the world over a period of 32 years (1974–2006) were investigated. Selection of the 1404 strains was done among the approximately 4000 strains collection of the BCCN (*Brucella* Culture Collection Nouzilly), based on classical biotyping and on the animal/human/geographic origin over the time period considered. MLVA16 was performed on extracted DNAs using high throughput capillary electrophoresis. The 16 loci were amplified in four multiplex PCR reactions. This large scale study firstly confirmed the accuracy of MLVA16 typing for *Brucella* species and biovar identification and its congruence with the recently described Extended Multilocus Sequence Analysis. In addition, it allowed identifying novel MLVA11 (based upon 11 slowly evolving VNTRs) genotypes representing an increase of 15% relative to the previously known *Brucella* MLVA11 genotypes. Cluster analysis showed that among the MLVA16 genotypes some were genetically more distant from the major classical clades. For example new major clusters of *B. abortus* biovar 3 isolated from cattle in Sub-Saharan Africa were identified. For other classical species and biovars this study indicated also genotypic expansion within the population structure of classical *Brucella* species. MLVA proves to be a powerful tool to rapidly assess genetic diversity of bacterial populations on a large scale, as here on a large collection of strains of the genomically homogeneous genus *Brucella*. The highly discriminatory power of MLVA appears of particular interest as a first step for selection of *Brucella*

strains for whole-genome sequencing. The MLVA data of this study were added to the public *Brucella* MLVA database at <http://microbesgenotyping.i2bc.paris-saclay.fr>. Current version *Brucella_4_3* comprises typing data from more than 5000 strains including *in silico* data analysis of public whole genome sequence datasets.

Keywords: *Brucella*, MLVA, population structure, genotyping, animal, human

INTRODUCTION

Brucellae are Gram-negative, facultative intracellular bacteria that can infect many species of animals and man. Until the 1990s six species were classically recognized within the genus *Brucella*: *B. abortus*, *B. melitensis*, *B. suis*, *B. ovis*, *B. canis*, and *B. neotomae* (Corbel and Brinley Morgan, 1984; Moreno et al., 2002; Godfroid et al., 2011). This classification was mainly based on differences in pathogenicity, host preference, and phenotypic characteristics (Alton et al., 1988). With the advent of modern molecular typing methods and whole genome sequencing a number of new species representing mostly wildlife isolates have been validly published. In chronological order it concerns the species (i) *B. ceti* and *B. pinnipedialis* isolated from marine mammals, with cetaceans (dolphin, porpoise, and whale species) and pinnipeds (various seal species) as preferred hosts respectively (Foster et al., 2007); (ii) *B. microti* isolated initially from the common vole but found later also in red foxes and in soil (Scholz et al., 2008a,b, 2009); (iii) *B. inopinata* isolated from human (Scholz et al., 2010); (iv) *B. papionis* isolated from baboons (Whatmore et al., 2014); and (v) the latest *B. vulpis* species isolated from red foxes (Scholz et al., 2016b). Novel *Brucella* strains representing potentially novel species have also been isolated from Australian rodents (Tiller et al., 2010a), a wide variety of frog species (Eisenberg et al., 2012; Fischer et al., 2012; Scholz et al., 2016a; Soler-Lloréns et al., 2016; Al Dahouk et al., 2017; Kimura et al., 2017; Mühldorfer et al., 2017), and surprisingly also from fish namely from a bluespotted ribbontail ray (*Taeniura lymma*) (Eisenberg et al., 2017). The genus *Brucella* nowadays is thus not restricted to mammal species. Particular attention is required to survey and study those novel isolates which may represent a potential risk to human health with possible associated difficulty of diagnosis and consecutive treatment. A good example to emphasize this problem is the novel *Brucella* sp. strain BO2, isolated from a patient with chronic destructive pneumonia (Tiller et al., 2010b), for which the animal or environmental reservoir has not been identified yet.

During the 1980s the six classical species were found by DNA–DNA hybridization to be highly genetically related (more than 90% DNA relatedness) which was later confirmed by whole genome sequencing (Paulsen et al., 2002). Consequently, from a strict genomic point of view, *Brucella* could be considered as a monospecific genus (Vergner et al., 1985). However, for both medical and historical reasons the multispecies concept has been kept. Indeed the different lineages induce specific pathologies in farm animals as well as different risks of transmission and long-lasting disease in humans if antibiotic treatment is not applied adequately.

The species *B. melitensis*, *B. abortus*, and *B. suis* are further subdivided into biovars based on phenotypic characterization, such as serotyping, phage typing, sensitivity to dyes, or metabolic profiles (Alton et al., 1988). These classical phenotyping techniques have a limited discriminatory power and are mostly available in reference laboratories only. Some of them are time-consuming, require manipulating the living agent, and due to a lack of standardization of the typing reagents, they sometimes raise difficulties in the interpretation of the results. Therefore, several molecular typing methods have been developed since the end of the 1990s, especially when *Brucella* genome sequences became available. The most commonly used today are Multilocus Sequence Typing (MLST) and Multiple Loci VNTR (Variable Number of Tandem Repeats) Analysis (MLVA) (Le Flèche et al., 2006; Whatmore et al., 2007). Both methodologies are sufficiently highly discriminatory and provide a clustering of strains that is globally in accordance with the currently recognized *Brucella* species and biovars. Moreover, they have allowed identifying subtypes within each species or biovar based on geographic origin or host specificity. A good example for this are the marine mammal brucellae consisting currently of the species *B. ceti* and *B. pinnipedialis*. No biovars have been defined for these species, but nevertheless both species constitute a diverse set of distinct genotypes in both MLST and MLVA that are in clear congruence with the marine mammal host from which they were isolated (Groussaud et al., 2007; Maquart et al., 2009). Based on the latest published extended MLST scheme with 21 loci, over 100 sequence types (STs) were identified for the whole *Brucella* population structure, including 16 STs for marine mammal brucellae (Whatmore et al., 2016). From numerous studies both MLVA and MLST have proved to be useful to assess genetic diversity of *Brucella* strains and to identify and classify newly emerging or atypical isolates as novel species within the genus *Brucella* (Scholz and Vergnaud, 2013), which was not possible based on phenotypic characterization alone. In addition, both MLVA and MLST are robust and accurate and their implementation as rapid diagnostic assays may likely replace in the future the classical phenotyping scheme of *Brucella* species and biovar.

Since 10 years, numerous studies have been published independently using MLVA technology but mostly on a limited number of *Brucella* strains (less than 300) from specific geographic origins or hosts. The objective of the present study was to assess genetic diversity of *Brucella* spp. by MLVA on a larger scale. Thus, 1404 animal or human isolates covering all parts of the world over a period of 32 years (1974–2006), hosted by INRA in the *Brucella* Culture Collection Nouzilly (BCCN), were investigated. Data were compared for congruency with those of MLST when available, to try to determine the advantages

and complementarity of each methodology. This was facilitated by taking advantage of the availability of whole genome sequence data from which both MLVA and MLST genotypes could be deduced by *in silico* analysis.

MATERIALS AND METHODS

Bacterial Strains

Selection of the 1404 strains of this study was done among the approximately 4000 strains collection of the BCCN (*Brucella* Culture Collection Nouzilly), based on classical biotyping, and covering all geographic origins and hosts of the world over the period 1974–2006. Information on these strains is provided in Supplementary Figure S1 and Supplementary Table S1. Culture, DNA extraction, and PCR were performed using standard methods.

MLVA

MLVA16 [Multiple Loci VNTR (Variable Number of Tandem Repeats) Analysis (MLVA) using 16 chromosomal loci] was performed as described previously (Scholz and Vergnaud, 2013), using high throughput capillary electrophoresis on a Beckman CEQ8000 machine. The 16 loci were amplified in four multiplex PCR reactions. The composition of each multiplex is indicated in Supplementary Table S2.

MLST and MLVA *in Silico* Analysis of Available Genome Sequence Data

Multilocus Sequence Typing codes of complete genomes or *de novo* assemblies from reads archives were deduced *in silico* using the BioNumerics (Applied-Maths) version 7.6.2 tools. The scheme for MLST coding was recovered from the *Brucella* MLST database at <https://pubmlst.org/brucella/>.

The scripts used to deduce MLVA codes of complete genomes or draft assemblies are deposited at <https://github.com/dpchris/MLVA>. In order to estimate the read length necessary for a correct reconstruction of tandem repeats length from read archives, artificial reads data were produced from complete genome sequences using artificial fastq generator (Frampton and Houlston, 2012). The reads were then assembled using SPAdes version 3.9 (Bankevich et al., 2012).

Supplementary Table S3 indicates that reads longer than 200 bp can be used to reconstruct all VNTRs with a reasonable success rate, whereas only some VNTRs can be confidently reconstructed with shorter reads.

Whole Genome SNP Analysis

Sequencing reads were mapped on a reference genome using BioNumerics version 7.6.2. The *B. melitensis* 16M assembly GCA_000740415.1 was used as reference after concatenating chromosome I accession number CP007763.1 and chromosome II accession number CP007762.1 in a single file. SNPs were called within BioNumerics using the strict closed dataset option. Minimum spanning trees were produced with the hypothetical missing links option.

RESULTS AND DISCUSSION

Global Clustering Analysis of MLVA Data

Figure 1 shows the MLVA11 genotype distribution of 4971 *Brucella* strains which include previously published strains and the 1404 strains of this study listed in Supplementary Table S1. In total 377 MLVA11 genotypes were defined, of which 63 new ones from this study. At the species level the largest contribution in this study was *B. melitensis*, with 1049 strains analyzed from diverse geographic origins and hosts (see Supplementary Figures S1, S2). Previously, three major clusters within *B. melitensis* were defined, based on MLVA data, in agreement with a preferred geographic location, and called “Americas,” “West Mediterranean,” and “East Mediterranean” (Le Flèche et al., 2006). This clustering was subsequently confirmed by MLST (Whatmore et al., 2016). As can be seen in Figure 1B most of the 1050 *B. melitensis* strains studied are uniformly distributed within the East Mediterranean or West Mediterranean clades, of which some are new for the East Mediterranean clade. A lower proportion of strains were distributed in the Americas clade. The 213 *B. abortus* strains of this study were predominantly found in the MLST21-defined clade called *B. abortus* B. The remaining 142 strains of this study, classified within a species, were mainly *B. suis* biovar 2 ($n = 92$), followed by *B. suis* biovar 1 ($n = 30$) and a few strains of *B. canis* ($n = 1$), *B. ovis* ($n = 2$), and *B. neotomae* ($n = 7$). Most of them clustered with previously described MLVA11 genotypes. These different species/biovars were clearly separated from each other and from the other major *Brucella* species. Recently reported strains isolated from Australian rodents representing a potential novel *Brucella* species were also included in this study, and MLVA11 confirmed them as a specific separate *Brucella* lineage (Tiller et al., 2010a). A large number of marine mammal *Brucella* strains ($n = 295$), of the species *B. ceti* and *B. pinnipedialis*, has been previously characterized by MLVA (Maquart et al., 2009), and are included in Figure 1. Species *B. ceti* and *B. pinnipedialis* form distinct MLVA11 clades from the other *Brucella* species. Species *B. microti*, and *B. suis* biovars 4 and 5 are similarly shown and form also distinct clades. *B. suis* biovar 5 represents a distant clade relative to the species *B. suis*, that does not cluster with any of the other biovars including *B. canis*, known to be closely genetically related to *B. suis*.

Taking all MLVA11 data together ($n = 4971$), and in agreement with global animal or human brucellosis epidemiology, since the 1970s *B. melitensis* is the predominant species followed by *B. abortus* and *B. suis*.

B. melitensis

If we take a closer look at the largest panel of strains of this study belonging to the species *B. melitensis*, in the MLVA11 based minimum spanning tree shown in Figure 2, we confirm a distribution reflecting geographic origins previously defined by MLVA (Le Flèche et al., 2006), i.e., East Mediterranean, West Mediterranean, and the Americas. Most of the strains belonged to the East Mediterranean group which actually comprises strains from Europe, the Middle-East, and Asia (Figure 2C). A more precise geographic origin is indicated in Supplementary

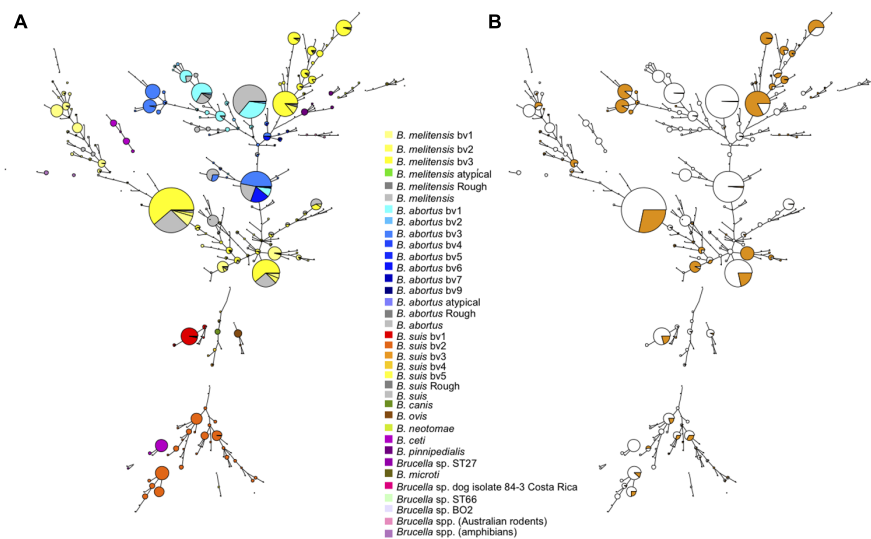


FIGURE 1 | Global view of the genetic diversity of *Brucella* spp. provided by MLVA11. Entries with a full MLVA11 dataset were used to produce a minimum spanning tree based upon 4998 entries, allowing hypothetical missing links. This includes 1404 *Brucella* strains from the present study, and 375 *in silico* deduced data (from 48 assemblies and 327 sequence reads archives). 377 MLVA11 genotypes are defined. **(A)** Strains are color coded according to species and biovar as indicated. **(B)** The proportion of strains from the present study is reflected by the colored sector in each circle.

B. melitensis

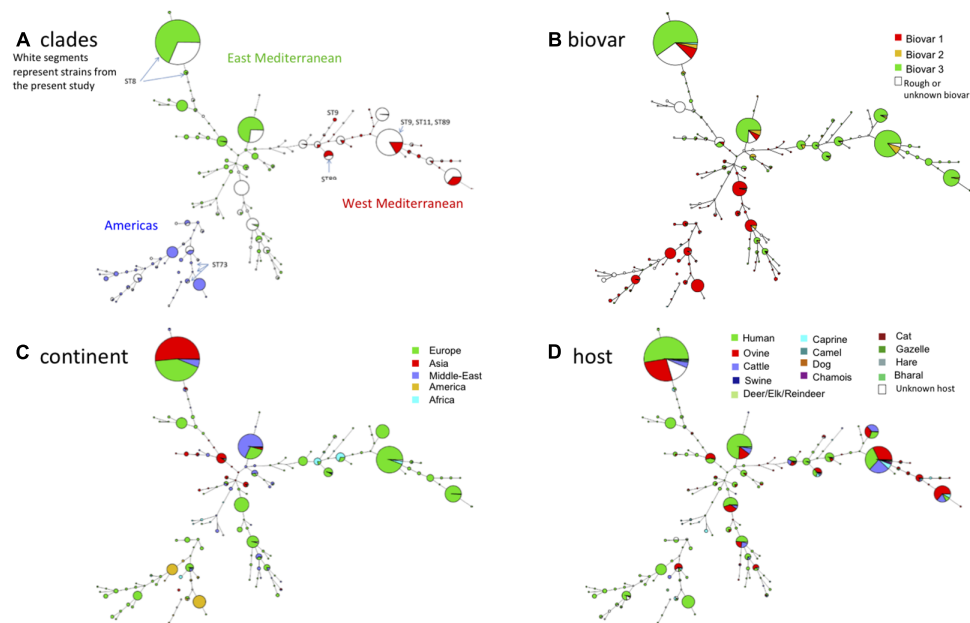


FIGURE 2 | *B. melitensis* intraspecies diversity view provided by MLVA11. 2320 among the 4971 entries with a full MLVA11 dataset belong to *B. melitensis*. 1049 entries are from this study, 17 are *in silico* entries (nine complete genomes and eight entries based on sequence reads archives) and 1254 are compiled from MLVA publications. The same MLVA11 minimum spanning tree was color-coded according to different characteristics. **(A)** Color coding according to assignment to East Mediterranean, West Mediterranean, or Americas groups except for strains typed in the course of the present study (white). The MLST21 genotypes deduced from whole genome sequence data are indicated. **(B)** Color-coding according to biovar (white when unknown). **(C)** Color-coding according to geographic origin defined at continent level. **(D)** Color-coding according to host (white when unknown).

Figure S1. It must be noted that for Europe most strains were from Spain, France, or Greece. The West Mediterranean group consisted mostly of strains from Europe (Mediterranean

countries) and to a lesser extent of strains from Africa, while the Americas group was mainly composed of strains from the Americas and from Europe (Figure 2C).

As observed before and also in agreement with MLST (Whatmore et al., 2016) (corresponding ST types of MLVA clades are indicated in **Figure 2A**), there was no clear relationship between genotype and biovar of *B. melitensis* (**Figure 2B**). In summary the following observations are fully congruent with MLST data (i) strains of the “Americas” clades are essentially of biovar 1, (ii) the “West Mediterranean” clades are mainly composed of biovar 3 strains and some contain a minority of biovar 2 strains, (iii) the “East Mediterranean” clades are more heterogeneous and comprise strains belonging to all three biovars, but biovar 2 remains minor and is likely a minor biovar within species *B. melitensis*. *B. melitensis* biovars are solely classified based on serological reaction using polyclonal antibodies directed against the main surface antigen consisting of the O chain of the outer membrane lipopolysaccharide (LPS). Structurally and antigenically this O chain is not highly diverse among the *Brucella* species and biovars, and therefore strains are classified by use of established anti-A or anti-M monospecific serum only within three serotypes, namely A+ (or A-dominant), M+ (or M-dominant), and A+M+ strains (Alton et al., 1988; Zygmunt et al., 2015). Those that do not react with these monospecific sera usually lack the O chain and are classified as rough type (R). Each of these serotypes exists also within the major species *B. abortus* and *B. suis*, but unlike *B. melitensis*, these species comprise other biovar markers than the serotype (Alton et al., 1988). As suggested in the MLVA study of Le Flèche et al. (2006) and confirmed by the MLST study of Whatmore et al. (2016), the biovar concept in the case of *B. melitensis* appears of limited epidemiological value and MLVA or MLST may better fulfill questions regarding epidemiology and tracking epidemic strains.

Regarding the host distribution of *B. melitensis*, the main hosts were as expected ovine and human, followed by cattle and caprine (**Figure 2D**). Strains from these hosts were quite uniformly distributed within the Americas, East or West Mediterranean MLVA clades. *B. melitensis* was also encountered in less frequent or unexpected hosts such as camel (mostly dromedary), cat, dog, swine including wildlife hosts such as chamois, bharal, elk, hare, gazelle, or reindeer.

B. abortus

The species *B. abortus* could be subdivided by MLVA in three clades congruent with the clades B, C1, and C2 of MLST (Whatmore et al., 2016). The correspondence with MLST STs is indicated in **Figure 3A**. Most strains of this study were of clade B and originated from Africa (Sub-Saharan, see Supplemental Figure S1 for details), mostly isolated from cattle and some from dromedary, zebu, or human (**Figures 3C,D**). Clade B strains predominantly belonged to biovar 3 (**Figure 3B**). Clade C strains, although more limited in number in this study, appeared more widely distributed over the other continents America, Asia, and Europe (**Figure 3C**) and comprised other *B. abortus* biovars such as biovar 1, 2, 6, and 9 (**Figure 3B**). They were mostly isolated from cattle but one C2 clade (corresponding to ST5 in MLST) comprised also buffalo strains.

B. suis* – *B. canis

Figure 4 shows the *B. suis* and *B. canis* MLVA clades distribution with the corresponding MLST STs. *B. suis* biovar 4 and *B. canis* are known to be phylogenetically closely related and this is also supported by the MLVA or MLST data. On the other hand, *B. suis* biovar 5 appears far more distant. Most strains of this study belonged to *B. suis* biovar 1 or biovar 2. The large proportion of biovar 2 strains from Western Europe correspond to an emergence of this biovar in European countries. A change in agricultural practices namely rearing in open fields of swine bringing them in close contact with wildlife reservoirs, mainly wild boar and hare might be responsible for this emergence (Godfroid et al., 2011). Some MLVA clades comprised strains isolated from the three predominant hosts (swine, wild boar, hare) (**Figure 4D**). Some more distant clades consisted exclusively of swine or hare isolates. *B. suis* biovar 1 strains formed distinct clades from biovar 2 with a major one corresponding to MLST21 ST75 (**Figure 4A**). Those strains were more widely distributed with a majority from South America, followed by Europe, North America, and Oceania (**Figure 4C**). The major host for this biovar is swine, but the clade corresponding to ST75 comprised also wild boar, hare, and human isolates (**Figure 4D**).

***Brucella* spp. From Rodents and Human Isolate BO2**

Over the past decade there has been growing interest for *Brucella* spp. isolated from rodents because they may constitute a reservoir for novel *Brucella* species that may be potential novel zoonotic pathogens. Some of them have been evaluated in mouse or cellular models of infection (Jiménez de Bagüés et al., 2010, 2014). Among these novel species, *B. microti* has firstly been isolated from the common vole in the Czech Republic (Hubálek et al., 2007; Scholz et al., 2008b), but was later also identified in the red fox from Austria (Scholz et al., 2009), and most recently in wild boar from Hungary (Rónai et al., 2015). Of interest is that *B. microti* has also been isolated from soil 7 years after its first isolation from common voles at the same location, suggesting that this species persists in soil (Scholz et al., 2008a). The diversity of *B. microti* strains has been previously assessed by MLVA (Al Dahouk et al., 2012). In this study we analyzed other strains from rodents, namely a set of strains belonging to the species *B. neotomae*, two strains of *B. suis* biovar 5, and a set of strains isolated from Australian rodents and the human *Brucella* sp. strain BO2 isolated from a lung biopsy from a patient presenting chronic destructive pneumonia (Tiller et al., 2010b). The latter strains (from Australian rodents and BO2) represent potential novel species phylogenetically closer to *B. inopinata* than the classical *Brucella* species (Tiller et al., 2010a). **Figure 5** shows MLVA cluster analysis of these strains and the corresponding MLST ST in comparison with the *B. microti* strains previously published (Al Dahouk et al., 2012). The four groups of rodent strains and human isolate BO2 are clearly separated with no apparent epidemiological link. As a

*B. abortus***A** clade

White segments represent strains from the present study

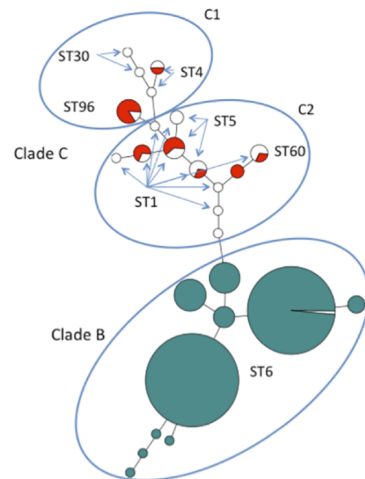
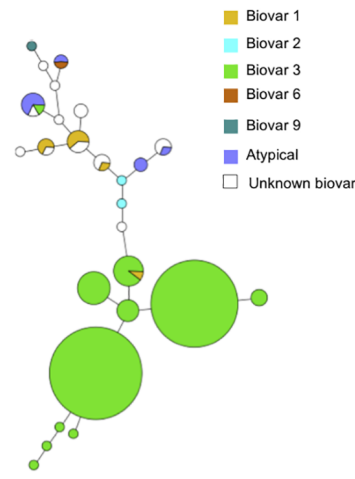
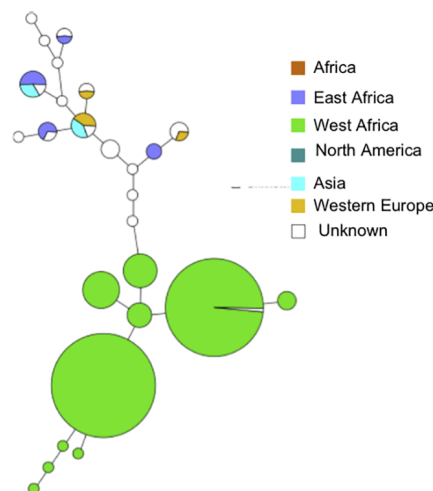
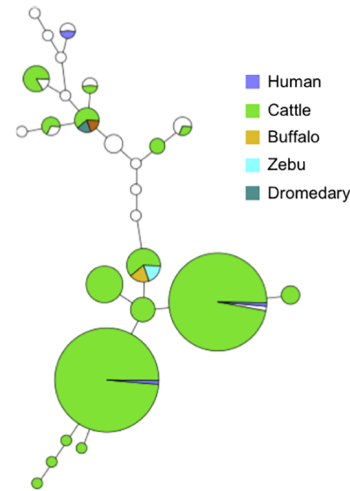
**B** biovar**C** continent**D** host

FIGURE 3 | *B. abortus* intraspecies diversity view provided by MLVA11. 232 entries are used including 213 *B. abortus* strains from this study and 19 representative entries from *in silico* data. The same MLVA11 minimum spanning tree was color-coded according to different characteristics. **(A)** Color coding according to assignment to *B. abortus* clade C or *B. abortus* clade B. Uncolored (white) entries correspond to *in silico* data. The MLST21 ST genotype for the white entries is indicated and was used to deduce the A, B, or C clade assignment defined by Whatmore et al. (2016). A tentative assignment of clades C1 and C2 is also proposed. **(B)** Color coding according to biovar (white when unknown). **(C)** Color-coding according to geographic origin defined at continent level (white when unknown). **(D)** Color-coding according to host (white when unknown).

consequence, from these and previous molecular data provide no clue regarding the animal or environmental reservoir for the human *Brucella* sp. isolate BO2. Although only a limited number of rodent strains are currently available ($n = 37$ in **Figure 5**), intra-species diversity is observed by MLVA within each species represented, except *B. suis* biovar 5. Regarding host diversity only *B. microti* appears not restricted to rodents (**Figure 5C**).

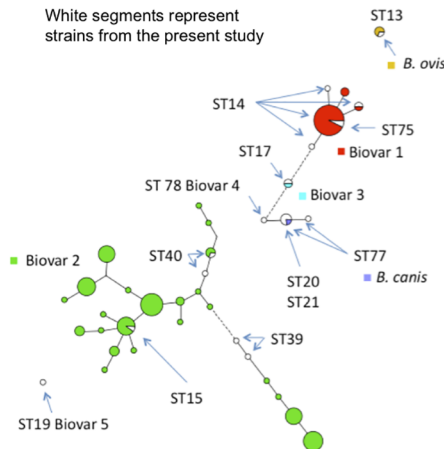
Taking Advantage of Available Whole Genome Sequence Data to Link MLVA Clusters Onto MLSA-Based Phylogeny

MLVA is an efficient clustering tool but with moderate phylogenetic value on its own. Phylogeny can be recovered indirectly by anchoring MLVA genotypes on a phylogenetic framework, as provided by whole or partial (as in MLST) genome

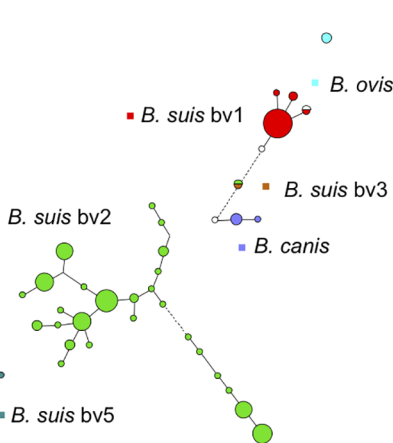
B. suis/canis

A

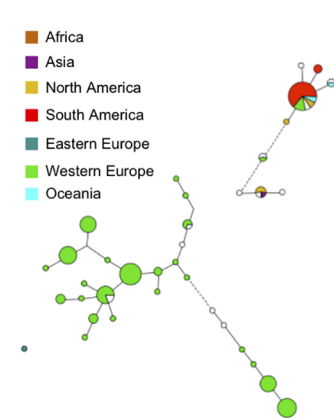
White segments represent strains from the present study



B



C



D

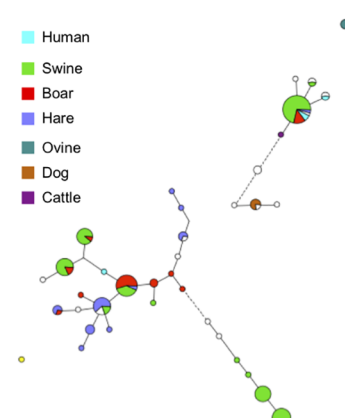


FIGURE 4 | *B. suis*, *B. canis*, and *B. ovis* intraspecies diversity according to MLVA11. The minimum spanning tree was drawn with data from 138 entries including 120 strains from this study and 18 representative entries from *in silico* data. **(A)** Color coding according to species and biovar, *B. suis* bv1, bv2, bv3, *B. canis*, or *B. ovis*. Uncolored (white) entries correspond to *in silico* data. The MLST21 ST genotypes for the white entries are indicated. **(B)** Color coding according to biovar (white when unknown). **(C)** Color-coding according to geographic origin defined at continent level (white when unknown). **(D)** Color-coding according to host (white when unknown).

analysis. This can be done if a representative set of strains has been typed with both methods as described by Riehm et al. (2012). In theory, both MLVA and MLST data can be deduced from whole genome sequence data. We recovered fifty-four complete *Brucella* genomes from the EBI-ENA public databases. Seventeen correspond to 14 reference strains (strains *B. abortus* 870, *B. melitensis* 16M, and *B. suis* 1330 were sequenced twice independently), which we have also typed *in vitro* by MLVA via electrophoresis of PCR amplification products. The *in vitro* and *in silico* deduced MLVA11 genotypes were identical with three exceptions. *B. abortus* C68 full genome is *in silico* coded 2 at locus Bruce06 whereas it is *in vitro* coded 3. The duplicate full genome sequences of strains 870 and 16M differ respectively

at locus Bruce06 and Bruce42 by a one repeat unit difference. One of the two genome sequences is in agreement with *in vitro* typing data. These two loci are fairly stable so that the most likely explanation for these discrepancies is an incorrect assembly of the corresponding tandem repeat in the generation of one of the full genome sequences. Consequently, most complete genome assemblies appear to correctly reconstruct the tandem repeat loci used in the MLVA11 assay. Because more than 1000 *Brucella* sequence reads archives are currently accessible in public depositories, we have evaluated the read length which allows reconstruction of a given tandem repeat with a moderate error rate. For this purpose we have produced artificial sequence reads of different length from each of the complete genomes.

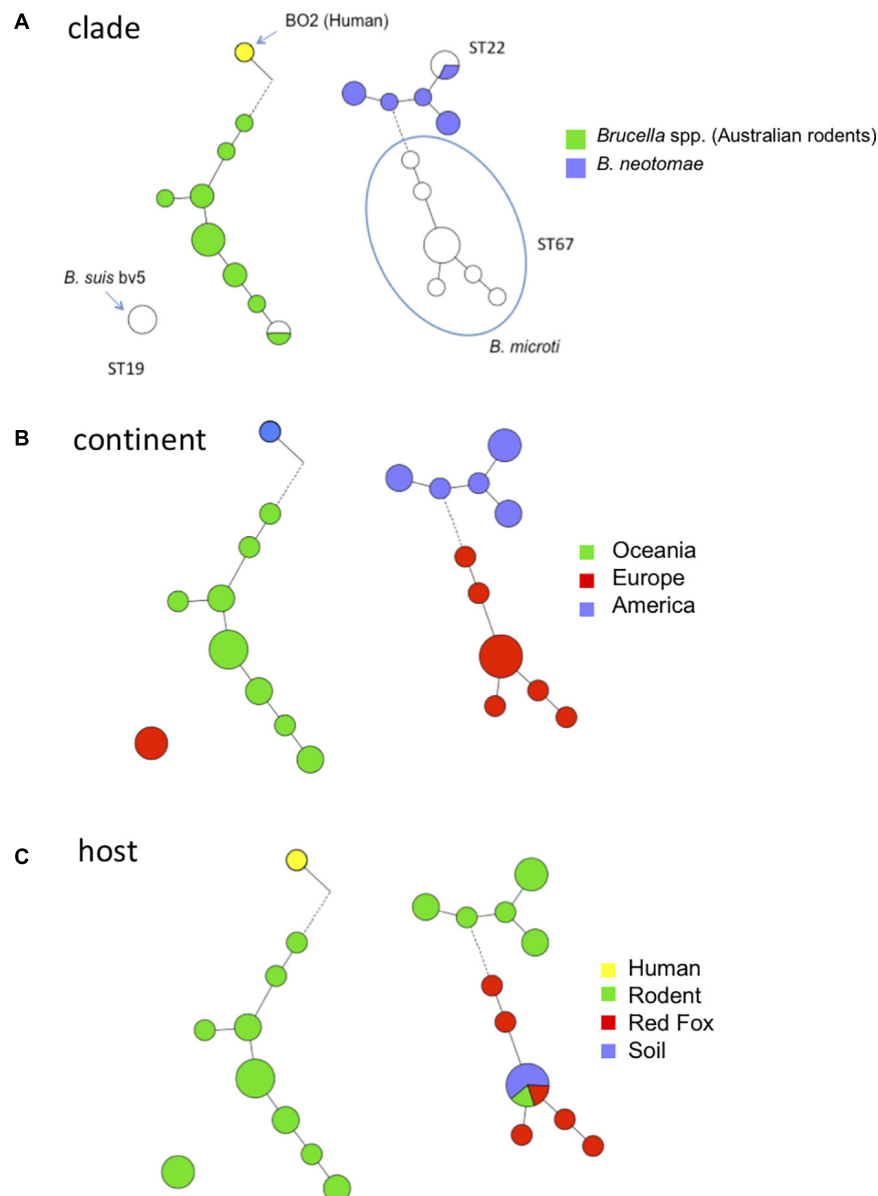
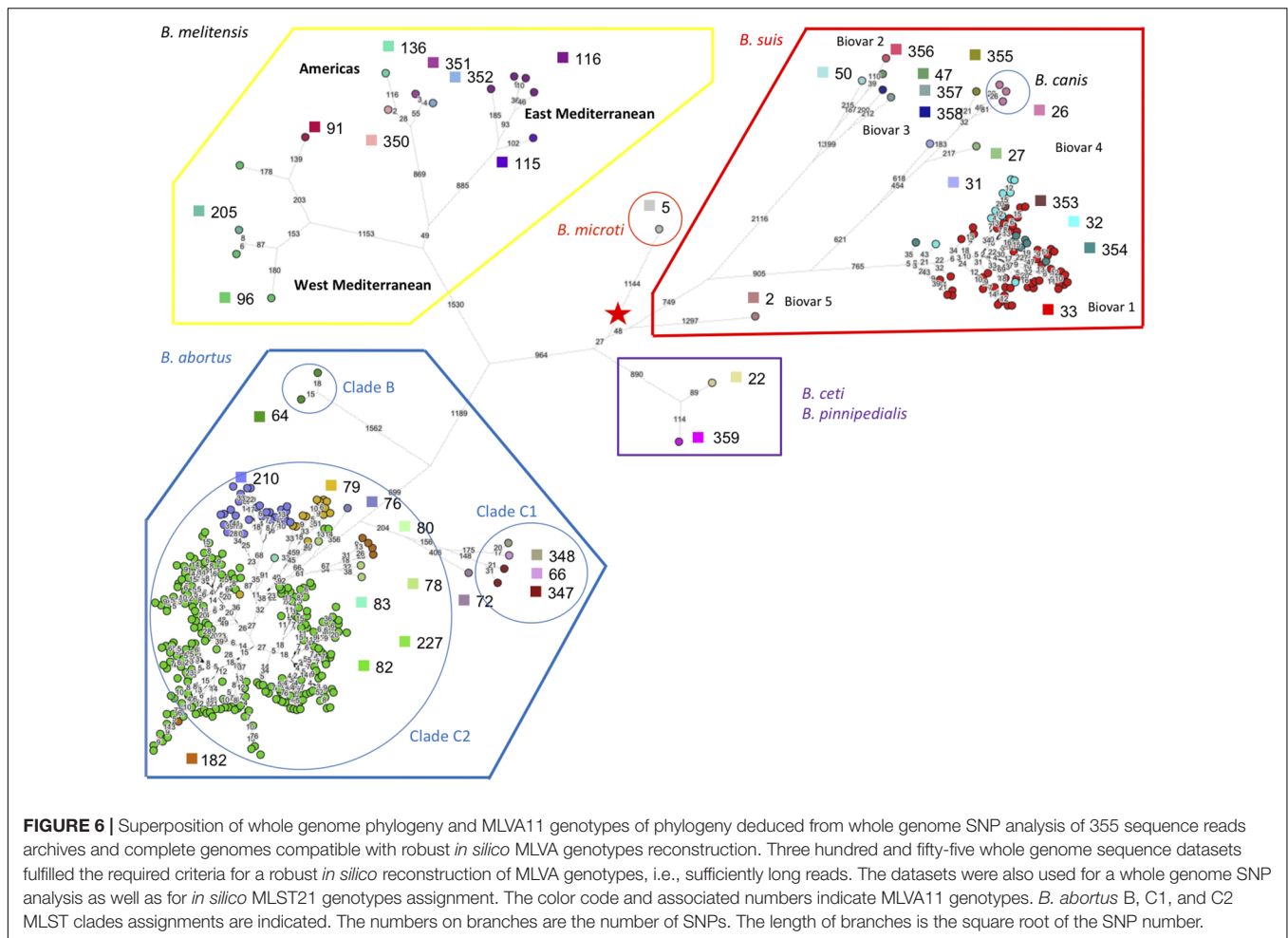
Rodent *Brucella* spp., *B. microti* and *B. neotomae*

FIGURE 5 | MLVA11 diversity of rodent *Brucella* spp., *B. microti*, *B. neotomae* and human *Brucella* sp. isolate BO2. Thirty-seven entries are used including 21 strains from this study (*B. neotomae*, *Brucella* spp. from Australian rodents, and human *Brucella* sp. isolate BO2), six representative entries from *in silico* data and data from 10 previously reported strains including *B. microti*. **(A)** Color coding according to species and biovar. Uncolored (white) entries correspond to *in silico* or previously published data. The MLST21 ST genotype is indicated. **(B)** Color-coding according to geographic origin defined at continent level. **(C)** Color-coding according to host.

We then reassembled the genomes using Spades version 3.9 and *in silico* deduced the resulting MLVA genotype. Supplementary Table S3 shows that all alleles which could be assembled from 250 bp long reads have a correct size. In contrast, shorter reads are often incorrectly assembled. Loci Bruce06, Bruce42, Bruce55, and Bruce21 are the most challenging in terms of reassembly at least when using Spades 3.9 and reads up to

200 bp long. When an *in silico* MLVA reconstruction corresponds to an unknown MLVA11 genotype, we suggest to confirm it by PCR amplification and sequencing the loci that are responsible for the new genotype.

Next we assembled public sequence reads archives with reads of appropriate length according to the previous simulation. For example, Illumina MiSeq 250 bp paired ends files allow to



confidently reconstitute all VNTR loci, whereas reads archives with shorter reads are used to reconstruct only some loci as deduced from Supplementary Table S3. From these assemblies, MLVA and MLST data were extracted *in silico*. Full MLVA11 and MLST9 (according to Whatmore et al., 2007) genotypes could be recovered for 355 datasets including the complete genome sequences. **Figure 6** shows a minimum spanning tree deduced from whole genome SNP analysis. The tree is in agreement with the MLVA clade assignment. The three clades within *B. melitensis*, previously identified by MLVA and MLST, were well-resolved. Within *B. suis*, the clusters initially defined by biotyping (biovars 1 to 5) and further supported by MLVA and MLST, were also well-preserved. The *B. suis* biovar 5 lineage defines the first split within the *B. suis* species. From the split, 1297 SNPs define the branch leading to biovar 5. In contrast, the speed of branch expansion is twice relative to *B. suis* biovar 2 (up to 2648 SNPs). According to the figure, the rate of expansion of the different lineages appears generally variable. More than 4,000 SNPs occur from the root indicated by the red star in the figure to the tip within the *B. melitensis* West Mediterranean clade. *B. microti* defines the shortest branch with approximately 1000 SNPs from root to tip. **Figure 6** thus illustrates how both MLST and MLVA can be used to assign a strain to a

position on the phylogenetic tree produced by whole genome SNP analysis.

CONCLUSION

Both MLVA and MLST constitute valuable complementary tools to investigate genetic diversity and molecular epidemiology of *Brucella* species and biovars. In addition to their ability to identify rapidly pathogenic *Brucella* species or to their recognized contribution to identify novel *Brucella* species, they both are able to discriminate below the biovar level, down to a strain level representative of a geographic origin or particular host.

Multilocus Sequence Typing as classically done, i.e., via sequencing of nine (MLST9) or 21 (MLST21) PCR amplification products might soon become too expensive compared to the running of draft whole genome sequencing, which has much greater added value. Nevertheless, MLST genotypes are a very valuable way of naming lineages, and can be readily deduced from whole genome sequences as used in this study.

MLVA is a convenient first line assay for outbreak investigations, fast quality check of strain identity in a collection, and identification of outliers, i.e., strains which should be

sequenced in priority as they may represent new lineages. With more than 5,000 strains in the current version of the online database, it is likely that most of the existing genotype diversity has now been uncovered and that the discovery of new MLVA11 genotypes will be limited.

From a practical point of view, MLVA can be run with a variety of equipment including regular agarose gels (Le Flèche et al., 2006), monoplex capillary electrophoresis (De Santis et al., 2013), or multiplex PCR multicolor capillary electrophoresis (Garofolo et al., 2013). Target loci can be selected to suit a specific epidemiological background. In a given area, only a few MLVA11 genotypes will be encountered. It will not be necessary to type all 11 loci, and conversely it will be very valuable to include additional, more discriminatory VNTRs not included in the MLVA16 assay. When MLVA was initially developed, a subset of loci was selected for practical reasons among a large collection of potentially interesting markers (Bricker et al., 2003; Le Flèche et al., 2006; Whatmore et al., 2006). Owing to the accessibility of whole genome sequencing, tailored optimized MLVA assays can now be developed. For this purpose, one only needs to draft sequence a few local representative strains, deduce the MLVA profile at all known *Brucella* VNTR loci, identify the relevant VNTRs, and use these in a new assay. We have shown here that sequencing reads with a length of 250 bp or more will provide accurate assemblies. The advent of sequencing machines providing long reads may further simplify the process. *In silico* MLVA typing requires a correct determination of the length of the tandem repeat, but is not very demanding in terms of internal sequence accuracy.

REFERENCES

- Al Dahouk, S., Hofer, E., Tomaso, H., Vergnaud, G., Le Flèche, P., Cloeckert, A., et al. (2012). Intraspecific biodiversity of the genetically homologous species *Brucella microti*. *Appl. Environ. Microbiol.* 78, 1534–1543. doi: 10.1128/AEM.06351-6311
- Al Dahouk, S., Köhler, S., Occhialini, A., Jiménez de Bagüés, M. P., Hammerl, J. A., Eisenberg, T., et al. (2017). *Brucella* spp. of amphibians comprise genomically diverse motile strains competent for replication in macrophages and survival in mammalian hosts. *Sci. Rep.* 7:44420. doi: 10.1038/srep44420
- Alton, G. G., Jones, L. M., Angus, R. D., and Verger, J. M. (1988). *Techniques for the Brucellosis Laboratory*. Paris: INRA.
- Bankevich, A., Nurk, S., Antipov, D., Gurevich, A. A., Dvorkin, M., Kulikov, A. S., et al. (2012). SPAdes: a new genome assembly algorithm and its applications to single-cell sequencing. *J. Comput. Biol.* 19, 455–477. doi: 10.1089/cmb.2012.0021
- Bricker, B. J., Ewalt, D. R., and Halling, S. M. (2003). *Brucella* 'HOOF-prints': strain typing by multi-locus analysis of variable number tandem repeats (VNTRs). *BMC Microbiol.* 3:15. doi: 10.1186/1471-2180-3-15
- Corbel, M. J., and Brinley Morgan, W. J. (1984). "Genus *Brucella* meyer and shaw 1920, 173AL," in *Bergey's Manual of Systematic Bacteriology*, Vol. 1, eds N. R. Krieg and J. G. Holt (Baltimore, MD: Williams and Wilkins), 377–390.
- De Santis, R., Ancora, M., De Massis, F., Ciammaruconi, A., Zilli, K., Di Giannatale, E., et al. (2013). Molecular strain typing of *Brucella abortus* isolates from Italy by two VNTR allele sizing technologies. *Mol. Biotechnol.* 55, 101–110. doi: 10.1007/s12033-013-9659-9653
- Eisenberg, T., Hamann, H. P., Kaim, U., Schlez, K., Seeger, H., Schauerte, N., et al. (2012). Isolation of potentially novel *Brucella* spp. from frogs. *Appl. Environ. Microbiol.* 78, 3753–3755. doi: 10.1128/AEM.07509-7511

AUTHOR CONTRIBUTIONS

GV, CP, AC, and MZ conceived and designed the study. GV, AC, and MZ analyzed the data and drafted the manuscript. YH, GV, and CP performed experimental work and data management and control. DC performed *in silico* data analyses. BD upgraded the MicrobesGenotyping web site and underlying database. IJ oversaw strains provision, DNA preparation, and biotyping.

FUNDING

This work was funded by Direction Générale de l'Armement grant REI 10 34 003 and by Agence Nationale de la Recherche grant ANR-14-ASMA-0002-02.

ACKNOWLEDGMENTS

We thank Philippe Le Flèche and Rim Bouchouicha for their help in setting-up the capillary electrophoresis assay. This work has benefited from the assistance and expertise of the I2BC Informatics Support team.

SUPPLEMENTARY MATERIAL

The Supplementary Material for this article can be found online at: <https://www.frontiersin.org/articles/10.3389/fmicb.2018.01545/full#supplementary-material>

- Eisenberg, T., Riße, K., Schauerte, N., Geiger, C., Blom, J., and Scholz, H. C. (2017). Isolation of a novel 'atypical' *Brucella* strain from a bluespotted ribbontail ray (*Taeniura lymma*). *Antonie Van Leeuwenhoek* 110, 221–234. doi: 10.1007/s10482-016-0792-794
- Fischer, D., Lorenz, N., Heuser, W., Kämpfer, P., Scholz, H. C., Lierz, M. (2012). Abscesses associated with a *Brucella inopinata*-like bacterium in a big-eyed tree frog (*Leptopelis vermiculatus*). *J. Zoo Wildl. Med.* 43, 625–628. doi: 10.1638/2011-0005R2.1
- Foster, G., Osterman, B. S., Godfroid, J., Jacques, I., and Cloeckert, A. (2007). *Brucella ceti* sp. nov. and *Brucella pinnipedialis* sp. nov. for *Brucella* strains with cetaceans and seals as their preferred hosts. *Int. J. Syst. Evol. Microbiol.* 57, 2688–2693. doi: 10.1099/ijs.0.65269-0
- Frampton, M., and Houlston, R. (2012). Generation of artificial FASTQ files to evaluate the performance of next-generation sequencing pipelines. *PLoS One* 7:e49110. doi: 10.1371/journal.pone.0049110
- Garofolo, G., Ancora, M., and Di Giannatale, E. (2013). MLVA16 loci panel on *Brucella* spp. using multiplex PCR and multicolor capillary electrophoresis. *J. Microbiol. Methods* 92, 103–107. doi: 10.1016/j.mimet.2012.11.007
- Godfroid, J., Scholz, H. C., Barbier, T., Nicolas, C., Wattiau, P., Fretin, D., et al. (2011). Brucellosis at the animal/ecosystem/human interface at the beginning of the 21st century. *Prev. Vet. Med.* 102, 118–131. doi: 10.1016/j.prevetmed.2011.04.007
- Groussaud, P., Shankster, S. J., Koylass, M. S., Whatmore, A. M. (2007). Molecular typing divides marine mammal strains of *Brucella* into at least three groups with distinct host preferences. *J. Med. Microbiol.* 56, 1512–1518. doi: 10.1099/jmm.0.47330-0
- Hubálek, Z., Chalupský, V., Juricová, Z., and Sevcíková, L. (2007). Brucellosis of the common vole (*Microtus arvalis*). *Vector Borne Zoonotic Dis.* 7, 679–687. doi: 10.1089/vbz.2007.0143

- Jiménez de Bagüés, M. P., Iturralde, M., Arias, M. A., Pardo, J., Cloeckert, A., and Zygmunt, M. S. (2014). The new strains *Brucella inopinata* BO1 and *Brucella* species 83-210 behave biologically like classic infectious *Brucella* species and cause death in murine models of infection. *J. Infect. Dis.* 210, 467–472. doi: 10.1093/infdis/jiu102
- Jiménez de Bagüés, M. P., Ouahrani-Bettache, S., Quintana, J. F., Mitjana, O., Hanna, N., Bessoles, S., et al. (2010). The new species *Brucella microti* replicates in macrophages and causes death in murine models of infection. *J. Infect. Dis.* 202, 3–10. doi: 10.1086/653084
- Kimura, M., Une, Y., Suzuki, M., Park, E. S., Imaoka, K., and Morikawa, S. (2017). Isolation of *Brucella inopinata*-like bacteria from white's and denny's tree frogs. *Vector Borne Zoonotic Dis.* doi: 10.1089/vbz.2016.2027 [Epub ahead of print].
- Le Flèche, P., Jacques, I., Grayon, M., Al Dahouk, S., Bouchon, P., Denoeud, F., et al. (2006). Evaluation and selection of tandem repeat loci for a *Brucella* MLVA typing assay. *BMC Microbiol.* 6:9. doi: 10.1186/1471-2180-6-9
- Maquart, M., Le Flèche, P., Foster, G., Tryland, M., Ramisse, F., Djønne, B., et al. (2009). MLVA16 typing of 295 marine mammal *Brucella* isolates from different animal and geographic origins identifies 7 major groups within *Brucella ceti* and *Brucella pinnipedialis*. *BMC Microbiol.* 9:145. doi: 10.1186/1471-2180-9-145
- Moreno, E., Cloeckert, A., and Moriyón, I. (2002). *Brucella* evolution and taxonomy. *Vet. Microbiol.* 90, 209–227. doi: 10.1016/S0378-1135(02)00210-9
- Mühldorfer, K., Wibbelt, G., Szentiks, C. A., Fischer, D., Scholz, H. C., Zschöck, M., et al. (2017). The role of 'atypical' *Brucella* in amphibians: are we facing novel emerging pathogens? *J. Appl. Microbiol.* 122, 40–53. doi: 10.1111/jam.13326
- Paulsen, I. T., Seshadri, R., Nelson, K. E., Eisen, J. A., Heidelberg, J. F., Read, T. D., et al. (2002). The *Brucella suis* genome reveals fundamental similarities between animal and plant pathogens and symbionts. *Proc. Natl. Acad. Sci. U.S.A.* 99, 13148–13153. doi: 10.1073/pnas.192319099
- Riehm, J. M., Vergnaud, G., Kiefer, D., Damdindorj, T., Dashdavaa, O., Khurelsukh, T., et al. (2012). *Yersinia pestis* lineages in Mongolia. *PLoS One* 7:e30624. doi: 10.1371/journal.pone.0030624
- Rónai, Z., Kreizinger, Z., Dán, Á., Drees, K., Foster, J. T., Bányai, K., et al. (2015). First isolation and characterization of *Brucella microti* from wild boar. *BMC Vet. Res.* 11:147. doi: 10.1186/s12917-015-0456-z
- Soler-Lloréns, P. F., Quance, C. R., Lawhon, S. D., Stuber, T. P., Edwards, J. F., Ficht, T. A., et al. (2016). A *Brucella* spp. isolate from a Pac-Man frog (*Ceratophrys ornata*) reveals characteristics departing from classical *Brucellae*. *Front. Cell. Infect. Microbiol.* 6:116. doi: 10.3389/fcimb.2016.00116
- Scholz, H. C., Hofer, E., Vergnaud, G., Le Flèche, P., Whatmore, A. M., Al Dahouk, S., et al. (2009). Isolation of *Brucella microti* from mandibular lymph nodes of red foxes, *Vulpes vulpes*, in lower Austria. *Vector Borne Zoonotic Dis.* 9, 153–156. doi: 10.1089/vbz.2008.0036
- Scholz, H. C., Hubalek, Z., Nesvadbova, J., Tomaso, H., Vergnaud, G., Le Flèche, P., et al. (2008a). Isolation of *Brucella microti* from soil. *Emerg. Infect. Dis.* 14, 1316–1317. doi: 10.3201/eid1408.080286
- Scholz, H. C., Hubalek, Z., Sedláček, I., Vergnaud, G., Tomaso, H., Al Dahouk, S., et al. (2008b). *Brucella microti* sp. nov., isolated from the common vole *Microtus arvalis*. *Int. J. Syst. Evol. Microbiol.* 58, 375–382. doi: 10.1099/ijls.0.65356-65350
- Scholz, H. C., and Vergnaud, G. (2013). Molecular characterisation of *Brucella* species. *Rev. Sci. Tech.* 32, 149–162. doi: 10.20506/rst.32.1.2189
- Scholz, H. C., Mühldorfer, K., Shilton, C., Benedict, S., Whatmore, A. M., Blom, J., et al. (2016a). The change of a medically important genus: worldwide occurrence of genetically diverse novel *Brucella* species in exotic frogs. *PLoS One* 11:e0168872. doi: 10.1371/journal.pone.0168872
- Scholz, H. C., Nöckler, K., Göllner, C., Bahn, P., Vergnaud, G., Tomaso, H., et al. (2010). *Brucella inopinata* sp. nov., isolated from a breast implant infection. *Int. J. Syst. Evol. Microbiol.* 60, 801–808. doi: 10.1099/ijls.0.011148-11140
- Scholz, H. C., Revilla-Fernández, S., Al Dahouk, S., Hammerl, J. A., Zygmunt, M. S., Cloeckert, A., et al. (2016b). *Brucella vulpis* sp. nov., isolated from mandibular lymph nodes of red foxes (*Vulpes vulpes*). *Int. J. Syst. Evol. Microbiol.* 66, 2090–2098. doi: 10.1099/ijsem.0.000998
- Tiller, R. V., Gee, J. E., Frace, M. A., Taylor, T. K., Setubal, J. C., Hoffmaster, A. R., et al. (2010a). Characterization of novel *Brucella* strains originating from wild native rodent species in North Queensland, Australia. *Appl. Environ. Microbiol.* 76, 5837–5845. doi: 10.1128/AEM.00620-610
- Tiller, R. V., Gee, J. E., Lonsway, D. R., Gribble, S., Bell, S. C., Jennison, A. V., et al. (2010b). Identification of an unusual *Brucella* strain (BO2) from a lung biopsy in a 52 year-old patient with chronic destructive pneumonia. *BMC Microbiol.* 10:23. doi: 10.1186/1471-2180-10-23
- Verger, J. M., Grimont, F., Grimont, P. A. D., and Grayon, M. (1985). *Brucella*, a monospecific genus as shown by deoxyribonucleic acid hybridization. *Int. J. Syst. Bacteriol.* 35, 292–295. doi: 10.1099/00207713-35-3-292
- Whatmore, A. M., Davison, N., Cloeckert, A., Al Dahouk, S., Zygmunt, M. S., Brew, S. D., et al. (2014). *Brucella papionis* sp. nov., isolated from baboons (*Papio* spp.). *Int. J. Syst. Evol. Microbiol.* 64, 4120–4128. doi: 10.1099/ijls.0.065482-65480
- Whatmore, A. M., Koylass, M. S., Muchowski, J., Edwards-Smallbone, J., Gopaul, K. K., and Perrett, L. L. (2016). Extended multilocus sequence analysis to describe the global population structure of the genus *Brucella*: phylogeography and relationship to biovars. *Front. Microbiol.* 7:2049. doi: 10.3389/fmicb.2016.02049
- Whatmore, A. M., Perrett, L. L., and MacMillan, A. P. (2007). Characterisation of the genetic diversity of *Brucella* by multilocus sequencing. *BMC Microbiol.* 7:34. doi: 10.1186/1471-2180-7-34
- Whatmore, A. M., Shankster, S. J., Perrett, L. L., Murphy, T. J., Brew, S. D., Thirlwall, R. E., et al. (2006). Identification and characterization of variable-number tandem-repeat markers for typing of *Brucella* spp. *J. Clin. Microbiol.* 44, 1982–1993. doi: 10.1128/JCM.02039-05
- Zygmunt, M. S., Bundle, D. R., Ganesh, N. V., Guiard, J., Cloeckert, A. (2015). Monoclonal antibody-defined specific C epitope of *Brucella* O-polysaccharide revisited. *Clin. Vaccine Immunol.* 22, 979–982. doi: 10.1128/CVI.00225-15

Conflict of Interest Statement: The authors declare that the research was conducted in the absence of any commercial or financial relationships that could be construed as a potential conflict of interest.

Copyright © 2018 Vergnaud, Hauck, Christiany, Daoud, Pourcel, Jacques, Cloeckert and Zygmunt. This is an open-access article distributed under the terms of the Creative Commons Attribution License (CC BY). The use, distribution or reproduction in other forums is permitted, provided the original author(s) and the copyright owner(s) are credited and that the original publication in this journal is cited, in accordance with accepted academic practice. No use, distribution or reproduction is permitted which does not comply with these terms.



BASI74, a Virulence-Related sRNA in *Brucella abortus*

Hao Dong^{1†}, Xiaowei Peng^{2†}, Yufu Liu^{2,3†}, Tonglei Wu⁴, Xiaolei Wang⁵, Yanyan De⁶, Tao Han¹, Lin Yuan¹, Jiabo Ding², Chuanbin Wang^{1*} and Qingmin Wu^{6*}

¹ China Animal Disease Control Center, Beijing, China, ² Department of Inspection Technology Research, China Institute of Veterinary Drug Control, Beijing, China, ³ College of Veterinary Medicine, South China Agricultural University, Guangzhou, China, ⁴ Key Laboratory of Preventive Veterinary Medicine of Hebei Province, Hebei Normal University of Science and Technology, Qinhuangdao, China, ⁵ Institute of Animal Husbandry and Veterinary Medicine, Beijing Academy of Agriculture and Forestry Sciences, Beijing, China, ⁶ Key Laboratory of Animal Epidemiology and Zoonosis, Ministry of Agriculture, College of Veterinary Medicine, China Agricultural University, Beijing, China

OPEN ACCESS

Edited by:

Michel Stanislas Zygmunt,
Institut National de la Recherche
Agronomique (INRA), France

Reviewed by:

Alessandra Occhialini,
Université de Montpellier, France
Gregory T. Robertson,
Colorado State University,
United States

*Correspondence:

Chuanbin Wang
nvdcwang@sina.com
Qingmin Wu
wuqm@cau.edu.cn

[†] These authors have contributed
equally to this work

Specialty section:

This article was submitted to
Infectious Diseases,
a section of the journal
Frontiers in Microbiology

Received: 21 March 2018

Accepted: 24 August 2018

Published: 13 September 2018

Citation:

Dong H, Peng X, Liu Y, Wu T, Wang X,
De Y, Han T, Yuan L, Ding J, Wang C
and Wu Q (2018) BASI74,
a Virulence-Related sRNA in *Brucella*
abortus. Front. Microbiol. 9:2173.
doi: 10.3389/fmicb.2018.02173

Brucella spp. are intracellular pathogens that infect a wide variety of mammals including humans, posing threats to the livestock industry and human health in developing countries. A number of genes associated with the intracellular trafficking and multiplication have so far been identified in *Brucella* spp. However, the sophisticated post-transcriptional regulation and coordination of gene expression that enable *Brucella* spp. to adapt to changes in environment and to evade host cell defenses are not fully understood. Bacteria small RNAs (sRNAs) play a significant role in post-transcriptional regulation, which has already been confirmed in a number of bacteria but the role of sRNAs in *Brucella* remains elusive. In this study, we identified several different sRNAs in *Brucella* spp., and found that over-expression of a sRNA, tentatively termed BASI74, led to alternation in virulence of *Brucella* in macrophage infection model. The expression level of BASI74 increased while *Brucella abortus* 2308 was grown in acidic media. In addition, BASI74 affected the growth ratio of the *Brucella* cells in minimal media and iron limiting medium. Using a two-plasmid reporter system, we identified four genes as the target of BASI74. One target gene, BABI1154, was predicted to encode a cytosine-N4-specific DNA methyltransferase, which protects cellular DNA from the restriction endonuclease in *Brucella*. These results show that BASI74 plays an important role in *Brucella* survival in macrophage infection model, speculatively by its connection with stress response or impact on restriction-modification system. Our study promotes the understanding of *Brucella* sRNAs, as well as the mechanism by which sRNAs use to influence *Brucella* physiology and pathogenesis.

Keywords: *Brucella*, sRNA, virulence, post-transcriptional regulation, stress response, intracellular survival

INTRODUCTION

Brucella spp. as well as other bacteria are capable of quickly adapting to changing conditions to survive. Successful adaptation depends on changes in gene expression, which may take place at both transcriptional level and post-transcriptional level. Compared to a wide range of studies in transcriptional regulation, e.g., transcriptional regulators (Dong et al., 2013), two-component regulators (Abdou et al., 2013), quorum sensing systems (Brambila-Tapia and Perez-Rueda, 2014),

only a limited number of studies focused on post-transcriptional regulation [especially small RNAs (sRNAs)] in *Brucella* spp.

Small RNAs usually have a length of 50–300 nt and most of them base-pair with mRNA and regulate mRNA stability or mRNA translation efficiency. According to the location of their genes on the chromosomes, sRNAs can be divided into two groups: (a) *cis*-acting sRNAs with the capacity of extensive base pairing, and (b) trans-encoded sRNAs, having limited potential of base pairing with the target mRNAs (Waters and Storz, 2009).

Previous studies have demonstrated that some sRNAs are involved in bacterial virulence in various pathogens (such as *Listeria*, *Salmonella*, *Vibrio*, and *Yersinia*). Two sRNAs (AbcR1 and AbcR2) regulating *Brucella* virulence were identified, and AbcR1 and AbcR2 double mutant was defective in both macrophage infection model and mice chronic infection model (Caswell et al., 2012; Sheehan and Caswell, 2017). One sRNA (BSR0602), which modulated *Brucella melitensis* intracellular survival was also reported (Wang et al., 2015). Based on the results of strand-specific RNA deep-sequencing approach, 1321 sRNAs were found in *B. melitensis* 16 M, and one sRNA, BSR0441, involved in bacterial virulence in both macrophages and mice infection models was also found (Zhong et al., 2016).

In previous studies, we integrated the output of two published sRNA detection programs (sight and napp), and found a total of 129 sRNAs candidates, out of which 7 from 20 sRNA candidates were verified by RT-PCR (Dong et al., 2014). In this study, additional 43 sRNA from 109 remaining candidates were detected by RT-PCR and the role of all verified sRNAs in virulence of *Brucella* was examined by over-expression in the wild type strain *B. abortus* 2308. We identified and characterized one sRNA (BAS174) that significantly changed *Brucella* virulence in macrophage infection model.

MATERIALS AND METHODS

Bacteria Strains and Culture Conditions

We performed a routine cultivation of *Escherichia coli* strains in Luria-Bertani (LB) broth or on LB agar plates with appropriate antibiotic supplementation, if necessary. The *Brucella* strains were routinely grown in tryptic soy broth (TSB, BD company) at 37°C or on tryptic soy agar medium incubated at 37°C under 5% CO₂. Additionally, we added chloramphenicol (30 µg/mL), when we cultured the *Brucella* strains with chloramphenicol resistance. All of the bacterial strains were stored at –80°C and supplemented with 25% (v/v) glycerol. In order to determine the expression levels of the BAS174 under different conditions, we cultured *B. abortus* 2308 in TSB (pH 4.5), TSB (10 mM 2,2'-dipyridyl), and BMM (*Brucella* minimum medium) for 4 h or in TSB (2.5 mM H₂O₂) for 30 min.

Mice and Ethics Statement

Female 4- to 6-week-old BALB/c mice were obtained from Beijing Vital River Laboratory Animal Technology Co., Ltd. All animals were handled in strict accordance with the Experimental Animal Regulation Ordinances defined by the China National Science and Technology Commission; the study was approved by the

animal ethics committee of China Institute of Veterinary Drug Control.

RNA Isolation and Reverse Transcription Polymerase Chain Reaction

We extracted the total RNA of *B. abortus* 2308 under different stress conditions and different growth stages using Bacterial RNA Kit (Omega) and reverse-transcribed into cDNA using random primers, as previously described (Liu et al., 2012). We performed RT-PCR to verify the expression of the sRNA candidates. 1 µl of cDNA sample (without dilution) or total RNA (negative control) was used as template for the PCR. The specific primers of BAS174 used for RT-PCR are listed in **Supplementary Table S1**. We analyzed the PCR products using a 2% agarose gel by electrophoresis, and the bands with the appropriate sizes were cut and sequenced by the Beijing Genomics Institute (Shenzhen, China).

Construction of Small RNA Over-expression Strains

Each putative sRNA encoding sequence (containing the predicted sRNA sequence, about 300 nt upstream and 300 nt downstream sequences) inserted into pBBR1-MCS6 was analyzed to make sure it contains a putative promoter sequence. The constructed over-expression plasmids were verified by sequencing. For construction of sRNA over-expression strains, the pBBR1-MCS6 plasmid with putative sRNA encoding sequence was electroporated into *B. abortus* 2308, and then cells were plated onto TSA containing chloramphenicol for selection of positive clones. In addition, the over-expression strains were further verified by PCR using universal primers.

Construction of BAS174 Deletion Mutant

Construction of recombinant plasmid and selection of marked deletion mutant were performed as previously reported (Zhang et al., 2009). The primers used to construct the recombinant plasmid were listed in **Supplementary Table S1**.

Quantitative RT-PCR

In order to detect the expression levels of the sRNAs under different stress conditions described above, we performed RT-qPCR as previously described (Dong et al., 2013). Samples were run in triplicate and amplified in a 20 µl reaction system containing 10 µl 2 × SYBR® Premix Ex Taq™ II (TAKARA), 100 nM forward and reverse primers, and 1 µl appropriately diluted cDNA sample. Primers used for RT-qPCR are provided in **Supplementary Table S1**. 16S rRNA, expression of which is relatively constant in bacteria, was used as a reference gene.

Cellular Infections

To investigate intracellular survival of the pathogen, we evaluated the multiplication of *B. abortus* 2308 and its derived strains in J774A.1 murine macrophages. The assays were performed as previously described (Zhang et al., 2009).

Mouse Infections

Mice were inoculated intraperitoneally with 100 μ l (10^5 CFU) of 2308-BAS174 and the parental strain *B. abortus* 2308. Five mice of one group were euthanized via carbon dioxide asphyxiation at 1 and 4 weeks post-infection. At each time point, the spleens were harvested, weighed, and then homogenized in 1 ml of peptone saline. Serial dilutions were prepared, and 100- μ l aliquots of each dilution (including the undiluted organ) were plated in duplicate onto TSA plates or TSA plates with 30 μ g/mL chloramphenicol (Zhang et al., 2009).

Stress Assays

We performed the stress response assays as previously reported with slight modifications as following: the *Brucella* strains derived from a single clone were grown for 48 h in 4 ml TSB medium. The bacterial cells (initial density of 1×10^6 CFU/ml) were grown in BMM at 37°C with continuous shaking. The concentration of bacteria was measured every 2 days. The number of colony forming units per milliliter was obtained by plating a series of 1:10 dilutions on TSA plates.

To test if over-expression of BAS174 affected bacterial survival under acidic environments, the *Brucella* strains (with an initial density of 1×10^7 CFU/ml) were cultured in TSB (pH 4.5) and the concentration of bacteria was measured at 2 h and 9 h post-inoculation.

In order to determine if over-expression of BAS174 affected bacterial survival under oxidation stress, bacterial strains were adjusted to a concentration of 1×10^9 CFU/ml, and 100 μ l of each bacterial strains were seeded on a TSA plate, with a 5.5 mm sterile filter paper disk in the center of each plate. We placed 10 μ l of a 30% solution of H₂O₂ onto each disk and incubated at 37°C with 5% CO₂. After 72 h of incubation, the zones of inhibition around each disk were measured.

In order to detect if over-expression of BAS174 affected the iron utilization, we cultured the *Brucella* strains in an iron limitation medium (TSB with 2.5, 5, and 10 mM2,2'-dipyridyl) for 48 h. The bacteria were cultured in this medium at the same initial density (1×10^6 CFU/ml), and we then determined the CFUs at 48 h for each strain.

Bioinformatics Data Analysis

To determine the position of putative promoter sequence, the upstream sequences of each verified sRNAs were analyzed using BDGP: Neural Network Promoter Prediction¹, with the parameters for the software set at their default settings.

We predicted the target genes for the sRNA using CopraRNA², with the parameters for the software set at their default settings (Wright et al., 2009).

Verification of the Target Gene Regulated by BAS174 and β -Galactosidase Assays

The *E. coli*-based reporter system used for verification of genes regulated by BAS174 was constructed as previously described

(Dong et al., 2014). The primers used to amplify BAS174 and the putative target sequences are listed in **Supplementary Table S1**, and the plasmids used in this study can be found in **Supplementary Table S2**.

Statistical Analysis

Differences between the means of the experimental and control groups were analyzed using the independent samples *t*-test

TABLE 1 | Verified sRNA in this work.

sRNA Name	sRNA start	end	Length of sRNA (nt)
BAS I 365	24475	24577	102
BAS I 371	29595	29988	393
BAS I 387	47061	47307	246
BAS I 22	100793	100872	79
BAS I 23	100828	100944	116
BAS I 262	128868	129114	246
BAS I 35	254741	254855	114
BAS I 62	521937	522023	86
BAS I 74	713147	713233	86
BAS I 84	815539	815617	78
BAS I 244	1098391	1098472	81
BAS I 245	1099846	1100145	299
BAS I 122	1173218	1173318	100
BAS I 130	1221129	1221226	97
BAS I 133	1249641	1249811	170
BAS I 137	1289949	1290101	152
BAS I 151	1441442	1441521	79
BAS I 273	1445660	1445799	139
BAS I 9	1490038	1490143	105
BAS I 283	1500367	1500491	124
BAS I 176	1603445	1603565	120
BAS I 304	1648877	1649137	260
BAS I 306	1662860	1663033	173
BAS I 193	1688162	1688286	124
BAS I 214	1971684	1971765	81
BAS I 344	2005699	2006063	364
BAS I 345	2017052	2017142	90
BAS I 218	2032657	2032746	89
BAS I 221	2056362	2056509	147
BAS I 228	2084505	2084582	77
BAS II 152	873615	873740	125
BAS II 36	295058	295164	106
BAS II 47	433815	433936	121
BAS II 149	75638	75764	126
BAS II 37	309649	309775	126
BAS II 99	1099166	1099368	202
BAS II 39	325182	325397	215
BAS II 133	508838	509001	163
BAS II 5	580622	580840	218
BAS II 73	824439	824525	86
BAS II 150	824439	824613	174
BAS II 74	824439	824637	198
BAS II 117	381044	381193	149

¹http://www.fruitfly.org/seq_tools/promoter.html

²<http://rna.informatik.uni-freiburg.de>

included in the program SPSS 17.0. Differences were considered significant at p -values of <0.05 .

RESULTS

Identification of Additional 43 sRNAs Expressed in *Brucella abortus* 2308

Our previous studies had identified 129 sRNAs candidates of *Brucella* using bioinformatics methods, and 7 of 20 tested sRNA candidates were verified to be present (Dong et al., 2014). In this study, we extracted the total RNA of *B. abortus* strain 2308 and detected if the remaining 109 sRNA candidates were expressed using RT-PCR. A total of 43 sRNAs could be detected by RT-PCR and sequencing (Table 1), out of which the RT-PCR result of 24 sRNAs were shown in Figure 1.

Identification of sRNA Over-expressed Strains With Reduced Survival Compared With Parental Strain in Macrophages

In this study, several *cis*-encoded sRNAs were verified, and it was impossible to construct mutants of *cis*-encoded sRNAs without affecting their neighboring target genes. To address this problem, we over-expressed all the 43 verified sRNAs in the wild type *Brucella* strain, and detected if the virulence of these over-expressed strains were altered.

Overall, the virulence of 42 sRNA over-expression strains were almost equivalent to that of 2308 and 2308-pBBR1, while over-expression of the sRNA BAS174(named 2308-BAS174) significantly reduced *Brucella* virulence in the macrophage infection model at 48h post-infection ($p < 0.01$) (Table 2).

Over-expression of BAS174 Affected the Virulence of *B. abortus* 2308

To further confirm the relationship between BAS174 and reduced survival ability in macrophages, a BAS174-deletion strain(named Δ BAS174) was constructed and the virulence of 2308-BAS174 and Δ BAS174 in J774A.1 macrophages was detected at different time points.

Before the macrophage infection assay, the expression of BAS174 was detected in both 2308-BAS174 and Δ BAS174. The results of RT-qPCR showed that the expression levels of BAS174 were not significantly different between 2308 and Δ BAS174, while that of 2308-BAS174 was about 8-fold higher than that of 2308(Supplementary Table S3). According to the blast result of BAS174 sequence in *B. abortus* 2308, several highly homologous sequences were found in both chromosomes, I and II (Supplementary Table S4).

As shown in Figure 2, the intracellular bacteria load of 2308-BAS174 was significantly reduced at 48 h post-infection compared to that of 2308 and 2308-pBBR1 ($p < 0.01$). However, the survival ratio of Δ BAS174 showed no difference, compared with that of 2308 at each time point.

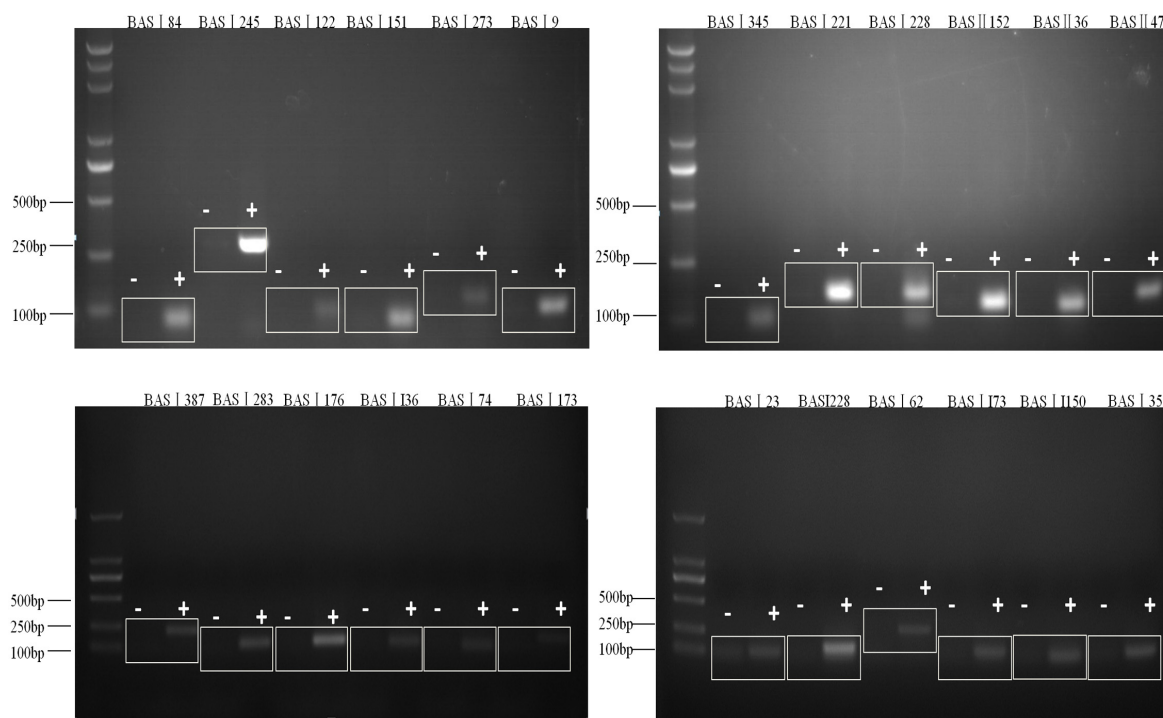
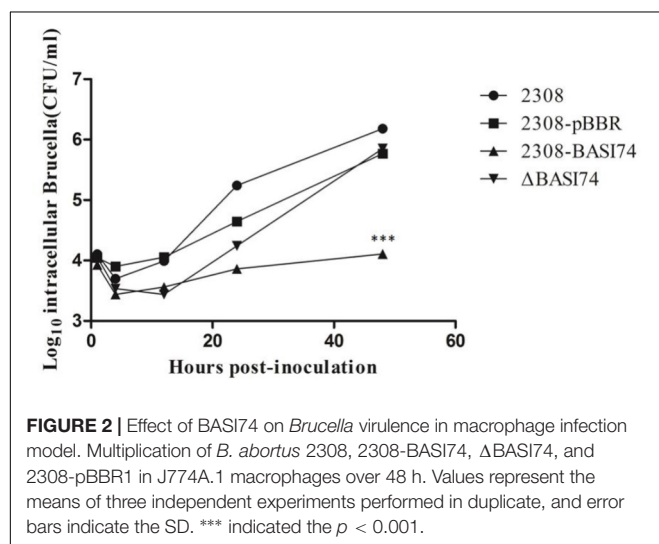


FIGURE 1 | Verification of sRNAs in *B. abortus* 2308. RT-PCR verification of the transcriptional unit of sRNA candidates. RNA prepared from *B. abortus* 2308 grown to stationary phase at 37°C was used for RT-PCR. The regions to be amplified were shown by bars with numbers. "+" represents reactions with reverse transcriptase and "-" represents reactions without reverse transcriptase.

TABLE 2 | Multiplication ability of sRNA over expression strains in J774A.1 macrophages.

sRNA Name	1 h CFU	Over-expression strain/WT(1 h)	48 h CFU	Over-expression strain/WT(48 h)	sRNA Name	1 h CFU	Over-expression strain/WT(1 h)	48 h CFU	Over-expression strain/WT (48 h)
BAS I 74	1.98E + 03	33.51%	9.17E + 03	0.61%	BAS I 306	8.42E + 02	14.23%	4.98E + 05	33.40%
BAS I 22	9.67E + 02	16.34%	4.05E + 05	27.14%	BAS I 344	8.66E + 03	146.32%	8.61E + 05	57.70%
BAS I 23	8.33E + 02	14.08%	2.45E + 05	16.42%	BAS I 345	8.42E + 02	14.23%	2.28E + 05	15.30%
BAS I 35	1.28E + 03	21.55%	1.23E + 05	8.27%	BAS I 365	2.24E + 03	37.89%	4.16E + 05	27.87%
BAS I 62	2.71E + 03	45.77%	2.62E + 05	17.54%	BAS I 371	9.33E + 02	15.77%	5.83E + 05	39.04%
BAS I 9	8.33E+02	14.08%	7.52E + 05	50.38%	BAS I 387	5.42E + 03	91.55%	1.02E + 06	68.16%
BAS I 84	2.80E + 03	47.32%	4.33E + 05	29.04%	BAS II 5	2.01E + 03	33.94%	3.66E + 05	24.52%
BAS I 122	1.10E + 03	18.59%	1.15E + 06	77.08%	BAS II 36	8.42E + 02	14.23%	3.18E + 05	21.34%
BAS I 130	8.67E + 03	146.48%	1.10E + 06	73.39%	BAS II 37	1.15E + 03	19.44%	6.55E + 05	43.90%
BAS I 133	1.63E + 03	27.46%	5.52E + 05	36.97%	BAS II 39	1.57E + 03	26.48%	3.68E + 05	24.69%
BAS I 137	3.11E + 03	52.53%	8.50E + 05	56.97%	BAS II 47	1.99E + 03	33.67%	4.15E + 05	27.81%
BAS I 151	1.91E + 03	32.25%	7.80E + 05	52.28%	BAS II 73	9.08E + 02	15.35%	3.22E + 05	21.56%
BAS I 176	2.28E + 03	38.45%	2.84E + 05	19.05%	BAS II 74	1.15E + 03	19.49%	6.33E + 05	42.45%
BAS I 193	1.49E + 03	25.22%	5.88E + 05	39.43%	BAS II 99	1.60E + 03	27.04%	3.33E + 05	22.34%
BAS I 214	2.31E+03	39.01%	5.47E + 05	36.64%	BAS II 117	5.42E + 03	91.55%	6.23E + 05	41.78%
BAS I 218	1.79E + 03	30.29%	5.58E + 05	37.42%	BAS II 133	3.27E + 03	55.21%	9.51E + 05	63.73%
BAS I 221	8.33E + 03	140.83%	1.25E + 06	83.44%	BAS II 149	1.50E + 03	25.35%	4.96E + 05	33.23%
BAS I 228	1.81E + 03	30.56%	1.00E + 06	67.02%	BAS II 152	2.90E + 03	49.01%	8.02E + 05	53.73%
BAS I 244	5.50E + 03	92.95%	9.47E + 05	63.45%	BAS II 150	1.50E + 03	25.35%	4.96E + 05	33.23%
BAS I 245	1.03E + 03	17.46%	8.27E + 05	55.41%	2308-pBBR1	2.14E + 03	36.20%	1.00E + 06	67.09%
BAS I 262	9.25E + 02	15.63%	3.97E + 05	26.59%	2308	5.92E + 03	100.00%	1.49E + 06	100.00%
BAS I 273	8.42E + 02	14.23%	3.95E + 05	26.47%					
BAS I 283	7.08E + 03	119.71%	5.17E + 05	34.63%					
BAS I 304	1.28E + 03	21.68%	4.19E + 05	28.09%					



To evaluate the virulence *in vivo*, BALB/c mice were infected with both 2308-BAS174 and *B. abortus* 2308. Compared with the parental strain 2308, the spleen weight of 2308-BAS174 infected mice was significantly lighter at both 1 week ($p < 0.01$)

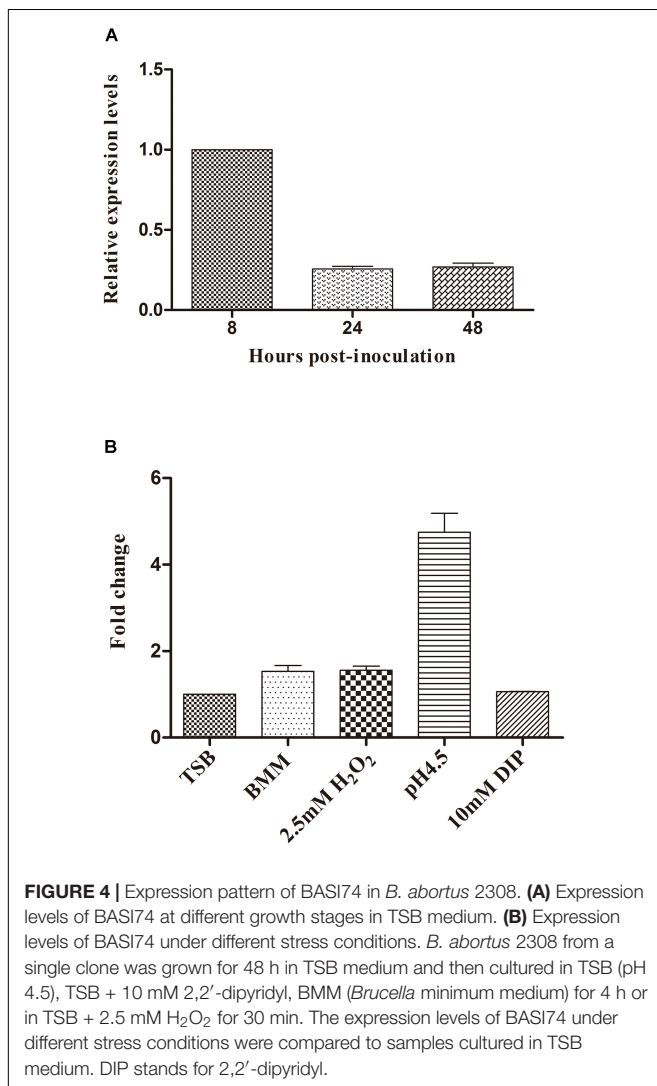
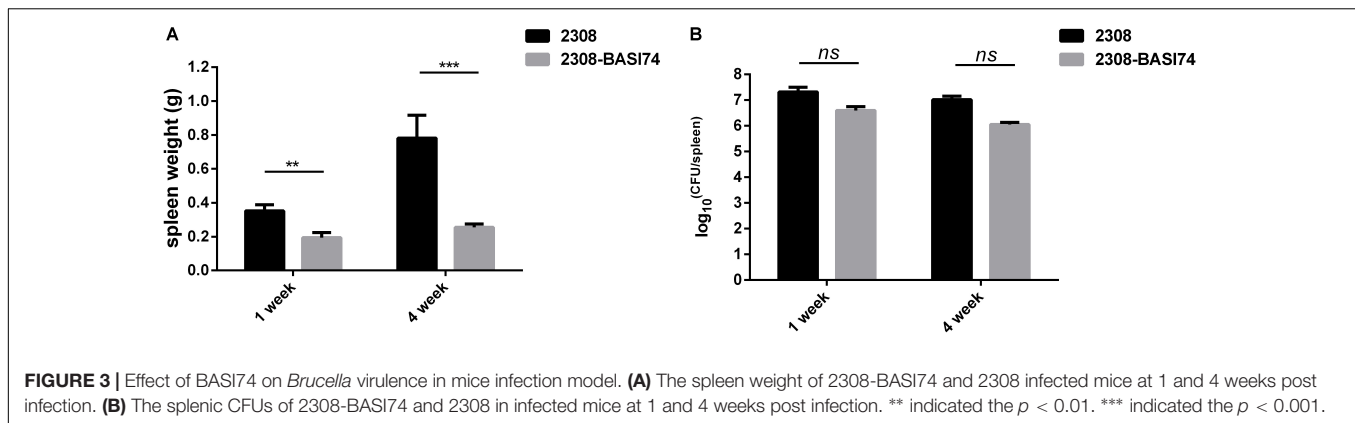
and 4 weeks ($p < 0.001$) post-infection (Figure 3A), while no significant difference was observed in the splenic CFUs between 2308-BAS174 and 2308-infected groups at each time point ($p > 0.05$) (Figure 3B).

Expression Pattern of BAS174 in *B. abortus* 2308

RT-qPCR with RNA samples isolated from the bacteria grown under different stress conditions or harvested at different stages was performed in order to characterize the expression pattern of BAS174. We found that BAS174 was produced at all growth phases, and the expression level increased to the peak at 8 h post-incubation (Figure 4A). The expression levels of BAS174 were not significantly changed under iron deficiency (10 mM 2,2'-dipyridyl for 4 h) or oxidative (2.5 mM H₂O₂ for 30 min) stress, or even in BMM compared with in normal TSB culture. However the level of BAS174 increased more than 4-fold under acidic (pH 4.5 for 4 h) stress than in normal TSB control (Figure 4B).

The BAS174 Was Involved in Stress Responses

The characteristics of 2308-BAS174 in macrophages promoted us to study the underlying mechanisms. Previous studies have demonstrated that many sRNAs are related to stress response, and



that of 2308-pBBR1 and 2308. Neither did we find significant differences of growth ratio among these three strains in the H₂O₂ disk sensitivity assays (**Figure 5B**). In BMM culture, the growth ratio of 2308-BAS174 gradually deviated since 4 days post-incubation compared with that of 2308 and 2308-pBBR1 cells, and turned out to be significantly lower at 8 days post-incubation ($p < 0.05$) (**Figure 5C**). In addition, the survival ratio of the 2308-BAS174 was much lower than that of 2308 and 2308-pBBR1 when cultured in iron limited TSB (10 mM 2,2'-dipyridyl) for 48 h (**Figure 5D**). These data revealed that BAS174 was involved in growth in iron-limiting medium and BMM.

Identification of Targets Regulated by BAS174

To identify the genes regulated by the BAS174 RNA, we performed an *in silico* analysis with sTarPicker (see footnote 2).

As shown in **Table 3**, for BAB1_1361, BAB1_1335, the β -galactosidase activity of the strains containing the combination of the sRNA-encoding plasmid and target *lacZ* fusion plasmids were significantly reduced compared with the vector and *lacZ* fusion plasmids combination group. On the contrary, co-expression of BAS174 with the 5'-UTR of BAB1_1154 or BAB1_0847 *lacZ* fusion plasmids significantly increased the β -galactosidase activity. For BAB1_0097 and BAB1_0343, no obvious difference was observed between the BAS174 and vector group. Except for that of BAB1_1154 (encoding cytosine-N4-specific DNA methyltransferase), functions of all other three targets were still unknown.

To further determine whether these targets were regulated by BAS174, the expression level of four putative targets was tested by RT-qPCR in both Δ BAS174 and 2308-BAS174. As shown in **Table 4**, the transcriptional level of all four verified targets was upregulated in 2308-BAS174, while none of the four targets was affected in the Δ BAS174.

therefore the survival ability of the over-expression strains under different stress conditions was tested.

As shown in **Figure 5A**, the survival ratio of 2308-BAS174 cultured in an acidic medium for 9 h was almost the same as

DISCUSSION

Previous studies have demonstrated that sRNAs were related with the proper expression of virulence factors in a variety of

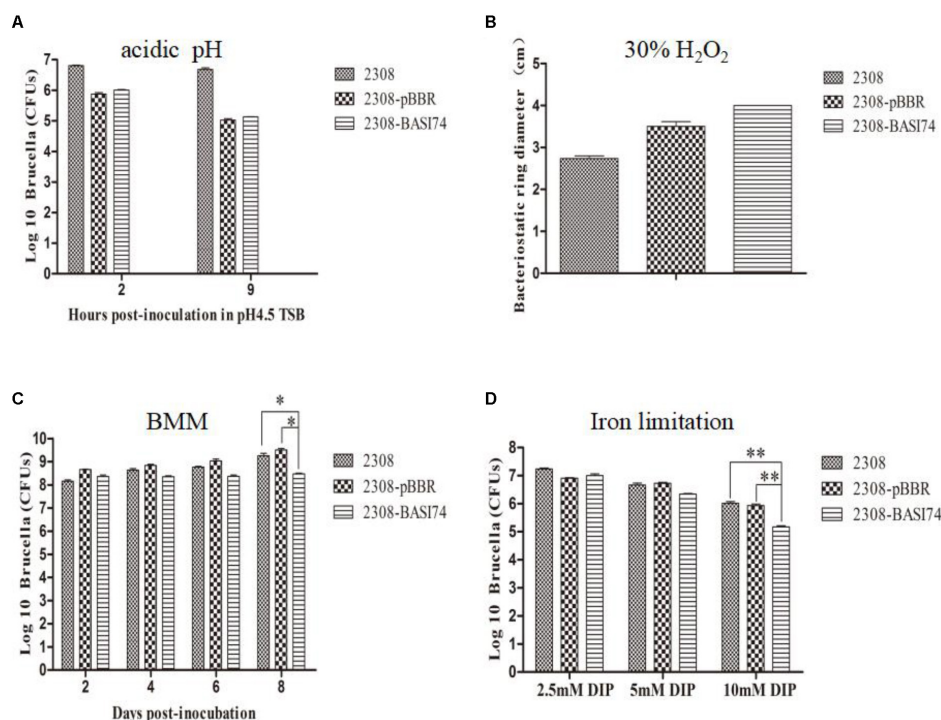


FIGURE 5 | Growth behavior of strains over-producing BAS174 under different stress conditions. **(A)** Over-expression of BAS174 did not affect the survival ratio of *B. abortus* in acidic medium (TSB pH 4.5). **(B)** The 2308-BAS174 strain had equal sensitivity to 30% H₂O₂ compared to two control strains. **(C)** BAS174 affected bacteria growth in *Brucella* minimum medium. **(D)** Over-expression of BAS174 reduced the survival ratio of *B. abortus* under iron-limiting condition. Values represent the means of three independent experiments, and error bars indicate the SD. * indicated the $p < 0.05$. ** indicated the $p < 0.01$.

TABLE 3 | Verification of the interaction between BAS174 and putative target sequences.

Putative target genes	β -galactosidase activity (Miller units)		Fold change BAS174/vector	p -value
	pUT18C	pUT18C-BAS174		
BAB1_0097	9.21 \pm 2.23	11.61 \pm 2.71	1.26	0.8093
BAB1_0343	3.15 \pm 1.21	2.01 \pm 0.83	0.64	0.1253
BAB1_0847	15.57 \pm 2.77	23.65 \pm 2.57	1.52	<0.05
BAB1_1154	14.99 \pm 2.41	47.18 \pm 1.935	3.15	<0.001
BAB1_1335	4.18 \pm 0.32	1.36 \pm 0.48	0.33	<0.05
BAB1_1361	5.48 \pm 1.81	2.03 \pm 1.64	0.37	<0.05

The data were expressed as averages \pm standard deviations (SD). Three independent experiments were performed.

pathogenic bacteria (Papenfert and Vogel, 2010), and several recent studies also showed that sRNAs directly correlated with the virulence of organisms such as *Listeria* (Mraheil et al., 2011),

TABLE 4 | The transcriptional levels of four verified target genes in 2308-BAS174 and Δ BAS174.

Gene	Fold change	
	2308-BAS174 vs. 2308	Δ BAS174 vs. 2308
BAB1_1361	4.52	1.32
BAB1_1335	2.69	1.17
BAB1_1154	7.89	0.93
BAB1_0847	3.89	0.77

Salmonella (Gong et al., 2011), *Vibrio* (Song et al., 2008), *Yersinia* (Koo et al., 2011), and *Brucella* (Caswell et al., 2012).

In this study, it was interesting to find that over-expression of BAS174 locus reduced *Brucella* virulence in macrophages, while deletion of putative BAS174 encoding sequence did not affect *Brucella* virulence. The results of RT-qPCR showed that the transcriptional level of BAS174 between 2308 and Δ BAS174 were not significantly changed, while that of 2308-BAS174 was about 8-fold higher than that of 2308, which might possibly explain the difference of virulence between 2308-BAS174 and Δ BAS174. We speculated that there possibly existed more than one locus encoding BAS174 in the genome of 2308.

Further, we observed a consistent trend in the downstream target genes. The transcriptional level of four verified target genes

were changed more than 2-fold in 2308-BAS174, while none of the four targets was affected in Δ BAS174.

In a previous study, it was also demonstrated that over-expression of sRNAs could result in more dramatic effects on their regulated targets than sRNAs deletion (Koo et al., 2011). Our result was consistent with data previously reported.

Taken together, these data indicated that the reason that Δ BAS174 could not significantly affect the virulence of *Brucella* strains might be explained by the redundancy in genetic structure and function.

Previous studies demonstrated that AbcR sRNAs had redundant and compensatory functions in *B. abortus* 2308 (Caswell et al., 2012). In addition, the four Qrr sRNAs involved in the regulation of quorum sensing are redundant in *Vibrio cholerae* (Lenz et al., 2004). In our study, the probable multiple copies of BAS174 might indicate the important role of this sRNA, and the redundancy of this sRNA may be an evolutionary adaption ensuring the proper expression of essential genes.

As a facultative intracellular pathogen, *B. abortus* encounters formidable environmental stresses such as nutrient deprivation during its interactions with the host cells (Roop et al., 2009). In addition, *Brucella* strains required iron transporters for the expression of wild type virulence in natural and experimental hosts (Roop, 2012). Our results that 2308-BAS174 exhibited lower growth in iron-limiting and nutrient deprivation medium indicated that the attenuation of 2308-BAS174 was probably related with its reduced tolerance under these two types of stresses.

Although 2308-BAS174 was attenuated in macrophage infection model, no significant difference of virulence was observed in the mice infection assay at different time points (Figure 3B). This disagreement of *Brucella* virulence tested by macrophage and mice infection models was not uncommon. In the study of *Brucella* quorum sensing regulator BlxR, the Δ blxR strain exhibited reduced growth in macrophages, while this mutant was not highly attenuated in mice (Rambow-Larsen et al., 2008). Besides, it was worthy noting that the spleen weight of the mice infected with 2308-BAS174 was significantly lighter than that of 2308 in mice infection models at both 1 and 4 weeks post-infection. This observation, which was also found in the mice infection assay of *Brucella* attenuated strain, indicated that the 2308-BAS174 might induce a different immune response in the mice infection model.

REFERENCES

- Abdou, E., Deredjian, A., Jimenez, D. B. M., Kohler, S., and Jubier-Maurin, V. (2013). RegA, the regulator of the two-component system RegB/RegA of *Brucella suis*, is a controller of both oxidative respiration and denitrification required for chronic infection in mice. *Infect. Immun.* 81, 2053–2061. doi: 10.1128/IAI.00063-13
- Brambila-Tapia, A. J., and Perez-Rueda, E. (2014). A functional and phylogenetic comparison of quorum sensing related genes in *Brucella melitensis* 16M. *J. Microbiol.* 52, 709–715. doi: 10.1007/s12275-014-3570-x
- Caswell, C. C., Gaines, J. M., Ciborowski, P., Smith, D., Borchers, C. H., Roux, C. M., et al. (2012). Identification of two small regulatory RNAs linked to virulence in *Brucella abortus* 2308. *Mol. Microbiol.* 85, 345–360. doi: 10.1111/j.1365-2958.2012.08117.x

Previous studies have demonstrated that bacterial DNA methyltransferases were not only associated with restriction-modification systems, but also with chromosome replication, transcription, repair, and many other fundamental processes (Reisenauer et al., 1999). In addition, some recent studies have demonstrated that DNA adenine methylation play an important role in host-pathogen interactions (Marinus and Casadesus, 2009). In *B. abortus*, the CcrM DNA methyltransferase was also reported to be essential for viability, and its over-expression attenuated intracellular replication in murine macrophages (Robertson et al., 2000). In *Helicobacter pylori*, C5-cytosine methylation also affects the expression of several genes related to motility, adhesion, and virulence (Kumar et al., 2012). However, the cytosine-N4-specific DNA methyltransferase can hardly be related with bacterial virulence. As a *trans*-encoded sRNA, BAS174 could regulate more than one target mRNA. In this study, we only verified the top six putative targets with the highest scores in the prediction result, and more targets of BAS174 needs to be verified in the future. Thus, we hypothesized that over-expression of BAS174 might have various effects on more different targets including the target gene BAB1_1154 encoding DNA methylation.

AUTHOR CONTRIBUTIONS

HD wrote the paper. XP, YL, TW, and XW performed the experiments. CW and QW conceived and designed the experiments. YD, TH, LY, and JD analyzed the data.

FUNDING

This work was supported by the National Natural Science Foundation of China (Nos. 31602055 and 31372446) and the National Basic Research Program of China (973 Program) (No. 2010CB530202).

SUPPLEMENTARY MATERIAL

The Supplementary Material for this article can be found online at: <https://www.frontiersin.org/articles/10.3389/fmicb.2018.02173/full#supplementary-material>

- Dong, H., Liu, W., Peng, X., Jing, Z., and Wu, Q. (2013). The effects of MucR on expression of type IV secretion system, quorum sensing system and stress responses in *Brucella melitensis*. *Vet. Microbiol.* 166, 535–542. doi: 10.1016/j.vetmic.2013.06.023
- Dong, H., Peng, X., Wang, N., and Wu, Q. (2014). Identification of novel sRNAs in *Brucella abortus* 2308. *FEMS Microbiol. Lett.* 354, 119–125. doi: 10.1111/1574-6968.12433
- Gong, H., Vu, G. P., Bai, Y., Chan, E., Wu, R., Yang, E., et al. (2011). A *Salmonella* small non-coding RNA facilitates bacterial invasion and intracellular replication by modulating the expression of virulence factors. *PLoS Pathog.* 7:e1002120. doi: 10.1371/journal.ppat.1002120
- Koo, J. T., Alleyne, T. M., Schiano, C. A., Jafari, N., and Lathem, W. W. (2011). Global discovery of small RNAs in *Yersinia pseudotuberculosis* identifies *Yersinia*-specific small, noncoding RNAs required for virulence.

- Proc. Natl. Acad. Sci. U.S.A. 108, E709–E717. doi: 10.1073/pnas.1101655108
- Kovach, M. E., Phillips, R. W., Elzer, P. H., Roop, R. M. II, and Peterson, K. M. (1994). pBBR1MCS: a broad-host-range cloning vector. *Biotechniques* 16, 800–802.
- Kumar, R., Mukhopadhyay, A. K., Ghosh, P., and Rao, D. N. (2012). Comparative transcriptomics of *H. pylori* strains AM5, SS1 and their hpyAVIBM deletion mutants: possible roles of cytosine methylation. *PLoS One* 7:e42303. doi: 10.1371/journal.pone.0042303
- Lenz, D. H., Mok, K. C., Lilley, B. N., Kulkarni, R. V., Wingreen, N. S., and Bassler, B. L. (2004). The small RNA chaperone Hfq and multiple small RNAs control quorum sensing in *Vibrio harveyi* and *Vibrio cholerae*. *Cell* 118, 69–82. doi: 10.1016/j.cell.2004.06.009
- Liu, W., Dong, H., Liu, W., Gao, X., Zhang, C., and Wu, Q. (2012). OtpR regulated the growth, cell morphology of *B. melitensis* and tolerance to beta-lactam agents. *Vet. Microbiol.* 159, 90–98. doi: 10.1016/j.vetmic.2012.03.022
- Marinus, M. G., and Casades, J. (2009). Roles of DNA adenine methylation in host-pathogen interactions: mismatch repair, transcriptional regulation, and more. *FEMS Microbiol. Rev.* 33, 488–503. doi: 10.1111/j.1574-6976.2008.00159.x
- Mraheil, M. A., Billion, A., Mohamed, W., Mukherjee, K., Kuenne, C., Pischmarov, J., et al. (2011). The intracellular sRNA transcriptome of *Listeria monocytogenes* during growth in macrophages. *Nucleic Acids Res.* 39, 4235–4248. doi: 10.1093/nar/gkr033
- Papenfert, K., and Vogel, J. (2010). Regulatory RNA in bacterial pathogens. *Cell Host Microbe* 8, 116–127. doi: 10.1016/j.chom.2010.06.008
- Rambow-Larsen, A. A., Rajashekara, G., Petersen, E., and Splitter, G. (2008). Putative quorum-sensing regulator BlxR of *Brucella melitensis* regulates virulence factors including the type IV secretion system and flagella. *J. Bacteriol.* 190, 3274–3282. doi: 10.1128/JB.01915-07
- Reisenauer, A., Kahng, L. S., McCollum, S., and Shapiro, L. (1999). Bacterial DNA methylation: a cell cycle regulator? *J. Bacteriol.* 181, 5135–5139.
- Robertson, G. T., Reisenauer, A., Wright, R., Jensen, R. B., Jensen, A., Shapiro, L., et al. (2000). The *Brucella abortus* CcrM DNA methyltransferase is essential for viability, and its overexpression attenuates intracellular replication in murine macrophages. *J. Bacteriol.* 182, 3482–3489. doi: 10.1128/JB.182.12.3482-3489.2000
- Roop, R. N. (2012). Metal acquisition and virulence in *Brucella*. *Anim. Health Res. Rev.* 13, 10–20. doi: 10.1017/S1466252312000047
- Roop, R. N., Gaines, J. M., Anderson, E. S., Caswell, C. C., and Martin, D. W. (2009). Survival of the fittest: how *Brucella* strains adapt to their intracellular niche in the host. *Med. Microbiol. Immunol.* 198, 221–238. doi: 10.1007/s00430-009-0123-8
- Sheehan, L. M., and Caswell, C. C. (2017). A 6-nucleotide regulatory motif within the AbcR small RNAs of *Brucella abortus* mediates host-pathogen interactions. *mBio* 8:e00473-17. doi: 10.1128/mBio.00473-17
- Song, T., Mika, F., Lindmark, B., Liu, Z., Schild, S., Bishop, A., et al. (2008). A new *Vibrio cholerae* sRNA modulates colonization and affects release of outer membrane vesicles. *Mol. Microbiol.* 70, 100–111. doi: 10.1111/j.1365-2958.2008.06392.x
- Wang, Y., Ke, Y., Xu, J., Wang, L., Wang, T., Liang, H., et al. (2015). Identification of a novel small non-coding RNA modulating the intracellular survival of *Brucella melitensis*. *Front. Microbiol.* 6:164. doi: 10.3389/fmicb.2015.00164
- Waters, L. S., and Storz, G. (2009). Regulatory RNAs in bacteria. *Cell* 136, 615–628. doi: 10.1016/j.cell.2009.01.043
- Wright, P. R., Georg, J., Mann, M., Sorescu, D. A., Richter, A. S., Lott, S., et al. (2014). CopraRNA and IntaRNA: predicting small RNA targets, networks and interaction domains. *Nucleic Acids Res.* 42, W119–W123. doi: 10.1093/nar/gku359
- Zhang, X., Ren, J., Li, N., Liu, W., and Wu, Q. (2009). Disruption of the BMEI0066 gene attenuates the virulence of *Brucella melitensis* and decreases its stress tolerance. *Int. J. Biol. Sci.* 5, 570–577. doi: 10.7150/ijbs.5.570
- Zhong, Z., Xu, X., Li, X., Liu, S., Lei, S., Yang, M., et al. (2016). Large-scale identification of small noncoding RNA with strand-specific deep sequencing and characterization of a novel virulence-related sRNA in *Brucella melitensis*. *Sci. Rep.* 6:25123. doi: 10.1038/srep25123

Conflict of Interest Statement: The authors declare that the research was conducted in the absence of any commercial or financial relationships that could be construed as a potential conflict of interest.

Copyright © 2018 Dong, Peng, Liu, Wu, Wang, De, Han, Yuan, Ding, Wang and Wu. This is an open-access article distributed under the terms of the Creative Commons Attribution License (CC BY). The use, distribution or reproduction in other forums is permitted, provided the original author(s) and the copyright owner(s) are credited and that the original publication in this journal is cited, in accordance with accepted academic practice. No use, distribution or reproduction is permitted which does not comply with these terms.



Characterization of Cell Envelope Multiple Mutants of *Brucella ovis* and Assessment in Mice of Their Vaccine Potential

Rebeca Singh Sidhu-Muñoz^{1,2}, Pilar Sancho¹, Axel Cloeckeaert³, Michel Stanislas Zygmunt³, María Jesús de Miguel⁴, Carmen Tejedor¹ and Nieves Vizcaino^{1,2*}

¹ Departamento de Microbiología y Genética, Universidad de Salamanca, Salamanca, Spain, ² Instituto de Investigación Biomédica de Salamanca, Salamanca, Spain, ³ Plasticité Génomique, Biodiversité, Antibiorésistance (PGBA), UR1282 – Infectiologie Animale, Santé Publique (IASP-311), Institut National de la Recherche Agronomique Centre Val de Loire, Nouzilly, France, ⁴ Unidad de Producción y Sanidad Animal, Centro de Investigación y Tecnología Agroalimentaria de Aragón, Instituto Agroalimentario de Aragón – IA2, Zaragoza, Spain

OPEN ACCESS

Edited by:

Rustam Aminov,
University of Aberdeen,
United Kingdom

Reviewed by:

Bi-Hung Peng,
The University of Texas Medical
Branch at Galveston, United States
Renato de Lima Santos,
Universidade Federal de Minas
Gerais, Brazil

*Correspondence:

Nieves Vizcaino
vizcaino@usal.es

Specialty section:

This article was submitted to
Infectious Diseases,
a section of the journal
Frontiers in Microbiology

Received: 29 June 2018

Accepted: 31 August 2018

Published: 20 September 2018

Citation:

Sidhu-Muñoz RS, Sancho P,
Cloeckeaert A, Zygmunt MS,
de Miguel MJ, Tejedor C and
Vizcaino N (2018) Characterization
of Cell Envelope Multiple Mutants
of *Brucella ovis* and Assessment
in Mice of Their Vaccine Potential.
Front. Microbiol. 9:2230.
doi: 10.3389/fmicb.2018.02230

Brucella ovis is a non-zoonotic *Brucella* species lacking specific vaccine. It presents a narrow host range, a unique biology relative to other *Brucella* species, and important distinct surface properties. To increase our knowledge on its peculiar surface and virulence features, and seeking to develop a specific vaccine, multiple mutants for nine relevant cell-envelope-related genes were investigated. Mutants lacking Omp10 plus Omp19 could not be obtained, suggesting that at least one of these lipoproteins is required for viability. A similar result was obtained for the double deletion of *omp31* and *omp25* that encode two major surface proteins. Conversely, the absence of major Omp25c (proved essential for internalization in HeLa cells) together with Omp25 or Omp31 was tolerated by the bacterium. Although showing important *in vitro* and *in vivo* defects, the $\Delta omp10 \Delta omp31 \Delta omp25c$ mutant was obtained, demonstrating that *B. ovis* PA survives to the simultaneous absence of Omp10 and four out seven proteins of the Omp25/Omp31 family (i.e., Omp31, Omp25c, Omp25b, and Omp31b, the two latter naturally absent in *B. ovis*). Three multiple mutants were selected for a detailed analysis of virulence in the mouse model. The $\Delta omp31 \Delta cgs$ and $\Delta omp10 \Delta omp31 \Delta omp25c$ mutants were highly attenuated when inoculated at 10^6 colony forming units/mouse but they established a persistent infection when the infection dose was increased 100-fold. The $\Delta omp10 \Delta ugpB \Delta omp31$ mutant showed a similar behavior until week 3 post-infection but was then totally cleared from spleen. Accordingly, it was retained as vaccine candidate for mice protection assays. When compared to classical *B. melitensis* Rev1 heterologous vaccine, the triple mutant induced limited splenomegaly, a significantly higher antibody response against whole *B. ovis* PA cells, an equivalent memory cellular response and, according to spleen colonization measurements, better protection against a challenge with virulent *B. ovis* PA. Therefore, it would be a good candidate to be evaluated in the natural host as

a specific vaccine against *B. ovis* that would avoid the drawbacks of *B. melitensis* Rev1. In addition, the lack in this attenuated strain of Omp31, recognized as a highly immunogenic protein during *B. ovis* infection, would favor the differentiation between infected and vaccinated animals using Omp31 as diagnostic target.

Keywords: *Brucella ovis*, outer membrane, virulence, recombinant vaccine, Omp31, Omp25/Omp31 family, cyclic glucans, lipoprotein

INTRODUCTION

Brucella ovis is a Gram-negative bacterial species belonging to the genus *Brucella*. It is a non-zoonotic species mainly provoking epididymitis and other genital lesions in rams, although it has also been associated with increased perinatal mortality in lambs and placentitis, abortions, and infertility in ewes (OIE, 2017b). It causes significant economic losses worldwide and lacks commercially available specific vaccine. *B. ovis* lipopolysaccharide (LPS) is devoid of O-polysaccharide (O-PS) chains and is defined as rough (R) LPS (R-LPS). *B. ovis* and *B. canis* are the sole species of the *Brucella* genus constituted exclusively by R strains that are virulent for their natural hosts. This characteristic differentiates them from smooth (S) brucellae that require O-PS for full virulence (e.g., *B. melitensis*, *B. abortus*, or *B. suis*). *B. melitensis* Rev1, currently used for vaccination against ovine and caprine brucellosis caused by *B. melitensis*, is considered the best available vaccine against *B. ovis* (OIE, 2017a). However, this vaccine is banned in countries or regions where infection by *B. melitensis* is eradicated because, among other drawbacks, it induces antibodies that interfere with the serological diagnosis of infections caused by S brucellae. Therefore, the development of a specific vaccine for the prophylaxis of *B. ovis* infection is a matter of interest. Considering that the best available vaccines against brucellosis caused by S *Brucella* strains are homologous S attenuated strains (Nicoletti, 2010), the search for a *B. ovis* attenuated vaccine strain seems an interesting approach. The first step to achieve this goal is the identification of virulence factors that can be removed from *B. ovis*, to minimize its deleterious effects on the host, but without compromising its immunogenicity.

Comparatively to its S counterparts, little is known about the virulence of *B. ovis*, although a species-specific ABC transporter (Silva et al., 2011, 2013) and some classical virulence factors described in S species have been identified as necessary for its virulence (Martín-Martín et al., 2012; Sá et al., 2012; Macedo et al., 2015). O-PS chains mask other outer membrane (OM) components in S strains (Clockaert et al., 2002), hindering their interaction with host cells, antibodies, and other elements of the immune system. According to the surface exposure of OM molecules other than LPS in R *B. ovis*, a more important role in the interaction with host cells and virulence than in S strains would be expected. However, several OM proteins (OMPs) and OM-related genes necessary for full virulence in S strains seem not required in *B. ovis* experimental infection models (Martín-Martín et al., 2012; Sidhu-Muñoz et al., 2016). This observation reveals

differences among the brucellae regarding the role of the OM molecules in host–pathogen interactions, differences that might be associated with their heterogeneity regarding OM-related properties (Martín-Martín et al., 2011; Vizcaíno and Clockaert, 2012), host-preference, and pathogenicity. Although the *Brucella* species share a high level of DNA homology, an increased number of pseudogenes and insertion sequences has been detected in *B. ovis*, when compared to zoonotic S *Brucella* (Tsolis et al., 2009). This feature led to hypothesize that its narrow host-range and tissue tropism (almost exclusively restricted to ovine male genital tract) is in part consequence of genome degradation (Tsolis et al., 2009). However, despite this genome degradation, that among others affects O-PS biosynthetic genes and several OMPs (Tsolis et al., 2009), *B. ovis* causes a chronic infection in its natural host and in laboratory animals (Caro-Hernández et al., 2007; Silva et al., 2011; OIE, 2017b), which would also support a specific pattern of interaction between the host and the bacterial OM.

With the aim of increasing our knowledge about the contribution of cell envelope components to OM-related properties and virulence of *B. ovis* and as a tool to develop a specific live attenuated vaccine, in this work we have constructed and characterized a panel of *B. ovis* multiple mutants in genes related to the cell envelope that either code for major OMPs or either are individually required in S *Brucella* strains, but not in *B. ovis*, for virulence (Caro-Hernández et al., 2007; Martín-Martín et al., 2012; Sidhu-Muñoz et al., 2016). Genes targeted in multiple mutations were: (i) *omp31*, *omp25*, and *omp25c* that code for major OMPs in *B. ovis* (Clockaert et al., 2002; Martín-Martín et al., 2009); (ii) *omp10* and *omp19* that encode two minor OM lipoproteins (Tibor et al., 1999) required in *B. abortus* 544 for full virulence (Tibor et al., 2002); (iii) *bepC* that encodes a TolC-homolog protein necessary in *B. suis* 1330 for full virulence (Posadas et al., 2007); (iv) *bacA* that encodes an integral inner membrane protein involved in lipid A acylation, cell-envelope properties, and virulence in *B. abortus* 2308 (LeVier et al., 2000; Roop et al., 2002; Ferguson et al., 2004; Parent et al., 2007); and (v) *ugpB* that encodes SP41, a surface protein involved in invasion of *B. suis* 1330 to HeLa cells (Castañeda-Roldán et al., 2006). Beside these genes that are not individually required for virulence in *B. ovis* PA, multiple mutations also included *cgs*, involved in the synthesis of periplasmic cyclic β -1,2-glucans (C β Gs) (Iñón de Iannino et al., 1998; Haag et al., 2010) and necessary for full virulence in *B. abortus* 2308 (Briones et al., 2001). The Δ *cgs* mutant of *B. ovis* PA was also highly attenuated when it was intraperitoneally inoculated at a dose of 10^6 colony

forming units (CFU)/mouse (Martín-Martín et al., 2012), but when the dose usually employed for protection experiments (10^8 CFU/mouse) (Sancho et al., 2014; Soler-Lloréns et al., 2014; Silva et al., 2015b) was used, the bacterial counts in spleen increased to levels that were close to those of the parental strain (unpublished results). Several combinations of deleted genes were tempted in the panel of multiple mutants, although, keeping in mind the development of an attenuated vaccine, the inclusion of Δcgs and $\Delta omp31$ mutations was prioritized for two reasons: (i) to study how the addition of new mutations could increase the attenuation of the Δcgs single mutant to appropriate levels for an attenuated vaccine, and (ii) *Omp31* is an abundant OMP in the OM of *B. ovis* PA (Martín-Martín et al., 2009), it is the most immunogenic OMP in the course of *B. ovis* infection (Kittelberger et al., 1998) and its interest for a serological diagnosis favoring the differentiation between infected and vaccinated animals (DIVA diagnosis) has also been evidenced (Vizcaino et al., 2001b).

MATERIALS AND METHODS

Bacterial Strains, Culture Conditions, and Plasmids

Brucella ovis PA and *B. melitensis* Rev1 were obtained from BCCN (*Brucella* Culture Collection Nouzilly, maintained at the Institut National de la Recherche Agronomique, Nouzilly, France), and the other *B. ovis* strains are listed in Table 1. Recombinant plasmids used for mutagenesis of *cgs* (BOV_RS00535), *bacA* (BOV_RS01960), *omp10* (BOV_RS10700), *omp19* (BOV_RS09115), *bepC* (BOV_RS04655), and *ugpB* (BOV_RS13470), and the corresponding single mutants derived from parental *B. ovis* PA have previously been described (Martín-Martín et al., 2012; Sidhu-Muñoz et al., 2016). *B. ovis* $\Delta omp31$ (BOV_RS12205) and $\Delta omp25$ (BOV_RS3460) single nonpolar mutants (Table 1) were obtained from parental *B. ovis* PA as described below. Multiple mutants (Table 1) were constructed from initial single mutants where one or two of the mentioned genes were additionally deleted. The $\Delta omp31$ -k and $\Delta omp25$ -k mutant strains (*omp31* or *omp25* replaced by a kanamycin resistance cassette) and the same mutants complemented with the corresponding *omp31* or *omp25* (BOV_RS00575) wild type genes ($\Delta omp31$ -k com and $\Delta omp25$ -k com strains) were previously obtained (Caro-Hernández et al., 2007).

Brucella ovis strains and the *B. melitensis* Rev1 attenuated vaccine were cultured in tryptic soy agar or tryptic soy broth (Pronadisa-Laboratorios Conda, Torrejón de Ardoz, Spain) both supplemented with 0.3% yeast extract (Pronadisa-Laboratorios Conda, Torrejón de Ardoz, Spain) and 5% horse serum (Gibco-Life Technologies, Grand Island, NY, United States) (TSA-YE-HS and TSB-YE-HS, respectively). Incubations were performed at 37°C in a 5% CO₂ atmosphere and, in the case of TSB-YE-HS liquid medium, under agitation at 120 rpm. When required, streptomycin (Strep; 50 µg/ml) (Sigma-Aldrich, St. Louis, MO, United States)

was added to the culture medium of *B. melitensis* Rev1 (Strep-resistant strain). Similarly, when necessary for the selection of the recombinant *B. ovis* strains, kanamycin (50 µg/ml) or 5% sucrose (Sigma-Aldrich, St. Louis, MO, United States) was added. Assays with the *B. ovis* strains, including $\Delta omp31$ -k, $\Delta omp25$ -k, $\Delta omp31$ -k com, and $\Delta omp25$ -k com strains, were performed in the absence of antibiotics.

Plasmid pGEM-T Easy (Promega, Madison, WI, United States) was used to clone PCR-amplified fragments and pCVD-KanD (Martín-Martín et al., 2012) was the suicide plasmid employed to insert the mutant genes into parental *B. ovis* PA. They were propagated in *Escherichia coli* JM109 or CC118 (λ pir), respectively, that were incubated at 37°C in Luria Bertani medium supplemented, when required, with ampicillin or kanamycin (50 µg/ml). Their derived recombinant plasmids constructed during this work are mentioned below.

DNA Primers and Mutagenesis

DNA primers (IDT, Leuven, Belgium) used for the construction and verification of the *B. ovis* $\Delta omp31$, $\Delta omp25$, and $\Delta omp25c$ single and multiple nonpolar mutants are listed in Table 2. The additional primers used to check the multiple mutants were previously described (Martín-Martín et al., 2012; Sidhu-Muñoz et al., 2016).

For the construction of the recombinant plasmids used in the mutagenesis process, inactivation of *omp31*, *omp25*, and *omp25c* was performed by in-frame deletion with overlapping PCR (Martín-Martín et al., 2012). Briefly, the 5'- and 3'-ends of each target gene, together with about 300–700 pb upstream or downstream, respectively, were separately amplified by PCR with two pairs of primers (31MUT-F + 31OVL-R and 31OVL-F + 31MUT-R for *omp31*, 25MUTZ-F + 25OVL-R and 25OVL-F + 25MUTZ-R for *omp25*, 25cdMUT-F + 25cOVL-R and 25cOVL-F + 25cdMUT-R) (Table 2). The two amplified fragments were fused, through the overlapping sequences located in the internal primers (primers OVL-F and OVL-R) (Table 2), in a PCR reaction with the two external primers of each fragment (31MUT-F + 31MUT-R for *omp31*, 25MUTZ-F + 25MUTZ-R for *omp25*, and 25cdMUT-F + 25cdMUT-R for *omp25c*). The resulting mutant genes were cloned in pGEM-T Easy, verified by DNA sequencing, and subsequently cloned in pCVD-KanD to give pPS31OVL02, pNV25OVL02, and pNV25cOVL02, respectively. Plasmids were introduced in *B. ovis* PA by electroporation and the selection of bacteria with the corresponding plasmid integrated in the chromosome (intermediate strains), through a single homologous recombination event, was performed on TSA-YE-HS plates with kanamycin. The selected intermediate strains were plated onto TSA-YE-HS supplemented with 5% sucrose to give either the desired mutant strain (wild-type gene replaced by the inactivated gene) or a strain reverting to the parental genotype (Rv). They were differentiated by PCR amplification with the two primers external to each side of the deleted gene (amplified fragment with higher size in

TABLE 1 | Most relevant bacterial strains used in this work, growth characteristics, and preliminary evaluation of virulence.

Brucella ovis strains ^a	Deleted gene/s and strain abbreviation in the text	Log CFU/ml OD ₆₀₀ = 0.2 ^b	Log CFU/spleen at week (W) p.i. ^c			
			(dose 10 ⁶ CFU)		(dose 10 ⁸ CFU)	
			W3	W7	W3	W7
<i>B. ovis</i> PA (BCCN 76-250)	Parental strain, PA	9.09 ± 0.04	6.90	5.85	7.62	6.31
Single mutants						
<i>B. ovis</i> -pPS31OVL02M	$\Delta omp31$	8.80 ± 0.10*	5.44	5.79	–	–
<i>B. ovis</i> -pNV25OVL02M	$\Delta omp25$	9.08 ± 0.07	6.87	4.92	–	–
<i>B. ovis</i> -PNV25cA	$\Delta omp25c-k$	8.93 ± 0.03*	7.20	5.61	–	–
<i>B. ovis</i> -pNVcgs03M	Δcgs	8.88 ± 0.08*	0.45	0.53	6.20	5.53
<i>B. ovis</i> -pNVbacA03M	$\Delta bacA$	9.12 ± 0.07	6.48	5.64	–	–
<i>B. ovis</i> -pNV1002M	$\Delta omp10$	8.84 ± 0.04*	6.91	5.79	–	–
<i>B. ovis</i> -pNV1902M	$\Delta omp19$	8.92 ± 0.05*	6.51	5.90	–	–
<i>B. ovis</i> -pNVBepC02M	$\Delta bepC$	9.15 ± 0.08	6.17	5.28	–	–
<i>B. ovis</i> -pNVSP4102M	$\Delta ugpB$	9.10 ± 0.03	7.72	6.30	–	–
Double mutants						
<i>B. ovis</i> $\Delta omp31$ -pNV1902M	$\Delta omp31 \Delta omp19$	8.78 ± 0.04*	5.25	5.92	–	–
<i>B. ovis</i> $\Delta omp31$ -pNVBepC02M	$\Delta omp31 \Delta bepC$	8.80 ± 0.04*	6.78	5.75	–	–
<i>B. ovis</i> $\Delta omp31$ -pNVSP4102M	$\Delta omp31 \Delta ugpB$	8.82 ± 0.06*	5.90	6.32	–	–
<i>B. ovis</i> $\Delta omp31$ -pNVcgs03M	$\Delta omp31 \Delta cgs$	8.49 ± 0.09*	–	–	5.16	4.95
<i>B. ovis</i> $\Delta omp25$ -pNVcgs03M	$\Delta omp25 \Delta cgs$	8.56 ± 0.06*	–	–	5.52	5.15
<i>B. ovis</i> $\Delta omp25$ -pNV25cOVL02M	$\Delta omp25 \Delta omp25c$	8.82 ± 0.06*	6.91	6.32	–	–
<i>B. ovis</i> Δcgs -pNVSP4102M	$\Delta cgs \Delta ugpB$	8.89 ± 0.04*	–	–	5.24	4.80
<i>B. ovis</i> Δcgs -pNVBepC02M	$\Delta cgs \Delta bepC$	8.87 ± 0.07*	–	–	5.45	4.63
<i>B. ovis</i> $\Delta omp10$ -pPS31OVL02M	$\Delta omp10 \Delta omp31$	8.89 ± 0.07*	6.72	6.66	–	–
<i>B. ovis</i> $\Delta omp10$ -pNVSP4102M	$\Delta omp10 \Delta ugpB$	8.91 ± 0.06*	7.29	5.66	–	–
<i>B. ovis</i> $\Delta omp10$ -pNVcgs03M	$\Delta omp10 \Delta cgs$	8.82 ± 0.09*	–	–	5.21	5.39
<i>B. ovis</i> $\Delta omp19$ -pNVcgs03M	$\Delta omp19 \Delta cgs$	8.79 ± 0.03*	–	–	6.07	5.99
<i>B. ovis</i> $\Delta omp19$ -pNVSP4102M	$\Delta omp19 \Delta ugpB$	8.88 ± 0.03*	6.57	5.36	–	–
<i>B. ovis</i> $\Delta bepC$ -pNVSP4102M	$\Delta bepC \Delta ugpB$	9.10 ± 0.05	7.37	5.63	–	–
<i>B. ovis</i> $\Delta bacA$ -pPS31OVL02M	$\Delta bacA \Delta omp31$	8.81 ± 0.02*	6.05	5.36	–	–
Triple mutants						
<i>B. ovis</i> $\Delta omp10 \Delta ugpB$ -pPS31OVL02M	$\Delta omp10 \Delta ugpB \Delta omp31$	8.76 ± 0.18*	0.47	0.57	5.53	0.52
<i>B. ovis</i> $\Delta omp10 \Delta omp31$ -pNV25cOVL02M	$\Delta omp10 \Delta omp31 \Delta omp25c$	8.49 ± 0.04*	2.57	3.26	5.30	5.70
<i>B. ovis</i> $\Delta omp31 \Delta omp10$ -pNV25cOVL02M	$\Delta omp31 \Delta omp10 \Delta omp25c$	8.39 ± 0.03*	2.42	2.03	–	–
<i>B. ovis</i> $\Delta omp31 \Delta cgs$ -pNV1002M	$\Delta omp31 \Delta cgs \Delta omp10$	8.61 ± 0.07*	–	–	5.53	5.73
<i>B. ovis</i> $\Delta omp31 \Delta cgs$ -pNV1902M	$\Delta omp31 \Delta cgs \Delta omp19$	8.71 ± 0.05*	–	–	5.07	4.61
<i>B. ovis</i> $\Delta omp31 \Delta bepC$ -pNVSP4102M	$\Delta omp31 \Delta bepC \Delta ugpB$	8.86 ± 0.12*	7.65	6.00	–	–
Other previous mutants used as controls						
<i>B. ovis</i> PNV31A	$\Delta omp31-k$	8.85 ± 0.03*	–	–	–	–
<i>B. ovis</i> PNV31A-com	$\Delta omp31-k$ com	8.89 ± 0.03*	–	–	–	–
<i>B. ovis</i> PNV25c-com	$\Delta omp25c-k$ com	8.99 ± 0.06	–	–	–	–

^aLog CFU/spleen 3 and 7 weeks after intraperitoneal infection with 1×10^6 or 1×10^8 CFU/mouse. One mouse was used per time point in this preliminary assay of virulence. –, not determined. ^bThe *B. ovis* mutants derive from *B. ovis* PA, which was obtained from BCCN (Brucella Culture Collection Nouzilly, Institut National de la Recherche Agronomique, Nouzilly, France). *B. ovis* Δcgs , $\Delta bacA$, $\Delta omp10$, $\Delta omp19$, $\Delta bepC$, and $\Delta ugpB$ were previously described (Martín-Martín et al., 2012; Sidhu-Muñoz et al., 2016). *B. ovis* PA $\Delta omp25c-k$ and $\Delta omp31-k$ were also previously obtained replacing *omp25c* and *omp31*, respectively, by a kanamycin resistance cassette; they were complemented with wild-type *omp25c* and *omp31*, respectively, to give *B. ovis* $\Delta omp25c-k$ com and *B. ovis* $\Delta omp31-k$ com (Caro-Hernández et al., 2007). The other *B. ovis* mutants were obtained in this work. ^cThe asterisk (*) indicates statistically significant differences ($P < 0.05$), compared to the parental strain. Log CFU/ml of bacterial suspensions adjusted to an OD₆₀₀ value of 0.2. The results are expressed as the mean ± SD of three assays.

Rv strains than in mutant strains) and a second PCR with an external primer and a primer annealing inside the deleted fragment (primers 31-MAT, 25-MAT, and 25c-MAT) (Table 2). The latter PCR reaction produces no amplification in mutant strains.

For multiple gene mutagenesis, single mutants listed in Table 1 were subjected to a second mutagenesis round with a recombinant plasmid containing another inactivated gene. A third round of mutagenesis was conducted on some selected double mutants to inactivate a third gene. The selection of

TABLE 2 | Primers used in this work for the construction and verification of *omp25*, *omp25c*, and *omp31* single and multiple mutants^a.

Primer name	Nucleotide sequence 5'–3' ^b	Target gene or plasmid ^c
Construction of <i>B. ovis</i> PA mutants		
25MUTZ-F	CGACCTTATCCTCCTGAA	<i>omp25</i>
25OVL-R	GACGATTACGAGAGACTT	<i>omp25</i>
25OVL-F	<u>AAGTCTCTCGTAATCGTC</u> AAGCTGGACACGCAGGAT	<i>omp25</i>
25MUTZ-R	TTTGCGACGTTTTGCTGG	<i>omp25</i>
25cdMUT-F	TGCGTGGTTTCAGATTCG	<i>omp25c</i>
25cOVL-R	AGCCTTGAGCTTCATGAT	<i>omp25c</i>
25cOVL-F	<u>ATCATGAAGCTCAAGGCT</u> GCTTACAAGTTCTGATAG	<i>omp25c</i>
25cMUT-R	AGCCGTAACCAACTGAC	<i>omp25c</i>
31MUT-F	AGAATAAACACATGCC	<i>omp31</i>
31OVL-R	GATGGACGCCAAAATTAC	<i>omp31</i>
31OVL-F	<u>GTAATTTGGCGTCCATC</u> GTCGGTCTGAACATACAG	<i>omp31</i>
31MUT-R	GCTGAATGCGGAGATGGT	<i>omp31</i>
Additional primers for the verification of recombinant plasmids and mutants		
Universal-F	GTTTTCCAGTCACGAC	pGEM-T Easy
Universal-R	CAGGAAACAGCTATGAC	pGEM-T Easy
25-Sec	GGACCGCGCAAACGTAATT	<i>omp25</i>
25-MAT	GCCGACGCCATCCAGGAA	<i>omp25</i>
25c-MAT	GCTGACGCCGTCATTGAA	<i>omp25c</i>
31-MAT	GCCGACGTGGTTGTTTCT	<i>omp31</i>

^aPrimers for the verification of proper deletion of other genes have been previously described (Martin-Martin et al., 2012; Sidhu-Muñoz et al., 2016).

^bUnderlined sequences in 25OVL-F, 25cOVL-F, and 31OVL-F correspond to regions overlapping with 25OVL-R, 25cOVL-R, and 31OVL-R, respectively. ^cTarget gene is the *B. ovis* gene to be deleted or PCR-amplified for the verification of mutant strains. Primers Universal-F and Universal-R target pGEM-T Easy and its derived recombinant plasmids at both sides of the cloned insert and were used for sequencing of the DNA insert. The remaining primers target the *B. ovis* genome and were designed according to the published genome sequence of *B. ovis* 63/290 (ATCC 25840) (accession numbers NC_009505 and NC_009504 for chromosome I and II, respectively).

mutant strains was performed with specific PCRs targeting each inactivated locus.

Growth Pattern, Autoagglutination, and Susceptibility Assays

Growth characteristics of the mutant strains in TSA-YE-HS plates and TSB-YE-HS liquid medium were compared to those of parental *B. ovis* PA. Numbers of CFU/ml corresponding to bacterial suspensions in PBS with optical density scores at 600 nm (OD₆₀₀) of 0.2 were determined for each mutant by triplicate plating on TSA-YE-HS of the properly diluted suspensions. The initial suspensions were prepared from bacteria cultured in TSA-YE-HS plates for 44 h. Colony size was photographed 5 days after plating and colonies enumerated 8 days after plating. Growth curves were established for triplicate bacterial suspensions in TSB-YE-HS medium (30 ml) with initial OD₆₀₀ readings of 0.05 that were incubated at 37°C under agitation (120 rpm) and a 5% CO₂ atmosphere. OD₆₀₀

scores were measured through a 120-h period, and CFU/ml numbers were evaluated at the beginning of the experiment (t₀), and after 24, 52, and 77 h of incubation (t₂₄, t₅₂, and t₇₇, respectively), by plating the properly diluted cultures on TSA-YE-HS.

The autoagglutination assay was performed as described previously (Caro-Hernández et al., 2007; Martín-Martín et al., 2012) by measuring the evolution, over 48 h of static incubation, of the OD₆₀₀ values of bacterial suspensions with initial readings of 0.8 (100% OD₆₀₀) in TSB-YE-HS. Susceptibility to 1 mg/ml of polymyxin B (Sigma-Aldrich, St. Louis, MO, United States) and 0.1 mg/ml of sodium deoxycholate (Sigma-Aldrich, St. Louis, MO, United States) in PBS was expressed as the percentage of survival after 80 min of exposure. It was determined by comparison of the numbers of CFU in untreated (incubation in PBS, 100% survival) and treated bacterial suspensions (Caro-Hernández et al., 2007; Martín-Martín et al., 2011). The results were expressed as means ± standard deviation (SD) of three assays.

Mapping of Cell Envelope Antigens

Reactivity of *B. ovis* mutants with MAbs specific for cell-envelope antigens (Table 3) was measured by indirect enzyme-linked immunosorbent assay (iELISA) as previously described (Soler-Lloréns et al., 2014). MAbs specific for *Brucella* peptidoglycan (PG), R-LPS, S-LPS, Omp2b, Omp10, Omp16, Omp19, Omp25, Omp31, or periplasmic BP26 were used (Cloeckaert et al., 1990, 1991, 1996a,b; Vizcaino et al., 2001b; Seco-Mediavilla et al., 2003). Briefly, 96-well plates were coated overnight at room temperature with sonicated (mild homogenization for 10 s at 40% intensity in a Sonic Dismembrator model 120, Thermo Fisher Scientific, Waltham, Ma, United States) bacterial suspensions in PBS (OD₆₀₀ = 1),

TABLE 3 | Main characteristics of the monoclonal antibodies used in this work.

Monoclonal antibody ^a	Specificity	Abbreviation
A68/15B06/C08	Omp2b	C08
A68/07G11/C10	Omp10	C10
A76/08C03/G03	Omp16	G03
A76/18B02/D06	Omp19	D06
A59/10F09/G10	Omp31	G10
A59/05F01/C09	Omp25	C09
A18/13D02/F05	Omp25	F05
A76/08H09/A02	Omp25	A02
V78/09B12/B02	BP26	B02
V78/02E08/F03	BP26	F03
V78/04D01/A10	BP26	A10
V78B/04G07/H05	BP26	H05
A76/03D06/A09	PG	A09
A76/12G12/F12	S-LPS	F12
A68/03F03/D05	R-LPS	D05

^aThe MAbs were obtained and characterized previously (Cloeckaert et al., 1990, 1991, 1992, 1996a,b; Zygmunt et al., 1994; Seco-Mediavilla et al., 2003).

which were prepared from cultures in TSA-YE-HS plates. MABs (hybridoma supernatant) diluted 1/2 and a goat anti-mouse IgG-horseradish peroxidase conjugate (Bio-Rad, Hercules, CA, United States) diluted 1:9000 were used as primary and secondary antibodies, respectively. Antigen-antibody binding was revealed by incubation for 20 min with TMB as substrate for peroxidase and subsequent addition of a 1 M HCl-based stop solution (Interchim, Montluçon, France). The results were expressed as means \pm SD of the values recorded at 450 nm (OD₄₅₀) in a Labsystems Multiskan Ascent microplate reader (Thermo Fisher Scientific) for three repeats by MAb and strain.

Additionally, sodium dodecyl sulfate polyacrylamide gel electrophoresis (SDS-PAGE) and immunoblot were also performed and carried out as previously described (Vizcaíno et al., 2001b; Martín-Martín et al., 2009). Briefly, bacterial suspensions concentrated to OD₆₀₀ values of 20 were prepared in H₂O with the different *B. ovis* strains. They were submitted to SDS-PAGE on a Protean II xi cell (Bio-Rad, Hercules, CA, United States) and either stained with Coomassie blue (Bio-Rad, Hercules, CA, United States) or transferred to a nitrocellulose membrane in a semidry electroblotter (Amersham, GE Healthcare, Little Chalfont, United Kingdom). Prestained protein marker VI (Applichem-Panreac, Barcelona, Spain) was used as protein standard. Nitrocellulose strips were saturated with skim milk and then incubated with sera obtained, as described before (Martín-Martín et al., 2009), by immunization of rabbits with Omp31b, Omp25c, Omp25d, and Omp22 purified recombinant proteins. Binding of the secondary antibody – a goat anti-rabbit IgG-peroxidase conjugate (Sigma-Aldrich, St. Louis, MO, United States) – was detected with a 4-chloro-1-naphthol substrate solution.

Infection Assays on Murine Macrophage and HeLa Cells

Infection assays of murine macrophage-like J774.A1 cells (DSMZ ACC170) and epithelial HeLa (ATCC CCL-2TM) cells were performed as described previously (Sidhu-Muñoz et al., 2016). Briefly, 2×10^4 J774.A1 macrophages or 1.5×10^4 HeLa cells/well were seeded on 96-well sterile microplates and incubated for 24 h at 37°C under a 5% CO₂ atmosphere. After incubation for 2 h with the *B. ovis* strains (4×10^6 CFU/well for macrophages or 8×10^6 CFU/well for HeLa cells) and killing of extracellular bacteria by incubation with gentamycin for 1 h, intracellular bacteria were enumerated in three wells per strain after lysis of the phagocytes with H₂O [t0 post-infection (p.i.)] (Sidhu-Muñoz et al., 2016). The remaining wells were maintained in the presence of gentamycin and intracellular bacteria were similarly determined at 20 (t20) and 44 h (t44) p.i. The results were expressed as means \pm SD of the log CFU/well at each selected p.i. time point (t0, t20, and t44) and are representative of at least two experiments.

Mice and Ethics Statement

Female 6-week-old BALB/c mice (Charles River Laboratories, Chatillon-sur-Chalaronne, France), received 1 week

previously, were used. They were randomly distributed into experimental groups and kept with water and food *ad libitum* in the animal experimentation facilities of the University of Salamanca (registration number PAE SA-001) or the Unidad de Producción y Sanidad Animal, Instituto Agroalimentario de Aragón-IA2 (CITA-Universidad de Zaragoza) (registration number ES502970012005).

Procedures with mice were designed according to Spanish and European legislation regarding the use of animals in research (RD 53/2013 and directive 2010/63/UE). Microbiological practices and animal experimentation were approved by the Biosecurity and Bioethics Committees of the University of Salamanca, and authorized by the competent authority of Junta de Castilla y León, Spain. The Animal Welfare Committee of the CITA (Spain) also reviewed and approved the protocols.

Virulence Assays and Antibody Response in Mice

Preliminary evaluation of virulence in mice was performed by intraperitoneal inoculation of 10^6 or 10^8 CFU/mouse depending on the previous information about each single mutant (Martín-Martín et al., 2012; Sidhu-Muñoz et al., 2016). One mouse was used per strain, dose and time of analysis and splenic colonization was evaluated 3 or 7 weeks (W3 and W7) p.i. as described previously (Sancho et al., 2014). These time points in parental *B. ovis* PA correspond to the acute and chronic phase of infection, respectively (Caro-Hernández et al., 2007; Martín-Martín et al., 2012; Sidhu-Muñoz et al., 2016).

Spleen colonization of the selected mutants – according to the results of the preliminary analysis – was evaluated at W3 and W7 p.i. in mice inoculated intraperitoneally with 10^6 CFU, and at W1, W3, W5, W7, and W11 p.i. in mice inoculated intraperitoneally with 10^8 CFU. Five mice per strain and time point were used. The results were expressed as means \pm SD ($n = 5$) of the log of CFU/spleen for each strain and time point. The identity of the recovered colonies was checked by PCR. Antibodies specific for *B. ovis* PA were determined by iELISA (Sancho et al., 2014) in sera obtained from submandibular blood from the same mice. Briefly, a suspension in PBS of heat-inactivated *B. ovis* PA whole cells (OD₆₀₀ = 1) was used as the coating antigen of 96-well plates and a goat antimouse IgG-peroxidase conjugate (Sigma-Aldrich, St. Louis, MO, United States) was used as the secondary antibody. OD₄₀₅ readings were recorded on a Multiskan Go Microplate Reader (Thermo Fisher Scientific) after 30 min incubation at room temperature with the substrate solution constituted by 1 mM 2,2'-azino-di-(3-3-ethylbenzothiazoline-sulfonic acid) (ABTS; Sigma-Aldrich, St. Louis, MO, United States) and 2 mM H₂O₂ (Sigma-Aldrich, St. Louis, MO, United States) in 0.1 M citrate, pH 4.2. Antibody titers in serum were defined as the inverse of the highest serum dilution scoring an OD₄₀₅ value twice as high as that obtained with the blank (mean OD₄₀₅ of six wells in which serum was replaced by dilution buffer). The results were represented as means \pm SD

of the log of the titers obtained with five mice analyzed individually.

Vaccine Efficacy and Immune Response of *B. ovis* $\Delta omp10\Delta ugpB\Delta omp31$

BALB/c mice were inoculated intraperitoneally with PBS, 10^5 CFU of the classical vaccine *B. melitensis* Rev1, or 10^8 CFU of the attenuated mutant *B. ovis* $\Delta omp10\Delta ugpB\Delta omp31$. Seven weeks later, corresponding with the time point where the *B. ovis* vaccine was cleared from spleen, five mice per group were either challenged with 2×10^5 CFU of *B. ovis* PA, or processed for the evaluation of the antibody and cellular immune responses specific for *B. ovis* PA. Determination of virulent *B. ovis* PA in spleen was evaluated 3 weeks after experimental challenge (Sancho et al., 2014). The CFU number of virulent *B. ovis* PA in mice vaccinated with *B. melitensis* Rev 1 was obtained by subtracting the values obtained in TSA-YE-HS-Strep medium from those obtained in the same medium without antibiotic. Results were expressed as means \pm SD ($n = 5$) of the log CFU/spleen of *B. ovis* PA for each vaccination group.

IgG titers in serum were analyzed, as described above, in five mice per group 7 weeks after vaccination by using heat-inactivated *B. ovis* PA whole cells as the coating antigen in a iELISA test. Additionally, IgG isotypes were determined under the same conditions but using goat anti-mouse IgG₁-, IgG_{2a}-, or IgG_{2b}-peroxidase conjugates (Santa Cruz Biotechnology, Dallas, TX, United States). The same mice were processed as previously described (Sancho et al., 2014) to evaluate the cytokine response of splenocytes to a second stimulus with *B. ovis* PA. Briefly, spleen cells from immunized mice were cultured in 24-well sterile plates and stimulated by exposure to heat-inactivated (1 h at 65°C) *B. ovis* PA whole cells (10^7 CFU/well), 10 μ g/ml of the mitogen concanavalin A (Sigma-Aldrich, St. Louis, MO, United States) as a positive control of cell proliferation, or culture medium as a negative control. After 72 h of incubation, the culture supernatants were harvested to evaluate the levels of interferon- γ (IFN- γ), tumor necrosis factor- α (TNF- α), IL-10, and IL-12(p40). They were determined by sandwich ELISA with OptEIA™ Mouse Sets specific to each cytokine, as instructed by the manufacturer (BD Biosciences, San Diego, CA, United States). Two wells were used for each experimental condition and mouse. The results for each vaccination group were expressed as means \pm SD of the cytokine amount (ng/well) in the supernatants of splenocytes obtained from five individual mice. The results obtained with the positive and negative controls (concanavalin A and RPMI as stimulating agents, respectively) were as expected and are not shown.

Statistical Analysis

Statistical comparisons between means were performed using analysis of variance. The significance of the differences ($P < 0.05$) between the experimental groups was determined with the *post hoc* Fisher's protected least significant differences (PLSD) test. To simplify the figures and tables, no ranking of P -values has been established and all significant differences are marked as $P < 0.05$.

RESULTS

Genotypic Characterization of the Mutants

The *B. ovis* mutants (Table 1) were genotypically characterized as described in the section "Materials and Methods." Two PCR reactions were settled for each inactivated gene, one reaction with external primers to each side of the deleted locus (amplified fragment of lower size in mutant strains than in parental strain), and a second reaction with an external primer to the deleted loci and a primer annealing inside the deleted region (no amplification in mutant strains). All single and multiple mutants gave the expected results for each inactivated gene (data not shown).

Although not all combinations of single genes shown in Table 1 were tempted in multiple mutants, two combinations were specially assayed without success: a double mutant in lipoproteins Omp10 and Omp19 and a double mutant in major Omp25 and Omp31 proteins. Despite multiple attempts, the intermediate strains for these double mutants always reverted to the single mutant initial genotype. Similarly, two independent *omp25c* intermediate strains always reverted to the parental genotype and, consequently, the non-polar $\Delta omp25c$ single mutant was not obtained. However, the non-polar deletion of *omp25c*, with plasmid pNV25cOVL02, was successful in the $\Delta omp25\Delta omp25c$ double mutant and in the $\Delta omp10\Delta omp31\Delta omp25c$ and $\Delta omp31\Delta omp10\Delta omp25c$ triple mutants. The *omp25c*-k mutant, where *omp25c* was replaced by a kanamycin resistance cassette (Caro-Hernández et al., 2007), was used in this work for comparisons with the non-polar $\Delta omp25c$ double and triple mutants.

Growth Characteristics of the Mutants

The numbers of CFU in bacterial suspensions with OD₆₀₀ values of 0.2 were determined for each mutant in TSA-YE-HS plates. Bacterial counts obtained for $\Delta omp25$, $\Delta bepC$, $\Delta ugpB$, and $\Delta bacA$ single mutants and for $\Delta bepC\Delta ugpB$ double mutant did not significantly differ from those observed with the parental strain. On the contrary, $\Delta omp31$, $\Delta omp25c$ -k, $\Delta omp10$, $\Delta omp19$, Δcgs , and the remaining multiple mutants showed, in different degrees, lower CFU values than *B. ovis* PA (Table 1). The $\Delta omp31\Delta cgs$ double mutant and its derived triple mutants, the $\Delta omp25\Delta cgs$ mutant and the $\Delta omp10\Delta omp31\Delta omp25c$ and $\Delta omp31\Delta omp10\Delta omp25c$ triple mutants (bearing the same three genes inactivated but in a different order) showed the lowest CFU/ml values in TSA-YE-HS plates (Table 1). The numbers of CFU/ml obtained for each mutant were used for the calculation of the bacterial doses in further experiments.

In addition, the size of the colonies in TSA-YE-HS was monitored over time and recorded 5 days after inoculation (see some representative results in Figure 1A). Colony size of the $\Delta omp25$, $\Delta bacA$, $\Delta bepC$, $\Delta ugpB$, $\Delta omp25c$ -k, $\Delta bepC\Delta ugpB$, and $\Delta omp25\Delta omp25c$ mutants was undistinguishable from that of the parental strain (see *B. ovis* PA and the $\Delta omp25\Delta omp25c$ mutant in Figure 1A). Growth of the $\Delta omp10$ and $\Delta omp19$ mutants was slightly delayed when compared to the parental

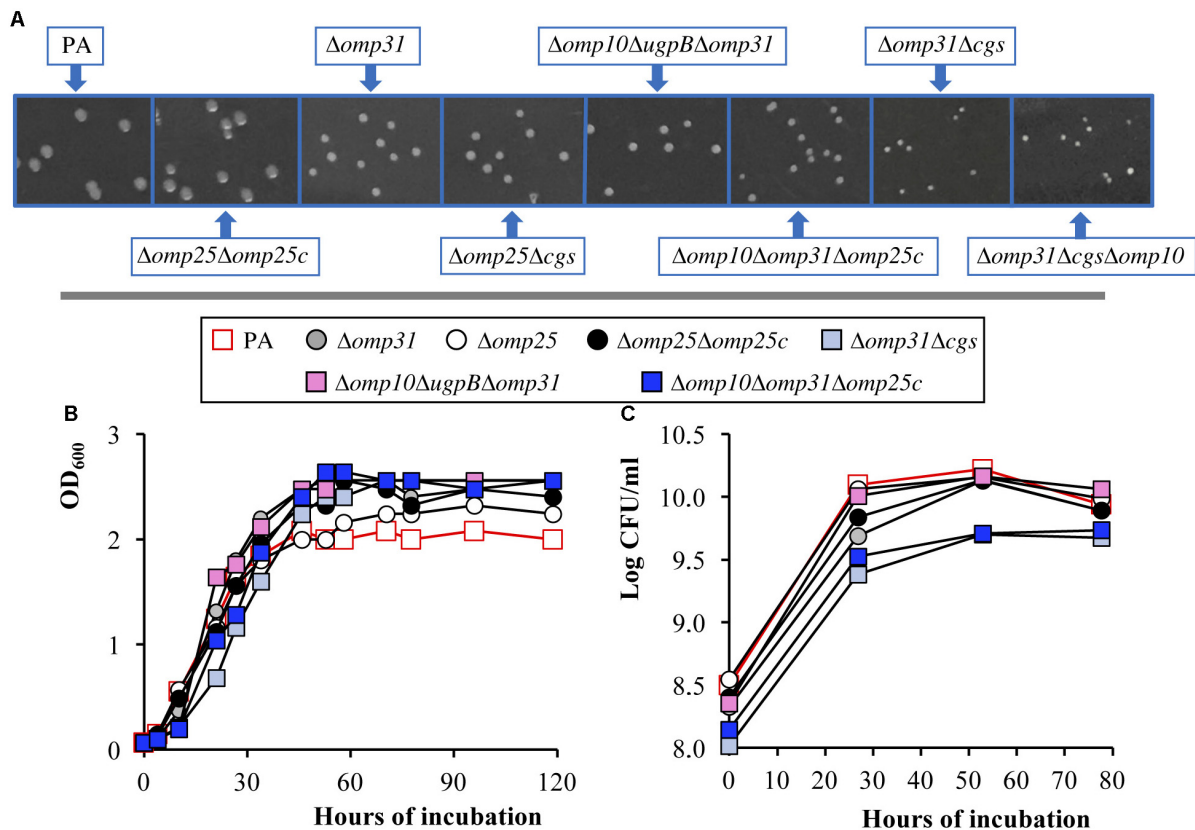


FIGURE 1 | Growth pattern of *B. ovis* PA and selected mutants in TSA-YE-HS (A) and TSB-YE-HS (B,C). Colony size in TSA-YE-HS (A) was photographed 5 days after inoculation. Plates were taken in the same picture and a section of each strain was extracted to compose the final panel. Growth in TSB-YE-HS liquid medium was determined by the evolution with time of the OD₆₀₀ values (B) and of the bacterial CFU/ml numbers (C). The SD of three assays, which was always lower than 5% of the mean, is not shown. To simplify the figure, relevant statistically significant differences ($P < 0.05$) are mentioned in the text.

strain but the initial differences in colony size were not apparent after 5 days of incubation (data not shown). Colonies of the $\Delta omp31$ and Δcgs single mutants appeared hardly visible 72 h after inoculation, 24 h later than those of the *B. ovis* PA parental strain, and were smaller than those of the parental strain after 5 days (see $\Delta omp31$ in Figure 1A). A similar or higher delay, depending on the strain, was detected with colonies of their multiple mutants. Despite the triple gene deletion, the $\Delta omp10\Delta ug p B \Delta omp31$ mutant showed a colony growth pattern undistinguishable from that of the single $\Delta omp31$ mutant (Figure 1A). The most important growth defects were observed with the $\Delta omp31\Delta cgs$ mutant and its derived triple mutants (with the additional deletion of *omp10* or *omp19*), whose colonies started to be detected 96 h after inoculation and showed the smallest size after 5 days of incubation (Figure 1A). Colonies of the $\Delta omp10\Delta omp31\Delta omp25c$ and $\Delta omp31\Delta omp10\Delta omp25c$ triple mutants were also detected after 96 h of incubation but, at day 5 post-inoculation, they were bigger (see colonies of the $\Delta omp10\Delta omp31\Delta omp25c$ mutant that are representative for both mutants) than those of *B. ovis* $\Delta omp31\Delta cgs$ (Figure 1A).

The $\Delta omp31\Delta cgs$, $\Delta omp10\Delta omp31\Delta omp25c$, and $\Delta omp10\Delta ug p B \Delta omp31$ mutants (selected according to the results obtained in the evaluation of virulence described below),

the $\Delta omp25\Delta omp25c$ mutant (selected because it lacks two major OMPs in *B. ovis* PA) and their corresponding single mutants were also analyzed regarding growth in TSB-YE-HS liquid medium (Figures 1B,C). Cultures were adjusted to OD₆₀₀ values of 0.05 and incubated at 37°C under agitation (120 rpm) and a 5% CO₂ atmosphere. As expected, according to the correlation OD₆₀₀-CFU/ml in solid medium previously determined, values of CFU/ml at t0 for mutants with inactivated *omp31* or *cgs* were lower than those of *B. ovis* PA ($P < 0.05$), the $\Delta omp31\Delta cgs$ and $\Delta omp10\Delta omp31\Delta omp25c$ mutants presenting the lowest values ($P < 0.05$) (Figure 1C). However, the CFU/ml values of the $\Delta omp31$ and $\Delta omp10\Delta ug p B \Delta omp31$ mutants at the beginning of the stationary phase (approximately t52) were similar to those of *B. ovis* PA ($P > 0.05$), which correlates with the higher OD₆₀₀ scores observed with these mutants by this time ($P < 0.05$). Although the $\Delta omp31\Delta cgs$ and $\Delta omp10\Delta omp31\Delta omp25c$ mutants, those showing the most important growth defects in solid medium (Figure 1A), also had higher OD₆₀₀ values at this moment ($P < 0.05$), their CFU/ml counts never reached the maximum level of *B. ovis* PA (detected at t52) (Figures 1B,C). The Δcgs , $\Delta omp25$, $\Delta omp25c$, and $\Delta omp25\Delta omp25c$ mutants had slightly higher OD₆₀₀ scores in the stationary phase, when compared to the parental strain, but

not important differences in the CFU/ml values (**Figures 1B,C** and data not shown). The $\Delta omp10$ and $\Delta ugpB$ mutants behaved similarly to the parental strain (data not shown).

Virulence in the Mouse Model

For a preliminary assay of virulence, aiming to select the most relevant mutants, mice were inoculated with 10^6 CFU of the parental strain or its derived mutants and bacteria were enumerated in spleen at W3 and W7 p.i. The multiple *cgs* mutants were excluded from this first analysis, since the single Δcgs mutant showed poor spleen colonization in a previous study (Martín-Martín et al., 2012). Only those mutants that, when compared to the parental strain, showed bacterial counts lower than 1.5 logarithmic units were considered as probably attenuated and they were later inoculated in a dose of 10^8 CFU/mouse. Uniquely the Δcgs , $\Delta omp10\Delta ugpB\Delta omp31$, $\Delta omp10\Delta omp31\Delta omp25c$, and $\Delta omp31\Delta omp10\Delta omp25c$ mutants met this requirement and, together with the Δcgs multiple mutants, were evaluated with the increased dose (except *B. ovis* $\Delta omp31\Delta omp10\Delta omp25c$ that bears the same mutations as the $\Delta omp10\Delta omp31\Delta omp25c$ but in a different order). All these mutants were present in spleen at W3 p.i. but the CFU were between 1 and 2.5 log units lower than those obtained with the parental strain (**Table 1**). All *cgs* mutants and *B. ovis* $\Delta omp10\Delta omp31\Delta omp25c$ had similar splenic counts at W7 p.i., which were not drastically different from those observed at W3 p.i., while the $\Delta omp10\Delta ugpB\Delta omp31$ mutant was not detected in spleen at W7 p.i. (**Table 1**).

According to these results, the $\Delta omp31\Delta cgs$, $\Delta omp10\Delta ugpB\Delta omp31$, and $\Delta omp10\Delta omp31\Delta omp25c$ mutants were retained for a detailed evaluation of virulence and the selection of vaccine candidates. First, to statistically verify the previous results, the spleen colonization was evaluated in five mice per group at W3 and W7 after intraperitoneal infection with 10^6 CFU (**Figure 2A**). The spleen weight (**Figure 2B**) and the levels in serum of IgG reacting against *B. ovis* PA whole cells (**Figure 2C**) were also determined. As expected, spleen infection of *B. ovis* PA was noteworthy at both sampling points – with mean values ranging between log 6 and 7 of CFU/spleen – while the three mutants presented a poor colonization under these conditions (**Figure 2A**). Spleen infection of the mutants was undetectable in several mice per group, although two out five mice inoculated with the $\Delta omp10\Delta omp31\Delta omp25c$ mutant gave values of about log 5 CFU/spleen at W7 p.i. (**Figure 2A**). Spleen weight and IgG titers in serum were also significantly higher ($P < 0.05$) in mice inoculated with the parental strain (**Figures 2B,C**).

The same parameters described above were evaluated at several time points over a 11-week period in mice inoculated with 10^8 CFU of each strain (**Figures 2D–F**), the dose usually employed for evaluation of attenuated strains as vaccines (Sancho et al., 2014; Soler-Lloréns et al., 2014; Silva et al., 2015b). The parental strain showed high levels of spleen infection through the entire experiment with mean log CFU/spleen values of 5.99 at W1 p.i. and a peak at W3 p.i. of 7.64. *B. ovis* PA counts decreased thereafter but were still high at the end of the experiment (mean log CFU/spleen values of 5.01 at W11) (**Figure 2D**). The $\Delta omp31\Delta cgs$ and $\Delta omp10\Delta omp31\Delta omp25c$ mutants displayed

lower levels of splenic infection at W1, with mean CFU/spleen values 1–1.5 log lower than those of the parental strain ($P < 0.05$). However, although their maximum CFU/spleen scores (about log 6 at W3–W5 p.i.) did never reach those of *B. ovis* PA (log 7.64 at W3 p.i.), they persisted in spleen with similar values to those of the parental strain at W11 p.i. ($P > 0.05$) (**Figure 2D**). The spleen colonization of the $\Delta omp10\Delta ugpB\Delta omp31$ mutant did not show statistically significant differences with the parental strain at W1 p.i., but the bacterial counts did not increase at W3 p.i. and decreased thereafter until the detection limit of infection at W7 p.i. ($P < 0.05$) (**Figure 2D**).

At W1 p.i., the spleen weight in mice infected with 10^8 CFU of the parental strain (0.102 ± 0.030 g) was analogous to that currently obtained with mice inoculated with PBS and that was also observed in the PBS group used to determine the production of cytokines by splenocytes in the experiment described below (0.096 ± 0.005 g) ($P > 0.05$). However, a prominent splenomegaly was detected at W3 p.i. (0.478 ± 0.020 g/spleen) which, although decreased after W3 p.i., persisted until the end of the experiment (0.205 ± 0.046 g/spleen) ($P < 0.05$) (**Figure 2E**). On the contrary, the *B. ovis* mutants did never reach mean values of 0.200 g/spleen (**Figure 2E**). At W1 p.i., all groups of mice had low levels of IgG reactive with whole cells of *B. ovis* PA. An important increase of the antibody response was detected at W3 p.i. in all groups ($P < 0.05$), except in mice vaccinated with the $\Delta omp31\Delta cgs$ mutant ($P > 0.05$). At W5 p.i. and thereafter, mice inoculated with the parental strain or the $\Delta omp31\Delta cgs$ and $\Delta omp10\Delta omp31\Delta omp25c$ mutants displayed IgG titers of about log 4, while mice inoculated with *B. ovis* $\Delta omp10\Delta ugpB\Delta omp31$ gave titers in the order of 0.5 logarithmic units higher ($P < 0.05$) than those detected in the *B. ovis* PA group (**Figure 2F**).

Autoagglutination and Susceptibility Assays

In addition to the three selected mutants, other relevant mutants were included in the remaining studies by their interest to increase the knowledge about the *B. ovis* cell envelope. Several tests related to the OM properties of *Brucella* spp. (i.e., autoagglutination and resistance to polymyxin B and sodium deoxycholate) (Martín-Martín et al., 2011; Vizcaino and Cloeckaert, 2012) were performed. In the autoagglutination assay, most of the single mutants behaved as the *B. ovis* PA parental strain ($P > 0.05$), remaining in suspension until the end of the experiment (**Figure 3** and data not shown). The exceptions were *B. ovis* $\Delta omp31$ – with %OD₆₀₀ values of about 30 and 10% after 24 and 48 h of static incubation, respectively – and the Δcgs and $\Delta omp25c$ -k mutants, whose %OD₆₀₀ values gradually decreased until 70% at the end of the experiment ($P < 0.05$ when compared to the parental strain) (**Figure 3**). The *omp31* multiple mutants behaved similarly to the single mutant, although the $\Delta omp10\Delta omp31\Delta omp25c$ and $\Delta omp31\Delta omp10\Delta omp25c$ mutants agglutinated more quickly (they were almost completely settled after 10 h) ($P < 0.05$) (**Figure 3**). *B. ovis* $\Delta omp25\Delta cgs$ behaved like the single Δcgs mutant while *B. ovis* $\Delta omp25\Delta omp25c$ did not show differences with the parental strain ($P > 0.05$) (**Figure 3**).

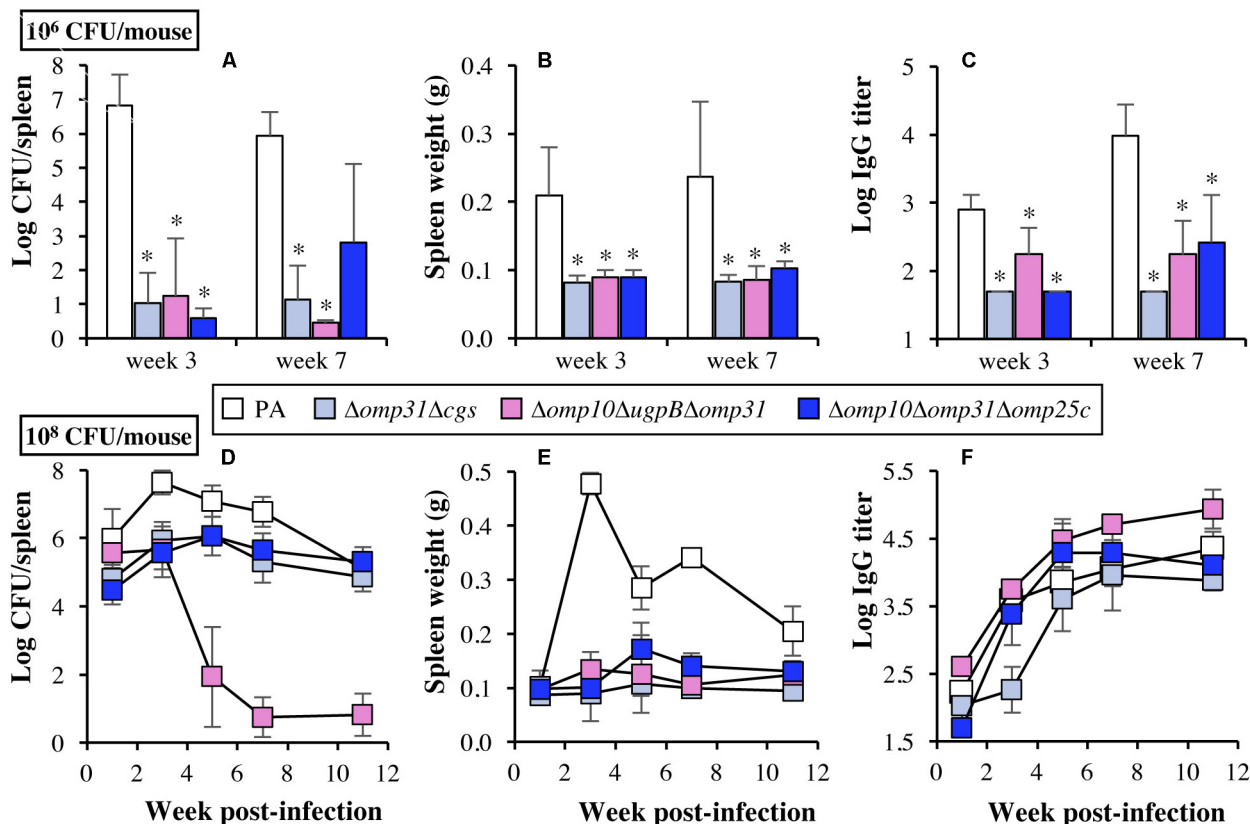


FIGURE 2 | Bacterial spleen colonization (A,D), spleen weight (B,E), and IgG response in serum against *B. ovis* PA whole cells (C,F) in BALB/c mice. Mice ($n = 5$ per group and time point) were inoculated intraperitoneally with 10^6 (upper panels) or 10^8 (lower panels) CFU/mouse of *B. ovis* PA or $\Delta omp31 \Delta cgs$, $\Delta omp10 \Delta ug p B \Delta omp31$, and $\Delta omp10 \Delta omp31 \Delta omp25c$ mutants. Statistically significant differences in upper panels, compared to parental *B. ovis* PA, are marked with an asterisk. To simplify the figure, relevant statistically significant differences in lower panels ($P < 0.05$) are mentioned in the text. Detection limit for antibody titers is log 1.7. As a reference for panels B and E, spleen weight of mice inoculated with PBS ($n = 5$) for the protection experiment described in Figure 8 was 0.096 ± 0.005 (W7 post-inoculation).

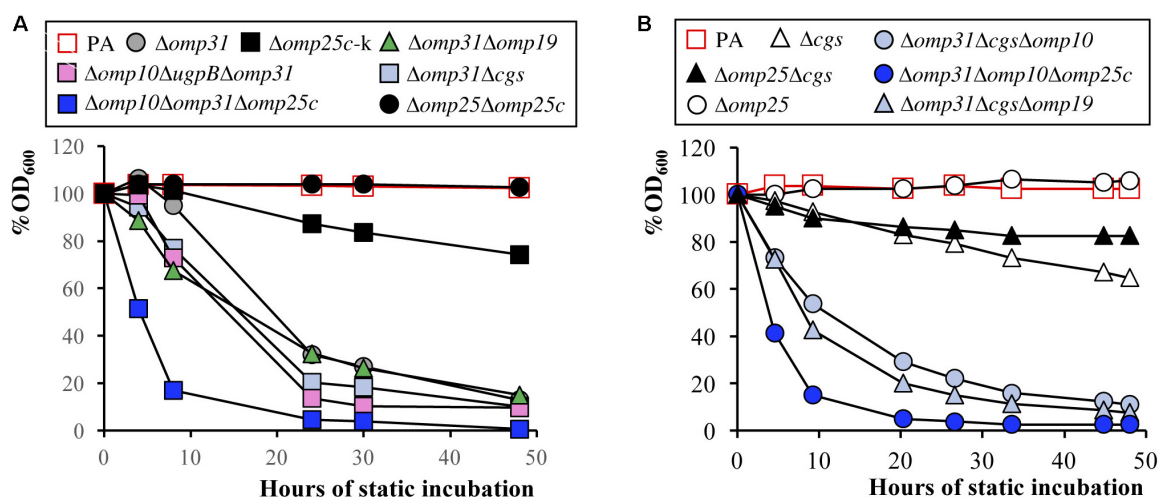


FIGURE 3 | Autoagglutination assay with bacterial suspensions of initial OD₆₀₀ readings of 0.8 (100% OD₆₀₀). The percentage of the OD₆₀₀ values was determined over 48 h of static incubation. Panels A and B represent results of two independent experiments. The SD of three assays, which was always lower than 5% of the mean, is not shown. To simplify the figure, relevant statistically significant differences ($P < 0.05$) are mentioned in the text.

Brucella ovis $\Delta bacA$ and the *B. ovis* $\Delta bacA \Delta omp31$ double mutant were more resistant than *B. ovis* PA to polymyxin B exposure for 80 min (Table 4). On the contrary, *B. ovis* $\Delta omp25 \Delta omp25c$, and the $\Delta omp31$ single and multiple mutants – except the previously mentioned $\Delta bacA \Delta omp31$ mutant – showed higher susceptibility to polymyxin B than the parental strain (Table 4). The lowest survival percentages were obtained with the $\Delta omp10 \Delta omp31 \Delta omp25c$ and $\Delta omp31 \Delta omp10 \Delta omp25c$ mutants (less than 10% survival). Only the $\Delta omp31 \Delta cgs$ double mutant and its derived $\Delta omp31 \Delta cgs \Delta omp10$ and $\Delta omp31 \Delta cgs \Delta omp19$ triple mutants were more susceptible to sodium deoxycholate than the parental strain (about 30% survival versus 86% survival, respectively) (Table 4).

Mapping of Cell Envelope Antigens

The reactivity of the *B. ovis* mutants with MABs raised against *Brucella* S-LPS, R-LPS, PG, major and minor OMPs, and periplasmic BP26 was analyzed by iELISA (Figure 4 and data not shown). As expected, the MAB-specific against S-LPS did

not react with any mutant or with the parental strain (data not shown) and *omp31*, *omp25*, *omp10*, or *omp19* single and multiple mutants did not react with the respective MABs (see Figure 4 for representative results). No relevant differences were observed between the parental strain and the mutants regarding reactivity with MABs specific against Omp31 (except with mutants lacking *omp31*), Omp10 (except with mutants lacking *omp10*), Omp16, Omp2b, PG, and R-LPS. On the contrary, all *omp31* mutants showed a stronger reaction with MAB C09 (specific against Omp25) and *omp19* mutants showed a stronger reaction with MAB B02, specific against BP26 (Figure 4, upper panels and data not shown). Accordingly, several *omp31* mutants were tested in iELISA with three MABs specific against Omp25, while *omp19* mutants were tested with four anti-BP26 MABs. All the $\Delta omp31$ and $\Delta omp19$ mutants showed a stronger reactivity with the anti-Omp25 and anti-BP26 MABs, respectively (Figures 4G,H), which confirmed the results obtained in the previous analysis.

The protein profile of the most relevant strains was evaluated by SDS-PAGE followed by Coomassie blue staining (Figure 5A). Proteins were also transferred to nitrocellulose to assess the reactivity with sera raised against the proteins of the Omp25/Omp31 family. A serum against Omp25c was used to detect both Omp25c and Omp25 since these proteins display cross-reacting epitopes (Martín-Martín et al., 2009), while the detection of Omp31 was performed with a serum raised against Omp31b (an OMP absent in *B. ovis*) that strongly cross-react with Omp31 (Martín-Martín et al., 2009). Omp25d and Omp22 were detected by reactivity with their respective anti-sera (Martín-Martín et al., 2009).

A multiple band pattern, dependent on the electrophoretic conditions, is frequently observed in SDS-PAGE for Omp25, Omp25c, and Omp31 (Cloëckaert et al., 1990; Martín-Martín et al., 2009). Two protein bands corresponding to Omp25c were detected by immunoblot in parental *B. ovis* PA and were absent in all *omp25c* mutants (Figure 5B). Additionally, the intensity of the upper band in *omp31* mutants was higher than that observed with the parental strain (Figure 5B). Absence of the lower band of Omp25c in the $\Delta omp25c$ mutants was also evident in the SDS-PAGE gel (Figure 5A, lanes $\Delta omp25c-k$, $\Delta omp25 \Delta omp25c$, and $\Delta omp10 \Delta omp31 \Delta omp25c$) while the absence of the upper band was only apparent in the $\Delta omp10 \Delta omp31 \Delta omp25c$ triple mutant (Figure 5A). This result can be explained by the fact that this mutant also lacks Omp31, which is a major OMP that exhibits an electrophoretic mobility similar to that of Omp25c (Figure 5A) and, consequently, masks the absence of the upper Omp25c band in the other $\Delta omp25c$ mutants.

Omp25 was detected between the two Omp25c bands except in the *omp25* mutants. Absence of Omp25 in these mutants was evidenced in both the SDS-PAGE gel (Figure 5A) and the immunostained nitrocellulose (Figure 5B) (see $\Delta omp25$, $\Delta omp25 \Delta cgs$, and $\Delta omp25 \Delta omp25c$ lanes in comparison with PA lanes). With both techniques, the Omp25 band of the $\Delta omp31$ mutants was more intense than in *B. ovis* PA. Omp31 was detected in immunoblot and with the same intensity in all the strains, except those lacking the encoding gene (Figure 5C). Absence of Omp31 in these latter

TABLE 4 | Susceptibility of *B. ovis* PA and selected mutants to polymyxin B and Na deoxycholate.

Brucella ovis strains ^b	% Survival after exposure to ^a :	
	Polymyxin B (1 mg/ml)	Na deoxycholate (0.1 mg/ml)
<i>B. ovis</i> PA	69.03 ± 6.12	86.25 ± 5.74
Single mutants		
$\Delta omp31$	27.47 ± 3.04*	83.74 ± 3.09
$\Delta omp25$	65.84 ± 7.17	92.94 ± 4.06
$\Delta omp25c-k$	65.99 ± 4.72	95.89 ± 7.15
Δcgs	77.96 ± 11.80	79.82 ± 9.07
$\Delta bacA$	84.10 ± 5.49*	87.38 ± 8.28
$\Delta omp10$	62.04 ± 3.46	91.20 ± 4.22
$\Delta omp19$	67.27 ± 7.05	83.19 ± 7.75
$\Delta ugpB$	77.59 ± 11.67	90.66 ± 9.42
Double mutants		
$\Delta omp31 \Delta omp19$	25.68 ± 2.94*	90.49 ± 7.79
$\Delta omp31 \Delta ugpB$	20.66 ± 0.57*	92.65 ± 3.64
$\Delta omp31 \Delta cgs$	31.20 ± 14.30*	32.14 ± 1.27*
$\Delta omp25 \Delta cgs$	61.71 ± 7.30	92.35 ± 5.18
$\Delta omp25 \Delta omp25c$	45.23 ± 5.10*	91.36 ± 9.59
$\Delta omp10 \Delta omp31$	33.31 ± 4.58*	84.66 ± 6.36
$\Delta omp10 \Delta ugpB$	64.22 ± 5.36	77.93 ± 9.26
$\Delta bacA \Delta omp31$	88.06 ± 18.61*	86.90 ± 5.51
Triple mutants		
$\Delta omp10 \Delta ugpB \Delta omp31$	30.50 ± 9.94*	88.52 ± 6.22
$\Delta omp10 \Delta omp31 \Delta omp25c$	1.65 ± 0.36*	76.74 ± 9.37
$\Delta omp31 \Delta omp10 \Delta omp25c$	7.19 ± 4.38*	80.40 ± 7.49
$\Delta omp31 \Delta cgs \Delta omp10$	37.84 ± 9.43*	33.63 ± 1.78*
$\Delta omp31 \Delta cgs \Delta omp19$	33.30 ± 3.68*	34.39 ± 2.94*

^aResults are expressed as the mean ± SD of three assays. Statistically significant differences ($P < 0.05$), compared to the parental strain, are marked with an asterisk.

^bSee legend to Figure 1 for strain characteristics.

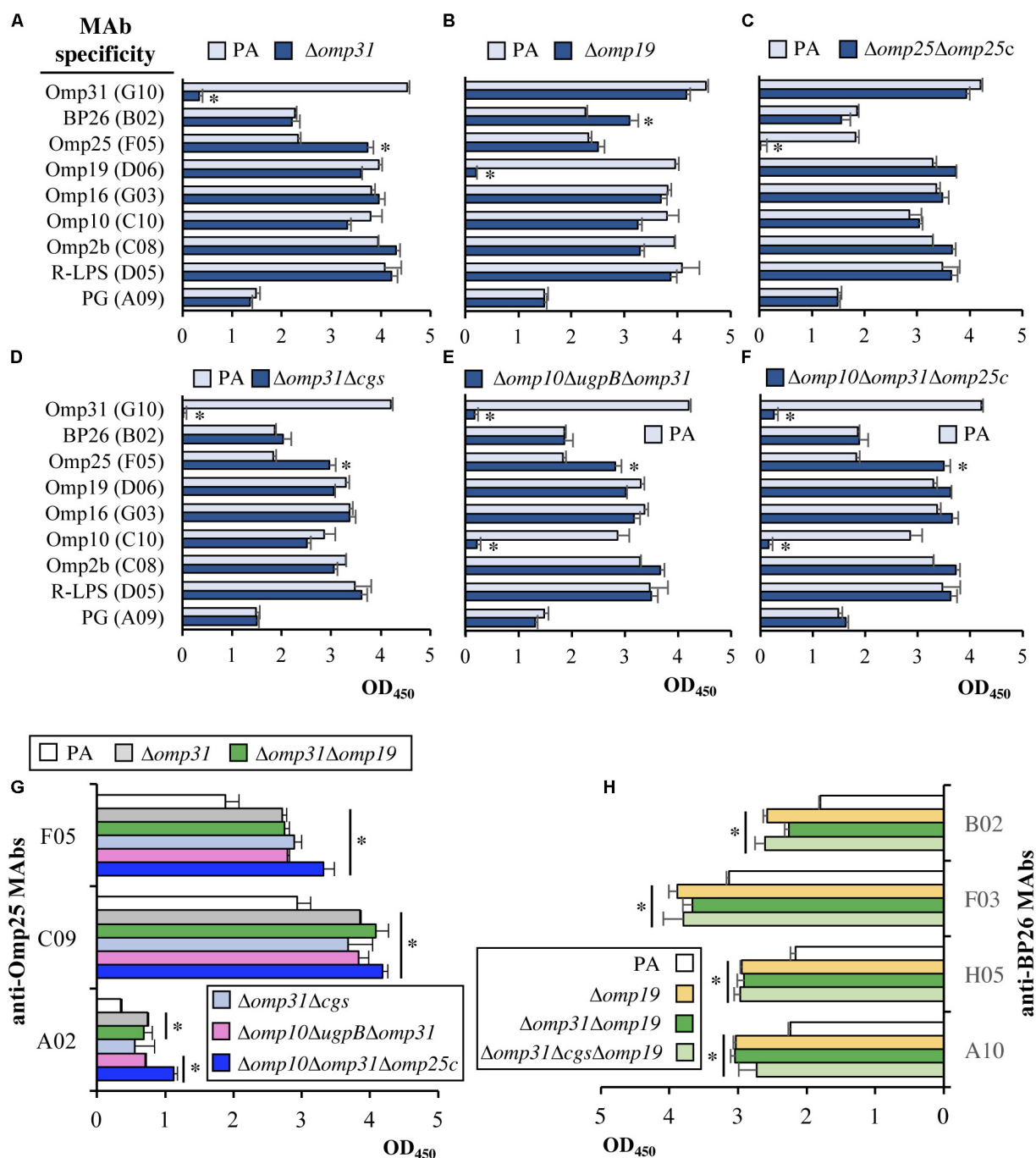


FIGURE 4 | Reactivity by iELISA of MAbs against cell envelope antigens with *B. ovis* PA and selected mutants. The reactivity of MAbs specific against PG, R-LPS, the BP26 periplasmic protein, the Omp2b, Omp31, and Omp25 major OMPS, and the Omp10, Omp16, and Omp19 OM lipoproteins (A–F) was tested with most of the mutant strains obtained in this work. Representative results are shown in panels A–F and others are commented in the text. Differences between the mutant strains and the parental strain were considered relevant for further analysis when, in addition to being statistically significant ($P < 0.05$), the mean values differed more than 25% (marked with an asterisk). Reactivity of $\Delta omp31$ single and multiple mutants with several anti-Omp25 MAbs (G), and of $\Delta omp19$ mutants with several anti-BP26 MAbs (H), is also shown. Statistically significant differences between the mutant strains and the parental strain ($P < 0.05$) in panels G and H, are marked with an asterisk.

mutants was also evident in the SDS–PAGE gel (Figure 5A). The Omp22 band was revealed in *B. ovis* PA and the analyzed mutants, while Omp25d – that has only been

observed in a complemented mutant overexpressing the protein (Martín-Martín et al., 2009) – was not detected (data not shown).

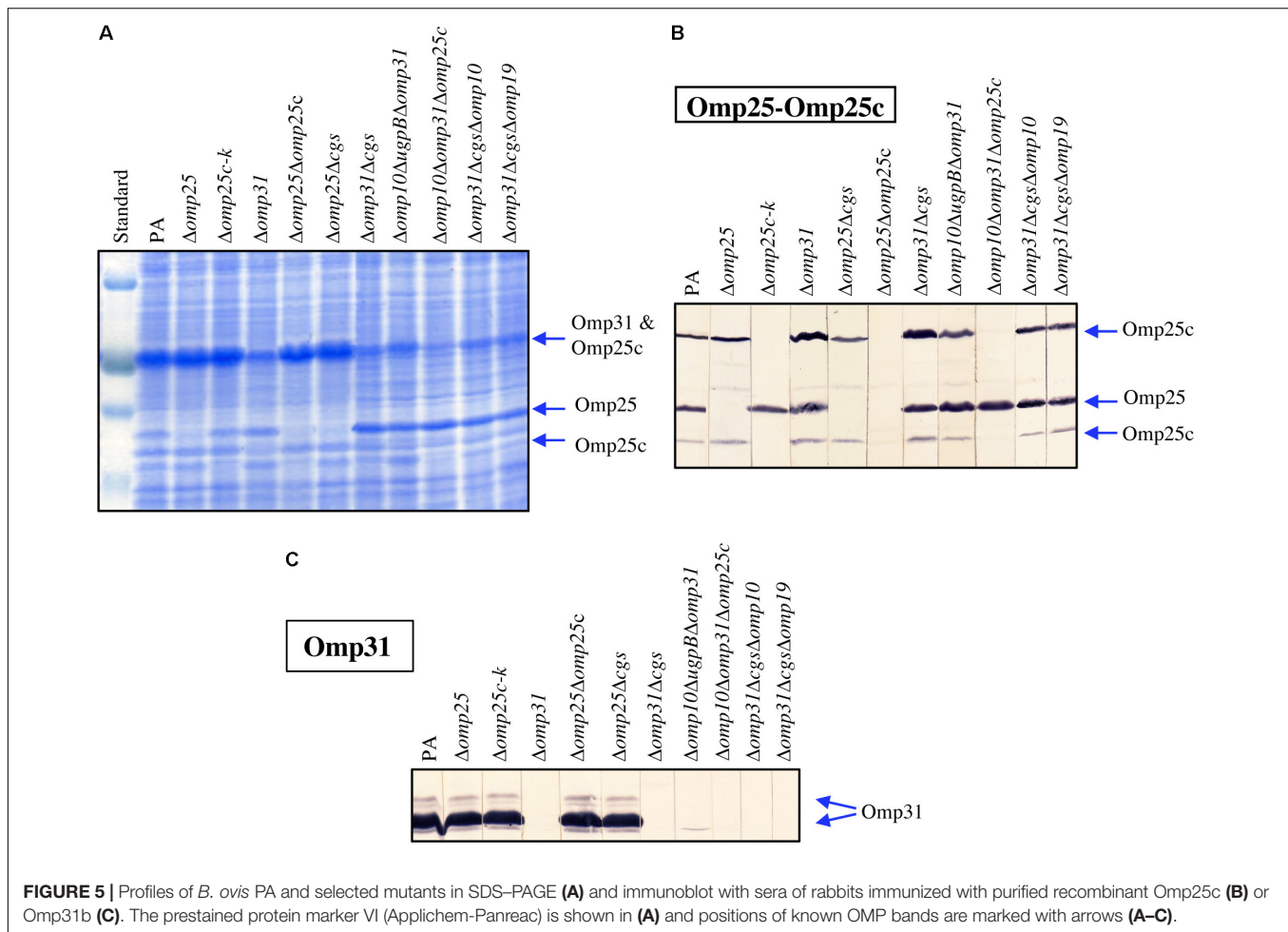


FIGURE 5 | Profiles of *B. ovis* PA and selected mutants in SDS-PAGE (A) and immunoblot with sera of rabbits immunized with purified recombinant Omp25c (B) or Omp31b (C). The prestained protein marker VI (Applichem-Panreac) is shown in (A) and positions of known OMP bands are marked with arrows (A–C).

Cellular Models of Infection

The intracellular behavior of *B. ovis* PA and the most relevant mutants was evaluated in J774.A1 murine macrophages and HeLa cells. No significant differences between strains ($P > 0.05$) were observed regarding internalization in J774.A1 macrophages (Figure 6, upper panels). However, although the intracellular bacterial numbers decreased at t20 with all the strains, the reduction was more pronounced with strains $\Delta omp25\Delta omp25c$ (Figure 6A), $\Delta omp25\Delta cgs$, $\Delta omp31\Delta cgs$, and its derived triple mutants (Figure 6C), and with *B. ovis* $\Delta omp10\Delta ugpB\Delta omp31$ and $\Delta omp10\Delta omp31\Delta omp25c$ (Figure 6B) ($P < 0.05$). After this moment, all strains were able to replicate, reaching intracellular CFU numbers at t44 about 1 log unit higher than those detected at t20 for each strain ($P < 0.05$) (Figure 6, upper panels).

In HeLa cells, the $\Delta omp25c$ mutants ($\Delta omp25c-k$, $\Delta omp25\Delta omp25c$, $\Delta omp10\Delta omp31\Delta omp25c$, and $\Delta omp31\Delta omp10\Delta omp25c$) showed a deficient internalization, with intracellular CFU at t0 in the order of 1–1.5 log units lower than those determined for *B. ovis* PA ($P < 0.05$). On the contrary, all mutants bearing the *omp31* deletion, except those with the $\Delta omp25c$ genotype (*B. ovis* $\Delta omp10\Delta omp31\Delta omp25c$ and $\Delta omp31\Delta omp10\Delta omp25c$), showed an increased internalization

in HeLa cells, with CFU at t0 about 1 log higher than those of the parental strain ($P < 0.05$) (Figure 6, lower panels). All strains suffered a reduction ($P < 0.05$) of intracellular CFU at t20 while at t44 the bacterial numbers were, in general, similar to those obtained at t20 (Figure 6, lower panels).

Searching for an explanation to the internalization differences observed in HeLa cells, the $\Delta omp25c-k$ mutant complemented with the wild-type gene and the $\Delta omp31-k$ mutant together with its complemented strain (Caro-Hernández et al., 2007) were also analyzed regarding internalization in HeLa cells (CFU determined at t0) and their behavior in immunoblot with sera reacting with Omp31 and Omp25c (Figure 7). Complementation of the $\Delta omp25c-k$ mutant restored its ability to enter HeLa cells like the parental strain (Figure 7A) and the production of Omp25c (Figures 6B,C). The complemented $\Delta omp31-k$ mutant recovered the ability to produce Omp31, but its level was lower than that of the parental strain (Figures 7B,D). This fact was concomitant with a higher intensity of Omp25c bands, when compared to *B. ovis* PA that, however, did not reach the intensity observed with the $\Delta omp31$ and $\Delta omp31-k$ mutants (Figure 7C). Internalization of the complemented $\Delta omp31-k$ mutant in HeLa cells was similar to that of the $\Delta omp31$ mutant

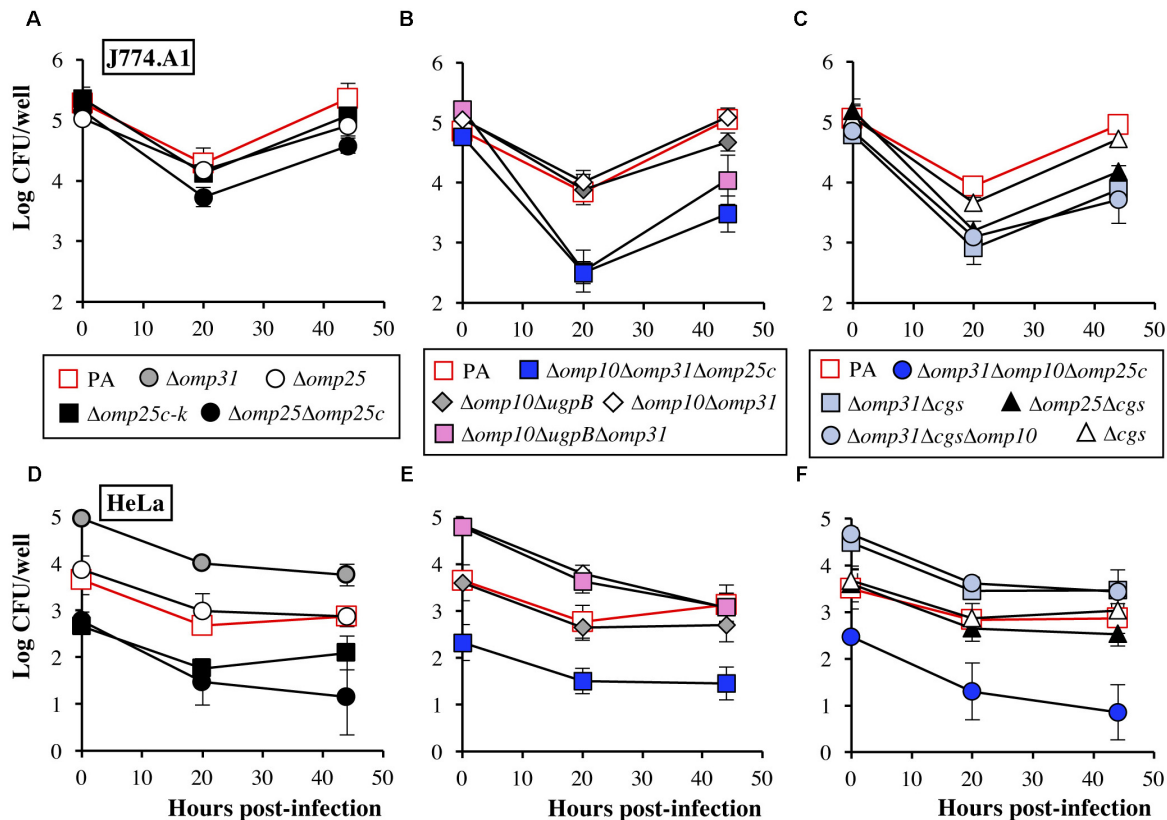


FIGURE 6 | Internalization and intracellular behavior of *B. ovis* PA and selected mutants in J774.A1 murine macrophages (A–C) and HeLa cells (D–F). The results are expressed as the means \pm SD ($n = 3$) of the log CFU/well at each time point. To simplify the figure, relevant statistically significant differences ($P < 0.05$) are mentioned in the text.

and significantly higher than that observed with the parental strain (Figure 7A).

Efficacy as Vaccine of *B. ovis* $\Delta omp10\Delta ugpB\Delta omp31$

The usefulness as vaccine of *B. ovis* $\Delta omp10\Delta ugpB\Delta omp31$ against *B. ovis* PA was evaluated in mice and compared to that of the *B. melitensis* Rev1 heterologous vaccine. Spleen colonization of the challenge strain was evaluated 3 weeks after infection (Figure 8F) and the humoral (Figure 8E) and cellular (Figures 8A–D) immune response was evaluated at the time point selected for the challenge with the virulent strain (W7 post-vaccination).

Weight of spleens obtained at W7 post-vaccination from mice inoculated with the $\Delta omp10\Delta ugpB\Delta omp31$ mutant (0.104 ± 0.012 g) did not show statistically significant differences with that of mice inoculated with PBS (0.096 ± 0.005 g), while splenomegaly ($P < 0.05$) was detected in mice vaccinated with *B. melitensis* Rev1 (0.136 ± 0.011 g) (data not shown). Additionally, *B. melitensis* Rev1 was detected in spleen (log CFU/spleen values of 3.66 ± 0.07), while the $\Delta omp10\Delta ugpB\Delta omp31$ mutant was cleared by this time (data not shown).

Splenocytes were stimulated with *B. ovis* PA whole cells to evaluate, by specific ELISA tests, the production of cytokines. Splenocytes of mice inoculated with PBS secreted limited amounts of IFN- γ , while about 30 and 60 times higher levels ($P < 0.05$) were detected in the groups vaccinated with the $\Delta omp10\Delta ugpB\Delta omp31$ mutant and *B. melitensis* Rev1, respectively (Figure 8A). In a lesser extent, splenocytes from vaccinated mice also produced more IL-10 ($P < 0.05$) than those obtained from mice of the PBS group (mean values of 14.7, 9.9, and 1.4 ng/well for the *B. melitensis* Rev1, *B. ovis* $\Delta omp10\Delta ugpB\Delta omp31$, and PBS groups, respectively) (Figure 8C). Regarding the production of TNF- α , splenocytes from mice vaccinated with the two *Brucella* attenuated strains secreted about double amounts (mean values of 3 ng/well) than those obtained from the unvaccinated control group ($P < 0.05$) (Figure 8B). No statistically significant differences were observed between groups concerning the production of IL-12(p40) (Figure 8D).

At the time of challenge, mice inoculated with PBS 7 weeks earlier showed low titers (close to the detection limit of log 1.7) of serum antibodies of the IgG₁, IgG_{2a}, and IgG_{2b} subclasses able to react with *B. ovis* PA whole cells in iELISA (Figure 8E). On the contrary, mice vaccinated with *B. ovis* $\Delta omp10\Delta ugpB\Delta omp31$ had titers of the three IgG subclasses (ranging from log

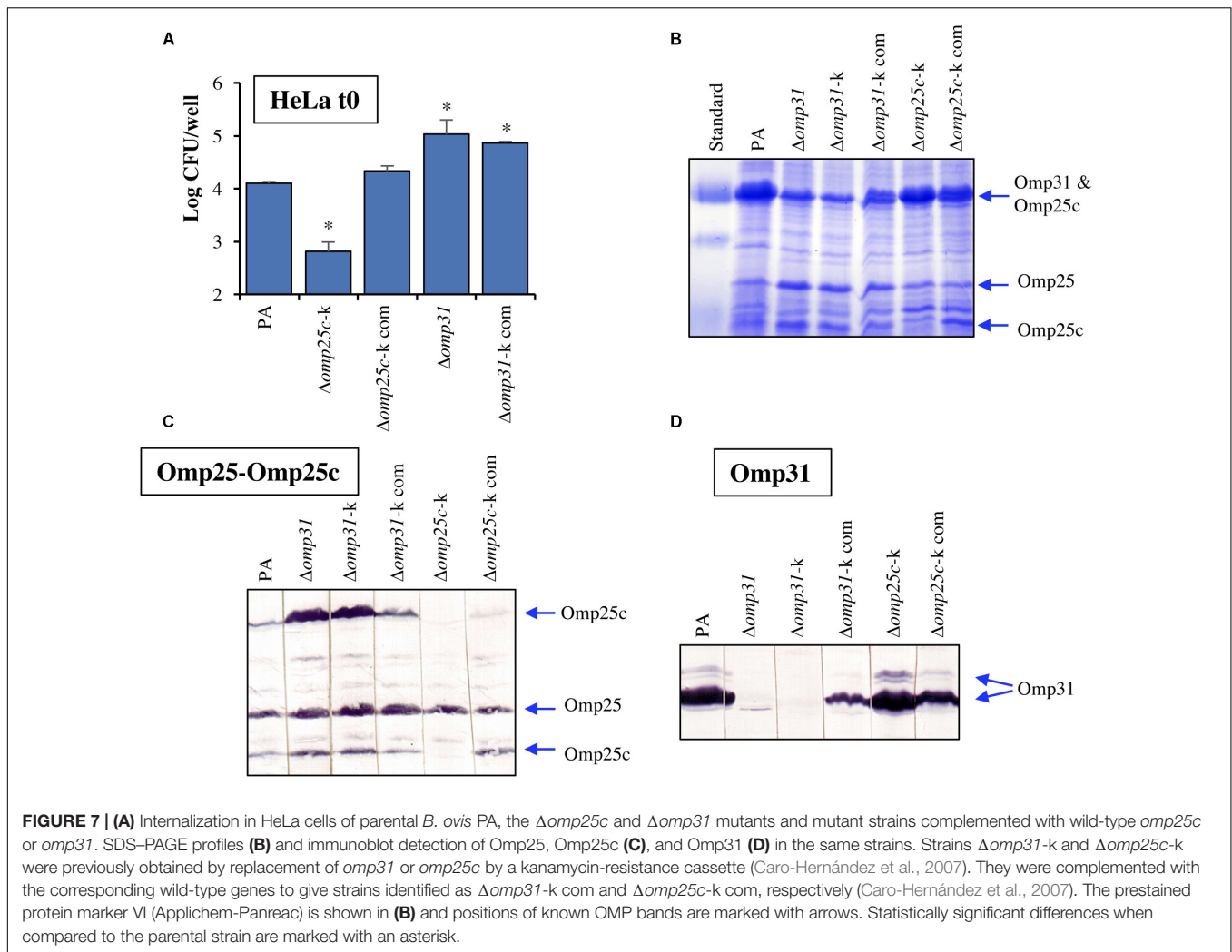


FIGURE 7 | (A) Internalization in HeLa cells of parental *B. ovis* PA, the $\Delta omp25c$ and $\Delta omp31$ mutants and mutant strains complemented with wild-type *omp25c* or *omp31*. SDS-PAGE profiles **(B)** and immunoblot detection of Omp25, Omp25c **(C)**, and Omp31 **(D)** in the same strains. Strains $\Delta omp31$ -k and $\Delta omp25c$ -k were previously obtained by replacement of *omp31* or *omp25c* by a kanamycin-resistance cassette (Caro-Hernández et al., 2007). They were complemented with the corresponding wild-type genes to give strains identified as $\Delta omp31$ -k com and $\Delta omp25c$ -k com, respectively (Caro-Hernández et al., 2007). The prestained protein marker VI (Applichem-Panreac) is shown in **(B)** and positions of known OMP bands are marked with arrows. Statistically significant differences when compared to the parental strain are marked with an asterisk.

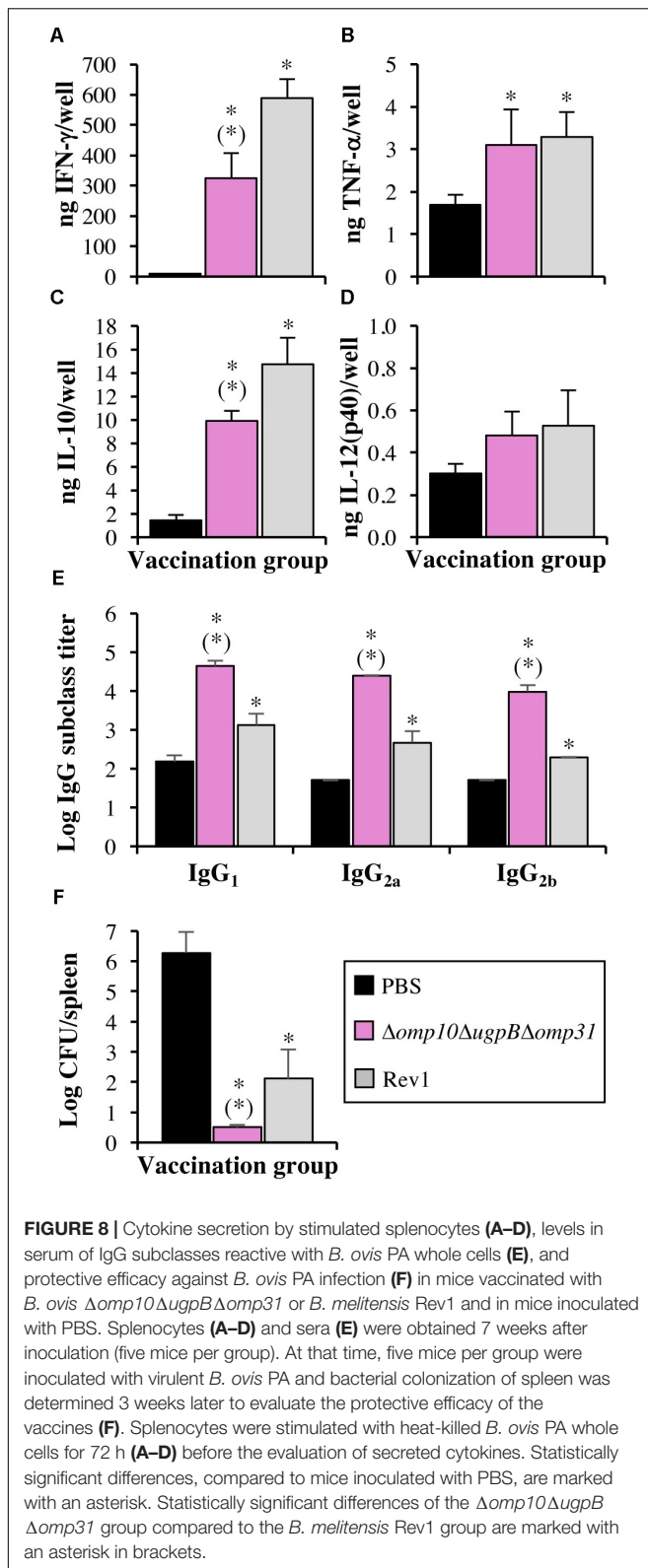
3.99 ± 0.16 for IgG_{2b} to log 4.65 ± 0.13 for IgG₁) that were about 1.5 log units higher ($P < 0.05$) than those detected in mice vaccinated with the *B. melitensis* Rev1 heterologous vaccine. Within each vaccination group, no relevant differences were observed between the three IgG subclasses (**Figure 8E**).

The homologous *B. ovis* $\Delta omp10 \Delta ugpB \Delta omp31$ vaccine was not detected in spleen 3 weeks after the experimental challenge while it prevented spleen colonization of virulent *B. ovis* PA (CFU/spleen counts were under the detection limit) (**Figure 8F**). When compared to control mice inoculated with PBS, vaccination with heterologous *B. melitensis* Rev1 also drastically reduced the spleen colonization of *B. ovis* PA (**Figure 8F**), but both the vaccine strain and the challenge strain were detected in some mice.

DISCUSSION

With the aim to increase our knowledge about the OM and virulence of *B. ovis* and to develop a specific homologous attenuated vaccine, multiple deletion mutants targeting nine

genes related to the OM were obtained and characterized. Two of these genes encode Omp10 and Omp19, two lipoproteins that are conserved in *Brucella* (Cloeckaert et al., 1990; Tibor et al., 1994, 1996) and have orthologs in other phylogenetically related bacteria able to establish interactions with eukaryotic cells either as symbionts or as pathogens (e.g., *Ochrobactrum*, *Bartonella*, *Rhizobium*, *Ensifer*, *Sinorhizobium*) (Cloeckaert et al., 1999; Barquero-Calvo et al., 2009). This observation suggests their relevant role for the bacterium and, in fact, both lipoproteins have been linked to the virulence of *B. abortus* 544 (Tibor et al., 2002). Surprisingly, the individual absence of Omp10 and Omp19 in the OM of *B. ovis* PA did not affect its virulence or modified notably its OM-related properties (Sidhu-Muñoz et al., 2016). On the contrary, the multiple assays we have performed to achieve the simultaneous deletion of *omp10* and *omp19* in *B. ovis* PA were unsuccessful. Since OM lipoproteins are thought to anchor the OM through the lipid moiety and contribute to the stability of the cell envelope (Goolab et al., 2015), Omp10 and Omp19 could have an interchangeable role necessary to maintain the OM integrity. Nevertheless, the amount of Omp10 in *B. ovis* $\Delta omp19$ and the amount of Omp19 in the $\Delta omp10$ mutant does not



seem to be increased (Figure 4B and data not shown), although the absence of one of these lipoproteins, in the presence of the other, could also be compensated by an increase in other cell

envelope proteins. In this respect, a higher reactivity with MAbs against BP26 suggestive of increased levels of this periplasmic protein was detected in the mutants bearing the *omp19* deletion (Figure 4H). Contrasting with the impossibility to obtain the double $\Delta omp10 \Delta omp19$ mutant, the simultaneous absence of major Omp31 together with Omp10 or Omp19 lipoprotein was well tolerated in *B. ovis* PA, since the respective double mutants do not have prominent defects in virulence (Table 1) and the other phenotypic changes are associated to the deletion of *omp31* (Table 4, Figures 3, 5, 6, and data not shown). Similarly, deletion of *ugpB* on the $\Delta omp10$ or $\Delta omp19$ genetic background did not affect the virulence (Table 1), and the alterations detected after deletion of *cgs* on the same mutants resembled those detected with the *B. ovis* Δcgs single mutant (Table 1).

Other target surface antigens were Omp31, Omp25, and Omp25c that are abundant OMPs in *B. ovis* (Cloeckaert et al., 2002; Martín-Martín et al., 2009; Vizcaino and Cloeckaert, 2012) and the main members of the Omp25/Omp31 family that is constituted by seven homologous OMPs (Salhi et al., 2003; Vizcaino et al., 2004; Vizcaino and Cloeckaert, 2012). Orthologs of this family of OMPs have been found in *Bartonella quintana* (Minnick et al., 2003) and other Rhizobiales (e.g., *Rhizobium leguminosarum*, *Agrobacterium tumefaciens*, or *O. anthropi*), which suggests that the redundancy of these OMPs provides an advantage that could be related with the compensatory effect between these proteins previously reported (Salhi et al., 2003; Caro-Hernández et al., 2007; Martín-Martín et al., 2009; Vizcaino and Cloeckaert, 2012). This compensatory effect is in accordance with the apparent increase of Omp25 and Omp25c that was observed with all *omp31* mutants, except those also lacking *omp25c* where Omp25c was not detected (Figures 4, 5). On the contrary, *omp25* and *omp25c* mutants and even the double $\Delta omp25 \Delta omp25c$ mutant did not show higher levels of Omp31 (Figures 4, 5). In addition, this latter double mutant did not suffer important defects regarding *in vitro* growth (Figure 1) or virulence in mice (Table 1). These observations could be indicative of a more relevant role for Omp31, whose absence in the OM would require a compensation with another paralog that would not be necessary when Omp25 or Omp25c are missing.

However, considering that our attempts to obtain a *B. ovis* PA double mutant defective in Omp31 and Omp25 were fruitless, it seems probable that the presence in the bacterial surface of one of these two major OMPs is a requirement at least for *in vitro* survival. This assertion is in contradiction with the availability of $\Delta omp25$ mutants in *B. abortus* (Edmonds et al., 2002; Manterola et al., 2007), a *Brucella* species naturally lacking Omp31 due to a 25-kb deletion involving its encoding gene (Vizcaino et al., 2001a). Nevertheless, unlike *B. ovis* where *omp31b* is a pseudogene (Vizcaino et al., 2004), *B. abortus* strains synthesize Omp31b (Martín-Martín et al., 2009), an OMP sharing 67% of amino acid identity with Omp31 (Salhi et al., 2003) and that could compensate for the absence of Omp31 in this species. Research aiming to construct the $\Delta omp25 \Delta omp31b$ double mutant in the *B. abortus* genetic background would help to a better understanding of the relationships between the members of the Omp25/Omp31 family.

According to the availability of the $\Delta omp10\Delta omp31\Delta omp25c$ and $\Delta omp31\Delta omp10\Delta omp25c$ mutants (with the same deleted genes in a different order), *B. ovis* PA survives to the simultaneous absence of Omp10 lipoprotein and major Omp31 and Omp25c, together with the natural lack of Omp31b and Omp25b (Martín-Martín et al., 2009). However, both mutants suffered important phenotypic changes, such as strong *in vitro* growth defects, quick autoagglutination, remarkable susceptibility to polymyxin B, increased killing by murine macrophages in the first 20 h of infection, defective internalization in HeLa cells, and limited spleen colonization in mice inoculated with 10^6 CFU. Nevertheless, not only both strains replicate in murine macrophages after 20 h of infection (**Figure 6B** and data not shown) but at least *B. ovis* $\Delta omp10\Delta omp31\Delta omp25c$ can establish a chronic infection in mice, with important levels of spleen colonization, when inoculated at 10^8 CFU/mouse (**Figure 2D**).

Another finding regarding the Omp25/Omp31 family, and that was further confirmed by confocal microscopy (data not shown), is that all *omp25c* mutants are impaired for internalization in HeLa cells (**Figures 6D–F**), while all strains bearing the $\Delta omp31$ mutation (except the triple mutants also bearing the *omp25c* deletion) internalize more efficiently than the parental strain (**Figures 6D–F** and data not shown). Since immunoblot assays showed that $\Delta omp31$ mutants had higher levels of Omp25c, we postulated that Omp25c is involved in the internalization of *B. ovis* PA in HeLa cells. This hypothesis is supported by the immunoblots and HeLa cells assays performed with *omp31* and *omp25c* mutant and complemented strains (**Figure 7**). Whether this characteristic is specific for HeLa cells, for human cells or for non-professional phagocytes independently of the animal species remains to be studied.

As expected (Martín-Martín et al., 2012) the Δcgs mutant did not suffer drastic changes in the *in vitro* characteristics, but was the only single mutant that was attenuated in the murine model when it was inoculated at 10^6 CFU/mouse (**Table 1**). However, a 100-fold increase of the inoculation dose led to high splenic infection levels at both the acute and chronic phase of infection (**Table 1**) and to a kinetics of spleen colonization resembling that observed in mice experimentally infected with 10^6 CFU of the parental strain (data not shown; see the equivalent spleen colonization profile of the $\Delta omp31\Delta cgs$ mutant in **Figure 2**). According to the similarities between the parental strain and the Δcgs mutant regarding their behavior in the cellular models of professional and non-professional phagocytes used in this work (**Figures 6C,F**) the attenuation of the Δcgs mutant of *B. ovis* PA does not seem to be due to killing inside phagocytic cells. However, since we have used individual cell lines, a defective interaction with one or more types of professional and/or non-professional phagocytes of BALB/c mice cannot be discarded. In fact, Δcgs mutants of *B. abortus* 2308 and S19 are defective in both HeLa cells (Briones et al., 2001; Arellano-Reynoso et al., 2005; Roset et al., 2006, 2014) and peritoneal macrophages of C57BL/6 mice (Arellano-Reynoso et al., 2005) but, on the contrary, they behave as the parental strains in bone marrow cells also obtained from C57BL/6 mice (Salcedo et al., 2008; Roset et al., 2014). Another possible explanation for the

attenuation of *B. ovis* Δcgs could be related to the association that has been established between C β Gs and a dual pro- and anti-inflammatory response that transiently recruits neutrophils and suggests a controlled local inflammatory response (Degos et al., 2015). This controlled inflammatory response might be important for the establishment of the *Brucella* infection, since survival and replication inside phagocytes is a characteristic trait of *Brucella* that provides the bacterium with a safe environment. A strong inflammatory process would trigger a detrimental immune response against the pathogen but, on the contrary, a diminished inflammatory response in the absence of C β Gs would reduce the presence of suitable target cells for *Brucella* replication and, therefore, could influence the outcome of infection.

The $\Delta omp31\Delta cgs$ double mutant, defective in a major OMP and in periplasmic C β Gs, maintained or exacerbated the most severe phenotype of the corresponding single mutants. Thus, the susceptibility to DOC (**Table 4**) and *in vitro* growth defects were more prominent in the $\Delta omp31\Delta cgs$ mutant than in the single mutants, which would be in accordance with cell envelope modifications compromising the permeability of the bacterial cell to nutrients and toxic compounds. Strikingly, despite its important *in vitro* growth impairment and its increased killing during the first stage of infection in murine macrophages (**Figure 6C**), the $\Delta omp31\Delta cgs$ mutant behaved similarly to the Δcgs mutant in the mouse model, except for a lower spleen colonization at W3 p.i. (**Table 1**, **Figure 2**, and data not shown). Additionally, a third deletion of *omp10* or *omp19* did not produce apparent differences with respect to the $\Delta omp31\Delta cgs$ mutant in any of the characteristics evaluated and attenuation of the Δcgs mutant was not drastically intensified by the deletion of *omp10*, *omp19*, *bepC*, *ugpB*, or *omp25* (**Table 1**).

Similarly to *B. ovis* $\Delta omp31\Delta cgs$, the $\Delta omp10\Delta omp31\Delta omp25c$ mutant suffered a higher decrease of the intracellular CFU during the first 20 h of macrophage infection but both mutants multiplied properly after that moment (**Figures 6B,C**). This ability to replicate intracellularly might explain why, despite their impairment to infect mice at doses of 10^6 CFU/mouse, they persisted at least until week 11 p.i. – with splenic counts equivalent to those of the parental strain at that moment – when 10^8 CFU were inoculated (**Figure 2**). Increased killing inside professional phagocytes at the onset of infection could have dramatic effects on the outcome of infection when the lower dose of infection is used. However, higher doses of infection would allow some bacteria to escape to the bactericidal mechanisms of phagocytes and reach the replicative niche to establish a persistent infection thereafter. At least in part, the higher reduction of intracellular CFU at t20 could be related to a defective growth inside the phagocytes – mimicking that observed *in vitro* for both mutants (**Figure 1**) – and that might be due to alterations in OM permeability to nutrients and/or toxic compounds. On the other side, both mutants showed an opposed internalization pattern in HeLa non-professional phagocytes (**Figures 6E,F**) that does not correlate with their similar attenuation in mice. Since, in addition, other single and multiple mutants with analogous profiles in HeLa cells were not attenuated in mice (e.g., *B. ovis* $\Delta omp10\Delta omp31$ and $\Delta omp25\Delta omp25c$) (**Table 1** and **Figure 6**), an altered behavior in

HeLa cells of a *B. ovis* mutant does not imply attenuation in the mouse model.

The $\Delta omp10\Delta ugpB\Delta omp31$ mutant behaved in macrophages similarly to the $\Delta omp31\Delta cgs$ and $\Delta omp10\Delta omp31\Delta omp25c$ mutants (Figure 6B). However, although during the first 3 W p.i. the three mutants showed a similar pattern of spleen colonization in mice (Figure 2), the $\Delta omp10\Delta ugpB\Delta omp31$ mutant was progressively cleared from spleen thereafter (Figure 2D). Therefore, additional defects, preventing the establishment of a chronic infection, must be present in the $\Delta omp10\Delta ugpB\Delta omp31$ mutant. It must be noted that after W5 p.i., concomitantly with the splenic dampening of CFU, the antibody response induced by *B. ovis* PA $\Delta omp10\Delta ugpB\Delta omp31$ was higher than that observed in mice infected with the parental strain (Figure 2F) ($P < 0.05$), despite the higher spleen colonization of the latter (Figure 2A). This increased humoral immunity might contribute to the clearance of the mutant but, at the same time, be a relevant characteristic for an attenuated vaccine. Clearing of the mutant after W3 p.i. could also be related with defects impairing its colonization and/or survival inside reservoir cells involved in sustaining the chronic phase of infection. In the case of *B. abortus*, alternatively activated macrophages – more abundant during the chronic phase of infection – have been described as preferential target cells for survival and replication in mice (Xavier et al., 2013). This preference has been related with an increase in glucose availability in these cells (Xavier et al., 2013), which adds new evidence about the relevant role of metabolism in the acute phase of infection and/or in sustaining persistent *Brucella* infection (Hong et al., 2000; Ronneau et al., 2016; Barbier et al., 2018). Since transport through membranes of metabolic substrates, metals, and other compounds is a key mechanism for bacterial homeostasis, the changes in the bacterial surface suffered by the $\Delta omp10\Delta ugpB\Delta omp31$ mutant might lead to an altered transport of essential molecules that could impair survival in the reservoir cells. However, these changes would not have dramatic effects under *in vitro* growth conditions, at least in the culture medium used in this work (Figure 1).

According to its attenuation profile, the $\Delta omp10\Delta ugpB\Delta omp31$ mutant was considered the best candidate to evaluate its vaccine properties against in the mouse model. Three weeks after the challenge, when *B. ovis* PA reaches its peak of infection in unvaccinated mice (Figure 2), neither the virulent strain nor the vaccine strain were detected in spleen, while both strains were detected – although in low levels – in some mice vaccinated with *B. melitensis* Rev1 (Figure 8F). The protective activity of *B. ovis* $\Delta omp10\Delta ugpB\Delta omp31$ was accompanied by a good antibody response against *B. ovis* PA whole cells that was significantly higher than that obtained with *B. melitensis* Rev1 by the time of challenge (Figure 8F) and even higher ($P < 0.05$) than that observed in mice infected with the parental strain (Figure 2F). The development of specific antibodies is critical for the protective activity against *B. melitensis* of both killed and live strains (Vitry et al., 2014) and was described as even more relevant than cell-mediated immunity in protecting against *B. ovis* infection (Jiménez de Bagüés et al., 1994). Accordingly, the strong humoral immune response elicited by

B. ovis $\Delta omp10\Delta ugpB\Delta omp31$ could account for its remarkable protective activity against *B. ovis*. The similar levels of specific IgG₁, IgG_{2a}, and IgG_{2b} suggest a mixed Th1/Th2 response, also observed with other *B. ovis* PA attenuated mutants (Sancho et al., 2014), that is considered as an advantage for attenuated live vaccines in controlling both early and late events in *Brucella* infections (Vitry et al., 2014). *B. ovis* $\Delta omp10\Delta ugpB\Delta omp31$ also induced a memory immune response evidenced by the profile of cytokine secretion obtained with splenocytes of vaccinated mice after re-stimulation with *B. ovis* PA whole cells (Figure 8). The cytokine response, at least regarding the parameters evaluated in this work, resembled that obtained with the classical vaccine *B. melitensis* Rev1, the best available vaccine against *B. ovis* with proved protective activity in the natural host (OIE, 2017b). Both vaccination groups showed remarkable levels of IFN- γ , key cytokine for the control of *Brucella* infections (Zhan and Cheers, 1993; Murphy et al., 2001; Figure 8). Important secretion of IL-10, described as an anti-inflammatory cytokine that also suppresses phagolysosome fusion in macrophages contributing to *Brucella* survival in the host (Corsetti et al., 2013; Hop et al., 2018), was also detected in both vaccination groups (Figure 8). However, since both vaccines provided good protection against infection, this increase in IL-10 levels could reflect a strong activation of the immune response after a second exposure, that would neutralize the pathogen but that could also have detrimental effects for the host and would need to be controlled.

Although mutants should be evaluated simultaneously to establish accurate comparisons, and other experimental conditions in the murine model would provide a more accurate information (e.g., different challenge doses, interval vaccination-challenge), the level of protection conferred by the $\Delta omp10\Delta ugpB\Delta omp31$ mutant against *B. ovis* infection seems better than that previously described for other *B. ovis* attenuated vaccines inoculated by the i.p. route (Sancho et al., 2014; Soler-Lloréns et al., 2014; Silva et al., 2015b). Additionally, a $\Delta abcAB$ mutant of *B. ovis*, which is defective in a species-specific ABC transporter (Silva et al., 2011) and that even encapsulated did not provide good protection level in mice (Silva et al., 2015b), protected against *B. ovis* in rams (Silva et al., 2015a). Accordingly, the results obtained in this work encourage the evaluation of *B. ovis* $\Delta omp10\Delta ugpB\Delta omp31$ as vaccine in the natural host. Moreover, the usefulness of *B. ovis* $\Delta omp31\Delta cgs$ and $\Delta omp10\Delta omp31\Delta omp25c$ in rams should not be discarded, since the mouse model – although considered a good approach to evaluate the virulence of *Brucella* strains – has limitations (Kahl-McDonagh and Ficht, 2006; Grilló et al., 2012) and some virulent mutants in the mouse model were found attenuated in the natural host (Bellaire et al., 2003). Additionally, considering that they are avirulent in mice at low doses of infection, that they do not reach the maximum levels of infection at higher infection doses (Figure 2) and that they barely induce inflammation in spleen (Figure 2), the $\Delta omp31\Delta cgs$ and $\Delta omp10\Delta omp31\Delta omp25c$ mutants might be unable to produce epididymitis in rams. In addition to the protective properties, the three attenuated mutants would provide diagnostic advantages. They would not interfere with the serological diagnosis of infections caused by smooth *Brucella* and, since they are defective in major Omp31

that has been proposed as an interesting diagnostic antigen for *B. ovis* infection (Vizcaíno et al., 2001b), they would favor the differentiation between vaccinated and infected animals by using Omp31 as diagnostic antigen.

In addition to the development of a vaccine candidate against *B. ovis*, the results obtained in this work provide new information about the relationships among cell-envelope molecules of *B. ovis* and the peculiar characteristics of its OM. This knowledge could help to explain why *B. ovis*, despite its reported genome degradation (Tsolis et al., 2009), establishes persistent infections in its natural host whereas rough mutants derived from *S. Brucella* do not or why its pathogenicity differs from that of *B. melitensis* in the same preferred host.

AUTHOR CONTRIBUTIONS

NV, RS-M, and PS conceived the study and wrote the paper. RS-M, PS, NV, MM, CT, AC, and MZ performed the experimental work. All authors participated in the presentation

and discussion of the results and in the revision of the manuscript.

FUNDING

Financial support to RS-M (FPI Grant BES-2012-057056) and this work was provided by the Ministerio de Economía y Competitividad (MINECO) of Spain (Grants AGL2008-04514-C03-03, AGL2011-30453-C04-02, AGL2014-58795-C4-4-R – cofinanced with FEDER funds – and AGL2014-58795-C4-3-R). Funding was also provided by Aragon Government (Grupo de investigación en desarrollo A13-17D).

ACKNOWLEDGMENTS

We thank the staff of the animal experimentation and DNA sequencing facilities of the University of Salamanca for their helpful collaboration.

REFERENCES

- Arellano-Reynoso, B., Lapaque, N., Salcedo, S., Briones, G., Ciocchini, A. E., Ugalde, R., et al. (2005). Cyclic β -1,2-glucan is a brucella virulence factor required for intracellular survival. *Nat. Immunol.* 6, 618–625. doi: 10.1038/nri1202
- Barbier, T., Zúñiga-Ripa, A., Moussa, S., Plovier, H., Sternon, J. F., Lázaro-Antón, L., et al. (2018). *Brucella* central carbon metabolism: an update. *Crit. Rev. Microbiol.* 44, 182–211. doi: 10.1080/1040841X.2017.1332002
- Barquero-Calvo, E., Conde-Álvarez, R., Chacón-Díaz, C., Quesada-Lobo, L., Martirosyan, A., Guzmán-Verri, C., et al. (2009). The differential interaction of *Brucella* and *Ochrobactrum* with innate immunity reveals traits related to the evolution of stealthy pathogens. *PLoS One* 4:e5893. doi: 10.1371/journal.pone.0005893
- Bellaire, B. H., Elzer, P. H., Hagius, S., Walker, J., Baldwin, C. L., and Roop, R. M. II (2003). Genetic organization and iron-responsive regulation of the *Brucella abortus* 2,3-dihydroxybenzoic acid biosynthesis operon, a cluster of genes required for wild-type virulence in pregnant cattle. *Infect. Immun.* 71, 1794–1803. doi: 10.1128/IAI.71.4.1794-1803.2003
- Briones, G., Iñón de Iannino, N., Roset, M., Vigliocco, A., Paulo, P. S., and Ugalde, R. A. (2001). *Brucella abortus* cyclic β -1,2-glucan mutants have reduced virulence in mice and are defective in intracellular replication in HeLa cells. *Infect. Immun.* 69, 4528–4535. doi: 10.1128/IAI.69.7.4528-4535.2001
- Caro-Hernández, P., Fernández-Lago, L., de Miguel, M. J., Martín-Martín, A. I., Cloeckaert, A., Grilló, M. J., et al. (2007). Role of the Omp25/Omp31 family in outer membrane properties and virulence of *Brucella ovis*. *Infect. Immun.* 75, 4050–4061. doi: 10.1128/IAI.00486-07
- Castañeda-Roldán, E. I., Ouahrani-Bettache, S., Saldaña, Z., Avelino, F., Rendón, M. A., Dornand, J., et al. (2006). Characterization of SP41, a surface protein of *Brucella* associated with adherence and invasion of host epithelial cells. *Cell. Microbiol.* 8, 1877–1887. doi: 10.1111/j.1462-5822.2006.00754.x
- Cloeckaert, A., Debbarh, H. S., Zygmunt, M. S., and Dubray, G. (1996a). Production and characterisation of monoclonal antibodies to *Brucella melitensis* cytosoluble proteins that are able to differentiate antibody responses of infected sheep from rev. 1 vaccinated sheep. *J. Med. Microbiol.* 45, 206–213.
- Cloeckaert, A., de Wergifosse, P., Dubray, G., and Limet, J. N. (1990). Identification of seven surface-exposed *Brucella* outer membrane proteins by use of monoclonal antibodies: immunogold labeling for electron microscopy and enzyme-linked immunosorbent assay. *Infect. Immun.* 58, 3980–3987.
- Cloeckaert, A., Jacques, I., Bosseray, N., Limet, J. N., Bowden, R., Dubray, G., et al. (1991). Protection conferred on mice by monoclonal antibodies directed against outer-membrane-protein antigens of *Brucella*. *J. Med. Microbiol.* 34, 175–180. doi: 10.1099/00222615-34-3-175
- Cloeckaert, A., Tibor, A., and Zygmunt, M. S. (1999). *Brucella* outer membrane lipoproteins share antigenic determinants with bacteria of the family Rhizobiaceae. *Clin. Diagn. Lab. Immunol.* 6, 627–629.
- Cloeckaert, A., Verger, J. M., Grayon, M., Zygmunt, M. S., and Grépinet, O. (1996b). Nucleotide sequence and expression of the gene encoding the major 25-kilodalton outer membrane protein of *Brucella ovis*: evidence for antigenic shift, compared with other *Brucella* species, due to a deletion in the gene. *Infect. Immun.* 64, 2047–2055.
- Cloeckaert, A., Vizcaíno, N., Paquet, J. Y., Bowden, R. A., and Elzer, P. H. (2002). Major outer membrane proteins of *Brucella* spp.: past, present and future. *Vet. Microbiol.* 90, 229–247. doi: 10.1016/S0378-1135(02)00211-0
- Cloeckaert, A., Zygmunt, M. S., de Wergifosse, P., Dubray, G., and Limet, J. N. (1992). Demonstration of peptidoglycan-associated *Brucella* outer-membrane proteins by use of monoclonal antibodies. *J. Gen. Microbiol.* 138, 1543–1550. doi: 10.1099/00221287-138-7-1543
- Corsetti, P. P., de Almeida, L. A., Carvalho, N. B., Azevedo, V., Silva, T. M., Teixeira, H. C., et al. (2013). Lack of endogenous IL-10 enhances production of proinflammatory cytokines and leads to *Brucella abortus* clearance in mice. *PLoS One* 8:e74729. doi: 10.1371/journal.pone.0074729
- Degos, C., Gagnaire, A., Banchereau, R., Moriyón, I., and Gorvel, J. P. (2015). *Brucella* C β G induces a dual pro- and anti-inflammatory response leading to a transient neutrophil recruitment. *Virulence* 6, 19–28. doi: 10.4161/21505594.2014.979692
- Edmonds, M. D., Cloeckaert, A., and Elzer, P. H. (2002). *Brucella* species lacking the major outer membrane protein Omp25 are attenuated in mice and protect against *Brucella melitensis* and *Brucella ovis*. *Vet. Microbiol.* 88, 205–221. doi: 10.1016/S0378-1135(02)00110-4
- Ferguson, G. P., Datta, A., Baumgartner, J., Roop, R. M. II, Carlson, R. W., and Walker, G. C. (2004). Similarity to peroxisomal-membrane protein family reveals that *Sinorhizobium* and *Brucella* BacA affect lipid-A fatty acids. *Proc. Natl. Acad. Sci. U.S.A.* 101, 5012–5017. doi: 10.1073/pnas.0307137101
- Goolab, S., Roth, R. L., van Heerden, H., and Crampton, M. C. (2015). Analyzing the molecular mechanism of lipoprotein localization in *Brucella*. *Front. Microbiol.* 6:1189. doi: 10.3389/fmicb.2015.01189
- Grilló, M. J., Blasco, J. M., Gorvel, J. P., Moriyón, I., and Moreno, E. (2012). What have we learned from brucellosis in the mouse model? *Vet. Res.* 43:29. doi: 10.1186/1297-9716-43-29
- Haag, A. F., Myka, K. K., Arnold, M. F., Caro-Hernández, P., and Ferguson, G. P. (2010). Importance of lipopolysaccharide and cyclic β -1,2-glucans in

- Brucella*-mammalian infections. *Int. J. Microbiol.* 2010:124509. doi: 10.1155/2010/124509
- Hong, P. C., Tsois, R. M., and Ficht, T. A. (2000). Identification of genes required for chronic persistence of *Brucella abortus* in mice. *Infect. Immun.* 68, 4102–4107. doi: 10.1128/IAI.68.7.4102-4107.2000
- Hop, H. T., Reyes, A. W. B., Huy, T. X. N., Arayan, L. T., Min, W., Lee, H. J., et al. (2018). Interleukin 10 suppresses lysosome-mediated killing of *Brucella abortus* in cultured macrophages. *J. Biol. Chem.* 293, 3134–3144. doi: 10.1074/jbc.M117.805556
- Ignón de Iannino, N., Briones, G., Tolmasky, M., and Ugalde, R. A. (1998). Molecular cloning and characterization of *cgs*, the *Brucella abortus* cyclic β (1-2) glucan synthetase gene: genetic complementation of *Rhizobium meliloti* *ndvB* and *Agrobacterium tumefaciens* *chvB* mutants. *J. Bacteriol.* 180, 4392–4400.
- Jiménez de Bagüés, M. P., Elzer, P. H., Blasco, J. M., Marín, C. M., Gamazo, C., and Winter, A. J. (1994). Protective immunity to *Brucella ovis* in BALB/c mice following recovery from primary infection or immunization with subcellular vaccines. *Infect. Immun.* 62, 632–638.
- Kahl-McDonagh, M. M., and Ficht, T. A. (2006). Evaluation of protection afforded by *Brucella abortus* and *Brucella melitensis* unmarked deletion mutants exhibiting different rates of clearance in BALB/c mice. *Infect. Immun.* 74, 4048–4057. doi: 10.1128/IAI.01787-05
- Kittelberger, R., Diack, D. S., Vizcaíno, N., Zygmunt, M. S., and Cloeckert, A. (1998). Characterization of an immuno-dominant antigen in *Brucella ovis* and evaluation of its use in an enzyme-linked immunosorbent assay. *Vet. Microbiol.* 59, 213–227. doi: 10.1016/S0378-1135(97)00196-X
- LeVier, K., Phillips, R. W., Grippe, V. K., Roop, R. M. II, and Walker, G. C. (2000). Similar requirements of a plant symbiont and a mammalian pathogen for prolonged intracellular survival. *Science* 287, 2492–2493. doi: 10.1126/science.287.5462.2492
- Macedo, A. A., Silva, A. P., Mol, J. P., Costa, L. F., Garcia, L. N., Araújo, M. S., et al. (2015). The *abcEDCBA*-encoded ABC transporter and the *virB* operon-encoded type IV secretion system of *Brucella ovis* are critical for intracellular trafficking and survival in ovine monocyte-derived macrophages. *PLoS One* 10:e0138131. doi: 10.1371/journal.pone.0138131
- Manterola, L., Guzmán-Verri, C., Chaves-Olarte, E., Barquero-Calvo, E., de Miguel, M. J., Moriyón, I., et al. (2007). BvrR/BvrS-controlled outer membrane proteins Omp3a and Omp3b are not essential for *Brucella abortus* virulence. *Infect. Immun.* 75, 4867–4874. doi: 10.1128/IAI.00439-07
- Martín-Martín, A. I., Caro-Hernández, P., Sancho, P., Tejedor, C., Cloeckert, A., Fernández-Lago, L., et al. (2009). Analysis of the occurrence and distribution of the Omp25/Omp31 family of surface proteins in the six classical *Brucella* species. *Vet. Microbiol.* 137, 74–82. doi: 10.1016/j.vetmic.2008.12.003
- Martín-Martín, A. I., Sancho, P., de Miguel, M. J., Fernández-Lago, L., and Vizcaíno, N. (2012). Quorum-sensing and BvrR/BvrS regulation, the type IV secretion system, cyclic glucans, and BacA in the virulence of *Brucella ovis*: similarities to and differences from smooth brucellae. *Infect. Immun.* 80, 1783–1793. doi: 10.1128/IAI.06257-11
- Martín-Martín, A. I., Sancho, P., Tejedor, C., Fernández-Lago, L., and Vizcaíno, N. (2011). Differences in the outer membrane-related properties of the six classical *Brucella* species. *Vet. J.* 189, 103–105. doi: 10.1016/j.tvjl.2010.05.021
- Minnick, M. F., Sappington, K. N., Smitherman, L. S., Andersson, S. G., Karlberg, O., and Carroll, J. A. (2003). Five-member gene family of *Bartonella quintana*. *Infect. Immun.* 71, 814–821. doi: 10.1128/IAI.71.2.814-821.2003
- Murphy, E. A., Sathiyaseelan, J., Parent, M. A., Zou, B., and Baldwin, C. L. (2001). Interferon-gamma is crucial for surviving a *Brucella abortus* infection in both resistant C57BL/6 and susceptible BALB/c mice. *Immunology* 103, 511–518. doi: 10.1046/j.1365-2567.2001.01258.x
- Nicoletti, P. (2010). Brucellosis: past, present and future. *Prilozi* 31, 21–32.
- OIE (2017a). “Chapter 2.1.4. Brucellosis (*Brucella abortus*, *B. melitensis* and *B. suis*) (infection with *B. abortus*, *B. melitensis* and *B. suis*)”, in *Manual of Diagnostic Tests and Vaccines for Terrestrial Animals*. Paris: OIE. Available at: http://www.oie.int/fileadmin/Home/eng/Health_standards/tahm/2.01.04_BRUCELLOSIS.pdf
- OIE (2017b). “Chapter 2.7.8. Ovine epididymitis (*Brucella ovis*)”, in *Manual of Diagnostic Tests and Vaccines for Terrestrial Animals*. Paris: OIE. Available at: http://www.oie.int/fileadmin/Home/eng/Health_standards/tahm/2.07.08_OVIN_EPIDID.pdf
- Parent, M. A., Goenka, R., Murphy, E., Levier, K., Carreiro, N., Golding, B., et al. (2007). *Brucella abortus* *bacA* mutant induces greater pro-inflammatory cytokines than the wild-type parent strain. *Microbes Infect.* 9, 55–62. doi: 10.1016/j.micinf.2006.10.008
- Posadas, D. M., Martín, F. A., Sabio y García, J. V., Spera, J. M., Delpino, M. V., Baldi, P., et al. (2007). The TolC homologue of *Brucella suis* is involved in resistance to antimicrobial compounds and virulence. *Infect. Immun.* 75, 379–389. doi: 10.1128/IAI.01349-06
- Ronneau, S., Moussa, S., Barbier, T., Conde-Álvarez, R., Zúñiga-Ripa, A., Moriyón, I., et al. (2016). *Brucella*, nitrogen and virulence. *Crit. Rev. Microbiol.* 42, 507–525. doi: 10.3109/1040841X.2014.962480
- Roop, R. M. II, Robertson, G. T., Ferguson, G. P., Milford, L. E., Winkler, M. E., and Walker, G. C. (2002). Seeking a niche: putative contributions of the *hfq* and *bacA* gene products to the successful adaptation of the brucellae to their intracellular home. *Vet. Microbiol.* 90, 349–363. doi: 10.1016/S0378-1135(02)00220-1
- Roset, M. S., Ciocchini, A. E., Ugalde, R. A., and Ignón de Iannino, N. (2006). The *Brucella abortus* cyclic β -1,2-glucan virulence factor is substituted with O-ester-linked succinyl residues. *J. Bacteriol.* 188, 5003–5013. doi: 10.1128/JB.0086-06
- Roset, M. S., Ibañez, A. E., de Souza Filho, J. A., Spera, J. M., Minatel, L., Oliveira, S. C., et al. (2014). *Brucella* cyclic β -1,2-glucan plays a critical role in the induction of splenomegaly in mice. *PLoS One* 9:e101279. doi: 10.1371/journal.pone.0101279
- Sá, J. C., Silva, T. M., Costa, E. A., Silva, A. P., Tsois, R. M., Paixão, T. A., et al. (2012). The virB-encoded type IV secretion system is critical for establishment of infection and persistence of *Brucella ovis* infection in mice. *Vet. Microbiol.* 159, 130–140. doi: 10.1016/j.vetmic.2012.03.029
- Salcedo, S. P., Marchesini, M. I., Lelouard, H., Fugier, E., Jolly, G., Balor, S., et al. (2008). *Brucella* control of dendritic cell maturation is dependent on the TIR-containing protein Btp1. *PLoS Pathog.* 4:e21. doi: 10.1371/journal.ppat.0040021
- Salhi, I., Boigegrain, R. A., Machold, J., Weise, C., Cloeckert, A., and Rouot, B. (2003). Characterization of new members of the group 3 outer membrane protein family of *Brucella* spp. *Infect. Immun.* 71, 4326–4332. doi: 10.1128/IAI.71.8.4326-4332.2003
- Sancho, P., Tejedor, C., Sidhu-Muñoz, R. S., Fernández-Lago, L., and Vizcaíno, N. (2014). Evaluation in mice of *Brucella ovis* attenuated mutants for use as live vaccines against *B. ovis* infection. *Vet. Res.* 45:61. doi: 10.1186/1297-9716-45-61
- Seco-Mediavilla, P., Verger, J. M., Grayon, M., Cloeckert, A., Marín, C. M., Zygmunt, M. S., et al. (2003). Epitope mapping of the *Brucella melitensis* BP26 immunogenic protein: usefulness for diagnosis of sheep brucellosis. *Clin. Diagn. Lab. Immunol.* 10, 647–651. doi: 10.1128/CDLI.10.4.647-651.2003
- Sidhu-Muñoz, R. S., Sancho, P., and Vizcaíno, N. (2016). *Brucella ovis* PA mutants for outer membrane proteins Omp10, Omp19, SP41, and BepC are not altered in their virulence and outer membrane properties. *Vet. Microbiol.* 186, 59–66. doi: 10.1016/j.vetmic.2016.02.010
- Silva, A. P., Macêdo, A. A., Costa, L. F., Rocha, C. E., Garcia, L. N., Farias, J. R., et al. (2015a). Encapsulated *Brucella ovis* lacking a putative ATP-binding cassette transporter (Δ abcBA) protects against wild type *Brucella ovis* in rams. *PLoS One* 10:e0136865. doi: 10.1371/journal.pone.0136865
- Silva, A. P., Macêdo, A. A., Costa, L. F., Turchetti, A. P., Bull, V., Pessoa, M. S., et al. (2013). *Brucella ovis* lacking a species-specific putative ATP-binding cassette transporter is attenuated but immunogenic in rams. *Vet. Microbiol.* 167, 546–553. doi: 10.1016/j.vetmic.2013.09.003
- Silva, A. P., Macêdo, A. A., Silva, T. M., Ximenes, L. C., Brandão, H. M., Paixão, T. A., et al. (2015b). Protection provided by an encapsulated live attenuated Δ abcBA strain of *Brucella ovis* against experimental challenge in a murine model. *Clin. Vaccine Immunol.* 22, 789–797. doi: 10.1128/CI.00191-15
- Silva, T. M., Paixão, T. A., Costa, E. A., Xavier, M. N., Sá, J. C., Moustakas, V. S., et al. (2011). Putative ATP-binding cassette transporter is essential for *Brucella ovis* pathogenesis in mice. *Infect. Immun.* 79, 1706–1717. doi: 10.1128/IAI.01109-10
- Soler-Lloréns, P., Gil-Ramírez, Y., Zabalza-Baranguá, A., Iriarte, M., Conde-Álvarez, R., Zúñiga-Ripa, A., et al. (2014). Mutants in the lipopolysaccharide of *Brucella ovis* are attenuated and protect against *B. ovis* infection in mice. *Vet. Res.* 45:72. doi: 10.1186/PREACCEPT-4884962711194249
- Tibor, A., Decelle, B., and Letesson, J. J. (1999). Outer membrane proteins Omp10, Omp16, and Omp19 of *Brucella* spp. are lipoproteins. *Infect. Immun.* 67, 4960–4962.

- Tibor, A., Saman, E., de Wergifosse, P., Cloeckaert, A., Limet, J. N., and Letesson, J. J. (1996). Molecular characterization, occurrence, and immunogenicity in infected sheep and cattle of two minor outer membrane proteins of *Brucella abortus*. *Infect. Immun.* 64, 100–107.
- Tibor, A., Wansard, V., Bielartz, V., Delrue, R. M., Danese, I., Michel, P., et al. (2002). Effect of *omp10* or *omp19* deletion on *Brucella abortus* outer membrane properties and virulence in mice. *Infect. Immun.* 70, 5540–5546. doi: 10.1128/IAI.70.10.5540-5546.2002
- Tibor, A., Weynants, V., Denoel, P., Lichtfouse, B., De Bolle, X., Saman, E., et al. (1994). Molecular cloning, nucleotide sequence, and occurrence of a 16.5-kilodalton outer membrane protein of *Brucella abortus* with similarity to PAL lipoproteins. *Infect. Immun.* 62, 3633–3639.
- Tsolis, R. M., Seshadri, R., Santos, R. L., Sangari, F. J., García Lobo, J. M., de Jong, M. F., et al. (2009). Genome degradation in *Brucella ovis* corresponds with narrowing of its host range and tissue tropism. *PLoS One* 4:e5519. doi: 10.1371/journal.pone.0005519
- Vitry, M. A., Hanot Mambres, D., De Trez, C., Akira, S., Ryffel, B., Letesson, J. J., et al. (2014). Humoral immunity and CD4 + Th1 cells are both necessary for a fully protective immune response upon secondary infection with *Brucella melitensis*. *J. Immunol.* 192, 3740–3752. doi: 10.4049/jimmunol.1302561
- Vizcaino, N., Caro-Hernández, P., Cloeckaert, A., and Fernández-Lago, L. (2004). DNA polymorphism in the *omp25/omp31* family of *Brucella* spp.: identification of a 1.7-kb inversion in *Brucella cetaceae* and of a 15.1-kb genomic island, absent from *Brucella ovis*, related to the synthesis of smooth lipopolysaccharide. *Microbes Infect.* 6, 821–834. doi: 10.1016/j.micinf.2004.04.009
- Vizcaino, N., and Cloeckaert, A. (2012). “Biology and genetics of the *Brucella* outer membrane,” in *Brucella Molecular Microbiology and Genomics*, eds I. López-Goñi and D. O’Callaghan (Norfolk: Caister Academic Press), 133–161.
- Vizcaino, N., Cloeckaert, A., Zygmunt, M. S., and Fernández-Lago, L. (2001a). Characterization of a *Brucella* species 25-kilobase DNA fragment deleted from *Brucella abortus* reveals a large gene cluster related to the synthesis of a polysaccharide. *Infect. Immun.* 69, 6738–6748.
- Vizcaino, N., Kittelberger, R., Cloeckaert, A., Marín, C. M., and Fernández-Lago, L. (2001b). Minor nucleotide substitutions in the *omp31* gene of *Brucella ovis* result in antigenic differences in the major outer membrane protein that it encodes compared to those of the other *Brucella* species. *Infect. Immun.* 69, 7020–7028. doi: 10.1128/IAI.69.11.7020-7028.2001
- Xavier, M. N., Winter, M. G., Spees, A. M., den Hartigh, A. B., Nguyen, K., Roux, C. M., et al. (2013). PPAR γ -mediated increase in glucose availability sustains chronic *Brucella abortus* infection in alternatively activated macrophages. *Cell Host Microbe* 14, 159–170. doi: 10.1016/j.chom.2013.07.009
- Zhan, Y., and Cheers, C. (1993). Endogenous gamma interferon mediates resistance to *Brucella abortus* infection. *Infect. Immun.* 61, 4899–4901.
- Zygmunt, M. S., Cloeckaert, A., and Dubray, G. (1994). *Brucella melitensis* cell envelope protein and lipopolysaccharide epitopes involved in humoral immune responses of naturally and experimentally infected sheep. *J. Clin. Microbiol.* 32, 2514–2522.

Conflict of Interest Statement: The authors declare that the research was conducted in the absence of any commercial or financial relationships that could be construed as a potential conflict of interest.

Copyright © 2018 Sidhu-Muñoz, Sancho, Cloeckaert, Zygmunt, de Miguel, Tejedor and Vizcaino. This is an open-access article distributed under the terms of the Creative Commons Attribution License (CC BY). The use, distribution or reproduction in other forums is permitted, provided the original author(s) and the copyright owner(s) are credited and that the original publication in this journal is cited, in accordance with accepted academic practice. No use, distribution or reproduction is permitted which does not comply with these terms.



OPEN ACCESS

Edited by:

Konstantin V. Korotkov,
University of Kentucky, United States

Reviewed by:

Diego J. Comerci,
Instituto de Investigaciones
Biotecnológicas (IIB-INTECH),
Argentina
Suzana P. Salcedo,
UMR5086 Microbiologie Moléculaire
et Biochimie Structurale (MMSB),
France

*Correspondence:

Maite Iriarte
miriart@unav.es
Raquel Conde-Álvarez
rconde@unav.es

[†] Present address:

Yolanda Gil-Ramírez,
Centro Nacional de Tecnología y
Seguridad Alimentaria, San Adrian,
Spain
Estrella Martínez-Gómez,
Unidad de Gestión Clínica de Aparato
Digestivo, Servicio de Farmacología
Clínica, Instituto de Investigación
Biomédica de Málaga – IBIMA,
Hospital Universitario Virgen de la
Victoria, Universidad de Málaga,
CIBERehd, Málaga, Spain

Specialty section:

This article was submitted to
Infectious Diseases,
a section of the journal
Frontiers in Microbiology

Received: 21 June 2018

Accepted: 07 September 2018

Published: 27 September 2018

Citation:

Salvador-Bescós M, Gil-Ramírez Y,
Zúñiga-Ripa A, Martínez-Gómez E,
de Miguel MJ, Muñoz PM,
Cloeckaert A, Zygmunt MS, Moriyón I,
Iriarte M and Conde-Álvarez R (2018)
WadD, a New *Brucella*
Lipopolysaccharide Core
Glycosyltransferase Identified by
Genomic Search and Phenotypic
Characterization.
Front. Microbiol. 9:2293.
doi: 10.3389/fmicb.2018.02293

WadD, a New *Brucella* Lipopolysaccharide Core Glycosyltransferase Identified by Genomic Search and Phenotypic Characterization

Miriam Salvador-Bescós¹, Yolanda Gil-Ramírez^{1†}, Amaia Zúñiga-Ripa¹,
Estrella Martínez-Gómez^{1†}, María J. de Miguel², Pilar M. Muñoz², Axel Cloeckaert³,
Michel S. Zygmunt³, Ignacio Moriyón¹, Maite Iriarte^{1*} and Raquel Conde-Álvarez^{1*}

¹ Instituto de Salud Tropical, Instituto de Investigación Sanitaria de Navarra, and Departamento de Microbiología y Parasitología, Universidad de Navarra, Pamplona, Spain, ² Unidad de Tecnología en Producción y Sanidad Animal, Centro de Investigación y Tecnología Agroalimentaria, Instituto Agroalimentario de Aragón – IA2 (CITA – Universidad de Zaragoza), Zaragoza, Spain, ³ Institut National de la Recherche Agronomique, Université François Rabelais de Tours, UMR 1282, Nouzilly, France

Brucellosis, an infectious disease caused by *Brucella*, is one of the most extended bacterial zoonosis in the world and an important cause of economic losses and human suffering. The lipopolysaccharide (LPS) of *Brucella* plays a major role in virulence as it impairs normal recognition by the innate immune system and delays the immune response. The LPS core is a branched structure involved in resistance to complement and polycationic peptides, and mutants in glycosyltransferases required for the synthesis of the lateral branch not linked to the O-polysaccharide (O-PS) are attenuated and have been proposed as vaccine candidates. For this reason, the complete understanding of the genes involved in the synthesis of this LPS section is of particular interest. The chemical structure of the *Brucella* LPS core suggests that, in addition to the already identified WadB and WadC glycosyltransferases, others could be implicated in the synthesis of this lateral branch. To clarify this point, we identified and constructed mutants in 11 ORFs encoding putative glycosyltransferases in *B. abortus*. Four of these ORFs, regulated by the virulence regulator MucR (involved in LPS synthesis) or the BvrR/BvrS system (implicated in the synthesis of surface components), were not required for the synthesis of a complete LPS neither for virulence or interaction with polycationic peptides and/or complement. Among the other seven ORFs, six seemed not to be required for the synthesis of the core LPS since the corresponding mutants kept the O-PS and reacted as the wild type with polyclonal sera. Interestingly, mutant in ORF BAB1_0953 (renamed *wadD*) lost reactivity against antibodies that recognize the core section while kept the O-PS. This suggests that WadD is a new glycosyltransferase adding one or more sugars to the core lateral branch. WadD mutants were more sensitive than the parental strain to components

of the innate immune system and played a role in chronic stages of infection. These results corroborate and extend previous work indicating that the *Brucella* LPS core is a branched structure that constitutes a steric impairment preventing the elements of the innate immune system to fight against *Brucella*.

Keywords: lipopolysaccharide (LPS), bacterial pathogenesis, vaccine development, virulence factor, glycosyltransferase, brucellosis, *Brucella*

INTRODUCTION

Members of the genus *Brucella* are the etiologic agents of brucellosis, a worldwide spread zoonosis that affects ruminants, camelids, swine, dogs, and several forms of marine and terrestrial wildlife and causes abortions, infertility, and the subsequent economic losses in livestock. Humans become infected via direct contact with affected animals and through consumption of unpasteurized dairy products, and develop a chronic and debilitating condition that requires prolonged antibiotic treatment, being lethal in 1–5% of untreated cases (Ariza, 1999). Because of its impact on animal production and Public Health, it is estimated that brucellosis imposes a heavy burden in the developing world (McDermott et al., 2013).

The genus includes several nominal species that show host preferences¹. Those that have been known for a long time (often referred to as “classical” *Brucella* species) include *B. abortus* and *B. melitensis* (the *brucellae* that infect domestic ruminants), *B. suis* (infecting swine, reindeer, hares, and several species of wild rodents), *B. canis* (infecting dogs), *B. ovis* (not zoonotic and restricted to sheep), and *B. neotomae* (infecting the desert woodrat). Because of their early identification and their economic and public health importance, *B. abortus*, *B. melitensis*, and *B. suis* are the best-characterized members of the genus, and all of them produce smooth (S) glossy colonies, a morphology that reflects the existence of a lipopolysaccharide (LPS) carrying an O-polysaccharide (O-PS) linked to the core-lipid A section that anchors the molecule to the outer membrane (OM). These *Brucella* spp. behave as facultative intracellular parasites of professional and non-professional phagocytes, an ability that depends on a number of virulence factors, chiefly a type IV secretion system and a peculiar OM structure. Critical OM components such as the S-LPS, lipoproteins, and ornithine lipids differ in relevant molecular details from the homologous molecules that in other bacteria bear the pathogen-associated molecular patterns (PAMP) readily detected by innate immunity pattern recognition receptors (PRRs). Consequently, these *brucellae* induce comparatively low and delayed proinflammatory responses, which create a time window allowing the pathogen to traffic intracellularly in dendritic cells and macrophages to reach a safe niche before effective phagocyte activation takes place (Lapaque et al., 2005; Barquero-Calvo et al., 2007; Palacios-Chaves et al., 2011). In this regard, the *Brucella* S-LPS carries the most significant PAMP modifications and is thus a major virulence factor (Lapaque et al., 2005).

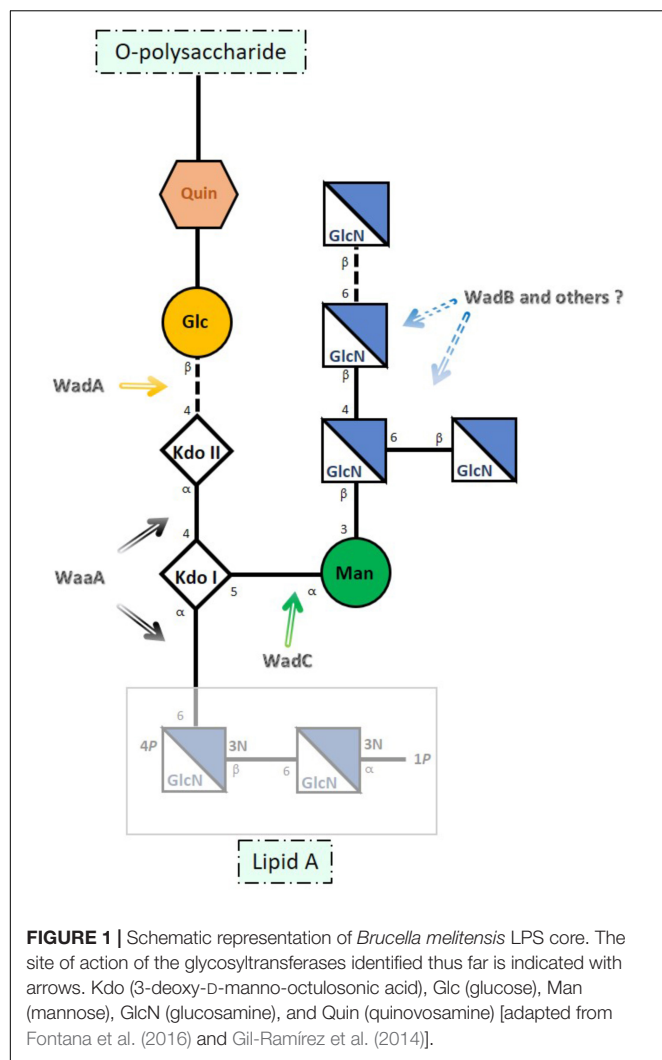
Whereas the structure of the O-PS (a *N*-formylperosamine homopolymer) and its role in virulence in animal models and in the natural host have been known for a long time, the importance of the core and its structure have only recently been established.

The core of *B. melitensis* LPS (Figure 1) is a branched oligosaccharide built of lipid A-linked 3-deoxy-D-manno-2-octulosonic acid (Kdo), glucose, 2-amino-2,6-dideoxy-D-glucose (quinovosamine), mannose, and 2-amino-2-deoxy-D-glucose [glucosamine (GlcN)] (Iriarte et al., 2004; Conde-Álvarez et al., 2012; Kubler-Kielb and Vinogradov, 2013; Gil-Ramírez et al., 2014; Fontana et al., 2016). This structure accounts for the *Brucella* LPS core overlapping epitopes (Rojas et al., 1994) an inner one comprising the Kdo residues plus the glucose bridging KdoII with the O-PS and an outer epitope encompassing the mannose and GlcN residues (Iriarte et al., 2004; González et al., 2008; Fontana et al., 2016). This last epitope plays a critical role in the binding of monoclonal antibodies (MoAbs) such as A68/24G12/A08 and A08/24D08/G09 (Conde-Álvarez et al., 2012; Fontana et al., 2016).

Accordingly, the reactivity with R-LPS-specific MoAbs strongly suggests that the structure elucidated for *B. melitensis* is conserved in the classical species (Bowden et al., 1995; Zygmunt et al., 2012). Moreover, availability of the corresponding structure of several mutants has also allowed assigning genes that upon mutation generate LPSs that lack [i.e., rough (R) LPS] or carry O-PS (Figure 1). Gene *wadA* corresponds to the enzyme linking KdoII and glucose, *wadC* to the mannosyltransferase acting on KdoI, and *wadB* to a glucosaminyltransferase involved in the assembly of the GlcN branch (González et al., 2008; Conde-Álvarez et al., 2012; Gil-Ramírez et al., 2014). These genes are highly conserved in the classical *Brucella* species (Monreal et al., 2003; Iriarte et al., 2004; González et al., 2008; Conde-Álvarez et al., 2012; Gil-Ramírez et al., 2014; Soler-Lloréns et al., 2016) and as expected, all *Brucella* genomes also carry a *waaA* homolog, the essential gene coding for the Kdo transferase of Gram-negative bacteria (Raetz and Whitfield, 2002; Iriarte et al., 2004). However, since most but not all glycosyltransferases involved in LPS synthesis are monofunctional (Raetz and Whitfield, 2002), it remains to be determined whether glucosaminyltransferases other than WadB are required for the synthesis of the GlcN branch.

Based on the complete structure of the core and the phenotype of mutants in *wadB* and *wadC*, it is postulated that the lack of acidic groups other than the two Kdo and lipid A phosphates and the mannose-GlcN branch account for the role of *Brucella* core in virulence both in cellular and animal models. By virtue

¹<http://www.bacterio.net/-allnamesac.html>



of the density of amino groups and close position to the inner core and lipid A, the GlcN tetrasaccharide both neutralizes and sterically protects those inner anionic groups, thereby hampering binding of bactericidal peptides and PRRs such as the activators of the antibody-independent classical complement pathway and MD2, the TLR4 co-receptor. Accordingly, core defects bolster proinflammatory responses causing an activation of innate immunity earlier than that of the wild type, thereby generating attenuation (Conde-Álvarez et al., 2012; Gil-Ramírez et al., 2014; Soler-Lloréns et al., 2014; Fontana et al., 2016). Also, although both *wadB* and *wadC* mutants maintain an intact O-PS, attenuation in mice is more severe for the latter (Conde-Álvarez et al., 2012; Gil-Ramírez et al., 2014; Fontana et al., 2016) strongly suggesting a correlation between the extent of core damage and the intensity of the immunoactivation that brings about attenuation. A complete elucidation of the genetics of *Brucella* LPS core could confirm such a correlation and, since LPS core mutants represent a tool for developing a new generation of brucellosis vaccines (Conde-Álvarez et al., 2013; Zhao et al., 2017), also provide a graded array of possibilities.

With these possibilities in mind, we investigated *B. abortus* 2308 genes annotated as glycosyltransferases for their possible involvement in LPS core synthesis and relevant biological effects.

MATERIALS AND METHODS

Bacterial Strains and Growth Conditions

The bacterial strains and plasmids used in this study are listed in **Supplementary Table S1**. All bacteria were grown either on tryptic soy agar (TSA, Pronadisa) plates or in tryptic soy broth (TSB, Scharlau) or Mueller-Hinton broth (Becton Dickinson, Difco) at 37°C. Where indicated, growth media were supplemented with kanamycin (Km) at 50 mg/ml, nalidixic acid (Nal) at 25 mg/ml, ampicillin (Amp) at 100 mg/ml, and/or 5% sucrose. Bacterial growth rates were determined at 37°C in Mueller-Hinton broth (Becton Dickinson, Difco), using a Bioscreen C apparatus (Lab Systems). All strains were stored in skim milk at -80°C. Work with *Brucella* was performed at the Biosafety Level 3 (BSL-3) laboratory facilities of the “Centro de Investigación Médica Aplicada de la Universidad de Navarra” (CIMA) and “Centro de Investigación y Tecnología Agroalimentaria de Aragón” (CITA), Spain.

DNA Manipulations and Analyses

Sequence data were obtained from *Kyoto Encyclopedia of Genes and Genomes* (KEGG²). Searches for DNA and protein homologies between *Brucella* species and other α -proteobacteria such as *Ochrobactrum*, *Rhizobium*, or *Agrobacterium* were carried out using KEGG, *Basic Local Alignment Sequence Tool* (BLAST³), and *Clustal Omega*⁴ from the *European Molecular Biology Laboratory – European Bioinformatics Institute* (EMBL-EBI⁵). New glycosyltransferase identification, using *B. abortus* 2308 was supported by *Carbohydrate-Active enZymes* database (CAZy⁶). Primers were designed using *Primer 3* input⁷ and synthesized by Sigma-Aldrich. Plasmid DNA was extracted with *Qiaprep spin Miniprep* (Qiagen GmbH). When needed, DNA was purified from agarose gels using *Qiaquick Gel* extraction kit (Qiagen) and sequenced by the *Servicio de Secuenciación* of CIMA.

Construction of Mutants

Open-reading frames (ORFs) BAB2_0133, BAB2_0135, BAB2_0105, and BAB1_1620 were mutagenized by in frame non-polar deletion in *B. abortus* 2308W (**Supplementary Table S1**).

For the construction of *Ba*ΔBAB2_0133 mutant, we first generated two PCR fragments: oligonucleotides BAB2_0133-F1 (5'-GCGTTGGACAAGTTGAGGTT-3') and BAB2_0133-R2 (5'-CATAGCGGTCGGTTAAATGC-3') were used to

²<http://www.genome.jp/kegg/>

³<http://blast.ncbi.nlm.nih.gov/Blast.cgi>

⁴<http://www.ebi.ac.uk/Tools/msa/clustalo>

⁵<http://www.ebi.ac.uk/>

⁶<http://www.cazy.org>

⁷<http://bioinfo.ut.ee/primer3-0.4.0/>

amplify a 572 base pairs (bp) fragment including codons 1–38 of BAB2_0133, as well as 458 bp upstream of the BAB2_0133 start codon. Oligonucleotides BAB2_0133-F3 (5'-GTATCGCCAGCCAATTTACGTCCGTATTGGAAGCCAAGA-3') and BAB2_0133-R4 (5'-CAGTAACAAAAGGCCGCTAT-3') were used to amplify a 442 bp fragment including codons 299–326 of BAB2_0133 and 355 bp downstream of the BAB2_0133 stop codon. Both fragments were ligated by overlapping PCR using oligonucleotides F1 and R4 for amplification, and the complementary regions between R2 and F3 for overlapping. The resulting fragment, containing the BAB2_0133 deletion allele, was cloned into pCR2.1 (Invitrogen), to generate plasmid pMSB-01, sequenced to ensure the maintenance of the reading frame, subsequently subcloned into the *Bam*HI and the *Xba*I sites of the suicide plasmid pJQK (Scupham and Triplett, 1997) and transformed into competent *E. coli* S17 λ pir (Simon et al., 1983). The resulting suicide pJQK-derived plasmid was introduced into *B. abortus* 2308 by conjugation. The first recombination event (integration of the suicide vector in the chromosome) was selected by Nal and Km resistance, and the second recombination (excision of the mutator plasmid leading to construction of the mutant by allelic exchange) was selected by Nal and sucrose resistance and Km sensitivity. The resulting colonies were screened by PCR with primers F1 and R4 which amplified a fragment of 1014 bp in the mutant and 1794 bp in the sibling strain that keeps the wild-type gene. Primers BAB2_0133-F1 and BAB2_0133-R5 (5'-AAGACCCAGTAGTTAGCACT-3') amplified a fragment of 919 bp only in the wild-type strain. The mutation generated results in the loss of the 80% of the ORF.

Ba Δ BAB2_0135 mutant was constructed following the same procedure and using oligonucleotides BAB2_0135-F1 (5'-TGGCGGCCGCTCTAGAACACCGGACTGCCTGATAA-3') and BAB2_0135-R2 (5'-CGGGCAATTTCCGGCATAG-3') that amplified a 240 bp fragment including codons 1–40 of BAB2_0135, as well as 120 bp upstream of the BAB2_0135 start codon, and oligonucleotides BAB2_0135-F3 (5'-CTATGCCGAAATTGCCCGCCGGTTTGGAATGCCGGTCAA-3') and BAB2_0135-R4 (5'-ATCCACTAGTTCTAGTTATGTAGCCGCCACCGTTT-3') that amplified a 232 bp fragment including codons 441–478 of BAB2_0135 and 115 bp downstream of the BAB2_0135 stop codon. The resulting colonies were screened by PCR with primers F1 and R4 that amplified a fragment of 472 bp in the mutant and 1672 bp in the sibling strain that keeps the wild-type gene. Primers BAB2_0135-F1 and BAB2_0135-R5 (5'-CGATTGCCAGTCCCAGAAAG-3') amplified a fragment of 628 bp only in the wild-type strain. The mutation generated results in the loss of the 84% of the ORF.

For the construction of *Ba* Δ BAB2_0105 mutant, oligonucleotides BAB2_0105-F1 (5'-GCGTGTCTACAGCCATGAA-3') and BAB2_0105-R2 (5'-CCGCCGAAATGTAGGAAGTG-3') amplified a 198 bp fragment including codons 1–33 of BAB2_0105, as well as 99 bp upstream of the BAB2_0105 start codon. Oligonucleotides BAB2_0105-F3 (5'-CACTTCCTACATTTCCGGCGGTATGTTGGATTGGGACGGG

T-3') and BAB2_0105-R4 (5'-GCCGAATATGACGCTTGCTA-3') amplified a 154 bp fragment including codons 307–330 of BAB2_0105 and 79 bp downstream of the BAB2_0105 stop codon. The resulting colonies were screened by PCR with primers F1 and R4 which amplified a fragment of 352 bp in the mutant and 1171 bp in the sibling strain which keeps the wild-type gene. Primers BAB2_0105-F1 and BAB2_0105-R5 (5'-CAAAGACCGGATATTGCGGG-3') amplified a fragment of 550 bp only in the wild-type strain. The mutation results in the loss of the 83% of the ORF.

Ba Δ BAB1_1620 mutant was constructed using oligonucleotides 1620-F1 (5'-GTACGCGGTCGTAGCTCAGT-3') and 1620-R2 (5'-CTCAAAGTACGACGCCATGA-3'), that amplified a 475 bp fragment including codons 1–23 of BAB1_1620 as well as 406 bp upstream of the ORF start codon. Oligonucleotides 1620-F3 (5'-TCATGGCGTCTCAGTTTGAGATAGCCCAACGTCACCAAAA-3') and 1620-R4 (5'-CTCTGCAATTCCTGCGATCA-3') were used to amplify a 410 bp fragment including codons 241–261 of the BAB1_1620 ORF and 347 bp downstream of the BAB1_1620 stop codon. Both fragments were ligated, cloned into pCR2.1 to generate plasmid pYRI-16, and subcloned into the suicide pJQK (pYRI-17). After conjugation with *B. abortus*, the resulting colonies were screened by PCR with primers 1620-F1 and 1620-R4 which amplified a 885 bp fragment in the mutant and 1536 bp in the parental strain. The mutation generated results in the loss of the 83% of the BAB1_1620 ORF.

The rest of the ORFs were mutagenized by recombination and gene disruption using as suicide vectors pJQK or pSKoriT (Tibor et al., 2002) carrying an internal fragment of the ORF.

For the construction of *Ba*::pJQK-BAB1_0114 mutants, we generated a PCR fragment using oligonucleotides BAB1_0114-F1 (5'-TCAACAAATCGGCCAAGGAC-3') and BAB1_0114-R2 (5'-GTCACGCGGTCAAAGTGG-3') which amplified a 481 bp fragment containing the region that codes for amino acids 248–407. The fragment was cloned into pCR2.1, to generate plasmid pMSB-17, sequenced and subcloned into the *Bam*HI and the *Xba*I sites of the suicide plasmid pJQK to obtain pMSB-28, and then transformed into competent *E. coli* S17 and transferred into *B. abortus* 2308 by conjugation. The integration of the suicide vector and disruption of the target gene were selected by Nal and Km resistance and by PCR combining BAB1_0114-F3 (5'-CCTATATTCCCCAGGCCGTT-3') with M13 Forward (5'-CTGGCCGTCGTTTTAC-3') or with M13 Reverse (5'-CAGGAAACAGCTATGAC-3'). These last two primers hybridize in the suicide vector inserted in the chromosome. BAB1_0114-F3 and M13 Forward amplified a fragment of 881 bp only in the mutant strain. Following the same strategy, we constructed the rest of insertion mutants:

Mutant *Ba*::pSKoriT-BAB1_0417 was obtained using oligonucleotides BAB1_0417-F1 (5'-TGATCGACCATGGCTCGG-3') and BAB1_0417-R2 (5'-TCAAGCCTGACCAGAAAGCC-3') which amplified a 295 bp fragment of BAB1_0417 (codon 37–134). The fragment was first cloned in pCR2.1 (pMSB-05), subcloned into the suicide plasmid pSKoriT

(pMSB-06), and transferred into *B. abortus* 2308 by conjugation. Primers M13 Reverse and BAB1_0417-F3 (5'-CTGTTTCCCGACCAGCTTG-3') amplified a fragment of 649 bp only in the mutant.

Oligonucleotides BAB2_0693-F1 (5'-CACTGCAAGCCG GTTACAAT-3') and BAB2_0693-R2 (5'-TGCAACGAAAT TCTGTCCGG-3') were used for the construction of *Ba::pJQK-BAB2_0693* mutant. F1 and R2 amplified a fragment of 416 bp (codons 249–386). We generated plasmid pMSB-16, subsequently subcloned into the suicide plasmid pJQK (pMSB-24), and conjugated into *B. abortus* 2308. Primers M13 Forward and BAB2_0693-F3 (5'-ACGAGCGCTATGATTTCGTC-3') amplified a fragment of 684 bp only in the mutant.

For the construction of *Ba::pJQK-BAB1_0932* mutants we used oligonucleotides BAB1_0932-F1 (5'-GCCGTCGTCCT GAATGTTAC-3') and BAB1_0932-R2 (5'-GCCATTATCCAG TGCAGCC-3') which amplified a 420 bp fragment of BAB1_0932 (codons 354–493). We generated plasmid pMSB-28, subsequently subcloned into the suicide plasmid pJQK (pMSB-29), and conjugated into *B. abortus* 2308. The resulting Nal–Km-resistant colonies were screened by PCR. Primers M13 Reverse and BAB1_0932-F3 (5'-GGCC GAGAATGGCTATATCA-3') amplified a fragment of 915 bp only in the mutant.

Mutant *Ba::pSKoriT-BAB1_0326* was obtained using oligonucleotides BAB1_0326-F1 (5'-GCACTCAACCGCT CAATTG-3') and BAB1_0326-R2 (5'-AGCACCGCATATTCA AAGGC-3') which amplified a 368 bp fragment of BAB1_0326 (codons 261–383) that was cloned into pCR2.1 to obtain pMSB-07. The fragment was then subcloned into the suicide pSKoriT (pMSB-10), and conjugated into *B. abortus* 2308. The resulting Nal–Km-resistant colonies were screened by PCR. Primers M13 Reverse and BAB1_0326-F3 (5'-ATGTTGCCATGTCGCTGTTT-3') amplified a fragment of 678 bp only in the mutant strain.

Construction of *Ba::pJQK-BAB1_0607* mutants was carried out using oligonucleotides BAB1_0607-F1 (5'-GCCAATGTCGTTCTCTCAA-3') and BAB1_0607-R2 (5'-CTTGGTGTCAGCCCCCTTTTC-3') which amplified a 449 bp fragment of BAB1_0607 (codons 278–427). We generated the pCR2.1-derived plasmid pMSB-19, then subcloned into the suicide plasmid pJQK (pMSB-21), and conjugated into *B. abortus* 2308. Primers M13 Forward and BAB1_0607-F3 (5'-TTCTTTCCAATGAGCGCACC-3') amplified a fragment of 800 bp only in the mutant.

We constructed two different mutants in ORF BAB1_0953 (*wadD*). The first, *Ba::pSKoriT-BAB1_0953*, carried the suicide vector inserted in the gene and was obtained with oligonucleotides BAB1_0953-F1 (5'-ACTTTTCGCCGAGCAACAAA-3') and BAB1_0953-R2 (5'-AGGCACGGTTTCATAGACGA-3') which amplified a 358 bp fragment of BAB1_0953 (codons 112–230). We generated plasmid pMSB-11, subsequently subcloned into the suicide plasmid pSKoriT (pMSB-12), and conjugated into *B. abortus*

2308. Primers M13 Forward and BAB1_0953-F3 (5'-GCTGGCTTCATGAAATCCGT-3') amplified a fragment of 612 bp in mutant.

We also constructed a non-polar *wadD* mutant (*BaΔwadD*) by in frame deletion. Oligonucleotides *wadD*-F1 (5'-TCTATAATGAGAGGCGGCTTTT-3') and *wadD*-R2 (5'-AGAAGTGCTGGTCCTGTTGT-3') were used to amplify a 304 (bp) fragment including codons 1–50 of BAB1_0953, as well as 154 bp upstream of the BAB1_0953 start codon. Oligonucleotides *wadD*-F3 (5'-ACAACAGGACCAGCACTT CTATCCTCACCTGCCATTCAA-3') and *wadD*-R4 (5'-CTGGTACTAGACGCCCTGTT-3') were used to amplify a 175 bp fragment including codons 281–324 of BAB1_0953 and 43 bp downstream of the BAB1_0953 stop codon. Both fragments were ligated by overlapping PCR using oligonucleotides F1 and R4 for amplification, and the complementary regions between R2 and F3 for overlapping. The resulting fragment, containing the BAB1_0953 deletion allele, was cloned directly into pJQK by the *InFusion* cloning system (Clontech) to generate pMSB-34. This suicide vector was sequenced to ensure the maintenance of the reading frame and transferred into *B. abortus* 2308 by conjugation. The resulting colonies were screened by PCR with primers F1 and R4 that amplified a fragment of 479 bp in the mutant and 1169 bp in the sibling strain which keeps the wild-type gene. Primers *wadD*-F1 and *wadD*-R5 (5'-AGGCACGGTTTCATAGACGA-3') amplified a fragment of 844 bp only in the wild-type strain. The mutation generated results in the loss of the 71% of the ORF and the mutant was called *BaΔwadD*.

Complementation of *wadD* Mutants

For complementation experiments, we performed a stable insertion of the miniTn7 transposon into the chromosome of *BaΔwadD* (Choi and Schweizer, 2006). For this purpose, we first generated a PCR product using oligonucleotides Tn7-*wadD*-F1 (5'-CGGGCTGCAGGAATTGCGATTCTTTGTGCCAGAT-3') and Tn7-*wadD*-R2 (5'-GCTTCTCGAGGAATTATCATCG CCGCATTGAAGAC-3'), which amplified a 1771 bp fragment including codons 1–323 of BAB1_0953 together with 481 bp upstream of the ORF start codon including the putative *wadD* promoter and 318 bp downstream the ORF stop codon. This PCR product was cloned into the corresponding sites of the linearized pUC18 R6KT miniTn7T Km^R vector (Llobet et al., 2009) to generate plasmid pMSB-44. The plasmid was sequenced to ensure the maintenance of the reading frame transformed into *E. coli* S17 and transferred to *BaΔwadD* mutant by tetra-parental conjugation between *E. coli* S17 (pMSB44), *E. coli* SM10 λpir (pTNS2), and *E. coli* HB101 (pRK2013). The conjugants harboring pMSB-44 were selected by plating the mating mixture onto TSA–Nal–Km plates that were incubated at 37°C for 4 days. To confirm that the transposon was inserted between genes *glmS* and *recG* (Choi and Schweizer, 2006), we performed PCR using different oligonucleotides: Tn7F (5'-TGGCTAAAGCAAACCTCTTCATTT-3') and Tn7R (5'-GCGGATTTGTCTACTCAGG-3') allowed to confirm that the Tn7 was inserted, oligonucleotides *Glms_B* (5'-GT CCTTATGGGAACGGACGT-3') and PTn7-R (5'-CACAGC

ATAACTGGACTGATT-3') confirmed that the transposon was inserted immediately after the gene *glmS*, and RecG-R (5'-TATATTCTGGCGAGCGATCC-3') and PTn7-L (5'-ATTAGCTTACGACGCTACACCC-3') confirmed that the transposon was inserted before the gene *recG* (Choi and Schweizer, 2006). The resulting strain was named *BaΔwadD::Tn7-PwadD*.

Crystal Violet Exclusion Test

To study if the mutants had smooth (complete LPS) or rough (*O*-PS-lacking LPS) phenotype, 5 ml of a crystal violet solution at 0.1 mg/ml in distilled water were used to cover isolated colonies on TSA plates for 20 s. Smooth colonies excluded crystal violet and looked white, whereas rough colonies captured crystal violet and looked violet.

LPS Extraction and Characterization

LPS was extracted by the proteinase-K sodium dodecyl sulfate (SDS) protocol (Dubray and Limet, 1987; Garin-Bastuji et al., 1990) with some modifications. Bacteria grown overnight in 10 ml of TSB were killed with 0.5% phenol during 3 days in agitation at 37°C. After that, samples were weighed and pipetted into small polycarbonate cap tubes and then suspended by ultrasounds in 2% SDS–60 mM Tris–HCl buffer (pH 6.8) at a concentration of 0.5 g (wet weight) of bacteria per 10 ml of buffer. Samples were then heated at 100°C for 10 min, and lysates were cooled to 55°C. This treatment was followed by digestion with 60 µl of proteinase-K at 2.5 mg/ml in HCl–Tris per ml of sample (Merck KGaA) for 3 h at 55°C, and overnight incubation at 20°C. Afterward, they were centrifuged at 20,000 × *g* for 30 min at room temperature, and the LPS was precipitated from the supernatant by addition of 3 volumes of methanol containing 1% sodium acetate-saturated methanol at –20°C. After 60 min, the precipitate was harvested by centrifugation at 5,000 × *g* for 15 min at 4°C and resuspended by sonication in 10 ml of distilled water. After a second methanol precipitation and centrifugation, the pellets were resuspended by sonication in 2–3 ml of 60 mM HCl–Tris (pH 6.8) and left at 37°C. Then samples were treated with 20 µl/ml of RNase and DNase stock solutions at 0.5 mg/ml in HCl–Tris (MP Biomedicals and Sigma–Aldrich, respectively) at 37°C for 30 min. Subsequently, the LPS was treated again with 5 µl/ml of proteinase K at 2.5 mg/ml in HCl–Tris, at 55°C for 3 h and then, at room temperature overnight. After a third methanol precipitation in the same conditions described above, the pellet containing LPS was recovered in 1 ml of distilled water and frozen at –20°C.

SDS–PAGE and Western Blots

Samples were mixed 1:1 with Sample buffer 2× (Bio-Rad), heated at 100°C for 10 min, and analyzed in Tris–HCl–glycine-12, 15, or 18% polyacrylamide gels (37.5:1 acrylamide/methylene-bisacrylamide ratio). Fifteen microliters of each sample were run at 30 mA constant current for 140 min. Finally, LPS molecules were revealed by the periodate-alkaline silver method (Tsai and Frasch, 1982).

For Western blot, gels were electro-transferred onto PVDF sheets (Whatman, Schleicher & Schuell, WESTRAN S.; 0.2 µm pore size) in a transfer buffer (pH 8.3) containing 0.025 M

Tris, 0.192 M glycine, and 20% (vol/vol) methanol. Transfer was performed at a constant voltage of 8 V and 200 mA for 30 min in a Trans-Blot Semi-Dry Transfer Cell (Bio-Rad). Antibodies used were MoAbs A68/24D08/G09 and A68/24G12/A08, which recognize core epitopes (Bowden et al., 1995), and a polyclonal serum from a rabbit infected with *B. melitensis* 16 M and bled at day 45.

Enzyme-Linked Immunosorbent Assay (ELISA)

Enzyme-Linked Immunosorbent Assay using whole bacteria (sonicated cells) as the antigen were performed as described previously (Cloeckaert et al., 1993a). MoAbs used were directed against *O*-PS, R-LPS, and the OM lipoproteins Omp10, Omp16, and Omp19 (Cloeckaert et al., 1990, 1993a,b, 1998). The anti-R-LPS MoAbs used were A68/03F03/D05 (IgG2b), A68/10A06/B11 (IgM), A68/24D08/G09 (IgG1), and A68/24G12/A08 (IgG3). The MoAbs specific for the *O*-PS epitopes were 2E11 (IgG3; M epitope), 12G12 [IgG1; C (A = M) epitope], 07F09 [IgG1; C (A = M) epitope], 12B12 [IgG3; C (M > A) epitope], 18H08 [IgA; C/Y (A = M) epitope], 04F9 [IgG2a; C/Y (A > M) epitope], and 05D4 [IgG1; C/Y (A > M) epitope]. The MoAbs specific for OM lipoproteins were A68/08E07/B11 (Omp10; IgG2a), A68/04G01/C06 (Omp16; IgG2a), A76/08C03/G03 (Omp16; IgG2a), and A76/10D03/H02 (Omp19; IgG2b). All MoAbs were used as hybridoma supernatants in ELISA.

Sensitivity to Polycationic Bactericidal Peptides

The minimal inhibitory concentration (MIC) of polymyxin B and poly-L-ornithine (both from Sigma–Aldrich) were determined in Mueller–Hinton medium. Exponentially growing bacteria were adjusted to an OD equivalent to 1 of the McFarland scale, and exposed to serial dilutions of the bactericidal peptides. MICs were determined by technical duplicates after 2 days of incubation at 37°C. Experiments were performed in triplicate.

Sensitivity to the Bactericidal Action of Non-immune Serum

Exponentially growing bacteria were adjusted to 10⁴ Colony Forming Units (CFU)/ml in saline and dispensed in duplicate in microtiter plates (30 µl/well) containing 60 µl of new-born bovine serum. After 90 min of incubation at 37°C with gentle agitation, complement action was blocked by adding brain heart infusion (BHI) broth (150 µl/well). After mixing the BHI broth with the bacterial suspension, 75 µl were plated by triplicate on TSA plates. Five days after incubation at 37°C, results were expressed as the percentage of CFU recovered with respect to control samples where new-born bovine serum was substituted by PBS. The experiment was repeated three different times.

Virulence in Mice

Seven-week-old female BALB/c mice (ENVIGO, Harlan) were lodged in cages in BSL-3 facilities with water and food

ad libitum for 2, 8, or 12 weeks. Six groups of five mice each were inoculated with *Ba*Δ*wadD* or *Ba*-parental. Inocula were prepared in sterile PBS and each mouse was administered intraperitoneally approximately with 5×10^4 CFU in 0.1 ml. To assess the exact dose retrospectively, dilutions of each inoculum were plated by triplicate on TSA plates. Spleen CFUs in infected mice were counted at 2, 8, and 12 weeks after inoculation. The CFU counts were normalized by logarithmic transformation and the mean log CFU/spleen values and the standard deviations were calculated. The spleens were weighed and homogenized in 9 volumes of PBS and serial 10-fold dilutions were accomplished and plated by triplicate on TSA plates. After 5 days of incubation at 37°C the colonies were checked by crystal violet exclusion test and PCR.

Statistical Analysis

Statistical significance for sensitivity to normal serum was evaluated with one-way ANOVA followed by Dunnett's multiple comparisons test ($***p < 0.0001$). For virulence analysis, statistical significance between the parental strain and the *wadD* mutant was evaluated using Student's *t*-independent-samples test ($*p < 0.05$).

RESULTS

Screening for Putative LPS Core Glycosyltransferases

A bioinformatic search in the Carbohydrate-Active Enzymes database CAZy⁸ revealed 23 ORFs in the genome of *B. abortus* 2308 (Supplementary Table S1) that could code for glycosyltransferases. We excluded from further analysis BAB1_0108-*cgs*, which is involved in cyclic glucan synthesis (Briones et al., 2001), BAB1_1786-*mtgA* and BAB1_1450-*murG*, both related to peptidoglycan synthesis, BAB1_1171-*lpxB*, probably implicated in lipid A formation (Iriarte et al., 2004), and BAB1_0553-*wbkA*, BAB1_0563-*wbkE*, BAB1_1000-*wboA* and BAB1_1000-*wboB*, four genes that belong to the O-PS synthesis route (McQuiston et al., 1999; Godfroid et al., 2000; González et al., 2008). Similarly, four ORFs correspond to those glycosyltransferases already known to be involved in the synthesis of the LPS core: BAB1_0639-*wadA* (Monreal et al., 2003), BAB1_0351-*wadB* (Gil-Ramírez et al., 2014), BAB1_1522-*wadC* (Conde-Álvarez et al., 2012), and BAB2_0209-*waaA* (Iriarte et al., 2004) (see the section "Introduction"). The remaining 11 ORFs are listed in Table 1, and data on their presence in other *Brucella* spp. and genetic location are in the Supplementary Material (Supplementary Table S2 and Supplementary Figure S1). Of these, seven (BAB1_0953, BAB2_0105, BAB2_0133, BAB2_0135, BAB1_1620, BAB1_0607, and BAB1_0932) were highly conserved in all *Brucella* spp., but four (BAB2_0693, BAB1_0417, BAB1_0114, and BAB1_0326) presented significant differences when compared to *B. abortus* sequences, mainly due to frameshifts generating shorter proteins

(Supplementary Table S2). Perusal of the literature revealed some information on 4 of those 11 putative glycosyltransferases. Expression of BAB1_0326, BAB2_0133, and BAB2_0135 has been shown to be controlled by MucR, a general virulence regulator in *Brucella* (Caswell et al., 2013). However, although it has been reported that *B. abortus* and *B. melitensis* *mucR* mutants have a defective LPS core, the glycosyltransferases involved have not been identified (Caswell et al., 2013; Mirabella et al., 2013). Also, BAB1_1620 expression has been reported to be controlled by BvrR/BvrS, a master regulator of *Brucella* virulence that modulates OM homeostasis and undetermined aspects of LPS structure (Manterola et al., 2005; Viadas et al., 2010).

We first analyzed the MucR and BvrR/BvrS controlled ORFs for involvement in LPS synthesis. To this end, we constructed an insertion mutant in BAB1_0326 (since the downstream ORF is oriented in the opposite direction) as well as non-polar deletion mutants in BAB2_0133 and BAB2_0135 (both part of an operon), and BAB1_1620 (which, although isolated, is surrounded by genes implicated in the cell cycle). These four mutants maintained the S phenotype in the crystal violet assay, suggesting that they kept an intact O-PS. Then, SDS-proteinase-K LPSs were analyzed by SDS-PAGE and Western blot with both a polyclonal serum against *S. brucellae* and anti-core MoAbs A68/24G12/A08 and A68/24D08/G09, using as controls LPS from *B. abortus* 2308W (*Ba*-parental), a *B. abortus* *wadC* mutant (*Ba*Δ*wadC*), and a *R. per* mutant (*Ba*Δ*per*) (Martínez-Gómez et al., 2018). The LPS of the four mutants presented S and R fractions with migration profiles identical to those of *Ba*-parental LPS and reacted similarly with the serum and MoAbs (Supplementary Figure S2) strongly suggesting that the corresponding ORFs are not required for normal LPS synthesis. When we complemented these observations by inoculating BALB/c mice with BAB2_0133, BAB2_0135, and BAB1_1620 mutants, they produced CFU/spleen that did not differ from those of *Ba*-parental at weeks 2 ($p = 0.99$; 0.75 and 0.45, respectively) and 8 ($p = 0.95$; 0.99 and 0.99) after infection. Moreover, mutants in BAB2_0133 and BAB1_1620 behaved similarly to *Ba*-parental in polycationic peptide resistance, and the former also performed as *Ba*-parental in sensitivity to normal serum (Supplementary Figure S3). These results are consistent with the idea that the putative glycosyltransferases regulated by MucR or BvrR/BvrS are not involved in the synthesis of LPS or of other components implicated in virulence, at least under the conditions used in this study.

To investigate whether the remaining seven putative glycosyltransferases (BAB1_0953, BAB2_0105, BAB2_0693, BAB1_0607, BAB1_0114, BAB1_0932, and BAB1_0417) were required for LPS synthesis, we constructed *B. abortus* 2308W insertion mutants in each of them. All mutants were S by the crystal violet assay and the analysis of the extracted LPS showed S fractions with a migration profile like that of *Ba*-parental and reacted similarly with the anti *S-Brucella* polyclonal serum (Figure 2 and Supplementary Figure S4). Interestingly, although keeping the S fraction, mutant in BAB1_0953 lost reactivity in the R fraction, suggesting a

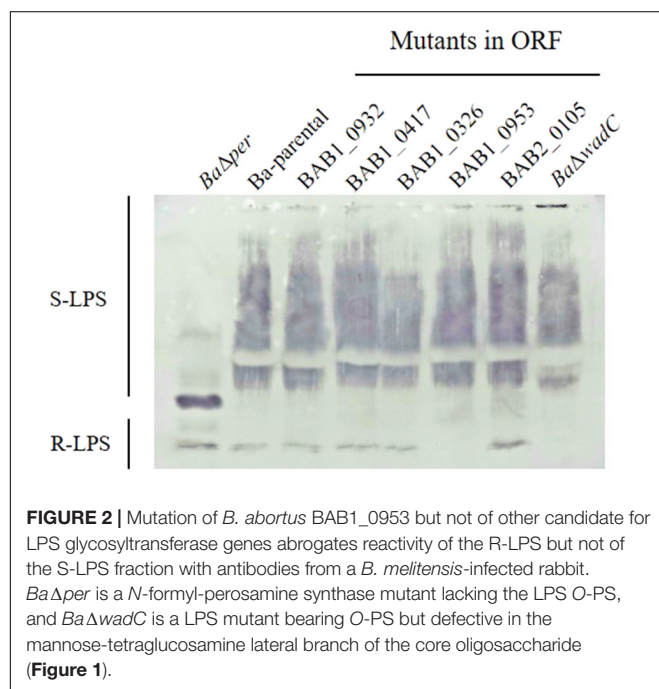
⁸<http://www.cazy.org>

TABLE 1 | ORF coding for *B. abortus* hypothetical glycosyltransferases, family to which they belong, predicted function, and the corresponding mutant LPS phenotype by Western blot analysis.

ORF	Family	Predicted function (KEGG)	Mutant LPS reactivity	
			O-PS ^a	R-LPS ^b
BAB1_0326	2	Glycosyltransferase	+	+
BAB2_0133	2	Glycosyltransferase	+	+
BAB2_0105	2	Glycosyltransferase	+	+
BAB2_0693	2	Glycosyltransferase	+	+
BAB1_0953	2	Glycosyltransferase	+	–
BAB1_1620	25	Glycosyltransferase	+	+
BAB1_0607	51	Penicillin-binding protein 1A transpeptidase domain – Glycosyltransferase	+	+
BAB1_0114	51	Penicillin-binding protein transpeptidase domain: ATP/GTP-binding site motif A (P-loop) – Glycosyltransferase	+	+
BAB1_0932	51	Penicillin-binding protein 1A transpeptidase domain – Glycosyltransferase	+	+
BAB2_0135	83	Possible dolichyl-phosphate-mannose-protein mannosyltransferase family protein	+	+
BAB1_0417	nc ^c	Conserved hypothetical protein	+	+

^aReactivity to polyclonal serum from a rabbit infected with *B. melitensis* 16M. ^bReactivity to monoclonal antibodies anti-R-LPS: A68/24G12/A08 and A68/24D08/G09.

^cGlycosyltransferase family non-classified.



defect in the core and/or lipid A epitope(s) recognized by polyclonal sera of infected animals (Rojas et al., 2001). Since this was not observed for the other mutants, we investigated further BAB1_0953 and the phenotype associated with its mutation.

BAB1_0953 Encodes WadD, a Previously Unidentified Glycosyltransferase Involved in the Synthesis of the LPS Core Lateral Branch

BAB1_0953 is an isolated gene and the adjacent ORFs are encoded in the complementary strand. Thus, it was very

unlikely that a polar effect caused the LPS phenotype of the insertion mutant. However, to rule out such a possibility, we constructed a non-polar deletion mutant, hereafter named *BaΔwadD* following the nomenclature previously established for *Brucella* LPS core genes (Reeves et al., 1996; Gil-Ramírez et al., 2014). *BaΔwadD* LPS showed a migration profile similar to that of *Ba*-parental in the high molecular weight S-LPS fraction and an increased mobility in the R-LPS one. Western-blot analysis with a polyclonal serum showed that, while the former fraction kept the reactivity with this serum, the latter failed to react indicating a significant alteration of the core-lipid A epitopes. To assign the defect to the core oligosaccharide, we probed the LPS with MoAbs A68/24G12/A08 and A68/24D08/G09, the binding of which to the R-LPS requires an intact mannose-GlcN tetrasaccharide (Conde-Álvarez et al., 2012; Fontana et al., 2016). Both antibodies failed to react with the R-LPS fraction and this failure was reverted upon insertion of a complete *wadD* gene in the bacterial chromosome of the deletion mutant (*BaΔwadD*::Tn7-PwadD). Moreover, this complementation restored both the migration pattern of the R-LPS fraction to the level of the *Ba*-parental LPS and the reactivity with the polyclonal serum (Figure 3). An ELISA with several anti-core MoAbs and whole bacteria confirmed the core defect (Figure 4, upper panel).

We only observed small but constant differences in reactivity of *Ba*-parental and *BaΔwadD* with anti-Outer Membrane Proteins (OMP) antibodies (Figure 4, lower panel). Although considering the limitations of the method used, this suggests that the presence of the O-PS and the defect in the core LPS could generate a steric hindrance that would allow the access of antibodies to the OMPs (Bowden et al., 1995) or the possibility that *wadD* mutation could affect the amount of LPS in the OM or how it is inserted in the bacterial surface.

Although as signaled above, the final confirmation would require a complete chemical analysis, all these results

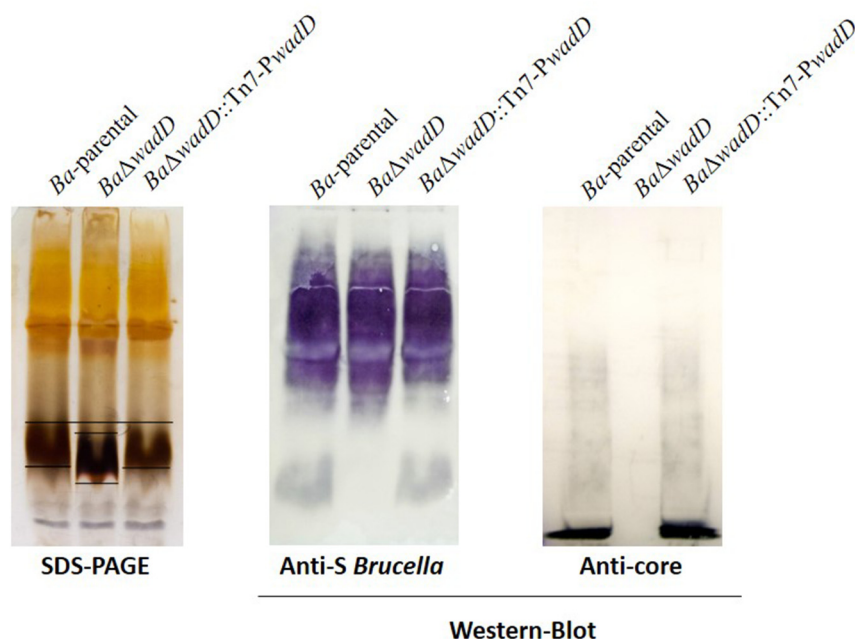


FIGURE 3 | Mutation of *wadD* generates an LPS core defect. Left panel, SDS-PAGE electrophoresis and silver staining of SDS-proteinase K extracts; central panel, Western blot analysis of SDS-proteinase K extracts with a polyclonal serum of a *B. melitensis*-infected rabbit; right panel, Western blot analysis of SDS-proteinase K extracts with monoclonal anti-core antibody A68/24G12/A08.

strongly suggest that *wadD* encodes a previously unidentified glycosyltransferase involved in the synthesis of the core lateral branch.

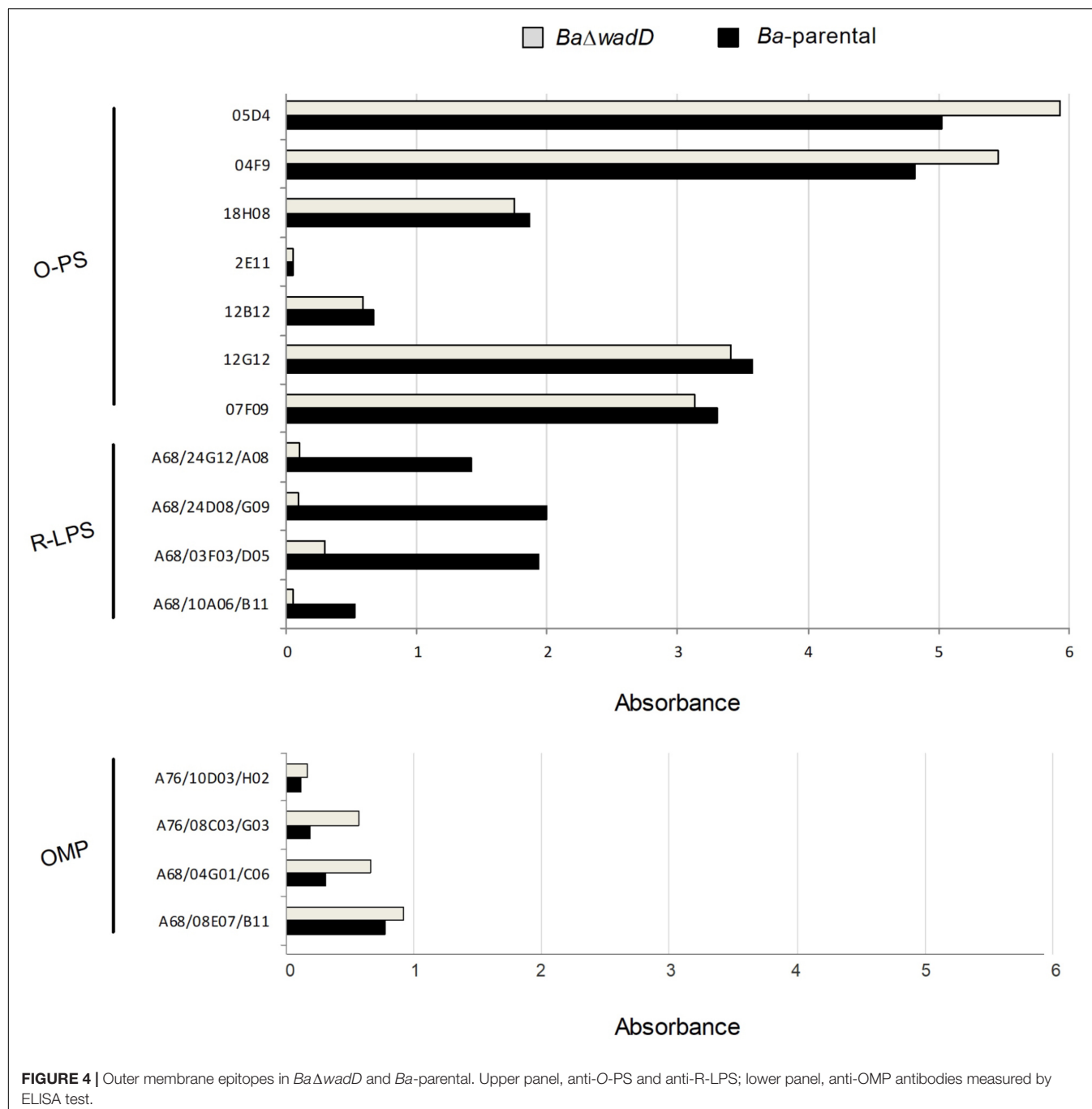
WadD Orthologs Are Present in all *Brucella* spp. but in a Recently Characterized Isolate From Amphibians

In silico analysis (Supplementary Figure S5) showed that *wadD* was highly conserved in the core *brucellae* including the “classical” spp. *B. melitensis*, *B. suis* (smooth LPS), and *B. ovis* and *B. canis* (rough LPS) and also in other “non-classical” smooth *Brucella* spp.: *B. pinnipedialis*, *B. microti*, *B. ceti*, and *B. vulpis*. We also analyzed the presence of *wadD* in the group of early-diverging *brucellae* that depart from the classical spp. and includes *B. inopinata* strain BO1, *B. inopinata*-like strain BO2, an isolated strain from native rodents in Australia (NF2653), and the *Brucella* spp. recently isolated from amphibians. These early-diverging *Brucella* produce an atypical LPS (Scholz et al., 2010; Tiller et al., 2010; Soler-Lloréns et al., 2016; Al Dahouk et al., 2017). Unexpectedly, *wadD* was present in all of them but absent in *Brucella* spp. B13-0095, one of the four *Brucella* strains isolated from frogs that have been completely sequenced (Soler-Lloréns et al., 2016). In contrast, this strain conserves *wadB* and *wadC*. Finally, WadD was 72 and 71% homologous to *Ochrobactrum anthropi* and *O. intermedium* orthologs, respectively, two species that also belong to the α -2 *Proteobacteria* subclass and are the closest genetic neighbors of *Brucella*.

Dysfunction of *wadD* Generates Increased Sensitivity to Cationic Peptides and Normal Serum

To test if the core defect displayed by *BaΔwadD* affected resistance to polycationic peptides, we used poly-L-ornithine, a mildly bactericidal cationic peptide and the two known core mutants *BaΔwadB* and *BaΔwadC* plus the parental strain as controls. The results (Figure 5A) showed that *wadD* dysfunction brought about a sensitivity similar to that of *BaΔwadB* but inferior to that of *BaΔwadC*. These differences in sensitivity were not due to growth defects because *BaΔwadD* had a growth rate similar to that of *Ba-parental*, and experiments with the highly bactericidal lipopeptide polymyxin B confirmed the role of *wadD* (*BaΔwadD* MIC = 0.094 μ g/ml versus MIC = 2 μ g/ml for both the mutant complemented with wild-type *wadD* and *Ba-parental*).

S. brucellae are resistant to the bactericidal action of normal serum, a property associated with both the O-PS hindrance to inner OM targets such as OMPs and the PAMP modifications of the core that reduce binding of the complement activators of the antibody-independent classical pathway (Conde-Álvarez et al., 2012; Gil-Ramírez et al., 2014; Fontana et al., 2016). We compared the sensitivity to newborn bovine and ovine serum of *Ba-parental* and *wadB*, *wadC*, or *wadD* mutants and observed that the three core mutants were more sensitive than *Ba-parental*. The effect was more remarkable for mutant *wadC* than for *wadD* or *wadB* mutants (Figure 5B).



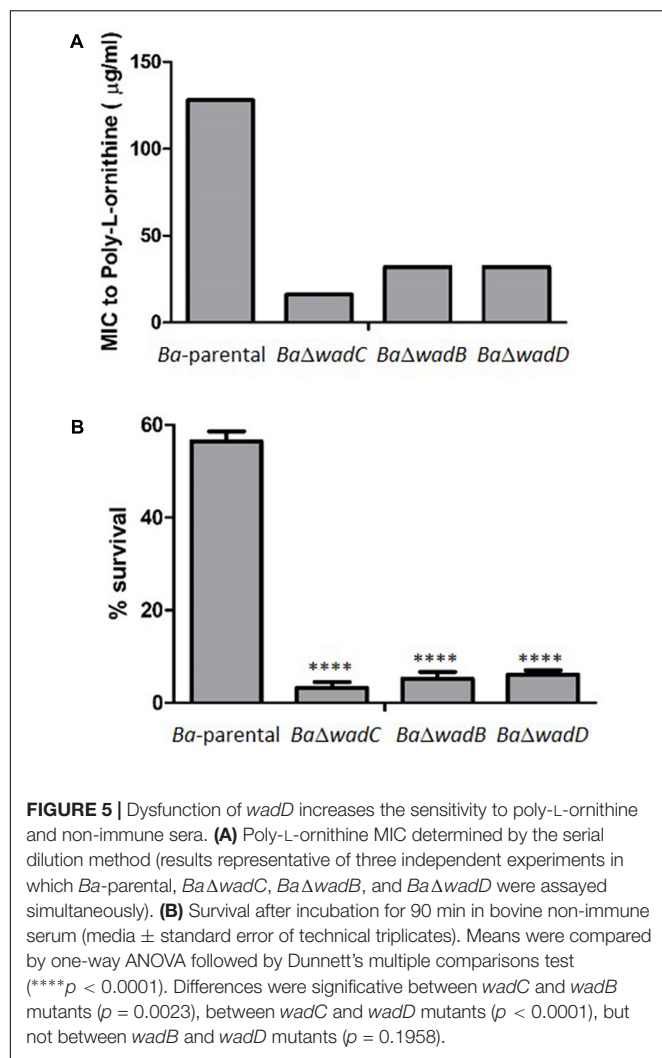
Dysfunction of *wadD* Generates Attenuation Detectable in the Chronic Phase in the Mouse Model

To analyze the role of *wadD* in virulence, we infected BALB/c mice ($n = 5$) with *Ba*Δ*wadD* or *Ba*-parental and compared the CFU/spleen at weeks 2, 8, and 12 (Figure 6). At weeks 8 and 12 post-infection, the CFU numbers of *Ba*Δ*wadD* were significantly lower than those of *Ba*-parental ($p = 0.0003$ and $p = 0.0073$, respectively), showing that *wadD* is required for full *Brucella* virulence in mice. This result is in line with previous observations

with *wadB* and *wadC* mutants (Conde-Álvarez et al., 2012; Gil-Ramírez et al., 2014) and further confirms that an intact LPS core is necessary for virulence.

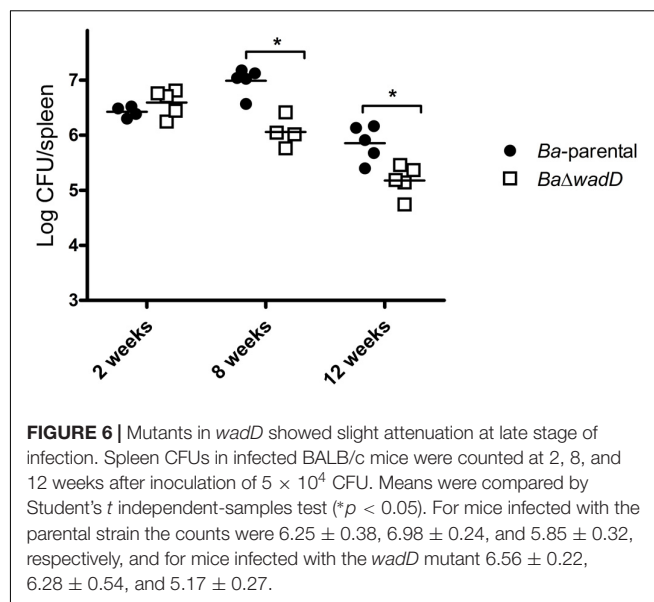
DISCUSSION

In this work, we have analyzed the role of ORFs BAB1_0114, BAB1_0417, BAB2_0693, BAB1_0932, BAB1_0607, BAB2_0105, BAB1_1620, BAB2_0133, BAB2_0135, and BAB1_0326 annotated as glycosyltransferases in the *B. abortus* genome.



Our results indicate that mutants in these ORFs react similarly to the parental strain in the S and R-LPS fractions and suggest that, in the studied conditions and with the available techniques, they seem not to be required for the synthesis of a complete LPS. Interestingly, the last three ORFs have been shown to be controlled by *mucR*, a regulator of *Brucella* virulence. Although it has been reported that *B. abortus* and *B. melitensis* *mucR* mutants have a defect in the core LPS (Caswell et al., 2013; Mirabella et al., 2013), the glycosyltransferases responsible for this defect have not been identified. In this work we have shown that mutation of the *mucR*-regulated putative glycosyltransferases BAB2_0133, BAB2_0135, and BAB1_0326 (Caswell et al., 2013) does not affect the synthesis of the core, at least in the growth conditions tested. Nevertheless, since the expression of these genes seems to be repressed by *mucR* (Caswell et al., 2013), a single mutation in the ORF could not be sufficient for the complete clarification of their role in LPS synthesis and further work would be required.

We have also analyzed in detail the role of the hypothetical glycosyltransferase BAB1_1620, as it is regulated by the master two-component regulator BvrR/BvrS that controls *Brucella*



virulence and the expression of surface components. According to our results, this ORF is not required for the synthesis of a complete LPS and is not implicated in surface-dependent characteristics that confer resistance to polycationic peptides or in virulence in the mouse model.

More interestingly, we report the identification of *wadD*, a gene encoding a previously unidentified glycosyltransferase involved in the synthesis of the core section not linked to the O-PS and thus, corroborate and extend previous work indicating that the *Brucella* LPS core is a branched structure that constitutes a steric impairment preventing the elements of the innate immune system to fight against *Brucella* (Conde-Álvarez et al., 2012; Kubler-Kielb and Vinogradov, 2013; Gil-Ramírez et al., 2014; Fontana et al., 2016), and contribute to *Brucella* virulence.

The discovery of genes *wadC* and *wadB*, involved in the synthesis of the lateral branch not linked to the O-PS, was critical for the understanding of the structure and the role of the core section in virulence. It has been clearly demonstrated that in a *wadC* mutant, the complete core lateral branch is absent because this mutant cannot incorporate the mannose residue that is the depart of the lateral branch and it links to the lipid A-core section (Conde-Álvarez et al., 2012; Fontana et al., 2016). In accordance, deletion of *wadC* results in higher sensitivity to polycationic peptides and complement, better recognition by the CD14–MD2–TLR4 receptor complex, maturation of dendritic cells, secretion of pro-inflammatory cytokines (including Th1-type cytokines IL-12 and IFN- γ), and attenuation in mice (Conde-Álvarez et al., 2012; Fontana et al., 2016). A *wadB* mutant is also more sensitive to elements of the innate immune system and shows attenuation in mice, although not to the levels of the *wadC* mutant (Gil-Ramírez et al., 2014). As we show here, disruption of *wadD* in *B. abortus* leads to a S strain with a core defect less severe than that of the *wadC* mutant, more sensitive to polycationic peptides and normal serum than the parental strain and attenuated in the murine model. Interestingly, its sensitivity

to polycationic peptides is similar to that of the *wadB* mutant (Gil-Ramírez et al., 2014) and not as strong as that of the *wadC* mutant (Conde-Álvarez et al., 2012), that has lost the complete branch, and its role in virulence became apparent already at 8 weeks post-infection.

The resistance to polycationic peptides and the bactericidal action of normal serum of mutant *wadD* strongly suggest a role in thwarting some effectors of innate immunity and that this could be manifested in the early stages of infection. However, to observe these effects would depend on the virulence model used. Indeed, the results obtained in an *in vitro* test, where the bacteria are put directly in contact with the polycationic peptides or with the serum can not be completely extrapolated to all situations in the *in vivo* model where other factors apart from polycationic peptides and complement are clearly taking part during the infection process. Still, the mouse model is the only well-characterized laboratory model for *Brucella* virulence studies and requires that mice are inoculated by the IP route. By this route, bacteria are not in contact with polycationic peptides or serum proteins at the beginning of the infection process as they are taken up and transported to the spleen rapidly. Nevertheless, the attenuation observed for *Brucella* LPS core mutants is caused by an early activation of innate immunity, as we have proved before (Conde-Álvarez et al., 2012; Fontana et al., 2016).

Our results would be compatible with the loss of one or few glucosamine residues in the lateral branch of the *wadD* mutant, and with the fact that removal of these residues would cause an increase in overall negative charge of the remaining LPS inner section that will facilitate the binding of polycationic peptides.

According to chemical studies performed in *B. melitensis*, the core lateral branch contains a mannose and four glucosamines residues assembled as follows: β -D-GlcpN-(1 \rightarrow 6)- β -D-GlcpN-(1 \rightarrow 4)-[β -D-GlcpN-(1 \rightarrow 6)]- β -D-GlcpN-(1 \rightarrow 3)- α -D-Manp-(1 \rightarrow 5) (Figure 1). Taking into account that *wadC*, *wadB*, and *wadD* are perfectly conserved in *B. melitensis* and *B. abortus*, and since WadC adds the mannose (Conde-Álvarez et al., 2012; Fontana et al., 2016), in all likelihood the four glucosamines should be added by WadB (Gil-Ramírez et al., 2014) and WadD. These glucosamines are bound to each other by β -(1 \rightarrow 6), or β -(1 \rightarrow 4) links, and the one bound to mannose by β -(1 \rightarrow 3) is also linked to two glucosamine residues, both in β -(1 \rightarrow 6) and β -(1 \rightarrow 4). If WadB and WadD are the only glycosyltransferases involved in the assembly of the glucosamine tetrasaccharide and its binding to the mannose residue, one of them (or both) could be multi-functional and thus able to add sugars in different linkage. Most glycosyltransferase enzymes involved in lipooligosaccharide (LOS) or LPS core biosynthesis are responsible for one type of sugar addition onto the growing chain (Raetz and Whitfield, 2002). However, some bacterial glycosyltransferase enzymes of the GT-2 family, to which WadD belongs, can be multi-functional and are characterized by the presence of tandems of two active domains (DXD) on one polypeptide, as is the case of Lgt3, responsible for the addition of three glucoses with different linkages [β -(1-3), β -(1-4), and β -(1-6)] onto the inner core of *Moraxella catarrhalis* LOS (Coutinho et al., 2003; Luke-Marshall et al., 2013). Interestingly,

WadD from *B. melitensis*, *B. abortus*, and all the orthologs in the other *Brucella* spp. conserves two DXD domains, opening the door to the possibility of a bi-functional role for this glycosyltransferase (Supplementary Figure S5). This DXD domain is not present in WadB. Nevertheless, the understanding of the particular role of each glycosyltransferase in the linkage of the different glucosamines to form the pentasaccharide (glucosamine tetrasaccharide bound to mannose) would require the elucidation of the core chemical structure of *wadB* and *wadD* mutants.

Contrary to most of the genes encoding glycosyltransferases implicated in the synthesis of the LPS, that are clustered in the same or related regions of the *Brucella* genome (Vemulapalli et al., 2000; Monreal et al., 2003; Rajashekara et al., 2004, 2008; González et al., 2008), *wadC*, *wadB*, and *wadD* (BAB1_1522, BAB1_0351, and BAB1_0953, respectively), although all situated in chromosome I, are isolated and surrounded by other ORFs apparently not related to LPS synthesis. This, and the fact that some other genes involved in the synthesis of the core (*manBcore* and *manCcore*) are situated in chromosome II (Monreal et al., 2003; González et al., 2008), makes even more intriguing the identification of genes needed for the synthesis of *Brucella* core LPS and its lateral branch. Thus, although we think all glycosyltransferases have been identified, we can not rule out that other glycosyltransferases could be required for the assembly of the pentasaccharide that forms the core lateral branch.

In a chemical characterization of the core LPS previously performed in a *B. melitensis* strain different from the one used in our studies, a glucose residue was found linked to the mannose that is the depart of the lateral branch, and, if this were the case, a new glycosyltransferase could be needed (Kubler-Kielb and Vinogradov, 2013). However, it should be taken into account that the LPS extraction method and the *B. melitensis* biovar used for the determination of the core structure in this experiment were different from those used in our genetic and biochemical studies (Figure 1). It is important to notice that the chemical structure we discuss in Figure 1 has been elucidated in the same *B. melitensis* strain where the *wadC* gene was mutated (Fontana et al., 2016) and, in this case, no glucose residues were detected. The fact that, as discussed above, *wadC*, *wadB*, and *wadD* are perfectly conserved in *B. melitensis*, reinforces the interpretation of our results, and the idea that the glycosyltransferases encoded by the last two genes would be involved in the assembly of glucosamine residues.

Nevertheless, we should consider that, although the phenotype of *wadC* mutant in *B. melitensis* and *B. abortus* is similar (Conde-Álvarez et al., 2012; Fontana et al., 2016), previous results suggest that there could exist differences in the structure of the core in these two *Brucella* spp., since they react differently with MoAbs against core epitopes (González et al., 2008). Moreover, we have already seen that some of the studied ORFs (and discarded in our first screening since they reacted as the parental strain in the rough and smooth LPS fractions) present differences between *B. abortus* and *B. melitensis* (Supplementary Table S2). Thus, we could not discard them as the responsible for these differences. To understand the final role of *wadB*, *wadC*, and *wadD*, it would

be necessary to analyze and compare the chemical structure of the core section in mutants in these genes in both spp.

ETHICS STATEMENT

Female BALB/c mice (ENVIGO, Harlan) were kept in cages with water and food *ad libitum* under P3 biosafety conditions in the facilities of CIMA (registration code ES31 2010000132) or CITA (registration code ES502970012005) 2 weeks before and during the experiments. The procedures were in accordance with the current European (directive 86/609/EEC) and Spanish (RD 53/2013) legislations, supervised by the Animal Welfare Committee of the University of Navarra or CITA, and authorized by “Gobierno de Navarra” (protocol number 134-14) or “Gobierno de Aragón” (protocol number R108/2009).

AUTHOR CONTRIBUTIONS

MI, RC-Á, IM, and MS-B conceived the study. MS-B, YG-R, AZ-R, EM-G, MM, PM, AC, and MZ carried out the experimental work. MI, IM, RC-Á, and MS-B wrote the paper. All authors participated in the presentation and discussion of the results.

REFERENCES

- Al Dahouk, S., Köhler, S., Occhialini, A., Jiménez de Bagüés, M. P., Hammerl, J. A., Eisenberg, T., et al. (2017). *Brucella* spp. of amphibians comprise genomically diverse motile strains competent for replication in macrophages and survival in mammalian hosts. *Sci. Rep.* 7:44420. doi: 10.1038/srep44420
- Ariza, J. (1999). Brucellosis: an update. the perspective from the Mediterranean basin. *Rev. Med. Microbiol.* 10, 125–135.
- Barquero-Calvo, E., Chaves-Olarte, E., Weiss, D. S., Guzmán-Verri, C., Chacón-Díaz, C., Rucavado, A., et al. (2007). *Brucella abortus* uses a stealthy strategy to avoid activation of the innate immune system during the onset of infection. *PLoS One* 2:e631. doi: 10.1371/journal.pone.0000631
- Bowden, R., Cloeckaert, A., Zygmunt, M., Bernard, S., and Dubray, G. (1995). Surface exposure of outer membrane protein and lipopolysaccharide epitopes in *Brucella* species studied by enzyme-linked immunosorbent assay and flow cytometry. *Infect. Immun.* 63, 3945–3952.
- Briones, G., Iñón de Iannino, N., Roset, M., Vigliocco, A., Paulo, P. S., and Ugalde, R. A. (2001). *Brucella abortus* cyclic beta-1,2-glucan mutants have reduced virulence in mice and are defective in intracellular replication in HeLa cells. *Infect. Immun.* 69, 4528–4535. doi: 10.1128/IAI.69.7.4528-4535.2001
- Caswell, C. C., Elhassanny, A. E., Planchin, E. E., Roux, C. M., Weeks-Gorospe, J. N., Ficht, T. A., et al. (2013). Diverse genetic regulon of the virulence-associated transcriptional regulator MucR in *Brucella abortus* 2308. *Infect. Immun.* 81, 1040–1051. doi: 10.1128/IAI.01097-12
- Choi, K. H., and Schweizer, H. P. (2006). mini-Tn7 insertion in bacteria with single attTn7 sites: example *Pseudomonas aeruginosa*. *Nat. Protoc.* 1, 153–161. doi: 10.1038/nprot.2006.24
- Cloeckaert, A., De Wergifosse, P., Dubray, G., and Limet, J. N. (1990). Identification of seven surface-exposed *Brucella* outer membrane proteins by use of monoclonal antibodies: immunogold labeling for electron microscopy and enzyme-linked immunosorbent assay. *Infect. Immun.* 58, 3980–3987.
- Cloeckaert, A., Jacques, I., Bowden, R., Dubray, G., and Limet, J. N. (1993a). Monoclonal antibodies to *Brucella* rough lipopolysaccharide: characterization and evaluation of their protective effect against *B. abortus*. *Res. Microbiol. Paris* 144, 475–484. doi: 10.1016/0923-2508

FUNDING

This research was supported by the Institute for Tropical Health funders (Obra Social la CAIXA, “Fundaciones Caja Navarra” and “Roviralta, PROFAND, Ubesol, ACUNSA,” and “Artai”) and grants MINECO (AGL2014-58795-C4-1-R). MS-B is the recipient of a Ph.D. Fellowship funded by the “Asociación de Amigos de la Universidad de Navarra.” Work at CITA-Spain was also sustained by Grants from MINECO (AGL2008-04514-C03-03/GAN and AGL2014-58795-C4-3-R).

ACKNOWLEDGMENTS

The authors thank A. Delgado-López for excellent technical assistance.

SUPPLEMENTARY MATERIAL

The Supplementary Material for this article can be found online at: <https://www.frontiersin.org/articles/10.3389/fmicb.2018.02293/full#supplementary-material>

- Cloeckaert, A., Weynants, V., Godfroid, J., Verger, J.-M., Grayon, M., and Zygmunt, M. S. (1998). O-polysaccharide epitopic heterogeneity at the surface of *Brucella* spp. studied by enzyme-linked immunosorbent assay and flow cytometry. *Clin. Diagn. Lab. Immunol.* 5, 862–870.
- Cloeckaert, A., Zygmunt, M. S., Dubray, G., and Limet, J. N. (1993b). Characterization of O-polysaccharide specific monoclonal antibodies derived from mice infected with the rough *Brucella melitensis* strain B115. *J. Gen. Microbiol.* 139, 1551–1556. doi: 10.1099/00221287-139-7-1551
- Conde-Álvarez, R., Arce-Gorvel, V., Gil-Ramírez, Y., Iriarte, M., Grilló, M. J., Gorvel, J. P., et al. (2013). Lipopolysaccharide as a target for brucellosis vaccine design. *Microb. Pathog.* 58, 29–34. doi: 10.1016/j.micpath.2012.11.011
- Conde-Álvarez, R., Arce-Gorvel, V., Iriarte, M., Manček-Keber, M., Barquero-Calvo, E., Palacios-Chaves, L., et al. (2012). The lipopolysaccharide core of *Brucella abortus* acts as a shield against innate immunity recognition. *PLoS Pathog.* 8:e1002675. doi: 10.1371/journal.ppat.1002675
- Coutinho, P. M., Deleury, E., Davies, G. J., and Henrissat, B. (2003). An evolving hierarchical family classification for glycosyltransferases. *J. Mol. Biol.* 328, 307–317. doi: 10.1016/S0022-2836(03)00307-3
- Dubray, G., and Limet, J. (1987). Evidence of heterogeneity of lipopolysaccharides among *Brucella* biovars in relation to A and M specificities. *Ann. Inst. Pasteur. Microbiol.* 138, 27–37.
- Fontana, C., Conde-Álvarez, R., Stähle, J., Holst, O., Iriarte, M., Zhao, Y., et al. (2016). Structural studies of lipopolysaccharide defective mutants from *Brucella melitensis* identify a core oligosaccharide critical in virulence. *J. Biol. Chem.* 291, 7727–7741. doi: 10.1074/jbc.M115.701540
- Garin-Bastuji, B., Bowden, R. A., Dubray, G., and Limet, J. N. (1990). Sodium dodecyl sulfate-polyacrylamide gel electrophoresis and immunoblotting analysis of smooth-lipopolysaccharide heterogeneity among *Brucella* biovars related to A and M specificities. *J. Clin. Microbiol.* 28, 2169–2174.
- Gil-Ramírez, Y., Conde-Álvarez, R., Palacios-Chaves, L., Zúñiga-Ripa, A., Grilló, M.-J., Arce-Gorvel, V., et al. (2014). The identification of wadB, a new glycosyltransferase gene, confirms the branched structure and the role in virulence of the lipopolysaccharide core of *Brucella abortus*. *Microb. Pathog.* 73, 53–59. doi: 10.1016/j.micpath.2014.06.002
- Godfroid, F., Cloeckaert, A., Taminiau, B., Danese, I., Tibor, A., De Bolle, X., et al. (2000). Genetic organisation of the lipopolysaccharide O-antigen biosynthesis region of *Brucella melitensis* 16M (wbk). *Res. Microbiol.* 151, 655–668. doi: 10.1016/S0923-2508(00)90130-X

- González, D., Grilló, M.-J. M., De Miguel, M. M.-J., Ali, T., Arce-Gorvel, V., Delrue, R. R.-M., et al. (2008). Brucellosis vaccines: assessment of *Brucella melitensis* lipopolysaccharide rough mutants defective in core and O-polysaccharide synthesis and export. *PLoS One* 3:e2760. doi: 10.1371/journal.pone.0002760
- Iriarte, M., González, D., Delrue, R.-M., Monreal, D., Conde, R., López-Goñi, I., et al. (2004). "Brucella lipopolysaccharide: structure, biosynthesis and genetics," in *Brucella. Molecular and Cellular Biology* (Wymondham: Horizon Bioscience), 159–192.
- Kubler-Kielb, J., and Vinogradov, E. (2013). The study of the core part and non-repeating elements of the O-antigen of *Brucella* lipopolysaccharide. *Carbohydr. Res.* 366, 33–37. doi: 10.1016/j.carres.2012.11.004
- Lapaque, N., Moriyon, I., Moreno, E., and Gorvel, J.-P. (2005). *Brucella* lipopolysaccharide acts as a virulence factor. *Curr. Opin. Microbiol.* 8, 60–66. doi: 10.1016/j.mib.2004.12.003
- Llobet, E., March, C., Giménez, P., and Bengoechea, J. A. (2009). *Klebsiella pneumoniae* OmpA confers resistance to antimicrobial peptides. *Antimicrob. Agents Chemother.* 53, 298–302. doi: 10.1128/AAC.00657-08
- Luke-Marshall, N. R., Edwards, K. J., Sauberman, S., St Michael, F., Vinogradov, E. V., Cox, A. D., et al. (2013). Characterization of a trifunctional glucosyltransferase essential for *Moraxella catarrhalis* lipooligosaccharide assembly. *Glycobiology* 23, 1013–1021. doi: 10.1093/glycob/cwt042
- Manterola, L., Moriyón, I., Moreno, E., Sola-Landa, A., Weiss, D. S., Koch, M. H. J., et al. (2005). The lipopolysaccharide of *Brucella abortus* BvrS/BvrR mutants contains lipid A modifications and has higher affinity for bactericidal cationic peptides. *J. Bacteriol.* 187, 5631–5639. doi: 10.1128/JB.187.16.5631-5639.2005
- Martínez-Gómez, E., Stähle, J., Gil-Ramírez, Y., Zúñiga-Ripa, A., Zaccheus, M., Moriyón, I., et al. (2018). Genomic insertion of a heterologous acetyltransferase generates a new lipopolysaccharide antigenic structure in *Brucella abortus* and *Brucella melitensis*. *Front. Microbiol.* 9:1092. doi: 10.3389/FMICB.2018.01092
- McDermott, J., Grace, D., and Zinsstag, J. (2013). Economics of brucellosis impact and control in low-income countries. *Rev. Sci. Tech.* 32, 249–261.
- McQuiston, J. R., Vemulapalli, R., Inzana, T. J., Schurig, G. G., Sriranganathan, N., Fritzinger, D., et al. (1999). Genetic characterization of a Tn5-disrupted glycosyltransferase gene homolog in *Brucella abortus* and its effect on lipopolysaccharide composition and virulence. *Infect. Immun.* 67, 3830–3835.
- Mirabella, A., Terwagne, M., Zygmunt, M. S., Cloeckert, A., De Bolle, X., and Letesson, J. J. (2013). *Brucella melitensis* MucR, an orthologue of *Sinorhizobium meliloti* MucR, is involved in resistance to oxidative, detergent, and saline stresses and cell envelope modifications. *J. Bacteriol.* 195, 453–65. doi: 10.1128/JB.01336-12
- Monreal, D., Grilló, M. J., González, D., Marín, C. M., De Miguel, M. J., López-Goñi, I., et al. (2003). Characterization of *Brucella abortus* O-polysaccharide and core lipopolysaccharide mutants and demonstration that a complete core is required for rough vaccines to be efficient against *Brucella abortus* and *Brucella ovis* in the mouse model. *Infect. Immun.* 71, 3261–3271. doi: 10.1128/iai.71.6.3261-3271.2003
- Palacios-Chaves, L., Conde-Álvarez, R., Gil-Ramírez, Y., Zúñiga-Ripa, A., Barquero-Calvo, E., Chacón-Díaz, C., et al. (2011). *Brucella abortus* ornithine lipids are dispensable outer membrane components devoid of a marked pathogen-associated molecular pattern. *PLoS One* 6:e16030. doi: 10.1371/journal.pone.0016030
- Raetz, C. R. H., and Whitfield, C. (2002). Lipopolysaccharide endotoxins. *Annu. Rev. Biochem.* 71, 635–700. doi: 10.1146/annurev.biochem.71.110601.135414
- Rajashankara, G., Covert, J., Petersen, E., Eskra, L., and Splitter, G. (2008). Genomic island 2 of *Brucella melitensis* is a major virulence determinant: functional analyses of genomic islands. *J. Bacteriol.* 190, 6243–6252. doi: 10.1128/JB.00520-08
- Rajashankara, G., Glasner, J. D., Glover, D. A., and Splitter, G. A. (2004). Comparative whole-genome hybridization reveals genomic islands in *Brucella* species. *J. Bacteriol.* 186, 5040–5051. doi: 10.1128/JB.186.15.5040-5051.2004
- Reeves, P. R., Hobbs, M., Valvano, M. A., Skurnik, M., Whitfield, C., Coplin, D., et al. (1996). Bacterial polysaccharide synthesis and gene nomenclature. *Trends Microbiol.* 4, 495–503. doi: 10.1016/S0966-842X(97)82912-5
- Rojas, N., Freer, E., Weintraub, A., Ramirez, M., Lind, S., and Moreno, E. (1994). Immunochemical identification of *Brucella abortus* lipopolysaccharide epitopes. 1, 206–213. doi: 10.1111/j.1439-0450.2001.00476.x
- Rojas, N., Zamora, O., Cascante, J., Garita, D., and Moreno, E. (2001). Comparison of the antibody response in adult cattle against different epitopes of *Brucella abortus* lipopolysaccharide. *J. Vet. Med. Ser. B* 48, 623–629. doi: 10.1111/j.1439-0450.2001.00476.x
- Scholz, H. C., Nockler, K., Gollner, C., Bahn, P., Vergnaud, G., Tomaso, H., et al. (2010). *Brucella inopinata* sp. nov., isolated from a breast implant infection. *Int. J. Syst. Evol. Microbiol.* 60, 801–808. doi: 10.1099/ij.s.0.011148-0
- Scupham, A. J., and Triplett, E. W. (1997). Isolation and characterization of the UDP-glucose 4-epimerase-encoding gene, galE, from *Brucella abortus* 2308. *Gene* 202, 53–59. doi: 10.1016/S0378-1119(97)00453-8
- Simon, R., Priefer, U., and Pühler, A. (1983). A broad host range mobilization system for in vivo genetic engineering: transposon mutagenesis in gram negative bacteria. *Biotechnology* 1, 784–791. doi: 10.1038/nbt1183-784
- Soler-Lloréns, P. F., Quance, C. R., Lawhon, S. D., Stuber, T. P., Edwards, J. F., Ficht, T. A., et al. (2016). A *Brucella* spp. isolate from a Pac-Man Frog (*Ceratophrys ornata*) reveals characteristics departing from classical *Brucellae*. *Front. Cell. Infect. Microbiol.* 6:116. doi: 10.3389/fcimb.2016.00116
- Soler-Lloréns, P., Gil-Ramírez, Y., Zabalza-Baranguá, A., Iriarte, M., Conde-Álvarez, R., Zúñiga-Ripa, A., et al. (2014). Mutants in the lipopolysaccharide of *Brucella ovis* are attenuated and protect against *B. ovis* infection in mice. *Vet. Res.* 45:72. doi: 10.1186/s13567-014-0072-0
- Tibor, A., Wansard, V., Bielartz, V., Delrue, R.-M., Danese, I., Michel, P., et al. (2002). Effect of omp10 or omp19 deletion on *Brucella abortus* outer membrane properties and virulence in mice. *Infect. Immun.* 70, 5540–5546. doi: 10.1128/IAI.70.10.5540-5546.2002
- Tiller, R. V., Gee, J. E., Frace, M. A., Taylor, T. K., Setubal, J. C., Hoffmaster, A. R., et al. (2010). Characterization of novel *Brucella* strains originating from wild native rodent species in North Queensland, Australia. *Appl. Environ. Microbiol.* 76, 5837–5845. doi: 10.1128/AEM.00620-10
- Tsai, C.-M., and Frasch, C. E. (1982). A sensitive silver stain for detecting lipopolysaccharides in polyacrylamide gels. *Anal. Biochem.* 119, 115–119. doi: 10.1016/0003-2697(82)90673-X
- Vemulapalli, R., He, Y., Buccolo, L. S., Boyle, S. M., Sriranganathan, N., and Schurig, G. G. (2000). Complementation of *Brucella abortus* RB51 with a functional wboA gene results in O-antigen synthesis and enhanced vaccine efficacy but no change in rough phenotype and attenuation. *Infect. Immun.* 68, 3927–3932. doi: 10.1128/IAI.68.7.3927-3932.2000
- Viadas, C., Rodríguez, M. C., Sangari, F. J., Gorvel, J.-P., García-Lobo, J. M., and López-Goñi, I. (2010). Transcriptome analysis of the *Brucella abortus* BvrR/BvrS two-component regulatory system. *PLoS One* 5:e10216. doi: 10.1371/journal.pone.0010216
- Zhao, Y., Hanniffy, S., Arce-Gorvel, V., Conde-Álvarez, R., Oh, S., Moriyón, I., et al. (2017). Immunomodulatory properties of *Brucella melitensis* lipopolysaccharide determinants on mouse dendritic cells in vitro and in vivo. *Virulence* 9, 465–479. doi: 10.1080/21505594.2017.1386831
- Zygmunt, M. S., Jacques, I., Bernardet, N., and Cloeckert, A. (2012). Lipopolysaccharide heterogeneity in the atypical group of novel emerging *Brucella* species. *Clin. Vaccine Immunol.* 19, 1370–1373. doi: 10.1128/CVI.00300-12

Conflict of Interest Statement: The authors declare that the research was conducted in the absence of any commercial or financial relationships that could be construed as a potential conflict of interest.

Copyright © 2018 Salvador-Bescós, Gil-Ramírez, Zúñiga-Ripa, Martínez-Gómez, de Miguel, Muñoz, Cloeckert, Zygmunt, Moriyón, Iriarte and Conde-Álvarez. This is an open-access article distributed under the terms of the Creative Commons Attribution License (CC BY). The use, distribution or reproduction in other forums is permitted, provided the original author(s) and the copyright owner(s) are credited and that the original publication in this journal is cited, in accordance with accepted academic practice. No use, distribution or reproduction is permitted which does not comply with these terms.



Comparative Genomics and *in vitro* Infection of Field Clonal Isolates of *Brucella melitensis* Biovar 3 Did Not Identify Signature of Host Adaptation

Marion Holzapfel¹, Guillaume Girault¹, Anne Kerié^{2,3}, Claire Ponsart¹, David O'Callaghan^{2,3} and Virginie Mick^{1*}

¹ EU/OIE/FAO and National Reference Laboratory for Brucellosis, Animal Health Laboratory, Anses/Paris-Est University, Maisons-Alfort, France, ² VBMI, INSERM, U1047, Université de Montpellier, Nîmes, France, ³ CNR Laboratoire Expert Brucella, Service de Microbiologie, CHU Caremeau, Nîmes, France

OPEN ACCESS

Edited by:

Michel Stanislas Zygmunt,
Institut National de la Recherche
Agronomique (INRA), France

Reviewed by:

Jeffrey T. Foster,
Northern Arizona University,
United States
Menachem Banai,
Kimron Veterinary Institute, Israel

*Correspondence:

Virginie Mick
virginie.mick@anses.fr

Specialty section:

This article was submitted to
Infectious Diseases,
a section of the journal
Frontiers in Microbiology

Received: 18 July 2018

Accepted: 02 October 2018

Published: 22 October 2018

Citation:

Holzapfel M, Girault G, Kerié A,
Ponsart C, O'Callaghan D and Mick V
(2018) Comparative Genomics
and *in vitro* Infection of Field Clonal
Isolates of *Brucella melitensis* Biovar 3
Did Not Identify Signature of Host
Adaptation. *Front. Microbiol.* 9:2505.
doi: 10.3389/fmicb.2018.02505

Brucella spp. are responsible for brucellosis, a widespread zoonosis causing reproductive disorders in animals. Species-classification within this monophyletic genus is based on bacteriological and biochemical phenotyping. Traditionally, *Brucella* species are reported to have a preferential, but not exclusive mammalian host. However, this concept can be challenged since many *Brucella* species infect a wide range of animal species. Adaptation to a specific host can be a driver of pathogen variation. It is generally thought that *Brucella* species have highly stable and conserved genomes, however the degree of genomic variation during natural infection has not been documented. Here, we investigated potential genetic diversity and virulence of *Brucella melitensis* biovar 3 field isolates obtained from a single outbreak but from different host species (human, bovine, small ruminants). A unique MLVA-16 pattern suggested all isolates were clonal. Comparative genomic analyses showed an almost non-existent genetic diversity among isolates (only one SNP; no architectural rearrangements) and did not highlight any signature specific to host adaptation. Similarly, the strains showed identical capacities to enter and replicate in an *in vitro* model of macrophage infection. In our study, the absence of genomic variability and similar virulence underline that *B. melitensis* biovar 3 is a broad-host-range pathogen without the need to adapt to different hosts.

Keywords: brucellosis, *Brucella melitensis*, host preference, whole genome sequencing, comparative genomics, macrophage infection, adaptation

INTRODUCTION

Brucellosis, caused by bacteria of the *Brucella* genus, is a widespread zoonosis causing reproductive disorders in animals and a debilitating infection in humans. *Brucella* classification is based on bacteriological and biochemical phenotypes (Ficht, 2010). Traditionally, different species were reported to have a preferential mammalian host, however in reality, spill over into a wide range of animal species has been reported. *B. melitensis*, for example, primarily responsible for disease in domestic small ruminants (sheep and goats), also causes natural infections in bovids, camelids and

wild ruminants (e.g., ibex) (Office International des Epizooties [OIE], 2016) (Garin-Bastuji et al., 2014), and is the major species responsible for human infections.

Comparative genomics have allowed us to identify the key steps in the evolution of *Brucella* from a soil organism to a stealth pathogen. This has involved the acquisition of a battery of virulence factors followed by a toning down of virulence (Wattam et al., 2014). What is not understood is how the different species have adapted to their 'preferential' host, or the time line of this adaptation. Despite the strong sequence homogeneity within the genus (>94% nucleotide identity) (Wattam et al., 2009), genome-wide studies suggest genetic variation, especially pseudogenization, i.e., due to IS711 insertion and point mutations within marine *Brucella* genomes (Suárez-Esquivel et al., 2017), might play a key role in *Brucella* host preference as the bacteria evolved with their respective preferential hosts (Chain et al., 2005). In a recent report, Ke and collaborators suggested that *B. melitensis* rapidly accumulates mutations during *in vivo* passage, however this observation is not supported by the high levels of sequence conservation seen between the genome sequences available in Genbank (Ke et al., 2012).

In this study we investigate seven clonal isolates of *B. melitensis* biovar 3 (bv3) isolated from different mammalian hosts during a well characterized outbreak in southern France. We used *in vitro* virulence assays and comparative genomics to determine whether genetic variation is required for the ability to infect different hosts.

MATERIALS AND METHODS

Bacterial Strains

Seven isolates (Supplementary Table S1) collected over a 1-year period (2000–2001) from a restricted geographical area (Drôme, South-East France) from different host species: human ($n = 1$); bovine ($n = 2$); small ruminants (sheep and goat) ($n = 4$) were biotyped using standard procedures (Office International des Epizooties [OIE], 2016). Records regarding this epidemiological event available at the National Reference Laboratory (NRL) for brucellosis were examined. At least one abortion occurred amongst infected animals, probably in small ruminant. Epidemiological and serological investigations conducted to the slaughtering of the herd.

B. melitensis reference strains 16M (bv1) and Ether (bv3) (Supplementary Table S1) were included in this study.

Molecular Analyses and Comparative Genomics

Genomic DNA was extracted using High Pure DNA Template Preparation kit (Roche Diagnostics, France), according to the manufacturer's recommendations. Real Time-PCR and MLVA-16 assays were performed as previously described (Al Dahouk et al., 2007; Bounaadja et al., 2009).

Genome sequencing was performed on an Illumina HiSeq2500 platform (2 × 250 bp paired-end reads). Raw

reads were trimmed using Trimmomatic (Bolger et al., 2014) and quality controls were conducted with FastQC (Andrews, 2010). Mapping assemblies against reference concatenated genomes (i.e., both chromosomes I and II are concatenated together in a single file) of Ether and 16M were performed using Bionumerics v7.6.2 [Burrows-Wheeler Aligner BWA (Li and Durbin, 2009)], as well as *de novo* assembly using SPAdes v3.9. Annotations were performed with Prokka (Seemann, 2014) and alignments with progressiveMAUVE (Darling et al., 2010) and BLAST Ring Image Generator (BRIG) 0.95 (Alikhan et al., 2011). Genome assemblies were evaluated with QUAST 4.6.3 (Gurevich et al., 2013).

Single Nucleotide Polymorphism (SNP) and clustering (maximum-parsimony) analyses were performed using Bionumerics v7.6.2 (wgSNP-module). Applied filters removed indels, repeated regions and rRNAs with minimum ten bp-distance between SNPs. Non-synonymous, synonymous and intergenic SNPs were identified against 16M. Local alignment of interesting regions were done with ClustalW (Thompson et al., 1994) via MEGA 6 (Tamura et al., 2013).

To functionally analyze genomes, Roary v3.6.1 (Page et al., 2015) was used to generate matrices of presence/absence of core (i.e., genes present in all genomes included in the study) and accessory (i.e., not core genes) genes among seven investigated genomes, or among seven genomes vs. 16M. Scoary (Brynildsrud et al., 2016) was used to associate the presence/absence of genes/SNPs to given clustering according to host-range.

Sequences were deposited in European-Nucleotide-Archive (Study PRJEB26921) (Supplementary Table S1).

Macrophage Infection Assays

Murine J774.1 macrophages (ATCC® TIB-67™) were cultivated and infected with *Brucella* using a standard gentamycin protection protocol as described previously (Soler-Llorens et al., 2016). All experiments were performed in triplicate and independently repeated three times.

The ability of infection of different field isolates was represented as the *Brucella* penetration index (BPI) and the *Brucella* multiplication index (BMI). BPI was defined as the percentage of the inoculum inside macrophages at 2 h post-inoculation (PI); BMI as the ratio of CFU in cell lysates at 48 h PI to CFU at 2 h PI. Results were analyzed using a non-parametric Kruskal-Wallis test (GraphPad Prism program) with significant p -values < 0.05.

RESULTS

Seven investigated isolates were confirmed as *B. melitensis* bv3 using classical microbiological and molecular methods. All seven isolates had identical phenotypes. All isolates had an identical MLVA-16 pattern: Bruce06 3U; Bruce08 5U; Bruce11 3U; Bruce12 13U; Bruce42 1U; Bruce43 1U; Bruce45 3U; Bruce55 3U; Bruce18 7U; Bruce19 42U; Bruce21 8U; Bruce04 8U; Bruce07 5U; Bruce09 12U; Bruce16 8U; Bruce30 3U. This suggests that the isolates were clonal.

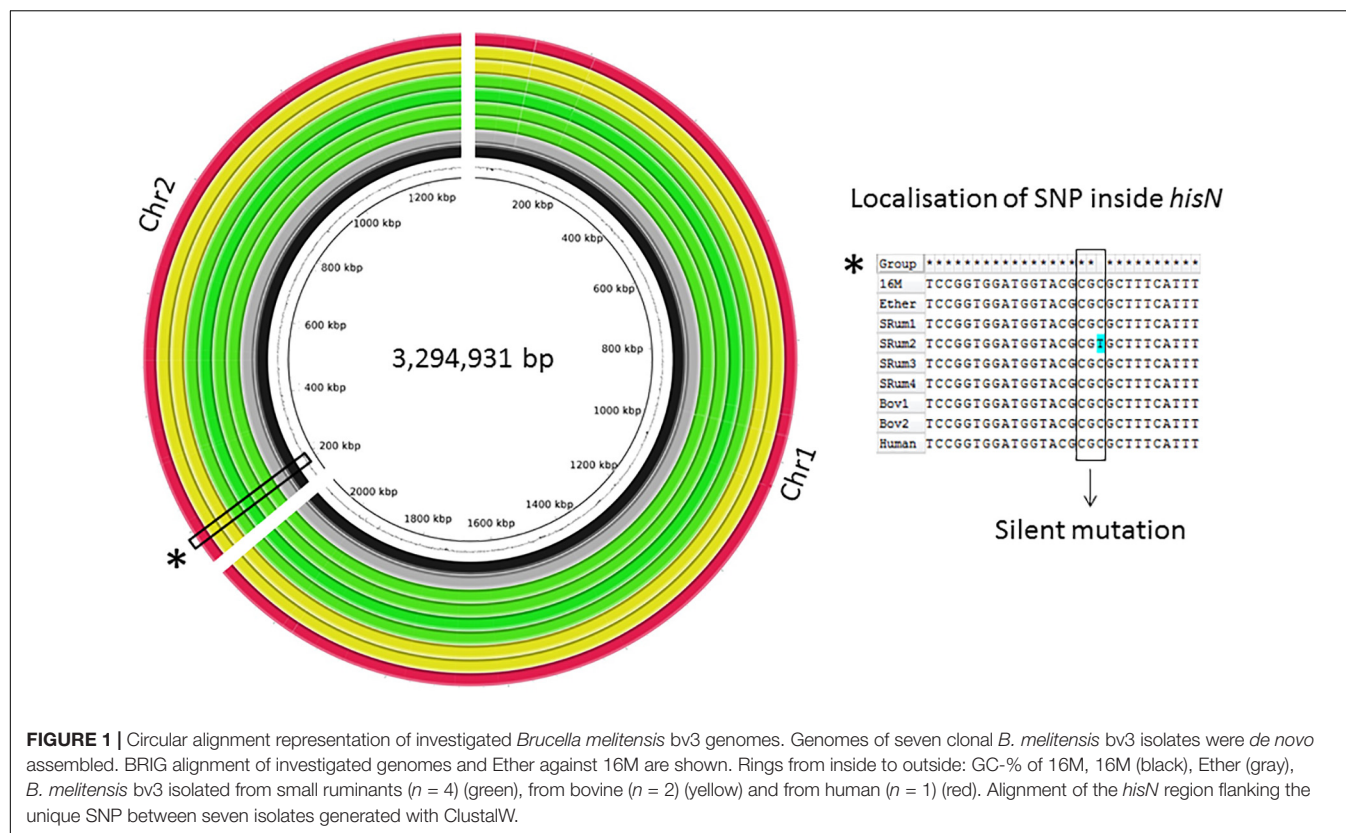


FIGURE 1 | Circular alignment representation of investigated *Brucella melitensis* bv3 genomes. Genomes of seven clonal *B. melitensis* bv3 isolates were *de novo* assembled. BRIG alignment of investigated genomes and Ether against 16M are shown. Rings from inside to outside: GC-% of 16M, 16M (black), Ether (gray), *B. melitensis* bv3 isolated from small ruminants ($n = 4$) (green), from bovine ($n = 2$) (yellow) and from human ($n = 1$) (red). Alignment of the *hisN* region flanking the unique SNP between seven isolates generated with ClustalW.

Comparative Genomics

The global genomic architecture of the seven strains was consistent with those of published *B. melitensis* genomes (i.e., presence of two chromosomes). The field isolates had a genome size of approximately 3.3 Mbp, a G-C content similar to that of the Ether genome (57.24% vs. 57.22%) with 3,210–3,218 predicted protein-encoding genes (QUAST). After filtering, a total of 2,748 SNPs were identified among all studied strains vs. 16M, but only one SNP was observed amongst the seven field strains, in an ovine isolate (**Figure 1**). This C-to-T substitution at position 267 of the *hisN* gene coding for histidinol-phosphatase (BME_RS10415) is a silent mutation. Manual analysis also showed a bovine isolate harbored another SNP in *hisN* (A-to-G at nucleotide 599) that was discarded by automated analysis; this lead to an Asp200Gly modification of HisN.

Genome-wide comparison from *de novo* assemblies showed a perfect collinearity of the seven genomes as well as with those of 16M and Ether, highlighting absence of genomic rearrangements (**Figure 1**). Further comparison regarding the pan-genome, i.e., among seven genomes, highlighted a total amount of 3,196 predicted genes, including 3,141 core genes and 55 accessory genes. The strains showed a full complement of previously described virulence factors (He, 2012).

Macrophage Infection Assays

The virulence of the isolates was compared within an *in vitro* murine macrophage infection model. The seven bv3 isolates showed similar ability to infect and multiply in macrophages as

the reference strain. In our conditions, *B. melitensis* bv3 small ruminant isolates had slightly but significantly lower BPI values than 16M ($p = 0.02$), unlike human and bovine isolates ($p > 0.99$ and $p = 0.19$, respectively) (**Figure 2B**). BPI values showed no significant difference among isolates whatever host-species ($p = 0.34$ for human vs. small ruminants to >0.99 for other comparisons) (**Figure 2B**). At 48 h PI, BMI observed between 16M vs. isolates ($p > 0.99$ for all comparisons) and among isolates did not show significant difference ($p = 0.26$ bovine vs. human; $p = 0.37$ bovine vs. small ruminants; $p > 0.99$ human vs. small ruminants) correlated with host-species (**Figure 2C**). Indeed, multiplication inside macrophages was similar to the intracellular growth of reference 16M (**Figure 2A**), and statistically identical among tested isolates.

DISCUSSION

Brucella species have been classically assigned to preferential, but not exclusive animal hosts. Hence, *B. melitensis* is associated with infection of small ruminants and *B. abortus* with cattle. There have, however been numerous reports of *B. melitensis* causing abortion in cattle (Verger et al., 1989; Alvarez et al., 2011; El-Diasty et al., 2018). In this study, we characterized seven *B. melitensis* bv3 field isolates, considered as epidemiologically related because isolated from a same outbreak (same geographical area, same time-period), but from different mammalian hosts. As it was not possible to distinguish between the strains

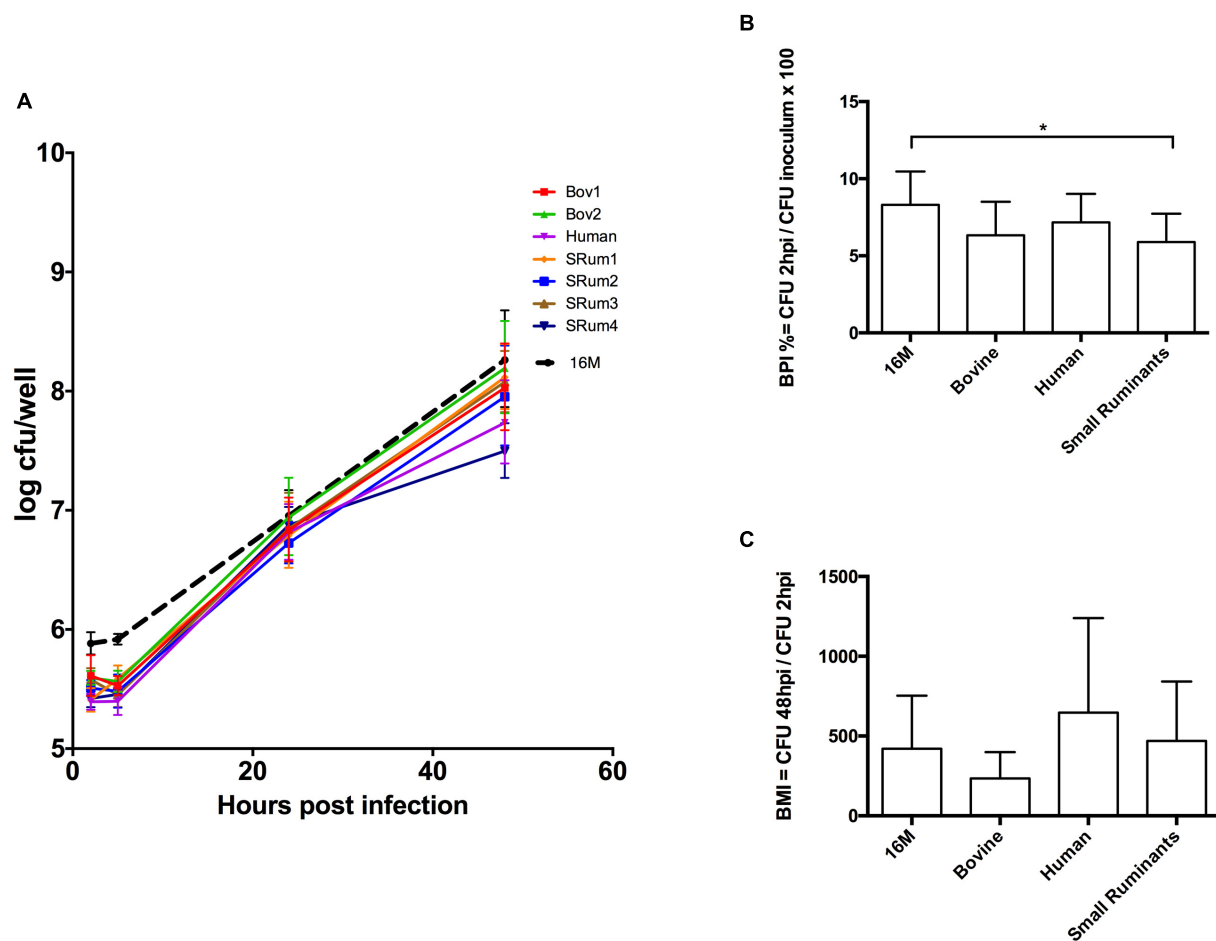


FIGURE 2 | Macrophage infection assay with clonal *B. melitensis* bv3 isolates from different host-range. **(A)** Intracellular growth of *Brucella* isolates inside murine macrophages J774A.1. Each point is performed in triplicates from three independent experiments and represents the \log_{10} of the mean \pm SD CFU/well. **(B)** Adhesion/Invasion capacity of *Brucella* isolates. **(C)** *Brucella* multiplicity index. Isolates are grouped into three host-categories – bovine ($n = 2$), human ($n = 1$) and small ruminants ($n = 4$)– and compared to the reference *B. melitensis* biovar 1str. 16M. Error bars denote standard errors. Statistical significance of each group was determined by Kruskal-Wallis test. * $p < 0.05$. Bov1/2, *B. melitensis* bv3 isolated from bovine; Human, *B. melitensis* bv3 isolated from human; SRum1/2/3/4, *B. melitensis* bv3 isolated from small ruminants.

phenotypically and the strains all had the same single identical pattern in MLVA-16, we considered the seven strains as clonal, according to the definition of a “clone” from Tenover et al. (1995) isolates that are indistinguishable from each other by a variety of genetic tests (e.g., PFGE, multilocus enzyme electrophoresis, or ribotyping) or that are so similar that they are presumed to be derived from a common parent. Consequently, this study mimics an *in vivo* experimental infection aiming to determine whether genetic modifications are induced during the short-time adaptation of *B. melitensis* to a transition of environment, i.e., different host species, host being considered as driver of pathogen variation. Adaptation is defined as the process of change by which an organism or species becomes better suited to its environment (Ryall et al., 2012).

Comparison with the genomes of two *B. melitensis* reference strains showed perfect synteny. Our in-depth comparative genomics analyses revealed an almost non-existent genetic diversity among the seven *Brucella* field isolates, with only one

SNP confirming that there is no signature of adaptation to different host-species. Most importantly, our data is in complete contrast with the study from Ke et al. (2012) who reported over 5,000 SNPs after 13 weeks mouse passage of *B. melitensis* 16M and suggested that *Brucella* accumulates a large number of adaptive mutations during chronic infection.

The seven field isolates showed identical virulence in murine macrophages. *B. melitensis* clearly has the intrinsic capacity to infect a wide range of mammalian hosts without the need to adapt. It is more likely that the traditional host preference was due to the epidemiology and lack of contact between infected small ruminants and other livestock. Domestic dogs and cats, and feral swine are occasionally infected with *Brucella* through contact with infected livestock (Stoffregen et al., 2007; Lucero et al., 2008; Hinic et al., 2010; Wareth et al., 2017). *B. melitensis* bv3 has also been isolated from Nile catfish, probably infected by contaminated animal waste in the water contamination, showing the broad spectrum of hosts (El-Tras et al., 2010). Some *Brucella*

species have a more restricted host range. *B. suis* bv2, which is endemic in wild boar and hares in much of Europe, shows low levels of pathogenicity for ruminants and for humans (Mailles et al., 2017). Genome analysis showed a large inversion and a number of INDELs and SNPs, although none were predicted to affect known virulence factors (Ferreira et al., 2017). The clearest example of host restriction is *B. ovis*, which is almost only pathogenic for sheep, with some studies reporting clinical sign in Red Deer (Ridler et al., 2012). Here a clear process of genome degradation and accumulation of pseudogenes is evident (Tsolis et al., 2009). Genomic decay seems to be associated with a host-restricted pattern, whereas intact genes are present in broad-host-range pathogens (Kirzinger and Stavrinides, 2012). The absence of pseudogenes and/or of genomic rearrangement among genomes studied here underlines that *B. melitensis* bv3 remains a broad-host-range pathogen.

In conclusion, this study shows that *B. melitensis* does not require any adaptive mutations when infecting different mammalian hosts. We cannot exclude the possibility that adaptation to a different host requires differential expression of specific genes that cannot be detected with the simple experimental models that we use.

AUTHOR CONTRIBUTIONS

VM and DO conceived the study. CP obtained funding. MH and GG performed genomics analyses. MH and AK performed

macrophage infection assays. MH, GG, CP, and VM performed data interpretation. MH, DO, and VM wrote the paper. All authors read and approved the manuscript content.

FUNDING

MH was supported by a Ph.D. fellowship the (CIFRE grant) French Direction Générale de l'Armement (DGA and IDVet). This work was supported by European Union Reference Laboratory for Brucellosis, INSERM, Université de Montpellier and Santé Publique France.

ACKNOWLEDGMENTS

The authors wish to express their gratitude to Maëlys Kevin and Benoit Durand for critical and supportive comments.

SUPPLEMENTARY MATERIAL

The Supplementary Material for this article can be found online at: <https://www.frontiersin.org/articles/10.3389/fmicb.2018.02505/full#supplementary-material>

TABLE S1 | Field *Brucella* isolates investigated in this study and reference strains from public databases.

REFERENCES

- Al Dahouk, S., Fleche, P. L., Nockler, K., Jacques, I., Grayon, M., Scholz, H. C., et al. (2007). Evaluation of *Brucella* MLVA typing for human brucellosis. *J. Microbiol. Methods* 69, 137–145. doi: 10.1016/j.mimet.2006.12.015
- Alikhan, N. F., Petty, N. K., Ben Zakour, N. L., and Beatson, S. A. (2011). BLAST ring image generator (BRIG): simple prokaryote genome comparisons. *BMC Genomics* 12:402. doi: 10.1186/1471-2164-12-402
- Alvarez, J., Saez, J. L., Garcia, N., Serrat, C., Perez-Sancho, M., Gonzalez, S., et al. (2011). Management of an outbreak of brucellosis due to *B. melitensis* in dairy cattle in Spain. *Res. Vet. Sci.* 90, 208–211. doi: 10.1016/j.rvsc.2010.05.028
- Andrews, S. (2010). *FastQC: A Quality Control tool for High Throughput Sequence Data*. Available at: <http://www.bioinformatics.babraham.ac.uk/projects/fastqc>
- Bolger, A. M., Lohse, M., and Usadel, B. (2014). Trimmomatic: a flexible trimmer for illumina sequence data. *Bioinformatics* 30, 2114–2120. doi: 10.1093/bioinformatics/btu170
- Bounaadja, L., Albert, D., Chenais, B., Henault, S., Zygmunt, M. S., Poliak, S., et al. (2009). Real-time PCR for identification of *Brucella* spp.: a comparative study of IS711, bcsP31 and per target genes. *Vet. Microbiol.* 137, 156–164. doi: 10.1016/j.vetmic.2008.12.023
- Bryndisrud, O., Bohlin, J., Scheffer, L., and Eldholm, V. (2016). Rapid scoring of genes in microbial pan-genome-wide association studies with Scoary. *Genome Biol.* 17:238. doi: 10.1186/s13059-016-1108-8
- Chain, P. S., Comerici, D. J., Tolmasky, M. E., Larimer, F. W., Malfatti, S. A., Vergez, L. M., et al. (2005). Whole-genome analyses of speciation events in pathogenic *Brucellae*. *Infect. Immun.* 73, 8353–8361. doi: 10.1128/IAI.73.12.8353-8361.2005
- Darling, A. E., Mau, B., and Perna, N. T. (2010). Progressivemaue: multiple genome alignment with gene gain, loss and rearrangement. *PLoS One* 5:e11147. doi: 10.1371/journal.pone.0011147
- El-Diasty, M., Wareth, G., Melzer, F., Mustafa, S., Sprague, L. D., and Neubauer, H. (2018). Isolation of *Brucella abortus* and *Brucella melitensis* from seronegative cows is a serious impediment in brucellosis control. *Vet. Sci.* 5:E28. doi: 10.3390/vetsci5010028
- El-Tras, W. F., Tayel, A. A., Eltholth, M. M., and Guitian, J. (2010). *Brucella* infection in fresh water fish: evidence for natural infection of Nile catfish, *Clarias gariepinus*, with *Brucella melitensis*. *Vet. Microbiol.* 141, 321–325. doi: 10.1016/j.vetmic.2009.09.017
- Ferreira, A. C., Correa de Sa, M. I., Dias, R., and Tenreiro, R. (2017). MLVA-16 typing of *Brucella suis* biovar 2 strains circulating in Europe. *Vet. Microbiol.* 210, 77–82. doi: 10.1016/j.vetmic.2017.09.001
- Ficht, T. A. (2010). *Brucella* taxonomy and evolution. *Future Microbiol.* 5, 859–866. doi: 10.2217/fmb.10.52
- Garin-Bastuji, B., Hars, J., Drapeau, A., Cherfa, M. A., Game, Y., Le Horgne, J. M., et al. (2014). Reemergence of *Brucella melitensis* in wildlife, France. *Emerg. Infect. Dis.* 20, 1570–1571. doi: 10.3201/eid2009.131517
- Gurevich, A., Saveliev, V., Vyahhi, N., and Tesler, G. (2013). QUAST: quality assessment tool for genome assemblies. *Bioinformatics* 29, 1072–1075. doi: 10.1093/bioinformatics/btt086
- He, Y. (2012). Analyses of *Brucella* pathogenesis, host immunity, and vaccine targets using systems biology and bioinformatics. *Front. Cell Infect. Microbiol.* 2:2. doi: 10.3389/fcimb.2012.00002
- Hinic, V., Brodard, I., Petridou, E., Filioussis, G., Contos, V., Frey, J., et al. (2010). Brucellosis in a dog caused by *Brucella melitensis* rev 1. *Vet. Microbiol.* 141, 391–392. doi: 10.1016/j.vetmic.2009.09.019
- Ke, Y., Yang, X., Wang, Y., Bai, Y., Xu, J., Song, H., et al. (2012). Genome sequences of *Brucella melitensis* 16m and its two derivatives 16m1w and 16m13w, which evolved in vivo. *J. Bacteriol.* 194:5489. doi: 10.1128/JB.01293-12
- Kirzinger, M. W., and Stavrinides, J. (2012). Host specificity determinants as a genetic continuum. *Trends Microbiol.* 20, 88–93. doi: 10.1016/j.tim.2011.11.006
- Li, H., and Durbin, R. (2009). Fast and accurate short read alignment with burrows-wheeler transform. *Bioinformatics* 25, 1754–1760. doi: 10.1093/bioinformatics/btp324

- Lucero, N. E., Ayala, S. M., Escobar, G. I., and Jacob, N. R. (2008). *Brucella* isolated in humans and animals in latin America from 1968 to 2006. *Epidemiol. Infect.* 136, 496–503. doi: 10.1017/S0950268807008795
- Mailles, A., Ogielska, M., Kemiche, F., Garin-Bastuji, B., Brieu, N., Burnus, Z., et al. (2017). *Brucella suis* biovar 2 infection in humans in France: emerging infection or better recognition? *Epidemiol. Infect.* 145, 2711–2716.
- Office International des Epizooties [OIE] (2016). *Brucellosis (Brucella abortus, B. melitensis and B. suis)* (Infection with *abortus*, *B.*, *B. melitensis* and *B. suis*). Paris: OIE Terrestrial Manual.
- Page, A. J., Cummins, C. A., Hunt, M., Wong, V. K., Reuter, S., Holden, M. T., et al. (2015). Roary: rapid large-scale prokaryote pan genome analysis. *Bioinformatics* 31, 3691–3693. doi: 10.1093/bioinformatics/btv421
- Ridler, A. L., West, D. M., and Collett, M. G. (2012). Pathology of *Brucella ovis* infection in red deer stags (*Cervus elaphus*). *New Zealand Vet. J.* 60, 146–149. doi: 10.1080/00480169.2011.638269
- Ryall, B., Eydallin, G., and Ferenci, T. (2012). Culture history and population heterogeneity as determinants of bacterial adaptation: the adaptomics of a single environmental transition. *Microbiol. Mol. Biol. Rev.* 76, 597–625. doi: 10.1128/MMBR.05028-11
- Seemann, T. (2014). Prokka: rapid prokaryotic genome annotation. *Bioinformatics* 30, 2068–2069. doi: 10.1093/bioinformatics/btu153
- Soler-Llorens, P. F., Quance, C. R., Lawhon, S. D., Stuber, T. P., Edwards, J. F., Ficht, T. A., et al. (2016). A *Brucella* spp. Isolate from a pac-man frog (*Ceratophrys ornata*) reveals characteristics departing from classical *Brucellae*. *Front. Cell Infect. Microbiol.* 6:116. doi: 10.3389/fcimb.2016.00116
- Stoffregen, C., Olsen, S. C., Wheeler, C. J., Bricker, B. J., Palmer, M. V., Jensen, A. E., et al. (2007). Diagnostic characterization of a feral swine herd enzootically infected with *Brucella*. *J. Vet. Diagn. Invest.* 19, 227–237.
- Suárez-Esquivel, M., Baker, K. S., Ruiz-Villalobos, N., Hernandez-Mora, G., Barquero-Calvo, E., Gonzalez-Barrientos, R., et al. (2017). *Brucella* genetic variability in wildlife marine mammals populations relates to host preference and ocean distribution. *Genome Biol. Evol.* 9, 1901–1912. doi: 10.1093/gbe/evx137
- Tamura, K., Stecher, G., Peterson, D., Filipski, A., and Kumar, S. (2013). MEGA6: molecular evolutionary genetics analysis version 6.0. *Mol. Biol. Evol.* 30, 2725–2729. doi: 10.1093/molbev/mst197
- Tenover, F. C., Arbeit, R. D., Goering, R. V., Mickelsen, P. A., Murray, B. E., Persing, D. H., et al. (1995). Interpreting chromosomal DNA restriction patterns produced by pulsed-field gel electrophoresis: criteria for bacterial strain typing. *J. Clin. Microbiol.* 33, 2233–2239.
- Thompson, J. D., Higgins, D. G., and Gibson, T. J. (1994). CLUSTAL W: improving the sensitivity of progressive multiple sequence alignment through sequence weighting, position-specific gap penalties and weight matrix choice. *Nucleic Acids Res.* 22, 4673–4680.
- Tsolis, R. M., Seshadri, R., Santos, R. L., Sangari, F. J., Lobo, J. M., de Jong, M. F., et al. (2009). Genome degradation in *Brucella ovis* corresponds with narrowing of its host range and tissue tropism. *PLoS One* 4:e5519. doi: 10.1371/journal.pone.0005519
- Verger, J. M., Garin-Bastuji, B., Grayon, M., and Mahé, A. M. (1989). La brucellose bovine à *Brucella melitensis* en France. *Ann. Rech. Vet.* 20, 93–102.
- Wareth, G., Melzer, F., El-Diasty, M., Schmooch, G., Elbauomy, E., Abdel-Hamid, N., et al. (2017). Isolation of *Brucella abortus* from a dog and a cat confirms their biological role in re-emergence and dissemination of bovine brucellosis on dairy farms. *Transbound. Emerg. Dis.* 64, e27–e30. doi: 10.1111/tbed.12535
- Wattam, A. R., Williams, K. P., Snyder, E. E., Almeida, NF Jr, Shukla, M., Dickerman, A. W., et al. (2009). Analysis of ten *Brucella* genomes reveals evidence for horizontal gene transfer despite a preferred intracellular lifestyle. *J. Bacteriol.* 191, 3569–3579. doi: 10.1128/JB.01767-08
- Wattam, A. R., Foster, J. T., Mane, S. P., Beckstrom-Sternberg, S. M., Beckstrom-Sternberg, J. M., Dickerman, A. W., et al. (2014). Comparative phylogenomics and evolution of the *Brucellae* reveal a path to virulence. *J. Bacteriol.* 196, 920–930. doi: 10.1128/JB.01091-13

Conflict of Interest Statement: The authors declare that the research was conducted in the absence of any commercial or financial relationships that could be construed as a potential conflict of interest.

Copyright © 2018 Holzapfel, Girault, Keriell, Ponsart, O'Callaghan and Mick. This is an open-access article distributed under the terms of the Creative Commons Attribution License (CC BY). The use, distribution or reproduction in other forums is permitted, provided the original author(s) and the copyright owner(s) are credited and that the original publication in this journal is cited, in accordance with accepted academic practice. No use, distribution or reproduction is permitted which does not comply with these terms.



Phenotypic and Molecular Characterization of *Brucella microti*-Like Bacteria From a Domestic Marsh Frog (*Pelophylax ridibundus*)

OPEN ACCESS

Edited by:

Holger C. Scholz,
Institut für Mikrobiologie der
Bundeswehr, Germany

Reviewed by:

Yuehua Ke,
Centers for Disease Control and
Prevention (CDC), United States
Alice Rebecca Wattam,
Virginia Tech, United States
Alessandra Occhialini,
Université de Montpellier, France
Adrian Whatmore,
Animal and Plant Health Agency,
United Kingdom

*Correspondence:

Virginie Mick
virginie.mick@anses.fr

† Present Address:

Maryne Jaÿ,
ANSES, Laboratoire de Lyon, UMR
Mycoplasmoses des Ruminants,
Lyon, France Université de Lyon,
VetAgro Sup, UMR Mycoplasmoses
des Ruminants, Marcy L'Etoile, France

‡ These authors have contributed
equally to this work

Specialty section:

This article was submitted to
Veterinary Infectious Diseases,
a section of the journal
Frontiers in Veterinary Science

Received: 29 June 2018

Accepted: 24 October 2018

Published: 15 November 2018

Citation:

Jaÿ M, Girault G, Perrot L, Taunay B,
Vuilmet T, Rossignol F, Pitel P-H,
Picard E, Ponsart C and Mick V (2018)
Phenotypic and Molecular
Characterization of *Brucella*
microti-Like Bacteria From a Domestic
Marsh Frog (*Pelophylax ridibundus*).
Front. Vet. Sci. 5:283.
doi: 10.3389/fvets.2018.00283

Maryne Jaÿ^{1†}, Guillaume Girault^{1†}, Ludivine Perrot¹, Benoit Taunay¹, Thomas Vuilmet¹,
Frédérique Rossignol², Pierre-Hugues Pitel³, Elodie Picard⁴, Claire Ponsart¹ and
Virginie Mick^{1*}

¹ ANSES/Paris-Est University, EU/OIE/FAO and National Reference Laboratory for Brucellosis, Animal Health Laboratory,
Maisons-Alfort, France, ² DDPP de la Drôme, Valence, France, ³ LABEO, Caen, France, ⁴ LABEO-Orne, Alençon, France

Several *Brucella* isolates have been described in wild-caught and “exotic” amphibians from various continents and identified as *B. inopinata*-like strains. On the basis of epidemiological investigations conducted in June 2017 in France in a farm producing domestic frogs (*Pelophylax ridibundus*) for human consumption of frog’s legs, potentially pathogenic bacteria were isolated from adults showing lesions (joint and subcutaneous abscesses). The bacteria were initially misidentified as *Ochrobactrum anthropi* using a commercial identification system, prior to being identified as *Brucella* spp. by MALDI-TOF assay. Classical phenotypic identification confirmed the *Brucella* genus, but did not make it possible to conclude unequivocally on species determination. Conventional and innovative bacteriological and molecular methods concluded that the investigated strain was very close to *B. microti* species, and not *B. inopinata*-like strains, as expected. The methods included growth kinetic, antimicrobial susceptibility testing, RT-PCR, Bruce-Ladder, Suis-Ladder, RFLP-PCR, AMOS-ERY, MLVA-16, the ectoine system, 16S rRNA and *recA* sequence analyses, the LPS pattern, *in silico* MLST-21, comparative whole-genome analyses (including average nucleotide identity ANI and whole-genome SNP analysis) and HRM-PCR assays. Minor polyphasic discrepancies, especially phage lysis and A-dominant agglutination patterns, as well as, small molecular divergences suggest the investigated strain should be considered a *B. microti*-like strain, raising concerns about its environmental persistence and unknown animal pathogenic and zoonotic potential as for other *B. microti* strains described to date.

Keywords: Brucellosis, *Brucella microti*, domestic frog, *Pelophylax ridibundus*, Europe

INTRODUCTION

Based on bacteriological features, host preference and pathogenicity, the taxonomy of the *Brucella* genus (<http://www.bacterio.net/brucella.html>) currently identifies 12 species split into (i) “core” *Brucella* species, including the six “classical” species (*Brucella melitensis*, *B. abortus*, *B. suis*, *B. canis*, *B. ovis*, *B. neotomae*; <http://www.oie.int/fr/normes/code-terrestre/acces-en-ligne/>), *B. ceti* and *B. pinnipedialis* isolated from marine mammals (1, 2), and the recently described

B. papionis from baboons (3), and *ii*) the emerging atypical *Brucella* species (4–6). The atypical *Brucella* species include fast-growing *B. microti* initially isolated from common voles (7) and reported from soil (8) and red fox (9), *B. inopinata* BO1 isolated from a breast implant (10), *B. vulpis* from red fox (11), as well as, unclassified isolates: BO2 isolated from a patient with chronic destructive pneumonia (12), probably representing a novel lineage of *B. inopinata*, and novel Australian rodent isolates (13). Interestingly, the atypical *Brucella* isolates are phenotypically close to *Ochrobactrum* spp., a soil-associated facultative human pathogen (14), but genetically close to the *Brucella* genus. Molecular data show that Australian rodent isolates are related to *B. inopinata* and strain BO2, although *B. microti* is genetically close to the core phylogenetic clade of *Brucella*, especially to *B. suis* 1330 (15).

Brucella infections have been described in wild-caught and captive-bred anuran species native to Africa, South and Central America, and Australia, from animals showing systemic or localized infections (16–22), as well as, from other apparently healthy individuals (23). These exotic frog strains are affiliated with the atypical *Brucella* group, genetically close to *B. inopinata* (24), (18).

Although human infections due to *B. inopinata* have been reported (10, 12), its zoonotic potential remains unclear. Likewise, the pathogenicity of atypical *Brucella* bacteria and their transmission among amphibians are unknown (25).

This study presents the isolation and phenotypic identification of a new *Brucella* field isolate from *Pelophylax ridibundus*, a domestic frog on a breeding farm, as well as, its in-depth genomic characterization.

RESULTS AND DISCUSSION

Detection of a Presumptive *Brucella* Field Isolate From the Domestic Frog *P. ridibundus*

In June 2017, epidemiological investigations were conducted for research purposes on a frog farm in France breeding the first domesticated strain of *P. ridibundus* Rivan92[®], selected by the French National Institute for Agricultural Research (INRA) for human consumption (frog's legs). Animals were sampled randomly from the farm, based on development stages and ponds (3 batches of tadpoles, 1 batch of 20 small frogs and 2 batches of 8 adults) for pan-pathogen examination. All the selected batches were apparently healthy except for one batch of adults that showed lesions: swollen joint ($n = 1$) and subcutaneous edema ($n = 2$), confirmed at necropsy. After necropsy, bacteriological analyses were performed on 6 pools of individuals (whole animal for early stages [20g] and internal organs for adults), and on visible lesions. A number of regular, brownish colonies, reaching 2 mm after 48 h, were isolated from the only adult batch showing lesions. Testing using the commercial API20-NE identification system (Biomérieux, France) pointed to *Ochrobactrum anthropi*. MALDI-TOF assay (Bruker Daltonics, France) run on a spot of pure culture overlaid with 1 μ L of HCCA matrix indicated *Brucella* spp. using the Biotyper

Security-Related (SR) database (26). *Brucella* misidentification using commercial biochemical tests is frequently reported (27); (28), and can result in laboratory-acquired infections (29, 30). Isolates were subsequently sent to the national reference laboratory for reliable identification and refined characterization.

Phenotypic Identification

Standard phenotypic identification (31) confirmed the *Brucella* genus (Table 1), without concluding unequivocally on species determination. Interestingly, strain biotyping traits were not strictly consistent with the *B. inopinata*-like profile previously described in anurans, in particular due to phage lysis. Surprisingly, phenotypic features (Table 1) were closer to the *B. microti* reference strain CCM 4915, except for the A-dominant agglutination pattern, already described for one *B. microti* fox isolate (32).

Growth kinetics in nutritive tryptic soy and M9 minimal broths confirmed faster growth than classical fastidious *Brucella* for the investigated frog strain, named 17-2122-4144, with a generation time identical to *B. microti* CCM 4915 (i.e., approximately 4 h in our growth conditions).

Moreover, antimicrobial susceptibility testing (AST) performed by the disk and E-test methods highlighted an

TABLE 1 | Classical phenotypic characterization of the frog isolate investigated in this study vs. *B. inopinata*, *B. inopinata*-like strains isolated from exotic frogs, and *B. microti* field/reference strains.

	<i>B. inopinata</i>	<i>B. inopinata</i> -like	<i>B. microti</i>	17-2122-4144
Morphology	S	S	S ^a	S
CO ₂	–	–	–	–
H ₂ S	+	– ^b	– ^c	–
Oxidase	+	+	+	+
Urease	+ rapid	+ ^d	+ slow	+ slow
A	–	– ^e	– ^f	+
M	+ weak	– ^e	+ ^g	–
R	–	–	–	–
Thionin	+	+	+	+
Fuchsin	+	+	+	+
Tb RTD	–	–	–	–
Tb 10 ⁴ RTD	+ PL	–	+	+
Wb RTD	ND	–	+	+
Iz RTD	ND	–	+	+
R/C RTD	ND	–	ND	–

R/S, Colony morphology (Rough/Smooth); CO₂, CO₂ requirement; H₂S, H₂S production; Agglutination with monospecific A, M and R (rough) antisera; Dye (thionin and basic fuchsin) concentration 20 μ g.mL^{–1} in serum dextrose medium (1/50,000); +, Growth or Lysis by phages; –, No growth or no lysis; PL, Partial lysis.

^aSome rough isolates from soil.

^bSome isolates positive.

^cOne strain positive.

^dVarious rates.

^eSome isolates A+ M–.

^fOne fox isolate: A+ M–.

^gRough isolates from soil: A+, M+, R+; (31, 32).

identical pattern of susceptibility to the main anti-*Brucella* antibiotics of veterinary and human interest: doxycycline (DX), rifampicin (RIF), streptomycin (STM), ofloxacin (OFX), and sulfamethoxazole/trimethoprim (SMX/TMP) for the strain 17-2122-4144 vs *B. microti* CCM 4915.

Molecular Analysis

Conventional genus- and species-specific PCR methods (33) were performed (Table 2). The real-time PCR assays confirmed that the investigated strain belongs to the *Brucella* genus. The obtained Bruce-Ladder pattern was shared with the *B. microti* and *B. suis* biovar 2 reference strains and was distinct from other *Brucella* reference and vaccine strains. The Suis-Ladder method split the biovars of *B. suis*, *B. canis* and *B. microti* as previously described (32), and concluded that there was a single pattern between *B. microti* and the investigated strain.

Although most conventional molecular techniques did not make it possible to differentiate between CCM 4915 and 17-2122-4144, minor differences were observed regarding RFLP results (34): the restriction profile of the *omp2b* target digested by *EcoRI* for 17-2122-4144 was distinct from the CCM 4915 profile, but similar to the *B. pinnipedialis* reference strain B2/94. Interestingly, the AMOS-ERY profile of the studied strain (2 fragments of 1.3 kbp and 1.2 kbp) was divergent from classical *Brucella* spp. profiles, as well as, from the atypical *B. microti* (one single 1.3 kbp fragment), but close to *B. suis* reference strains (1.3 and 1.2 kbp).

In addition to classical molecular approaches, phylogenomic methods were used (Table 2). Unsurprisingly, MLVA-16 results showed that 17-2122-4144 clustered within *B. microti* reference strains CCM 4915 and CCM 4916 and together with the 10 field strains reported to date (Figure 1; Supplementary Figure 1), close to the *B. neotomae* reference strain 5K33 (32).

De novo assembly showed a genome with a total length of 3,335,258 bp, vs 3.37 Mbp for *B. inopinata* BO1 and 3.34 Mbp for *B. microti* CCM 4915. Moreover, the total number of predicted genes per genome (evaluated by QUAST) for 17-2122-4144 (3,141 genes) is very similar to CCM 4915 (3,145 genes), closer than for BO1 (3,220 genes). ANI exhibited maximum identity with *B. microti* CCM 4915 (99.89%); 98.33% identity with *B. inopinata* and 97.77–98.2% with 3 frog *Brucella* genomes from the NCBI database (24). Similarly, a bacteriophage-related 11,742 bp insertion, previously described as present only in *B. microti* isolates (15), was also found within the investigated genome. Further analyses using Roary and Scoary to compare gene presence or absence did not underline any gene signature specific to the investigated field isolate vs. *B. inopinata* BO1, *B. microti* CCM 4915 and *B. melitensis* bv1 16M. Moreover, the ectoine system, conferring salt and temperature resistance, described in atypical *Brucella* (24), was absent in 17-2122-4144, as well as, BO1 and CCM 4915. Similarly, 16S rRNA and *recA* comparative analyses (27) confirmed that 17-2122-4144 was closely related to *B. microti*, with absence of 5 *rrs* mutations in 17-2122-4144 and CCM 4915, systematically present in *B. inopinata* and *B. inopinata*-like strains, and presence of a single *recA* *B. microti*-specific SNP in 17-2122-4144 (24, 25, 32).

In line with previous studies (4, 5, 25, 35), we assessed *in silico* the LPS profile of the investigated isolate, especially focusing on the genes essential for LPS synthesis: the *wbk* region, *wboA* and *wboB* genes, the *manBCA* region, as well as, the *tagH* and *rfbD* genes. Regions of the investigated isolate were strikingly similar to *B. microti*. In addition, our analysis concluded presence of the *wboA*, *wboB* and *manBCA* genes (unlike bullfrog strains, BO2 and B13-0095) and absence of the *rmlACBD* region and *tagH* gene found in BO2 and B13-0095 in the investigated genome.

TABLE 2 | Molecular characterization of the frog isolate investigated in this study vs. *B. inopinata*, *B. inopinata*-like strains isolated from exotic frogs, and *B. microti* field/reference strains.

	<i>B. inopinata</i>	<i>B. inopinata</i> -like	<i>B. microti</i>	17-2122-4144
RT-PCR	+	+	+	+
Bruce-Ladder	NR	NR	<i>Bmic/Bsuis</i> bv2	<i>Bmic/Bsuis</i> bv2
Suis-Ladder	NR	NR	<i>B. microti</i>	<i>B. microti</i>
RFLP	NR	NR	<i>B. microti</i>	Different from <i>B. microti</i>
AMOS-ERY	NR	NR	<i>B. microti</i>	Close to <i>B. suis</i>
MLVA16	<i>B. inopinata</i>	NR	<i>B. microti</i>	<i>B. microti</i>
ANI* (%)	98.33	97.77–98.2	99.89	100
11.7 kbp insertion	–	–	+	+
Ectoine system	–	+	–	–
16S rRNA (5 mutations)	+	+	–	–
<i>recA</i> (<i>B. microti</i> -specific SNP)	–	–	+	+
LPS pattern	<i>B. inopinata</i>	Close to <i>B. inopinata</i>	<i>B. microti</i>	<i>B. microti</i>
MLST-21	<i>B. inopinata</i>	Close to <i>B. inopinata</i>	<i>B. microti</i>	Close to <i>B. microti</i>
HRM PCR	NR	NR	<i>B. microti</i>	<i>B. microti</i>
wgSNP	<i>B. inopinata</i>	<i>B. inopinata</i> -like	<i>B. microti</i>	<i>B. microti</i>

*ANI values are calculated on the basis of the reference strain vs. the frog strain investigated in this study; NR, not reported; *Bmic/Bsuis* bv2, the pattern is shared with *B. microti* and *B. suis* bv 2 reference strains; +, presence; –, absence; *B. microti*, the pattern is a unique signature among *B. microti* strains described to date; *B. inopinata*, the pattern is a unique signature among *B. inopinata* strains described to date; *B. inopinata*-like, the pattern is a unique signature among *B. inopinata*-like strains described to date (25).

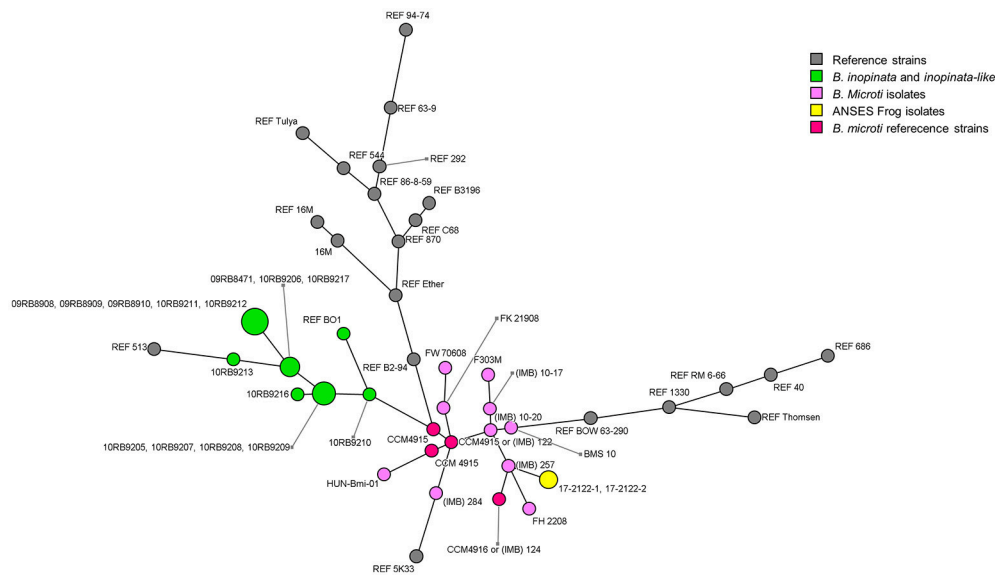


FIGURE 1 | Minimum Spanning Tree of MLVA-16 genotypes of the frog strain investigated in this study, *B. microti* isolates published to date, and all *Brucella* reference strains. *B. microti* isolates are distinguished by different colors: yellow for the frog strain investigated in this study; pink for previously published isolates (32); red for *B. microti* reference strains; other reference strains are colored in gray.

Interestingly, the *rfbD* gene was present in 17-2122-4144, but disrupted by numerous stop codons, as in *B. microti* CCM 4915. Our results show that the LPS profile of the novel isolate matches that described in *B. microti*.

In silico MultiLocus Sequence Typing-21 (MLST-21) confirmed this genetic proximity of 17-2122-4144 with *B. microti* CCM 4915. Except for the *mutL* gene involved in DNA mismatch repair, which harbored a point mutation at position 1149 (E383V), the MLST-21 pattern was strictly identical between the novel frog isolate and *B. microti*.

In parallel, *B. microti* and *B. inopinata*-specific High Resolution Melting (HRM) PCR assays were designed and performed against 17-2122-4144, emphasizing a profile similar to *B. microti* and divergent from *B. inopinata*. Phylogenetic comparative whole-genome SNP analysis showed that 17-2122-4144 is very close to *B. microti* CCM 4915 (323 SNPs without filtering, 73 SNPs in an overall phylogeny context) among the classical *Brucella* group (Figure 2; Supplementary Table 2), unlike strains previously isolated from frogs that clustered with *B. inopinata* in the “early-diverging” *Brucella* group (25).

Taxonomic Conclusions

The investigated frog strain is very close to *B. microti* species, and not to *B. inopinata*-like strains, as might be expected given the current taxonomy of strains isolated from frogs. Despite minor polyphasic discrepancies, 17-2122-4144 is qualified as a *B. microti*-like strain.

B. microti has been isolated from wild animals, such as the common vole *Microtus arvalis* (36), (7), wild boars (37), and red foxes (9), and is described as persistent over a long period in soil (8), suggesting the existence of environmental reservoirs. Interestingly, although *B. microti* is suspected to induce epizootic

mortality in the common vole (36), isolated cases from other described hosts seem to be asymptomatic, with no associated clinical signs (9, 37), suggesting asymptomatic carriage. In addition, the replication ability of *B. microti* was demonstrated in mouse macrophages (25, 38) and its pathogenic potential was shown to cause death in murine models (38–40) and lesions in chicken embryo models (41).

Anthropogenic interference has previously been reported to impact brucellosis prevalence in wildlife (42), raising questions on the influence of natural selection and selective breeding on *B. microti* fitness. Long-term environmental persistence outside the host and the putative ubiquitous nature of the *B. microti*-like strain investigated in this study, as well as, its unknown—but suspected—animal pathogenic and zoonotic potential, raise possible concerns for animal and public health. Further epidemiological investigations in wild frogs, as well as, in the natural environment might be required to offer new insights regarding bacterial carriage and possible clinical expression, depending on housing conditions. Moreover, *in vitro* cell infection experiments, as well as, *in vivo* infections will be required to determine the pathogenic potential of the *B. microti*-like isolates from frogs, in accordance with previous approaches applied to amphibian strains (25).

This study is the first isolation of *B. microti*-like bacteria from *P. ridibundus* on a domestic frog farm in France.

MATERIALS AND METHODS

Bacterial Strains and Genomes

Strains and/or genomes used in this study are listed in Supplementary Table 1.

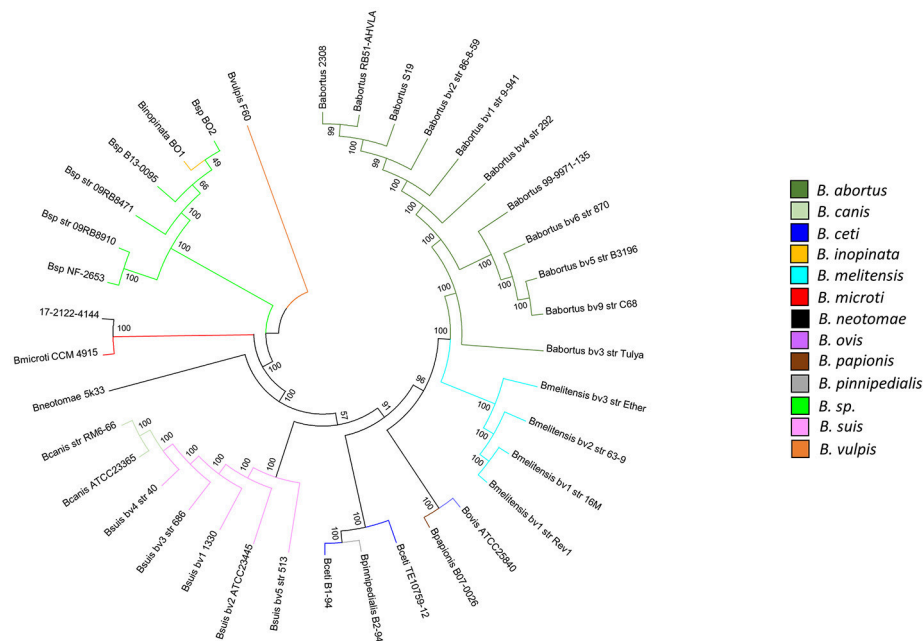


FIGURE 2 | Phylogenetic comparative whole-genome SNP analysis of the frog strain investigated in this study and all *Brucella* reference strains. The dendrogram was constructed using the maximum likelihood method with 200 bootstrap repetitions (36,590 SNPs). Species are distinguished by different colors. A log scale is used in this tree, allowing a better distinction between isolates.

Phenotypic Identification

Isolates were characterized using standard procedures (31) in BSL-3 facilities. AST was performed by the disk (Thermo Scientific - Oxoid) and E-test (Biomérieux) diffusion methods on Mueller-Hinton agar plates, supplemented with 5% sheep blood (DX, RIF, STM, OFX, SMX/TMP), following the recommendations of the Clinical and Laboratory Standards Institute (43). Growth kinetics were performed in nutritive tryptic soy and on M9 minimal broths (44). Stationary phase cultures were diluted to an OD₆₀₀ of 0.03 and grown in 75 cm² cell culture flasks at 37°C. OD₆₀₀ was measured every hour, and each point was serially diluted and plated on *Brucella* agar to determine colony-forming units. Each strain was assayed in triplicate.

Molecular Analysis

Genomic DNA was extracted using the High Pure PCR template preparation kit (Roche Diagnostics, France), according to the manufacturer's instructions.

Real-Time PCR (45), Bruce-Ladder (46), Suis-Ladder (47), RFLP-PCR (34), AMOS-ERY (48) and MLVA-16 (49) assays were performed as previously described. All tests have been carried out in duplicate (i.e., from 2 independent isolates). Clustering analysis was performed by using a minimum spanning tree (MST) and the cophenetic correlation coefficient with the UPGMA algorithm from MLVA data (Bionumerics v7.6.2; Applied Maths, Belgium), as well as, a maximum likelihood tree based on the Jukes Cantor model (with 200 repetitions

for bootstrap) from WGS data (Bionumerics 7.6.2 and MEGA software v. 6).

Whole-genome sequencing (Illumina HiSeq2500 platform, 100X) was performed. *De novo* assembly was performed using the SPAdes v3.9 algorithm. QUAST 4.6.3 was used to assess assembly robustness by gathering extensive assembly statistics. Nucleotide sequences of contigs from this work were deposited in the European Nucleotide Archive (EMBL-EBI) –Bioproject: <http://www.ebi.ac.uk/ena/data/view/PRJEB26927>; Accession Number: ERZ654921–. Average Nucleotide Identity (ANI) values were calculated using Jspecies (50). Phylogenetic SNP distances were determined using the Bionumerics v7.6.2 wgSNP-module. Roary v3.6.1 and Scoary were used to generate and compare matrices of gene presence/absence. Polymorphism of 16S rRNA (27), *recA* (27), the ectoine system (24), the LPS pattern (4, 5, 25, 35) as well as, the presence of a bacteriophage-related 11,742 bp insertion (15) were studied as previously described, using Bionumerics v7.6.2 for multiple sequence alignments. The 21 locus scheme (MLST-21) was determined *in silico* as previously described (33, 51).

HRM PCR assays were carried out as previously described (52) using the Bmic_1F (5'-AACTGCCGGATGTGAAAAAG-3') and Bmic_1R (5'-AAGGATCGAGGCGTCATAAA-3') primers.

AUTHOR CONTRIBUTIONS

MJ, GG, and VM designed the study and wrote the paper. FR, P-HP, and EP carried out preliminary identification studies. MJ and BT performed standard bacteriology. LP and GG performed

growth kinetics and antimicrobial susceptibility tests. LP, BT, TV, and GG contributed to molecular studies. GG and VM performed bioinformatics analyses. GG, MJ, CP, and VM performed data interpretation. All authors read and approved the manuscript content.

FUNDING

The first steps of investigation were supported by a grant from the *Conseil Regional de Normandie*. This work was supported by the European Union Reference Laboratory for Brucellosis.

ACKNOWLEDGMENTS

We are grateful to Vincent Sester and Madeleine Carle for their technical support and all the staff at local laboratory LVD61, in

particular Kathy Rocton, and local and central veterinary services DDPP26, especially Françoise Jacquet.

SUPPLEMENTARY MATERIAL

The Supplementary Material for this article can be found online at: <https://www.frontiersin.org/articles/10.3389/fvets.2018.00283/full#supplementary-material>

Supplementary Figure 1 | MLVA-16 analysis of the frog strain investigated in this study, *B. microti* isolates published to date and all *Brucella* reference strains. The dendrogram was constructed with the cophenetic correlation coefficient and UPGMA algorithm. *B. microti* isolates are distinguished by different colors: yellow for the frog strain investigated in this study; pink for previously published isolates (32); red for *B. microti* reference strains; other reference strains are colored in gray.

Supplementary Table 1 | *Brucella* strains used in this study.

Supplementary Table 2 | List of identified SNPs among the novel frog isolate investigated in this study and *Brucella* strains, as well as, location of mutations found within 17-2122-4144 vs. CCM4915.

REFERENCES

- Cloekaert A, Verger J-M, Grayon M, Paquet J-Y, Garin-Bastuji B, Foster G, et al. Classification of *Brucella* spp. isolated from marine mammals by DNA polymorphism at the *omp2* locus. *Microbes Infect Institut Pasteur*. (2001) 3:729–38. doi: 10.1016/S1286-4579(01)01427-7
- Foster G, Osterman BS, Godfroid J, Jacques I, Cloekaert A. *Brucella ceti* sp. nov. and *Brucella pinnipedialis* sp. nov. for *Brucella* strains with cetaceans and seals as their preferred hosts. *Int J Syst Evol Microbiol*. (2007) 57:2688–93. doi: 10.1099/ijs.0.65269-0
- Whatmore AM, Davison N, Cloekaert A, Al Dahouk S, Zygmunt MS, Brew SD, et al. *Brucella papionis* sp. nov. isolated from baboons (*Papio* spp.). *Int J Syst Evol Microbiol*. (2014) 64:4120–8. doi: 10.1099/ijs.0.065482-0
- Wattam AR, Inzana TJ, Williams KP, Mane SP, Shukla M, Almeida NF, et al. Comparative genomics of early-diverging *Brucella* strains reveals a novel lipopolysaccharide biosynthesis pathway. *mBio* (2012) 3:e00246–12. doi: 10.1128/mBio.00246-12
- Zygmunt MS, Jacques I, Bernardet N, Cloekaert A. Lipopolysaccharide heterogeneity in the atypical group of novel emerging *Brucella* species. *Clin Vaccine Immunol*. (2012) 19:1370–3. doi: 10.1128/CI.00300-12
- Scholz HC, Vergnaud G. Molecular characterisation of *Brucella* species. *Rev Sci Tech Off Int Epiz*. (2013) 32:149–62. doi: 10.20506/rst.32.1.2189
- Scholz HC, Hubalek Z, Sedlacek I, Vergnaud G, Tomaso H, Al Dahouk S, et al. *Brucella microti* sp. nov. isolated from the common vole *Microtus arvalis*. *Int J Syst Evol Microbiol*. (2008) 58:375–82. doi: 10.1099/ijs.0.65356-0
- Scholz HC, Hubalek Z, Nesvadbova J, Tomaso H, Vergnaud G, Le Fleche P, et al. Isolation of *Brucella microti* from soil. *Emerg Infect Dis*. (2008) 14:1316–7. doi: 10.3201/eid1408.080286
- Scholz HC, Hofer E, Vergnaud G, Le Fleche P, Whatmore AM, Al Dahouk S, et al. Isolation of *Brucella microti* from mandibular lymph nodes of red foxes, *Vulpes vulpes*, in lower Austria. *Vector Borne Zoonotic Dis*. (2009) 9:153–6. doi: 10.1089/vbz.2008.0036
- Scholz HC, Nockler K, Gollner C, Bahn P, Vergnaud G, Tomaso H, et al. *Brucella inopinata* sp. nov. isolated from a breast implant infection. *Int J Syst Evol Microbiol*. (2010) 60:801–8. doi: 10.1099/ijs.0.011148-0
- Scholz HC, Revilla-Fernandez S, Al Dahouk S, Hammerl JA, Zygmunt MS, Cloekaert A, et al. *Brucella vulpis* sp. nov., a novel *Brucella* species isolated from mandibular lymph nodes of red foxes (*Vulpes vulpes*) in Austria. *Int J Syst Evol Microbiol*. (2016) 66:2090–8. doi: 10.1099/ijs.0.000998
- Tiller R, Gee J, Lonsway D, Gribble S, Bell S, Jennison A, et al. Identification of an unusual *Brucella* strain (BO2) from a lung biopsy in a 52 year-old patient with chronic destructive pneumonia. *BMC Microbiol*. (2010) 10:23. doi: 10.1186/1471-2180-10-23
- Tiller RV, Gee JE, Frace MA, Taylor TK, Setubal JC, Hoffmaster AR, et al. Characterization of novel *Brucella* strains originating from wild native rodent species in North Queensland, Australia. *Appl Environ Microbiol*. (2010) 76:5837–45. doi: 10.1128/AEM.00620-10
- Al Dahouk S, Scholz HC, Tomaso H, Bahn P, Gollner C, Karges W, et al. Differential phenotyping of *Brucella* species using a newly developed semi-automated metabolic system. *BMC Microbiol*. (2010) 10:269. doi: 10.1186/1471-2180-10-269
- Audic S, Lescot M, Claverie JM, Scholz HC. *Brucella microti*: the genome sequence of an emerging pathogen. *BMC Genomics* (2012) 10:352. doi: 10.1186/1471-2164-10-352
- Fischer D, Lorenz N, Heuser W, Kampfer P, Scholz HC, Lierz M. Abscesses associated with a *Brucella inopinata*-like bacterium in a big-eyed tree frog (*Leptopelis vermiculatus*). *J Zoo Wildl Med*. (2012) 43:625–8. doi: 10.1638/2011-0005R2.1
- Whatmore AM, Dale EJ, Stubberfield E, Muchowski J, Koylass M, Dawson C, et al. Isolation of *Brucella* from a White's tree frog (*Litoria caerulea*). *JMM Case Rep*. (2015) 2:e17. doi: 10.1099/jmmcr.0.000017
- Muhldorfer K, Wibbelt G, Szentiks CA, Fischer D, Scholz HC, Zschock M, et al. The role of 'atypical' *Brucella* in amphibians: are we facing novel emerging pathogens? *J Appl Microbiol*. (2017) 122:40–53. doi: 10.1111/jam.13326
- Eisenberg T, Risse K, Schauerte N, Geiger C, Blom J, Scholz HC. Isolation of a novel 'atypical' *Brucella* strain from a bluespotted ribbontail ray (*Taeniura lymma*). *Antonie Van Leeuwenhoek* (2017) 110:221–34. doi: 10.1007/s10482-016-0792-4
- Eisenberg T, Hamann HP, Kaim U, Schlez K, Seeger H, Schauerte N, et al. Isolation of potentially novel *Brucella* spp. from frogs. *Appl Environ Microbiol*. (2012) 78:3753–5. doi: 10.1128/AEM.07509-11
- Helmick KE, Garner MM, Rhyan J, Bradway D. Clinicopathologic features of infection with novel *Brucella* organisms in captive waxy tree frogs (*Phyllomedusa sauvagii*) and Colorado River Toads (*Incilius Alvarius*). *J Zoo Wildl Med*. (2018) 49:153–61. doi: 10.1638/2017-0026R1.1
- Soler-Llorens PF, Quance CR, Lawhon SD, Stuber TP, Edwards JF, Ficht TA, et al. A *Brucella* spp. isolate from a pac-man frog (*Ceratophrys ornata*) reveals characteristics departing from classical *Brucellae*. *Front Cell Infect Microbiol*. (2016) 6:116. doi: 10.3389/fcimb.2016.00116
- Kimura M, Une Y, Suzuki M, Park ES, Imaoka K, Morikawa S. Isolation of *Brucella inopinata*-like bacteria from White's and Denny's tree frogs. *Vector Borne Zoonotic Dis*. (2017) 17:297–302. doi: 10.1089/vbz.2016.2027
- Scholz HC, Muhldorfer K, Shilton C, Benedict S, Whatmore AM, Blom J, et al. The change of a medically important genus: worldwide occurrence of genetically diverse novel *Brucella* species in exotic frogs. *PLoS ONE* (2016) 11:e0168872. doi: 10.1371/journal.pone.0168872

25. Al Dahouk S, Kohler S, Occhialini A, Jimenez de Bagues MP, Hammerl JA, Eisenberg T, et al. *Brucella* spp. of amphibians comprise genomically diverse motile strains competent for replication in macrophages and survival in mammalian hosts. *Sci Rep*. (2017) 7:44420. doi: 10.1038/srep44420
26. Ferreira L, Vega Castano S, Sanchez-Juanes F, Gonzalez-Cabrero S, Menegotto F, Orduna-Domingo A, et al. Identification of *Brucella* by MALDI-TOF mass spectrometry. Fast and reliable identification from agar plates and blood cultures. *PLoS ONE* (2010) 5:e14235. doi: 10.1371/journal.pone.0014235
27. Scholz HC, Pfeiffer M, Witte A, Neubauer H, Al Dahouk S, Wernery U, et al. Specific detection and differentiation of *Ochrobactrum anthropi*, *Ochrobactrum intermedium* and *Brucella* spp. by a multi-primer PCR that targets the recA gene. *J Med Microbiol*. (2008) 57:64–71. doi: 10.1099/jmm.0.47507-0
28. Poonawala H, Marrs Conner T, Peaper DR. The brief case: misidentification of *Brucella melitensis* as *Ochrobactrum anthropi* by matrix-assisted laser desorption ionization-time of flight mass spectrometry (MALDI-TOF MS). *J Clin Microbiol*. (2018) 56:e00914–17. doi: 10.1128/JCM.00914-17
29. Traxler RM, Lehman MW, Bosserman EA, Guerra MA, Smith TL. A literature review of laboratory-acquired brucellosis. *J Clin Microbiol*. (2013) 51:3055–62. doi: 10.1128/JCM.00135-13
30. Yang J, Ren X, Xue W, Yu X. Misidentification of *Brucella* and a review of the literature. *Rev Med Microbiol*. (2015) 26:85–7. doi: 10.1097/MRM.0000000000000038
31. OIE. Brucellosis (*Brucella abortus*, *B. melitensis* and *B. suis*) (Infection with *B. abortus*, *B. melitensis* and *B. suis*). Paris: OIE Terrestrial Manual (2016).
32. Al Dahouk S, Hofer E, Tomaso H, Vergnaud G, Le Fleche P, Cloeckaert A, et al. Intraspecific biodiversity of the genetically homologous species *Brucella microti*. *Appl Environ Microbiol*. (2012) 78:1534–43. doi: 10.1128/AEM.06351-11
33. Whatmore AM. Current understanding of the genetic diversity of *Brucella*, an expanding genus of zoonotic pathogens. *Infect Genet Evol*. (2009) 9:1168–84. doi: 10.1016/j.meegid.2009.07.001
34. Al Dahouk S, Tomaso H, Prenger-Berninghoff E, Spletstoesser WD, Scholz HC, Neubauer H. Identification of *Brucella* species and biotypes using polymerase chain reaction-restriction fragment length polymorphism (PCR-RFLP). *Crit Rev Microbiol*. (2005) 31:191–6. doi: 10.1080/10408410500304041
35. Cardoso PG, Macedo GC, Azevedo V, Oliveira SC. *Brucella* spp noncanonical LPS: structure, biosynthesis, and interaction with host immune system. *Microb Cell Fact*. (2006) 5:13. doi: 10.1186/1475-2859-5-13
36. Hubalek Z, Scholz HC, Sedlacek I, Melzer F, Sanogo YO, Nesvadbova J. Brucellosis of the common vole (*Microtus arvalis*). *Vector Borne Zoonotic Dis*. (2007) 7:679–87. doi: 10.1089/vbz.2007.0143
37. Ronai Z, Kreizinger Z, Dan A, Drees K, Foster JT, Banyai K, et al. First isolation and characterization of *Brucella microti* from wild boar. *BMC Vet Res*. (2015) 11:147. doi: 10.1186/s12917-015-0456-z
38. Jimenez de Bagues MP, Ouahrani-Bettache S, Quintana JF, Mitjana O, Hanna N, Bessoles S, et al. The new species *Brucella microti* replicates in macrophages and causes death in murine models of infection. *J Infect Dis*. (2010) 202:3–10. doi: 10.1086/653084
39. Jimenez de Bagues MP, de Martino A, Quintana JF, Alcaraz A, Pardo J. Course of infection with the emergent pathogen *Brucella microti* in immunocompromised mice. *Infect Immun*. (2011) 79:3934–9. doi: 10.1128/IAI.05542-11
40. Jimenez de Bagues MP, Iturralde M, Arias MA, Pardo J, Cloeckaert A, Zygmunt MS. The new strains *Brucella inopinata* BO1 and *Brucella* species 83–210 behave biologically like classic infectious *Brucella* species and cause death in murine models of infection. *J Infect Dis*. (2014) 210:467–72. doi: 10.1093/infdis/jiu102
41. Wareth G, Bottcher D, Melzer F, Shehata AA, Roesler U, Neubauer H, et al. Experimental infection of chicken embryos with recently described *Brucella microti*: pathogenicity and pathological findings. *Comp Immunol Microbiol Infect Dis*. (2015) 41:28–34. doi: 10.1016/j.cimid.2015.06.002
42. Mick V, Le Carrou G, Corde Y, Game Y, Jay M, Garin-Bastuji B. *Brucella melitensis* in France: persistence in wildlife and probable spillover from alpine ibex to domestic animals. *PLoS ONE* (2014) 9:e94168. doi: 10.1371/journal.pone.0094168
43. CLSI. *Performance Standards for Antimicrobial Susceptibility Testing: Twenty-Fifth Informational Supplement*. Wayne: Clinical and Laboratory Standards Institute (2015).
44. Sambrook J, Fritsch E, Maniatis T. *Molecular Cloning: A Laboratory Manual*. Melbourne: C. S. H. Laboratory (1989).
45. Bounaadja L, Albert D, Chenais B, Henault S, Zygmunt MS, Poliak S, et al. Real-time PCR for identification of *Brucella* spp.: a comparative study of *IS711*, *bcsp31* and *per* target genes. *Vet Microbiol*. (2009) 137:156–64. doi: 10.1016/j.vetmic.2008.12.023
46. Lopez-Goni I, Garcia-Yoldi D, Marin CM, de Miguel MJ, Munoz PM, Blasco JM, et al. Evaluation of a multiplex PCR assay (Bruce-ladder) for molecular typing of all *Brucella* species, including the vaccine strains. *J Clin Microbiol*. (2008) 46:3484–7. doi: 10.1128/JCM.00837-08
47. Lopez-Goni I, Garcia-Yoldi D, Marin CM, de Miguel MJ, Barquero-Calvo E, Guzman-Verri C, et al. New Bruce-ladder multiplex PCR assay for the biovar typing of *Brucella suis* and the discrimination of *Brucella suis* and *Brucella canis*. *Vet Microbiol*. (2011) 154:152–5. doi: 10.1016/j.vetmic.2011.06.035
48. Ocampo-Sosa AA, Aguero-Balbin J, Garcia-Lobo JM. Development of a new PCR assay to identify *Brucella abortus* biovars 5, 6 and 9 and the new subgroup 3b of biovar 3. *Vet Microbiol*. (2005) 110:41–51. doi: 10.1016/j.vetmic.2005.06.007
49. Le Fleche P, Jacques I, Grayon M, Al Dahouk S, Bouchon P, Denoeuf F, et al. Evaluation and selection of tandem repeat loci for a *Brucella* MLVA typing assay. *BMC Microbiol*. (2006) 6:9. doi: 10.1186/1471-2180-6-9
50. Richter M, Rossello-Mora R. Shifting the genomic gold standard for the prokaryotic species definition. *PNAS* (2009) 106:19126–31. doi: 10.1073/pnas.0906412106
51. Whatmore AM, Koylass MS, Muchowski J, Edwards-Smallbone J, Gopaul KK, Perrett LL. Extended multilocus sequence analysis to describe the global population structure of the genus *Brucella*: phylogeography and relationship to biovars. *Front Microbiol*. (2016) 7:2049. doi: 10.3389/fmicb.2016.02049
52. Girault G, Wattiau P, Saqib M, Martin B, Vorimore F, Singha H, et al. High-resolution melting PCR analysis for rapid genotyping of *Burkholderia mallei*. *Infect Genet Evol*. (2018) 63:1–4. doi: 10.1016/j.meegid.2018.05.004

Conflict of Interest Statement: The authors declare that the research was conducted in the absence of any commercial or financial relationships that could be construed as a potential conflict of interest.

Copyright © 2018 Jay, Girault, Perrot, Taunay, Vuilmet, Rossignol, Pitel, Picard, Ponsart and Mick. This is an open-access article distributed under the terms of the Creative Commons Attribution License (CC BY). The use, distribution or reproduction in other forums is permitted, provided the original author(s) and the copyright owner(s) are credited and that the original publication in this journal is cited, in accordance with accepted academic practice. No use, distribution or reproduction is permitted which does not comply with these terms.



Transcriptomic Analysis of the *Brucella melitensis* Rev.1 Vaccine Strain in an Acidic Environment: Insights Into Virulence Attenuation

Mali Salmon-Divon^{1*}, Tamar Zahavi¹ and David Kornspan^{2*}

¹ Genomic Bioinformatics Laboratory, Department of Molecular Biology, Ariel University, Ariel, Israel, ² Department of Bacteriology, Kimron Veterinary Institute, Bet Dagan, Israel

OPEN ACCESS

Edited by:

Axel Cloeckaert,
Institut National de la Recherche
Agronomique (INRA), France

Reviewed by:

Caterina Guzmán-Verri,
National University of Costa Rica,
Costa Rica
Ramesh Vemulapalli,
Texas A&M University, United States
Thomas A. Ficht,
Texas A&M University, United States

*Correspondence:

Mali Salmon-Divon
malisa@ariel.ac.il
David Kornspan
davidko@moag.gov.il

Specialty section:

This article was submitted to
Infectious Diseases,
a section of the journal
Frontiers in Microbiology

Received: 24 October 2018

Accepted: 30 January 2019

Published: 14 February 2019

Citation:

Salmon-Divon M, Zahavi T and
Kornspan D (2019) Transcriptomic
Analysis of the *Brucella melitensis*
Rev.1 Vaccine Strain in an Acidic
Environment: Insights Into Virulence
Attenuation. *Front. Microbiol.* 10:250.
doi: 10.3389/fmicb.2019.00250

The live attenuated *Brucella melitensis* Rev.1 (Elberg-originated) vaccine strain is widely used to control the zoonotic infection brucellosis in small ruminants, but the molecular mechanisms underlying the attenuation of this strain have not been fully characterized. Following their uptake by the host cell, *Brucella* replicate inside a membrane-bound compartment—the *Brucella*-containing vacuole—whose acidification is essential for the survival of the pathogen. Therefore, identifying the genes that contribute to the survival of *Brucella* in acidic environments will greatly assist our understanding of its molecular pathogenic mechanisms and of the attenuated virulence of the Rev.1 strain. Here, we conducted a comprehensive comparative transcriptome analysis of the Rev.1 vaccine strain against the virulent reference strain 16M in cultures grown under either normal or acidic conditions. We found 403 genes that respond differently to acidic conditions in the two strains (FDR < 0.05, fold change ≥ 2). These genes are involved in crucial cellular processes, including metabolic, biosynthetic, and transport processes. Among the highly enriched genes that were downregulated in Rev.1 under acidic conditions were acetyl-CoA synthetase, aldehyde dehydrogenase, cell division proteins, a cold-shock protein, GroEL, and VirB3. The downregulation of these genes may explain the attenuated virulence of Rev.1 and provide new insights into the virulence mechanisms of *Brucella*.

Keywords: *Brucella melitensis* 16M, *Brucella melitensis* Rev.1, acid stress, attenuation, virulence, transcriptomic analyses, RNA-Seq

INTRODUCTION

Brucella are facultative intracellular bacteria that are responsible for brucellosis—a zoonotic infection that causes abortions and sterility in ruminants, pigs, dogs, and rodents, and a severely debilitating febrile illness in humans (Ko and Splitter, 2003; von Barmen et al., 2012). One factor that crucially contributes to the virulence of *Brucella* is their ability to survive within various host cells, where they are inaccessible to the humoral immune response of the host (Delrue et al., 2004). Following uptake by the host cells, *Brucella* create a unique, highly acidic intracellular niche—the *Brucella*-containing vacuole (BCV)—in which they reside and multiply (Celli, 2006; Starr et al., 2008). The acidification of the BCV is essential for inducing the major *Brucella* virulence determinant, the type-IV secretion system (T4SS; Porte et al., 1999; Boschirola et al., 2002;

Köhler et al., 2002; Ke et al., 2015) which is encoded by the *virB* locus in their chromosomes. As the T4SS system (and, especially, the proteins VirB3–6 and VirB8–11) plays a crucial role in inhibiting the host immune response and in the intracellular survival and replication of *Brucella* within the host cells (Comerci et al., 2001; den Hartigh et al., 2008; Ke et al., 2015; Smith et al., 2016), the ability of *Brucella* to survive within the acidic conditions of the BCV is key to their pathogenesis and can be used to study the underlying mechanisms (Roop et al., 2009).

Porte et al. (1999) reported that the pH in phagosomes containing live *Brucella suis* decreases to 4.0 within 1 h following infection, and that this value persists for at least 5 h. Thus, one can assume the existence of a complex, transcription-level regulation network, which responds to specific cellular signals that enable the bacteria to survive in the acidic BCV environment. Indeed, two recent comparative transcriptome analyses employed RNA-seq to determine the changes in *Brucella* gene expression in cultures containing normal-pH media (namely, pH_{7.3}) versus those containing low-pH media (pH_{4.4}), thereby revealing novel molecular mechanisms leading to *Brucella* pathogenicity (Liu et al., 2015, 2016). Notably, one gene that was shown to play an important role in the resistance of *Brucella* to low-pH conditions is BMEI1329, which encodes a two-component response regulator gene in the transcriptional regulation pathway of *Brucella melitensis* (Liu et al., 2016).

Brucella melitensis, which infects goats and sheep mainly around the Mediterranean and the Persian Gulf, is the most pathogenic *Brucella* species for humans (Poester et al., 2013). Among the brucellosis vaccines used in high-prevalence regions, a widely used one utilizes the live attenuated Rev.1 *B. melitensis* strain (Avila-Calderón et al., 2013). This strain, originally developed from the virulent *B. melitensis* 6056 strain by Elberg and Herzberg in the mid-1950s, successfully protects and reduces abortions in small ruminants (Herzberg and Elberg, 1953; Banai, 2002), but it remains infectious for humans and causes abortions in small ruminants vaccinated during the last trimester of gestation. To improve brucellosis vaccines, we need to better understand the mechanisms underlying the virulence attenuation of the Rev.1 vaccine strain (as compared with that of other, pathogenic strains), but these mechanisms are yet unclear.

In a recent study, we sequenced and annotated the whole genome of the original Elberg *B. melitensis* Rev.1 vaccine strain (passage 101, 1970) and compared it to that of the virulent *B. melitensis* 16M strain (Salmon-Divon et al., 2018a,b). We found that, as compared with 16M, Rev.1 contains non-synonymous and frameshift mutations in important virulence-related genes—including genes involved in lipid metabolism, stress response, regulation, amino acid metabolism, and cell-wall synthesis—which we assumed are related to the attenuated virulence of this strain. In this study, we aimed to extend these findings to elucidate the intracellular survival mechanisms of the virulent 16M strain versus the vaccine Rev.1 strain. To this end, and in light of the importance of the acidic BCV environment for the virulence of *Brucella* species, we employed RNA-seq to comprehensively compare the transcriptome of the Rev.1 and 16M strains, each grown under either low- or normal-pH conditions, under the hypothesis that

the gene expression patterns of the two strains will differ between the two conditions. Our analysis revealed several candidate genes that may be related to the attenuated virulence of Rev.1 and may, therefore, facilitate the design of improved brucellosis vaccines.

MATERIALS AND METHODS

Bacteria Strains and Culture Conditions

Bacterial strains used in the present study were *B. melitensis* 16M (INRA *Brucella* Culture Collection)—the commonly used, virulent, wild-type biotype 1 strain—and the original attenuated *B. melitensis* Rev.1 vaccine strain (passage 101, 1970). For comparative assays, both the Rev.1 and 16M strains were cultured for 72 h on tryptic soy agar (TSA) plates at 37°C under 5% CO₂. The low-pH treatment assay was performed as reported previously (Liu et al., 2016). Briefly, bacteria were grown with shaking for 24 h in 10 ml of a tryptic soy broth (TSB; pH_{7.3}) at 37°C, with an initial density of 1×10^7 CFU/ml. The final bacterial densities were adjusted to 5×10^8 CFU/ml (OD₆₀₀ \cong 0.4) before the low-pH treatment, in which 1 ml of the culture was centrifuged at $7000 \times g$, resuspended in a pH_{4.4} TSB culture, and incubated for 4 h at 37°C. In the control group, bacteria were cultured in a pH_{7.3} TSB and incubated at 37°C for 4 h. After incubation, cell cultures were collected and centrifuged at $7000 \times g$, and then the supernatants were removed and an RNA Protect Reagent (Qiagen, Hilden, Germany) was added to the pellets to prevent RNA degradation. Five different biological replicates were used for each strain under each type of condition (total 20 samples). All the work with *Brucella* strains was performed at a biosafety level 3 laboratory in the Kimron Veterinary Institute, Bet Dagan, Israel.

RNA Isolation

The total RNA of the 16M and Rev.1 strains was isolated using the RNeasy Mini Kit (Qiagen) with a DNase treatment (Qiagen). RNA was eluted from the column using RNase-free water. RNA quality was measured by Bioanalyzer (Agilent, Waldbronn, Germany). Libraries were prepared using the ScriptSeq RNA-Seq Library Preparation Kit (Illumina, Inc., San Diego, CA, United States). Library quantity and pooling were measured by Qubit [dsDNA high sensitivity (HS); Molecular Probes, Inc., Eugene, OR, United States]. The pool was size-selected by using a 4% agarose gel. Library quality was measured by TapeStation (HS; Agilent). For RNA-seq, the NextSeq 500 high output kit V2 was used (Illumina, Inc.). The reads were single end at the length of 75 bp (~10 million reads per sample). Sample denaturation and loading were conducted according to the manufacturer's instructions. Library preparation and RNA-seq were conducted at the Center for Genomic Technologies at the Hebrew University of Jerusalem, Jerusalem, Israel.

Reverse Transcriptase PCR (RT-PCR)

To confirm the RNA-seq results, five upregulated or downregulated genes from the RNA-seq analysis were selected and a RT-PCR was used to confirm the expression changes of these genes in both strains (16M and Rev.1) and conditions

(low- and normal-pH). PCR primers were designed using Primer-BLAST (Ye et al., 2012) and are listed in **Supplementary Table S1**. Complementary DNA (cDNA) was obtained by a reverse transcription of 850 ng total RNA at a final reaction volume of 20 μ l, containing 4 μ l qScript Reaction Mix, and 1 μ l qScript Reverse Transcriptase (Quantabio, Beverly, MA, United States). Quantitative RT-PCR assays were purchased from Biosearch Technologies (Petaluma, CA, United States) and used according to the manufacturer's instructions. PCR reactions were conducted in a final reaction volume of 10 μ l containing 20 ng of cDNA template, 5 μ l of PerfeCTa SYBR Green FastMix, ROX (Quantabio), and 1 μ l of primer mix. All reactions were run in triplicate and the reference gene 16S rRNA was amplified in a parallel reaction for normalization.

RNA-Seq Analysis

Following quality control with FastQC¹, the reads were processed to trim adaptors and low-quality bases by using Trim Galore software². The EDGE-pro v1.3.1 software (Magoc et al., 2013) was used with the default parameters to map reads to the *B. melitensis* 16M reference genome (GCF_000007125.1), filter out multi-aligned reads, and estimate the expression levels of each gene. To convert the EDGE-pro output to a count-table format, the "edgeToDeseq.perl" script (provided with the software) was used. Normalization and differential gene expression analysis were conducted with the edgeR (Robinson et al., 2010) and Limma R packages (Smyth, 2005), using as input the count table generated by EDGE-pro. Briefly, genes that did not show more than 1 count per million (CPM) mapped reads in at least three samples were filtered out. Then, a TMM normalization (Robinson and Oshlack, 2010) was applied, followed by voom transformation (Law et al., 2014). Linear models to assess differential gene expression were generated by fitting a model with a coefficient for all factor combinations (strain and low-pH treatment) and then extracting the comparisons of interest, which also included the interaction between strain and treatment effects. The aim of adding the interaction term in this experimental setup was to detect genes that respond differently to pH treatment in Rev.1 compared to 16M; we named these genes "interaction genes." Only genes that demonstrated a fold change ≥ 2 and an FDR ≤ 0.05 were considered significant. Sequencing reads from this study were deposited in the NCBI SRA repository under the accession number PRJNA498082. The significantly upregulated or downregulated genes were subjected to a gene ontology enrichment analysis using ClusterProfiler (Yu et al., 2012) with a cutoff of FDR < 0.05 . To perform the gene ontology analysis, we first generated a database annotation package for *B. melitensis* 16M using the "makeOrgPackage" command from the AnnotationForge R package (Carlson, 2018). As input, we used the GO annotation, downloaded from QuickGO (Binns et al., 2009). Additional comparisons of the biological processes were performed with the Comparative GO web server (Fruzangohar et al., 2013) using all the upregulated and downregulated genes. Multidimensional scaling analysis (MDS)

was conducted using the "plotMDS" command within the edgeR (Robinson et al., 2010) package. A heatmap of the 403 genes that respond differently to acidic conditions in the two strains was generated using the "heatmap3" R package (Zhao et al., 2014), employing 1-Pearson correlation as the distance measure and "complete" as the linkage method. Genes were categorized into five clusters based on the generated dendrogram, and genes within each cluster were characterized based on Clusters of Orthologous Groups (COGs) annotations. For this purpose, protein sequences of the clustered genes were searched against a local COG BLAST database, which was downloaded from NCBI using the reverse position-specific BLAST (RPS-BLAST) tool (Marchler-Bauer et al., 2013). The expectation value (E) threshold was set to 0.01 and the BLAST output was parsed using an updated version of the cdd2cog.pl script³ to obtain the assignment statistics of the COGs. The number of genes within each heatmap cluster belonging to each COG assignment was calculated, and the ontologies with the highest number of genes were indicated in the heatmap.

Cell Infection Test

JEG-3 (ATCC® HTB-36™) human trophoblasts were grown in Eagle's Minimum Essential Medium (EMEM; ATCC® 30-2003™) with 10% fetal bovine serum. For intracellular replication experiments, 2×10^5 cells were seeded in a 24-well plate and cultured overnight at 37°C under 5% CO₂. Monolayers of cells were infected with the 16M or Rev.1 strains at a multiplicity of infection (MOI) of 500 (100 μ l of bacterial suspension per well). To synchronize the infection, the infected plates were centrifuged at 400 g for 5 min at room temperature, followed by a 75 min incubation at 37 °C in an atmosphere containing 5% CO₂. The cells were then washed three times with PBS and re-incubated for another 60 min in a medium containing 50 μ g/ml gentamicin to eliminate extracellular bacteria, after which the number of internalized bacteria was measured (time zero of the culture). To assess the intracellular bacterial growth, the concentration of gentamicin was reduced to 5 μ g/ml. To monitor the intracellular survival of the bacteria at various times post-infection, the infected cells were lysed for 10 min with 0.1% Triton X-100 in water and serial dilutions of the lysates were plated on TSA plates to enumerate the colony-forming units. Three identical wells were evaluated at each time for each strain. Experiments were repeated three times, independently.

RESULTS

We used RNA-seq to conduct a comprehensive comparative transcriptomic analysis of the gene expression profiles of the Rev.1 (vaccine) and 16M (virulent) *B. melitensis* strains, grown either under low-pH conditions that mimic the intracellular niche of the BCV (pH_{4.4}; referred to here as the "low- pH" group) or normal-pH conditions (pH_{7.3}; "normal-pH" group). The raw sequence outputs for each group are presented in **Table 1**. An MDS analysis revealed four clusters, of which all bacterial

¹<http://www.bioinformatics.babraham.ac.uk/projects/fastqc>

²http://www.bioinformatics.babraham.ac.uk/projects/trim_galore/

³<https://github.com/aleimba/bac-genomics-scripts/tree/master/cdd2cog>

TABLE 1 | The list of raw data sequence output for the normal- and low-pH groups of *B. melitensis* 16M and Rev.1.

Sample	Number of reads	Number of mapped reads	Number of unique reads	Number of multireads
c16M_1	10100002	9936571	9166680	769891
c16M_2	11159803	10971670	9999629	972041
c16M_3	11578986	11368597	10406648	961949
c16M_4	11983881	11809453	10675444	1134009
c16M_5	10342149	10171502	9243044	928458
e16M_1	12883209	11245980	10323376	922604
e16M_2	13370804	11211603	10325228	886375
e16M_3	13314490	10637845	9800648	837197
e16M_4	12717414	10407763	9768405	639358
e16M_5	12523271	10787022	10183357	603665
cRev1_1	9453360	9143362	8564979	578383
cRev1_2	12195263	11691352	10853987	837365
cRev1_3	13145448	12644912	11557656	1087256
cRev1_4	10815300	10207826	9459182	748644
cRev1_5	11052077	10371169	9553236	817933
eRev1_1	11005387	10756038	10093466	662572
eRev1_2	10892535	10654239	9949716	704523
eRev1_3	10208763	9979844	9441165	538679
eRev1_4	12700928	12464941	12176241	288700
eRev1_5	10150825	9873463	9665201	208262

c: control (normal pH) group; e: experimental (low pH) group.

samples within each cluster are closely related, emphasizing the high quality and reproducibility of the data (Figure 1).

Below, we first report the genes that are differentially expressed (DE) between the Rev.1 and 16M strains, each grown under normal-pH conditions. Then, for each separate strain, we report the genes that are DE between bacteria grown under normal-pH conditions and those grown under low-pH conditions. Finally,

we report possible interactions between the strain and its unique response to acidic conditions.

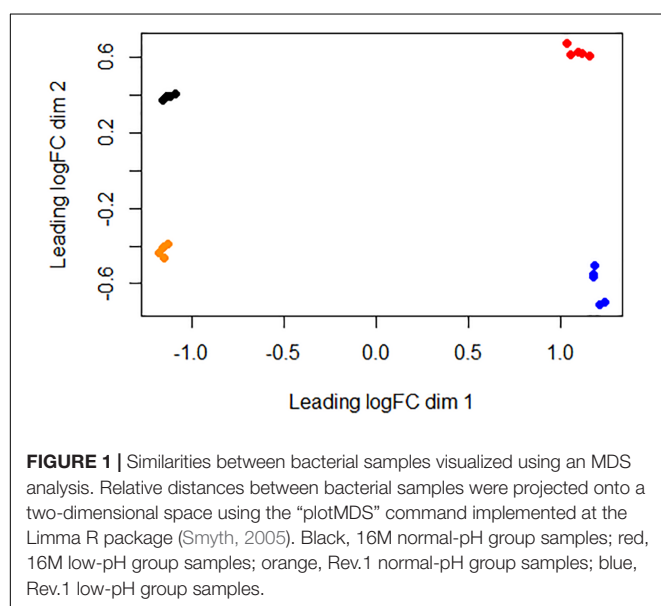
Differential Gene Expression Between *B. melitensis* Rev.1 and 16M Grown Under Normal-pH Conditions

When both Rev.1 and 16M were grown under normal-pH conditions (pH_{7.3}), our comparative transcriptomic analysis revealed 242 genes that were DE (FDR < 0.05, fold change ≥ 2; **Supplementary Table S2**) between the two strains, of which 172 genes were upregulated and 70 genes were downregulated in Rev.1 versus 16M. The most enriched biological processes associated with the DE genes were transport-related processes (Figure 2), while the most enriched molecular functions were cation transmembrane transporter, oxidoreductase, hydrolase, and ATPase activities (Figure 3). Twelve of the 242 DE genes encode for proteins that were previously reported in a proteomic analysis to be overexpressed in Rev.1 versus 16M (Table 2), including BMEI0704 (which encodes bacterioferritin) and six genes that encode ABC transporters (Forbes and Gros, 2001).

Next, we compared the genes that we found to be DE between the two strains to a list of *Brucella* virulence genes obtained from the *Brucella* Bioinformatics Portal (Xiang et al., 2006). Out of the 212 *B. melitensis* virulence genes that were reported in the *Brucella* Bioinformatics Portal, our transcriptomic analysis indicated eight genes that were upregulated and eight genes that were downregulated in Rev.1 versus 16M (Table 3), including six genes that encode transporters, of which three are annotated as sugar transporters.

Differential Gene Expression Between *B. melitensis* 16M Grown Under Low- and Normal-pH Conditions

In total, 773 genes in the 16M strain were DE (FDR < 0.05, fold change ≥ 2) between bacteria grown under normal- and low-pH conditions, of which 374 were upregulated and 399 were downregulated in the low-pH group versus the normal-pH group (Supplementary Table S3). The most enriched biological processes within these DE genes were transport, oxidation-reduction, and nucleoside triphosphate biosynthetic processes (Figure 2), and the most enriched molecular functions were ion and cation transmembrane transporters, oxidoreductase activities, and transition metal ion binding (Figure 3). Recently, Liu et al. (2016) reported 113 genes that are DE (using FDR < 0.05 and fold change ≥ 8) between normal- and low-pH conditions in 16M. Of these genes, 104 were also annotated in our analysis, of which 72 were DE (~70%; FDR < 0.05, fold change ≥ 2; Supplementary Table S4) between the two conditions, including 24 genes that were upregulated and 48 genes that were downregulated in the low-pH group versus the normal-pH group. Notably, the two-component response regulator BMEI1329, which is involved in the acid resistance of *B. melitensis* (Liu et al., 2016) was upregulated to a similar extent



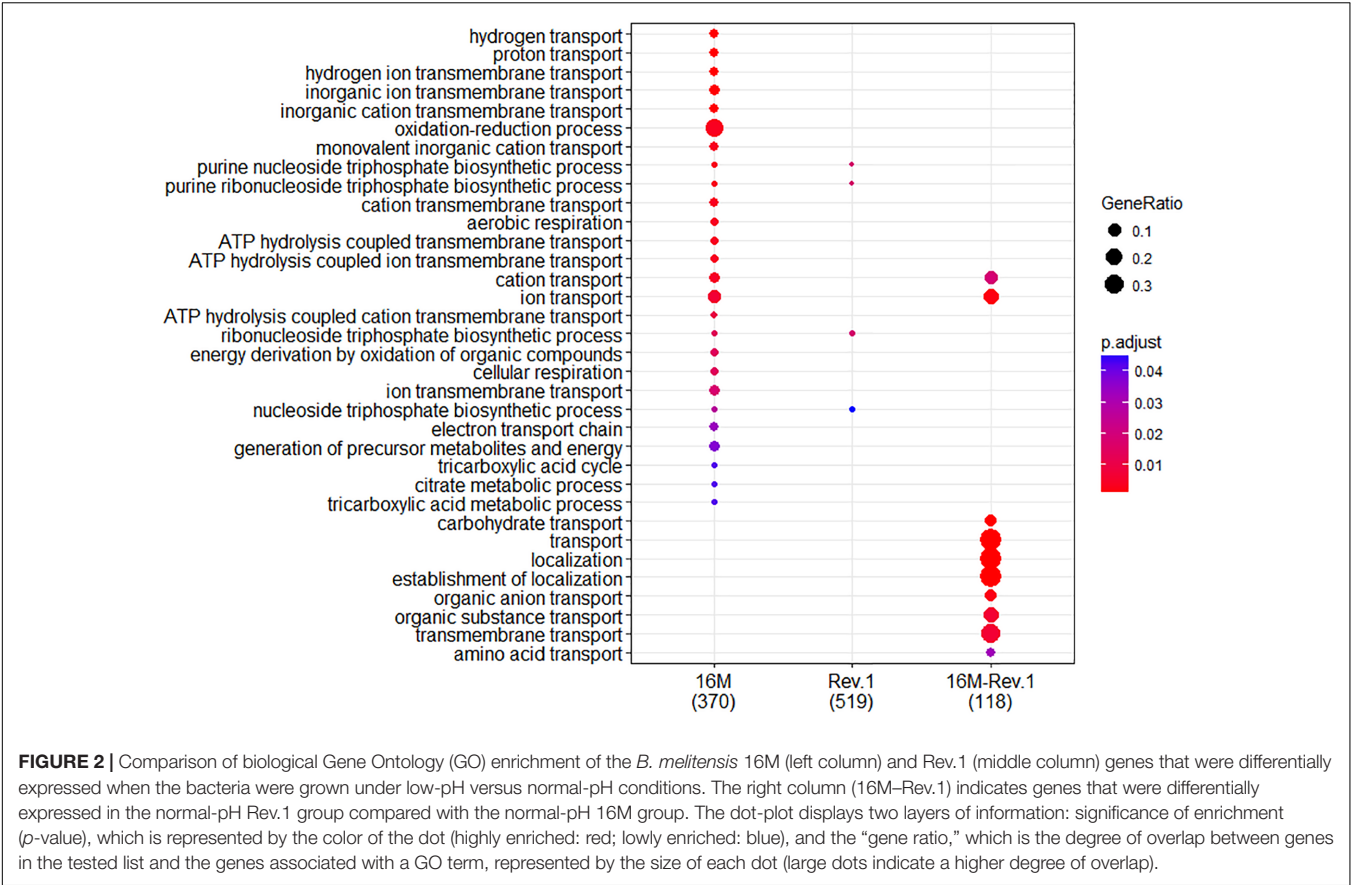


FIGURE 2 | Comparison of biological Gene Ontology (GO) enrichment of the *B. melitensis* 16M (left column) and Rev.1 (middle column) genes that were differentially expressed when the bacteria were grown under low-pH versus normal-pH conditions. The right column (16M–Rev.1) indicates genes that were differentially expressed in the normal-pH Rev.1 group compared with the normal-pH 16M group. The dot-plot displays two layers of information: significance of enrichment (*p*-value), which is represented by the color of the dot (highly enriched: red; lowly enriched: blue), and the “gene ratio,” which is the degree of overlap between genes in the tested list and the genes associated with a GO term, represented by the size of each dot (large dots indicate a higher degree of overlap).

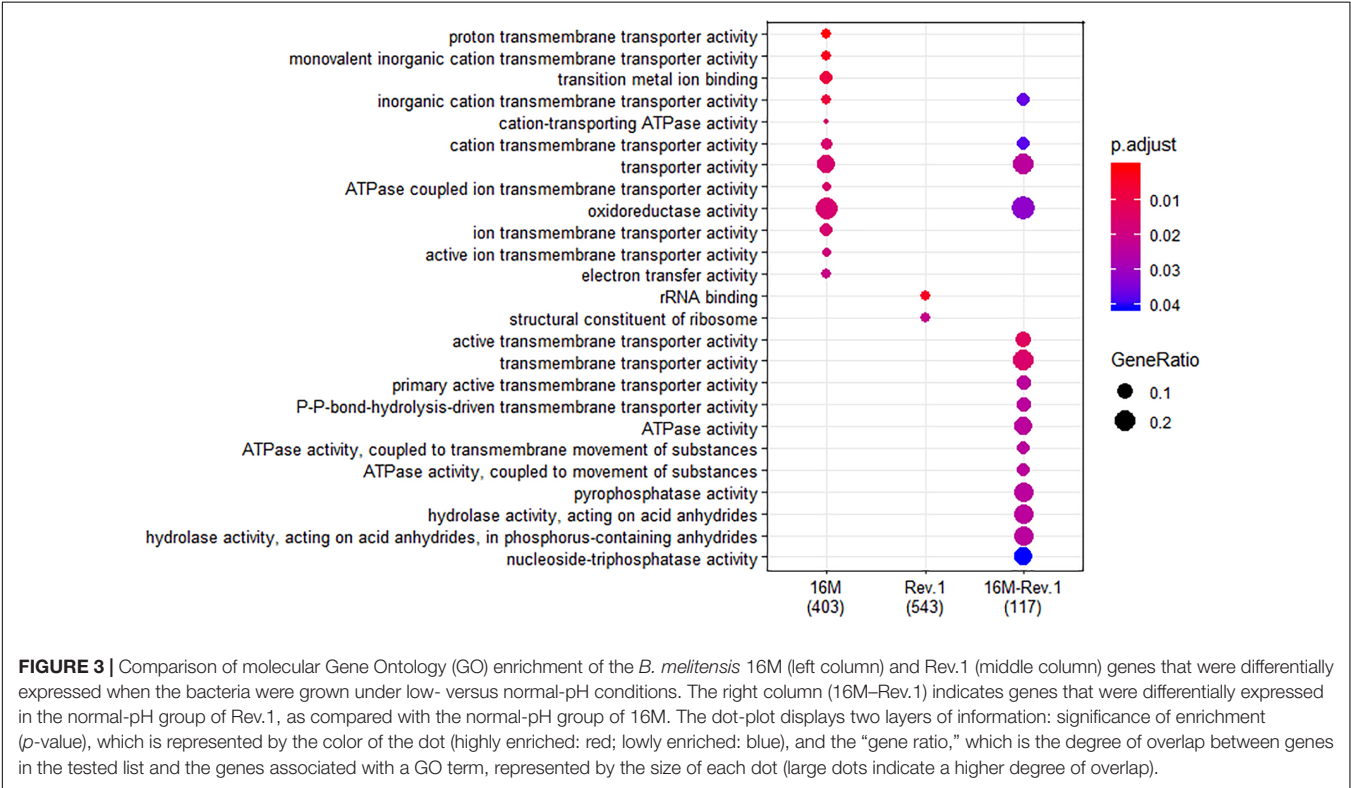


FIGURE 3 | Comparison of molecular Gene Ontology (GO) enrichment of the *B. melitensis* 16M (left column) and Rev.1 (middle column) genes that were differentially expressed when the bacteria were grown under low- versus normal-pH conditions. The right column (16M–Rev.1) indicates genes that were differentially expressed in the normal-pH group of Rev.1, as compared with the normal-pH group of 16M. The dot-plot displays two layers of information: significance of enrichment (*p*-value), which is represented by the color of the dot (highly enriched: red; lowly enriched: blue), and the “gene ratio,” which is the degree of overlap between genes in the tested list and the genes associated with a GO term, represented by the size of each dot (large dots indicate a higher degree of overlap).

TABLE 2 | List of DE genes found in the reported proteomic analysis.

Gene ID	Gene description	RNA-seq/proteome
BMEI0372	Response regulator	Overexpression/overexpression
BMEI1211	Amino acid ABC transporter substrate-binding protein	Overexpression/overexpression
BMEI1390	ABC transporter substrate-binding protein	Overexpression/overexpression
BMEI1923	Isovaleryl-CoA dehydrogenase	Overexpression/overexpression
BMEI0203	ABC transporter substrate-binding protein	Overexpression/overexpression
BMEI0344	ABC transporter permease	Overexpression/overexpression
BMEI0550	Glycine/betaine ABC transporter substrate-binding protein	Overexpression/overexpression
BMEI0590	Sugar-binding periplasmic protein	Overexpression/overexpression
BMEI0633	Branched-chain amino acid ABC transporter substrate-binding protein	Overexpression/overexpression
BMEI0704	Bacterioferritin	Overexpression/overexpression
BMEI0746	2-Oxo acid dehydrogenase subunit E2	Overexpression/overexpression
BMEI0747	Alpha-ketoacid dehydrogenase subunit beta	Overexpression/overexpression

(namely, a fold-change of ~ 4.55) in our analysis and in that of Liu et al. (2016).

Differential Gene Expression Between *B. melitensis* Rev.1 Grown Under Normal- and Low-pH Conditions

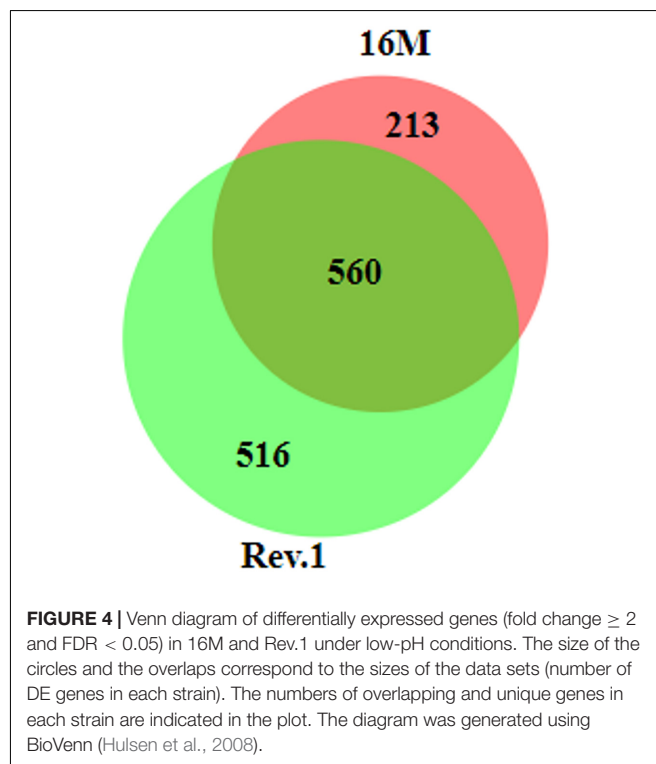
In total, 1076 genes in the Rev.1 strain were DE (FDR < 0.05, fold change ≥ 2) between the low-pH and normal-pH groups, of which 519 genes were upregulated and 557 genes were downregulated in the low-pH versus the normal-pH group (Supplementary Table S5). The most enriched biological process within these DE genes was the nucleoside triphosphate biosynthetic process (Figure 2), and the most enriched molecular functions were rRNA binding and a structural constituent of the ribosome (Figure 3).

The Effects of Low-pH Conditions on Gene Expression in *B. melitensis* 16M and Rev.1: A Comparison

In total, 560 genes that were DE between the low-pH and normal-pH conditions were common to both 16M and Rev.1, while 213 and 516 of the DE genes were unique to either 16M or Rev.1, respectively (Figure 4). A comparison of the genes that uniquely changed their expression between the low-pH and normal-pH groups in Rev.1 to those that uniquely changed their expression between the two conditions in 16M, in relation to their GO categories, revealed that the main biological processes that were highly enriched in Rev.1 were translation, metabolic process, and transport (transmembrane, amino acid, carbohydrate, and protein),

TABLE 3 | List of DE genes found in the *Brucella* Bioinformatics Portal.

Gene ID	Gene description	Up/downregulation (Rev.1 versus 16M)
BMEI0451	2-Isopropylmalate synthase	Upregulation
BMEI0545	DUF475 domain-containing protein	Downregulation
BMEI0624	Ketol-acid reductoisomerase	Downregulation
BMEI0626	PLP-dependent aminotransferase family protein	Upregulation
BMEI0796	Hypothetical protein	Downregulation
BMEI1759	Methionine synthase	Downregulation
BMEI1837	DUF3131 domain-containing protein	Downregulation
BMEI0056	Magnesium-translocating P-type ATPase	Upregulation
BMEI0077	Isochorismate synthase	Upregulation
BMEI0361	Sugar ABC transporter ATP-binding protein	Upregulation
BMEI0591	Sugar ABC transporter permease	Upregulation
BMEI0761	Thiol reductant ABC exporter subunit CydC	Downregulation
BMEI0762	Thiol reductant ABC exporter subunit CydD	Downregulation
BMEI0923	ABC transporter substrate-binding protein	Upregulation
BMEI0931	Class Ib ribonucleoside-diphosphate reductase assembly flavoprotein NrdI	Downregulation
BMEI1053	glucose/galactose transporter	Upregulation



whereas multiple biological processes were enriched in 16M, including pathogenesis, cell division, cell cycle, and cell wall organization (Supplementary Table S6).

Interaction Genes: Determination of a Possible Link Between Gene Expression, Environmental Stress, and a Specific Strain

In the analyses described above, we assumed that the two major parameters that could affect gene expression—the specific *B. melitensis* strain (Rev.1 versus 16M) and the environmental pH (4.4 versus 7.3)—are independent. Therefore, we adopted a naive approach and detected the effect of the acidic environment on gene expression in each strain separately, then compared the final list of DE genes. Our next step was to identify the potential dependency between strain and environmental pH, i.e., we sought to detect genes that respond differently to acidic stress in Rev.1 versus 16M. To this end, we added the “interaction” term to our statistical model, which revealed 403 genes that can be referred to as “interaction genes” (FDR < 0.05, fold change ≥ 2 ; **Supplementary Table S7**) and may potentially shed light on the attenuation mechanisms of Rev.1. Annotating these “interaction genes” revealed that the most enriched biological processes were related to metabolic, biosynthetic, and transport processes; the most enriched molecular functions were related to catalytic, hydrolase, nucleotide binding, oxidoreductase, and transporter activities; and the most enriched cellular compartments were related to integral components of the membrane (**Supplementary Tables S8–S10**). To identify genes that are potentially involved in the attenuation and survival of Rev.1, we searched the interaction genes for those that are associated with bacterial virulence and survival within the host and found four highly downregulated genes involved in metabolism processes and mitigation of acidic and oxidative stresses (**Table 4**). A heatmap of the 403 detected interaction genes, categorized into five clusters, is presented in **Figure 5**, and the list of genes within each cluster is shown in **Supplementary Table S11**. Finally, we created a GO Network based on 133 interaction genes with FDR < 0.05 and fold change ≥ 2.8 (**Figure 6**); as expected, the most enriched GO was related to transport and metabolic processes.

RT-qPCR Validation of the RNA-Seq Results

To ensure technical reproducibility and to validate the data generated from the RNA-seq experiment, we conducted a real-time qPCR analysis of five selected genes (BMEI0027, BMEI0591, BMEI1980, BMEI1116, and BMEI1040), from both strains (16M and Rev.1), grown under either low- or normal-pH conditions. The mRNA levels of all genes obtained by the

RT-qPCR were in high accordance with those obtained by our RNA-seq analysis (**Supplementary Table S1**).

Differential Survival of *B. melitensis* 16M and Rev.1 Within JEG-3 Human Trophoblastic Cells

As shown by Porte et al. (1999), the acidic environment during the early phase of infection is necessary for the survival and multiplication of *Brucella* in host cells. Therefore, we investigated the ability of the virulent 16M and the attenuated Rev.1 strains to infect and replicate within the human trophoblastic cell line JEG-3. As expected, the number of bacteria that were replicated over time (4 and 24 h) was higher in 16M than in Rev.1 (**Figure 7**).

DISCUSSION

To elucidate the molecular mechanisms underlying the attenuation of the *B. melitensis* Rev.1 vaccine strain, we conducted a comparative transcriptomic analysis between Rev.1 and its virulent counterpart, 16M, each grown under either normal- or low-pH conditions. When the two strains were grown under normal-pH conditions, Rev.1 showed a marked upregulation, as compared with 16M, of various genes that encode ABC transporters—a large and widespread family of proteins (Garmory and Titball, 2004). ABC transporters, which export solutes, antibiotics, and extracellular toxins, play a role in various cellular processes, such as translational regulation and DNA repair (Garmory and Titball, 2004), and the number of ABC systems appears to depend upon the bacterial adaptation to its environment (Garmory and Titball, 2004; Tanaka et al., 2018). The upregulation of ABC transporter-related genes in the attenuated Rev.1 strain should be considered in light of two other findings. First, Rev.1 showed an upregulated expression of BMEI0704, which encodes for bacterioferritin (**Table 2**). Notably, iron plays an important role in the survival of pathogens within host cells (Collins, 2003), and during infection, macrophages actively export iron from the phagosome (which is the replicative niche of *Brucella*; Forbes and Gros, 2001); it was previously suggested that Rev.1 may have lost the ability to regulate bacterioferritin synthesis and degradation (Eschenbrenner et al., 2002). Second, Rev.1 showed a downregulated expression of BMEI1759 (**Table 3**), which encodes for the vitamin B12-dependent methyltransferase, MetH (Lestrade et al., 2000). As MetH is involved in methionine biosynthesis, its downregulation in Rev.1 may have impaired amino acid metabolism in this strain. Taken together, these findings suggest that an improper regulation of essential metabolic pathways, including iron and amino acid metabolism, may have affected the ABC transporter activity, leading to down/upregulation of specific transporters to compensate for the gain/loss of critical metabolites.

To further understand the molecular mechanisms underlying Rev.1 attenuation, we examined the “interaction genes,” i.e., the main genes that are influenced differently by the acidic treatment in Rev.1 and in 16M. These interaction genes are probably the key genes involved in the attenuation of Rev.1, and are,

TABLE 4 | Potentially key genes involved in the attenuation of Rev.1.

Gene ID	Gene	Fold change
BMEI0815	Acetyl-coenzyme A (acetyl-CoA) synthetase	16.9
BMEI1747	Aldehyde dehydrogenase	5.06
BMEI1980	DNA starvation/stationary phase protection protein Dps	3.3
BME_RS02600	Cold-shock protein	2.19

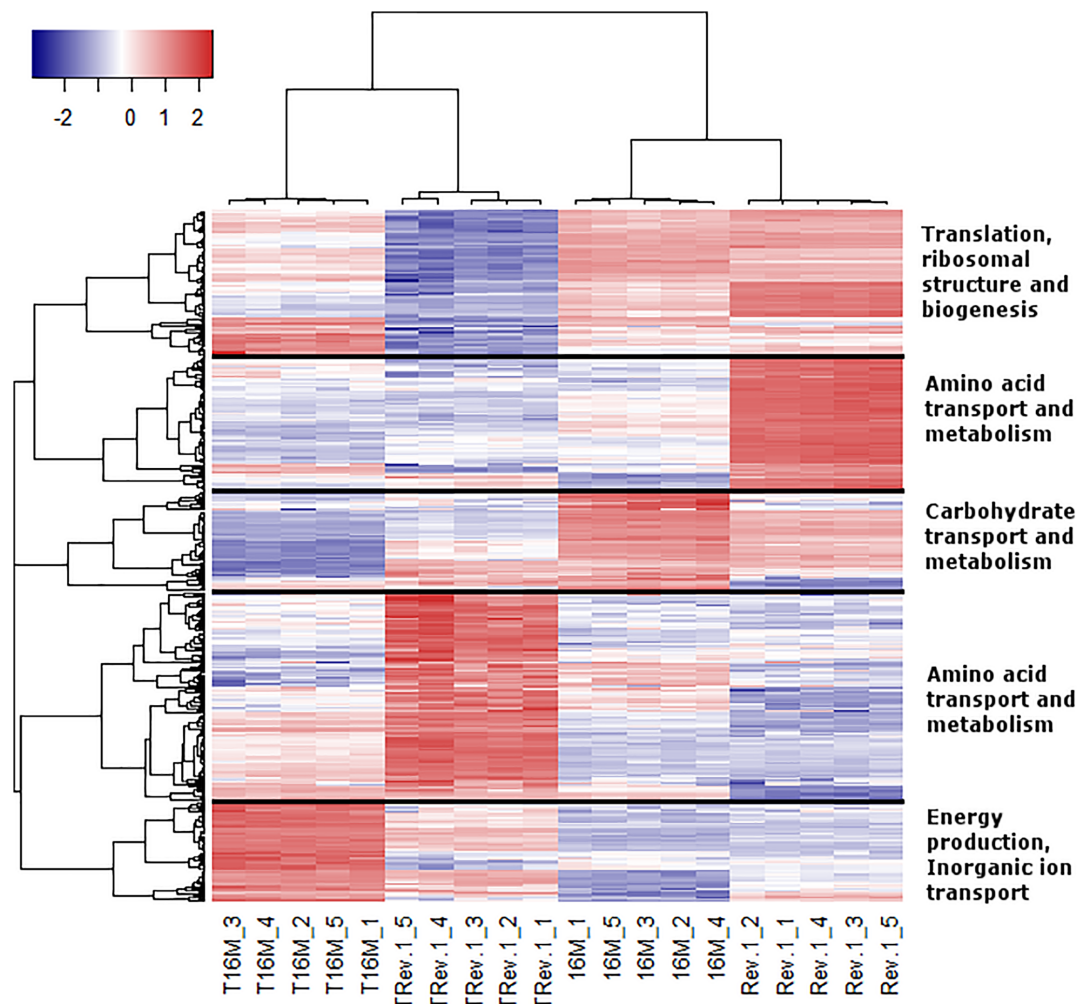


FIGURE 5 | Heatmap representing the expression profiles of the 403 interaction genes. Rows represent genes and columns represent bacterial samples. Red and blue pixels indicate upregulated and downregulated genes (Rev.1 versus 16M), respectively. The hierarchical clustering was generated using 1-Pearson correlation as the distance measure, and “complete” as the linkage method. Genes were categorized into five clusters based on the generated dendrogram, and genes within each cluster were characterized based on Clusters of Orthologous Groups (COGs) annotations.

therefore, of particular interest. Among these interaction genes, we found that acetyl-coenzyme A (acetyl-CoA) synthetase was significantly downregulated in the low-pH group of Rev.1, as compared with the low-pH group of 16M. Acetyl-CoA is the molecule by which glycolytic pyruvate enters the tricarboxylic acid cycle, it is a crucial precursor of lipid synthesis, and it acts as a sole donor of the acetyl groups for acetylation (Pietrocola et al., 2015). Previous studies revealed a clear association between the metabolism of *Brucella* and its persistence in its hosts (Hong et al., 2000; Lestrade et al., 2000; Barbier et al., 2011). The significantly high downregulation of acetyl-CoA synthetase in Rev.1 may decrease the levels of acetyl-CoA production, thereby affecting crucial metabolic processes that may potentially have a major contribution to bacterial attenuation.

Pathogenic bacteria must deal with oxidative stress emanating from the host immune response during invasion and persistent infection (Cabiscol et al., 2000; Singh et al.,

2013). We found several key interaction genes that were significantly downregulated in Rev.1, as compared with 16M, and which encode proteins involved in oxidative stress: aldehyde dehydrogenase (ALDH), the DNA starvation/stationary phase protection protein Dps, and a cold-shock protein (CSP). Prokaryotic and eukaryotic ALDHs metabolize endogenous and exogenous aldehydes to mitigate oxidative stress, (Singh et al., 2013) and an upregulation of bacterial ALDH was shown to occur following exposure to environmental or chemical stressors. It was suggested that such an upregulation is a critical element in the response of bacteria to oxidative stress (Singh et al., 2013). Dps was shown to protect *Escherichia coli* from oxidative stress, UV and gamma irradiation, iron and copper toxicity, thermal stress, and acid and base shocks (Martinez and Kolter, 1997; Nair and Finkel, 2004; Karas et al., 2015). CSP-A activity was found to be associated with the ability of *B. melitensis* to resist acidic and H₂O₂ stresses, especially during the mid-log-phase

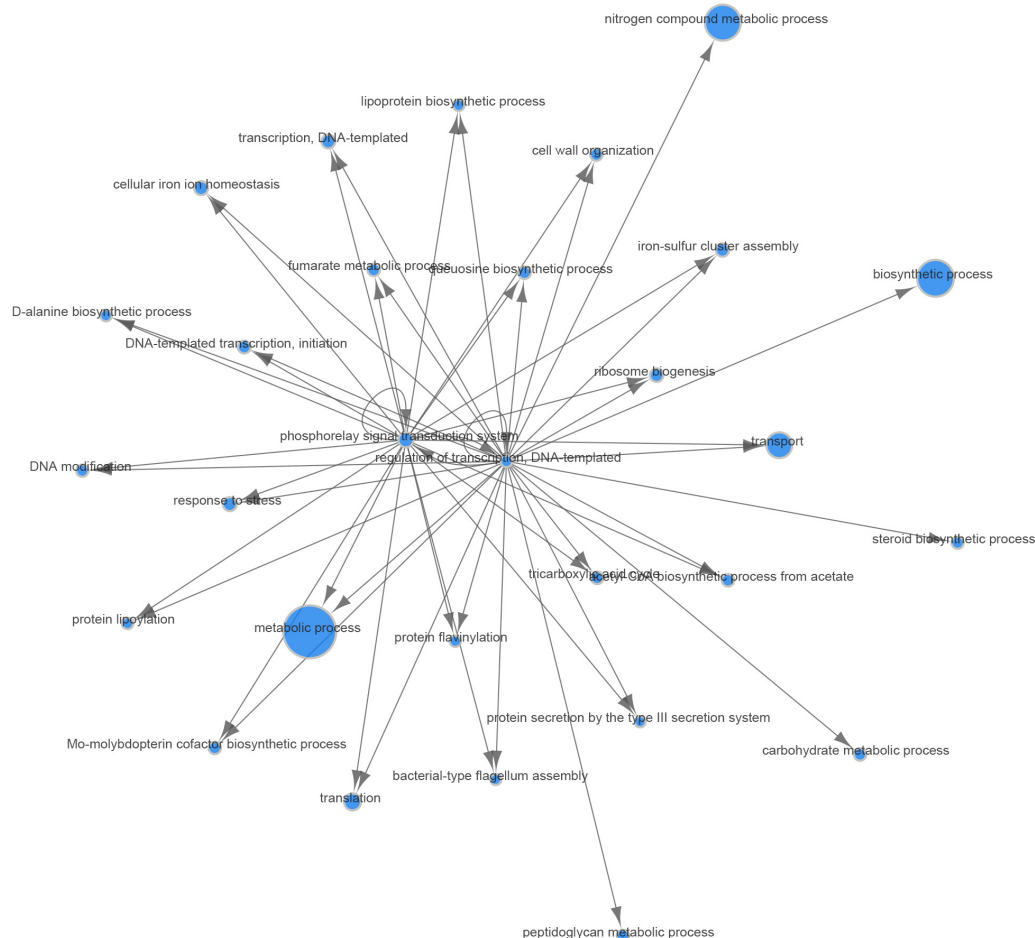


FIGURE 6 | Gene Ontology (GO) network of genes responding differently to low-pH conditions in the Rev.1 versus 16M strains. Of the 403 interaction genes (FDR < 0.05, fold change ≥ 2) expressed differently in Rev.1 versus 16M, the 133 most significant genes (FDR < 0.05, fold change ≥ 2.8) were selected and their GO network was generated using the Comparative GO tool (Fruzangohar et al., 2013). The node sizes represent the level of GO enrichment.

(Wang et al., 2014), and it was suggested that the *Brucella* CSP highly contributes to its virulence, most likely by facilitating its adaptation to the harsh environmental circumstances within the host (Wang et al., 2014). Taken together, it is possible that the downregulation of these key interaction genes in Rev.1 results in its inability to cope with oxidative stress in the host, thus contributing to bacterial attenuation.

As compared with Rev.1, 16M demonstrated a downregulation (FDR < 0.05, fold change ≥ 2) of interaction genes that encode for four proteins of the SUF system and the heat-shock protein IbpA, which were shown to be involved in the resistance to heat and oxidative stress (Kitagawa et al., 2000; Angelini et al., 2008; Outten, 2015). In *E. coli*, the SUF pathway plays a major role in preserving Fe-S cluster biosynthesis under oxidative stress conditions (Angelini et al., 2008; Outten, 2015). The small heat shock proteins (sHsps) IbpA and IbpB were previously suggested to be involved in the resistances to heat and oxidative stress, as overexpression of *ibpA* and *ibpB* in *E. coli* increased the resistance to heat and superoxide stress (Kitagawa

et al., 2000). Our transcriptomic analysis revealed enhanced enrichment within the molecular function of oxidoreductase activity in the low-pH group of 16M, but not in the low-pH group of Rev.1. As oxidoreductase protects bacteria against oxidative stress (Lumppio et al., 2001), we assume that the enhanced expression of the SUF system and IbpA by Rev.1, as compared with 16M, compensates for its impaired oxidoreductase activity, thereby enabling survival within the harsh oxidative intracellular environment of the host.

As compared with the low-pH group of 16M, the low-pH group of Rev.1 showed a downregulation (FDR < 0.05, fold change ~ 2) of five key interaction genes BME_RS02910, BMEI0584, BMEI0583, BME_RS13825, and BMEI1943 that encode for FtsZ, FtsA, FtsQ, FtsK, and DnaA respectively, all of which participate in critical stages of the cell cycle (Margolin, 2005; Sherratt et al., 2010; van den Ent et al., 2008; Bell and Kaguni, 2013; Loose and Mitchison, 2014). This finding may indicate that, in the acidic conditions of the BCV, the replication capabilities

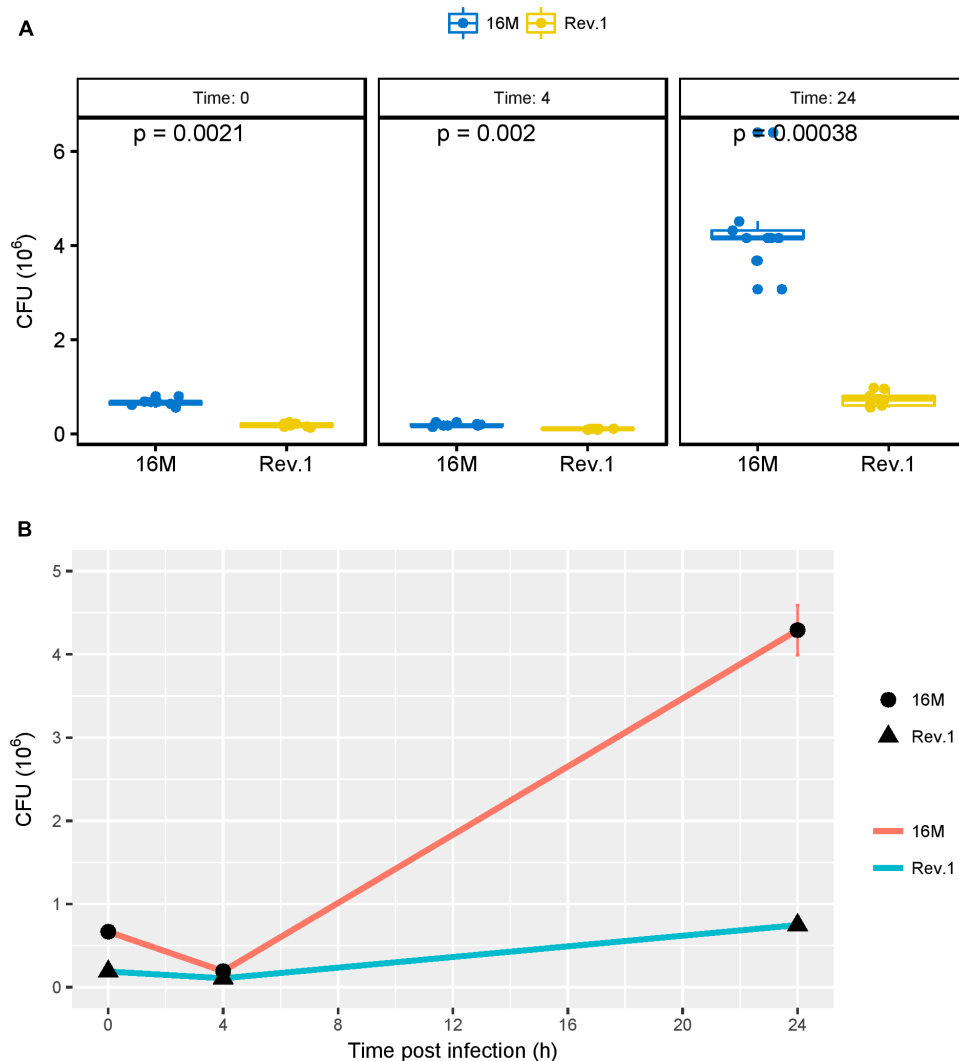


FIGURE 7 | Bacterial burden, measured as colony forming units (CFUs) over time. JEG-3 trophoblasts were infected with bacteria at a MOI of 500, and CFUs were determined 0, 4, and 24 h thereafter. **(A)** Boxplots representing the distribution of 16M (blue) and Rev.1 (yellow) bacterial count replicates, measured 0, 4, and 24 h following infection. *P*-values were calculated using two-sample Wilcoxon test. **(B)** Scatter plot indicating the change in bacterial counts over time (means \pm SD) following infection. Three replicate wells were evaluated at each time for each strain.

of Rev.1 are reduced, which lowers their intracellular survival compared to 16M. The significantly lower intracellular survival of Rev.1 in trophoblasts (**Figure 7**) supports this conclusion.

Under low-pH conditions, Rev.1 also showed a downregulation of the interaction gene BMEII1048 that encodes the molecular chaperone, GroEL (FDR < 0.05, fold change \sim 2). Molecular chaperons facilitate protein folding, preventing protein denaturation, and are involved in various cellular processes, including DNA replication, UV mutagenesis, bacterial growth, and RNA transcription (Maleki et al., 2016). Under acidic conditions, partially unfolded proteins may emerge (Mendoza et al., 2017) and molecular chaperones may stabilize them to prevent their acid-induced aggregation. Indeed, the *Helicobacter pylori* GroEL homolog, HSP60, was shown to be

induced upon acid stress (Mendoza et al., 2017). Thus, the downregulation of the interaction gene encoding GroEL in Rev.1 under low-pH conditions may lead to the accumulation of partially unfolded and desaturated proteins, leading to bacterial attenuation.

Finally, the interaction gene BMEII0027, which encodes for the T4SS protein VirB3, was upregulated (FDR < 0.05, fold change \sim 2) in the low-pH group of 16M, as compared with the low-pH group of Rev.1. This may have a harmful effect on the survival of Rev.1 within host cells, as VirB3 was shown to be essential for *Brucella* virulence because, together with VirB4, VirB6, VirB8, and the N-terminus of VirB10, it comprises the inner membrane complex of the T4SS apparatus (Ke et al., 2015).

Notably, the Rev.1 upregulated interaction gene BMEII1116 that encodes the HTH-type quorum sensing-dependent

transcriptional regulator VjbR, was shown to contribute to the virulence and survival of *Brucella* by regulating the expression of various virulence factors (Delrue et al., 2005; Weeks et al., 2010). It is possible that this interaction gene somewhat compensates for the lower expression of highly important virulent genes, such as VirB3, in Rev.1.

CONCLUSION

Through a comparative transcriptomic analysis, we revealed DE key genes involved in various crucial pathways, which are either upregulated or downregulated under acidic conditions in Rev.1, as compared with 16M. We suggest that these genes—and, especially, those mentioned in **Table 4**—are involved in the molecular mechanisms underlying Rev.1 attenuation, although further characterization through mutation and knockout experiments is required to conclusively determine the role of these genes in acid

resistance and virulence attenuation of the *B. melitensis* Rev.1 strain.

AUTHOR CONTRIBUTIONS

MS-D and DK conceived and coordinated the study. DK conducted the bacteriology work, acidic experiments, acquired the samples, and extracted RNA. MS-D analyzed the data. TZ performed the real-time PCR validation experiments. All authors interpreted the data, drafted the manuscript, and approved the content for publication.

SUPPLEMENTARY MATERIAL

The Supplementary Material for this article can be found online at: <https://www.frontiersin.org/articles/10.3389/fmicb.2019.00250/full#supplementary-material>

REFERENCES

- Angelini, S., Gerez, C., Ollagnier-de Choudens, S., Sanakis, Y., Fontecave, M., Barras, F., et al. (2008). NfuA, a new factor required for maturing Fe/S proteins in *Escherichia coli* under oxidative stress and iron starvation conditions. *J. Biol. Chem.* 283, 14084–14091. doi: 10.1074/jbc.M70940.5200
- Avila-Calderón, E. D., Lopez-Merino, A., Sriranganathan, N., Boyle, S. M., and Contreras-Rodríguez, A. (2013). A history of the development of *Brucella* vaccines. *Biomed. Res. Int.* 2013:743509. doi: 10.1155/2013/743509
- Banai, M. (2002). Control of small ruminant brucellosis by use of *Brucella melitensis* Rev.1 vaccine: laboratory aspects and field observations. *Vet. Microbiol.* 90, 497–519.
- Barbier, T., Nicolas, C., and Letesson, J. J. (2011). *Brucella* adaptation and survival at the crossroad of metabolism and virulence. *FEBS Lett.* 585, 2929–2934. doi: 10.1016/j.febslet.2011.08.011
- Bell, S. P., and Kaguni, J. M. (2013). Helicase loading at chromosomal origins of replication. *Cold Spring Harb. Perspect. Biol.* 5:a010124. doi: 10.1101/cshperspect.a010124
- Binns, D., Dimmer, E., Huntley, R., Barrell, D., O'Donovan, C., and Apweiler, R. (2009). QuickGO: a web-based tool for gene ontology searching. *Bioinformatics* 25, 3045–3046. doi: 10.1093/bioinformatics/btp536
- Boschiroli, M. L., Ouahrani-Bettache, S., Foulongne, V., Michaux-Charachon, S., Bourg, G., Allardet-Servent, A., et al. (2002). The *Brucella suis* virB operon is induced intracellularly in macrophages. *Proc. Natl. Acad. Sci. U.S.A.* 99, 1544–1549. doi: 10.1073/pnas.032514299
- Cabiscol, E., Tamarit, J., and Ros, J. (2000). Oxidative stress in bacteria and protein damage by reactive oxygen species. *Int. Microbiol.* 3, 3–8.
- Carlson M, P. H. (2018). *AnnotationForge: Code for Building Annotation Database Packages*. Available at: <https://bioconductor.org/packages/release/bioc/html/AnnotationForge.html>
- Celli, J. (2006). Surviving inside a macrophage: the many ways of *Brucella*. *Res. Microbiol.* 157, 93–98. doi: 10.1016/j.resmic.2005.10.002
- Collins, H. L. (2003). The role of iron in infections with intracellular bacteria. *Immunol. Lett.* 85, 193–195.
- Comerci, D. J., Martínez-Lorenzo, M. J., Sieira, R., Gorvel, J. P., and Ugalde, R. A. (2001). Essential role of the VirB machinery in the maturation of the *Brucella abortus*-containing vacuole. *Cell. Microbiol.* 3, 159–168.
- Delrue, R.-M., Deschamps, C., Léonard, S., Nijskens, C., Danese, I., Schaus, J.-M., et al. (2005). A quorum-sensing regulator controls expression of both the type IV secretion system and the flagellar apparatus of *Brucella melitensis*. *Cell. Microbiol.* 7, 1151–1161. doi: 10.1111/j.1462-5822.2005.00543.x
- Delrue, R.-M., Lestrade, P., Tibor, A., Letesson, J.-J., and De Bolle, X. (2004). *Brucella* pathogenesis, genes identified from random large-scale screens. *FEMS Microbiol. Lett.* 231, 1–12.
- den Hartigh, A. B., Rolán, H. G., de Jong, M. F., and Tsolis, R. M. (2008). VirB3 to VirB6 and VirB8 to VirB11, but not VirB7, are essential for mediating persistence of *Brucella* in the reticuloendothelial system. *J. Bacteriol.* 190, 4427–4436. doi: 10.1128/JB.00406-08
- Eschenbrenner, M., Wagner, M. A., Horn, T. A., Kraycer, J. A., Mujer, C. V., Hagius, S., et al. (2002). Comparative proteome analysis of *Brucella melitensis* vaccine strain Rev.1 and a virulent strain, 16M. *J. Bacteriol.* 184, 4962–4970.
- Forbes, J. R., and Gros, P. (2001). Divalent-metal transport by NRAMP proteins at the interface of host-pathogen interactions. *Trends Microbiol.* 9, 397–403.
- Fruzangohar, M., Ebrahimie, E., Ogunniyi, A. D., Mahdi, L. K., Paton, J. C., and Adelson, D. L. (2013). Comparative GO: a web application for comparative gene ontology and gene ontology-based gene selection in bacteria. *PLoS One* 8:e58759. doi: 10.1371/journal.pone.0058759
- Garmory, H. S., and Titball, R. W. (2004). ATP-binding cassette transporters are targets for the development of antibacterial vaccines and therapies. *Infect. Immun.* 72, 6757–6763. doi: 10.1128/IAI.72.12.6757-6763.2004
- Herzberg, M., and Elberg, S. (1953). Immunization against *Brucella* infection. I. Isolation and characterization of a streptomycin-dependent mutant. *J. Bacteriol.* 66, 585–99.
- Hong, P. C., Tsolis, R. M., and Ficht, T. A. (2000). Identification of genes required for chronic persistence of *Brucella abortus* in mice. *Infect. Immun.* 68, 4102–4107.
- Hulsen, T., de Vlieg, J., and Alkema, W. (2008). BioVenn – A web application for the comparison and visualization of biological lists using area-proportional Venn diagrams. *BMC Genomics* 9:488. doi: 10.1186/1471-2164-9-488
- Karas, V. O., Westerlaken, I., and Meyer, A. S. (2015). The DNA-binding protein from starved cells (Dps) utilizes dual functions to defend cells against multiple stresses. *J. Bacteriol.* 197, 3206–3215. doi: 10.1128/JB.00475-15
- Ke, Y., Wang, Y., Li, W., and Chen, Z. (2015). Type IV secretion system of *Brucella* spp. and its effectors. *Front. Cell. Infect. Microbiol.* 5:72. doi: 10.3389/fcimb.2015.00072
- Kitagawa, M., Matsumura, Y., and Tsuchido, T. (2000). Small heat shock proteins, IbpA and IbpB, are involved in resistances to heat and superoxide stresses in *Escherichia coli*. *FEMS Microbiol. Lett.* 184, 165–171.
- Ko, J., and Splitter, G. A. (2003). Molecular host-pathogen interaction in brucellosis: current understanding and future approaches to vaccine development for mice and humans. *Clin. Microbiol. Rev.* 16, 65–78.
- Köhler, S., Porte, F., Jubier-Maurin, V., Ouahrani-Bettache, S., Teyssier, J., and Liautaud, J.-P. (2002). The intramacrophagic environment of *Brucella suis* and bacterial response. *Vet. Microbiol.* 90, 299–309.

- Law, C. W., Chen, Y., Shi, W., and Smyth, G. K. (2014). Voom: precision weights unlock linear model analysis tools for RNA-seq read counts. *Genome Biol.* 15:R29. doi: 10.1186/gb-2014-15-2-r29
- Lestrade, P., Delrue, R. M., Danese, I., Didembourg, C., Taminiau, B., Mertens, P., et al. (2000). Identification and characterization of in vivo attenuated mutants of *Brucella melitensis*. *Mol. Microbiol.* 38, 543–551.
- Liu, Q., Liu, X., Yan, F., He, Y., Wei, J., Zhang, Y., et al. (2016). Comparative transcriptome analysis of *Brucella melitensis* in an acidic environment: identification of the two-component response regulator involved in the acid resistance and virulence of *Brucella*. *Microb. Pathog.* 91, 92–98. doi: 10.1016/j.micpath.2015.11.007
- Liu, W., Dong, H., Li, J., Ou, Q., Lv, Y., Wang, X., et al. (2015). RNA-seq reveals the critical role of OtpR in regulating *Brucella melitensis* metabolism and virulence under acidic stress. *Sci. Rep.* 5:10864. doi: 10.1038/srep10864
- Loose, M., and Mitchison, T. J. (2014). The bacterial cell division proteins FtsA and FtsZ self-organize into dynamic cytoskeletal patterns. *Nat. Cell Biol.* 16, 38–46. doi: 10.1038/ncb2885
- Lumppio, H. L., Shen, N. V., Summers, A. O., Voordouw, G., and Kurtz, D. M. (2001). Rubrerythrin and rubredoxin oxidoreductase in *Desulfovibrio vulgaris*: a novel oxidative stress protection system. *J. Bacteriol.* 183, 101–108. doi: 10.1128/JB.183.1.101-108.2001
- Magoc, T., Wood, D., and Salzberg, S. L. (2013). EDGE-pro: estimated degree of gene expression in prokaryotic genomes. *Evol. Bioinform.* 9, 127–136. doi: 10.4137/EBO.S11250
- Maleki, F., Khosravi, A., Nasser, A., Taghinejad, H., and Azizian, M. (2016). Bacterial heat shock protein activity. *J. Clin. Diagn. Res.* 10, BE01–BE3. doi: 10.7860/JCDR/2016/14568.7444
- Marchler-Bauer, A., Zheng, C., Chitsaz, F., Derbyshire, M. K., Geer, L. Y., Geer, R. C., et al. (2013). CDD: conserved domains and protein three-dimensional structure. *Nucleic Acids Res.* 41, D348–D352. doi: 10.1093/nar/gks1243
- Margolin, W. (2005). FtsZ and the division of prokaryotic cells and organelles. *Nat. Rev. Mol. Cell Biol.* 6, 862–871. doi: 10.1038/nrm1745
- Martinez, A., and Kolter, R. (1997). Protection of DNA during oxidative stress by the nonspecific DNA-binding protein Dps. *J. Bacteriol.* 179, 5188–5194.
- Mendoza, J. A., Weinberger, K. K., and Swan, M. J. (2017). The Hsp60 protein of *Helicobacter pylori* displays chaperone activity under acidic conditions. *Biochem. Biophys. Rep.* 9, 95–99. doi: 10.1016/j.bbrep.2016.11.011
- Nair, S., and Finkel, S. E. (2004). Dps protects cells against multiple stresses during stationary phase. *J. Bacteriol.* 186, 4192–4198. doi: 10.1128/JB.186.13.4192-4198.2004
- Outten, F. W. (2015). Recent advances in the Suf Fe-S cluster biogenesis pathway: beyond the *Proteobacteria*. *Biochim. Biophys. Acta* 1853, 1464–1469. doi: 10.1016/j.bbamcr.2014.11.001
- Pietrocola, F., Galluzzi, L., Bravo-San Pedro, J. M., Madeo, F., and Kroemer, G. (2015). Acetyl coenzyme A: a central metabolite and second messenger. *Cell Metab.* 21, 805–821. doi: 10.1016/j.cmet.2015.05.014
- Poester, F. P., Samartino, L. E., and Santos, R. L. (2013). Pathogenesis and pathobiology of brucellosis in livestock. *Rev. Sci. Tech.* 32, 105–115.
- Porte, F., Liautard, J. P., and Köhler, S. (1999). Early acidification of phagosomes containing *Brucella suis* is essential for intracellular survival in murine macrophages. *Infect. Immun.* 67, 4041–4047.
- Robinson, M. D., McCarthy, D. J., and Smyth, G. K. (2010). edgeR: a bioconductor package for differential expression analysis of digital gene expression data. *Bioinformatics* 26, 139–140. doi: 10.1093/bioinformatics/btp616
- Robinson, M. D., and Oshlack, A. (2010). A scaling normalization method for differential expression analysis of RNA-seq data. *Genome Biol.* 11:R25. doi: 10.1186/gb-2010-11-3-r25
- Roop, R. M., Gaines, J. M., Anderson, E. S., Caswell, C. C., and Martin, D. W. (2009). Survival of the fittest: how *Brucella* strains adapt to their intracellular niche in the host. *Med. Microbiol. Immunol.* 198, 221–238. doi: 10.1007/s00430-009-0123-8
- Salmon-Divon, M., Banai, M., Bardenstein, S., Blum, S. E., and Kornspan, D. (2018a). Complete genome sequence of the live attenuated vaccine strain *Brucella melitensis* Rev.1. *Genome Announc.* 6:e00175-18. doi: 10.1128/genomeA.00175-18
- Salmon-Divon, M., Yehekel, A., and Kornspan, D. (2018b). Genomic analysis of the original Elberg *Brucella melitensis* Rev.1 vaccine strain reveals insights into virulence attenuation. *Virulence* 9, 1436–1448. doi: 10.1080/21505594.2018.1511677
- Sherratt, D. J., Arciszewska, L. K., Crozat, E., Graham, J. E., and Grainge, I. (2010). The *Escherichia coli* DNA translocase FtsK. *Biochem. Soc. Trans.* 38, 395–398. doi: 10.1042/BST0380395
- Singh, S., Brocker, C., Koppaka, V., Chen, Y., Jackson, B. C., Matsumoto, A., et al. (2013). Aldehyde dehydrogenases in cellular responses to oxidative/electrophilic stress. *Free Radic. Biol. Med.* 56, 89–101. doi: 10.1016/j.freeradbiomed.2012.11.010
- Smith, E. P., Miller, C. N., Child, R., Cundiff, J. A., and Celli, J. (2016). Postrepletion roles of the *Brucella* VirB type IV secretion system uncovered via conditional expression of the VirB11 ATPase. *MBio* 7:e01730-16. doi: 10.1128/mBio.01730-16
- Smyth, G. K. (2005). “Limma: linear models for microarray data,” in *Bioinformatics and Computational Biology Solutions Using R and Bioconductor*, eds R. Gentleman, V. Carey, and S. Dudoit (Berlin: Springer), 397–420.
- Starr, T., Ng, T. W., Wehrly, T. D., Knodler, L. A., and Celli, J. (2008). *Brucella* intracellular replication requires trafficking through the late endosomal/lysosomal compartment. *Traffic* 9, 678–694. doi: 10.1111/j.1600-0854.2008.00718.x
- Tanaka, K. J., Song, S., Mason, K., and Pinkett, H. W. (2018). Selective substrate uptake: the role of ATP-binding cassette (ABC) importers in pathogenesis. *Biochim. Biophys. Acta* 1860, 868–877. doi: 10.1016/j.bbame.2017.08.011
- van den Ent, F., Vinkenvleugel, T. M. F., Ind, A., West, P., Veprintsev, D., Nanninga, N., et al. (2008). Structural and mutational analysis of the cell division protein FtsQ. *Mol. Microbiol.* 68, 110–123. doi: 10.1111/j.1365-2958.2008.06141.x
- von Bargen, K., Gorvel, J.-P., and Salcedo, S. P. (2012). Internal affairs: investigating the *Brucella* intracellular lifestyle. *FEMS Microbiol. Rev.* 36, 533–562. doi: 10.1111/j.1574-6976.2012.00334.x
- Wang, Z., Wang, S., and Wu, Q. (2014). Cold shock protein A plays an important role in the stress adaptation and virulence of *Brucella melitensis*. *FEMS Microbiol. Lett.* 354, 27–36. doi: 10.1111/1574-6968.12430
- Weeks, J. N., Galindo, C. L., Drake, K. L., Adams, G. L., Garner, H. R., and Ficht, T. A. (2010). *Brucella melitensis* VjbR and C12-HSL regulons: contributions of the N-dodecanoyl homoserine lactone signaling molecule and LuxR homologue VjbR to gene expression. *BMC Microbiol.* 10:167. doi: 10.1186/1471-2180-10-167
- Xiang, Z., Zheng, W., and He, Y. (2006). BBP: *Brucella* genome annotation with literature mining and curation. *BMC Bioinformatics* 7:347. doi: 10.1186/1471-2105-7-347
- Ye, J., Coulouris, G., Zaretskaya, I., Cutcutache, I., Rozen, S., and Madden, T. L. (2012). Primer-BLAST: a tool to design target-specific primers for polymerase chain reaction. *BMC Bioinformatics* 13:134. doi: 10.1186/1471-2105-13-134
- Yu, G., Wang, L.-G., Han, Y., and He, Q.-Y. (2012). clusterProfiler: an R package for comparing biological themes among gene clusters. *Omics A J. Integr. Biol.* 16, 284–287. doi: 10.1089/omi.2011.0118
- Zhao, S., Guo, Y., Sheng, Q., and Shyr, Y. (2014). Advanced heat map and clustering analysis using heatmap3. *Biomed. Res. Int.* 2014, 1–6. doi: 10.1155/2014/986048

Conflict of Interest Statement: The authors declare that the research was conducted in the absence of any commercial or financial relationships that could be construed as a potential conflict of interest.

Copyright © 2019 Salmon-Divon, Zahavi and Kornspan. This is an open-access article distributed under the terms of the Creative Commons Attribution License (CC BY). The use, distribution or reproduction in other forums is permitted, provided the original author(s) and the copyright owner(s) are credited and that the original publication in this journal is cited, in accordance with accepted academic practice. No use, distribution or reproduction is permitted which does not comply with these terms.



Genomic Characterization Provides New Insights for Detailed Phage-Resistant Mechanism for *Brucella abortus*

OPEN ACCESS

Edited by:

Michel Stanislas Zygmunt,
Institut National de la Recherche
Agronomique (INRA), France

Reviewed by:

Menachem Banai,
Kimron Veterinary Institute, Israel
Antonio Battisti,
Istituto Zooprofilattico Sperimentale
delle Regioni Lazio
e Toscana (IZSLT), Italy
Alba Patricia,
Istituto Zooprofilattico Sperimentale
delle Regioni Lazio e Toscana (IZSLT),
Italy, in collaboration with reviewer AB
Guillaume Girault,
National Agency for Sanitary Safety
of Food, Environment and
Labor (ANSES), France

*Correspondence:

Yao-xia Kang
kxaaa@126.com
Yung-Fu Chang
yc42@cornell.edu
Xiao-Kui Guo
microbiology@sjtu.edu.cn
YongZhang Zhu
yhzhu@hotmail.com

[†] These authors have contributed
equally to this work

Specialty section:

This article was submitted to
Infectious Diseases,
a section of the journal
Frontiers in Microbiology

Received: 03 December 2018

Accepted: 11 April 2019

Published: 03 May 2019

Citation:

Li X-m, Kang Y-x, Lin L, Jia E-H,
Piao D-R, Jiang H, Zhang C-C, He J,
Chang Y-F, Guo X-K and Zhu Y (2019)
Genomic Characterization Provides
New Insights for Detailed Phage-
Resistant Mechanism for *Brucella*
abortus. *Front. Microbiol.* 10:917.
doi: 10.3389/fmicb.2019.00917

Xu-ming Li^{2†}, Yao-xia Kang^{1*†}, Liang Lin¹, En-Hou Jia¹, Dong-Ri Piao³, Hai Jiang³,
Cui-Cai Zhang^{3,4}, Jin He², Yung-Fu Chang^{6*}, Xiao-Kui Guo^{5*} and YongZhang Zhu^{5*}

¹ Baotou Municipal Center for Disease Control and Prevention, Baotou, China, ² State Key Laboratory of Agricultural Microbiology, College of Life Science and Technology, Huazhong Agricultural University, Wuhan, China, ³ State Key Laboratory for Infectious Disease Prevention and Control, Collaborative Innovation Center for Diagnosis and Treatment of Infectious Diseases, National Institute for Communicable Disease Control and Prevention, Beijing, China, ⁴ Collaborative Innovation Centre for Diagnosis and Treatment of Infectious Diseases, Zhejiang University, Hangzhou, China, ⁵ Department of Immunology and Microbiology, Institutes of Medical Sciences, Shanghai Jiao Tong University School of Medicine, Shanghai, China, ⁶ Department of Population Medicine and Diagnostic Sciences, College of Veterinary Medicine, Cornell University, Ithaca, NY, United States

As the causative agent of cattle brucellosis, *Brucella abortus* commonly exhibits smooth phenotype (by virtue of colony morphology) that is characteristically sensitive to specific *Brucella* phages, playing until recently a major role in taxonomical classification of the *Brucella* species by the phage typing approach. We previously reported the discrepancy between traditional phenotypic typing and MLVA results of a smooth phage-resistant (SPR) strain Bab8416 isolated from a 45-year-old custodial worker with brucellosis in a cattle farm. Here, we performed whole genome sequencing and further obtained a complete genome sequence of strain Bab8416 by a combination of multiple NGS technologies and routine PCR sequencing. The detailed genetic differences between *B. abortus* SPR Bab8416 and large smooth phage-sensitive (SPS) strains were investigated in a comprehensively comparative genomic study. The large indels between *B. abortus* SPS strains and Bab8416 showed possible divergence between two evolutionary branches at a far phylogenetic node. Compared to *B. abortus* SPS strain 9-941 (Bab9-941), the specific re-arrangement event in Bab8416 displaying a closer linear relationship with *B. melitensis* 16M than other *B. abortus* strains resulted in the truncation of c-di-GMP synthesis, and 3 c-di-GMP-metabolizing genes, were present in Bab8416 and *B. melitensis* 16M, but absent in Bab9-941 and other *B. abortus* strains, indicating potential SPR-associated key determinants and novel molecular mechanisms. Moreover, despite almost completely intact smooth LPS related genes, only one mutated OmpA family protein of Bab8416, functionally related to flagellar and efflux pump, was newly identified. Several point mutations were identified to be Bab8416 specific while a majority of them were verified to be *B. abortus* ST2 characteristic. In conclusion, our study therefore identifies new SPR-associated factors that could play a role in refining and updating *Brucella* taxonomic schemes and provides resources for further detailed analysis of mechanism for *Brucella* phage resistance.

Keywords: *Brucella abortus*, phage resistance, comparative genomics, genome typing, phylogenetic analysis

INTRODUCTION

Brucellosis is one of the most serious zoonotic infectious diseases worldwide, and is caused by pathogenic species of *Brucella* genus. Up to now, 12 species were defined into the genus *Brucella* (Godfroid et al., 2013). Six of them, including *B. melitensis*, *B. abortus*, *B. suis*, *B. canis*, *B. ovis*, and *B. neotomae*, belong to the “classical” or “traditional” *Brucella* species¹. Generally, all *Brucella* species with nucleotide similarities > 90% are genetically closely related (Al Dahouk et al., 2010).

Traditional *Brucella* typing is primarily based on different phenotypic characteristics (Garcia et al., 1988; Jahans et al., 1997; Moreno et al., 2002; Sanogo et al., 2013), including colony morphology, CO₂ requirement, H₂S production, substrate utilization, growth on serum dextrose agar dye plate, agglutination with monospecific sera, *Brucella* phage lysis profiles at routine test dilution (RTD) and host preference (Jones et al., 1968; Morris et al., 1973; Rigby et al., 1989). The three major species in terms of disease and economic impact for man, *B. melitensis*, *B. abortus* and *B. suis* are further subdivided into multiple biovars (*bv*) based on a range of phenotypic and serological characteristics. For example, *B. abortus* is subdivided into *bv* 1–6 and 9 (Pappas et al., 2006). Furthermore, despite the close genetic relationship of several genetic loci (e.g., 16S rRNA, 98.7%) and a biochemical profile similar to *Ochrobactrum* spp., several non-classical *Brucella* species like *B. microti* and *B. inopinata* are often easily misidentified using traditional biochemical typing methods (Scholz et al., 2008a,b). Among these routine phenotypic characterizations, *B. abortus* with smooth Lipopolysaccharide (LPS) was identified to be sensitive to *Brucella* phages like Berkeley2 (BK2), Tbilisi (Tb), Weybridge (Wb), and Izatnagar (Iz) (FAO/WHO, 1986). This useful test is significant for differentiating *B. abortus* from other *Brucella* species (Jones et al., 1968; Morris et al., 1973).

Since SPR *B. abortus* was initially reported in Corbel and Morris (1974), there have been few studies on this distinct phenotype over the last four decades. The susceptibility of smooth *B. abortus* strains to lysis by *Brucella* phages is commonly used to type various *Brucella* species. We have recently reported the identification of the first SPR *B. abortus* strain Bab8416 from a brucellosis patient in China (Kang et al., 2015). The phage activity of Bab8416 is similar to that of *B. melitensis* *bv* 1 strain 16M and showed special biochemical characteristics distinct from that of all *B. abortus* biovars. It was not lysed by Tb, Iz, and Wb phage in 1 × RTD and 10⁴ × RTD, but lysed by BK2 phage in 1 × RTD and 10² × RTD. Due to the unusual discrepancy between phenotypic profiles, Bab8416 could not be precisely classified to any of the existing *B. abortus* biovars. In this study, we completed the genome sequence of Bab8416 through a combination of next-generation sequencing (NGS) and common PCR-based gap closure and investigated genomic differences between Bab8416 and other *Brucella* strains for gene association in corresponding biochemical or physiological profiles.

¹<http://www.bacterio.net/brucella.html>

MATERIALS AND METHODS

Ethics Statement

This study and the protocol were carried out in accordance with the recommendations of ethics committee of the local disease control and Prevention Research Center of the Inner Mongolia Autonomous Region and Baotou City. The patient gave written informed consent for participation in this study and publication of his identifiable information, in accordance with the Declaration of Helsinki. The detailed information of strain Bab8416 referred to our previous study (Kang et al., 2015).

Genome Sequencing, Assembly and Annotation

Using 454 GS-FLX system, a total of 190,817 reads were obtained with the average length of 566 bp. Twenty-two contigs with lengths more than 500 bp and average coverage of 33.2X were obtained by Newbler using default parameters. Using the genome of *B. abortus* 9-941 as a reference, the order of the contigs was sorted and gap closure using common PCR was performed with ContigsScape (Tang et al., 2013). To fix the homopolymer sequencing errors systemically caused by 454 GS-FLX sequencing system, another 180 bp Paired End (PE) library was constructed and sequenced by the Illumina HiSeq 2000 system. Genome sequencing results were refined by short reads using Pilon with default parameters (Walker et al., 2014). The coding genes were predicted by Prodigal (Hyatt et al., 2010) and these genes were annotated by BLAST against NCBI non-redundant (NR), COG, KEGG, TrEMBL, Swissprot databases with *e* value cutoff of 1e-5 and GO terms assigned to the annotated genes using BLAST2GO pipeline (Conesa et al., 2005). The tRNAs were detected by tRNAscan-SE (v1.23) (Schattner et al., 2005) and rRNAs were identified by blasting homologous rRNA sequences against the Bab8416 genome.

Whole Genome Collinear Analysis

Firstly, *oriC* site was identified in both references and Bab8416 genome using Ori-Finder 2 and was set to be the first base of Bab8416 genome (Luo et al., 2014). Then, whole genome sequence alignments between these two genomes were processed by MUMmer 3.23 package (Kurtz et al., 2004).

Brucella MLVA Typing and MLST Typing

Multiple-locus variable number tandem repeat analysis (MLVA) assay was employed and the markers were obtained by PCR (Jiang et al., 2013b). The MLVA markers of Bab8416 were compared to the MLVA database². The multilocus sequence typing (MLST) schemes of *Brucella* species using 9 conserved housekeeping genes were performed as previously described (Whatmore et al., 2007).

SNP Calling

All the draft genomes were linked to be two pseudo chromosomes by taking *B. abortus* 9-941 genome as a reference and the

²<http://mlva.u-psud.fr/brucella/>

sequences were gaped with 'NNNN.' The SNPs were firstly identified by Mauve (Darling et al., 2010) using the genome sequences in this study and after "N" removed, the remaining SNP were finally exported for further analysis.

Gene Family Identification and Phylogenetic Analysis

Thirty-nine available *Brucella* reference genomes were utilized to perform comparative genomic and phylogenetic analyses, including all known *Brucella* species and all of seven biovars of *B. abortus*. Three strains with lower contig numbers and high coverage in each biovar of *B. abortus* were selected. All genes of the selected strains were ortholog clustered by PGAP (Zhao et al., 2012), a pipeline for pan-genome analysis, and genes with both coverage and identity higher than 90% were considered to be the same ortholog cluster. Hence, a total of 2,014 single copy gene families were identified and a super gene was constructed for phylogenetic analysis by combining all sequences of these genes into one ortholog cluster. A maximum likelihood phylogenetic tree was constructed by Phylml 3.0 (Guindon et al., 2010) using HKY85 nucleotide substitution model with a bootstrap value of 1000. In addition, in order to investigate the regions of differences (RD) from pan-genome analysis, we further added 200 *B. melitensis* genomes and 197 *B. abortus* genomes for detailed screening and characterization by using BLASTN program.

Virulence Factor Screening

We downloaded all the virulence factor from Virulence Factors Database (VFDB) (Chen et al., 2005), and we aligned all the protein sequences of the strain Bab8416 to the VFDB using BLASTP program available at NCBI server (ncbi-blast-2.7.1+) with both coverage and identity higher than 80%.

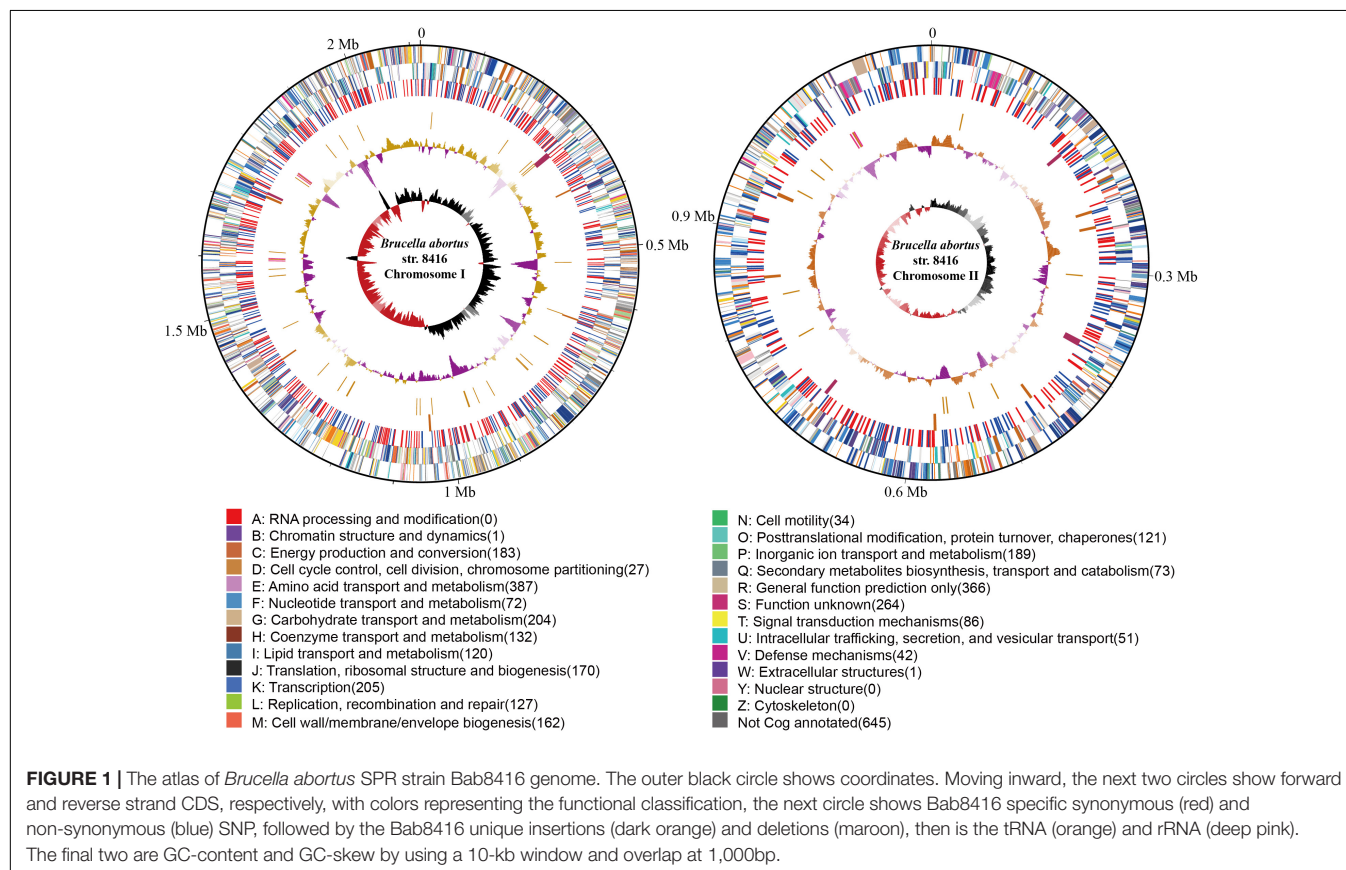
Data Access

The genome sequence and annotations were submitted to GenBank database with accession number CP008774–CP008775. All the reference genomes used in this paper were obtained from PATRIC (Wattam et al., 2017).

RESULTS AND DISCUSSION

Genome Features

The genome size of strain Bab8416 is 3.2 Mb, and it consists of two circular chromosomes: a large chromosome of 2,116,946 bp and a smaller one of 1,156,123 bp. The average GC content of two chromosomes was 57.22% (Crasta et al., 2008; Tsolis et al., 2009). A total of 3,295 Coding DNA sequences (CDSs) have been computationally predicted. The summarized message of Bab8416 genome is showing in **Figure 1**. The average length of CDS was 856 bp and 2,272 CDSs (68.95%) were assigned definite biological function as well as 1,023 (31.05%) are hypothetical proteins. **Figure 2** is showing GO function class of the annotated genes.



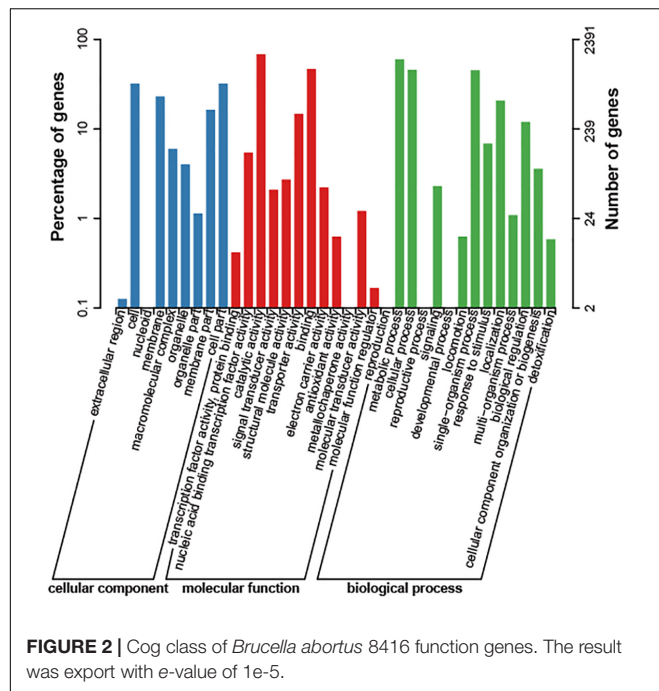


FIGURE 2 | Cog class of *Brucella abortus* 8416 function genes. The result was export with e-value of 1e-5.

Inconsistent Phenotypic and Molecular Typing Results

Except for resistance to phage Iz, Tb, and Wb shown in **Table 1**, the physiological and biochemical profiles of strain Bab8416 was more closely related to smooth *B. abortus* bv 9 (Morris et al., 1973). In addition, electron microscopy was used to investigate phage Tb/Bab8416 interaction (**Figure 3**); absorption but no lysis of host bacteria was observed. Here, we performed additional MLVA typing (Le Fleche et al., 2006; Al Dahouk et al., 2007; Van Belkum, 2007; Valdezate et al., 2009). While no 100% match could be found in MLVA database, the top 20 matches consistently with *B. abortus* bv. 3 (**Figure 4**).

Without coincident results in both traditional phenotyping and modern MLVA genotyping, we further employed MLST method (Whatmore et al., 2007). Twenty-seven *Brucella* sequence types (STs) were initially identified and more STs have been found (Whatmore et al., 2016). Bab8416 was identified as an ST2 in this study.

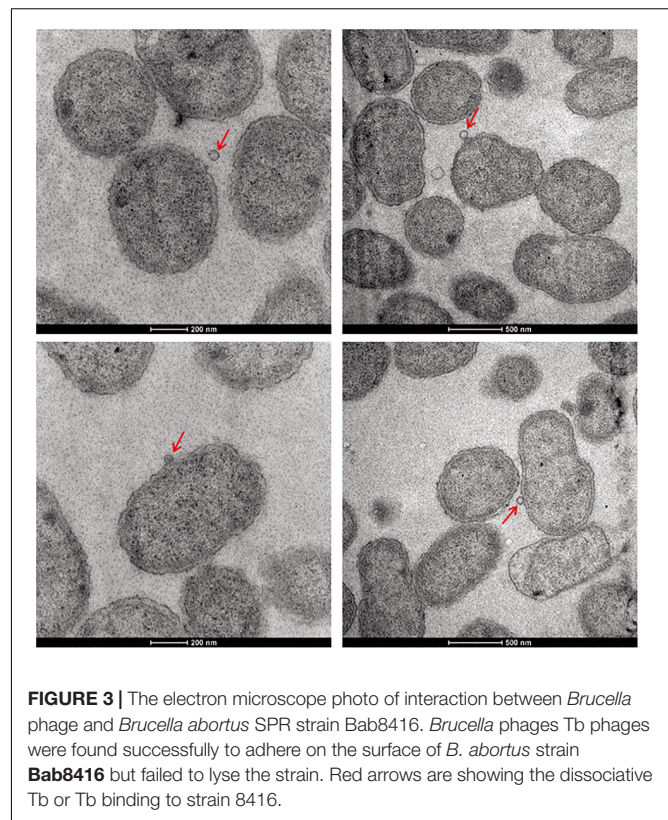


FIGURE 3 | The electron microscope photo of interaction between *Brucella* phage and *Brucella abortus* SPR strain Bab8416. *Brucella* phages Tb phages were found successfully to adhere on the surface of *B. abortus* strain **Bab8416** but failed to lyse the strain. Red arrows are showing the dissociative Tb or Tb binding to strain 8416.

Phylogenetic Analysis

Determining the evolutionary context of Bab8416 is essential for a detailed comparative genomic analysis and to account for the inconformity of the former two typing results from different strains and isolates of *Brucella* (Crasta et al., 2008). A total of 2,014 single copy genes were identified within 25 *B. abortus* strains with three strains in each biovar and *B. melitensis* str. 16M as one outgroup being used to build a maximum likelihood phylogenetic tree (**Figure 5**). Many strains within the same biovar are not closely genetically related; conversely, several strains in different biovars have been shown to be closely related. This finding indicates that traditional physiological and biochemical typing designations of biovars within *B. abortus* do not reflect genetic linkage patterns.

TABLE 1 | Physiological and biochemical typing details of *B. abortus* Bab8416 compared with other standard strains.

No	Growth characteristics				Monospecific sera		Phages at RTD				Interpretation
	CO ₂ requirement	H ₂ S production	TH	BF	A	M	Tb	Wb	Iz	BK2	
1	—	+	+	+	—	+	—	—	—	+	<i>B. abortus</i> 8416
2	±	+	+	+	+	—	+	+	+	+	<i>B. abortus</i> 3a
3	—	+	+	+	—	+	+	+	+	+	<i>B. abortus</i> 9
4	—	—	+	+	—	+	—	—	+	+	<i>B. melitensis</i> 16M

TH, Thionin at 20 µg/ml (1/50,000); BF, Basic fuchsin at 20 µg/ml (1/50,000); Phages: Tb, Tbilisi; Wb, weybridge; BK2, Berkeley type 2; Fi, Firenze; RTD, Routine test dilution: +, positive; -, negative.

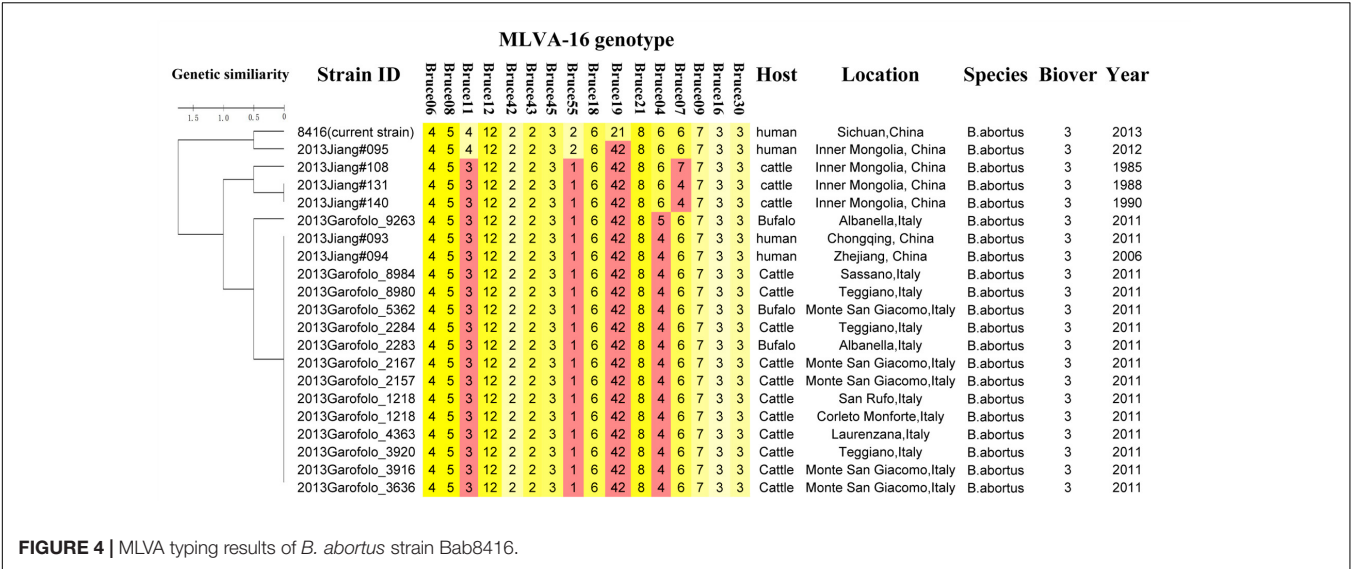


FIGURE 4 | MLVA typing results of *B. abortus* strain Bab8416.

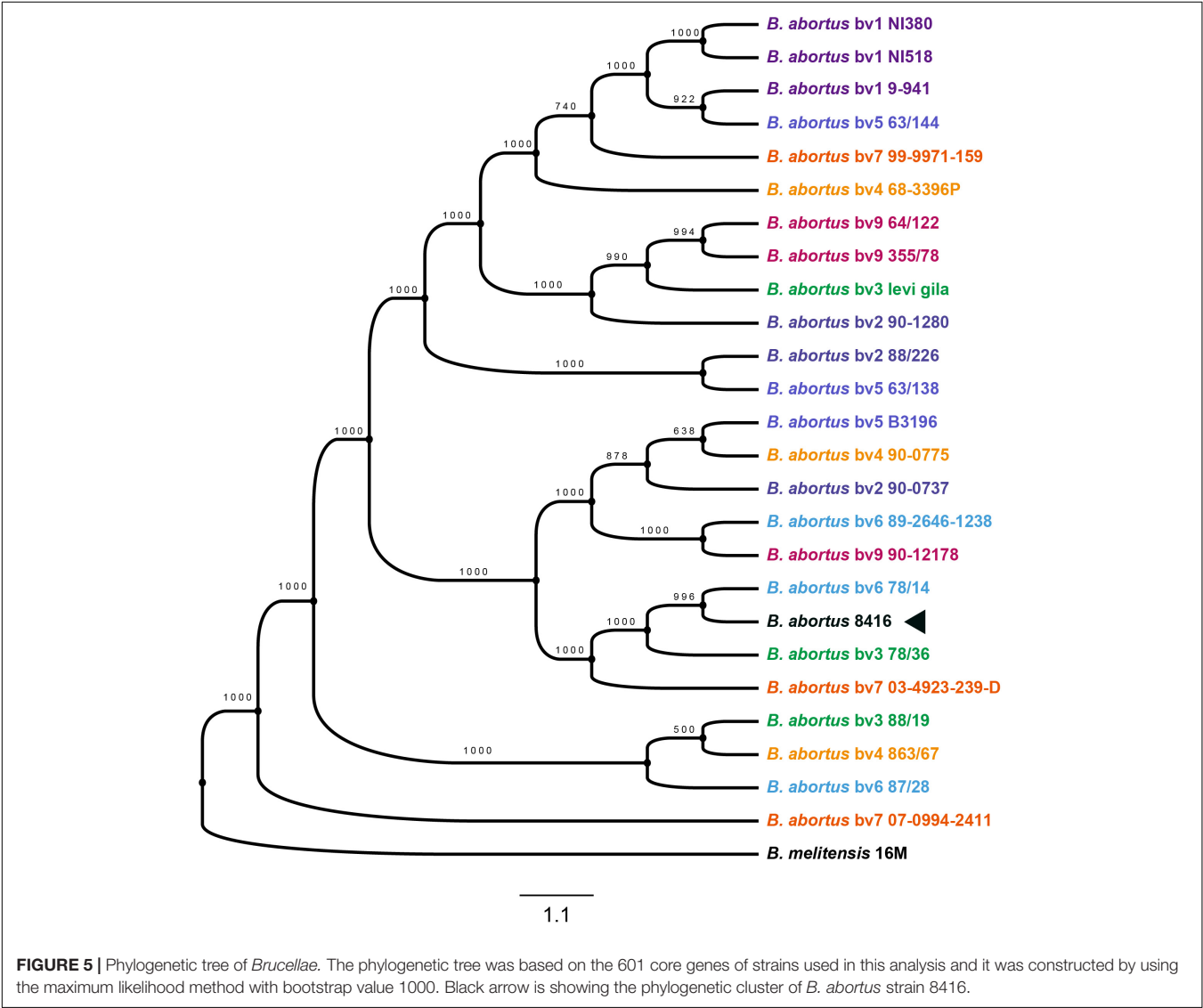


FIGURE 5 | Phylogenetic tree of *Brucellae*. The phylogenetic tree was based on the 601 core genes of strains used in this analysis and it was constructed by using the maximum likelihood method with bootstrap value 1000. Black arrow is showing the phylogenetic cluster of *B. abortus* strain 8416.

TABLE 2 | Genome features of these strains used in comparative analysis.

Strains	Genome status	Biovar	Contig	CDS
<i>B. abortus</i> 8416	Complete	–	2	3295
<i>B. abortus</i> 9-941	Complete	1	2	3085
<i>B. abortus</i> 104M	WGS	–	92	3303
<i>B. abortus</i> 2308-A	WGS	1	9	3072
<i>B. abortus</i> 544	WGS	–	9	3120
<i>B. abortus</i> NCTC 8038	WGS	–	10	3044
<i>B. abortus</i> Tulya	WGS	3	10	3261

Comparative Genomics

As draft genomes often generate low resolution results in studies measuring genetic variation, we conducted a comparative genomic analysis using complete genomes as previously described (Ricker et al., 2012; Zhang et al., 2012). *B. abortus* strain 9-941 (Bab9-941) was a typical SPS strain with the complete genome published. Here, we chose Bab9-941 as a reference for comparative genomic analysis and the genome features of *B. abortus* used and were listed in Table 2.

Chromosome Arrangement

In comparison with Bab9-941, a large fragment (420 kb) re-arrangement in small chromosome of Bab8416 was found by using MUMmer (Figure 6). Re-arrangements in *Brucella* species

have been previously reported (Sieira et al., 2000; Jiang et al., 2013a), however, this one proved to be exceptional. Compared with other *B. abortus* genomes observed here, the re-arrangement in Bab8416 was specific and displayed a closer linear relationship with *B. melitensis* 16M than the other *B. abortus* genomes. As mentioned above, Bab8416 shared the same phage typing status with *B. melitensis* bv 1 strain 16M; strongly similar genomic structures were also shown to exist between these two strains.

Nevertheless, neither IS elements nor tRNA operons usually responsible for genome re-arrangement were detected in the terminal region of the Bab8416 re-arrangement sequence. Three genes, *BMEII0292*, *BMEII0293*, and *BMEII1009*, were truncated or incomplete at the terminal fragment in other *B. abortus* strains. Both *BMEII0292* and *BMEII1009* contain a GGDEF domain that enables them to generate the cyclic di-GMP (c-di-GMP), a kind of secondary messenger central in regulating bacteria adaptive responses. In addition, analysis of protein-protein interactions using STRING database (Franceschini et al., 2013) indicated that *BMEII0293* encodes a hypothetical protein that is tightly associated with the synthesis and degradation of c-di-GMP. In *B. melitensis*, 11 c-di-GMP-metabolizing proteins had been inferred to regulate c-di-GMP metabolism (Petersen et al., 2011). The structure of these 11 genes were verified to be intact in Bab8416, but *BMEII0929*, *BMEII0292* and *BMEII1009*, were found absent in Bab941 and some *B. abortus* strains.

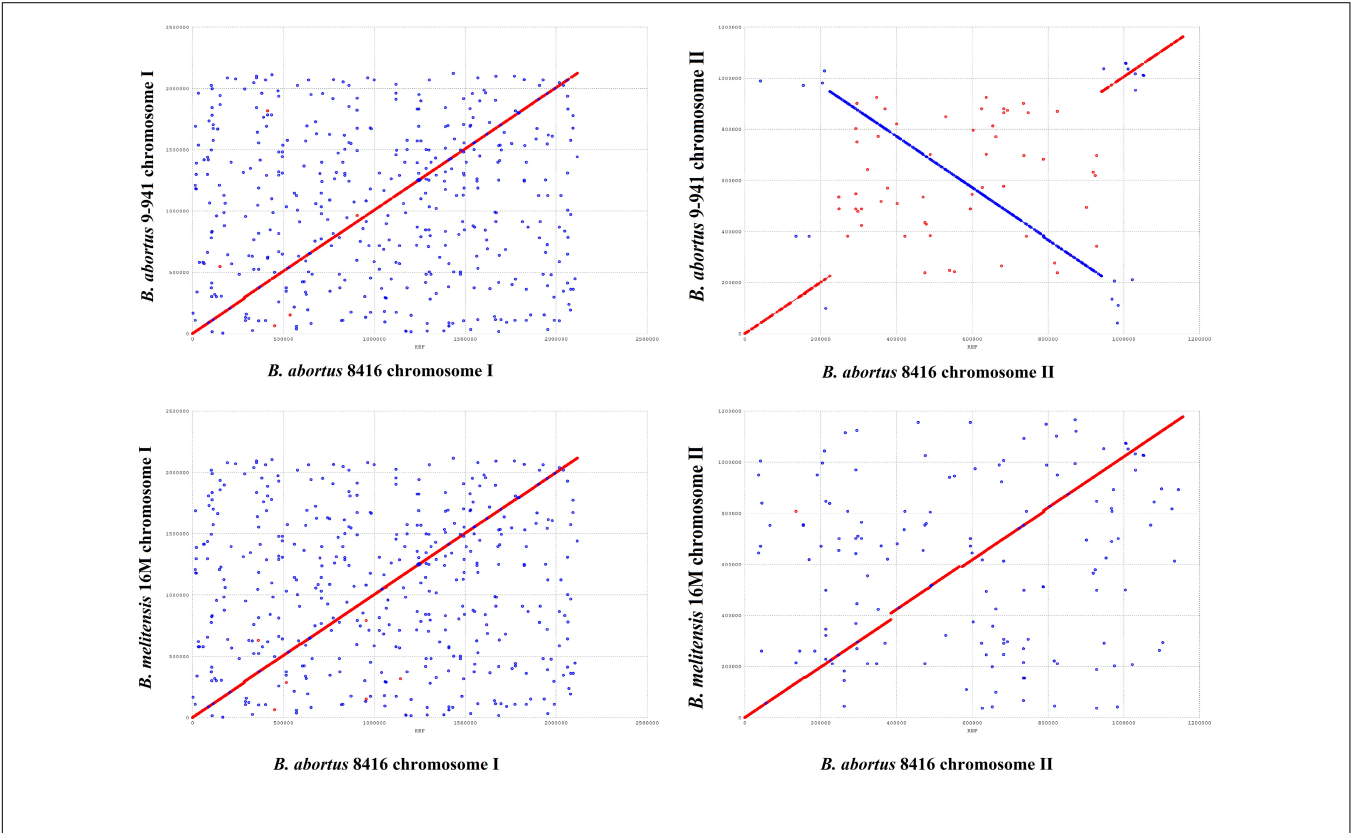


FIGURE 6 | Genome arrangement of *Brucella abortus* strain Bab8416 small Chromosome. The four complete *B. abortus* genomes, including *B. abortus* Bab8416, were compared to *B. abortus* Bab9-941 and arrangements only appeared in small Chromosome of *B. abortus* Bab8416.

TABLE 3 | ORFs related to deletions in *B. abortus* str.8416 compared to *B. abortus* 9–941 genome.

	BAB9-941 coordinate		Region length	Associated genes	Gene length	Gene length % in RD region	Gene functions
Chr1	Deletion	80475..80812	338	BruAb1_0072	2,271	14.88%	Hypothetical protein
	Deletion	85269..85303	35	BruAb1_0075	750	4.82%	Amino acid efflux LysE family protein
	Deletion	88412..88434	23	BruAb1_0079	384	0.52%	Hypothetical protein
	RD1	287585..295517	7,933	BruAb1_0284	1,767	100.00%	Phage integrase family site specific recombinase
				BruAb1_0286	195	100.00%	Hypothetical protein
				BruAb1_0287	618	100.00%	Resolvase family site-specific recombinase
				BruAb1_0289	228	100.00%	Hypothetical protein
				BruAb1_0290	285	100.00%	Hypothetical protein
				BruAb1_0291	261	100.00%	Hypothetical protein
				BruAb1_0292	390	100.00%	Hypothetical protein
				BruAb1_0371	1,128	2.84%	ABC transporter substrate-binding protein
	Deletion	1040055..1040246	193	BruAb1_1057	1,596	4.04%	DEAD/DEAH box helicase
	Deletion	1774700..1774731	32	BruAb1_1803	405	8.21%	30S ribosomal protein S16
	Deletion	1795037..1795098	62	BruAb1_1825	711	8.90%	Hypothetical protein
Chr2	Deletion	156432..156703	272	BruAb2_0168	5,952	17.87%	Outer membrane transporter
	RD2	158847..159637	791	BruAb2_0377	1,335	62.76%	FAD-binding oxidoreductase
				BruAb2_0378	420	100.00%	Hypothetical protein
				BruAb2_0379	1,011	100.00%	Epimerase
				BruAb2_0380	1,455	100.00%	Aminotransferase
	Deletion	620905..620941	37	BruAb2_0616	1,143	3.25%	Major facilitator family transporter
	RD4	701096..701938	843	BruAb2_0690	477	100.00%	IS711, transposase orfB
				BruAb2_0691	312	100.00%	Transposase orfA
	Deletion	711185..711248	64	BruAb2_0698	1,296	7.27%	Branched-chain alpha-keto acid dehydrogenase subunit E2

TABLE 4 | ORFs in insertions in *B. abortus* 8416 compared to *B. abortus* 9-941 genome.

BAB8416 coordinate		Region length	Associated ORFs	Gene length	ORF length % in Insertions	Gene Function
Chr1	15707..15843	137	BAB8416_I0012	1155	11.86%	ABC transporter, substrate-binding protein
	374342..374383	42	BAB8416_I0362	2019	2.08%	Xanthine dehydrogenase, molybdenum binding subunit
	643653..643790	138	BAB8416_I0630	1104	12.50%	ATP/GTP-binding site motif A
	1035800..1037009	1210	BAB8416_I1044	651	100.00%	Diguanylate cyclase/phosphodiesterase domain
	1040674..1040705	32	BAB8416_I1049	480	6.67%	Multidrug resistance protein A
	1409719..1409750	32	BAB8416_I1431	195	16.41%	FIG00450652: hypothetical protein
Chr2	4629..4760	132	BAB8416_II0007	912	14.47%	Nucleoside ABC transporter, permease protein 2
	10010..10058	49	BAB8416_II0012	726	6.75%	4'-phosphopantetheinyl transferase entD
	231155..231181	27	BAB8416_II0234	570	4.74%	Nitric oxide reductase activation protein NorE
	248732..248754	23	BAB8416_II0253	828	2.78%	Various polyols ABC transporter, ATP-binding component
	459512..459556	45	BAB8416_II0463	1335	3.37%	Branched-chain alpha-keto acid dehydrogenase, E1 component, alpha subunit
	572539..572616	78	BAB8416_II0569	1203	6.48%	Acetyl-CoA acetyltransferase
	849446..849532	87	BAB8416_II0843	1107	7.86%	RND efflux membrane fusion protein
	942069..942905	837	BAB8416_II0941	1047	46.51%	Putative Heme-regulated two-component response regulator
			BAB8416_II0942	1233	14.27%	L-2-hydroxyglutarate oxidase

Deletions and Insertions

Compared with SPS Bab9-941, 49 indels (≥ 20 bps), including 25 deletions and 24 insertions, were found in the Bab8416 genome (Tables 3, 4). A 16.5 kb region is absent from Bab8416 genome and a 3.2 kb region appears to be unique. Only four large

regions (> 500 bp) were represented by deletions, one Region of Differences (RD) 1 in chromosome I and three (RD2–RD4) in small chromosome. Genes lost in these regions are determined by referencing the annotation of *B. abortus* 9–941. The details of deletions and associated ORFs are shown in Table 3.

Eight genes, *BruAb1_0284-0292*, were located in RD1 region. *BruAb1_0284* and *BruAb1_0287* are specific recombinases, belonging to phage integrase and resolvase families, respectively. *BruAb1_0285* and *BruAb1_0288* were annotated as pseudo genes and the others were labeled hypothetical proteins. In addition, we further detected the RD1 region in 200 *B. melitensis* genomes and 197 *B. abortus* genomes by using BLASTn. In all of *B. melitensis* 200 strains we could not found any sequence similar with RD1. While 127 out of 197 *B. abortus* strains could be found the sequences with identity higher than 99% and coverage over 90% (**Supplementary Table S4**). These evidences above showed that RD1 was exclusively specific to *B. abortus* and the insert event should occur after the differentiation of the most recent common ancestor of *B. abortus* 9–941 and Bab8416. RD2 and another small deletion are involved in the locus of an outer membrane transporter, *BruAb2_0168*. An earlier study confirmed that this locus was conserved between *B. abortus* (Halling et al., 2005), but variation is present in Bab8416. RD3 contains four genes, *BruAb2_0377* to *BruAb2_0380*. *BruAb2_0377* encodes FAD-binding oxidoreductase. *BruAb2_0378* was defined as a hypothetical protein. *BruAb2_0379* encodes an epimerase that catalyzes the transformation of dTDP-glucose to dTDP-4-oxo-6-deoxy-D-glucose. *BruAb2_0380* encodes an amino transferase that participates in arginine and proline metabolism, metabolic pathways and biosynthesis of secondary metabolites. Two intact genes and one partial gene are encoded by RD4. The two complete genes, *BruAb2_0690* and *BruAb2_069*, encode transposase.

Inserted regions specific to Bab8416 are shown in **Table 4**. Among the 20 Bab8416 specific regions, six regions are located at intergenic spacer (IGS) and fifteen ORFs are involved in the other 14 insertions. All of these ORFs are annotated with known functions.

Variant ORFs

The variant ORFs were identified by BLASTn method. The results are shown in **Table 5**. In consideration of the prediction discrepancy and the restriction of software, we searched these

ORFs within these five genomes. BLASTn results showed that 144 Bab9-941 ORFs were found deleted or incomplete in Bab8416 and 129 Bab8416 ORFs were found to be Bab8416 specific. These deletions may be partly responsible for the unusual *Brucella* phage status of Bab8416.

SNPs

A total of 1,373 SNPs were identified between Bab8416 and Bab9-941. Using *B. abortus* 9–941 as a reference, 336 SNPs were intergenic and 1,036 SNPs were located in the ORFs. In addition, 518 genes-encoding proteins showed amino acid changes caused by 632 non-synonymous SNPs. As the SNP number was large, we inferred that these markers appeared in Bab8416 could be the characteristics of ST2. Since no other complete genomes of ST2 were available, we chose to utilize the existing draft genomes. In consideration of insuring the quality of sequencing and assembly, only the draft genomes with contig numbers less than 12 were selected. The MLST typing results of these genomes are shown in **Supplementary Table S1**. Fifteen out of 95 genomes were identified to be ST2. We tested the SNPs between the 16 ST2 genomes and found that overwhelming majority (95.05%) of former identified SNPs were verified to be potential markers of ST2 strains and only 68 SNPs appeared to be Bab8416 specific. The detailed SNP annotations are present in **Supplementary Table S2** and the Bab8416 specific SNP involved genes are presented in **Supplementary Table S3**.

LPS Synthesis

Lipopolysaccharide is tightly associated with the virulence of pathogens and the efficiency of corresponding vaccines. *Brucella* with rough lipopolysaccharide (R-LPS) was lysed by *Brucella* phage R/C, and is host specific (Hammerl et al., 2017). In *Brucella*, genes essential in synthesizing LPS and developing a smooth phenotype have been located at the Wbk region of chromosome I (Godfroid et al., 2000; Gonzalez et al., 2008; Zygmunt et al., 2009). Inactivation of formyltransferase (*wbkC*) gene is the significant factor that contributes to rough phenotype (Lacerda et al., 2010). BLASTn results showed that none of these genes were deleted/missing in Bab8416. Four non-synonymous mutations were identified in Bab8416 LPS genes, only one (*BruAb1_1699*) was found not belonging to ST2. This gene encodes an OmpA family protein, which is tightly related to flagellar protein production and also related to the efflux pump.

Virulence Factors

Bab8416 was isolated from a patient with clinical brucellosis, indicating that this strain was virulent. The presence of 23 *Brucella* virulence factors confirmed by VFDB was tested in the Bab8416 isolate. Bab8416 was found to have a full complement of these loci. BLASTp results showed that eleven genes were 100% identical, eight genes had point mutations, and short deletions were found in the other four genes with only one deletion being present in *VFG2217*. In addition, compared to *BAB1_0069*, a putative outer membrane protein considered to be a virulence factor, a 133 amino acid deletion is present in this locus of Bab8416. We inferred these changes might exert some influence

TABLE 5 | Classification of *B. abortus* strain Bab8416 specific SNPs associated ORFs.

Function class	ORF numbers
Amino acid transport and metabolism	5
Carbohydrate transport and metabolism	3
Cell envelope biogenesis, outer membrane	3
Cell motility and secretion	3
Coenzyme metabolism	2
Function unknown	1
General function prediction only	2
Inorganic ion transport and metabolism	7
Lipid metabolism	1
Nucleotide transport and metabolism	1
Transcription	3
Translation, ribosomal structure and biogenesis	5
Not in COGs	27

on the virulence of Bab8416 but not that much to cause high level attenuation as it is still a pathogenic bacterium.

CONCLUSION

Combining NGS sequencing technology and comparative genomics analysis, the complete genome sequence of *B. abortus* SPR strain Bab8416 was obtained and specific genetic characteristics of *B. abortus* SPR were comprehensively investigated in this study. Study of smooth LPS related genes showed that Bab8416 does share same LPS key genes with other *B. abortus* SPR strains, which supported veracity of previous phenotype screening results. The gold standard for *Brucella* characterization is still based on specific properties of the bacteria. None of the available molecular typing methods covers all currently known species and biovars of the genus *Brucella* (Hammerl et al., 2017). The difference between biotyping and genotyping of some special strain need further analysis not only on genomic but protein expressive level, because the host strains co-evolute with their special phages. The importance of individual amino acids of the tail collar protein for the host range of the *Brucella* phages has not yet been investigated. To avoid diverging lysis patterns, examine the phage genomes by sequencing were recommended if the lysis results are inconsistent on the same indicator strains (Hammerl et al., 2017).

Bab8416 has a genetic profile different from that typically found in most *B. abortus* strains. The arrangement sequences in small chromosome resulted in the truncation of c-di-GMP synthesis. The indels within SPS and SPR *B. abortus* showed that two evolutionary branches might have diverged at a far phylogenetic node. Plentiful point mutations were identified to be Bab8416 specific while the majority of the point mutations were verified to be ST2 characteristic of *B. abortus*. While few Bab8416 SNPs were identified, SNPs might still exert a significant

influence on phage typing status. Despite the unique genetic characteristics of Bab8416 uncovered in this study, full details of its resistance to phage have not yet been elucidated at the genomic level. Our findings established some novel molecular mechanisms underlying *Brucella* sensitivity to brucellaphages that might contribute to improving our understanding on *Brucella* phenotyping.

AUTHOR CONTRIBUTIONS

X-ML and Y-XK performed genomic sequencing and comparative genomic analyses and wrote the manuscript. LL, E-HJ, and D-RP performed *Brucella* MLVA typing and phage typing. HJ, C-CZ, and JH performed *Brucella* MLST typing and PCR sequencing. Y-FC, X-KG, and YZ designed the whole experiments and revised the manuscript.

FUNDING

This study was supported by the National Natural Science Foundation of China (81460319 and 81360444).

ACKNOWLEDGMENTS

We would like to thank Dr. L. Gary Adams, for his critical reading of this manuscript.

SUPPLEMENTARY MATERIAL

The Supplementary Material for this article can be found online at: <https://www.frontiersin.org/articles/10.3389/fmicb.2019.00917/full#supplementary-material>

REFERENCES

- Al Dahouk, S., Fleche, P. L., Nockler, K., Jacques, I., Grayon, M., Scholz, H. C., et al. (2007). Evaluation of brucella MLVA typing for human brucellosis. *J. Microbiol. Methods* 69, 137–145. doi: 10.1016/j.mimet.2006.12.015
- Al Dahouk, S., Scholz, H. C., Tomaso, H., Bahn, P., Gollner, C., Karges, W., et al. (2010). Differential phenotyping of brucella species using a newly developed semi-automated metabolic system. *BMC Microbiol.* 10:269. doi: 10.1186/1471-2180-10-269
- Chen, L., Yang, J., Yu, J., Yao, Z., Sun, L., Shen, Y., et al. (2005). VFDB: a reference database for bacterial virulence factors. *Nucleic Acids Res.* 33, D325–D328.
- Conesa, A., Gotz, S., Garcia-Gomez, J. M., Terol, J., Talon, M., and Robles, M. (2005). Blast2GO: a universal tool for annotation, visualization and analysis in functional genomics research. *Bioinformatics* 21, 3674–3676. doi: 10.1093/bioinformatics/bti610
- Corbel, M. J., and Morris, J. A. (1974). Studies on a smooth phage-resistant variant of *Brucella abortus*. I. Immunological properties. *Br. J. Exp. Pathol.* 55, 78–87.
- Crasta, O. R., Folkerts, O., Fei, Z., Mane, S. P., Evans, C., Martino-Catt, S., et al. (2008). Genome sequence of *Brucella abortus* vaccine strain S19 compared to virulent strains yields candidate virulence genes. *PLoS One* 3:e2193. doi: 10.1371/journal.pone.0002193
- Darling, A. E., Mau, B., and Perna, N. T. (2010). progressiveMauve: multiple genome alignment with gene gain, loss and rearrangement. *PLoS One* 5:e11147. doi: 10.1371/journal.pone.0011147
- FAO/WHO (1986). Joint FAO/WHO expert committee on brucellosis. *World Health Organ. Tech. Rep. Ser.* 740, 1–132.
- Franceschini, A., Szklarczyk, D., Frankild, S., Kuhn, M., Simonovic, M., Roth, A., et al. (2013). STRING v9.1: protein-protein interaction networks, with increased coverage and integration. *Nucleic Acids Res.* 41, D808–D815. doi: 10.1093/nar/gks1094
- Garcia, M. M., Brooks, B. W., Ruckerbauer, G. M., Rigby, C. E., and Forbes, L. B. (1988). Characterization of an atypical biotype of *Brucella abortus*. *Can. J. Vet. Res.* 52, 338–342.
- Godfroid, F., Cloeckaert, A., Taminiau, B., Danese, I., Tibor, A., De Bolle, X., et al. (2000). Genetic organisation of the lipopolysaccharide O-antigen biosynthesis region of brucella melitensis 16M (wbk). *Res. Microbiol.* 151, 655–668. doi: 10.1016/s0923-2508(00)90130-x
- Godfroid, J., Al Dahouk, S., Pappas, G., Roth, F., Matope, G., Muma, J., et al. (2013). A "One Health" surveillance and control of brucellosis in developing countries: moving away from improvisation. *Comp. Immunol. Microbiol. Infect. Dis.* 36, 241–248. doi: 10.1016/j.cimid.2012.09.001
- Gonzalez, D., Grillo, M. J., De Miguel, M. J., Ali, T., Arce-Gorvel, V., Delrue, R. M., et al. (2008). Brucellosis vaccines: assessment of *Brucella melitensis* lipopolysaccharide rough mutants defective in core and O-polysaccharide synthesis and export. *PLoS One* 3:e2760. doi: 10.1371/journal.pone.0002760
- Guindon, S., Dufayard, J. F., Lefort, V., Anisimova, M., Hordijk, W., and Gascuel, O. (2010). New algorithms and methods to estimate maximum-likelihood phylogenies: assessing the performance of PhyML 3.0. *Syst. Biol.* 59, 307–321. doi: 10.1093/sysbio/syq010

- Halling, S. M., Peterson-Burch, B. D., Bricker, B. J., Zuerner, R. L., Qing, Z., Li, L. L., et al. (2005). Completion of the genome sequence of *Brucella abortus* and comparison to the highly similar genomes of *Brucella melitensis* and *Brucella suis*. *J. Bacteriol.* 187, 2715–2726. doi: 10.1128/jb.187.8.2715-2726.2005
- Hammerl, J. A., Gollner, C., Jackel, C., Scholz, H. C., Nockler, K., Reetz, J., et al. (2017). Genetic diversity of brucella reference and non-reference phages and its impact on brucella-typing. *Front. Microbiol.* 8:408. doi: 10.3389/fmicb.2017.00408
- Hyatt, D., Chen, G. L., Locascio, P. F., Land, M. L., Larimer, F. W., and Hauser, L. J. (2010). Prodigal: prokaryotic gene recognition and translation initiation site identification. *BMC Bioinformatics* 11:119. doi: 10.1186/1471-2105-11-119
- Jahans, K. L., Foster, G., and Broughton, E. S. (1997). The characterisation of *Brucella* strains isolated from marine mammals. *Vet. Microbiol.* 57, 373–382. doi: 10.1016/s0378-1135(97)00118-1
- Jiang, H., Du, P., Zhang, W., Wang, H., Zhao, H., Piao, D., et al. (2013a). Comparative genomic analysis of *Brucella melitensis* vaccine strain M5 provides insights into virulence attenuation. *PLoS One* 8:e70852. doi: 10.1371/journal.pone.0070852
- Jiang, H., Wang, H., Xu, L., Hu, G., Ma, J., Xiao, P., et al. (2013b). MLVA genotyping of *Brucella melitensis* and *Brucella abortus* isolates from different animal species and humans and identification of *Brucella suis* vaccine strain S2 from cattle in China. *PLoS One* 8:e76332. doi: 10.1371/journal.pone.0076332
- Jones, L. M., Merz, G., and Wilson, J. (1968). Phage typing reactions on *Brucella* species. *Appl. Microbiol.* 16, 1179–1190.
- Kang, Y. X., Li, X. M., Piao, D. R., Tian, G. Z., Jiang, H., Jia, E. H., et al. (2015). Typing discrepancy between phenotypic and molecular characterization revealing an emerging biovar 9 variant of smooth phage-resistant *B. abortus* Strain 8416 in China. *Front. Microbiol.* 6:1375. doi: 10.3389/fmicb.2015.01375
- Kurtz, S., Phillippy, A., Delcher, A. L., Smoot, M., Shumway, M., Antonescu, C., et al. (2004). Versatile and open software for comparing large genomes. *Genome Biol.* 5:R12.
- Lacerda, T. L., Cardoso, P. G., Augusto De Almeida, L., Camargo, I. L., Afonso, D. A., Trant, C. C., et al. (2010). Inactivation of formyltransferase (wbkC) gene generates a *Brucella abortus* rough strain that is attenuated in macrophages and in mice. *Vaccine* 28, 5627–5634. doi: 10.1016/j.vaccine.2010.06.023
- Le Fleche, P., Jacques, I., Grayon, M., Al Dahouk, S., Bouchon, P., Denoeud, F., et al. (2006). Evaluation and selection of tandem repeat loci for a *Brucella* MLVA typing assay. *BMC Microbiol.* 6:9. doi: 10.1186/1471-2180-6-9
- Luo, H., Zhang, C. T., and Gao, F. (2014). Ori-Finder 2, an integrated tool to predict replication origins in the archaeal genomes. *Front. Microbiol.* 5:482. doi: 10.3389/fmicb.2014.00482
- Moreno, E., Cloeckert, A., and Moriyon, I. (2002). *Brucella* evolution and taxonomy. *Vet. Microbiol.* 90, 209–227. doi: 10.1016/s0378-1135(02)00210-9
- Morris, J. A., Corbel, M. J., and Phillip, J. I. (1973). Characterization of three phages lytic for *Brucella* species. *J. Gen. Virol.* 20, 63–73. doi: 10.1099/0022-1317-20-1-63
- Pappas, G., Papadimitriou, P., Akritidis, N., Christou, L., and Tsianos, E. V. (2006). The new global map of human brucellosis. *Lancet Infect. Dis.* 6, 91–99. doi: 10.1016/s1473-3099(06)70382-6
- Petersen, E., Chaudhuri, P., Gourley, C., Harms, J., and Splitter, G. (2011). *Brucella melitensis* cyclic di-GMP phosphodiesterase BpdA controls expression of flagellar genes. *J. Bacteriol.* 193, 5683–5691. doi: 10.1128/JB.00428-11
- Ricker, N., Qian, H., and Fulthorpe, R. R. (2012). The limitations of draft assemblies for understanding prokaryotic adaptation and evolution. *Genomics* 100, 167–175. doi: 10.1016/j.ygeno.2012.06.009
- Rigby, C. E., Cerqueira-Campos, M. L., Kelly, H. A., and Surujballi, O. P. (1989). Properties and partial genetic characterization of Nepean phage and other lytic phages of *Brucella* species. *Can. J. Vet. Res.* 53, 319–325.
- Sanogo, M., Abatih, E., Thys, E., Fretin, D., Berkvens, D., and Saegerman, C. (2013). Importance of identification and typing of brucellae from west african cattle: a review. *Vet. Microbiol.* 164, 202–211. doi: 10.1016/j.vetmic.2013.02.009
- Schattner, P., Brooks, A. N., and Lowe, T. M. (2005). The tRNAscan-SE, snoscan and snoGPS web servers for the detection of tRNAs and snoRNAs. *Nucleic Acids Res.* 33, W686–W689.
- Scholz, H. C., Al Dahouk, S., Tomaso, H., Neubauer, H., Witte, A., Schloter, M., et al. (2008a). Genetic diversity and phylogenetic relationships of bacteria belonging to the ochrobactrum-brucella group by recA and 16S rRNA gene-based comparative sequence analysis. *Syst. Appl. Microbiol.* 31, 1–16. doi: 10.1016/j.syapm.2007.10.004
- Scholz, H. C., Pfeffer, M., Witte, A., Neubauer, H., Al Dahouk, S., Wernery, U., et al. (2008b). Specific detection and differentiation of *Ochrobactrum anthropi*, *Ochrobactrum intermedium* and *Brucella* spp. by a multi-primer PCR that targets the recA gene. *J. Med. Microbiol.* 57, 64–71. doi: 10.1099/jmm.0.47507-0
- Sieira, R., Commerci, D. J., Sanchez, D. O., and Ugalde, R. A. (2000). A homologue of an operon required for DNA transfer in *Agrobacterium* is required in *Brucella abortus* for virulence and intracellular multiplication. *J. Bacteriol.* 182, 4849–4855. doi: 10.1128/jb.182.17.4849-4855.2000
- Tang, B., Wang, Q., Yang, M., Xie, F., Zhu, Y., Zhuo, Y., et al. (2013). ContigScape: a cytoscape plugin facilitating microbial genome gap closing. *BMC Genomics* 14:289. doi: 10.1186/1471-2164-14-289
- Tsolis, R. M., Seshadri, R., Santos, R. L., Sangari, F. J., Lobo, J. M., De Jong, M. F., et al. (2009). Genome degradation in *Brucella ovis* corresponds with narrowing of its host range and tissue tropism. *PLoS One* 4:e5519. doi: 10.1371/journal.pone.0005519
- Valdezate, S., Navarro, A., Rubio, V., Garin-Bastuji, B., Albert, D., Hernandez, P., et al. (2009). Emergence of a clonal lineage of *Brucella abortus* biovar 3 in clinical cases in Spain. *J. Clin. Microbiol.* 47, 2687–2688. doi: 10.1128/jcm.00756-09
- Van Belkum, A. (2007). Tracing isolates of bacterial species by multilocus variable number of tandem repeat analysis (MLVA). *FEMS Immunol. Med. Microbiol.* 49, 22–27. doi: 10.1111/j.1574-695x.2006.00173.x
- Walker, B. J., Abeel, T., Shea, T., Priest, M., Abouelliel, A., Sakthikumar, S., et al. (2014). Pilon: an integrated tool for comprehensive microbial variant detection and genome assembly improvement. *PLoS One* 9:e112963. doi: 10.1371/journal.pone.0112963
- Wattam, A. R., Davis, J. J., Assaf, R., Boisvert, S., Brettin, T., Bun, C., et al. (2017). Improvements to PATRIC, the all-bacterial bioinformatics database and analysis resource center. *Nucleic Acids Res.* 45, D535–D542. doi: 10.1093/nar/gkw1017
- Whatmore, A. M., Koylass, M. S., Muchowski, J., Edwards-Smallbone, J., Gopaul, K. K., and Perrett, L. L. (2016). Extended multilocus sequence analysis to describe the global population structure of the genus *brucella*: phylogeography and relationship to biovars. *Front. Microbiol.* 7:2049. doi: 10.3389/fmicb.2016.02049
- Whatmore, A. M., Perrett, L. L., and Macmillan, A. P. (2007). Characterisation of the genetic diversity of *Brucella* by multilocus sequencing. *BMC Microbiol.* 7:34. doi: 10.1186/1471-2180-7-34
- Zhang, X., Goodsell, J., and Norgren, R. B. (2012). Limitations of the rhesus macaque draft genome assembly and annotation. *BMC Genomics* 13:206. doi: 10.1186/1471-2164-13-206
- Zhao, Y., Wu, J., Yang, J., Sun, S., Xiao, J., and Yu, J. (2012). PGAP: pan-genomes analysis pipeline. *Bioinformatics* 28, 416–418. doi: 10.1093/bioinformatics/btr655
- Zygmunt, M. S., Blasco, J. M., Letesson, J. J., Cloeckert, A., and Moriyon, I. (2009). DNA polymorphism analysis of *Brucella* lipopolysaccharide genes reveals marked differences in O-polysaccharide biosynthetic genes between smooth and rough *Brucella* species and novel species-specific markers. *BMC Microbiol.* 9:92. doi: 10.1186/1471-2180-9-92

Conflict of Interest Statement: The authors declare that the research was conducted in the absence of any commercial or financial relationships that could be construed as a potential conflict of interest.

Copyright © 2019 Li, Kang, Lin, Jia, Piao, Jiang, Zhang, He, Chang, Guo and Zhu. This is an open-access article distributed under the terms of the Creative Commons Attribution License (CC BY). The use, distribution or reproduction in other forums is permitted, provided the original author(s) and the copyright owner(s) are credited and that the original publication in this journal is cited, in accordance with accepted academic practice. No use, distribution or reproduction is permitted which does not comply with these terms.



Genetic and Phenotypic Characterization of the Etiological Agent of Canine Orchiepididymitis Smooth *Brucella* sp. BCCN84.3

OPEN ACCESS

Edited by:

Armanda Bastos,
University of Pretoria, South Africa

Reviewed by:

Sidharath Dev Thakur,
Chaudhary Sarwan Kumar Himachal
Pradesh Krishi Vishvavidyalaya, India
Jacques Xavier Godfroid,
UiT The Arctic University of
Norway, Norway

*Correspondence:

Edgardo Moreno
emoreno@racsa.co.cr

Specialty section:

This article was submitted to
Veterinary Infectious Diseases,
a section of the journal
Frontiers in Veterinary Science

Received: 23 February 2019

Accepted: 20 May 2019

Published: 07 June 2019

Citation:

Guzmán-Verri C, Suárez-Esquivel M,
Ruiz-Villalobos N, Zygmunt MS,
Gonnet M, Campos E, Viquez-Ruiz E,
Chacón-Díaz C, Aragón-Aranda B,
Conde-Álvarez R, Moriyón I,
Blasco JM, Muñoz PM, Baker KS,
Thomson NR, Cloeckert A and
Moreno E (2019) Genetic and
Phenotypic Characterization of the
Etiological Agent of Canine
Orchiepididymitis Smooth *Brucella* sp.
BCCN84.3. *Front. Vet. Sci.* 6:175.
doi: 10.3389/fvets.2019.00175

Caterina Guzmán-Verri^{1,2}, Marcela Suárez-Esquivel¹, Nazareth Ruiz-Villalobos¹, Michel S. Zygmunt³, Mathieu Gonnet³, Elena Campos⁴, Eunice Viquez-Ruiz¹, Carlos Chacón-Díaz², Beatriz Aragón-Aranda⁵, Raquel Conde-Álvarez⁵, Ignacio Moriyón⁵, José María Blasco⁶, Pilar M. Muñoz⁶, Kate S. Baker^{7,8}, Nicholas R. Thomson⁷, Axel Cloeckert³ and Edgardo Moreno^{1*}

¹ Programa de Investigación en Enfermedades Tropicales (PIET), Escuela de Medicina Veterinaria, Universidad Nacional, Heredia, Costa Rica, ² Facultad de Microbiología, Centro de Investigación en Enfermedades Tropicales, Universidad de Costa Rica, San José, Costa Rica, ³ ISP, INRA, Université François Rabelais de Tours, Nouzilly, France, ⁴ Centro Nacional de Referencia en Bacteriología, Instituto Costarricense de Investigación y Enseñanza en Nutrición y Salud (INCIENSA), Cartago, Costa Rica, ⁵ IDISNA and Departamento de Microbiología y Parasitología, Instituto de Salud Tropical, Universidad de Navarra, Pamplona, Spain, ⁶ Unidad de Producción y Sanidad Animal, Instituto Agroalimentario de Aragón-IA2, CITA-Universidad de Zaragoza, Zaragoza, Spain, ⁷ Pathogen Genomics, Wellcome Trust Sanger Institute, Hinxton, United Kingdom, ⁸ Institute for Integrative Biology, University of Liverpool, Liverpool, United Kingdom

Members of the genus *Brucella* cluster in two phylogenetic groups: classical and non-classical species. The former group is composed of *Brucella* species that cause disease in mammals, including humans. A *Brucella* species, labeled as *Brucella* sp. BCCN84.3, was isolated from the testes of a Saint Bernard dog suffering orchiepididymitis, in Costa Rica. Following standard microbiological methods, the bacterium was first defined as “*Brucella melitensis* biovar 2.” Further molecular typing, identified the strain as an atypical “*Brucella suis*.” Distinctive *Brucella* sp. BCCN84.3 markers, absent in other *Brucella* species and strains, were revealed by fatty acid methyl ester analysis, high resolution melting PCR and *omp25* and *omp2a/omp2b* gene diversity. Analysis of multiple loci variable number of tandem repeats and whole genome sequencing demonstrated that this isolate was different from the currently described *Brucella* species. The smooth *Brucella* sp. BCCN84.3 clusters together with the classical *Brucella* clade and displays all the genes required for virulence. *Brucella* sp. BCCN84.3 is a *species nova* taxonomical entity displaying pathogenicity; therefore, relevant for differential diagnoses in the context of brucellosis. Considering the debate on the *Brucella* species concept, there is a need to describe the extant taxonomical entities of these pathogens in order to understand the dispersion and evolution.

Keywords: *Brucella*, *Brucella melitensis*, *Brucella suis*, *Brucella canis*, brucellosis, dog, species, epididymitis

INTRODUCTION

The *Brucella* genus comprises two phylogenetically related clusters: classical and non-classical (1). The former cluster is a compact group composed of *Brucella melitensis*, *Brucella abortus*, *Brucella suis*, *Brucella canis*, *Brucella neotomae*, *Brucella ceti*, *Brucella pinnipedialis*, *Brucella ovis*, *Brucella microti*, *Brucella papionis*, and *Brucella* sp. F5/99. All these species infect and produce disease in mammals, displaying host preference. Members of this cluster are non-motile, devoid of plasmids and their genomes show nucleotide identities of >99% (1, 2). The first six *Brucella* species of this cluster are zoonotic and can infect humans (3–5).

Non-classical *Brucella* species, also known as the “BO clade,” cluster in a discrete group that includes the fast-growing *Brucella inopinata* and BO2 strains isolated in humans as well as *Brucella* species living in frogs (1). *Brucella vulpis*, isolated from red foxes in Australia, is more distant to BO clade and contains unique genetic information related to soil bacteria not encoded in classical *Brucella* organisms (1). Bacteria of the BO clade and *B. vulpis* display nucleotide identities of 97–98% with those of the classical clade. The species of this cluster also share genes with the soil bacteria *Ochrobactrum* spp. and show key sequence differences in central genes such as 16S rRNA and *recA*, as distinctive features (1). With the sole exception of *B. inopinata*, these *Brucella* species possess an O-chain lipopolysaccharide (LPS) structure that departs from that of the classical *Brucella* species (1, 6). This feature hampers the straightforward recognition of non-classical *Brucella* infections in animals.

Identification of the classical *Brucella* species and strains by traditional bacteriological and molecular methods is not straightforward. This is due to the high phenotypic and genotypic resemblance among different members of the genus (3, 7).

For this reason, many *Brucella* strains isolated from various animal species have been misclassified or not fully characterized (8, 9). One clear example of clinical relevance has been the discovery of *B. neotomae* as a human pathogen, which was wrongly classified as an atypical *B. abortus* strain by classical bacteriological methods (10). With the advent of sophisticated molecular tools and whole genome sequence analysis (WGSA), the correct identification of *Brucella* species was achieved (1, 4).

Here, we describe the phenotypic and genotypic properties of a new classical pathogenic smooth *Brucella* sp., isolated from a Saint Bernard dog suffering orchiepididymitis. After its primary isolation in 1984 in Costa Rica (11), the strain was first assigned as an atypical strain of *B. melitensis* biovar 2 (12).

MATERIALS AND METHODS

Clinical Case and Bacterial Isolation

A 4-year male domestic Saint Bernard dog from the Central Valley of Costa Rica showing testicular lesions, was brought to the Hospital of the Veterinary School of the National University, in 1984. After hospitalization, the owner was informed of all procedures and clinical studies and gave her written consent. All protocols and actions undertaken to diagnose the disease were under the Veterinary Hospital guidance established in 1980. The protocols used in 1984, were those approved by the “Ley General de Salud” N° 5395, and “Disposiciones sobre Matrícula y Vacunación de Perros” N° 2391.

After anamnesis and clinical examination, the dog was subjected to surgery and both testes removed. Rose Bengal test (13) was used to determine the presence of antibodies against smooth *Brucella*. Histopathological examination of the testes was performed following previous protocols (14). For bacterial isolation, blood and testicular samples were cultured in blood-agar plates. The plates were incubated at 37°C under the presence

TABLE 1 | Microbiological characterization of *Brucella* sp. BCCN84.3 and comparison with *Brucella* reference strains.

Strains	RTD phage lysis ^a				CO ₂ requirement	Urease	Serum agglutination against ^b		Growth on dyes, µg/mL ^c				
	Tb	Wb	Iz	R/C			A	M					
									Thionin	Basic fuchsin	O safranin		
	10	20	10	20					100				
<i>Brucella</i> sp. BCCN84.3 ^d	–	+	+	–	No	+	+	–	+	+	+	+	+
<i>B. abortus</i> 2308W	+	+	+	–	No	+	+	–	–	–	+	+	+
<i>B. suis</i> 1330	–	+	+	–	No	+	+	–	+	+	–	–	–
<i>B. melitensis</i> 16M	–	–	+	–	No	+	–	+	+	+	+	+	+
<i>B. ovis</i> 63/290	–	–	–	+	Yes	+	–	–	+	–	–	–	–
<i>B. canis</i> CR12	–	–	–	+	No	+	–	–	+	–	–	–	–
<i>B. neotomae</i> 5K/33	+	–	+	+	No	+	+	–	–	–	–	–	–
<i>B. microti</i> CCM 4915	–	+			No	+	–	+	+	+	+	+	
<i>B. ceti</i> , B1/94	–	+	–	–	No	+	+	–	+	+	+	+	+
<i>B. pinnipedialis</i> B2/94	–	–	+	–	Yes	+	+	–	+	+	+	+	+

^aRTD, routine test dilution of phages Tbilisi (Tb), Weybridge (Wb), Izatnagar (Iz), and rough type Wb derivative (R/C).

^bSerum against LPS epitopes, measured as agglutination with monospecific serum.

^cDye concentrations expressed in µg/mL of culture medium and plates incubated under 10% CO₂ atmosphere.

^dThe strain was oxidase positive and readily produced H₂S.

or the absence of 10% CO₂ atmosphere. The bacterial colonies were identified as *Brucella* sp. at the Bacteriology Laboratory of INCIENSA, Costa Rica (11). The isolate (code *Brucella* sp. BCCN84.3) was freeze-dried and submitted for further bacteriological and molecular typing, as described below.

Bacterial Phenotypic Characterization

The *Brucella* sp. BCCN84.3 was subjected to classical bacteriological typing (Table 1) following established protocols (13). Reference *Brucella* strains were used for comparative purposes (Supplementary Table 1). Total lipids were extracted and analyzed as described elsewhere (15) and resolved on silica gel 60 high-performance TLC plates (Merck Chemicals) using n-propanol/propionic acid/chloroform/water (3:2:2:1) and developed by charring with 15% (v/v) sulfuric acid in ethanol (16). Processing of the fatty acid methyl ester for taxonomical identification and dendrogram assembly were carried out as described before (17). Extraction of LPS by SDS-proteinase K protocol was performed as described previously (18). LPS was analyzed in 12 or 15% polyacrylamide gels and stained by the periodate-alkaline silver method (19). An immune serum obtained from *B. melitensis* 16M infected rabbits (20), either plain or absorbed with cells from rough Per mutant strain derived from *B. abortus* 2308W, was used for assessing anti-smooth-LPS reactivity. Immune serum obtained from *B. abortus* Per immunized rabbit (21) was used for anti-rough-LPS reactivity. Western blots and ELISA with a collection of monoclonal antibodies (Mabs) for the detection of specific *Brucella* surface antigens were performed as described elsewhere (22, 23). Susceptibility to polymyxin B was determined by estimating the minimal inhibitory concentration on Müller-Hinton agar (Becton Dickinson, Izasa), following the e-test (Liofilchem, Werfen) method (24).

Genotypic and Phylogenetic Characterization

Bacterial DNA was extracted with DNeasy Blood & Tissue kit from QIAGEN or Promega Wizard Genomic DNA Purification kit as per manufacturer's instructions. DNA was stored at -70°C until used. Bruce-ladder v2.0 PCR for the differentiation of *Brucella* species and strains was carried following previous protocols (25). Suis-ladder PCR assay for *B. suis* biovar typing and the discrimination of *B. suis* and *B. canis* was performed as described before (26).

Two different real-time PCRs, for the detection of *Brucella* genus and *B. suis* were performed as previously described (27). Additionally, two different high-resolution melting PCR assays (HRM-PCR) for the specific detection and discrimination of *B. canis* and *B. melitensis* were performed following previous protocols (27), using a DNA concentration of 1.5 ng/μL and a Type-it HRM-PCR Kit (QIAGEN) in a reaction volume of 25 μL with a Rotor-Gene Q (QIAGEN). Control DNAs from *B. canis* RM 6/66, *B. melitensis* 16M, *B. suis* 1330 and *B. neotomae* 5K/33 were extracted with DNeasy Blood & Tissue kit from QIAGEN, and stored at -80°C until used. The conditions were one cycle at 50°C for 2 min and one cycle at 95°C for 10 min, followed by 40 cycles at 95°C for 5 s and a cycle at 60°C for 30 s, with data

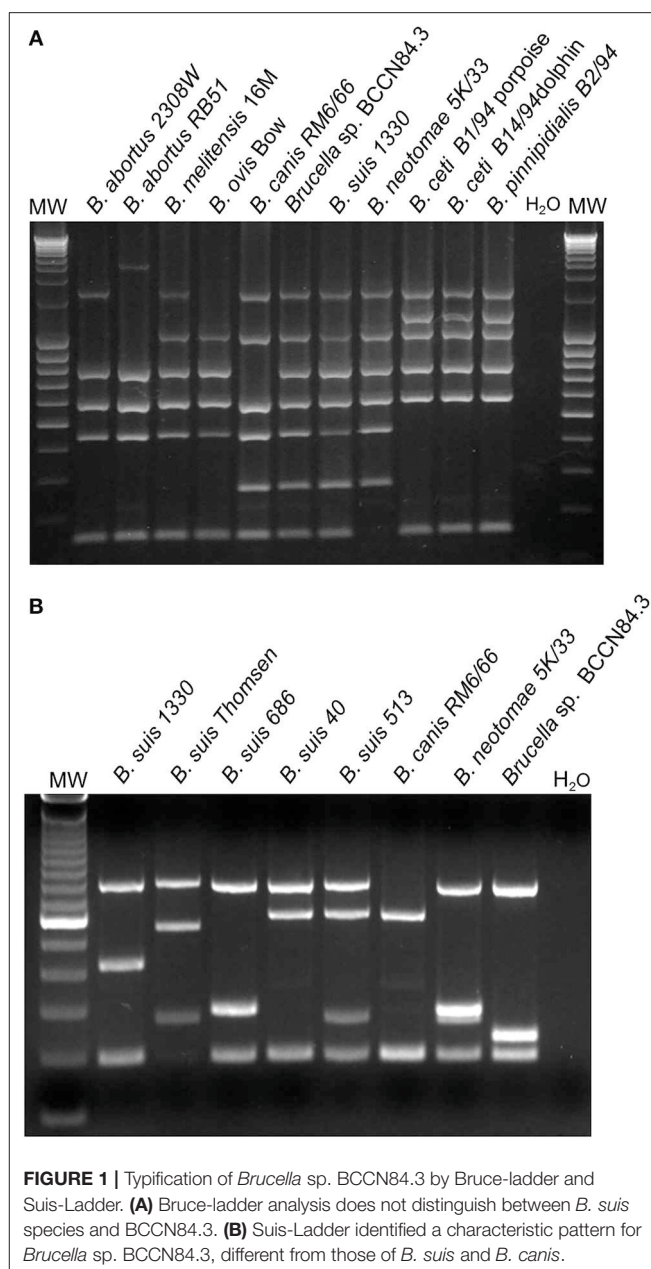


FIGURE 1 | Typification of *Brucella* sp. BCCN84.3 by Bruce-ladder and Suis-Ladder. (A) Bruce-ladder analysis does not distinguish between *B. suis* species and BCCN84.3. (B) Suis-Ladder identified a characteristic pattern for *Brucella* sp. BCCN84.3, different from those of *B. suis* and *B. canis*.

acquired at 60°C in the green channel. After amplification, an HRM-PCR was performed when needed from 73 to 88°C at a rate of 0.03°C per step.

Multiple loci variable number of tandem repeats analysis (MLVA16) and the corresponding cladograms were generated according to described protocols (17, 28) using the MLVA-NET database (29). Values obtained for each MLVA16 marker are in Supplementary Data Sheet 1.

WGSa was performed at the Wellcome Trust Sanger Institute on Illumina platforms according to in-house protocols (30, 31). For WGSa assembly and alignment sequencing reads were *de novo* assembled using a Velvet Optimiser (32). In order to overcome possible genome deviation

through serial cultivation, the strain deposited in 1984 in the *Brucella* Culture Collection Nouzilly (BCCN) was also sequenced and deposited at DDBJ/ENA/GenBank under the accession NQLX000000000; Accession *Brucella* sp. BCCN84.3 (NQLX000000000; BioSample SAMN07488835). WGSa from representative *Brucella* strains used for comparative purposes were obtained from GenBank (**Supplementary Data Sheet 1**). Low length and N50 scaffold sequences were not included in the analysis. Automatic annotation of the assembly was performed with the Prokka program (33). Genome sequence data was deposited at the European Nucleotide Archive under accession code ERS568777 and at DDBJ/ENA/GenBank under the accession NQLX000000000; BioSample SAMN07488835 (**Supplementary Data Sheet 1**). The 9 and 21 loci schemes of Multi Locus Sequence typing (MLST) were performed *in*

silico by BLAST comparison with a set of specific primers (34) and the assembled scaffolds as input. The results were confirmed by querying the matched sequences or “amplicons” at the *Brucella* MLST Database (<https://pubmlst.org/brucella/>) (**Supplementary Data Sheet 1**).

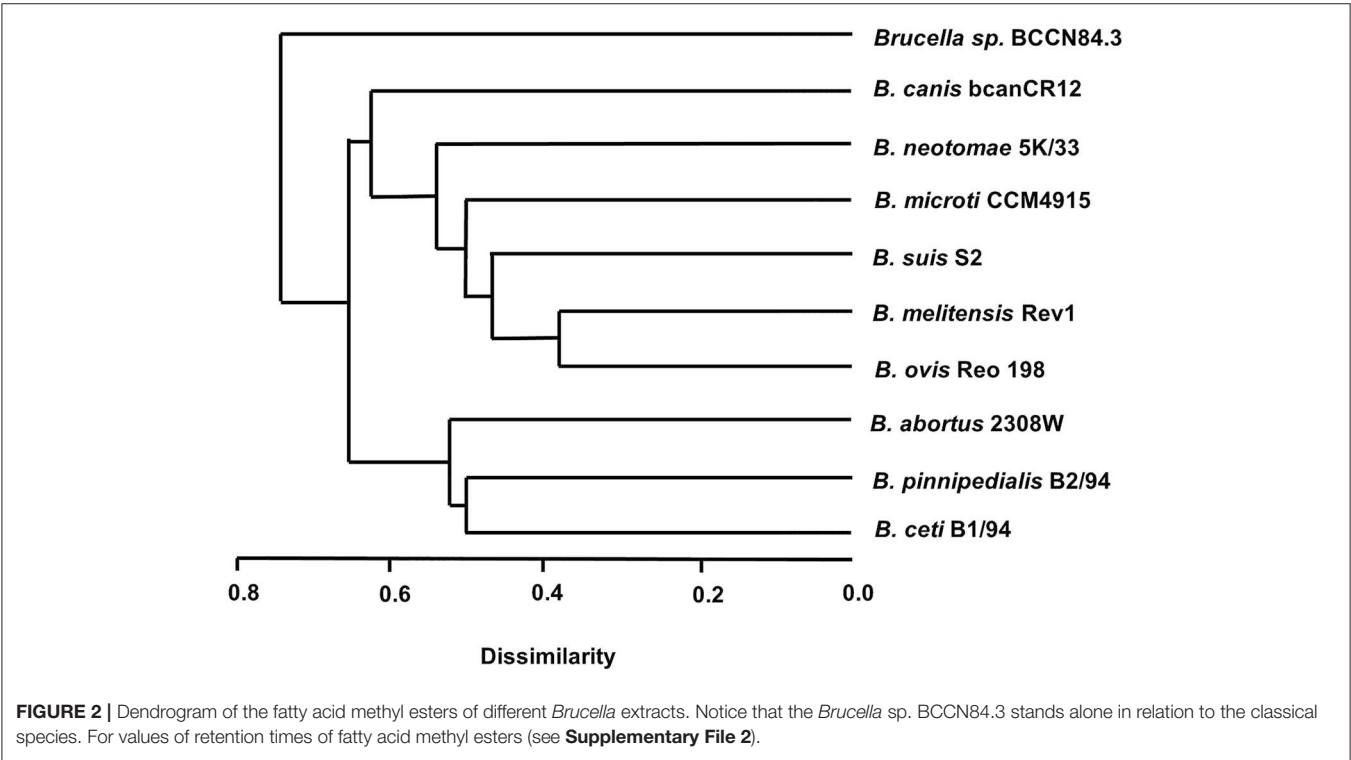
Phylogenetic Reconstruction

Two *Ochrobactrum* species and *Brucella* isolates were used for phylogenetic reconstruction (**Supplementary Data Sheet 1**). The 25 WGSa were aligned by *bwa* and mapped with SMALT v.0.7.4 against *B. suis* 1330, with an average mapping of 89.41% when excluding *Ochrobactrum*. Single Nucleotide Polymorphisms (SNPs) were called using SAMtools (35), and 451213 variable sites were extracted using SNP sites (36). The general features of all 25 assemblies annotated by Prokka were used to perform

TABLE 2 | Cell envelope characteristics of *Brucella* sp. BCCN84.3 and comparison with reference *Brucella* strains.

	Major lipids		Reactivity with serum to		Resistance to cationic peptides (PmxB MIC µg/ml)
	Phospholipids	Aminolipids	O-chain	R-LPS	
<i>Brucella</i> sp. BCCN84.3	PC; PE; PG; CL	OL	A>M	+	12
<i>B. canis</i> CR12	PC; PE; PG; CL	OL	–	+	12
<i>B. microti</i> CCM 4915	PC; PE; PG; CL	OH-OL; OL	A>M	–	>16
<i>B. melitensis</i> 16M	PC; PE; PG; CL	OL	M>A	+	16
<i>B. suis</i> 1330	PC; PE; PG; CL	OL	A>M	+	16
<i>B. abortus</i> 2308W	PC; PE; PG; CL	OL	A>M	+	4

PC, phosphatidylcholine; PE, phosphatidylethanolamine; PG, phosphatidylglycerol; CL, cardiolipine, OL, ornithine lipids; OH-OL, hydroxylated ornithine lipids; PmxB, polymixin B.



a pangenome analysis (36). Both SNPs and core genome alignments were individually used to each produce a maximum likelihood phylogenetic reconstruction with RAxML v8.2 (37). The phylogenetic trees were rooted using *Ochrobactrum anthropi* ATCC49188 and *Ochrobactrum intermedium* LMG3301.

A Specific Search for Regions of Interest

Regions of interest were searched through *bwa* alignment and SMALT mapping, or BLAST comparison against *B. canis* ATCC RM6/66 (NC_010103.1-NC_010104.1), *B. suis* 1330 (NC_004310.3-NC_004311.2), *B. abortus* 9-941 (NC_006932.1-NC_006933.1), *B. abortus* 2308W (ERS568782), *B. melitensis* 16M (NC_003317.1-NC_003318.1), and *B. microti* CCM 4915

(NC_013119.1-NC_013118.1). The number of SNPs, insertions and deletions in each gene were recorded. BLAST comparisons between *Brucella* sp. BCCN84.3, *B. canis* RM6/66 and *B. suis* 1330 were performed and visualized with the Artemis Comparison Tool (38). The presence of recombination events was analyzed by Genealogies Unbiased By recomBINations In Nucleotide Sequences (39) and visualized by Phandango (40). Southern blot analysis was performed as described previously (41) using the IS elements IS711 and ISBme1 as probes on EcoRI-digested DNA.

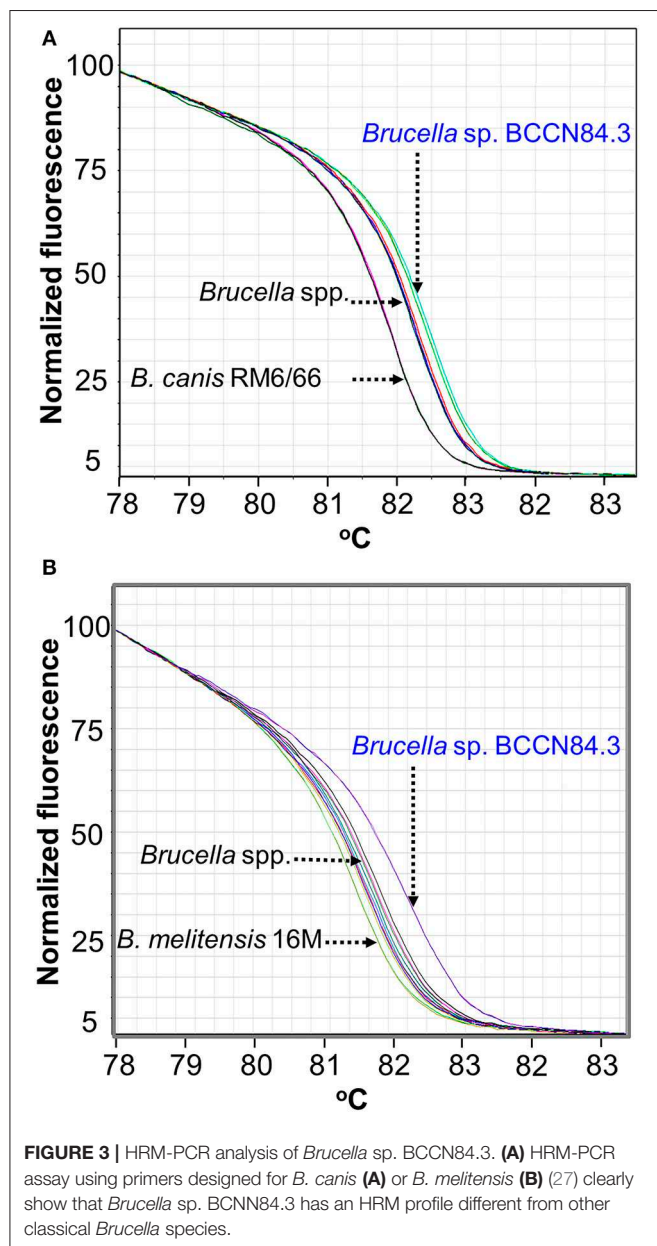
For phylogenetic reconstruction, comparisons among *omp2a* (BAW_10633) and *omp2b* (BAW_10634) porin gene sequences were assessed through multiple sequence alignments. Characterization of *Omp2a* and *omp2b* have been used as molecular tools for the description of *Brucella* species since 2007 (42), Sanger sequence data from 14 classical *Brucella* strains were visualized, edited, aligned, and analyzed in MEGA version 7 (43). The resulting alignment of 1,223 positions was used to build a phylogenetic tree by the maximum likelihood method based on the Tamura-Nei model (44). The tree with the highest log likelihood was selected. All the positions containing gaps or missing data were eliminated. Initial trees for the heuristic search were obtained automatically by applying the Neighbor-Join and BioNJ algorithms to a matrix of pairwise distances estimated using the maximum composite likelihood approach and then by selecting the topology with a superior log-likelihood value.

RESULTS

The anamnesis revealed that the Saint Bernard dog was imported from the United States as a puppy to Costa Rica, in 1980. The animal lived in the city of Heredia, Costa Rica and was never in contact with farm animals or mated. Upon arrival to the Veterinary Medicine School, the dog showed unwillingness to walk, general lethargy, refusal to eat, aspermia, fever, enlargement of the scrotum and testicles with local dermatitis and scrotal pain. The animal did not show any rashes, abdominal pain, visceral enlargement or local adenopathy. Platelets and leukocyte counts were normal. Pathological inspection showed bilateral enlargement of the epididymis and inflammation as well mild necrosis of both testes. Histopathological examination of testicular tissue revealed necrotizing foci and granulomatous inflammation. Since the serum of the animal showed positive agglutination in Rose Bengal test for brucellosis, it was not necessary to perform any other serological tests. The presumptive clinical diagnosis was orchiepididymitis due to brucellosis.

Serological diagnosis was confirmed by isolation of smooth *Brucella* sp. from testicular tissue after 1 week of culture in blood agar. The dog was treated orally with doxycycline (20 mg/Kg), three times a day for 14 days. Then streptomycin (11 mg/Kg) was administrated intramuscular every 12 h during 14 days. After treatment the dog showed improvement; however, the animal was not followed afterward.

Since the isolate displayed an atypical bacteriological profile (11), the strain was sent to the Station de Pathologie de la Reproduction, INRA, Centre de Tours-Nouzilly, France, for typing. The strain presented an atypical oxidative metabolic



profile with particularly high levels for L-glutamic acid and L-asparagine utilization. The strain was coded as *Brucella* sp. BCCN84.3 and identified as an atypical *B. melitensis* biovar 2 (12). Moreover, Bruce-ladder did not distinguish between *B. suis* biotype 1 and *Brucella* sp. BCCN84.3 (Figure 1A). However, the *Brucella* sp. BCCN84.3 strain displayed a different Suis-ladder profile departing from *B. suis* and *B. canis* strains (Figure 1B).

Conventional phenotyping did not allow ascription to any of the currently accepted *Brucella* nominal species (Tables 1, 2). However, the *Brucella* sp. BCCN84.3 fatty acid methyl esters profile suggested a different taxonomical rank (Figure 2). Likewise, plus-minus real-time PCR analysis using DNA from *Brucella* sp. BCCN84.3 was positive for the *Brucella* genus and *B. suis*. HRM-PCR analysis using specific primers for *B. canis* (Figure 3A) or *B. melitensis* (Figure 3B) showed that the profile of the BCCN84.3 strain was unique as compared to classical *Brucella* species.

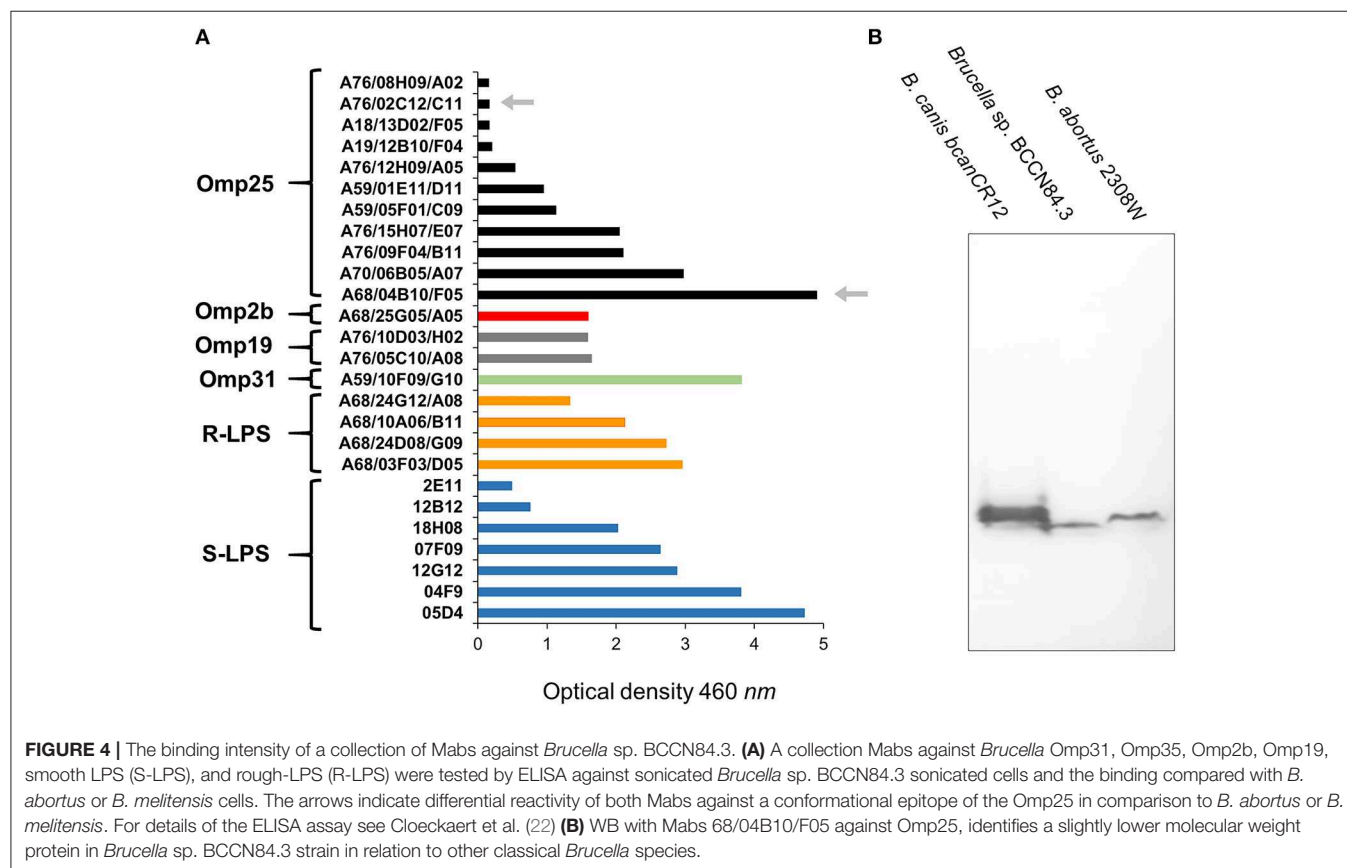
Following previous experiments (22, 45, 46), no significant differences in bindings against *Brucella* sp. BCCN84.3 rough-LPS, smooth-LPS, Omp2b, Omp19, and Omp31 were detected by ELISA (Figure 4A). In contrast, when compared with other brucellae (46), a distinct profile against the *Brucella* sp. BCCN84.3 Omp25 was attained (Figure 4A). Mab A68/04B10/F05 against the Omp25 conformational epitope reacted with *Brucella* sp. BCCN84.3, the Mab A76/02C12/C11 (also directed against a conformational epitope, 43) reaction was negative. A slightly lower molecular weight of the Omp25

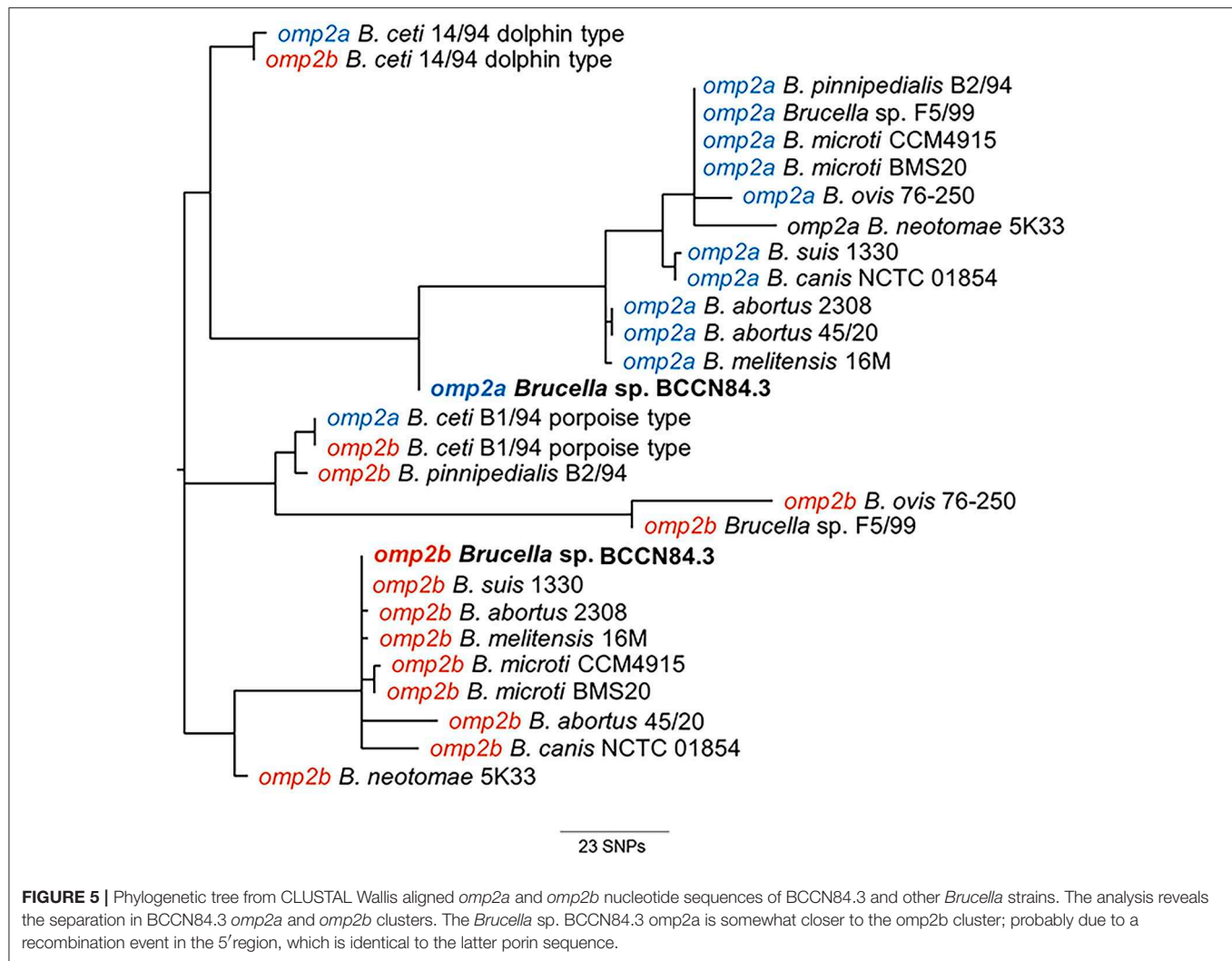
was identified in the *Brucella* sp. BCCN84.3, as compared to the *B. canis* and *B. abortus* counterparts (Figure 4B). This pattern agrees with the length of *omp25* (BAW_10696 locus), which is slightly shorter than other *omp25* genes of classical *Brucella* species.

Phylogenetic analysis of the *Brucella* sp. BCCN84.3 porin sequences showed a separation in the *omp2a* and *omp2b* corresponding clusters (Figure 5). However, the *Brucella* sp. BCCN84.3 *omp2a* was somewhat closer to the *omp2b* cluster, due to a putative recombination event in a region close to the 5', which is identical to the porin sequence of the latter (47).

The *Brucella* sp. BCCN84.3 formed a distinct branch in relation to other species, as revealed by the MLVA16 analysis (Figure 6). This result is in agreement with a previous analysis, using a somewhat different MLVA strategy (48). WGS demonstrated that the overall genomic structure of the *Brucella* sp. BCCN84.3 isolate corresponds to a new species of classical brucellae, with a size of 3.26 Mb. Parallel sequencing of the strain conserved in the BCCN collection (named *Brucella* sp. BCCN84.3) confirmed the stability of the genome. When both WGS were compared, no deletions or insertions were found between the strains and, only three SNPs were detected at intergenic regions.

As other classical brucellae, *Brucella* sp. BCCN84.3 presents two chromosomes with no plasmids, no major recent recombination events (Figure 7) and a similar number of anomalous regions (Figure 8). The genes encoding for





virulence factors such as smooth type LPS, VirB operon, Bac, cyclic glucans, flagellum-like, and BvrR/BvrS system are conserved (**Supplementary Data Sheet 1**). The *B. canis* genomic island GI_{FeGSH} coding for iron uptake enzymes and parts of the glutathione pathway (49) is not present in the *Brucella* sp. BCCN84.3. Putative genes in loci BAW_10265 coding for the TIR domain-containing protein BtpA claimed to be a VirB effector of the type IV secretion system and to modulate microtubule dynamics (50), and for putative integrases (BAW_10237; BAW_10274) are also absent. The *manBOAg* (BAW_10538) putatively involved in the synthesis of mannose of the LPS core (51) was 48 bp shorter than the *B. melitensis* (BMEI1396) and about the same size as *B. ovis* (BOV_0540) and *B. abortus* 2308W (BAW_10538) counterparts. The number of *IS711* elements identified by southern blot ranged from 6 to 7. Due to the repetitive nature of the IS elements, determination of the exact number by WGSa on Illumina platforms was not possible.

A total of 205,055 SNPs were found among the *Brucella* genomes (**Supplementary Data Sheet 1**) and were used for phylogenetic analysis using *O. anthropi* and *O. intermedium*

cluster as an outgroup. The general topology of the SNPs based tree was consistent with previous studies (1). *Brucella* sp. BCCN84.3 showed 7,281 polymorphic sites as compared to *B. suis* 1330, of those 5,911 were located in coding regions with a dN/dS ratio of 0.54 (p -value = 0.00). This shows a compact cluster harboring classical *Brucella* species and a more dispersed clade harboring the BO group (**Figure 9**). Within the classical cluster, *Brucella* sp. BCCN84.3 branches alone (**Figure 9**). This branching order does not fully agree with the classical MLVA16 dispersion. *In silico* identical matches of the 9 loci included in the MLST-9 profile were not able to classify the *B. abortus* sp. BCCN84.3 into a sequence type. The 21 loci MLST profile did not provide more information, 20 loci showed identical match, except for the *ddlA* locus, that partially matched to the allele 26, so no further typing was achieved by this scheme.

DISCUSSION

Canine brucellosis, caused by *B. canis*, is difficult to diagnose by serological assays due to the extensive cross-reaction of antigens with smooth brucellae (52, 53). The unambiguous diagnosis of

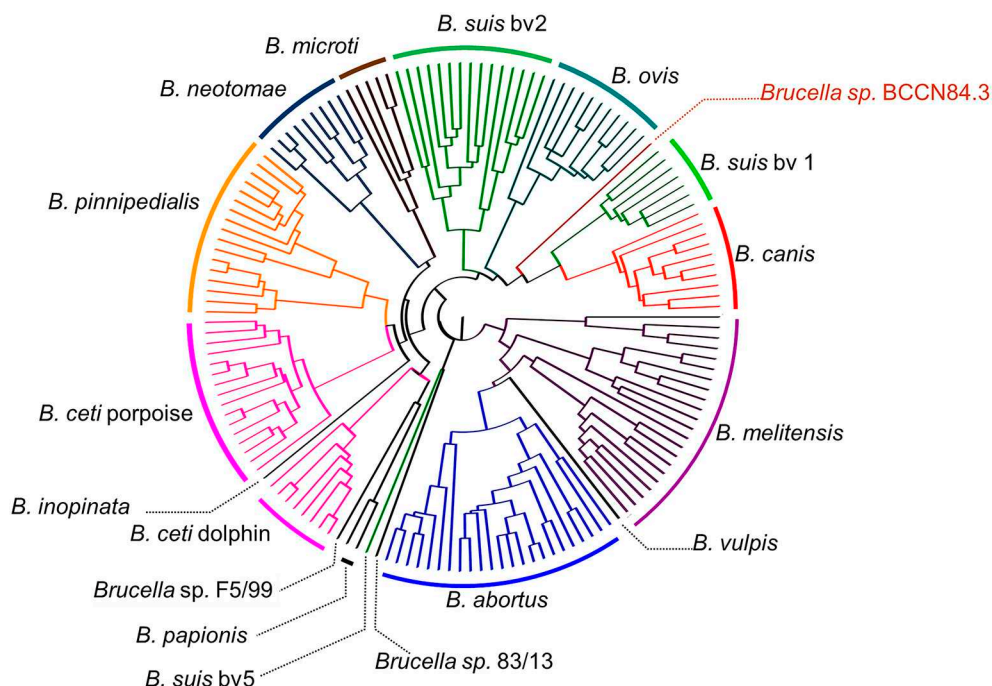


FIGURE 6 | Dendrogram based on MLVA16 analysis of *Brucella* species and strains representatives. The *Brucella* sp. BCCN84.3 showed a MLVA16 profile different from that of the classical smooth *Brucella* species; consistent with a previous report using a different MLVA strategy (48). MLVA-NET for *Brucella*. MLVA web service, CNRS. <http://microbesgenotyping.i2bc.paris-saclay.fr/> (accessed 21 December, 2017).

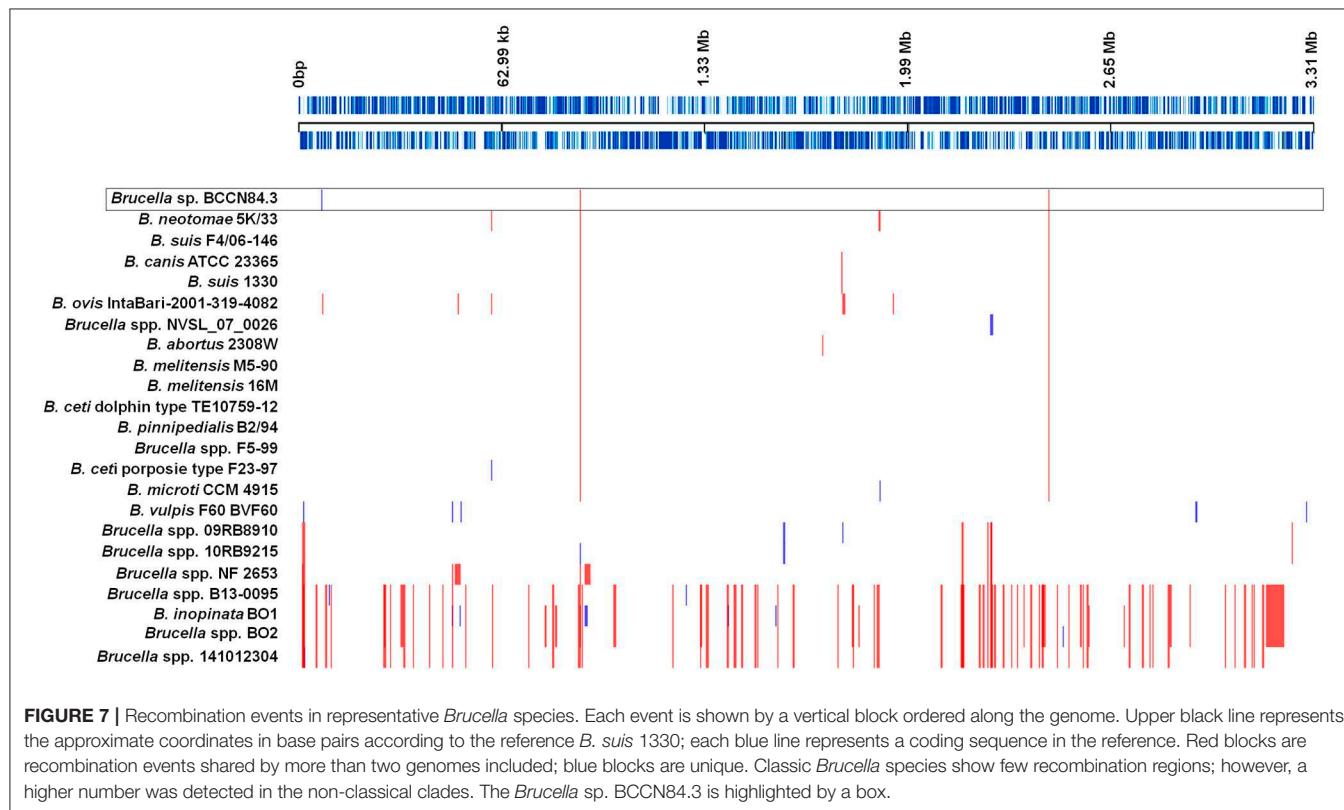
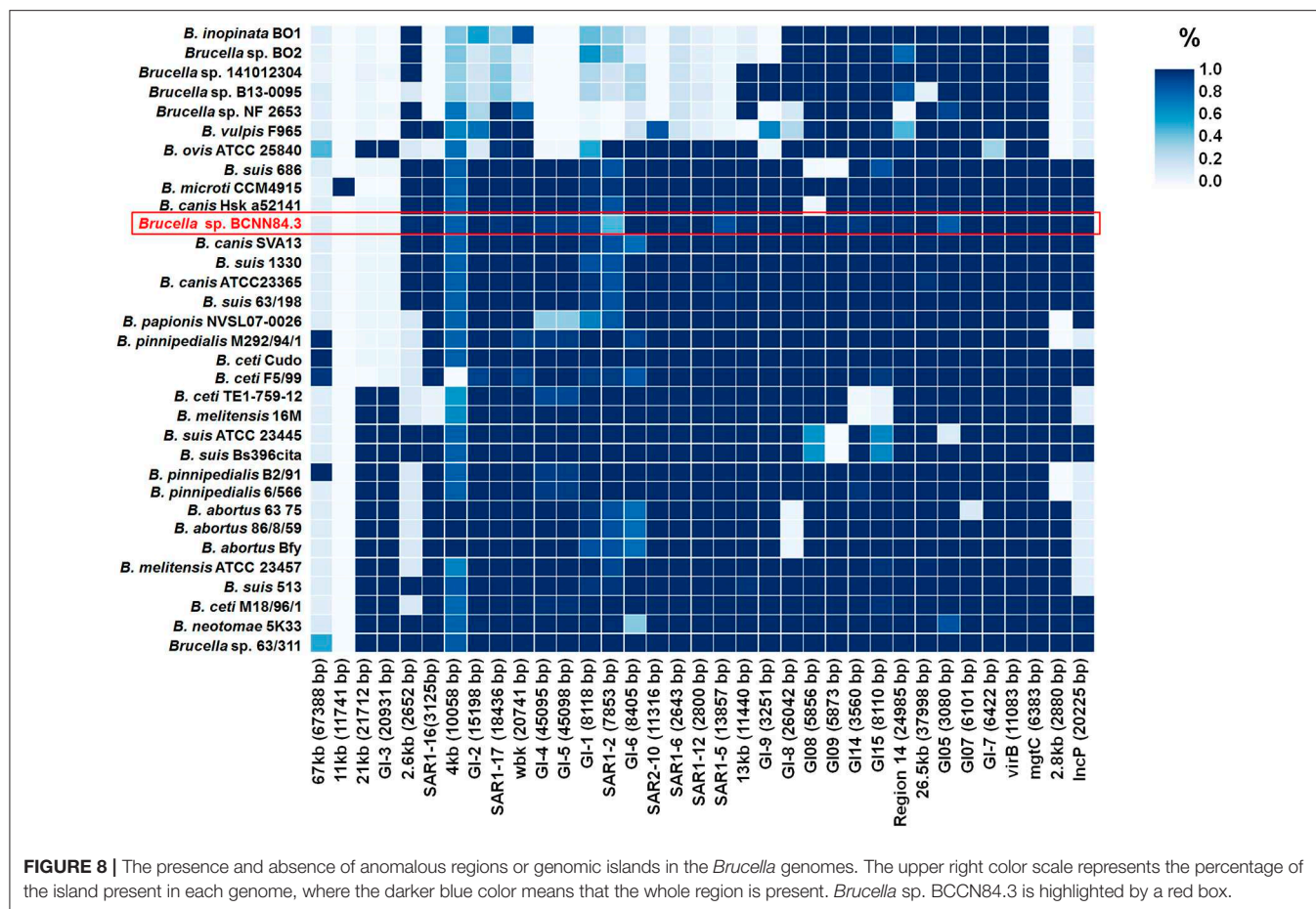


FIGURE 7 | Recombination events in representative *Brucella* species. Each event is shown by a vertical block ordered along the genome. Upper black line represents the approximate coordinates in base pairs according to the reference *B. suis* 1330; each blue line represents a coding sequence in the reference. Red blocks are recombination events shared by more than two genomes included; blue blocks are unique. Classic *Brucella* species show few recombination regions; however, a higher number was detected in the non-classical clades. The *Brucella* sp. BCCN84.3 is highlighted by a box.

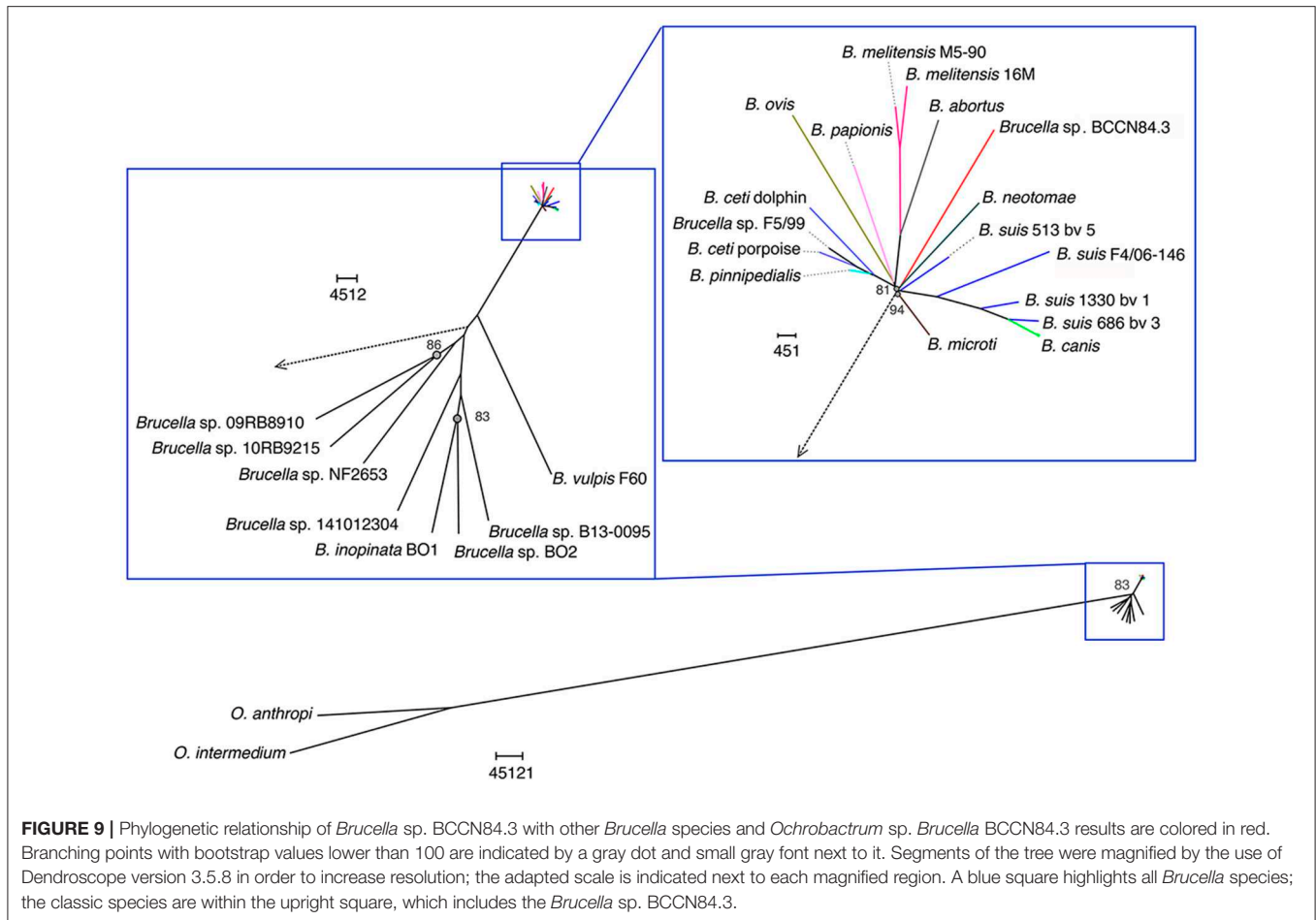


B. canis infections is just carried out after the isolation and identification of the bacterium (14) or molecular typing (26, 54). In contrast, when positive serological reactions against smooth brucellae arise in dogs presenting clinical signs of brucellosis, the presumptive diagnosis seems straightforward and commonly attributed to *B. melitensis*, *B. abortus* or *B. suis* (55–59). However, a detailed identification of the smooth *Brucella* strains isolated from dogs is seldom performed.

We were unable to trace the source of the Saint Bernard dog infection. The dog was imported as a puppy from the United States to Costa Rica. Whether the infection remained latent or it was acquired *de novo* in Costa Rica, is unknown. This is not trivial since there are several reports describing “atypical *B. suis* strains” isolated from dogs in different countries, including in the United States. For instance, in the same year as the *Brucella* sp. BCCN84.3 was isolated, a collection of “atypical *B. suis*” strains, which were also unusually resistant to fuchsin, were described in various countries (60). A new *B. suis* biovar was suggested for these atypical strains, some of them isolated from dogs and humans. Likewise, in the same year, an “atypical *B. suis* biotype 1” was also isolated in Brazil, from the testes of a dog suffering orchitis (61). In a survey carried out in 674 dogs in Georgia, United States, it was established that nine dogs presented positive serological reactions against

smooth *Brucella* antigens (58). *Brucella* organisms were isolated from the canine testes displaying necrotizing, suppurative epididymitis and orchitis. After conventional biochemical assays and 16SrRNA sequencing, the bacterial strains were assigned to the “*B. suis*” group. Unfortunately, these latter isolates were destroyed, precluding any further detailed characterization. More recently, several dogs were reported to be infected with “*B. suis*” in Australia; even though not all dogs were in contact with wild boars (62). In all these studies the bacterial strains were identified by conventional methods or rRNA PCR analysis; though, none of these methods are capable to unambiguously discern among the various *Brucella* classical species (63). The initial bacteriological characterization of the *Brucella* sp. BCCN84.3 was also misleading. It was only after genomic analyses that it became clear that the strain belonged to a new taxonomic entity.

From the genomic perspective, the *Brucella* sp. BCCN84.3 is a new taxonomical entity, since it departs phylogenetically from other strains, being the closest relative *B. neotomae* but distinct from this species. The total number of SNPs between *Brucella* sp. BCCN84.3 and *B. suis* 1330 (7281 SNPs) is bigger than the number between *B. suis* and *B. abortus* (6790 SNPs), two well-recognized species. It is also closer to the number that separates *B. ovis* st. IntaBari-2001-319-4082 from *B. suis*



st. 1330 (7499 SNPs). Considering the zoonotic potential of *Brucella* species, a correct identification by molecular methods is becoming mandatory. Moreover, in the light of distinct host preferences (64) and differences in WGS (1), the various *B. suis* strains need to be taxonomically reevaluated, since they seem to represent a collection of different *Brucella* species. In particular *B. suis* biovar 5 isolated from rodents which branches closer to *B. microti* (4) and the two clusters composed, on one hand by *B. suis* biovars 2 and 3, and on the other hand by *B. suis* biovars 1 and 4 (4). The problem with this latter cluster is the close phylogenetic relationship of *B. canis* with *B. suis* biovar 4 (4), which requires an idiosyncratic solution. The correct classification of *Brucella* species is particularly relevant in countries like Costa Rica, in which *B. melitensis* and *B. suis* are absent (65), or in countries in which bovine, caprine, and swine brucellosis have been eradicated from livestock, but that still have pathogenic *Brucella* infecting wildlife (66). In this regard, the differential diagnosis of the various *Brucella* species and strains is a requirement for taking the infection source.

Brucella sp. BCCN84.3 is a *species nova*. More isolates of this bacterium are necessary and additional epidemiological and biological information needs to be collected before assigning the corresponding taxonomical species name. In spite of this, and

taking into account the difficulties surrounding the debate on the *Brucella* species concept (5, 7), it is mandatory to describe the extant taxonomical entities in order to understand the dispersion and evolution of these important pathogens.

The fact that *Brucella* sp. BCCN84.3. has the ability to invade the reproductive tract of dogs, may favor the venereal transmission of this bacterium, as it the case of *B. canis* which rapidly disperse in kennel facilities. We do not know the zoonotic potential of *Brucella* sp. BCCN84.3. However, it is a smooth strain that possesses all the virulent machinery for being pathogenic for humans and other animals. Moreover, the fact that it was isolated from a domestic dog increases the zoonotic risk.

DATA AVAILABILITY

Publicly available datasets were analyzed in this study. This data can be found here: <https://www.ebi.ac.uk/ena/data/view/ERS568777>.

ETHICS STATEMENT

This is a clinical case. The dog was brought by its owner for therapy. Following the regular arrangements for hospitalization,

the owner was informed for all procedures and clinical studies and gave her written consent. All protocols and actions undertaken to diagnose the disease were under the Veterinary Hospital guidance established in 1980. The protocols used in 1984, were those approved by the Ley General de Salud N° 5395, and Disposiciones sobre Matrícula y Vacunación de Perros N° 2391.

AUTHOR CONTRIBUTIONS

EM, CG-V, and AC conceived the study. EM, CG-V, IM, NT, and JB obtained funding. EC and EM performed the isolation of the bacterium. CC-D performed fatty acid analysis. CG-V, MS-E, KB, AC, NR-V, MZ, EV-R, and MG performed genomics analyses. RC-Á, BA-A, and IM performed the LPS and lipid characterization. JB, EC, PM, and IM performed the bacteriological analysis. EM, CG-V, MS-E, AC, NR-V, NT, MG, and CC-D performed data interpretation. EM and CG-V wrote the paper. All authors read and approved the manuscript content.

FUNDING

This work was supported by FEES-CONARE, Costa Rica; Fondo Institucional de Desarrollo Académico (FIDA), Universidad Nacional; Wellcome Trust; CITA-INIA, Spain (project Bru-Epidia 291815-FP7/ERANET/ANIHWA); MINECO (AGL2014-58795-CA), and Aragon Government (Consolidated Group A14). Authors from the Sanger Institute were supported by Wellcome Trust (098051). NR-V was partially sponsored by a scholarship from the University of Costa Rica. KB was founded by a Wellcome Trust Postdoctoral Training Fellowship for

Clinicians (106690/Z/14/Z). MS-E was granted with a fellowship from SEP, Universidad de Costa Rica.

ACKNOWLEDGMENTS

We would like to thank Gordon Dougan (Sanger Institute, UK) and Esteban Chaves (CIET, Universidad de Costa Rica) for their helpful discussions. The genetic resources mentioned in this paper were accessed according to the Biodiversity Law #7788 and the Convention on Biological Diversity of Costa Rica, under the terms of respect to an equal and fair distribution of benefits among those who provided such resources under CONAGEBIO Costa Rica permit # R-028-203-OT.

SUPPLEMENTARY MATERIAL

The Supplementary Material for this article can be found online at: <https://www.frontiersin.org/articles/10.3389/fvets.2019.00175/full#supplementary-material>

Supplementary Table S1 | Control and reference *Brucella* species and strains used for typing.

Supplementary Data Sheet 1 | (i) Excel files displaying the *Brucella* strains used in MLVA16; (ii) the *Brucella* sp. BCCN84.3 WGS statistics, the metadata of WGS included in the phylogenetic reconstruction; (iii) the SNPs summary in comparison to *B. suis* 1330 as reference, (iv) the mutations found in *Brucella* sp. BCCN84.3 in genes related to virulence as compared to the indicated locus/gene name; (v) the genomic islands the comprises metadata of WGS included in the analysis and genomic islands reference information; (vi) the metadata of sequences included in the phylogenetic reconstruction using omp2a and omp2b genes, and; (vii) the retention time of the fatty acid methyl ester to construct dendrogram of **Figure 2**.

REFERENCES

- Soler-Lloréns PF, Quance CR, Lawhon SD, Stuber TP, Edwards JF, Ficht TA, et al. A *Brucella* spp. Isolate from a Pac-Man Frog (*Ceratophrys ornata*) reveals characteristics departing from classical brucellae. *Front Cell Infect Microbiol.* (2016) 6:116. doi: 10.3389/fcimb.2016.00116
- Scholz HC, Mühlendorfer K, Shilton C, Benedict S, Whatmore AM, Blom J, et al. The change of a medically important genus: worldwide occurrence of genetically diverse novel *Brucella* species in exotic frogs. *PLoS ONE.* (2016) 11:e0168872. doi: 10.1371/journal.pone.0168872
- Moreno E, Moriyón I. The genus *Brucella*. In: Dworkin M, Falkow SR, Rosenberg E, Schleifer KH, Stackebrandt E, editors. *The Prokaryotes*, Part 1, section 3.1. New York, NY: Springer-Verlag (2006). p. 315–456.
- Suárez-Esquível M, Ruiz-Villalobos N, Jiménez-Rojas C, Barquero-Calvo E, Chacón-Díaz C, Viquez-Ruiz E, et al. *Brucella neotomae* infection in humans, Costa Rica. *J Emerg Infect Dis.* (2017) 23:997–1000. doi: 10.3201/eid2306.162018
- Whatmore AM. Current understanding of the genetic diversity of *Brucella*, an expanding genus of zoonotic pathogens. *Infect Genet Evol.* (2009) 9:1168–84. doi: 10.1016/j.meegid.2009.07.001
- Zygmunt MS, Jacques I, Bernardet N, Cloeckaert A. A Lipopolysaccharide heterogeneity in the atypical group of novel emerging *Brucella* species. *Clin Vaccine Immunol.* (2012) 19:1370–3. doi: 10.1128/CI.00300-12
- Moreno E, Cloeckaert A, Moriyón I. *Brucella* evolution and taxonomy. *Vet Microbiol.* (2002) 90:209–27. doi: 10.1016/S0378-1135(02)00210-9
- Meyer ME. Inter- and intra-strain variants in the genus *Brucella*. *Dev Biol Stand.* (1984) 56:73–83.
- Zheludkov MM, Tsirelson LE. Reservoirs of *Brucella* infection in nature. *Biol Bull.* (2010) 37:709–15. doi: 10.1134/S106235901007006X
- Villalobos-Vindas JM, Amuy E, Barquero-Calvo E, Rojas N, Chacón-Díaz C, Chaves-Olarte E, et al. Brucellosis caused by the wood rat pathogen *Brucella neotomae*: two case reports. *J Med Case Rep.* (2017) 11:352. doi: 10.1186/s13256-017-1496-8
- Sequeira A, Campos E, Mendoza L, San-Román MA, Moreno E. Identificación de especies y biotipos de *Brucella* aisladas en Costa Rica. *Turrialba.* (1984) 34:525–6.
- Verger JM, Grimont F, Grimont PAD, Grayon M. *Brucella*, a monospecific genus as shown by deoxyribonucleic acid hybridization. *Int J Syst Bacteriol.* (1985) 35:292–5. doi: 10.1099/00207713-35-3-292
- Alton GG, Jones LM, Pietz DE. Laboratory techniques in brucellosis. *Monogr Ser World Health Organ.* (1975) 55:1–163.
- Carmichael LE, Kenney RM. Canine brucellosis: the clinical disease, pathogenesis, and immune response. *J Am Vet Med Assoc.* (1970) 156:1726–34.
- Bligh EG, Dyer WJ. A rapid method of total lipid extraction and purification. *Can J Biochem Physiol.* (1959) 37:911–7. doi: 10.1139/y59-099
- Palacios-Chaves L, Zúñiga-Ripa A, Gutiérrez A, Gil-Ramírez Y, Conde-Álvarez R, Moriyón I, et al. Identification and functional analysis of the cyclopropane fatty acid synthase of *Brucella abortus*. *Microbiology.* (2012) 158(Pt 4):1037–44. doi: 10.1099/mic.0.055897-0
- Isidoro-Ayza M, Ruiz-Villalobos N, Pérez L, Guzmán-Verri C, Muñoz PM, Alegre F, et al. *Brucella ceti* infection in dolphins from the Western Mediterranean sea. *BMC Vet Res.* (2014) 10:206. doi: 10.1186/s12917-014-0206-7

18. Garin-Bastuji B, Bowden RA, Dubray G, Limet JN. Sodium dodecyl sulfate-polyacrylamide gel electrophoresis and immunoblotting analysis of smooth-lipopolysaccharide heterogeneity among *Brucella* biovars related to A and M specificities. *Clin Microbiol.* (1990) 28:2169–74.
19. Tsai CM, Frasch CE. A sensitive silver stain for detecting lipopolysaccharides in polyacrylamide gels. *Anal Biochem.* (1982) 119:115–9. doi: 10.1016/0003-2697(82)90673-X
20. Aragón V, Díaz R, Moreno E, Moriyón I. Characterization of *Brucella abortus* and *Brucella melitensis* native haptens as outer membrane O-type polysaccharides independent from the smooth lipopolysaccharide. *J Bacteriol.* (1996) 178:1070–9. doi: 10.1128/jb.178.4.1070-1079.1996
21. Monreal D, Grillo MJ, González D, Marín CM, De Miguel MJ, López-Goñi I, et al. Characterization of *Brucella abortus* O-polysaccharide and core lipopolysaccharide mutants and demonstration that a complete core is required for rough vaccines to be efficient against *Brucella abortus* and *Brucella ovis* in the mouse model. *Infect Immun.* (2003) 71:3261–71. doi: 10.1128/IAI.71.6.3261-3271.2003
22. Cloeckaert A, Verger JM, Grayon M, Vizcaino N. Molecular and immunological characterization of the major outer membrane proteins of *Brucella*. *FEMS Microbiol Lett.* (1996) 145:1–8. doi: 10.1016/0378-1097(96)00373-4
23. Ramírez P, Bonilla JA, Moreno E, León P. Electrophoretic transfer of viral proteins to nitrocellulose sheets and detection with peroxidase-bound lectins and protein A. *J Immunol Methods.* (1983) 62:15–22. doi: 10.1016/0022-1759(83)90105-9
24. Freer E, Pizarro-Cerdá J, Weintraub A, Bengoechea JA, Moriyón I, Hultenby K, et al. The outer membrane of *Brucella ovis* shows increased permeability to hydrophobic probes and is more susceptible to cationic peptides than are the outer membranes of mutant rough *Brucella abortus* strains. *Infect Immun.* (1999) 67:6181–6.
25. López-Goñi I, García-Yoldi D, Marín CM, de Miguel MJ, Muñoz PM, Blasco JM, et al. Evaluation of a multiplex PCR assay (Bruce-ladder) or molecular typing of all *Brucella* species, including the vaccine strains. *J Clin Microbiol.* (2008) 46:3484–7.
26. López-Goñi I, García-Yoldi D, Marín CM, de Miguel MJ, Barquero-Calvo E, Guzmán-Verri C, et al. New bruce-ladder multiplex PCR assay for the biovar typing of *Brucella suis* and the discrimination of *Brucella suis* and *Brucella canis*. *Vet Microbiol.* (2011) 154:152–5. doi: 10.1016/j.vetmic.2011.06.035
27. Winchell JM, Wolff BJ, Tiller R, Bowen MD, Hoffmaster AR. Rapid identification and discrimination of *Brucella* isolates by use of real-time PCR and high-resolution melt analysis. *J Clin Microbiol.* (2010) 48:697–702. doi: 10.1128/JCM.02021-09
28. Maquart M, Le Flèche P, Foster G, Tryland M, Ramisse F, Dønne B, et al. MLVA-16 typing of 295 marine mammal *Brucella* isolates from different animal and geographic origins identifies 7 major groups within *Brucella ceti* and *Brucella pinnipedialis*. *BMC Microbiol.* (2009) 9:145. doi: 10.1186/1471-2180-9-145
29. Grissa I, Bouchon P, Pourcel C, Vergnaud G. On-line resources for bacterial microevolution studies using MLVA or CRISPR typing. *Biochimie.* (2008) 90:660–8. doi: 10.1016/j.biochi.2007.07.014
30. Quail MA, Kozarewa I, Smith F, Scally A, Stephens PJ, Durbin RR, et al. A large genome centre's improvements to the Illumina sequencing system. *Nat Methods.* (2009) 5:1005–10. doi: 10.1038/nmeth.1270
31. Quail MA, Otto TD, Gu Y, Harris SR, Skelly TF, McQuillan JA, et al. Optimal enzymes for amplifying sequencing libraries. *Nat Methods.* (2011) 9:10–1. doi: 10.1038/nmeth.1814
32. Zerbino DR, Birney E. Velvet: algorithms for *de novo* short read assembly using de Bruijn graphs. *Genome Res.* (2008) 18:821–9. doi: 10.1101/gr.074492.107
33. Seemann T. Prokka: rapid prokaryotic genome annotation. *Bioinformatics.* (2014) 30:2068–9. doi: 10.1093/bioinformatics/btu153
34. Whatmore AM, Koylass MS, Muchowski J, Edwards-Smallbone J, Gopaul KK, Perrett LL. Extended multilocus sequence analysis to describe the global population structure of the genus *Brucella*: phylogeography and relationship to biovars. *Front Microbiol.* (2016) 7:2049. doi: 10.3389/fmicb.2016.02049
35. Li H, Handsaker B, Wysoker A, Fennell T, Ruan J, Homer N, et al. The sequence alignment/map format and SAMtools. *Bioinformatics.* (2009) 25:2078–9. doi: 10.1093/bioinformatics/btp352
36. Page AJ, Taylor B, Delaney AJ, Soares J, Seemann T, Keane JA, et al. SNP-sites: rapid efficient extraction of SNPs from multi-FASTA alignments. *Microb Genomics.* (2016) 2:e000056. doi: 10.1099/mgen.0.000056
37. Stamatakis A. RAxML-VI-HP: maximum likelihood-based phylogenetic analyses with thousands of taxa and mixed models. *Bioinformatics.* (2006) 22:2688–90. doi: 10.1093/bioinformatics/btl446
38. Carver TJ, Rutherford KM, Berriman M, Rajandream MA, Barrell BG, Parkhill J. ACT: the Artemis Comparison Tool. *Bioinformatics.* (2005) 21:3422–3. doi: 10.1093/bioinformatics/bti553
39. Croucher NJ, Page AJ, Connor TR, Delaney AJ, Keane JA, Bentley SD, et al. Rapid phylogenetic analysis of large samples of recombinant bacterial whole genome sequences using Gubbins. *Nucleic Acids Res.* (2014) 43:e15. doi: 10.1093/nar/gku1196
40. Hadfield J, Croucher NJ, Goater RJ, Abudahab K, Aanensen DM, Harris SR. Phandango: an interactive viewer for bacterial population genomics. *Bioinformatics.* (2017) 34:292–3. doi: 10.1093/bioinformatics/btx610
41. Cloeckaert A, Bernardet N, Koylass MS, Whatmore AM, Zygmunt MS. Novel IS711 chromosomal location useful for identification of marine mammal *Brucella* genotype ST27, which is associated with zoonotic infection. *J Clin Microbiol.* (2011) 49:3954–9. doi: 10.1128/JCM.05238-11
42. Foster G, Osterman BS, Godfroid J, Jacques I, Cloeckaert A. *Brucella ceti* sp. nov. and *Brucella pinnipedialis* sp. nov. for *Brucella* strains with cetaceans and seals as their preferred hosts. *Int J Syst Evol Microbiol.* (2007) 57(Pt 11):2688–93. doi: 10.1099/ijs.0.65269-0
43. Kumar S, Stecher G, Tamura K. MEGA7: molecular evolutionary genetics analysis version 7.0 for bigger datasets. *Mol Biol Evol.* (2016) 33:1870–74. doi: 10.1093/molbev/msw054
44. Tamura K, Nei M. Estimation of the number of nucleotide substitutions in the control region of mitochondrial DNA in humans and chimpanzees. *Mol Biol Evol.* (1993) 10:512–26.
45. Cloeckaert A, Jacques I, Bowden RA, Dubray G, Limet JN. Monoclonal antibodies to *Brucella* rough lipopolysaccharide: characterization and evaluation of their protective effect against *B. abortus*. *Res Microbiol.* (1993) 144:475–844. doi: 10.1016/0923-2508(93)90055-7
46. Cloeckaert A, Verger JM, Grayon M, Zygmunt MS, Grépinet O. Nucleotide sequence and expression of the gene encoding the major 25-kilodalton outer membrane protein of *Brucella ovis*: evidence for antigenic shift, compared with other *Brucella* species, due to a deletion in the gene. *Infect Immun.* (1996) 64:2047–55.
47. Cloeckaert A, Vizcaino N, Paquet JY, Bowden RA, Elzer PH. Major outer membrane proteins of *Brucella* spp.: past, present and future. *Vet Microbiol.* (2002) 90:229–34. doi: 10.1016/S0378-1135(02)00211-0
48. Le-Flèche P, Jacques I, Grayon M, Al-Dahouk S, Bouchon P, Denoed F, et al. Evaluation and selection of tandem repeat loci for a *Brucella* MLVA typing assay. *BMC Microbiol.* (2006) 6:9. doi: 10.1186/1471-2180-6-9
49. Wahab T, Skarp A, Båverud V, Kaden R. GIFE-GSH: a new genomic island might explain the differences in *Brucella* virulence. *Open J Anim Sci.* (2017) 7:141–8. doi: 10.4236/ojas.2017.72012
50. Felix C, Kaplan-Türköz B, Ranaldi S, Koelblen T, Terradot L, O'Callaghan D, et al. The *Brucella* TIR domain containing proteins BtpA and BtpB have a structural WxxxE motif important for protection against microtubule depolymerisation. *Cell Commun Signal.* (2014) 12:53. doi: 10.1186/s12964-014-0053-y
51. González D, Grillo MJ, De Miguel MJ, Ali T, Arce-Gorvel V, Delrue RM, et al. Brucellosis vaccines: assessment of *Brucella melitensis* lipopolysaccharide rough mutants defective in core and O-polysaccharide synthesis and export. *PLoS ONE.* (2008) 3:e2760. doi: 10.1371/journal.pone.0002760
52. Diaz R, Jones LM, Wilson JB. Antigenic relationship of the gram-negative organism causing canine abortion to smooth and rough brucellae. *J Bacteriol.* (1968) 95:618–24.
53. Moreno E, Jones LM, Berman DT. Immunochemical characterization of rough *Brucella* lipopolysaccharides. *Infect Immun.* (1984) 43:779–82.
54. Corrente M, Franchini D, Decaro N, Greco G, D'Abramo M, Greco MF, et al. Detection of *Brucella canis* in a dog in Italy. *New Microbiol.* (2010) 33:337–41.

55. Bicknell SR, Bell RA. *Brucella abortus* in the bitch: subclinical infection associated with urinary excretion. *J Hyg.* (1979) 82:249–54. doi: 10.1017/S0022172400025663
56. Forbes LB. *Brucella abortus* infection in 14 farm dogs. *J Am Vet Med Assoc.* (1990) 96:911–6.
57. Islamov RZ. Transmission of *Brucella melitensis* to the offspring of dogs. *Veterinarya.* (1973) 12:62.
58. Ramamoorthy S, Woldemeskel M, Ligett A, Snider R, Cobb R, and Rajeev S. *Brucella suis* infection in dogs, Georgia, USA. *Emerg Infect Dis.* (2011) 17:2386–7. doi: 10.3201/eid1712.111127
59. Wareth G, Melzer F, El-Diasty M, Schmooch G, Elbauomy E, Abdel-Hamid N, et al. Isolation of *Brucella abortus* from a dog and a cat confirms their iological role in re-emergence and dissemination of bovine brucellosis on dairy farms. *Transbound Emerg Dis.* (2016). 64:e27–30. doi: 10.1111/tbed.12535
60. Corbel MJ, Thomas EL, Garcia-Carillo C. Taxonomic studies on some atypical trains of *Brucella suis*. *Br Vet J.* (1984) 140:34–43. doi: 10.1016/0007-1935(84)90055-1
61. Correa WM, Correa CNM, Iamaguti P. Canine brucellosis caused by *Brucella suis* iotype 1 atypical. *Arq Bras Med Vet Zootec.* (1984) 36:397–406.
62. Mor SM, Wiethoelter AK, Lee A, Moloney B, James DR, Malik R. Emergence of *Brucella suis* in dogs in New South Wales, Australia: clinical findings and implications or zoonotic transmission. *BMC Vet Res.* (2016) 12:199. doi: 10.1186/s12917-016-0835-0
63. Moreno E. Genome evolution within the alpha Proteobacteria: why do some acteria not possess plasmids and others exhibit more than one different chromosome? *FEMS Microbiol Rev.* (1998) 22:255–75. doi: 10.1016/S0168-6445(98)00016-3
64. Alton GG. *Brucella suis*. in: Nielsen K, Duncan B, editors. *Animal Brucellosis*. Boca Raton, FL: CRC Press, Inc (1990). pp. 244–422.
65. Hernández-Mora G, Bonilla-Montoya R, Barrantes-Granados O, Esquivel-Suárez A, Montero-Caballero D, González-Barrientos R, et al. Brucellosis in mammals of Costa Rica: an epidemiological survey. *PLoS ONE.* (2017) 12:e0182644. doi: 10.1371/journal.pone.0182644
66. Mick V, Le Carrou G, Corde Y, Game Y, Jay M, Garin-Bastuji B. *Brucella melitensis* in France: persistence in wildlife and probable spillover from Alpine ibex to omestic animals. *PLoS ONE.* (2014) 9:e94168. doi: 10.1371/journal.pone.0094168

Conflict of Interest Statement: The authors declare that the research was conducted in the absence of any commercial or financial relationships that could be construed as a potential conflict of interest.

Copyright © 2019 Guzmán-Verri, Suárez-Esquivel, Ruíz-Villalobos, Zygmunt, Gonnet, Campos, Viquez-Ruiz, Chacón-Díaz, Aragón-Aranda, Conde-Álvarez, Moriyón, Blasco, Muñoz, Baker, Thomson, Cloeckert and Moreno. This is an open-access article distributed under the terms of the Creative Commons Attribution License (CC BY). The use, distribution or reproduction in other forums is permitted, provided the original author(s) and the copyright owner(s) are credited and that the original publication in this journal is cited, in accordance with accepted academic practice. No use, distribution or reproduction is permitted which does not comply with these terms.



Genetic Diversity of *Brucella melitensis* in Kazakhstan in Relation to World-Wide Diversity

Elena Shevtsova¹, Gilles Vergnaud², Alexandr Shevtsov^{1*}, Alexandr Shustov¹, Kalysh Berdimuratova¹, Kasim Mukanov¹, Marat Syzdykov³, Andrey Kuznetsov³, Larissa Lukhnova³, Uinkul Izbanova³, Maxim Filipenko^{1,4,5} and Yerlan Ramankulov^{1,6}

¹ National Center for Biotechnology, Nur-Sultan, Kazakhstan, ² Institute for Integrative Biology of the Cell (I2BC), CEA, CNRS, Univ. Paris-Sud, Université Paris-Saclay, Gif-sur-Yvette, France, ³ Kazakh Scientific Center for Quarantine and Zoonotic Diseases, Almaty, Kazakhstan, ⁴ Institute of Chemical Biology and Fundamental Medicine, Novosibirsk, Russia, ⁵ Synthetic Biology Department, Novosibirsk State University, Novosibirsk, Russia, ⁶ School of Science and Technology, Nazarbayev University, Nur-Sultan, Kazakhstan

OPEN ACCESS

Edited by:

Axel Cloeckaert,
Institut National de la Recherche
Agronomique (INRA), France

Reviewed by:

Herbert Tomaso,
Friedrich-Loeffler-Institut, Germany
Jacques Xavier Godfroid,
UiT The Arctic University of Norway,
Norway

*Correspondence:

Alexandr Shevtsov
ncbshevtsov@gmail.com

Specialty section:

This article was submitted to
Infectious Diseases,
a section of the journal
Frontiers in Microbiology

Received: 03 March 2019

Accepted: 31 July 2019

Published: 13 August 2019

Citation:

Shevtsova E, Vergnaud G, Shevtsov A, Shustov A, Berdimuratova K, Mukanov K, Syzdykov M, Kuznetsov A, Lukhnova L, Izbanova U, Filipenko M and Ramankulov Y (2019) Genetic Diversity of *Brucella melitensis* in Kazakhstan in Relation to World-Wide Diversity. *Front. Microbiol.* 10:1897. doi: 10.3389/fmicb.2019.01897

We describe the genetic diversity of 1327 *Brucella* strains from human patients in Kazakhstan using multiple-locus variable-number tandem repeat (VNTR) analysis (MLVA). All strains were assigned to the *Brucella melitensis* East Mediterranean group and clustered into 16 MLVA11 genotypes, nine of which are reported for the first time. MLVA11 genotype 116 predominates (86.8%) and is present all over Kazakhstan indicating existence and temporary preservation of a “founder effect” among *B. melitensis* strains circulating in Central Eurasia. The diversity pattern observed in humans is highly similar to the pattern previously reported in animals. The diversity observed by MLVA suggested that the epidemiological status of brucellosis in Kazakhstan is the result of the introduction of a few lineages, which have subsequently diversified at the most unstable tandem repeat loci. This investigation will allow to select the most relevant strains for testing these hypotheses via whole genome sequencing and to subsequently adjust the genotyping scheme to the Kazakhstan epidemiological situation.

Keywords: *Brucella melitensis*, Kazakhstan, genotyping, genetic diversity, multiple-locus variable-number tandem repeat (VNTR) analysis (MLVA)

INTRODUCTION

Brucellosis is a zoonotic infection affecting many mammals including marine species as well as humans. Infection is endemic in many countries of the world, the etiological agent being a Gram-negative bacteria of the genus *Brucella*. Among the 12 species currently proposed in this genus, *Brucella melitensis*, *B. abortus*, and *B. suis* are highly dangerous for humans and cause disease with severe complications and chronic process (Meyer, 1990; Godfroid et al., 2011). Rare cases of infection of people with other *Brucella* species are also recorded (Ficht, 2010). Despite its low mortality rates, brucellosis is a very important public health problem in Kazakhstan. Husbandry suffer direct economic losses from brucellosis due to reduced productivity, culling of livestock and costs of associated measures. In spite of the control strategies, brucellosis remains a major economic problem for agriculture, with an annual direct cost of more than \$45 million and a social problem in health care with an average disability-adjusted life year of 0.5 per case (Charypkhan et al., 2019).

In addition, aerosol transmission and low infectious doses (10–100 bacteria) potentially allow using *Brucella* in acts of bioterrorism (Pappas et al., 2006b; Neubauer, 2010; Doganay and Doganay, 2013).

Control of animal infections is essential to prevent human infections. In developed countries, epidemiological measures were successfully undertaken to eliminate brucellosis in domestic animals, resulting in that all human cases are recorded among migrants, or associated with traveling to endemic areas, consumption of imported products, and in rare cases contacts with wild animals (Gwida et al., 2012). On the contrary, in many countries of the Mediterranean region, Southern and Central America, Africa, Asia, Arabian Peninsula, Indian subcontinent, Eastern Europe, and Middle East, the brucellosis epidemiological situation remains complex allowing to describe it as a continuing epidemic (Nicoletti, 2010).

Given the zoonotic nature of brucellosis, identification of sources of the infection and tracking of transmission paths are of high importance for epidemiologic surveillance. Reliable discrimination among *Brucella* species and biovars are important for treatment, due to differences in pathogenicity between various *Brucella*. DNA-based genotyping methods are preferred because molecular methods minimize the risks of infection of laboratory personnel and phenotypic methods have a much lower discriminatory power. For *Brucella*, a number of genotyping methods have been proposed including AMOS-PCR, Bruce-ladder, tandem-repeats polymorphism [multiple-locus VNTR analysis (MLVA)] and whole genome SNP analysis (wgSNP). wgSNP analysis is by far the most powerful and robust approach, but its current cost does not allow yet to use it as a routine first line assay (Ledwaba et al., 2019). MLVA typing is a compromise in terms of discriminatory power, cost and speed to provide an overview of genetic diversity and assist the selection of strains for whole genome sequencing (Scholz and Vergnaud, 2013). Availability of freely accessible databases with MLVA genotypes allow to track the spreading of specific *Brucella* biovars globally (Kattar et al., 2008; Kilic et al., 2011; Ferreira et al., 2012; Vergnaud et al., 2018). Fundamental for this work is genotyping and consolidation of data from all endemic regions.

Kazakhstan is located in the center of Eurasia. It covers a territory of 2.725 million km² for 18 million inhabitants. The country shares land borders with Russia, China, Kyrgyzstan, Uzbekistan, Turkmenistan. With regard to brucellosis, Kazakhstan is a hyperendemic area considering the very high incidence rates in the human population and farm animals (Pappas et al., 2006a). According to evaluations in the Former Soviet Union (FSU), more than 40% of newly diagnosed brucellosis cases are from Kazakhstan (Studentsov, 1975). From 1999 to 2016, 38,557 new cases of human brucellosis were recorded, with annual counts of cases ranging from 1443 (2014) to 3596 (2004) (Syzydykov et al., 2013; Shevtsova et al., 2016; Daugaliyeva et al., 2018). Within these 18 years, the majority of cases (89.5%) occurred in southern and eastern Kazakhstan (Almaty, Zhambyl, Kyzylorda, East-Kazakhstan, and South-Kazakhstan regions). 75% of the cases of newly diagnosed brucellosis were in the age group 10–39 years, and 85.8% were rural residents. Most strains recovered from patients

were identified as *B. melitensis* (Mizanbayeva et al., 2009). The epidemiological situation correlates with occurrence of brucellosis in small ruminants, e.g., the mentioned geographic regions hold more than 70% of all identified seropositive animals among small ruminants (data collected during 2008–2015) (Espembetov et al., 2017). From 2006 to 2015, the average level of seropositive small ruminants ranged from 0.15 to 0.3% with an increase in 2008 (0.65%) and 2013 (0.5%). The fluctuation from 0.01 to 2.5% of the percentage of seropositive animals at the district level is uncorrelated with the level of infection in humans (Daugaliyeva et al., 2018; Charypkhan et al., 2019). In cattle, the incidence of seropositive animals varied from 0.3 in 2006 to 0.6% in 2013–2015. The high incidence of brucellosis reported in cattle during 2009–2011 (1.85%) is most probably an artifact originating from a change in diagnostic procedures used in Kazakhstan. During this period, all cattle was screened using only an indirect enzyme-linked immunosorbent assay (iELISA) and classical methods such as the rose Bengal test (RBT), serum agglutination test (SAT), and complement fixation test (CFT) were not used for confirmation of the brucellosis diagnosis, until the low specificity of the iELISA became evident. Starting from 2012, the classical methods were again made compulsory for confirmation of brucellosis diagnosis which resulted in reduction of the reported incidence (Espembetov et al., 2017). In addition to the main reservoir hosts, brucellosis caused by *B. melitensis* or *B. abortus* is registered in camels, horses, and dogs (Zheludkov and Tsirelson, 2010). *Brucella* antibodies have been detected in more than 60 wild mammals (Shevtsova et al., 2016).

The high morbidity and large territory of Kazakhstan make it essential to describe the genetic diversity and distribution of genotypes among circulating strains of *Brucella* in order to support efforts for disease control. Previous reports have described the genetic diversity of *Brucella* isolated from animals in Kazakhstan (Shevtsov et al., 2015; Shevtsova et al., 2016; Daugaliyeva et al., 2018; Yespembetov et al., 2019). The purpose of the present study was to determine the genetic diversity of the strains infecting humans at the whole country scale.

MATERIALS AND METHODS

Ethics Statement

A formal institutional ethical review process and approval was not required for this study as all strains investigated here were collected as a part of standard clinical investigation of patients with suspected brucellosis and the strains were anonymized. All *Brucella* strains used in this study were obtained from the collection maintained by the Masgut Aykimbayev Kazakh Scientific Center of Quarantine and Zoonotic Diseases (KSCQZD) in accordance to Kazakhstan regulations.

Clinical Strains Characterization

A total of 1383 *Brucella* strains were isolated from patients seropositive to brucellosis antigen (agglutination test 1:200 and higher) during 2015–2016 in 13 regional infectious diseases hospitals. The hemocultures were produced by the two-phase method proposed by Castaneda (Castaneda, 1947;

Yagupsky, 1999). All strains were Gram negative, agglutinated with polyvalent brucellosis serum, had oxidase and catalase activity, did not produce H₂S, synthesized urease, and were capable of growing in plain atmospheric conditions. Biotyping was performed by KSCQZD by routine test (Al Dahouk et al., 2003).

DNA Preparation, Genotyping, and Data Analysis

Bacterial culture was scrapped from the surface of the solid agar medium, resuspended in 500 µl Tris 10 mM EDTA 1 mM pH 8 (TE) buffer and inactivated by adding an equal volume of chloroform. DNA was isolated using the QIAamp DNA Mini Kit (Qiagen, United States). Species identification was confirmed

by the multiplex PCR “Bruce-ladder” assay (Lopez-Goni et al., 2008). The 16S rDNA fragment was sequenced to confirm taxonomic identification of the genus and to exclude presence of extraneous microflora.

Markers proposed by Le Flèche et al. (2006) and Al Dahouk et al. (2007) were used for MLVA. The 16 loci are commonly divided into three panels. The first panel (also called MLVA8) consists of the eight tandem repeat loci with the largest repeat units, Bruce06, Bruce08, Bruce12, Bruce42, Bruce43, Bruce45, and Bruce55. The eight other tandem repeats have smaller repeat units up to eight base-pairs. The second panel (panel 2A) includes Bruce18, Bruce19, and Bruce21. Panel 2B includes the last five loci: Bruce04, Bruce07, Bruce09, Bruce16, and Bruce30. The combination of panels MLVA8 and 2A is called MLVA11, while the combination of all three panels (16 loci) is designated MLVA16. The MLVA11 panel allows for species identification in the *Brucella* genus and grouping of strains in accordance to the global geographic distribution. The panel 2B loci are highly discriminatory and their combination with MLVA11 is used in tracking local outbreaks. New variable-number tandem repeat (VNTR) alleles were confirmed by sequencing the PCR product.

Primers for multiplex PCR and their combinations were used as previously described (Garofolo et al., 2013; Shevtsov et al., 2015). PCR amplification products were diluted 1/70, and aliquots (3 µl) of the diluted samples were run on a capillary electrophoresis machine (DNA Analyzer 3730xl, Applied Biosystems, Japan), using the POP7 polymer and LIZ 1200 size standard. Size analysis of VNTR repeats was performed using GeneMapper 4.1 (Applied Biosystems).

To visualize clustering relations, maximum parsimony analysis dendrograms were constructed using BioNumerics 7.6 (Applied Maths, Sint-Martens-Latem, Belgium). The Hunter and Gaston diversity index (HGDI) was used to describe discriminatory capacity of each locus, as well as of the panels MLVA8, MLVA11, and MLVA16 (Hunter and Gaston, 1988). Computations were performed using the Internet resources at www.hpa-bioinfotools.org.uk/cgi-bin/DICI/DICI.pl. Geographic coordinates (longitude, latitude) were deduced from available geographic origin data using the BioNumerics geographical plugin. The geographic location map was drawn using QGIS 3.4.8-Madeira (QGIS Geographic Information System. Open Source Geospatial Foundation)¹.

TABLE 1 | Hunter and Gaston diversity index (HGDI) for loci and MLVA panels for 1327 *B. melitensis* strains from human patients in Kazakhstan.

Locus	Diversity index	Confidence interval	Number of genotypes observed	Max(pi)*
Bruce06	0.000	0.000–0.006	1	1.000
Bruce08	0.025	0.020–0.031	3	0.987
Bruce11	0.000	0.000–0.006	1	1.000
Bruce12	0.000	0.000–0.006	1	1.000
Bruce42	0.000	0.000–0.006	1	1.000
Bruce43	0.142	0.130–0.153	4	0.924
Bruce45	0.000	0.000–0.006	1	1.000
Bruce55	0.000	0.000–0.006	1	1.000
MLVA8	0.163	0.150–0.175	7	0.913
Bruce18	0.049	0.041–0.056	3	0.975
Bruce19	0.052	0.044–0.059	6	0.974
Bruce21	0.000	0.000–0.006	1	1.000
MLVA11	0.242	0.228–0.256	16	0.868
Bruce04	0.770	0.764–0.775	11	0.349
Bruce07	0.292	0.277–0.306	6	0.835
Bruce09	0.016	0.012–0.021	4	0.992
Bruce16	0.786	0.782–0.791	12	0.320
Bruce30	0.632	0.624–0.640	6	0.503
MLVA16	0.989	0.988–0.989	310	0.050

*Max(pi) = fraction of samples that have the most frequent repeat number in this locus (range 0.0–1.0).

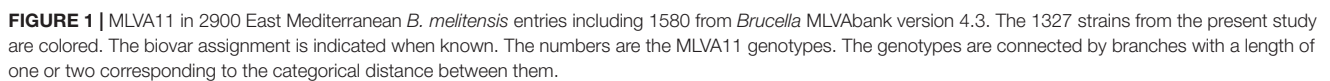
TABLE 2 | HGDI for the panel 2B for East Mediterranean *B. melitensis* from various countries.

Country	Bruce04	Bruce07	Bruce09	Bruce16	Bruce30	Number of strains
Kazakhstan	0.770	0.292	0.016	0.786	0.632	1327
France	0.851	0.720	0.858	0.880	0.540	479
Spain	0.807	0.778	0.371	0.814	0.680	403
China	0.750	0.114	0.109	0.834	0.754	303
Turkey	0.762	0.487	0.195	0.782	0.737	233
Italy	0.798	0.784	0.894	0.817	0.070	225
Portugal	0.760	0.737	0.321	0.777	0.451	149
Peru	0	0.164	0.689	0.18	0	114
Greece	0.774	0.279	0.57	0.778	0.75	78

RESULTS

A total of 1383 strains *Brucella* collected from 13 regions of Kazakhstan were studied. All strains could be assigned to the *Brucella* genus based on analysis of a fragment of the nucleotide sequence of 16S rDNA and to *B. melitensis* according to the Bruce-ladder profile. The biovar was established for 500 strains. Ninety-five (19%) were assigned to biovar 1, six (1.2%) to biovar 2 and 399 (79.8%) were assigned to biovar 3 (**Supplementary Table S1**). The 16 VNTR loci constituting the MLVA assay were successfully amplified in all DNAs. Five samples showed a mixed

¹<http://qgis.org>



alleles (106 bp, called 17 and 208 bp called 51) were observed in three strains (NCB#h-3378, NCB#h-3379, and NCB#h-3409) and one strain (NCB#h-2223), respectively. These new alleles were confirmed by sequencing of the PCR products.

The HGDI index of the 16 VNTR loci and of panels MLVA8, MLVA11, MLVA16 are indicated in **Table 1**. In panel MLVA11, only 5 among the 11 loci were polymorphic in the present collection. In panel 2B, all five loci were variable, with loci Bruce07 and Bruce09 being the least variable. The HGDI for MLVA8 and MLVA11 were 0.163 and 0.242, respectively. The HGDI for MLVA16 was 0.989. In countries with more than

TABLE 3 | Distribution of genotypes by MLVA8 and MLVA11 in Kazakhstan.

MLVA11 profile	MLVA8 genotype (number of strains/%)	MLVA11 genotype (number of isolates/%)
1-5-3-13-2-2-3-2-4-41-8*	42 (1211/91.25)	116(1152/86.8)
1-5-3-13-2-2-3-2-5-41-8		180(29/2.18)
1-5-3-13-2-2-3-2-4-46-8		297(20/1.51)
1-5-3-13-2-2-3-2-3-41-8		342(2/0.15)
1-5-3-13-2-2-3-2-4-17-8		388(4/0.3)†
1-5-3-13-2-2-3-2-4-36-8		389/(3/0.23)†
1-5-3-13-2-2-3-2-4-51-8		393(1/0.15)†
1-5-3-13-2-3-3-2-4-41-8	63 (89/6.71)	111(80/6.03)
1-5-3-13-2-3-3-2-4-46-8		386(6/0.45)†
1-5-3-13-2-3-3-2-4-36-8		392(2/0.15)†
1-5-3-13-2-3-3-2-4-43-8		394(1/0.15)†
1-3-3-13-2-2-3-2-4-41-8	62 (11/0.83)	114(11/0.83)
1-5-3-13-2-1-3-2-4-41-8	114 (7/0.53)	291(7/0.53)
1-4-3-13-2-2-3-2-4-41-8	115 (4/0.3)	387(4/0.3)†
1-5-3-13-2-4-3-2-4-41-8	196 (3/0.23) †	390(3/0.23)†
1-4-3-13-2-3-3-2-4-41-8	197(2/0.15) †	391(2/0.15)†

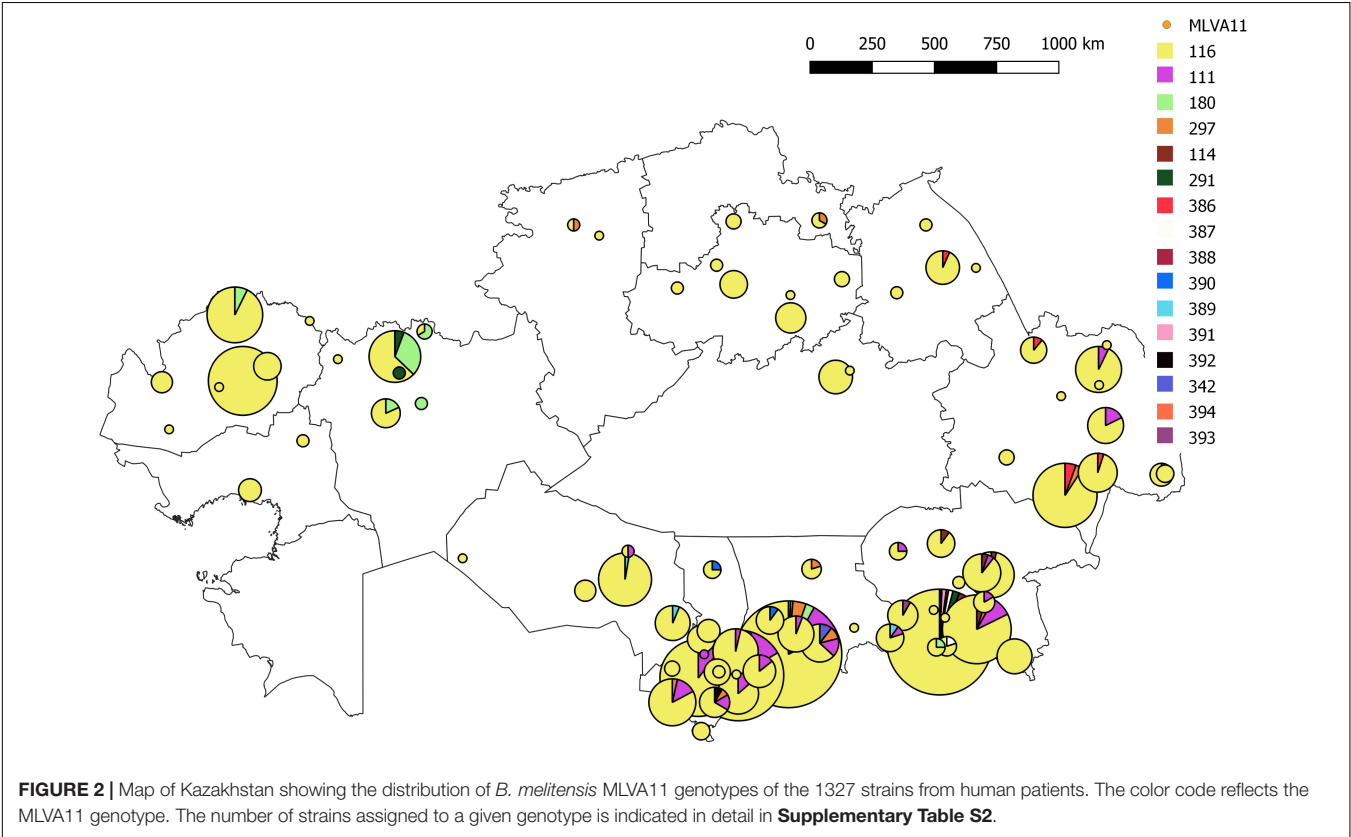
*MLVA8 in bold.†New genotype.

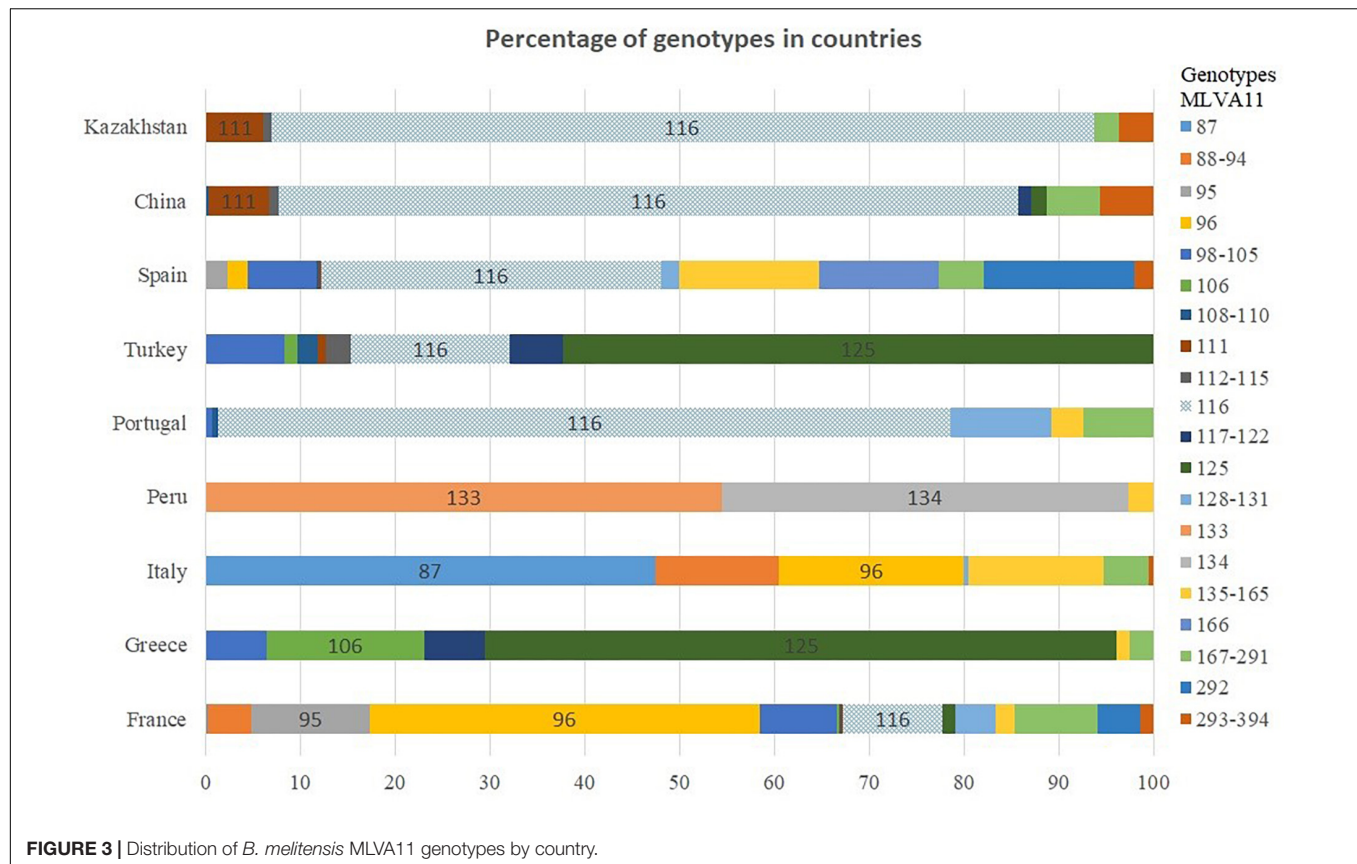
50 entries in MLVA bank, variable HGDI levels could be observed (Table 2). In Asian countries including Kazakhstan, panel2B loci Bruce07 and Bruce09 consistently showed low HGDI values. Locus Bruce30 is invariable in strains sampled from Africa and South America, and moderately variable in

Italy. In most European countries, all loci of the panel 2B are highly discriminatory.

All *B. melitensis* isolates isolated in Kazakhstan cluster within the East Mediterranean group congruently defined by MLVA, MLST and wgSNP (Whatmore et al., 2016; Vergnaud et al., 2018). In agreement with previous observations, all three *B. melitensis* biovars are observed within the East Mediterranean group. In the whole *Brucella* genus, 383 MLVA11 genotypes are defined, 100 of which belong to the East Mediterranean group (Figure 1). The 1327 *B. melitensis* strains from human patients isolated in Kazakhstan were clustered into 16 genotypes, nine of which numbered 386–394 have not been reported previously (Table 3). The most prevalent, genotype 116, was found in 86.8% of samples, genotype 111 in 6.03%, genotype 180 in 2.18%, and genotype 297 in 1.51%. The 12 other genotypes are rare (<1%). Genotype 116 is widespread in Kazakhstan whereas genotype 111 is detected in the hyperendemic areas in the southern part of Kazakhstan. The other genotypes have small prevalence in Kazakhstan and tend to be present in Southern Kazakhstan although genotypes 180 and 297 were also recovered in Northern Kazakhstan (Figure 2 and Supplementary Table S2).

The MLVA genotypes deposited in *Brucella* MLVAbank version 4_3 can be used to compare the incidence of these genotypes in different regions of the world. Genotypes 116 and 111 represent 50 and 3.2%, respectively of the more than 1500 East Mediterranean strains present in MLVAbank (Supplementary Table S1). In Portugal and China, genotype 116 accounts for more than 77% of cases, 37% in Spain and the





prevalence descends further in Turkey (16%) and France (10%) (**Figure 3**). Genotype 116 is predominant in Asian countries, as is evidenced by the identification of only this genotype in *B. melitensis* isolates from India and Mongolia, although the sampled populations were small. Genotype 111 is also relatively frequent in Asia. The rare genotypes 291 and 387 have been found only in Kazakhstan and China, whereas genotype 114 was found only in Kazakhstan and Turkey. Genotype 125, which is the second most frequent (18.5%) in East Mediterranean strains represented in MLVAbank and is the most prevalent genotype in Greece and Turkey, was not detected in Kazakhstan.

The MLVA16 clustered the 1327 strains into 310 genotypes, 131 of which were represented by a single isolate, 53 by two isolates, and 33 by three isolates. The most prevalent genotype was found in 66 strains (**Figure 4**). Among the 29 most frequent genotypes (found in 10 or more isolates) one genotype with 17 isolates was restricted to one geographic region (West Kazakhstan), whereas other most prevalent genotypes were present in a wider area. Among 61 medium-prevalence genotypes (e.g., found in four to nine samples), geographic linkage was established for ten genotypes: four genotypes are confined to Almaty region, five genotypes to East Kazakhstan, and one to West Kazakhstan. **Figure 5** shows the diversity of genotypes observed in humans, together with diversity previously reported in animals (Shevtsov et al., 2015).

Clustering analysis using all 16 VNTR loci (MLVA16) was conducted including *B. melitensis* East Mediterranean data

from MLVAbank. Shared genotypes were found for 83 (among 313) genotypes representing more than 57% of the isolates (**Figure 6**). The highest number of shared genotypes was found for strains circulating in China and Kazakhstan. Fifty-four MLVA16 genotypes are common between 530 isolates from Kazakhstan and 172 strains from China. Shared genotypes were also observed with *Brucella* strains isolated in other Asian and European countries. Eleven MLVA16 genotypes were present in a large geographic space, including Kazakhstan (242 isolates), China and other Asian and Middle-East countries (Turkey, Saudi Arabia, India, Mongolia, and Kuwait). Identical MLVA16 genotypes were observed among strains from Kazakhstan and Syria (one genotype, one strain for each country), Kazakhstan and Afghanistan (1 genotype, 10 and 1 strain(s), respectively), Kazakhstan and India (one genotype, one strain from each country), Kazakhstan and Saudi Arabia (1 genotype, 10 and 1 strain(s), respectively), Kazakhstan and Turkey (5 genotypes, 26 and 7 strains, respectively). Ten MLVA16 genotypes from Kazakhstan (comprising 37 strains) were found in European countries: Spain (6 genotypes, 11 strains), Portugal (4 genotypes, 6 strains), and France and Belgium (2 genotypes, 2 strains).

DISCUSSION

We report here the largest investigation of the genetic diversity of *Brucella* in a single country. More than 1300 strains were

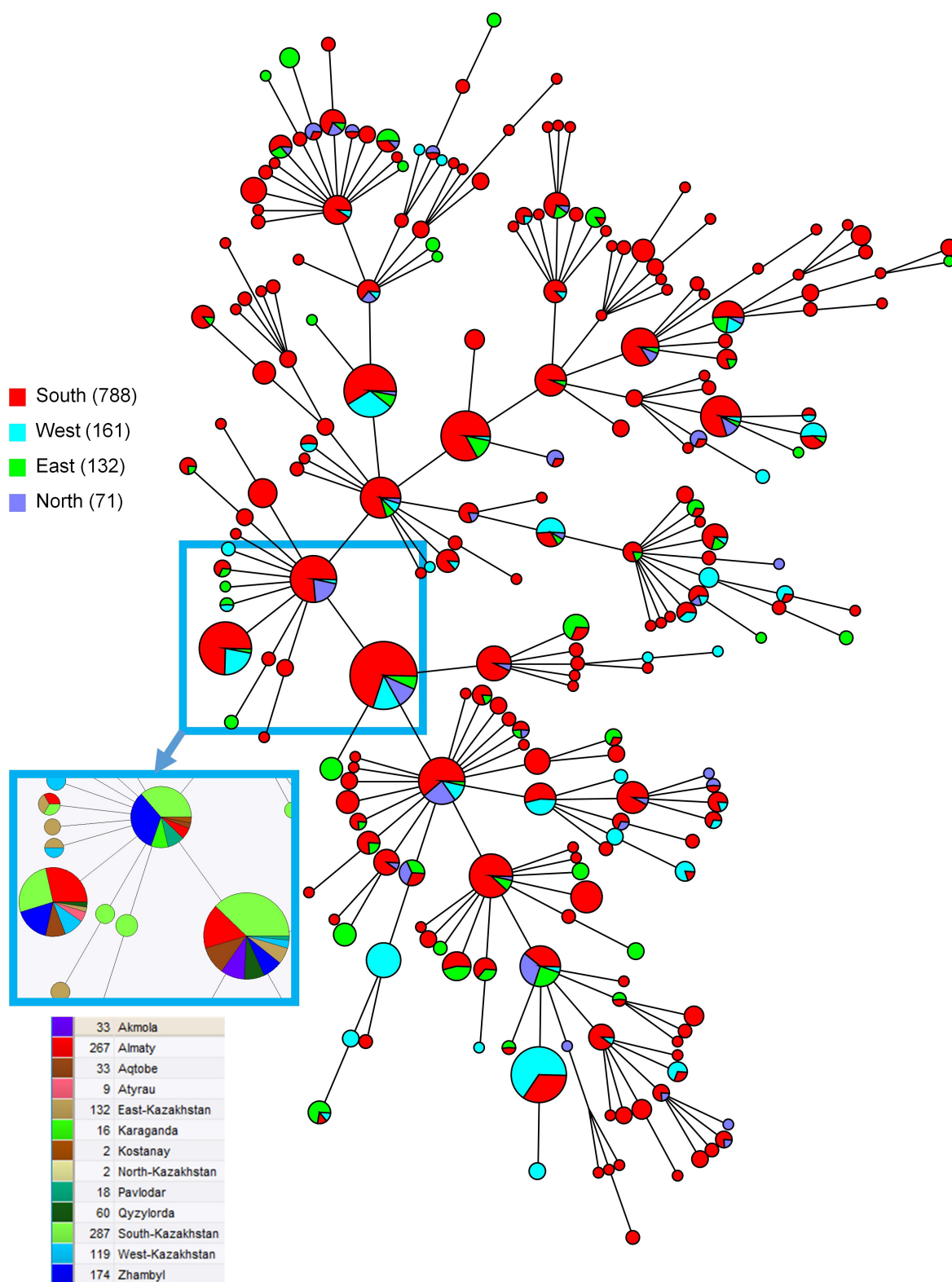


FIGURE 4 | Maximum parsimony analysis using MLVA16 for 1152 genotype 116 *B. melitensis* strains isolated from humans in Kazakhstan. The color code reflect the geographic origin of the strains (South: Almaty, Qyzylorda, Zhambyl, South-Kazakhstan; West: Aqtobe, Atyrau, West Kazakhstan; East: East Kazakhstan; North: Akmola, Kostanay, Karaganda, Pavlodar, North Kazakhstan). Inset: color code by region for a subset of the most frequent MLVA16 genotypes showing their wide geographic spreading. Branch lengths correspond to one up to two differences among the 16 values constituting the MLVA16 genotype.

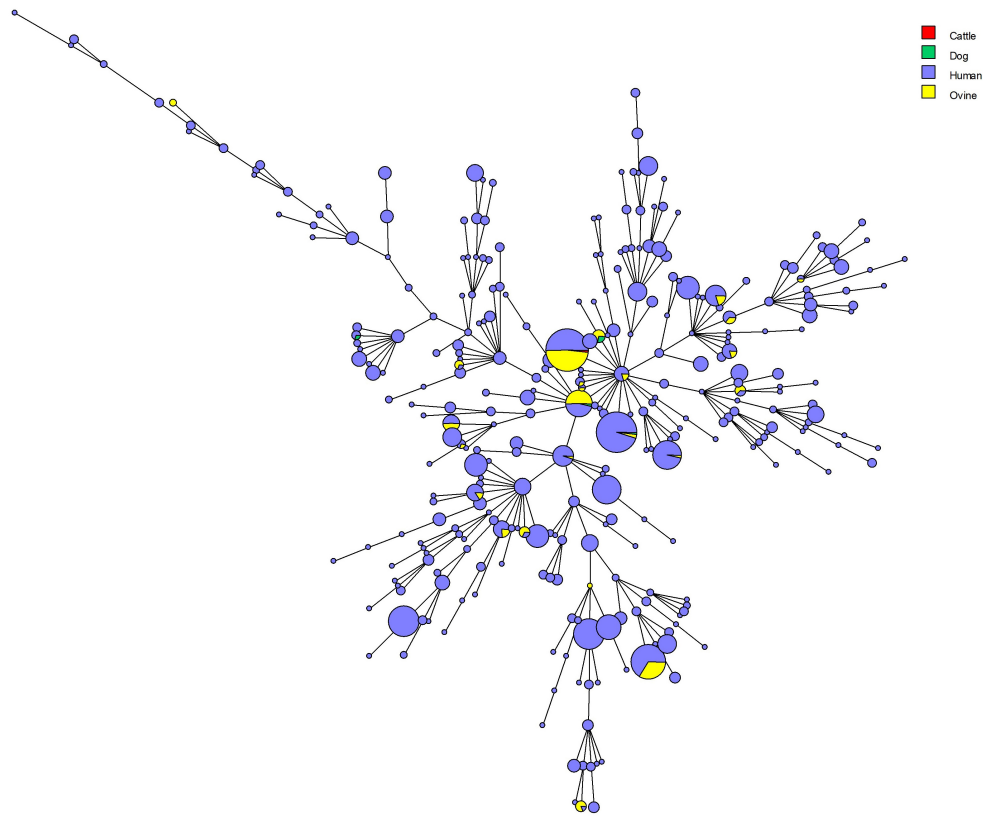


FIGURE 5 | Maximum parsimony analysis using MLVA16 data from 1455 *B. melitensis* strains isolated from humans and animals in Kazakhstan. The color code reflects the host origin (cattle: 1 strain, genotype 116; dog: 5 strains, 2 belong to genotype 111, 3 to genotype 116; human: 1327 strains; sheep: 122 strains).

collected from human patients and genotyped using tandem repeats polymorphism. Despite the fact that both *B. melitensis* and *B. abortus* are circulating among farm animals, and that the live vaccines from strains Rev1 (*B. melitensis* “Americas”), S19, SR82, and RB51 (*B. abortus*) are used in Kazakhstan, all strains from humans in this study were identified as *B. melitensis* “East-Mediterranean” (Shevtsova et al., 2016; Daugaliyeva et al., 2018). *B. melitensis* biovar 3 is predominant in this collection (79.8%), whereas biovars 1 and 2 account for 19 and 1.2%, respectively. Predominance of biovar 3 is typical in neighboring countries as well as in the whole Eurasian region (FAO, 2010; Liu et al., 2017). The results obtained show a very good correlation between the genotypes present in livestock in Kazakhstan and the genotypes observed in humans, as expected if infections occurred locally. Brucellosis is a typical zoonotic disease and better monitoring of *Brucella* circulation in animal populations will hopefully contribute to the successful control of human brucellosis.

Multiple-locus VNTR analysis genotyping assigned all strains to the *B. melitensis* “East-Mediterranean” group with predominance of the MLVA11 genotypes 116 and 111 (86.8 and 6.03%, respectively). The recovery of genotype 116 across most of Kazakhstan may be explained by extensive movement of livestock between regions by nomadic herders. The nomadic style is a historic way of livestock husbandry in Kazakhstan and was preserved until the beginning of the 20th century. Nomadism

implies regular movement of herds to new pastures many times per year (Mukhatova, 2014). Similarly, uncontrolled movement of livestock is described as the main source for geographic propagation of the infection (Syzydykov et al., 2014).

In contrast, genotype 111 is almost exclusively observed in South Kazakhstan, Almaty, Zhambyl, East-Kazakhstan, and Qyzylorda regions. These regions suffer from the most aggravated epidemiological situation. They account for 70% of infected sheep in Kazakhstan (during 5-year observation, 2011–2015), and hold 67% of small ruminants population in the country (Syzydykov et al., 2014; Espembetov et al., 2017). Two of the mentioned Kazakhstan’s regions share long borders with China. Information is lacking on genetic diversity in the other countries bordering Kazakhstan along the southwestern border.

The distribution of MLVA genotypes in Kazakhstan circulating in animals and humans closely replicated the genotypic distribution in the brucellosis-hyperendemic regions of Northern China, and more than 50% of the isolates from Kazakhstan have analogs among strains from China. This similarity supposedly reflects a common circulation in the neighboring countries, although it is not clear if the cross-border circulation still exist. MLVA typing does not allow establishing at what historical epoch the genotypic structure shaped into its current form. Trade ties and livestock exchange between the countries have long history, archeological finds

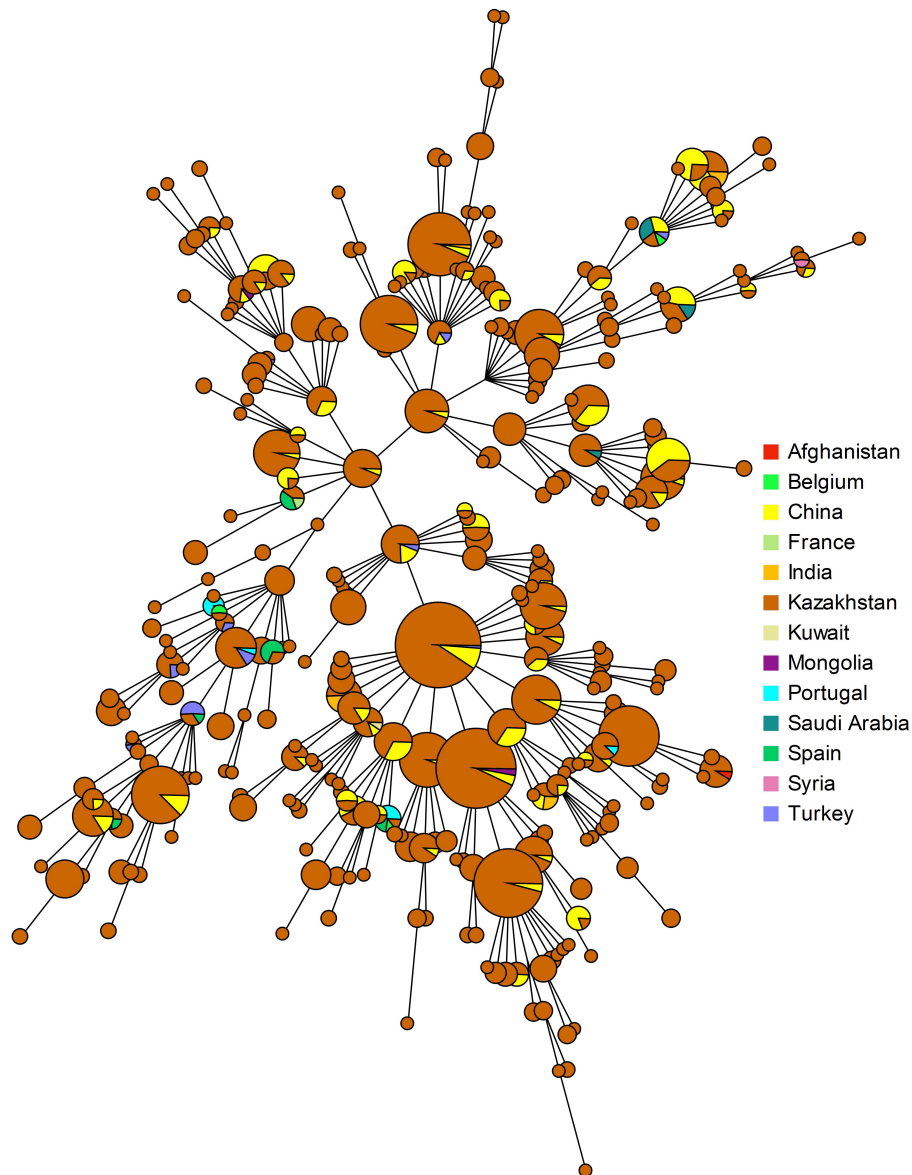


FIGURE 6 | Geographic origin of strains present in MLVAbank Brucella_4_3 and showing an MLVA16 genotype present in Kazakhstan.

indicate trade relations between the nomadic peoples who inhabited Central Asia and China long before the Common Era (CE) (Dicosmo, 1996). In addition, 4500 years ago, seasonal nomadic pastoralist routes were formed from modern southern Kazakhstan to Xinjiang Uygur Autonomous Region, covering the territory of more than 70% of the high-mountain route of the silk road (Frachetti et al., 2017). Cross-border nomadic pastoralism played an important role in the functioning of the Silk Road until the 15th century CE (Hermes et al., 2018). Trade relations between China and nomadic pastoralists of Kazakhstan continued until the formation of the Soviet Union. During the Soviet period, cattle was run from Mongolia to the Western parts of the Soviet Union passing through Kazakhstan (Kuznetsov, 1962). In modern history there is no trade in live

cattle between Kazakhstan and China, but actively developing trade in livestock products.

CONCLUSION

Multiple-locus VNTR analysis genotyping constitute a convenient medium-resolution classification assay for large-scale investigations. Follow-up studies based on whole genome sequencing of selected strains will be necessary to more precisely decipher the dynamics of strain circulation both within Kazakhstan and with Kazakhstan's neighboring countries. Such studies will also permit to design new low-cost genotyping assays tailored for Central Asia. These assays may be based on

a combination of selected tandem repeats including currently unused loci and of key SNPs.

DATA AVAILABILITY

The datasets generated for this study can be found in <http://microbesgenotyping.i2bc.paris-saclay.fr>.

AUTHOR CONTRIBUTIONS

GV edited the original manuscript. AShe conceptualized and designed the experiments. AShe, ES, and GV analyzed the data. ES, AShe, ASHu, KB, KM, MF, and YR were involved in the genotyping and wrote the manuscript. MS, AK, LL, and UI did

bacteriological researches and wrote the manuscript. All authors have read and approved the final version of the manuscript.

FUNDING

This study was supported by the Ministry of Education and Science of the Kazakhstan (Grant No. AP05133053).

SUPPLEMENTARY MATERIAL

The Supplementary Material for this article can be found online at: <https://www.frontiersin.org/articles/10.3389/fmicb.2019.01897/full#supplementary-material>

REFERENCES

- Al Dahouk, S., Le Flèche, P., Nockler, K., Jacques, I., Grayon, M., Scholz, H. C., et al. (2007). Evaluation of *Brucella* MLVA typing for human brucellosis. *J. Microbiol. Methods* 69, 137–145. doi: 10.1016/j.mimet.2006.12.015
- Al Dahouk, S., Tomaso, H., Nockler, K., Neubauer, H., and Frangoulidis, D. (2003). Laboratory-based diagnosis of brucellosis—a review of the literature. Part I: techniques for direct detection and identification of *Brucella* spp. *Clin. Lab.* 49, 487–505.
- Castaneda, M. R. (1947). A practical method for routine blood cultures in brucellosis. *Proc. Soc. Exp. Biol. Med.* 64:114. doi: 10.3181/00379727-64-15717
- Charypkhan, D., Sultanov, A. A., Ivanov, N. P., Baramova, S. A., Taitubayev, M. K., and Torgerson, P. R. (2019). Economic and health burden of brucellosis in Kazakhstan. *Zoonoses Public Health* 66, 487–494. doi: 10.1111/zph.12582
- Daugaliyeva, A., Sultanov, A., Usserbayev, B., Baramova, S., Modesto, P., Adambayeva, A., et al. (2018). Genotyping of *Brucella melitensis* and *Brucella abortus* strains in Kazakhstan using MLVA-15. *Infect. Genet. Evol.* 58, 135–144. doi: 10.1016/j.meegid.2017.12.022
- Dicosmo, N. (1996). Ancient xinjiang between central asia and china - the nomadic factor. *Anthropol. Archeol. Eurasia* 34, 87–101
- Doganay, G. D., and Doganay, M. (2013). *Brucella* as a potential agent of bioterrorism. *Recent Pat. Antiinfect. Drug Discov.* 8, 27–33.
- Espembetov, B. A., Syrvn, N. S., and Zinina, N. N. (2017). Monitoring and analysis of the epizootic situation of animal brucellosis in Kazakhstan in 2011–2015. *Bull. Ulyanovsk State Agric. Acad.* 37, 92–96. doi: 10.18286/1816-4501-2017-1-92-96
- FAO (2010). *Brucella Melitensis in Eurasia and the Middle East*. Rome: FAO Animal Production and Health Proceedings.
- Ferreira, A. C., Chambel, L., Tenreiro, T., Cardoso, R., Flor, L., Dias, I. T., et al. (2012). MLVA16 typing of portuguese human and animal *Brucella melitensis* and *Brucella abortus* isolates. *PLoS One* 7:e42514. doi: 10.1371/journal.pone.0042514
- Ficht, T. (2010). *Brucella taxonomy and evolution*. *Future Microbiol.* 5, 859–866. doi: 10.2217/fmb.10.52
- Frachetti, M. D., Smith, C. E., Traub, C. M., and Williams, T. (2017). Nomadic ecology shaped the highland geography of Asia's silk roads. *Nature* 543, 193–198. doi: 10.1038/nature21696
- Garofolo, G., Ancora, M., and Di Giannatale, E. (2013). MLVA-16 loci panel on *Brucella* spp. using multiplex PCR and multicolor capillary electrophoresis. *J. Microbiol. Methods* 92, 103–107. doi: 10.1016/j.mimet.2012.11.007
- Godfroid, J., Scholz, H. C., Barbier, T., Nicolas, C., Wattiau, P., Fretin, D., et al. (2011). Brucellosis at the animal/ecosystem/human interface at the beginning of the 21st century. *Prev. Vet. Med.* 102, 118–131. doi: 10.1016/j.prevetmed.2011.04.007
- Gwida, M., Neubauer, H., Ilhan, Z., Schmoock, G., Melzer, F., Nockler, K., et al. (2012). Cross-border molecular tracing of brucellosis in Europe. *Comp. Immunol. Microbiol. Infect. Dis.* 35, 181–185. doi: 10.1016/j.cimid.2011.12.012
- Hermes, T. R., Frachetti, M. D., Bullion, E. A., Maksudov, F., Mustafokulov, S., and Makarewicz, C. A. (2018). Urban and nomadic isotopic niches reveal dietary connectivities along central Asia's silk roads. *Sci. Rep.* 8:5177. doi: 10.1038/s41598-018-22995-22992
- Hunter, P. R., and Gaston, M. A. (1988). Numerical index of the discriminatory ability of typing systems: an application of Simpson's index of diversity. *J. Clin. Microbiol.* 26, 2465–2466.
- Kattar, M. M., Jaafar, R. F., Araj, G. F., Le Flèche, P., Matar, G. M., Abi Rached, R., et al. (2008). Evaluation of a multilocus variable-number tandem-repeat analysis scheme for typing human *Brucella* isolates in a region of brucellosis endemicity. *J. Clin. Microbiol.* 46, 3935–3940. doi: 10.1128/JCM.00464-468
- Kilic, S., Ivanov, I. N., Durmaz, R., Bayraktar, M. R., Ayaslioglu, E., Uyanik, M. H., et al. (2011). Multiple-locus variable-number tandem-repeat analysis genotyping of human *Brucella* isolates from Turkey. *J. Clin. Microbiol.* 49, 3276–3283. doi: 10.1128/JCM.02538-2510
- Kuznetsov, V. S. (1962). *Kazakhsko-Kitayskiye Torgovyye Otnosheniya v Kontse XVIII veke [Kazakh-Chinese trade relations at the end of the XVIII century]*. Almaty: Publishing house of the Academy of Sciences of the Kazakh SSR.
- Le Flèche, P., Jacques, I., Grayon, M., Al Dahouk, S., Bouchon, P., Denoeud, F., et al. (2006). Evaluation and selection of tandem repeat loci for a *Brucella* MLVA typing assay. *BMC Microbiol.* 6:9. doi: 10.1186/1471-2180-6-9
- Ledwaba, M. B., Gomo, C., Lekota, K. E., Le Flèche, P., Hassim, A., Vergnaud, G., et al. (2019). Molecular characterization of *Brucella* species from Zimbabwe. *PLoS Negl. Trop. Dis.* 13:e0007311. doi: 10.1371/journal.pntd.0007311
- Liu, Z. G., Di, D. D., Wang, M., Liu, R. H., Zhao, H. Y., Piao, D. R., et al. (2017). MLVA genotyping characteristics of human *Brucella melitensis* isolated from ulanqab of inner mongolia. China. *Front. Microbiol.* 8:6. doi: 10.3389/fmicb.2017.00006
- Lopez-Goni, I., Garcia-Yoldi, D., Marin, C. M., de Miguel, M. J., Munoz, P. M., Blasco, J. M., et al. (2008). Evaluation of a multiplex PCR assay (Bruce-ladder) for molecular typing of all *Brucella* species, including the vaccine strains. *J. Clin. Microbiol.* 46, 3484–3487. doi: 10.1128/JCM.00837-838
- Maquart, M., Le Flèche, P., Foster, G., Tryland, M., Ramisse, F., Djonje, B., et al. (2009). MLVA-16 typing of 295 marine mammal *Brucella* isolates from different animal and geographic origins identifies 7 major groups within *Brucella ceti* and *Brucella pinnipedialis*. *BMC Microbiol.* 9:145. doi: 10.1186/1471-2180-9-145
- Meyer, M. E. (1990). "Evolutionary development and taxonomy of the genus *Brucella*," in *Advances in Brucellosis Research*, ed. L. G. Adams (Galveston, TX: Texas A&M University Press), 12–35.
- Mizanbayeva, S., Smits, H. L., Zhalilova, K., Abdoel, T. H., Kozakov, S., Ospanov, K. S., et al. (2009). The evaluation of a user-friendly lateral flow assay for the serodiagnosis of human brucellosis in Kazakhstan. *Diagn. Microbiol. Infect. Dis.* 65, 14–20. doi: 10.1016/j.diagmicrobio.2009.05.002
- Mukhatova, O. (2014). Kazakh economy In XVII–XVIII centuries. 3rd world conference on educational technology researches 2013. *Wcetr* 2013, 218–223. doi: 10.1016/j.sbspro.2014.04.107
- Neubauer, H. (2010). Brucellosis: new demands in a changing world. *Prilozi* 31, 209–217.

- Nicoletti, P. (2010). Brucellosis: past, present and future. *Prilozi* 31, 21–32.
- Pappas, G., Papadimitriou, P., Akritidis, N., Christou, L., and Tsianos, E. V. (2006a). The new global map of human brucellosis. *Lancet Infect. Dis.* 6, 91–99. doi: 10.1016/S1473-3099(06)70382-70386
- Pappas, G., Panagopoulou, P., Christou, L., and Akritidis, N. (2006b). *Brucella* as a biological weapon. *Cell. Mol. Life Sci.* 63, 2229–2236. doi: 10.1007/s00018-006-6311-6314
- Scholz, H. C., and Vergnaud, G. (2013). Molecular characterisation of *Brucella* species. *Rev. Sci. Tech.* 32, 149–162. doi: 10.20506/rst.32.1.2189
- Shevtsov, A., Ramanculov, E., Shevtsova, E., Kairzhanova, A., Tarlykov, P., Filipenko, M., et al. (2015). Genetic diversity of *Brucella abortus* and *Brucella melitensis* in Kazakhstan using MLVA-16. *Infect. Genet. Evol.* 34, 173–180. doi: 10.1016/j.meegid.2015.07.008
- Shevtsova, E., Shevtsov, A., Mukanov, K., Filipenko, M., Kamalova, D., Sytnik, I., et al. (2016). Epidemiology of brucellosis and genetic diversity of *Brucella abortus* in kazakhstan. *PLoS One* 11:e0167496. doi: 10.1371/journal.pone.0167496
- Studentsov, È. P. (1975). *Brutsellez zhivotnykh [Brucellosis in animals]*. Almaty: Kaynar.
- Syzdykov, M. S., Kuznetsov, A. N., Kazakov, S. V., Daulbayeva, S. F., Duysenova, A. K., Berezovskiy, D. V., et al. (2014). Analiz prostranstvenno-vremennogo raspredeleniya brutselloza cheloveka i zhivotnykh s ispol'zovaniyem Geograficheskikh informatsionnykh tekhnologiy—[Analysis of the spatial and temporal distribution of human and animal brucellosis using Geographic information technology]. *Gigiyena, epidemiologiya i immunobiologiya - [Hygiene, Epidemiology and Immunobiology]* 72, 24–26.
- Syzdykov, M. S., Kuznetsov, A. N., Kazakov, S. V., Espembetov, B. A., and Duysenova, A. K. (2013). Spatio-temporal analysis of the incidence of brucellosis using GIS technology [in Rus.]. *Med. Kyrgyzstan* 4, 148–151.
- Vergnaud, G., Hauck, Y., Christiany, D., Daoud, B., Pourcel, C., Jacques, I., et al. (2018). Genotypic expansion within the population structure of classical *Brucella* species revealed by MLVA16 Typing of 1404 *Brucella* isolates from different animal and geographic origins, 1974–2006. *Front. Microbiol.* 9:1545. doi: 10.3389/fmicb.2018.01545
- Whatmore, A. M., Koylass, M. S., Muchowski, J., Edwards-Smallbone, J., Gopaul, K. K., and Perrett, L. L. (2016). Extended multilocus sequence analysis to describe the global population structure of the genus *Brucella*: phylogeography and relationship to biovars. *Front. Microbiol.* 7:2049. doi: 10.3389/fmicb.2016.02049
- Whatmore, A. M., Shankster, S. J., Perrett, L. L., Murphy, T. J., Brew, S. D., Thirlwall, R. E., et al. (2006). Identification and characterization of variable-number tandem-repeat markers for typing of *Brucella* spp. *J. Clin. Microbiol.* 44, 1982–1993. doi: 10.1128/JCM.02039-2035
- Yagupsky, P. (1999). Detection of *Brucellae* in blood cultures. *J. Clin. Microbiol.* 37, 3437–3442.
- Yespembetov, B. A., Syrym, N. S., Zinina, N. N., Sarmykova, M. K., Konbayeva, G. M., Basybekov, S. Z., et al. (2019). Phenotypic and genotypic characteristics of *Brucella* isolates from the republic of kazakhstan. *Trop Anim. Health Prod.* doi: 10.1007/s11250-019-01941-y [Epub ahead of print].
- Zheludkov, M. M., and Tsirelson, L. E. (2010). Reservoirs of *Brucella* infection in nature. *Biol. Bull.* 37, 709–715. doi: 10.1134/s106235901007006x

Conflict of Interest Statement: The authors declare that the research was conducted in the absence of any commercial or financial relationships that could be construed as a potential conflict of interest.

Copyright © 2019 Shevtsova, Vergnaud, Shevtsov, Shustov, Berdimuratova, Mukanov, Syzdykov, Kuznetsov, Lukhnova, Izbanova, Filipenko and Ramankulov. This is an open-access article distributed under the terms of the Creative Commons Attribution License (CC BY). The use, distribution or reproduction in other forums is permitted, provided the original author(s) and the copyright owner(s) are credited and that the original publication in this journal is cited, in accordance with accepted academic practice. No use, distribution or reproduction is permitted which does not comply with these terms.



Polymorphisms in *Brucella* Carbonic Anhydrase II Mediate CO₂ Dependence and Fitness *in vivo*

Juan M. García Lobo^{1,2}, Yelina Ortiz^{1,2}, Candela Gonzalez-Riancho^{1,2},
Asunción Seoane^{1,2}, Beatriz Arellano-Reynoso³ and Félix J. Sangari^{1,2*}

¹ Instituto de Biomedicina y Biotecnología de Cantabria (IBBT), CSIC – Universidad de Cantabria, Santander, Spain,

² Departamento de Biología Molecular, Universidad de Cantabria, Santander, Spain, ³ Departamento de Microbiología, Delegación Coyoacán, Facultad de Medicina Veterinaria y Zootecnia, Universidad Nacional Autónoma de México, Mexico City, Mexico

OPEN ACCESS

Edited by:

Axel Cloeckaert,
Institut National de la Recherche
Agronomique (INRA), France

Reviewed by:

Amaia Zúñiga-Ripa,
University of Navarra, Spain
Jean-Jacques Letesson,
University of Namur, Belgium

*Correspondence:

Félix J. Sangari
sangarif@unican.es

Specialty section:

This article was submitted to
Infectious Diseases,
a section of the journal
Frontiers in Microbiology

Received: 31 May 2019

Accepted: 12 November 2019

Published: 10 December 2019

Citation:

García Lobo JM, Ortiz Y,
González-Riancho C, Seoane A,
Arellano-Reynoso B and Sangari FJ
(2019) Polymorphisms in *Brucella*
Carbonic Anhydrase II Mediate CO₂
Dependence and Fitness *in vivo*.
Front. Microbiol. 10:2751.
doi: 10.3389/fmicb.2019.02751

Some *Brucella* isolates are known to require an increased concentration of CO₂ for growth, especially in the case of primary cultures obtained directly from infected animals. Moreover, the different *Brucella* species and biovars show a characteristic pattern of CO₂ requirement, and this trait has been included among the routine typing tests used for species and biovar differentiation. By comparing the differences in gene content among different CO₂-dependent and CO₂-independent *Brucella* strains, we have confirmed that carbonic anhydrase (CA) II is the enzyme responsible for this phenotype in all the *Brucella* strains tested. *Brucella* species contain two CAs of the β family, CA I and CA II; genetic polymorphisms exist for both of them in different isolates, but only those putatively affecting the activity of CA II correlate with the CO₂ requirement of the corresponding isolate. Analysis of these polymorphisms does not allow the determination of CA I functionality, while the polymorphisms in CA II consist of small deletions that cause a frameshift that changes the C-terminus of the protein, probably affecting its dimerization status, essential for the activity. CO₂-independent mutants arise easily *in vitro*, although with a low frequency ranging from 10⁻⁶ to 10⁻¹⁰ depending on the strain. These mutants carry compensatory mutations that produce a full-length CA II. At the same time, no change was observed in the sequence coding for CA I. A competitive index assay designed to evaluate the fitness of a CO₂-dependent strain compared to its corresponding CO₂-independent strain revealed that while there is no significant difference when the bacteria are grown in culture plates, growth *in vivo* in a mouse model of infection provides a significant advantage to the CO₂-dependent strain. This could explain why some *Brucella* isolates are CO₂ dependent in primary isolation. The polymorphism described here also allows the *in silico* determination of the CO₂ requirement status of any *Brucella* strain.

Keywords: *Brucella*, carbonic anhydrase, CO₂ requirement, fitness, protein structure

INTRODUCTION

Brucella species are facultative intracellular Gram-negative coccobacilli that cause brucellosis, the most prevalent zoonosis with more than 500,000 human cases reported worldwide every year (Pappas et al., 2006). *Brucella* isolates are routinely identified and classified by biochemical and phenotypical characteristics like urease activity, CO₂ dependence, H₂S production, erythritol and

dye sensitivity, lysis by *Brucella*-specific bacteriophages, agglutination with monospecific sera, or even host preference (Alton et al., 1988). The first observations pertaining to *Brucella* and CO₂ were made by Nowak in 1908 (Duncan, 1928), who noticed that *Brucella abortus* was more easily isolated from the host tissues when the concentration of oxygen in the atmosphere was reduced, but it was Wilson (1931) who established the requirement of CO₂ for growth in these isolates. This requirement is not universal within *Brucellaceae*, and the different species and biovars show a characteristic pattern of CO₂ dependence. Within the classical species, *B. abortus* biovars 1, 2, 3, and 4 and some isolates from biovar 9, as well as *Brucella ovis*, require an increased concentration of CO₂ for growth, especially in the case of primary cultures obtained directly from infected animals. Within the more recently described species, most strains of *Brucella pinnipedialis* require supplementary CO₂ for growth, and most of *Brucella ceti* do not (Foster et al., 1996). The CO₂ dependence may be lost by subculturing *in vitro*, with an estimated frequency of 3×10^{-10} per cell division (Marr and Wilson, 1950), and this is what happened with well-known laboratory *B. abortus* biovar 1 strains like 2308 or S19, which grow in ambient air.

Facultative intracellular bacteria face two environmental conditions with very dissimilar concentrations of carbon dioxide (CO₂). Inside mammalian cells, CO₂ concentration may be as high as 5%, while atmospheric concentration is currently estimated at 0.04%. CO₂ and bicarbonate (HCO₃⁻) are essential growth factors for bacteria, and they can be interconverted spontaneously at significant rates (Gladstone et al., 1935; Smith et al., 1999). The reversible hydration of CO₂ into HCO₃⁻ can also be catalyzed by carbonic anhydrase (CA), a ubiquitous metalloenzyme fundamental to many biological functions including photosynthesis, respiration, and CO₂ and ion transport. The CA superfamily (CAs, EC 4.2.1.1) has been found in all the three domains of life (Eubacteria, Archaea, and Eukarya), and it currently includes seven known families (α -, β -, γ -, δ -, ζ -, η -, and θ -CAs) of distinct evolutionary origin (Supuran, 2018). The conversion of CO₂ into HCO₃⁻ is accelerated in the presence of CA and has the effect of ensuring correct CO₂ concentration for carboxylating enzymes involved in central, amino acid, and nucleotide metabolism (Merlin et al., 2003).

Carbonic anhydrase has been shown to be required to support growth under ambient air in a number of microorganisms like *Ralstonia eutropha* (Kusian et al., 2002), *Escherichia coli* (Hashimoto and Kato, 2003; Merlin et al., 2003), *Corynebacterium glutamicum* (Mitsuhashi et al., 2004), and *Saccharomyces cerevisiae* (Aguilera et al., 2005). Growth of CA mutants of these organisms was only possible under an atmosphere with high levels of CO₂, a phenomenon that is explained by the availability of bicarbonate, which is a substrate for various carboxylation reactions of physiological importance. These reactions are catalyzed by several housekeeping enzymes, like 5'-phosphoribosyl-5-amino-4-imidazole carboxylase (EC 4.1.1.21), phosphoenolpyruvate carboxylase (EC 4.1.1.31), carbamoyl phosphate synthetase (EC 6.3.4.16), pyruvate carboxylase (EC 6.4.1.1), and acetyl-CoA carboxylase (EC 6.4.1.2). They catalyze key steps of pathways for the biosynthesis

of not only physiologically essential but also industrially useful metabolites, such as amino acids, nucleotides, and fatty acids (Mitsuhashi et al., 2004). A role for CA in the intracellular pH regulation has also been demonstrated in some bacteria (Marcus et al., 2005).

Brucella species contain two different β -CAs, first identified in *Brucella suis* 1330 and thus named β_{s1330} CAI and β_{s1330} CAII. Both CAs contain the amino acid residues involved in the binding of the Zn ion (typical of the β family of CAs), as well as those involved in the catalytic site. Their activity has been verified *in vitro*, and it is slightly higher in β_{s1330} CAII than in β_{s1330} CAI (Joseph et al., 2010, 2011). Pérez-Etayo et al. (2018) compared CA I and CA II activity (activity defined empirically as that allowing growth in a normal atmosphere, the same definition used throughout this study) in several strains of *B. suis*, *B. abortus*, and *B. ovis* and determined that CA II is not functional in CO₂-dependent *B. abortus* and *B. ovis*, thus establishing a correlation between CA activity and CO₂ dependence. They also observed that CA I is active in *B. suis* 1330 or 513, but not in *B. abortus* 2308W, 292, and 544. Moreover, although an active CA I alone is enough to support CO₂-independent growth of *B. suis* in rich media, it is not able to do it in minimal media or to support CO₂-independent growth of *B. abortus* at all. A similar result was also obtained by Varesio et al. (2019) that identified BcaA_{BOV} (CA II) as the enzyme responsible for the growth of *B. ovis* in a standard, unsupplemented atmosphere (0.04% CO₂), in this case, by whole-genome sequencing (WGS) of CO₂-independent mutants. Interestingly, they also reported that a CO₂ downshift *B. ovis* initiates a gene expression program that resembles the stringent response and results in transcriptional activation of its type IV secretion system. This shift is absent in *B. ovis* strains carrying a functional copy of CA.

The classical biotyping mentioned above, despite its limitations and the emergence of new molecular approaches to identify and classify *Brucella* at different taxonomic levels, is still extensively used by reference laboratories, often side by side with the molecular methods (Garin-Bastuji et al., 2014). However, although there is a known link between phenotype and its genetic cause in some traits like urease activity or erythritol sensitivity (Sangari et al., 1994, 2007, 2010), there is still a gap between the information provided by the molecular methods and the phenotype of *Brucella* isolates. With the availability of more genome sequences, it should be possible to reduce this gap by comparing the phenotypic characteristics of *Brucella* strains with their genome content. Comparative genomics of whole-genome sequences is especially interesting in bacterial pathogenesis studies (Hu et al., 2011). Pathogenomics can be considered as a particular case of comparative genomics, and it has been extensively used for the identification of putative virulence factors in bacteria, by comparing virulent and avirulent isolates (Pallen and Wren, 2007), although in principle it could be applied to the elucidation of any phenotypic trait. The genus *Brucella* is a very homogeneous one, with over 90% identity on the basis of DNA–DNA hybridization assays within the classical species, and this results in relatively minor genetic variation between species that sometimes result in striking differences. As an example, only 253 single-nucleotide polymorphisms

(SNPs) separate *Brucella canis* from its nearest *B. suis* neighbor (Foster et al., 2009), but their host specificity differs widely, while *B. canis* is almost entirely restricted to the Canidae family, *B. suis* has a wide host range that includes pigs, dogs, rodents, hares, horses, reindeer, musk oxen, wild carnivores, and humans. Similarly, there are only 39 SNPs consistently different between the vaccine strain *B. abortus* S19 and strains *B. abortus* 9-941 and 2308, two well-known virulent isolates (Crasta et al., 2008). In the last years, a large number of *Brucella* genomes representing all species and biovars have been sequenced, and all this wealth of information is already resulting in new molecular epidemiology and typing methods (O'Callaghan and Whatmore, 2011). We have tested the potential of pathogenomics to unveil phenotypic traits in *Brucella* by defining the pangenome/pseudogenes of a set of *Brucella* strains and comparing it with the CO₂ dependence of those strains. This process has allowed us to identify CA II as the enzyme responsible for growth of the bacteria at atmospheric CO₂ concentrations and extend the analysis to new species of *Brucella*. All the sequenced genomes of *Brucella* contain two β -CA genes, but only those that carry a defective β -CA II require supplemental CO₂. Reversion of this phenotype happens *in vitro* at a low frequency and is accompanied by a compensatory mutation that results in a full-length β -CA II product. We have also tested the hypothesis that the presence of a truncated β -CA II would have a competitive advantage *in vivo*, as a way to explain why a mutation with such a low frequency could get fixed in some *Brucella* species and biovars. A competitive assay shows that one of such mutants is significantly enriched in a mouse model of infection when compared with its corresponding full-length β -CA II strain. This could explain why CO₂-dependent strains are selected *in vivo*. The polymorphisms affecting β -CA II encoding genes allow the prediction of the CO₂ dependence status of any given strain, thus having the potential to replace the classical assay to characterize *Brucella* isolates.

MATERIALS AND METHODS

Bacterial Strains and Growth Conditions

The bacterial strains and plasmids used in this work are listed in **Table 1**. *Brucella* strains were grown at 37°C for 48–96 h in a 5% CO₂ atmosphere in *Brucella* broth (BB) or agar (BA) medium (Pronadisa, Spain). Media were supplemented with 10% fetal bovine serum (FBS) to grow *B. ovis*. All experiments with live *Brucella* were performed in a Biosafety Level 3 (BSL3) facility at the Department of Molecular Biology of the University of Cantabria, and animal infections with *Brucella* were conducted at the University of Cantabria animal facilities, also under BSL3 conditions.

Bioinformatic Methods

Genomic and protein sequences of the different *Brucella* species were obtained from GenBank and the Broad Institute¹. To allow easy comparison between the genes and pseudogenes in the different *Brucella* species, we constructed the panproteome of

TABLE 1 | Strains and plasmids used in this study.

Strains	Main characteristics	References
<i>Brucella</i>		
<i>Brucella abortus</i> 544	Biotype 1, CO ₂ dependent	Alton et al. (1988)
<i>B. abortus</i> 86/8/59	Biotype 2, CO ₂ dependent	Alton et al. (1988)
<i>B. abortus</i> Tulya	Biotype 3, CO ₂ dependent	Alton et al. (1988)
<i>B. abortus</i> 292	Biotype 4, CO ₂ dependent	Alton et al. (1988)
<i>B. abortus</i> A-579	Biotype 3, CO ₂ dependent	Alton et al. (1988)
<i>B. abortus</i> 2308W	Biotype 1, CO ₂ independent	Suárez-Esquivel et al. (2016)
<i>Brucella ovis</i> 63/290	CO ₂ dependent	Alton et al. (1988)
<i>Brucella pinnipedialis</i> B2/94	CO ₂ dependent	Foster et al. (1996)
<i>B. abortus</i> 2308 Δ Ba2308wCAI mutant	CO ₂ independent	This study
<i>B. abortus</i> 292mut1	CO ₂ independent	This study
Plasmids		
pDS132	Suicide mobilizable plasmid	Philippe et al. (2004)
pFJS267	pDS132: Δ Ba2308wCA	This study

a selected set of 10 strains with the most complete genome annotation at that time (**Supplementary Table S1**). To construct this set, we started with all the coding sequences (CDSs) annotated in the *B. suis* 1330 genome. Next, we found the most probable functional counterparts for the *n* pseudogenes annotated in *B. suis* 1330. The pseudogene list was taken directly from the original annotation of the *B. suis* 1330 genome. Finally, we added those CDSs in indels from the other genomes not present in *B. suis* 1330. We assigned a new gene name to every CDS in our set following the Bru1_xxxx and Bru2_xxxx nomenclature, depending on the location of the gene in the *B. suis* genome. CDSs from indels were also renamed with a nomenclature, BRU1_iXXXX, the “i” indicating their origin from indels absent in *B. suis* 1330. The file pan_pep provided in the **Supplementary Material** is a multifasta protein file containing the sequence of all 3,496 CDSs present at least once in any of the used genomes and constitutes the first version of the *Brucella* panproteome. The genes and pseudogenes annotated in these genomes were tabulated and assigned to one of the different gene families present in those genomes. In this way, we constructed a spreadsheet with the pseudogenes in each genome using a uniform nomenclature. The analysis of the CA sequences at both the DNA and protein levels was extended to a group of 35 *Brucella* genomes (**Supplementary Table S2**).

A structural theoretical model of *Brucella* Ba2308CAII was generated by molecular threading using the protein homology and recognition engine Phyre2 (Kelley et al., 2015), taking the atomic coordinates of the best hit as template. The pdb model generated was visualized using the PyMOL Molecular Graphics System, version 1.3 (Schrödinger, LLC, Portland, OR, United States).

Primers used in this study (**Table 2**) were designed with Primer 3² and synthesized by Sigma-Aldrich.

¹<https://www.broadinstitute.org/projects/brucella>

²<http://bioinfo.ut.ee/primer3-0.4.0/>

TABLE 2 | Oligonucleotides used in this work.

BS192_0456.F	CATGCTGGAACCAAAGTTGA
BS192_0456.R	CGTTTCCGCAAGCTGTAAAT
BS191_1911.F	GGGTTCCACAGGGTTCATTT
BS191_1911.R	GACGGCAAATAATTGCATGA
U_BAB2_0449. SacI.F	GAGCTCTGAGCACAACCTGCAAAATC
U_BAB2_0449.R	GGCGAATGATCGTTCTTCAT
D_BAB2_0449.F	ATGAAGAACGATCATTGCGCGGATCCTGCCAAC
	CGGCAGATAAT
D_BAB2_0449. XbaI.R	TCTAGAGGGGGAGGCTTCTAGTTT

Isolation of CO₂-Independent Mutants in CO₂-Dependent *Brucella* Strains

Different CO₂-dependent *Brucella* strains from our collection were streaked onto BA plates and grown in a 5% CO₂ atmosphere. Individual colonies were then re-streaked in duplicate plates and incubated at 5% CO₂ and ambient atmosphere to check for the correct CO₂ dependence phenotype. They were grown as a lawn in fresh BA plates, and the growth was resuspended in phosphate-buffered saline (PBS). The suspension was serially diluted, and each dilution seeded in duplicate in BA plates. One dilution series was incubated at 5% CO₂ to enumerate the number of bacteria in the inoculum, while the second was incubated at ambient atmosphere to select for CO₂-independent colonies. The mutation rate was expressed as number of mutants per number of initial bacteria. Individual mutants were selected, and genomic DNA was obtained by using the InstaGene matrix as described by the supplier (Bio-Rad Laboratories, United Kingdom). *CA I* and *CA II* complete sequences from the different strains were amplified by PCR with oligonucleotides BS192_0456.F/R and BS191_1911.F/R, respectively, and sequenced to determine if there was any change compared to the corresponding parental sequence.

Infection and Intracellular Viability Assay of *Brucella abortus* in J774 Cells

J774.A1 macrophage-like cells [American Type Culture Collection (ATCC), TIB-67] were cultured in RPMI medium with 2 mM L-glutamine and 10% FBS at 37°C in 5% CO₂ and 100% humidity. Confluent monolayers were trypsinized, and 2×10^5 cells per well were incubated for 24 h before infection in 24-well tissue culture plates. Macrophages were infected with *Brucella* strains in triplicate wells at an MOI of 50. After infection for 30 min, the wells were washed five times with sterile PBS and further incubated for 30 min in RPMI with 2 mM L-glutamine, 10% FCS, and 50 µg gentamicin per milliliter to kill extracellular bacteria. That was taken as time 0 post infection, and the medium was changed to contain 10 µg gentamicin per milliliter. The number of intracellular viable *B. abortus* was determined at different time points by washing three times with PBS and lysing infected cells with 0.1% Triton X-100 in H₂O and plating a series of 1:10 dilutions on BA plates for colony-forming unit (CFU) determination.

Competitive Infection Assays

The following protocol was approved by the Cantabria University Institutional Laboratory Animal Care and Use Bioethics Committee and was carried out in accordance with the Declaration of Helsinki and the European Communities Council Directive (86/609/EEC). Comparison of fitness between CO₂-dependent and isogenic CO₂-independent strains was done through a competitive infection assay in order to minimize animal-to-animal variation. BALB/c mice (CIFRA, Spain) were injected with 1:1 mixtures of *B. abortus* 292 (CO₂ dependent, wild type) and *B. abortus* 292mut1 (a spontaneous Ba292CAII CO₂-independent mutant). Two hundred microliters of a suspension containing approximately 10⁸ bacteria was administered intraperitoneally to a group ($n = 6$) of 6- to 8-week-old female BALB/c mice. Mice were sacrificed 8 weeks after infection, and the liver and spleen were removed aseptically and homogenized with 5 ml of BB containing 20% glycerol. Samples were serially diluted and plated in quadruplicate on BA plates. Half of the plates were incubated with 5% CO₂, and the other half at ambient atmosphere. Additionally, colonies grown at 5% CO₂ were replica-plated and incubated at both CO₂ concentrations, to measure the ratio of CO₂-dependent and CO₂-independent colonies in two independent ways. For *in vitro* competitive index (CI) assays, BA plates were seeded, forming a lawn with the infection mix, and incubated at 37°C with 5% CO₂ for 8 weeks, with repeated subculture in fresh BA plates every 4–5 days in the same conditions. The ratio of CO₂-dependent and CO₂-independent colonies was determined with the same protocol as the *in vivo* CI. The CI was calculated as the ratio of mutant to wild-type bacteria recovered at the end of the experiment divided by the ratio of mutant to wild-type bacteria in the inoculum, and the differences between groups were analyzed by Student's two-tailed *t* test with significance set at $P < 0.05$.

RESULTS

Identification of the Gene Responsible for the CO₂ Dependence in *Brucella abortus*

The first evidence of the involvement of CA in the CO₂ dependence phenotype came from the analysis of pseudogenes in the 10 fully annotated *Brucella* genomes (**Supplementary Table S1**). After tabulation of the pseudogenes, their presence along with the different species was compared with the target phenotype; in this particular case, we interrogated the spreadsheet *n_pseudos.xls* (**Supplementary Material**) to find out which genes are pseudogenes only in those strains in our list that are CO₂ dependent, *B. abortus* 9-941, and *B. ovis*. Three genes met this criterion, namely, Bru1_1050, which encodes for a multidrug resistance efflux pump; Bru1_1827, which encodes for CA II; and Bru2_1236, encoding for an adenosylmethionine-8-amino-7-oxononanoate aminotransferase.

Given the requirement of CA for growth of other microorganisms at ambient CO₂ concentrations and to check if Bru1_1827 could be responsible for the CO₂ dependence

FIGURE 1 | Continued

C337 also appears in CO₂-independent *B. abortus* biovar 1 strains, like S19, 2308, or NTCC 8038, but in these cases, there are additional mutations that recover the original open reading frame (ORF), two extra nucleotides in strain 2308, or one nucleotide deletion in *B. abortus* NCTC 8038 and S19. These changes do

not affect the conserved amino acid residues typical of β -CAs involved in the catalytic cycle, that is, the four zinc-binding residues, Cys44, Asp46, Hys105, and Cys108, and the catalytic dyad Asp46 and Arg48 (**Figure 1B**). Some of the strains analyzed here (*B. suis* 1330 and *B. abortus* strains 2308W, 292, and 544) were also analyzed by Pérez-Etayo et al. (2018), and our results are in complete agreement.

There is one discrepancy involving *B. abortus* Tulya, a biovar 3 strain that according to the literature (Alton et al., 1988) should be CO₂ dependent, but according to our analysis, it codes for a full-length CA II, thus being grouped with the CO₂-independent isolates. To solve this apparent puzzle, we plated a sample of *B. abortus* Tulya from our laboratory stock and determined its CO₂ dependence. Contrary to the original reference strain phenotype and in agreement with our *in silico* analysis, this isolate was indeed CO₂ independent. The complete *BaTulya* CAII was amplified by PCR from our strain and sequenced, confirming the published sequence. This strain originated from the collection kept in the Centro de Investigación y Tecnología Agroalimentaria de Aragón (CITA), Zaragoza, Spain, where it is also labeled as being CO₂ independent, suggesting that this is not the result of a contamination or selection of a CO₂-independent mutant in our hands.

As *Brucella* species code for two different CAs (Joseph et al., 2010), we repeated the analysis for the CA I CDSs. Although several isolates contain a polymorphism consisting of a 24-nt deletion between two 11-nt direct repeats or different SNPs (**Supplementary Figure S1**), there was no obvious correlation between the presence of these polymorphisms and CO₂ dependence. Pérez-Etayo et al. (2018) demonstrated that CA I from *B. abortus* strains 2308W, 292, and 544 is inactive, while that from *B. suis* strains 1330 and 513 is active, although it can only mediate CO₂ independence in complex media and in a rather prototrophic host. Comparison of *Bsuis*513CAI and *Babortus*2308WCAI reveals a difference of only one amino acid, the valine at position 74 being replaced by a glycine.

***Brucella* CO₂-Independent Spontaneous Mutants Present a Modified CA II Sequence**

Comparison of some of the CA II sequences of *B. abortus* biovar 1 CO₂-independent strains like 2308, S19, or NCTC 8038 with those of the other *Brucella* CO₂-dependent and independent isolates suggests that reversion of the CO₂ requirement is coincidental with the introduction of compensatory mutations able to reverse the initial frameshift described above. CO₂-independent mutants have been previously reported to appear at a low frequency (3×10^{-10}) in cultures of CO₂-dependent strains by subculturing *in vitro* in the absence of supplementary CO₂ (Marr and Wilson, 1950). We measured the frequency of the reversion in six CO₂-dependent strains from our laboratory collection, by growing duplicate cultures with or without CO₂. We first checked the phenotype of all the strains by streaking them in a BA that was incubated without added CO₂. All the strains but *B. abortus* Tulya, as reported above, failed to grow in these conditions, in agreement with the published phenotype.

TABLE 3 | Observed frequency of appearance of CO₂-independent mutants in different *Brucella* strains.

Strain	Frequency of mutants
<i>Brucella abortus</i> 292	2.72×10^{-8}
<i>B. abortus</i> 544	5.95×10^{-8}
<i>B. abortus</i> 86/8/59	1.14×10^{-9}
<i>B. abortus</i> A-579	2.29×10^{-10}
<i>Brucella ovis</i> 63/290	3.38×10^{-6}
<i>Brucella pinnipedialis</i> B2/94	5.5×10^{-6}

We then plated o/n cultures from the CO₂-dependent strains to obtain colonies grown at ambient atmosphere and calculated the frequency of revertants for those strains (**Table 3**). The *B. abortus* strains had a similar frequency to the one described by Mar and Wilson (1950), 10^{-8} to 10^{-10} , but *B. ovis* and *B. pinnipedialis* had a higher frequency of reversion, 10^{-6} . In an exploratory effort to identify a possible cause for these differences in mutation rates, we analyzed the presence and identity between strains of the most obvious proteins that could be involved in this phenotype, like DNA polymerases, MutT, MutS, and MutD. Blastp analysis showed that, in all the cases, the protein not only was present in all strains but also had a 100% identity, so we could not find any difference that could explain our results. Maybe the analysis of the frequency of reversion in more CO₂-dependent strains will reveal if this is a species, biovar, or even isolate phenotype. We selected a few revertants from each strain and amplified by PCR the CA I and CA II coding regions. The amplicons were then sequenced to determine if any compensatory mutation had appeared in those loci. In all cases, we found compensatory mutations in the same region, around nucleotides 333–343. All mutations in this hot spot resulted in full-length CA II proteins (**Figure 2**), or in the case of *B. pinnipedialis*, a C-to-T change that reverts the Leu-to-Pro substitution. In this case, we also found the insertion of a nucleotide triplet (CGC or CCG) at the hot spot, which results in the addition of an extra amino acid, either Ala113 or Arg113, that is, the same position where the extra codon in *Ba*2308CAII is located. Although some of the compensatory mutations appear several times, the most common situation was to find different mutations for the same sequence.

As expected, reversion of the CO₂ dependence phenotype did not produce any change in the CDSs of CA I, reinforcing the hypothesis that CA II plays the main role in CO₂ independence.

Structural Modeling of *Babortus*2308CAI and *Babortus*2308CAII

A single amino acid substitution, Val74 in *Bsuis*513CAI to Gly74 in *Babortus*2308WCAI, putatively renders the protein inactive, while the mutations in CA II in CO₂-dependent *Brucella* isolates do not affect the region where the active center is located, at the N-terminal part of the protein (**Figure 1B**). Moreover, a non-conservative Leu186Pro substitution, far from the active center, is enough to induce CO₂ dependence in the *B. pinnipedialis* strains analyzed. To better understand the effect of the observed mutations, a structural theoretical model of *Ba*2308CAI and *Ba*2308CAII was built with Phyre2. The modeled structures closely


```

301
A579      GTGGT GATGGG CCACGG GCGTTG CGGTGG CATCAAGG CGGCGCTCGACACTGAAAGCGC
A579mut1  GTGGT GATGGG CCACGG GCGTTG CGGTGG CATGGCGGC-GGCGCTCGACACTGAAAGCGC
A579mut2  GTGGT GATGGG CCACGG GCGTTG CGGTGG CATCAAGG CGGC-CTCGACACTGAAAGCGC
          *****

301
86/8/59   GTGGT GATGGG CCACGG GCGTTG CGGTGG CATCAAGG CGG--GCGCTCGACACTGAAAGC
86/8/59mut1 GTGGT GATGGG CCACGG GCGTTG CGGTGG CATCAAGG CGGCGGCGCTCGACACTGAAAGC
86/8/59mut2 GTGGT GATGGG CCACGG GCGTTG CGGTGG CATCAAGG CGG--GC-CTCGACACTGAAAGC
          *****

301
292       GTGGT GATGGG CCACGG GCGTTG CGGTGG CATCAAGG CGGCGCTCGACACTGAAAGCGC
292mut1   GTGGT GATGGG CCACGG GCGTTG CGGTGG CATCAAGG CGGC-CTCGACACTGAAAGCGC
292mut4   GTGGT GATGGG CCACGG GCGTTG CGGTGG CATCAAGG -CGGCGCTCGACACTGAAAGCGC
          *****

481
63/290    TCGATCCGCTATTGCTGGCTAATCTGCGCACTTTCCCTTG GCGTGGATATTCTGGAGAA
63_290mut01 TCGATCCGCTATTGCTGGCTAATCTGCGCACTTTCCCTTG -CGTGGATATTCTGGAGAA
63_290mut08 TCGATCCGCTATTGCTGGCTAATCTGCGCACTTTCCCT-GCGTGGATATTCTGGAGAA
63_290mut09 TCGATCCGCTATTGCTGGCTAATCTGCGCACTTTCCCTTG G-GTGGATATTCTGGAGAA
          *****

301
B2/94     GTGGT GATGGG CCACGG GCGTTG CGGTGG CATCAAGG ---GGCGCTCGACACTGAAAGC
B2/94mut1 GTGGT GATGGG CCACGG GCGTTG CGGTGG CATCAAGG CGGGGCGCTCGACACTGAAAGC
B2/94mut2 GTGGT GATGGG CCACGG GCGTTG CGGTGG CATCAAGG CGGGGCGCTCGACACTGAAAGC
          *****

541
B2/94     AAGGGCAAGCTCACCCGCATGGCGCATGGTTCGATATTTTGACCGGCGAATTGTGGGTG
B2/94mut1 AAGGGCAAGCTCACCTGCATGGCGCATGGTTCGATATTTTGACCGGCGAATTGTGGGTG
B2/94mut2 AAGGGCAAGCTCACCTGCATGGCGCATGGTTCGATATTTTGACCGGCGAATTGTGGGTG
          *****

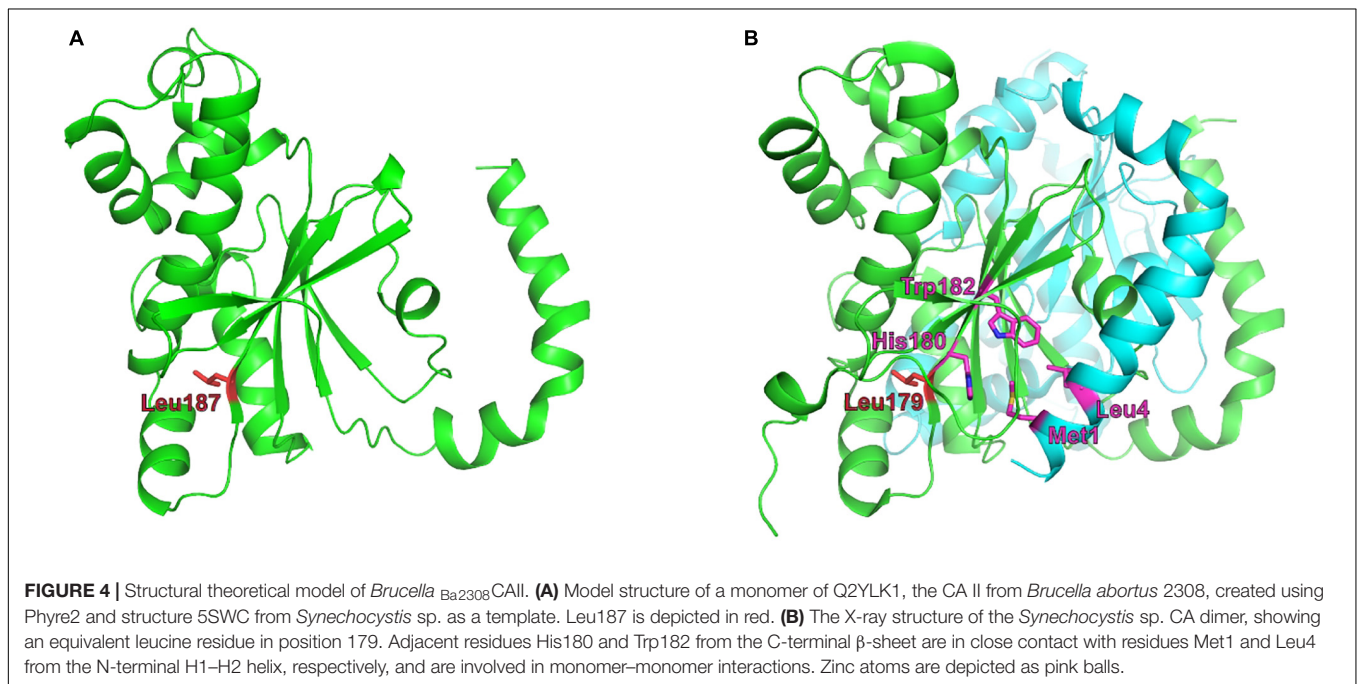
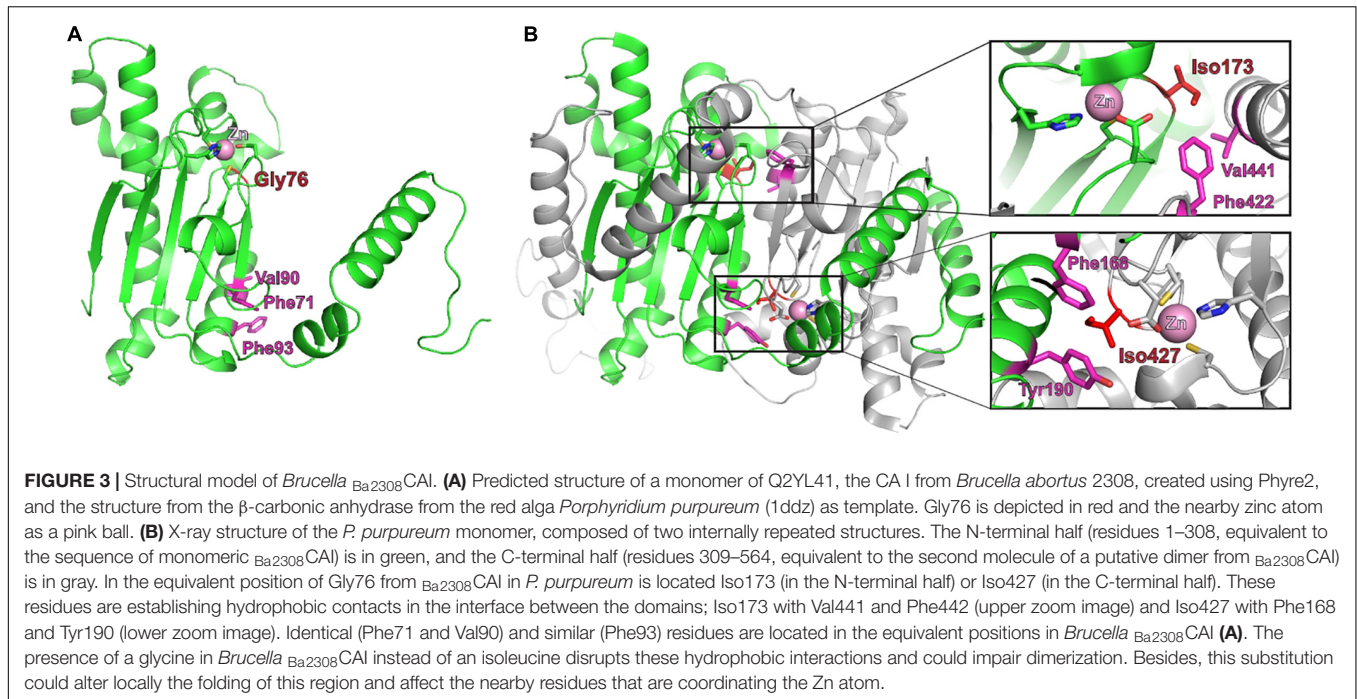
```

FIGURE 2 | Nucleotide changes in CA II from selected CO₂-independent mutants of different *Brucella* strains. Partial sequence of the regions where the original CO₂-dependent strains had the mutations that caused the defective phenotype (shown in red), and the changes observed after selection and sequencing of different spontaneous CO₂-independent mutants (shown in blue).

resembled those of other β -CAs that have been crystalized, displaying matches with a 100% confidence.

The closest structural homolog to Ba2308 CAI is 1DDZ, a β -CA from the red alga *Porphyridium purpureum* (Mitsubishi et al., 2000), with a 45% identity. Each 1DDZ monomer contains two internally repeated structures, each one homologous to Ba2308 CAI. Overlapping of the modeled structures shows how the mutated residue Gly76 lies in close proximity to the coordinated zinc atom and also to the dimer interface (Figure 3). In the

equivalent position of Val76 in Bsuis513 CAI, 1DDZ contains Ile173 or Ile427, both among the most hydrophobic of amino acids. These residues are establishing hydrophobic contacts in the interface between the domains: Iso173 with Val441 and Phe442 (upper zoom image) and Iso427 with Phe168 and Tyr190 (lower zoom image). Identical (Phe71 and Val90) and similar (Phe93) residues are located in the equivalent positions in *Brucella* Ba2308 CAI. The presence of a glycine in *Brucella* Ba2308 CAI instead of an isoleucine disrupts these hydrophobic interactions



and could impair dimerization. Besides, this substitution could locally alter the folding of this region and affect the nearby residues that are coordinating the Zn atom. In both cases, the structure and consequently the activity of the protein would be affected. Indeed, a Val-to-Gly substitution, located in the dimerization surface, was shown to interfere with dimerization of citrate synthase from *Thermoplasma acidophilum* (Kocabiyik and Erduran, 2000), not only reducing its catalytic activity (about 10-fold) but also decreasing its thermal and chemical stability.

The model structure obtained for Ba_{2308} CAII is shown in **Figure 4**, along with the dimer structure of the best hit obtained, 5SWC, showing a 29% of identity and 100% confidence. 5SWC is the β -CA CcaA from *Synechocystis* sp. PCC 6803. As Ba_{2308} CAII contains an extra codon, the residue highlighted in red, Leu187, is the equivalent residue to the Leu186Pro change that is present in the CO₂-dependent *B. pinnipedialis* strains.

In this structure, the protein crystallizes as a dimer, with the N-terminal arm composed of two α -helical segments (H1

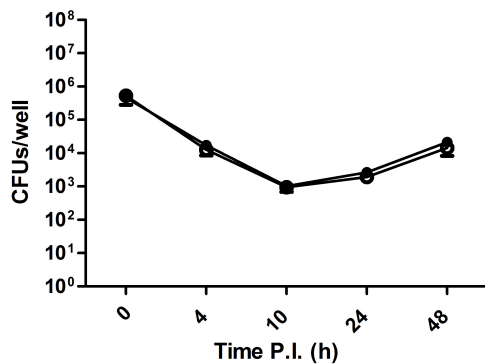


FIGURE 5 | Infection and intracellular viability assay of *Brucella abortus* in J774 mouse macrophages *in vitro*. J774 macrophages were infected with either *B. abortus* 292 or the CO₂-independent spontaneous mutant *B. abortus* 292mut1, at a multiplicity of infection (MOI) of 50. Samples from triplicate wells were obtained at 0, 4, 10, 24, and 48 h post infection and enumerated by dilution and plating. ●, *B. abortus* 292; ○, *B. abortus* 292mut1.

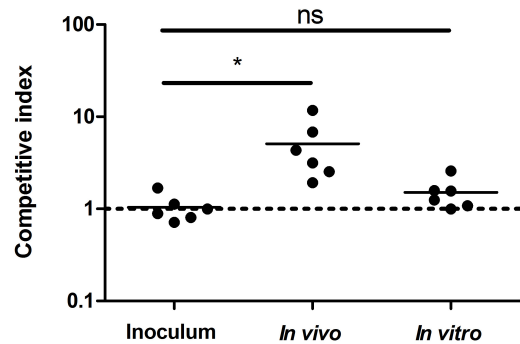


FIGURE 6 | Competitive index assay of a mixture of *Brucella abortus* 292 and its corresponding CO₂-independent spontaneous mutant *B. abortus* 292mut1. The competitive index was calculated by dividing the output ratio of mutant to wild-type bacteria by the input ratio of mutant to wild-type bacteria, in the two groups tested, regarding the original inoculum. Thus, for strains with the same fitness, the result should be 1. The differences between groups were analyzed by Student's two-tailed *t* test with significance set at **P* < 0.05. ns, non-significant.

and H2) that extend away from the rest of the molecule and make significant contacts with the last β -sheet with an adjacent monomer (in the case of Ba2308CAII His188 with Met1 and Trp191 with Leu4). This interaction between monomers has been determined as crucial for the establishment of the dimer (Cronk et al., 2001). In the case of *B. abortus* strains 86/8/59, 9-941, and 292, the premature stop would cause the complete loss of the C-terminal end of the protein, including the last β -sheet, involved in the formation of the dimer. *B. ovis* ATCC 25840 shows also a completely altered C-terminus, and although the new amino acid sequence would remain folded as a β -sheet, it shows a completely different amino acid composition that would prevent the establishment of the right molecular interactions between the adjacent monomers. Regarding the last mutation observed in CO₂-dependent strains, the SNP present in *B. pinnipedialis* strains M163/99/10, M292/94/1, and B2/94 causes a non-conservative amino acid substitution, Leu186Pro. The model predicts that this change will occur at the last β -sheet, in the area of interaction with the N-terminus of the adjacent monomer. Proline is an amino acid that confers an exceptional conformational rigidity and as such is a known disruptor of both α -helices and β -sheets. This being the case, this substitution is predicted to disrupt the dimerization of *Brucella* CA II.

Competitive Infection Assays

Strain 2308 is not only a CO₂-independent *Brucella* isolate but also one of the most widely used virulent challenge strains, while S19, also a CO₂-independent *Brucella* isolate, is an attenuated vaccine strain. *In vitro* cell assays using J774 macrophages did not detect any difference in virulence between a CO₂-dependent *B. abortus* 292 strain and its corresponding CO₂-independent revertant (Figure 5). Additionally, we could not find any report in the literature that suggests that the CO₂ dependence phenotype is related to virulence; however, there is one puzzling fact; despite the expected low frequency of a frameshift mutation, somehow, this mutation is fixed in several species and biovars of

Brucella. It is then reasonable to think of it as having a biological advantage in specific situations. CI assays have been used to reveal subtle differences in fitness between two strains, and intra-animal experiments help to minimize inherent inter animal biological variation and also improve the identification of mutations or isolates with reduced or improved competitive fitness within the host (Falkow, 2004). As this could be the case with Ba2308WCAII, we performed a CI experiment using *B. abortus* 292 and one of its CO₂-independent mutants, 292mut1. As a control, we grew the same initial mixture in BA plates that were incubated at 37°C with 5% CO₂, to know if any change in CI could be attributed to just the CO₂ concentration, or there was some other factor that could be attributed to growth within an animal. Results are shown in Figure 6. During the course of the experiments in mice, there was a significant enrichment of the strain carrying the truncated form of Ba2308WCAII *B. abortus* 292, when compared with the CO₂-independent revertant able to produce a complete active form of Ba2308WCAII. There was not a significant change in the ratio of both strains in liver or spleen, so the colony counts were combined in each mouse to show the ratio in that mice. At the same time, there was no significant enrichment/change in the ratio in cultures grown on plates. This suggests that inactivation of Ba292CAII has some fitness advantage *in vivo* and could eventually result in the displacement of its corresponding CO₂-independent counterpart. This hypothesis could explain why, despite the low frequency of mutation, CO₂-dependent strains appear on primary isolation. As there are some other species and biotypes of *Brucella* that are CO₂ dependent on primary isolation, we could infer that the fitness advantage is also present in those species and biotypes.

DISCUSSION

Diagnosis of brucellosis is usually achieved by serological detection in both animals and humans. This could be enough

to warrant the initiation of response measures, like the start of antibiotic therapy in humans or immobilization or sacrifice of animals. However, isolation, identification, and subtyping of brucellae not only are definitive proof of infection but also allow epidemiological surveillance. Depending on the laboratory, this process is carried out by a combination of classical and modern molecular methods. The classical typing methods consist in the phenotypic characterization of the isolates, using biochemical and immunological tests (CO₂ requirement; H₂S production; urease activity; agglutination with monospecific A, R, and M sera; growth on media with thionin or basic fuchsin; or sensitivity to erythritol), and susceptibility to lytic *Brucella* phages (Alton et al., 1988). These methods require culture of the bacteria, are usually time-consuming and laborious, and do not offer good discriminatory power. Moreover, in the last few years, the field has experienced a revolution with the advent of new molecular methods, resulting in the description of new species and a better understanding of the population structure of the genus *Brucella*. Thus, the classical methods are being replaced or complemented by modern molecular methods. These methods range from PCR detection systems targeting different loci (like *ery*, *bcs*p31, or IS711), which allow species and even biovar differentiation (Mayer-Scholl et al., 2010; López-Goñi et al., 2011), to the multilocus sequence analysis (MLSA) that has been successfully used to describe the phylogenetic relationships of isolates and the global population structure of the genus *Brucella* (Whatmore et al., 2016). More recently, with the advent of WGS and especially with the drop in sequencing prices, WGS has been proposed to be the new routine typing method, particularly in groups with a high degree of similarity at the biochemical or serological levels (Chattaway et al., 2017), like *Brucellaceae*. But these methods are still far from being routine in most brucellosis laboratories, particularly in developing countries, and the classical methods are still routinely used in reference laboratories. Although genomic information offers the potential to unveil most of the phenotypic traits in bacteria, there are still important attributes that are not evident in the genome sequence. Thus, there is a gap between the classical typing schemes and the molecular methods, and some features still cannot be attributed to any specific genetic trait. In the case of *Brucella*, host specificity is particularly interesting, as it is yet impossible to predict from the genome sequence. It is reasonable to think that as molecular typing improves, we should advance in closing the gaps between classical and molecular typing, and we would be able to predict the full virulence and host specificity of a given isolate by analyzing the genome content. We have started to address this gap by looking at the genomic differences between *Brucella* isolates regarding one of the classical tests for typing, namely, CO₂ requirement.

Brucella abortus biovars 1, 2, 3, and 4 and some isolates from biovar 9, as well as *B. ovis*, require an increased concentration of CO₂ for growth, as do most strains of *B. pinnipedialis*, but only some of *B. ceti*. We selected 10 *Brucella* strains, which have been sequenced and annotated and whose CO₂ dependence status was known, to construct a *Brucella* pangenome based on the *B. suis* 1330 genome annotation. This resulted in a collection of 3,496 CDSs. We next compared the distribution

of pseudogenes (as annotated in the databases) and absent genes with CO₂ dependence, resulting in only three candidate genes: Bru1_1050, which encodes for a multidrug resistance efflux pump; Bru1_1827, which encodes for CA II; and Bru2_1236, which encodes for an adenosylmethionine-8-amino-7-oxononanoate aminotransferase. The most obvious candidate was CA II, as it has been shown to be required to grow under ambient air in a number of microorganisms. To confirm our initial result, we extracted and aligned the DNA and amino acid sequences of CA II from an extended set of sequenced strains with a known CO₂ phenotype. Those strains that are able to grow in atmospheric concentrations of CO₂ carry a full-length copy of the protein, while those that are not contain truncated or mutated versions of the proteins. *Brucella* species also carry a second CA, CA I, but the polymorphisms found at both the DNA and protein levels do not allow us to infer CO₂ dependence. This result is in agreement with that reported by Pérez-Etayo et al. (2018) and Varesio et al. (2019) and further extends the range of strains tested.

A direct application of this result would be the determination of the CO₂ dependence status of any given strain by determining the sequence at the CA II locus. This is actually the case in *B. abortus* Tulya, where our analysis predicted that our stock should be CO₂ independent, as it was the original stock from CITA. Laboratory determination of the phenotype confirmed the *in silico* result. This approach could be used to determine or at least narrow down candidate genes for different phenotypes, obviously with monogenic traits being the easier to determine.

We have found three different mutations that caused dependence of added CO₂, two independent insertions (C337 and G523) that either cause a premature stop or change completely the C-terminus of the protein, and an SNP that changes a leucine for a proline in the last β -sheet. All bacterial β -CAs crystallized so far are active as dimers or tetramers and inactive as monomers, and all of them have the N-terminal α -helix arm that extends away from the rest of the molecule and makes significant contact with the last β -sheet of an adjacent monomer (Supuran, 2016). In all the cases observed in this work, the mutations do not affect the active site, but all of them potentially change the sequence and structure of the protein at the C-terminus, so the most obvious hypothesis is that it is the modified structure of the proteins that causes the loss of activity. Inactive *Brucella* CA II proteins either lack the last β -sheet completely or have a very different sequence composition that disrupts this last β -sheet. The substitution of a leucine by a proline in the β -sheet is a particular example of this latter case, as proline is known to be a very disruptive amino acid for both α -helix and β -sheet structures. As these contacts seem to be important for dimerization, we can hypothesize that all the mutations found in CA II will have a strong impact in the dimerization or multimerization of CA II that will remain as a monomer, losing its activity (which we have defined as that allowing growth in a normal atmosphere). But there is a caveat in this reasoning. We, as well as others (Pérez-Etayo et al., 2018), have been unable to obtain a full-length mutant of CA II, despite being able to obtain a CA I (both data not shown). Moreover, a transposon sequencing analysis shows that CA II is essential, at

least for *B. abortus* 2308 (Sternon et al., 2018). This experiment was apparently carried out without added CO₂, so the result is not unexpected. It would be interesting to know if, performed in the presence of 5–10% CO₂, they would have observed insertions only in the C-terminus of the protein, where the mutations in the natural CO₂-dependent isolates accumulate. This means that the C-terminal part of the protein still carries out at least some of its functions as a monomer. We have not found any information regarding the activity of β -CAs as monomers, but in the α -CA from *Thermovibrio ammonificans*, the destabilization of the tetramer by reduction of the cysteines results in the dissociation of the tetrameric molecule into monomers with lower activity and reduced thermostability. It seems reasonable to think that this is the case also for *Brucella* CA II.

Carbonic anhydrase II catalyzes the fixation of CO₂ with high efficiency when forming dimers, but the low efficiency of the carboxylation reaction when acting as a monomer would require the presence of higher amounts of CO₂.

A similar situation could be taking place in the case of CA I. Modeling of the structure of Babortus2308CAI allows us to hypothesize the role of the only residue of difference with Bsuis513CAI that has to be responsible for the absence of activity in the first one. Its localization close to the Zn atom and to the dimer interface probably results in the destabilization of the dimer, lowering, or abolishing its activity. However, it would be necessary to purify and characterized biochemically the monomers of both Babortus2308CAI and Babortus2308CAII to confirm our model.

These mutations can only be selected in high-CO₂ environments, like those present inside animals, where high CA II activity would be dispensable, as this atmosphere generates enough bicarbonate in solution as to fulfill the metabolic requirement of the bacteria (Nishimori et al., 2009). We have determined the frequency of appearance of CO₂-independent isolates, and although there is a huge variation between strains, it ranges from 10⁻⁶ to 10⁻¹⁰, as previously described. Despite their low frequency, somehow these mutations got selected in several species and biovars of *Brucella*, suggesting that they provide some biological advantage. To test this hypothesis, we performed a competitive assay both *in vitro* and *in vivo*. This assay resulted in a significant enrichment of the strain carrying an inactive CA in animals, but not in cultured plates. Pérez-Etayo et al. (2018) assayed the bacterial loads of *B. ovis* PA and *B. ovis* PA Tn7Ba2308WCAII in the spleens of BALB/c mice at 3 and 8 weeks post infection and found that there was no significant difference between a CO₂-dependent strain and its corresponding CO₂-independent strain at the level of multiplication in the mouse model. This apparent contradiction with our own results could be due to the different species used or to the different experiment used to test this hypothesis. When researchers try to determine subtle differences in fitness between two given strains, a competitive assay has a higher discrimination power (Eekels et al., 2012; Shames et al., 2017), as any effect is amplified over time. Although the ultimate reason behind this

competitive advantage is currently unknown, it would explain why some strains and biovars of *Brucella* are dependent of CO₂ in primary isolation, despite the low frequency of mutation. It is also noteworthy that this phenotype is only observed in certain species and biovars, suggesting that the competitive advantage of the CA II mutants only applies to a subset of host/pathogen pairs. As CA II is essential, the mutant strains still would have to produce the protein, and thus, the metabolic gain should be negligible for them. Another possibility would be that the dimer form of the enzyme is too active in a high-CO₂ environment and causes a deleterious acidification in the bacteria. By evolving this sophisticated system that reversibly alters the dimerization state of the protein, *Brucella* is able to adjust to the different requirements encountered during its biological cycle.

DATA AVAILABILITY STATEMENT

All datasets generated for this study are included in the article/**Supplementary Material**.

ETHICS STATEMENT

The animal study was reviewed and approved by the Cantabria University Institutional Laboratory Animal Care and Use Bioethics Committee.

AUTHOR CONTRIBUTIONS

FS conceived and coordinated the study, conducted the bacteriology work, and wrote the manuscript. JG analyzed the data and wrote the manuscript. YO, CG-R, AS, and BA-R conducted the bacteriology work. All authors interpreted the data, corrected the manuscript, and approved the content for publication.

FUNDING

This work was supported by grants BFU2011-25658 from the Spanish Ministry of Science and Innovation, and by grant 55JU07.64661 from the University of Cantabria to FS. BA-R was supported by a Scholarship received from DGAPA-UNAM PASPA program. The authors want to acknowledge help from María J. Lucas and Elena Cabezon in the drawing and interpretation of crystallographic data.

SUPPLEMENTARY MATERIAL

The Supplementary Material for this article can be found online at: <https://www.frontiersin.org/articles/10.3389/fmicb.2019.02751/full#supplementary-material>

REFERENCES

- Aguilera, J., Van Dijken, J. P., De Winde, J. H., and Pronk, J. T. (2005). Carbonic anhydrase (Nce103p): an essential biosynthetic enzyme for growth of *Saccharomyces cerevisiae* at atmospheric carbon dioxide pressure. *Biochem. J.* 391, 311–316. doi: 10.1042/bj20050556
- Alton, G. G., Jones, L. M., Angus, R. D., and Verger, J. M. (1988). *Techniques for the Brucellosis Laboratory*. Paris: INRA.
- Chattaway, M. A., Schaefer, U., Tewolde, R., Dallman, T. J., and Jenkins, C. (2017). Identification of *Escherichia coli* and *Shigella* species from Whole-Genome sequences. *J. Clin. Microbiol.* 55, 616–623. doi: 10.1128/JCM.01790-16
- Crasta, O. R., Folkerts, O., Fei, Z., Mane, S. P., Evans, C., Martino-Catt, S., et al. (2008). Genome sequence of *Brucella abortus* vaccine strain s19 compared to virulent strains yields candidate virulence genes. *PLoS One* 3:e2193. doi: 10.1371/journal.pone.0002193
- Cronk, J. D., Endrizzi, J. A., Cronk, M. R., O'Neill, J. W., and Zhang, K. Y. J. (2001). Crystal structure of *E. coli* β -carbonic anhydrase, an enzyme with an unusual pH-dependent activity. *Protein Sci.* 10, 911–922. doi: 10.1110/ps.46301
- Duncan, J. T. (1928). The identification of *Brucella abortus* from human sources. *Trans. R. Soc. Trop. Med. Hyg.* 22, 269–272. doi: 10.1016/S0035-9203(28)90099-1
- Eekels, J. J., Pasternak, A. O., Schut, A. M., Geerts, D., Jeeninga, R. E., and Berkhout, B. (2012). A competitive cell growth assay for the detection of subtle effects of gene transduction on cell proliferation. *Gene Ther.* 19, 1058–1064. doi: 10.1038/gt.2011.191
- Falkow, S. (2004). Molecular Koch's postulates applied to bacterial pathogenicity—a personal recollection 15 years later. *Nat. Rev. Microbiol.* 2, 67–72. doi: 10.1038/nrmicro799
- Foster, G., Jahans, K. L., Reid, R. J., and Ross, H. M. (1996). Isolation of *Brucella* species from cetaceans, seals and an otter. *Vet. Rec.* 138, 583–586. doi: 10.1136/vr.138.24.583
- Foster, J. T., Beckstrom-Sternberg, S. M., Pearson, T., Beckstrom-Sternberg, J. S., Chain, P. S., Roberto, F. F., et al. (2009). Whole-genome-based phylogeny and divergence of the genus *Brucella*. *J. Bacteriol.* 191, 2864–2870. doi: 10.1128/JB.01581-08
- Garin-Bastuji, B., Mick, V., Le Carrou, G., Allix, S., Perrett, L. L., Dawson, C. E., et al. (2014). Examination of taxonomic uncertainties surrounding *Brucella abortus* bv. 7 by phenotypic and molecular approaches. *Appl. Environ. Microbiol.* 80, 1570–1579. doi: 10.1128/AEM.03755-13
- Gladstone, G. P., Fildes, P., and Richardson, G. M. (1935). Carbon dioxide as an essential factor in the growth of bacteria. *Br. J. Exp. Pathol.* 16, 335–348.
- Hashimoto, M., and Kato, J. (2003). Indispensability of the *Escherichia coli* carbonic anhydrases YadF and CynT in cell proliferation at a low CO₂ partial pressure. *Biosci. Biotechnol. Biochem.* 67, 919–922. doi: 10.1271/bbb.67.919
- Hu, B., Gary, X., Chien-Chi, L., Shawn, R. S., and Patrick, S. G. C. (2011). Pathogen comparative genomics in the next-generation sequencing era: genome alignments, pangenomics and metagenomics. *Brief. Funct. Genomics* 10, 322–333. doi: 10.1093/bfpg/elfr042
- Joseph, P., Ouahrani-Bettache, S., Montero, J. L., Nishimori, I., Minakuchi, T., Vullo, D., et al. (2011). A new β -carbonic anhydrase from *Brucella suis*, its cloning, characterization, and inhibition with sulfonamides and sulfamates, leading to impaired pathogen growth. *Bioorgan. Med. Chem.* 19, 1172–1178. doi: 10.1016/j.bmc.2010.12.048
- Joseph, P., Turtaut, F., Ouahrani-Bettache, S., Montero, J. L., Nishimori, I., Minakuchi, T., et al. (2010). Cloning, characterization, and inhibition studies of a beta-carbonic anhydrase from *Brucella suis*. *J. Med. Chem.* 53, 2277–2285. doi: 10.1021/jm901855h
- Kelley, L. A., Mezulis, S., Yates, C. M., Wass, M. N., and Sternberg, M. J. E. (2015). The Phyre2 web portal for protein modeling, prediction and analysis. *Nat. Protoc.* 10, 845–858. doi: 10.1038/nprot.2015.053
- Kocabiyyik, S., and Erduran, I. (2000). The effect of valine substitution for glycine in the dimer interface of citrate synthase from thermoplasma acidophilum on stability and activity. *Biochem. Biophys. Res. Commun.* 275, 460–465. doi: 10.1006/bbrc.2000.3310
- Kusian, B., Sultemeyer, D., and Bowien, B. (2002). Carbonic anhydrase is essential for growth of *Ralstonia eutropha* at ambient CO₂ concentrations. *J. Bacteriol.* 184, 5018–5026. doi: 10.1128/jb.184.18.5018-5026.2002
- Larkin, M. A., Blackshields, G., Brown, N. P., Chenna, R., McGettigan, P. A., McWilliam, H., et al. (2007). Clustal W and clustal X version 2.0. *Bioinformatics* 23, 2947–2948. doi: 10.1093/bioinformatics/btm404
- López-Goní, I., García-Yoldi, D., Marín, C. M., de Miguel, M. J., Barquero-Calvo, E., Guzmán-Verri, C., et al. (2011). New Bruce-ladder multiplex PCR assay for the biovar typing of *Brucella suis* and the discrimination of *Brucella suis* and *Brucella canis*. *Vet. Microbiol.* 154, 152–155. doi: 10.1016/j.vetmic.2011.06.035
- Marcus, E. A., Moshfegh, A. P., Sachs, G., and Scott, D. R. (2005). The periplasmic alpha-carbonic anhydrase activity of *Helicobacter pylori* is essential for acid acclimation. *J. Bacteriol.* 187, 729–738. doi: 10.1128/jb.187.2.729-738.2005
- Marr, A. G., and Wilson, J. B. (1950). Genetic aspects of the added carbon dioxide requirements of *Brucella abortus*. *Proc. Soc. Exp. Biol. Med.* 75, 438–440. doi: 10.3181/00379727-75-18224
- Mayer-Scholl, A., Draeger, A., Göllner, C., Scholz, H. C., and Nöckler, K. (2010). Advancement of a multiplex PCR for the differentiation of all currently described *Brucella* species. *J. Microbiol. Methods* 80, 112–114. doi: 10.1016/j.mimet.2009.10.015
- Merlin, C., Masters, M., McAteer, S., and Coulson, A. (2003). Why is carbonic anhydrase essential to *Escherichia coli*? *J. Bacteriol.* 185, 6415–6424. doi: 10.1128/jb.185.21.6415-6424.2003
- Mitsuhashi, S., Mizushima, T., Yamashita, E., Yamamoto, M., Kumasaka, T., Moriyama, H., et al. (2000). X-ray structure of beta-carbonic anhydrase from the red alga, *Porphyridium purpureum*, reveals a novel catalytic site for CO(2) hydration. *J. Biol. Chem.* 275, 5521–5526. doi: 10.1074/jbc.275.8.5521
- Mitsuhashi, S., Ohnishi, J., Hayashi, M., and Ikeda, M. (2004). A gene homologous to beta-type carbonic anhydrase is essential for the growth of *Corynebacterium glutamicum* under atmospheric conditions. *Appl. Microbiol. Biotechnol.* 63, 592–601. doi: 10.1007/s00253-003-1402-8
- Nishimori, I., Minakuchi, T., Onishi, S., Vullo, D., Cecchi, A., Scozzafava, A., et al. (2009). Carbonic anhydrase inhibitors. Cloning, characterization and inhibition studies of the cytosolic isozyme III with anions. *J. Enzyme Inhib. Med. Chem.* 24, 70–76. doi: 10.1080/14756360801907143
- O'Callaghan, D., and Whatmore, A. M. (2011). *Brucella* genomics as we enter the multi-genome era. *Brief. Funct. Genomics* 10, 334–341. doi: 10.1093/bfpg/elfr026
- Pallen, M. J., and Wren, B. W. (2007). Bacterial pathogenomics. *Nature* 449, 835–842. doi: 10.1038/nature06248
- Pappas, G., Papadimitriou, P., Akritidis, N., Christou, L., and Tsianos, E. V. (2006). The new global map of human brucellosis. *Lancet Infect. Dis.* 6, 91–99. doi: 10.1016/s1473-3099(06)70382-6
- Pérez-Etayo, L., de Miguel, M. J., Conde-Álvarez, R., Muñoz, P. M., Khames, M., Iriarte, M., et al. (2018). The CO₂-dependence of *Brucella ovis* and *Brucella abortus* biovars is caused by defective carbonic anhydrases. *Vet. Res.* 49:85. doi: 10.1186/s13567-018-0583-1
- Philippe, N., Alcaraz, J. P., Coursange, E., Geiselmann, J., and Schneider, D. (2004). Improvement of pCVD442, a suicide plasmid for gene allele exchange in bacteria. *Plasmid* 51, 246–255. doi: 10.1016/j.plasmid.2004.02.003
- Rognes, T., Flouri, T., Nichols, B., Quince, C., and Mahé, F. (2016). VSEARCH: a versatile open source tool for metagenomics. *PeerJ* 4:e2584. doi: 10.7717/peerj.2584
- Sangari, F. J., Cayón, A. M., Seoane, A., and García-Lobo, J. M. (2010). *Brucella abortus ure2* region contains an acid-activated urea transporter and a nickel transport system. *BMC Microbiol.* 10:107. doi: 10.1186/1471-2180-10-107
- Sangari, F. J., García-Lobo, J. M., and Agüero, J. (1994). The *Brucella abortus* vaccine strain B19 carries a deletion in the erythritol catabolic genes. *FEMS Microbiol. Lett.* 121, 337–342. doi: 10.1016/0378-1097(94)90314-x
- Sangari, F. J., Seoane, A., Rodríguez, M. C., Agüero, J., and García Lobo, J. M. (2007). Characterization of the urease operon of *Brucella abortus* and assessment of its role in virulence of the bacterium. *Infect. Immun.* 75, 774–780. doi: 10.1128/IAI.01244-06
- Shames, S. R., Liu, L., Havey, J. C., Schofield, W. B., Goodman, A. L., and Roy, C. R. (2017). Multiple *Legionella pneumophila* effector virulence phenotypes revealed through high-throughput analysis of targeted mutant libraries. *Proc. Natl. Acad. Sci. U. S. A.* 114, E10446–E10454. doi: 10.1073/pnas.1708553114
- Smith, K. S., Jakubczik, C., Whittam, T. S., and Ferry, J. G. (1999). Carbonic anhydrase is an ancient enzyme widespread in prokaryotes. *Proc. Natl. Acad. Sci. U.S.A.* 96, 15184–15189. doi: 10.1073/pnas.96.26.15184

- Sternon, J. F., Godessart, P., Gonçalves de Freitas, R., Van der Henst, M., Poncin, K., Francis, N., et al. (2018). Transposon sequencing of *Brucella abortus* uncovers essential genes for growth in vitro and inside macrophages. *Infect. Immun.* 86:e00312-18. doi: 10.1128/IAI.00312-18
- Suárez-Esquivel, M., Ruiz-Villalobos, N., Castillo-Zeledón, A., Jiménez-Rojas, C., Roop II, R. M., Comerci, D. J., et al. (2016). *Brucella abortus* strain 2308 wisconsin genome: importance of the definition of reference strains. *Front. Microbiol.* 7:1557. doi: 10.3389/fmicb.2016.01557
- Supuran, C. T. (2016). Structure and function of carbonic anhydrases. *Biochem. J.* 473, 2023–2032. doi: 10.1042/BCJ20160115
- Supuran, C. T. (2018). Carbonic anhydrases and metabolism. *Metabolites* 8:E25. doi: 10.3390/metabo8020025
- Varesio, L. M., Willett, J. W., Fiebig, A., and Crosson, S. (2019). A carbonic anhydrase pseudogene sensitizes select *Brucella* lineages to low CO₂ tension. *J. Bacteriol.* 201:e00509-19. doi: 10.1128/JB.00509-19
- Wattam, A. R., Foster, J. T., Mane, S. P., Beckstrom-Sternberg, S. M., Beckstrom-Sternberg, J. M., Dickerman, A. W., et al. (2014). Comparative phylogenomics and evolution of the Brucellae reveal a path to virulence. *J. Bacteriol.* 196, 920–930. doi: 10.1128/JB.01091-13
- Whatmore, A. M., Koylass, M. S., Muchowski, J., Edwards-Smallbone, J., Gopaul, K. K., and Perrett, L. L. (2016). Extended multilocus sequence analysis to describe the global population structure of the genus *Brucella*: phylogeography and relationship to biovars. *Front. Microbiol.* 7:2049. doi: 10.3389/fmicb.2016.02049
- Wilson, G. S. (1931). The gaseous requirements of *Br. abortus* (Bovine type). *Brit. J. Exper. Path.* 12, 88–92.
- Conflict of Interest:** The authors declare that the research was conducted in the absence of any commercial or financial relationships that could be construed as a potential conflict of interest.

Copyright © 2019 García Lobo, Ortiz, González-Riancho, Seoane, Arellano-Reynoso and Sangari. This is an open-access article distributed under the terms of the Creative Commons Attribution License (CC BY). The use, distribution or reproduction in other forums is permitted, provided the original author(s) and the copyright owner(s) are credited and that the original publication in this journal is cited, in accordance with accepted academic practice. No use, distribution or reproduction is permitted which does not comply with these terms.



Taxonomic Organization of the Family *Brucellaceae* Based on a Phylogenomic Approach

Sébastien O. Leclercq, Axel Cloeckeaert and Michel S. Zygmunt*

INRA, Infectiologie et Santé Publique, Université de Tours, Nouzilly, France

OPEN ACCESS

Edited by:

Dongsheng Zhou,
Beijing Institute of Microbiology
and Epidemiology, China

Reviewed by:

Jens Andre Hammerl,
Federal Institute for Risk Assessment
(BfR), Germany
Jeffrey T. Foster,
Northern Arizona University,
United States

*Correspondence:

Michel S. Zygmunt
michel.zygmunt@inrae.fr

Specialty section:

This article was submitted to
Infectious Diseases,
a section of the journal
Frontiers in Microbiology

Received: 02 October 2019

Accepted: 20 December 2019

Published: 30 January 2020

Citation:

Leclercq SO, Cloeckeaert A and
Zygmunt MS (2020) Taxonomic
Organization of the Family
Brucellaceae Based on
a Phylogenomic Approach.
Front. Microbiol. 10:3083.
doi: 10.3389/fmicb.2019.03083

Deciphering the evolutionary history of pathogenic bacteria and their near neighbors may help to understand the genetic or ecological bases which led to their pathogenic behavior. The *Brucellaceae* family comprises zoonotic pathogenic species belonging to the genus *Brucella* as well as the environmental genus *Ochrobactrum* for which some species are considered as opportunistic pathogens. Here, we used a phylogenomic approach including a set of 145 *Brucellaceae* genomes representative of the family diversity and more than 40 genomes of the order *Rhizobiales* to infer the taxonomic relationships between the family's species. Our results clarified some unresolved phylogenetic ambiguities, conducting to the exclusion of *Mycoplana* spp. out of the family *Brucellaceae* and the positioning of all *Brucella* spp. as a single genomic species within the current *Ochrobactrum* species diversity. Additional analyses also revealed that *Ochrobactrum* spp. separate into two clades, one comprising mostly environmental species while the other one includes the species considered as pathogens (*Brucella* spp.) or opportunistic pathogens (mainly *O. anthropi*, *O. intermedium*, and *O. pseudintermedium*). Finally, we show that *O. intermedium* is undergoing a beginning of genome reduction suggestive of an ongoing ecological niche specialization, and that some lineages of *O. intermedium* and *O. anthropi* may shift toward an adaption to the human host.

Keywords: *Brucella*, *Ochrobactrum*, *Rhizobiales*, *Mycoplana*, phylogenomic reconstruction

INTRODUCTION

The *Brucellaceae* is a family of Gram negative bacteria, member of the order *Rhizobiales* within the class *Alphaproteobacteria*. The family was named after the genus *Brucella*, a facultative intracellular pathogen responsible for the zoonotic disease brucellosis, which causes major economical burden in livestock and human health concerns worldwide (Ficht, 2010; Garin-Bastuji et al., 2014). First described *Brucella* species were specifically associated with livestock animals, such as sheep and goats for *B. melitensis*, cattle for *B. abortus*, and pigs for *B. suis*, in which they can cause abortions and other reproductive diseases. These species are highly transmissible to humans through direct contacts with infected animals, aerosols, or consumption of raw-milk dairy products, and can produce chronic, debilitating infections. Other pathogenic *Brucella* species were later described, such as *B. canis* causing infection in dogs and which is also pathogenic in humans, and *B. ovis* causing epididymitis in rams (Buddle, 1956; Carmichael and Bruner, 1968). Other species have been isolated from wildlife and consist in their order of description of (i) *B. neotomae* isolated

from rodents (Stoener and Lackman, 1957), (ii) *B. ceti* and *B. pinnipedialis* isolated from marine mammals (Foster et al., 2007), (iii) *B. microti* initially isolated from the common vole but later found in a wider variety of animals such as red foxes, wild boar and even frogs (Jay et al., 2018; Scholz et al., 2008b), (iv) *B. papionis* isolated from baboons (Whatmore et al., 2014), and (v) *B. vulpis* isolated from red foxes (Scholz et al., 2016). More genetically distant *Brucella* strains comprising several potential new species, have been also reported (Tiller et al., 2010; Eisenberg et al., 2012, 2016). To date only one species of this group of strains has validly been published as *B. inopinata*, and consists of a single human isolate for which the animal or environmental reservoir has not yet been identified (De et al., 2008; Scholz et al., 2010). The pathogenic status for humans of the newly described wildlife or environmental species is currently not well understood although some human clinical isolates with a similar genetic background have been reported (Sohn et al., 2003; McDonald et al., 2006; Scholz et al., 2010; Tiller et al., 2010; Cloeckert et al., 2011). One of the striking specificity of the *Brucella* genus is its extreme homogeneity at the genetic level, with more than 90% DNA-DNA hybridization between species (Verger et al., 1985). Despite this lack of diversity, the phylogenetic relationship between species was extensively investigated using various genetic tools and more recently with the availability of whole-genome sequences, and are now well resolved (Foster et al., 2009; Wattam et al., 2014; Al Dahouk et al., 2017). The current classification includes 12 *Brucella* species commonly classified as ‘classical’ or ‘atypical’, depending on their phenotypical characteristics and their phylogenetic relationships (Scholz et al., 2018).

The other well-studied genus in the family *Brucellaceae* is *Ochrobactrum*. There are currently 18 *Ochrobactrum* species described, with the recent re-classification of *O. lupini* as an *O. anthropi* synonym (Gazolla Volpiano et al., 2019), which are mostly considered as environmental bacteria. For example, *O. tritici*, *O. oryzae*, and *O. cystisi* were first isolated from plant rhizosphere (Lebuhn et al., 2000; Tripathi et al., 2006; Zurdo-Pineiro et al., 2007), *O. anthropi*, *O. grignonense*, *O. intermedium* can be isolated from bulk soil (Lebuhn et al., 2000; Scholz et al., 2008a), while the type strain of *O. thiophenivorans* was isolated from wastewater (Kämpfer et al., 2007). Nonetheless, some few species, such as *O. anthropi*, *O. intermedium*, *O. pseudintermedium*, *O. haematophilum*, were initially isolated from human clinical cases (Holmes et al., 1988; Velasco et al., 1998; Kämpfer et al., 2007, 2008; Teyssier et al., 2007) and among them the two first seem to be the main species involved in opportunistic human infections (Teyssier et al., 2005). The other members of the family *Brucellaceae* family are the more distant *Pseudochrobactrum*, *Paenochrobactrum*, *Falsochrobactrum*, *Mycoplana* and *Daeguia* genera, composed of four, three, two, two, and one species, respectively (Yoon et al., 2008; Kämpfer et al., 2014; Kämpfer and Glaeser, 2015; Urakami and Segers, 2015; Sun et al., 2019). Although *Paenochrobactrum*, *Pseudochrobactrum*, and *Falsochrobactrum* genera seem to be true *Brucellaceae*, the inclusion of the two latter genera in the family is still a matter of debate (Kämpfer and Glaeser, 2015). The phylogenetic relationships between *Brucellaceae*

species have been much less thoroughly investigated than those belonging strictly to the genus *Brucella*, and most studies relied on the comparison of the small subunit 16S rRNA or the *recA* gene. The most comprehensive analysis of *Brucellaceae* species to date, that included more than one hundred strains, showed that the use of these single markers results in different tree topologies depending on the locus and the phylogenetic reconstruction algorithm, and with low to very low branching support throughout the topology (Scholz et al., 2008a). Such lack of resolution was confirmed by a number of other studies which each reported a unique tree topology using the same markers (Teyssier et al., 2007; Huber et al., 2009; Kämpfer et al., 2013, 2015; Chai et al., 2015; Gazolla Volpiano et al., 2019; Krzyżanowska et al., 2019). Nonetheless, a striking common observation of these various studies is that the genus *Brucella* was consistently embedded within the *Ochrobactrum* genus diversity, although no definitive conclusion about the taxonomic status of *Brucella* spp. could be drawn because of the underlying lack of phylogenetic resolution. Limited multilocus sequence typing (MLST) or Internal Transcribed Spacer (ITS) region-based analyses were also performed but were hampered by a small set of genes, a small set of species, or poorly supported branching, and still resulted in conflicting results (Zurdo-Pineiro et al., 2007; Aujoulat et al., 2014; Burygin et al., 2019; Gazolla Volpiano et al., 2019; Krzyżanowska et al., 2019). More recently, whole genome phylogenetic studies started to emerge but generally focused on a limited number of isolates of few species and could not provide a comprehensive view of the phylogenetic relationships at the family level or even at the *Ochrobactrum* genus level (Gazolla Volpiano et al., 2019; Krzyżanowska et al., 2019). Finally, the question of the *Brucellaceae* positioning among the *Rhizobiales* order have not been thoroughly investigated to date. Depending on the studies, the *Brucellaceae* family is a sister group of the *Bartonellaceae*, the *Rhizobiaceae*, or the *Phyllobacteriaceae* (Gupta and Mok, 2007; Scholz et al., 2008a; Kämpfer et al., 2015). In the present study, the taxonomic organization of the *Brucellaceae* genera and their species among the *Rhizobiales* order was determined at the genomic scale using a representative sample of genome sequences available in GenBank, and the inter-relationship between members of the family *Brucellaceae* was investigated using a comprehensive phylogenomic analysis including most GenBank genomes and newly sequenced isolates.

MATERIALS AND METHODS

Genome Sequences

The 101 non-*Brucella* *Brucellaceae* genomes available in the GenBank assembly summary file as of 07/14/2019 were downloaded from the NCBI FTP repository¹ in fasta format. Since almost 800 *Brucella* genomes were available at the time of this study and that the phylogenomic organization of the genus was already thoroughly investigated before (Wattam et al., 2014; Al Dahouk et al., 2017), only 12 genomes spanning the diversity of the classical and non-classical *Brucella* species were

¹ftp.wip.ncbi.nlm.nih.gov/genomes/genbank

used in our analyses (**Supplementary Table S1**). A set of 43 diverse non-*Brucellaceae* *Rhizobiales* genomes listed as ‘reference’ or ‘representative’ genomes in the NCBI database were also downloaded, as well as the genome of two *Caulobacteriales* (*Caulobacter vibrioides* and *Parvularcula bermudensis*) to serve as outgroups. GenBank assembly identifiers of all downloaded genomes are given in **Supplementary Table S1**. Additionally, the genomes of 32 *Ochrobactrum* spp. isolates were sequenced and added to the analysis. For the 32 isolates, bacterial DNA was extracted with DNeasy Blood & Tissue kit from QIAGEN. Genome sequencing was performed by Genoscreen (Lille, France) on an Illumina MiSeq apparatus (paired end 250 bp), with an average of 60x coverage per genome, except for the *Ochrobactrum* sp. strain Kaboul genome which was sequenced on a Pacific Bioscience SMRT device. Resulting reads were quality trimmed with Trimmomatic v.0.33 (Bolger et al., 2014) and assembled using the Spades v.3.11.1 assembly software (Bankevich et al., 2012). Information and accession/assembly number of these newly sequenced genomes are given in **Supplementary Table S2**.

Phylogenomic Analyses

All genomic nucleotide sequences were first annotated with PROKKA 1.12 (Seemann, 2014) using the same parameters, i.e., default parameters with no search of ribosomal and transfer RNA, to ensure consistent ORF detection among all sequences. At this stage, the genome sequence of *O. anthropi* SUBG007 was excluded from further analysis because of an excessive number of very short predicted proteins, suggesting a poor assembly quality. The remaining annotated proteomes were then used to create two datasets. Dataset 1 included all non-*Brucellaceae* *Rhizobiales* proteomes, the two *Caulobacteriales* proteomes, and 25 *Brucellaceae* proteomes representative of the family diversity. Dataset 2 included all downloaded and locally sequenced *Brucellaceae* proteomes as well as four other *Rhizobiales* proteomes to serve as outgroups. Proteomes of *Bartonella* species were not selected as outgroups despite being the closest *Brucellaceae*’s family because their highly reduced genomes would lower the number of proteins shared with the *Brucellaceae* and reduce the power of the analysis. Protein orthology relationships were inferred for both datasets independently using the OrthoMCL pipeline (Li et al., 2003) based on all-against-all BlastP hits with an *e*-value of 10^{-20} . Among the 20,319 and 16,717 orthology groups returned, respectively 145 and 195 were retained because they included only orthologs (detected only once in each proteome) and were present in 100% and at least 95% of all proteomes, including all outgroups. We used 95% ortholog prevalence threshold for the *Brucellaceae* analysis because this dataset included a number of genomes originating from metagenomic data (**Supplementary Table S1**) for which some conserved genomic regions were missing. Proteins of each orthogroup were aligned independently using MAFFT v.7.310 (Katoh and Standley, 2013) with the L-INS-I method and the resulting alignments were concatenated in a single large alignment for each dataset, of 78512 and 79,793 residues respectively, in which missing proteins in some orthogroups were replaced by tracks of gaps. To select the

model of protein evolution that best fitted our two datasets, we performed a PROTTEST 3.4.2 preanalysis (Darriba et al., 2011). The program returned the LG model (Le and Gascuel, 2008) with a gamma model of rate heterogeneity, a proportion of invariable sites, and an empirical residue frequency as the best model for both datasets. RAXML v8.2.11 (Stamatakis, 2006) was used to compute a maximum likelihood tree for each concatenated alignment, using the rapid bootstrap algorithm with the protein model returned by the PROTTEST analysis (GAMMAILGF) and 100 bootstraps. Additional phylogenomic reconstructions were computed to test the positioning of *Falsochrobactrum* spp. genomes within the resulting trees. Each reconstruction was performed on the same selection of 25 *Brucellaceae* genomes used in Dataset 1 (and the genome of *Mesorhizobium loti* as an outgroup), for which *F. ovis* genome, *F. shanghaiense* genome, or none were discarded, respectively. Trees were calculated for these three combinations using each of the 145 and 195 orthogroups alignments obtained from Dataset 1 (*Rhizobiales* analysis) and Dataset 2 (*Brucellaceae* analysis), with RaxML and the same parameters as in the two first calculations. All trees were displayed and annotated using the iTOL v.4 web interface (Letunic and Bork, 2019).

16S rRNA Sequence Alignment Analysis

The 16S rRNA sequence was extracted from each *Brucellaceae* genome used in Dataset 1 and were completed with 15 16S rRNA sequences from type strains of all *Brucellaceae* species with no genome available, downloaded from NCBI. The sequence of some other *Rhizobiales* were also added for comparison purposes. Pooled fasta were aligned using MUSCLE (Edgar, 2004) with default parameters using Ugene v.1.30 (Okonechnikov et al., 2012). The alignment was manually inspected and unexpectedly similar sequence stretches found in phylogenetically distant strains were considered as hallmarks of past recombination events.

gANI Analysis

All *Brucellaceae* annotated genomes from Dataset 2 were subjected to a pairwise gANI calculation using ANIcalculator v.1 (Varghese et al., 2015) with rRNA genes excluded. As recommended in Varghese et al. (2015), all genome pairs with a gANI value > 96.5 were considered belonging to the same species.

Core and Pan-Proteome Analysis

Core and pan proteomes were computed independently on *Brucellaceae* phylogenetic clades including at least five isolates and corresponding to species according to the gANI criterion. Five genomes of *O. intermedium*, 10 genomes of *O. anthropi* and 4 genomes of *O. pseudogrignone* clades were excluded from the analysis because they were reconstructed from metagenomic sequencing and lacked large core-genome regions, which resulted in inconsistent results. Additionally, no contig of strain BH3 (*O. pituitosum* clade) matched the second chromosome of *Ochrobactrum*, suggesting incomplete sequencing. This genome was therefore also excluded from the analysis. Calculations were performed using a in-house procedure (detailed below)

and were then confirmed using the Roary software (Page et al., 2015) with a 95% blastp minimum identity, and genes defined as core when present in 100% of isolates. The in-house procedure started with a within-species all-vs.-all blastp comparison with an *e*-value of 10^{-20} , at least 80% coverage of both sequences, and a post-treatment filtering to keep only hits with $\geq 95\%$ amino-acid identity. All filtered result files were parsed to group proteins into homology clusters, by recursively combining hits matching to the same proteins. For each homology group, the number of core and pan protein-coding genes were defined as the minimum and maximum number of homologues in a single genome, respectively. Core and pan numbers were summed over all homology groups to obtain the total core and pan genomes. Both calculations (in-house and Roary) returned core and pan genomes of each genomic species. Because each species has a different number of sequenced genomes, accumulation curves for the core and accessory (pan minus core) genomes were calculated as follows: for each x between 1 and N , with N the total number of genomes in the group, 50 random combinations of x genomes among N were selected, and their core and accessory genomes were estimated.

RESULTS AND DISCUSSION

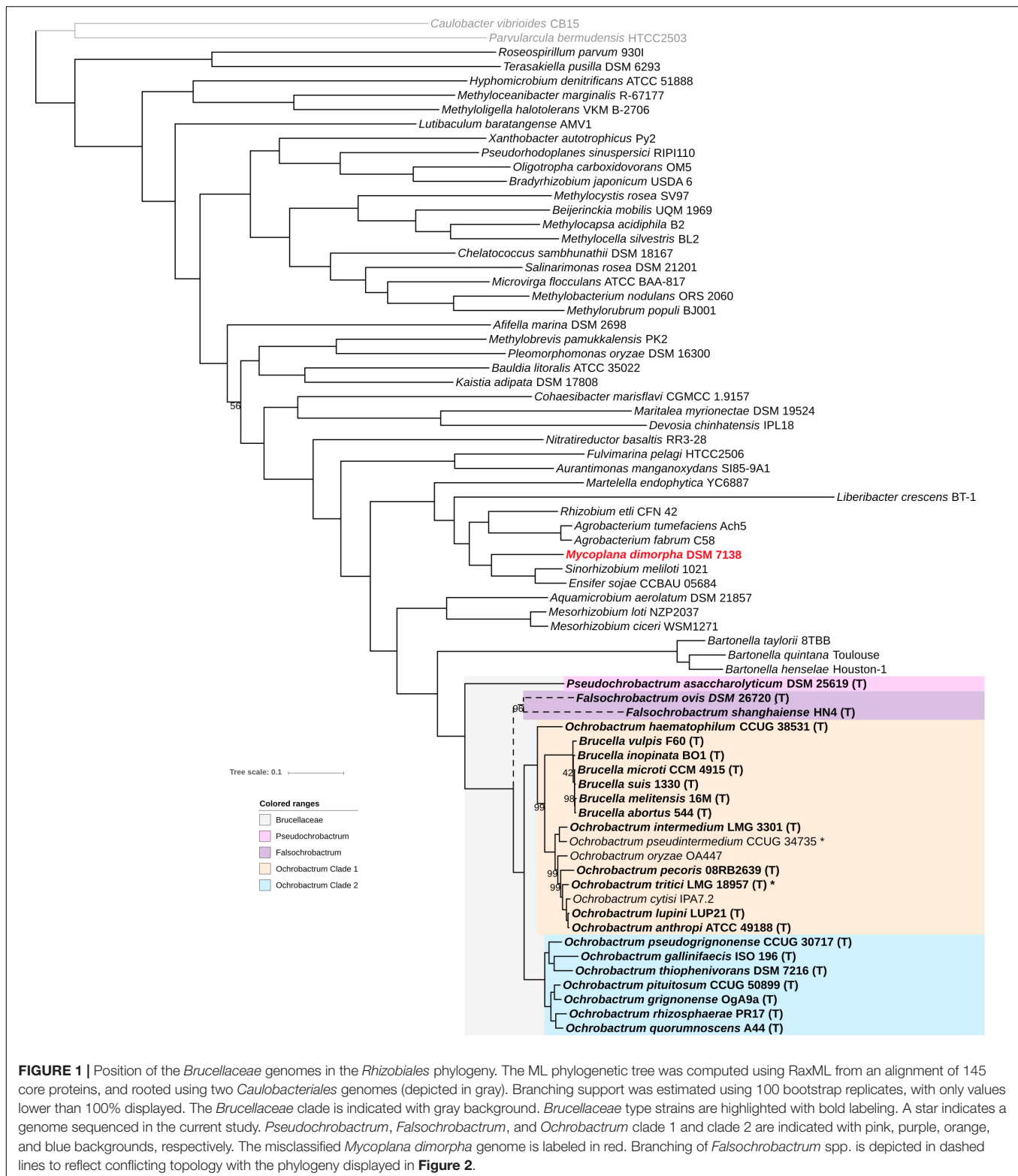
Phylogenomic Positioning of the Family Brucellaceae in the Order Rhizobiales

Forty-three complete and draft genomes representative of the *Rhizobiales* diversity and 25 genomes representative of the *Brucellaceae* diversity from the NCBI ftp repository (Supplementary Table S1) were selected, and a phylogenomic tree from a set of 145 proteins shared by all genomes (core proteins) was constructed. As seen in Figure 1, the high number of compared proteins resulted in an almost completely resolved tree, with all but one bootstrap values being $\geq 98\%$. The tree structure generally reflects the currently accepted *Rhizobiales* families grouping, with few exceptions. Consistent with 16S rRNA and *recA* analyses, *Pseudochrobactrum* and *Falsochrobactrum* spp. form a monophyletic group with other *Ochrobactrum* and *Brucella* spp. On the contrary, the *Mycoplana dimorpha* genome investigated here branches with maximum bootstrap support distant to the *Brucellaceae* family, and actually within the family *Rhizobiaceae* (Figure 1). *Mycoplana stricto sensu* have been variously included into the *Mycobacteriaceae*, the *Pseudomonadaceae*, or even left unclassified before ending up into the *Brucellaceae* (Urakami and Segers, 2015). However, this classification was not based on phylogenetic studies, and most current phylogenies actually branches the genus outside the *Brucellaceae* (Yanagi and Yamasato, 1993; Scholz et al., 2008a; Kämpfer and Glaeser, 2015). This results provide the first robust taxonomic position for *Mycoplana*, which indicates that the genus should be transferred from the *Brucellaceae* to the *Rhizobiaceae*. Our fully resolved tree also indicates that the sister group of the *Brucellaceae* family is the *Bartonellaceae* family with

100% confidence. This result is consistent with another phylogenomic study that spanned the whole α -Proteobacteria diversity and therefore included only a few *Brucella* species as representative of the *Brucellaceae* (Gupta and Mok, 2007). Finally, the extensive *Rhizobiales* genome diversity used here provide a clear delineation of the *Brucellaceae* family and confirms that no other *Rhizobiales* species/genus are part of the family.

Phylogenomic Relationships Among Brucellaceae

Our next objective was to better understand the intra-family phylogenetic relationships between *Brucellaceae* species. In the topology observed in Figure 1, *Pseudochrobactrum asaccharolyticum* branches at the root of the *Brucellaceae*, and *Falsochrobactrum* spp. branch as a sister clade of all *Ochrobactrum* and *Brucella* species. All these other species are then separated into two main clades. The first clade includes *Ochrobactrum* species *haematophilum*, *pseudintermedium*, *intermedium*, *oryzae*, *pecoris*, *tritici*, *cytisi*, and *anthropi-lupini*. The triad *anthropi-lupini/cytisi/tritici* was generally well resolved in most previous phylogenies, but the position of *O. oryzae*, *O. pecoris*, and *O. haematophilum* was much less consistent. 16S rRNA-based analyses usually branch *O. oryzae* with *O. pseudintermedium* and *O. gallinifacies*, away from the *anthropi/tritici* clade, although *recA* analyses provided results in agreement with our phylogenomic analysis (Scholz et al., 2008a; Huber et al., 2009; Gazolla Volpiano et al., 2019; Krzyżanowska et al., 2019). Similarly, *O. pecoris* usually branches within or as a sister taxon of *Ochrobactrum* Clade 2 (see below) in 16S rRNA-based phylogenies, with sometimes a close connection to *O. rhizosphaerae* and *O. pituitosum* (Kämpfer et al., 2011, 2013, 2015; Krzyżanowska et al., 2019), while the MLST phylogeny more accurately branched it with the other members of *Ochrobactrum* Clade 1 (Aujoulat et al., 2014). For *O. haematophilum*, no single-locus or even multi-locus analysis could have resolved its correct position with high support (Scholz et al., 2008a; Aujoulat et al., 2014; Gazolla Volpiano et al., 2019), suggesting that its deep branching at the root of Clade 1 precludes from retrieving enough phylogenetic signal when only few genes are used. It should also be noted that all *Brucella* species form a monophyletic cluster inside Clade 1 with maximum support. The inclusion of *Brucella* among *Ochrobactrum* species was recurrently observed within previous studies, but the exact positioning have never been conclusively resolved (Zurdo-Pineiro et al., 2007; Huber et al., 2009; Kämpfer et al., 2015; Burygin et al., 2019). Specifically, the species *O. intermedium* was named after its supposed closest relationship to *Brucella* spp. using serological cross-reactivity, polymyxin resistance, and 16S rRNA-based phylogeny (Velasco et al., 1998), a clustering also observed in most 16S rRNA-based analyses (Kämpfer et al., 2007, 2008; Teyssier et al., 2007; Zurdo-Pineiro et al., 2007; Scholz et al., 2008a; Huber et al., 2009). Here we show that *Brucella* spp. branch as a sister group of a clade including the *Ochrobactrum* species *pseudintermedium*, *intermedium*, *oryzae*, *perocis*, *cytisi*, *tritici*, and *anthropi-lupini*. It indicates that *O. intermedium* is



actually more genetically related to most *Ochrobactrum* spp. of Clade 1 than to *Brucella* spp.

Clade 2 includes *Ochrobactrum* species *gallinifacis*, *thiophenivorans*, *pseudorignonense*, *quorumnoscens*, *rhizosphaerae*,

grignonense, and *pituitosum*. These species consistently group together in most 16S rRNA-based phylogenetic analyses, but usually as an internal *Ochrobactrum* clade and with *O. gallinifacis* excluded (Chai et al., 2015;

Gazolla Volpiano et al., 2019; Krzyżanowska et al., 2019). On the contrary, *recA* and multilocus phylogenies usually separated correctly this group from the other *Ochrobactrum* spp. (Aujoulat et al., 2014; Kämpfer et al., 2015; Gazolla Volpiano et al., 2019), suggesting that some recombination events in the 16S rRNA region have blurred the phylogenetic signal for this clade.

Comparison of the 16S rRNA Region

The numerous discrepancies revealed in the previous section between our phylogenomic analysis and 16S rRNA-based phylogenies prompted us to investigate in more detail the 16S rRNA sequence of the *Brucellaceae*. We constructed an alignment using the 16S rRNA sequence extracted from all *Brucellaceae* genomes and several outgroups from **Figure 1**, completed with 16S rRNA sequences for the *Brucellaceae* type strains not available as genome sequences in the NCBI database. The resulting alignment show numerous likely recombined regions involving diverse *Ochrobactrum* and non-*Ochrobactrum* species (see **Table 1** and **Supplementary Figure S1**). For instance, the *O. gallinifaecis* ISO 196 16S rRNA sequence is highly recombined, with three independent inferred recombined regions, all three of them shared with non-*Ochrobactrum* species or possibly with *Aquamicrobium aerolatum* from the family *Phyllobacteriaceae* (**Table 1**). These observed recombination events are likely the reason for the incorrect positioning of *O. gallinifaecis* outside *Ochrobactrum* clade 2 in previous 16S rRNA-based phylogenies. Interestingly, one of them is shared with *O. pseudintermedium* and two with *O. oryzae*, two species usually grouped along with *O. gallinifaecis* in 16S rRNA phylogenies. The grouping of *O. pecoris* with *Ochrobactrum* clade 2 in 16S rRNA phylogenies is also probably caused by the recombination event inferred at positions 75–91 of the alignment, which also involves *O. rhizosphaerae*, *O. pituitosum*, and *O. daejeonense* (**Table 1**). Another recombined region is inferred at pos. 927–979 in the alignment and involves the whole clade including *O. tritici*, *O. cytisi*, and *O. anthropi-lupini* with *Ochrobactrum* Clade 2 (**Table 1**). Since this region is one of the highly variable region of the 16S rRNA sequence (see **Supplementary Figure S1**), the resulting inter-species similarity likely weighted on the positioning of *Ochrobactrum* Clade 2 within *Ochrobactrum* Clade 1 in former studies. Likewise, it forces the *O. anthropi-tritici* clade to branch out of *Ochrobactrum* Clade 1, leaving *O. intermedium* as an apparent sister clade of the *Brucella* spp. in these studies. Finally, a number of other discrepancies were noticed in the 16S rRNA alignment (green boxes in **Supplementary Figure S1**), which contributes to the general unreliability of phylogenies based on the 16S rRNA sequence. In contrast, no obvious recombined region involving specifically *Mycoplana* and any member of the *Brucellaceae* was observed, consistent with its highly supported positioning among the family *Rhizobiaceae*.

Falsochrobactrum Species Phylogenetic Positioning

To go further in the taxonomic analysis of the *Brucellaceae*, a new core-proteins tree was constructed, including all non-*Brucella* *Brucellaceae* genomes available in GenBank at the

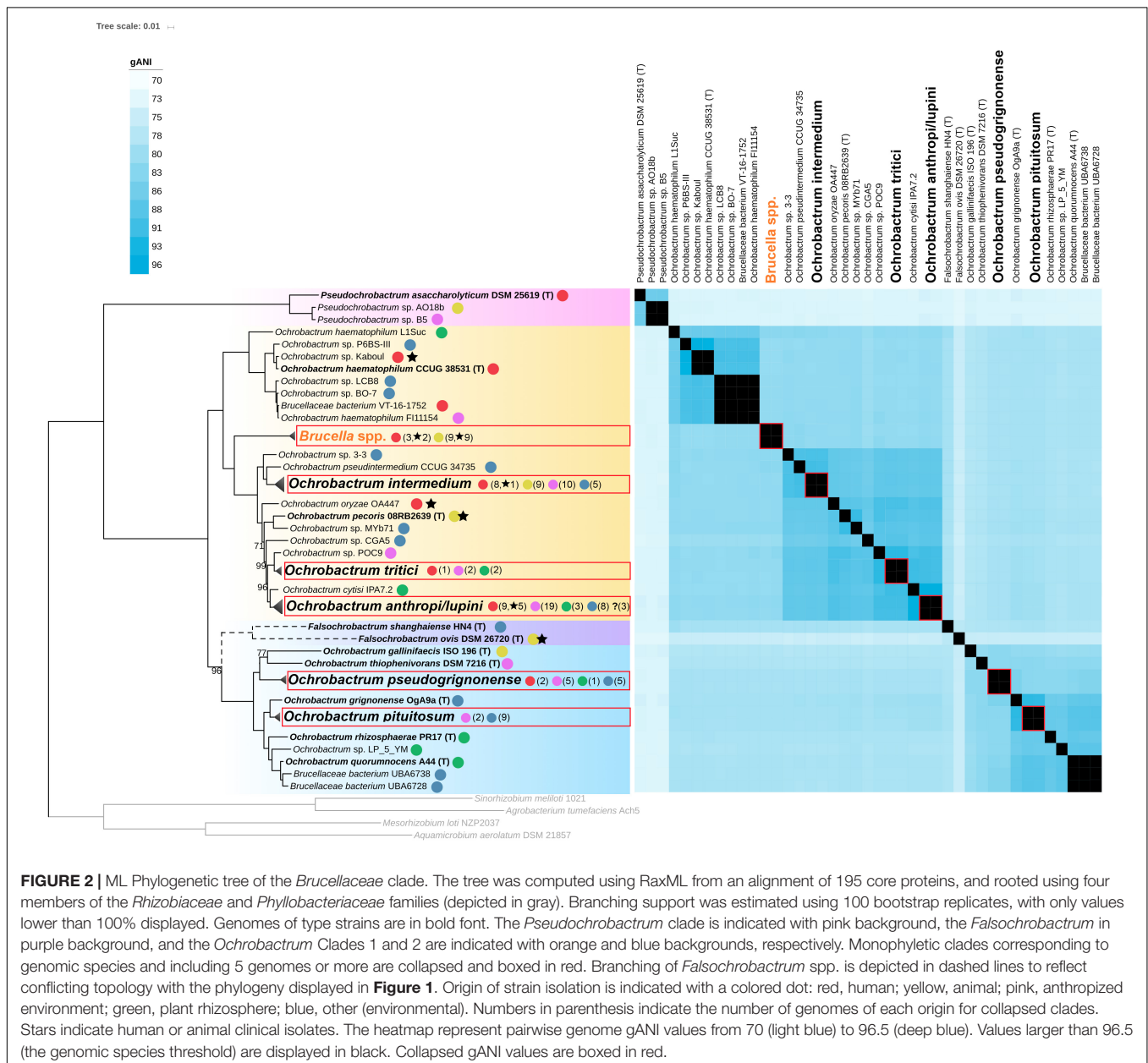
TABLE 1 | Inferred recombination regions in 16S rRNA sequence of Brucellaceae isolates.

	<i>O. oryzae</i>	<i>O. pseudintermedium</i>	<i>O. quorumnoscens</i>	<i>O. rhizosphaerae</i> <i>O. pituitosum</i> <i>O. daejeonense</i>	<i>Ochrobactrum</i> Clade 2	<i>Paenochrobactrum</i> spp.	<i>Pseudochrobactrum</i> spp. <i>Falsochrobactrum</i> spp.	<i>D. caeni</i>	<i>A. aerolatum</i>
<i>O. gallinifaecis</i> ISO 196 (T)	63–178*	63–178				63–178		371–378	
<i>O. pecoris</i> 08RB2639 (T)	519–577		371–378	75–91		519–577 75–91	519–577		519–577
<i>O. anthropi-tritici</i> clade					927–979				

*Numbers refer to positions in the 16S rRNA alignment provided in **Supplementary Figure S1**.

time of the study (15th of July, 2019), 12 *Brucella* genomes representative of the diversity of the genus, and 32 novel *Ochrobactrum* genomes sequenced in the present study (see **Supplementary Tables S1, S2**). The topology of this new tree is highly congruent with the topology observed for the *Brucellaceae* type strains in the *Rhizobiales* tree, except for the position of *Falsochrobactrum* spp. (**Figure 2** and **Supplementary Figure S2**). Indeed, although the two *Falsochrobactrum* species cluster together in both topologies, they branch with maximum support as a distinct genus in the *Rhizobiales* tree (**Figure 1**) but within the *Ochrobactrum* diversity in the *Brucellaceae* tree (**Figure 2**). To test whether this discrepancy was caused by the set of included genomes or by the set of core proteins

used, additional phylogenetic trees were constructed using the same representative *Brucellaceae* type strains with/without *Falsochrobactrum* genomes, and with each core protein dataset. When the two *Falsochrobactrum* genomes are included in the analysis, both calculations provide the same topology than the original trees (see **Supplementary Figures S3A,B**). When each single *Falsochrobactrum* genome is included alone, the branching is similar whatever the protein dataset: outside the *Ochrobactrum* clade for *F. ovis*, and inside the *Ochrobactrum* clade for *F. shanghaiense* (see **Supplementary Figures S3C–F**). This inconsistent positioning suggests that extensive recombination events occurred in *F. shanghaiense* or *F. ovis*, or both, and questions the classification of *Falsochrobactrum* spp. as a new



genus, at least from a genomic point of view. Unfortunately, the deep branching of these genomes within the *Brucellaceae* and the lack of sequenced close relatives hamper any further investigation using existing algorithm of recombination detection. The *Falsolechrobacterium* spp. phylogenetic position in the family *Brucellaceae* thus cannot be accurately determined in the present study, and its resolution will require additional sequencing effort.

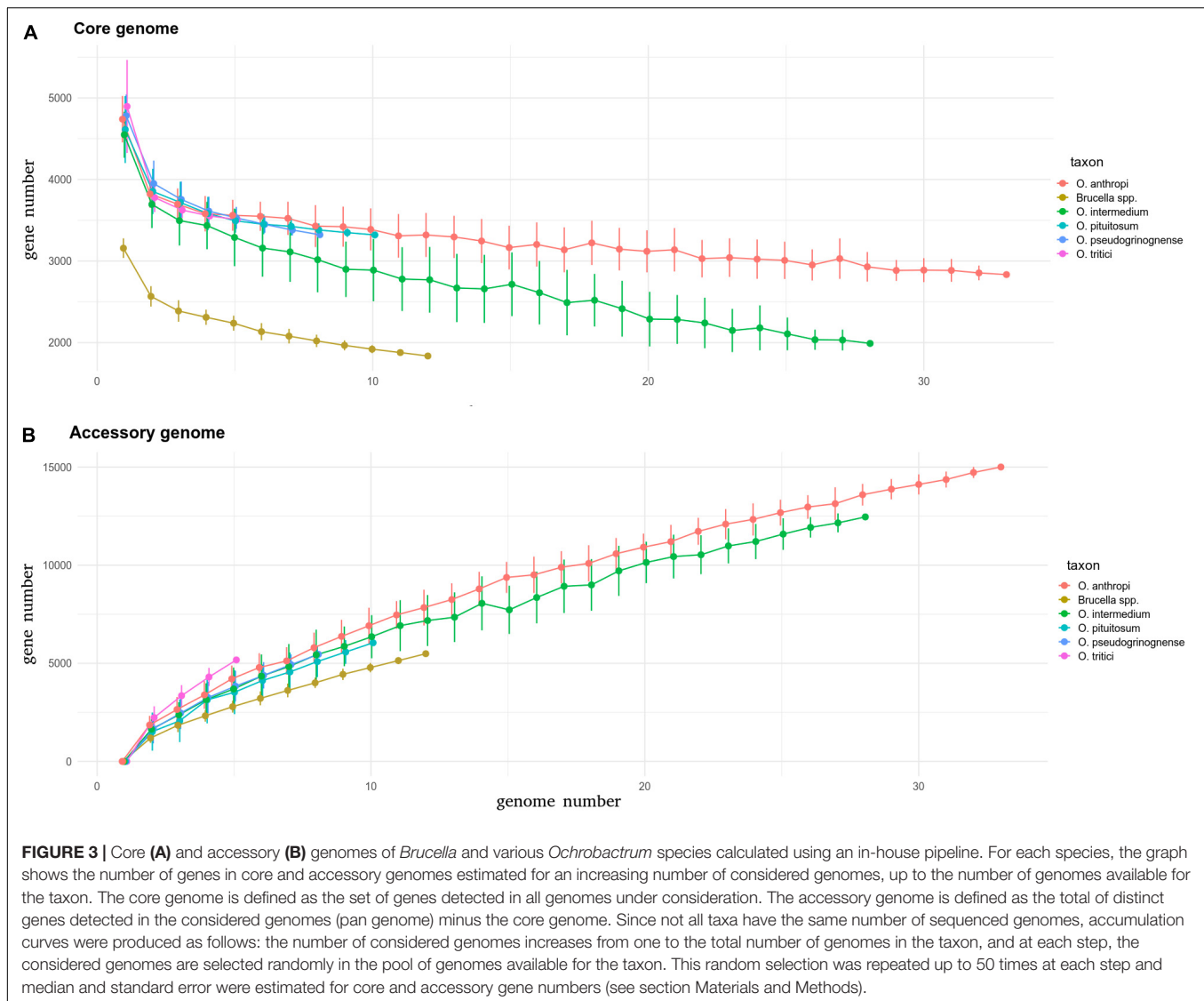
Delimitation of *Ochrobactrum* Genomic Species

The high resolution of our *Brucellaceae* core protein phylogeny emphasized the presence of clusters that generally overlap with the species names given to isolates (see **Supplementary Figure S2**). To delineate even more precisely species boundaries at the genomic level, an all-versus-all gANI comparison was conducted on the *Brucellaceae* genomes. A gANI score is a measure of genomic relatedness which can be viewed as an *in silico* DNA-DNA hybridization (Goris et al., 2007), and benchmarking on more than 13,000 genomes representative of most of the accepted bacterial species indicated that a genome pair with a gANI value > 96.5 can be considered belonging to the same species (Varghese et al., 2015). In the following sections, cluster of genomes with a gANI higher than this threshold are named genomic species, to avoid any ambiguity with taxonomically accepted species. In our phylogenomic framework, most clusters with genomes harboring the same species name match a single genomic species, supporting the robustness of the gANI indicator to detect species boundaries. The *O. haematophilum* cluster is an exception, with two genomes (*O. haematophilum* L1SUC and *O. haematophilum* FI11154) distantly related to the type strain genome, with 86.37 and 90.21 gANI values, respectively (**Figure 2**). The strain FI11154 was identified as *O. haematophilum* solely on the closest relationship of its 16S rRNA sequence to the *O. haematophilum* type strain (Diaz et al., 2018) while no information about the characterization process is available for strain L1SUC. It is thus likely that these two strains do not belong to the species *O. haematophilum* and should return to an unidentified *Ochrobactrum* sp. status until more thorough characterization. The gANI analysis also indicated that *O. cytisi* IPA7.2 can be clearly separated from *O. anthropi* genomes (gANI in the range 95.47–95.99) despite a very close phylogenetic relationship (**Figure 2**). Although the sequenced strain is not the type strain of the species, a multilocus analysis showed previously that IPA7.2 is phylogenetically closer to the *O. cytisi* type strain than to any *O. anthropi* strain (Burygin et al., 2019). These results support the status of *O. cytisi* as a separate species, a status which have been recently questioned based on 16S rRNA, MLSA and DDH analyses (Gazolla Volpiano et al., 2019). On the contrary, gANI calculation indicates that all *Brucella* genomes included in this study, which span the whole diversity of currently known *Brucella* species, actually belong to the same genomic species. This result is fully consistent with previous DNA-DNA hybridization and 16S rRNA analyses and support the concept that all currently known members of the genus *Brucella* constitute in fact a single

species, at least from a genetic point of view (Verger et al., 1985). The genomic species delineation finally confirmed that *O. lupini* isolates fall in the diversity of the *O. anthropi* species (Gazolla Volpiano et al., 2019) and revealed that a number of genome sequences available in GenBank were incorrectly identified. Indeed, phylogenomic and gANI analyses indicate that *O. anthropi* FRAF13 belongs to the *tritici* clade, *O. pituitosum* AA2 to the *pseudogrignonense* clade, and both *O. rhizospherae* SJY1 and *O. thiophenivorans* MYb6 to the *pituitosum* clade (see **Supplementary Figure S2**).

Core and Accessory Genomes Among *Ochrobactrum* Species

After considering these species boundaries at the genomic level, five *Ochrobactrum* species have more than four sequenced genomes, with a diversity suitable for core and pan genome estimations. Among them, *O. anthropi* and *O. intermedium* were the most heavily sequenced, with 43 and 33 genomes available, respectively. *O. pituitosum*, *O. pseudogrignonense*, and *O. tritici* followed, with 11, 8, and 5 genomes available, respectively. All these species have ~4300–5000 protein-coding genes, with no significant difference between species (**Figure 3A**, ANOVA test, $p = 0.061$). By comparison, the genomes of the 12 *Brucella* isolates, known to have experienced genomic reduction (Wattam et al., 2014), harbor ~3200 protein-coding genes on average. When the core genome of each species is estimated, differences emerge. While the species *anthropi*, *pituitosum*, *pseudogrignonense*, and *tritici* species show a similar decreasing curve with an increasing number of observed genomes, *O. intermedium* exhibits a faster and stronger decrease (**Figure 3A**). When 28 genomes are included in the comparison (the maximum possible for *O. intermedium* after discarding incompletely sequenced genomes), the core genome of *O. intermedium* is almost 1000 genes smaller than those of *O. anthropi*, a result supported by two independent calculation methods (see Section Materials and Methods, **Supplementary Figure S4A**). Such difference is not compensated by a larger accessory genome (all non-core protein-coding genes) for which all *Ochrobactrum* species except *O. tritici* show a similar increase in the accessory genome with increasing number of genomes observed (**Figure 3B** and see **Supplementary Figure S4B**). Overall, these results suggest that *O. intermedium* could be subject of pervasive gene disruption, with no or very few gene inactivation yet fixed in the population. Genome-wide gene disruption is considered as one of the first steps of genome reduction, usually caused by the reduction of effective population size following ecological niche specialization, such as host-adaptation (Toft and Andersson, 2010). Consistent with our observation, an ongoing process of genome reduction in *O. intermedium* have already been proposed, based on the recurrent deletion of large genomic regions in different strains (Aujoulat et al., 2014). The authors of this study compared the population structure and isolation site of 65 *O. intermedium* isolates and concluded that the species may undergo a niche specialization toward an environment related to medical and industrial



technologies. Another study suggested that *O. intermedium* may be specializing to the animal gastric niche, based on co-isolation and genetic features shared with the stomach-adapted human pathogen *Helicobacter pylori* (Kulkarni et al., 2014). The large number of human-related *O. intermedium* isolates (Scholz et al., 2008a; Aujoulat et al., 2014), sometimes from human clinical cases (Velasco et al., 1998; Moller et al., 1999), as well as their intrinsic resistance to polymyxin E (Velasco et al., 1998), a trait shared with *Brucella* spp., also suggest that *O. intermedium* may shift to an animal-associated and potential pathogenic lifestyle.

Ecological Niches of *Brucellaceae* Species

The intriguing observation made for *O. intermedium* genomes suggests that isolation sources for the sequenced strains may inform us on its potential niche specialization. We therefore

compiled this information for all the *Brucellaceae* and classified them into five main sources: human clinical, human-related environments, vertebrate animals (including strains causing diseases), plant rhizosphere, and natural environment (including invertebrate animals such as worms). The distribution of these main sources among the *Brucellaceae* tree revealed a clear separation between *Ochrobactrum* Clade 1 and Clade 2, with almost all human, human-related, and animal isolates being localized in Clade 1 while Clade 2 comprises mainly environmental and plant-associated isolates (Figure 2). Strikingly, Clade 1 is actually those in which the *Brucella* spp. belong to, suggesting that this taxonomic lineage may harbor genetic determinants facilitating a preferential association with animal hosts, including humans. At the species level, *O. intermedium* shows the lowest proportion of environmental isolates and many isolates sampled in poultry (all isolates identified as xx/2009 and xx/2015 in Supplementary Figure S2), in line with a niche specialization

toward a human-associated environment. Moreover, an internal *O. intermedium* highly supported clade is exclusively composed of human isolates which includes two strains isolated from gastric disorder in association with *H. pylori* (Kulkarni et al., 2013, 2014) and the type strain of clinical origin (see **Supplementary Figure S2**). Whether this clade represents an ongoing pathogenic lineage should be carefully investigated with a more comprehensive epidemiological analysis. Similarly, more than 50% of the *O. anthropi* human isolates cluster in a well-supported clade that includes only human-related isolates (see **Supplementary Figure S2**). This cluster matches remarkably well the clonal complex CC4 observed by Romano et al. (2009) with 3 common strains, a complex exclusively composed of human clinical isolates in their study. Our results thus fully support the proposal of these authors that this lineage may represent a human-specialized opportunistic pathogen lineage among the environmental *O. anthropi* species.

CONCLUSION

In summary, this study used a phylogenomic approach to investigate the taxonomic relationship of the family *Brucellaceae*. Our results confirmed the taxonomic position of the family *Brucellaceae* within the order of *Rhizobiales*, with the family *Bartonellaceae* containing the closest relatives. The family *Brucellaceae* includes, using this approach, the following current genera: *Pseudochrobactrum*, *Falsochrobactrum*, *Ochrobactrum*, and *Brucella*. The genus *Mycoplana*, described previously as belonging to the *Brucellaceae*, is actually positioned within the *Rhizobiaceae* and thus outside the *Brucellaceae*. Within the family *Brucellaceae*, while our approach confirmed the genus status of *Ochrobactrum* and *Pseudochrobactrum*, that of *Falsochrobactrum* was not totally resolved and that of *Brucella* appeared questionable. The various *Ochrobactrum* species clustered into two main clades. The first one includes *Brucella* spp. and the main opportunistic pathogenic *Ochrobactrum* species, such as *O. anthropi*, *O. intermedium*, *O. pseudintermedium*, and *O. haematophilum*. The second clade comprises the other *Ochrobactrum* species that seem currently not involved in opportunistic infections and are only exceptionally associated with humans. The robustness of the phylogenetic inferences we obtained here using two set of marker proteins and two sets of input genomes, compared to what was previously reported with single locus markers, emphasizes the help that genomic information can bring to characterize the taxonomic status of potential new species or genera. Nevertheless, according to our gANI analysis, the use of the 16S rRNA marker appears to be quite reliable to assign isolates to known species and should still be used for this purpose. Finally, the present work provides new elements on the question of the *Brucella* species delineation, and its status as a genus. Species definition has been problematic for numerous bacterial taxa because of a lack of a strong and universally accepted theoretical basis (Gevers et al., 2005). Our finding that all *Brucella* species can be considered as a single species according to gANI

scores is actually also supported by the approach of the Genome Taxonomy Database (GTDB²) (Parks et al., 2018). This approach is an alternative to the official prokaryotic taxonomic nomenclature in which taxonomic ranks are defined according to a strict monophyly among groups and thresholds based on corrected genomic distances. Interestingly, under the GTDB framework, *Brucella* remains a genus, consisting of a single species as initially proposed by Verger et al. (1985). However, *Ochrobactrum* would be separated into three genera corresponding to the *O. haematophilum* clade, the *O. anthropi/tritici/intermedium* clade, and the *Ochrobactrum* clade 2 of the present study. The resulting GTDB classification remains, however, to be validated.

DATA AVAILABILITY STATEMENT

The datasets generated for this study can be found in the ncbi Biosample, SAMN12821270, SAMN12821271, SAMN12821272, SAMN12821273, SAMN12821274, SAMN12821275, SAMN12821276, SAMN12821277, SAMN12821278, SAMN12821279, SAMN12821280, SAMN12821281, SAMN12821282, SAMN12821283, SAMN12821284, SAMN12821285, SAMN12821286, SAMN12821287, SAMN12821288, SAMN12821289, SAMN12821290, SAMN12821291, SAMN12821292, SAMN12821293, SAMN12821294, SAMN12821295, SAMN12821296, SAMN12821297, SAMN12821298, SAMN12821299, SAMN12821300, and SAMN12821301.

AUTHOR CONTRIBUTIONS

AC and MZ conceived and designed the study. SL performed *in silico* data analyses. SL, AC, and MZ analyzed the data and drafted the manuscript.

FUNDING

This work was funded by Agence Nationale de la Recherche Grant ANR-14-ASMA-0002-02.

ACKNOWLEDGMENTS

We would like to thank Holger Scholz and Michel Thibault for supplying *Ochrobactrum* strains. We would also like to thank Nelly Bernardet and Isabelle Foubert for expert technical assistance and Mathieu Gonnet for preliminary genome analyses.

SUPPLEMENTARY MATERIAL

The Supplementary Material for this article can be found online at: <https://www.frontiersin.org/articles/10.3389/fmicb.2019.03083/full#supplementary-material>

²<http://gtdb.ecogenomic.org/>

REFERENCES

- Al Dahouk, S., Köhler, S., Occhialini, A., de Bagues, M. P. J., Hammerl, J. A., Eisenberg, T., et al. (2017). *Brucella* spp. of amphibians comprise genomically diverse motile strains competent for replication in macrophages and survival in mammalian hosts. *Sci. Rep.* 7:44420. doi: 10.1038/srep44420
- Aujoulat, F., Romano-Bertrand, S., Masnou, A., Marchandin, H., and Jumas-Bilak, E. (2014). Niches, population structure and genome reduction in *Ochrobactrum intermedium*: clues to technology-driven emergence of pathogens. *PLoS One* 9:e83376. doi: 10.1371/journal.pone.0083376
- Bankevich, A., Nurk, S., Antipov, D., Gurevich, A. A., Dvorkin, M., Kulikov, A. S., et al. (2012). SPAdes: a new genome assembly algorithm and its applications to single-cell sequencing. *J. Comput. Biol.* 19, 455–477. doi: 10.1089/cmb.2012.0021
- Bolger, A. M., Lohse, M., and Usadel, B. (2014). Trimmomatic: a flexible trimmer for illumina sequence data. *Bioinformatics* 30, 2114–2120. doi: 10.1093/bioinformatics/btu170
- Buddle, M. B. (1956). Studies on *Brucella ovis* (n.sp.), a cause of genital disease of sheep in New Zealand and Australia. *J. Hyg.* 54, 351–364. doi: 10.1017/s0022172400044612
- Burygin, G. L., Kargapolova, K. Y., Kryuchkova, Y. V., Avdeeva, E. S., Gogoleva, N. E., Ponomaryova, T. S., et al. (2019). *Ochrobactrum cytisi* IPA7.2 promotes growth of potato microplants and is resistant to abiotic stress. *World J. Microbiol. Biotechnol.* 35:55. doi: 10.1007/s11274-019-2633-x
- Carmichael, L. E., and Bruner, D. W. (1968). Characteristics of a newly-recognized species of *Brucella* responsible for infectious canine abortions. *Cornell Vet.* 484, 579–592.
- Chai, L., Jiang, X., Zhang, F., Zheng, B., Shu, F., Wang, Z., et al. (2015). Isolation and characterization of a crude oil degrading bacteria from formation water: comparative genomic analysis of environmental *Ochrobactrum intermedium* isolate versus clinical strains. *J. Zhejiang Univ. Sci. B* 16, 865–874. doi: 10.1631/jzus.b1500029
- Cloekaert, A., Bernardet, N., Koylass, M. S., Whatmore, A. M., and Zygmunt, M. S. (2011). Novel IS711 chromosomal location useful for identification of marine mammal *Brucella* genotype ST27, which is associated with zoonotic infection. *J. Clin. Microbiol.* 49, 3954–3959. doi: 10.1128/JCM.05238-11
- Darriba, D., Taboada, G. L., Doallo, R., and Posada, D. (2011). ProtTest 3: fast selection of best-fit models of protein evolution. *Bioinformatics* 27, 1164–1165. doi: 10.1093/bioinformatics/btr088
- De, B. K., Stauffer, L., Koylass, M. S., Sharp, S. E., Gee, J. E., Helsel, L. O., et al. (2008). Novel *Brucella* strain (BO1) associated with a prosthetic breast implant infection. *J. Clin. Microbiol.* 46, 43–49. doi: 10.1128/JCM.01494-07
- Diaz, M., Wegmann, U., Akinyemi, N., Oguntuyinbo, F. A., Sayavedra, L., Mayer, M. J., et al. (2018). Complete genome sequence of *Ochrobactrum haematophilum* FI11154, isolated from kunu-zaki, a nigerian millet-based fermented food. *Genome Announc.* 6:e00428-18. doi: 10.1128/genomeA.00428-18
- Edgar, R. C. (2004). MUSCLE: multiple sequence alignment with high accuracy and high throughput. *Nucleic Acids Res.* 32, 1792–1797. doi: 10.1093/nar/gkh340
- Eisenberg, T., Hamann, H.-P., Kaim, U., Schlez, K., Seeger, H., Schauerte, N., et al. (2012). Isolation of potentially novel *Brucella* spp. from frogs. *Appl. Environ. Microbiol.* 78, 3753–3755. doi: 10.1128/aem.07509-11
- Eisenberg, T., Riße, K., Schauerte, N., Geiger, C., Blom, J., and Scholz, H. C. (2016). Isolation of a novel “atypical” *Brucella* strain from a bluespotted ribbontail ray (*Taeniura lymma*). *Antonie Van Leeuwenhoek* 110, 221–234. doi: 10.1007/s10482-016-0792-4
- Ficht, T. A. (2010). *Brucella* taxonomy and evolution. *Future Microbiol.* 5, 859–866. doi: 10.2217/fmb.10.52
- Foster, G., Osterman, B. S., Godfroid, J., Jacques, I., and Cloekaert, A. (2007). *Brucella ceti* sp. nov. and *Brucella pinnipedialis* sp. nov. for *Brucella* strains with cetaceans and seals as their preferred hosts. *Int. J. Syst. Evol. Microbiol.* 57, 2688–2693. doi: 10.1099/ijs.0.65269-0
- Foster, J. T., Beckstrom-Sternberg, S. M., Pearson, T., Beckstrom-Sternberg, J. S., Chain, P. S. G., Roberto, F. F., et al. (2009). Whole-genome-based phylogeny and divergence of the genus *Brucella*. *J. Bacteriol.* 191, 2864–2870. doi: 10.1128/jb.01581-08
- Garin-Bastuji, B., Hars, J., Drapeau, A., Cherfa, M. A., Game, Y., Le Horgne, J. M., et al. (2014). Reemergence of *Brucella melitensis* in wildlife. France. *Emerg. Infect. Dis.* 20, 1570–1571. doi: 10.3201/eid2009.131517
- Gazolla Volpiano, C., Hayashi Sant’Anna, F., Ambrosini, A., Brito Lisboa, B., Kayser Vargas, L., and Passaglia, L. M. P. (2019). Reclassification of *Ochrobactrum lupini* as a later heterotypic synonym of *Ochrobactrum anthropi* based on whole-genome sequence analysis. *Int. J. Syst. Evol. Microbiol.* 69, 2312–2314. doi: 10.1099/ijs.0.003465
- Gevers, D., Cohan, F. M., Lawrence, J. G., Spratt, B. G., Coenye, T., Feil, E. J., et al. (2005). Opinion: re-evaluating prokaryotic species. *Nat. Rev. Microbiol.* 3, 733–739. doi: 10.1038/nrmicro1236
- Goris, J., Konstantinidis, K. T., Klappenbach, J. A., Coenye, T., Vandamme, P., and Tiedje, J. M. (2007). DNA-DNA hybridization values and their relationship to whole-genome sequence similarities. *Int. J. Syst. Evol. Microbiol.* 57, 81–91. doi: 10.1099/ijs.0.64483-0
- Gupta, R. S., and Mok, A. (2007). Phylogenomics and signature proteins for the alpha *Proteobacteria* and its main groups. *BMC Microbiol.* 7:106. doi: 10.1186/1471-2180-7-106
- Holmes, B., Popoff, M., Kiredjian, M., and Kersters, K. (1988). *Ochrobactrum anthropi* gen. nov., sp. nov. from human clinical specimens and previously known as group vd. *Int. J. Syst. Evol. Microbiol.* 38, 406–416. doi: 10.1099/00207713-38-4-406
- Huber, B., Scholz, H. C., Kämpfer, P., Falsen, E., Langer, S., and Busse, H.-J. (2009). *Ochrobactrum pituitosum* sp. nov., isolated from an industrial environment. *Int. J. Syst. Evol. Microbiol.* 60, 321–326. doi: 10.1099/ijs.0.011668-0
- Jay, M., Girault, G., Perrot, L., Taunay, B., Vuilmet, T., Rossignol, F., et al. (2018). Phenotypic and molecular characterization of *Brucella microti*-like bacteria from a domestic marsh frog (*Pelophylax ridibundus*). *Front. Vet. Sci.* 5:283. doi: 10.3389/fvets.2018.00283
- Kämpfer, P., Glaeser, S., Busse, H.-J., Eisenberg, T., and Scholz, H. (2013). *Falsochrobactrum ovis* gen. nov., sp. nov., isolated from a sheep. *Int. J. Syst. Evol. Microbiol.* 63, 3841–3847. doi: 10.1099/ijs.0.049627-0
- Kämpfer, P., and Glaeser, S. P. (2015). “*Brucellaceae*,” in *Bergey’s Manual of Systematics of Archaea and Bacteria*, eds W. B. Whitman, F. Rainey, P. Kämpfer, M. Trujillo, J. Chun, and P. DeVos, (Hoboken, NJ: John Wiley & Sons, Inc.) doi: 10.1002/9781118960608.fbm00166.pub2
- Kämpfer, P., Glaeser, S. P., and Holmes, B. (2015). “*Ochrobactrum*,” in *Bergey’s Manual of Systematics of Archaea and Bacteria*, eds W. B. Whitman, F. Rainey, P. Kämpfer, M. Trujillo, J. Chun, and P. DeVos, (Hoboken, NJ: John Wiley & Sons, Inc.) doi: 10.1002/9781118960608.fbm00809.pub2
- Kämpfer, P., Poppel, M. T., Wilharm, G., Glaeser, S. P., and Busse, H.-J. (2014). *Paenochrobactrum pullorum* sp. nov. isolated from a chicken. *Int. J. Syst. Evol. Microbiol.* 64, 1724–1728. doi: 10.1099/ijs.0.061101-0
- Kämpfer, P., Scholz, H. C., Huber, B., Falsen, E., and Busse, H.-J. (2007). *Ochrobactrum haematophilum* sp. nov. and *Ochrobactrum pseudogrignone* sp. nov., isolated from human clinical specimens. *Int. J. Syst. Evol. Microbiol.* 58:1271. doi: 10.1099/ijs.0.65899-0
- Kämpfer, P., Sessitsch, A., Schlöter, M., Huber, B., Busse, H.-J., and Scholz, H. C. (2008). *Ochrobactrum rhizosphaerae* sp. nov. and *Ochrobactrum thiophenivorans* sp. nov., isolated from the environment. *Int. J. Syst. Evol. Microbiol.* 58, 1426–1431. doi: 10.1099/ijs.0.65407-0
- Kämpfer, P., Huber, B., Busse, H.-J., Scholz, H. C., Tomaso, H., Hotzel, H., et al. (2011). *Ochrobactrum pecoris* sp. nov., isolated from farm animals. *Int. J. Syst. Evol. Microbiol.* 61, 2278–2283. doi: 10.1099/ijs.0.027631-0
- Katoh, K., and Standley, D. M. (2013). MAFFT multiple sequence alignment software version 7: improvements in performance and usability. *Mol. Biol. Evol.* 30, 772–780. doi: 10.1093/molbev/mst010
- Krzyżanowska, D. M., Maciag, T., Ossowicki, A., Rajewska, M., Kaczynski, Z., Czerwicka, M., et al. (2019). *Ochrobactrum quorumnocens* sp. nov., a quorum quenching bacterium from the potato rhizosphere, and comparative genome analysis with related type strains. *PLoS One* 14:e0210874. doi: 10.1371/journal.pone.0210874
- Kulkarni, G., Dhotre, D., Dharne, M., Shetty, S., Chowdhury, S., Misra, V., et al. (2013). Draft genome of *Ochrobactrum intermedium* strain M86 isolated from non-ulcer dyspeptic individual from India. *Gut Pathogens* 5:7. doi: 10.1186/1757-4749-5-7

- Kulkarni, G. J., Shetty, S., Dharne, M. S., and Shouche, Y. S. (2014). Genome sequencing analysis reveals virulence-related gene content of *Ochrobactrum intermedium* strain 229E, a urease-positive strain isolated from the human gastric niche. *FEMS Microbiol. Lett.* 359, 12–15. doi: 10.1111/1574-6968.12549
- Le, S. Q., and Gascuel, O. (2008). An improved general amino acid replacement matrix. *Mol. Biol. Evol.* 25, 1307–1320. doi: 10.1093/molbev/msn067
- Lebuhn, M., Achouak, W., Schloter, M., Berge, O., Meier, H., Barakat, M., et al. (2000). Taxonomic characterization of *Ochrobactrum* sp. isolates from soil samples and wheat roots, and description of *Ochrobactrum tritici* sp. nov. and *Ochrobactrum grignonense* sp. nov. *Int. J. Syst. Evol. Microbiol.* 50, 2207–2223. doi: 10.1099/00207713-50-6-2207
- Letunic, I., and Bork, P. (2019). Interactive tree of life (iTOL) v4: recent updates and new developments. *Nucleic Acids Res.* 47, W256–W259. doi: 10.1093/nar/gkz239
- Li, L., Stoeckert, C. J. J., and Roos, D. S. (2003). OrthoMCL: identification of ortholog groups for eukaryotic genomes. *Genome Res.* 13, 2178–2189. doi: 10.1101/gr.1224503
- McDonald, W. L., Jamaludin, R., Mackereth, G., Hansen, M., Humphrey, S., Short, P., et al. (2006). Characterization of a *Brucella* sp. strain as a marine-mammal type despite isolation from a patient with spinal osteomyelitis in New Zealand. *J. Clin. Microbiol.* 44, 4363–4370. doi: 10.1128/jcm.00680-06
- Moller, L. V., Arends, J. P., Harmsen, H. J., Talens, A., Terpstra, P., and Slooff, M. J. (1999). *Ochrobactrum intermedium* infection after liver transplantation. *J. Clin. Microbiol.* 37, 241–244.
- Okonechnikov, K., Golosova, O., and Fursov, M. (2012). Unipro UGENE: a unified bioinformatics toolkit. *Bioinformatics* 28, 1166–1167. doi: 10.1093/bioinformatics/bts091
- Page, A. J., Cummins, C. A., Hunt, M., Wong, V. K., Reuter, S., Holden, M. T. G., et al. (2015). Roary: rapid large-scale prokaryote pan genome analysis. *Bioinformatics* 31, 3691–3693. doi: 10.1093/bioinformatics/btv421
- Parks, D. H., Chuvochina, M., Waite, D. W., Rinke, C., Skarshewski, A., Chaumeil, P. A., et al. (2018). A standardized bacterial taxonomy based on genome phylogeny substantially revises the tree of life. *Nat. Biotechnol.* 36, 996–1004. doi: 10.1038/nbt.4229
- Romano, S., Aujoulat, F., Jumas-Bilak, E., Masnou, A., Jeannot, J.-L., Falsen, E., et al. (2009). Multilocus sequence typing supports the hypothesis that *Ochrobactrum anthropi* displays a human-associated subpopulation. *BMC Microbiol.* 9:267. doi: 10.1186/1471-2180-9-267
- Scholz, H. C., Banai, M., Cloeckert, A., Kämpfer, P., and Whatmore, A. M. S. (2018). *Brucella* in *Bergey's Manual of Systematics of Archaea and Bacteria*, eds W. B. Whitman, F. Rainey, P. Kämpfer, M. Trujillo, J. Chun, and P. DeVos, (Hoboken, NJ: John Wiley & Sons, Inc.) doi: 10.1002/9781118960608.gbm00807.pub2
- Scholz, H. C., Dahouk, S. A., Tomaso, H., Neubauer, H., Witte, A., Schloter, M., et al. (2008a). Genetic diversity and phylogenetic relationships of bacteria belonging to the *Ochrobactrum-Brucella* group by *recA* and 16S rRNA gene-based comparative sequence analysis. *Syst. Appl. Microbiol.* 31, 1–16. doi: 10.1016/j.syapm.2007.10.004
- Scholz, H. C., Hofer, E., Hammerl, J. A., Zygmunt, M. S., Cloeckert, A., Koylass, M., et al. (2016). *Brucella vulpis* sp. nov., a novel *Brucella* species isolated from mandibular lymph nodes of red foxes (*Vulpes vulpes*) in Austria. *Int. J. Syst. Evol. Microbiol.* 66, 2090–2098. doi: 10.1099/ijsem.0.000998
- Scholz, H. C., Hubalek, Z., Sedlacek, I., Vergnaud, G., Tomaso, H., Dahouk, S. A., et al. (2008b). *Brucella microti* sp. nov., isolated from the common vole *Microtus arvalis*. *Int. J. Syst. Evol. Microbiol.* 58, 375–382. doi: 10.1099/ijse.0.65356-0
- Scholz, H. C., Nockler, K., Gollner, C., Bahn, P., Vergnaud, G., Tomaso, H., et al. (2010). *Brucella inopinata* sp. nov., isolated from a breast implant infection. *Int. J. Syst. Evol. Microbiol.* 60, 801–808. doi: 10.1099/ijse.0.011148-0
- Seemann, T. (2014). Prokka: rapid prokaryotic genome annotation. *Bioinformatics* 30, 2068–2069. doi: 10.1093/bioinformatics/btu153
- Sohn, A. H., Probert, W. S., Glaser, C. A., Gupta, N., Bollen, A. W., Wong, J. D., et al. (2003). Human neurobrucellosis with intracerebral granuloma caused by a marine mammal *Brucella* spp. *Emerg Infect. Dis.* 9, 485–488. doi: 10.3201/eid0904.020576
- Stamatakis, A. (2006). RAxML-VI-HP: maximum likelihood-based phylogenetic analyses with thousands of taxa and mixed models. *Bioinformatics* 22, 2688–2690. doi: 10.1093/bioinformatics/btl446
- Stoener, H. G., and Lackman, D. B. (1957). A new species of *Brucella* isolated from the desert wood rat *Neotoma lepida*. *Am. J. Vet. Res.* 18, 947–951.
- Sun, L., Yao, L., Gao, X., Huang, K., Bai, N., Lyu, W., et al. (2019). *Falsochrobactrum shanghaiense* sp. nov., isolated from paddy soil and emended description of the genus *Falsochrobactrum*. *Int. J. Syst. Evol. Microbiol.* 69, 778–782. doi: 10.1099/ijsem.0.003236
- Teyssier, C., Marchandin, H., Jean-Pierre, H., Diego, I., Darbas, H., Jeannot, J. L., et al. (2005). Molecular and phenotypic features for identification of the opportunistic pathogens *Ochrobactrum* spp. *J. Med. Microbiol.* 54, 945–953. doi: 10.1099/jmm.0.46116-0
- Teyssier, C., Marchandin, H., Masnou, A., Dusart, G., and Jumas-Bilak, E. (2007). *Ochrobactrum pseudintermedium* sp. nov., a novel member of the family Brucellaceae, isolated from human clinical samples. *Int. J. Syst. Evol. Microbiol.* 57, 1007–1013. doi: 10.1099/ijse.0.64416-0
- Tiller, R. V., Gee, J. E., Lonsway, D. R., Gribble, S., Bell, S. C., Jennison, A. V., et al. (2010). Identification of an unusual *Brucella* strain (BO2) from a lung biopsy in a 52 year-old patient with chronic destructive pneumonia. *BMC Microbiol.* 10:23. doi: 10.1186/1471-2180-10-23
- Toft, C., and Andersson, S. G. E. (2010). Evolutionary microbial genomics: insights into bacterial host adaptation. *Nat. Rev. Genet.* 11, 465–475. doi: 10.1038/nrg2798
- Tripathi, A. K., Verma, S. C., Chowdhury, S. P., Lebuhn, M., Gattinger, A., and Schloter, M. (2006). *Ochrobactrum oryzae* sp. nov., an endophytic bacterial species isolated from deep-water rice in India. *Int. J. Syst. Evol. Microbiol.* 56, 1677–1680. doi: 10.1099/ijse.0.63934-0
- Urakami, T., and Segers, P. (2015). “Mycoplana,” in *Bergey's Manual of Systematics of Archaea and Bacteria*, eds W. B. Whitman, F. Rainey, P. Kämpfer, M. Trujillo, J. Chun, and P. DeVos, (Hoboken, NJ: John Wiley & Sons, Inc.) doi: 10.1002/9781118960608.gbm00808
- Varghese, N. J., Mukherjee, S., Ivanova, N., Konstantinidis, K. T., Mavrommatis, K., Kyrpides, N. C., et al. (2015). Microbial species delineation using whole genome sequences. *Nucleic Acids Res.* 43, 6761–6771. doi: 10.1093/nar/gkv657
- Velasco, J., Romero, C., Lopez-Goni, I., Leiva, J., Diaz, R., and Moriyon, I. (1998). Evaluation of the relatedness of *Brucella* spp. and *Ochrobactrum anthropi* and description of *Ochrobactrum intermedium* sp. nov., a new species with a closer relationship to *Brucella* spp. *Int. J. Syst. Bacteriol.* 48, 759–768. doi: 10.1099/00207713-48-3-759
- Verger, J. M., Grimont, F., Grimont, P. A. D., and Grayon, M. (1985). *Brucella*, a monospecific genus as shown by deoxyribonucleic acid hybridization. *Int. J. Syst. Evol. Microbiol.* 35, 292–295.
- Wattam, A. R., Foster, J. T., Mane, S. P., Beckstrom-Sternberg, S. M., Beckstrom-Sternberg, J. M., Dickerman, A. W., et al. (2014). Comparative phylogenomics and evolution of the *Brucellae* reveal a path to virulence. *J. Bacteriol.* 196, 920–930. doi: 10.1128/jb.01091-13
- Whatmore, A. M., Davison, N., Cloeckert, A., Dahouk, S. A., Zygmunt, M. S., Brew, S. D., et al. (2014). *Brucella papionis* sp. nov., isolated from baboons (*Papio* spp.). *Int. J. Syst. Evol. Microbiol.* 64, 4120–4128. doi: 10.1099/ijse.0.065482-0
- Yanagi, M., and Yamasato, K. (1993). Phylogenetic analysis of the family Rhizobiaceae and related bacteria by sequencing of 16S rRNA gene using PCR and DNA sequencer. *FEMS Microbiol. Lett.* 107, 115–120. doi: 10.1111/j.1574-6968.1993.tb06014.x
- Yoon, J. H., Kang, S.-J., Park, S., and Oh, T.-K. (2008). *Daeguia caeni* gen. nov., sp. nov., isolated from sludge of a textile dye works. *Int. J. Syst. Evol. Microbiol.* 58, 168–172. doi: 10.1099/ijse.0.65483-0
- Zurdo-Pineiro, J. L., Rivas, R., Trujillo, M. E., Vizcaino, N., Carrasco, J. A., Chamber, M., et al. (2007). *Ochrobactrum cytisi* sp. nov., isolated from nodules of *Cytisus scoparius* in Spain. *Int. J. Syst. Evol. Microbiol.* 57, 784–788. doi: 10.1099/ijse.0.64613-0

Conflict of Interest: The authors declare that the research was conducted in the absence of any commercial or financial relationships that could be construed as a potential conflict of interest.

Copyright © 2020 Leclercq, Cloeckert and Zygmunt. This is an open-access article distributed under the terms of the Creative Commons Attribution License (CC BY). The use, distribution or reproduction in other forums is permitted, provided the original author(s) and the copyright owner(s) are credited and that the original publication in this journal is cited, in accordance with accepted academic practice. No use, distribution or reproduction is permitted which does not comply with these terms.



Omp2b Porin Alteration in the Course of Evolution of *Brucella* spp.

Axel Cloeckaert^{1*}, Gilles Vergnaud² and Michel S. Zygmunt¹

¹ INRAE, UMR ISP, Université de Tours, Nouzilly, France, ² Institute for Integrative Biology of the Cell (I2BC), CEA, CNRS, Université Paris-Saclay, Gif-sur-Yvette, France

OPEN ACCESS

Edited by:

Miklos Fuzi,
Semmelweis University, Hungary

Reviewed by:

Zeliang Chen,
Shenyang Agricultural University,
China
Jens Andre Hammerl,
Federal Institute for Risk Assessment
(BfR), Germany

*Correspondence:

Axel Cloeckaert
Axel.Cloeckaert@inrae.fr

Specialty section:

This article was submitted to
Infectious Diseases,
a section of the journal
Frontiers in Microbiology

Received: 09 December 2019

Accepted: 07 February 2020

Published: 24 February 2020

Citation:

Cloeckaert A, Vergnaud G and
Zygmunt MS (2020) Omp2b Porin
Alteration in the Course of Evolution
of *Brucella* spp.
Front. Microbiol. 11:284.
doi: 10.3389/fmicb.2020.00284

The genus *Brucella* comprises major pathogenic species causing disease in livestock and humans, e.g. *B. melitensis*. In the past few years, the genus has been significantly expanded by the discovery of phylogenetically more distant lineages comprising strains from diverse wildlife animal species, including amphibians and fish. The strains represent several potential new species, with *B. inopinata* as solely named representative. Being genetically more distant between each other, relative to the “classical” *Brucella* species, they present distinct atypical phenotypes and surface antigens. Among surface protein antigens, the Omp2a and Omp2b porins display the highest diversity in the classical *Brucella* species. The genes coding for these proteins are closely linked in the *Brucella* genome and oriented in opposite directions. They share between 85 and 100% sequence identity depending on the *Brucella* species, biovar, or genotype. Only the *omp2b* gene copy has been shown to be expressed and genetic variation is extensively generated by gene conversion between the two copies. In this study, we analyzed the *omp2* loci of the non-classical *Brucella* spp. Starting from two distinct ancestral genes, represented by Australian rodent strains and *B. inopinata*, a stepwise nucleotide reduction was observed in the *omp2b* gene copy. It consisted of a first reduction affecting the region encoding the surface L5 loop of the porin, previously shown to be critical in sugar permeability, followed by a nucleotide reduction in the surface L8 loop-encoding region. It resulted in a final *omp2b* gene size shared between two distinct clades of non-classical *Brucella* spp. (African bullfrog isolates) and the group of classical *Brucella* species. Further evolution led to complete homogenization of both *omp2* gene copies in some *Brucella* species such as *B. vulpis* or *B. papionis*. The stepwise *omp2b* deletions seemed to be generated through recombination with the respective *omp2a* gene copy, presenting a conserved size among *Brucella* spp., and may involve short direct DNA repeats. Successive Omp2b porin alteration correlated with increasing porin permeability in the course of evolution of *Brucella* spp. They possibly have adapted their porin to survive environmental conditions encountered and to reach their final status as intracellular pathogen.

Keywords: *Brucella*, Omp2 porin, loop, diversity, gene conversion, evolution

INTRODUCTION

Members of the genus *Brucella* are Gram-negative, facultative, intracellular bacteria that can infect many species of animals and man. Until the 1990s, six species were classically recognized within the genus *Brucella*: *B. abortus*, *B. melitensis*, *B. suis*, *B. ovis*, *B. canis*, and *B. neotomae* (Corbel and Brinley Morgan, 1984; Moreno et al., 2002; Godfroid et al., 2011). This classification was mainly

based on differences in pathogenicity, host preference, and phenotypic characteristics (Alton et al., 1988). Since then, with the help of modern molecular typing methods [e.g. Multiple Loci Sequence Analysis (MLSA) and Multiple Loci VNTR Analysis (MLVA)] and whole genome sequencing (WGS), a number of new species representing mostly wildlife isolates and showing very different phenotypes have been validly published. In chronological order it concerns the species (i) *B. ceti* and *B. pinnipedialis* isolated from marine mammals, with cetaceans (dolphin, porpoise, and whale species) and pinnipeds (various seal species) as preferred hosts, respectively (Foster et al., 2007); (ii) *B. microti* isolated initially from the common vole but found later also in red foxes, in soil, and most recently in marsh frogs (Scholz et al., 2008a,b, 2009; Jaý et al., 2018); (iii) *B. inopinata* isolated from human (Scholz et al., 2010); (iv) *B. papionis* isolated from baboons (Whatmore et al., 2014); and (v) the latest *B. vulpis* species isolated from red foxes (Scholz et al., 2016a). Novel *Brucella* strains representing potentially novel species have also been isolated from Australian rodents (Tiller et al., 2010a), a wide variety of frog species (Eisenberg et al., 2012; Fischer et al., 2012; Scholz et al., 2016b; Soler-Lloréns et al., 2016; Al Dahouk et al., 2017; Kimura et al., 2017; Mühldorfer et al., 2017), and surprisingly also from fish namely from a bluespotted ribbontail ray (*Taeniura lymma*) (Eisenberg et al., 2017). The genus *Brucella* nowadays is thus not restricted to mammal species. The most recent potential new species reported is isolated from a dog in Costa Rica in the early 1980s (Guzmán-Verri et al., 2019).

Brucella spp. consist nowadays of two major groups. The first represents the species termed “classical” and consists of the six initially recognized species together with the more recent species *B. ceti*, *B. pinnipedialis*, *B. microti*, and *B. papionis*. The further subdivision in MLSA or MLVA genotypes proved to be helpful for subtyping of some species. For example *B. ceti* genotype ST23 is currently mainly found in several cetacean species (porpoise, dolphin, whale), whereas *B. ceti* genotype ST26 seems more restricted to dolphin species (Maquart et al., 2009; Whatmore et al., 2016; Vergnaud et al., 2018). The first group has been characterized and investigated in detail because of its importance in causing disease in animals and humans. The second major group is represented by lineages phylogenetically more distant from the classical species and still poorly characterized. This group comprises several distinct subgroups consisting of isolates from diverse wildlife animal species cited above, i.e. Red foxes, Australian rodents, several frog species, the isolate from a ray fish, and interestingly also two isolates from human cases. These subgroups represent several potential new species, with *B. inopinata*, isolated from a human case, as solely named representative. Being genetically more distant between each other, relative to the classical *Brucella* species, they present distinct atypical phenotypes and surface antigens. For example several amphibian subgroups and the human isolate *Brucella* sp. BO2 present distinct unidentified O antigens, that are not typable by polyclonal or monoclonal antibodies used for serotyping of the classical species (Tiller et al., 2010b; Zygmunt et al., 2012; Al Dahouk et al., 2017).

Among outer membrane proteins, the Omp2 porins have been shown to display the highest diversity within the classical *Brucella* species, which allowed to differentiate them at the species, biovar, or genotype level (Ficht et al., 1990, 1996; Cloekaert et al., 1995, 2001). More precisely, the porins are encoded by the *omp2* locus, consisting of two closely related genes *omp2a* and *omp2b*, separated by approximately 830 bp and oriented in opposite directions (Ficht et al., 1989; Marquis and Ficht, 1993). Gene diversity is extensively generated by recombination between both copies called also gene conversion (Santoyo and Romero, 2005), thus resulting in *omp2a* and *omp2b* gene copies sharing from 82 to 100% nucleotide identity depending on the species, biovar or genotype. The highest divergence between the gene copies in classical species was found in *B. microti* and *B. melitensis* (82.4 and 83.4% identity, respectively, see **Supplementary Figure S1**). In contrast, complete homogenization of the copies (100% identity) was observed for *B. ceti* ST26 or *B. papionis* (**Supplementary Figure S1**). Several other situations may be observed and in former studies *Brucella* strains were sometimes described in a simple way as carrying either (i) both the *omp2a* and *omp2b* gene copies (e.g. *B. melitensis*), (ii) two *omp2a* gene copies (e.g. *B. ovis*), or (iii) two *omp2b* gene copies (e.g. *B. ceti*) (Ficht et al., 1990, 1996; Cloekaert et al., 2001). The release of additional sequences showed that the situation is more complex because of the existence of numerous intermediate situations, including also *B. ovis* whose gene copies are actually not 100% *omp2a* identical. Only the *omp2b* gene copy has been shown to be expressed (Marquis and Ficht, 1993), and the genetic exchanges that may occur with its *omp2a* counterpart may affect the sugar permeability of the expressed porin as previously shown for naturally chimeric Omp2a and Omp2b porin variants (Paquet et al., 2001). The evaluated Omp2a variant showed a more efficient pore in sugar diffusion than the Omp2b variant. Differences in their respective L5 surface-exposed loop were suggested to play a major role in permeability, the L5 loop of Omp2a being shorter and containing less negatively charged residues than that of Omp2b.

Porins being important first line players to resist and adapt to environmental conditions, in the present study we analyzed the *omp2* loci and their encoded porins from non-classical *Brucella* spp. to identify possible evolutionary paths that may have contributed to the adaptation to their final status as intracellular mammal or human pathogens.

MATERIALS AND METHODS

Brucella strains analyzed were from previous studies (Scholz et al., 2010, 2016a; Tiller et al., 2010a,b; Zygmunt et al., 2012; Al Dahouk et al., 2017; Eisenberg et al., 2017), and are listed in the **Supplementary Figure S1**. Bacterial cultures and DNA extraction were performed as described previously (Cloekaert et al., 1995). For the African bullfrog isolates of this study, DNA was extracted from killed bacterial cells provided by Dr. S. Al Dahouk (BfR, Berlin, Germany). PCR amplification of the *omp2a* and *omp2b* genes was performed as described previously (Cloekaert et al., 1995, 2001). The PCR products were sequenced at Genome

Express (Meylan, France). Nucleotide sequence analysis and alignments were done using Clustal Omega at EBI¹. GenBank nucleotide accession numbers are indicated in **Supplementary Figure S1**. *omp2* sequences were aligned using BioNumerics version 7.6.3 (Applied Maths, Belgium) with default parameters and the multiple alignment was used to produce a Maximum Parsimony tree. Comparative Omp2 protein analyses were done using a previously published Omp2a and Omp2b predicted and functionally validated topology model (Paquet et al., 2001).

Whole genome SNP (wgSNP) analysis was done as previously described (Vergnaud et al., 2018). Full genome sequences and assemblies were converted into artificial reads. SNPs were identified by mapping sequencing reads on a reference genome within BioNumerics. Assembly GCF_000007125 (*B. melitensis* 16 M) was used as reference. The Bio-Neighbor joining algorithm

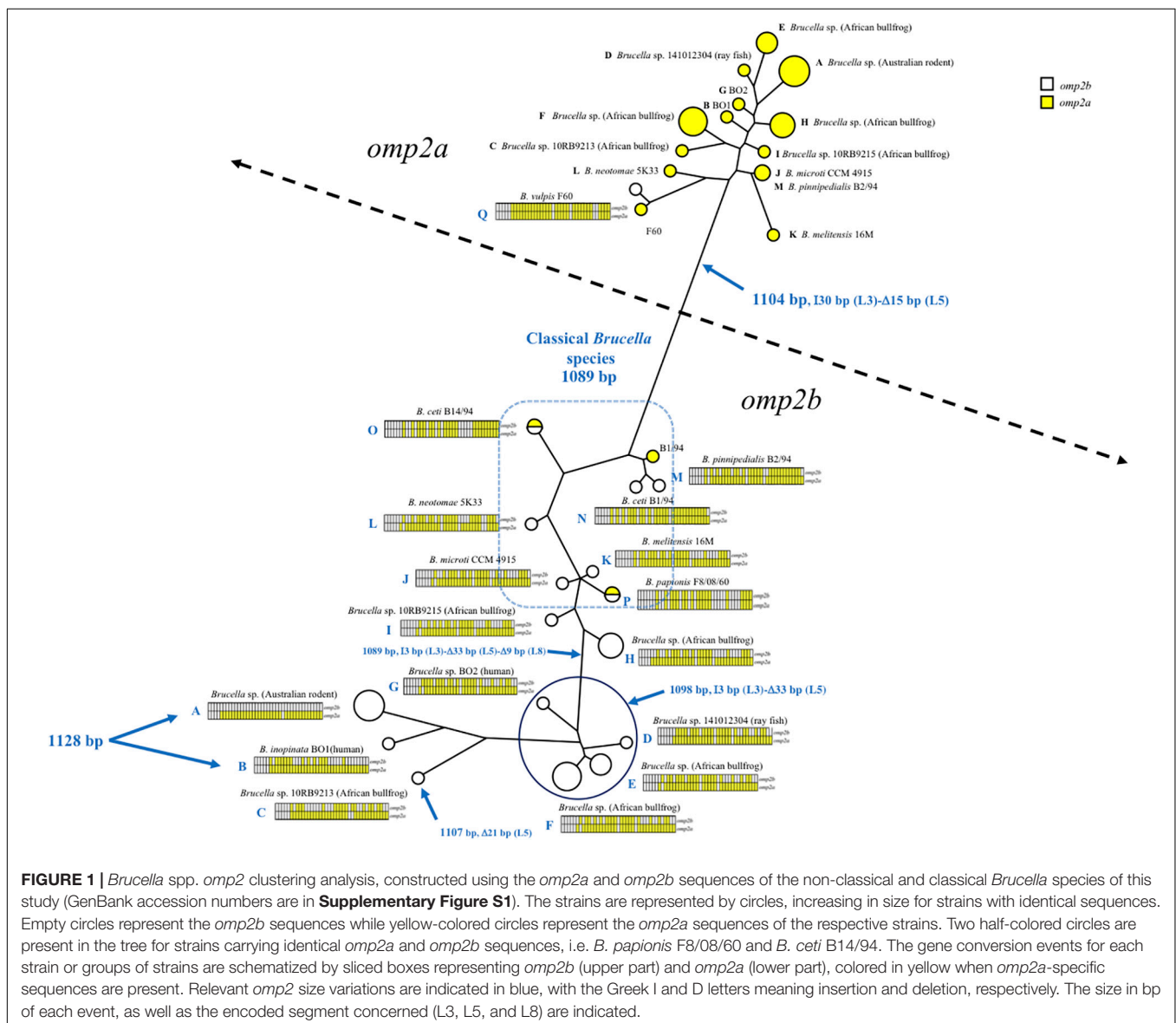
with bootstrap analysis embedded in BioNumerics was used for clustering analysis (Gascuel, 1997).

RESULTS AND DISCUSSION

Global View of *omp2* Gene Diversity in *Brucella* spp.

As shown in **Figures 1, 2** and **Supplementary Figure S1**, *omp2* sequence diversity analysis allowed to separate the non-classical *Brucella* spp. of this study in nine distinct groups (A to I), that correlated perfectly well with other previously published molecular methods such as MLSA, MLVA, IS711 profiling, or whole genome phylogeny (**Figure 3**). A second observation was a relative lower nucleotide sequence identity between their respective *omp2a* and *omp2b* gene copy ranging from 78.9 to

¹ www.ebi.ac.uk/Tools/msa/clustalo/



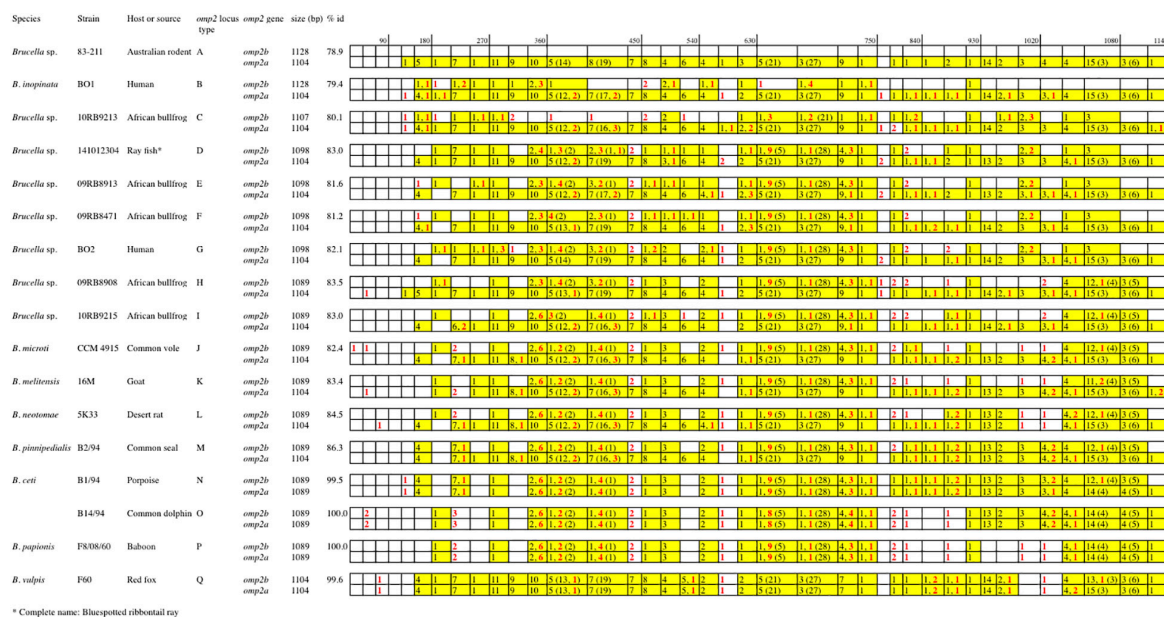


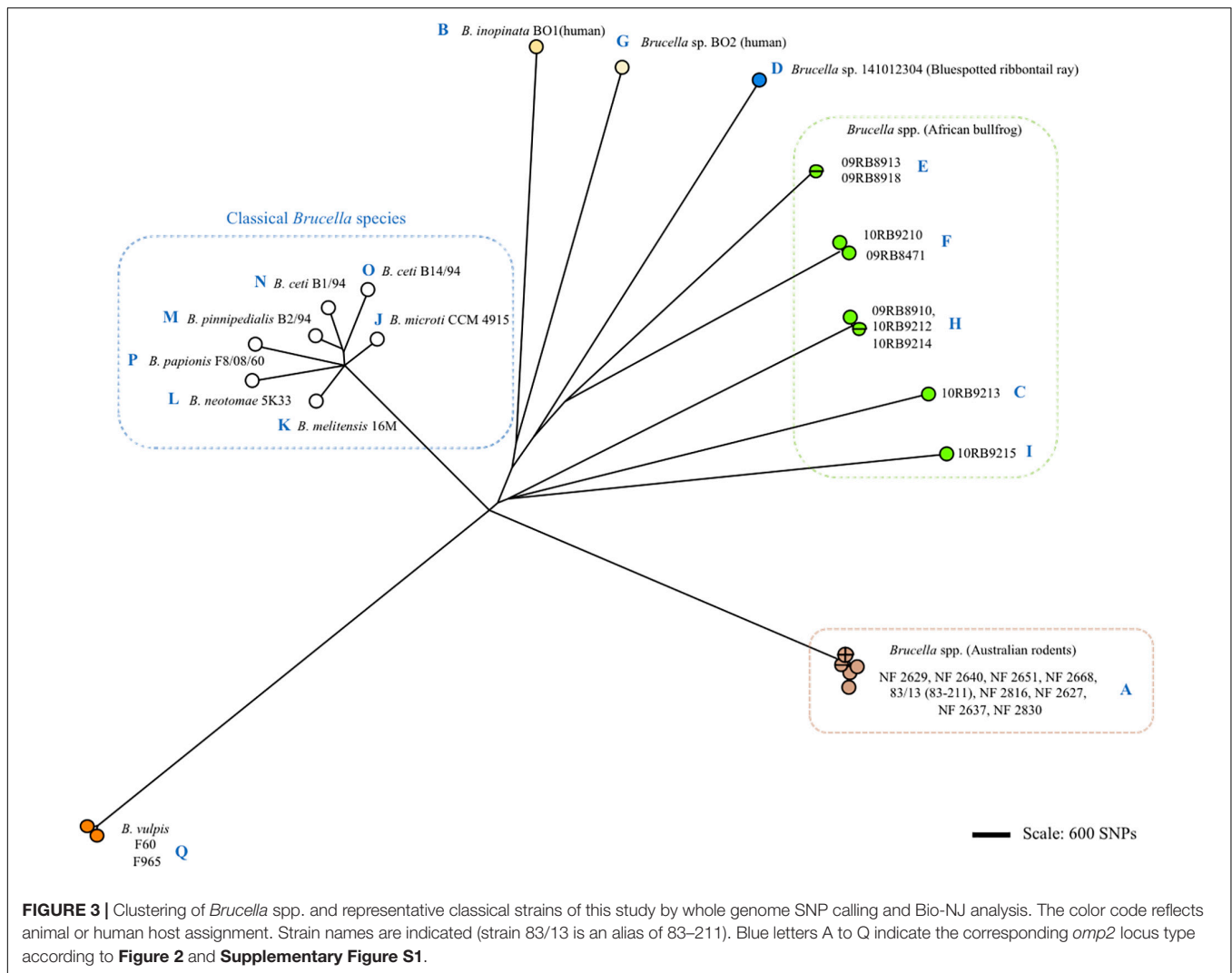
FIGURE 2 | Schematic multiple nucleotide sequence alignment of the *omp2a* and *omp2b* genes of *Brucella* strains. This schematic representation was done according to the detailed alignment shown in the **Supplementary Figure S1**. Nucleotide sequences are represented by rectangles divided into boxes of 30 nucleotides. The *Brucella* sp. 83-211 *omp2b* gene sequence was used as a reference (white boxes). The boxes containing *omp2a*-specific nucleotides are colored in yellow. The numbers in the corresponding boxes indicate the number of *omp2a*-specific nucleotides present in the sequence considered. Numbers in parentheses represent insertions and deletions. Numbers in red indicate nucleotide differences that are not due to gene conversion.

83.5%, in comparison to those of classical *Brucella* species ranging from 82.4 to 100% (**Figure 2** and **Supplementary Figure S1**). Considering all *omp2* sequences from both classical and non-classical *Brucella* spp., two separate clusters were observed in the clustering analysis. The “*omp2a*” cluster appeared less diverse than the “*omp2b*” cluster (**Figure 1**). All *omp2a* representatives shared the same size (1104 bp). In contrast, the size of *omp2b* representatives varied from 1089 to 1128 bp. To analyze in more detail the molecular basis behind this diversity, in particular recombination events, we have used the two most divergent *omp2* gene copies, namely those of *Brucella* spp. isolated from Australian rodents, to designate them as either reference *omp2a* and reference *omp2b* gene copy. It actually provided a more comprehensive evolutionary picture, establishing a clearer link between classical and non-classical strains, than if the most divergent gene copies observed in the classical species only had been used as in previous studies (eg. *B. melitensis* or *B. microti*) (Cloekaert et al., 2001; Al Dahouk et al., 2012). It also allowed to explain *omp2b* gene size variation, through stepwise genetic reduction, from the size observed for Australian rodent strains to that of the classical *Brucella* species. Starting from these designated reference *omp2a* and *omp2b* gene copies, the effect of genetic recombination events was observed in all groups of strains. Recombination events are schematized in **Figure 1** by boxes containing either uncolored segments (*omp2b*) or yellow-colored segments (containing *omp2a*-specific nucleotides) along the groups of strains studied, and these genetic changes are more detailed in **Figure 2**. The events observed consisted mostly of converting some specific *omp2b* regions into *omp2a*, but the

opposite situation (converting *omp2a* regions to *omp2b*) also occurred for some genotypes, resulting in almost complete (e.g. *B. vulpis* or *B. ceti* ST23) or complete (e.g. *B. ceti* ST26 or *B. papionis*) homogenization of both gene copies. Of note is that homogenization did not involve the same *omp2* regions for the examples cited above (see **Figure 2**), resulting in the placement of the homogenized copies in either the *omp2a* or the *omp2b* cluster of the *omp2* clustering analysis, for, respectively, *B. vulpis* and the other species/genotypes (**Figure 1**).

Regarding *omp2b* gene size variation, departing from a 1128 bp-sized *omp2b* gene as represented in Australian rodent *Brucella* spp. (group A) and the human *B. inopinata* BO1 isolate (group B), a number of consecutive indel events were observed including: (i) a deletion of 21 bp in the surface-encoding loop L5 in *Brucella* sp. 10RB9213 isolated from an African bullfrog; (ii) a deletion of 33 bp in the same region in four groups of isolates representing two groups from African bullfrogs (groups E and F), one isolate from ray fish (strain 141012304, group D) and the human isolate BO2 (group G); and (iii) and a 9 bp deletion in the region encoding the L8 surface-exposed loop was detected in two groups of African bullfrog strains (H and I), to reach the *omp2b* size of classical species (1089 bp). Those latter African bullfrog *Brucella* spp. thus present the same *omp2b* size as the classical species represented in **Figure 1** (from *B. microti* to the marine mammal species *B. ceti* and *B. pinnipedialis*).

Relative to *omp2b* of classical species (1089 bp), the 1104 bp-sized *omp2a* differs by an insertion of 30 bp in the region encoding the L3 surface loop and a deletion of 15 bp in the region encoding the L5 surface loop (**Figure 1**). The conserved size of the



omp2a gene copy in both the non-classical and classical species suggests that, as previously observed for classical species (Ficht et al., 1996; Cloekaert et al., 2002), this gene copy may have been used to convert its *omp2b* counterpart and thus generate the successive *omp2b* gene deletions in the course of evolution of the non-classical species.

Porin Evolution in the Global Phylogenomic Background Diversity of *Brucella* spp.

Although the Omp2b diversity generated through gene conversion appeared sequential, it did not correlate with the global phylogeny of *Brucella* spp. as shown in **Figure 3**. More precisely, we did not observe a clear sequential evolutionary link among the non-classical species which appeared genetically far more distant between each other than is reflected by the diversity of their *omp2* locus. It may be explained by the essential functional nature of the Omp2b porin (Laloux et al., 2010), that actually would allow only variation depending on the

external or intracellular environmental pressure and favor convergent evolution. In addition, although some SNPs were observed between *omp2* sequences (indicated in **Figures** and **Supplementary Figures S1–S3**), Omp2b variation relied mainly on gene conversion and not on SNP variation as for the whole phylogeny of *Brucella* spp.

Genetic Loss and Functional Alteration of the Omp2b Porin

As described above *omp2a* or *omp2b* insertions or deletions were predominantly located in regions encoding three predicted surface exposed loops, namely L3, L5, and L8 (Paquet et al., 2001). **Figure 4** shows a nucleotide sequence alignment of each region of representative strains of this study, complete sequence alignment is shown in **Supplementary Figure S2**. The L3 encoding region is characterized by either a 33 bp or 30 bp deletion in *omp2b* relative to *omp2a* in *omp2* groups A, B, and C *Brucella* strains and the other groups, respectively. This 3 bp difference is difficult to explain according to the sequence alignment, but nevertheless in the shorter deletion, *omp2a*-specific sequence fragments remain

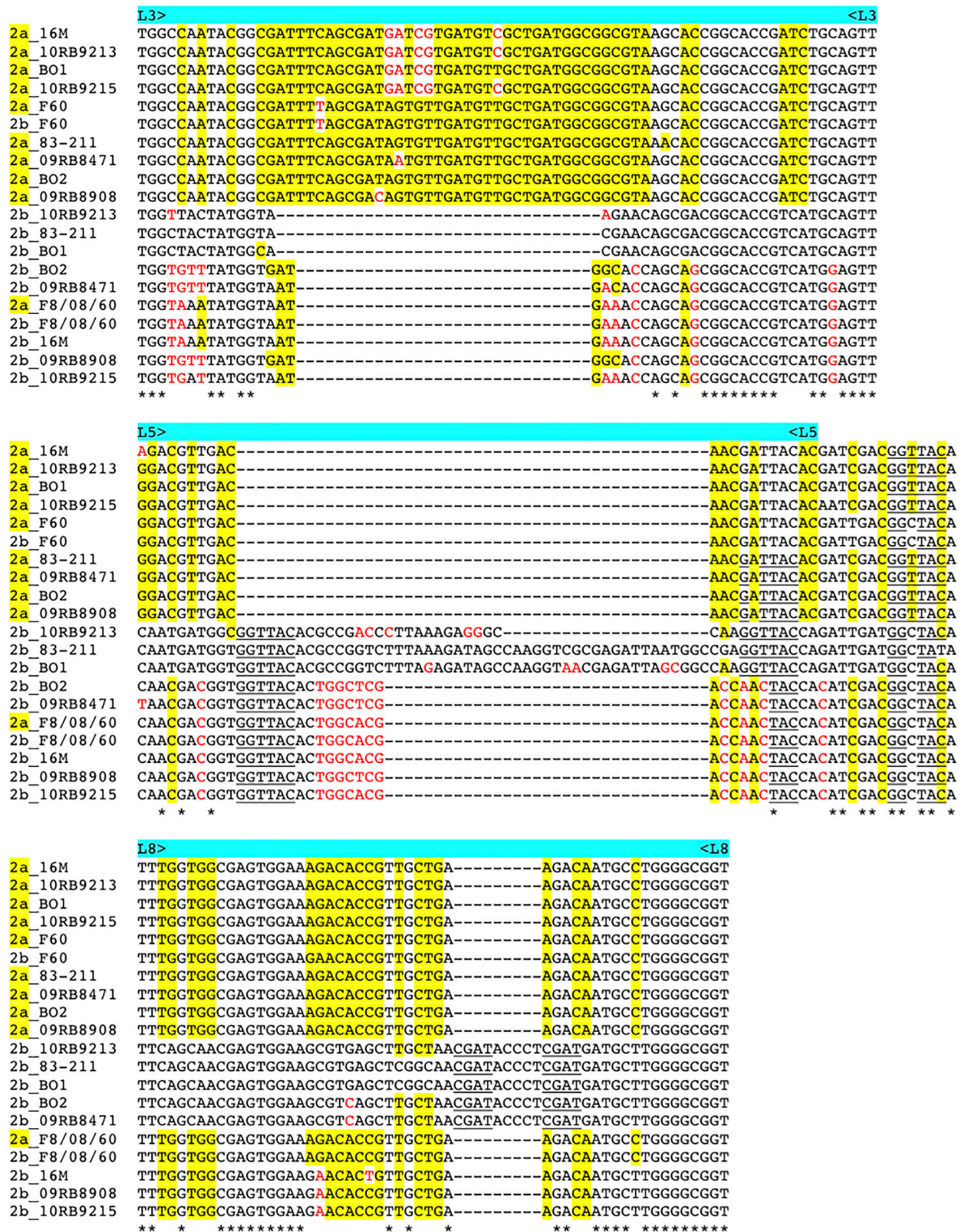


FIGURE 4 | Multiple nucleotide sequence alignment of the *omp2* segments encoding the L3, L5, and L8 loops (upper, middle, and lower panel, respectively), from representative strains containing insertions or deletions. Strains and *omp2* genes used are indicated on the left of each segment, *omp2a* genes are indicated as 2a in yellow. *omp2a*-specific nucleotides are highlighted in yellow, according to the *omp2a* and *omp2b* reference sequences used from *Brucella* sp. 83-211. Nucleotides colored in red indicate differences that are not due to gene conversion, according to the same reference sequences. Direct DNA repeats are underlined. *Indicates identical nucleotides.

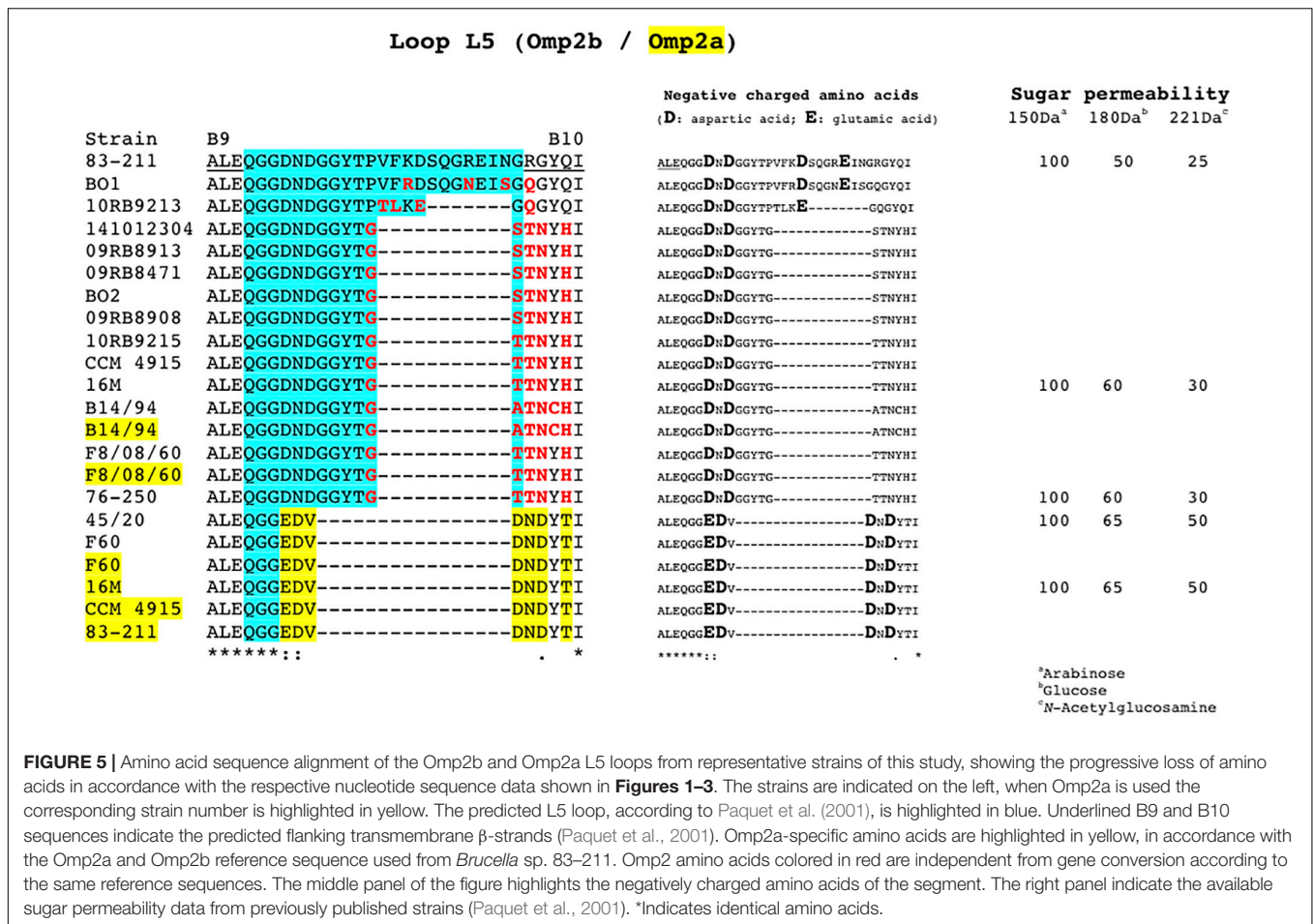


FIGURE 5 | Amino acid sequence alignment of the Omp2b and Omp2a L5 loops from representative strains of this study, showing the progressive loss of amino acids in accordance with the respective nucleotide sequence data shown in **Figures 1–3**. The strains are indicated on the left, when Omp2a is used the corresponding strain number is highlighted in yellow. The predicted L5 loop, according to Paquet et al. (2001), is highlighted in blue. Underlined B9 and B10 sequences indicate the predicted flanking transmembrane β -strands (Paquet et al., 2001). Omp2a-specific amino acids are highlighted in yellow, in accordance with the Omp2a and Omp2b reference sequence used from *Brucella* sp. 83-211. Omp2 amino acids colored in red are independent from gene conversion according to the same reference sequences. The middle panel of the figure highlights the negatively charged amino acids of the segment. The right panel indicate the available sugar permeability data from previously published strains (Paquet et al., 2001). *Indicates identical amino acids.

suggesting that the deletion in *omp2b* resulted from an intra-molecular recombination event between *omp2a* and *omp2b* for this specific region. The L3 loop has been shown to play a major role as constriction loop in most bacterial porins (Jap and Walian, 1996). However, in *Brucella* spp. this loop did not appear critical for sugar permeability according to a previous study (Paquet et al., 2001). According to the same study the L5 loop appeared to be a critical determinant in *Brucella* porin sugar permeability and could participate in the formation of the pore “external mouth,” which serves to prescreen the solute in porins of known structure (Paquet et al., 2001). Consistent with this, two deletions, a first of 21 bp and the second of 33 bp, in the L5 encoding region of the Omp2b porin were identified in the present study, starting from the *omp2* groups A and B strains to reach a minimal L5 size in the other groups of strains, with J to O strains representing the classical *Brucella* species (**Figures 1, 4**). In addition, it must be noted that *omp2b* from *B. vulpis* (group P in **Figures 1, 2**) represents a separate situation as its *omp2b* copy has converted to *omp2a* in the L5 region with a concomitant additional 15 bp deletion relative to other *omp2b* sequences (**Figure 4**), thus making it the shortest Omp2b encoding L5 region of strains of this study. A similar situation has been reported previously for *B. abortus* strain 45/20 for which the same *omp2b* to *omp2a* sequence conversion was

observed in this segment (Paquet et al., 2001). The different L5 situations are detailed in the nucleotide sequence alignment of **Figure 4**. In addition to segmental gene conversion-mediated exchanges between the respective *omp2a* and *omp2b* gene copy, short 6 bp direct DNA repeats may have contributed to generate the different deletions observed in the L5-encoding segment. At the amino acid sequence level it resulted in the loss of either 7 or 11 amino acids including one or two negatively charged residues, respectively (**Figure 5**), that may possibly be important on ion conductance and ion selectivity of the L5 loop (Paquet et al., 2001). According to previous data, the sequential loss of amino acids observed correlates with increased sugar permeability to reach the highest permeation rate for porin variants containing the shortest Omp2a-type L5 loop (**Figure 5**; Paquet et al., 2001).

The last genetic reduction observed in the sequential course of Omp2b porin evolution shown in **Figure 1**, consisted of a 9 bp deletion in the region encoding the surface L8 loop, and it finally ended up to the size of *omp2b* and the respective Omp2b porin protein observed for the classical species. As shown in **Figure 5** this short deletion, as observed for the L5 segment, may be the result of gene conversion using the respective *omp2a* copy as template, and two short 4 bp direct repeats may also have contributed to create this deletion. In addition it created an *omp2a*-like segment at the 3' end of the respective

omp2b sequence, which did not appear as clearly when using as references *omp2a* and *omp2b* genes from classical species (e.g. *B. melitensis* 16 M) (Cloekaert et al., 2001). As a consequence group H and I non-classical *Brucella* spp. (African bullfrog isolates), possess Omp2b porins with an Omp2a-like L8 surface loop at the amino acid sequence level, as seen in all classical *Brucella* species (Supplementary Figure S3). The L8 surface loop was previously shown to be an important target site recognized by monoclonal antibodies directed against conformational epitopes of the Omp2b porin (Paquet et al., 2001). We thus predict that the genetic loss in the L8 encoding region has created antigenic variability of the corresponding protein in the course of evolution of *Brucella* spp., and possibly may have affected antibody induction and recognition in some animal species. In several bacterial species gene conversion appears to have a prime importance in the generation of antigenic variation, an interesting mechanism whereby some bacterial pathogens are able to avoid the host immune system (Santoyo and Romero, 2005). For example, in *Anaplasma marginale* the major surface protein Msp2 is encoded by a single expression site, and diversity is achieved by gene conversion of chromosomally encoded *msp2* pseudogenes (Graça et al., 2015). A model was proposed where *msp2*, through gene conversion, progressively incorporates changes to produce an *msp2* repertoire capable of generating sufficient antigenic variants to escape immunity and establish persistent infection (Graça et al., 2019). We may see a similar situation from the present *omp2* study, with the progressive changes of the Omp2b porin cited above, altering the porin both functionally and antigenically.

CONCLUSION

This study provided evidence for a progressive genetic loss in the *omp2b* gene encoding the major outer membrane porin, from non-classical *Brucella* spp. to the classical pathogenic *Brucella*

species. This genetic loss appears mainly mediated by segmental gene conversion events with its silent *omp2a* gene copy, and concerns especially the regions encoding the L5 surface loop for porin function and the L8 loop for antigenic variability. The progressive loss in the L5 loop correlates with increasing sugar permeability of the porin, and could be related to environmental adaptation to survive conditions from a possible extracellular aquatic environment (e.g. amphibian or fish) to the intracellular macrophagic environment of the classical pathogenic species causing disease in livestock and humans.

DATA AVAILABILITY STATEMENT

The new sequence data of this study were deposited in Genbank. The accession numbers are listed in Supplementary Figure S1.

AUTHOR CONTRIBUTIONS

AC conceived and designed the study. AC, GV, and MZ analyzed the data, and drafted the manuscript.

ACKNOWLEDGMENTS

We thank Nelly Bernardet for expert technical assistance and Dr. S. Al Dahouk (BfR, Berlin, Germany) for providing killed bacterial cells used to extract DNA analyzed in this study.

SUPPLEMENTARY MATERIAL

The Supplementary Material for this article can be found online at: <https://www.frontiersin.org/articles/10.3389/fmicb.2020.00284/full#supplementary-material>

REFERENCES

- Al Dahouk, S., Hofer, E., Tomaso, H., Vergnaud, G., Le Flèche, P., Cloekaert, A., et al. (2012). Intraspecies biodiversity of the genetically homologous species *Brucella microti*. *Appl. Environ. Microbiol.* 78, 1534–1543. doi: 10.1128/AEM.06351-11
- Al Dahouk, S., Köhler, S., Occhialini, A., Jiménez de Bagüés, M. P., Hammerl, J. A., Eisenberg, T., et al. (2017). *Brucella* spp. of amphibians comprise genomically diverse motile strains competent for replication in macrophages and survival in mammalian hosts. *Sci. Rep.* 7:44420. doi: 10.1038/srep44420
- Alton, G. G., Jones, L. M., Angus, R. D., and Verger, J. M. (1988). *Techniques for the Brucellosis Laboratory*. Paris: INRA.
- Cloekaert, A., Verger, J. M., Grayon, M., and Grépinet, O. (1995). Restriction site polymorphism of the genes encoding the major 25 kDa and 36 kDa outer-membrane proteins of *Brucella*. *Microbiology* 141, 2111–2121. doi: 10.1099/13500872-141-9-2111
- Cloekaert, A., Verger, J. M., Grayon, M., Paquet, J. Y., Garin-Bastuji, B., Foster, G., et al. (2001). Classification of *Brucella* spp. isolated from marine mammals by DNA polymorphism at the *omp2* locus. *Microbes Infect.* 3, 729–738. doi: 10.1016/s1286-4579(01)01427-7
- Cloekaert, A., Vizcaino, N., Paquet, J. Y., Bowden, R. A., and Elzer, P. H. (2002). Major outer membrane proteins of *Brucella* spp.: past, present and future. *Vet. Microbiol.* 90, 229–247. doi: 10.1016/s0378-1135(02)00211-0
- Corbel, M. J., and Brinley Morgan, W. J. (1984). “Genus *Brucella* meyer and shaw 1920, 173AL,” in *Bergey's Manual of Systematic Bacteriology*, eds N. R. Krieg, and J. G. Holt, (Baltimore, MD: Williams and Wilkins), 377–390.
- Eisenberg, T., Hamann, H. P., Kaim, U., Schlez, K., Seeger, H., and Schauerte, N. (2012). Isolation of potentially novel *Brucella* spp. from frogs. *Appl. Environ. Microbiol.* 78, 3753–3755. doi: 10.1128/AEM.07509-11
- Eisenberg, T., Riße, K., Schauerte, N., Geiger, C., Blom, J., and Scholz, H. C. (2017). Isolation of a novel ‘atypical’ *Brucella* strain from a bluespotted ribbontail ray (*Taeniura lymma*). *Antonie Van Leeuwenhoek* 110, 221–234. doi: 10.1007/s10482-016-0792-4
- Ficht, T. A., Bearden, S. W., Sowa, B. A., and Adams, L. G. (1989). DNA sequence and expression of the 36-kilodalton outer membrane protein gene of *Brucella abortus*. *Infect. Immun.* 57, 3281–3291. doi: 10.1128/iai.57.11.3281-3291.1989
- Ficht, T. A., Bearden, S. W., Sowa, B. A., and Marquis, H. (1990). Genetic variation at the *omp2* porin locus of the *brucellae*: species-specific markers. *Mol. Microbiol.* 4, 1135–1142. doi: 10.1111/j.1365-2958.1990.tb00688.x
- Ficht, T. A., Husseinen, H. S., Derr, J., and Bearden, S. W. (1996). Species-specific sequences at the *omp2* locus of *Brucella* type strains. *Int. J. Syst. Bacteriol.* 46, 329–331. doi: 10.1099/00207713-46-1-329

- Fischer, D., Lorenz, N., Heuser, W., Kämpfer, P., Scholz, H. C., and Lierz, M. (2012). Abscesses associated with a *Brucella inopinata*-like bacterium in a big-eyed tree frog (*Leptopelis vermiculatus*). *J. Zoo Wildl. Med.* 43, 625–628. doi: 10.1638/2011-0005r2.1
- Foster, G., Osterman, B. S., Godfroid, J., Jacques, I., and Cloekaert, A. (2007). *Brucella ceti* sp. nov. and *Brucella pinnipedialis* sp. nov. for *Brucella* strains with cetaceans and seals as their preferred hosts. *Int. J. Syst. Evol. Microbiol.* 57, 2688–2693. doi: 10.1099/ijs.0.65269-0
- Gascuel, O. (1997). BIONJ: an improved version of the NJ algorithm based on a simple model of sequence data. *Mol. Biol. Evol.* 14, 685–695. doi: 10.1093/oxfordjournals.molbev.a025808
- Godfroid, J., Scholz, H. C., Barbier, T., Nicolas, C., Wattiau, P., Fretin, D., et al. (2011). Brucellosis at the animal/ecosystem/human interface at the beginning of the 21st century. *Prev. Vet. Med.* 102, 118–131. doi: 10.1016/j.prevetmed.2011.04.007
- Graça, T., Ku, P. S., Silva, M. G., Turse, J. E., Hammac, G. K., and Brown, W. C. (2019). Segmental variation in a duplicated *msh2* pseudogene generates *Anaplasma marginale* antigenic variants. *Infect. Immun.* 87:e00727-18.
- Graça, T., Paradiso, L., Broschat, S. L., Noh, S. M., and Palmer, G. H. (2015). Primary structural variation in *Anaplasma marginale* Msp2 efficiently generates immune escape variants. *Infect. Immun.* 83, 4178–4184. doi: 10.1128/IAI.00851-815
- Guzmán-Verri, C., Suárez-Esquivel, M., Ruiz-Villalobos, N., Zygmunt, M. S., Gonnet, M., Campos, E., et al. (2019). Genetic and phenotypic characterization of the etiological agent of canine orchitis epididymitis smooth *Brucella* sp. BCCN84.3. *Front. Vet. Sci.* 6:175. doi: 10.3389/fvets.2019.00175
- Jap, B. K., and Walian, P. J. (1996). Structure and functional mechanism of porins. *Physiol. Rev.* 76, 1073–1088. doi: 10.1152/physrev.1996.76.4.1073
- Jaý, M., Girault, G., Perrot, L., Taunay, B., Vuilmet, B., Rossignol, F., et al. (2018). Phenotypic and molecular characterization of *Brucella microti*-like bacteria from a domestic marsh frog (*Pelophylax ridibundus*). *Front. Vet. Sci.* 5:283. doi: 10.3389/fvets.2018.00283
- Kimura, M., Une, Y., Suzuki, M., Park, E. S., Imaoka, K., and Morikawa, S. (2017). Isolation of *Brucella inopinata*-like bacteria from White's and Denny's tree frogs. *Vector Borne Zoonotic Dis.* 17, 297–302. doi: 10.1089/vbz.2016.2027
- Laloux, G., Deghelt, M., de Barys, M., Letesson, J. J., and De Bolle, X. (2010). Identification of the essential *Brucella melitensis* porin Omp2b as a suppressor of Bax-induced cell death in yeast in a genome-wide screening. *PLoS One* 5:e13274. doi: 10.1371/journal.pone.0013274
- Maquart, M., Le Flèche, P., Foster, G., Tryland, M., Ramisse, F., Djønne, B., et al. (2009). MLVA16 typing of 295 marine mammal *Brucella* isolates from different animal and geographic origins identifies 7 major groups within *Brucella ceti* and *Brucella pinnipedialis*. *BMC Microbiol.* 9:145. doi: 10.1186/1471-2180-9-145
- Marquis, H., and Ficht, T. A. (1993). The *omp2* gene locus of *Brucella abortus* encodes two homologous outer membrane proteins with properties characteristic of bacterial porins. *Infect. Immun.* 61, 3785–3790. doi: 10.1128/iai.61.9.3785-3790.1993
- Moreno, E., Cloekaert, A., and Moriyón, I. (2002). *Brucella* evolution and taxonomy. *Vet. Microbiol.* 90, 209–227. doi: 10.1016/s0378-1135(02)00210-9
- Mühldorfer, K., Wibbelt, G., Szentiks, C. A., Fischer, D., Scholz, H. C., Zschöck, M., et al. (2017). The role of 'atypical' *Brucella* in amphibians: are we facing novel emerging pathogens? *J. Appl. Microbiol.* 122, 40–53. doi: 10.1111/jam.13326
- Paquet, J. Y., Diaz, M. A., Genevros, S., Grayon, M., Verger, J. M., de Bolle, X., et al. (2001). Molecular, antigenic, and functional analyses of Omp2b porin size variants of *Brucella* spp. *J. Bacteriol.* 183, 4839–4847. doi: 10.1128/jb.183.16.4839-4847.2001
- Santoyo, G., and Romero, D. (2005). Gene conversion and concerted evolution in bacterial genomes. *FEMS Microbiol. Rev.* 29, 169–183. doi: 10.1016/j.femsre.2004.10.004
- Scholz, H. C., Hofer, E., Vergnaud, G., Le Flèche, P., Whatmore, A. M., Al Dahouk, S., et al. (2009). Isolation of *Brucella microti* from mandibular lymph nodes of red foxes, *Vulpes vulpes*, in lower Austria. *Vector Borne Zoonotic Dis.* 9, 153–156. doi: 10.1089/vbz.2008.0036
- Scholz, H. C., Hubalek, Z., Nesvadbova, J., Tomaso, H., Vergnaud, G., Le Flèche, P., et al. (2008b). Isolation of *Brucella microti* from soil. *Emerg. Infect. Dis.* 14, 1316–1317. doi: 10.3201/eid1408.080286
- Scholz, H. C., Hubalek, Z., Sedláček, I., Vergnaud, G., Tomaso, H., Al Dahouk, S., et al. (2008a). *Brucella microti* sp. nov., isolated from the common vole *Microtus arvalis*. *Int. J. Syst. Evol. Microbiol.* 58, 375–382. doi: 10.1099/ijs.0.65356-65350
- Scholz, H. C., Mühldorfer, K., Shilton, C., Benedict, S., Whatmore, A. M., Blom, J., et al. (2016b). The change of a medically important genus: worldwide occurrence of genetically diverse novel *Brucella* species in exotic frogs. *PLoS One* 11:e0168872. doi: 10.1371/journal.pone.0168872
- Scholz, H. C., Nöckler, K., Göllner, C., Bahn, P., Vergnaud, G., Tomaso, H., et al. (2010). *Brucella inopinata* sp. nov., isolated from a breast implant infection. *Int. J. Syst. Evol. Microbiol.* 60, 801–808. doi: 10.1099/ijs.0.011148-11140
- Scholz, H. C., Revilla-Fernández, S., Al Dahouk, S., Hammerl, J. A., Zygmunt, M. S., Cloekaert, A., et al. (2016a). *Brucella vulpis* sp. nov., isolated from mandibular lymph nodes of red foxes (*Vulpes vulpes*). *Int. J. Syst. Evol. Microbiol.* 66, 2090–2098. doi: 10.1099/ijsem.0.000998
- Soler-Lloréns, P. F., Quance, C. R., Lawhon, S. D., Stuber, T. P., Edwards, J. F., Ficht, T. A., et al. (2016). A *Brucella* spp. isolate from a Pac-Man frog (*Ceratophrys ornata*) reveals characteristics departing from classical *Brucellae*. *Front. Cell. Infect. Microbiol.* 6:116. doi: 10.3389/fcimb.2016.00116
- Tiller, R. V., Gee, J. E., Frace, M. A., Taylor, T. K., Setubal, J. C., Hoffmaster, A. R., et al. (2010a). Characterization of novel *Brucella* strains originating from wild native rodent species in North Queensland, Australia. *Appl. Environ. Microbiol.* 76, 5837–5845. doi: 10.1128/AEM.00620-610
- Tiller, R. V., Gee, J. E., Lonsway, D. R., Gribble, S., Bell, S. C., Jennison, A. V., et al. (2010b). Identification of an unusual *Brucella* strain (BO2) from a lung biopsy in a 52 year-old patient with chronic destructive pneumonia. *BMC Microbiol.* 10:23. doi: 10.1186/1471-2180-10-23
- Vergnaud, G., Hauck, Y., Christiany, D., Daoud, B., Pourcel, C., Jacques, I., et al. (2018). Genotypic expansion within the population structure of classical *Brucella* species revealed by MLVA16 typing of 1404 *Brucella* isolates from different animal and geographic origins, 1974–2006. *Front. Microbiol.* 9:1545. doi: 10.3389/fmicb.2018.01545
- Whatmore, A. M., Davison, N., Cloekaert, A., Al Dahouk, S., Zygmunt, M. S., Brew, S. D., et al. (2014). *Brucella papionis* sp. nov., isolated from baboons (*Papio* spp.). *Int. J. Syst. Evol. Microbiol.* 64, 4120–4128. doi: 10.1099/ijs.0.065482-65480
- Whatmore, A. M., Koylass, M. S., Muchowski, J., Edwards-Smallbone, J., Gopaul, K. K., and Perrett, L. L. (2016). Extended multilocus sequence analysis to describe the global population structure of the genus *Brucella*: phylogeography and relationship to biovars. *Front. Microbiol.* 7:2049. doi: 10.3389/fmicb.2016.02049
- Zygmunt, M. S., Jacques, I., Bernardet, N., and Cloekaert, A. (2012). Lipopolysaccharide heterogeneity in the atypical group of novel emerging *Brucella* species. *Clin. Vaccine Immunol.* 19, 1370–1373. doi: 10.1128/CVI.00300-312

Conflict of Interest: The authors declare that the research was conducted in the absence of any commercial or financial relationships that could be construed as a potential conflict of interest.

Copyright © 2020 Cloekaert, Vergnaud and Zygmunt. This is an open-access article distributed under the terms of the Creative Commons Attribution License (CC BY). The use, distribution or reproduction in other forums is permitted, provided the original author(s) and the copyright owner(s) are credited and that the original publication in this journal is cited, in accordance with accepted academic practice. No use, distribution or reproduction is permitted which does not comply with these terms.



Application of Whole Genome Sequencing and Pan-Family Multi-Locus Sequence Analysis to Characterize Relationships Within the Family *Brucellaceae*

Roland T. Ashford^{1*}, Jakub Muchowski¹, Mark Koylass^{1†}, Holger C. Scholz² and Adrian M. Whatmore¹

OPEN ACCESS

Edited by:

David W. Ussery,
University of Arkansas for Medical
Sciences, United States

Reviewed by:

David O'Callaghan,
Université de Montpellier, France
Martin W. Hahn,
University of Innsbruck, Austria

*Correspondence:

Roland T. Ashford
Roland.Ashford@apha.gov.uk

† Present address:

Mark Koylass,
AstraZeneca, Cambridge,
United Kingdom

Specialty section:

This article was submitted to
Evolutionary and Genomic
Microbiology,
a section of the journal
Frontiers in Microbiology

Received: 22 November 2019

Accepted: 25 May 2020

Published: 14 July 2020

Citation:

Ashford RT, Muchowski J,
Koylass M, Scholz HC and
Whatmore AM (2020) Application
of Whole Genome Sequencing
and Pan-Family Multi-Locus
Sequence Analysis to Characterize
Relationships Within the Family
Brucellaceae.
Front. Microbiol. 11:1329.
doi: 10.3389/fmicb.2020.01329

¹ Department of Bacteriology, Animal and Plant Health Agency, Weybridge, United Kingdom, ² Department of Bacteriology and Toxinology, Bundeswehr Institute of Microbiology, Munich, Germany

The bacterial family *Brucellaceae* is currently composed of seven genera, including species of the genus *Brucella*, a number of which are significant veterinary and zoonotic pathogens. The bacteriological identification of pathogenic *Brucella* spp. may be hindered by their close phenotypic similarity to other members of the *Brucellaceae*, particularly of the genus *Ochrobactrum*. Additionally, a number of novel atypical *Brucella* taxa have recently been identified, which exhibit greater genetic diversity than observed within the previously described species, and which share genomic features with organisms outside of the genus. Furthermore, previous work has indicated that the genus *Ochrobactrum* is polyphyletic, raising further questions regarding the relationship between the genus *Brucella* and wider *Brucellaceae*. We have applied whole genome sequencing (WGS) and pan-family multi-locus sequence analysis (MLSA) approaches to a comprehensive panel of *Brucellaceae* type strains, in order to characterize relationships within the family. Phylogenies based on WGS core genome alignments were able to resolve phylogenetic relationships of 31 non-*Brucella* spp. type strains from within the family, alongside type strains of twelve *Brucella* species. A phylogeny based on concatenated pan-family MLSA data was largely consistent with WGS based analyses. Notably, recently described atypical *Brucella* isolates were consistently placed in a single clade with existing species, clearly distinct from all members of the genus *Ochrobactrum* and wider family. Both WGS and MLSA methods closely grouped *Brucella* spp. with a sub-set of *Ochrobactrum* species. However, results also confirmed that the genus *Ochrobactrum* is polyphyletic, with seven species forming a separate grouping. The pan-family MLSA scheme was subsequently applied to a panel of 50 field strains of the family *Brucellaceae*, isolated from a wide variety of sources. This analysis confirmed the utility of the pan-*Brucellaceae* MLSA scheme in placing field isolates in relation to recognized type strains. However, a significant number of these isolates did not cluster with currently identified type strains, suggesting the existence

of additional taxonomic diversity within some members of the *Brucellaceae*. The WGS and pan-family MLSA approaches applied here provide valuable tools for resolving the identity and phylogenetic relationships of isolates from an expanding bacterial family containing a number of important pathogens.

Keywords: *Brucella*, *Brucellaceae*, multi-locus locus sequence analysis, pan-family, phylogeny, *Ochrobactrum*

INTRODUCTION

The bacterial family *Brucellaceae* (class *Alphaproteobacteria*, order *Rhizobiales*) is currently comprised of seven genera; *Brucella*, *Daeguia*, *Falsolechrobacterium*, *Mycoplana*, *Ochrobactrum*, *Paenochrobactrum*, and *Pseudochrobactrum* (Kämpfer and Glaeser, 2019). The family contains species with a wide range of habitat or host preferences, encompassing obligate intracellular pathogens of animals (e.g., *Brucella melitensis*), opportunistic pathogens often associated with nosocomial infections (e.g., *Ochrobactrum anthropi*), plant associated pathogens and symbionts (e.g., *O. lupini*) and organisms isolated from the natural and anthropogenic environment (e.g., *Paenochrobactrum glaciei* and *Pseudochrobactrum lubricantis*, respectively).

The type genus *Brucella* (Scholz et al., 2018) contains the causative agents of brucellosis, which remains one of the most important zoonotic diseases globally, with more than 500,000 new cases reported each year (Pappas et al., 2006). For several decades the genus *Brucella* was described as consisting of six “classical” species (*B. abortus*, *B. melitensis*, *B. ovis*, *B. suis*, *B. canis*, and *B. neotomae*), with well characterized mammalian host preferences (Corbel, 2006). Subsequently, additional species have been described, with the genus expanding to include *B. pinnipedialis* and *B. ceti* isolated from marine mammals (Foster et al., 2007), *B. microti* from voles (Scholz et al., 2008b), *B. inopinata* isolated from a human infection (Scholz et al., 2010), *B. papionis* from baboons (Whatmore et al., 2014) and *B. vulpis*, isolated from foxes (Scholz et al., 2016a). Additionally, a number of novel atypical strains from human and other mammalian hosts have been described, but await formal classification (Tiller et al., 2010a,b; Guzmán-Verri et al., 2019). These species and strains reflect an ongoing expansion of the known host range and genetic diversity of the genus. In particular, *B. microti*, *B. inopinata* and *B. vulpis* have been described as “atypical” *Brucella* species, exhibiting either atypical phenotypic traits (*B. microti*), or greater genetic diversity (*B. inopinata* and *B. vulpis*).

In addition to the novel atypical *Brucella* species and strains identified from mammalian hosts there is an expanding body of literature describing the isolation of *Brucella* sp. organisms from poikilothermic hosts, namely amphibians (Eisenberg et al., 2012; Whatmore et al., 2015; Scholz et al., 2016b; Soler-Lloréns et al., 2016) and cartilaginous fish (Eisenberg et al., 2017). In many cases, these isolates have initially been misidentified as *Ochrobactrum anthropi* on the basis of automated phenotyping or mass spectrometry (Eisenberg et al., 2017). However, further genetic investigation has identified the isolates as representing distinct *Brucella* lineages (Scholz et al., 2016b). Such isolates fall outside of the core *Brucella*, exhibiting greatest similarity to previously described atypical

isolates from mammals (*B. inopinata* and *B. vulpis*). Analyses based on whole genome sequencing (WGS) have indicated that, whilst such amphibian isolates maintain a high degree of genetic homology with core *Brucella* species, they exhibit a degree of horizontal gene transfer, with the incorporation of genomic regions exhibiting sequence identity to soil living or facultatively pathogenic *Alphaproteobacteria*, most notably from the genus *Ochrobactrum* (Scholz et al., 2016b; Al Dahouk et al., 2017).

The genus *Ochrobactrum*, is the largest within the family *Brucellaceae*, and has expanded significantly in the past decade (Kämpfer et al., 2018). The genus currently consists of 18 validly published species, plus a number of others awaiting valid publication. It has previously been noted that the genus *Ochrobactrum* appears to be polyphyletic (Kämpfer et al., 2013). Furthermore, studies based on sequencing of single locus targets (most commonly 16S ribosomal RNA or *recA*), have generated conflicting results on phylogenetic relationships within the family.

These issues highlight the well described problems of inferring phylogenetic relationships from single genetic loci, including lack of resolution, stochastic variation and the influence of recombination or horizontal gene transfer (Gevers et al., 2005). Previously, few studies had attempted to apply a multi-locus analysis approach to interrogate phylogenetic relationships within the family *Brucellaceae*. Aujoulat et al. (2014) applied an existing multi-locus sequence typing scheme for *Ochrobactrum anthropi* (Romano et al., 2009) to a wider panel of type strains from 14 *Ochrobactrum* species and two *Brucella* species. These authors again identified the genus *Ochrobactrum* as polyphyletic, with a robust clade containing *O. anthropi* and *O. intermedium* and five other species grouping distinctly from a less well supported clade containing the remaining *Ochrobactrum* type strains and the two *Brucella* species included. However, this analysis did not incorporate the full diversity of either *Ochrobactrum* or *Brucella*, or the remaining five genera which make up the family.

More recently, a number of studies have combined multi-locus sequencing and whole genome sequencing (WGS) based approaches to address specific taxonomic issues within the genus *Ochrobactrum*. Gazolla Volpiano et al. (2019) for example, identified *O. lupini* as a heterotypic synonym of *O. anthropi*. Similarly, Krzyzanowska et al. (2019) used a combination of these approaches to investigate the relationship of a proposed novel *Ochrobactrum* species (*O. quorumnocens*) to previously described members of the genus.

Very recently, Leclercq et al. (2019) used WGS data to investigate relationships within the family *Brucellaceae*, as well as its position within the wider *Rhizobiales*. These authors confirmed the genus *Brucella* to be a monophyletic grouping

within the genus *Ochrobactrum*, and that *Ochrobactrum* spp. divide into two distinct clades. However, Leclercq et al. (2019) did not incorporate type strains reflecting the full taxonomic diversity of either *Ochrobactrum* or *Brucella*. Additionally, the remaining genera within the *Brucellaceae* were either under-represented (*Pseudochrobactrum* and *Mycoplana*) or absent (*Paenochrobactrum* and *Daeguia*).

The continuing expansion of the recognized genetic diversity of the genus *Brucella*, and the uncertainty regarding phylogenetic relationships amongst members of related genera, highlight the need for a comprehensive multi-gene phylogeny of the *Brucellaceae*. Here, we describe the parallel application of WGS and multi-locus sequence analysis (MLSA) approaches to investigate phylogenetic relationships within the family. The pan-family MLSA method developed incorporates loci identical those used in existing schemes for *Brucella* species (Whatmore et al., 2007, 2016) thereby permitting the comparison of data generated under both schemes. Subsequently, we have applied the pan-family MLSA scheme to panels of field isolates, to assess its utility in establishing relationships with extant species.

MATERIALS AND METHODS

Type Strains

The taxonomic status of species within the *Brucellaceae* was retrieved via the online resource *List of Prokaryotic Names with Standing in Nomenclature* (Euzéby, 1997; Parte, 2014 accessed 14/11/2019). The type strains of all *Brucella* species were available from the collection of the APHA *Brucella* Reference Laboratory. The type strains of other species identified as belonging to the family *Brucellaceae* were purchased from established culture collections (Table 1). Strains were grown on solid media at optimal conditions as described by the supplier. A single pure colony from each agar plate was transferred to 100 µl of molecular grade water and cells were lysed by heating at 100°C for 10 min. Type strain 16S rRNA sequences were retrieved from the National Centre for Biotechnology Information (NCBI) database.

Additional Atypical *Brucella* sp. Strains

In addition to *Brucellaceae* type strains, atypical *Brucella* sp. from both mammalian and cold-blooded hosts were included in phylogenetic analyses (Table 2). These included previously described atypical isolates from a human patient (BO2: Tiller et al., 2010b) and from Australian rodents (Tiller et al., 2010a). These latter strains (referred to here as 83/13 and 83/4) were originally isolated as part of the same cohort as the Australian rodent strain NF2653 (Cook et al., 1966). Additionally, a number of more recently described atypical isolates from amphibians were analyzed. Isolate UK8/14 was recovered from a White's tree frog (Whatmore et al., 2015). Six African bullfrog strains from the 21 previously analyzed by Scholz et al. (2016b) were also selected, on the basis of representing all sequence types from this panel in the existing *Brucella* MLSA scheme (09RB8471: ST63; 09RB8910: ST64; 09RB8913: ST65; 10RB9205: ST66; 10RB9215: ST67 and 10RB9213: ST68 (Al Dahouk et al., 2017).

Field Strains

The performance of the MLSA scheme was further evaluated using field isolates provided by the Bundeswehr Institute of Microbiology (Munich, Germany) and obtained by the Animal and Plant Health Agency (Weybridge, United Kingdom) via brucellosis surveillance activities. In the former case, these represented a diverse panel of *Ochrobactrum* spp. from a variety of sources and geographical locations, confirmed as *Ochrobactrum* sp. by both 16S rRNA and *recA* sequencing (see Scholz et al., 2008a for full details). A panel of 37 isolates was examined (Table 3), representing major clades identified by *recA* sequence analysis (Scholz et al., 2008a). DNA was prepared as previously described (Scholz et al., 2008a). In the case of Animal and Plant Health Agency (APHA) isolates ($n = 13$), these were submitted as suspect *Brucella* sp. of veterinary origin but subsequently identified as non-*Brucella* members of the *Brucellaceae* by 16S rRNA sequencing (Wragg et al., 2014) (Table 3). Pure cultures were stored frozen in either Luria Broth with 15% glycerol or using proprietary MicroBank tubes (ProLab Diagnostics, United Kingdom). Frozen strains were revived by plating onto sheep blood and/or nutrient agar and incubating at 28°C for 24–48 h. Crude thermo-lysates from single colonies were prepared as described above.

Multi-Locus Sequence Analysis (MLSA)

Genomic targets for the pan-*Brucellaceae* MLSA scheme were selected from a larger panel of 21 loci used in an existing scheme for the *Brucella* genus (Whatmore et al., 2016). Alignments of sequences retrieved from NCBI were constructed for all 21 *Brucella* genus MLSA loci using CLUSTALW, implemented in the Lasergene software suite (version 12, DNASTAR Inc., WI, United States), for processing by the degenerate primer design program HYDEN (Linhart and Shamir, 2007) using default settings (25 bp in length, up to 1 mis-match in the 5' and 3' region allowed). Further iterations of primers were generated as alternatives, by modifying these default settings (primer length, number of mis-matches allowed and the level of degeneracy allowed across the primer).

Thermo-lysates from *Brucellaceae* type strains (generated as described above) were used to evaluate MLSA targets and optimize PCR conditions, to identify a panel of loci which amplified reliably using a standard thermal profile and reaction conditions. Optimal reaction conditions were identified as 5.0 µl of Roche 10x PCR buffer, 200 µM final concentration of dNTPs, 1.25 units of FastStart *Taq* polymerase, 2 mM of MgCl₂, 0.4 µM of forward and reverse primers and 1 µl of template DNA (thermo-lysate), in a total reaction volume of 50 µl. Amplification was performed using an Eppendorf MasterCyclerPro (Eppendorf, Germany), with the following thermal cycle: 94°C for 5 min. followed by 35 cycles of 94°C for 1 min., 55°C for 1 min. and 72°C for 1 min. and a final extension step of 72°C for 7 min. Products were separated by agarose gel electrophoresis to confirm that only a single product of the expected size was present. PCR

TABLE 1 | Type strains of species belonging to the *Brucellaceae*, used for whole genome sequence analysis and pan-family multi-locus sequence analysis (genus type species shown in bold).

Genus	Species	Type strain	Valid publication	WGS data
<i>Brucella</i>	<i>B. abortus</i>	NCTC 10093 ^T	Meyer and Shaw (1920)	GCA_000739315.1
	<i>B. canis</i>	NCTC 10854 ^T	Carmichael and Bruner (1968)	GCF_000018525.1
	<i>B. ceti</i>	NCTC 12891 ^T	Foster et al. (2007)	GCF_000662035.2
	<i>B. inopinata</i>	BO1 ^T	Scholz et al. (2010)	GCF_000182725.1
	<i>B. melitensis</i>	NCTC 10094^T	Meyer and Shaw (1920)	GCF_000007125.1
	<i>B. microti</i>	CCM 4915 ^T	Scholz et al. (2008b)	GCF_000022745.1
	<i>B. neotomae</i>	NCTC 10084 ^T	Stoenner and Lackman (1957)	GCF_900446125.1
	<i>B. ovis</i>	NCTC 10512 ^T	Buddle (1956)	GCF_900446135.1
	<i>B. papionis</i>	NCTC 13660 ^T	Whatmore et al. (2014)	SRR4038994
	<i>B. pinnipedialis</i>	NCTC 12890 ^T	Foster et al. (2007)	GCF_000221005.1
	<i>B. suis</i>	NCTC 10316 ^T	Huddleson (1929)	GCF_000007505.1
	<i>B. vulpis</i>	DSM 101715 ^T	Scholz et al. (2016a)	GCA_900000005.1
<i>Daeguia</i>	<i>D. caeni</i>	CCUG 54520^T	Yoon et al. (2008)	This study*
<i>Falchochromobacter</i>	<i>F. ovis</i>	LMG 27356^T	Kämpfer et al. (2013)	This study
	<i>F. shanghaiense</i>	HN4 ^T	Sun et al. (2019)	GCF_003149535.1
<i>Mycoplana</i>	<i>M. dimorpha</i>	DSM 7138^T	Gray and Thornton (1928)	This study
	<i>M. ramosa</i>	DSM 7292 ^T	Urakami et al. (1990)	This study*
<i>Ochrobactrum</i>	<i>O. anthropi</i>	LMG 3331^T	Holmes et al. (1988)	GCF_000017405.1
	<i>O. ciceri</i>	DSM 22292 ^T	Imran et al. (2010)	This study
	<i>O. cytisi</i>	DSM 19778 ^T	Zurdo-Piñero et al. (2007)	This study
	<i>O. daejeonense</i>	JCM 16234 ^T	Woo et al. (2011)	This study
	<i>O. endophyticum</i>	DSM 29930 ^T	Li et al. (2016)	This study*
	<i>O. gallinifaecis</i>	DSM 15295 ^T	Kämpfer et al. (2003)	GCF_006476605.1
	<i>O. grignonense</i>	LMG 18954 ^T	Lebuhn et al. (2000)	This study
	<i>O. haematophilum</i>	CIP 109452 ^T	Kämpfer et al. (2007a)	This study
	<i>O. intermedium</i>	LMG 3301 ^T	Velasco et al. (1998)	GCF_000182645.1
	<i>O. lupini</i> ^a	DSM 16930 ^T	Trujillo et al. (2005)	This study
	<i>O. oryzae</i>	DSM 17471 ^T	Tripathi et al. (2006)	This study
	<i>O. pecoris</i>	CCUG 60088 ^T	Kämpfer et al. (2011)	GCF_006376675.1
	<i>O. pituitosum</i>	DSM 22207 ^T	Huber et al. (2010)	This study
	<i>O. pseudintermedium</i>	DSM 17490 ^T	Teyssier et al. (2007)	GCF_008932435.1
	<i>O. pseudogrignonense</i>	CIP 109451 ^T	Kämpfer et al. (2007a)	This study
	<i>O. quorumnocens</i> ^b	LMG 30544 ^T	Krzyzanowska et al. (2019)	GCF_002278035.1
	<i>O. rhizosphaerae</i>	DSM 19824 ^T	Kämpfer et al. (2008)	This study
	<i>O. thiophenivorans</i>	DSM 7216 ^T	Kämpfer et al. (2008)	This study
	<i>O. tritici</i>	LMG 18957 ^T	Lebuhn et al. (2000)	GCF_008932295.1
<i>Paenochrobactrum</i>	<i>P. gallinarii</i>	CCUG 57736^T	Kämpfer et al. (2010)	This study*
	<i>P. glaciei</i>	JCM 15115 ^T	Romanenko et al. (2008); Kämpfer et al. (2010)	This study*
	<i>P. pullorum</i>	LMG 28095 ^T	Kämpfer et al. (2014)	This study*
<i>Pseudochrobactrum</i>	<i>P. asaccharolyticum</i>	CCUG 46016^T	Kämpfer et al. (2006)	This study
	<i>P. kiredjianiae</i>	DSM 19762 ^T	Kämpfer et al. (2007b)	This study*
	<i>P. lubricantis</i>	CCUG 56963 ^T	Kämpfer et al. (2009)	This study*
	<i>P. saccharolyticum</i>	CCUG 33852 ^T	Kämpfer et al. (2006)	This study

Strains marked with an asterisk (*) were sequenced for the first time for this study. ^a *O. lupini* identified as a heterotypic synonym of *O. anthropi*; ^b *O. quorumnocens* not yet validly published.

products were then purified by passage through QIAquick PCR purification columns (Qiagen, United Kingdom) and sequenced in both directions using the same forward and reverse primers as used for initial PCR amplification. The Big Dye Terminator Cycle Sequencing Kit (version 3.1, Applied Biosystems, Carlsbad, CA, United States) was used according to manufacturer's instructions, with capillary electrophoresis on

an ABI 3130xl DNA Analyzer (Applied Biosystems, Carlsbad, CA, United States). In a small number of cases an amplified product of the correct size was extracted from an agarose gel following electrophoresis and purified using the MinElute Gel Extraction Kit (Qiagen, United Kingdom), according to manufacturer's instructions. Purified PCR products were then sequenced as described.

TABLE 2 | Atypical *Brucella* sp. strains used for whole genome sequence analysis and pan-family multi-locus sequence analysis.

Strain ID	Source	Reference	Accession number
BO2	Human lung biopsy	Tiller et al. (2010b)	GCA_000177135.1
83/13	Australian rodent	–	GCA_000157875.1
83/4	Australian rodent	–	–
NF2653	Australian rodent	Wattam et al. (2012)	GCA_000177155.1
UK8/14	Whites tree frog (<i>Litoria caerulea</i>)	Whatmore et al. (2015)	–
09RB8471	African bull frog (<i>Pyxicephalus edulis</i>)	Al Dahouk et al. (2017)	GCA_001971625.1
09RB8910	African bull frog (<i>Pyxicephalus edulis</i>)	Al Dahouk et al. (2017)	GCA_001971805.1
09RB8913	African bull frog (<i>Pyxicephalus edulis</i>)	Al Dahouk et al. (2017)	GCA_009664925.1
10RB9205	African bull frog (<i>Pyxicephalus edulis</i>)	Al Dahouk et al. (2017)	–
10RB9213	African bull frog (<i>Pyxicephalus edulis</i>)	Al Dahouk et al. (2017)	GCA_009664915.1
10RB9215	African bull frog (<i>Pyxicephalus edulis</i>)	Al Dahouk et al. (2017)	GCA_900092405.1
141012304	Ribbontail ray (<i>Taeniura lymma</i>)	Eisenberg et al. (2017)	GCA_900095155.1
B13-0095	Pac-Man frog (<i>Ceratophrys ornata</i>)	Soler-Lloréns et al. (2016)	GCA_001742815.1

Sanger sequence data were manipulated using the Lasergene software suite (version 12, DNASTAR Inc., WI, United States), to produce a trimmed consensus sequence file for each strain and locus. Consensus sequences were used to perform phylogenetic analyses, for both individual loci and concatenated sequences (in the following order: *gpd*, *dnaK*, *trpE*, *csdB*, *leuA*, and *acnA*). The Lasergene MegAlign module was used to estimate percentage similarity between sequences. Other summary statistics were calculated using MEGA5 (version 5.2; Tamura et al., 2011). Three type strains were not available when MLSA work was undertaken (*O. endophyticum* DSM 29930^T; *O. quorumnecens* LMG 30544^T; *F. shanghaiense* HN4^T), and therefore MLSA sequences were retrieved from WGS data as described below. Similarly, MLSA data for three atypical *Brucella* sp. isolates (141012304, B13-0095 and NF2653) were extracted from WGS data available on NCBI. Phylogenetic analyses for MLSA data were performed using MEGA5. Maximum likelihood trees were constructed using a general time reversible substitution model (gamma distribution plus invariant sites), with percentage bootstrap confidence levels of internal branches calculated from 1000 re-samplings of the original data. Sequence data from *Rhizobium etli* CFN42^T (*Rhizobiales*; *Rhizobiaceae*; assembly accession GCF_000092045.1) were included and defined as an out-group in all analyses.

Whole Genome Sequencing (WGS)

Whole genome sequencing data from type strains were either retrieved from publically available databases (NCBI), or generated for this study (Table 1). For this purpose DNA was extracted from crude thermo-lysates, using the Qiagen DNEasy Blood and Tissue Kit (Qiagen, Manchester, United Kingdom). Library preparation was performed using the Nextera XT Library Preparation Kit (Illumina Inc., San Diego, CA, United States) according to the manufacturer's protocol. Libraries were sequenced on the Illumina MiSeq platform, using the MiSeq v2 Reagent Kit (Illumina Inc., San Diego, CA, United States), producing 150 bp paired-end reads.

Raw sequence data were processed using the Nullarbor pipeline (version 2.0¹), which integrates a number of previously published bioinformatic tools. Briefly, quality assessment and trimming of raw read data was performed using Trimmomatic (version 0.39; Bolger et al., 2014). *De novo* assembly of raw reads was performed using the SPAdes assembler (version 3.13.1; Bankevich et al., 2012). *De novo* assembled genomes were then annotated using Prokka (version 1.13.1; Seemann, 2014). Genomes retrieved from publically available databases (either as finished genomes or whole genome shotgun assembly contigs) were likewise annotated using Prokka. Where an assembled genome was not available via NCBI then short-read data were downloaded from the NCBI SRA database and assembled as described. Genomic average nucleotide identity (ANI) estimates were calculated from fasta formatted genome assemblies, using FastANI (version 1.3; Jain et al., 2018).

In order to generate pan-genomes from WGS data, Roary (version 3.13.0; Page et al., 2015) was used, with a minimum sequence identity of 70% and gene presence in ≥99% of isolates to be identified as a core gene. Core genome sequence alignments were generated using MAFFT (Katoh et al., 2002). Core genome alignments were used to produce maximum likelihood phylogenies with RAXML-NG (Kozlov et al., 2019) applying a general time reversible model (gamma distribution plus invariant sites), with 100 bootstraps. The resulting phylogenies were viewed and further annotated using MEGA5. *Rhizobium etli* CFN42^T (*Rhizobiales*; *Rhizobiaceae*; assembly accession GCF_000092045.1) was included and defined as an out-group. Additional outgroup strains were incorporated in some analyses to investigate the placement of *Mycoplana* spp. (*Agrobacterium tumefaciens* Ach5: GCF_000971565.1; *Aquamicrobium aerolatum* DSM 21857^T: GCF_900113935.1; *Ensifer adhaerens* ATCC 33212^T: GCF_000697965.2; *Ensifer sojiae* DSM 26426^T: GCF_000261485.1; *Mesorhizobium ciceri*: WSM 1271: GCF_000185905.1; *Mesorhizobium loti* NZP 2037^T: GCF_001676765.1; *Rhizobium etli* CFN42^T: GCF_000092045.1; *Sinorhizobium meliloti* DSM 30135^T: GCF_000006965.1).

¹<https://github.com/tseemann/nullarbor>

TABLE 3 | Field strains used for evaluation of the pan-*Brucellaceae* multi-locus sequence analysis scheme.

Strain ID ^a	Source	Geographic origin	Identity ^b
CCM 7036 (D)	<i>Phlebotomus duboscqi</i>	Czechia	<i>O. intermedium</i>
CCUG 1047 (D)	Dextran	Sweden	<i>O. anthropi</i>
CCUG 12860 (D)	Human blood	Sweden	<i>O. anthropi</i>
CCUG 16508 (D)	n/a	France	<i>O. anthropi</i>
CCUG 17894 (D)	Contaminant	Sweden	<i>O. anthropi</i>
CCUG 1821 (D)	Cattle dip trays	Australia	<i>O. tritici</i>
CCUG 29689 (D)	Human blood	Sweden	<i>O. tritici</i>
CCUG 32009 (D)	Paint	Sweden	<i>O. anthropi</i>
CCUG 33786 (D)	Human blood	Sweden	<i>O. anthropi</i>
CCUG 34735 (D)	Water	Sweden	<i>O. pseudintermedium</i>
CCUG 39736 (D)	Human blood	Sweden	<i>O. intermedium</i>
CCUG 43465 (D)	Paper mill	Sweden	<i>O. pseudintermedium</i>
CCUG 43892 (D)	Human Ear	Norway	<i>O. pseudogrignonense</i>
CCUG 7349 (D)	n/a	n/a	<i>O. anthropi</i>
CLM 26 (D)	Soil	Germany	<i>O. anthropi</i>
CLM 6 (D)	Soil	Germany	<i>O. anthropi</i>
DSM 20150 (D)	Urine of leech	Germany	<i>O. anthropi</i>
LMG 2134 (D)	Cattle dip trays	Australia	<i>O. tritici</i>
LMG 2136 (D)	Sewage plant	Sweden	<i>O. anthropi</i>
LMG 3298 (D)	Blood	United States	<i>O. anthropi</i>
LMG 3306 (D)	Soil	France	<i>O. intermedium</i>
LMG 35 (D)	Human sputum	Denmark	<i>O. anthropi</i>
LMG 394 (D)	Exudate	United States	<i>O. anthropi</i>
LMG 401 (D)	Cervix	United States	<i>O. tritici</i>
LMG 5425 (D)	Urine	United Kingdom	<i>O. intermedium</i>
LMG 5426 (D)	Urine	United Kingdom	<i>O. intermedium</i>
LMG 5442 (D)	Throat	United States	<i>O. anthropi</i>
LMG 5444 (D)	Human	United States	<i>O. anthropi</i>
LMG 5446 (D)	Bladder	United States	<i>O. intermedium</i>
LMG 379 (D)	Ear	United States	<i>O. intermedium</i>
RR (D)	Industrial environment	Austria	<i>O. intermedium</i>
OgA9c (D)	Soil	France	<i>O. grignonense</i>
TA13 (D)	Industrial environment	Austria	<i>O. intermedium</i>
TA93 (D)	Industrial environment	Austria	<i>O. tritici</i>
TD30 (D)	Industrial environment	Austria	<i>O. intermedium</i>
WS1830 (D)	Wheat rhizoplane	Germany	<i>O. tritici</i>
WS1846 (D)	<i>Oryza sativa</i>	India	<i>O. oryzae</i>
R5/07 (UK)	<i>Bos taurus</i>	United Kingdom	<i>Pseudochrobactrum</i> sp.
R16/08-3UT (UK)	<i>Capra hircus</i>	Italy	<i>Pseudochrobactrum</i> sp.
R17/08-1UD (UK)	<i>Bubalus bubalis</i>	Italy	<i>Pseudochrobactrum</i> sp.
R22/05 (UK)	<i>Bos taurus</i>	United Kingdom	<i>Pseudochrobactrum</i> sp.
R24/05 (UK)	<i>Bos taurus</i>	United Kingdom	<i>Pseudochrobactrum</i> sp.
UK2/05 (UK)	<i>Bos taurus</i>	United Kingdom	<i>Pseudochrobactrum</i> sp.
UK3/11-1 (UK)	<i>Ovis aries</i>	United Kingdom	<i>Paenochrobactrum</i> sp.
UK5/07 (UK)	<i>Bos taurus</i>	United Kingdom	<i>Pseudochrobactrum</i> sp.
UK14/09 (UK)	<i>Bos taurus</i>	United Kingdom	<i>Pseudochrobactrum</i> sp.
UK20/09 (UK)	<i>Bos taurus</i>	United Kingdom	<i>Pseudochrobactrum</i> sp.
UK34/07-2 (UK)	<i>Bos taurus</i>	United Kingdom	<i>Pseudochrobactrum</i> sp.
VLA10/07-E (UK)	<i>Phocoena phocoena</i>	United Kingdom	<i>Pseudochrobactrum</i> sp.
VLA07/50 (UK)	<i>Phocoena phocoena</i>	United Kingdom	<i>Ochrobactrum</i> sp.

^a Strains denoted (D) provided by Bundeswehr Institute of Microbiology (Munich, Germany); strains denoted (UK) obtained by the Animal and Plant Health Agency (Weybridge, United Kingdom). ^b Identity based on published data (strains denoted D: see Scholz et al., 2008a) or analysis of 16S rRNA sequence (strains denoted UK).

RESULTS

WGS Core Genome Analyses and Selection of MLSA Loci

Summary statistics for *de novo* genome assemblies are provided in **Supplementary Table S1**. Of those type strain genomes sequenced for this study (see **Table 1**) the genome size ranged from 3.2 to 5.8 Mb, corresponding to between 3030 and 5542 annotated coding sequences (**Supplementary Table S1**). The mean GC content of these genomes ranged from 48.6% to 63.5%. Pan genome analysis of annotated assemblies identified a core genome of 450 genes amongst the 43 type strains included in the analysis (plus *R. etli* CFN42^T). The concatenated core genome alignment of these genes comprised 449,688 bp. Inclusion of additional outgroup strains reduced the core genome to 410 genes (419,690 bp), whilst inclusion of atypical *Brucella* strains resulted in a core genome of 400 genes (395,037 bp).

Six loci were identified which amplified reliably in all type species of the *Brucellaceae*, using the standard thermal profile and reaction conditions described, and were therefore incorporated into the pan-family MLSA scheme (**Supplementary Table S2**). All loci represent informative housekeeping genes of the type conventionally used in MLSA. Mean GC content in the six loci ranged from 54.5% to 59.4%, with an average of 57.0% across all loci. The proportion of polymorphic sites in each of the six loci, across all *Brucellaceae* type species, ranged from 42.34% (*dnaK*) to 53.50% (*trpE*), with an average of 48.37%. Nucleotide diversity (π) in the six loci ranged from 0.1256 (*dnaK*) to 0.1975 (*trpE*), whilst nucleotide diversity across the entire 3,004 bp concatenated sequence was 0.1532 (**Supplementary Table S2**).

Sequence Diversity Indices From WGS and MLSA

The level of genomic ANI and MLSA nucleotide identity observed within and between genera of the *Brucellaceae* varied considerably (**Table 4** and **Supplementary Table S3**). As anticipated, the highest intra-generic ANI values were observed within the *Brucella* (average 99.1%) whilst the lowest average ANI value was seen amongst *Falschochromobacter* (average 77.9%). The largest intra-generic range (highest to lowest) in ANI values was observed within the *Ochrobactrum* genus (75.4–98.5%). Between genera, the highest ANI was observed between *Brucella* and *Ochrobactrum* (80.9%), whilst the lowest was between *Mycoplana* and *Paenochrobactrum* or *Pseudochrobactrum* (both 74.3%). The same pattern was observed in nucleotide identity estimates derived from MLSA data (**Table 4**). Again, nucleotide identity within the genus *Brucella* was very high (average 99.3%). Average nucleotide identity within the other genera of the *Brucellaceae* ranged from 79.4% (*Falschochromobacter*) to 93.7% (*Pseudochrobactrum*). The largest intra-generic range (highest to lowest) in nucleotide identity was observed within the *Ochrobactrum* (78.2–99.7%). Between genera, the highest level of average nucleotide identity was observed between *Brucella* and *Ochrobactrum* (86.9%), whilst the lowest was between *Mycoplana* and *Paenochrobactrum* (70.7%).

TABLE 4 | Intra-generic (bold) and inter-generic similarity of seven genera of the family *Brucellaceae*, measured by genomic ANI values from WGS data (bottom left matrix) and nucleotide identity from concatenated MLSA data (upper right matrix).

Genus (n species)	<i>Brucella</i> (n = 12)	<i>Daeguia</i> (n = 1)	<i>Falschochromobacter</i> (n = 2)	<i>Mycoplana</i> (n = 2)	<i>Ochrobactrum</i> (n = 19)	<i>Paenochrobactrum</i> (n = 3)	<i>Pseudochrobactrum</i> (n = 4)
<i>Brucella</i>	99.3 (98–100) 99.1 (97.5–99.9) 79.4 (79.4–79.5)	86.0 (85.8–86.1)	82.0 (79.9–84.1)	77.7 (77.4–77.9)	86.9 (82.2–88.9)	76.8 (76.7–77.2)	78.4 (78.0–78.8)
<i>Daeguia</i>		NA NA	81.3 (80.3–82.3)	78.4 (78.3–78.5)	85.2 (81.3–86.8)	78.9 (78.5–79.4)	79.6 (79.0–80.1)
<i>Falschochromobacter</i>			79.4 (79.4–79.4) 77.9 (77.9–77.9) 74.8 (74.2–75.4)	74.7 (71.8–78.2)	81.8 (76.2–84.8)	76.8 (75.1–78.7)	77.1 (75.8–78.0)
<i>Mycoplana</i>				93.5 (93.5–93.5) 84.8 (84.8–84.8) 75.1 (74.4–76.4)	77.4 (73.7–81.2)	70.7 (70.2–71.0)	72.6 (71.3–73.2)
<i>Ochrobactrum</i>					88.0 (78.2–99.7) 82.2 (75.4–98.5) 75.8 (74.8–76.4)	77.3 (74.3–78.6)	78.6 (75.4–80.2)
<i>Paenochrobactrum</i>						92.3 (90.4–95.6) 88.4 (86.3–92.3) 77.1 (76.8–77.5)	79.6 (79.2–80.5)
<i>Pseudochrobactrum</i>							93.7 (92.1–97.5) 88.7 (85.8–97.1)

Values are expressed as the average for each group (with range), NA, not available where genus represented by a single species.

As anticipated, measures of sequence similarity for WGS (percentage ANI) and MLSA (percentage nucleotide identity) showed very high levels of agreement [Figure 1A; semi-logarithmic regression: $Y = -283.2 + 193 \cdot \log(X)$; $R^2: 0.89$]. The relationship between genomic ANI and MLSA nucleotide identity was further investigated by comparing their values for all species, relative to the *Brucellaceae* type species *B. melitensis* NCTC 10094^T (Figure 1B). Most notable was the very large dispersion of *Ochrobactrum* species, which were split into distinct groups by both metrics (Groups A and B as defined in section “Phylogenetic Analyses Based on WGS”), with one outlier (*O. endophyticum*) highly divergent from other members of the genus. Similarly, the two *Falsochrobactrum* species were characterized by very different levels of diversity relative to *B. melitensis*.

Further investigation of genomic ANI values (Figure 2) demonstrated that all pairwise comparisons between species within the genus *Brucella* exceeded 97.5%. Furthermore, a number of other intra-generic pairings with very high ANI values were identified. Specifically, within the genus *Ochrobactrum*, *O. ciceri* and *O. intermedium* were identified as sharing 98.5% genomic ANI, whilst *O. anthropi* and *O. lupini* (the latter already identified as a homotypic synonym of the former) shared 97.9% ANI. Outside of the *Brucella* and *Ochrobactrum* genera, the highest ANI value observed was between *Pseudochrobactrum lubricantis* and *P. sacchrolyticum* (97.1%).

Phylogenetic Analysis of *Brucellaceae* Type Strains

Phylogenetic Analyses Based on WGS

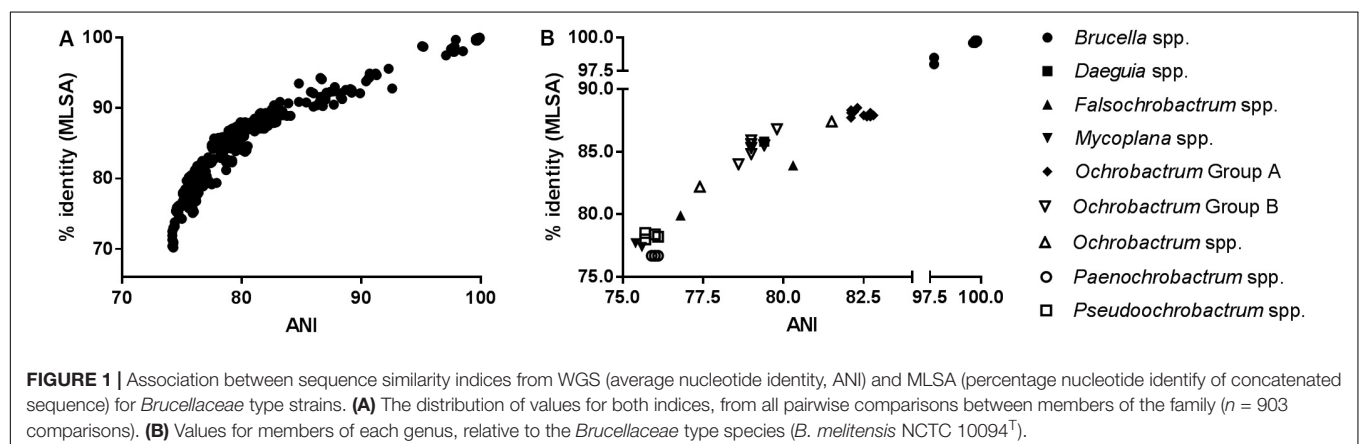
Maximum likelihood analysis based on the core genome alignment from *Brucellaceae* type strains resulted in an almost fully resolved phylogeny (Figure 3A), with the only nodes lacking full bootstrap support sitting within the genus *Brucella*. Nonetheless, the monophyly of this genus was highly supported. The genus *Ochrobactrum* was identified as polyphyletic. A sister group to the *Brucella* consisted of 10 *Ochrobactrum* species (Figure 3A: Group A), containing *O. anthropi* – *O. lupini* – *O. cytisi* – *O. tritici* – *O. pecoris* – *O. oryzae* – *O. ciceri* – *O. intermedium* – *O. pseudintermedium* – *O. daejeonense*.

A single species (*O. haematophilum*), branched basally, to form a sister group to the clade containing these two taxa (*Ochrobactrum* Group A and *Brucella* spp.). A second group of seven *Ochrobactrum* species (Figure 3A: Group B) formed a sister group to the *Brucella* and all other *Ochrobactrum* species (with the exception of *O. endophyticum*). This clade was comprised of *O. grignonense* – *O. pituitosum* – *O. quorumnecens* – *O. rhizosphaerae* – *O. pseudogrignonense* – *O. thiophenivorans* – *O. gallinifacis*.

Maximum likelihood phylogeny based on WGS data indicated that *Falsochrobactrum* spp. formed a sister clade to *Ochrobactrum* Group B. Further phylogenies were estimated using the WGS dataset (both with and without additional outgroups), removing each species in turn (*F. ovis* and *F. shanghaiense*). The phylogenies produced were identical in their placement of the two *Falsochrobactrum* species, which were individually placed as a sister taxon to *Ochrobactrum* Group B (Supplementary Figure S1). The single *Daeguia* species (*D. caeni*) branched basally to *Brucella* spp., *Ochrobactrum* Groups A and B and *Falsochrobactrum* spp. Both *Paenochrobactrum* spp. and *Pseudochrobactrum* spp. formed well-supported sister taxa in a single clade. A single *Ochrobactrum* species (*O. endophyticum*) branched basally to all members of the family, other than *Mycoplana* spp. (Figure 3A). Maximum likelihood phylogenetic analysis incorporating eight outgroup strains from the wider *Rhizobiales* indicated that *Mycoplana* spp. were placed with type strains of *Sinorhizobium meliloti* DSM 30135^T and *Ensifer* spp. (*E. sojae* DSM 26426^T and *E. adhaerens* ATCC 33212^T), of the family *Rhizobiaceae*, rather than with members of the *Brucellaceae* (Supplementary Figure S1).

Phylogenetic Analysis Based on MLSA

Phylogenetic analyses based on concatenated sequences (3,004 bp) for all *Brucellaceae* type strains demonstrated that the pan-family MLSA scheme was able to distinguish all members of the taxon, with reasonable levels of bootstrap support in the majority of cases (Figure 3B). A single strongly supported clade containing all currently recognized *Brucella* species was evident. The species of *Ochrobactrum* included in the analysis of concatenated sequences formed three distinct clades. The first of these clades (Figure 3B: Group A) consisted



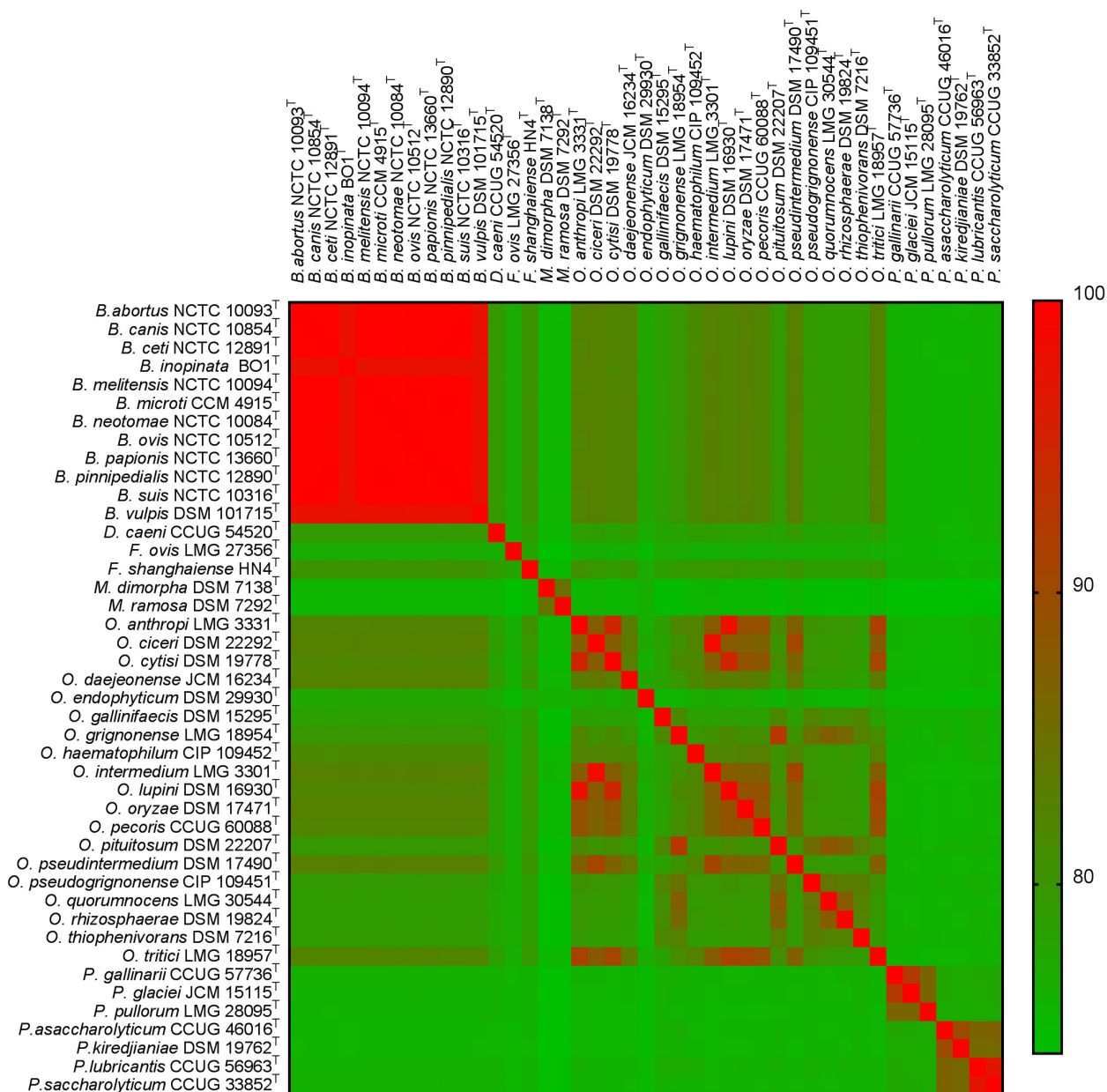
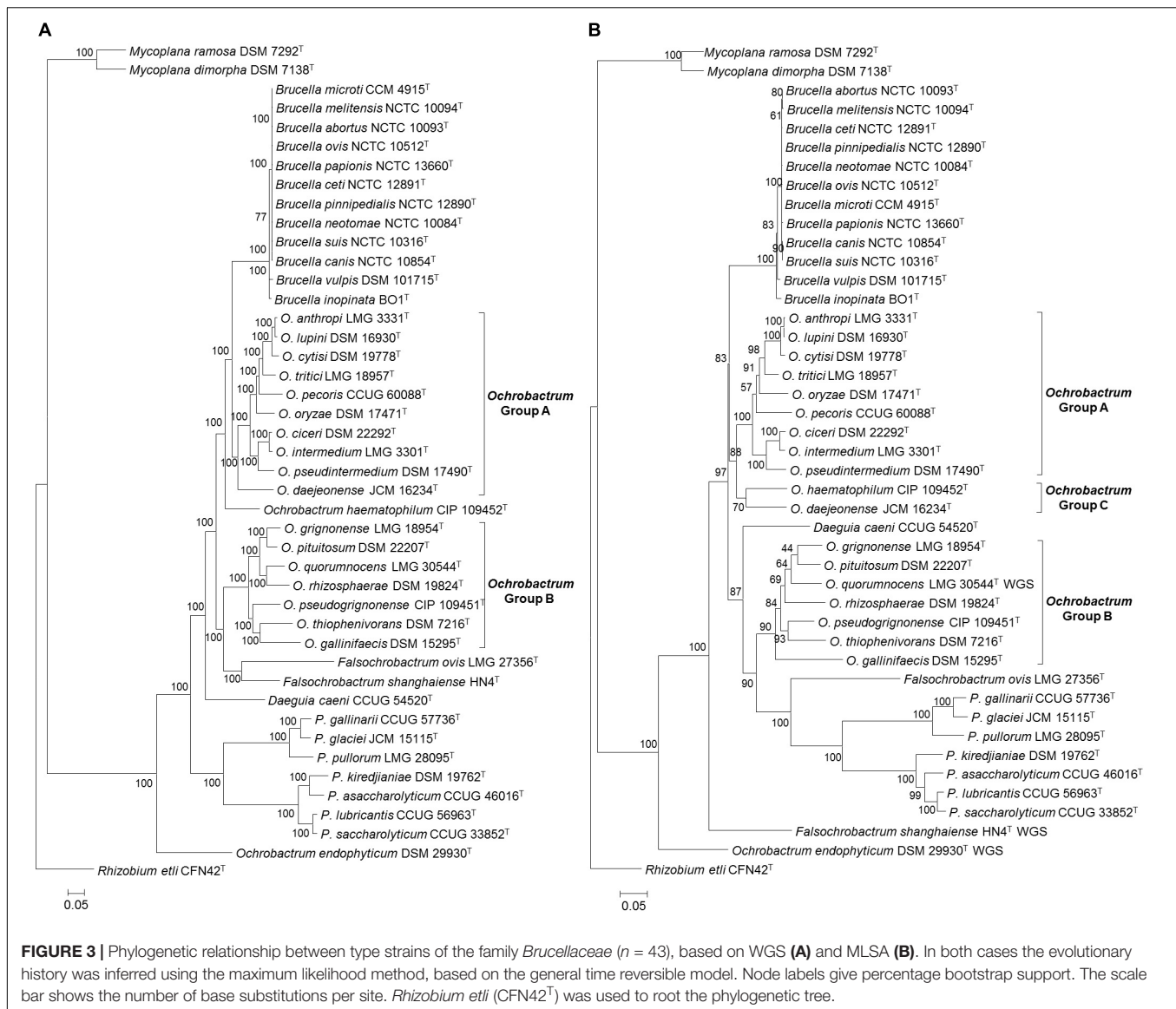


FIGURE 2 | Heatmap of genomic average nucleotide identity (ANI) values for pairwise comparisons between all type strains of the family *Brucellaceae* ($n = 43$).

of nine species, containing the grouping of *O. anthropi* – *O. lupini* *O. cytisi* – *O. tritici* – *O. oryzae* – *O. pecoris* – *O. ciceri* – *O. intermedium* – *O. pseudintermedium*. However, the node separating *O. pecoris* from other members of this clade was weakly supported. A second *Ochrobactrum* clade (**Figure 3B**: Group B) contained seven species (*O. grignonense* – *O. pituitosum* – *O. quorumnocens* – *O. rhizosphaerae* – *O. pseudogrignonense* – *O. thiophenivorans* – *O. gallinifacis*) and grouped more closely with a clade containing *Pseudochrobactrum* spp., *Paenochrobactrum* spp. and *Falsochrobactrum ovis* than with the *Ochrobactrum* Group A clade. Bootstrap support for nodes within this grouping of seven *Ochrobactrum*

species was generally low, with the exception of the nodes dividing *O. gallinifacis* from all others, and dividing *O. thiophenivorans* from *O. pseudogrignonense*. A third clade of two *Ochrobactrum* species (**Figure 3B**: Group C: *O. daejeonense* and *O. haematophilum*) formed a distinct sister clade to Group A, though with only moderate bootstrap support. A well-supported clade contained *Pseudochrobactrum* spp., *Paenochrobactrum* spp. and *Falsochrobactrum ovis*, with *F. ovis* branching basally to form a sister taxon to the other two genera. The recently described *F. shanghaiense*, however, branched basally to all other *Brucellaceae* type strains, with the exception of a single *Ochrobactrum* species (*O. endophyticum*) and *Mycoplana* spp.



Daeguia caeni was placed as a sister taxon to *Ochrobactrum* Group B and *Pseudochrobactrum* spp., *Paenochrobactrum* spp. and *F. ovis*.

Phylogenetic Analyses Based on Individual MLSA Loci and 16S rRNA Sequence

Maximum-likelihood phylogenies for each locus are shown in **Supplementary Figure S2**. In all cases, a single clade containing *Brucella* type species, including divergent atypical species (*B. inopinata* and *B. vulpis*) was identified, with a high level of support (bootstrap values of 100% for all loci). Only one locus (*trpE*) indicated the existence of a monophyletic *Ochrobactrum* clade. All other loci indicated that the genus was polyphyletic. A group of species, corresponding to *Ochrobactrum* Group A (as identified in analysis of both WGS and MLSA datasets), was evident for all loci except *acnA*. Within *Ochrobactrum* Group A, *O. anthropi* and *O. lupini* were consistently shown to be

very closely related, with *O. cytisi* also consistently grouping with the former species, but somewhat divergent. Similarly, *O. ciceri* and *O. intermedium* were consistently identified as highly similar, with *O. pseudintermedium* forming a slightly divergent sister taxon. The relative position of the seven species within *Ochrobactrum* Group B (as identified in analysis of both WGS and MLSA datasets) was not consistent between loci, and generally had low levels of bootstrap support. Both *O. daejeonense* and *O. haematophilum* were inconsistently placed, and often weakly supported, in analyses of data from individual loci. Analysis of individual MLSA loci consistently identified well supported *Pseudochrobactrum* and *Paenochrobactrum* groups, as sister taxa. The position of the two *Falsobacterium* species was variable, however, and they were not placed in a unified taxon in any single locus analysis. The placement of the single *Daeguia* species was highly variable in analyses based on individual loci, and frequently had low levels of bootstrap support. In

the majority of cases *O. endophyticum* branched basally to all members of the family except *Mycoplana* spp., and clearly distinct from other *Ochrobactrum* species. Finally, data from individual loci other than *gpd* identified the two *Mycoplana* species as branching basally to all other members of the family.

As observed in previous studies, analysis of almost full-length 16S rRNA sequences from *Brucellaceae* type strains did not provide sufficient resolution to correctly place species, even at the genus level (Supplementary Figure S2).

Atypical *Brucella* Isolates

Inclusion of atypical *Brucella* isolates with type strains of the family *Brucellaceae* clearly identified them as belonging within the genus *Brucella*, with maximum bootstrap support for a

monophyletic genus (Figures 4A,C). Additionally, both WGS and MLSA based approaches identified the six classical *Brucella* species, plus the more recently described *B. ceti*, *B. pinnipedialis*, *B. microti* and *B. papionis* as forming a well-supported group of ten core species, with limited diversity between them (Figures 4B,D). Outside of these core species, the basal branching order of atypical *Brucella* species and strains within the genus was relatively weakly supported by both WGS and MLSA datasets, with low bootstrap values for several nodes (Figures 4B,D). Amongst these isolates there were only a small number of groupings well supported by bootstrap values using MLSA data. Strains from Australian rodents (83/4, 83/13 and NF2653) formed a well-supported clade (Figure 4D), as did two strains from African bullfrogs (*Brucella* sp. 09RB8471 and 10RB9205).

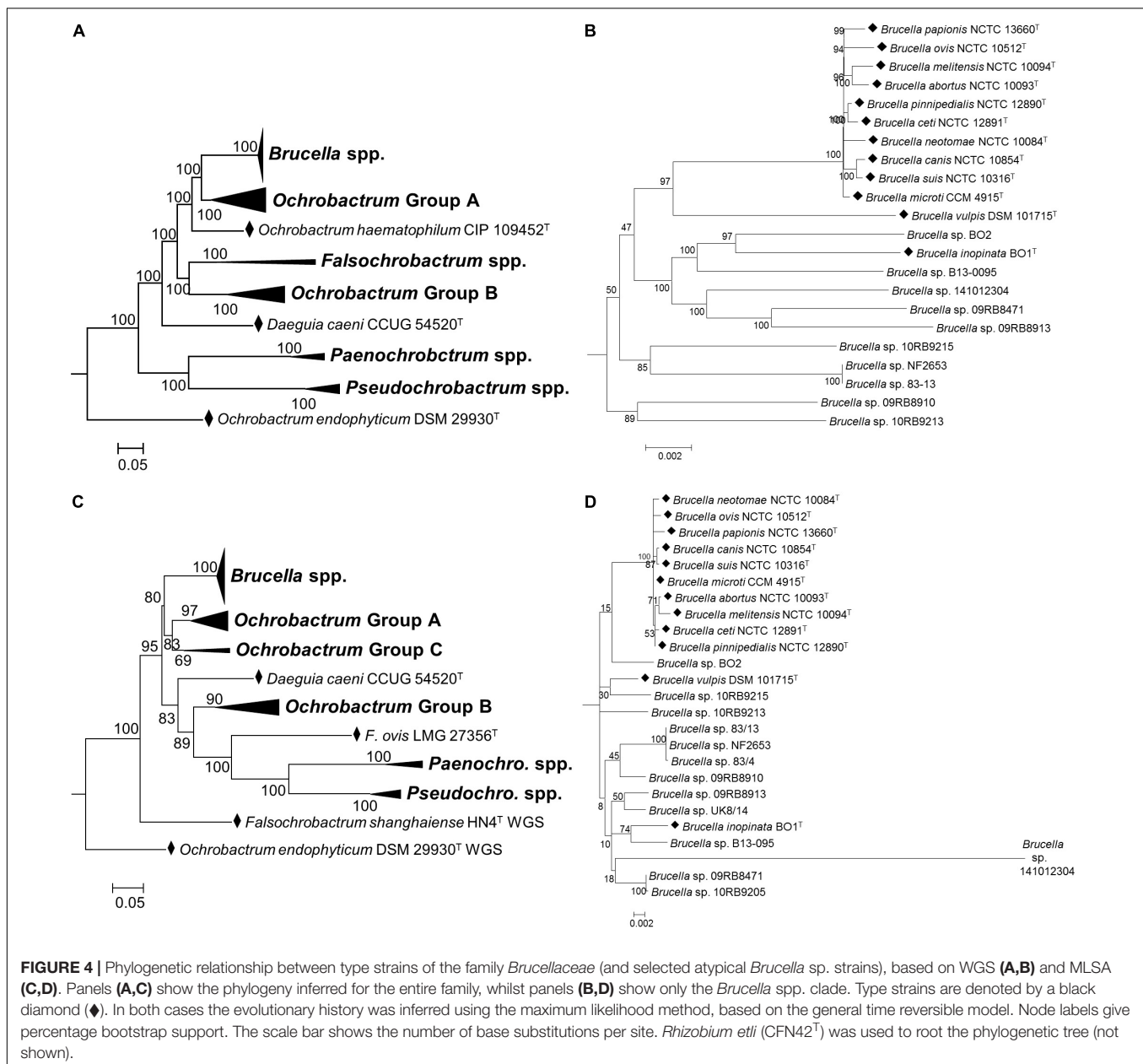


FIGURE 4 | Phylogenetic relationship between type strains of the family *Brucellaceae* (and selected atypical *Brucella* sp. strains), based on WGS (A,B) and MLSA (C,D). Panels (A,C) show the phylogeny inferred for the entire family, whilst panels (B,D) show only the *Brucella* spp. clade. Type strains are denoted by a black diamond (◆). In both cases the evolutionary history was inferred using the maximum likelihood method, based on the general time reversible model. Node labels give percentage bootstrap support. The scale bar shows the number of base substitutions per site. *Rhizobium etli* (CFN42^T) was used to root the phylogenetic tree (not shown).

Based on MLSA data the human-associated strain *B. inopinata* formed a moderately well-supported group with a novel isolate from an amphibian (*Brucella* sp. B13-095), and distinct from the other atypical human isolate *Brucella* sp. BO2. In contrast, WGS based analysis identified these human associated isolates as sister taxa, with the amphibian isolate *Brucella* sp. B13-095 branching basally (Figure 4B). Branch lengths based on MLSA data indicated that *Brucella* sp. 141012304, isolated from a cartilaginous fish, was highly divergent from other atypical strains. Branch lengths of atypical *Brucella* strains calculated from WGS data, however, indicated a more consistent level of divergence from core species.

Field Isolates

In order to assess the value of the pan-family MLSA scheme in placing field isolates, subsequent analysis incorporated panels of field isolates, alongside type strains of all species within the *Brucellaceae*. This demonstrated that the MLSA scheme assigned field isolates to phylogenetic locations largely consistent with their identities assigned on the basis of phenotypic, *recA* and/or 16S rRNA sequence analysis (Figure 5).

Isolates previously identified as *Ochrobactrum anthropi* formed a well-supported clade containing the type strains of *O. anthropi* – *O. cytisi* and *O. lupini*. However, isolates did not fall into three separate clusters corresponding to the three species but rather represented a continuum of diversity. Only five *O. anthropi* field strains clustered with the type strain for the species. A further ten *O. anthropi* field strains grouped more closely with *O. cytisi* although with low levels of bootstrap support for the node separating them from the well supported *O. anthropi* – *O. lupini* cluster. A single field isolate (VLA07/50) grouped within the *O. anthropi* – *O. cytisi* and *O. lupini* clade with a high degree of bootstrap support, but appeared to be sufficiently divergent from other strains within the cluster to potentially represent a novel species. Interestingly, this isolate originated from a harbor porpoise (*Phocoena phocoena*) and hence may represent a marine or marine-mammal associated strain.

A sister clade to the *O. anthropi* – *O. cytisi* and *O. lupini* grouping contained the type strain of *O. tritici* and all field isolates identified as belonging to this species. A sister clade to the grouping of *O. anthropi* – *O. cytisi* – *O. lupini* and *O. tritici* contained the type species of *O. pseudintermedium* – *O. ciceri* and *O. intermedium* and associated field isolates. All field isolates of *O. pseudintermedium* grouped with their respective type strain (DSM 17490^T). In the case of *O. intermedium*, five of the ten field isolates grouped most closely with the type strain (LMG 3301^T), though with a continuum of diversity from the parent species. Four *O. intermedium* field strains clustered more closely with the *Ochrobactrum ciceri* type strain (DSM 22292^T). A single *O. intermedium* field strain (CCM 7036) branched basally to the cluster containing type species of *O. intermedium* – *O. ciceri* and associated field isolates, indicating additional diversity within this group that may merit description of further species. A single field isolate originally identified as *O. oryzae* (WS 1846), clustered with the *O. intermedium* type strain and field isolates. The location of the type strain for this species (DSM 17471^T) was relatively poorly supported.

A single field isolate grouped with the type strains of both *O. grignonense* and *O. pseudogrignonense* (field isolates OgA9c and CCUG 43892, respectively). In the case of the former (OgA9c), this strain was isolated simultaneously to the type strain, and from the same material (Lebuhn et al., 2000) which is reflected in their sequence homology. Strain CCUG 43892 was isolated independently from the type strain of *O. pseudogrignonense* (CIP 109451^T), but formally described at the same time (Kämpfer et al., 2007a) due to their phenotypic and genetic similarity. This is reflected in the high level of bootstrap support for their placement together, though branch lengths indicate a degree of sequence divergence in the six MLSA loci described here.

With the exception of a single strain, United Kingdom field isolates (obtained via surveillance, for exclusion as *Brucella*), were identified as either *Pseudochrobactrum* sp. or *Paenochrobactrum* sp. by 16S sequencing (Table 3). *Pseudochrobactrum* sp. field strains formed a diverse cluster with the type strains of *P. lubricantis* and *P. saccharolyticum* suggesting these species poorly reflect actual diversity of these bacterial groups. In particular, a group of five field isolates within this grouping formed two distinct and well-supported clusters of two and three isolates, respectively. The single *Paenochrobactrum* sp. field strain (UK3/11-1) grouped in a single well-supported clade with type strains of the three described *Paenochrobactrum* species, and was identified as most closely resembling *P. glaciei*.

DISCUSSION

In this study, we have investigated phylogenetic relationships within the *Brucellaceae*, using a comprehensive WGS dataset incorporating all currently described species and a pan-family MLSA approach developed to be compatible with existing *Brucella* schemes.

Increasingly, WGS approaches are being used to generate data for phylogenetic placement of novel bacterial isolates. Nonetheless, the pan-family MLSA approach developed here remains valuable, in providing a defined list of genomic targets for future phylogenetic analysis and a comprehensive database of both reference and field isolates for comparison. Additionally, whilst the generation of WGS data for bacterial isolates is increasing, such data is absent for a large number of strains described before the approach became widespread. Again, the data generated in the current work will permit their integration into future multi-gene analyses incorporating results derived from both whole genome and “first-generation” sequencing methods. As an example of this approach, Krzyzanowska et al. (2019) recently described a putative novel *Ochrobactrum* species (*Ochrobactrum quorumnocens* sp. nov.) isolated from the potato rhizosphere. These authors applied a comparative genomic analysis with related *Ochrobactrum* type strains, using WGS data from the novel isolate and six existing species. These data were used to apply an MLSA based approach using concatenated nucleotide sequences of three genes: 16S rRNA gene, *groEL* and *gyrB*. Retrieval of data for the genes adopted in the current work would permit the comparison

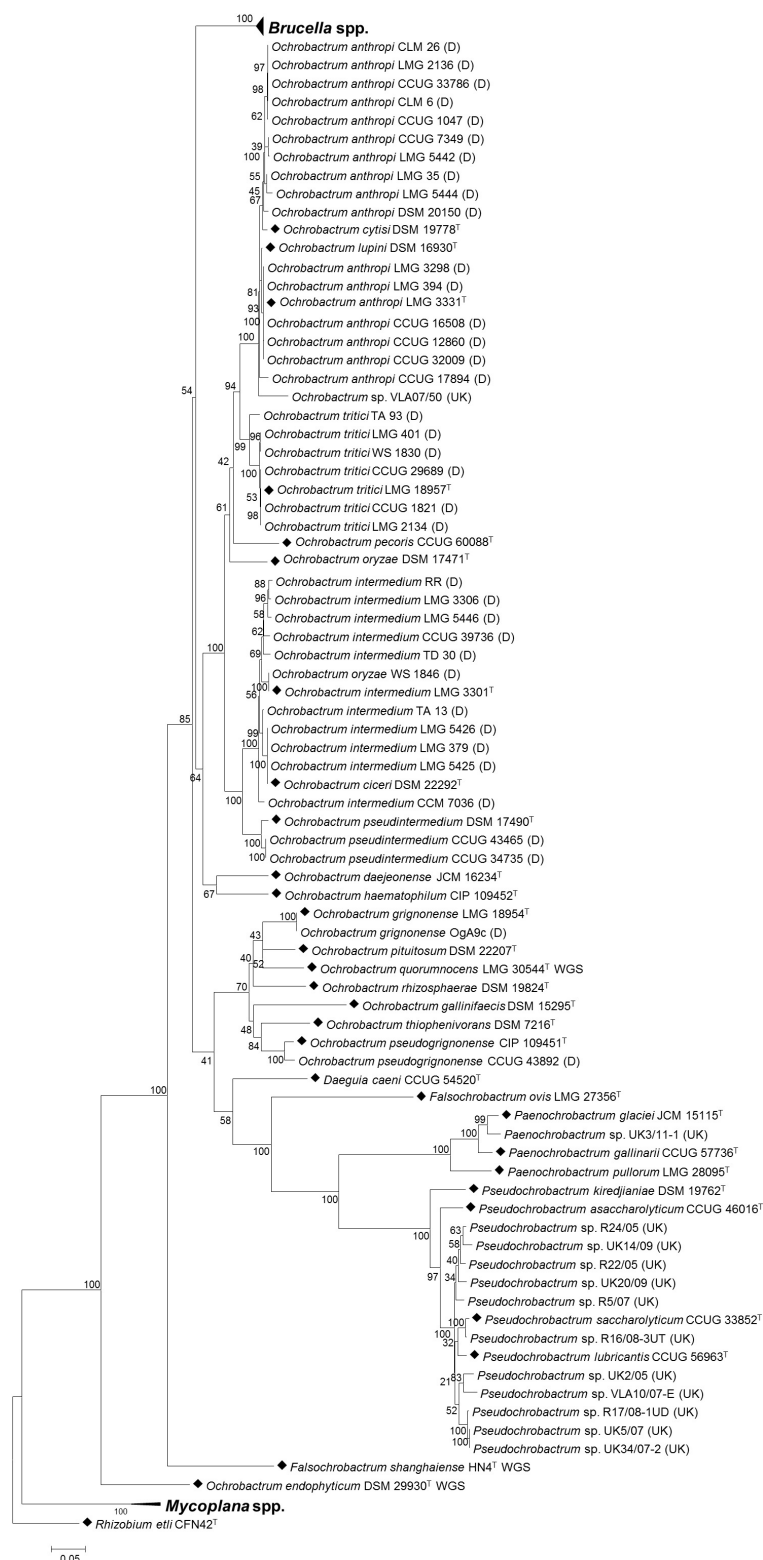


FIGURE 5 | Phylogenetic relationship between type strains of the family *Brucellaceae* ($n = 43$) and field strains ($n = 50$), based on multi-locus sequence analysis. Type strains are denoted by a black diamond (◆), whilst strains from Bundeswehr Institute of Microbiology, Germany are denoted (D) and field strains from the Animal and Plant Health Agency, United Kingdom are denoted (UK). The evolutionary history was inferred using the maximum likelihood method, based on the general time reversible model. Node labels give percentage bootstrap support. The scale bar shows the number of base substitutions per site. *Rhizobium etli* (CFN42^T) was used to root the phylogenetic tree.

of this novel strain to a wider diversity of species within the *Brucellaceae*.

Our work provides an additional tool to understand strains where conventional diagnostic approaches are confounded. Recently described “atypical” *Brucella* sp. isolates can be confused with *Ochrobactrum* sp. by diagnostic approaches such as API 20NE tests (Scholz et al., 2010; Tiller et al., 2010b; Soler-Lloréns et al., 2016). These isolates can also confound identification by matrix-assisted laser desorption/ionization time-of-flight (MALDI-TOF) mass spectrometry (MS), an increasingly widely used front-line tool in bacterial diagnostics (Cunningham and Patel, 2013). Thus there are examples where atypical *Brucella* either return no reliable identification or are misidentified as *B. melitensis* (Whatmore et al., 2015; Mühldorfer et al., 2017). The pan-family MLSA approach applied here clearly identified that all atypical strains incorporated into the analysis are much more closely related to *Brucella* than to *Ochrobactrum*.

The WGS and MLSA approaches applied here are of value in informing the ongoing debate concerning *Brucella* taxonomy and evolution, and allow accurate placement and understanding of the relationships of these organisms with extant isolates. Both methods identified a monophyletic *Brucella* clade, with a highly conserved group of ten core species and greater diversity in recently identified atypical strains. Basal branches in this clade were, however, relatively weakly supported by both methods. Nonetheless, based on currently accepted practices for defining species based on genomic ANI values (Varghese et al., 2015) all *Brucella* strains incorporated into our analyses would represent a single species. *Brucella* taxonomy continues to be controversial both at the intra-genus level and in terms of relationships with closely related species. The previous re-designation of the then six original “core” *Brucella* species as a single species based on genetic homogeneity (Verger et al., 1985) was reversed, based on community preference for a nomenclature that reflected clear differences in epidemiology and pathogenic potential of the nomenclatures (Osterman and Moriyón, 2006). The current study emphasizes the genetic homogeneity of the expanded core group, in contrast to the greater diversity seen in the recently emerged atypical *Brucella*. Attempts to describe emerging amphibian isolates as new species failed because of the heterogeneity of the isolates (Al Dahouk et al., 2017) and their placement here confirms that there are currently few distinct clusters of isolates among the atypical *Brucella* that would readily facilitate description of any well-defined new species. A more pragmatic, though not cladistic, solution may be to update the species description for *B. inopinata*, originally based on only a single isolate (BO1), taking into account the large number of recently described strains, and potentially classify all atypical *Brucella* as *B. inopinata*. Arguments that these isolates should not be members of the genus *Brucella*, as currently defined, are not supported by the genetic relationships observed here, as they clearly remain well separated from the closest *Ochrobactrum* isolates.

The current work supports previous findings, based on single-gene, multi-locus and whole genome analyses, which indicated that the genus *Ochrobactrum* represents a polyphyletic

grouping (Kämpfer et al., 2013; Aujoulat et al., 2014; Leclercq et al., 2019). Our study provides the most comprehensive analysis to date of the composition of these groupings, and their relationships to other members of the family. Both WGS and MLSA based analyses identified two main clusters, with *Ochrobactrum* Group A (*O. anthropi*, *O. lupini*, *O. cytisi*, *O. tritici*, *O. pecoris*, *O. oryzae*, *O. ciceri*, *O. intermedium*, *O. pseudintermedium*) forming a well-supported sister taxa to all *Brucella* species. The position of two further species (*O. daejeonense* and *O. haematophilum*) diverged slightly between the two methods, though both were placed with the *Brucella*-*Ochrobactrum* Group A clade (with WGS indicating *O. haematophilum* to branch basally to this group). A further *Ochrobactrum* clade (Group B) contained seven species (*O. gallinifaecis* – *O. quorumnocens* – *O. rhizosphaerae* – *O. grignonense* – *O. pituitosum* – *O. pseudogrignonense* – *O. thiophenivorans*) and formed a sister taxon to the *Brucella* – *Ochrobactrum* Group A clade in WGS based analyses (An *Ochrobactrum* group of the same composition was identified in MLSA based analysis, but in this case it was placed as a sister taxon to the clade containing *Pseudochrobactrum* spp., *Paenochrobactrum* spp. and *Falsochrobactrum ovis*). Recently, Leclercq et al. (2019) applied a phylogenomic approach to identify similar polyphyletic *Ochrobactrum* clades to those identified here. These authors suggest that there is a separation in the ecological niche of species belonging to *Ochrobactrum* groups A and B, with the former characterized by human and animal derived isolates, and the latter mainly composed of environmental and plant-associated isolates. Grouping type strains by their source of isolation did not reveal any association between *Ochrobactrum* groups and human/animal origin of isolation in the current study (Fisher’s exact test, $P > 0.05$ for both WGS and MLSA data).

Two *Ochrobactrum* species (*O. daejeonense* and *O. haematophilum*) were inconsistently placed, and often weakly supported, in analyses of data from individual loci. Examples of incongruence in placement between single gene trees of *Ochrobactrum* species are supportive of previous suggestions that horizontal gene transfer may be a driving force in the evolution of both atypical *Brucella* (Scholz et al., 2016b) and other free-living members of the *Brucellaceae* (Aujoulat et al., 2014). This is in contrast to the situation in the core *Brucella* which have been considered largely clonal with only rare horizontal gene transfer events contributing to speciation (Whatmore et al., 2007; Wattam et al., 2014).

Analyses in the current work (WGS, MLSA, individual gene and 16S rRNA based) indicated that *O. endophyticum* (DSM 29930^T) is not located within the *Ochrobactrum* groupings described above, but instead forms a distinct taxon, basal to other members of the family (with the exception of *Mycoplana* spp., though see below). Analysis of WGS data incorporating additional outgroup species (**Supplementary Figure S1**) also indicated that *O. endophyticum* remained basal to other members of the *Brucellaceae*, but was more closely related to them than the nearest taxonomic neighbors included in the analysis (*Mesorhizobium* spp. and *Aquamicrobium aerolatum*). Clarification of the true taxonomic position of *O. endophyticum*

will require the incorporation of additional strains outside of the *Brucellaceae*, but it appears that it may require amendment.

Analysis of WGS and MLSA data from *Brucellaceae* type strains identified *O. anthropi* and *O. lupini* to be closely related, consistent with a recent analysis based on WGS data, which proposed that *O. lupini* should be re-classified as a later heterotypic synonym of *O. anthropi* (Gazolla Volpiano et al., 2019). These authors also highlighted the high level of similarity observed between *O. anthropi/O. lupini* and *O. cytisi*, and recommended WGS of the type strain for the latter species, to clarify its position. Incorporation of WGS data for *O. cytisi* DSM 19778^T in the current study indicated that it is correctly identified as an independent species (adopting the threshold of 96.5% proposed by Varghese et al., 2015) with genomic ANI values of 95.2% and 95.1% relative to *O. anthropi/O. lupini*, respectively. Leclercq et al. (2019) drew the same conclusion based on sequencing of a non-type strain of *O. cytisi* (IPA7.2). High levels of similarity, consistent with possible re-classification as a single species were observed between type strains of *O. ciceri* and *O. intermedium* (genomic ANI of 98.5%) and *P. lubricantis* and *P. saccharolyticum* (genomic ANI of 97.1%).

Furthermore, it is also clear from the inclusion of field isolates into multi-locus analysis of *Brucellaceae* that there is much previously unrecognized diversity that is not reflected in currently identified species. Notable diversity was evident within the *O. anthropi* – *O. cytisi* – *O. lupini*, *O. intermedium* – *O. ciceri* and *P. saccharolyticum* – *P. lubricantis* groupings, resulting in a lack of clear monophyletic lineages for any of these taxa once field isolates were incorporated.

Basal branching orders within type strain phylogenies were largely consistent between WGS and MLSA based approaches (Figure 3). One instance where this was not the case, however, was in the placement of *Falsochrobactrum*. Both *F. ovis* and *F. shanghaiense* were placed as a sister taxon to *Ochrobactrum* Group B in analyses based on WGS data. Conversely, in analyses using MLSA, the taxon was split, with *F. ovis* placed as a sister taxon to the *Paenochrobactrum* spp., and *Pseudochrobactrum* spp. group, and *F. shanghaiense* placed basal to all member of the family other than *O. endophyticum* and *Mycoplana* spp. Leclercq et al. (2019) reported inconsistent placement of *Falsochrobactrum* spp. using a whole genome dataset, with the location differing when both species were included relative to when either was included independently. However, neither placement was fully supported by bootstrap values in their analyses. The inclusion of a more comprehensive panel of related species and, potentially, the larger number of loci employed, provides greater confidence in the placement of these species in WGS analyses from the present study, as evidenced by the level of bootstrap support achieved. Nonetheless, it is clear from levels of sequence similarity observed within this genus (both genomic ANI and MLSA nucleotide identity) that these two species are highly divergent (Figure 1 and Table 4).

Finally, incorporation of additional outgroup strains in analyses of WGS data in the current work has demonstrated that *Mycoplana* spp. were placed with maximum bootstrap support within the family *Rhizobiaceae* rather than within the *Brucellaceae*. This is consistent with the

findings of Leclercq et al. (2019) who incorporated a dataset encompassing the wider order *Rhizobiales* and demonstrated the same placement of *Mycoplana* spp. with *Ensifer* and *Sinorhizobium* species.

CONCLUSION

The work presented here provides a comprehensive multi-gene analysis of the phylogeny of an expanding bacterial family, which includes a number of significant human and veterinary pathogens. It further demonstrates the importance of a multi-gene approach, be it WGS or MLSA based, in establishing robust relationships within this group. This work has demonstrated that the genus *Brucella* as currently described forms a well-separated monophyletic group, despite its on-going expansion to incorporate genetically diverse strains from a wide range of host species. Furthermore, the work confirms *Ochrobactrum* to be polyphyletic. The analysis of non-type strains of some members of *Brucellaceae* reveals that there remains significant genetic diversity not captured within existing species. The tools and databases developed in this study provide a valuable resource against which to place novel isolates and begin to identify new groups.

DATA AVAILABILITY STATEMENT

WGS data generated for this study can be found in the NCBI SRA database under BioProject PRJNA638390. MLSA data can be found in either the *Brucella* PubMLST database (<https://pubmlst.org/brucella/>) or in the NCBI GenBank database (accession numbers given in Supplementary Table S4).

AUTHOR CONTRIBUTIONS

RA analyzed the data and drafted the manuscript. JM and MK undertook experimental work and data analysis. HS provided strains and contributed to the manuscript. AW conceived of and designed the study and contributed to the manuscript. All authors contributed to the article and approved the submitted version.

FUNDING

Brucellosis research at APHA is supported by the United Kingdom Department for Environment, Food and Rural Affairs (Defra). Development and implementation of the pan-family MLSA scheme was specifically funded as part of project SE0313.

SUPPLEMENTARY MATERIAL

The Supplementary Material for this article can be found online at: <https://www.frontiersin.org/articles/10.3389/fmicb.2020.01329/full#supplementary-material>

REFERENCES

- Al Dahouk, S., Köhler, S., Occhialini, A., Jiménez de Bagüés, M. P., Hammerl, J. A., Eisenberg, T., et al. (2017). *Brucella* spp. of amphibians comprise genomically diverse motile strains competent for replication in macrophages and survival in mammalian hosts. *iSci. Rep.* 7:44420. doi: 10.1038/srep44420
- Aujoulat, F., Romano-Bertrand, S., Masnou, A., Marchandin, H., and Jumas-Bilak, E. (2014). Niches, population structure and genome reduction in *Ochrobactrum intermedium*: clues to technology-driven emergence of pathogens. *PLoS One* 9:e83376. doi: 10.1371/journal.pone.0083376
- Bankevich, A., Nurk, S., Antipov, D., Gurevich, A. A., Dvorkin, M., Kulikov, A. S., et al. (2012). SPAdes: a new genome assembly algorithm and its applications to single-cell sequencing. *J. Comput. Biol.* 19, 455–477. doi: 10.1089/cmb.2012.0021
- Bolger, A. M., Lohse, M., and Usadel, B. (2014). Trimmomatic: a flexible trimmer for Illumina sequence data. *Bioinformatics* 30, 2114–2120. doi: 10.1093/bioinformatics/btu170
- Buddle, M. B. (1956). Studies on *Brucella ovis* (n.sp.), a cause of genital disease of sheep in New Zealand and Australia. *J. Hyg. (Lond)* 54, 351–364. doi: 10.1017/s0022172400044612
- Carmichael, L. E., and Bruner, D. W. (1968). Characteristics of a newly-recognized species of *Brucella* responsible for infectious canine abortions. *Cornell Vet.* 48, 579–592.
- Cook, I., Campbell, R. W., and Barrow, G. (1966). Brucellosis in North Queensland rodents. *Aust. Vet. J.* 42, 5–8. doi: 10.1111/j.1751-0813.1966.tb04603.x
- Corbel, M. J. (2006). *Brucellosis in Humans and Animals*. Geneva: World Health Organization.
- Cunningham, S. A., and Patel, R. (2013). Importance of using Bruker's security-relevant library for Biotyper identification of *Burkholderia pseudomallei*, *Brucella* species, and *Francisella tularensis*. *J. Clin. Microbiol.* 51, 1639–1640. doi: 10.1128/JCM.00267-13
- Eisenberg, T., Hamann, H.-P., Kaim, U., Schlez, K., Seeger, H., Schauerte, N., et al. (2012). Isolation of potentially novel *Brucella* spp. from frogs. *Appl. Environ. Microbiol.* 78, 3753–3755. doi: 10.1128/aem.07509-11
- Eisenberg, T., Rife, K., Schauerte, N., Geiger, C., Blom, J., and Scholz, H. C. (2017). Isolation of a novel 'atypical' *Brucella* strain from a bluespotted ribbontail ray (*Taeniura lymma*). *Antonie Van Leeuwenhoek* 110, 221–234. doi: 10.1007/s10482-016-0792-4
- Euzéby, J. P. (1997). List of bacterial names with standing in nomenclature: a folder available on the Internet. *Int. J. Syst. Bacteriol.* 47, 590–592. doi: 10.1099/00207713-47-2-590
- Foster, G., Osterman, B. S., Godfroid, J., Jacques, I., and Cloeckart, A. (2007). *Brucella ceti* sp. nov. and *Brucella pinnipedialis* sp. nov. for *Brucella* strains with cetaceans and seals as their preferred hosts. *Int. J. Syst. Evol. Microbiol.* 57, 2688–2693. doi: 10.1099/ijs.0.65269-0
- Gazolla Volpiano, C., Sant, H., Anna, F., Ambrosini, A., Brito Lisboa, B., et al. (2019). Reclassification of *Ochrobactrum lupini* as a later heterotypic synonym of *Ochrobactrum anthropi* based on whole-genome sequence analysis. *Int. J. Syst. Evol. Microbiol.* 69, 2312–2314. doi: 10.1099/ijsem.0.003465
- Gevers, D., Cohan, F. M., Lawrence, J. G., Spratt, B. G., Coenye, T., Feil, E. J., et al. (2005). Re-evaluating prokaryotic species. *Nat. Rev. Microbiol.* 3, 733–739. doi: 10.1038/nrmicro1236
- Gray, P. H. H., and Thornton, H. G. (1928). Soil bacteria that decompose certain aromatic compounds. *Zentralbl. Bakteriell. Parasitenkd. Infektionskr. Hyg. Abteilung II* 73, 74–96.
- Guzmán-Verri, C., Suárez-Esquivel, M., Ruiz-Villalobos, N., Zygmunt, M. S., Gonnet, M., Campos, E., et al. (2019). Genetic and phenotypic characterization of the etiological agent of canine orchepididymitis smooth *Brucella* sp. BCCN84.3. *Front. Vet. Sci.* 6:175. doi: 10.3389/fvets.2019.00175
- Holmes, B., Popoff, M., Kiredjian, M., and Kersters, K. (1988). *Ochrobactrum anthropi* gen. nov., sp. nov. from human clinical specimens and previously known as group Vd. *Int. J. Syst. Evol. Microbiol.* 38, 406–416. doi: 10.1099/00207713-38-4-406
- Huber, B., Scholz, H. C., Kämpfer, P., Falsen, E., Langer, S., and Busse, H. J. (2010). *Ochrobactrum pituitosum* sp. nov., isolated from an industrial environment. *Int. J. Syst. Evol. Microbiol.* 60, 321–326. doi: 10.1099/ijs.0.011668-0
- Huddleson, I. F. (1929). The differentiation of the species of genus *Brucella*. *Michigan State Coll. Agric. Exp. Station Tech. Bull.* 100, 1–16.
- Imran, A., Hafeez, F. Y., Frühling, A., Schumann, P., Malik, K. A., and Stackebrandt, E. (2010). *Ochrobactrum ciceri* sp. nov., isolated from nodules of *Cicer arietinum*. *Int. J. Syst. Evol. Microbiol.* 60, 1548–1553. doi: 10.1099/ijs.0.013987-9
- Jain, C., Rodriguez-R, L. M., Phillippy, A. M., Konstantinidis, K. T., and Aluru, S. (2018). High throughput ANI analysis of 90K prokaryotic genomes reveals clear species boundaries. *Nat. Commun.* 9:5114. doi: 10.1038/s41467-018-07641-9
- Kämpfer, P., Buczolits, S., Albrecht, A., Busse, H.-J., and Stackebrandt, E. (2003). Towards a standardized format for the description of a novel species (of an established genus): *Ochrobactrum gallinifacies* sp. nov. *Int. J. Syst. Evol. Microbiol.* 53, 893–896. doi: 10.1099/ijs.0.02710-0
- Kämpfer, P., Glaeser, S., Busse, H.-J., Eisenberg, T., and Scholz, H. (2013). *Falsobacterium ovis* gen. nov., sp. nov., isolated from a sheep. *Int. J. Syst. Evol. Microbiol.* 63, 3841–3847. doi: 10.1099/ijs.0.049627-0
- Kämpfer, P., and Glaeser, S. P. (2019). "Brucellaceae," in *Bergey's Manual of Systematics of Archaea and Bacteria*, eds W. B. Whitman, F. Rainey, P. Kämpfer, M. Trujillo, J. Chun, P. DeVos, et al. (Hoboken, NJ: John Wiley & Sons, Inc). doi: 10.1002/9781118960608.fbm00166.pub2
- Kämpfer, P., Glaeser, S. P., and Holmes, B. (2018). "Ochrobactrum," in *Bergey's Manual of Systematics of Archaea and Bacteria*, eds W. B. Whitman, F. Rainey, P. Kämpfer, M. Trujillo, J. Chun, P. DeVos, et al. (Hoboken, NJ: John Wiley & Sons, Inc). doi: 10.1002/9781118960608.fbm00809.pub2
- Kämpfer, P., Huber, B., Busse, H. J., Scholz, H. C., Tomaso, H., Hotzel, H., et al. (2011). *Ochrobactrum pecoris* sp. nov., isolated from farm animals. *Int. J. Syst. Evol. Microbiol.* 61, 2278–2283. doi: 10.1099/ijs.0.027631-0
- Kämpfer, P., Huber, B., Lodders, N., Warfolomeow, I., Busse, H.-J., and Scholz, H. C. (2009). *Pseudochrobactrum lubricantis* sp. nov., isolated from a metal-working fluid. *Int. J. Syst. Evol. Microbiol.* 59, 2464–2467. doi: 10.1099/ijs.0.008540-0
- Kämpfer, P., Martin, E., Lodders, N., Jackel, U., Huber, B. E., Schumann, P., et al. (2010). *Paenochrobactrum gallinarii* gen. nov., sp. nov., isolated from air of a duck barn, and reclassification of *Pseudochrobactrum glaciei* as *Paenochrobactrum glaciei* comb. nov. *Int. J. Syst. Evol. Microbiol.* 60, 1493–1498. doi: 10.1099/ijs.0.015842-0
- Kämpfer, P., Poppel, M. T., Wilharm, G., Glaeser, S. P., and Busse, H. J. (2014). *Paenochrobactrum pullorum* sp. nov. isolated from a chicken. *Int. J. Syst. Evol. Microbiol.* 64, 1724–1728. doi: 10.1099/ijs.0.061101-0
- Kämpfer, P., Rosselló-Mora, R., Scholz, H. C., Welinder-Olsson, C., Falsen, E., and Busse, H.-J. (2006). Description of *Pseudochrobactrum* gen. nov., with the two species *Pseudochrobactrum asaccharolyticum* sp. nov. and *Pseudochrobactrum saccharolyticum* sp. nov. *Int. J. Syst. Evol. Microbiol.* 56, 1823–1829. doi: 10.1099/ijs.0.64256-0
- Kämpfer, P., Scholz, H. C., Huber, B., Falsen, E., and Busse, H.-J. (2007a). *Ochrobactrum haematophilum* sp. nov. and *Ochrobactrum pseudogrignone* sp. nov., isolated from human clinical specimens. *Int. J. Syst. Evol. Microbiol.* 57, 2513–2518. doi: 10.1099/ijs.0.65066-0
- Kämpfer, P., Scholz, H., Huber, B., Thummens, K., Busse, H.-J., Maas, E. W., et al. (2007b). Description of *Pseudochrobactrum kiredjianiae* sp. nov. *Int. J. Syst. Evol. Microbiol.* 57, 755–760. doi: 10.1099/ijs.0.64714-0
- Kämpfer, P., Sessitsch, A., Schlöter, M., Huber, B., Busse, H. J., and Scholz, H. C. (2008). *Ochrobactrum rhizosphaerae* sp. nov. and *Ochrobactrum thiophenivorans* sp. nov., isolated from the environment. *Int. J. Syst. Evol. Microbiol.* 58, 1426–1431. doi: 10.1099/ijs.0.65407-0
- Katoh, K., Misawa, K., Kuma, K.-I., and Miyata, T. (2002). MAFFT: a novel method for rapid multiple sequence alignment based on fast Fourier transform. *Nucleic Acids Res.* 30, 3059–3066. doi: 10.1093/nar/gkf436
- Kozlov, A. M., Darriba, D., Flouri, T., Morel, B., and Stamatakis, A. (2019). RAXML-NG: a fast, scalable and user-friendly tool for maximum likelihood phylogenetic inference. *Bioinformatics* 35, 4453–4455. doi: 10.1093/bioinformatics/btz305
- Krzyzanowska, D. M., Maciag, T., Ossowicki, A., Rajewska, M., Kaczyński, Z., Czerwicka, M., et al. (2019). *Ochrobactrum quorumnecens* sp. nov., a quorum quenching bacterium from the potato rhizosphere, and comparative genome analysis with related type strains. *PLoS One* 14:e0210874. doi: 10.1371/journal.pone.0210874

- Lebuhn, M., Achouak, W., Schloter, M., Berge, O., Meier, H., Barakat, M., et al. (2000). Taxonomic characterization of *Ochrobactrum* sp. isolates from soil samples and wheat roots, and description of *Ochrobactrum tritici* sp. nov. and *Ochrobactrum grignonense* sp. nov. *Int. J. Syst. Evol. Microbiol.* 50, 2207–2223. doi: 10.1099/00207713-50-6-2207
- Leclercq, S. O., Cloeckaert, A., and Zygmunt, M. S. (2019). Taxonomic organization of the family *Brucellaceae* based on a phylogenomic approach. *Front. Microbiol.* 10:3083. doi: 10.3389/fmicb.2019.03083
- Li, L., Li, Y. Q., Jiang, Z., Gao, R., Nimaichand, S., Duan, Y. Q., et al. (2016). *Ochrobactrum endophyticum* sp. nov., isolated from roots of *Glycyrrhiza uralensis*. *Arch. Microbiol.* 198, 171–179. doi: 10.1007/s00203-015-1170-8
- Linhart, C., and Shamir, R. (2007). Degenerate primer design: theoretical analysis and the HYDEN program. *Methods Mol. Biol.* 402, 221–244. doi: 10.1007/978-1-59745-528-2_11
- Meyer, K. F., and Shaw, E. B. (1920). A comparison of the morphological, cultural and biochemical characteristics of *B. abortus* and *B. melitensis*, Studies on the genus *Brucella* nov. gen. I. *J. Infect. Dis.* 27, 173–184.
- Mühldorfer, K., Wibbelt, G., Szentiks, C. A., Fischer, D., Scholz, H. C., Zschöck, M., et al. (2017). The role of 'atypical' *Brucella* in amphibians: are we facing novel emerging pathogens? *J. Appl. Microbiol.* 122, 40–53. doi: 10.1111/jam.13326
- Osterman, B., and Moriyón, I. (2006). International committee on systematics of prokaryotes; subcommittee on the taxonomy of *Brucella*. *Int. J. Syst. Evol. Microbiol.* 56, 1173–1175. doi: 10.1099/ijs.0.64349-0
- Page, A. J., Cummins, C. A., Hunt, M., Wong, V. K., Reuter, S., Holden, M. T. G., et al. (2015). Roary: rapid large-scale prokaryote pan genome analysis. *Bioinformatics* 31, 3691–3693. doi: 10.1093/bioinformatics/btv421
- Pappas, G., Papadimitriou, P., Akritidis, N., Christou, L., and Tsianos, E. V. (2006). The new global map of human brucellosis. *Lancet Infect. Dis.* 6, 91–99. doi: 10.1016/S1473-3099(06)70382-6
- Parte, A. C. (2014). LPSN—list of prokaryotic names with standing in nomenclature. *Nucleic Acids Res.* 42, D613–D616. doi: 10.1093/nar/gkt1111
- Romanenko, L. A., Tanaka, N., Frolova, G. M., and Mikhailov, V. V. (2008). *Pseudochrobactrum glaciei* sp. nov., isolated from sea ice collected from Peter the Great Bay of the Sea of Japan. *Int. J. Syst. Evol. Microbiol.* 58, 2454–2458. doi: 10.1099/ijs.0.65828-0
- Romano, S., Aujoulat, F., Jumas-Bilak, E., Masnou, A., Jeannot, J.-L., Falsen, E., et al. (2009). Multilocus sequence typing supports the hypothesis that *Ochrobactrum anthropi* displays a human-associated subpopulation. *BMC Microbiol.* 9:267. doi: 10.1186/1471-2180-9-267
- Scholz, H. C., Banai, M., Cloeckaert, A., Kämpfer, P., and Whatmore, A. M. (2018). "Brucella," in *Bergey's Manual of Systematics of Archaea and Bacteria*, eds W. B. Whitman, F. Rainey, P. Kämpfer, M. Trujillo, J. Chun, P. DeVos, et al. (Hoboken, NJ: John Wiley & Sons, Inc). doi: 10.1002/9781118960608.gbm00807.pub2
- Scholz, H. C., Al Dahouk, S., Tomaso, H., Neubauer, H., Witte, A., Schloter, M., et al. (2008a). Genetic diversity and phylogenetic relationships of bacteria belonging to the *Ochrobactrum-Brucella* group by *recA* and 16S rRNA gene-based comparative sequence analysis. *Syst. Appl. Microbiol.* 31, 1–16. doi: 10.1016/j.syapm.2007.10.004
- Scholz, H. C., Hubalek, Z., Sedláček, I., Vergnaud, G., Tomaso, H., Al Dahouk, S., et al. (2008b). *Brucella microti* sp. nov., isolated from the common vole *Microtus arvalis*. *Int. J. Syst. Evol. Microbiol.* 58, 375–382. doi: 10.1099/ijs.0.65356-0
- Scholz, H. C., Nöckler, K., Göllner, C., Bahn, P., Vergnaud, G., Tomaso, H., et al. (2010). *Brucella inopinata* sp. nov., isolated from a breast implant infection. *Int. J. Syst. Evol. Microbiol.* 60, 801–808. doi: 10.1099/ijs.0.011148-0
- Scholz, H. C., Revilla-Fernandez, S., Al Dahouk, S., Hammerl, J. A., Zygmunt, M. S., Cloeckaert, A., et al. (2016a). *Brucella vulpis* sp. nov., isolated from mandibular lymph nodes of red foxes (*Vulpes vulpes*). *Int. J. Syst. Evol. Microbiol.* 66, 2090–2098. doi: 10.1099/ijs.0.000998
- Scholz, H. C., Muehldorfer, K., Shilton, C., Benedict, S., Whatmore, A. M., Blom, J., et al. (2016b). The change of a medically important genus: worldwide occurrence of genetically diverse novel *Brucella* species in exotic frogs. *PLoS One* 11:e0168872. doi: 10.1371/journal.pone.0168872
- Seemann, T. (2014). Prokka: rapid prokaryotic genome annotation. *Bioinformatics* 30, 2068–2069. doi: 10.1093/bioinformatics/btu153
- Soler-Lloréns, P. F., Quance, C. R., Lawhon, S. D., Stuber, T. P., Edwards, J. F., Ficht, T. A., et al. (2016). A *Brucella* spp. isolate from a Pac-Man Frog (*Ceratophrys ornata*) reveals characteristics departing from classical *Brucellae*. *Front. Cell. Infect. Microbiol.* 6:116. doi: 10.3389/fcimb.2016.00116
- Stoener, H. G., and Lackman, D. B. (1957). A new species of *Brucella* isolated from the desert wood rat, *Neotoma lepida* Thomas. *Am. J. Vet. Res.* 18, 947–951.
- Sun, L., Yao, L., Gao, X., Huang, K., Bai, N., Lyu, W., et al. (2019). *Falsobacterium shanghaiense* sp. nov., isolated from paddy soil and emended description of the genus *Falsobacterium*. *Int. J. Syst. Evol. Microbiol.* 69, 778–782. doi: 10.1099/ijs.0.003236
- Tamura, K., Peterson, D., Peterson, N., Stecher, G., Nei, M., and Kumar, S. (2011). MEGA5: molecular evolutionary genetics analysis using maximum likelihood, evolutionary distance, and maximum parsimony methods. *Mol. Biol. Evol.* 28, 2731–2739. doi: 10.1093/molbev/msr121
- Teyssier, C., Marchandin, H., Jean-Pierre, H., Masnou, A., Dusart, G., and Jumas-Bilak, E. (2007). *Ochrobactrum pseudintermedium* sp. nov., a novel member of the family *Brucellaceae*, isolated from human clinical samples. *Int. J. Syst. Evol. Microbiol.* 57, 1007–1013. doi: 10.1099/ijs.0.64416-0
- Tiller, R. V., Gee, J. E., Frace, M. A., Taylor, T. K., Setubal, J. C., Hoffmaster, A. R., et al. (2010a). Characterization of novel *Brucella* strains originating from wild native rodent species in North Queensland, Australia. *Appl. Environ. Microbiol.* 76, 5837–5845. doi: 10.1128/aem.00620-10
- Tiller, R. V., Gee, J. E., Lonsway, D. R., Gribble, S., Bell, S. C., Jennison, A. V., et al. (2010b). Identification of an unusual *Brucella* strain (BO2) from a lung biopsy in a 52 year-old patient with chronic destructive pneumonia. *BMC Microbiol.* 10:23. doi: 10.1186/1471-2180-10-23
- Tripathi, A. K., Verma, S. C., Chowdhury, S. P., Lebuhn, M., Gatteringer, A., and Schloter, M. (2006). *Ochrobactrum oryzae* sp. nov., an endophytic bacterial species isolated from deep-water rice in India. *Int. J. Syst. Evol. Microbiol.* 56, 1677–1680. doi: 10.1099/ijs.0.63934-0
- Trujillo, M. E., Willems, A., Abril, A., Planchuelo, A.-M., Rivas, R., Ludeña, D., et al. (2005). Nodulation of *Lupinus albus* by strains of *Ochrobactrum lupini* sp. nov. *Appl. Environ. Microbiol.* 71, 1318–1327. doi: 10.1128/AEM.71.3.1318-1327.2005
- Urakami, T., Oyanagi, H., Araki, H., Suzuki, K.-I., and Komagata, K. (1990). Recharacterization and emended description of the genus *Mycoplana* and description of two new species, *Mycoplana ramosa* and *Mycoplana segnis*. *Int. J. Syst. Evol. Microbiol.* 40, 434–442. doi: 10.1099/00207713-40-4-434
- Varghese, N. J., Mukherjee, S., Ivanova, N., Konstantinidis, K. T., Mavrommatis, K., Kyrpides, N. C., et al. (2015). Microbial species delineation using whole genome sequences. *Nucleic Acids Res.* 43, 6761–6771. doi: 10.1093/nar/gkv657
- Velasco, J., Romero, C., Lopez-Goni, I., Leiva, J., Diaz, R., and Moriyon, I. (1998). Evaluation of the relatedness of *Brucella* spp. and *Ochrobactrum anthropi* and description of *Ochrobactrum intermedium* sp. nov., a new species with a closer relationship to *Brucella* spp. *Int. J. Syst. Bacteriol.* 48, 759–768. doi: 10.1099/00207713-48-3-759
- Verger, J.-M., Grimont, F., Grimont, P. A. D., and Grayon, M. (1985). *Brucella*, a monospecific genus as shown by deoxyribonucleic acid hybridization. *Int. J. Syst. Evol. Microbiol.* 35, 292–295. doi: 10.1099/00207713-35-3-292
- Wattam, A. R., Foster, J. T., Mane, S. P., Beckstrom-Sternberg, S. M., Beckstrom-Sternberg, J. M., Dickerman, A. W., et al. (2014). Comparative phylogenomics and evolution of the *Brucellae* reveal a path to virulence. *J. Bacteriol.* 196, 920–930. doi: 10.1128/jb.01091-13
- Wattam, A. R., Inzana, T. J., Williams, K. P., Mane, S. P., Shukla, M., Almeida, N. F., et al. (2012). Comparative genomics of early-diverging *Brucella* strains reveals a novel lipopolysaccharide biosynthesis pathway. *mBio* 3:e00246-12. doi: 10.1128/mBio.00388-12
- Whatmore, A. M., Dale, E. J., Stubberfield, E., Muchowski, J., Koylass, M., Dawson, C., et al. (2015). Isolation of *Brucella* from a White's tree frog (*Litoria caerulea*). *JMM Case Rep.* 2015:2. doi: 10.1099/jmmcr.0.000017
- Whatmore, A. M., Davison, N., Cloeckaert, A., Al Dahouk, S., Zygmunt, M. S., Brew, S. D., et al. (2014). *Brucella papionis* sp. nov., isolated from baboons

- (*Papio* spp.). *Int. J. Syst. Evol. Microbiol.* 64, 4120–4128. doi: 10.1099/ijs.0.065482-0
- Whatmore, A. M., Koylass, M. S., Muchowski, J., Edwards-Smallbone, J., Gopaul, K. K., and Perrett, L. L. (2016). Extended multilocus sequence analysis to describe the global population structure of the genus *Brucella*: phylogeography and relationship to biovars. *Front. Microbiol.* 7:2049. doi: 10.3389/fmicb.2016.02049
- Whatmore, A. M., Perrett, L. L., and MacMillan, A. P. (2007). Characterisation of the genetic diversity of *Brucella* by multilocus sequencing. *BMC Microbiol.* 7:34. doi: 10.1186/1471-2180-7-34
- Woo, S. G., Ten, L. N., Park, J., and Lee, M. (2011). *Ochrobactrum daejeonense* sp. nov., a nitrate-reducing bacterium isolated from sludge of a leachate treatment plant. *Int. J. Syst. Evol. Microbiol.* 61, 2690–2696. doi: 10.1099/ijs.0.025510-0
- Wragg, P., Randall, L., and Whatmore, A. M. (2014). Comparison of Biolog GEN III MicroStation semi-automated bacterial identification system with matrix-assisted laser desorption ionization-time of flight mass spectrometry and 16S ribosomal RNA gene sequencing for the identification of bacteria of veterinary interest. *J. Microbiol. Methods* 105, 16–21. doi: 10.1016/j.mimet.2014.07.003
- Yoon, J. H., Kang, S. J., Park, S., and Oh, T. K. (2008). *Daeguia caeni* gen. nov., sp. nov., isolated from sludge of a textile dye works. *Int. J. Syst. Evol. Microbiol.* 58, 168–172. doi: 10.1099/ijs.0.65483-0
- Zurdo-Piñero, J. L., Rivas, R., Trujillo, M. E., Vizcaino, N., Carrasco, J. A., Chamber, M., et al. (2007). *Ochrobactrum cytisi* sp. nov., isolated from nodules of *Cytisus scoparius* in Spain. *Int. J. Syst. Evol. Microbiol.* 57, 784–788. doi: 10.1099/ijs.0.64613-0

Conflict of Interest: The authors declare that the research was conducted in the absence of any commercial or financial relationships that could be construed as a potential conflict of interest.

Copyright © 2020 Ashford, Muchowski, Koylass, Scholz and Whatmore. This is an open-access article distributed under the terms of the Creative Commons Attribution License (CC BY). The use, distribution or reproduction in other forums is permitted, provided the original author(s) and the copyright owner(s) are credited and that the original publication in this journal is cited, in accordance with accepted academic practice. No use, distribution or reproduction is permitted which does not comply with these terms.

Advantages of publishing in Frontiers



OPEN ACCESS

Articles are free to read
for greatest visibility
and readership



FAST PUBLICATION

Around 90 days
from submission
to decision



HIGH QUALITY PEER-REVIEW

Rigorous, collaborative,
and constructive
peer-review



TRANSPARENT PEER-REVIEW

Editors and reviewers
acknowledged by name
on published articles

Frontiers

Avenue du Tribunal-Fédéral 34
1005 Lausanne | Switzerland

Visit us: www.frontiersin.org

Contact us: frontiersin.org/about/contact



REPRODUCIBILITY OF RESEARCH

Support open data
and methods to enhance
research reproducibility



DIGITAL PUBLISHING

Articles designed
for optimal readership
across devices



FOLLOW US

@frontiersin



IMPACT METRICS

Advanced article metrics
track visibility across
digital media



EXTENSIVE PROMOTION

Marketing
and promotion
of impactful research



LOOP RESEARCH NETWORK

Our network
increases your
article's readership